

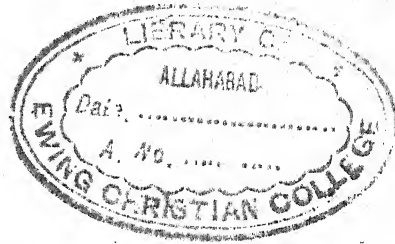
THE PHYSICAL REVIEW

A JOURNAL OF EXPERIMENTAL AND
THEORETICAL PHYSICS

CONDUCTED BY

THE

AMERICAN PHYSICAL SOCIETY



BOARD OF EDITORS

Managing Editor: John T. TATE, University of Minnesota, Minneapolis;
K. K. DARROW, E. C. KEMBLE, F. L. MOHLER; J. A. GRAY, G. E. M. JAUNCEY,
J. H. VAN VLECK; G. BREIT, P. W. BRIDGMAN, L. W. MCKEEHAN.

VOLUME 29, SECOND SERIES

JANUARY-JUNE, 1927

THE PHYSICAL REVIEW

MINNEAPOLIS, MINN.

The Collegiate Press
GEORGE BANTA PUBLISHING COMPANY
MENASHA, WISCONSIN

CONTENTS

JANUARY, 1927

Electron Distribution in the Atoms of Crystals. Sodium Chloride and Lithium, Sodium and Calcium Fluorides - - - - -	R. J. HAVIGHURST	1
Measurements and Interpretation of the Intensity of X-rays Reflected from Sodium Chloride Aluminum - - - - -	J. A. BEARDEN	20
The Crystal Structure of Magnesium Di-Zincide - - - - -	JAMES B. FRIAUF	34
Absorption in the Region of Soft X-rays - - - - -	ELIZABETH R. LAIRD	41
Line Spectra of the Isotopes of Mercury and Chlorine - - - - -	FRANCIS A. JENKINS	50
Quantum Analysis of the Band Spectrum of Aluminum Oxide ($\lambda 5200-\lambda 4650$) - - - - -	WILLIAM C. POMEROY	59
Oxygen Bands in the Ultra-Violet - - - - -	VIVIAN M. ELLSWORTH AND J. J. HOPFIELD	79
Many-Lined Spectrum of Sodium Hydride - - - - -	E. H. JOHNSON	85
Band Spectrum of Calcium Hydride - - - - -	E. HULTHÈN	97
Correlation of the Fluorescent and Absorption Spectra of Iodine - - - - -	F. W. LOOMIS	112
Absorption Coefficient of Helium for its own Radiation - - - - -	A. WOLF AND B. B. WEATHERBY	135
Electron Collisions in Carbon Monoxide - - - - -	F. L. MOHLER AND PAUL D. FOOTE	141
Influence of a Magnetic Field on the Dielectric Constant of a Diatomic Dipole Gas - - - - -	LINUS PAULING	145
Differences in the Time Lags of the Faraday Effect behind the Magnetic Field in Various Liquids - - - - -	J. W. BEAMS AND FRED ALLISON	161
Resistance of Copper Wires at Very High Frequencies - - - - -	W. M. ROBERDS	165
Principal Magnetic Susceptibilities of Crystals - - - - -	I. I. RABI	174
Scattering of Particles by an Einstein Center - - - - -	T. TAKEUCHI	186
Breakdown of Atoms at High Pressures - - - - -	P. W. BRIDGMAN	188
Continuous Motion Produced by Vibration - - - - -	W. B. MORTON AND A. MCKINSTRY	192
Book Reviews - - - - -		197
PROCEEDINGS OF THE AMERICAN PHYSICAL SOCIETY		
Chicago Meeting, November 26-27, 1926; Minutes and Abstracts 1-57; Author Index - - -		204

FEBRUARY, 1927

Crystal Structure of Magnesium Platino-cyanide Heptahydrate - - - - -	RICHARD M. BOZWORTH AND F. E. HAWORTH	223
Series Spectra of Boron, Carbon, Nitrogen, Oxygen and Fluorine - - - - -	I. S. BOWEN	231
Velocity Distribution of Electrons Issuing from Small Holes - - - - -	ROBERT H. DALTON AND WARREN P. BAXTER	248
Photoelectric Emission as a Function of Composition in Sodium-Potassium Alloys - - - - -	HERBERT E. IVES AND G. R. STILWELL	252
Symmetrical Top in the Undulatory Mechanics - - - - -	R. DE L. KRONIG AND I. I. RABI	262
Energy of the Crossed-Orbit Model of the Hydrogen Molecule - - - - -	ELMER HUTCHISSON	270
Electron Affinity of Hydrogen and the Second Ionization Potential of Lithium - - - - -	LINUS PAULING	285
Measurement of Index of Refraction of Gases at Higher Temperatures - - - - -	E. W. CHENEY	292
Determination of the Dielectric Constant of Air by a Discharge Method - - - - -	A. P. CARMAN AND K. H. HUBBARD	299
Magnetic Moment of the Hydrogen Atom - - - - -	T. E. PHIPPS AND J. B. TAYLOR	309
Magnetic Properties of Evaporated Nickel and Iron Films - - - - -	R. L. EDWARDS	321
Hall Effect in Bismuth with Small Magnetic Fields - - - - -	C. W. HEAPS	332
Temperature Distribution Along a Filament - - - - -	V. BUSH AND KING E. GOULD	337
Book Reviews - - - - -		346
PROCEEDINGS OF THE AMERICAN PHYSICAL SOCIETY		
Philadelphia Meeting, December 28, 29, 30, 1926; Minutes and Abstracts 1-77; Author Index - - -		350

CONTENTS

MARCH, 1927

Reflection of X-rays by Crystals as a Problem in the Reflection of Radiation by Parallel Planes	SAMUEL K. ALLISON	375
Spark Spectrum of Copper (Cu II)	A. G. SHENSTONE	380
Electronic States and Band Spectrum Structure in Diatomic Molecules: III, Intensity Relations	ROBERT S. MULLIKEN	391
Rotational Terms in the MgH Bands	WILLIAM W. WATSON AND PHILIP RUDNICK	413
Excitation of Spectra by Atomic Hydrogen	F. L. MOHLER	419
Multiplets in Two Electron Systems of the First Long Period	R. C. GIBBS AND H. E. WHITE	426
Electron Scattering in Helium	E. G. DYMOND	433
Ionization and Resonance Potentials in Gallium and Indium	CHARLES W. JARVIS	442
Photoelectric Properties of Thoroughly Outgassed Platinum	LEE A. DU BRIDGE	451
Excitation of Fluorescence in Fluorescein	E. H. KENNARD	466
Compound Interferometer for Fine Structure Work	WILLIAM V. HOUSTON	478
Absolute Method for Measuring the Velocity of Fluids	H. E. HARTIG AND H. B. WILCOX	485
Book Reviews		491

APRIL, 1927

Carbon Atom Model and the Structure of Diamond-	R. B. LINDSAY	497
Series Spectra of Ionized Phosphorus, P_{II}	I. S. BOWEN	510
Diffusion of Imprisoned Resonance Radiation in Mercury Vapor	MARK W. ZEMANSKY	513
On the Surface Heat of Charging	LEWI TONKS AND IRVING LANGMUIR	524
Piezoelectricity of Crystal Quartz-	L. H. DAWSON	532
Transformation Period of the Initial Positive Air Ion	LEILA M. VALASEK	542
Resonance in Alternating Currents Containing a Single Harmonic	FREDERIC H. MILLER	546
Thermo-Electric Effect in Single Crystal Zinc	ERNEST G. LINDER	554
Magnetic Permeability of Iron and Magnetite in High Frequency Alternating Fields	G. R. WAIT	566
Phenomena Depending on the Change of Elastic Frequencies in Solid Bodies with Pressure	F. ZWICKY	579
Direct Comparison of the Loudness of Pure Tones	B. A. KINGSBURY	588
Book Reviews		601

PROCEEDINGS OF THE AMERICAN PHYSICAL SOCIETY

New York Meeting, February 25-26, 1927; Minutes and Abstracts 1-47; Author Index - 604

MAY, 1927

X-ray Isochromats of Copper Taken in Different Directions Relative to the Cathode Stream	WARREN W. NICHOLAS	619
Polarization Factor in X-ray Reflection	PAUL KIRKPATRICK	632
Electronic States and Band Spectrum Structure in Diatomic Molecules. IV. Hund's Theory; Second Positive Nitrogen and Swan Bands; Alternating Intensities	ROBERT S. MULLIKEN	637
Screening Constants from Optical Data	O. LAPORTE	650
Multiplets in Three Electron Systems of the First Long Period	R. C. GIBBS AND H. E. WHITE	655
Absorption Spectra of Ga, In, Mn, Cr, Ni and Co in Underwater Sparks	ALPHEUS SMITH AND MORRIS MUSKAT	663
Stages in the Excitation of the Spectrum of Indium	JOHN G. FRAYNE AND CHARLES W. JARVIS	673
Secondary Radiation and Polarization of Resonance Radiation in Cadmium	WALTER A. MACNAIR	677
Ionization by Collisions of the Second Kind in the Rare Gases	GAYLORD P. HARNWELL	683
Changes in the Photoelectric Threshold of Mercury	HUGH K. DUNN	693
On Atomic Properties Which Make an Element a Metal-	K. F. HERZFELD	701
Absorption of Radio Waves in the Upper Atmosphere	E. O. HULBURTT	706
Electrical Measurements at Radio Frequencies	S. L. BROWN AND M. Y. COLBY	717
Dielectric Constants and Magnetic Susceptibilities in the New Quantum Mechanics. Part I. General Proof of the Langevin-Debye Formula	J. H. VAN VLECK	727
Book Reviews		745

PROCEEDINGS OF THE AMERICAN PHYSICAL SOCIETY

Los Angeles Meeting, March 5, 1927; Minutes and Abstracts 1-31; Author Index - - - 748

CONTENTS

v

JUNE, 1927

Theory of the Intensity of Scattered X-rays - - - - -	G. E. M. JAUNCEY	757
Effect of Chemical Combination on X-ray Absorption - - - - -	W. B. MOREHOUSE	765
Heat Energy of X-rays - - - - -	ROY KEGERREIS	775
On the Calculation of the Spectroscopic Terms Derived from Equivalent Electrons - - - - -	HENRY NORRIS RUSSELL	782
Terms Arising from Similar and Dissimilar Electrons - - - - -	R. C. GIBBS, D. T. WILBER AND H. E. WHITE	790
Line Intensities in the Hydrogen Chloride Fundamental Band - - - - -	D. G. BOURGIN	794
Relative Intensities of Some Lines in the Mercury Spectrum - - - - -	JOSEPH VALASEK	817
Probability of Ionization of Mercury Vapor by Electron Impact - - - - -	T. J. JONES	822
Ionization by Collisions of the Second Kind in Mixtures of Hydrogen and Nitrogen with the Rare Gases - - - - -	GAYLORD P. HARNWELL	830
Number of Radiating Atoms in a Hydrogen Discharge Tube - - - - -	W. H. CREW AND E. O. HULBURT	843
Study of the Polarization of Light from Hydrogen Canal Rays - - - - -	K. L. HERTEL	848
Electron Emission from Thoriated Tungsten - - - - -	S. DUSHMAN AND JESSIE W. EWALD	857
Neutralization of the Deflecting Field in a Braun Tube with External Electrodes - - - - -	L. T. JONES AND A. M. CRAVATH	871
Index of Refraction of Water for Short Continuous Waves - - - - -	L. E. McCARTY AND L. T. JONES	880
High Frequency Resistance of a Bureau of Standards Type Variable Air Condenser - - - - -	S. L. BROWN, C. F. WIEBUSCH AND M. Y. COLBY	887
Note on the Plane Wave in a Gas - - - - -	SATYENDRA RAY	892
Book Reviews - - - - -		894
PROCEEDINGS OF THE AMERICAN PHYSICAL SOCIETY		
Washington Meeting, April 22, 23, 1927; Minutes and Abstracts 1-94; Author Index - - - - -		901
Index to Volume 29 - - - - -		937



Second Series

January, 1927

No. 29, No. 1.

THE
PHYSICAL REVIEW

ELECTRON DISTRIBUTION IN THE ATOMS OF CRYSTALS.
SODIUM CHLORIDE AND LITHIUM, SODIUM AND
CALCIUM FLUORIDES

By R. J. HAVIGHURST*

ABSTRACT

Determination of electron density by means of a Fourier analysis. The application of the correspondence principle by Epstein and Ehrenfest to Duane's quantum theory of diffraction leads to the conclusion that the electron density, $\rho(xyz)$, at any point in the unit cell of a crystal may be represented by a Fourier's series the general term of which is

$$A_{n_1 n_2 n_3} \sin(2\pi n_1 x/a_1 - \delta_{n_1}) \sin(2\pi n_2 y/a_2 - \delta_{n_2}) \sin(2\pi n_3 z/a_3 - \delta_{n_3})$$

$A_{n_1 n_2 n_3}$ is proportional to the structure factor for x-ray reflection from the $(n_1 n_2 n_3)$ plane, where n_1 , n_2 , and n_3 are the Miller indices multiplied by the order of reflection. Considerations of symmetry fix the values of the phase constants, and the assumption that the coefficients are all positive at the center of the heaviest atom in the unit cell fixes the algebraic signs. For crystals of the rock-salt or fluorite types the series becomes a simple cosine series in which the values of the structure factors previously determined by the author may be used as coefficients. If the atoms are assumed to possess spherical symmetry, the number of electrons in a spherical shell of radius r and thickness dr is $U dr = 4\pi r^2 p dr$ and the total number of electrons in the atom is equal to the integral of $U dr$. A. H. Compton has obtained the same expression for the electron density in a crystal, as well as a series expression for $U dr$, on the basis of classical theory.

Results of the Fourier analysis. Application of this method of analysis to the calculated F curve from a model sodium ion shows that the series converge rapidly when the F values are uncorrected for the effect of thermal agitation, and that reliable results may be obtained after extrapolation of the experimental F curves for light atoms to zero values of F . Curves are given which show the variation of electron density along the cube edges of the unit cells of NaCl, LiF, and NaF, and along the cube diagonal of CaF₂. U curves for the different atoms, showing the variation of U with r , give the following information: (1) the points of the crystal lattice are occupied by ions (no *a priori* assumptions have been made concerning the amount of electricity associated with a lattice point); (2) the sum of the radii of any two ions in a crystal is approximately equal to the distance of closest approach as determined by ordinary crystal analysis; (3) the electron distributions in the Na⁺ of NaF and NaCl are markedly different, while the distributions in F⁻ from all three fluorides are practically identical; (4) there is evidence of the existence of electrons in shells which are in rough agreement with Stoner's scheme of electron distribution.

* National Research Fellow.

INTRODUCTION

THE most direct means in our possession of determining the electron distribution in atoms lies in the use of experimental measurements on the scattering powers of these atoms for x-rays. From the F curves for crystals, which represent the variation of the scattering power with angle of scattering, individual F curves for the component atoms may be obtained, and the problem consists of finding the electron arrangements which will account for the experimental values of F . The experimental data used in this paper have been obtained by a powdered crystal method¹ which is free from error due to primary and secondary extinction.

Before considering the method of Fourier analysis which the author has used, we may mention the method of trial, used by A. H. Compton² and by Bragg, James and Bosanquet,³ in which the F values for various assumed distributions are calculated and the distribution giving results which are in best agreement with the experimental data is taken as correct. This method as applied by Bragg, James and Bosanquet to the atoms of rock salt gives distributions which are in rough agreement with those obtained by the Fourier analysis. However, a direct method has obvious advantages over a method of trial.

DETERMINATION OF ELECTRON DISTRIBUTION BY FOURIER ANALYSIS

The first suggestion of the use of a Fourier's series to express the distribution of diffracting power in a crystal seems to have been made by W. H. Bragg,⁴ but the method was not put into practice until quite recently,^{5,6} after the application of the correspondence principle by Epstein and Ehrenfest⁷ to Duane's⁸ quantum theory of diffraction. Epstein and Ehrenfest showed that any diffraction grating may be considered to be made up of a large number of superposed "sinusoidal gratings," and that the intensity of the diffracted beam in any order is proportional to the square of the coefficient of the corresponding term in the Fourier's series representing the density of diffracting power.

¹ Havighurst, Phys. Rev. 28, 869 (1926).

² A. H. Compton, Phys. Rev. 9, 49 (1917).

³ W. L. Bragg, James and Bosanquet, Phil. Mag. 44, 433 (1922).

⁴ W. H. Bragg, Phil. Trans. Roy. Soc. A215, 253 (1915).

⁵ Duane, Proc. Nat. Acad. Sci. 11, 489 (1925).

⁶ Havighurst, Proc. Nat. Acad. Sci. 11, 502, 507 (1925). The electron density curves given in these preliminary papers give only relative values of the density and in addition are subject to errors arising from two sources—first, the constant term of the series was neglected, and second, the experimental F curves were not extrapolated to zero.

⁷ Epstein and Ehrenfest, Proc. Nat. Acad. Sci. 10, 133 (1924).

⁸ Duane, Proc. Nat. Acad. Sci. 9, 159 (1923).

By the reverse process, we may deduce the density of diffracting power in a grating by substituting the square roots of the measured intensities of diffraction as coefficients in the Fourier's series. In a book recently published,⁹ A. H. Compton has given a thorough discussion of the application of Fourier analysis to the problem of electron distribution on the basis of the classical theory. He derives the equations given below and applies the analysis to the data of Bragg, James and Bosanquet on rock salt with results which will be compared with those of the author.

Linear electron density. Consider a one-dimensional grating which contains Z electrons within a grating space a . The general term in the Fourier's series representing the linear density is⁷ $A_n \sin(2\pi nx/a - \delta_n)$, where n is the order of diffraction and δ_n is a phase constant. The linear density of diffracting power, P_x , at a point x in the grating is represented by the series

$$P_x = \sum_n A_n \sin(2\pi nx/a - \delta_n) \quad (1)$$

where $A_n = F_n/a$ and F_n is the structure factor for the diffraction of the n th order. $F_0 = Z$, and the summation is taken over all values of n , positive and negative.

Volume electron density. The three-dimensional analogue of the general term in the Fourier's series given above is

$$A_{n_1 n_2 n_3} \sin(2\pi n_1 x/a_1 - \delta_{n_1}) \sin(2\pi n_2 y/a_2 - \delta_{n_2}) \sin(2\pi n_3 z/a_3 - \delta_{n_3}). \quad (2)$$

for the series representing the volume density, $\rho(xyz)$, of diffracting power at a point in the unit cell of a crystal. a_1 , a_2 , and a_3 are the lengths of sides of the unit cell. Unless we fix the values of the δ 's, we find that the series based on (2) does not give a unique distribution of diffracting power; that is, an indefinitely large number of distributions will produce beams of rays of precisely the same intensities in the same directions. In order to obtain a unique distribution of diffracting power it is necessary to make two assumptions.

The first assumption is that the distribution of diffracting power conforms to the symmetry of the crystal. This symmetry fixes the values of the δ 's. For example, if the crystal has three mutually perpendicular planes of symmetry and if we take the intersections of these planes as the axes of coordinates, the terms in the series can contain cosines only, for they must have the same values when we reverse the algebraic sign of

⁹ A. H. Compton, "X-Rays and Electrons," Chap 5. Van Nostrand and Co., 1926. For the privilege of using the manuscript of this work, the author desires to express his thanks to Professor Compton.

either x , y or z . In this case, therefore, the δ 's must be odd multiples of $\pi/2$. The symmetry conditions often determine, also, the values of certain coefficients A as being equal to one another. If the crystal possesses such complete symmetry as that of NaCl, all the A 's having the same values of n_1 , n_2 , and n_3 , but interchanged in any manner, must be equal to each other.

The second assumption has to do with the algebraic signs of the coefficients A , which, being square roots of measured quantities, are undetermined as to sign by the diffraction data. In general, the intersections of planes or axes of symmetry in a crystal must be points of maximum or minimum density, and if there is an atom at such a point, it is natural to suppose that $\rho(xyz)$ is a maximum there. There may be other points in the unit cell at which $\rho(xyz)$ has maximum values; it is probable that the greatest maximum value of the density corresponds to the center of the heaviest atom, and that the terms in the Fourier's series are all positive at that point. We assume, therefore, that if we take the origin of coordinates at the center of the heaviest atom, all the coefficients in the Fourier's series have positive values. For the crystals of high symmetry and simple structure which are considered in this paper, the effect of these assumptions upon the form of the Fourier's series is easily worked out. The author has published elsewhere¹⁰ a treatment of a more complicated crystal structure by this method.

A further assumption must be made before we can properly speak of electron distributions obtained from diffraction data. The density of diffracting power must be assumed to be proportional to the electron density. This means that all the electrons of an atom are equivalent in scattering power for x-rays, a statement to which objection may possibly be raised; for it is not certain that the inner and outer electrons of a heavy atom are equally effective as scatterers.

We may now write down the Fourier's series expressing the electron density $\rho(xyz)$ at a point (xyz) in the unit cell of a cubic crystal of the rock-salt or fluorite type, with the origin of coordinates at the center of the heaviest atom:

$$\rho(xyz) = \sum_{n_1} \sum_{n_2} \sum_{n_3} A_{n_1 n_2 n_3} \cos 2\pi n_1 x / a \cos 2\pi n_2 y / a \cos 2\pi n_3 z / a \quad (3)$$

where $n_1 n_2 n_3$ are the Miller indices of the different crystal planes multiplied by the order of reflection; $A_{n_1 n_2 n_3} = 4F_{n_1 n_2 n_3}/a^3$ and $F_{000} = Z =$ the number of electrons per molecule, there being four molecules in the unit cell. It should be noted that the experimental values of F used in this

¹⁰ Havighurst, J. Am. Chem. Soc. 48, 2113 (1926).

paper contain the Debye temperature factor, so that in Eq. (3), which gives the time average of the electron density in the unit cell, the amplitude of thermal agitation is superposed upon the actual distances of the electrons from their atomic centers.

Radial distribution of electrons. From the determinations of electron density we may get information concerning the radial distribution of electrons in the separate atoms. The number of electrons in a spherical shell of radius r , thickness dr , and density ρ is

$$Udr = 4\pi r^2 \rho dr \quad (4)$$

The area under the curve of U plotted against r gives directly the number of electrons in the atom. It seems proper to assume spherical symmetry of the electron density, as is done by this procedure, but the question will be raised again later.

Compton⁹ has derived an expression for the radial distribution which does not require the evaluation of a three-dimensional series. The number of electrons in a spherical shell is represented by a series:

$$Udr = 4\pi r/D \sum_1^{\infty} (2nF_n/D) \sin(2\pi nr/D) dr \quad (5)$$

where D is the spacing of the set of atomic planes which are perpendicular to r and F_n is the *atomic* structure factor for the order n (or for reflection by planes of spacing D/n). Upon the assumption of spherical symmetry, any convenient spacing D in the region covered by the atomic F curve may be used as the first order spacing; but the series becomes negative when r/D is greater than 0.5, consequently the radius of the atom must be less than $D/2$ if the values of U in the neighborhood of $D/2$ are to be considered as dependable. The author's U curves determined for the same atom by the two different methods of Eqs. (4) and (5) are in satisfactory agreement.

It is important that we now have a method (the integration of $U dr$) of determining the number of electrons grouped about a point in a crystal lattice without having made any assumption concerning the existence of ions. Indeed, we have not even assumed the existence of atoms or molecules in the exact sense that is ordinarily understood by the use of these terms—we have simply supposed that there are certain maxima of diffracting power in the unit cell of a crystal. Now that we are in possession of a method of counting the number of electrons associated with these maxima, we find ourselves able to decide what these lumps of diffracting power are—ions, neutral atoms, or molecules.

APPLICATION OF FOURIER ANALYSIS TO A MODEL ATOM

Before an adequate idea of the limits of accuracy of the Fourier analysis can be obtained, it is necessary to know something about the convergence of the series used. The coefficients of the series come from experimental F curves which must be extrapolated to zero values of F . The questions to be answered are: (1) does the actual F curve of an atom fall to zero and remain there or does it maintain appreciable positive and negative values out to very small interplanar spacings? and (2) do the series of Eqs. (3) and (5) converge for these values?

The best method of deciding these questions appears to be that of calculating the F curve for a model atom and subjecting it to the Fourier analysis. This procedure has been carried through for a model sodium ion under assumptions designed to make a satisfactory Fourier analysis more difficult than in the cases of the light atoms to be studied experimentally. The sodium ion is built up of ten electrons on three concentric spherical shells, as follows:

2 electrons on a shell of radius 0.1A

6 electrons on a shell of radius 0.3A

2 electrons on a shell of radius 0.9A

The F values for this ion may be readily calculated from the expression¹¹

$$f = \sum (\sin \xi) / \xi$$

where

$$\xi = (4\pi r \sin \theta) / \lambda = 2\pi r n / d$$

TABLE I
F values for sodium model ion. $F = f e^{-0.0063n^2}$

<i>n</i>	<i>f</i>	<i>F</i>	<i>n</i>	<i>f</i>	<i>F</i>	<i>n</i>	<i>f</i>
0	10.	10.	18	.51	.066	38	-.34
1	9.53	9.48	20	1.17	.093	40	-.08
2	8.42	8.22	22	1.24	.059	44	-.02
4	5.90	5.33*	24	0.98	.025	48	-.44
6	4.45	3.55	26	.69	.010	52	-.47
8	3.01	2.01	28	.01	.000	56	-.07
10	1.14	0.61	30	-.53		60	.40
12	0.20	.08	32	-.73	-.0011	70	.02
14	.14	.04	34	-.83		80	.29
16	.14	.028	36	-.82	-.00022	100	-.01

and the summation is taken over each of the electrons. As a convenient first order spacing we shall choose 5.628A. The f values are given in Table I, along with F values which have been obtained by applying a temperature factor to f as follows:

¹¹ Hartree, Phil. Mag., 50, 289 (1925).

$$F = f e^{-(b \sin^2 \theta) / (2\lambda^2)} = f e^{-2 n^2 / d^2} = f e^{-0.0063 n^2}$$

This evaluation of the Debye factor is based upon W. H. Bragg's figure for rock-salt, $b/(2\lambda^2) = 2.06$, which will at least give the order of magnitude of the temperature effect. In Fig. 1 are shown the f and F values plotted against $\sin \theta$ for $\lambda = 0.1126\text{A}$. This wave-length was chosen because it makes $\sin \theta = 0.01$ for $d/n = 5.628$ and allows the F values for 100 orders of reflection to be plotted. The author's measurements with $\lambda = 0.710\text{A}$ would stop at a point equivalent to $\sin \theta = 0.12$ in the figure.

Of the series in Eqs. (3) and (5), the sine series of (5) will converge the more slowly because the coefficient F is multiplied by n . Let us consider the question of its convergence. It is evident that the series

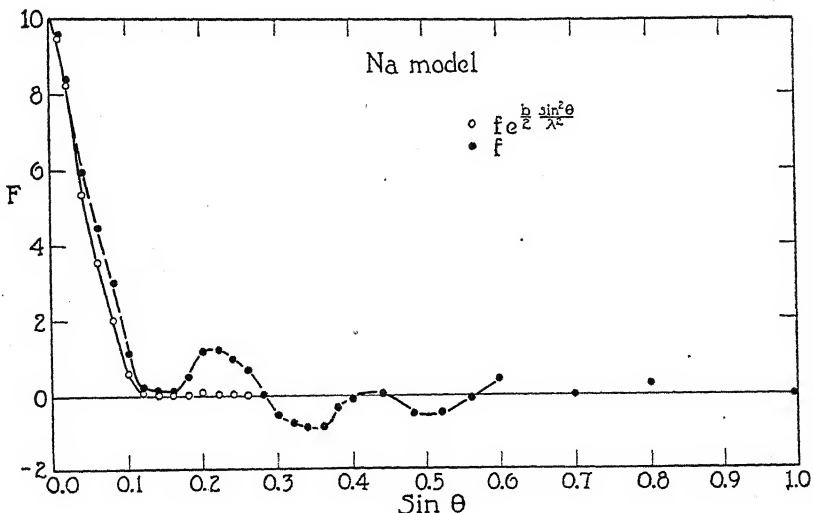


Fig. 1. F curves for a model sodium ion.

when evaluated with the f 's of Table I is probably not convergent, for in some instances $f_n > f_0/n$. The application of the temperature factor to f introduces a negative exponential n^2 , consequently the F values of the table undoubtedly satisfy the conditions for convergence. Looking at the question from another point of view, we see that the series of Eq. (5), if used with the f values of Table I, would have to give a radial distribution showing infinite values of U at the r values of the three shells, and zero values of U at all other points. The effect of thermal agitation, however, is to spread out the shells into what is a more or less continuous distribution of electrons and the series representing U for this case should converge rather rapidly.

The series of Eq. (5) has been evaluated with the f and F values of Table I and $D = 2.814\text{A}$. U is plotted against r in Fig. 2. In the heavy-line curve in the upper part of the figure, which was obtained by using the first twenty f terms, down to $n = 40$ in the table, the three shells are beginning to emerge as predominant peaks. The broken-line curves, representing the series when cut off at the end of five and eleven terms,

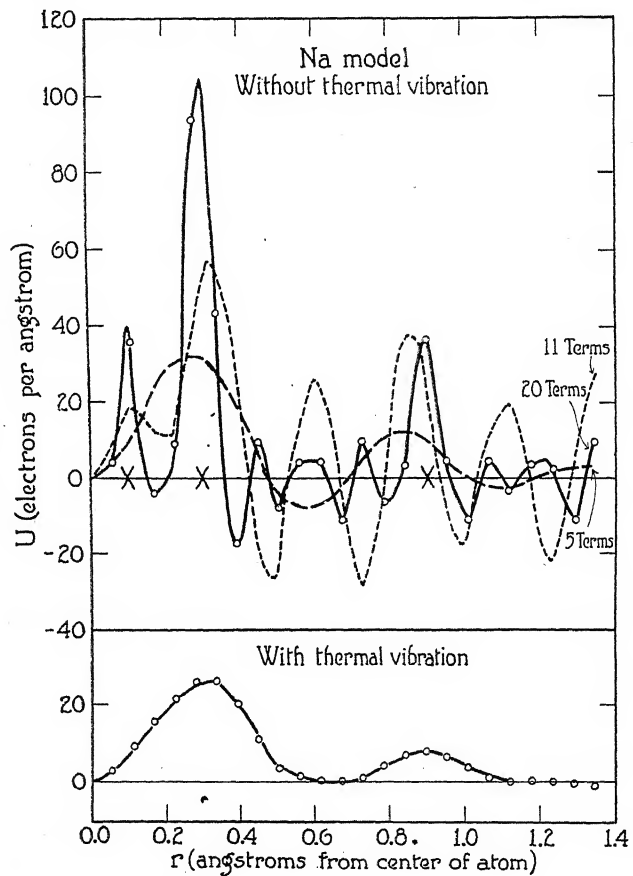


Fig. 2. Radial electron distribution in model sodium ion.

help to indicate the unsatisfactory nature of the analysis when used upon an atom which has its electrons arranged on a few stationary shells. When evaluated for 12 terms, down to $n = 24$, with the F values of Table I, the series gives the lower curve of the figure. Its area is 9.6 electrons. The effect of thermal agitation has smoothed over the shells distinctly. When the series is cut off at the end of the sixth term, which would be the limit of the author's measurements, the curve coincides so

nearly with that of the figure that it was impossible to draw it in separately. Now elliptical and interpenetrating orbits aid thermal agitation in producing a practically continuous electron distribution, hence it seems reasonable to extrapolate the experimental F curves rather quickly to zero values of F . The value of the retention of the temperature factor

TABLE II

in the experimental F curves as a means of securing a rapidly convergent series and therefore of obtaining a more trustworthy Fourier analysis is clearly demonstrated. In an effort to determine the error due to the extrapolations which have been made for the purpose of this analysis, the author plans to continue the investigation of F curves out to smaller interplanar spacings by the use of radiation of shorter wave-length, and of apparatus which permits the measurement of reflections out to $\theta = 90^\circ$.

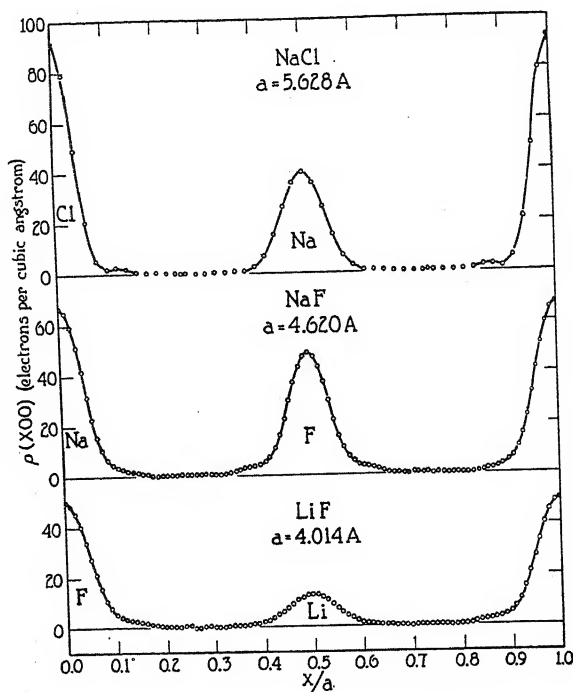


Fig. 3. Electron density in crystals.

ELECTRON DISTRIBUTION IN CRYSTALS

We may now calculate electron distributions from Eq. (3), and on the basis of the author's F curves extrapolated to zero, with considerable confidence in the results. The F values to be used as coefficients, given in Table II, are, as a rule, identical with the measured values given in the previous paper, although in a few cases where measured points fell noticeably off a smooth curve, interpolated values are substituted. Interpolated values are given for the reflections which were not measured, while below the dotted lines the points were all taken from extrapolated curves.

The electron density, $\rho(x00)$, along the cube edge of the unit cell of the crystals here considered is

$$\rho(x00) = 4/a^3 \sum_{n_1} \sum_{n_2} \sum_{n_3} F_{n_1 n_2 n_3} \cos 2\pi n_1 x/a \quad (6)$$

The curves of $\rho(x00)$ plotted against x/a are given in Fig. 3. Going out from the center of an atom, they all show the same rapid decrease of electron density at the start, followed usually by a rather sharp change of slope which produces a hump on the U curve. One feature of these curves cannot be observed clearly, because the scale of the figure is too small; for each curve there is only one very narrow region between the

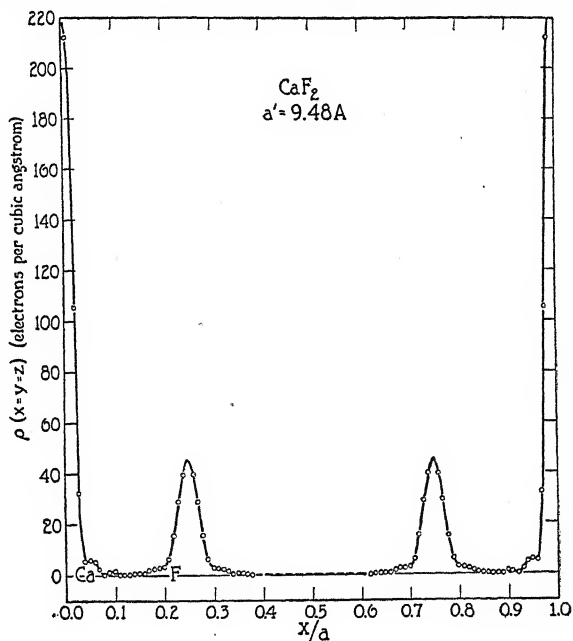


Fig. 4. Electron density in CaF₂.

atoms where the density becomes practically zero. In other words, the atoms extend physically well out into the unit cell, almost touching each other, although the electron density over a large part of the region is very small. There is a sharp drop to zero density at the limit of the atom, which is much more evident in the U curves, where ρ is magnified by multiplication by n^2 . The electron distributions in other directions through the unit cell have been calculated from Eq. (3), giving curves similar to those of the figure.

The $\rho(x00)$ curve from CaF₂ has no peak at its middle, for there is merely a series of Ca atoms along the cube edges of the unit cell. In order

to get evidence of the existence of fluorine peaks, it is necessary to work out the curve for $\rho(x=y=z)$, the density along the cube diagonal. Not only is the three dimensional series, required in this case, a much more laborious one to evaluate than the one-dimensional series of Eq. (5), but also the F curve for Ca falls rather slowly toward zero, so that the extrapolation would have to be made out to very high values of the n 's, still further increasing the labor of evaluating the series. Consequently an indirect method of determining $\rho(x=y=z)$ was adopted. The F curve for Ca was extrapolated and the values for the higher orders of the (111) planes determined. $U dr$ values were determined from Eq. (5) on the basis of the $F(111)$ data, and, from the curve of U against r , $\rho(x=y=z)$ was calculated for the desired values of r by Eq. (4). By a similar procedure with the U curve of fluorine from CaF_2 , the $\rho(x=y=z)$ values for fluorine were obtained. The two sets of data have been united in the curve of Fig. 4. There is, of course, no data to cover the middle of the curve, which is a region of zero density. Incidentally, the fact that the F curves for heavy atoms fall rather slowly to zero indicates that they are not very suitable for this Fourier analysis.

TABLE III
Atomic F values for use in Fourier's series

Plane	Ca^{++}	CaF_2	F^{-*}	Na^{+}	NaCl	Cl^{-}	Na^{+}	NaF	F^{-}	Li^{+}	LiF	F^{-}	Mean Fluorine F^{-**}
111	15.90	7.35	8.80	13.60	8.35	7.15	1.26	5.89	1.26	0.88	2.72	7.35	3.32
222	10.75	3.20	5.46	7.84	4.90	3.49	0.41	1.30	0.41	0.65	1.62		
333	7.32	1.75	3.05	5.15	2.65	1.59	0.14	0.65	0.14	0.37	0.55		0.86
444	5.30	1.05	1.60	3.40	1.30	0.94	0.28	0.28	0.28	0.28	0.27		
555	3.97	0.65	0.72	2.10	0.72	0.53	0.06	0.37	0.06	0.37	0.55		
666	2.80	0.27	0.10	1.15	0.28	0.28	0.28						
777	2.10			0.31									
888	1.22												
999	0.30												
200	15.00			8.58				1.25					
400	9.80			4.62				0.73					
600	6.15			2.23				0.24					
800	4.55			1.00				0.11					
10 00	2.95			0.20				0.02					
12 00	2.15												
14 00	1.10												
16 00	0.10												

* Values taken from F_F curve with $D(111)=2.67\text{\AA}$.

** $D(111)=2.67\text{\AA}$.

RADIAL ELECTRON DISTRIBUTION IN ATOMS

We have seen that the radial distribution may be determined by the use of Eq. (4) or Eq. (5). In most cases the writer has used both methods, and the results have always been in satisfactory agreement. Table III contains atomic F values for use in Eq. (5), for the different orders of the (100) and (111) planes, the values being taken from smooth curves and those below the dotted lines being extrapolated.

The U curves invariably show humps which seem to indicate the existence of definite electron shells. While the evidence for and against the actual existence of these humps will be considered later, it is interesting on the assumption of their reality to compare the electron arrangements which they give with Stoner's¹² scheme for the distribution of electrons in atoms.

Stoner's arrangement for the argon atom (chlorine or calcium ion) is as follows:

2 K electrons with n	1,	j	1,	k	1
2 L		2,	1,		1
2 L		2,	1,		2
4 L		2,	2,		2
2 M		3,	1,		1
2 M		3,	1,		2
4 M		3,	2,		2

The neon atom (Na^+ or F^- ion) corresponds to the above arrangement without the M electrons. The inner quantum number, j , need not be considered here.

Sodium and chlorine. The full-line curve in Fig. 5 represents U for Na in NaCl . The curve is almost identical with one obtained by Compton⁹ by a similar analysis of the results of Bragg, James and Bosanquet.¹³ The area under the curve is 10.4 electrons, indicating that we have here a positive Na^+ ion. The area of the hump B is approximately 2, while that of A is 8. Upon the basis of Stoner's scheme, we should interpret these humps as follows: A contains the 2 K electrons and the 6 circular L electrons; B contains the 2 L electrons with elliptical orbits.

There was some difficulty in obtaining a U curve from Eq. (5) for chlorine, as Cl occupies much more space than Na. The $U(111)$ curve does not extend to the limit of the atom, as it is based upon too small a spacing. Compton solved this difficulty by extrapolating the F curve for Cl toward $\sin \theta = 0$, upon the assumption that $F_0 = 18$, and using a

¹² Stoner, Phil. Mag. **48**, 719 (1924).

¹³ W. L. Bragg, James and Bosanquet, Phil. Mag. **42**, 1 (1921).

larger spacing for D in the series. This requires the assumption, which we wish to avoid, of an ionized chlorine atom, consequently we must rely chiefly upon the U values obtained from $\rho(x00)$ which are in agreement with the $U(111)$ values as far as the latter may be used. The area under the curve of Fig. 6 is 17.85 electrons, indicating the existence of

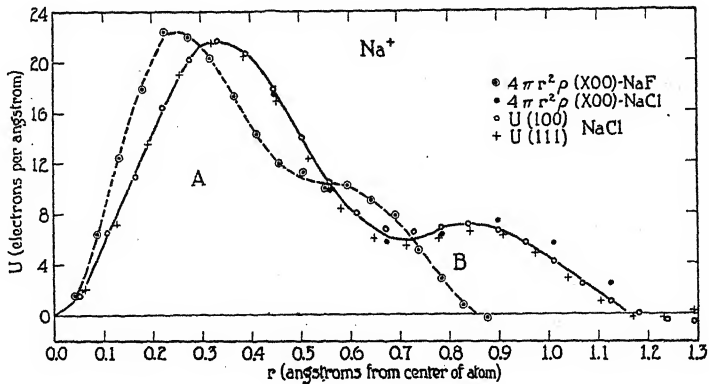


Fig. 5. Radial electron distribution in Na^+ .

the Cl^- ion. The hump A contains 10 electrons, which are probably those belonging to the K and L levels, leaving us with 8 M electrons to account

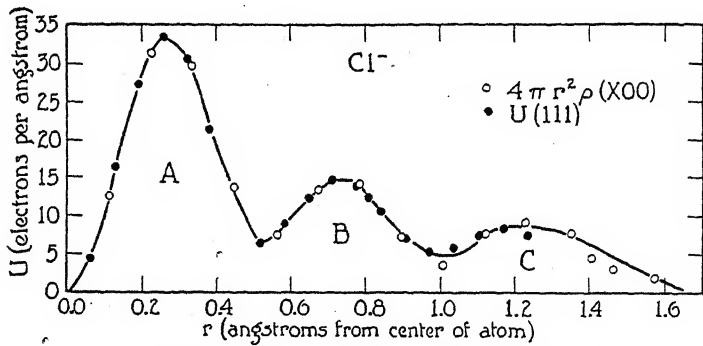


Fig. 6. Radial electron distribution in Cl^- .

for. The areas of B and C are more nearly 5 and 3 than 6 and 2, although the latter values might be taken to indicate the presence of six 3_2 electrons in orbits of moderate eccentricity, and two 3_1 electrons in orbits of greater eccentricity. Hartree's¹¹ calculations, however, indicate that the effective radii of the 3_2 and 3_1 electrons are practically the same. In this connection it should be stated that according to calculations by both

Hartree and Compton, an electron in an interpenetrating orbit spends much the larger part of its time in the outer portion of its orbit, so that its effective radius for the purpose of x-ray scattering and its maximum radius are very nearly the same. Compton's curve for Cl, based upon the data of Bragg, James and Bosanquet which are very nearly identical with those of the author, but also based upon an F curve extrapolated toward $\sin \theta = 0$, shows an extra hump, while the radius of the atom is 2.0A. This discrepancy throws some doubt upon the reality of these humps.

Calcium. The U curve for Ca given in Fig. 7 is strikingly similar to that for Cl^- , except that the electrons are contained within a radius less than two thirds that of the chlorine ion. Almost a positive proof of the existence of the Ca^{++} ion in the lattice is to be seen in the fact that the area under the curve is exactly 18 electrons, for the neutral atom would

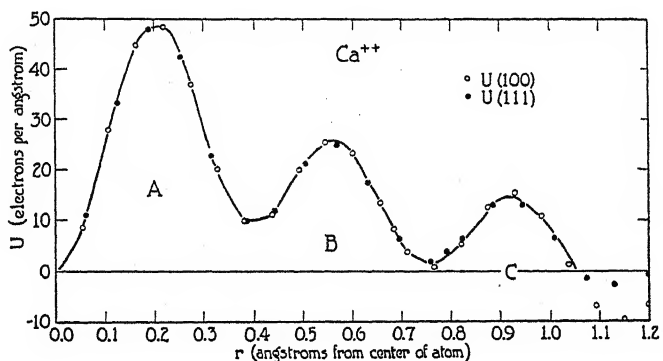


Fig. 7. Radial electron distribution in Ca^{++} .

contain 20 electrons. The area of hump *A* is 10 electrons, while *B* and *C* contain 6 and 2 electrons respectively.

Sodium in sodium fluoride. The broken-line curve of Fig. 5 is the U curve of Na from NaF. A very interesting difference exists between the sodium ion in the two compounds, an apparent compression of the whole ion having taken place in NaF. As the area under the curve is only 9.2 electrons, the analysis is not particularly satisfactory in this instance, but the addition of sufficient area to bring the electron content to 10 would not make the two distributions alike. One is brought to the conclusion that the forces acting upon the ion in the two crystals are of rather different magnitudes.

Lithium. The U curve for lithium, given in Fig. 8, is the least satisfactory of the group, because we meet the same absolute amount of error,

due to deficiencies of the experimental data and of the analysis, in electron densities which are very small, so that the percentage errors are large.

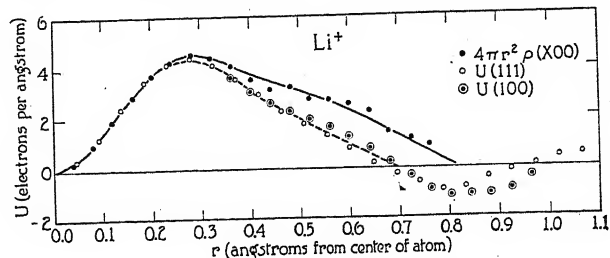


Fig. 8. Radial electron distribution in Li^+ .

There is a noticeable difference between the U curves obtained in different ways, and these curves can be changed considerably by different methods of smoothing out the experimental F curve for Li. The difference between the results obtained from Eq. (5) and those from Eq. (4) is undoubtedly due to the fact that the experimental F values were used without change in the determination of $\rho(x00)$, while the F curve of Li, upon which is based the $U(111)$ curve, being determined by subtraction of rather large and nearly equal ($F+\text{Li}$) and ($F-\text{Li}$) values, showed considerable irregularity and was smoothed out. However, the area under the full-line curve is 2.0 electrons, and there is no reason to believe that we are dealing with anything but the Li^+ ion with two K electrons.

Fluorine. As has been pointed out, the F curves for fluorine from all three fluorides are very closely similar, hence it was not considered necessary to reproduce separate U curves for each crystal. The values used in obtaining Fig. 9 were taken from the mean F curve of fluorine,

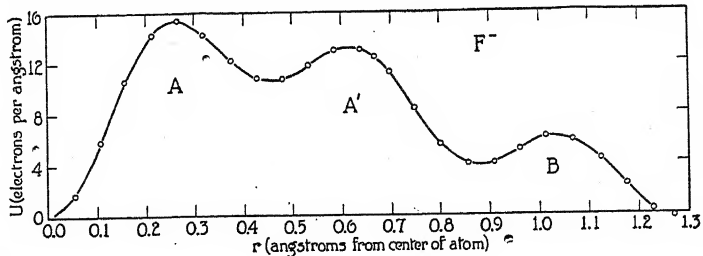


Fig. 9. Radial electron distribution in F^- .

given in the previous paper, D for the first order being 2.67 Å. U curves from the individual F curves have also been worked out, and they show

only unimportant differences at large values of r . Corresponding to the F^- ion, the area under the curve is 9.95 electrons. The striking thing about this curve is the existence of the A' hump. We should, of course, assign B to the two L electrons in elliptical orbits, as in the case of Na^+ , but there is nothing in the sodium curve to correspond with A' . Whether in the spreading out of the electron atmosphere which takes place during the formation of a negative ion the inner electron groups separate somewhat, or whether the A' hump is merely due to a deficiency of the analysis, is uncertain.

DISCUSSION OF RESULTS

The results of the foregoing analysis may be grouped into two classes: those which allow an unambiguous interpretation, and those which do not. Let us consider the first class.

(1) It appears to be definitely proven that the lattice points of the crystals are occupied by ions. Commencing with no *a priori* assumption as to the amount of electricity associated with a lattice point, we have found in each case that the number of electrons was almost exactly the same as the number in the ion which might be expected to reside at that point.

(2) The Fourier analysis determines definitely the radius of the ion. The volume density curves fall quite accurately to zero over a small region between the ions, while the U curves determine sharply the radii. Comparison of the distance of closest approach of ions as determined by ordinary x-ray analysis with the sum of the radii of the ions determined in this analysis shows that the sum of the radii is in every case very slightly less than the distance of closest approach. We accordingly are led to form the usual picture of the unit cell of a crystal: one which contains a number of spherical electron systems practically in contact with each other and distributed regularly over the lattice points, each system having a dense electron atmosphere near its center which becomes extremely rarefied at its outer limit. Whether the valence electrons remain between ions all the time, rotate about pairs of ions, or pass completely over to the negative ions, is not decided; all we may be certain of is that the diffracting power of a valence electron unites with that of a negative ion.

The ionic radii of Wasastjerna,¹⁴ discussed in a recent paper on interatomic distances by W. L. Bragg,¹⁵ and which are based upon a theoretical consideration of atomic force-fields, correspond exceedingly closely with the radii determined in this analysis.

¹⁴ Wasastjerna, Soc. Scient. Fenn. Comm. Phys. Math. 38, 1 (1923).

¹⁵ W. L. Bragg, Phil. Mag. 2, 258 (1926).

(3) The electron distribution of an atom may be modified by the external forces which act upon it in a crystal. The Na^+ ion is found to possess different electron distributions in NaF and NaCl , probably because of a combination of differences in chemical, crystal lattice and thermal forces. On the other hand, the electron distributions of F^- are practically the same in LiF , NaF and CaF_2 .

Turning now to results which are somewhat ambiguous, we are met at once with the question of the reality of the humps in the curves of radial distribution. There is reason to believe that a shell-like electron structure exists in atoms, and the results of this analysis are in rough agreement with the predictions of Stoner's scheme. The persistence of the humps in both Ca^{++} and Cl^- , although one ion has only two-thirds as large a radius as the other, is evidence of their reality. On the other hand, we have the discrepancy between Compton's U curve for Cl^- and that of the author, the two curves being obtained from practically the same data by slightly different methods of analysis. Also there is a subsidiary hump in the U curve for F^- which is not readily explained. Perhaps the best method of investigating this question of shell structure would be to study a model argon atom in the manner of the investigation carried out above for the sodium ion.

Although we have assumed spherical symmetry of the electron distributions for the purposes of a part of this analysis, such an assumption cannot be completely justified. Probably the atoms in crystals of low symmetry are not spherically symmetrical, but the nearest approach to this condition would be expected in a cubic crystal of high symmetry. It is impossible to decide from existing experimental data upon intensity of reflection that spherical symmetry does not exist, the irregularities of the F curves being in general so small that they could be ascribed to experimental error. Any lack of symmetry would be expected to show on the U curves at large values of r , and there are differences between these curves when they are evaluated for reflections in different directions through the crystal, but these differences also may be attributed to deficiencies in the analysis.

A further point which has been raised in connection with the use of experimental F curves for the determination of electron distributions has to do with the effect of the Compton scattering. Since the amount of radiation scattered with a change of wave-length increases with the angle of scattering, it might be supposed that this increase takes place at the expense of the energy scattered with unmodified wave-length. That is, the F curve might drop off at large angles for two reasons—first, because of the spatial distribution of electrons in the atoms, and second,

because an increasing fraction of the secondary radiation is being scattered with a change of wave-length and hence is not subject to interference. This idea seems not unreasonable, yet, on the other hand, there is reason for the belief that the two scattering processes take place side by side without influencing each other. It seems that the foregoing analysis, which gives electron distributions containing the proper number of electrons and of the dimensions to be expected from the results of ordinary crystal analysis, is a strong argument for the reliability of the experimental F curves and speaks definitely in favor of the idea that the Compton scattering is a separate and distinct process from the ordinary scattering.

In conclusion, the author wishes to express his appreciation of the aid and advice of Professor William Duane, who suggested this problem.

JEFFERSON PHYSICAL LABORATORY,
HARVARD UNIVERSITY,
July 20, 1926.

MEASUREMENTS AND INTERPRETATION OF THE
INTENSITY OF X-RAYS REFLECTED FROM
SODIUM CHLORIDE AND ALUMINUM

By J. A. BEARDEN

ABSTRACT

Measurements of the intensity of x-rays reflected from sodium chloride have been made by three methods: (1) *Reflection from a single crystal*, (2) *Reflection from a plate of powdered crystals*, (3) *Reflection from a powdered plate using the transmission method*. The results from single and powdered crystal measurements are not in agreement, showing that there is possibly an uncorrected extinction effect in the single crystal measurements. The results from both powdered crystal methods are in very close agreement.

Using the Fourier series formula for the electron distribution derived by Compton, *electron distribution curves* for sodium and chlorine have been obtained. The difference in the electron distribution curves for powdered and single crystals indicates that the absolute intensity measurements must be made accurate to within 1 percent before confidence can be placed in the results. It is also shown that the portion of the experimental curves extrapolated to large angles of reflection is very important.

Similar measurements and curves have been obtained for aluminum. The distribution curve and also the *F* curve are more satisfactory than those obtained for sodium and chlorine, showing that the experimental values for aluminum are probably more accurate than the rock salt measurements.

VARIOUS writers¹⁻¹⁰ have obtained theoretical expressions for the intensity of x-ray reflection, and although by independent methods, most of the formulas are in agreement with each other. The following formulas which have been derived by Compton¹⁰ for the three most important cases of crystals, are directly applicable to experimental results:

(1) Reflection from single crystals:

$$\frac{W\omega}{P} = \frac{1}{4\mu} n^2 \lambda^3 F^2 \frac{e^4}{m^2 c^4} \left\{ \frac{1 + \cos^2 2\theta}{\sin 2\theta} \right\} = \frac{Q}{2\mu}. \quad (1)$$

¹ P. Debye, Ann. d. Physik, **43**, 49 (1914).

² C. G. Darwin, Phil. Mag. **27**, 315 and 675 (1914).

³ C. G. Darwin, Phil. Mag. **43**, 800 (1922).

⁴ W. H. Bragg, Phil. Trans. **215**, 253 (1915).

⁵ A. H. Compton, Phys. Rev. **9**, 29 (1917).

⁶ W. L. Bragg, James and Bosanquet, Phil. Mag. **41**, 309 (1921).

⁷ H. A. Wilson, Phys. Rev. **18**, 396 (1921).

⁸ P. P. Ewald, Phys. Zeits. **22**, 29 (1925).

⁹ W. Duane, Proc. Nat. Acad. Sci. **11**, 489 (1925).

¹⁰ A. H. Compton, X-Rays and Electrons.

W represents the total amount of energy reflected by the crystal as it is turned past the angle θ with a uniform angular velocity ω , P the power in the primary x-ray beam, μ the effective absorption coefficient of the crystal, n the number of atoms per unit volume of the crystal, λ the wavelength of the x-rays used, e the charge on the electron, m the mass of the electron, c the velocity of light, $(1 + \cos^2\theta)$ the polarization factor, and F is termed the structure factor and is defined by the equation

$$F = Z \int_{-a}^a p(z) \cos\left(\frac{4\pi z}{\lambda} \sin \theta\right) dz \quad (2)$$

where a is the maximum possible distance of an electron from its atomic layer, Z is the number of electrons in the atom and $p(z)$ represents the probability that an electron will be at a distance between z and $z+dz$ from the mid-plane of the layer of atoms to which it belongs.

(2) Reflection from a plate of powdered crystals:

$$\frac{P_s}{P} = Q \frac{p}{16\pi} \frac{l}{\mu r} \frac{\rho'}{\rho} \frac{1}{\sin \theta} \quad (3)$$

(3) Reflection from a powdered plate using the transmission method:

$$\frac{P_s}{P} = Q \frac{p}{4\pi} \frac{l}{r} \frac{h\rho'}{\rho} \frac{1}{\sin 2\theta} \quad (4)$$

In these equations, P_s represents the power in the beam reflected by the powdered crystals at an angle θ , P the power in the incident x-ray beam, Q is defined by Eq. (1), p is the number of surfaces in a crystal of the type considered, l is the length of the slit in the ionization chamber, h is the thickness of the crystal mass, r is the distance of the ionization chamber slit from the crystal mass, ρ' is the density of the crystal mass, ρ is the density of the individual crystals, and μ is the effective absorption coefficient of the crystal mass. Thus F is the only quantity occurring in Eqs. (1), (3) and (4) which cannot be directly measured. Its value may be calculated, however, when the other factors in these equations have been determined.

From the value of F as calculated from the above formulas it is possible to gain some knowledge of the distribution of the electrons in the atoms composing the crystal. The method of Fourier series is doubtless the best method that has been developed for obtaining a knowledge of the electronic distribution. The method was first suggested by W. H. Bragg⁴ but in a manner which did not give satisfactory results. Duane⁵ has applied Epstein and Ehrenfest's¹¹ quantum treatment of the problem

¹¹ Epstein and Ehrenfest, Proc. Nat. Acad. Sci. 10, 133 (1924).

of Fraunhofer diffraction to the determination of the electronic distribution and has obtained results which are in a very usable form. His equation for the electron distribution is in the form of a 3 dimensional Fourier series. It has been applied by Havighurst¹² to the electron distribution of several crystals with interesting results. Compton¹⁰ working on the basis of classical electrodynamics has arrived at the same expression as that found by Duane⁹ for the electron density at any point in the crystal. Assuming the atoms in the crystal to have spherical symmetry, Compton¹⁰ has derived the following single Fourier series equation for the radial electron distribution in the atom.

$$U = \frac{8\pi r}{D^2} \sum_{n=1}^{\infty} n F_n \sin \frac{2\pi nr}{D} \quad (5)$$

In this equation U represents the number of electrons per Angstrom measured from the center of the atom, r the distance from the center of the atom in Angstroms, D the arbitrary grating space in Angstroms, F_n the value of the structure factor for the n th order of reflection and n the order of reflection.

The total number of electrons in the atom may be found by integrating Eq. (5). If D is taken large enough so that there will be no overlapping of the atoms, we may integrate the equation between the limits $r=0$ and $r=D/2$. Integrating we find

$$Z = -2 \sum (-1)^n F_n \quad (6)$$

where Z represents the total number of electrons in the atom, n and F_n have the same meaning as in Eq. (5). Since Z is known this equation becomes very useful in making extrapolations in the experimental F_n curves to small angle of reflection.

The object of the present work was: (1) To compare the values of F as determined from the three methods indicated in Eqs. (1), (3) and (4) as a possible check on the validity of the equations. (2) To compare the electron distribution curves using these values of F in Eq. (5). (3) To determine the distribution of electrons in aluminum by the same method.

APPARATUS

In making absolute measurements of intensity the ionization method was employed. These measurements necessitate using x-rays of a single wave-length. The best method of securing really monochromatic x-rays is to use a beam which has been reflected from a crystal. In the work of

¹² R. J. Havighurst, Proc. Nat. Acad. Sci. 11, 502 and 507 (1925).

Bragg and his collaborators¹³ this method was used only for the first order reflection, whereas in this experiment the method has been used for all orders of reflection. In this way the error introduced in choosing a base line for measuring relative intensities is greatly reduced. The disposition of the apparatus was similar to that first employed by Compton.¹⁴ Fig. 1 shows the arrangement of the apparatus used throughout the present experiment. X-rays from a molybdenum-target water-cooled x-ray tube were incident upon the crystal C_1 which was set to reflect the

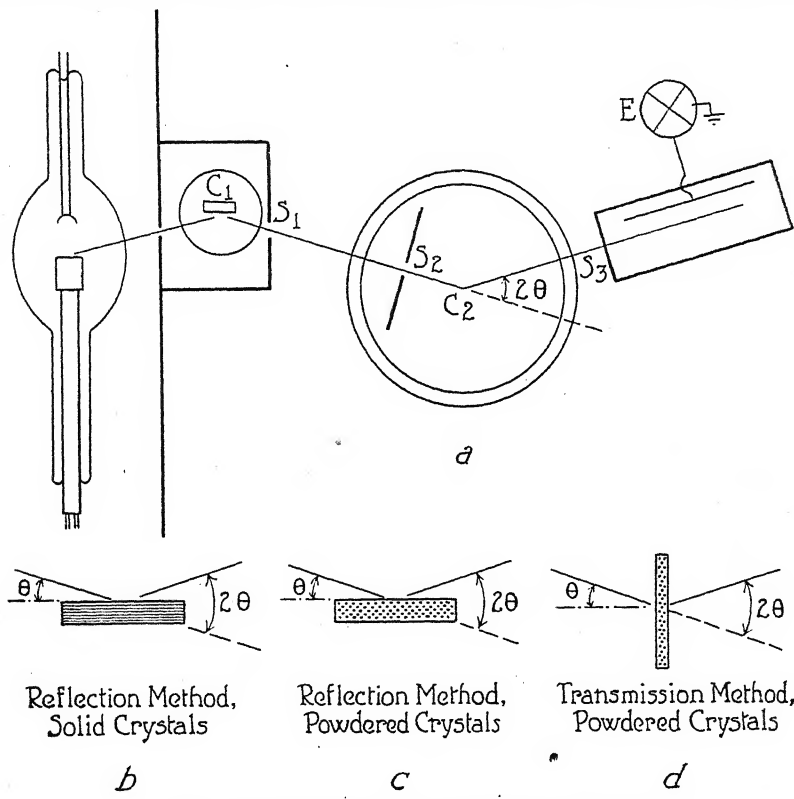


Fig. 1. Apparatus and method of mounting crystals.

$\text{K}\alpha$ lines of molybdenum. These lines were further collimated by slits S_1 and S_2 , so that the width of the beam passing across the spectrometer table C_2 was less than 0.8 mm. The x-ray spectrometer was designed by Compton for this particular type of work. The ionization chamber was about 12 cm in diameter so that it was almost impossible for β -rays produced by the x-rays to be absorbed by the walls or electrode of the

¹³ W. L. Bragg, James and Bosanquet, Phil. Mag. 41, 309 (1921) and 42, 1 (1921).

¹⁴ A. H. Compton, Phys. Rev. 10, 95 (1917).

ionization chamber. This is an important point in all measurements of absolute intensities as it was found that by using ionization chambers less than 5 cm in diameter, errors of more than 50 percent could easily be made unless the slits were extremely small and the ionization chamber accurately set parallel to the x-ray beam being measured. The ionization chamber was filled with methyl bromide and the ionization current measured by a Compton electrometer the sensitivity of which was about 5 meters per volt. The slit S_3 was in all cases wide enough to include the entire beam reflected by the crystal C_2 .

In order to secure enough intensity to make accurate measurements on the higher orders of reflection it was necessary to operate the x-ray tube at 45 to 50 milliamperes using a potential of 70 kilovolts. For the first

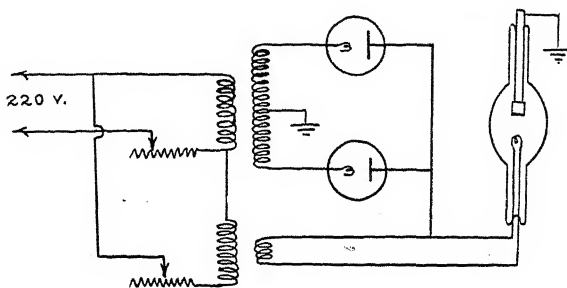


Fig. 2. Diagram of electrical connections.

order reflections it was possible to reduce the current to 30 milliamperes and the voltage to 35 kilovolts thereby eliminating any second order x-rays that might be reflected by the crystal C_1 . In order that the relative intensities and also the absolute measurements could be made with accuracy it was necessary to have a source of x-rays that would be constant over a long period of time. Several of the ordinary methods of obtaining constant current through the tube at constant voltage were tried but it was found that an arrangement suggested by W. D. Coolidge gave the best results. As a constant source of x-rays is essential to many x-ray problems a diagram of the connections is shown in Fig. 2. Using this arrangement it was possible to keep the source of x-rays constant to within 1 percent over a period of several hours. The rectifiers in this circuit were two 85 kv. 8.5 kw. kenotrons.

The time during which the x-rays were allowed to pass through the ionization chamber was controlled by an electromagnet which operated

a lead slit in the path of the x-ray beam C_1C_2 . The electromagnet was operated by a Victor x-ray timing switch. By this method it was found that any period of time up to 30 seconds could be reproduced to within 0.01 of a second. The method of taking readings was to allow the x-rays to pass through the ionization chamber for a definite length of time producing a certain deflection of the electrometer which could be read very accurately.

EXPERIMENTS ON ROCK SALT

Single crystal. Probably the most complete and accurate previous work that has been done on the intensity of x-ray reflection is that of Bragg, James and Bosanquet¹³ using the single crystal method. It was thought advisable to repeat their experiments for two reasons. (1) Their results are considered to be reasonably accurate and therefore would serve as a possible check on the writer's apparatus, suitable for determining the possibility of systematic errors which might not have been detected otherwise. (2) The measurements could be extended to the higher orders of reflection using the monochromatic x-rays instead of the direct radiation from the tube as was used by Bragg and his collaborators,¹³ thence obtaining a higher degree of precision than was probably attained in their experiments.

The apparatus used was exactly as that shown in Fig. 1, Part *a*, with the single crystal mounted as shown in Part *b* of the same figure. The ionization chamber with the slit S_3 0.5 cm wide was set at an angle 2θ so as to receive the entire line reflected by the crystal as the crystal was rotated through its angle of reflection for the particular order being measured. The power of the reflected beam was measured at intervals of 5 minutes of arc in the usual manner of obtaining ionization spectra. The time required to map out such a reflection was only a few minutes and in every case in which the results have been retained the intensity of the source was the same after the curve was taken as before. The crystal was then removed from the spectrometer table and the power in the incident beam C_1C_2 was measured. The ratio of the area under the reflection curve to the power in the direct beam gave the absolute reflecting power of the crystal. Instead of making absolute measurements on all the orders of reflection as above, it was found better to make the absolute measurements only on the first few orders of reflection and then to compare the higher orders of reflection with the first. Measurements were made in this manner on all of the more important planes of rock salt.

The other experimental value that is needed in Eq. (1) in order to determine F is the effective absorption coefficient μ . In the experiments

of Bragg, James and Bosanquet¹³ corrections were made for secondary extinction. Since the difference in wave-length of the rhodium x-rays used by Bragg and his collaborators¹³ and the molybdenum $K\alpha$ rays used by the writer is small, the extinction coefficient has been assumed to be proportional to the absorption coefficient in the two experiments. That is, in order to obtain the effective absorption for the present experiment, we have taken the normal absorption coefficient for the molybdenum $K\alpha$ line and added to this the relative percent correction for secondary extinction as determined in the experiment of Bragg, James and Bosanquet.¹³ Using this value of the absorption coefficient with the measured absolute reflecting power we can calculate the numerical value of the structure factor F . In order to compare the experimental results of this experiment with those of Bragg, James and Bosanquet¹³ it is necessary to compare the values of F as they are independent of the experimental conditions and depend only on the order of reflection. The values of F calculated from the writer's experiment are shown plotted against the sine of the reflecting angle θ in Fig. 3, curves D and G . The points thus plotted fall on the curve drawn within two or three percent representing the values of $F_{Cl} + F_{Na}$ and $F_{Cl} - F_{Na}$. Using the experimental values given by Bragg, James and Bosanquet¹³ and calculating in a similar manner the values of F one obtains values most of which are slightly higher than those shown by the broken line D . If one takes the values of F from their F curves it is found that they do not agree accurately with the values which I calculate from their experimental results. The difference is in many cases as much as 5 percent and in general the values taken from the curves are lower than the values calculated from the experimental data. The difference is probably due to some correction that has been applied in one case and not in the other. The values obtained by the writer seem to be in better agreement with the values calculated from their experimental results than with their F curves.

Reflection from a plate of powdered rock salt crystals. In this method a plate of powdered crystals as shown in Part c of Fig. 1 replaced the single crystal used in the last method. The crystal plate was prepared by pressing the finely powdered crystals into a plate about 4 mm thick, then in order to eliminate the orientation produced at the surface by the compressing block, about 1 mm of the surface was shaved off. This surface was placed at an angle θ with the primary beam and the ionization chamber at an angle 2θ . The width of the slit S_3 in the ionization chamber was so adjusted as to include the entire beam reflected by the crystal mass. It was only necessary to make one measurement on a reflection,

then remove the crystal plate and measure the power in the direct beam. As in the last case, it was found better to measure this ratio directly only for the first few orders of reflection and then compare the other orders of reflection with the first.

The values obtained by this method are, within experimental error, in exact accord with the results obtained by the transmission method and so will not be given separately.

Reflection from a powdered plate using the transmission method. In the transmission method, shown in Part d of Fig. 1, a plate of the powdered crystals is placed on the center of the spectrometer table and the x-rays allowed to pass through the crystal plate instead of being reflected as was done in the last case. The thickness of the crystal plate was made equal to the reciprocal of the absorption coefficient, which is the correct thickness to give the maximum intensity in the reflected lines. The normal to the surface of the plate was set at an angle θ with the primary beam and the ionization chamber at an angle 2θ . As in the last method the ionization chamber slit S_3 was adjusted so as to include the entire line reflected by crystal mass. Instead of removing the plate to measure the power in the direct beam as was done in the other two methods, the crystal plate was left on the spectrometer table with the normal to the surface making zero angle with the incident beam. The power in the beam transmitted through the plate was then measured with the ionization chamber set at zero angle. The advantage of measuring the power in the incident beam in this manner is that the absorption coefficient does not enter into the theoretical formula for the intensity of reflection. Theoretically primary extinction would also be negligible if the crystals were as small as 10^{-6} cm, but experimentally¹⁵ it is found in the case of rock salt that primary extinction is of little importance even for crystals as large as 10^{-3} cm. This means that a crystal of rock salt is by no means a perfect crystal. Since the extinction is thus negligible the results obtained with the powdered crystals should be more precise than the results from single crystal measurements.

The absolute intensity measurements obtained by the transmission method were substituted in Eq. (4) from which the values of the structure factor F were calculated for the various planes and orders of reflection. These values are plotted against the sine of the reflecting angle θ in Fig. 3, curves C and G. The curve G represents both powdered and single crystal $F_{\text{Cl}} - F_{\text{Na}}$ as the values were so nearly the same that they could not be distinguished. It will be noticed that the curves representing

¹⁵ R. J. Havighurst, Proc. Nat. Acad. Sci. 12, 375 (1926).

$F_{\text{Cl}} + F_{\text{Na}}$ for the single and powdered crystals do not agree except for the (100) plane and in the higher orders of reflection. It is believed that this difference is too great to be an experimental error. The difference is more likely due to the fact that sufficient correction has not been made for secondary extinction in the single crystal measurements. It was for the first order of the (100) plane that Bragg, James and Bosanquet¹³ made their most careful correction of secondary extinction, and for this point the two methods agree fairly well. Also it has been shown that extinction is inappreciable for the higher orders of reflection and here again we find the two methods in agreement. It seems justifiable to conclude that for the single crystals sufficient correction has not been made for secondary extinction in the orders of reflection which do not agree with the values obtained by the powdered method.

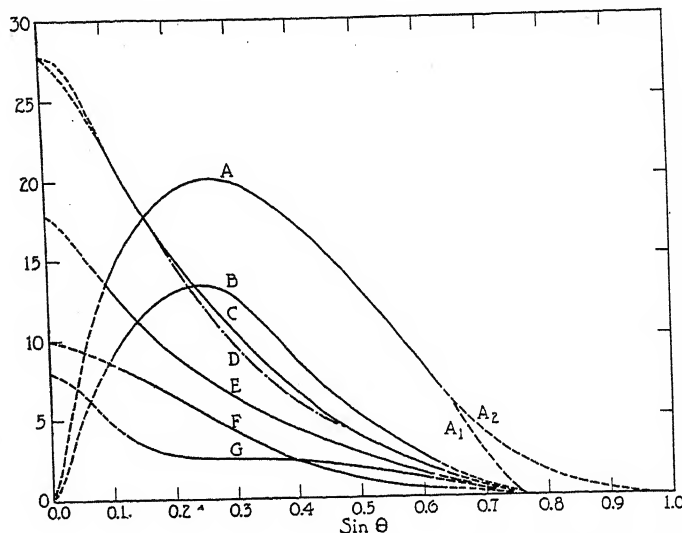


Fig. 3. Curves D and G represent the $F_{\text{Cl}} + F_{\text{Na}}$ and $F_{\text{Cl}} - F_{\text{Na}}$ values respectively for single crystals. Curves C and E represent the corresponding values for powdered crystals. F and G represent the F_{Cl} and F_{Na} values respectively, A and B are the corresponding nF_n curves.

From Fig. 3 it will be seen that experimental determinations of F have only been made up to an angle whose sine is 0.6. The reason for this is that the intensity of the reflected rays for higher orders of reflection is less than one three-millionths of the intensity in the incident beam, and measurements of such intensity are extremely difficult to make. Any extrapolation beyond the last experimental point is doubtful as will be shown in the discussion of the electron distribution curves. Probably the best extrapolation is to extend the curve smoothly to the axis, but

this is only a guess as it is quite possible for the curve to cross the axis, that is, for the values of F to become negative.

The curves E and D represent the F_{Cl} and the F_{Na} values which are derived directly from the $F_{\text{Cl}} - F_{\text{Na}}$ and the $F_{\text{Cl}} + F_{\text{Na}}$ curves for powdered crystals. If the values of F are taken from these two curves and multiplied by the corresponding order of reflection we obtain the curves A and B which represent the powdered crystal nF_n values which are used in Eq. (5) to obtain the electron distribution curves. The order here refers to the arbitrary grating space D used in Eq. (5). The broken part of the curves correspond to the extrapolated portions of the curves.

ELECTRON DISTRIBUTIONS CURVES FOR SODIUM AND CHLORINE

Compton¹⁰ has calculated the electron distributions for sodium and chlorine from Eq. (5) using the single crystal measurements of Bragg, James and Bosanquet.¹³ Since the absolute values obtained by the

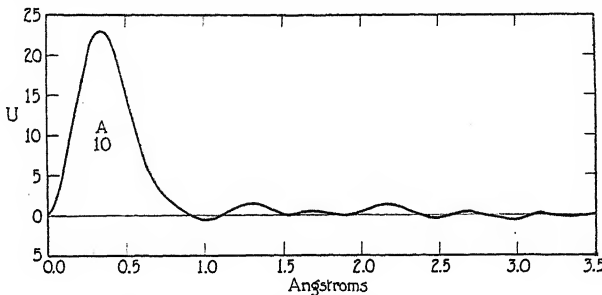


Fig. 4. Sodium electron distribution curve.

writer are in agreement with these measurements, separate distribution curves for the single crystal measurements will not be given.

Sodium. Substituting the sodium nF_n values from curve B , Fig. 3, in the electron distribution Eq. (5) one obtains the electron density as a function of the distance from the center of the atom. Plotting the density against the distance from the center of the atom we obtain the curve in Fig. 4. The value of the arbitrary grating space D used in constructing this curve was 7.1A, a large grating space being used in order to study the distribution of the electrons in the individual atomic layers. This curve shows only one large peak which is at 0.4A and a number of small erratic oscillations which, as has been pointed out by Compton,¹⁰ are probably due to experimental errors. Integrating the peak A we find that it represents a little less than 10 electrons. The resolving power of the present method is not great enough to separate the K and L electrons into separate peaks but gives only the average position of all the electrons in the atom.

Comparing the electron distribution curve for sodium obtained from the powdered crystal values with the curve obtained by Compton¹⁰ using the single crystal measurements we find that they do not agree as closely as one might wish. The second peak at 0.9A containing 2 electrons as found by Compton¹⁰ does not occur at all in the curve obtained by the writer from powdered crystal measurements. This indicates that a high degree of precision must be attained in the experimental determinations before confidence can be placed in the distribution curves. It must be remembered, however, that the sodium experimental values are dependent upon the difference in the atomic reflecting power of chlorine and sodium. Hence the intensity reflected is very weak and the probable experimental errors are greatly increased. About the only safe conclusions to be reached in the case of sodium are—(1) Most of the electrons are

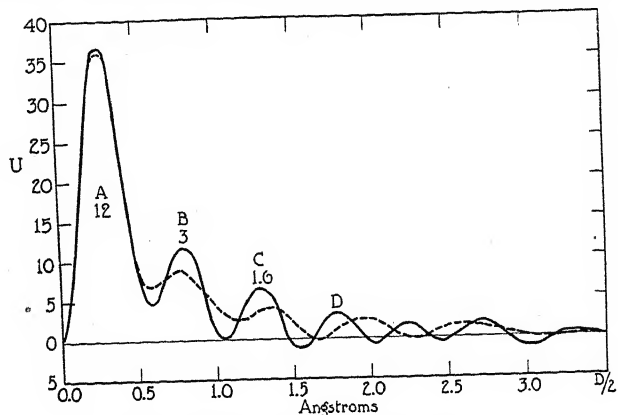


Fig. 5. Chlorine electron distribution curve.

concentrated at a distance between 0.4A and 0.5A from the center of the atom. (2) The radius of the sodium atom is probably less than 1.2A.

Chlorine. For chlorine we will not only make a comparison of the distribution curves for single and powdered crystals, but also the effect of different extrapolations beyond the last experimental point of the F curves on the electron distribution curves. Substituting the nF_n values from curve A , Fig. 3, in Eq. (5) as above, one obtains the electron distribution curves shown in Fig. 5. The solid line represents the electronic distribution if one uses the extrapolation A_1 from the nF_n curve A in Fig. 3, and the dotted line the extrapolation A_2 of the same nF_n curve. These curves are very different from the sodium curve in that there are several important peaks and the density of electrons is much greater near the center of the atom. The difference in the two chlorine curves for the different extrapolations shows clearly the importance of the extrapolated

part of the experimental curves in Fig. 3. The general form and position of the peaks are quite similar to the curves obtained by Compton¹⁰ from the single crystal measurements but the sizes of the peaks are different. The peaks in these curves are much better resolved than those obtained from the single crystal measurements. If we integrate the area under the separate peaks we find that the peak *A* represents 12 electrons, *B* 3 electrons, *C* 1.6 electrons and the remaining peaks 1.4 electrons. The fact that we get fractional parts of an electron in the peaks beyond 1.4 probably means that the experimental values are not accurate enough to give exact distributions in the exterior part of the atom. In the corresponding curves for single crystals measurements Compton¹⁰ obtained 10 electrons in peak *A*, 4 in *B*, 2 in *C* and 2 in *D*. The difference

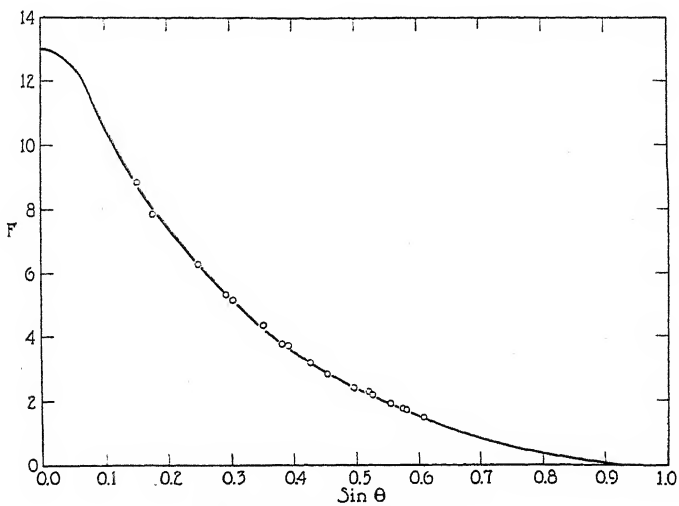


Fig. 6. *F* curve for aluminum.

in the magnitude of the distribution for the different peaks indicates as in sodium that a high degree of precision must be obtained before considerable confidence can be placed in the results. To the writer it seems that the absolute intensity measurements must be made precise to less than 1 percent in order to obtain reliable distribution curves in a crystal such as rock salt. This estimate, of course, refers to the actual value of the different peaks and not to the general form of the curve or to the approximate distribution of the electrons. It seems safe to conclude that the distribution of electrons in chlorine is different from that in sodium and that the radius of the chlorine atom is greater than that of the sodium atom. Any definite conclusions concerning the detailed structure of chlorine or sodium seems unwarranted.

INTENSITY MEASUREMENTS AND THE ELECTRON DISTRIBUTION
OF ALUMINUM

Experiments were made on aluminum in exactly the same manner as described in the transmission method for rock salt. The F_n curve for aluminum is shown in Fig. 6. The extrapolation made for the higher orders of reflection was merely a smooth continuation of the experimental curve. The extrapolation for small angles of reflection was made as before using Eq. (6). For aluminum it was necessary to use two points from this extrapolated portion of the curve because there are no reflections from aluminum crystals at angles smaller than $\sin \theta = .15$. Substituting in the Fourier series Eq. (5), the electron distribution curve shown in Fig. 7 was obtained. The area under the curve out to 1.75A represents very accurately 13 electrons, and the area from 1.75A out to the center of the atomic plane $D/2$ is very nearly zero. Resolving the

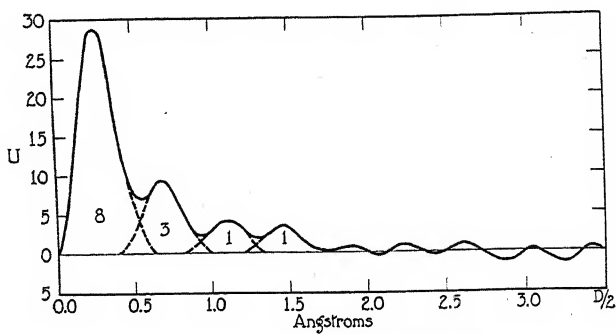


Fig. 7. Aluminum electron distribution curve.

curve as before and measuring the areas under the peaks it is found that peak *A* represents 8 electrons, *B* 3 electrons, *C* 1 electron and *D* 1 electron. In each case the values are accurate whole numbers as near as planimeter measurements could be made. As remarked in the case of sodium and chlorine the oscillations beyond 1.75A are probably due to experimental errors. Their size is proportional to r and hence cannot account for any appreciable part of the four peaks *A*, *B*, *C* and *D*.

Thus from aluminum we get results which appear to be more precise than those obtained from rock salt. The values of F_n fall on a very smooth curve indicating a higher degree of precision than was obtained in the case of rock salt. The resolution of the electron distribution curve into four components such that each contained a whole number of electrons is somewhat arbitrary, but the resolution in each case seems to be a reasonable one.

CONCLUSIONS

It is by no means certain that the theoretical equations on which this discussion is based are correct. For these expressions are based upon the classical electrodynamics, whose reliability applied to problems of the present type is open to question, in view of its failure to account for such phenomena of x-ray scattering as the Compton and allied effects. Nevertheless, as far as these experiments have been made they seem to support in every way the theoretical developments. This is borne out by the following facts: (1) The probable radius of the atom as determined by this means is in no case an impossible radius. (2) The distribution of the electrons in the atom is quite consistent with distributions determined by other methods. (3) Using the electron distribution curves obtained by Compton¹⁰ from the single crystal measurements, Bieler has calculated the magnetic susceptibility of the chlorine and sodium ion, which is of the same order of magnitude as is found experimentally. There is thus no evidence of any failure of the classical electrodynamics as applied to calculations of the intensity of x-ray reflection.

In conclusion the writer wishes to express his appreciation to Professor A. H. Compton for suggesting the problem and for his advice and assistance in this work. He is also indebted to Mr. C. S. Barrett for his assistance in the computations.

RYERSON PHYSICAL LABORATORY,
UNIVERSITY OF CHICAGO.
September 4, 1926.

THE CRYSTAL STRUCTURE OF MAGNESIUM DI-ZINCIDE

BY JAMES B. FRIAUF

ABSTRACT

Crystals of the intermetallic compound, $MgZn_2$, were prepared and the crystal structure was determined from x-ray data furnished by Latie and rotation photographs. The crystal was found to have hexagonal axes with $a=5.15\text{A}$ and $c=8.48\text{A}$. The unit cell contains four molecules. The effect of absorption in the crystal in determining the wave-length giving a maximum intensity of reflection in Laue photographs was used to confirm the dimensions of the unit cell. The atoms have the positions:

Zn: $u, \bar{u}, \frac{1}{4}; 2\bar{u}, \bar{u}, \frac{1}{4}; u, 2u, \frac{1}{4}; \bar{u}, u, \frac{3}{4}; 2u, u, \frac{3}{4}; \bar{u}, 2\bar{u}, \frac{3}{4}; 0, 0, 0; 0, 0, \frac{1}{2}$

Mg: $\frac{1}{3}, \frac{2}{3}, v; \frac{1}{3}, \frac{2}{3}, \frac{1}{2} - v; \frac{2}{3}, \frac{1}{3}, \frac{1}{2} + v; \frac{2}{3}, \frac{1}{3}, \bar{v}$.

Where $u=0.830$ and $v=0.062$. The least distance between two magnesium atoms is 3.15A , between two zinc atoms, 2.52A , and between a magnesium and a zinc atom, 3.02A .

THE constitution diagram for the binary system, magnesium-zinc,^{1,2} has a pronounced maximum corresponding to the formation of an intermetallic compound, $MgZn_2$, which forms eutectics with both constituents. Since both magnesium and zinc crystallize in the hexagonal close-packed arrangement, a determination of the crystal structure of their compound was thought to be of interest.

Crystals of the compound were formed by melting together the calculated amounts of magnesium and zinc under a molten mixture of sodium and potassium chlorides to prevent oxidation. The melt was then allowed to cool slowly in the electric furnace, about four hours being taken to cool from ten degrees above to ten degrees below the melting point of the compound, 595°C . In this way a mass of crystals was obtained from which individual crystals were separated for the production of Laue and spectral photographs.

Two rotation photographs taken with the x-rays from a molybdenum water-cooled tube on an x-ray spectrograph of the kind described by Wyckoff,³ furnished data for the determination of the size and shape of the unit cell. As no information on the crystal class or axial ratio of crystals of this compound was found in the literature, a consideration of the secondary spectra as well as of the principal spectrum was necessary in order to obtain the quadratic form which gives the spacings of the planes. These spacings can be computed from the positions of the re-

¹ Grube, Z. anorg. Chemie 49, 80 (1906).

² Bruni and Sandonnini, Z. anorg. Chemie 78, 276 (1912).

³ Wyckoff, The Structure of Crystals (New York, 1924), p. 164.

lections on the plate and furnish information of the same nature as that available from a powder photograph.

Table I gives the data from a rotation photograph. The observed spacings are the means of those calculated from the reflections produced by the $K\alpha$ doublet and the $K\beta$ line of molybdenum for all the planes of the same form showing on the plate. These spacings were compared with the charts given by Hull and Davey,⁴ and were found to agree with the

TABLE I
Spacing between planes of magnesium di-zincide. The spacings are found to agree with the spacings for a hexagonal unit cell having $a=5.15\text{A}$, $c=8.48\text{A}$, $c/a=1.646$

Plane	Observed spacing	Calculated spacing	Plane	Observed spacing	Calculated spacing
00.1(2)	4.241A	4.240A	12.3	1.449	1.448
10.3	2.377	2.388	00.1(6)	1.411	1.413
11.2	2.204	2.201	20.5	1.351	1.350
00.1(4)	2.122	2.120	12.4	1.321	1.320
10.1(2)	1.966	1.974	11.6	1.244	1.239
10.4	1.916	1.915	20.6	1.198	1.194
20.3	1.746	1.751	20.7	1.071	1.065
12.1	1.658	1.653	00.1(8)	1.062	1.060

spacings for a hexagonal unit cell having $a=5.15\text{A}$ and $c=8.48\text{A}$. Since the crystal was rotated about one of the a axes for this photograph, the assignment of indices obtained from the chart was checked by comparing the computed values of the x and y coordinates with the observed. The fact that certain reflections could not occur because of the limited rotation of the crystal could also be used in some cases to distinguish between planes having nearly the same spacings. On another photograph taken with the crystal rotating about the c axis, only the principal spectrum was measured. This gave $a=5.15\text{A}$ which is in agreement with the value just given. The third column of the table gives the values for the spacings computed from the dimensions of the unit cell.

This unit cell agrees with the data from Laue photographs taken with the white radiation from a tungsten target. When the wave-lengths of the x-rays producing the spots on symmetrical and unsymmetrical Laue photographs were calculated on the basis of this unit cell, no values were found less than the short wave-length limit, about 0.24A , of the x-rays used. The curves showing the intensity of reflection from different planes of the same form reflecting at different wave-lengths in unsymmetrical Laue photographs, start from the short wave-length limit, rise to a maximum between 0.36A and 0.40A , and then decrease for longer wave-lengths. The presence of a maximum intensity so far below the wave-length of the silver absorption edge is due to absorption in the crystal.

⁴ Hull and Davey, Phys. Rev. 17, 549 (1921).

The photographic intensity, I , of the white radiation from a tungsten target operated at 50 kv can be approximately represented⁵ between the short wave-length limit, λ_0 , and the wave-length of the silver absorption edge, 0.485A, by the equation

$$I = B(\lambda - \lambda_0)$$

where B is a constant. This must be modified, however, if the crystal is strongly absorbing. For a first approximation it can be assumed that all the rays producing spots on a Laue photograph are absorbed for a distance equal to the thickness of the crystal. The absorption coefficient can be computed from data given by Richtmyer and Warburton⁶ for the atomic scattering and fluorescent absorption coefficients. Since the absorption due to scattering is small and nearly independent of the wave-length,⁶ it will have no other effect than to decrease the value of the constant, B , but the fluorescent absorption, which is proportional to the cube of the wave-length, will cause greater weakening of the longer wave-lengths and the maximum intensity is accordingly shifted to the short wave-length side of the silver absorption edge. The density of the crystal, 5.16, its thickness, about 0.3 mm, and the computed absorption coefficient give

$$I' = B'(\lambda - \lambda_0)e^{-22\lambda^3}$$

where I' is the photographic intensity of the white radiation after passing through the crystal, and B' is the constant, B , multiplied by the factor which represents the common decrease in intensity of all wave-lengths due to scattering. The curve given by this equation has a maximum at 0.36A and agrees in form with the curves showing the intensity of reflection as a function of the wave-length, thus furnishing additional evidence for the correctness of the unit cell chosen.

The density was determined by weighing in a specific gravity bottle after breaking the sample into small pieces in order to avoid, as far as possible, inclusion of blowholes. Two determinations gave 5.164 and 5.155. Using the value 5.16 for the density, the computed number of molecules in the unit cell was found to be 3.93, the deficiency from the integral number, 4, doubtless being due to the fact that the density determined by the use of a specific gravity bottle is likely to be less than the density determined by x-ray measurements, unless porosity of the sample can be completely eliminated.

Smaller unit cells, containing 1, 2, or 3 molecules were found to be inconsistent with the data available.

⁵ Wyckoff, *The Structure of Crystals* (New York, 1924), p. 142.

⁶ Richtmyer and Warburton, *Phys. Rev.* 22, 539 (1923).

A Laue photograph taken with the incident beam of x-rays parallel to the principal axis of the crystal had a six-fold symmetry axis intersected by six planes of symmetry. The space-group giving the arrangement of atoms in the crystal must consequently be isomorphous with one of the point-groups D_3^h , C_6^v , D_6 or D_{6h}^4 . Reference to a tabulation of the results of the theory of space-groups⁷ shows the possible ways of arranging four (magnesium) and eight (zinc) atoms in the unit cell. The arrangements which are possible if it is assumed that the magnesium atoms are equivalent and that the zinc atoms are likewise equivalent, are inconsistent with the Laue data and the assumption of equivalence of all chemically like atoms must consequently be relinquished. With the freedom of choice thus allowed there are numerous ways of arranging the atoms. The zinc atoms may be in two groups, each of four equivalent positions; two groups, one of six and one of two equivalent positions; or in some other combination giving the required number of atoms. The number of possible combinations for the magnesium atoms is somewhat less. The choice of the correct atomic arrangement is simplified by the observation that many of the groups of six equivalent positions lie in a single plane parallel to the base of the unit cell. If, however, six zinc atoms which constitute more than half the reflecting power of all the atoms contained in the unit cell, are arranged in such a plane, the absence of odd order reflections from 00.1 and the observation that the fourth order reflection from 00.1 is stronger than the second order cannot be satisfactorily explained. Groups of six equivalent positions having such an arrangement are consequently excluded from further consideration.

The only structures which are possible with these restrictions and which offer any possibility of accounting for the observed intensity relations are those arising from the space-groups D_{3h}^4 , C_{6v}^4 , D_6^6 , and D_{6h}^4 . Of the structures which can be obtained from the space-groups D_6^6 and D_{6h}^4 the only one not conflicting with the data is that in which the atoms have the following positions:

$$\text{Zn: } u, \bar{u}, \frac{1}{4}; 2\bar{u}, \bar{u}, \frac{1}{4}; u, 2u, \frac{1}{4}; \bar{u}, u, \frac{3}{4}; 2u, u, \frac{3}{4}; \bar{u}, 2\bar{u}, \frac{3}{4}; 0, 0, 0; 0, 0, \frac{1}{2}$$

$$\text{Mg: } \frac{1}{3}, \frac{2}{3}, v; \frac{1}{3}, \frac{2}{3}, \frac{1}{2} - v; \frac{2}{3}, \frac{1}{3}, \frac{1}{2} + v; \frac{2}{3}, \frac{1}{3}, \bar{v}$$

This arrangement is obtained by placing the magnesium atoms in one group of four equivalent positions and the zinc atoms in two groups of, respectively, six and two equivalent positions. A consideration of the type of structure involved shows that it is sufficient to consider only values of the parameters satisfying the conditions $0 \leq u \leq 0.5$ and -0.25

⁷ Wyckoff, The Analytical Expression of the Results of the Theory of Space Groups (Washington, 1922).

$\leq v \leq 0.25$. If it is assumed that there is a reasonable distance between the two magnesium atoms in the same vertical line, v will be restricted to the middle half of its possible range.

The amplitude factor, S , is computed from

$$S = (A^2 + B^2)^{\frac{1}{2}}$$

where A and B have their usual significance of sine and cosine summations,⁸ and is zero for first order reflections from planes of the forms $\{h\ h \cdot 2p+1\}$ irrespective of the values of u and v . No first order reflections from any such planes were found on any of the Laue photographs, although planes of the forms 22.1, 33.1, 44.3, 55.3, and 44.5 were in a position to give first order reflections at a favorable wave-length. Another characteristic feature of this structure is that the magnesium atoms contribute nothing to the amplitude factors for first order reflections from planes of the forms $\{0\ 3h \cdot 2p+1\}$. The intensities of such reflections are consequently useful in determining the positions of the zinc atoms, and show that u can not have values differing greatly from 0, $\frac{1}{6}$, $\frac{1}{3}$, or $\frac{1}{2}$. Consideration of the amplitude factors for other planes shows that the only values of u giving general agreement with the requirements of the Laue data are those in the neighborhood of $u = \frac{1}{6}$. The observed intensity relations for the planes 26.3, 26.5 and 26.7 can then be satisfied by giving v a small negative value.

TABLE II

Extent of the agreement between estimated intensity and amplitude factor using for the parameters the values $u = 0.170$ and $v = -0.062$

Plane	Spacing	Estimated intensity	$n\lambda$	Amplitude factor	Plane	Spacing	Estimated intensity	$n\lambda$	Amplitude factor
12.1	1.65A	32	0.37	31	16.4	0.65	3	0.36	72
03.1	1.46	4	0.46	15	07.3	0.62	5	0.37	108
13.1	1.22	20	0.36	38	35.3	0.62	4.8	0.38	89
04.1	1.10	90	0.43	171	35.4	0.61	3	0.43	84
02.1(2)	1.08	70	0.76	132	26.3	0.60	5	0.36	114
23.1	1.01	12	0.41	46	22.3(2)	0.58	6	0.80	149
23.2	0.99	6	0.37	30	26.5	0.58	10	0.35	191
14.2	0.95	60	0.36	153	07.6	0.58	2.5	0.41	71
05.3	0.85	11	0.38	77	13.3(2)	0.57	9	0.74	164
33.2	0.84	36	0.38	152	35.7	0.56	1.4	0.44	68
24.1	0.84	28	0.31	170	26.7	0.55	5	0.42	136
24.3	0.81	23	0.40	116	08.3	0.55	2.5	0.30	113
12.2(2)	0.78	3	0.91	29	17.6	0.54	2.5	0.36	83
15.3	0.77	11	0.43	83	08.5	0.53	5	0.35	192
15.4	0.75	12	0.41	98	04.3(2)	0.51	5	0.73	164
03.1(2)	0.73	8	0.75	83	18.4	0.50	1	0.32	108
34.3	0.71	4.2	0.39	77	08.7	0.50	2.5	0.36	134
25.2	0.70	10	0.36	155	46.5	0.49	3	0.36	190
03.2(2)	0.70	50	0.77	237	27.8	0.48	1	0.38	149
34.4	0.69	8	0.37	111	46.7	0.47	1	0.34	134
16.3	0.66	5	0.39	98					

⁸ Wyckoff, The Structure of Crystals (New York, 1924), p. 107.

With the values of u and v restricted in this way it was found by trial that satisfactory agreement with the data was obtained for $u=0.170$ and $v=-0.062$. The extent of the agreement is shown in Table II, which gives the data from an unsymmetrical Laue photograph. The table shows the spacing of the plane producing the reflection, the intensity as estimated visually by comparison with a plate which had been given a series of graduated exposures, the product of the order of reflection by the wave-length producing the reflection, and the amplitude factor computed for the values of the parameters given on the assumption that the reflecting powers of the zinc and magnesium atoms are proportional to their atomic numbers. In comparing the intensities of two planes, if the plane with the smaller spacing gives the greater intensity under comparable conditions of wave-length, it must have a greater amplitude factor. As previously stated, the maximum intensity falls between 0.36A and 0.40A and the intensities in the table have been given in this region when possible.

This two-parameter structure is the simplest which will give agreement with the data available. The only other possible structures are a three-parameter structure derived from D_{sh}^4 and a five-parameter structure derived from C_{6v}^4 . Neither of these two more general structures can be eliminated, but consideration indicates that neither will give satisfactory agreement with the data except for values of the parameters which reduce them to forms closely approaching that of the two-parameter structure, and it is consequently concluded that this structure, or a more general structure, so similar as to be indistinguishable from it, represents the crystal structure of MgZn_2 when u and v have the values given.

This structure can be described in an alternative way without the use of a negative parameter by setting $u=0.830$ and $v=0.062$. Fig. 1 shows the arrangement of atoms in the unit cell. The least distance between two magnesium atoms is 3.15A , between two zinc atoms 2.52A and between a magnesium and a zinc atom 3.02A . The values computed from the atomic radii determined from the crystal structures of magnesium and zinc are respectively 3.22A , 2.67A , and 2.95A . If the zinc atoms at $0,0,0$ and $0,0,\frac{1}{2}$ are called zinc atoms of the first kind and the others, zinc atoms of the second kind, each magnesium atom is surrounded by three zinc atoms of the first kind and nine of the second kind, all twelve zinc atoms having very nearly the same distances from the magnesium atom. Each zinc atom of the first kind is equidistant from six zinc atoms of the second kind, while the nearest neighbors of each zinc atom of the second kind are two zinc atoms of the same kind.

Each magnesium atom in magnesium di-zincide is equidistant from

three other magnesium atoms and at very nearly the same distance from a fourth. In the structure found, these four atoms are at the corners of a tetrahedron which is so nearly regular that with changes in the values of the axial ratio and the parameter, v , of less than one percent, each magnesium atom would be surrounded by four others at the corners of a regular tetrahedron having the inclosed atom at its center. This is the arrangement which Bragg⁹ has suggested for the oxygen atoms in ice, and is given by two interpenetrating hexagonal close-packed arrangements of which one has been displaced vertically with respect to the

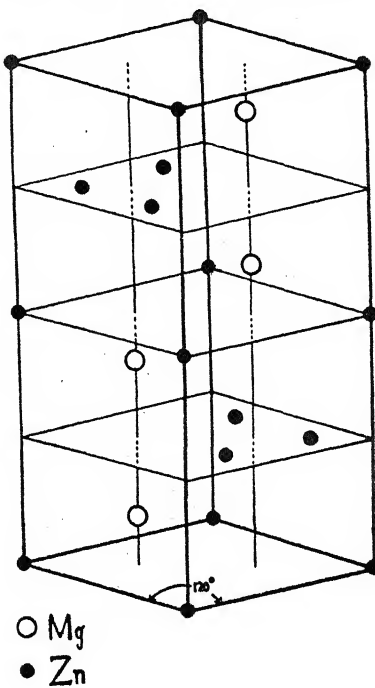


Fig. 1. Arrangement of atoms in the unit cell of MgZn_2 .

other; through a distance equal to $\frac{3}{8}c$. There is no such obvious similarity between the way in which the zinc atoms are arranged in magnesium di-zincide and in metallic zinc, and the structure which has been found for this compound is apparently different from any which has been previously described.

In conclusion, the writer wishes to express his thanks to Dr. R. G. Dickinson for reading the manuscript and suggesting some modifications.

THE BUREAU OF METALLURGICAL RESEARCH,
CARNEGIE INSTITUTE OF TECHNOLOGY,
PITTSBURGH, PENNSYLVANIA.

April 19, 1926.

⁹ W. H. Bragg, Proc. Phys. Soc. London 34, 98 (1922).

ABSORPTION IN THE REGION OF SOFT X-RAYS

By ELIZABETH R. LAIRD

ABSTRACT

Energy of soft x-rays from a tungsten-coated nickel target as a function of potential from 40 to 610 v.—Soft x-rays from the target were allowed to fall on a solid solution consisting of $\text{CaSO}_4 + 2$ percent MnSO_4 . The square of the time of duration of the thermoluminescence produced was assumed to be proportional to the total energy of the x-rays. The results indicate that in the range 40–610 v., the total energy varies approximately as the square of the potential applied to the tube.

Absorption of soft x-rays (40–610 v.) by thin celluloid films.—By interposing a thin celluloid film, about $25 \text{ m}\mu$ thick, between the target and the thermoluminescent substance, the transmission of the film was measured for various values of the applied potential from 40 to 610 volts. The transmission varied from 0.0 percent at 40 volts (minimum wave-length 310A) to 57 percent at 610 volts (minimum wave-length 20A). The results are in general agreement with the hypothesis that the absorption varies as the cube of the wavelength, that K absorption discontinuities in celluloid occur between 300 and 600 volts and that the x-rays cover a wide spectral region. A photographic method of investigating absorption is also described. The results are fairly consistent with those obtained otherwise but the method suffers from the fact that the photographic plate is not equally sensitive to energy of different wavelengths.

Absorption of soft x-rays (300–600 v.) in air and H_2 .—Computation based on previous measurements give for air values of $\mu/\rho = 6.0, 6.25, 7.0, 7.6 \times 10^3$ at 600, 500, 400, and 300 volts respectively. These figures agree fairly well with those given by Holweck in O_2 and N_2 . For H_2 the value of μ/ρ is calculated to be about 1.8×10^4 which is larger than the value given by Holweck and larger than is to be expected from the results for air.

THE absorption of various substances, but especially of thin celluloid films, for soft x-rays was measured by the author¹ in 1914 for the range 300 to 1300 volts, and was found to change little with the voltage. In all cases however, the radiation had to pass through one window-film in addition to the substance whose transmission was being measured, and this made the interpretation of the results doubtful. Later the absorption of films between 30 and 40 $\text{m}\mu$ thick was measured by an optical method,² using the vacuum spectrograph, and it was estimated that from 1700A down to 900A a thin celluloid film transmits from 50 to 20 percent, and below not much over 5 percent. The transmission was followed to about 450A and was thought to extend lower.

¹ Laird, Ann. d. Physik 46, 105 (1915).

² Laird, Phys. Rev. 15, 543 (1920).

Holweck³ also measured the absorption of soft x-rays (10.8 to 1230 volts) by films 80 μ thick using a method similar to the author's, i.e. one in which the radiation had to pass an absorbing window in addition to the film in question. He found the transmission in the Lyman-Millikan region approximately the same as that found by the author by the purely optical method, but his films were thicker. In the region of soft x-rays from 300 volts to 1200 volts he found likewise no substantial change in transmission, and likewise attributed this to the effect of the window. That with this filtering the absorption in this region follows approximately the law $I = I_0 e^{-\mu d}$ is shown by the figures in Table I computed from the earlier data.

TABLE I

	Holweck			
Thickness:	1.6	0.9	0.3	0.08
I/I_0 :	0.17	0.4	0.7	0.92
$(1/d) \log (I_0/I)$:	0.48	0.44	0.52	0.45

On account of the usefulness of these films it was thought desirable to investigate the transmission by a method that would not involve the previous filtering of the radiation

There are difficulties in using the photoelectric method without a window, as seen by the discrepancies in the results of different investigators who have used this method, hence a thermoluminescent method was chosen which seemed likely to give at least a general orientation on the problem. The apparatus is suggested by Fig. 1. A tungsten coil, as used in 100-watt, 110-volt lamps furnished by the General Electric Company, served as cathode and gave ample electron current at from 0.62 to 0.64 amp. heating current. The voltage was furnished by small storage cells and wireless *B* batteries, and was measured from the negative end of the filament by a Weston voltmeter. The potential drop across the filament was from 8 to 10 volts. The anti-cathode was of nickel, v-shaped. It was placed about 2 mm from the filament cathode and hence was soon covered with a layer of tungsten. To produce the vacuum a diffusion pump, with carbon dioxide cooling, following a Gaede mercury pump with phosphorous pentoxide drying was used. The pressure on the Gaede pump side was from .0008 to .00001 mm Hg as measured while the filament current was on. A channelled metal piece *D*, with a magnet *MM* was used to prevent any stray corpuscular radiation from reaching the thermoluminescent substance *T*. The latter was a solid solution of $\text{CaSO}_4 + 2$ percent MnSO_4 , well heated, spread on resistance ribbon wire bent to form a plate. It could be

³ Holweck, Ann. d. physique 17, 5 (1922).

heated and the thermoluminescence observed *in situ*. This substance was not at all sensitive to the light from the tungsten filament. Exposures up to six hours with the filament lighted gave no effect. In one experiment when a leak suddenly developed during a run, it was noticed that after the short-time luminescence ceased, there persisted a faint luminescence of long duration. This effect was reproduced later when at the end of an experiment air was admitted as a test. The effect was

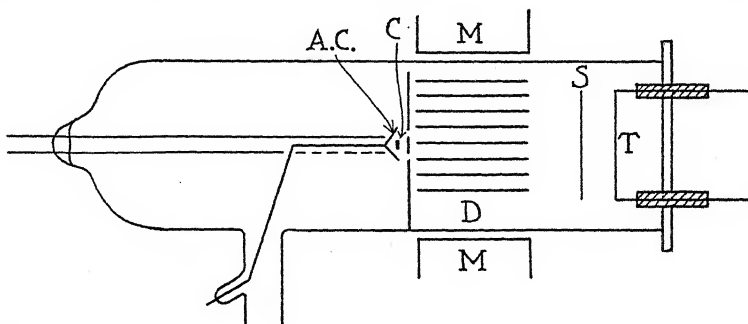


Fig. 1. Diagram of apparatus.

therefore ascribed to a change in the thermoluminescent substance caused by the presence of air or a trace of moisture. In investigations on Entladungsstrahlen it has previously been observed that luminescence may be caused by ordinary light in this same detector when it was insufficiently heated before using.

In front of the thermoluminescent substance was a screen *S*, with two groups of three openings (see Fig. 2). In the one group 4 and 6 were open while 5 was covered with thin celluloid. In the other, 1 and

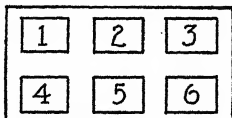


Fig. 2. Diagram of screen.

3 were covered with celluloid and 2 with fluorite. It may be said at once that only once, with 630 volts on the tube, I thought possibly I saw a faint flash of light under the fluorite. After a six-hour exposure at 40 volts there was no visible fluorescence under the fluorite.

It has been estimated in connection with earlier experiments⁴ that the square of the time during which the thermoluminescence is visible

⁴ Laird, Phys. Rev. 30, 293 (1910).

is roughly proportional to the total quantity of radiation received, and the results given by C. A. Pierce⁵ make this plausible. It is not supposed that this holds exactly, as the times would depend on the threshold of vision, but comparison of the duration of visibility for exposures of different lengths at the same voltage showed that the radiation received is more nearly proportional to the square than to the first power of the time, and this square has been used in computations of transmission.

The procedure was to expose the thermoluminescent substance for a given time to the radiation from the anti-cathode with a given potential difference on the tube and then, with metronome and stopwatch, to measure the time that the luminosity under the holes and under the celluloid lasts. From this the transmission was computed. In observing the thermoluminescence I had the help, on a number of occasions, of Mr. Smyth, curator of the department. We found good agreement in our observations. The results are given in Table II and are, in general, averages of several trials. Two exposures at 40 volts were made, each lasting six hours, the thermoluminescence with no screen lasted 11 sec. but no luminosity was seen under the celluloid. It was thought that a 5 percent transmission should have been visible, but as it would be faint it might have been missed. It is not intended to attach importance to

TABLE II
Transmission of soft x-rays through a celluloid film

Volts on tube	Transmission through thin celluloid	Minimum wave- length	Volts on tube	Transmission through thin celluloid	Minimum wave- length
40	0.00	310A	310	.24	40A
60	.06	206	360	.32	34
75	.06	164	390	.54	32
115	.09	107	480	.46	26
220	.13	56	540	.44	23
270	.11	46	610	.57	20
295	.21	42			

the slightly higher values of transmission given at 220 volts and at 390 volts. In the first case one of four observations was decidedly larger than the others, and in the second only one observation was made. The potential as given is measured to the center of the filament. The last column contains the corresponding minimum wave-length computed in the usual way.

A computation was made of the theoretical absorption of celluloid, assuming it composed of two parts pyroxylin and one part camphor

by weight, and also assuming that each atom absorbs independently of the others. The formula

$$\tau a/\rho = .0106(n + .02n_L)N^4\lambda^3$$

was used to compute the coefficient of absorption for the different substances present, where n is zero until the wave-length is reached at which K absorption begins, and then equals two, and n_L is the number of L-electrons per atom. One may suppose that for wave-lengths greater than 50A the absorption for carbon, nitrogen and oxygen is of type L only, and that K absorption has begun for carbon at 40A, for nitrogen at 30A, and for oxygen at 25A. The result of this computation is shown in Table III for a film 100 m μ thick. To find from these figures the effect to be expected in a given experiment, one needs to know the distribution of energy in the spectrum for a given voltage, and

TABLE III

λ in A:	15	20	25	30	35	40	50	60	90	120	150
Transmission:	.90	.78	.61	.71	.64	.51	.79	.67	.26	.04	.002

the variation in sensitiveness of the detector for different wave-lengths. Graphs were made of the Kuhlenkampf equation in the form,

$$E_\lambda = [A(1/\lambda_0 - 1/\lambda) + B]/\lambda^2$$

and then the computed transmission factors were used to draw curves representing the approximate distribution of energy after passing the film. Radiation of wave-length longer than 120A was neglected and uniform energy sensitiveness of the thermoluminescent detector was assumed. The ratio of the areas under the curves then gives the transmission. At 1230 volts this was computed to be 62 percent, at 615 volts 56 percent, a relatively small change, and at 246 volts the transmission would be less than 25 percent, but through a second film would be 50 percent of what had passed the first. It is seen that theoretically, because of (a) the rapidly diminishing factor, λ^3 , in the absorption coefficient, combined with the introduction between 40A and 20A of the various K terms, and (b) the integration of the effect over a considerable spectrum range, the result is to produce an absorption of soft x-rays which does not vary greatly in the range considered. It is also seen that theoretically, for voltages above 300, the effect of a celluloid window would be to cut off wave-lengths greater than 90A almost completely, but to transmit the whole range of shorter wave-lengths in the general radiation. Films made from the same solution as used in this work measured 25 m μ in equivalent thickness. When one compares computation and experiment one sees therefore that while the theoretical result is in general

agreement in the sense of predicting, for the transmission of general radiation at low voltages, small values, which gradually increase as the voltage increases and then remain approximately constant over a certain range, that the actual absorption is greater than predicted. From Table I one may see that for agreement with the earlier experiments these films should transmit 95 percent of a filtered radiation at 600 volts. While the luminescence at 600 volts is quite strong the total duration under the film is appreciably less than under the free opening, the difference being greater than the figure 95 percent would imply. Any corpuscular rays mixed with the radiation would have the effect of diminishing the apparent transmission, but tests made with the metal carrying the thermoluminescent substance insulated and at positive and at negative potentials showed no difference, hence it is certain that a corpuscular radiation was not involved. This difference between the present and earlier results has been however already explained, at least in part, by the fact that the filtered radiation of the earlier experiments had already lost the easily absorbed part. That the computation describes the phenomenon as nearly as it does is interesting because one could not expect an atomic formula to hold exactly in this region. Holweck³ made the statement (l. c. p. 37) that a film which transmits 92 percent before the carbon K discontinuity transmits only 9 percent of a radiation of slightly shorter wave-length. He thus accounted for the uniform transmission from 300 volts on by assuming that beyond this potential the window-film transmitted only the same longer wave-lengths. This is evidently not in accord with the facts.

A comparison of the total energy in the radiation at different voltages for the same electron current, as estimated by the thermoluminescence produced, suffers both from the difficulty of estimating quantitatively the thermoluminescence, and the uncertainty as to whether the same proportion of the total radiation is being utilized at different voltages when on account of diaphragms the whole surface of the anticathode does not act as source. In a general way the results would agree with the hypothesis that the energy increases with the square of the voltage, but there is a big scattering of points. The effect of a one-minute exposure at 15 m.a. electron current at 600 volts is about the same as for a five-minute exposure at 300 volts, and is estimated to be more than twice as great as for a six-hour exposure with 4 m.a. current at 40 volts.

As another means of investigating this region of radiation it was thought desirable to try a photographic method. This introduced the

³ E. L. Nichols and E. Merritt, Studies in Luminescence, p. 91.

difficulty of eliminating effects from direct or reflected filament light, and necessitated the use of a Wehnelt cathode which could be used at a dull red temperature. With this cathode, even when the McLeod gauge between the tube and diffusion pump registered no pressure, one could with rested eye in a dark room usually detect some luminosity in the tube, perhaps on the walls of the glass. The arrangement as finally used was as indicated in Fig. 3, in which *G* is a grid in an opening in a piece of mica, *AC* is the plate serving as source of radiation, *S* is a long tubular slit, *A* is a shelf on which absorbing screens may be placed, *P* is the photographic plate which may be moved along by a ground glass joint. A horseshoe magnet was used to deflect sidewise any corpuscular rays passing down the slit. There were three openings in the screen *A*,

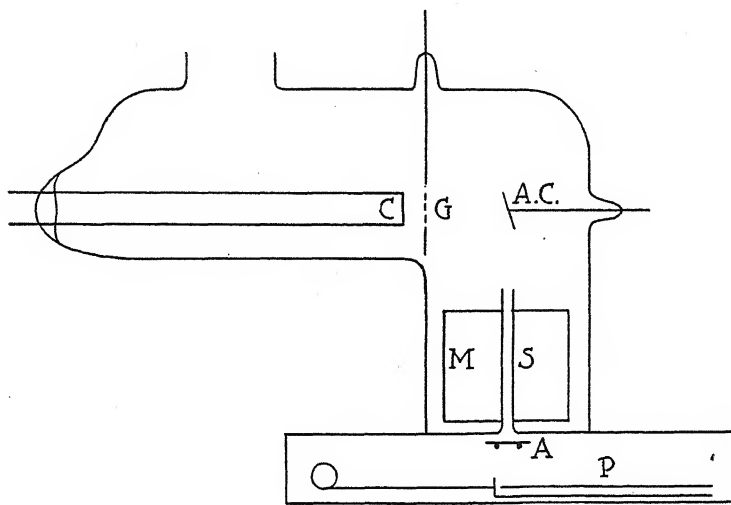


Fig. 3. Arrangement of apparatus for the photographic method.

one was covered with thin quartz, and one with a celluloid film. With this arrangement there was no photographic effect due to the hot filament, but when the potential was applied to the tube slight effects showing the presence of a small amount of ultra-violet light were found at various times under the quartz.

In these experiments liquid air was used on the mercury trap, and after the tube was exhausted, it was run for from one and a half to three hours before the definite exposures were made. The pumps were kept going continuously. Several exposures were made on one plate. The effect of different times of exposure with the same voltage, and of different voltages was thus tested. It was at once

apparent that the photographic effect did not increase with voltage so rapidly as the thermoluminescence or ionization does. To give the same darkening the product of electron current and time of exposure was more nearly inversely as the voltage than as its square, or was varied even more slowly than this. The interpretation of absorption records is hence difficult, since if the energy in the longer wave-lengths is more effective in producing a photographic effect than the same quantity of energy in the shorter wave-lengths, then the transmission through a film which transmits the shorter wave-lengths relatively better will appear less than by a method which more nearly measures the total energy of the radiation.

The darkening of the plate was measured by a thermocouple densitometer. Estimates of the transmission were made both by comparing the time of exposure, with film interposed, and that exposure without the film which gave most nearly the same darkening, and by comparing the density with and without film from a simultaneous exposure. These gave at 600 and 845 volts a transmission between 40 and 50 percent, and at 265 volts between 30 and 40 percent. In some experiments two absorbing films of different thickness were used, and as expected the ratio of transmission through thick to that through thin was greater than the above. These experiments served then to confirm in a general way the results obtained by other methods. It may be added that a five-minute exposure with 0.4 m.a. plate current at 600 volts gave a good photographic effect.

ABSORPTION IN GASES

In 1920, data were given⁶ from which could be computed the coefficient of absorption of air in the region from 600 to 300 volts, by giving ionization currents produced at different air pressures in an ionization chamber. The source of error was the difficulty in maintaining a constant electron current. There is an error in the published table, the electrometer deflections at 2 mm pressure and at 7.5 mm pressure being for 2 and 1.5 min. respectively instead of for 1 min. as stated. These gave for μ/ρ the values 6, 6.25, 7, 7.6×10^3 at 600, 500, 400 and 300 volts respectively. Another set of values not taken with this in view, and probably not as accurate because of greater inconstancy in the source of radiation, gave at 600 volts 5.4×10^3 . These values are quite close to those given by Holweck, viz. $\log \mu/\rho$ for nitrogen 3.68 and for oxygen somewhat larger. Holweck examined the absorption for nitrogen over a wide region, and found it substantially constant between 300 and 1200 volts. He ex-

⁶ Laird and Barton, Phys. Rev. 15, 303 (1920).

plained this also as the effect of the transmission of an approximately unchanged wave-length by the celluloid window. Considerations similar to those employed for celluloid show that also here, with just one discontinuity to be expected in the region, there is still but slight change in the integrated absorption phenomena, if one assumes a distribution of energy such as was computed previously for the radiation after passing a window. The average value of μ/ρ as so computed for the case of 600 volts is however 1.2×10^4 , corresponding to a much larger absorption than that found, instead of smaller as in the case of the celluloid. One may question whether the absorption is strictly atomic.

Some earlier experiments⁷ were also made with hydrogen, and while not made for this purpose serve to indicate that while μ in cm^{-1} for hydrogen is smaller than for air, μ/ρ would be larger, 1.8×10^4 , contrary to the result given by Holweck and to the usual theory. Assuming his value for μ at a pressure of 3 mm in the ionization vessel used, one should have only about 2 percent of the maximum ionization, and the large difference between this and the result found by the author is not easy to explain. Perhaps reflection from the walls play a larger part than is thought. I hope to try this by a slightly different method.

The work on developing and using the photographic method for these experiments and those on reflection reported earlier, was done at the Sloane Physical Laboratory, Yale University. It is a pleasure to thank Professor Zeleny and Professor Swann for their great kindness in placing the facilities of the laboratory at my disposal.

MOUNT HOLYOKE COLLEGE,
August 7, 1926.

⁷ I. c. pp. 301, 302.

THE LINE SPECTRA OF THE ISOTOPES OF MERCURY AND CHLORINE

BY FRANCIS A. JENKINS¹

ABSTRACT

Comparison, for Hg and Cl, of wave-lengths and relative intensities in line spectra from samples of varying isotopic composition.—Two sample-pairs of mercury with atomic weight differences of 0.124 and 0.180 and one sample pair of chlorine with a difference of 0.097 were examined spectroscopically. An echelon (resolving power about 400,000) and a plane grating (resolving power 478,000 in the fifth order) were used. The spectra of the mercuries with the smaller atomic weight separation showed for the lines $\lambda\lambda 5461, 4359, 4078$ and 4047 no wave-length differences greater than the error of measurement ($3 \times 10^{-4}\text{A}$). The first two of these lines, obtained, with the use of a special source from the mercuries of the greater atomic weight separation, were studied to see if differences in the relative intensities of the satellites could be brought out. None was found. The results, therefore, do not favor the isotopic origin of the satellites. The spectra of the two chlorine samples, when examined with the echelon showed distinct evidence of differences in wave-length. The heavier chlorine almost invariably gave the smaller wave-length. The displacements were of the order of 0.001A , and only two or three times the error of their determination. A convenient source of the chlorine spectrum is described.

THE only direct experimental evidence of a difference in the electronic spectra of isotopes is that first brought forward by Aronberg,² who found the line $\lambda 4058$ in the arc spectrum of ordinary lead to have a wavelength 0.0043A shorter than the same line in the spectrum of lead extracted from a uranium ore. This result has since been confirmed and extended to other lead lines in later independent investigations.³ It is important that the effect observed by Aronberg was a distinct shift of the line, and not a mere broadening on one side, which we should expect if ordinary lead were a mixture of isotopes of mass 206 and 208. The latter effect was noted, however, by Grebe and Konen⁴ in their comparison of the lines of the lead band spectrum. Even if we assume ordinary lead to be a third isotope, it is difficult to explain Aronberg's result, since his uranium lead was not free from ordinary lead. Although the shift which we observe in a line when the relative proportions of the isotopes are altered is most reasonably ascribed to a re-distribution of

¹ National Research Fellow.

² Aronberg, *Astrophys. J.* **47**, 96 (1918).

³ Comprehensive reviews of the subject of isotope spectra have been given by Aston, "Isotopes," 2nd ed., Ch. X (1924) and by Joos, *Phys. Zeits.* **26**, 357 (1925).

⁴ Grebe and Konen, *Phys. Zeits.* **22**, 546 (1921).

intensities in a close multiplet whose components arise in the several isotopes, it has not been experimentally proven to be due to this effect.

The results of other investigations of the spectra of the lead isotopes agree as to the direction of the shifts (the lines from the heavier lead always had the smaller wave-length), and fairly well as to their magnitude. Discrepancies in the latter were attributed to the different purity of the samples of radioactive lead, and correspond roughly with the atomic weight data. Merton⁵ compared the wave-lengths of several of the brighter arc lines, and found that the shifts varied, sometimes by as much as 50 percent, for different lines. Recent work by Mlle. Pierette,⁶ however, has failed to confirm this: the displacements were found to be constant over the range of wave-lengths studied.

The circumstance that we have been unable completely to separate the isotopes of other non-radioactive elements in appreciable quantities has left the theoretical interpretation of these results in a rather unsatisfactory state. The simple Bohr equation³ for the change of the Rydberg constant with the nuclear mass, although strictly accurate only for an atom having one planetary electron, was thought to give an upper limit for the actual shift for complex atoms. However, as Bohr has pointed out,⁷ the equation is probably not at all valid for lines involving S-states, since the electron in these orbits penetrates the shells of other electrons and passes very near the nucleus. The energy of the orbit would be largely determined during this close approach, and a difference in the distribution of the nuclear field of force in the isotopes might thus account for the unexpected magnitude of the shift observed for some lead lines.

In order to obtain further information on these uncertain points, the writer has made a comparison of the spectra of samples of mercury of different atomic weight, which were made available for this investigation through the kindness of Professor W. D. Harkins. A similar comparison has also been made for chlorine, which was likewise obtained from him.⁸ The atomic weight difference for both elements was brought about by long-continued fractional diffusions, and in both cases represents an appreciable change in the proportions of the isotopes.

⁵ Merton, Proc. Roy. Soc. 100A, 84 (1921).

⁶ Pierette, Comptes rendus 180, 1589 (1925).

⁷ Bohr, Nature 109, 745 (1922).

⁸ This separation of the mercury isotopes was obtained by using the extremely rapid and efficient method devised by McMilliken (Jour. Am. Chem. Soc. 45, 1592 (1923)). The results have not yet been published. The chlorine samples were produced by independent work on the heavy fraction from the diffusion of HCl (Harkins and Hayes, Jour. Am. Chem. Soc. 43, 1803 (1921)), and on the light fraction (Harkins and Jenkins, Jour. Am. Chem. Soc. 48, 58 (1926)).

The mercury spectrum in particular has interested those searching for spectroscopic evidence of isotopes, since the numerous satellites of its lines were thought to be related to its complex composition.⁹ While it is now generally conceded that the satellites have no direct connection with the isotopes,¹⁰ the results of Nagaoka, Sugiura, and Mishima,⁹ which they held to demonstrate such a relation, can be tested by investigating the "partially separated" isotopes, as Nagaoka suggested later.¹¹ Although the separation for mercury is small in terms of the atomic weight change, we might expect a considerable difference in the relative proportions of the lightest and heaviest isotopes in the two fractions because of the large atomic weight interval. Assuming the more accurate isotopic constitution recently reported by Aston,¹² the exact changes in the proportions of all isotopes, corresponding to a given atomic weight change, may be calculated. This has been done for the two best samples, which differed by 0.18 atomic weight units, using the equations of Mulliken and Harkins.¹³ The results show that, while the proportions of most of the isotopes are nearly the same in each, the fraction of isotope 198 in the heavier mercury is 20 percent smaller than in the lighter mercury, and the fraction of isotope 204 is 27 percent greater. A comparison of the intensities of the satellites of a given line from the two samples thus affords an experimental test of the theories mentioned above.

The separation for chlorine, expressed as an atomic weight difference, was less than that for mercury. However, because of its smaller atomic weight, the *relative* difference for chlorine is three times that for mercury. We may suppose that, although the components of the hypothetical isotopic chlorine doublets should show smaller changes in relative intensity than should be found in the isotopic components for mercury, their frequency difference should be much greater than the differences for mercury. Since, in the absence of a quantitative theory for this effect, it is impossible to say what difference should exist between the spectra of these isotopic samples, and how it will manifest itself at the dispersion

⁹ See, for example, Nagaoka, Sugiura, and Mishima, Nature 113, 459 (1924); Jap. J. Phys. 2, 121, 167 (1923) and McLennan, Ainslie and Cale, Proc. Roy. Soc. 102A, 33 (1922). These theories have lost some force since Aston's recent discovery (Ref. 12), of the absence of an isotope of mass 197, and neither is supported by the intensity relations among the satellites. The work of Metcalfe and Venkatesachar (Nature 115, 15 (1925); Proc. Roy. Soc. 105A, 520 (1924)), on the long-column radiation and absorption of the mercury lines seems to favor the isotopic origin of some of the satellites.

¹⁰ Runge, Nature 113, 781 (1924); Joos, Ref. 3.

¹¹ Nagaoka, Nature 114, 245 (1924).

¹² Aston, Nature 116, 208 (1925).

¹³ Mulliken and Harkins, Jour. Am. Chem. Soc. 44, 37 (1922).

used, the comparison of wave-lengths and intensities has been made as accurate and complete as possible for both mercury and chlorine.

COMPARISON OF THE MERCURY LINES

The spectra of two small mercury arcs containing the isotopic mercury were compared using a 30-plate Michelson echelon, and later an 8-inch plane grating in the fifth order. Owing to its greater dispersion, the echelon gave more accurate wave-length comparisons, although its resolving power was slightly less than that of the grating. The optical system for the echelon photographs consisted of a collimator, the echelon, a large glass prism, and a lens of 4 m focal length to form the image. The slit was horizontal, and was fitted with a slide which could expose either of two adjacent portions 1 mm long. The collimator passed a beam of parallel light directly into the echelon, which was placed so that its steps ascended toward the collimating lens. After leaving the echelon, the light passed through the prism, which was in the usual position and hence crossed with the echelon—a very convenient arrangement for isolating the individual lines of a spectrum when they are not too numerous. The lens and plate-holder were mounted at either end of a light-tight metal pipe.

It is well known that the relative intensities of the satellites of the mercury lines vary somewhat with the conditions in the source. In order to minimize this effect, the two mercury arcs were made with identical dimensions, operated with the same current, and connected with the same vacuum line. They were placed close together in a rectangular jar of running water, and one could be lowered slightly so that a comparison photograph could be made without moving the condensing lens. A heavy metal box surrounded the echelon, and the apparatus was mounted on solid piers in a constant-temperature room. These precautions were necessary to avoid false shifts of the adjacent spectra. The time of exposure was short (3 to 5 minutes for the brightest lines), with these mercury arcs. The arc is established between two small pools of mercury and passes through a short horizontal length of tubing 3 mm in diameter. The light from the constriction is very intense, while the definition of the lines is still very good owing to the efficient cooling.

Other mercury sources giving very sharp lines were used later, and are worthy of mention. For the grating photographs, a water-cooled arc lamp constructed from the figure shown by Wood¹⁴ proved very satisfactory, though its lack of intensity necessitated long exposures. In examining the mercury with the largest atomic weight difference, it

¹⁴ Wood, Phil. Mag. 50, Fig. 1, 765 (1925).

was found convenient to excite the spectrum in a Geissler tube discharge through helium at 1 cm pressure, with a droplet of mercury in the tube. The lines from this source, when it was operated with a small current from a transformer, were bright and extremely sharp, and the method had the advantage of requiring only a trace of the valuable mercury. The spectra of Fig. 1 (B) were taken in this way.

Fig. 1 (A) shows one of the comparison plates for the green mercury line. Several plates of this kind were taken for each of the lines $\lambda\lambda 5461$, 4359, 4078 and 4047, all of which involve *S*-terms in the series notations. The most accurate wave-length comparisons were obtained with these plates. Relative measurements were made for all of the satellites, as well as the central components. With a Gaertner comparator graduated

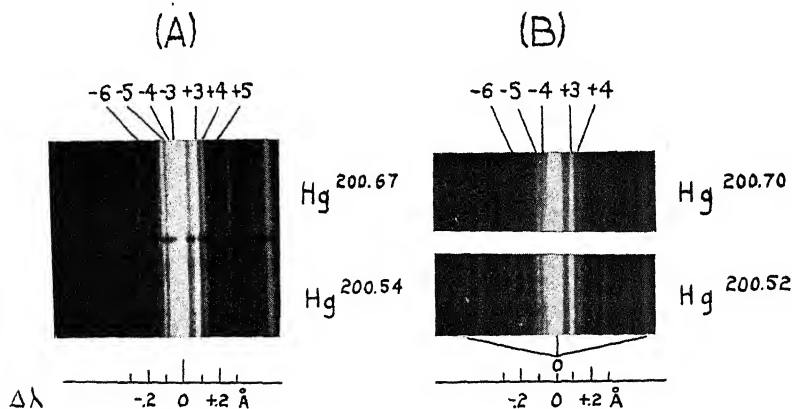


Fig. 1. Comparison of green mercury line from isotopic sources. (A) From vacuum arcs. This illustrates the method of wave-length comparisons. The slight haziness in the upper pattern was due to a droplet of mercury which condensed in the constriction of the arc. (B) From Geissler tubes containing helium and mercury. Note the identical intensity distribution among the satellites.

These photographs were taken with the echelon. The central band may be seen in 2 and 3 orders, respectively, in (A) and (B). The three in (B) are marked below. The atomic weight of the mercury giving the line is indicated at the right in each case. The satellites are numbered outward from the central band, which consists of five unresolved lines. Lines not marked are ghosts, which always appeared on the high-frequency side of the brighter lines. The wave-length separations are indicated by the scales drawn below.

in .001 mm, settings were made alternately on the same line in the two spectra, and the difference in the two readings could be reproduced to within a few ten-thousandths of an angstrom. All the shifts measured were $3 \times 10^{-4}\text{\AA}$ or less, and were about equal to the probable error of measurement in each case. As typical of these results, the values obtained for the brighter components of $\lambda 5461$ may be quoted: -6, 0.0000 \AA

± 0.0001 ; $-5, -0.0003 \pm 0.0002$; $-4, -0.0002 \pm 0.0002$; central component, -0.0001 ± 0.0003 ; $+3, +0.0001 \pm 0.0002$; $+4, 0.0000 \pm 0.0002$. A positive sign indicates that the line from the heavier mercury gave the smaller wave-length. A survey of all the data indicates a random distribution in regard to both sign and magnitude, and it is evident that all the wave-lengths resolved are very exactly equal in these isotopic samples of mercury (atomic weight difference 0.124 units). If the shift for mercury were similar to that for lead, and proportional to the atomic weight difference, we should expect the shifts to be $+0.0007$.

The relative intensities of the satellites were always visually the same in the two patterns. Some preliminary photometric measurements were made, but failed to show any consistent variation. The two spectra were so nearly alike that in some cases, where the patterns were particularly well matched, it was very difficult to distinguish the dividing line. Further confirmation of the identical intensity distribution was obtained from the spectra of the mercury with the larger separation (atomic weight difference 0.180 units), using the helium-mercury sources mentioned above (see Fig. 1 (B)). Plates were taken for the lines $\lambda\lambda 5461$ and 4359. For these, a small comparison prism was employed, so that they were not as suitable for the determination of wave-length differences. The spectra were adjacent, however, and the relative intensities of the satellites could be accurately compared. No difference could be detected for either line; whereas, if the satellites of a line were given out by the isotopes, those corresponding to 198 and 204 should show intensity differences of $1/5$ and $1/4$, as has been explained. It is possible, as McLennan has suggested for $\lambda 5461$, that the real isotopic satellites lie within the central group (-3 to $+3$), which was not resolved with these instruments.¹⁵ The entirely negative results obtained here would be expected if this were the case. They are, however, certainly contrary to any hypothesis attributing the *outer* satellites to the isotopes.

COMPARISON OF THE CHLORINE LINES

For studying the chlorine lines, a special discharge tube was used, provided with a trough-shaped platinum cathode. Silver chloride prepared from the isotopic chlorine was fused on the surface of the cathode. The tube was then highly evacuated and filled with purified hydrogen to a pressure of 1 mm. This was necessary to maintain the constant radiation of the chlorine spectrum required for long exposures. When it was excited by a large induction coil, the chlorine lines appeared in the bright green glow above the cathode, which was viewed end-on.

¹⁵ But see Ref. 9.

The only hydrogen line in the region investigated, H β , was easily distinguished by its diffuseness in the high-dispersion spectra. It is interesting to note that the chlorine lines from this source have an intensity distribution remarkably different from that given by a tube containing chlorine gas.¹⁶

Here again the echelon proved best adapted to an accurate comparison of wave-lengths. The exposures were of from 5 to 7 hours duration, so that the spectra were necessarily photographed simultaneously. This was accomplished with a small total-reflection prism placed as near as possible to the slit. The latter was set vertical, and the echelon placed so that its dispersion was horizontal and in the same direction as that of the prism which followed. The image was formed by a lens of much shorter focus (1 m), which increased the intensity and possessed the added advantage that the whole visible spectrum could be photographed on the same plate. The sources were operated in series from the same induction coil, and plates were taken where they were interchanged, to bring out any artificial shifts.

In the first few trials a difficulty was experienced in accurately comparing the positions of a line in the two spectra, since, with the small image, the lines had a marked curvature. This was met by superimposing a comparison spectrum of mercury, so that measurements could be made from a point in a sharp mercury line to the corresponding point in a chlorine line. The mercury lines were exposed by placing a mercury lamp for a few seconds in the positions which had been occupied by the two chlorine sources, without moving either condensing lens.

Fig. 2 shows one of the plates which were taken in this way. No attempt has been made to ascertain the fine-structure of the chlorine lines from these photographs, but it is evident from the reproduction that most of them are relatively simple. The wave-length designations in the echelon spectra are somewhat arbitrary, but probably most of them are correct. A bright line in the echelon spectrum, appearing in two or more orders, was usually found in the approximate position of a line in the spectrum with the prism alone, and was designated by the wave-length of the latter.

The coincidences of twelve of the brighter lines were measured by the method mentioned above. The sharp satellites in the superimposed mercury patterns were used as reference lines. Four plates served for these comparisons. For two of these, the light from the heavier chlorine had passed into the collimator directly; while that from the lighter

¹⁶ For instance, as shown by Hagenback and Konen, "Atlas of Emission Spectra," (1905) chart 249. The chlorine was used at a fairly high pressure.

chlorine was reflected by the comparison prism. For the other two, the position of the sources was interchanged. If, as before, the shift is given a positive sign when the heavier sample showed the shorter wave-length, the four brightest lines gave the following results: $\lambda 5392$, $+0.0012A \pm 0.0007$; 5218 , $+0.0008 \pm 0.0006$; 4741 , $+0.0011 \pm 0.0003$; 4133 , $+0.0001 \pm 0.0002$. All four plates gave the shift as positive for $\lambda 4741$, the line which gave the most definite indications of a displacement. A further series of measurements was made for these four lines, averaging a large number of settings on each line. The values thus obtained were (in the same order as above), 0.0006 ± 0.0005 ; 0.0008 ± 0.0003 ; 0.0012 ± 0.0002 , and -0.0004 ± 0.0003 . This is typical of the accuracy with which the results could be reproduced. Although it is true that the shifts for the first three lines are not far above the probable error of their determination, the writer considers that they represent a real difference in these spectra. It seems significant that a large majority of the values obtained were positive, the direction of shift required by the Bohr theory. The negative shifts were always small and the lines among the faintest.

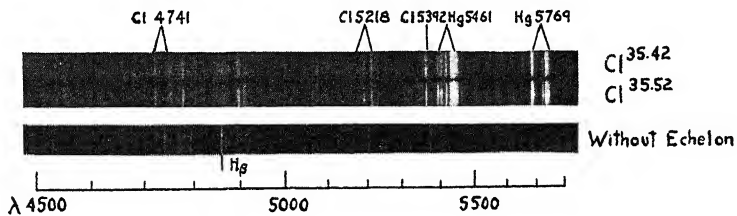


Fig. 2. Comparison of chlorine lines from isotopic sources. The upper strip shows echelon spectra of the chlorine samples, the atomic weight of which is given at the right. Three of the lines which gave the best measurements are marked above; two of them appear in two orders. The green and yellow lines of mercury were here superimposed to furnish reference lines. Most of the measurements in this region were made from the satellite -6 of the green line. A prism spectrum of the chlorine lines in this region is shown in the lower strip, and the wave-lengths are roughly indicated by the scale.

The lines $\lambda\lambda 5078$ and 4133 , however, could be measured accurately and the results for each appeared to be equally distributed about zero. No difference in the character of the lines, or in their relative intensities, could be found on any of the plates.

A further increase in the precision of the measurements would be necessary if conclusions are to be drawn from the numerical values of the shifts. This would require a low-temperature source to decrease the intrinsic width of the lines. The spectra of the mercury isotopes deserve further study: it would be of great value to compare the lines with instruments capable of resolving the closer components, and to carry

out more accurate photometric measurements of the intensities of the satellites in these isotopic samples. The separation for mercury obtained by Harkins and his collaborators is almost twice that hitherto reported, while that achieved for chlorine (one part in 365 of the atomic weight), is by far the largest relative change that has been given for any element. Unless new methods of separation are devised, it seems improbable that material much better than that used for the present investigation will be available for some time.

The writer wishes to express his indebtedness to Professor Harkins, who kindly furnished the isotopic chlorine and mercury for this work, and to Professor H. B. Lemon, who made many valuable suggestions during its progress. The experiments were carried out in the Chemistry and Physics departments of the University of Chicago.

JEFFERSON PHYSICAL LABORATORY,
HARVARD UNIVERSITY.
August 20, 1926.

THE QUANTUM ANALYSIS OF THE BAND SPECTRUM OF
ALUMINUM OXIDE ($\lambda 5200-\lambda 4650$)

BY WILLIAM C. POMEROY

ABSTRACT

Frequencies of lines in band spectrum of AlO.—The spectrograms were taken by R. T. Birge, using a new form of aluminum arc of his design. A table of frequencies of all measured lines is given, extending over ranges of 135, 70 and 65 lines of both branches of the (0,0), (0,1) and (1,0) bands respectively. No perturbations were observed within the range of measurement. Complete numerical formulas expressing the frequencies of all individual band lines within the range of measurement are given. The doublet separations are found to agree in bands of the same final vibration state. Numerical formulas for the doublet separation are given, in which the coefficients are consistent with the theory applied to the mean of doublet components.

Quantum analysis of the band spectrum of AlO.—A new method of locating band origins and verifying the combination principle is given, which applies particularly to bands in which no perturbations are observed. The method is direct and considers every possible choice of origins. The combination principle is verified for these bands over a range of 50 consecutive lines. Expressing the molecular energy terms due to vibration and rotation by $E = E^n + F = E^n + B_n m^4 + D_n m^4 + F_n m^6 + H_n m^8 + \dots$ the coefficients are evaluated for the vibration states $n=0$ and $n=1$, by a method suggested by Kemble. The coefficients are consistent with their theoretical relations, involving the vibration frequency, as deduced by Kratzer, Kemble and Birge. Further, the coefficients are used to evaluate sets of rotational energy terms by means of which the frequencies of all lines within the range of measurement are represented well within the limits of experimental error. The numerical formulas for the frequencies of band lines are therefore of theoretical significance rather than purely empirical.

Molecular constants of the AlO molecule.—The moments of inertia of the AlO molecule for infinitely small vibration are found to be $(46.02 \pm 0.02) \times 10^{-40}$ and $(43.38 \pm 0.02) \times 10^{-40}$ gm cm² for the initial and final states respectively, and the corresponding distances of nuclear separation, 1.665×10^{-8} and 1.617×10^{-8} cm. The constants of an assumed law of force of the form $F = K_1(r - r_0) + K_2(r - r_0)^2 + K_3(r - r_0)^3 + \dots$ are evaluated. Expressions for K_2 and K_3 are new and are due to Birge.

INTRODUCTION

THIS paper¹ is concerned with a detailed analysis of the (0,0)($\lambda 4842$), (0,1)($\lambda 5079$), and (1,0)($\lambda 4648$) bands² of AlO according to the

¹ Preliminary results of this work have been reported to the American Physical Society in the following abstracts: W. C. Pomeroy and R. T. Birge, Phys. Rev. 27, 107 (1926) (Abstract 21). William C. Pomeroy, Phys. Rev. 27, 640 (1926) (Abstract 11).

² Bands are designated (n' , n'') where n' and n'' are the vibration quantum numbers of the initial and final states respectively, in emission.

quantum theory³ and the testing of recently developed theoretical relations by which the elements of the rotational energy terms are connected with vibrational energy constants. These relations permit the representation of long band series by functions which are of theoretical significance rather than purely empirical.⁴

These bands, the so-called aluminum bands of the blue and green, are degraded to the red. As will appear from the detailed discussion to follow, they have no *Q* branch and the *P* and *R* branches consist of doublets of the violet cyanogen type. The variation of doublet separation with the rotation quantum number, *k*, is nearly linear to about *k* = 100.5, actually increasing somewhat more rapidly than *k*. The departure of the frequencies of lines from a second degree law of variation is immediately apparent from the fact that the lines of one branch shift with respect to those of the other branch, overlap, and finally cross over, this occurring twice within the measured range of the (0,0) band. This crossing, which is unique in band spectra, was first recognized by Birge and is illustrated by the numbering of the *P* and *R* lines in the accompanying spectrograms, Fig. 1. The assignment of vibration quantum numbers to these bands was made independently by Birge⁵ and by Mecke.⁶

Beginning with the work of Thalen (1866), Mörikofer⁷ has given a brief but complete review of the studies of the band spectra of aluminum up to the year 1924. For the most part these are concerned either with the representation of band edges only, or with the question as to whether it is the metal or the oxide which is responsible for the band emission. In a recent comparison of emitters of band spectra, Mulliken,⁸ using the results of the present work together with other data, has shown conclusively that these bands are due to the oxide, AlO.

As early as 1891, Hasselberg⁹ had measured the wave-lengths of about 3000 lines in the band spectrum of aluminum, photographed with the aid of a plane grating. These are tabulated by Watts in his "Index of

³ A brief account of the quantum theory of band spectra is contained in Sommerfeld, "Atombau und Spektrallinien," 4th edition, Ch. 9. A detailed account is given in the recent report of the National Research Council on "Molecular Spectra in Gases" (in press). The manuscript of this report was rendered available to the writer through the kindness of R. T. Birge, one of its co-authors. The nomenclature of the report has been adopted throughout this paper.

⁴ With reference to the empirical representation of long band series, see R. T. Birge, *Astrophys. J.* **46**, 85 (1917); *Phys. Rev.* **13**, 360 (1919).

⁵ R. T. Birge, *Phys. Rev.* **25**, 240 (1925) (Abstract 21).

⁶ R. Mecke, *Phys. Zeits.* **26**, 217 (1925).

⁷ W. Mörikofer, Dissertation, Basel (1925).

⁸ R. S. Mulliken, *Phys. Rev.* **26**, 561 (1925).

⁹ B. Hasselberg, *Svensk. Vet. Akad. Handl. N. F.* **24**, Nr. 15 (1891).

Spectra." Later, Lauwartz,¹⁰ using a concave grating, photographed the bands and made an analysis of structure lines with the object of testing Deslandres' law on long band series. He measured the wave-lengths of four bands designated after Hasselberg as $A(\lambda 4471)$, $B(\lambda 4648)$, $C(\lambda 4842)$ and $D(\lambda 5079)$ and represented the frequencies of the lines of each band by four series which we now recognize as the separate components of the doublets of the R and P branches¹¹ respectively. In each series, for three arbitrary lines, he evaluated the constants a and b and the parameter n in the formula

$$1/\lambda = a + bn^2 \quad (1)$$

and calculated the frequencies of all lines in the series. Having compared observed and calculated frequencies, he concluded that Deslandres' law holds within the limits of experimental error only to 50 or 60 lines from the head of the band.¹²

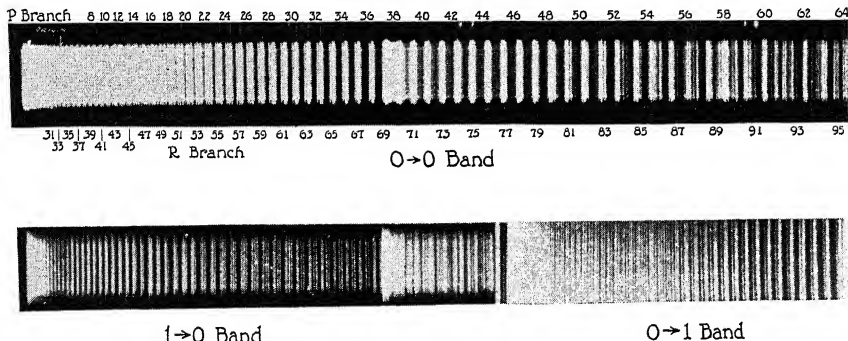


Fig. 1. Spectrograms of a portion of the band spectrum of AlO. The numerals attached to the (0,0) band indicate the quantum number of the final state corresponding to each doublet. The complete overlapping of P_{42} and R_{74} is clearly apparent.

Recently Eriksson and Hulthén¹³ have published some results of their analysis of these bands which are not in agreement with those of the

¹⁰ J. Lauwartz, Zeit. f. wiss. Phot. 1, 160 (1903).

¹¹ According to Deslandres' formulation, there are two series starting at the head of a band. The first of these—Lauwartz' C_3C_4 (in the case of the $\lambda 4842$ band)—includes not only all of the P branch, but also that portion of the R branch between the head and the origin. The other series—Lauwartz' C_1C_2 —includes the remaining portion of the R branch. However, at a point about 50 lines from the head, where the C_1C_2 series actually crosses the C_3C_4 , Lauwartz failed to recognize the crossing, hence from this point to the red, his C_1C_2 , instead of being the R branch, is actually the P branch, with a similar error for the series C_3C_4 .

¹² It is of interest to note here that, according to the results of this paper, the assumption of a second degree law of variation leads to an error of about 24 cm^{-1} in the frequencies of lines which are about 160 lines distant from the head of the (0,0) band.

¹³ Eriksson and Hulthén, Zeits. f. Physik 34, 775 (1925).

writer. Their location of origins is based upon data which allow a verification of the combination principle only for the final states, and leads to an assignment of rotational quantum numbers which causes the doublet separation to exhibit a marked discontinuity at the origin, while the writer finds no evidence of such a discontinuity. The present assignment of rotation quantum numbers is based upon a complete verification of the combination principle and the exclusion of all other possibilities of assignment, which facts should establish its correctness. The satellite system observed on their spectrograms does not appear on those measured by the writer, possibly because of differences in conditions of excitation.

THE SPECTROGRAMS AND THEIR MEASUREMENT

The following analysis is based upon the writer's measurements of spectrograms taken by R. T. Birge in 1915 in the second order of the 21 foot concave grating of the University of Wisconsin with a dispersion of about 1.33\AA per mm. As a source of emission, Birge devised a new form of aluminum arc, the lower electrode (anode) consisting of a 1/2 in. carbon rod into which short lengths of 1/8 in. aluminum rod were inserted so as to project about 1/2 in. above the end of the carbon. A solid 1/2 in. carbon rod served as the cathode. The arc was operated at 160 volts and with as high a value of current as was possible without causing the aluminum to collapse (about 9 amps.). The discharge from the cathode was confined to the aluminum tip of the anode rendering it in the spheroidal state as in the Pfund iron arc. The spectrograms, which contained considerably more data than had previously been obtained, were measured with the 200 mm comparator purchased by Professor Birge through the generosity of the Rumford Fund Committee. The standards of wave-length used were those of Meggers, Kiess and Burns.¹⁴ Both components of each doublet line were measured at least twice, in most cases on different spectrograms. For each doublet, the wave-lengths of the separate components, their difference and mean value were calculated. Each difference and mean was converted to wave numbers (cm^{-1}) and corrected to vacuum. Results for the most part should be accurate within 0.005\AA (0.02 cm^{-1}) or better for distinct lines. All series relations are based upon the mean of frequencies of the doublet components, the values of which are tabulated in Tables I, II and III. While it was expected that small irregularities in successive differences of frequencies would occur, none were observed which could be classed as perturbations, a fact which is quite significant.

¹⁴ Meggers, Kiess and Burns, "Redetermination of Secondary Standards of Wave-Length from the New International Arc," Bull. Bur. Stan. 19, 263 (1924).

VERIFICATION OF THE COMBINATION PRINCIPLE

In addition to the fact that no perturbations were observed within the range of measurement, the band lines faded out toward the origin to such an extent that the establishment of the origins by the usual criterion of missing lines was impossible. Their approximate locations were determined, however, by a visual examination of enlargements of spectrograms, bearing in mind that the intensities of lines of the *R* and *P* branches should be roughly symmetrical with respect to the origin. The method adopted for considering every possible choice of origins may be readily understood with reference to the following representation of the combination principle which is taken from the report of the National Research Council.³

$$R_j = F_{j+1}' - F_j'' \quad (2)$$

$$P_j = F_{j-1}' - F_j'' \quad (3)$$

$$R_j - P_j = F_{j+1}' - F_{j-1}' = 2\Delta F_j' \quad (4)$$

$$R_j - P_{j+2} = F_{j+2}'' - F_j'' = 2\Delta F_{j+1}'' \quad (5)$$

R and *P* represent the frequencies of lines, the subscript referring to the final state in emission. *F'* and *F''* are the initial and final rotational energy "term" values respectively, the functional form of which will be discussed later. *j* is an integer, the meaning of which is explained by the following considerations of nomenclature: according to experimental results which will be discussed later, the nuclear angular momentum, *m*, has been shown to have very nearly half integral values. If the *resultant* angular momentum is parallel with the nuclear, i.e., the electrons have no angular momentum about the figure axis, we write $m=j-\epsilon=k-\alpha$. Now, it is uncertain whether the resultant angular momentum is an integer (*j*) or a half integer (*k*). If the former, the electronic momentum $\epsilon (=j-m)$ is for these bands essentially 0.5, and if the latter, the electronic momentum $\alpha (=k-m)$ is essentially zero. The adoption of the integer $j (=k+\frac{1}{2})$ leads to the condition that missing lines correspond to $j'=0$, or $j''=0$.

Eqs. (2) and (3) may be regarded as defining the lines of the *R* and *P* branches of the band. $2\Delta F'$ and $2\Delta F''$ represent changes in the rotational term values for a change of two units in *j*, and may be termed "combination differences." According to the combination principle, all bands having the same initial vibration state should yield sets of values of $2\Delta F'$ which are numerically identical and similarly, all bands having the same final vibration state should give like sets of values of $2\Delta F''$. The problem then consists in assigning values of *j* to the lines of the three

bands such that the combination differences defined by Eqs. (4) and (5) will give the required agreement.

The following is a direct method by which every possible assignment of origins (or values of j) may be considered. Having arbitrarily designated each line by its numbering from the head, for each band an array of differences was constructed of the following form:

$$\begin{array}{ccccccc} R_s - P_t & R_s - P_{t+1} & R_s - P_{t+2} & \dots \\ R_{s+1} - P_t & R_{s+1} - P_{t+1} & R_{s+1} - P_{t+2} & \dots \\ R_{s+2} - P_t & R_{s+2} - P_{t+1} & R_{s+2} - P_{t+2} & \dots \\ \dots & \dots & \dots & \dots \end{array}$$

and each diagonal of each array was arbitrarily numbered. The form of

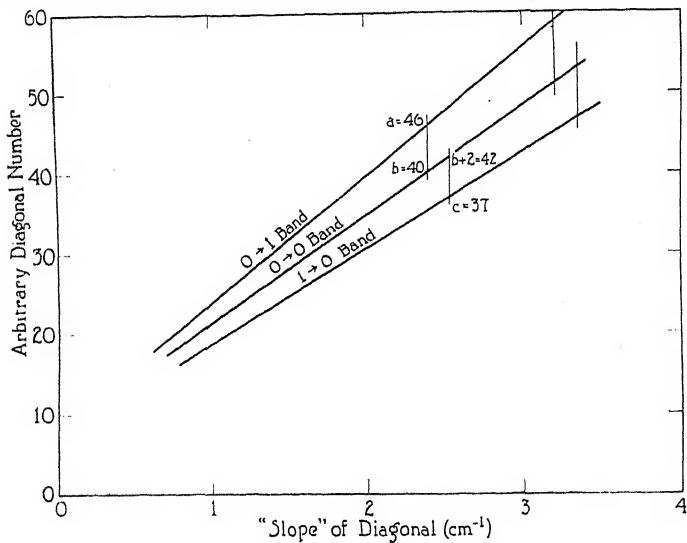


Fig. 2. Graphical construction employed in a direct verification of the combination principle.

each diagonal indicates that it represents a possible set of combination differences. The problem thus reduces to finding four diagonals which agree in pairs, two for the initial state and two for the final state. Now, suppose that a particular diagonal numbered b represents a set of values of $R_i - P_i$. Then a set of values of $R_i - P_{i+2}$ is given by the diagonal $b+2$. Thus, according to Eqs. (4) and (5), we must find a diagonal a of the (0,1) array which agrees with diagonal b of the (0,0) array (same initial vibration state), and a diagonal c of the (1,0) array which agrees with diagonal $b+2$ of the (0,0) array (same final vibration state). The process of finding the particular set of diagonals which gave agreement was greatly facilitated by plotting for each array the "slope" of diagonals (average of

approximately constant first differences) as a function of the arbitrary numbering. These slope curves were practically straight lines as shown in Fig. 2. Now, it is quite obvious that a pair of diagonals whose elements agree throughout must have the same slope, hence we examine the slope curves systematically and note every set of four diagonals for which the slopes agree in pairs, the two diagonals of the (0,0) array differing by two in numbering. Two such sets are indicated in the figure. We now refer back to the diagonals of the arrays by number and find that but one of these sets of four (in this case a , b , and $c = 46, 40$, and 37 respectively) gives agreement of absolute values of the elements of the diagonals. The combination principle is thus verified and the values of j determined to the exclusion of all other possibilities of assignment.

Having verified the combination principle and determined the combination differences, it is required to assign values of j to these differences and to the lines which were combined to give them. The approximate expression for any combination difference is¹⁵

$$2\Delta F = 4Bm \quad (6)$$

and its rate of change with m is $4B$, the diagonal slope mentioned above. The experimentally determined values of $m (= 2\Delta F/4B)$ are found to form a set of approximate half integers and each m is increased by approximately $\frac{1}{2}$ to give the integral j which designates the corresponding $2\Delta F$. Eq. (4) indicates that the value of j which designates each $2\Delta F'$ also applies to the corresponding R and P lines while Eq. (5) indicates that the value of j which designates each $2\Delta F''$ is to be diminished by 1 and increased by 1 to give the values of j which apply to the corresponding R and P lines respectively.

Tables I, II and III, arranged with j as argument, give the values of the frequencies of all measured lines (mean of doublet components corrected to vacuum) and the combination differences. The agreement between the values of $R_j - P_j$ for the (0,0) and the (0,1) bands and between the values of $R_j - P_{j+2}$ for the (0,0) and the (1,0) bands, indicates the accuracy with which the combination principle is verified.

¹⁵ See Eq. (20) below.

TABLE I
Frequencies and combination differences of all measured lines of the (0,0) band

j	R_j	P_j	$R_j - P_j$	$R_j - P_{j+2}$	j	R_j	P_j	$R_j - P_j$	$R_j - P_{j+2}$
6					13				
7		20626.53			14		20615.14		
8		24.82			15		12.98		
9		23.04			16		10.74		
10		21.18			17		08.46		
11		19.24			18		06.11		
12		17.24					03.67		

TABLE I—Continued

Frequencies and combination differences of all measured lines of the (0, 0) band

<i>j</i>	<i>Rj</i>	<i>P_j</i>	<i>R_j - P_j</i>	<i>R_j - P_{j+2}</i>	<i>j</i>	<i>Rj</i>	<i>P_j</i>	<i>R_j - P_j</i>	<i>R_j - P_{j+2}</i>
19		01.14			81	20590.80	20301.86	188.94	203.28
20		598.54			82	85.92	294.74	191.18	205.71
21		95.88			83	80.92	87.52	193.40	208.08
22		93.16			84	75.84	80.21	195.63	210.43
23	20644.46	90.33	54.13	59.96	85	70.68	72.84	197.84	212.80
24	43.94	87.45	56.49	62.48	86	65.44	65.41	200.03	215.16
25	43.37	84.50	58.87	65.02	87	60.12	57.88	202.24	217.50
26	42.73	81.46	61.27	67.56	88	54.71	50.28	204.43	219.81
27	42.00	78.35	63.65	70.08	89	49.25	42.62	206.63	222.18
28	41.20	75.17	66.03	72.60	90	43.68	34.90	208.78	224.51
29	40.33	71.92	68.41	75.11	91	38.09	27.07	211.02	226.89
30	39.40	68.60	70.80	77.65	92	32.36	19.17	213.19	229.19
31	38.38	65.22	73.16	80.16	93	26.58	11.20	215.38	231.50
32	37.30	61.75	75.55	82.68	94	20.71	03.17	217.54	233.83
33	36.13	58.22	77.91	85.22	95	14.74	195.08	219.66	236.12
34	34.88	54.62	80.26	87.75	96	08.73	86.88	221.85	238.45
35	33.56	50.91	82.65	90.26	97	02.59	78.62	223.97	240.72
36	32.18	47.13	85.05	92.78	98	396.42	70.27	226.15	243.04
37	30.71	43.30*	87.41	95.28	99	90.15	61.87	228.28	245.35
38	29.17	39.40	89.77	97.80	100	83.79	53.38	230.41	247.59
39	27.57	35.43	92.14	100.34	101	77.40	44.80	232.60	249.90
40	25.86	31.37	94.49	102.84	102	70.90	36.20	234.70	252.17
41	24.12	27.23	96.89	105.36	103	64.30	27.50	236.80	254.43
42	22.28	23.02	99.26	107.86	104	57.65	18.73	238.92	256.70
43	20.34	18.76	101.58	110.34	105	50.90	09.87	241.03	258.98
44	18.36	14.42	103.94	112.86	106	44.10	00.95	243.15	261.23
45	16.29	10.00	106.29	115.37	107	37.21	091.92	245.29	263.49
46	14.17	05.50	108.67	117.88	108	30.20	82.87	247.33	265.69
47	11.95	00.92	111.03	120.37	109	23.13	73.72	249.41	267.91
48	09.63	496.29	113.34	122.83	110	15.98	64.51	251.47	270.16
49	07.28	91.58	115.70	125.34	111	08.79	55.22	253.57	272.40
50	04.84	86.80	118.04	127.85	112	01.50	45.82	255.68	274.64
51	02.31	81.94	120.37	130.33	113	294.14	36.39	257.75	276.83
52	599.70	76.99	122.71	132.80	114	86.66	26.86	259.80	279.01
53	97.03	71.98	125.05	135.29	115	79.12	17.31	261.81	281.20
54	94.27	66.90	127.37	137.75	116	71.52	07.65	263.87	283.38
55	91.44	61.74	129.70	140.24	117	63.81	19997.92	265.89	285.59
56	88.52	56.52	132.00	142.68	118	56.01	88.13	267.88	287.73
57	85.55	51.20	134.35	145.15	119	48.16	78.22	269.94	289.90
58	82.51	45.84	136.67	147.66	120	40.24	68.28	271.96	292.09
59	79.37	40.40	138.97	150.10	121	32.22	58.26	273.96	294.22
60	76.17	34.85	141.32	152.55	122	24.13	48.15	275.98	296.38
61	72.88	29.27	143.61	155.00	123	15.96	38.00	277.96	298.53
62	69.50	23.62	145.88	157.43	124	07.71	27.75	279.96	300.67
63	66.03	17.88	148.15	159.85	125	199.40	17.43	281.97	302.81
64	62.51	12.07	150.44	162.29	126	91.00	07.04	283.96	304.94
65	58.94	06.18	152.76	164.76	127	82.54	896.59	285.95	307.08
66	55.27	00.22	155.05	167.20	128	73.98	86.06	287.92	309.18
67	51.55	394.18	157.37	169.66	129	65.30	75.46	289.84	311.23
68	47.69	88.07	159.62	172.08	130	56.61	64.80	291.81	313.35
69	43.80	81.89	161.91	174.51	131	47.82	54.07	293.75	315.43
70	39.80	75.61	164.19	176.93	132	38.93	43.26	295.67	317.52
71	35.75	69.29	166.46	179.35	133	29.97	32.39	297.58	319.57
72	31.59	62.87	168.72	181.75	134	20.93	21.41	299.52	321.62
73	27.38	56.40	170.98	184.20	135	11.85	10.40	301.45	323.70
74	23.10	49.84	173.34	186.59	136	02.65	799.31	303.34	325.73
75	18.72	43.18	175.54	188.97	137	093.40	88.15	305.25	327.78
76	14.30	36.51	177.79	191.41	138	84.60	76.92	307.14	329.82
77	09.75	29.75	180.00	193.80	139	74.64	65.62	309.02	331.84
78	05.14	22.89	182.25	196.17	140	65.15	54.24	310.93	333.85
79	00.45	15.95	184.50	198.59	141		42.80		
80	495.65	08.97	186.68	200.91	142		31.30		

*Band lines obscured by heads of other bands. Frequencies obtained by interpolation.

Representation of the structure lines of the bands. Let it now be required to formulate expressions for the frequencies of band lines on a definite theoretical basis. The theory which has been applied in this analysis has been outlined by Birge¹⁶ and further details are contained in the report of the National Research Council.³ The following account is intended as an explanation of the method of analysis used by the writer, rather than as a development of the theory.

TABLE II
Frequencies and combination differences of all measured lines of the (0,1) band

<i>j</i>	<i>R_j</i>	<i>P_i</i>	<i>R_j-P_i</i>	<i>R_j-P_{i+2}</i>	<i>j</i>	<i>R_j</i>	<i>P_i</i>	<i>R_j-P_i</i>	<i>R_j-P_{i+2}</i>
6					41	19668.20	19571.33	96.87	104.37
7					42	66.85	67.60	99.25	106.85
8	19659.68				43	65.43	63.83	101.60	109.33
9	58.00				44	63.94	60.00	103.94	111.83
10	56.21				45	62.36	56.10	106.26	114.30
11	54.40				46	60.76	52.11	108.65	116.80
12	52.52				47	59.08	48.06	111.02	119.27
13	50.60				48	57.33	43.96	113.37	121.74
14	48.60				49	55.51	39.81	115.70	124.21
15	46.54				50	53.64	35.59	118.05	126.65
16	44.40				51	51.70	31.30	120.40	129.11
17	42.21				52	49.69	26.99	122.70	131.58
18	39.96				53	47.63	22.59	125.04	134.03
19	37.66				54	45.50	18.11	127.39	136.46
20	35.29				55	43.29	13.60	129.69	138.90
21	32.86				56	41.04	09.04	132.00	141.37
22	30.38				57	38.73	04.39	134.34	143.83
23	27.84				58	36.32	499.67	136.65	146.20
24	25.22				59	33.87	94.90	138.97	148.76
25	22.53				60	31.37	90.06	141.31	151.15
26	19681.01	19.78	61.23	66.89	61	28.78	85.17	143.61	153.55
27	80.61	16.96	63.65	69.40	62	26.12	80.22	145.90	155.98
28	80.14	14.12	66.02	71.92	63	23.40	75.23	148.17	158.42
29	79.61	11.21	68.40	74.44	64	20.60	70.14	150.46	160.81
30	79.02	08.22	70.80	76.94	65	17.76	64.98	152.78	163.25
31	78.37	05.17	73.20	79.46	66	14.85	59.79	155.06	165.67
32	77.63	02.08	75.55	81.95	67	11.89	54.51	157.38	168.10
33	76.82	598.91	77.91	84.44	68	08.84	49.18	159.66	170.50
34	75.96	95.67	80.29	86.94	69	05.74	43.79	161.95	172.92
35	75.05	92.38	82.67	89.44	70	02.56	38.34	164.22	175.32
36	74.06	89.02	85.04	91.91	71	599.30	32.82	166.48	177.67
37	73.04	85.61	87.43	94.44	72	96.00	27.24	168.76	180.09
38	71.91	82.15	89.76	96.91	73	92.62	21.63	170.99	182.47
39	70.74	78.60	92.14	99.41	74	89.21	15.91	173.30	
40	69.50	75.00	94.50	101.90	75	85.66	10.15	175.51	

We assume the molecular energy "terms" due to vibration and rotation to be given by¹⁷

$$E = E^n + F = E^n + B_n m^2 + D_n m^4 + F_n m^6 + H_n m^8 + \dots \quad (7)$$

where $m = j - \epsilon = k - \alpha$.

¹⁶ R. T. Birge, Nature 116, 783 (1925); Phys. Rev. 27, 245 (1926).

¹⁷ For convenience we use the value of the energy "term" which is defined as energy in ergs divided by ch and is therefore measured in cm^{-1} .

Kemble,¹⁸ using only the first three terms of the right member of Eq. (7) has considered in some detail the dependence of E_n , B_n and D_n upon the value of the vibration quantum number, n , and the resulting relations between rotational and vibrational energy. The relations are much simplified by considering the special case of the non-vibrating molecule, i.e., $n=0$, for which the molecular energy, neglecting electronic, is entirely rotational and is given by

$$F = B_0 m^2 + D_0 m^4 + F_0 m^6 + H_0 m^8 + \dots \quad (8)$$

TABLE III

Frequencies and combination differences of all measured lines of the (1,0) band

j	R_i	P_i	$R_i - P_i$	$R_i - P_{i+2}$	j	R_i	P_i	$R_i - P_i$	$R_i - P_{i+2}$
6					46	21467.56	21359.71	107.85	117.89
7					47	64.93	54.73	110.20	120.38
8					48	62.19	49.67	112.52	122.85
9					49	59.37	44.55	114.82	125.34
10					50	56.49	39.34	117.15	127.84
11					51	53.49	34.03	119.46	130.28
12					52	50.44	28.65	121.79	132.79
13					53	47.30	23.21	124.09	135.29
14					54	44.05	17.65	126.40	137.76
15					55	40.72	12.01	128.71	140.22
16					56	37.32	06.29	131.03	142.72
17					57	33.83	00.50	133.33	145.15
18					58	30.26	294.60*	135.66	147.64
19	21462.88				59	26.58	88.67	137.91	150.08
20	60.13				60	22.85	82.62	140.23	152.54
21	57.29				61	19.00	76.50	142.50	154.98
22	54.36				62	15.08	70.31	144.77	157.42
23	21505.00	51.35	53.65	59.92	63	11.09	64.02	147.07	159.87
24	04.31	48.25	56.06	62.47	64	07.02	57.66	149.36	162.32
25	03.49	45.08	58.41	64.97	65	02.83	51.22	151.61	164.76
26	02.62	41.84	60.78	67.51	66	398.56	44.70	153.86	167.20
27	01.69	38.52	63.17	70.06	67	94.22	38.07	156.15	169.66
28	00.65	35.11	65.54	72.59	68	89.80	31.36	158.44	172.11
29	499.53	31.63	67.90	75.12	69	85.28	24.56	160.72	174.52
30	98.32	28.06	70.26	77.65	70	80.67	17.69	162.98	176.97
31	97.02	24.41	72.61	80.18	71	75.96	10.76	165.20	179.37
32	95.65	20.67	74.98	82.70	72	71.22	03.70	167.52	181.81
33	94.19	16.84	77.35	85.21	73	66.34	196.59	169.75	184.19
34	92.64	12.95	79.69	87.73	74	61.40	89.41	171.99	186.61
35	91.02	08.98	82.04	90.27	75	56.34	82.15	174.19	188.99
36	89.32	04.91	84.41	92.80	76	51.21	74.79	176.42	191.40
37	87.53	00.75	86.78	95.32	77	46.00	67.35	178.65	193.81
38	85.63	396.52*	89.11	97.80	78	40.70	59.81	180.89	196.19
39	83.71	92.21	91.50	100.34	79	35.31	52.19	183.12	198.57
40	81.65	87.83	93.82	102.85	80	29.83	44.51	185.32	200.93
41	79.50	83.37	96.13	105.34	81	24.26	36.74	187.52	203.33
42	77.29	78.80	98.49	107.84	82	18.60	28.90	189.70	205.69
43	74.97	74.16	100.81	110.35	83	12.87	20.93	191.94	208.07
44	72.59	69.45	103.14	112.88	84	07.06	12.91	194.15	
45	70.12	64.62	105.50	115.39	85		04.80		

*Band lines obscured by heads of other bands. Frequencies obtained by interpolation.

¹⁸ E. C. Kemble, J.O.S.A. 12, 1 (1926).

For this condition, D_0 , F_0 and H_0 have been evaluated in terms of other constants as follows:

$$D_0 = -4B_0^3/\omega^0 \quad (9)$$

$$F_0 = (2 - \bar{\alpha}\omega^0/6B_0^2)D_0^2/B_0 \quad (10)$$

$$H_0 = 3F_0D_0/B_0 - 5D_0^3/B_0^2 + F_0^2/D_0 - 8D_0^2x/3\omega^0 \quad (11)$$

Eq. (9) was obtained by Kratzer,¹⁹ Kemble¹⁸ and others while Eqs. (10) and (11) were first obtained by Birge.¹⁶ ω^0 and x have the same meaning as in Kratzer's equations¹⁹

$$\omega^n = \omega^0(1 - 2xn + \dots) \quad (12)$$

$$E^n = n\omega^0(1 - xn + \dots) \quad (13)$$

i.e., ω^0 is the vibration frequency for infinitely small amplitude expressed in cm^{-1} and $2\omega^0x$ is its initial rate of change with the vibration quantum number, n . From Eq. (13) it follows that

$$E^{n+1} - E^n = \omega^0 - (n + \frac{1}{2})2\omega^0x \quad (14)$$

Eq. (14) states that the difference of two adjacent vibration terms yields a frequency equal to the mean of the corresponding vibration frequencies.²⁰ We are thus enabled by extrapolation to determine the vibration frequency for the zero state, i.e., ω^0 . Values of ω^0 and ω^0x for these bands have been calculated by Birge (unpublished), using frequencies of band heads as vibration terms. The final analysis indicates, however, that the separation of band heads is in only approximate agreement with the separation of origins, hence these values are not exact.

As just noted, Eqs. (9), (10) and (11) apply only to the zero vibration state. For higher states, Kemble's formulas may be written

$$B_n = B_0 - \bar{\alpha}n \quad (15)$$

$$D_n = D_0 + \beta''n \quad (16)$$

thus defining

$$\bar{\alpha} = B_0 - B_1 \quad (17)$$

$$\beta'' = D_1 - D_0 \quad (18)$$

$\bar{\alpha}$ is required²¹ for the evaluation of F_0 in Eq. (10). β'' has been evaluated by the writer from Kemble's formulas as

$$\beta'' = (2 - 4H_0B_0^2/D_0^3 + 9B_0^2F_0^2/2D_0^4)12B_0^4/\omega^0 \quad (19)$$

¹⁹ A. Kratzer, Zeit. f. Physik 3, 289 (1920).

²⁰ This is of course only a particular instance of the so-called correspondence theorem.

²¹ Kratzer's α will be designated $\bar{\alpha}$ as defined by Eq. (17) and is not to be confused with the electronic momentum, α , previously defined.

Expressions for F_n and H_n for the higher vibration states have not yet been derived. For the present purpose, however, it is sufficient to assume that $F_1=F_0$ and that $H_1=H_0$.

Now, Eqs. (4) and (5) indicate the well known fact that the experimental data lead to the direct evaluation, not of F , but of $2\Delta F$, i.e., of the variation of F for a variation of two units in j . If ϵ (or α) is a constant, as will be assumed for the present, dF/dm and dF/dj are identical and it may easily be shown²² that the values of $2\Delta F/2$ differ from dF/dm by negligible amounts. Hence we obtain from Eq. (7)

$$2dF/dm = 2\Delta F = 4B_n m + 8D_n m^3 + 12F_n m^5 + 16H_n m^7 + \dots \quad (20)$$

and

$$\Delta F/m = 2B_n + 4D_n m^2 + 6F_n m^4 + 8H_n m^6 + \dots \quad (21)$$

The immediate problem to be solved may now be more definitely stated in terms of the above formulas. In Tables I, II and III are tabulated four sets of values of $2\Delta F$, two for the zero vibration state (initial and final molecular configuration respectively), and two for the vibration state, $n=1$. It is required to determine the four corresponding sets of coefficients in Eq. (7) yielding four sets of rotational energy terms, combinations of which will accurately represent the observed lines of the (0,0), (0,1) and (1,0) bands respectively. Further, it is required to compare the relations among calculated coefficients with the theoretical relations given by Eqs. (9), (10) and (11). The problem is largely a matter of the best method of handling the data, taking into account the amount of labor required and the accuracy of the final results. The method used herein is a combination of the methods of successive approximation and least squares and will be described in some detail.

With reference to Eq. (21) it may be noted that the left member may not be evaluated accurately until ϵ (or α) is known. Preliminary analysis shows, however, that in the case of bands such as the violet cyanogen bands or those discussed in this paper, the value of α is either zero or is very small. Hence, to a close approximation, m may be replaced by k .²³

Using the four sets of values of $2\Delta F$ tabulated in Tables I, II and III, values of $\Delta F/k$ were calculated and each $\Delta F/k$ was plotted as a function of k . Omitting the last two terms of Eq. (21) as a first approximation, values of B and D for each of the four cases were calculated from two suitable points on the $\Delta F/k : k$ curve. For the zero state, values of B_0 and D_0 thus determined and combined with the previously calculated values of ω^0 satisfied Eq. (9) within a fraction of a percent. Having determined

²² Report of National Research Council, Ch. IV, Eq. (78).

²³ More accurately, $\Delta F/k = 2B_n - 2B_n\alpha/k + 4D_n k^2 + 6F_n k^4 + \dots$

fairly accurate values of B_0 and D_0 , we calculate approximate values of F_0 and H_0 from Eqs. (10) and (11). $\bar{\alpha}$ may be taken as the difference between B_0 and B_1 as obtained from the $\Delta F/k : k$ curves, or may be found analytically from the approximate relation deduced from Eq. (21), with m replaced by k :

$$\Delta F_0/k - \Delta F_1/k = 2\bar{\alpha} - 16B_0^3k^2(1/\omega^{02} - 1/\omega^{12}) \quad (22)$$

Following Kemble's suggestion,¹⁸ we now transform Eq. (20) as

$$2\Delta F^* = 2\Delta F - 8D_n m^3 - 12F_n m^5 - 16H_n m^7 - \dots \quad (23)$$

$$= 4B_n m \quad (24)$$

$$= 4B_n(k - \alpha) \quad (25)$$

Now, as just noted, $m = k$ approximately, and D_n , F_n and H_n are small quantities compared to B_n . Therefore it is entirely legitimate to replace the unknown m by the known k in the third and higher degree terms of Eq. (23). By this substitution, a set of numerical values of $2\Delta F^*$ is obtained which should be linear in k provided that D_n , F_n and H_n are known with sufficient accuracy and α is constant. The outstanding feature of this method of solution is the transformation of the higher degree $2\Delta F : k$ curve into the linear $2\Delta F^* : k$ curve. This permits the use of all of the experimental data in the evaluation of $4B$ as the constant slope of the linear $2\Delta F^* : k$ curve as compared with the extrapolation of the lower end of the non-linear $2\Delta F : k$ curve to determine $4B$ as its limiting slope for $k = 0$.

The following procedure is carried out for both the initial and final states respectively. Considering first the zero vibration state, values of $2\Delta F^*$ were calculated by Eq. (23) using the observed values of $2\Delta F$ and the values of D_0 , F_0 and H_0 given by Eqs. (9), (10) and (11). In these equations the value of B_0 determined from the $\Delta F/k : k$ curve was used. The resulting set of Eqs. (25) considered as linear in k was solved by least squares, giving a better value of B_0 and also a value of α . Should the new value of B_0 differ sufficiently from its first approximation to affect D_0 , F_0 , and H_0 materially, a second solution is necessary. It may be mentioned here that the greatest obstacle to accuracy is the lack of trustworthy values of vibration frequency since we must resort to Eq. (9) in order to improve upon the values of D_0 obtained from the $\Delta F/k : k$ curves. Unfortunately an accurate set of vibration frequencies may be obtained only from an extended fine structure analysis which will determine a relatively large number of band origins rather closely. A set of values of $2\Delta F^*$ is now calculated by Eq. (25), using the results of the least squares solution, and the linearity of "observed" values is tested

by plotting differences of observed and calculated values of $2\Delta F^*$. Any appreciable trend in the residuals is to be corrected by an adjustment of coefficients.

Turning now to the vibration state $n=1$, we note that β'' may be calculated from Eq. (19), knowing the values of the coefficients B_0 , D_0 , F_0 and H_0 . The resulting value of D_1 may be compared with that obtained from the $\Delta F/k : k$ curve for the state $n=1$. It was assumed that $F_1=F_0$ and $H_1=H_0$, the error introduced being negligible since the contribution of these terms to the rotational energy is small within the range of measurement of the (1,0) and (0,1) bands. Values of $2\Delta F^*$ for $n=1$ are then calculated and the equations solved as described above.

Having evaluated the four sets of coefficients B , D , F and H , we calculate the four corresponding sets of rotational energy terms and the six sets of differences to be used in the representation of the six sets of lines, i.e., the P and R lines of the three measured bands. For each band, we write

$$R_j = \nu_0 + \frac{F_{j'+1}}{n'} - \frac{F_{j''}}{n''} \quad (26)$$

$$P_j = \nu_0 + \frac{F_{j'-1}}{n'} - \frac{F_{j''}}{n''} \quad (27)$$

where ν_0 is the frequency of the origin of the band. The calculated value of ν_0 for each of the three bands, using in Eqs. (26) and (27) the observed frequencies of lines and the calculated values of the rotational energy terms, should be constant throughout the range of measurement. As a matter of fact, although the variations were not large, they exceeded the limits of experimental error as might be expected from the fact that we are virtually building up a function from the values of successive differences.

This difficulty, however, may be overcome as follows: for each band, the differences between calculated values of ν_0 and an arbitrary constant (conveniently, a round number approximating the average) were plotted as a function of k , giving a curve of residuals with ordinates, $\Delta\nu$, ranging within a few tenths of a cm^{-1} . Each residual curve was expressed analytically by passing a curve through six arbitrary points to satisfy an equation of the form

$$\Delta\nu = A + ak + bk^2 + dk^4 + fk^6 + hk^8 \quad (28)$$

The coefficients in the above equation give the corrections to be applied to the differences of corresponding coefficients of the rotational energy terms which are concerned. For example, b of the (0,0) residual curve is the correction to be applied to the difference $(B_0' - B_0'')$. From the (0,1) and (1,0) curves we obtain the corrections to $(B_0' - B_1'')$ and

$(B_1' - B_0'')$ respectively. Having three correction equations containing the four unknowns, B_0' , B_0'' , B_1' , and B_1'' , there remains an element of arbitrariness in fixing the correction to each value of B . Similarly, for each of the sets of coefficients, D , F and H , we write three correction equations. In every case the corrections were small and were adjusted in such a manner that the final results satisfied Eqs. (9), (10) and (11) as nearly as possible.

It may be emphasized here that since the frequencies of long band series may be satisfactorily represented by a number of arbitrarily chosen forms of polynomial, the problem is not to find the form of function which best represents the band lines but rather to determine whether or not the lines of the bands can be represented accurately by means of rotational energy terms of the form of Eq. (8) in which the coefficients satisfy Eqs. (9), (10) and (11).

The final values of calculated coefficients follow:

$$\begin{aligned}
 B_0' &= 0.60190 \text{ cm}^{-1} & D_0' &= -1.1630 \times 10^{-6} \text{ cm}^{-1} \\
 B_0'' &= 0.63860 & D_0'' &= -1.1094 \times 10^{-6} \\
 B_1' &= 0.59737 & D_1' &= -1.1571 \times 10^{-6} \\
 B_1'' &= 0.63285 & D_1'' &= -1.1181 \times 10^{-6} \\
 \alpha_0' &= +0.0074 & F_0' = F_1' &= +0.440 \times 10^{-12} \text{ cm}^{-1} \\
 \alpha_0'' &= +0.0100 & F_0'' = F_1'' &= -0.530 \times 10^{-12} \\
 \alpha_1' &= +0.0050 & H_0' = H_1' &= 0.0 \\
 \alpha_1'' &= +0.0132 & H_0'' = H_1'' &= -5.2 \times 10^{-18} \\
 \bar{\alpha}' &= B_0' - B_1' = +0.00453 \text{ cm}^{-1} \\
 \bar{\alpha}'' &= B_0'' - B_1'' = +0.00575
 \end{aligned}$$

As a final test of the accuracy with which the frequencies of the lines of each band were represented with the use of the above coefficients, the four sets of rotational energy terms and the six sets of differences to be used in Eqs. (26) and (27) were recalculated. For each band, the appropriate differences were combined with the observational data of Tables I, II and III and in every case yielded a set of values of ν_0 which was constant within the limits of experimental error throughout the range of measurement. This fact was indicated by constructing for each band a table of differences between calculated and most probable values of ν_0 (not reproduced in this paper). These residuals showed no systematic trend and in every case the average of the absolute values was less than 0.02 cm^{-1} (0.005\AA) and very few exceeded 0.04 cm^{-1} (0.01\AA). The most

probable value of ν_0 was arbitrarily taken as its average from $j=30$ to $j=70$ thus avoiding the less reliable observational data for the smaller values of j and the less accurate values of the rotational energy terms for the larger values of j .

It is interesting to note the rather unusual occurrence of the coincidence of a band line with the origin. It was found that for the (1,0) band, the frequency of the line R_{30} is the same as that of the origin. In the case of the (0,1) band, one component of the line R_{40} very nearly coincides in position with the origin.²⁴ In such instances as these, the recognition of missing lines is difficult if not impossible.

Agreement of coefficients with theoretical relations. From Eq. (9), we find

$$\omega^0 = \sqrt{-4B_0^3/D_0} \quad (29)$$

The determination of ω^0 from the final calculated coefficients gives

$$\omega^0 = 866 \text{ cm}^{-1} \quad \omega^{0''} = 969 \text{ cm}^{-1}$$

whereas Birge, using frequencies of band heads as vibration terms has calculated

$$\omega^0 = 866 \text{ cm}^{-1} \quad \omega^{0''} = 970 \text{ cm}^{-1}$$

While this agreement is very close, it appears from the meager data available that these frequencies would be slightly higher if calculated from the frequencies of origins (see Eq. (36) ahead).

Substitution of the final calculated coefficients in Eq. (10) yields for the left members, initial and final states respectively, $+0.440 \times 10^{-12}$, and -0.530×10^{-12} and for corresponding right members $+0.439 \times 10^{-12}$ and -0.534×10^{-12} , a very satisfactory agreement.

The evaluation of the right member of Eq. (11), using Birge's values of $\omega^0/x' = 3.75$ and $\omega^{0''}/x'' = 7.00$ gives $H_0' = +0.9 \times 10^{-18}$ and $H_0'' = -5.2 \times 10^{-18}$ as compared with the finally adopted values of $H_0' = 0.0 \times 10^{-18}$ and $H_0'' = -5.2 \times 10^{-18}$. In view of the fact that the contribution of the term in x is relatively large and that the values of x are rather uncertain, we may assume that Eq. (11) is satisfied within the limits of experimental error.

Substitution of the final calculated coefficients in the right member of Eq. (18) gives for β'' , initial and final states respectively, $+0.0059 \times 10^{-6}$ and -0.0087×10^{-6} , while the right member of Eq. (19) gives for corresponding values, $+0.0055 \times 10^{-6}$ and -0.0085×10^{-6} . Considering the uncertainty of the values of H_0 , this agreement is quite satisfactory.

Lastly, Eq. (17) is satisfied exactly by the final calculated coefficients.

²⁴ This statement anticipates the discussion of doublet separation which is to follow.

The relatively good agreement indicated in the preceding discussion is rather conclusive evidence of the validity of the relations between rotational and vibrational constants given by Eqs. (9), (10) and (11), at least in the case of the bands discussed in this paper.

Accuracy of calculated coefficients. From a physical point of view, the constants in which we are most interested are α and B since these determine the electronic momentum, the moment of inertia and the nuclear separation. In the table of final calculated coefficients, a sufficient number of significant figures has been indicated to give a mathematically consistent evaluation of rotational energy terms to the nearest 0.001 cm^{-1} in order that differences may be given to the nearest 0.01 cm^{-1} . It is not to be inferred, however, that the coefficients have been determined with this degree of accuracy. The probable errors may be estimated on the basis of experience in the progressive steps of the calculation.

The values of B_0 are probably correct within two units in the fourth place, an accuracy of 0.03 percent, permitting the evaluation of the moment of inertia and nuclear separation with an accuracy exceeding that of any previous determination. The accuracy of the former is comparable with that with which Planck's constant is known, while that of the latter is limited primarily by the accuracy with which the relative atomic weights of Al and O are known. With regard to α , it is clear that a small change in the coefficients of the higher degree terms in $2\Delta F^*$ will quite appreciably affect the percent change in the intercept of the $2\Delta F^* : k$ curve, even though the absolute value of the change may be small. Thus, α may be in error by as much as 50 percent. For the remaining coefficients, the writer estimates the following accuracy: B_1 , 0.05 percent; D_0 , 0.25 percent; D_1 , 0.50 percent; F_0 and F_1 , 5 percent; H_0 and H_1 , 20 percent.

Calculation of molecular constants. The moments of inertia of the AlO molecule, for the zero vibration state, calculated from the relation²⁵

$$I_0 = h/8\pi^2 B_0 c = 27.70 \times 10^{-40}/B_0 \quad (30)$$

are, for the initial and final states respectively

$$I_0' = (46.02 \pm .02) \times 10^{-40} \text{ gm cm}^2$$

$$I_0'' = (43.38 \pm .02) \times 10^{-40} \text{ gm cm}^2$$

The corresponding distances of nuclear separation calculated from the relation²⁵

$$r_0^2 = I_0/\mu \quad (31)$$

²⁵ Formulas for moment of inertia and nuclear separation appear in the report of the National Research Council, Ch. IV, as Eqs. (134) and (187) respectively. The "reduced molecular weight" of the AlO molecule is 10.06 giving a "reduced mass."

$$\mu = 10.06 \times 1.650 \times 10^{-24} = 16.6 \times 10^{-24} \text{ gm}$$

where μ is the "reduced mass" of the molecule, are

$$r_0' = 1.665 \times 10^{-8} \text{ cm}$$

$$r_0'' = 1.617 \times 10^{-8} \text{ cm}$$

Calculation of the constants of the law of force. The derivation of Eqs. (9), (10) and (11) is based upon an assumed law of nuclear force of attraction of the form²⁶

$$F = K_1(r - r_0) + K_2(r - r_0)^2 + K_3(r - r_0)^3 + \dots \quad (32)$$

where $(r - r_0)$ represents the increase in the distance of nuclear separation. Eq. (10) and (11) were derived by Birge²⁷ by obtaining new expressions for K_2 and K_3 in terms of rotational energy constants. Together with the previously known expression for K_1 , these are

$$K_1 = -2hcB_0^2/D_0r_0^2 \quad (33)$$

$$K_2 = -(3D_0^2 - B_0F_0)3K_1/2r_0D_0^2 \quad (34)$$

$$K_3 = +(18F_0B_0D_0^2 - 25D_0^4 - 9F_0^2B_0^2 + 4H_0D_0B_0^2)hcB_0^2/r_0^4D_0^5 \quad (35)$$

in which all quantities have been defined previously.

The evaluation of these constants, using the numerical results of this analysis, gives for the initial and final states respectively

$$K_1' = +4.42 \times 10^5 \text{ dyne cm}^{-1} \quad K_1'' = +5.55 \times 10^5 \text{ dyne cm}^{-1}$$

$$K_2' = -1.12 \times 10^{14} \text{ dyne cm}^{-2} \quad K_2'' = -1.69 \times 10^{14} \text{ dyne cm}^{-2}$$

$$K_3' = +1.81 \times 10^{22} \text{ dyne cm}^{-3} \quad K_3'' = +2.60 \times 10^{22} \text{ dyne cm}^{-3}$$

The doublet separation. Contrary to conditions found in other band systems, the doublet separations for the (0,0) and (1,0) bands were found to agree, indicating a possible double rotational energy level in the *final* state. This may indicate a relatively stable initial state and hence explain the absence of perturbations which are usually associated with the initial state. The fact that $\omega'x'$ is small compared to $\omega''x''$ is possible further evidence of this conclusion.

Doublet separations were plotted as a function of k of the final state and the agreement for the (0,0) and (1,0) bands is indicated in Fig. 3. For the comparatively short range of measurement of the (0,1) band, the doublet separation was assumed to be linear, given by the equation

$$\Delta\nu = 0.014k \quad (36)$$

²⁶ The expressions for K_1 , K_2 and K_3 in terms of vibrational energy constants are given in the report of the National Research Council, Ch. IV, as Eqs. (189), (190), and (191) respectively, while the corresponding expressions in terms of rotational energy constants (here quoted) appear as Eqs. (194), (195), and (196) respectively.

²⁷ R. T. Birge, Nature 116, 783 (1925).

For the (0,0) and (1,0) bands, it was found that

$$\Delta\nu = 0.0116k + 12 \times 10^{-6}k^2 - 6.2 \times 10^{-11}k^4 \quad (37)$$

represented the doublet separation for both the *P* and the *R* branches. While $\Delta\nu$ could have been represented equally well by other polynomials, the significance of the above is the fact that the coefficients are com-

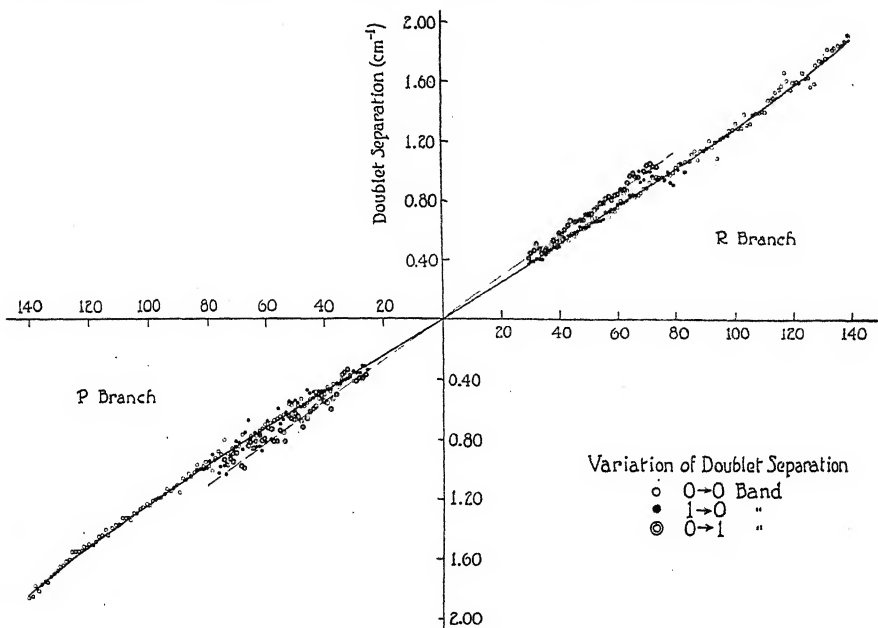


Fig. 3. Variation of doublet separation with rotation quantum number indicating that the doublet separation is a function of the final state.

patible with the theory applied to the mean of the doublet components. That is, we consider the double rotational energy term of the final state given by

$$\begin{aligned} F^{+-} &= F \pm \Delta\nu/2 \\ &= -2B(\alpha \mp \Delta\alpha/2)k + (B \pm \Delta B/2)k^2 + (D \pm \Delta D/2)k^4 \\ &= (B \pm \Delta B/2)m^2 + (D \pm \Delta D/2)m^4 \end{aligned} \quad (38)$$

where $m = k - \alpha \pm \Delta\alpha/2$.

If the theory which has been applied to the mean of the doublet components applies to the separate components as well, the relation between ΔD and ΔB must be, by Eq. (9)

$$\Delta D = -12B^2\Delta B/\omega^2 \quad (39)$$

and this relation is satisfied by the coefficients of k^4 and k^2 respectively in Eq. (37). Obviously, $\Delta\alpha/2$ is found by dividing the coefficient of the linear term by $4B$.

Final representation of individual band lines. The calculated frequencies of the respective origins of the three bands are

$$\begin{aligned} (0,0) \text{ Band}, \nu_0 &= 20635.27 \text{ cm}^{-1} \\ (0,1) \text{ Band}, \nu_0 &= 19669.75 \text{ cm}^{-1} \\ (1,0) \text{ Band}, \nu_0 &= 21498.30 \text{ cm}^{-1} \end{aligned} \quad (40)$$

The frequencies of individual band lines may now be written:

$$\begin{aligned} (0,0) \text{ Band} \quad R_{j^{+-}} &= 20635.27 + F'_{j+1} - F''_{j^{+-}} \\ &\quad n'=0 \quad n''=0 \\ P_{j^{+-}} &= 20635.27 + F'_{j-1} - F''_{j^{+-}} \\ &\quad n'=0 \quad n''=0 \\ (0,1) \text{ Band} \quad R_{j^{+-}} &= 19669.75 + F'_{j+1} - F''_{j^{+-}} \\ &\quad n'=0 \quad n''=1 \\ P_{j^{+-}} &= 19669.75 + F'_{j-1} - F''_{j^{+-}} \\ &\quad n'=0 \quad n''=1 \\ (1,0) \text{ Band} \quad R_{j^{+-}} &= 21498.30 + F'_{j+1} - F''_{j^{+-}} \\ &\quad n'=1 \quad n''=0 \\ P_{j^{+-}} &= 21498.30 + F'_{j-1} - F''_{j^{+-}} \\ &\quad n'=1 \quad n''=0 \end{aligned} \quad (41)$$

The subscripts in Eqs. (41) have been written to conform with Eqs. (2) and (3), although each F has been evaluated in powers of m . No confusion should arise, however, if it is understood that the F_m in the following expansions in powers of m has the same meaning as F_j in Eqs. (41), where j is greater than m by approximately one half.

Using the final calculated coefficients, the rotational energy terms of Eqs. (41) become

$$\begin{aligned} F_{m'} &= 0.60190m^2 - 1.1630 \times 10^{-6}m^4 + 0.440 \times 10^{-12}m^6 \\ &\quad n'=0 \quad \text{where } m=k-0.0074 \\ F_{m''} &= (0.63860 \pm 6.0 \times 10^{-6})m^2 - (1.1094 \times 10^{-6} \pm 3.1 \times 10^{-11})m^4 \quad (42) \\ &\quad n''=0 \quad - 0.530 \times 10^{-12}m^6 - 5.2 \times 10^{-18}m^8 \\ &\quad \text{where } m=k-0.01 \pm 0.00482 \\ F_{m'} &= 0.59737m^2 - 1.1571 \times 10^{-6}m^4 + 0.440 \times 10^{-12}m^6 \\ &\quad n'=1 \quad \text{where } m=k-.005 \\ F_{m''} &= 0.63285m^2 - 1.1181 \times 10^{-6}m^4 - 0.530 \times 10^{-12}m^6 - 5.2 \times 10^{-18}m^8 \\ &\quad n''=1 \quad \text{where } m=k-0.0132 \pm 0.00553 \end{aligned}$$

In conclusion, the writer wishes to express his deep appreciation of the continued interest and helpful advice, throughout the progress of this work, of Professor R. T. Birge, who suggested the problem and generously placed an excellent set of spectrograms at the writer's disposal.

PHYSICAL LABORATORY,
UNIVERSITY OF CALIFORNIA.
August, 1926.

OXYGEN BANDS IN THE ULTRA-VIOLET

BY VIVIAN M. ELLSWORTH AND J. J. HOPFIELD

ABSTRACT

The formula calculated by Birge for the first negative group of oxygen is

$$\nu = \frac{38308}{38108} + (887n' - 13.4n'^2) - (1859.9n'' - 16.53n''^2)$$

This is based upon data published by Johnson. The only transition to zero final state indicated by those data is the 6-0 and consequently there has been some doubt as to whether the first constant of the formula is correct. New photographs of this system show additional pairs of bands degraded to the red. Some of the new bands have been measured and found to represent the 7-0, 8-0, 9-0, 10-0, 9-1, 10-1 transitions as given by the formula above. The existence of the lowest final state represented by this formula is therefore established. The 0-9 band, not previously observed, is also present. Other new bands appear further to the ultra-violet. They have the appearance of belonging to the system, but are too faint to measure. It seems probable that these bands will be found to constitute from one to three progressions to still lower final states.

INTRODUCTION

FOUR systems of electronic bands of oxygen are known, two of which are due to the normal molecule and two to the ionized. A "system" includes all the bands representing a common electronic transition. Occurring simultaneously with this are transitions from a series of initial vibrational states to a series of final vibrational states, producing as a consequence the individual bands of the system.

Of the two systems due to normal oxygen, one is known in the solar spectrum¹ where it is produced by oxygen absorption in the earth's atmosphere. The other is the system which includes the absorption bands first observed by Schumann,² later extended and measured by Hopfield and Leifson³ and interpreted by Birge.⁴ This system lies in the region $\lambda\lambda 1950-1750$. Füchtbauer and Holm,⁵ in high temperature absorption, found other bands which they have interpreted as representing higher final states (initial in absorption) in the same system and Mulliken⁶ has recently shown that the seven Runge⁷ bands which appear in emission

¹ Heurlinger, Diss. Lund, S. 42 (1918); Kratzer, Ann. d. Physik 67, 134 (1922).

² Schumann, Smithsonian Contributions to Knowledge (1903).

³ Hopfield and Leifson, Phys. Rev. 25, 716 (1925); Leifson, Astrophys. J. 63, 73 (1926).

⁴ Birge and Sponer, Phys. Rev. 28, 259 (1926); Birge, Nat. Res. Coun., Report on Molecular Spectra, Ch. 4, Sec. 7.

⁵ Füchtbauer and Holm, Phys. Zeit. 26, 345 (1925).

⁶ Mulliken, private communication.

⁷ Runge, Physica 1, 254 (1921).

in the near ultra-violet ($\lambda\lambda 3850-2980$), are also a part of this system. Since the Schumann bands and the atmospheric bands are both produced by absorption in cold gas, the initial state (final in emission), must be the same for both and must be the normal state of the oxygen molecule.

The two band systems due to the ionized oxygen molecule are the first negative group, in the region $\lambda\lambda 4400-2000$, and the second negative group, or Schuster bands, in the visible. The latter are commonly observed in the greenish-yellow glow about the electrode of an oxygen discharge tube.

The first negative group has the peculiar intensity distribution which is not known in any other band systems except those of the β bands of nitrogen, due to NO, and the iodine bands. In these systems, all the bands having low quantum numbers in both the initial and final states are missing in emission. (See Table II.) The position of the 0-0 band can be located therefore only by extrapolation. It is the position of this band which determines the normal level of the ionized oxygen molecule. Bands of this system were observed and measured by Stark⁸ and later by Johnson.⁹ The latter arranged them in Deslandres progressions. We have photographed the same system and find additional members which are of importance in locating the position of the 0-0 band.

APPARATUS

The discharge tube, constructed of 1 cm Pyrex glass tubing, was of the π -shaped end-on type, the total length being about one meter. The oxygen was generated by electrolysis and passed through a phosphorus pentoxide drying tube. It entered the discharge tube through a valve at one electrode and was exhausted by the necessary pumps at the other. This valve was of the torsion capillary type recently developed by Hopfield¹⁰ for providing a continuous flow of gas. By means of it, unusual control of the gas flow into the discharge tube was possible and the pressure in the tube could be maintained constant at any desired value. Excitation was produced by an alternating current from an 11,500 volt, 10 kw transformer.

Two different spectrographs were used for photographing the spectrum. The first was a one meter concave grating. The slit, grating, and camera box containing the plate-holder were set up on an optical bench and properly adjusted for photographing the first order spectrum. The discharge tube when used with this apparatus, was provided with a quartz

⁸ Stark, Ann. d. Physik 43, 319 (1914).

⁹ Johnson, Proc. Roy. Soc. A105, 683 (1924).

¹⁰ Hopfield, J.O.S.A. 12, 391 (1926).

window. Later the discharge tube, without the quartz window, was connected directly to a vacuum grating spectrograph of 50 cm focal length. The receiver of the spectrograph and the discharge tube were exhausted by separate pumping systems. The advantage of this arrangement of pumps was that the pressure in the spectrograph could be reduced to practically zero, while that in the tube, although low, was high enough for the discharge to pass. In this way oxygen absorption in the receiver was eliminated.

Commercial films were used. They were lightly coated with a transparent mineral oil in order to increase their sensitivity toward the ultra-violet end of the spectrum.

EXPERIMENTAL

Spectrograms were made with currents varying from 0.008 to 0.6 amps. No difference in the number or intensity distribution of the bands was observed as a result of this wide variation in the current. The spectrogram *A* on Plate 1 was made with a current of 115 millamps. and an exposure of 13 hours. The pressure was almost as low as possible for a discharge to pass, about 0.02–0.03 mm of mercury. The spectrograms *B* and *D* were made with approximately the same current and pressure and exposures of 24 and 50 hours respectively.

THE SPECTROGRAMS

Fig. 1, *A*, *B*, and *D* show some of the new photographs. *A* was taken with the meter grating in air. It shows the portion toward the ultra-violet of the first negative group of oxygen and includes practically the same bands as those measured by Johnson⁹ in this region. The system consists of pairs of bands degraded to the red. The pairs, whose members are separated by a constant frequency difference of 200 units, are indicated on the plate. The last band which was measured by Johnson at this end of the spectrum is $\lambda 2318$. On each side of it on our spectrogram, there is a faint band for which Johnson published no measurement. Each of these faint bands have been found to differ from $\lambda 2318$ by 200 frequency units. Photograph *B* is one taken with the vacuum grating spectrograph. This photograph shows definitely eight new pairs of bands further to the ultra-violet. There is probably a ninth pair partially overlapping the last of these and on a similar photograph, *D*, two more pairs show. Accurate measurements of the new bands on these spectrograms could not be obtained because the oiled film warped during the long exposure so that the sharp focus was destroyed. On comparing these plates, however, with earlier ones taken by Hopfield, some of the new bands were found on them also and in good focus. One of these

earlier plates is shown in Fig. 1, C. The presence in the second order of the nitrogen triplets at $\lambda 1134$ and $\lambda 1200$ ¹¹ indicates that there was nitrogen impurity in the discharge tube when this spectrogram was made, whereas the new spectrograms are entirely free from nitrogen lines. The new oxygen bands identified on the earlier spectrogram are indicated by lines connecting B and C on the plate. Accurate wave-lengths of these bands were obtained from C. Both spectrograms show the second order of the strong ultra-violet triplet series of oxygen and the singlets $\lambda 999.4$ and $\lambda 1152.0$ also due to oxygen.¹² These lines were the standards used in measuring the bands. The wave-lengths and frequencies in vacuum,

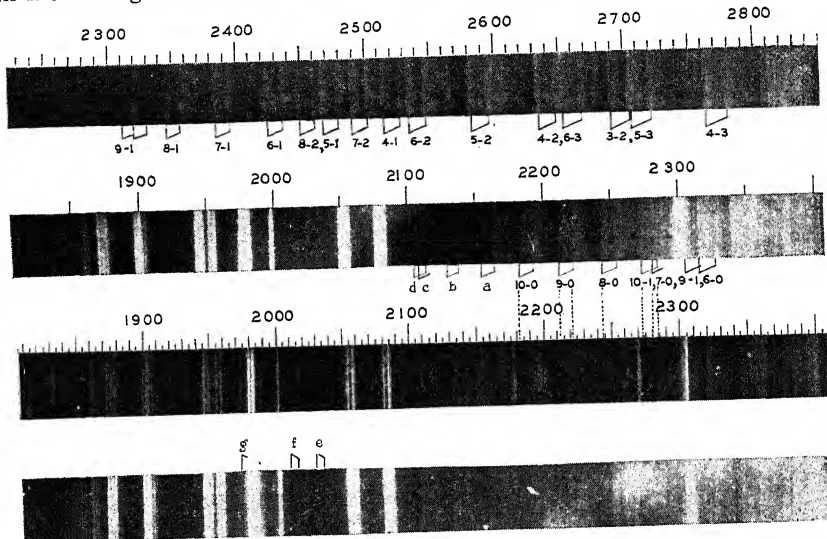


Fig. 1. Photograph of the first negative group of oxygen.

observed and calculated, are given in Table I. The difference between the calculated and observed values is constantly positive for the bands

TABLE I
Oxygen bands. Wave-lengths and frequencies in vacuum, observed and calculated

λ	$\nu(\text{obs.})$	$\nu(\text{calc.})$	$\Delta\nu$	λ	$\nu(\text{obs.})$	$\nu(\text{calc.})$	$\Delta\nu$
4399.4	22723	22708	-15	2285.79	43753	43794	+41
4363.1	22912	22908	-4	2275.34	43950	43994	+44
2328.7	42929	42947	+18	2246.93	44506	44546	+40
2317.9	43129	43147	+18	2224.35	44958	45005	+47
2307.2	43329	43361	+32	2213.78	45174	45205	+31
2291.83	43634	43660	+26			45638	-
2281.26	43837	43860	+23	2185.91	45789	45838	+49

¹¹ Hopfield, Phys. Rev. 27, 801 (1926).

¹² Hopfield, Astrophys. J. 49, 114 (1924).

toward the violet and can be accounted for by the method of using the comparator. The difference corresponds to a shift of the comparator setting toward the red by 0.04–0.06 mm.

THEORETICAL

The bands of this system are arranged diagrammatically in Table II in the usual manner. Only the short wave-length members of the pairs are given. The arrangement is substantially the same as that published by Johnson.⁹ The new bands are included and are indicated by stars. The vibrational quantum number of the initial state is indicated by n' and that of the final state by n'' . The lowest known state in either case is termed zero and other states are numbered in order. Progressions of initial states, or bands representing transitions from a series of initial states to a single final state, appear in columns in the table and pro-

TABLE II
Oxygen.—1st negative group
 $\nu = \frac{38308}{38108} + (887n' - 13.4n'^2) - (1859.9n'' - 16.53n''^2)$

n'	$n''=0$	1	2	3	4	5	6	7	8	9
0					OH	29427	27757	26104	29490	22912*
1					OH	OH	28611	26976		
2				OH	32853	OH	29466	27821		
3		37188		OH	33670	OH	OH			
4	39785	37978	36202		OH					
5	40551	38739	36953							
6	43126	41281	39474	37701						
7	43837*	41991	40181							
8	44506*	42668	40859							
9	45174*	43326*								
10	45789*	43950*								

*New bands.

gressions of final states in lines across the table. The frequency differences in both initial and final states are determined by the spacing of the respective vibrational energy levels. This spacing decreases as the quantum numbers increase, but the relative spacing in one state is different from that in another because of the difference in electronic configuration. For this reason, bands representing the same change in vibrational quantum number, as 0–1, 1–2 and 2–3, etc., are not superposed, but lie in a sequence in the spectrum.

The frequencies of a system of vibrational bands are expressed by the formula

$$\nu = \nu_0 + (\omega'n' - x'\omega'n'^2) - (\omega''n'' - x''\omega''n''^2)$$

Birge¹³ and Mecke¹⁴ each computed the constants of this formula from

¹³ Birge, Phys. Rev. 25, 240 (1925).

¹⁴ Mecke, Phys. Zeits. 26, 217 (1925).

the data published by Johnson.⁹ But Mecke omitted $\lambda 2318$ whose frequency is $\nu 43126$ and for that reason his quantum assignment and formula differ from those of Birge. The new work proves that this band should be included in the system. Its companion, although faint, appears, as well as four more pairs of bands to the same final state. These five pairs constitute a progression to a lower final state than the one designated as zero by Mecke.¹⁴ If there are no more progressions of this system further to the ultra-violet, the formula

$$\nu = \frac{38308}{38108} + (887n' - 13.4n'^2) - (1859.9n'' - 16.53n''^2)$$

calculated by Birge¹³, represents the system.

Bands appear, however, on *B* and *D* taken with the vacuum grating spectrograph, which cannot be identified on *C* because of the presence of impurity on the latter, and therefore cannot be measured accurately. Their positions are indicated by small letters. It seems probable from the appearance of these bands that they belong to the system and represent from one to three final states lower than those whose existence is already established. Further evidence for this conclusion is furnished by the result obtained by Birge and Sponer⁴ for the ionization potential of molecular oxygen from spectroscopic data. This value, based upon data which include the heat of dissociation of ionized oxygen calculated from the first negative group, is 14.1 volts. The experimental value obtained by Hogness and Lunn¹⁵ from positive ray analysis is 13 ± 1 volts. If the normal level of ionized oxygen is lower than that given by the formula above, the value of the heat of dissociation based upon the present data is too low. Each new progression to a lower final state, the presence of which is suggested by the dim bands on the new photographs, increases the value of the heat of dissociation of the ionized molecule by approximately 0.23 volts and consequently decreases the calculated value of the ionization potential of the neutral molecule by the same amount.¹⁶ The presence of two or three more progressions toward the ultra-violet in the spectrum of the first negative group would therefore result in better agreement between the experimental and calculated value for the ionization potential of molecular oxygen. The dim bands on the new photographs indicate that these progressions probably exist.

The authors are grateful to Professor R. T. Birge for suggestions in regard to the interpretation of this work.

DEPARTMENT OF PHYSICS,
UNIVERSITY OF CALIFORNIA,
September 10, 1926.

¹⁵ Hogness and Lunn, Phys. Rev. 27, 642(A), 732 (1926).

¹⁶ See Birge and Sponer (loc. cit.) for details.

THE MANY-LINED SPECTRUM OF SODIUM HYDRIDE

BY E. H. JOHNSON

ABSTRACT

A direct current arc was maintained between a water-cooled iron cathode and a sodium anode in a hydrogen atmosphere up to pressures of 3 or 4 cms. With potential differences from 20 to 30 volts, a many-lined spectrum was obtained in which several bands and branches have been identified in the region between $\lambda 3900$ and $\lambda 5100$. Computations involving the usual quantum assumptions have led to the determination of the following molecular magnitudes:—

$\lambda 4333$ band	
Initial state	Final state
$I' = 3.59 \times 10^{-40}$ gm cm ²	$I'' = 5.10 \times 10^{-40}$ gm cm ²
$r_0' = 1.51 \times 10^{-8}$ cms	$r_0'' = 1.80 \times 10^{-8}$ cms
$\lambda 4655$ band	
Initial state	Final state
$I' = 3.20 \times 10^{-40}$ gm cm ²	$I'' = 4.06 \times 10^{-40}$ gm cm ²
$r_0' = 1.42 \times 10^{-8}$ cms	$r_0'' = 1.60 \times 10^{-8}$ cms

Some deviations from current quantum formulas are pointed out.

THE object of the present work was to obtain an emission spectrum that could be ascribed definitely to a diatomic molecule consisting of one atom of sodium and one of hydrogen. Previous work with such hydrides indicated that the spectra to be expected would be of the complicated, many-lined type.¹

In the course of the present investigation many new points of technique had to be developed. The usual difficulties in handling metallic sodium were far exceeded by those which had to be overcome in securing the critical combination of conditions essential to the production of the desired spectrum. If this precise state were not maintained, quite a different spectrum was produced, either alone or so as to be dominant and altogether troublesome. Extensive work with widely different methods of excitation, showed the necessity of employing a relatively high gas pressure and a low-energy electric discharge so as to encourage molecular combinations and avoid all dissociative effects.

The essential parts of the apparatus that proved most satisfactory are shown in Fig. 1. The arc chamber was made from a heavy three-liter Pyrex flask in which the arc itself was maintained between a water cooled iron cathode 11 mm in diameter, and an anode consisting of several grams of metallic sodium in a porcelain cup 1.5 cms in diameter. The

¹ W. W. Watson has reported a many-lined spectrum due to a lithium hydride combination. See Abstract in Phys. Rev. 25, 887 (1925).

hydrogen with which the arc was surrounded during operation, was the commercial product drawn from steel cylinders. In so far as possible, all water and oxygen were removed by passing the gas through a hot tube containing copper and copper oxide, then over phosphorus pentoxide. It then passed through a charcoal trap which could be cooled in liquid air, although careful tests showed this step to have little if any advantage. A Geissler tube (not shown in the diagram) was permanently attached to the apparatus and always showed a pure hydrogen spectrum when the gas had been prepared as described.

Although the optimum pressure for the production of the desired spectra was found to be between 2 and 4 cms, the system was evacuated before each exposure by means of a Cenco Hyvac pump and a one-stage

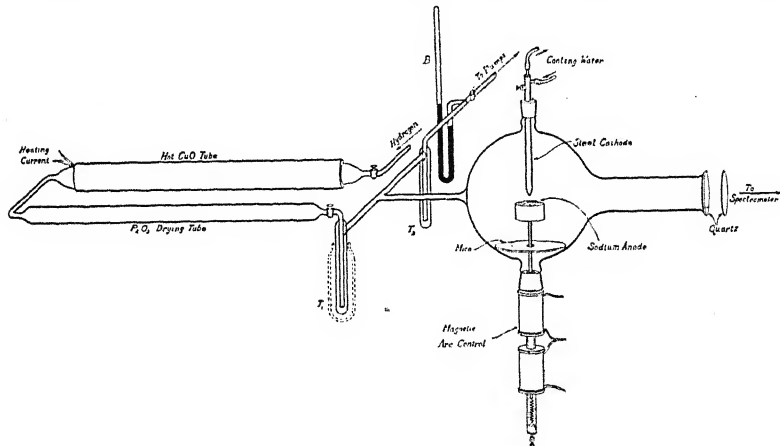


Fig. 1. General arrangement of apparatus.

mercury diffusion pump. Then, with fresh hydrogen, the pressure was raised to the desired value. A second trap in liquid air was introduced before the diffusion pump to prevent the passage of mercury vapor back to the arc chamber, if this became necessary.

The method developed for controlling the arc is shown in some detail in Fig. 2. Bartels² made similar adjustments by means of a hammer-shaped lever which passed out through a flexible joint in the wall of the evacuated chamber. Others have used ground joints or rods or screws passing through stuffed joints to manipulate one of the electrodes. In the present work, where the entire arc chamber was to be at fairly high temperatures during prolonged periods of time, it was found best to use a magnetic control wholly contained within the evacuated system. In-

² Bartels, Zeits. f. Physik 25, 378 (1924).

asmuch as this arrangement is adaptable to many kinds of vacuum arc work, a brief description will be given.

The glass tube *G* (Fig. 2) was sealed to the arc chamber so as to form a part of the same vacuum system. An inclosed brass rod *D* and a flexible wire *W* connected the porcelain anode cup *A* to the external binding post *P*. Two iron collars or lugs, *F₁* and *F₂*, were firmly secured to this rod, and between them was placed a loose hollow iron cylinder *E*, to act as an armature in the fields of the magnet coils, *M₁* and *M₂*. These were arranged in the circuit indicated at the left, so that by means of the

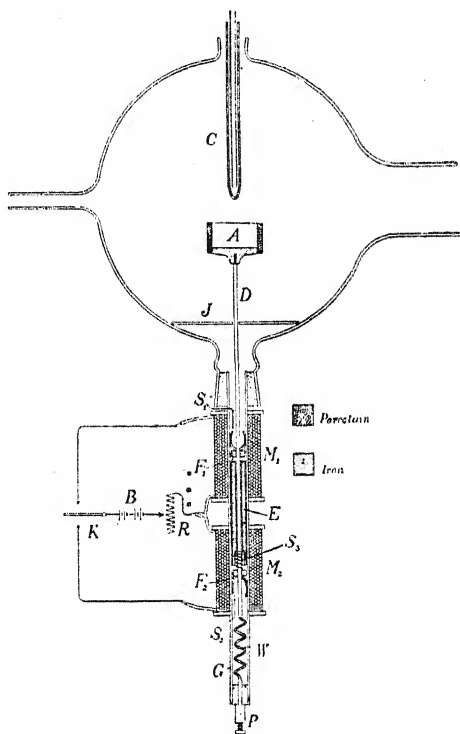


Fig. 2. Details of arc control.

reversing switch *K*, the armature could be jerked either upwards or downwards through a distance of a few millimeters. These two motions were equalized by the spring *S₃*, which was of sufficient strength to just support the armature freely at the mid-point of its range of action. The springs *S₁* and *S₂* were fitted into the glass tube with considerable friction and served to hold the moving system at any desired height. The striking force of the armature could be regulated by means of the rheostat *R*, so that the anode could be moved up or down by steps of several milli-

meters each, or by amounts so small as to be scarcely perceptible. Its operation in this respect left nothing to be desired. The winding of the coils was merely determined by trial so as to give the best operation with the particular system built.

The construction of the iron cathode is clearly shown in Figs. 1 and 2. A central brass tube permitted the continual flow of cold water right at the tip of the electrode. With this construction not the slightest trace of the iron spectrum was ever found on any of the plates. In fact, *in all cases*, a layer of metallic sodium a millimeter or so in thickness formed over the end of this electrode soon after the arc was struck, so that *all of the exposures were made with an arc source between electrodes of metallic sodium only*. Hence, the spectrum was not altered when the arc polarity was reversed.

The alkali metals differ greatly in their behavior under arc conditions, each requiring a somewhat specialized technique. In operating the sodium arc of the type described, considerable care is necessary because of the sudden expansion of the sodium on approaching the boiling point, and the explosive violence of its initial boiling. However, it is possible to maintain a satisfactory performance throughout exposures of eight hours or more.

The operating potential difference was usually from 20 to 30 volts. All photographs were made through a quartz window. Satisfactory spectrum plates were obtained with a Hilger quartz spectrograph and a 5-foot concave grating giving a dispersion of 16.8A per mm in the first order. All computations were based on measurements of first order plates obtained with a 21-foot concave grating, the dispersion being about 2.6A per mm.

EXPERIMENTAL RESULTS

A first examination of the photographic plates shows little more than a multitude of fine lines, with no very apparent order. On the whole they are suggestive of the secondary spectrum of hydrogen. However, direct comparison with hydrogen plates of the same dispersion, shows the spectra to be entirely different.

In attempting to order these lines into series one meets with all of the difficulties usually ascribed to the analysis of many-lined spectra. Diffuseness from various causes renders the precise measurement of many of the lines well-nigh impossible. The large number of lines present on the plates makes it not improbable that some of the anomalous intensities recorded are due to the superposition of lines properly belonging to other systems on weak members of the branches being investigated.

A parallel case is mentioned by Sandeman³ in discussing the difficulties in the analysis of the hydrogen secondary spectrum. Numerous attempts to improve the quality of the lines by altering the source conditions, such as current and pressure, were fruitless. Neither was there any appreciable increase in the sharpness of the lines when the grating slit was set at the smallest width practicable and the time of exposure greatly increased.⁴

In the tables of data and in the computations, vacuum frequencies have been employed, the necessary corrections having been made by means of the tables published by the Bureau of Standards.⁵ The wave-lengths are given in air values.

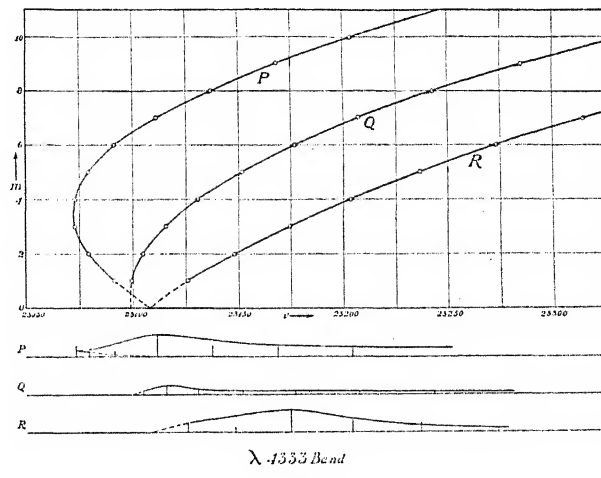


Fig. 3.

In ordering the lines into *P*, *Q* and *R* branches, the combination principle has been employed, as indicated in the following symbolic form:

$$R(m) - Q(m+1) = Q(m) - P(m+1).$$

The intensities of the lines were estimated visually when the plates were being measured. In the accompanying graphs (Figs. 3 and 4) it will be seen that the intensity curves follow the individual line intensities with few exceptions. In general they are of the form obtained by Richardson and Tanaka⁶ for the hydrogen secondary bands. With the exception of one rather doubtful portion of a branch, *all of these bands degrade*

³ Sandeman, Proc. Roy. Soc. Lond. A110, 326 (1926).

⁴ Eriksson and Hulthén mention a similar diffuseness of the lines in the AlO bands. See Zeits. f. Physik 34, 785 (1925).

⁵ Sci. Papers, 327 (1918). Also Bur. of Stan. Bull. 14, p. 731.

⁶ Richardson and Tanaka, Proc. Roy. Soc. Lond. A106, 663 (1924).

towards the violet. This is of special interest since Stücklen⁷ practically implied that the bands of all of the metals and metal hydrides in the first group of the periodic table degrade towards the red.

Frequently it has been stated that in emission bands consisting of *P*, *Q* and *R* branches, the *P* branch is stronger than the *R* branch. Dieke⁸ and others have brought forth a certain amount of theoretical argument for such a rule. However, as Eriksson and Hulthén⁹ have pointed out, experimental evidence does not justify such a generalization. It seems that the *P* branch may be much less intense than the *Q* or *R* branch, or again, all three may be of about the same intensity. This departure from

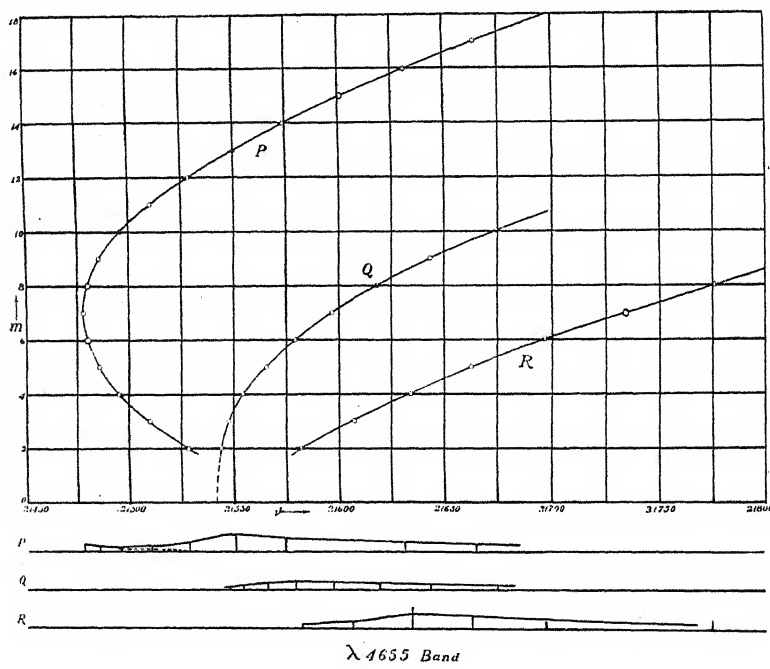


Fig. 4.

the "rule" is quite in keeping with the results obtained in the present investigation. The intensity distribution curves show approximately the same average intensity in the *P* and *R* branches, a fact which increases the difficulties in the analysis. In these bands, degrading as they all do, towards the shorter wave-lengths, the intensity maximum in a *P* branch is nearer the head than is that of the associated *R* branch. In the cases analyzed, the *Q* branches are by far the weakest of the three.

⁷ Stücklen, Zeits. f. Physik 34, 562 (1925).

⁸ Dieke, Zeits. f. Physik 33, 161 (1925).

⁹ Eriksson and Hulthén, Zeits. f. Physik 34, 775 (1925). "Über die Bandenspektra von Aluminium," see footnote, p. 777.

There was no evidence of a continuous spectrum on any of the plates, and no reversed lines.

In Tables IV, V, IX and X, giving the initial and final terms, parentheses have been placed around values in the columns of "means" in all cases where the numbers could be obtained from one quantity only. The gap responsible for this is evident in one of the two preceding columns. In some instances these are due to the absence of a line in the body of the branch, as will be seen by reference to the corresponding tables giving the wave-lengths and frequencies.

TABLE I
 $\lambda 4333$ Band. *P Branch.*

<i>m</i>	Intensity	λ (cms $\times 10^8$)	$\nu = 1/\lambda$	Differences
				1st
2	000	4332.909	23079.18	- 6.26
3	1	4332.870	23072.92	0
4	1	4332.870	23072.92	6.26
5	000	4332.909	23079.18	12.29
6	000	4329.389	23091.47	19.58
7	2	4325.721	23111.05	25.92
8	1	4320.876	23136.97	31.20
9	1	4315.056	23168.17	35.57
10	1	4308.442	23203.74	4.34

TABLE II
 $\lambda 4333$ Band. *Q Branch.*

<i>m</i>	Intensity	λ (cms $\times 10^8$)	$\nu = 1/\lambda$	Differences
				1st
1	000	4329.107	23099.45	5.51
2	000	4328.075	23104.96	10.59
3	00*	4324.880	23115.55	15.37
4	000	4323.217	23130.92	20.70
5	000*	4318.142	23151.62	25.15
6	000	4314.665	23176.77	30.52
7	000	4308.990	23207.29	35.62
8	000	4302.387	23242.91	42.43
9	1	4294.547	23285.34	48.13
10	00	4284.487	23333.47	5.70

*Double

TABLE III
 $\lambda 4333$ Band. *R Branch.*

<i>m</i>	Intensity	λ (cms $\times 10^8$)	$\nu = 1/\lambda$	Differences
				1st
				2nd
1	1	4322.957	23125.83	
2	000	4320.033	23147.97	22.14
3	2*	4313.846	23174.67	26.70
4	1	4308.442	23203.74	29.07
5	1	4302.316	23236.78	33.04
6	000	4296.820	23273.02	36.24
7	1	4287.904	23314.88	41.86

*Double

TABLE IV
 $\lambda 4333$ Band. *Initial terms.*
 $\Delta F' = R(m) - Q(m) = Q(m+1) - P(m+1)$

<i>m</i>	$R(m)$ - $Q(m)$	$Q(m+1)$ - $P(m+1)$	$\Delta F'(m)$ (mean)
1	26.38	25.78	26.08
2	43.01	42.63	42.82
3	59.12	58.00	58.56
4	72.82	72.44	72.63
5	85.16	85.30	85.23
6	96.25	96.24	96.24
7	107.59	105.94	106.76
8	—	117.17	(117.17)
9	—	129.73	(129.73)

TABLE V
 $\lambda 4333$ Band. *Final terms.*
 $\Delta F''(m) = R(m) - Q(m+1) = Q(m)$
- $P(m+1)$

<i>m</i>	$R(m)$ - $Q(m+1)$	$Q(m)$ - $P(m+1)$	$\Delta F''(m)$ (mean)
1	20.87	20.27	20.57
2	32.42	32.04	32.23
3	43.75	42.63	43.19
4	52.12	51.74	51.93
5	60.01	60.15	60.08
6	65.73	65.72	65.73
7	71.97	70.32	71.14
8	—	74.74	(74.74)
9	—	81.60	(81.60)

TABLE VI
 $\lambda 4655$ Band. *P Branch.*

<i>m</i>	Intensity	λ (cms $\times 10^8$)	$\nu = 1/\lambda$	Differences
				1st
				2nd
2	1	4643.804	21528.06	18.28
3	00	4647.750	21509.78	14.83
4	000	4652.255	21494.95	9.51
5	000	4653.016	21485.44	—
6	—	—	—	—
7	1	4656.031	21477.52	—
8	—	—	—	—

TABLE VI—Continued
 $\lambda 4655$ Band. P Branch.

<i>m</i>	Intensity	λ (cms $\times 10^8$)	$\nu = 1/\lambda$	Differences	
				1st	2nd
9	000	4654.399	21485.05	10.91	—
10	00	4652.036	21495.96	13.82	2.91
11	00	4647.750	21509.78	18.28	4.46
12	1	4643.804	21528.06	21.78	3.50
13	3	4639.110	21549.84	23.81	2.03
14	2	4633.989	21573.65	(26.86)	(3.05)
15	—	—	(21600.51)‡	(29.91)	(3.05)
16	2	4621.692	21631.05	32.96	(3.05)
17	1	4614.661	21664.01		

‡Interpolated values.

TABLE VII
 $\lambda 4655$ Band. Q Branch.

<i>m</i>	Intensity	λ (cms $\times 10^8$)	$\nu = 1/\lambda$	Differences	
				1st	2nd
2	000	4641.702	21543.82	3.53	—
3	000	4639.646	21547.35	6.65	3.12
4	00	4638.214	21554.00	11.24	4.59
5	000	4637.091	21565.24	13.82	2.58
6	0	4632.828	21579.06	17.60	3.78
7	00	4629.052	21596.66	21.26	3.66
8	00	4624.500	21617.92	25.20	3.94
9	00	4619.115	21643.12	30.97	5.77
10	00	4612.514	21674.09		

TABLE VIII
 $\lambda 4655$ Band. R Branch.

<i>m</i>	Intensity	λ (cms $\times 10^8$)	$\nu = 1/\lambda$	Differences	
				1st	2nd
2	000	4632.251	21581.75	25.72	—
3	000	4626.737	21607.47	26.41	0.69
4	2	4621.088	21633.88	28.65	2.24
5	1	4614.977	21662.53	34.44	5.79
6	000	4607.551	21696.97		
7	—	—	—		
8	0	4590.921	21776.04		

TABLE IX
 $\lambda 4655$ Band. Initial terms.
 $\Delta F' = R(m) - Q(m) = Q(m+1) - P(m+1)$

<i>m</i>	$R(m)$ - $Q(m)$	$Q(m+1)$ - $P(m+1)$	$\Delta F'(m)$ (mean)	<i>m</i>	$R(m)$ - $Q(m+1)$	$Q(m)$ - $P(m+1)$	$\Delta F''(m)$ (mean)
1	—	15.76	(15.76)	2	34.40	34.04	34.22
2	37.93	37.57	37.75	3	53.47	52.40	52.94
3	60.12	59.05	59.59	4	68.64	68.56	68.60
4	77.00	79.80	78.40	5	83.47	—	(83.47)
5	97.29	—	(97.29)	6	100.31	101.54	100.93
6	117.91	119.14	118.53	7	—	—	—
7	—	—	—	8	—	132.87	(132.87)
8	158.12	158.07	158.10	9	—	147.16	(147.16)
9	—	178.13	(178.13)	10	—	164.31	(164.31)
10	—	194.67	(194.67)	11	—	177.36	(177.36)

The work of Kratzer,¹⁰ and Kramers and Pauli¹¹ has resulted in the following general expression:

$$\Delta_1 F(j) = 2B(j + \frac{1}{2} \mp \epsilon) \mp \frac{B\epsilon\sigma^2}{j(j+1)} + \dots,$$

where j is the total angular momentum; σ is the component of the angular momentum of the electron normal to the vector angular momentum of the nuclei; ϵ is the component of the same vector parallel to the vector angular momentum of the nuclei.

The marked weakness of the Q branches in the bands analyzed in the present work suggests the application of this equation, using the lower (+) signs. By the assignment of probable j values (putting $j = m + s(\frac{1}{2})$, where s may have the values 0, ± 1 , ± 2 , etc.) and solving simultaneously the several similar expressions thus obtained so as to get the values of ϵ and σ , it is possible to draw some conclusion as to the general validity of the equation.

The restrictions prescribed by the theory in its present state are that while ϵ and σ may both have irrational values, ϵ should be of the order of $k/2$ (where k has the values 0, 1, 2, 3, etc.), and that σ should be unity or very small. Having made the substitutions thus required, we obtain initial and final values for $2B$.

Now,

$$2B = h/4\pi^2 I c,$$

whence the moment of inertia is given by

$$I = h/8\pi^2 c B$$

¹⁰ Kratzer, Naturwiss. 27, 577 (1923).

¹¹ Kramers and Pauli, Zeits. f. Physik 13, 351 (1923).

If we now assume that the body having this moment of inertia is a simple dipolar molecule, consisting of one atom of hydrogen and one atom of sodium, rotating about their common center of gravity, we can obtain the nuclear separation r_0 in the existing state. The values found in the above manner for the bands $\lambda 4333$ and $\lambda 4655$ are presented in Table XI.

TABLE XI
Molecular constants of sodium hydride

Initial state	Final state
$\lambda 4333$ Band	
$j = m$	$j = m$
$B' = 7.70$	$B'' = 5.42$
$\epsilon' = 0.325$	$\epsilon'' = 0.496$
$\sigma'^{1/2} = (-)0.156$	$\sigma''^{1/2} = (-)0.82$
$I' = 3.59 \times 10^{-40}$ gm cm ²	$I'' = 5.10 \times 10^{-40}$ gm cm ²
$r_0' = 1.51 \times 10^{-8}$ cms	$r_0'' = 1.80 \times 10^{-8}$ cms
$\lambda 4655$ Band	
$j = m - \frac{1}{2}$	$j = m$
$B' = 8.64$	$B'' = 6.81$
$\epsilon' = 0.645$	$\epsilon'' = 0.76$
$\sigma'^{1/2} = (-)5.37$	$\sigma''^{1/2} = (-)11.8$
$I' = 3.20 \times 10^{-40}$ gm cm ²	$I'' = 4.06 \times 10^{-40}$ gm cm ²
$r_0' = 1.42 \times 10^{-8}$ cms	$r_0'' = 1.60 \times 10^{-8}$ cms

CONCLUSION

From these values of I and r_0 we are justified in concluding that the carrier of these bands is actually the NaH dipole. They are entirely in accord with the trend of values found for other metal hydride molecules in the first part of the periodic table, which has been pointed out by Watson.¹²

These results have several other significant features. The j -values employed were retained as the most suitable ones after numerous computations with other values differing by half-integral steps. The values of ϵ are of the required order of $k/2$, where $k=1$, in the present cases. However, the values obtained for σ , which is the component of the angular momentum of the electron normal to the vector angular momentum of the nuclei, raise new questions. The general equation was developed with the signs \mp before the σ term, but the nature of this quantity (σ) requires the use of the positive sign if ϵ is to be positive, and this procedure, in the present work, leads to imaginary values of σ . It would seem that some modification of the general theory is necessary if it is to lead to an expression that can be applied closely to bands of the type investigated here. The same difficulty has been pointed out by Mecke.¹³

¹² Washington Meeting, Amer. Phys. Soc., Apr. 24, 1925. See Abstract No. 24, Phys. Rev. 25, 887 (1925).

¹³ Mecke, Zeits. f. Physik 36, 795 (1926).

In addition to the bands here described, a number of other branches have been traced out for appreciable distances. All agree in general character. There is considerable evidence that several of these bands are members of the same system. A further paper will deal with these extended series relations.

The writer wishes to express his appreciation to Dr. W. W. Watson at whose suggestion and under whose guidance the investigation covered in part in the present paper was carried out. Very excellent plates of the secondary spectrum of hydrogen for comparisons were continually available through the kindness of Dr. K. O. Lee. The author also wants to record his thanks to Professors Gale and Lemon for various suggestions.

RYERSON PHYSICAL LABORATORY,
UNIVERSITY OF CHICAGO.

June 2, 1926.

ON THE BAND SPECTRUM OF CALCIUM HYDRIDE

By E. HULTHÈN*

ABSTRACT

An arc of calcium burning in hydrogen at low pressure emits numerous bands in the region 6000–7000A. This spectrum was photographed at high dispersion and two groups of bands, shading toward the violet may be distinguished: the A groups with heads at $\lambda\lambda 7035, 7028, 6921, 6903$ and the B groups with heads at $\lambda\lambda 6389, 6382$. In addition to these, the arc emits an isolated C group—a single band in the ultra-violet at $\lambda 3533.6$. This group is identical with a band of calcium hydride recently studied by R. S. Mulliken. The structures of A, B and C are very different. The A group forms a doublet system (A_1, A_2) of *P-Q-R* branches. The bands of the B group have a similar structure to that of the violet cyanogen bands, signified by doublet P_1, P_2 and R_1, R_2 branches. The C group consists of a single band having *P-R* branches. In all bands the series deviate largely from polynomials of second degree. Thus, in B and C there is a remarkable "red-shift" of high numbered lines, accompanied by a sharp cut-off in their intensity. From combinations found between the *P-R* branches, conclusions are reached regarding the spectral terms in CaH. The A, B and C groups have a common final (*N*) electronic term with a rotational doubling ($\epsilon_2 = \pm \frac{1}{2}, \sigma_2 = 0$). The initial state of A forms an electronic doublet (A_1, A_2) with the emission electron in a σ -orbit ($\epsilon_1 = 0, \sigma_1 > 0$), thus explaining the appearance of *Q* branches in A. In B (initial) there is again a rotational doubling ($\epsilon_1 = \pm \frac{1}{2}, \sigma = 0$). In C (initial) only one ϵ component is present ($\epsilon_1 = -\frac{1}{2}, \sigma_1 = 0$). The departure from half-integral quantum numbers in C is avoided by accepting a large Kratzer's linear term $2\delta j$. The nuclear spacings in the CaH molecule are not in correlation with their vibration frequencies, violating a rule by Birge and Mecke. A comparison of the A group with the spectra of ZnH, CdH and HgH shows several interesting parallels, confirming the theory of Mulliken regarding these spectra.

ALTHOUGH the band spectrum of calcium hydride, discussed in this paper, has previously been noted by several investigators, no serious effort has been made to resolve and to measure accurately the great number of lines in the region 6000 to 7000A. The main interest seems to have been centered in identifying these bands in the sun-spot spectrum and from this point of view we may mention the works of C. M. Olmsted¹ and A. Eagle.² Olmsted presented evidence that the calcium hydride bands at $\lambda\lambda 6389, 6382$ appear in the sun spectrum. Eagle photographed the spectra of calcium, strontium and barium hydride in the region 6000–7000A. From his photographs the homologous structure of all three spectra appears clearly.

* International Education Board.

¹ C. M. Olmsted, *Astrophys. J.* 29, 66 (1908).

² A. Eagle, *Astrophys. J.* 30, 231 (1909).

In addition there is a single band of calcium hydride in ultra-violet at $\lambda\lambda 3533.6$, consisting of a small number of lines but having a very unusual structure. This band has recently been investigated by R. S. Mulliken.³

SOME GENERAL REMARKS REGARDING THE HYDRIDE BAND SPECTRA

Before entering into a detailed discussion of the band-spectrum of calcium hydride some general properties in the spectra of hydrides and their relations to the periodic table of elements may here be discussed. At present we know something about the hydride spectra of Cu, Ag, Au, —Mg, Ca, Sr, Ba,—Zn, Cd, Hg,—B, Al,—C,—N, P,—O. From theoretical interpretations of several of these spectra (moments of inertia, isotope effects, etc.), it is most probable that they are all emitted by a dipole of the element and a hydrogen atom. Besides the wide spacing of lines, which is an essential property of all hydrides, there is a clear conformity in the structure of bands belonging to elements of the same column in the periodic table. This is best illustrated by the table below.

TABLE I
Correlations in hydride band spectra

Hydrides	Shading direction	Band structure	Electronic frequencies
Cu, Ag, Au	Red	P, R	24910, 29900, 27342 38230
Mg, Ca, Sr, Ba	Violet	P_1P_2, Q_1Q_2, R_1R_2 .	19333.9 (Mg) ...
Zn, Cd, Hg	"	$P^{(1)}P^{(2)}, Q^{(1)}Q^{(2)}, R^{(1)}R^{(2)}$.	23263.6 22278.0 24933.9 23594.0 23279.0 28617.1
B, Al	Red	P, Q, R	23477 (Al)
C	Violet	$P_1^{(1)}P_2^{(1)}, P_1^{(2)}P_2^{(2)}, Q_1^{(1)}, \dots, R_1^{(1)}$	23161
	Red	P_1P_2, Q_1Q_2, R_1R_2 .	25715
N, P	Red	$P_1P_2P_3, Q_1Q_2Q_3, R_1R_2R_3$.	29750 (N)
O	Red	P_1P_2, Q_1Q_2, R_1R_2 .	32423

There is a remarkable alternation in the shading directions of bands belonging to the elements of the first columns. No pretensions are made, however, that this is a rule or that the notations regarding the band structures given in the table are complete. The spectrum of calcium hydride will illustrate these points.

SPECTRUM OF CALCIUM HYDRIDE

The calcium hydride bands in the region 6000–7000 Å form two groups of bands with more or less distinct heads at $\lambda\lambda 7035, 7028, 6921, 6903$ and $\lambda\lambda 6389, 6382$. The bands are all degraded toward the violet and though crowded with lines, are easily resolved under high dispersion.

³ R. S. Mulliken, Phys. Rev. 25, 509 (1925).

As source a calcium arc burning in hydrogen at low pressure was used. The arc ran steadily at 6 amp., 220 v., d.c., with a hydrogen pressure of about 20 mm. Under these conditions, with an exposure of from two to six hours, the spectrum was well developed in the first and second

TABLE II
The lines of the A band of calcium hydride

<i>j</i>	<i>P</i> ₁	<i>P</i> ₂	<i>Q</i> ₁	<i>Q</i> ₂	<i>R</i> ₁	<i>R</i> ₂
0			14399.92		14406.90	14470.58
1	14385.88		402.85		19.17	76.24
2	81.53	14428.52	05.77		31.15	82.45
3	76.94	17.51	08.62		42.79	89.14
4	71.95	06.71	11.45		54.10	96.10
6	66.80	396.46	14.30	14448.14	65.23	503.40
7	61.38	86.63	17.21	47.39	76.24	10.97
8	55.63	77.21	20.19	47.28	87.02	18.68
9	49.91	68.23	23.48	47.53	97.74	26.73
10	44.12	59.32	26.76	48.14	508.35	34.80
11	38.21	50.78	30.20	49.59	18.89	43.15
12	32.40	42.55	33.82	51.26	29.33	51.57
13	26.55	34.55	37.57	53.22	39.77	60.17
14	20.74	27.00	41.53	55.50	50.11	68.92
15	15.02	19.53	45.69	58.14	60.53	77.77
16	09.35	12.27	49.99	61.09	70.89	86.66
17	03.78	05.25	54.46	64.32	81.24	95.64
18	298.34	298.48	59.16	67.82	91.61	604.75
19	93.05	92.00	64.04	71.55	601.95	13.86
20	87.86	85.69	69.12	75.57	12.33	23.09
21	82.86	79.70	74.37	79.87	22.62	32.42
22	78.05	73.93	79.87	84.40	33.09	41.89
23	73.36	68.37	85.45	89.14	43.54	51.31
24	68.92	63.06	91.24	94.20	53.91	60.82
25	64.62	58.04	96.92	99.48	64.37	70.37
26	60.54	53.26	503.41	504.87	74.79	79.96
27	56.69	48.73	09.73	10.50	85.22	89.68
28	53.07	44.43	16.25	16.38	95.73	99.33
29	49.66	40.45	23.08	22.56	706.16	709.04
30	46.43	36.72	29.90	28.70	16.63	18.87
31	43.51	33.28	37.00	35.29	27.19	28.71
32	40.78	30.08	44.19	41.92	37.72	38.57
33	38.30	27.18	51.57	48.78	48.28	•48.28
34	36.05	24.47	59.14	55.81	58.70	
35	34.09	22.06	66.55	62.93	69.25	
36	32.34	19.96	74.46	70.38	79.89	
37	30.93	18.12	82.43	77.77		
38	29.68	16.54	90.62	85.51		
39	28.70	15.29	98.69	93.26		
40	27.97	14.20	607.09	601.25		
41	27.44	13.55	15.46	09.34		
42	27.18	12.94	24.03	17.58		
43		12.78		25.86		

order of a large concave grating (dispersion, 2.6 and 1.3A/mm respectively). The spectrum extends on both sides of the 6000–7000A region. However, these faint bands showed such a complicated array of numerous lines that no attempt was made to analyze them. Apparently they correspond to excited vibration levels of the two main groups at 6000–

TABLE III
The lines of the A' band of calcium hydride

<i>j</i>	<i>P</i> ₁	<i>P</i> ₂	<i>Q</i> ₁	<i>Q</i> ₂	<i>R</i> ₁	<i>R</i> ₂
0			14429.00			
1			32.04		14442.18	
2	14421.44		35.09		54.10	
3	17.21		38.00		65.94	
4	12.69		40.82		76.89	
5	07.94		43.54		88.28	
6	02.85	14432.66	46.31		98.64	14536.62
7	397.38	22.84	49.07		509.25	43.76
8	91.69	13.39	51.95	14483.25	19.56	51.09
9	85.88	04.37	54.87	83.02	29.90	58.69
10	80.01	395.49	57.93	83.02	39.94	66.74
11	74.07	86.89	61.09	83.25	50.11	74.46
12	68.06	78.75	64.32	83.98	60.17	82.49
13	62.13	70.72	67.82	85.03	70.02	90.62
14	56.25	62.94	71.55	86.46	80.02	98.97
15	50.42	55.63	75.34	88.28	89.96	607.35
16	44.71	48.25	79.24	90.42	99.88	15.85
17	39.14	41.24	83.50	93.00	609.84	24.44
18	33.70	34.55	87.81	95.58	19.73	33.09
19	28.40	27.98	92.25	98.64	29.68	41.89
20	23.28	21.75	96.92	501.83	39.73	50.79
21	18.24	15.70	501.83	05.47	49.74	59.73
22	13.38	09.94	06.73	09.24	59.73	68.63
23	08.67	04.31	11.95	13.31	69.70	77.64
24	04.31	299.08	17.45	17.60	79.74	86.68
25	299.99	93.86	23.08	22.16	89.68	95.73
26	95.87	89.06	28.70	26.73	99.70	704.95
27	92.00	84.33	34.44	31.82	709.74	14.12
28	88.39	80.11	40.57	37.00	19.83	23.38
29	84.85	76.07	46.81	42.30	29.86	32.64
30	81.68	72.18	53.12	48.06	39.91	41.89
31	78.57		59.60	53.63	49.93	51.15
32	75.87		66.35	59.60	59.89	
33	73.36		73.05	65.64		
34	70.88		80.02	71.95		

7000A. When a small amount of air or moisture was present in the arc-bulb, a continuous background appeared in the region 6300–6100A, sometimes rising to a bright intensity, covering the sharp lines of the hydride bands. This background belongs probably to the CaO spectrum and was easily suppressed by a permanent flow of hydrogen through the bulb.

In order to simplify our notations in the following we will refer to the long wave-length bands at $\lambda 7000$ as the A-group and to the bands at $\lambda\lambda 6389, 6382$ as the B-group. The overlapping faint bands in A and B are called A', B', respectively. The isolated band at $\lambda 3533$ already analyzed by Mulliken we refer to as the C-group. The lines of A, A',

TABLE IV
The lines of the B band of calcium hydride

<i>j</i>	<i>P</i> ₁	<i>P</i> ₂	<i>R</i> ₁	<i>R</i> ₂
0				15763.17
1		15745.12	15761.91	73.07
2	15745.12	37.87	70.73	83.20
3	36.53	30.86	79.91	93.75
4	28.43	24.11	89.51	804.58
5	20.70	17.78	99.54	15.73
6	13.48	11.81	809.93	27.21
7	06.72	06.23	20.65	38.99
8	00.33	01.00	31.70	51.08
9	694.40	696.17	43.11	63.42
10	88.83	91.69	54.82	76.04
11	83.59	87.60	66.81	88.93
12	78.90	83.84	78.99	902.04
13	74.47	80.48	91.45	15.38
14	70.32	77.42	904.14	28.97
15	66.69	74.70	17.08	42.76
16	63.35	72.32	30.09	56.76
17	60.34	70.42	43.47	70.84
18	57.64	68.65	56.99	85.12
19	55.26	67.18	70.53	99.49
20	53.23	66.15	84.30	16014.04
21	51.41	65.37	98.23	28.64
22	50.05	64.88	16012.17	43.35
23	49.02	64.55	26.25	58.11
24	48.09	64.55	40.39	72.94
25	47.34	64.88	54.61	87.74
26	47.00	65.37	68.82	102.62
27	47.00	66.15	83.12	17.41
28	47.11	67.18	97.33	32.25
29	47.52	68.28	111.52	46.92
30	48.09	69.64	25.68	61.65
31	48.86	71.18	39.74	76.13
32	49.82	72.81	53.75	90.53
33	50.92	74.59	67.63	
34	52.13	76.46	81.33	
35	53.52	78.48	94.83	
36	54.95	80.48		
37	56.49	82.61		
38	58.05	84.78		
39	59.63			
40	61.24			
41	62.81			

B, B' are in Tables II to V arranged in series. This arrangement includes practically all lines measured (approximately 800) and is based on the rules holding for band series and on the combination principle applied to band spectra.

TABLE V
The lines of The B' band of calcium hydride

j	P_1	P_2	R_1	R_2
0			15745.87	
1			54.45	
2	15729.45		63.39	15778.05
3	21.05		72.77	88.33
4	13.11		82.53	99.04
5	05.61	15703.86		
6	698.49	697.72	92.65	810.18
7	91.69	92.03	803.15	21.25
8	85.58	86.77	13.85	32.81
9	79.74	81.78	24.81	44.52
10	74.23	77.08	36.04	56.51
11	69.07	72.81	47.43	68.65
12	64.19	68.65	59.07	81.00
13	59.63	64.88	70.80	93.52
14	55.26	61.64	82.75	906.21
15	51.41	58.45	94.84	19.03
16	47.52	55.58	907.02	32.01
17	44.14	53.00	19.33	45.10
18	40.89	50.68	31.76	58.25
19	37.88	48.58	44.26	71.42
20	25.19	46.76	56.87	84.68
21	32.72	45.12	69.38	97.92
22	30.48	43.75	82.00	16011.17
23	28.40	42.53	94.65	24.38
24	26.54	41.50	16007.22	37.54
25	24.86	40.62	19.74	50.64
26	23.40	39.91	32.14	63.61
27	22.02	39.32	44.46	76.47
28	20.75	38.79	56.68	89.04
29	19.58	38.30	68.82	101.45
30	18.48	37.88	80.43	13.49
31	17.46	37.44	91.92	25.26
32	16.39	36.92	103.06	36.40
33	15.34	36.31	13.67	46.92
34	14.05	35.39		56.84
35	12.44			

BAND STRUCTURE

In Figs. 1 and 2 the groups B and A are graphically represented around their origins. The B group consists of two doublet branches P_1 , P_2 and R_1 , R_2 , overlapped by a faint B' band having a similar structure (P'_1 , P'_2 , R'_1 , R'_2) to that of B , only shifted a little toward the red. The

P_1, P_2 branches of B converge into two distinct heads at $\lambda\lambda 6382, 6389$.
The series of B and B' may be represented by polynomials:

$$P(j) = \sum_{k=0}^{\infty} \pi_k j^k, \quad R(j) = \sum_{k=0}^{\infty} \rho_k j^k, \quad (1)$$

where k is a positive integer.

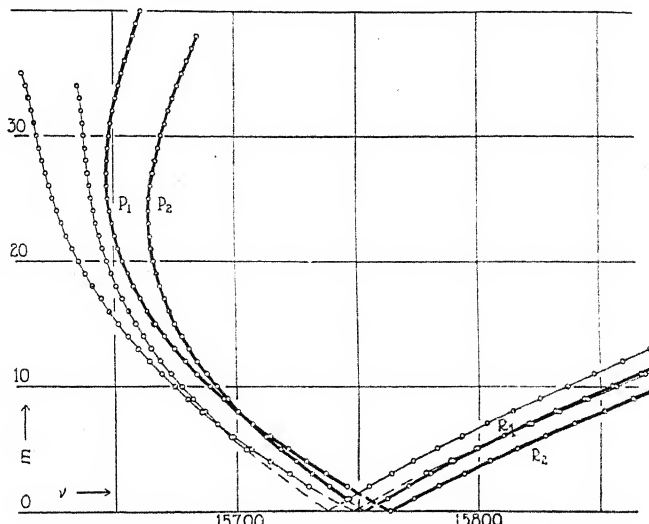


Fig. 1. Graphical representation of Group B bands.

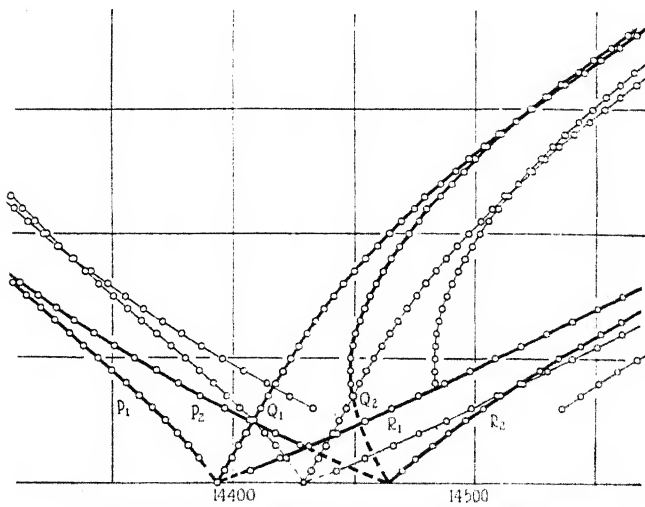


Fig. 2. Graphical representation of Group A bands.

According to the arrangement in the tables the lines $P_1(1), P_1(0), R_1(0)$ are missing in the P_1, R_1 series. In P_2, R_2 only $P_2(0)$ is missing.

The lines $P_1(2)$ and $P_2(1)$ coincide at 15745.12 but judged from the intensity of this line undoubtedly both are present. In the series of the B' band there is a great number of additional lines missing. Considering the relative faintness of this band it seems probable that the restrictions for missing lines are the same here as in B. For small j values the series may be represented by polynomials of the second degree ($k=0, 1, 2$) but for high j numbers there is a remarkable "red-shift" indicating the presence of the coefficients $\rho_4, \rho_6, \dots, \pi_4, \pi_6$ in (1). This is best observed in the P_1, P_2 series of the B' band, which do not converge into any heads, the spacing between the lines again increasing for the highest numbers observed. There is also an abrupt cut-off in the intensity of these series. Anomalies of this kind, but of still more prominent form, have already been noted by Mulliken³ in the C group of this spectrum and by Erikson and Hulthén⁴ in the spectrum of AlH. One is inclined to attribute these properties to an extreme molecular instability.^{3,4}

The A group (Fig. 2) may be considered as two bands, $A_1(P_1, Q_1, R_1)$ and $A_2(P_2, Q_2, R_2)$ having two different origins. As in B the A group is overlapped by the faint A', having a similar structure to that of A though here shifted toward the violet. The boundaries in A have a very unusual shape. Thus in A_1 and A_1' the series for small j values develop as if the bands were going to "shade" toward the red (ρ_2, π_2 in (1) are negative). From about $j=8$ the influence of higher terms of (1) appear and turn their "shading" into the opposite direction.

In A_1 and A_1' the lines $P_1(1), P_1(0)$ and $R_1(0)$ are missing, while the Q_1 branch can be traced down to its first line $Q_1(0)$. In A_2 and A_2' the Q_2 series vanish totally below $j=5$ and $j=6$ respectively. The absence of several lines around the band origin seems to be a common property for the short wave-length components in many spectra of doublet bands.⁵

As already mentioned the arrangements in Tables II to V are mainly based on the application of the combination principle to band spectra using simple assumptions regarding the nature of the emitter. Thus the lines are numbered according to the scheme:

$$\begin{aligned} P_i(j) &= \nu_0 + F(j-1, j_e') - f(j, j_e) \\ Q_i(j) &= \nu_0 + F(j, j_e') - f(j, j_e) \quad (i=1, 2) \\ R_i(j) &= \nu_0 + F(j+1, j_e') - f(j, j_e) \end{aligned}$$

⁴ G. Erikson and E. Hulthén, Zeits. f. Physik 34, 775 (1925).

⁵ Regarding the (C+H) spectrum see E. Hulthén, diss. Lund, 1923, p. 43, 45 OH spectrum, W. W. Watson, Astrophys. J. 60, 145 (1924). MgH spectrum, W. W. Watson and Ph. Rudnick, Astrophys. J. 63, 20 (1926).

where j is the quantum numbers for the total angular momentum and j_e the one for the resultant electronic angular momentum of the molecule. j_e may be divided into a σ component along the figure-axis of the dipole and an ϵ component perpendicular thereto. Different values of j_e correspond to rotational doublets as P_1P_2 and R_1R_2 in the B-group.

In Tables VI and VII the final and initial terms of rotation are isolated, using the following abbreviations:

$$\begin{aligned} R_i(j-1) - P_i(j+1) &= F_i(j+1) - F_i(j-1) = \Delta F_i(j) \\ R_i(j) - P_i(j) &= f_i(j+1) - f_i(j-1) = \Delta f_i(j) \end{aligned} \quad (3)$$

TABLE VI
Values of the final and initial terms of rotation in the band spectra of calcium hydride

j	A			B		C		A'		B'	
	Δf_1	Δf_2	Δf_1	Δf_2	Δf	Δf_1	Δf_2	Δf_1	Δf_2	Δf_1	Δf_2
1					25.30	25.37					
2	25.37			25.37	42.21	42.19	24.97			24.82	
3	42.23			42.30	59.09	59.04	41.41			41.34	
4	59.20	75.74	59.21	75.97	75.95	58.00			57.78	74.19	
5	75.99	92.68	76.03	92.77	92.78	74.04			74.28	90.61	
6	92.72	109.47	92.82	109.50	109.50	90.90			90.84	107.01	
7	109.60	126.19	109.60	126.21	126.19	106.95	123.23	123.23	107.07	123.41	
8	126.33	142.74	126.25	142.82	142.88	123.37	139.39	139.39	123.41	139.47	
9	142.90	159.36	142.87	159.39	159.33	139.55	155.60	155.60	139.62	155.73	
10	159.53	175.95	159.52	175.82	175.85	155.83	171.80	171.80	155.74	171.71	
11	175.95	192.25	175.92	192.20		171.88	187.99	171.85	187.86		
12	192.24	208.60	192.34	208.45		187.98	203.74	187.80	203.77		
13	208.59	224.57	208.67	224.62		203.92	219.55	203.81	219.36		
14	224.75	240.64	224.76	240.68		219.60	234.99	219.39	235.07		
15	240.76	256.65	240.79	256.65		235.31	250.72	235.23	250.63		
16	256.75	272.52	256.74	272.34		250.82	266.11	250.70	266.03		
17	272.55	288.18	272.45	288.11		266.18	281.30	266.13	281.33		
18	288.19	303.64	288.21	303.66		281.44	296.46	281.45	296.52		
19	303.75	319.06	303.76	318.97		296.45	311.34	296.57	311.49		
20	319.09	334.16	319.12	334.12		311.44	326.19	311.54	326.30		
21	334.28	349.16	334.25	349.16		326.35	340.85	326.39	340.93		
22	349.26	364.05	349.21	364.09		341.07	355.42	340.98	355.39		
23	364.17	378.83	364.08	378.80		355.42	369.55	355.46	369.67		
24	378.92	393.27	378.91	393.23		369.71	383.78	369.79	383.76		
25	393.37	407.56	393.39	407.57		383.87	397.62	383.82	397.63		
26	407.68	421.64	407.61	421.59		397.68	411.40	397.72	411.32		
27	421.72	435.53	421.71	435.44		411.31	424.84	411.39	424.82		
28	435.56	449.23	435.60	449.13		424.89	438.05	424.88	438.17		
29	449.30	462.61	449.24	462.61		438.15	451.20	438.20	451.16		
30	462.65	475.76	462.66	475.74		464.04		451.36	464.01		
31	475.85	488.79	475.86	488.84		476.57	476.61	464.04	476.57		
32	488.89	501.53	488.82	501.54		489.01		476.58	488.95		
33	501.67	514.10	501.62	514.07				489.01	501.01		
34	514.19	526.22	514.11	526.38				501.23	513.49		
35	526.36										
36	538.32			538.34							

Comparing the Δf of Table VI we find that they agree with each other for all groups, A, B, C. Consequently these groups are emitted by the same molecule and they have a common final state. Between Δf_1 and Δf_2 , the following relation exists:

$$\Delta f_1(j+1) = \Delta f_2(j) + c$$

where c is a very small constant (about 0.09 cm^{-1}). In the C group, where no doubling appears, there is a close agreement between the values of Δf and those of Δf_2 , which shows that they must be identical.

TABLE VII
Values of the final and initial terms of rotation in the band spectra of calcium hydride

The Q series in the A group do not fit into any simple scheme like that of (2) and probably not to any inter-combination between the F_i and f_i terms. Thus the numeration given in the tables is doubtful regarding these series. As in the P and R branches of A also here the long wavelength component Q_1 is far more intense than Q_2 for small j numbers. It is also worth noticing that while in P and R the intensity of the lines at first slowly increase with their enumeration, the lines of Q_1 almost at once gain their full strength.

In the B group our view of the structure seems to be complete and identical to that of the violet cyanogen bands. In order to explain the missing lines in these bands Kratzer⁶ excludes all transmissions from, or to, any states of $j=0$. From this postulate he concludes that the lines $R_2(0)$ and $P_2(1)$ in the "false doublets" formed by $R_1(j)$, $R_2(j-1)$ and $P_1(j)$, $P_2(j-1)$ must be missing. This could not be controlled in the CN spectrum because of the small separation of the doublets around the 0 lines. In the B group of CaH, however, these doublets are easily separated down to their origin and, contrary to the predictions of Kratzer, $R_2(0)$ and $P_2(1)$ are distinctly present.

In our scheme the missing lines are explained by excluding only those values of j which render

$$m = j - \epsilon < 0$$

m is the quantum number for the angular momentum of the nuclei. These properties are illustrated in Fig. 3.

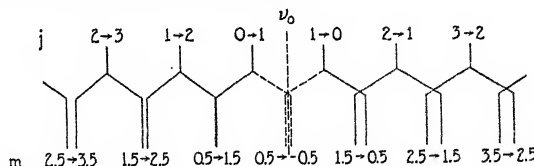


Fig. 3. Doublets separations in Group B bands.

In Fig. 4 the term structure for the entire spectrum is given by its electronic levels and additional vibration levels. While the N and B levels are noted as rotational doublets, we here refer to A_1 , A_2 as an electronic doublet. These and other notations in the figure will be explained further down.

ON THE NATURE OF THE EMITTER

The theory of diatomic molecules, as developed by Kratzer,⁶ Kramers and Pauli,⁷ gives the following expression for the spectral term due to the rotation or precession:

$$F(j) = B((j^2 - \sigma^2)^{\frac{1}{2}} \mp \epsilon)^2 \pm 2\delta((j^2 - \sigma^2)^{\frac{1}{2}} \mp \epsilon) + \dots \quad (4)$$

⁶ A. Kratzer, Ann. d. Physik 71, 72 (1923).

Here j , σ and ϵ are the notations given above (3). The double sign of ϵ , introduced by Kratzer, indicates that the corresponding vector can stand parallel or anti-parallel to that of m . ϵ is generally supposed to be accompanied by a double-signed δ term, giving account of the influence of the molecular rotation upon the electronic system. Applying the theory to the empirical results in our Tables VI and VII we have:

$$\Delta F(j) = 4B(j \mp \epsilon) \pm 2B\sigma^2\epsilon/(j^2 - 1) \pm 4\delta + \dots$$

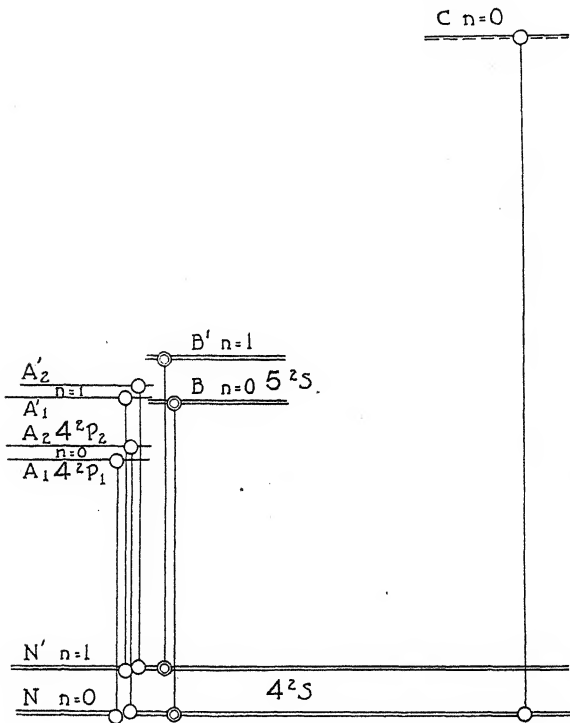


Fig. 4. The electronic levels in the CaH spectrum.

Obviously, as pointed out by several writers,⁸ it is here impossible to distinguish between ϵ and δ unless σ is not present. Further, σ can not be detected unless ϵ is not present. Unhappily, the real support for the σ , except for the appearance of Q branches and the postulate for missing lines, is given by only the first lines in a band series, and as these are

⁷ H. A. Kramers and W. Pauli, Zeits. f. Physik 13, 351 (1923).

⁸ For a more complete discussion of the Kramers and Pauli formula see: R. S. Mulliken, Systematic Relations between Electronic Structure and Band-Spectrum Structure I, II, III, Proc. Nat. Acad. Sci. 12, 144, 151, 338 (1926). In the following pages the writer in many cases follows the directions given in these very interesting papers.

mostly very faint or entirely missing, our knowledge about σ is very uncertain. ϵ and δ have to be considered from a theoretical point of view, ϵ usually assuming fractional values $\frac{1}{4}, \frac{1}{2}, \dots$ and δ being generally very small. In Table VIII the constants of (4) are given as calculated from the $\Delta F(j)$ of Tables VI and VII.

The σ values of A_1 , A_2 ($1/2$ and $3/2$ respectively) are chosen on the basis of the missing lines ($j-j_e \geq 0$). It is difficult to state whether in these terms a small ϵ is present or not. In any case it is interesting that all through the terms of the table a *distinct* ϵ appears in connection with an *inconsiderable* σ and *vice versa*.⁹ In the C group the value $\epsilon_1 = +\frac{3}{4}$ given by Mulliken³ is changed into $\epsilon_1 = -\frac{1}{2}$ on account of the close agreement between its final term with that of $N_2(\epsilon_2 = -\frac{1}{2})$ and on adoption of half-quantum numbers for band spectra. Thus δ in C turns out very large. However, considering the extremely unstable C term, indicated by the spectrum, this is not discouraging. It is also worth while to notice that according to our table no intercombination of the type $\pm\epsilon_1 \rightarrow \epsilon_2 \mp$ occur. In the next to last column of the table the nuclear spacings r_0 corresponding to the different states of the molecule are given.

TABLE VIII
Values of the constants in Eq. (4) calculated from the values of $\Delta F(j)$ in
Tables VI and VII

B	ϵ	σ	δ	$r_0 \cdot 10^8$	ν_0
N_1	4.225	$\pm\frac{1}{2}$	0	+0.011	2.01
N_2					
N_1'	4.125	$\pm\frac{1}{2}$	0	+0.011	2.03
N_2'					
A_1	4.09	0	$\frac{1}{2}$	—	2.03
A_2	4.49	0	$\frac{3}{2}$	—	1.94
A_1'	4.01	0	$\frac{1}{2}$	—	2.05
A_2'	4.38	0	$\frac{3}{2}$	—	1.97
B_1					
B_2	4.400	$\pm\frac{1}{2}$	0	-0.250	1.96
B_1'					
B_2'	4.308	$\pm\frac{1}{2}$	0	-0.250	1.98
C	4.912	$-\frac{1}{2}$	0	-1.04	1.88
					28353.04

From the simple theory of band spectra (Heurlinger, Lenz) we know that bands shaded toward the violet correspond to an increase of the nuclear spacing for the end configuration in the molecule. It is therefore somewhat confusing that though all bands of the spectrum are shaded toward the violet r_0 is larger for A_1 than for N_1 . The violet shading of A_1 , however, as already mentioned, may be considered as an effect of the higher terms in (1) or in (4).

⁹ In the spectrum of HgH Mulliken (l.c.) finds a small $\sigma^2\epsilon$ -term for the 2P_1 , 2S states. From a theoretical point of view, M. Born (Vorlesungen über Atom mechanik, Berlin, 1925, p. 140) excludes the simultaneous presence of σ and ϵ in (4).

In Fig. 4, A', B' have already been assigned as vibrational states ($n=1$) of N, A, B. This assumption is confirmed when we consider their r_0 values, which all show an increase compared to those of N, A, B. Theoretically this is explained by the unsymmetric character of the mutual force potential of the ions around their equilibrium position (r_0) in the molecule. The forces between the ions are indirectly measured by their vibration frequencies (ω) as these appear in band spectra and according to a rule by Birge¹⁰ and Mecke¹¹ (based on a great number of spectra) the forces increase when r_0 decreases. Thus from the r_0 values of Table VIII we would expect

$$\omega_{A_1} < \omega_N < \omega_B < \omega_{A_2} < \omega_C$$

while the spectrum shows:

$$\omega_{A_1} = \omega_{A_2} > \omega_N > \omega_B$$

In the C term no vibrational state appears.³ Considering the minimum nuclear spacing of this state in connection with its low degree of stability we may say that the CaH molecule acts throughout in opposition to the rule of Birge and Mecke.

ELECTRONIC LEVELS

According to the theory of the structure of molecules, as this has been developed recently by Birge, Mecke and Mulliken, the spectrum of a molecule agrees with that of the "corresponding atoms or molecules"—corresponding atoms and molecules having the same number of electrons in their coupled system. This comparison between the spectra of atoms and molecules has been worked out successfully for a number of diatomic molecules assigning their terms by S, P, D notations. In some cases a close agreement was found between the magnitudes and separations of the terms of corresponding atoms and molecules.

Here considering the elements in the second column of the periodic table, the spectra of ZnH, CdH, HgH show a doublet separation parallel to that of the $^3P_{1,2}$ of their metal atoms.¹² Applying the alternative and displacements laws as developed for band spectra, Mulliken⁹ and Mecke¹³ later on pointed out the parallel also existing between these separations and those of $^2P_{1,2}$ in Cu, Ag, Au—the corresponding atoms. It is now very satisfying, that the A group of CaH forms electronic doublets (A_1, A_2 and A'_1, A'_2) with separations roughly estimated to $\Delta\nu \sim 80 \text{ cm}^{-1}$,

¹⁰ R. T. Birge, Phys. Rev. 25, 240 (1925).

¹¹ R. Mecke, Zeits. f. Physik, 32, 823 (1925).

¹² E. Hulthén, Nature, Oct. 31 (1925).

¹³ R. Mecke, Zeits. f. Physik, 36, 795 (1926).

which are of the same magnitude as the $^2P_{1,2}$ of the potassium atom ($\Delta\nu=57.90\text{ cm}^{-1}$)—here the corresponding atom.

The A terms ($^2P_{1,2}$) of CaH may be pictured by an emission electron in a 4_2 orbit standing perpendicular (or nearly so) to the molecular figure axis. This explains the high stability of these states, a striking fact when we consider their various nuclear spacings.

The N level is assumed as the normal (2S) level as indicated by the fact that it makes the final state for three different electronic transitions in the molecule. The failure of the CaH bands in absorption¹⁴ is no serious argument against this assumption. Probably, the absorption of unstable molecules like those of MeH is a very complicated problem involving the stability and duration of the molecule. We know from the investigations of hydride spectra that the state of minimum energy does not necessarily mean a maximal nuclear stability (consider the spectra of CuH, HgH, AlH, OH).

In the N and B states the coupled electronic system of the molecule is assumed to be in the plane of the figure axis of the molecule ($\sigma=0$), its angular momentum standing parallel as well as anti-parallel to the axis of rotation ($\epsilon=\pm\frac{1}{2}$). Because of these similarities between N and B they are both assigned 2S levels (compare them with the terms of the violet CN bands). In the C state the electronic system again is of ϵ type ($\sigma=0$) here however only the anti-parallel direction ($\epsilon=-\frac{1}{2}$) of its angular momentum is present. Whether this is an effect due to the highly unstable characteristics of C or not, we do not know. Bands analogous to those of B and C have not yet been found in the spectra of ZnH, CdH and HgH.

Finally it may be mentioned that the band spectrum of MgH ($\lambda 5211$) apparently corresponds to the A group of CaH and thus should be assigned by a $^2P_{1,2}-^2S$ transition. Also here the doublet separation ($\Delta\nu \sim 20\text{ cm}^{-1}$) roughly agrees with that of the corresponding Na atom ($^2P_{1,2}=17$).

This work will be continued by an investigation on the spectra of strontium and barium hydride. The writer is indebted to the Director of this Laboratory, Professor H. M. Randall, for his very obliging and valuable interest in this work, and to the International Education Board for the award of a Fellowship.

DEPARTMENT OF PHYSICS,
UNIVERSITY OF MICHIGAN
Sept. 30, 1926.

¹⁴ E. Hulthén and R. V. Zumstein, Phys. Rev. 28, 13 (1926).

CORRELATION OF THE FLUORESCENT AND ABSORPTION SPECTRA OF IODINE

By F. W. LOOMIS

ABSTRACT

The lines near Hg5460 in Wood's fluorescent spectrum of iodine excited by the quartz mercury arc are identified with definite lines in the absorption spectrum. This identification furnishes the key to the analysis of the absorption spectrum. Values of the constants of the iodine spectrum, based on new measurements, are as follows: for the unexcited state $B_0'' = 0.037300 \pm 0.000003$, $I_0'' = 7.42 \times 10^{-38}$ g.cm², $r_0'' = 2.66 \times 10^{-8}$ cm; for the excited state $B'(26) = 0.023368 \pm 0.000005$, $I'(29) = 11.83 \times 10^{-38}$ g.cm², $r'(29) = 3.37 \times 10^{-8}$ cm; $C(29,0) = -0.013932$, $m_H''(29,0) = 1.677$. The identification, in the absorption bands, of both components of the fluorescent doublets makes possible the calculation of absolute rotation quantum numbers; and these furnish direct evidence for the hypothesis of half quantum numbers. Lines in Wood's magnetic rotation spectrum which show the "normal" direction of rotation are found to belong to *P* branches; those which show the opposite direction, to *R* branches.

Three new series of fluorescent doublets, $\nu(29,45\frac{1}{2})$, $\nu(29,50\frac{1}{2})$ and $\nu(29,51\frac{1}{2})$, extending to the -1 order, are found and formulated, and their relationship to bands (29,1) and (29,0) demonstrated.

Revised versions of Mecke's equations for band heads, based on corrected numbering, and of the constants of four red bands, based on new computations, are given; and the apparent occurrence of *Q* branches in the red bands is shown to be due to the fact that the values of these constants are such as to cause the lines of the *P* and *R* branches to coincide.

Calculated values of the constants of the fluorescent series, based on the results of the new absorption measurements, agree well with the values of these constants determined empirically from the fluorescent spectrum. Every detail is in agreement with the theory advanced by Lenz to account for the simple fundamental series of doublets excited by the narrow green mercury line.

ONE of the notable successes of the modern theory of band spectra is the explanation by Lenz¹ of the striking experiments of R. W. Wood² on the fluorescence of iodine vapor excited by monochromatic light. The spectrum reported by Wood was a series of approximately equally spaced doublets, of nearly constant frequency interval, extending from the doublet of "order" zero, whose short-wave component coincides with the exciting green mercury line, to the doublet of order 27, well down in the red. The simplicity of this spectrum offers a marked contrast to the very complex absorption spectrum, or to the fluorescent spectrum excited by white light. Nevertheless no explanation of it was put forward

¹ Lenz, Phys. Zeits. 21, 691 (1920).

² R. W. Wood, Researches in Physical Optics, II (1919); Phil. Mag. 35, 236 and 252 (1918).

until Lenz showed that it constitutes a clear example of the working of the Bohr selection principle for rotational quantum numbers. For, if only one absorption line is excited, all the excited molecules must be in the same state, having the same values of the vibrational quantum number n' and of the rotational quantum number j' . In the return transitions which accompany the emission of the fluorescent light the final value of j (i.e., j'') is limited, according to the Bohr selection principle, to $j'' = j' \mp 1$; while, if the vibration is anharmonic, all values of n'' are possible. The result is a series of lower energy levels arranged in fairly close pairs approximately evenly spaced; and a spectrum like that reported by Wood.

When the exciting green mercury line was broadened by using a quartz lamp run at a high temperature it covered seven apparent iodine lines and the resulting spectrum was more complex. It then consisted of groups of lines close to the original (the so-called "fundamental") doublets, tending toward the violet side of them in the groups of higher order, but having no apparent uniformity of pattern. Several new doublet series have, however, been found among these lines and empirically formulated by Mecke.^{3,4} The form of Mecke's empirical expression has been accounted for theoretically by Kratzer and Sudholt,⁵ in harmony with Lenz's theory of the fundamental doublet series; and they have been able to make a rough calculation of the moment of inertia of the iodine molecule from the numerical values of some of the constants in Mecke's series. Kemble and Witmer⁶ have extended and revised the work of Kratzer and Sudholt, have identified the bands in the absorption spectrum to which the excited lines of most of Mecke's series belong, and have made a more accurate computation of the moment of inertia.

An important objection to Lenz's theory, and one which holds equally against those of Kratzer and Sudholt, and Kemble and Witmer, has, however, been put forward by Mecke.⁴ He has studied the absorption spectrum, choosing four bands in the red region to avoid the complexity of the numerous overlapping bands in the green, and has found that these bands apparently consist only of Q (null) branches, corresponding in band spectrum theory to transitions with $j'' = j'$, whereas it is a necessary assumption of the Lenz theory that only transitions to $j'' = j' \mp 1$ should occur, and hence that the absorption bands should consist of R and P (positive and negative) branches.

³ Mecke, Zeits. f. Physik **7**, 73-85 (1921).

⁴ Mecke, Ann. d. Physik **71**, 104-134 (1923).

⁵ Kratzer and Sudholt, Zeits. f. Physik **33**, 144-152 (1925).

⁶ Kemble and Witmer, Phys. Rev. **28**, 633 (1926).

In the present paper the fluorescent lines in the zero order have been identified with definite lines in the absorption spectrum, and this identification has served as a clue to the unravelling of the complex overlapping absorption bands in the green. It is shown that they consist of *R* and *P* branches as required by the Lenz theory. Precise calculations of the absolute rotation quantum numbers, based on this identification, agree closely with the hypothesis of "half-quantum numbers." Accurate values of the moment of inertia and other constants of the iodine spectrum have been computed and an extrapolation into Mecke's red region has shown that his apparent finding of *Q* branches was due to an unfortunate accident in the selection of four bands in which the lines of the *R* and *P* branches overlapped so closely as to be inseparable with his resolution. Three new fluorescent series of a slightly different type are also reported and assigned to their place in the absorption spectrum. And the assignment of absorption lines to their *R* and *P* branches has made it possible to demonstrate the regularity in Wood's magnetic rotation spectrum.

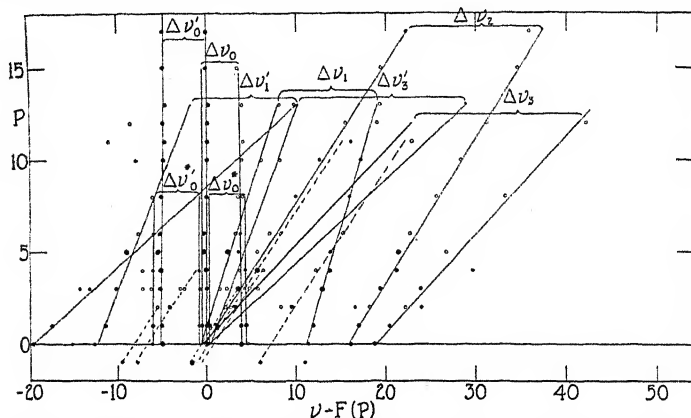


Fig. 1. Fluorescent series. The blackness of the points roughly indicate the intensities.

MECKE'S FLUORESCENT SERIES

The series in the fluorescent spectrum excited by the broad green line are exhibited in Fig. 1, which is like one made, but not published, by Mecke.⁷ Here the ordinate is *p*, the order⁸ of a group, and the abscissa is $\nu - F(p)$ where ν is the frequency of any line and

$$F(p) = 18307.5 - 213.667p + 0.592p^2 + 0.00207p^3 \quad (1)$$

⁷ L.c. page 75. R. W. Wood, Researches in Physical Optics, II, p. 33, published a similar diagram, but in terms of wave-length, in which the doublet series lie on curved lines and are consequently more difficult to pick out.

⁸ It is convenient to follow Wood's nomenclature in which a fluorescent line which coincides with some part of the exciting mercury line is called a "resonance line," the

is Mecke's formula for the series of main lines of the fundamental doublets. In this arrangement the main line of each fundamental doublet is brought to the axis of ordinates, and each doublet series is represented by a pair of nearly parallel straight lines. Nine of the ten doublet series which Mecke reported, slightly modified by Kratzer and Sudholt and by the writer, as explained below (see Table V), are indicated in Fig. 1 by continuous lines. The tenth, ν_2' , is omitted, because the writer has found it to be illusory. The broken lines represent new series to be described below.

Mecke's empirical formulas⁴ for his series are as follows:

$$\begin{array}{lll} \nu_0 = F(p) & + (3.8) & \nu_0' = F(p) & + (-5.0) \\ \nu_0^* = F(p) & + (4.5) & \nu_0^{*\prime} = F(p) & + (-6.0) \\ \nu_1 = F(p) + 0.66p + (11.6) & & \nu_1' = F(p) + 0.75p + (-12.5) & (2) \\ \nu_2 = F(p) + 1.33p + (16.0) & & \nu_2' = F(p) + 1.5p + (-?) \\ \nu_3 = F(p) + 1.95p + (19.0) & & \nu_3' = F(p) + 2.2p + (-19.7) \end{array}$$

where the quantities in parentheses are the doublet intervals and if omitted leave the expressions for the main lines, but if included give the companion lines. The constant terms in the parentheses will be denoted by d_i and the coefficients of p by γ_i . The "fundamental series" of doublets is ν_0' .

RECALCULATION OF MECKE'S ABSORPTION DATA

Mecke⁴ has measured the iodine absorption band heads in the region 5000–7000 Å and has shown that they all belong to the same band system, for which he publishes a formula in terms of two arbitrary parameters, n_1 and n_2 . For several reasons he concludes, correctly, that n_2 corresponds to n' , the upper level vibrational quantum number, but increases as n' decreases. As $n_2=26$ seems to be a limiting value he concludes that it is the zero of n' and sets $n'=26-n_2$. An inspection of Fig. 2 will show that this is only an approximation and that some future investigation may necessitate changing all the values of n' by a few units or half units. Since, however, only relative values of n' are needed in this paper, it is simplest to retain Mecke's assignments of n' for the present. Similarly, he concludes that n_1 corresponds to, and increases with, n'' , the lower level vibrational quantum number. And, since the coefficients of n_1 , n_1^2 , and n_1^3 are sensibly the same as those of p , p^2 and p^3 in the expression (1) for Wood's fluorescent doublets he

component of any doublet which is on the same side as the resonance line of the series to which it belongs is called the "main line;" and the other component the "companion line." The "order," p , is the ordinal number of a group, counted from the "group of zero order" which contains the resonance line.

justifiably identifies n_1 with p . He is, however, mistaken in concluding from Pringsheim's⁹ observation of antistokes groups as far as the -4 order, that the zero of n'' must be at least $n_1 = p = -4$. For, while it is true that the zero of a series having antistokes members must be at least as low as the lowest member, the fundamental series, for which $p = n_1$, does not contain any antistokes members; nor do any of the series (2)

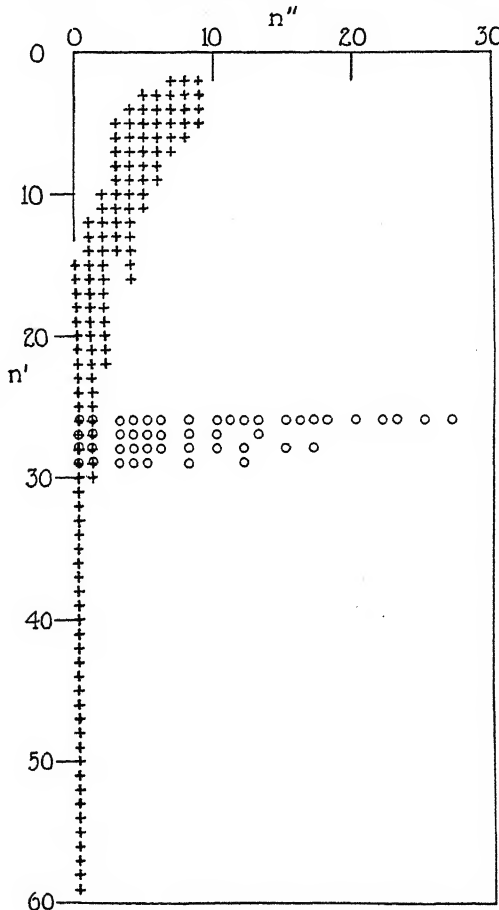


Fig. 2. Numbering of absorption bands.

which Mecke has found in the fluorescent spectrum, as can be seen from an inspection of Fig. 1, and as is evident from their γ 's, which, according to the theory of Kratzer and Sudholt, are so small that they must belong to series with the same \bar{n} , i.e., having the same number of vibrational quanta before excitation, as the fundamental series. It is a safe assertion

⁹ Pringsheim, Zeits. f. Physik 7, 206 (1921).

that the bands to which the zero order fluorescent lines of the fundamental series and of Mecke's series belong have the least possible value of n'' . There is at present no way to ascertain whether or not this minimum value is zero. Quite probably, in the light of the new quantum mechanics¹⁰ and by an analogy with the findings from isotope effect measurements by Mulliken¹¹ and Watson¹² in the spectra of BO and MgH, the minimum value will be $\frac{1}{2}$. However, we shall, in this paper, for simplicity, assume it to be zero and set $n'' = n_1 = p$ for the fundamental series and others having no antistokes members. For any series having \tilde{n} antistokes members, $n'' = n_1 = p + \tilde{n}$. No errors introduced in this way will be serious enough to affect our arguments. Using this numbering, the expression which represents Mecke's band heads becomes:

$$\nu(n', n'') = 15597.70 + (126.59n' - 0.755n'^2 - 0.0033n'^3) \\ - (213.76n'' - 0.596n''^2 - 0.0021n''^3) \quad (3)$$

Mecke's measurements of band heads are good only to about 0.5 cm^{-1} and Kemble and Witmer have shown that the heads lie within a few lines (2 in the green, or about 0.05 cm^{-1}) of the origin, so that Eq. (3) is equally valid for band origins, and can be compared with the usual theoretical expression

$$\nu(n', n'') = \nu_e + (\omega^{0'} n' - 2\omega^{0'} x' n'^2 \dots) \\ - (\omega^{0''} n'' - 2\omega^{0''} x'' n''^2 \dots) \quad (4)$$

Mecke¹³ mentions that Eq. (3) does not adequately represent the bands with large n'' 's, and probably terms in higher powers are required. It is the writer's intention to attempt to improve it when he has completed the accurate measurement of certain absorption bands on which he is now engaged.

The crosses in Fig. 2¹³ show all the absorption bands found by Mecke, plotted according to the assignment of n' and n'' numbering just explained. The circles show the bands to which the doublets in Mecke's fluorescent series belong, the values of n' being those assigned by Kemble and Witmer.

Mecke has also measured the individual lines of the four bands (4,7), (4,8), (5,7) and (5,8), which lie in the red, where the lines are less numerous and resolution easier than in the neighborhood of the green mercury line. He has found, as has been stated, that they appear to consist of Q branches and has represented them in the form

$$\nu = \nu_H + CM^2 \quad (5)$$

¹⁰ Heisenberg, Zeits. f. Physik **33**, 879-893 (1925).

¹¹ Mulliken, Phys. Rev. **25**, 259-294 (1925).

¹² Watson, Nature, May (1926).

¹³ Cf. Mecke's Fig. 4, l.c., p. 133.

where M represents the ordinal number, starting from the head, and C is approximately -0.008 . He states that, since he was unable to resolve the bands within about 30 lines of the heads, his numbering, M , may be wrong by a few units. The error in numbering is, however, a constant throughout the four bands; i.e., his relative numbering is correct. For, although a change of, say, $+1$ in the M 's of any of the pairs of bands in (7) would not result in a detectable combination defect, it would introduce into (7) a linear term of the order of $0.016M$ which is not admissible, since (7) is the difference of two equations like (5).

He has also found that C varies from band to band, as indeed it should, since¹⁴

$$C = B' - B'' = (B_0' - \alpha'n') - (B_0'' - \alpha''n''), \quad (6)$$

and he has represented the differences between corresponding lines of the four bands as follows:

$$\begin{aligned} \nu(4, 7, M) - \nu(4, 8, M) &= \nu(5, 7, M) - \nu(5, 8, M) = \text{const.} + 0.00011M^2 \\ \nu(4, 7, M) - \nu(5, 7, M) &= \nu(4, 8, M) - \nu(5, 8, M) = \text{const.} - 0.00015M^2 \end{aligned} \quad (7)$$

which means that $\alpha'' = 0.00011$ and $\alpha' = 0.00015$. Since the quantities C , α' and α'' are of fundamental importance in all the theories of the fluorescent series, and were only roughly evaluated, the writer has recomputed them from Mecke's data, in the following manner. M was determined for some of the first resolved lines in each band from Eq. (5) using both measured and extrapolated values of ν_H and approximate values of C . In this way it was found that all his M 's were approximately 4 units too large. If one is to assume that Mecke's apparent Q branches are really P and R branches whose lines coincide, the head must have an m either coincident with that of some line or midway between two lines;

¹⁴ This paper follows the notation usual in treating of band spectra; specifically that in the recent report on "Molecular Spectra in Gases" by a committee of the National Research Council. Primed letters refer to the upper energy level, double primed letters to the lower level, letters with a bar over them refer to the state of the molecule before absorption. n , j and m are the quantum numbers corresponding to vibration, total angular momentum and nuclear angular momentum respectively. The rotational energy is expressed as $\hbar Bm^2$, where $B = B_0 - \alpha n$, and $B_0 = \hbar/8\pi^2cI$, $I = mr^2/2$ being the moment of inertia; and α depends on the law of force between the nuclei. Since $j' - j'' = \pm 1$ it follows, if one sets $m' = j' - \rho'$ and $m'' = j'' - \rho''$, that $m' - m'' = \pm 1 - (\rho' - \rho'')$. The resulting expressions for the frequencies of band lines are:

$$\begin{aligned} \nu(n', n'', m', m'') &= \nu(n', n'') + B'm'^2 - B''m''^2 \\ &= \nu(n', n'') - B''[1 \mp 2(\rho' - \rho'') + (\rho' - \rho'')^2] + 2B''[\pm 1 - (\rho' - \rho'')]m' + Cm'^2 \end{aligned} \quad (a)$$

$$= \nu(n', n'') + B'[1 \mp 2(\rho' - \rho'') + (\rho' - \rho'')^2] + 2B'[\pm 1 - (\rho' - \rho'')]m'' + Cm''^2$$

where $C = B' - B''$ and the upper sign of each double sign refers to the R branch. $\nu(n', n'')$ is the band origin and is given by Eq. (4). These expressions are simplified, if one sets $\rho' = \rho''$ to $\nu = \nu - B'' \pm 2B''m' + Cm'^2 = \nu + B' \pm 2B'm'' + Cm''^2$, which is very probably correct in the light of results below.

i.e., the M 's must be either nearly integral or nearly half-integral. Much the best values which satisfy this condition are obtained by subtracting 4 from Mecke's M 's, leaving the corrected M 's integers and signifying that the head coincides with a line. The corrected M 's were then used in Eq. (5) to calculate, by least squares, the constants ν_H and C for band (5,8). The results were:

$$\nu_H(5,8) = 14540.44, \quad C(5,8) = -0.000808$$

The frequency differences between corresponding lines of different bands were then formulated, as in (7), by least squares, using the corrected M 's, with the following results:

$$\begin{aligned} \nu(4,7,M) - \nu(4,8,M) &= 204.51 + 0.000119M^2 \\ \nu(5,7,M) - \nu(5,8,M) &= 204.54 + 0.000118M^2 \\ \nu(5,7,M) - \nu(4,7,M) &= 119.54 - 0.000175M^2 \\ \nu(5,8,M) - \nu(4,8,M) &= 119.46 - 0.000156M^2 \end{aligned} \quad (8)$$

yielding the weighted mean values $\alpha'' = 0.00012$, $\alpha' = 0.00017$. The changes from Mecke's values of α' and α'' are largely due to the correction of the M 's. As Mecke's C needs only very slight correction, he presumably calculated it by the method of second differences, which is independent of the absolute numbering.

If we anticipate a little by taking $B''(0) = 0.0373$ from (11), we can combine it with the data just obtained to calculate, on the justifiable assumption that $\rho' - \rho'' = 0$ in Eq. (a), footnote 14, the line numbers of the band heads,

$$m_H'' = B' / (B'' - B') = B' / -C \quad (9)$$

and the frequencies of the origins,

$$\nu_0 = \nu_H - B' B'' / (B'' - B') \quad (10)$$

For

$$\begin{aligned} B''(8) &= B''(0) - 8\alpha'' = 0.03634 \\ B''(7) &= B''(0) - 7\alpha'' = 0.03646 \\ B'(5) &= B''(8) + C(5,8) = 0.02826 \\ B'(4) &= B'(5) + \alpha' = 0.02843 \\ B'(0) &= B'(5) + 5\alpha' = 0.02911 \end{aligned} \quad (11)$$

The results are exhibited in Table I.

TABLE I
Constants of the red bands

Band	B'	B''	C	m''_H	$\nu_H - \nu_0$
(5,7)	.02826	.03646	-.00820	3.45	0.126
(5,8)	.02826	.03634	-.00808	3.50	0.127
(4,7)	.02843	.03646	-.00803	3.54	0.129
(4,8)	.02843	.03634	-.00791	3.59	0.131

Now it will be shown below that the m 's of the iodine bands are half-integers, so that the numbers in the fifth column of Table I indicate that the heads of all four of these bands very nearly coincide with lines, and that consequently the lines of the P and R branches nearly cover each other. It is because of his unfortunate selection of these particular bands, coupled with the smallness of m_H'' , which brings the origins far within the unresolved region near the heads, that Mecke appeared to find Q branches. These values of m_H'' also check the correction of exactly -4 which was applied, above, to Mecke's M 's; for, if the heads closely coincide with lines, the M 's, which are line numbers counted from the heads, must be nearly integral.

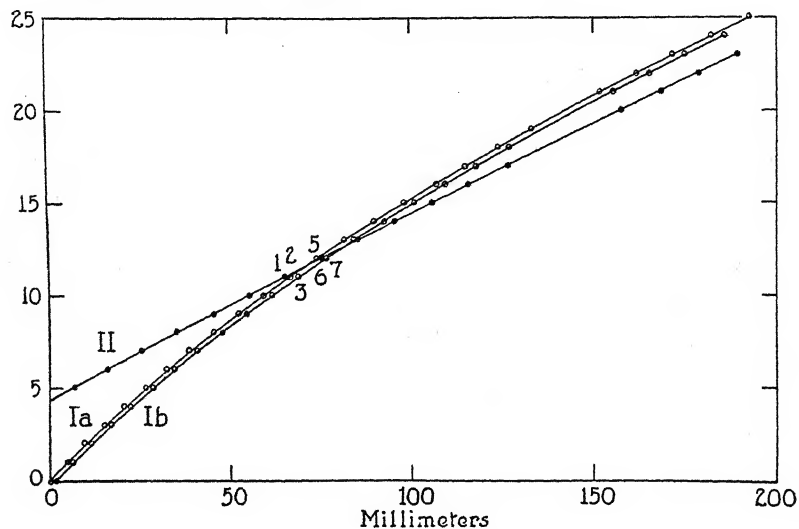


Fig. 3. Mecke's green series.

It would have been more pertinent to the problem had Mecke been able to measure the absorption spectrum in the neighborhood of the green mercury line which excites the fluorescence, but the density of lines was there too great for the resolution of his instrument. Wood photographed this region with his 40 foot spectrograph, but gives only the wave-lengths of the seven absorption lines which are covered by the wide green mercury line. He publishes a reproduction¹⁵ of a part of this spectrum, but it contains only one comparison line (Hg5460) and the scale can be only roughly determined as about 30 mm/ \AA . Mecke has found three series of regularly spaced lines in this reproduction which he calls Ia, Ib and II. They are shown in Fig. 3¹⁶ in which the abscissas

¹⁵ Wood, Researches in Physical Optics II, plate Ia. Phil. Mag. 35, 236-252 (1918) plate VIIa.

¹⁶ Mecke, l.c. Fig. 3, page 128.

are positions of lines on Wood's reproduction, in mm; and the ordinates are arbitrary parameters assigned by Mecke. The absorption lines which Wood has numbered 2 and 5 belong to series Ia, 3 and 7 to Ib, and 1 and 6 to II. Line 4 does not belong to any of them. Mecke mentions that series Ia and Ib, which are very similar, may be positive and negative branches, but considers them more probably electronic doublets.

IDENTIFICATION OF FLUORESCENT LINES IN THE ABSORPTION SPECTRUM

It has occurred to the writer, however, that there are good reasons for identifying these series Ia and Ib with the *R* and *P* branches which are required by the Lenz theory in the band which excites the fluorescent series ν_0 , ν_0^* , ν_0' and ν_0'' . These series, which all have $\gamma=0$, must according to Kratzer and Sudholt's equation^{17, 18}

$$\begin{aligned}\gamma_i &= 2\omega^{0''}x''(\bar{n}_i - \bar{n}_0') + \alpha''(\bar{m}_i^2 - \bar{m}_0'^2) \\ &= 1.192(\bar{n}_i - \bar{n}_0') + 0.00012(\bar{m}_i^2 - \bar{m}_0'^2)\end{aligned}\quad (12)$$

all be excited by lines in the same band, which must therefore contain four lines within the broad green mercury line. This is corroborated by calculation of the spacing, near Hg5460, between successive lines of the branch which excites the series ν_0' , from the values of *B*, *C* and \bar{m} of this band published by Kemble and Witmer or from the writer's revised values in this paper. The calculated spacing is¹⁴:

$$d\nu/dm = \pm 2B' + 2C\bar{m} = -0.82 \text{ cm}^{-1} \quad (13)$$

whereas the width of the mercury line is about 1.3 cm^{-1} . Now series Ia and Ib supply the four lines needed, and their spacing is about 7.45 mm on the reproduction, which corresponds to $d\nu/dm = -0.83 \text{ cm}^{-1}$ and agrees well with that just found from data on fluorescence. Moreover the position of the head of the band which excites ν_0' , calculated from fluorescent data, using Eq. (a), footnote 14, and Eq. (10) and the approximation $\rho' - \rho'' = 0$, is 18323, while the head of the series Ia and Ib is, according to Mecke's extrapolation¹⁹ at 18320.9, and by Eq. (3) $\nu_H(26,0)$

¹⁷ I.c., pp. 147 and 150.

¹⁸ Detailed proofs of this equation and of most of the others in this paper are to be found in the writer's Chap. VI of the recent report on "Molecular Spectra in Gases" by a committee of the National Research Council.

¹⁹ I.c., p. 128. Mecke also states that the fluorescent series ν_0 , ν_0^* , ν_0' and ν_0'' are surely excited by the absorption series to which lines 2, 3, 5 and 7 belong; ν_1 and ν_1' by the series containing lines 1 and 6; ν_2 and ν_2' by that containing line 4; and ν_3 and ν_3' by the series containing line 0, which coincides with a satellite of Hg5460. Except for ν_4 and ν_4' these assignments agree with the conclusions of the present paper. But Mecke does not arrive at any assignment of the individual fluorescent series to individual absorption lines.

=18320.97. Moreover line 11 of series Ib is Wood's absorption line 3 which nearly coincides with the narrow green mercury line and certainly excites the fundamental series ν_0' .

Wood has made a number of tentative suggestions, based on experiments in which the exciting light was varied by filtering with bromine vapor, etc., as to which absorption lines account for which fluorescent lines, but neither he nor others²⁰ have considered them conclusive, and as it turns out, many of them are wrong. The ascription of series ν_0' to absorption line 3, about which there can be no doubt, together with Mecke's arrangement of absorption spectrum lines into series Ia, Ib and II, is, however, enough of a start to permit the identification of the lines which excite the other fluorescent series with some certainty.

Series ν_0' and $\nu_0^{*''}$ have a negative doublet interval and their main lines must therefore belong to the *R* branch. It follows that series Ib is the *R* branch and that line Ib 12, the other line in this series within the green mercury line, excites $\nu_0^{*''}$. Lines Ia 11 and Ia 12 must excite series ν_0 and ν_0^* . Since the companion lines of series ν_0 have lower frequency than those of ν_0^* , its exciting line must also be the one with lower frequency, or Ia 12; and Ia 11 must excite ν_0^* . These assignments are checked by the corrected doublet intervals which they yield. The doublet intervals originally reported by Mecke, necessarily based on subtraction of the frequency of the center of the unresolved main line group from those of the observed companion lines, were as follows:

$$\Delta\nu_0 = +3.8 \quad \Delta\nu_0^* = +4.5 \quad \Delta\nu_0' = -5.0 \quad \Delta\nu_0^{*''} = -6.0$$

They should, since they are due to excitation of adjacent lines in the two branches of a single band, be equal in pairs. Now that we have identified the individual main lines of the several series we can use their measured frequencies (see Table II) to find much better values of the zero order $\Delta\nu$'s which are as follows:

$$\Delta\nu_0 = +4.4, \quad \Delta\nu_0^* = +4.3, \quad \Delta\nu_0' = -5.0, \quad \Delta\nu_0^{*''} = -5.2$$

It will be seen that they are very nearly equal in pairs, as they should be.

It is natural to expect that the next strongest absorption series in the λ5460 region will be the *R* and *P* branches of the band (27,0) which excites the fluorescent series ν_1' and ν_1 . The spacing between successive lines in either branch of this series, calculated as above, should be 2.11 cm^{-1} , whereas Mecke finds the single series, II, with a spacing of 10.0 mm corresponding to 1.12 cm^{-1} , or about half what one should expect. The natural conclusion is that alternate lines of this series II belong to the *R*, the others to the *P*, branch. Lines II 12 and II 11,

²⁰ Mecke, l.c., p. 127.

TABLE II
Identification of the zero order fluorescent lines on Wood's absorption spectrum reproduction

Series	Branch	Wood's number	Mecke's number	Exciting (main) line position on reproduction	$\nu - F(0)$	magnetic rotation	Branch	Wood's number	Companion line $\nu - F(0)$	Mecke's number	position on reproduction
ν_0^*	P	5	Ia 12	73.5	-0.53	+++++	R	5	+3.9	Ib 6	34.5
ν_0^*	P	2	Ia 11	66.4	+0.26		R	4	+4.6	Ib 5	28.3
ν_1	P	6	II 12	74.9	-0.68		R	3	+11.4	off	off
ν_1	P	4		70.4	-0.18		R	2	+16.1	.	.
ν_2	P	5		73.5	-0.53		R	1	+18.8	off	off
ν_3	P	3		68.7	0.00		P	7	-5.0	Ia 17	114.5
ν_0'	R	7	Ib 11	76.2	-0.83		P	8	-6.1	Ia 18	123.5
ν_0^*	R	1	II 11	64.9	+0.45		P	9	-12.2	II 22	178.6
				66.4	+0.26				-19.6		off

which are the two lines of this series within the green mercury line, should be assigned to series ν_1 and ν_1' respectively (and not vice-versa), because this gives corrected doublet intervals in the zero order, $\Delta\nu_1 = 12.0$ and $\Delta\nu_1' = -12.7$, which agree well with those in higher orders (see Fig. 7), while the alternative assignment gives $\Delta\nu_1 = 10.9$ and $\Delta\nu_1' = 11.6$, which do not.

Series ν_2 is assigned by Wood to absorption line 4 because it is the first new series to come out when the narrow mercury line, which lies between absorption lines 3 and 4, is broadened, either by raising the potential from 30 volts, which excites only the fundamental series, to 60 volts, or by using end-on emission. We can now be sure of this point because line 4 is the only absorption line shown on the reproduction, which has not been assigned by Mecke to his series Ia, Ib or II. Line 4 consequently belongs to the *P* branch of band (28,0) since ν_2 has a positive doublet interval. Mecke's series ν_2' is probably illusory. It is based on only 5 main lines and no companion lines, although the intensity of the two companions of a doublet should be equal unless they happen to be unequally reabsorbed. Moreover all the supposed main lines fit about equally well into other series. This point is confirmed by the writer's work on absorption bands in this region, described below, wherein it

is found that no line of the *R* branch of band (28,0) lies within the broad green mercury line.

No more lines within Hg5460 are left to account for series ν_3 and ν'_3 , but the writer's absorption measurements on band (29,0) show that a line on its *R* branch coincides with line 2 and one on its *P* branch with line 5. See Fig. 6. The above assignments are summarized in Table II.

Having identified the main lines in the absorption spectrum it is easy to pick out the corresponding companion lines by adding or subtracting the known doublet interval. The resulting correspondence is also shown in Table II. The fact that both main lines in the Ib series turn out to have companion lines in the Ia series, and vice versa, and that the companion line of II 11, an odd numbered line, is II 22, an even numbered line, is a good check on our interpretation of these three series.

Wood²¹ has investigated the rotation of the plane of polarization of mercury arc light passed through iodine vapor parallel to a strong magnetic field, and has reported that, for five of the absorption lines 1-7, the rotation is as shown in the seventh column of Table II. Here a + sign indicates the normal direction of rotation, the same as for the *D* lines of sodium. It will be seen that we have been forced to assign to a *P* branch every line which shows + magnetic rotation and to an *R* branch the line which shows - magnetic rotation. The apparent partial exception in line 2, which shows a + rotation and has been assigned to the *P* branch of band (26,0) and to the *R* branch of band (29,0), is accounted for by the faintness of the (29,0) lines this far from the origin. This result, by its regularity, tends to confirm our assignment of absorption lines. It may also be of value as a check on any proposed theory of the Zeeman effect in band spectra.

NEW ABSORPTION MEASUREMENTS: HALF QUANTUM NUMBERS

Having identified in the absorption spectrum both lines of the fluorescent doublets, we know which lines in the *R* and *P* branches of bands (26,0), (27,0), (28,0) and (29,0) have the same m' , and can easily deduce which have the same m'' . That is, we know the values of m' except for a single additive constant for each band; and similarly we know the values of m'' except for a possibly slightly different additive constant in each band. Thus (see Table II), lines Ia 17 and Ib 11 are the *P* and *R* branch components of the fundamental doublet of zero order, and must

²¹ Wood, Researches II, pp. 85-94; Wood and Ribaud, Phil. Mag. 27, 1009-1018 (1914). The magnetic rotation spectrum was made with vapor of high density and disclosed the existence of a new absorption line, 4', which does not show on the reproduction.¹⁶ This line has not yet been assigned to any band.

have the same m' . If one denotes m' in the P branch by $m'=a+A'$, where a is Mecke's arbitrary numbering, it then follows that in the R branch $m'=b+6+A'$. Similarly lines Ia 16 and Ib 12 must have the same m'' and if in the P branch $m''=a+A''$ then in the R branch $m''=b+4+A''$. It can easily be verified, by reference to Table II, that these equations also assign equal values of m' to both components of the doublets $\Delta\nu_0$, $\Delta\nu_0^*$ and $\Delta\nu_0^{**}$. We are now in a position to plot the frequency differences,¹⁴

$$\nu_R(m') - \nu_P(m') = 4B''(m_R'' + 1) = \nu_b(b) - \nu_a(b+6) = 4B''(b+5+A'')$$

and

$$\nu_R(m'') - \nu_P(m'') = 4B'(m_R' - 1) = \nu_b(b) - \nu_a(b+4) = 4B'(b+5+A'), \quad (14)$$

against Mecke's arbitrary R branch numbering, b ; to find $4B''$ and $4B'$ from the slopes of the graphs; and to determine A'' and A' and hence the absolute numbering of the lines from the points at which the frequency differences extrapolate to zero.

The writer did this at first using the wave-lengths of the fluorescent lines as reported by Wood to determine the scale of his absorption spectrum reproduction, on which companion lines are lacking. The values of B'' and B' so obtained, while they agreed satisfactorily with those calculated, as explained below, from the constants of the fluorescent series, could hardly be trusted to more than a few percent, since they depended on measurements made on a printed reproduction, which may have become distorted, which covered a very short region of the spectrum, and whose scale had to be found from fluorescent data of only moderate precision.

Much better results have, however, been obtained by analyzing some new plates of the iodine absorption spectrum taken with a 20 foot spectrograph by Wood and Klingaman for a forthcoming paper²² and kindly made available to the author in advance of publication. Starting from the lines picked out by fluorescence it has already proved possible to identify with certainty some 100 or 200 lines in each of several bands overlapping the green mercury line. The complete results of the analysis, which is still in progress, will be published later. But Fig. 4 represents the frequency differences (14), for band (26,0) plotted against b ; and their linear extrapolation to locate the origin of absolute numbering. It is apparent from the graph that the lines cannot intersect the axis at integral values of b . The equations of these graphs have been determined by least squares from the frequencies of many more lines than are plotted

²² Wood and Klingaman, Phil. Mag. (in press).

in Fig. 4; including those of several other bands, some of which were followed to values of m as high as 150. For these bands m^3 terms had to be added to Eqs. (14). The constants of interest here are:

$$\begin{aligned}
 B'(29) &= 0.023368 \pm 0.000005 & A' &= 17.5 \\
 B''(0) &= 0.037300 \pm 0.000003 & A'' &= 18.551 \pm 0.055 \\
 C(29, 0) &= -0.013932 & m''_H(Eq. 10) &= 1.677 \\
 I'(29) &= 11.83 \times 10^{-38} \text{ g. cm}^2 & r'(29) &= 3.37 \times 10^{-8} \text{ cm} \\
 I_0'' &= 7.42 \times 10^{-38} \text{ g. cm}^2 & r_0'' &= 2.66 \times 10^{-8} \text{ cm} \\
 I_0' &= 9.51 \times 10^{-38} \text{ g. cm}^2 & r_0' &= 3.01 \times 10^{-8} \text{ cm}
 \end{aligned} \tag{15}$$

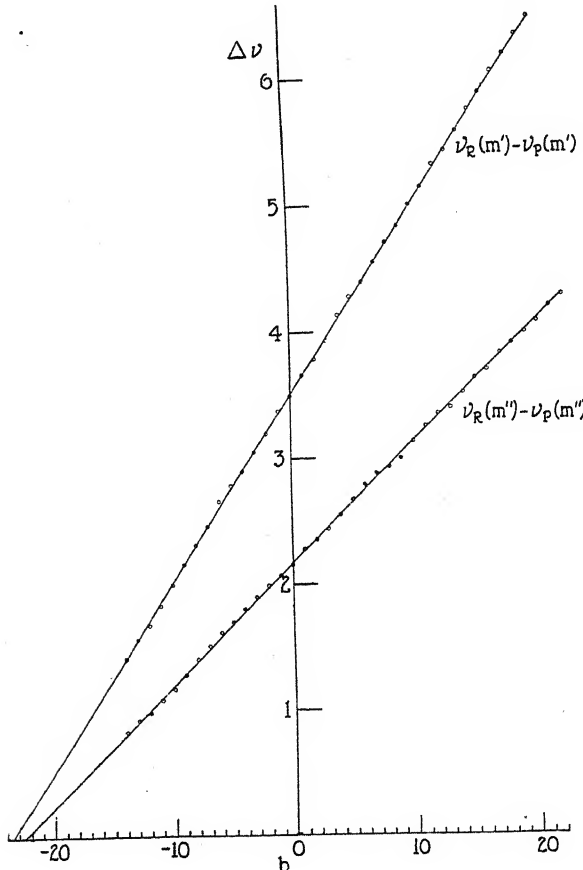


Fig. 4. Determination of the m' 's, m'' 's, B' and B'' for band (26,0).

These values of A' and A'' , or those of m' and m'' which are deduced from them and which are given in Table II together with those similarly deduced from other bands, are evidence for the doctrine of half quantum numbers; or at least definitely disprove the earlier hypothesis of integral

numbers, and are consistent with that of half-integral ones. They may perhaps be considered as direct evidence as any yet available on this point, since the assignment of the same m' to both members of a fluorescent doublet is indisputable. Because the computed m 's are half integers within their probable error, they have for simplicity been taken as exact half-integers in the writer's further analysis of the absorption bands, though slight deviations from half integers have been found in the bands of other substances.

TABLE III
Results of new absorption measurements

Band	i	m'	\bar{m}	frequency of companion line in absorption	frequency of companion line in fluorescence
(26,0)	0	29 ₁ ¹	30 ₂ ¹	18311.37	18311.4
	0*	28 ₂ ¹	29 ₁ ¹	18312.04	18312.1
	0'	34 ₂ ¹	33 ₂ ¹	18302.36	18302.5
	0*''	35 ₂ ¹	34 ₂ ¹	18301.36	18301.4
	1	80 ₂ ¹	81 ₂ ¹	18318.82	18318.9
(27,0)	1'	85 ₂ ¹	84 ₂ ¹	18295.22	18295.3*
	2	108 ₂ ¹	109 ₂ ¹	18323.45	18323.6
(28,0)	2'			none	none
	3	129 ₂ ¹	130 ₂ ¹	18326.23	18326.3
	3'	134 ₂ ¹	133 ₂ ¹	off plate	18287.9

*Wood gives 18294.8. The value in the table is from a remeasurement of his reproduction.

The measured frequencies, in the region covered by the zero order fluorescent group, of the absorption lines of the four bands, (26,0), (27,0), (28,0) and (29,0), which account for Mecke's fluorescent series, are plotted in Fig. 5 against the computed values of m' . The observed fluorescent doublets are also indicated, so that this figure serves to show the relationship between these doublets and the absorption spectrum. It will be seen that the requisite lines within Hg5460 have been found in these bands to account for all Mecke's fluorescent series except v_2' ; and reasons have been given for believing that this one is illusory. Band (30,0) is also plotted in Fig. 5 and it is evident that it contains no line within the wide green mercury line; which explains why there are no series v_4 and v_4' . It is perhaps worthy of note that the characteristic of band (27,0) which led Mecke to assign the lines of both branches to the single series II, i.e., the falling of the lines of one branch midway between those of the other, is part of the general picture. This can be seen by finding the vertical distance between the R and P branches of each band in Fig. 5. This quantity which might be written $m_R'(\nu) - m_P'(\nu)$ is 5.64, 5.50, 5.35, 5.20 and 5.07 for the bands (26,0) to (30,0) respectively. It changes regularly from band to band but happens to be exactly a half

integer for band (27,0), giving rise to the misleading appearance of this particular band. In fact, the analyses of bands (29,0), (30,0) and others in which fluorescent lines had not been identified, were started by making approximate extrapolations for $m_R'(\nu) - m_P'(\nu)$.

NEW FLUORESCENT SERIES WITH ANTISTOKES MEMBERS

The fundamental series of doublets definitely does not extend into the antistokes region, since prolonged exposures made by R. W. Wood with Cooper Hewitt excitation, though they brought out the positive orders with great intensity, failed to show any trace of the fundamental doublet series in the negative orders. It follows that the \bar{n} of the fundamental

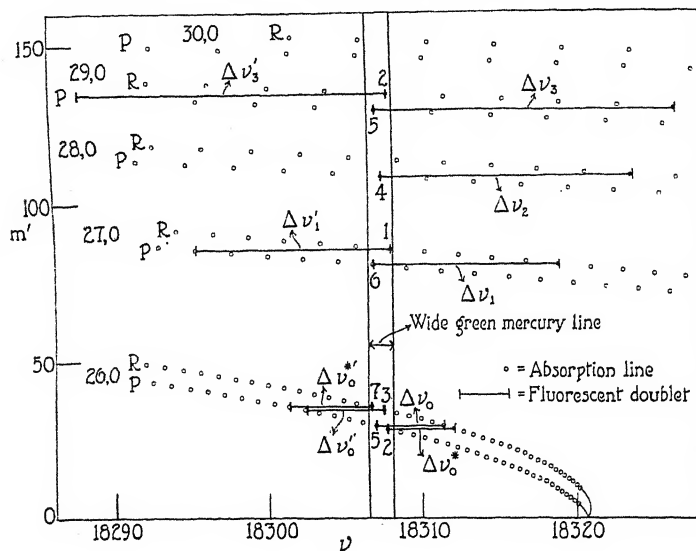


Fig. 5. Relation of the fluorescent doublets in the zero order of Mecke's series to their absorption bands.

series, i.e., the number of vibrational quanta which the molecules concerned in its emission possessed before excitation, must be the minimum possible value of n , presumably 0 or $\frac{1}{2}$. And, since Kratzer and Sudholt have proved that all Mecke's fluorescent series have the same \bar{n} , it follows that none of them can have antistokes members. The question then arises as to the origin of the group of five lines in the -1 order of the spectrum excited by the quartz lamp; and whether there are any lines in other orders which belong to the same fluorescent series. Wood does not record the wave-lengths of these lines, but they appear clearly on his reproduction.²³ The writer has measured them from the repro-

²³ R. W. Wood, Researches in Physical Optics II, Plates II m and y; Phil. Mag. 35, 236-252 (1918), Plate VII m .

TABLE IV
Lines of new fluorescent series, and corresponding absorption lines

Order	Fluorescent Lines			Band	Absorption Lines	
	-1	0	2		(29,0)	(29,1)
Doublet	$\nu - F(-1)$	$\nu - F(0)$	$\nu - F(2)$	$\nu - F(3)$	m' 45_1^1 P	$\nu - F(-1)$ -1.01 R
high		+0.25	+2.75	+4.2		+0.26 #2
1st low	-1.7	+0.75	+3.25	+4.8		+0.70 #0
2nd low		-0.35	+2.15	+3.5		-0.68 #6
high	+6.0	+7.2	+9.55	-4.15	51_1^1 45_1^1 P	+7.77
1st low	-7.8	-6.6	-8.25	-5.55	50_1^1 51_1^1 P	-8.08
2nd low	-9.6	+12.9?	+11.0	+16.65?	51_1^1 R	-9.60
unidentified						-8.31
high						

ductions and they are given in the third column of Table IV and plotted in Fig. 1. The accuracy is less than for the positive order lines which Wood measured on his plates. It is obvious from Fig. 1 that they do not, as they should not, belong to any of Mecke's series, which are indicated by continuous lines. On the reproduction the similarity of this group to the +2 group is striking; and also significant because the fundamental doublets are too faint to appear in the +2 order, and it is therefore likely that no lines belonging to Mecke's series will be found there, and that all the +2 lines belong to series containing antistokes members. On drawing straight lines, in Fig. 1, through the corresponding lines of groups -1 and +2 it is evident that several of them hit previously unassigned lines in higher orders, and very probably represent new fluorescent series. Three plausible new series of doublets can be identified, their main lines being resolved in the 2nd and 3rd orders, though appearing as a single strong hazy line in the reproduction of the -1 group. They are represented by approximately parallel lines with a γ of about 1.38. Computing \bar{m} roughly from the doublet interval and the constants which have been found for bands in this region by Eq. (14) and substituting in (12) it is evident that $\bar{n} - \bar{n}_0' = 1$, and that these series are excited by a band whose $n'' = 1$, and end in the -1 order. One can also use these \bar{m} 's in Eq. (a), footnote 14, and Eq. (10) to find the frequency of the head of the band to which they belong. The results identify

it as band (29,1) whose head calculated by (3) is at 18340.6 cm^{-1} . This identification is amply confirmed by the writer's measurements of the line frequencies of bands (29,1) and (29,0) on Wood and Klingaman's plates. One line in the *P* branch of (29,1) and one in its *R* branch are covered by the mercury line itself, and another *R* branch line is Wood's absorption line 0 which coincides with a satellite. These correspond to the one doublet with companion line on the high frequency side and the two with the companion lines on the low side. The frequencies of the lines in this band which have the same m' as the three lines which coincide with the green mercury line and its satellite, are given in Table IV, column 10. It will be seen that they are sensibly equal to the frequencies, in column 4, of the zero order lines in these new fluorescent series. The latter, which are apparently too faint to appear in fluorescence, were interpolated; in the case of the companion lines, by drawing straight lines in Fig. 1 between the corresponding points in the -1 and $+2$ orders; in the case of the main lines, by drawing lines through the 3 points representing the main lines of the $+2$ order, parallel to those just drawn through the companion lines. Moreover, the absorption lines of band (29,0) which have the same m' 's as those tabulated from band (29,1) agree with the fluorescent lines in the -1 order, as will be seen on comparing columns 9 and 3. These new series can consequently be safely identified as $\nu(n', m') = \nu(29, 45\frac{1}{2})$, $\nu(29, 50\frac{1}{2})$ and $\nu(29, 51\frac{1}{2})$.

Fig. 6, which is similar to Fig. 5, shows the relation of these (interpolated) zero order fluorescent doublets to the absorption spectrum. The constants of the new series are included in Table V. They are represented by the broken lines in Fig. 1.

The lines of band (29,1), which are rather faint near Hg5460, coincide with two of the six lines for which Wood has observed the magnetic rotation. A line on the *P* branch coincides with line 2, whose magnetic rotation is normal, and this agrees with the rule stated above. A line on the *R* branch, however, coincides with line 6, whose magnetic rotation is also normal, and this would constitute an exception to the rule were it not that line 6 has also been assigned to the *P* branch of band (27,0) which is much stronger.

NEW EQUATIONS FOR THE FLUORESCENT SERIES

The identification of the zero order fluorescent lines of Mecke's series in the absorption spectrum which can be much more accurately measured makes possible a considerably improved version of the Eqs. (2); for it precisely fixes one point on each line in Fig. 1. This is of particular importance in the case of the main lines, all of which Mecke of necessity

put through the origin, i.e., the center of the unresolved group, but which can now be sent through their appropriate absorption lines. It is also of assistance in the unresolved main line group of higher orders in the ν_0 , ν_0^* and ν_0^{**} series, which can be assumed to be arranged in about the same manner in the first few orders as in the zero order. The revised equations are of the form

$$\nu = F(p) + \epsilon + \gamma p + (d - \eta p) \quad (16)$$

where, as in (2), the quantities in parentheses are the doublet intervals, and if omitted or included give the main or companion lines series

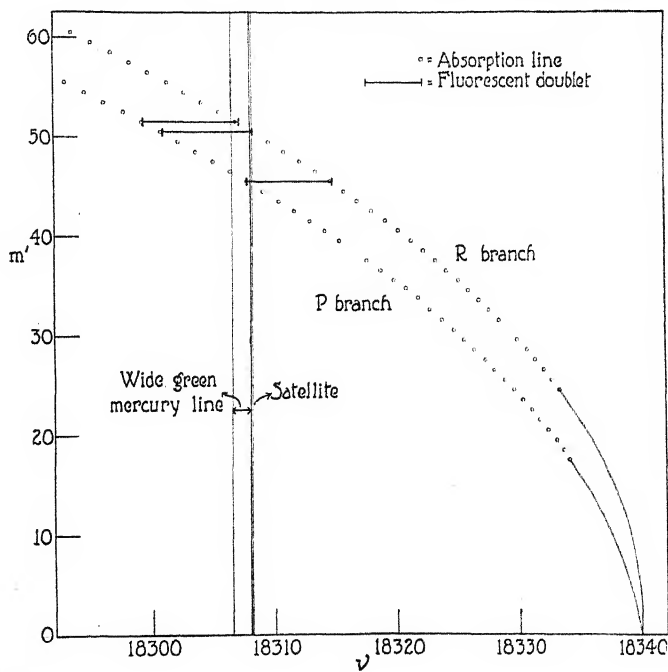


Fig. 6. Relation of the interpolated zero order fluorescent doublets of the three new series to band (29,1).

respectively. The constants of these equations are given in Table V. They are represented by the lines in Fig. 1. The terms ϵ_i are the frequencies of the absorption lines which excite the various series, relative to $F(0) = 18307.50$. The terms d_i are the doublet intervals in the zero order, taken from the absorption measurements. Mecke's γ_i 's have been retained as they are large enough to have been determined with accuracy. Kratzer and Sudholt published values of η_i , which represents the decrease of the doublet separation in higher orders, and computed the constant B_0'' from them, though only to perhaps 20 percent. But, because it is

TABLE V
Constants of the fluorescent series

Series	From fluorescence		From absorption			γ (Eq. 12)	$\eta = d\alpha''/B_0''$
	Empirical	γ	Empirical	ϵ	d		
ν_0	0.00	.025 ± ?	-0.53	+ 4.40	-0.02	.014	
ν_0^*	0.00		+0.26	+ 4.28	-0.03	.013	
ν_1	0.66	.062 ± .015	-0.68	+12.00	0.66	.039	
ν_2	1.33	.052 ± .006	-0.18	+16.13	1.30	.052	
ν_3	1.95		-0.53	+19.26	1.91	.062	
ν_0'	0.00	.021 ± .003	0.00	- 5.14	0.00	.017	
$\nu_0^{* \prime}$	0.00		-0.83	- 5.31	0.01	.017	
ν_1'	0.75		+0.45	-12.73	0.72	.041	
ν_3'	2.2		+0.26	-19.9*	2.00	.064	
$\nu(29,45\frac{1}{2})$	1.39		+0.26	+ 6.78	1.32	.022	
$\nu(29,50\frac{1}{2})$	1.38		+0.70	- 7.50	1.35	.024	
$\nu(29,51\frac{1}{2})$	1.35		-0.68	- 7.63	1.36	.025	

*from fluorescence.

possible to make somewhat better estimations of the variation in the doublet interval, now that the doublet interval of zero order is precisely known, the writer has thought it worth while to repeat their calculations. The intervals of all fluorescent doublets, of which both members can be

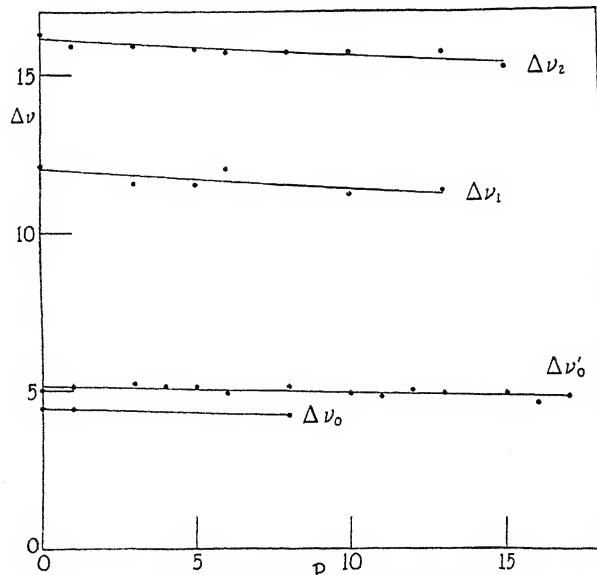


Fig. 7. Revised determination of η .

assigned to series without ambiguity, are plotted against p in Fig. 7. The lines which represent them have been put through the zero order $\Delta\nu$'s as measured in absorption and their slopes, η , determined by least squares. Nevertheless the mean value of $B_0'' = \alpha''d_i/\eta$; calculated from

them, using the revised $\alpha''=0.00012$, is 0.031 ± 0.003 and differs by twice its probable error from that in (15).

The results of the absorption measurements may now be used to calculate theoretically the constants of the fluorescent series. The d 's and e 's have, of course, already been taken from absorption data. The γ 's can be calculated from Eq. (12), taking the \bar{m} 's from column 4 of Table III, using the revised $\alpha''=0.00012$, and setting $\bar{n}_i - \bar{n}_0' = 0$ for all Mecke's series. For the new series extending to the -1 order, $\bar{n} - \bar{n}_0' = 1$; and $2\omega_0''x''$ can be taken from comparison of (4) with (3) as 1.19. The γ 's so calculated are given in column 6 of Table V, and are in excellent agreement with the observed values in column 2. The η 's calculated from the equation^{17,18}

$$\eta = d\alpha''/B_0'' \quad (17)$$

are given in column 7 and the agreement with observation is about as good as could be expected in a quantity so difficult to measure.

The first published estimate of the important constant B_0'' , which yields the moment of inertia of the unexcited iodine molecule, was Kratzer and Sudholt's value 0.032, based on the inaccurately determined quantities η_i . This was bettered by Kemble and Witmer who showed that it could be calculated from the quantities d_i , γ_i and α'' which are more accurately known. They published a weighted mean value of $B_0''=0.0343$, computed from Mecke's original d_i 's (2) and α'' . The writer²⁴ has also calculated this quantity with essentially the same equations as Kemble and Witmer, but using the revised α'' and values of d_i , which had been revised in accordance with the identification, on Wood's absorption spectrum reproduction, of the main lines of the zero order fluorescent group. The values calculated from the various fluorescent series agree well among themselves and the mean value, $B_0''=0.0367$ is probably as good a one as can be extracted from the data already published by Wood and Mecke.

Of course the value $B_0''=0.037300$ found from the writer's measurements of Wood and Klingaman's new absorption plates is very much more precise, but this also depends on the fluorescent spectrum, which furnished the clues without which the absorption spectrum could not have been unravelled.

²⁴ For the equations and details of this calculation the reader is referred to the writer's Chap. VI of the National Research Council Committee report on "Molecular Spectra in Gases." The precision gained by using the revised d_i 's is particularly apparent on comparing the discordant values of m''_H calculated by Kemble and Witmer and given in their Table III, with those in Table III of Chap. VI.

The most important conclusion of this paper is that the complex fluorescent spectrum excited by the quartz arc confirms, in every detail, the theory advanced by Lenz to account for the simple spectrum excited by the Cooper Hewitt arc.

NEW YORK UNIVERSITY,
Sept. 18, 1926.

ABSORPTION COEFFICIENT OF HELIUM FOR ITS OWN RADIATION

BY A. WOLF AND B. B. WEATHERBY

ABSTRACT

The absorption coefficient of helium for its own radiation in the extreme ultra-violet was measured for various pressures. In the range of pressure from 0.016 to 0.040 mm Hg the mass absorption coefficient was found to be 1.24×10^7 . For lower pressures the mass absorption coefficient increases rapidly with decrease in pressure.

INTRODUCTION

THE coefficient of absorption of gases for their own radiation is a subject of great importance in atomic theory. It is related both to the lack of sharpness of spectral lines and to the duration of the excited state of the atom. For a theoretical discussion of this subject reference may be made to an article of A. E. Milne.¹ Other recent contributions are by Hughes and Poindexter² (the determination of the absorption coefficient of helium) and by Goos and Meyer³ on the resonance radiation of mercury.

The object of our experiments was to determine the absorption coefficient of helium for its own line $1S-2P$ of wave-length 584.4A.

Lyman⁴ found that when the helium spectrum is excited by a continuous current discharge the line $1S-2P$ is by far the strongest shown on the plate. In addition to this line, only the principal series lines $1S-mP$ are strongly excited. If therefore we produce radiation in helium by electronic bombardment at a voltage lower than the excitation potential of the line $1S-3P$, we can expect that practically all the radiation will have the wave-length 584.4A. There is a further advantage in working with low voltage excitation since, even in the absence of any definite information on the subject, it is to be expected that spectral lines excited by low voltage electronic bombardment in a gas at low pressure will be sharp. This is of some importance because it is well known that absorption of resonance radiation varies greatly over the range of wave-lengths usually called a spectral line.

¹ A. E. Milne, Phil. Mag. 47, 209 (1924).

² Hughes and Poindexter, Phys. Rev. 23, 769 (1924).

³ Goos and Meyer, Zeits. f. Physik 35, 803 (1926).

⁴ Lyman, Astrophys. J. 60, 1 (1924).

APPARATUS AND METHOD

The method was essentially the following: Radiation was allowed to pass through a tube filled with helium and to fall on a nickel disk connected to a sensitive electrometer. The photo-electric current was measured by noting the time necessary for a given electrometer deflection and the intensity of radiation was assumed to be proportional to this current. The gas was then pumped out and the photo-electric current measured again. The ratio of the two currents was assumed to be equal to the ratio of the respective intensities of radiation. Although it is true that the photo-electric sensitivity of nickel may vary with pressure of gas, the fact that the ratios obtained under certain conditions were independent of the heat treatment of the nickel disk in vacuum shows that the variation is small.

Let d be the length of the absorption tube and I_2 and I_1 the respective photo-electric currents, then the linear absorption coefficient α can be computed from the relation

$$\alpha = (1/d) \log_e (I_2/I_1) \quad (1)$$

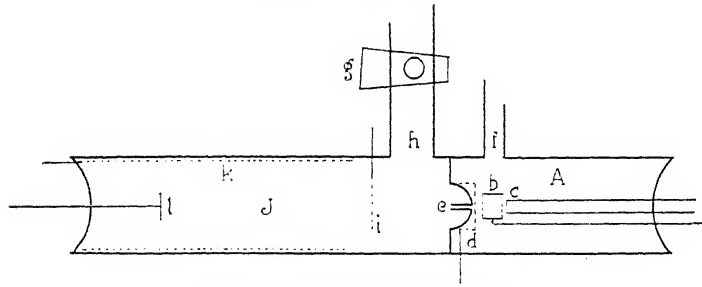


Fig. 1. Diagram of apparatus.

Since no material is known, which transmits radiation of the short wave-length investigated, it was necessary to introduce the radiation into the absorption tube through a fine capillary. The details of construction of the tube will be apparent from Fig. 1. In part A , electrons from the tungsten filament c (0.18 mm diameter) were accelerated by means of a suitable voltage applied to the nickel cylinder b (2 cm in diameter and 2 cm long). These electrons excited radiation inside the cylinder by collision with helium atoms. A fine nickel gauze d (mesh 70) was kept at -14 volts with respect to the negative end of the filament in order to prevent electrons from reaching the absorption tube J . Radiation passed into the absorption tube through a capillary tube e (1 mm in diameter and 1.2 cm long). A nickel disk l (18 mm diameter) was connected to the electrometer which served for measuring the

intensity of radiation. The collecting electrode k was kept at +10 volts. A grid of tungsten wire i , kept at -18 volts, collected any positive ions that might be present.

The absorption tube J was connected by glass tubing of large diameter with a set of mercury vapor diffusion pumps. A large bore stop-cock g made it possible to change the pressure in J . The high pressure side of the mercury vapor pumps was in turn connected with A . Three liquid air traps with charcoal at the bottom were placed between the pumps and A to insure the purity of helium when it was circulated. A liquid air trap and a tube with charcoal immersed in liquid air was also interposed between g and J . This is not shown in the diagram. The whole apparatus could be evacuated by another set of mercury vapor pumps backed by a Cenco oil pump.

The electrometer used in the experiments was of the Compton type. With 96 volts on the needle it had a sensitivity of 4400-9000 scale divisions per volt, depending on adjustment. The scale distance was 1.4 meters. As it was unnecessary to know the sensitivity it was tested only occasionally and used for computing the order of magnitude of the photo-electric currents obtained.

The tube was baked for several hours before readings were taken and the nickel cylinder b and disk l were out-gassed by means of an induction furnace. The helium was purified in a tube with charcoal immersed in liquid air before being admitted to the apparatus. A series of readings was then taken at various pressures.

The measurement of the absorption coefficient itself consisted mainly in the following procedure. Stop-cock g being kept closed, the radiation was excited in A and the photo-electric current to l was measured. Under these conditions the pressure in A and J was the same. Consequently, radiation leaving the capillary was partially absorbed before reaching l . Stop-cock g was then opened and the photo-electric current measured again. With the arrangement of apparatus that was used, the pressure in the absorption tube then dropped to $1/30$ its former value while that in A remained nearly constant. Radiation leaving the capillary was therefore the same, but, as the absorption in J was less, the photo-electric current was greater. The linear absorption coefficient was then evaluated with the aid of Eq. (1).

As there was a drop in pressure along the capillary, the length d in Eq. (1) was measured from the nickel disk l to the mid-point of the capillary. It was found to be 16.5 cm. The correction to be added to the voltage applied to b , to take account of initial electron velocities and contact potential differences, was determined by plotting the voltage

current curve for b and noting the ionization voltage. The current to b used in these experiments was about 10^{-3} amp. The order of magnitude of the photo-electric currents was 10^{-14} amp. The electrometer leakage current was also observed during the experiments and, whenever necessary, the measurements were corrected for this effect.

RESULTS

The linear coefficient of absorption α divided by the pressure in the absorption tube expressed in mm Hg gives a quantity β which is obviously proportional to the mass absorption coefficient, as all measurements were

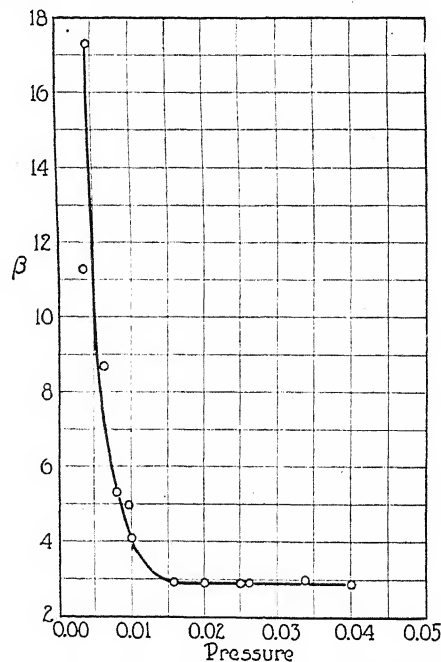


Fig. 2. Absorption coefficient as function of pressure.

taken at room temperature. The quantity β is also proportional to the contribution of individual atoms to absorption.

Fig. 2 gives the results of observations taken. The quantity β is here plotted against pressure. If the radiation could be regarded as monochromatic and if the probability of absorption of individual atoms did not depend on pressure or on the molecular fields of other atoms, β would be constant. From the diagram, however, it is seen that below a pressure of 0.016 mm Hg β increases rapidly with increasing pressure. In the range of pressure from 0.016 to 0.040 mm Hg β is constant within the errors of observation.

Its mean value in this range was computed from the following observations:

p :	0.040	0.034	0.026	0.025	0.020	0.020	0.016
β :	2.89	3.00	2.92	2.92	2.87	2.86	2.97
mean 2.92 ± 0.05							

These values were obtained with 22 volts applied between the negative end of the filament and the nickel cylinder. As the correction to be applied varied between 0 and +0.7 volt, this is seen to be well below the excitation potential of the line $1S - 3P$ which is 22.97 volts.⁵

The values of β for lower pressures are less accurate than for pressures above 0.016 mm Hg. The reasons are, first, the relatively greater correction for leakage current, and second, the increased proportion of impurities present. In general, impurities were found seriously to affect the observations and satisfactory results could only be obtained when careful precautions were taken to insure the purity of helium. This applied in particular to the necessity of eliminating mercury vapor.

Measurements were also made with bombarding voltages other than 22 volts. As the cathode was not equipotential, no exact results could be expected. It was however found that when the voltage approached the ionization voltage, the absorption coefficient decreased. At voltages below 21 volts the absorption coefficient was also much less.

INTERPRETATION OF RESULTS

From the method of evaluating the results it follows that they give merely the difference of absorption between helium at a certain pressure and at $1/30$ of that pressure. If absorption were independent of pressure it would be easy to calculate the total absorption coefficient. However, since the absorption coefficient varies with pressure the amount of the necessary correction is uncertain and therefore has not been calculated.

Radiation* entering the absorption tube has already been filtered by passing through a certain mass of gas. The increase of the absorption coefficient for low pressures shows the presence of a component for which the absorption is very strong. The fact that the absorption coefficient was found constant in a considerable range of pressure indicates that sufficiently filtered radiation would have an absorption coefficient independent of pressure. No certain conclusions could however be

⁵ Cf. Sommerfeld, Atombau 4th ed., p. 522.

* The objection might be raised that our results were due to excited helium atoms rather than radiation. Since, however, the electrometer current was very small for bombarding voltages lower than that corresponding to the line $1S - 2P$ and since a constant value of the absorption coefficient hardly could have been obtained if the effect of excited atoms was appreciable, this is not believed to be the case.

drawn as the measurements could not be extended to higher pressures. It should be stressed that the radiation used was always produced with the gas at the same pressure as that for which absorption was measured.

The mass absorption coefficient of the filtered radiation was determined as $(1.24 \pm 0.02) \times 10^7$. The limits of error here given cannot be claimed to have any absolute significance, but merely indicate how closely the measurements could be repeated.

If we wish to regard the individual helium atoms as disks or spheres absorbing all incident radiation of the particular wave-length considered, the diameter of the spheres would be 1.2A. This value is of the same order of magnitude as the diameter of the electronic orbits in helium. For lower pressures however, where the coefficient of absorption is higher, the diameter of the equivalent disk or sphere by far exceeds the diameter of electronic orbits, obviously presenting difficulties for the picture of absorption of radiation given by the theory of light quanta.

We wish to express our thanks to Professor C. B. Bazzoni for advice with regard to construction of apparatus and his interest in this investigation.

RESEARCH SECTION, RANDALL MORGAN PHYSICS LABORATORY,
UNIVERSITY OF PENNSYLVANIA,
PHILADELPHIA.
September 1, 1926.

ELECTRON COLLISIONS IN CARBON MONOXIDE*

BY F. L. MOHLER AND PAUL D. FOOTE

ABSTRACT

Critical potentials for electron impact in CO.—Critical potential measurements for CO are correlated with spectroscopic data. Observed values are: excitation, 5.8, 8.0, 10.1 volts; ionization 14.3 volts. The two lower values were obtained by the partial current method. Band spectra give 6.0, 8.0, 10.34 and 14.2 volts.

Probability of energy losses at electron impact in CO.—Denoting the 6 and 8 volt collisions by *a* and *b* respectively, energy losses corresponding to successive collisions of the type *a*, *aa*, *ba*, *baa*, and *bba* have a high probability while collisions of the type *b* and *bb* are relatively very infrequent. This peculiarity is also observed with the second group metals. The resemblance of CO to the second group metals is in accord with the spectral classification which makes the 6 volt level a 3P state and 8 volt level a 1P state.

SEVERAL years ago the authors obtained critical potential data for CO by use of a four-electrode tube in which the electron path for the most part was in a force free space. Measurements by the Lenard method showed a small effect at 10.1 volts and a large effect at 14.3 volts. Partial current curves indicated the presence of eight or more potentials of inelastic collision between 6 and 30 volts. These were recognized as successive electron collisions in which several molecules were excited to different states. At that time, however, we were unable to determine unambiguously the energies of the states involved, so that, aside from the mere listing of the observed potentials¹ no report of the work has been published.

Recently a fairly complete analysis of the CO band spectrum^{2,3} has been made and, as will be immediately apparent, our data are simply and logically interpretable on the basis of the known energy levels. The results are of more particular interest at the present time in that they furnish information relative to the probability of the different types of excitation.

Fig. 1 gives the energy diagram of the zero vibration states of CO. On the basis of the fine structure of the bands these levels can be designated according to the notation used for atomic spectra.³ As is shown in the figure the CO levels resemble those of a second group atom both in struc-

*Published by permission of the Director of the Bureau of Standards, Department of Commerce.

¹Foote and Mohler, Origin of Spectra, p. 188, (1922).

²Birge and Sponer, Phys. Rev. 28, 259 (1926).

³Mulliken, Phys. Rev. 28, 481 (1926).

ture and in relative energy values. It is to be expected that in general the zero vibration states will give at least approximately the critical potentials for excitation by electron collision though it is known that there may be cases where large vibration changes accompany excitation by electron collision. Duffendack and Fox⁴ give measurements of excitation potentials of the bands of CO and CO⁺ which in general confirm the spectroscopic results for the levels above 10 volts. We include as a broken line in Fig. 1 an additional level for which they find evidence. Our value 10.1 observed by the Lenard method probably measures the photoelectric effect resulting from excitation of the 10.34 volt level. There is good agreement on the

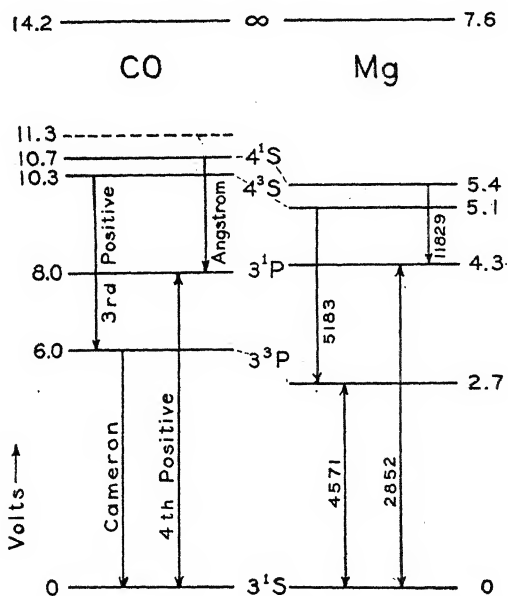


FIG. 1. Energy diagram of the zero vibration states of CO.

value of the ionization potential. Our result is 14.3 volts; Mackay⁵ obtained 14.1⁷ volts by direct measurement, and from excitation potentials of the CO⁺ bands the values 14.2² and 14.3⁴ are derived.

A typical partial current curve is shown in Fig. 2 while Table I, column 1, gives mean values for the potentials of inelastic collision obtained from about 20 curves with gas pressures ranging from .1 to .7 mm. These potentials can be explained by successive electron collisions involving loss of both 6 and 8 volts kinetic energy⁶ corresponding to the first two

⁴Duffendack and Fox, Sci. 64, 277 (1926).

⁵Mackay, Phys. Rev. 24, 319 (1924).

TABLE I
Inelastic collisions in CO

Observed potential*	Theoretical value	Type of collision	Magnitude of effect
6.4	6.0	<i>a</i>	strong
12.3	12.0	<i>aa</i>	medium
14.0	14.0	<i>ba</i>	strong
18.0	18.0	<i>aaa</i>	extremely weak
19.7	20.0	<i>baa</i>	medium
22.3	22.0	<i>bba</i>	medium
25.2	26.0	<i>baaa</i>	
27.7	28.0	<i>bbaa</i>	
30.9	30.0	<i>bbba</i>	weak and poorly resolved

*Cf. Origin of Spectra, p. 188.

excited states of CO. The mean values of the intervals give 5.8 and 8.0 volts. We denote the two types of collision by *a* and *b* respectively, and give in Table I, columns 2 and 3, the computed potentials and the corresponding type of collision. There is fair agreement between computed and observed values and one notes that all combinations of *a* and *b* do not occur. In particular, *b* and *bb* are missing while one might expect them to give a strong effect since *ba*, *baa* and *bba* are pronounced.

An exactly similar phenomenon is observed with metals of the second group.⁶ We include in Fig. 2 a curve obtained in mercury vapor, with a similar tube, which shows a striking resemblance both in the relative intensity of corresponding *a* and *b* combinations and in the absence of higher critical potentials. More refined methods of course show many other critical potentials in mercury but the two potentials here considered determine the general form of the curve.

The characteristic appearance of these curves is explained by the hypothesis that the probability of a collision of type *a* is large when the potential is nearly equal to *a* and decreases with increasing voltage, while the probability for a *b* collision is small at the potential corresponding to *b* and increases with the voltage. Thus, if for CO above 14 volts the *b* collision is much more probable than *a*, with the reverse condition at the lower voltages, precisely the group of potentials listed in the table should predominate. Evidence supporting a similar assumption for the second group metals has been advanced by Eldridge.⁷

On the basis of the spectral regularities, it has been assumed that CO is a structure with two valence electrons in n_1 orbits and the evidence concerning probabilities of electron collisions seems to lend strong support to this viewpoint. It has been argued that the valence electrons, 4 of

⁶Mohler, Foote and Meggers, Bur. Stds. Sci. Paper No. 403, (1920).

⁷Eldridge, Phys. Rev. 20, 456, (1922).

carbon and 6 of oxygen form in CO shells of 8 and 2 electrons giving a structure like magnesium. However, Birge and Sponer² present definite evidence that such an intimate sharing of electrons cannot be expected. An analysis of the vibration states of CO indicates that the molecule may be adiabatically separated into neutral atoms thus suggesting an entirely different electron configuration in which both atoms keep their full complement of electrons. From this viewpoint the striking resemblance of CO

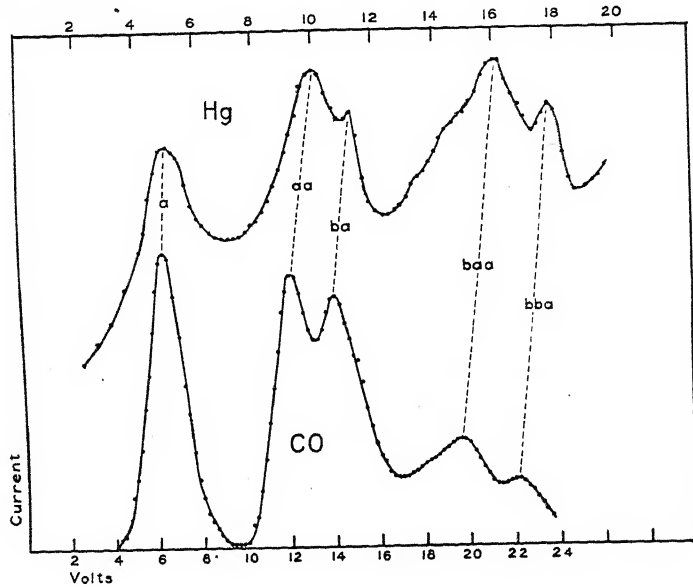


FIG. 2. Comparison of critical potential curves for CO and Hg vapor.

to a second group atom is quite astonishing. It may be noted that while N₂ also contains 10 valence electrons and closely resembles CO in most of its physical properties, yet the partial current curves are not similar. Under comparable experimental conditions N₂ shows a single series of inelastic collisions at intervals of about 8 volts.⁸

BUREAU OF STANDARDS,
WASHINGTON, D. C.
October 28, 1926.

⁸Mohler and Foote, Bur. Stds. Sci. Paper No. 400, (1920).

THE INFLUENCE OF A MAGNETIC FIELD ON THE DIELECTRIC CONSTANT OF A DIATOMIC DIPOLE GAS

By LINUS PAULING*

ABSTRACT

The investigation of the motion of a diatomic dipole molecule in crossed magnetic and electric fields shows that according to the old quantum theory there will be spatial quantization practically with respect to the direction of the magnetic field for experimentally realizable values of the field strengths. As a result of this the old quantum theory definitely requires that the application of a strong magnetic field to a gas such as hydrogen chloride produce a very large change in the dielectric constant of the gas. The theory of the dielectric constant of a diatomic dipole gas according to the new quantum mechanics, on the other hand, requires the dielectric constant not to depend upon the direction characterizing the spatial quantization, so that no effect of a magnetic field would be predicted. The effect is found experimentally not to exist; so that it provides an instance of an apparently unescapable and yet definitely incorrect prediction of the old quantum theory.

I. TREATMENT BY THE OLD QUANTUM THEORY

IN THE present paper we calculate the dielectric constant of a diatomic dipole gas in a magnetic field. We shall defer application of the new quantum dynamics until §II, and commence by employing the old quantum theory even though it is now obsolete. We include treatments by both theories because the difference in the results is very interesting and furnishes additional evidence for the new mechanics, inasmuch as in the old theory the dielectric constant is materially influenced by a magnetic field. This effect, which is absent in the new theory, arises from the fact that with sufficiently strong magnetic fields the direction characterizing the spatial quantization of the rotating molecules will be the direction of the magnetic field instead of that of the electric field. In order to determine the field strengths with which this transition occurs, it is necessary to determine the motion of the gas molecules in crossed electric and magnetic fields. The motion of a diatomic dipole molecule in an electric field has been treated by Hettner¹ and by W. Pauli, Jr.² The equations of motion can in this case be solved by means of the separation of variables. This procedure can also be followed for the motion of the molecule in a magnetic field alone, and in both a magnetic

* Fellow of the John Simon Guggenheim Memorial Foundation.

¹ G. Hettner, Zeits. f. Physik 2, 349 (1920).

² W. Pauli, Jr., *ibid.*, 6, 319 (1921).

and an electric field when the two fields are parallel; it cannot be used for crossed fields, however. The treatment given the problem of crossed fields in this paper is based on the methods of Bohr,³ and is somewhat similar to that given the problem of the hydrogen atom in crossed electric and magnetic fields by Klein⁴ and by Lenz.⁵

We shall for simplicity consider a diatomic molecule without resultant electronic angular momentum as a rigid assemblage of charged mass-points along a line. For our purposes it can be characterized by three quantities, the moment of inertia $A = \sum m_i r_i^2$, the electric moment $\mu = \sum \epsilon_i r_i$, and the electric moment of inertia or quadrupole moment $\kappa = \sum \epsilon_i r_i^2$, in which ϵ_i is the charge and m_i the mass of the i th mass-point, and r_i its distance from the center of mass of the molecule. The detailed consideration of the quantum-allowed states of motion of the

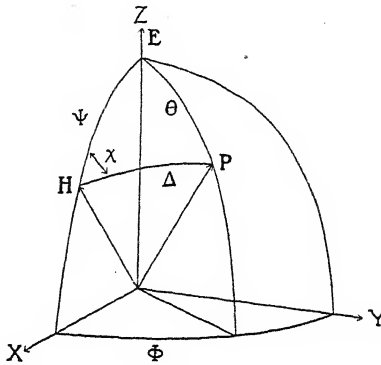


Fig. 1.

molecule given in the appendix of this paper leads to the result that except for terms of the order of magnitude of ω/ω_M the spatial quantization in crossed electric and magnetic fields is the same as for the magnetic field alone; namely, the total angular momentum vector P , of magnitude $p = j\hbar/2\pi$, has a component in the direction of the magnetic field vector H of magnitude $mh/2\pi$, and P further undergoes precessional motion about H with uniform angular velocity. ω and ω_M are given by the equations

$$\omega = 3\mu^2 E^2 A / 2p^3, \quad (1a)$$

$$\omega_M = \kappa H / 2A c, \quad (1b)$$

³ N. Bohr, "On the Quantum Theory of Line Spectra," Part II, Det Kgl. Danske Vid. Selsk. 8, IV, 1 (1918).

⁴ O. Klein, Zeits. f. Physik 22, 109 (1924).

⁵ W. Lenz, *ibid.* 24, 197 (1924).

in which E and H are the electric and magnetic field strengths respectively; $-\omega_M$ is the angular velocity of precession of P about H in the presence only of the magnetic field, and $-\omega \cos \Theta$, in which Θ is the angle between P and the electric field vector E , is the angular velocity of the precessional motion of P about E in the presence only of the electric field.

The dielectric constant of a diatomic dipole gas. Under the influence of an electric field a gas becomes electrically polarized in the direction of the field, the amount of polarization per unit volume being

$$P = \frac{3}{4\pi} \frac{\epsilon - 1}{\epsilon + 2} E = N \bar{\mu} + N \alpha E, \quad (2)$$

in which ϵ is the dielectric constant of the gas, N the number of molecules in unit volume, and α the deformation coefficient or coefficient of induced polarization of the gas. $\bar{\mu}$ is the average value of μ for all molecules in the gas, where $\bar{\mu}$ is the time-average of $\mu \cos \theta$ for one molecule in a given state of motion. An expression for $\bar{\mu}$ applicable to polyatomic molecules in general was obtained by Debye⁶ with the use of classical statistical mechanics; namely,

$$\bar{\mu} = \mu^2 E / 3kT. \quad (3)$$

The interpretation of the oscillation-rotation⁷ and the pure rotation⁸ band spectra of hydrogen chloride required that this result be abandoned; for with the old quantum theory these spectra showed that the rotational energy of the molecule was restricted to the series of values $W = (j^2 h^2) / 8\pi^2 A$, with $j = \frac{1}{2}, \frac{3}{2}, \frac{5}{2}, \dots \infty$. The expression for the dielectric constant of a diatomic dipole gas according to the old quantum theory was derived by W. Pauli, Jr.,⁹ in the following way. For a given molecule the average value of $\mu \cos \theta$ is

$$\bar{\mu} = \frac{\mu}{\tau} \int_0^\tau \cos \theta dt,$$

On substituting for dt its value given in Eq. (32) of the appendix, expanding in powers of $\mu E / \alpha$, and evaluating the resultant integrals by contour integration, one obtains the approximate result

$$\bar{\mu} = \frac{2\pi^2 A \mu^2 E}{h^2} \cdot \frac{1}{j^2} (3 \cos^2 \Theta - 1), \quad (4)$$

⁶ P. Debye, Physik. Zeits. 13, 97 (1912).

⁷ Colby, Astrophys. J. 58, 303 (1923).

⁸ Czerny, Zeits. f. Physik 34, 227 (1925).

in which Θ represents as before the angle between P and E . Assigning equal *a priori* probabilities to all of the possible quantum states characterized by the quantum numbers j and m , we have for the probability of a given state

$$w(j, m) = \frac{e^{-W/kT}}{\sum_i \sum_m e^{-W/kT}}, \quad (5)$$

and for $\bar{\mu}$ we have

$$\bar{\mu} = \sum_i \sum_m w(j, m) \cdot \mu(j, m). \quad (6)$$

When the electric field alone is present this expression can be easily evaluated, for then $\cos \Theta$ is equal to m/j , and

$$\bar{\mu}(j, m) = \frac{2\pi^2 A \mu^2 E}{h^2 j^2} \left(3 \frac{m^2}{j^2} - 1 \right), \quad (7)$$

and

$$\bar{\mu} = \mu^2 EC/kT, \quad (8)$$

with

$$C = \frac{\sum_i \sum_m \frac{1}{j^2} \left(3 \frac{m^2}{j^2} - 1 \right) e^{-\sigma j^2}}{4\sigma \sum_i \sum_m e^{-\sigma j^2}}, \quad (9)$$

in which $\sigma = h^2/8\pi^2 A k T$.

This is the result given by Pauli, who evaluated C by giving j and m integral values and assuming σ to be very small. Values of C as a function of σ have also been published by the writer,⁹ assuming the values $\frac{1}{2}, \frac{3}{2}, \frac{5}{2}, \dots \infty$ for j and $\pm \frac{1}{2}, \pm \frac{3}{2}, \pm \frac{5}{2}, \dots \pm j$ for m .

The influence of a strong magnetic field on the dielectric constant. If in addition to the electric field a strong magnetic field is present, the average value of $\mu \cos \theta$ for a molecule in a given state of motion will no longer be given by Eq. (4). We prove in the appendix that if the magnetic field is so strong that the ratio ω/ω_M is small compared with unity, the spatial quantization is relative to the direction of the magnetic field, about which P undergoes a uniform precession. Accordingly the cosine of the angle Δ between P and H will be equal approximately to m/j . We now have the trigonometric relation

$$\cos \Theta = \cos \psi \cos \Delta + \sin \psi \sin \Delta \cos \chi,$$

in which χ , as shown in the figure, increases uniformly from 0 to 2π during the precessional motion of P about H . From this relation we find

$$\frac{1}{2\pi} \int_0^{2\pi} (3\cos^2 \Theta - 1) d\chi = \left(\frac{3}{2} \cos^2 \psi - \frac{1}{2} \right) (3\cos^2 \Delta - 1),$$

⁹ L. Pauling, Proc. Nat. Acad. Sci. 12, 32 (1926); Phys. Rev. 27, 568 (1926).

and from this on substituting for $\cos \Delta$ its value m/j

$$(3\cos^2\Theta - 1)_{\text{average}} = \left(\frac{3}{2}\cos^2\psi - \frac{1}{2}\right)\left(3\frac{m^2}{j^2} - 1\right). \quad (10)$$

This equation shows that the effective polarization due to one molecule in the state characterized by the quantum numbers j and m is equal to $(\frac{3}{2}\cos^2\psi - \frac{1}{2})$ times its value in the absence of the magnetic field; i.e.,

$$\bar{\mu}_\psi(j, m) = \left(\frac{3}{2}\cos^2\psi - \frac{1}{2}\right)\bar{\mu}(j, m). \quad (11)$$

Since this multiplicative factor is independent of j and m , we may substitute Eq. (10) in (4) and obtain the result

$$\bar{\mu}_\psi = \left(\frac{3}{2}\cos^2\psi - \frac{1}{2}\right) \cdot \frac{\mu^2 E}{kT} \cdot C, \quad (12)$$

in which C has the value given by Eq. (9). We can consequently state that *in the presence of a strong magnetic field making an angle ψ with the electric field the polarization due to permanent dipoles will according to the old quantum theory be $(\frac{3}{2}\cos^2\psi - \frac{1}{2})$ times its value in the absence of the magnetic field.*¹⁰

The old quantum theory accordingly definitely requires that with the magnetic field nearly at right angles to the electric field gases such as hydrogen chloride should show a *negative polarization*, and a *dielectric constant smaller than unity*; the absolute value of the negative polarization should be equal to one-half of the usual positive polarization, except for the relatively small and always positive contribution due to deformation.

In view of the fact that the band spectra do not directly determine the possible values of the quantum number m , it is to be especially emphasized that this result regarding the effect of a magnetic field is completely independent of the assumption of particular values for this quantum number. The value of C , as shown in Eq. (9), does depend on this choice, but the ratio of $\bar{\mu}_\psi$ to $\bar{\mu}$ (Eqs. 12 and 8) is simply $\frac{3}{2}\cos^2\psi - \frac{1}{2}$, and so is independent of C .

It is of interest to consider the magnitude of the magnetic field strength necessary to make ω/ω_M small and so produce this effect. Using for A its value as determined by Czerny⁸ from the pure rotation absorption

¹⁰ This quantitatively predicted effect is not to be confounded with the effect qualitatively predicted by Ruark and Breit, Phil. Mag. 49, 504 (1925), and found experimentally not to exist by Weatherby and Wolf, Phys. Rev. 27, 769 (1926), for their effect involved molecules without a permanent electric moment, such as those of helium, oxygen, and air.

spectrum of hydrogen chloride, for μ the value found from its dielectric constant,⁹ for p the expression $jh/2\pi$, and for κ the estimate -1×10^{-25} E.S.U.,¹¹ we find from (1a,b) that ω/ω_M becomes small when

$$H \gg F^2/10,000j^3$$

in which H is the field strength in gauss, and F the electric field strength in volts/cm. It is at once apparent that this condition can be easily achieved experimentally.

II. TREATMENT BY THE NEW QUANTUM MECHANICS

According to the new quantum mechanics, the spatial rotator is characterized by two numbers j and m , such that j can assume the values $0, 1, 2, 3, \dots \infty$, and m the values $0, \pm 1, \pm 2, \pm 3, \dots \pm j$. The corresponding energy values, in the absence of an external field, are

$$W(j,m) = j(j+1)\hbar^2/8\pi^2A. \quad (13)$$

The energy-levels thus differ from those of the old quantum theory with half quantum numbers only by a constant additive quantity, and are in complete agreement with the infra-red spectral data.

The new quantum mechanics leads to a formula for the dielectric constant of a diatomic dipole gas greatly different from that given by the old quantum theory, as has been shown both by L. Mensing and W. Pauli, Jr.,¹² and by J. H. Van Vleck.¹³ The average polarization due to molecules with a given value of j not equal to zero vanishes, and only those molecules with $j=0$ produce any polarization under the influence of an external electric field. Hence the new quantum mechanics shows in this case much greater similarity to the classical theory than did the old quantum theory; for on the basis of the classical theory only those molecules with very small rotational energy, namely, less than μE , contributed to the polarization,¹⁴ while the old quantum theory stated that no such molecules were present.

The dielectric constant of a diatomic dipole gas. As shown by Mensing and Pauli and by Van Vleck, the polarization excited in a molecule by a static external electric field can be calculated by means of the Ladenburg-Kramers dispersion formula, derived on the basis of the Heisenberg

¹¹ This estimate is substantiated by the fact that Professor O. Stern has recently shown by a very sensitive adaptation of the experiment determining the bending of a molecular stream in a strong inhomogeneous magnetic field that a molecule of water vapor at around 0°C has a magnetic moment of the order of magnitude of 0.001 Bohr magnetons, which corresponds to a quadrupole moment of the order of that assumed for hydrogen chloride.

¹² L. Mensing and W. Pauli, Jr., Physik. Zeits. 27, 509 (1926); also C. Manneback, *ibid.* 27, 563 (1926).

¹³ J. H. Van Vleck, Nature, August 14, 1926.

¹⁴ Alexandrow, Physik. Zeits. 22, 258 (1921).

quantum mechanics by Born and Jordan¹⁵ and of the wave mechanics by Schrödinger,¹⁶ by placing the frequency of the impressed disturbance equal to zero. Placing the Z-axis parallel to the electric lines of force, corresponding to spatial quantization with respect to the electric field, we obtain for the polarization of a molecule characterized by the quantum numbers j and m the expression

$$\bar{\mu}(j, m) = 2\mu^2 E \sum'_{j', m'} \frac{z^2(j, m; j', m')}{h\nu(j, m; j', m')}, \quad (14)$$

in which $z(j, m; j', m')$ represents the term in the matrix z corresponding to the transition $j \rightarrow j'$, $m \rightarrow m'$, and $\nu(j, m; j', m')$ represents the corresponding frequency, considered positive in absorption and negative in emission; the summation is to be extended over all values of j' and m' for which $z(j, m; j', m')$ does not vanish. The values

$$z^2(j, m; j', m') = \frac{(j-m)(j+m)}{(2j-1)(2j+1)} \text{ for } m' = m, j' = j-1 \quad (15a)$$

$$= \frac{(j-m+1)(j+m+1)}{(2j+1)(2j+3)} \text{ for } m' = m, j' = j+1 \quad (15b)$$

$$= 0 \text{ otherwise}$$

have been derived by Mensing¹⁷ and by Dennison.¹⁸ On substituting these values, together with the values of $h\nu$ obtained from the energy-levels given by Eq. (13), we find for $j \neq 0$ the equation

$$\bar{\mu}(j, m) = \frac{8\pi^2 A \mu^2 E}{h^2} \cdot \frac{1}{(2j-1)(2j+3)} \left(3 \frac{m^2}{j(j+1)} - 1 \right). \quad (16)$$

For $j = 0$, however, only the jump with absorption can occur; from (15b) we accordingly find

$$\bar{\mu}(0, 0) = 8\pi^2 A \mu^2 E / 3h^2. \quad (17)$$

Since m does not occur in the energy expression (13), the probability of every value of m , with j constant, is the same. We may consequently find the average contribution to the polarization of molecules in the j th state by simply averaging $\bar{\mu}(j, m)$ as given in Eq. (16) over all values of m . On doing this zero is obtained for every state with j not zero:

$$\bar{\mu}(j) = \frac{1}{2j+1} \sum_{m=-j}^{+j} \bar{\mu}(j, m) = 0,$$

¹⁵ Born and Jordan, Zeits. f. Physik 34, 858 (1925).

¹⁶ Schrödinger, Ann. d. Physik 81, 109 (1926).

¹⁷ L. Mensing, Zeits. f. Physik 36, 814 (1926).

¹⁸ Dennison, Phys. Rev. 28, 318 (1926).

so that only molecules with $j=0$ are effective. From Eq. (5) the probability of this state is

$$w(0,0)=\left(\sum_{j=0}^{\infty} \sum_{m=-j}^{+j} e^{-\sigma j(j+1)}\right)^{-1}, \quad (18)$$

in which σ , as before, is $h^2/8\pi^2AkT$. We thus obtain the result that the total polarization of N molecules is

$$\bar{\mu}_z=N \cdot w(0,0) \cdot \bar{\mu}(0,0)=\frac{\mu^2 E}{3kT} \cdot \frac{1}{\sigma \sum_{j=0}^{\infty} (2j+1) e^{-\sigma j(j+1)}}. \quad (19)$$

For small values of σ ; i.e., for high temperatures, this reduces to the classical equation of Debye.

The dielectric constant in the presence of a magnetic field. We shall next calculate the polarization produced when the electric lines of force are parallel to the X - (or Y -) axis, and the characteristic direction Z of quantization is determined by some other influence, such as a strong magnetic field. We again use Eq. (14), except that for $x^2(j,m; j', m')$ we substitute $x^2(j,m; j', m')$ or $y^2(j,m; j', m')$, with the following values, given by Mensing and Dennison:

$$x^2(j,m; j', m') = y^2(j,m; j', m') = \frac{(j+m+1)(j+m+2)}{4(2j+1)(2j+3)} \quad (20a)$$

for $m'=m+1, j'=j+1$

$$= \frac{(j-m)(j-m-1)}{4(2j-1)(2j+1)} \quad (20b)$$

for $m'=m+1, j'=j-1$

$$= \frac{(j+m-1)(j+m)}{4(2j-1)(2j+1)} \quad (20c)$$

for $m'=m-1, j'=j-1$

$$= \frac{(j-m+1)(j-m+2)}{4(2j+1)(2j+3)} \quad (20d)$$

$= 0$ otherwise.

From 20a, b, c, and d we find for $j \neq 0$

$$\bar{\mu}_z(j,m) = \bar{\mu}_y(j,m) = -\frac{4\pi^2 A \mu^2 E}{h^2} \cdot \frac{1}{(2j-1)(2j+3)} \left(3 \frac{m^2}{j(j+1)} - 1 \right), \quad (21)$$

and from 20a and d for $j=0$

$$\bar{\mu}_z(0,0) = \bar{\mu}_y(0,0) = 8\pi^2 A \mu^2 E / 3h^2. \quad (22)$$

The polarization resulting when E and H are inclined at an angle ψ to each other may be found by taking the resultant of the polarizations produced by the components of E parallel and perpendicular to H , given by Eqs. (16), (17) and (21), (22). On doing this we find for all molecules with $j \neq 0$ the result

$$\bar{\mu}_\psi(j,m) = \left(\frac{3}{2} \cos^2 \psi - \frac{1}{2} \right) \bar{\mu}(j,m), \quad (23)$$

in complete agreement with the classical expression. For $j=0$, however, we find

$$\bar{\mu}_\psi(0,0) = \bar{\mu}(0,0). \quad (24)$$

The previous result regarding the influence of a magnetic field on the polarization does not follow, for on summing over m we find again that only those molecules in the lowest state, with $j=0$, contribute to the polarization. From the similarity of (17) and (22) it then follows immediately that the polarization μ_ψ is still given by the expression on the right-hand side of (19), and is consequently independent of the direction of quantization. Since for small values of electric and magnetic field strengths the only effect of applying a magnetic field to the gas will be to change the direction characteristic of the spatial quantization, we thus see that *on the basis of the new quantum mechanics a magnetic field should not influence the dielectric constant of a gas such as hydrogen chloride.*

Since this paper was submitted for publication, a note by Kronig¹⁹ has appeared in which it is stated that according to the new quantum mechanics a magnetic field should be without effect on the dielectric constant of a diatomic dipole gas.

III. COMPARISON WITH EXPERIMENT

The experiment suggested by the foregoing considerations was undertaken by Dr. L. M. Mott-Smith and C. R. Daily²⁰ in the Norman Bridge Laboratory of Physics of the California Institute of Technology, with the following results, which have been published in detail in the PHYSICAL REVIEW. Measurements were made on hydrogen chloride at pressures varying from 2 to 350 cm, using a sensitive heterodyne beat method of measuring the dielectric constant, and using the gas-handling technique described by Zahn.²¹ The magnetic field strength was about 4800 gauss, and the electric field strength only a few volts/cm, so that the quantization was very closely with respect to the magnetic field. At each pressure the dielectric constant was measured with the fields

¹⁹ Kronig, Proc. Nat. Acad. Sci. **12**, 488, 608 (1926).

²⁰ Mott-Smith and Daily, Phys. Rev. **28**, 978 (1926).

²¹ C. T. Zahn, Phys. Rev. **24**, 400 (1924).

both mutually parallel and mutually perpendicular. *In no case was any change in the dielectric constant detected*, within a limit of error of about one part in 100,000 in ϵ ; i.e., about 2 percent in the polarization for a pressure of 20 cm. The same result was also obtained with nitric oxide, NO.

APPENDIX

The motion of a diatomic dipole molecule in crossed fields according to the old quantum theory. The equation of motion of the idealized diatomic dipole molecule in an electric field E and a magnetic field H may be written vectorially as

$$A \frac{d}{dt}[\mathbf{r}\mathbf{v}] = \mu[\mathbf{r}\mathbf{E}] + \frac{\kappa}{c}[\mathbf{r}[\mathbf{v}\mathbf{H}]], \quad (25)$$

in which \mathbf{r} represents a unit vector in the direction of the axis of the molecule, and with the same sense as the electric moment. The velocity $d\mathbf{r}/dt$ is denoted by \mathbf{v} . By means of this equation we shall now determine the perturbing influence of the fields to the first approximation.

The unperturbed motion is characterized by four constants of integration. For our purposes it is desirable to choose as these constants the direction and magnitude of the total angular momentum vector (three constants) and the absolute phase of the motion. The perturbing fields produce changes in these quantities, the determination of which constitutes the perturbation problem. In order to find the perturbations for the angular momentum vector let us average each term of (25) through a length of time equal to the period of the unperturbed motion. If we define \mathbf{P} as the angular momentum vector averaged through the period of the unperturbed motion, the left side of Eq. (25) becomes $d\mathbf{P}/dt$, and we have

$$\frac{d\mathbf{P}}{dt} = \mu[\overline{\mathbf{r}\mathbf{E}}] + \frac{\kappa}{c}[\overline{\mathbf{r}[\mathbf{v}\mathbf{H}]}]. \quad (26)$$

The effect of the magnetic field. In order to evaluate the magnetic term in Eq. (26) we note that on account of the identity

$$[\mathbf{r}[\mathbf{v}\mathbf{H}]] + [\mathbf{H}[\mathbf{r}\mathbf{v}]] + [\mathbf{v}[\mathbf{H}\mathbf{r}]] = 0 \quad (27)$$

and the relation

$$\frac{d}{dt}[\mathbf{r}[\mathbf{H}\mathbf{r}]] = [\mathbf{v}[\mathbf{H}\mathbf{r}]] + [\mathbf{r}[\mathbf{H}\mathbf{v}]]$$

we may write

$$2[\mathbf{r}[\mathbf{v}\mathbf{H}]] = -[\mathbf{H}[\mathbf{r}\mathbf{v}]] - \frac{d}{dt}[\mathbf{r}[\mathbf{H}\mathbf{r}]].$$

To the first order of approximation we may now take the average value of these quantities through a period of the osculating unperturbed motion. The second term then becomes zero; and on substituting for $[\bar{r}v]$ its value P/A we obtain the equation

$$\frac{\kappa}{c} [\bar{r}[\bar{v}H]] = -\frac{\kappa}{2Ac} [HP]. \quad (28)$$

On substituting this result in (26) we observe that the effect of the magnetic field is to produce precessional motion of P about H , with the angular velocity $-\kappa H/2Ac$, in which $H = |H|$.

It can further be shown, by determining the Hamiltonian function in the way given by Schwarzschild, that the energy added by the magnetic field as it is increased adiabatically from zero to H is

$$\Psi_M = -\kappa(HP)/2Ac. \quad (29)$$

The effect of the electric field. It is found that the average value of $[\bar{r}E]$ taken through a period of the osculating field-free motion is zero; for the electric field produces only a second-order effect. In order to determine the perturbations due to the electric field it is accordingly necessary to consider not the osculating motion in the absence of both the electric and the magnetic field, but rather that in the presence of the electric field and the absence of the magnetic field.²² In this case the Hamiltonian function is

$$\mathcal{H} = \frac{1}{2A} \left(p_\theta^2 + \frac{p_\phi^2}{\sin^2\theta} \right) - \mu E \cos\theta, \quad (30)$$

in which ϕ and θ are the polar coordinates of the axis of the molecule, θ being measured with reference to E and ϕ with reference to an arbitrary zero-point. E is equal to $|E|$. The coordinate ϕ is cyclic; hence we may write

$$p_\phi = A \sin^2\theta \dot{\phi} = \alpha_2, \text{ a constant.} \quad (31)$$

Substituting this result in (30), and placing $p_\theta = A\dot{\theta}$ and $\mathcal{H} = \alpha_1$, the energy constant, we obtain

$$dt = A \{ 2A\alpha_1 - \alpha_2^2 \operatorname{cosec}^2\theta + 2A\mu E \cos\theta \}^{-1} d\theta. \quad (32)$$

²² I am indebted to Prof. J. H. Van Vleck for the observation that the justification for this procedure may be deduced by a different method developed by Bohr, Born, and others for perturbed degenerate systems. The electric term in the Hamiltonian function is much larger than the magnetic one, and so the former may be considered of the first order and the latter of the second. The former, however, gives only a second-order effect because its average value is zero to a first approximation. Born notes on p. 302 of his *Atommechanik* that in such cases it is possible to determine the secular perturbations by first averaging over the rapidly fluctuating first-order terms in the absence of the second-order perturbing terms, and hence it is legitimate for us to use the Hettner expression (36) even in the presence of a magnetic field.

Inasmuch as the old quantum theory required that the energy of the lowest quantum state be $\hbar^2/32\pi^2A$ in order to account for the pure rotation spectrum of hydrogen chloride, the quantity $\mu E/\alpha_1$ can be treated as very small in comparison with unity. It is accordingly permissible to expand the radical in the denominator and neglect higher powers of $\mu E/\alpha_1$.

We may use for the period τ of the variable θ the value corresponding to zero field; namely,

$$\tau = \pi(2A/\alpha_1)^{\frac{1}{2}} \quad (33)$$

In order to determine the motion of the vector P , we note that from Eqs. (31) and (32) we may write

$$d\phi = (\alpha_2/A \sin^2\theta)dt$$

In the time τ in which θ goes through a complete libration ϕ progresses from ϕ_0 to ϕ_τ , an angle given by the equation

$$\phi_\tau - \phi_0 = \frac{\alpha_2}{A} \int_0^\tau \frac{dt}{\sin^2\theta} = \alpha_2 \oint \frac{d\theta}{\sin^2\theta \{2A\alpha_1 - \alpha_2^2 \operatorname{cosec}^2\theta + 2A\mu E \cos\theta\}^{\frac{1}{2}}},$$

or, to the first approximation,

$$\phi_\tau - \phi_0 = 2\pi - \frac{3\pi\mu^2 E^2 \alpha_2}{8\alpha_1^2} \left(\frac{2}{A\alpha_1}\right)^{\frac{1}{2}}. \quad (34)$$

The system has undergone a pseudo-regular precession about the electric field, with a velocity which to the first approximation is found from Eq. (34), using the value of τ given by (33) and introducing for α_1 the value $p^2/2A$ and for α_2 the value $p \cos\Theta$, we thus find the velocity of precession to be $-(3\mu^2 E^2 A / 2p^3) \cos\Theta$. Since in the absence of the magnetic field this angular velocity provides a measure of the magnitude of dP/dt , and hence of $\mu[\mathbf{rE}]$, we are now able to write

$$\mu[\mathbf{rE}] = 3\mu^2 A (PE)[PE]/2p^4 \quad (35)$$

The contribution of the perturbing field to the energy function can be shown, as has been done by Hettner, to have the value

$$\psi_E = \frac{\mu^2 E^2 A}{4p^2} (1 - 3\cos^2\Theta). \quad (36)$$

The combined effect of an electric and a magnetic field. Substituting (28) and (35) in (26), we obtain the result

$$\frac{dP}{dt} = \frac{3\mu^2 A}{2p^4} (PE)[PE] - \frac{\kappa}{2Ac} [HP], \quad (37)$$

which shows that the average angular momentum vector P undergoes simultaneously precession about both the electric and the magnetic field, with the indicated velocities. The magnetic term of this equation differs from that of Klein and Lenz only in the replacement of $-e$ and m by κ and A ; the electric term is, however, completely different. For the first-order effect of the electric field is in our problem zero, and we have used the second-order term, corresponding in the case of the hydrogen atom to the quadratic Stark effect, which was neglected by Klein and Lenz.

Our differential equation is easily soluble in the scalar form. The Z -axis is chosen along E , and the X -axis in such a way that H lies in the XZ plane, making the angle ψ with E . Purely kinematically the following equations are then obtained from Eq. (37):

$$\frac{d\Phi}{dt} = -\omega \cos \Theta - \omega_z + \omega_z \cot \Theta \cos \Phi, \quad (38)$$

and

$$\frac{d\Theta}{dt} = \omega_z \sin \Phi, \quad (39)$$

in which

$$\omega_x = \omega_M \sin \psi \text{ and } \omega_z = \omega_M \cos \psi.$$

As shown in Fig. 1 the angles Θ and Φ are the polar coordinates of the vector P . Dividing (38) by (39), we obtain

$$\cos \Theta \cos \Phi - \sin \Theta \sin \Phi \frac{d\Phi}{d\Theta} = (\omega_z / \omega_x) \cos \Theta \sin \Theta + (\omega_z / \omega_x) \sin \Theta,$$

which on integration gives the equation

$$\cos \Phi \sin \Theta = -(\omega_z / \omega_x) \cos \Theta - (\omega / 2\omega_x) \cos^2 \Theta + B, \quad (40)$$

showing the relation between Θ and Φ during the perturbed motion. On substituting the value for $\cos \Phi$ given by this equation in (39) and integrating, we obtain

$$-\omega_x(t - t_0) = \int_{x_0}^x (a_0 \xi^4 + 4a_1 \xi^3 + 6a_2 \xi^2 + 4a_3 \xi + a_4)^{-\frac{1}{2}} d\xi \quad (41)$$

in which

$$x = \cos \Theta$$

and

$$a_0 = -\omega^2 / 4\omega_x^2$$

$$a_3 = \frac{\omega_z}{2\omega_x} B$$

$$a_1 = -\omega \omega_z / 4\omega_x^2$$

$$a_2 = -\frac{1}{6} \left(1 - \frac{\omega}{\omega_x} B + \frac{\omega_z^2}{\omega_x^2} \right) \quad a_4 = 1 - B^2.$$

Here x_0 is one of the roots of the equation

$$a_0 \xi^4 + 4a_1 \xi^3 + 6a_2 \xi^2 + 4a_3 \xi + a_4 = 0; \quad (42)$$

namely, it is the smaller of the two real roots lying between -1 and $+1$, between which x performs librations.

If we now make the substitution

$$\sigma = \frac{A_2}{2} + \frac{A_3}{\xi - x_0}, \quad s = \frac{A_2}{2} + \frac{A_3}{x - x_0},$$

Eq. (41) becomes

$$-\omega_x(t-t_0) = \int_s^\infty (4\sigma^3 - g_2\sigma - g_3)^{-\frac{1}{2}} d\sigma, \quad (43)$$

in which g_2 and g_3 are the invariants of Eq. (42) and have the values

$$\begin{aligned} g_2 &= a_0 a_4 - 4a_1 a_3 + 3a_2^2 \\ g_3 &= a_0 a_2 a_4 + 2a_1 a_2 a_3 - a_2^3 - a_0 a_3^2 - a_1^2 a_4, \\ \text{while } A_2 &= a_0 x_0^2 + 2a_1 x_0 + a_2 \\ A_3 &= a_0 x_0^3 + 3a_1 x_0^2 + 3a_2 x_0 + a_3. \end{aligned}$$

Now let e, e', e'' be the roots of the equation $4\sigma^3 - g_2\sigma - g_3 = 0$, and such that $e < e' < e'' < s < \infty$. We can then write

$$4\sigma^3 - g_2\sigma - g_3 = 4(\sigma - e)(\sigma - e')(\sigma - e'').$$

If we now make the substitution

$$\sin^2 \psi = \frac{e'' - e}{\sigma - e}, \quad \sin^2 \phi = \frac{e'' - e}{s - e}, \quad k^2 = \frac{e' - e}{e'' - e},$$

Eq. (43) becomes the following:

$$-\omega_x(t-t_0) = (e'' - e)^{-\frac{1}{2}} \int_0^\phi (1 - k^2 \sin^2 \psi)^{-\frac{1}{2}} d\psi.$$

This is the Legendre normal form of the elliptical integral of the first kind. We may accordingly write as the solution of our problem

$$-\omega_x(t-t_0) = (e'' - e)^{-\frac{1}{2}} F(\phi, k).$$

This last equation gives the relation between ϕ and t , and hence between Θ and t , for ϕ was obtained from Θ by means of the transformations given above. On substituting this expression for Θ in Eq. (40), a similar equation giving the relation between Φ and t is obtained.

Since the same elliptic function is thus shown to occur in the relations between both Θ and Φ and t , these two variables have the same period. Accordingly the secular perturbations are characterized by only one period, and the entire system by two, that of the unperturbed system and that due to the perturbing forces. If we represent by τ' the time required for one cycle in the precessional motion of P , we can evidently write

$$-\omega_x(e'' - e)^{\frac{1}{2}} \cdot \tau' = 2F(\pi/2, k) = 2K,$$

in which K is the complete elliptical integral of the first kind. The corresponding frequency of precession is

$$\nu = 1/\tau' = -\omega_z(e'' - e)^{1/2}/2K. \quad (44)$$

The determination of the quantum-allowed states of motion. The perturbed system is now non-degenerate, and two quantum conditions are required to determine a given state of motion. Bohr has shown that to the first order of small quantities one of these conditions is that characterizing the unperturbed motion; in this case

$$W_0 = I^2/8\pi^2 A = j^2 h^2/8\pi^2 A.$$

Moreover, he has remarked that to the same approximation the average contribution Ψ of the perturbing forces to the energy function must remain constant throughout the secular motion.

Reference to the kinematical relation between Φ and Θ (Eq. 40) verifies that Ψ is not a function of the time, for from (29) and (36) we find

$$\Psi = \Psi_B + \Psi_M = \frac{1}{2}\omega p - \omega_z p B. \quad (45)$$

The second quantum condition can now be obtained; for the second action variable I_2 must satisfy the relation

$$\delta\Psi = \nu \delta I_2.$$

There are, however, only two constants which determine the secular perturbations; one is the quantity B given by (40), and the other is a constant fixing the absolute phase of the motion of P . The second constant is of no significance with regard to the quantum conditions; so that the only variation that I_2 can experience must result from a variation in B . Hence we can write

$$\delta\Psi = \nu(dI_2/dB)\delta B,$$

or, collecting terms involving B and integrating,

$$I_2 = \int \frac{\partial\Psi}{\partial B} \cdot \frac{dB}{\nu} + \text{constant.}$$

The constant can be included in the quantity I_2 , which can then assume only the values allowed in case either the electric or the magnetic field is present alone. We are thus led, with the use of (44) and (45), to the following equation giving the second quantum condition:

$$2p \int (e'' - e)^{-1} K dB = I_2 = mh, \quad (46)$$

in which I_2 has been placed equal to its quantum-allowed value mh , m being the directional quantum number.

It can easily be shown that in case only one field is present or the fields are parallel or anti-parallel this equation leads to the spatial quantization obtained in the usual way by the separation of variables.

The system in the presence of an electric field small relative to the magnetic field. If the electric field is so small relative to the magnetic field that the quantity ω/ω_M is small compared with unity, the expression determining the action variable I_2 may be evaluated. In this case the two quantities a_0 and a_1 may be treated as small, and it is then possible to determine the three roots e , e' , and e'' of the equation $4\sigma^3 - g_2\sigma - g_3 = 0$ by the method of successive approximations. On doing this there result as a second approximation the expressions

$$e = \frac{a_2}{2} - \frac{4a_1a_3 - a_0a_4 - (12a_0a_2(3a_2a_4 - 2a_3^2))^{1/2}}{12a_2}$$

$$e' = \frac{a_2}{2} - \frac{4a_1a_3 - a_0a_4 + (12a_0a_2(3a_2a_4 - 2a_3^2))^{1/2}}{12a_2}$$

$$e'' = -a_2 + \frac{6a_1a_2a_3 - a_0a_3^2}{9a_2^2}.$$

By substituting these values in (46), using the well known series development for K , and integrating, neglecting powers higher than linear in ω/ω_M , there is obtained the equation

$$2\pi p B \sin \psi = mh \left[1 + \frac{\omega}{\omega_M} \left\{ 3\sin^3 \psi - \frac{mh}{8\pi p} \sin^2 \psi + \frac{mh}{4\pi p} \cos^2 \psi \right. \right. \\ \left. \left. + \frac{m^2 h^2}{16\pi^2 p^2} \sin \psi \cos^2 \psi - \frac{m^2 h^2}{8\pi^2 p^2} \sin^3 \psi \right\} \right]. \quad (47)$$

Furthermore, the quantity $B \sin \psi$ is given by the relation

$$B \sin \psi = \cos \Delta + (\omega/2\omega_M) \cos^2 \Theta, \quad (48)$$

in which Δ is the angle between P and H . Hence we have proved that except for corrections proportional to and of the order of magnitude of the first power of ω/ω_M the spatial quantization with crossed fields is the same as with the magnetic field alone; namely, that the component of angular momentum in the direction of the magnetic field must be equal to $mh/2\pi$.

In conclusion I wish to express my appreciation of the interest which Professor A. Sommerfeld has shown in this work, and to acknowledge my indebtedness to the John Simon Guggenheim Memorial Foundation and to the California Institute of Technology for their financial assistance.

PASADENA, CALIFORNIA, AND MUNICH, GERMANY.
September 10, 1926.

THE DIFFERENCES IN THE TIME LAGS OF THE FARADAY EFFECT BEHIND THE MAGNETIC FIELD IN VARIOUS LIQUIDS

By J. W. BEAMS* AND FRED ALLISON

ABSTRACT

Plane-polarized light from a zinc spark was passed through two liquid cells in succession. At the same time the current impulse through the spark passed, through leads of variable length, to oppositely wound solenoids surrounding the cells, where the magnetic fields rotated the plane of polarization of the light. By a proper adjustment of the positions of the cells and of the length of the lead wires it was possible to secure equal and opposite rotations of the plane of polarization in the two cells. Another liquid was then placed in one of the cells and its position changed until again the rotations were balanced. The distance the cell had to be moved, divided by the velocity of light, gave the difference in the time lag of the Faraday effect in the two liquids. The lag in carbon bisulphide behind that in hydrochloric acid was 0.3×10^{-9} sec. The lags in the following liquids behind that in carbon bisulphide were found to be (in 10^{-9} sec.): carbon tetrachloride 1.1; water 1.1; benzene 1.9; xylene 2.1; chloroform 2.4; toluene 2.5; amyl alcohol 4.0; bromoform 4.1. The precision of the results is about 0.3×10^{-9} sec., depending somewhat upon the liquid.

ALL transparent isotropic liquids when placed in a magnetic field acquire the property of rotating the plane of polarization, provided the light traverses the liquid in the direction of the lines of force. As long as the magnetic field is constant the rotation is constant, but if the field is reversed the rotation is reversed. This phenomenon is the well known Faraday effect.

Many attempts¹ have been made to detect a time interval between the removal of the magnetic field and the disappearance of the Faraday effect as well as the time interval between the application of the field and the appearance of the Faraday effect. Abraham and Lemoine² concluded from their experiments that the lag of the Faraday effect behind the magnetic field must be less than 10^{-8} sec. in the case of carbon bisulphide, while many others have shown that the magnetic rotatory polarization in an alternating field follows the variations of the field almost exactly and it has generally been concluded that if the above time lag exists, it is probably too small to measure. We have therefore thought it worth while to investigate this time lag by a very sensitive method by means of which a difference of 0.3×10^{-9} sec. in the lags of

* National Research Fellow.

¹ See Wood, Physical Optics, p. 500, Macmillan Co., 1923.

² Abraham and Lemoine, Comptes rendus 30, 499 (1900).

the Faraday effect behind the magnetic field in various liquids can be measured.

In Fig. 1, C is a parallel plate condenser with a capacity of 7×10^{-4} microfarads. A is a variable spark gap containing zinc electrodes, L a lens which renders the light from A parallel, F a light filter transmitting a narrow spectral region around the bright spark lines 4912, 4924A of zinc practically alone, while N_1 and N_2 are Nicol prisms. B_1 and B_2 are glass cells, made as nearly identical as possible, which contain the liquids under investigation. Each cell is provided with side tubes by means of which one liquid can be replaced by another. A helix of 18 turns of No. 18 copper wire is wound around each tube. T_1T_1 and T_2T_2 are cross wires by means of which the length of wire from A to B_1 and from A to B_2 can be lengthened or shortened symmetrically by the observer at E . The leads to B_2 were so arranged that B_2 could be moved in the direction of AN_1N_2 a distance of 4 or 5 meters without changing their lengths or distance apart. The source of high potential was an induction coil which

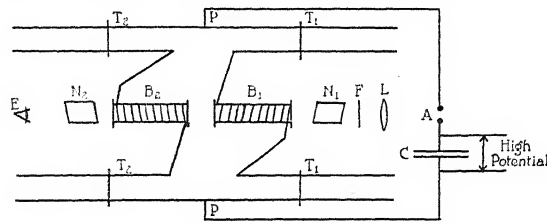


Fig. 1. Diagram of apparatus.

charged the condenser C 500 times per second. It might be noted here that there were no oscillations in C large enough to affect B_1 and B_2 , appreciably at least, after the initial discharge. This was verified experimentally.

Suppose B_1 and B_2 are first filled with carbon bisulphide and the condenser C is charged until the spark jumps across A . The electric impulse travels from A along the lead wires to P where it divides, equal and symmetrical parts passing over PT_1B_1 and PT_2B_2 . When the electric impulse reaches B_1 a magnetic field is established in the carbon bisulphide and hence because of the Faraday effect, light from the spark A made plane polarized by the Nicol N_1 has its plane of polarization rotated and will therefore pass the Nicol N_2 . On the other hand, if the other part of the electric impulse reaches B_2 over the path PT_2B_2 at a time equal to the distance between the centers of the cells divided by the velocity of light, after the arrival of the electric impulse at B_1 , the plane of polarization of the light is rotated back into its original direction provided the

helix around B_2 is so wound that the direction of the lines of force in B_2 is opposite to that of those in B_1 and that the magnitudes of the magnetic fields are identical. The length of the lead wires APT_1B_1 was first adjusted so that the electric impulse arrived at B_1 during the time that the spark lines 4912, 4924A of zinc were of maximum intensity.³ The length of APT_2B_2 was then adjusted by moving T_2T_2 until no light from A passed N_2 . This adjustment insures that the rotation of the plane of polarization produced in B_1 is exactly neutralized by the rotation in B_2 . If now B_2 is moved backward in the direction AN_1N_2 without changing the length or relative position of the lead wires APT_2B_2 , it was found that light passed N_2 . If, however, each of the lead wires APT_2B_2 was lengthened an amount equal to the distance through which B_2 was moved, the light was again extinguished, i.e., the velocity of the impulse along the lead wires was approximately equal to the velocity of light, which is in accord with many well known observations.

B_2 was placed immediately behind B_1 and the lead wires were adjusted so that no light passed N_2 . The carbon bisulphide in B_2 was then removed and carbon tetrachloride substituted in its place. Light from A then passed N_2 . B_2 was then moved back in the direction of N_2 and at a distance of 32 cm the light coming through N_2 passed through a distinct minimum.

When the same liquid, carbon bisulphide in this case, was in both B_1 and B_2 and the lead wires adjusted so that no light passed N_2 , then the magnetic fields in B_1 and B_2 were established and removed almost simultaneously, differing only by the time required for light to pass from B_1 to B_2 . When the carbon bisulphide was replaced by the carbon tetrachloride, the magnetic fields were still applied and relaxed together as before, but it was necessary to move B_2 back a distance of 32 cm in order to obtain a minimum amount of light through N_2 . The Faraday effect must therefore lag behind the magnetic field in carbon tetrachloride 1.1×10^{-9} sec. longer than in carbon bisulphide. Various other liquids when substituted for carbon tetrachloride showed distinct differences in time lags. The results are shown in the table together with the Verdet constant, and the magnetic susceptibility.

In practically all the above cases, because of differences in the magnitudes of the Verdet constants it was not possible completely to extinguish the light passing N_2 , but in every case a very sharp minimum occurred. By checking each liquid against the various other liquids having almost equal Verdet constants, the possible errors of reading a

³ Beams, J.O.S.A. & R.S.I. 13, 597 (1926).

minimum were somewhat reduced and the precision of the results given in the table is about 0.3×10^{-9} sec., although differing slightly for different liquids.

TABLE I

Liquid	*Verdet constant in minutes $\lambda = 5890\text{A}$	**Magnetic sus- ceptibility $K \times 10^6$ at 20°C	Time lag behind Carbon bisulphide Seconds
Hydrochloric acid HCl	0.0224 (15°C)	-0.83	-0.3×10^{-9}
Carbon tetrachloride CCl_4	0.0321 (15°C)	-0.72	1.1
Water H_2O	0.0130 (15°C)	-0.75	1.1
Benzene C_6H_6	0.0297 (20°C)	-0.69	1.9
Xylene C_8H_{10}	0.0221 (15°C)	-0.69	2.1
Chloroform CHCl_3	0.0164 (20°C)	-0.76	2.4
Toluene C_7H_8	0.0269 (28°C)	—	2.5
Amyl Alcohol $\text{C}_5\text{H}_{11}\text{OH}$	0.0131 (15°C)	-0.68	4.0
Bromoform CHBr_3	0.0317 (15°C)	-0.98	4.1
Carbon bisulphide CS_2	0.0441 (20°C)	-0.74	0

*From the Smithsonian Tables.

**Landolt-Börnstein Tabellen, 5. Auflage.

The fact that it was possible to obtain a sharp distinct minimum of the light transmitted by N_2 indicates that the time between the application of the magnetic field and the appearance of the Faraday effect is practically equal to the time between the removal of the magnetic field and the disappearance of the Faraday effect; or that the differences in the two above times are the same for the liquids investigated. It will be noted from the table that the differences in the time lags are not simple functions of the differences in the Verdet constants or the magnetic susceptibilities.

We wish to thank Professor L. G. Hoxton for his interest in the work and for placing apparatus at our disposal.

ROUSS PHYSICAL LABORATORY,
UNIVERSITY OF VIRGINIA.
September 3, 1926.

THE RESISTANCE OF COPPER WIRES AT VERY HIGH FREQUENCIES

By W. M. ROBERDS

ABSTRACT

At frequencies of the order of 10^7 cycles the distributed capacity of single loops of wire may cause sufficiently unequal current distribution in the loop to account for large apparent discrepancies between observed and calculated resistances. For a given frequency, more uniform current distribution is gained by decreasing the size of the loop and simultaneously increasing the capacity of the tuning condenser. Curves are plotted with ratio of observed to calculated resistance as ordinate and condenser setting as abscissa. For No. 20 copper wire at 0.86×10^7 cycles the ratio decreases to at least 1.05 as the current distribution along the wire is made more and more nearly uniform. For No. 16 oxide coated copper wire the ratio reduces to at least 1.35. The discrepancy in both cases is accounted for by the same value of condenser resistance. Observed resistance of a given loop is shown to vary greatly as condenser resistance is changed. Curves are run at 1.5×10^7 cycles on No. 20 bright copper wire, No. 20 oxide coated copper wire, and No. 20 silver wire. For all curves the ratio fell well below 1.45 and was still decreasing as far as data were taken. Since curves run on bright copper wire coincide with curves run on exactly the same wire after it had gained a heavy coating of oxide, it can be definitely stated that the presence of oxide has no appreciable effect on the resistance.

PREVIOUS experiments have shown a considerable discrepancy between observed and calculated values of the resistance of copper wires at frequencies of the order of 10^7 cycles. The results of one series of investigations¹ indicate that at a wave-length of 20 meters (1.5×10^7 cycles) the observed resistance of No. 18 copper wire is some four or five times the resistance as calculated from theoretical formulas. The object of the following experiments was to investigate whether such a discrepancy really exists.

The method of procedure was to construct a single rectangular loop of the wire whose resistance was to be measured and to couple this loop inductively to an oscillator radiating the desired frequency. It was found that if the loop was as near as 30 cm to the oscillator the current in the oscillator was reduced by about one percent as the loop was tuned. In order to avoid any effect due to coupling of loop and oscillator, the coupling was kept very loose. In no case was the loop nearer than one meter to the oscillator; in many cases it was over one and one-half meters away. The wave-length was measured by means of a wave-meter calibrated for short wave-lengths. The loop was tuned to the given

¹ Austin Bailey, Phys. Rev. 20, 154 (1922).

frequency by a variable condenser inserted in the loop. The current was measured with a sensitive thermocouple and galvanometer. The diagram of the apparatus is shown in Fig. 1. A known standard resistance of the order of that of the loop was then inserted and the loop again tuned. Then from the ratio of the "current in the loop without the standard resistance" to the "current when the standard resistance was in the loop," and from the known values of the thermocouple resistance and standard resistance, the resistance of the remainder of the loop could be found. The value thus found was compared with the value as calculated for the same length of wire by means of a standard formula.

The formula used was one deduced by A. Russell.² It is:

$$R_{a.c.} = R_{d.c.} \left[\frac{q}{2} \left(\frac{1}{2^{\frac{1}{2}}} + \frac{1}{2q} + \frac{3}{8q^2 2^{\frac{1}{2}}} - \frac{1}{2q^4 2^{\frac{1}{2}}} + \dots \right) \right]$$

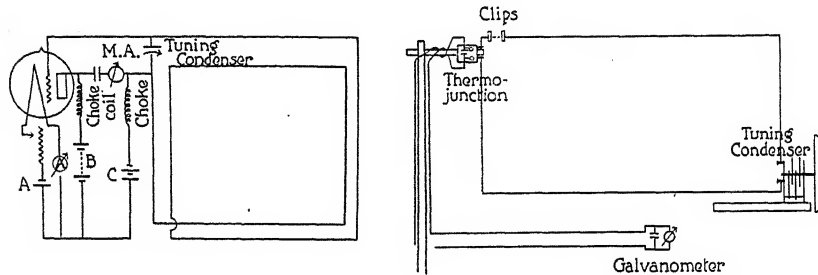


Fig. 1. Diagram of apparatus.

where q is defined by $q = \pi d(2\mu f/\rho)^{\frac{1}{2}}$ in which d is the diameter of the conductor, μ the permeability, f the frequency, and ρ the resistivity of the conductor in abohms per cc. Platinum wire 0.0069 cm in diameter was used as the inserted standard resistance. J. D. Stranathan³ has shown that platinum is normal in its resistance properties at high frequencies, and for wire of this size the calculated high frequency resistance is not two percent higher than the direct current resistance; hence it was considered safe to assume the calculated value of resistance for this wire to be correct. However, the Russell formula given above is only semi-convergent and cannot be applied in computing the resistance of wires the size of the platinum resistance wire here used. Therefore a formula due to Lord Rayleigh was used to get the resistance of the standard resistance wire. This formula is

² A. Russell, Phil. Mag. 17, 524 (1909).

³ J. D. Stranathan, Phys. Rev. 26, 500 (1925).

$$R_{a.c.} = R_{d.c.} \left(1 + \frac{h^2}{48} - \frac{h^4}{2880} + \frac{h^6}{58647} - \dots \right)$$

where $h = (\mu f \pi^2 d^2) / \rho$ in which μ , f , d and ρ represent the same quantities as in the Russell formula.

The galvanometer and thermocouple were calibrated by passing a known direct current through the thermojunction and observing the deflection of the galvanometer. The same current was sent in the reverse direction and again the galvanometer deflection noted. The average of these two deflections was taken as the deflection caused by an alternating current of the same intensity. Previous work in this laboratory⁴ has shown this procedure to be in error by considerably less than one percent when the galvanometer deflections for direct and reversed currents agree as closely as they did with the thermocouple used. Considering the smallness of the currents used, this accuracy is better than that which could have been obtained through calibrations made with the a.c. instruments at hand. Two calibration curves of the galvanometer and thermocouple were made, one before starting the series of experiments and one at the close. The two sets of data checked to less than one percent.

The resistance of the thermojunction was measured at each frequency used in the tests. This was accomplished by placing both the 'junction to be measured and another similar one in the same circuit and measuring the current in it with the second 'junction. The loop was tuned and maximum current observed. The 'junction whose resistance was desired was then replaced by a short piece of the standard resistance wire and the loop again tuned. The length of resistance wire was varied until the galvanometer showed exactly the same deflection as when the thermojunction was in the circuit. Then from the length of the standard wire the resistance of the 'junction could be calculated.

The size of platinum resistance wire used in the above procedure was so chosen that its length would be approximately equal to the distance between the 'junction terminals when their resistances were equal; in this way the dimensions of the loop remained unchanged when the resistance wire was substituted for the 'junction. In this manner the resistance of the thermojunction could be measured at any frequency to less than two percent. All direct current resistances were measured accurately with Wheatstone and Kelvin bridges.

The test loop was always twice as long as it was wide and was supported by means of cotton strings stretched taut. Such support helped to isolate the loop from solid dielectrics as well as to insulate it. No particular

⁴ J. D. Stranathan, Master's Thesis, 1924.

care was taken to insulate the galvanometer, though it was mounted on a dry wooden base. The condenser was inserted at the corner of the loop, as shown in Fig. 1, and was mounted rigidly on the corner of a small table. The thermojunction was mounted rigidly at the opposite corner of the loop since preliminary tests showed the maximum current in the loop to be at this point. Next to the thermojunction were two clips for insertion of standard resistance wire. A cotton string wound around a large pulley on the condenser shaft extended some distance away. By means of this the condenser could be tuned without the observer's being near the loop.

The tests were run as follows: the oscillator was tuned to the desired frequency and placed at about a meter and a half from the test loop. A piece of test wire (the same as that in the loop) was inserted between the clips and the loop tuned. The current I_c in the loop was then noted from the galvanometer deflection and calibration curve. The small piece of test wire was then replaced by the standard resistance wire r_p , the loop tuned and the current, I_p , noted. This process was repeated from three to five times for each measurement. In some cases different values of r_p were used for a single measurement. However, this did not always prove desirable because the value of r_p could be determined with far greater accuracy than the ratio I_p/I_c , when the latter was very different from 0.5. Therefore, such values of r_p were used as would give approximately 0.5 for I_p/I_c . Then if l is the length of the wire which is changed as just described, L the length of the wire in the loop which remains unchanged, R_t the resistance of the thermojunction at the given frequency, R_c the resistance of length L of the test wire, r_p the resistance of the inserted platinum wire of length l , and r_e the resistance of the inserted piece of test wire, then

$$I_p/I_c = (R_t + R_c + r_e)/(R_t + R_c + r_p)$$

Letting $M = I_p/I_c$ and noting that $r_e = lR_c/L$, we have

$$R_c = [(M - 1)R_t + r_p M]/[1 + (l/L) - M]$$

which gives the observed resistance of length L of the test wire. In this calculation the resistance of the condenser was entirely neglected. This, however, is not a legitimate procedure as has recently been shown by R. R. Ramsey,⁵ and Maibauer and Taylor,⁶ as also by the results of the present experiment.

⁵ R. R. Ramsey, Paper presented at Washington Meeting of Am. Phys. Soc., April, 1926.

⁶ A. E. Maibauer and T. Smith Taylor of Bakelite Corp. in paper presented at Kansas City meeting of Am. Phys. Soc., Dec., 1925.

Preliminary tests showed that if the size of the loop was varied the observed resistance per unit length of the wire in the loop varied greatly. Sensitive milliammeters placed at various points in the loop showed that the current varied greatly along the wire; the large variation was of course due to distributed capacity. Now since the resistance of a circuit is defined⁷ as the real part of the complex quantity z which is such that if the current i is the real part of $Ie^{j\omega t}$ and if the e.m.f. e is the real part of $Ee^{j\omega t}$, where I and E are real or complex quantities independent of the time t , where $j = (-1)^{\frac{1}{2}}$, and where e is the base of natural logarithms, then

$$E = zI$$

When this definition is applied to series circuits it is immaterial where e is applied or where i is measured. But in the loops here used the distributed capacity is in parallel with the variable condenser and the inductance of the loop, and hence the current i would not be uniform throughout the loop. Therefore, the resistance must be defined for each point in the loop or else the circumstances must be made such that the series condition is approximated. The more nearly the series conditions are attained the more nearly will the observed resistance approach the true resistance as above defined.

It was found that as the condenser capacity was increased and the size of the loop correspondingly decreased to keep the resonant frequency constant, the current throughout the loop became more and more nearly uniform, thus approaching the series conditions. Hence the observed resistance should approach a correct value.

In the following experiments, therefore, data were taken such that curves could be plotted of resistance against something that varied as the uniformity of the current in the loop. Since the current became more uniform as the condenser capacity was increased, the condenser setting was used as abscissa. Since the capacity of the condenser was not exactly proportional to the condenser setting no definite conclusions can be drawn from the exact shapes of the curves. The curves show better how the observed resistance approaches the calculated resistance if the ratio of the observed resistance to the calculated resistance is plotted as ordinate.

The data for the curve of Fig. 2 were taken at a frequency of 0.86×10^7 cycles (35 meters wave-length). The solid curve is for No. 20 cotton-covered copper wire. It is seen that this curve very definitely flattens out at a ratio of about 1.05. This would indicate that there might be a

⁷ Bureau of Standards Scientific Paper No. 430.

small resistance in the loop of which no account had been taken. A simple calculation showed that a resistance of 0.12 ohms would cause such a discrepancy. This is the order of the resistance of a low loss air condenser at these frequencies, as shown by R. R. Ramsey. A curve was then run on No. 16 heavily oxide-coated copper wire at the same frequency and the results are shown in the broken curve. It is seen that this curve does not come down nearly so far as the other. But since this wire was so much less in resistance than the No. 20 wire, a calculation similar to that above shows that here also, an unaccounted for resistance of about 0.15 ohms would account for the discrepancy. This value agrees with the previous result within the limit error.

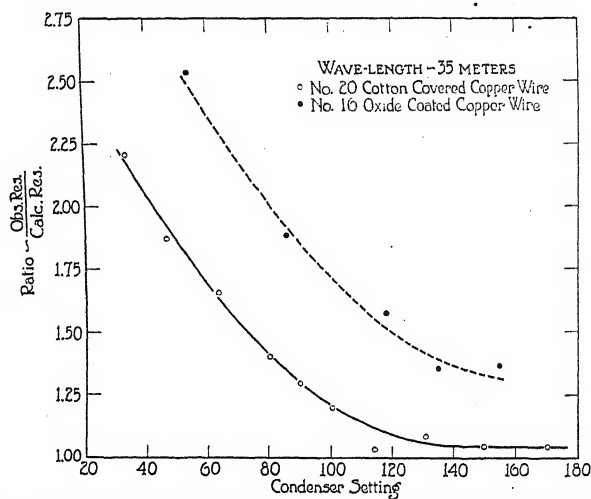


Fig. 2. Ratio of the observed resistance to the calculated resistance as a function of the condenser setting.

The curve of Fig. 3 was run on the No. 20 cotton-covered wire at 30 meters wave-length (10^7 cycles) and it shows the same form as the curves in Fig. 2. However, in this curve some changes were made in the condenser to see how it was affecting the resistance of the loop. The resistance plotted at point (1) of this curve was taken with the condenser just as it had been for the previous points in the curve. One plate of the condenser was removed so that at tuned position there was less "idle" area, that is, a larger proportion of the total area of the plates was opposed to another plate. Under these conditions the resistance found was as indicated at point (2). The spacing between the plates was next decreased and point (3) obtained. Then another plate was added, still with the closer spacing of the plates, and point (4) was obtained.

Another condenser was built with copper plates which had the advantage that the plates could be soldered together, whereas the aluminum plates could not be. With this condenser point (5) was obtained. Thus it is seen that slight changes in the condenser affected appreciably the observed resistance of the loop. It is also apparent that as the condenser capacity is increased by decreasing the spacing the resistance is lowered more than by decreasing the "idle" area of the plates. However, the changes in contact resistance between the plates was probably more responsible for the changes in resistance here observed than are the losses in the dielectric or plates.

Former investigators¹ have been led to believe that oxide which easily forms on copper causes an appreciable discrepancy between observed and calculated values of high frequency resistance. Therefore, in order

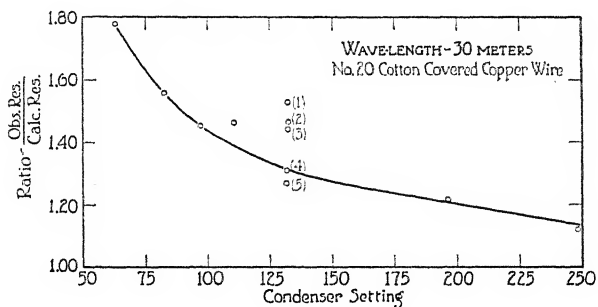


Fig. 3. Ratio of the observed resistance to the calculated resistance as a function of the condenser setting.

to see whether or not oxide on the wire made a great difference, the following experiments were carried out. A "resistance ratio"—"condenser setting" curve was run on No. 20 cotton covered copper wire at a wavelength of 20 meters (1.5×10^7 cycles). This is shown in the solid curve of Fig. 4. Some of the same wire was then carefully stripped of its insulation and laid out in the weather for ten weeks. At the end of that time it had gained a heavy brown coating of oxide. A curve was then run on it at 20 meters wave-length. This curve is shown as the dotted curve in Fig. 4. It is seen that these curves coincide within limits of error. If there is a difference, the oxide-coated wire has less resistance than the bright cotton insulated wire. Further tests showed that the resistance introduced by the cotton insulation was entirely negligible. These results prove conclusively that the presence of oxide has no appreciable effect upon the high frequency resistance of copper wire.

Another curve was run at the same wave-length on No. 20 silver wire. It is known that silver does not easily form an oxide and therefore any effects of oxide would be absent in this curve. This is shown in the dashed curve of Fig. 4. This curve shows a higher ratio of observed to calculated resistance than did the copper, but in general the shape is the same and it still is decreasing rapidly as far as data were taken.

In the foregoing tests the errors which are likely to occur all contribute to make the resistance ratio higher rather than lower than the actual values. All contact resistances and inaccurate tuning tended toward making the observed resistance high. Also the formula used for calculating the resistance applied only to long straight wires. Hence the corners of the loop as here used, and the interlocking magnetic fields of the sides of the loop, might be expected to raise its resistance somewhat.

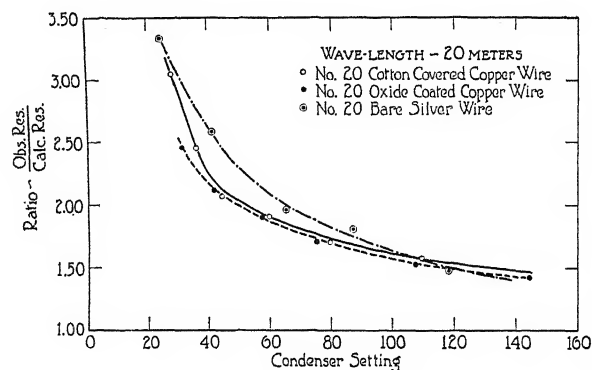


Fig. 4. Ratio of the observed resistance to the calculated resistance as a function of the condenser setting.

Therefore, it cannot be claimed that these curves are in error by less than five or six percent. Many points were repeated and the deviations were all less than this figure. Besides the above mentioned errors there is that introduced by the condenser resistance which recent investigations have shown is not negligible at the frequencies here used.

In conclusion it can be said that the foregoing results have shown that:

1. There is no great discrepancy between calculated and observed resistance of No. 20 copper wire at frequencies up to 1.5×10^7 cycles.
2. The differences which are found here are certainly due in the greatest part to condenser resistance.
3. If the acquisition of oxide by copper wires causes any change in resistance at all it is very small.

In closing the author wishes to express his appreciation and thanks to Professor J. D. Stranathan for his many helpful suggestions and his

continued interest throughout the investigation, and to Mr. Lawrence Lynn for his skill in the building of apparatus.

BLAKE PHYSICAL LABORATORY,
UNIVERSITY OF KANSAS.
September 1 1926

ON THE PRINCIPAL MAGNETIC SUSCEPTIBILITIES OF CRYSTALS

By I. I. RABI

ABSTRACT

A new method of measuring the principal magnetic susceptibilities of crystals.—The crystal to be measured is immersed in a solution, the susceptibility of which is varied, and the orientation of the crystal adjusted till there is no movement of the crystal due to the magnetic field. The susceptibilities of the solutions are then measured. From these values the principal susceptibilities can then be easily obtained. The method does not require any preparation of crystal sections, measurement of the magnetic field or gradient of the field. The range of application of this method is for volume susceptibilities of -0.9×10^{-6} to $+70 \times 10^{-6}$.

The principal magnetic susceptibilities of certain crystals.—The above method is applied to the measurement of principal susceptibilities of 14 crystals. Of these eleven are paramagnetic, and belong to the monoclinic double sulphate hexahydrate isomorphous series, $\text{MeSO}_4 \cdot \text{R}_2\text{SO}_4 \cdot 6\text{H}_2\text{O}$. With these crystals the results seem to indicate that, unlike the optical and crystallographic properties, the principal susceptibilities and their relative magnitudes depend almost entirely on the paramagnetic ion alone. The influence of the alkali or ammonium ion is secondary. In the series containing copper the greatest difference in maximum and minimum susceptibilities is 28% of the average susceptibility, in the nickel series 4%, in the Co series 32%, in the Fe series 16% and in the Mn series 1%. Of the diamagnetic crystals, NaNO_3 and KNO_3 , which are similar in their crystallographic properties to calcite and aragonite respectively, show similar magnetic properties.

THIS paper presents an experimental study of the principal magnetic susceptibilities of a series of chemically and crystallographically related crystalline compounds. The method involves the obtaining of solutions with the same susceptibilities as the crystal in definite known directions, and the measurement of the susceptibility of these solutions.

HISTORICAL

Measurements of the principal magnetic susceptibilities of crystals have been attempted by a number of investigators since the early qualitative work of Tyndall. Voigt and Kinoshita¹ measured a number of para- and diamagnetic crystals. Finke² in the same laboratory did some work on the well known monoclinic isomorphous series of double sulphates $\text{MeSO}_4\text{R}_2\text{SO}_4 \cdot 6\text{H}_2\text{O}$. More recently Jackson³ and Foex⁴

¹ Voigt and Kinoshita, Ann. der Physik 24, 492 (1907).

² Finke, Ann. d. Physik 31, 149 (1910).

³ Jackson, Phil. Trans. R. S. A. 224, 1 (1923); R. S. Proc., A, 104, 671 (1923).

⁴ Foex, Ann. d. Physique 16, 174 (1921).

have made measurements of paramagnetic crystals over great temperature ranges.

The experimental procedure in these attempts was to cut definite sections out of the crystal and to measure the force or torque on these sections. With a knowledge of the field and its gradient the susceptibilities could then be calculated. Another way was to compare the force or torque with that on a standard substance of the same dimensions.

It is evident that there exist in these methods many possibilities of error incident to the measuring of the field, the gradient of the field, the preparation of the crystal sections, the placing of the crystal in the field (especially in view of the great attraction toward the pole pieces in the case of strongly paramagnetic substances), the difference in various sections due to the non-homogeneity of the crystal, etc. In the present

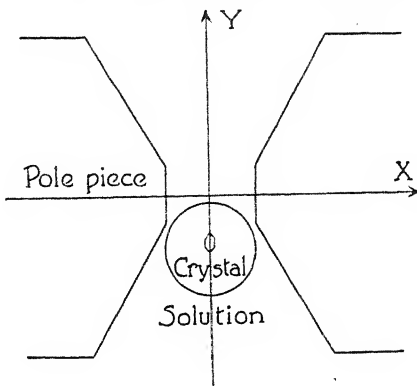


Fig. 1. Placing of crystal as seen from above.

investigation the aim has been to eliminate as far as possible these sources of error.

METHOD

The crystal is suspended vertically in the non-homogeneous field of a Weiss magnet as shown in Figs. 1 and 2. The suspension is a glass thread sufficiently thick to prevent any detectable turning of the crystal due to the action of the field. The thread is attached to a graduated head, giving the possibility of rotating the crystal. The crystal is first attached (with proper regard to orientation) to a fine glass thread about 10 cm long by means of the smallest possible amount of molten shellac. This thread in turn is attached to the rest of the suspension, the whole being about 75 cm long. The suspension is arranged symmetrically between the pole pieces (as shown in the diagrams), and the orientation

of the crystal about the axis of suspension is made definite by sending a narrow beam of light along the Y -axis and reflecting it back from a known face of the crystal. This together with the crystallographic data makes the orientation of the crystal completely known.

The crystal is suspended in a solution the susceptibility of which can be varied in the range of susceptibilities of the crystal. The container is pictured in the diagram. The arrangement makes it possible for the solution to be drawn out into another vessel and its susceptibility changed by the addition of other substances. Since all the crystals used in this research were water soluble, the solutions were first made saturated with respect to the material of the crystal used. This effectively prevented the dissolving of any of the crystals during the course of a run.

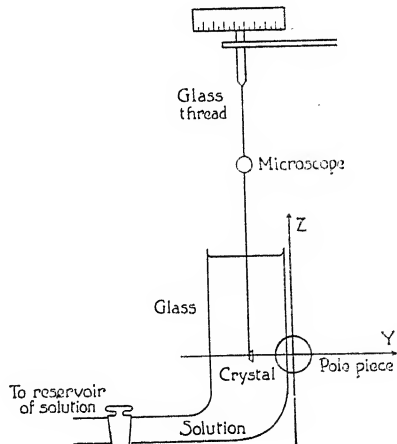


Fig. 2. Side-view of the crystal and suspension.

With substances the susceptibility of which is greater than that of water, the susceptibility of the solution is raised when necessary by the addition of a solution concentrated with respect to $MnCl_2$ and saturated with respect to the substance to be measured. The susceptibility is lowered by adding a solution saturated with respect to the substance. With materials of lower susceptibilities than water the susceptibility is lowered by adding a concentrated potassium iodide solution (saturated as above described) and raised by the addition of saturated solution.

The crystals were prepared from C.P. chemicals by the method described by Tutton.⁵ Only well formed crystals were used. The best size is about 3 to 4 mm thick and about the same in other dimensions.

⁵ Tutton, Crystallography and Practical Crystal Measurement, p. 14.

A movement of the crystal along the Y -axis is observed by means of the microscope. Motion along the X -axis is also observed. By means of the graduated head the crystal is adjusted till there is no movement along the X -axis when the field is turned on. The concentration of the solution is then varied till the field causes no motion along the Y -axis. The angles are read and a sample of the solution is drawn out. The crystal is then rotated through 90° when another position of zero movement along the X -axis is found. The susceptibility of the solution is then adjusted till there is no movement along the Y -axis, and another sample is taken. The crystal is then rehung so as to rotate about another axis and the same process is repeated.

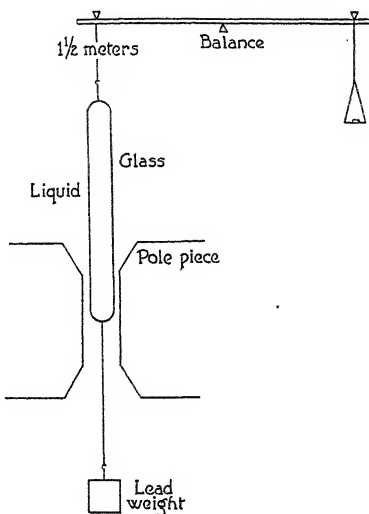


Fig. 3.

The susceptibility of the solution is measured⁶ by suspending a long glass tube (about 1 cm in diameter), filled with the solution, in the field of the magnet. Large pole pieces are used to secure a uniform field at the lower end of the tube. The tube is made long enough for the field at the upper end to be negligible. A lead weight is suspended from the lower end of the tube by means of silk thread. The weight is not necessary for weakly magnetic solutions. For strongly magnetic solutions the weight prevents the tube from going over to the pole piece. The glass for the tube is so chosen that the force of the field on the whole suspension without liquid is as small as possible. The force of the field is measured by means of a sensitive balance placed high enough to be

⁶ A. P. Wills, Phys. Rev. 6, 223 (1898).

away from the influence of the field. The net force on the liquid is compared to the net force on the same tube filled with pure water. Correcting for the susceptibility of the air, the two forces are to each other as the susceptibilities. The value of the susceptibility of water is taken as⁷ -0.720×10^{-6} . The field strength of the magnet is maintained constant throughout this part of the determination but its value need not be known.

THEORY OF THE METHOD

In general, when a substance is introduced into a magnetic field it will be polarized magnetically. The effect of this polarization will be to modify the magnetic intensity, which had previously existed, both in magnitude and direction. However, if the induced magnetization is small compared with the magnetic intensity this effect, for the purpose of this investigation, can be considered as negligible.⁸ The magnetic intensity will therefore be considered as unaltered by the introduction of the substance.

From the above and from the well known theorems of magnetostatics it follows that the force per unit volume which will be exerted on a weakly magnetic substance suspended in a magnetic field and surrounded by a solution will be;

$$\begin{aligned} F_x &= I_x \partial H_x / \partial x + I_y \partial H_x / \partial y + I_z \partial H_x / \partial z \\ &\quad - K_s [H_x \partial H_x / \partial x + \partial H_x / \partial y + \partial H_x / \partial z] \\ F_y &= I_x \partial H_y / \partial x + I_y \partial H_y / \partial y + I_z \partial H_y / \partial z \\ &\quad - K_s [H_x \partial H_y / \partial x + \partial H_y / \partial y + \partial H_y / \partial z] \\ F_z &= I_x \partial H_z / \partial x + I_y \partial H_z / \partial y + I_z \partial H_z / \partial z \\ &\quad - K_s [H_x \partial H_z / \partial x + H_y \partial H_z / \partial y + H_z \partial H_z / \partial z] \end{aligned} \quad (1)$$

where H is the magnetic intensity, I is the induced magnetic moment per unit volume or the intensity of magnetization, K_s is the susceptibility of the solution. There will be, in addition, surface traction on the interface of solid and solution of $(2\pi I_n)^2 - 2\pi I_{n_s}^2$ ⁹ per unit area. Since in these cases I_n is very small compared to the gradient of H these tractions are unimportant.

With respect to a system of axes $X Y Z$ fixed in the magnet, as shown in Figs. 1 and 2, it is evident from the symmetry of the field, and the vanishing of the curl and divergence of H , that when the substance is situated in the Y axis,

$$H_y = H_z = \partial H_y / \partial z = \partial H_z / \partial y = \partial H_z / \partial x = \partial H_x / \partial z = 0$$

⁷ A. P. Wills, Phys. Rev. 20, 188 (1905).

⁸ Maxwell, Electricity and Magnetism, 3rd Ed., pp. 69 and 73.

⁹ Larmor, Phil. Trans. R. S. A. 190, 248 (1897).

Eq. (1) can then be written,

$$F_x = I_y \partial H_x / \partial y, F_y = I_x \partial H_x / \partial y - K_s H_x \partial H_x / \partial y, F_z = 0 \quad (2)$$

In general for crystalline media, when there is no ferromagnetism it has been found by experiment that I is a linear vector function of H . Referred to an arbitrary set of axes $X'Y'Z'$ fixed in the crystal we have

$$\begin{aligned} I_{x_1} &= k_{11}H_{x_1} + k_{12}H_{y_1} + k_{13}H_{z_1} \\ I_{y_1} &= k_{21}H_{x_1} + k_{22}H_{y_1} + k_{23}H_{z_1} \\ I_{z_1} &= k_{31}H_{x_1} + k_{32}H_{y_1} + k_{33}H_{z_1} \end{aligned} \quad (3)$$

The k 's are the constant coefficients of magnetization. In general I will not have the same direction as H . However, there are three mutually perpendicular directions in which I and H will have the same direction. If we choose a set of axes $X''Y''Z''$ parallel to these directions, we have

$$I_{x''} = K_1 H_{x''}, I_{y''} = K_2 H_{y''}, I_{z''} = K_3 H_{z''}$$

These K 's are the principal susceptibilities and the corresponding system of axes are the principal magnetic axis. The principal axes and susceptibilities (K) can be found in terms of the "coefficients of magnetization" (k), from the theory of the linear vector function¹⁰. The problem now resolves itself into a determination of the six k 's ($k_{lm} = k_{ml}$)

Referred to XYZ fixed in the magnet let the direction cosines of X' be l_1, m_1, n_1 ; of Y', l_2, m_2, n_2 ; and of Z', l_3, m_3, n_3 . We then have

$$I_x = l_1 I_{x_1} + l_2 I_{y_1} + l_3 I_{z_1}, I_y = m_1 I_{x_1} + m_2 I_{y_1} + m_3 I_{z_1} \quad (4)$$

If the crystal is suspended with the Z' -axis parallel to the Z -axis and θ is the angle which the X' -axis makes with X it follows from Eqs. (3) and (4)

$$I_x/H_x = \frac{1}{2}(k_{11} + k_{22}) + \frac{1}{2}(k_{11} - k_{22})\cos 2\theta - k_{12}\sin 2\theta \quad (5)$$

$$I_y/H_x = \frac{1}{2}(k_{11} - k_{22})\sin 2\theta + k_{12}\cos 2\theta \quad (6)$$

For F_x to vanish it is evident from Eqs. (2), (5) and (6), that the right hand side of Eq. (6) must vanish yielding

$$\tan 2\theta = -2k_{12}/k_{11} - k_{22} \quad (7)$$

For F_y to vanish we must have by Eqs. (2) and (5)

$$I_x/H_x = K_s \quad (8)$$

In order that both F_x and F_y vanish simultaneously the conditions given by Eqs. (7) and (8) must both be fulfilled. It is evident from Eq. (5) that the values of θ imposed by Eq. (7) makes I_x either a maximum or a minimum, since the derivative of I_x with respect to θ is equal to $-I_y$. These values of θ recur at intervals of 90° in θ .

Let a_1 and a_2 respectively be the susceptibilities of the solutions necessary to bring about a balance in the maximum and minimum positions, and let θ_1 be the angle which the X' makes with the X -axis in

¹⁰ Gibbs-Wilson, Vector Analysis.

the maximum position when the crystal is suspended with the Z' -axis parallel to Z . It then follows from Eqs. (5), (7) and (8), after some algebraic manipulation that;

$$\begin{aligned} k_{11} &= \frac{1}{2}[a_1 + a_2 + (a_1 - a_2)\cos 2\theta_1]; \quad k_{22} = \frac{1}{2}[a_1 + a_2 - (a_1 - a_2)\cos 2\theta_1]; \\ k_{12} &= -\frac{1}{2}(a_1 - a_2)\sin 2\theta_1 \end{aligned} \quad (9)$$

Similarly let a_3, a_4, θ_2 be the corresponding values when Y is parallel to the axis of suspension and likewise a_5 and a_6 when X is parallel to Z the angle of suspension and θ is the angle between X and Y at a maximum position. By a procedure similar to the obtaining of Eqs. (5), (6), (7), (8) and (9) we have;

$$\begin{aligned} k_{33} &= \frac{1}{2}[a_3 + a_4 - (a_3 - a_4)\cos 2\theta_2] \\ k_{23} &= -\frac{1}{2}(a_3 - a_4)\sin 2\theta_2, \quad k_{13} = \frac{1}{2}(a_3 - a_4)\sin 2\theta_2 \end{aligned} \quad (10)$$

and also;

$$\begin{aligned} k_{11} &= \frac{1}{2}[a_5 + a_6 + (a_5 - a_6)\cos 2\theta_3] \\ k_{22} &= \frac{1}{2}[a_5 + a_6 - (a_5 - a_6)\cos 2\theta_3] \\ k_{33} &= \frac{1}{2}[a_5 + a_6 - (a_5 - a_6)\cos 2\theta_3] \end{aligned} \quad (11)$$

Eqs. (9) and (10) give the k 's in terms of the a 's and O 's. There are six equations to determine the six k 's. We have in addition Eq. 11 which gives us three independent values of k_{11} , k_{22} , and k_{33} . These can be averaged with the values obtained in Eqs. (9) and (10).

If the directions of the three principal magnetic axes are known, then the susceptibility of the solutions obtained by setting the crystal parallel to each of these axes in turn are the principal susceptibilities. If the position of one principal axis is known, the method is considerably simplified, since the other two axes are in the plane perpendicular to this direction.

We choose a set of co-ordinate axes in the crystal, with the Z -axis parallel to the known direction, suspending the crystal about this axis we determine a_1, a_2 and θ_1 as before. Setting the Z -axis parallel to H we determine a_3 . It is also well, but not necessary to determine a_4 in the perpendicular direction. It can be shown that;

$$K_1 = a_1, \quad K_2 = a_2, \quad K_3 = a_3 \quad (12)$$

where the K 's are the principal susceptibilities. The angle which the principal axis of maximum susceptibility in the XY plane makes with the X -axis in the crystal is $-\theta_1$. As a check on these results we have;

$$K_1 \cos^2 \theta_1 + K_2 \sin^2 \theta_1 = a_4 \quad (13)$$

The orientations and magnitudes of the magnetic axes are completely given by Eqs. (12).

If the crystal be isotropic, it is evident from Eq. (2) that when the concentration of the solution is adjusted so that the force vanishes, the susceptibility of the solution is equal to that of the crystal.

THE CRYSTALS

The crystals used were;

$\text{Cu}(\text{NH}_4)_2(\text{SO}_4)_2 \cdot 6\text{H}_2\text{O}$	$\text{Co}(\text{NH}_4)_2(\text{SO}_4)_2 \cdot 6\text{H}_2\text{O}$
$\text{CuK}_2(\text{SO}_4)_2 \cdot 6\text{H}_2\text{O}$	$\text{CoK}_2(\text{SO}_4)_2 \cdot 6\text{H}_2\text{O}$
$\text{CuRb}_2(\text{SO}_4)_2 \cdot 6\text{H}_2\text{O}$	$\text{CoRb}_2(\text{SO}_4)_2 \cdot 6\text{H}_2\text{O}$
$\text{Ni}(\text{NH}_4)_2(\text{SO}_4)_2 \cdot 6\text{H}_2\text{O}$	$\text{Mn}(\text{NH}_4)_2(\text{SO}_4)_2 \cdot 6\text{H}_2\text{O}$
$\text{NiK}_2(\text{SO}_4)_2 \cdot 6\text{H}_2\text{O}$	$\text{FeK}_2(\text{SO}_4)_2 \cdot 6\text{H}_2\text{O}$
$\text{NiRb}_2(\text{SO}_4)_2 \cdot 6\text{H}_2\text{O}$	$\text{NaNO}_3, \text{KNO}_3, \text{Sr}(\text{NO}_3)_2$

All except the last three are paramagnetic and belong to the well known isomorphous series. Tutton¹¹ in a series of elaborate investigations has shown that members of this series differ from each other

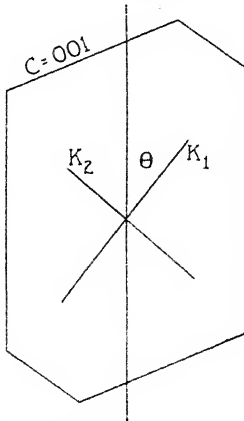


Fig. 4. Plane of symmetry of the double sulphate crystals.

only very slightly with regard to axial ratio, interfacial angles and refractive index. It is significant however that the above mentioned quantities show smaller changes when, for example, Co is substituted for Ni than when one alkali is substituted for another, or for an NH_4 group.

Of the diamagnetic crystals $\text{NaNO}_3, \text{KNO}_3, \text{Sr}(\text{NO}_3)_2$ the first two are of interest since their structures are very similar to that of calcite and aragonite already investigated by Voigt and Kinoshita.

With the monoclinic crystals the assumption was made that one of the principal magnetic axes lies in the axis of symmetry. Physically this means that in this direction the magnetization is parallel to the field, or in our notation I_y must vanish in all cases when this axis is parallel to H .

¹¹ Tutton, Proc. R. S. London **88**, 361 (1913); Trans. R. S. A. **216**, 1 (1916).

The above assumption was found to hold true in every case within the limit of error. Eqs. (9) were then used rather than (8). After a balance between solution and crystal was obtained the field was varied within wide limits, to ascertain whether there existed a dependence on field strength. None was found. This shows that it is very unlikely that any ferromagnetism exists in these crystals.

ACCURACY OF RESULTS

Because of surface forces where the glass thread emerges into the air, the pendulum cannot show differences in susceptibility much less than 10^{-8} . Very good checks have been obtained with that order of magnitude. Using the balance to measure the susceptibility of the liquid entails weighing to 0.5 mg, which is easily possible. However the percentage precision, as regards absolute values, is limited by our knowledge of the susceptibility of water. This is probably not known to better than 0.5 percent.

The fact that the suspension of the crystal has a different susceptibility from that of the crystal leads to a systematic fractional error roughly equal to the ratio of the volume of the suspension in the strong part of the field to the volume of the crystal. By a proper choice of thickness of thread this can be reduced to less than 0.2 percent.

The error due to the finite size of the crystal is unimportant. However there is an accidental error which arises from the fact that the crystal may not have its center of mass in the YZ plane. This error is reduced by suspending the crystal in that part of the field in which the gradient is small. This error does not appreciably affect the values of the a 's (Eq. 11) but may affect the value of the angles to the extent of about 2° . Since the value of the angle is obtained from four readings, two maxima and two minima each 180° apart, this error is practically balanced out.

In comparing these results for the double sulphates with those measured by Finke² and Jackson³, we find a very considerable disagreement. However the average mean value of the three principal susceptibilities of these measurements on the Co and Ni double sulphates agrees very well with a measurement by Jackson on the same crystals powdered. Finke's mean values do not so agree. Furthermore the consistency of these results as shown by Table I is a very good indication of their accuracy.

The average diamagnetic results are slightly lower than the values found from measurements in solution. This is another illustration of

the general phenomenon observed by Oxley,¹² a diminution of diamagnetic susceptibility on crystallization.

RESULTS AND DISCUSSION

Table I gives the results of the measurements of the double sulphate series. It is significant that while the Ni, Co and Fe salts have large differences in their principal susceptibilities, the Ni and Mn salts, though of almost identical crystal structure have only small differences in their principal susceptibilities. This would perhaps be explicable on the theory suggested by Foex⁴ that due to the forces of crystalline nature, there exists a potential energy which is a function of the direction. The direction of maximum susceptibility would then be the direction of minimum potential energy.

In view of the aforementioned similarities in the crystal structure of this series and the fact that smallest differences in refractive index, interfacial angle, and axial ratio are produced by varying the paramagnetic ion, it is difficult to concede that forces of a crystalline nature are responsible for these differences. In this connection it is interesting to note that rhombic $\text{NiSO}_4 \cdot 7\text{H}_2\text{O}$ has small differences in the principal susceptibilities, while in $\text{CoSO}_4 \cdot 7\text{H}_2\text{O}$, which is also rhombic, the differences are large. By Werner's coordination theory six molecules of water of crystallization are associated with the Co ion especially, and the seventh, with the SO_4 ion. The double sulphate is to be considered as a replacement of the water of crystallization by the alkali sulphate.

It is somewhat plausible that an ion with a spherical symmetrical external field would be free to rotate within its shell of H_2O molecules, whereas a departure from this symmetry would introduce forces opposing this rotation. On these considerations the differences in susceptibility would be ascribed to the assymmetry of the external field of the paramagnetic ion.

It would be interesting, in this connection, to examine crystals like
 $[\text{Co}(\text{NH}_3)_6]\text{Cl}_2$, $[\text{Ni}(\text{NH}_3)_6]\text{Cl}_2$

which are cubic, and the lattice structure of which is known, for differences of susceptibility in different directions. According to these views we should get differences similar to those found in the double sulphates.

The Weiss¹³ magneton numbers show very considerable deviations from whole numbers. As for the Bohr magneton numbers, it is difficult to decide from these data which computation is preferable; that is

¹² Oxley, Phil. Trans. R. S. A. **214**, 109 (1914).

¹³ Weiss, Phys. Zeits. **12**, 935 (1911).

TABLE I

Results of the measurements on the double sulphate series.

Axes 1 and 2 refer respectively to the maximum and minimum principal susceptibilities in the plane of symmetry of the crystal; axis 3 refers to the principal susceptibility perpendicular to the plane. The angle θ is the angle which the axis of maximum susceptibility in the plane of symmetry, makes with the C crystallographic axis; ϕ is the angle which the maximum refractive index, in the same plane, makes with the same axis. K is the volume susceptibility, χ is the mass susceptibility, χ_m the molecular susceptibility, χ_m' the molecular susceptibility with correction for diamagnetism. The quantity n is the number of Weiss magnetons, n' is the number of Bohr magnetons found by dividing n by 5, and n'' is the number of Bohr magnetons calculated according to Pauli-Sommerfeld, taking into account space quantization. The temperature is 27°C.

Compound	Axis	θ	ϕ	$K \times 10^6$	$\chi \times 10^6$	$\chi_m \times 10^6$	$\chi_m' \times 10^6$	n	n'	n''
$\text{Cu}(\text{NH}_4)_2 \cdot (\text{SO}_4)_2 \cdot 6\text{H}_2\text{O}$	1			6.80	3.52	1396	1550	9.48		
	2	-74°	-72°	5.40	2.80	1112	1260	8.54	2	1
	3			6.62	3.44	1364	1515	9.42		
$\text{CuK}_2(\text{SO}_4)_2 \cdot 6\text{H}_2\text{O}$	1			7.52	3.37	1478	1625	9.75		
	2	-99°	-162°	5.62	2.52	1104	1250	8.55	2	1
	3			6.83	3.12	1342	1490	9.34		
$\text{CuRb}_2(\text{SO}_4)_2 \cdot 6\text{H}_2\text{O}$	1			6.97	2.72	1437	1590	9.63		
	2	-76°	-64°	5.44	2.11	1122	1270	8.62	2	1
	3			6.78	2.63	1400	1550	9.52		
$\text{Ni}(\text{NH}_4)_2(\text{SO}_4)_2 \cdot 6\text{H}_2\text{O}$	1			20.2	10.5	4120	4270	15.8		
	2	-7°	-81°	19.9	10.35	4060	4210	15.7	3	2
	3			20.0	10.4	4080	4230	15.8		
$\text{NiK}_2(\text{SO}_4)_2 \cdot 6\text{H}_2\text{O}$	1			20.5	9.16	3980	4130	15.5		
	2	-17°	-84°	19.7	8.80	3820	3970	15.2	3	2
	3			19.6	8.76	3800	3950	15.2		
$\text{NiRb}_2(\text{SO}_4)_2 \cdot 6\text{H}_2\text{O}$	1			20.2	7.81	4110	4260	15.8		
	2	-19°	-77°	19.5	7.54	3970	4120	15.5	3	2
	3			19.6	7.58	3990	4140	15.6		
$\text{Co}(\text{NH}_4)_2(\text{SO}_4)_2 \cdot 6\text{H}_2\text{O}$	1			56.2	29.6	11610	11760	26.2		
	2	-13°	-80°	40.7	21.4	8410	8560	22.4	5	4
	3			48.9	25.7	10120	10270	24.5		
$\text{CoK}_2(\text{SO}_4)_2 \cdot 6\text{H}_2\text{O}$	1			57.6	25.9	11270	11420	25.9		
	2	-44°	-84°	44.6	20.1	8720	8870	22.8	5	4
	3			48.6	21.9	9510	9660	23.8		
$\text{CoRb}_2(\text{SO}_4)_2 \cdot 6\text{H}_2\text{O}$	1			56.3	22.0	11540	11690	26.1		
	2	-25°	-74°	42.9	16.7	8790	8940	22.9	5	4
	3			49.0	19.1	10040	10190	24.4		
$\text{FeK}_2(\text{SO}_4)_2 \cdot 6\text{H}_2\text{O}$	1			59.8	27.5	11840	11990	26.4		
	2	55°	-78°	52.1	23.9	10320	10470	24.8	5	4
	3			61.4	28.4	12160	12310	26.8		
$\text{Mn}(\text{NH}_4)_2(\text{SO}_4)_2 \cdot 6\text{H}_2\text{O}$	1			62.8	34.3	13320	13470	28.1		
	2	14°	-83°	62.6	34.2	13280	13430	28.1	6	5
	3			63.1	34.5	13380	13530	28.1		

the assignment of one Bohr magneton for each five Weiss magnetons, or the Sommerfeld-Pauli¹⁴ method based on space quantization, which would give,¹⁵

¹⁴ Pauli, Phys. Zeits. 21, 615 (1920); Epstein, Science 57, 532 (1923); Gerlach, Phys. Zeits. 24, 275 (1923); Sommerfeld, Phys. Zeits. 24, 360 (1923).

¹⁵ Sommerfeld, Atombau und Spektrallinien, 4th Ed., p. 631.

Bohr magnetons: 1 2 3 4 5
 Weiss magnetons:¹⁶ 8.6 14.1 19.2 24.4 29.4

TABLE II

Compound	Crystal system	Axis	Volume	Mass sus-	Molecular	Average
			$K \times 10^6$	$x \times 10^6$	$x_m \times 10^6$	molecular
NaNO_3	trigonal	trig axis	-0.788	-0.347	-29.5	-25.9
		\perp trig axis	-0.644	-0.284	-24.1	
CaCO_3 (calcite)*	trigonal	trig axis	-1.10	-0.406	-40.7	-37.8
		\perp trig axis	-0.98	-0.364	-36.4	
KNO_3	rhombic	c axis	-0.744	-0.353	-35.6	-31.7
		b axis	-0.620	-0.294	-29.7	
		a axis	-0.624	-0.296	-29.9	
CaCO_3 (aragonite)*	rhombic	c axis	-1.30	-0.444	-44.4	-40.8
		b axis	-1.14	-0.387	-38.7	
		a axis	-1.15	-0.392	-39.2	
$\text{Sr}(\text{NO}_3)_2$	cubic		-0.793	-0.271	-57.2	-57.2

*Voigt and Kinoshita loc. cit.

DIAMAGNETIC CRYSTALS

W. L. Bragg¹⁷ has recently published a theory accounting for the double refraction of calcite and aragonite on the basis of the mutual influence of the induced electric moments. This effect is specially great for the oxygen ions which lie close together, as shown by x-ray analysis. An attempt to explain the differences in diamagnetic susceptibility along the same lines shows that the internal field due to diamagnetic polarization is too small to account for the facts.

The writer wishes to express his thanks and appreciation to Professor A. P. Wills, under whose supervision this research was done, for his kind interest, suggestions and advice.

DEPARTMENT OF PHYSICS,
 COLUMBIA UNIVERSITY,
 August 16, 1926.

¹⁶ In Table I, the Bohr magneton numbers are given to the nearest integer since it is not to be expected that they will fit any one of three principal susceptibilities, or their average.

¹⁷ Bragg, Proc. R. S. London 105, 370 (1924).

SCATTERING OF PARTICLES BY AN EINSTEIN CENTER

By T. TAKEUCHI

ABSTRACT

The scattering of α -rays is considered by making use of the Jeffery-Nordstrom form of space time. The results obtained are similar to those of W. S. Kimball in that the relativity effect is found to be too small to be detected experimentally.

W. S. KIMBALL¹ has considered the scattering of alpha particles by a nucleus when Coulomb's inverse square law of force is replaced by a relativistic law corresponding to a fixed point center. But his substitution of the constant of integration $\gamma m/c^2$ which measures the strength of the center by ENe/c^2M (γ , Newton's gravitation constant; m , mass of the center; c , velocity of light in vacuo; Ne , nuclear charge; E , charge of the particle; M , its mass) upon which his results rest is not thought to be appropriate. The present author has attacked this problem using the Jeffrey-Nordstrom form of space time, which admits of a correct comparison of the scattering of atomic rays as required by the classical law² with the scattering when this law is replaced by a relativity law. However, the result shows that the amount of this relativity departure is too minute to be detected by experiments.

The field of the nucleus is defined by

$$ds^2 = -\gamma^{-1}dr^2 - r^2d\theta^2 - r^2\sin^2\theta d\phi^2 + \gamma c^2dt^2,$$

where

$$\gamma = 1 - 2km/c^2r + \kappa\epsilon^2/c^4r^2 \quad (\epsilon, \text{charge in e.s.u.}).$$

The equations of motion of a particle in this field are given in the following, simplified for orbits in the equatorial plane $\theta = \frac{1}{2}\pi$:

$$\gamma^{-1}(dr/ds)^2 + r^2(d\phi/ds)^2 - c^2\gamma(dt/ds)^2 + 1 = 0,$$

$$r^2d\phi/ds = h, \quad \gamma dt/ds = n - \epsilon\epsilon'/c^3m'r$$

ϵ' and m' denoting the charge and mass of the particle, h and n the constants of integration which have the following meanings

$h(c^2 - v^2)^{\frac{1}{2}} \approx hc = \text{constant of areas}; (c^2n^2 - 1)/n^2 = v^2, c \approx 1/n;$
where v denotes the initial velocity, at infinity.

¹W. S. Kimball, Phys. Rev. 23, 75 (1924).

²C. G. Darwin, Phil. Mag. 27, 499 (1914).

The equations of motion give, neglecting higher orders of small quantities,

$$\begin{aligned}(du/d\phi)^2 &= (c^2/h^2)(n - \epsilon\epsilon' u/c^3 m')^2 - (1/h^2 + u^2)(1 - 2\kappa m u/c^2 + \kappa\epsilon^2 u^2/c^4) \\ &\approx (c^2/h^2)(n^2 - 2\epsilon\epsilon' n u/c^3 m') - (1/h^2 + u^2) \\ &= (c^2 n^2 - 1)/h^2 - n^2 - 2\epsilon\epsilon' n u/h^2 m' c,\end{aligned}$$

where u stands for $1/r$. Accordingly

$$(du/d\phi)^2 = v^2/c^2 h^2 - u^2 - 2\epsilon\epsilon' u/c^2 h^2 m'$$

which agrees with the classical formula. No relativity correction term is obtained to this order of approximation.

TOKYO HIGHER TECHNICAL SCHOOL, JAPAN,
DEPARTMENT OF PHYSICS,
August 5, 1926.

THE BREAKDOWN OF ATOMS AT HIGH PRESSURES

By P. W. BRIDGMAN

ABSTRACT

Thermodynamic evidence supports the experimental suggestion of a previous paper that at ordinary temperatures sufficiently high pressures are capable of breaking down the quantum structure of atoms, reducing matter to an electrical gas of electrons and protons. We may, therefore look for atomic dissociation under two sorts of conditions: high temperatures and comparatively low pressures, such as we have in the stellar atmospheres, and high pressures and comparatively low temperatures, which we may surmise we have in the interiors of stars, possibly in stars like the sun, and almost certainly in stars of the enormous density of the dark Sirius type. The possibility of two sorts of dissociation, together with the more rapid increase of pressure than density when the diameter of a star is reduced, offers the possibility of a critical condition determining whether a star is of the dark Sirius type or not.

IN THE PHYSICAL REVIEW for January 1926 I called attention to a reversal in the behavior of certain properties of potassium (the atom of which has an abnormally loose structure) at high pressures and room temperature, which I suggested might indicate the initiation of an ultimate breakdown of the atom at much higher pressures and an approach to a gas of electrons and protons. Supporting this idea that a breakdown of the atoms is possible at high pressures, there is an argument from a theorem of Schottky's which I presented in the previous paper; furthermore we have the physical feeling that the quantum orbits to which the atom owes its structure ought not to be able to resist an indefinitely great force, and also the fact that there are stars of enormous densities. Nevertheless, the assumption of this sort of atomic disintegration involves certain apparent inconsistencies, for in the atmospheres of the stars we have direct spectroscopic evidence of atomic disintegration, as was first extensively shown by Saha, and simple thermodynamics shows that this decomposition *increases* with rising temperature and *decreases* with rising pressure. Since such decomposition at the high temperatures and greatly reduced pressures of the stellar atmospheres is only partial, it would appear at a first glance that there is no reason to expect any decomposition at all at ordinary temperatures and pressures of tens of thousands of atmospheres. It is the purpose of this note to present additional thermodynamic evidence suggesting that decomposition may nevertheless occur at high pressures and low temperatures, and to resolve the apparent inconsistency.

Let us examine the consequences of assuming that it is possible to apply sufficient pressure to a substance at room temperature to break the

atoms down into a perfect gas of electrons and protons. Under such a pressure the thermal expansion must assume the value appropriate to a perfect gas, and the specific heat must also become very much larger than that of a normal solid, because each electron makes its full individual contribution to specific heat. Now thermal expansion and specific heat cannot vary independently, but there is a thermodynamic connection, namely:

$$(\partial C_p / \partial p)_T = -\tau (\partial^2 v / \partial T^2)_p$$

Hence if C_p is to increase with pressure, $(\partial^2 v / \partial T^2)_p$ must be negative, which is the reverse of its usual behavior, because the thermal expansion at constant pressure of normal substances increases with rising temperature instead of decreasing. Now since the thermal expansion of a gas is much higher than that of a normal solid, a higher thermal expansion at low temperatures means a closer approach to the perfect gas condition at low temperatures. This indicates therefore that if a solid is decomposed by high pressure and made to approach the behavior of a gas, the approach to this condition will be most rapid at low temperatures. My experiments on potassium were made at low temperature.

This state of affairs is also consistent with other thermodynamic evidence. In the atmospheres of the stars atomic decomposition decreases with rising pressure; here it increases. Now a homogeneous reaction is driven by pressure in such a direction as to decrease the volume. In the stellar atmospheres, therefore, the volume of the neutral atoms is less than that of the ionized atoms and the detached electrons; this is a consequence of the comparatively low pressures. At high pressures, on the other hand, simple calculation shows that the electrical gas has a smaller volume than that of the undissociated atoms from which it comes. In normal substances under high pressures it appears therefore that the quantum orbits act like skeleton frameworks *distending* the structure; if these frameworks are destroyed, the substance collapses. It was shown in the previous paper that at 300°K the pressure at which the volume of the electrical gas is equal to that of the neutral atoms is of the order of a few 10,000 atmospheres, which is certainly a negligible pressure compared with cosmic possibilities. As temperature increases, the dissociated volume gains relatively to the undissociated volume in consequence of the high thermal expansion of the gas, thus bearing out the evidence above that the approach to gaseous decomposition is closest at low temperature.

In the stellar atmospheres decomposition increases with rising temperature at constant pressure; under our conditions it decreases. This means that in the stellar atmospheres heat must be absorbed by the dissociation, whereas under our conditions heat is given out. The reason for this dif-

ference is evident. Under atmospheric conditions the volumes are so large that the electron must be removed to a great distance against the electrostatic forces of the core during decomposition. There is a compensating effect arising from setting free the kinetic energy of the electrons in the quantum orbits, but this is only half the electrostatic effect. Under our conditions however the volume is small, and the electrons on the average are no further away from the core after decomposition than before. The electrical effect vanishes, therefore, leaving the kinetic effect outstanding. Now the kinetic energy of the electrons in the quantum orbits is much higher than the equipartition temperature energy at ordinary temperatures, so that heat must be given out rather than absorbed when an atom decomposes at high pressures. (Has this been considered as a source of stellar energy?) It is also evident, since the kinetic energy of the electrical gas is higher at the higher temperature, that this heat of dissociation decreases with rising temperature, again demanding that decomposition be greater at lower temperatures than high. Further, there is another effect tending to accentuate the reversal of sign of the heat of dissociation at high pressures. After the first few 10,000 atmospheres the internal energy of a solid increases when pressure increases at constant temperature. This increase of internal energy is divided in the ratio of two to one between energy of position and increased kinetic energy of the electrons in their orbits. This latter part is set free during dissociation, so that the heat of dissociation under high pressures is greater by this amount than would be indicated by our argument above applied to normal atoms at atmospheric pressure.

All the lines of evidence converge, therefore, to indicate a pure pressure decomposition of atoms at high pressures, and this decomposition is favored by low temperature. We must then visualize the condition of matter over extreme ranges of pressure and temperature somewhat as follows. The pressure-temperature plane is crossed by a diagonal band rising from low pressures and temperatures to high pressures and temperatures, within which matter exists in the normal form of neutral undissociated atoms as we know them. To one side of this band is the region of high temperature and low pressure in which the atoms are dissociated into a gas of electrons and protons, and it is in this region that we find matter in the stellar atmospheres. On the other side of the band, at high pressures and low temperatures, we also have matter dissociated into an electrical gas. We now have to ask to which of these two regions the apparently perfectly gaseous *interiors* of the stars belong. If to the first, we have decomposition in spite of high pressure, if to the second, in spite of high temperature. It seems almost certain that stars of densities of

50,000, like the dark companion of Sirius, indicate the second region. If the density is of the order of magnitude of unity, and nevertheless the star acts like a perfect gas (as does our sun, according to Eddington), we may suspect the first region, but perhaps even under these conditions the second region is not impossible.

Perhaps the following calculation is worth recording as suggesting possible orders of magnitude. Imagine an atom of atomic number 40, with the negative electricity all concentrated in a uniform spherical shell of radius 1.5×10^{-8} cm. Due to the mutual repulsion of its parts this shell is exposed to a distending pressure of approximately 3×10^{14} dynes/cm². The positive nucleus exerts an inward pressure of twice this; the difference, or 3×10^{14} dynes/cm², is the effective distending pressure of the quantum structure of the atom preventing collapse. The pressure in the interior of the sun is of the order of ten times higher, so that possibly we may expect pressure dissociation in the sun, although it seems more likely that we have the first sort of dissociation.

As far as I know, no adequate physical difference has been suggested to account for some stars with densities of 1.5 and others with 50,000. In view of the comparatively small range of mass of the stars this seems to demand some explanation. The possibility of two regions of dissociation seems to offer a clue. If the mass of a star is concentrated in spheres of decreasing radius, the pressure rises faster than the density. Thus if the sun were concentrated in a small sphere of density 50,000 times the present density, the pressure would be nearly 2,000,000 times greater (in general pressure varies as (density)^{4/3}). This sort of thing suggests instability and critical conditions, with the possibility of some stars in the second state of dissociation. If, however, the sun should turn out to be in the second condition, then we may perhaps recognize the possibility of two different stable states in the second condition, not unlike the two amorphous phases of ordinary matter of van der Waals.

A complete description of the state of affairs involves many complicated considerations. It is evident that the atoms in a star are in varying degrees of dissociation; according to the nature of the atom perhaps some of these are in the first condition, while others may be in the second. We need a detailed mathematical treatment of the comparatively simple problem of the equation of state of matter dissociated into electrons and protons under very high pressures without quantum conditions; this would show how nearly our assumption is realized of perfect gas behavior.

THE JEFFERSON PHYSICAL LABORATORY,
HARVARD UNIVERSITY, CAMBRIDGE, MASS.
October 4, 1926.

CONTINUOUS MOTION PRODUCED BY VIBRATION

BY W. B. MORTON AND A. MCKINSTRY

ABSTRACT

A special case of motion of this kind was discussed recently by A. T. Jones. In the present note attention is called to a number of other cases in which the precise mechanism is obscure. A simple form of the phenomenon occurs when a mass is made to slip along a rough inclined plane, without loss of contact, by making the plane oscillate. This is examined mathematically. It is found that the motion may be either upwards or downwards, according to the relation between the direction of oscillation and the inclination of the plane. The results have been roughly verified by experiment.

A PAPER with the above title was communicated to the British Association at the Belfast meeting in 1902. It appears in the Report for that year merely by its title¹; we deferred publication in the hope of doing further work on the subject, a hope which, for various reasons, was never realized. In a recent number of the PHYSICAL REVIEW Professor A. T. Jones² has discussed a very interesting case of the kind of motion referred to, viz., the rotation of the pulley in Melde's experiment. The present note is prompted by the appearance of his paper and may be of some interest as a sequel to it.

To begin with it may be worth while to draw up a list of cases of the transformation of oscillatory into continuous movement. The mode of action is perhaps not so difficult to understand, in general outline, as the complementary phenomenon, when oscillations are initiated and maintained by continuous motion, as in the sounding of an organ-pipe by a current of wind; but when we come down to detail a good deal still remains to be explained.

1. *The Chladni plate.* The motion of the sand to the nodal lines is one of the most familiar phenomena in physics but there appears to be a difference of opinion about the exact way in which this comes about. Lord Rayleigh³ regarded it as the result of haphazard hopping of the particles; when a grain by chance reaches a nodal line it remains there, and in time this happens to all the grains. Auerbach,⁴ on the other hand, proposed a theory by which the curvature of the plate in the moving parts caused the particles to be projected in a direction inclined to the vertical on the side towards the nodal line. On similar lines was the

¹ Report of B. A., p. 511 (1902).

² Jones, Phys. Rev. 27, 622 (1926).

³ Rayleigh, "Sound," Vol. I, p. 368.

⁴ Auerbach, in Winkelmann's "Handbuch," 2, "Akustik," p. 385.

explanation given by Zenneck⁵ of an effect which he observed, the rotation of a vibrating circular plate, free to move in its own plane, round its center. The motion was ascribed to a horizontal component in the reaction exerted on the plate by the support.

If a small particle of lead shot is flattened and laid on a Chladni plate, it will be found to make its way by a continuous movement to a nodal line. It would be interesting to examine what relation the paths so traced bear to the curved form of the plate.

Some anomalous effects observed by Savart⁶ are referred to in this connection by Lord Rayleigh.⁷ Here the nodal lines on opposite sides of a plate had different positions and the motion of the particles was continuous towards these positions. The explanation is found in a combination of transverse vibration with vibrations of the same period in the plane of the plate. In such cases "the movement of sand to the nodes, or to some of them, takes place in a more direct manner as the result of friction."

2. *Goold's "vortex-plate."* Very curious motions of sand-particles were discovered by Mr. Joseph Goold on steel plates of a long rectangular form when supported at proper points and rubbed along the edge of the long side. These plates were shown in London in 1906 at the Royal Society and the Physical Society, by Messrs. Newton and Co.⁷, and some specimens were then procurable from that firm. The dimensions of one which came to Belfast are $86.6 \times 10.0 \times 0.91$ cms. When the plate is properly excited two regions appear near the ends where the sand moves round and round in circles. A chain laid on the plate is gradually drawn into one of the vortices and coiled up there. We have probably here another case of coexistent vibrations of different modes, but no explanation of the very remarkable effects appears to have been published.

3. *Melde rotations.* An effect which we observed may be added to those described in Professor Jones' paper. If the axis of a pulley be made to vibrate, with no cord passing over the rim, the wheel will rotate when the point of a pencil is pressed against the rim. There are four points at which the direction of rotation reverses.

Another isolated phenomenon of this class was observed by Kundt.⁸

⁵ Zenneck, Ann. d. Physik **66**, 170 (1898).

⁶ Savart, a reference is given to "Ann. d. chim. **14**, 113 (1820).

⁷ In Nature **74**, 59 and 215 (1906) will be found merely a mention of the exhibition of the plate. The only description published, so far as we know, was in a book on "Harmonic Vibrations" published by Messrs. Newton and written jointly by Jos. Goold, Chas. E. Benham, Richard Kerr and L. R. Wilberforce.

⁸ Kundt, Pogg. Ann. **126** (1852).

A cork of slightly conical form fitting loosely inside a glass tube moved in the direction of its smaller cross-section when the tube was set in longitudinal oscillation.

The following trifling effect is perhaps new. It is usual, in showing lecture-experiments on the vibrations of strings, to use small paper riders cut in the form of an inverted V. These are thrown off the sonometer string at loops and remain in position at nodes. Let one of these be bent so that its side elevation is an arc of a circle. If the wire is gently twanged the bent rider will move along it in the direction towards which the paper is concave. If the two legs of the V are bent in opposite directions the rider remains at the same point of the wire and rotates. It would seem that the lamina, thrown upward from the wire, in its fall has time to rotate slightly so as to bring its concave side downward, possibly through the effect of air-resistance. In this way the notch of the rider comes back to the wire in a slightly displaced position.

Screwed-on nuts, etc., in machinery often "work loose" as a result of vibration; this so far as it goes, is a continuous movement and may, therefore, be included in the list.

In most of the instances which have been enumerated it is clear that an important part is played by the friction between the surfaces in contact. This suggests an examination of the simplest possible case. Let a block lie on a supporting plane to which is given a rectilinear oscillatory motion. If the block is to move in one piece with the plane it is necessary that the ratio of the tangential to the normal component of the reaction shall be less than the coefficient of friction. This implies that the acceleration of the plane shall not exceed a definite limiting value: when this is passed slip occurs in the direction opposite to the force of friction. We may suppose the limit reached by a gradual increase either of the frequency or the amplitude of the oscillations. The limiting values of the acceleration will, in general, be different for the two directions of slip. The motion which first occurs is that corresponding to the smaller value. If, by further increase of amplitude or frequency, the higher limit is also exceeded the net slip will still be in the former direction. It is unnecessary for our purpose to go into a detailed discussion of the course of the motion, which is a matter of some complexity.

Let us take first the case of a horizontal plane and suppose the line of oscillation to make angle α with the horizontal, sloping upwards to the right. Then the slip will occur to the right, i.e., in the direction of the horizontal component of the upward motion; for the limiting values of the acceleration are

$$g \sin \epsilon / \cos(\alpha - \epsilon), \text{ for slip to the right}$$

$$g \sin \epsilon / \cos(\alpha + \epsilon) \text{ for slip to the left}$$

where ϵ is the angle of friction.

Let now the plane have inclination β , where $\beta < \epsilon$, sloping upward to the right; so that the upward direction of vibration lies on the same side of the vertical as the surface of the plane. At first sight one might think that, when a block is kept up by friction on an incline, any kind of vibration would tend to bring it down. This is not so. It may easily be verified that the limiting values of the acceleration are now

$$g \sin(\epsilon + \beta) / \cos(\epsilon - \alpha + \beta) \text{ for upward slip}$$

$$g \sin(\epsilon - \beta) / \cos(\epsilon + \alpha - \beta) \text{ for downward slip.}$$

Putting these equal to each other we find the relation

$$\sin(\alpha - 2\beta) = \cos 2\epsilon \sin \alpha,$$

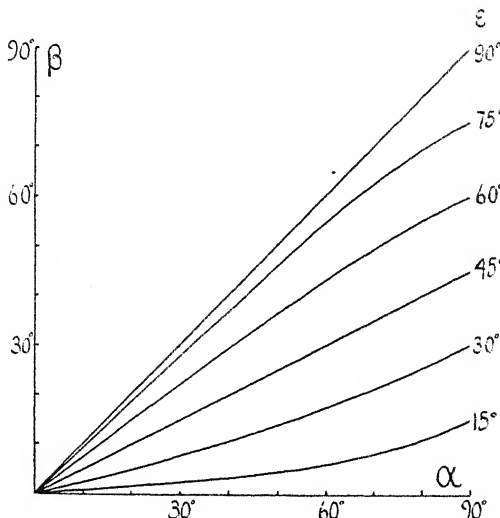


Fig. 1. Relation between pairs of critical values of α and β .

which gives a critical value of α for each β or of β for each α . With such a pair of values there will be no transport of the block. Increase of α or decrease of β gives upward motion, decrease of α or increase of β downward motion. If α is negative, i.e., if the direction of upward vibration and the plane are on opposite sides of the vertical, the slip is always downwards. In all this we are assuming that the acceleration is not great enough to make the block lose contact with the plane. The necessary acceleration for this to occur is $g \cos \beta / \sin(\alpha - \beta)$. Comparison with the slip-values shows that this is always greater than the upward slip-limit, and is greater than the downward one provided the coefficient of friction is less than

$$\cos(\alpha - 2\beta) / 2 \cos \beta \sin(\alpha - \beta).$$

The hopping motion is not further considered.

The relation between pairs of critical values of α, β is shown graphically on Fig. 1, each curve being drawn for a definite angle of friction which is marked at its right-hand end and which is also the ordinate at this end, where $\alpha=90^\circ$. This implies that vertical oscillations will always jolt upwards a mass which can lie at rest on a rough plane. For the special value $\epsilon=45^\circ$, i.e., coefficient of friction = 1, the graph is straight and $\beta=\frac{1}{2}\alpha$. The slope, $d\beta/d\alpha$, at the origin is $\sin^2\epsilon$ and at the upper ends all the curves have the slope $\frac{1}{2}$.

A few rough experiments were made to test this theory. A glass plate was mounted on a partly dismantled "Donkin's Harmonograph," and was made to oscillate by an electric motor at a rate which was varied by a regulating resistance. A definite direction of vibration having been set, the inclination of the plate to the horizontal was given a succession of small values. The speed was increased until a glass block placed on

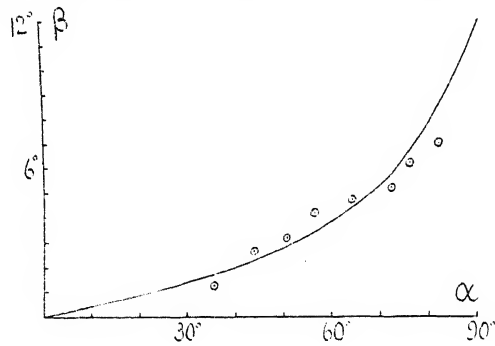


Fig. 2. Critical values of β for various values of α .

the plate moved in one direction or the other. In this way an estimate was made of the critical β for each α . It was found necessary to keep the surface of the glass warm by a heating coil to prevent the formation of a film of moisture which made the surfaces stick. The angles were read by a rather primitive clinometer. The result of a series of observations is shown on Fig. 2. The average value of $\sin(\alpha - 2\beta)/\sin \alpha_1$ which should have the constant value $\cos 2\epsilon$, was found to be .914, corresponding to $\epsilon=12^\circ$ approximately. The curve on Fig. 2 is the theoretical one corresponding to this value of ϵ , on a vertical scale for β which is five times that of Fig. 1. The agreement is perhaps as good as can be expected under the conditions of experiment.

QUEEN'S UNIVERSITY,
BELFAST.
July 28, 1926.

BOOK REVIEWS

Les Physiciens Hollandais et la Méthode Expérimentale en France au XVIII^e Siècle. PIERRE BRUNET.—This booklet is a careful and interesting study of the influence of British experimental physics of the seventeenth century upon eighteenth century scientific research and teaching in Holland, and the influence, in turn, of the three leading Dutch experimenters and writers, 'sGravesande, Desaguliers and Musschenbroek, upon experimental research in France. The Frenchmen, Du Fay, L'abbé Nollet, Voltaire, La Mettrie, all visited Holland and drew inspiration from the schools at Leyden and Utrecht. The invention of the Leyden jar was the outstanding achievement. Brunet gives considerable attention to the discussions, carried on in Holland and later in France, of methods of scientific research and of the use of hypotheses. The book has no alphabetical index. Pp. 153 Librairie Scientifique, Albert Blanchard, Paris, 1926. Price 14 Fr.

FLORIAN CAJORI

Méchanique Analytique et Théorie des Quanta. G. JUVET.—As the title indicates the author presents the principles and methods of analytical dynamics and celestial mechanics in a form suitable for their application to atomic problems. This occupies about two thirds of the text, which is divided into two parts, the remainder being devoted to methods for the quantization of multiply periodic systems. Although not a book for the beginner it should appeal strongly to the theoretical physicist, already familiar with the results of quantum theory, who wishes to broaden and complete his knowledge of advanced methods in dynamics. To the mathematician it should prove an attractive introduction to atomic dynamics.

In the treatment of dynamics the Hamiltonian action function is made to play a leading part, and the Hamilton-Jacobi equation is first introduced as a property of this integral. In the two chapters on perturbation theory there is a detailed account of the method of Delaunay and the methods of Bohlin and Lindstedt. In the treatment of the latter, which are the methods most extensively used in the quantum theory, the author has followed the presentation of Poincaré in his "Méthodes Nouvelles," but without discussion of the convergence of the series. This chapter should prove particularly useful, as the results are somewhat scattered and condensed in the original.

The section on the applications is devoted almost exclusively to the quantization of separable multiply periodic systems, and the reader may be somewhat disappointed at the lack of illustrative material. Only the relativity hydrogen atom and the Stark effect are discussed, and there are no examples of the perturbation methods, although a final chapter is given to a brief discussion of the work of Born and others on the use of the methods of Bohlin and Lindstedt.

The author's prediction that the quantum theory has not as yet attained a final form has been amply confirmed in the interim since publication. Nevertheless the methods of classical mechanics, so beautifully expounded in this little book will probably long continue to be of fundamental importance in atomic physics.—VI+151 pp., 2 figs. Librairie Scientifique Albert Blanchard, Paris, 1926. Price 20 francs, unbd.

F. C. HOYT

The Mystery of Mind. LEONARD T. TROLAND.—This elementary treatise on psychology has an interest for physicists, in view of the manner in which the author poses his problem. He is a Fellow of the American Physical Society as well as a teacher of psychology at Harvard, and it is therefore quite natural that he should seek his orientation in connection with the problem of the relation between the world of physical objects conceived in terms of the newest science, and the world of consciousness, which

latter he identifies with the world as it presents itself in the immediate experiences of our every-day lives. The difference between these two worlds is stressed to the utmost, so that not a single relation of resemblance between them remains; not even the space-time systems being identical, on account of the view of physical space and time necessitated by the theory of relativity. This difference, not to say divorce, between the two worlds, constitutes the "mystery of mind"; the problem of the author is to construct a bridge over this apparently impassable chasm. The exposition is couched in clear and simple language, and though elementary on both the physical and the psychological side, is thoroughly competent.

Does the author succeed in bridging his chasm? I will not attempt to spoil the reader's sense of mystery by outlining the proffered solution, but only offer a word or two in comment. Professor Troland sees more or less clearly that the nature of *perception* (as distinct from sensation) is the crux of the problem, and presents (pp. 90-94) a very ingenious theory of this concrete mental function. But he willfully rejects the hint given of the nature of thought and perception by the language, which always attaches an 'of' or an 'about' to the naming of the concrete mental functions; as *consciousness of, thought about, memory of, perception of, etc.* It thus suggests that perceiving as well as thinking is always an intentional act directed upon an object not itself. If this object is utterly unknown to the experience of daily life, then it must surely also remain unknown to the experience and reflection of the physicist, who naturally has no other foot-hold in experience than that which he shares with all human beings. Nevertheless, much can be learned from the author's formulation of the problem, the most pressing logical problem, perhaps, of the present day. Pp. 253, D. Van Nostrand Company, New York, 1926. Price \$3.00.

DAVID F. SWENSON

Colloid Chemistry—Theoretical and Applied. COLLECTED AND EDITED BY JEROME ALEXANDER. (VOL. I. THEORY AND METHODS.)—This is the first of a series of three volumes and is largely devoted to a consideration of the theoretical principles which underlie the study of colloids. The volumes which will follow will take up the applied aspects of Biology and Medicine and Technology. The book is a striking example of the degree of specialization which characterizes modern science. Only a few decades ago a "scientist" was supposed to be able to write authoritatively in all fields of natural science. Today in a single subject within a small field we have a further intense specialization. The volume contains 60 chapters, each written by a specialist in the particular subject under discussion. It is a truly international compilation, including authors from the United States, Canada, England, France, Germany, Sweden, China, Japan, Spain, and Holland. As one might expect, the chapters are almost wholly disconnected and there is a certain amount of duplication. However, the duplication is not a serious fault, for it sometimes affords the reader an opportunity to view the same problem through the eyes of two or more specialists. About three-fourths of the chapters are excellent and present a fairly exhaustive epitome of the subject under discussion. Part of the remaining chapters are either decidedly inferior in quality or deal in such vague generalities that it is difficult to see why they were included in a volume on "Theory and Methods." The remaining chapters deal almost wholly with industrial processes or applications and do not contribute either to theory or methodology.

The physicist and physical chemist should be especially interested in the chapters by von Weimarn, "Theory of the Colloid State of Matter" (p. 27-101); E. F. Burton, "Determination of Size and Mass of Colloidal Particles" (p. 165-173); W. D. Harkins, "Surface Energy and Surface Tension" (p. 192-264); H. R. Kruyt, "The Mechanism of Coagulation" (p. 306-322); A. Einstein, "Theory of the Opalescence of Homogeneous Liquids and Mixtures of Liquids in the Vicinity of the Critical State" (p. 323-339); L. Michaelis, "Electric Phenomena in Colloid Chemistry" (p. 471-506); Irving Lang-

muir, "The Effects of Molecular Dissymmetry on Some Properties of Matter" (p. 525-546); H. Freundlich, "Adsorption and Its Significance" (p. 575-599); E. C. Bingham, "Fluidity and Plasticity" (p. 720-726); E. Hatschek, "The Viscosity of Colloidal Solutions" (p. 738-750); and Sven Odén, "Sedimentation-Analysis" (p. 861-909).

The "editing" is apparently confined to the addition of occasional footnotes. In general, the printing, proof reading, and binding are well done. The volume should be of great assistance to those who are interested in the study of colloids either from the standpoint of the teacher or the research worker, for it brings together for the first time many isolated observations and divergent views, and to find all of this material in one volume will save many hours of library work. Pp. 974, 59 figs., The Chemical Catalog Company, N. Y., 1926. Price \$14.50.

ROSS AIKEN GORTNER

General Physics for Colleges. D. L. WEBSTER, H. W. FARWELL, AND E. R. DREW. REVISED EDITION.—While preserving the character and aims of the first edition,* the second edition is in many respects greatly improved. To quote from the preface, "The changes in the text are of all sorts, some in the addition of topics clearly called for, some in proofs or descriptions, and others such simple, but none the less important, changes as an improvement in typographical arrangement, enabling the student to locate more readily the definitions of technical terms. Likewise in the problems there are changes of many kinds, including additions of the easier types, a marked improvement in arrangement, and a simplification of the method of handling problems calling for original work in the collection of data." Almost every page has been to some extent revised, and considerable improvements have been made in the order of topics. The book has been increased in length by 150 pages, 22 of which are in the excellent chapter on statics. Among the new features may be mentioned frequent historical notes; references for supplementary reading; paragraphs on various subjects omitted in the first edition, for example musical intervals, and the equation of Van der Waals; explanatory captions printed under most of the figures; and the grouping of tables of constants at the end of the book. The sections on electricity and magnetism have been greatly improved. Many new problems have been included; in fact, the reviewer has found no other text in which the problems are as varied and as stimulating as these. The chapters on modern physics now occupy 174 pages. They have been very materially revised, brought down to date, and enlarged, and remain, as before, an admirable and notable feature of the book.—Pp. 707+xiii, 480 figs., Century Co., 1926. Price \$3.75.

W. G. CADY

Handbuch der Experimental Physik, Vol. I, Messmethoden und Messtechnik. L. HOLBORN AND E. VON ANGERER.—If the present volume is indicative of the character of the succeeding volumes of this undertaking, the new "Handbuch" will be prized by experimental physicists everywhere. It is being edited by W. Wien and F. Harms, with the coöperation of fifty colleagues in various European countries, whose names are sufficient guarantee for the high standard of the work. According to the ambitious statement in the general preface, "It is intended that the 'Handbuch' shall present the broad domain of this science, which, owing to the ever growing literature, the individual investigator can no longer survey by his own efforts, in such a way as to comprise with as much completeness as possible everything necessary for scientific and technical experimentation." About two thirds of this initial volume are devoted to the more fundamental methods and technique of measurement in the various branches of physics. A brief chapter on units is followed by a section on mechanics, heat, electricity, magnetism, and optics. The choice of topics and relative emphasis placed upon them seems somewhat strange, but presumably the balance will be restored in the remaining volumes.

* See review in this Journal, Vol. 23, p. 661, 1924.

Thus on the one hand considerable space is given to the evolution of the meter in terms of the wave-length of light; to the tube-driven tune-fork as a standard of time; and to photometry. On the other hand the remaining branches of optics are practically ignored in this volume, as well as all mention of experimental work in sound, elasticity and capillarity. The chapters on electricity are very condensed, many important methods of measurement being omitted. Granted that these and other omissions are to be made good in the volumes yet to come, there still remains the suspicion that the work, like most other large-scale collaborations, is likely to suffer from lack of coherence. However, the topics treated are dealt with in masterly fashion. The work is intended less for the student than for the trained experimental physicist, and it should prove useful for workers in allied sciences as well. It is evidently written in part for the "Ausland," since there are frequent references to units employed in France, Great Britain and the United States, and the number of citations of papers published in those countries is evidence of an unusual degree of thoroughness and impartiality. The remaining third of the volume forms an excellent treatise on laboratory technique. The chapters comprise the following subjects: substances used in the laboratory (including especially tungsten and quartz glass); soldering, welding, and cementing, (including the modern method of uniting glass with copper); manipulation of glass; silvering and the preparation of thin films (more might have been said on methods of sputtering); vacuum technique (but next to nothing on vacuum pumps!); metallic foil, fine wires, and quartz fibres; insulators and high resistances; thermo-elements (we miss, however, the modern vacuum thermo-element); an excellent chapter on photography; electric ovens, (the treatment of high temperature furnaces is inadequate); colloidal solutions; electro-plating; and a short chapter on miscellaneous "Kunstgriffe," including Eguchi's "electret." References to American sources are numerous. The index is excellent—an important virtue in a work of this sort.—xx+484 pp., 246 figs. Akademische Verlagsgesellschaft, Leipzig, 1926.

W. G. CADY

Handbuch der Elektrizität und des Magnetismus. Band V—Lieferung 1. L. GRAETZ.—This volume of the Graetz Handbuch is devoted to the problems of induction, alternating currents, electrical oscillations, and the methods of their production and detection. The policy followed is to present a skeleton of the theory and of the main experimental facts and to follow up by complete references to more recent work.

(a) Induction. In this chapter the induction of electric currents due to various causes is treated. Applications such as the earth inductor are discussed. Eight pages are devoted to unipolar induction. A reference to the discussion by Tate in the Bulletin of the National Research Council is apparently lacking. The bearing of the Lorentz transformation on the phenomenon is not discussed. Induction coils, interrupters, and rectifiers are treated next. Useful references to the breakdown potential of air and to the effects of frequency are given. Formulas for the calculation of self and mutual inductance of coils are presented in some detail. It is to be regretted, however, that no tables are printed. The most important bridge methods of measuring self inductance are mentioned. References to discussions of errors of measurement are also found. The results of the earlier work on skin effect are mentioned, though the later work is simply listed according to authors. The recent work of C. Snow at the Bureau of Standards is, of course, not mentioned. The applications of the theory of skin effect to resistance calculations are treated again in a later chapter. A numerical error in Sommerfeld's calculations is not mentioned there (3.7 instead of the correct 3.4 for the ratio of the resistance of closely coiled wire to straight wire at very high frequencies). The calculations of Abraham and Bloch are not discussed in this connection.

(b) Alternating currents. This section was prepared by J. Wiesent of Munich. The Argand diagram for alternating currents is discussed, but impedances are treated mostly

without the aid of complex number representation. Methods of producing alternating currents, multiple phase currents, and oscillographs are enumerated. The resistance for alternating currents is discussed briefly. Only 50 pages are devoted to this section, and so it cannot be complete from an engineering point of view. However, it gives the important physical facts.

(c) Electric oscillations. This chapter is again by L. Graetz. After a general discussion of the phenomena, the mathematical theory of two coupled circuits is given. The considerations of Bjerkness are presented concisely. A number of references are given in connection with the calculation of natural wave-lengths of coils. The shortest and the longest waves that have been obtained are mentioned. Various detectors of oscillations and methods of producing oscillations, electrical filters, Whiddington's ultra-micrometer, measurements of dielectric constants and absorption, electric dispersion in the region of Hertzian waves, and the work of Arkadiew on the magnetic permeability in alternating fields complete this section. A number of circuit diagrams for use with electron tubes are drawn.

In the first two sections the literature is covered through 1924. In the last the beginning of 1925 is included. The book is apparently intended to present most of the work done rather than to criticize it. v+262 pp., 190 figs. Johann Ambrosius Barth, 1926. Price 21,-brosch.

G. BREIT

Handbuch der Physik, Bd. IX. Theorien der Wärme.—H. GEIGER AND KARL SCHEEL.—The Handbuch aims to give a complete and critical summary of the state of both experimental and theoretical physics at the present time. It is not possible to give a detailed review of a work of so comprehensive a scope in a brief compass, and little more can be done than to indicate the contents. This volume contains the following articles:

(1) Classical Thermodynamics, 140 pp., by K. F. Herzfeld; (2) The Nernst Heat Theorem, 34 pp. by K. Bennewitz; (3) Statistical and Molecular Theories of Heat, 106 pp., by A. Smekal; (4) The Axiomatic Foundation of Thermodynamics by Carathéodory, 20 pp., by A. Landé; (5) Quantum Theory of the Large-Scale Thermodynamic State-Variables, 40 pp., by A. Byk; (6) The Kinetic Theory of Gases and Fluids, 131 pp., by G. Jäger; (7) The Production of Heat from Other Forms of Energy, 49 pp., by W. Jaeger; (8) Temperature Measurement, 90 pp., by F. Henning.

Each of these articles is the authoritative work of an expert in his own field, and the collection will be well nigh indispensable. The part of the whole volume concerned with questions of recent development, and the number of questions from all branches of physics which must be treated by thermodynamic methods will be in the nature of a revelation to those who are inclined to think of thermodynamics as a more or less exhausted subject or as restricted to a particular type of application. This book may well be used by advanced students as a text, since there is here presented in easily available form all the essential material for which one has had to search hitherto in a number of sources. 616 pp., Julius Springer, 1926. Price 49.20 R.M.

P. W. BRIDGMAN

Handbuch der Physik, Bd. XI. Anwendung der Thermodynamik. H. GEIGER AND KARL SCHEEL.—This volume contains the following articles:

1. Thermodynamics of the Production of the Electric Current, 41 pp., by W. Jaeger, Charlottenberg, 2. Thermal Conduction, 104 pp., by M. Jakob, Charlottenberg, 3. Thermodynamics of the Atmosphere, 45 pp., by A. Wegener, Graz, 4. Hygrometry, 11 pp., by M. Robitzsch, Lindenbergs, 5. Thermodynamics of the Stars, 37 pp., by E. Freundlich, Neubabelsberg, 6. Thermodynamics of Vital Processes, 34 pp., O. Meyerhof,

Berlin-Dahlem, 7. Production of Low Temperatures and Liquefaction of Gases, 68 pp., by W. Meissner, Berlin; 8. Production of High Temperatures, 85 pp., by Carl Muller, Charlottenberg, 9. Heat Transformations in Machines, 25 pp., by Kurt Neumann, Hanover.

Again we have a collection of authoritative articles, which every physicist will want to have easily available for reference. Some of the articles, particularly those on the production of high and low temperatures, give sufficient practical detail to make them valuable as manuals of laboratory practice. The article on the thermodynamics of the stars will be welcomed as collecting in accessible form recent matter of great interest. The inclusion of an article on the thermodynamics of vital processes is of great significance and is symptomatic of a growing feeling that the stage is nearly set for almost undreamed of developments in the application of physics to problems of biology. 454 pp. Julius Springer, price 37.20 M. bound.

P. W. BRIDGMAN

Handbuch der Physik, Bd. II. Elementare Einheiten und Ihre Messung. H. GEIGER AND KARL SCHEEL.—This volume contains the following articles: (1) Dimensions, Units, Systems of Measurement, J. Wallot; (2) Measurements of Length, F. Göpel; (3) Measurements of Angles, F. Göpel; (4) Measurements of Mass, W. Felgentraeger; (5) Space Measurement and Specific Gravity, Karl Scheel; (6) Measurements of Time, W. Schmundt, V. v. Niesiolowski-Gawin; and C. Cranz; (7) Measurements of Velocity, V. v. Niesiolowski-Gawin; (8) Production and Measurement of Pressure, H. Ebert; (9) Measurements of Gravity, A. Berroth; (10) General Physical Constants, F. Henning and W. Jaeger.

This book gives a useful collection of the sort of information that would be expected in a comprehensive series of this character, and should prove very convenient for general reference purposes. Anyone, however, who is interested in pushing his measurements to the limit practically attainable will probably have to go to the original sources. Thus in the section on weighing there is very little discussion of what the present possible limits of accuracy in weighing are, and the sections dealing with the subject of my own especial interest, high pressures, are entirely inadequate in the treatment of pressures higher than a few hundred atmospheres. One gets the impression from the diagrams and the references that technical developments outside of Germany have a less proportionate representation than those of Germany itself. Pp. 522, figs. 297, Julius Springer, 1926, price 39.60 R.M., 42:00 R.M. (bound).

P. W. BRIDGMAN

Handbuch der Physik, Band XXIII, Quanten. This volume is one of the well-known series now being published under the auspices of GEIGER and SCHEEL and so follows their policy of delegating the writing of particular chapters of each volume to experts in the particular field involved.

Chap. I, which is much the longest (278 pp.), is a very thorough compendium on *Quantum Theory* by W. PAULI. This is an authentic survey of outstanding excellence on the quantum theory of line spectra up to the advent of the new quantum mechanics, and is well adapted to the advanced reader who is interested in a really scholarly investigation of the theoretical problems connected with atomic structure and who can dispense with some of the elementary exposition found in the ordinary text-book on quantum theory. Pauli's monograph is devoted primarily to the spectroscopic aspects of the quantum theory, as the statistical and chemical applications, also some of the mathematics of multiply periodic motions, are reserved for other volumes of the handbook. The first third of Chap. I is on "general principles" such as adiabatic invariance, the correspondence principle, and the theories underlying the Compton effect, black body radiation, etc. This portion contains much excellent material not usually found

elsewhere, notably the discussion of spectroscopic stability, dispersion, and the sum-rules for intensities. Prof. Pauli might well have published his analysis of theories of damping constants and the breadth of spectral lines also in a research journal, as it is original and fills a real need. The second portion of Chap. I is devoted to the hydrogen atom, and is probably the most profound survey yet published of the various theoretical points connected with this topic, as such details as the second order Stark effect, etc., are considered. The third part of Pauli's chapter is concerned with the spectra of atoms with more than one electron, and contains good discussions of penetrating vs. non-penetrating orbits, multiplet theory, anomalous Zeeman effect, etc.

Although writing before the appearance of the new quantum mechanics, Prof. Pauli always very clearly emphasizes the inadequacies of the old quantum theory, and has in fact shown a remarkable premonition as to what features of this (such as the "sum-rules") would be permanent and what would not. In several cases he has even forecasted (as in discussing the second order and the inhomogeneous Stark effects) precisely the modifications in formulae which have since ensued with the new quantum mechanics.

Chap. II is a brief (27 pp.) but interesting critique by R. LADENBURG of the various experimental *Methods of Determining Planck's Constant h*.

Chap. III (126 pp.), by W. BOTHE, is called *The Absorption and Scattering of X-Rays*, but is more comprehensive than suggested by the title, as sixty pages are devoted to the properties of secondary corpuscular radiations, i.e., the photo- and Compton-electrons. This chapter should prove valuable both to the experimental and theoretical physicist, as it is a well-written account of a timely subject. The tabulation and clear delineation of the various kinds of absorption and scattering coefficients is excellent. The discussion of the Thomson scattering formula is purely from the conventional classical viewpoint, and unfortunately there is no mention of the quantum derivation of this formula by means of the Thomas-Kuhn relations (subsequently embodied in the new quantum mechanics) or even a cross-reference to Pauli's discussion of this topic on p. 92.

Chap. IV (44 pp.) is a good account of *Continuous X-ray Spectra* by H. KULENKAMPFF.

Chap. V (116 pp.), written by P. PRINGSHEIM, is entitled *Excitation of Emission by Radiation* and is devoted to various resonance radiation phenomena. Following a good discussion of the polarization of resonance radiation there is a section on the various effects of collisions of the second kind, such as quenching of radiation and "sensitized fluorescence." This should be particularly useful because good summaries of this recently developed experimental field are scarce. Considerable space is devoted to the fluorescence and phosphorescence of organic and complex inorganic molecules.

Chap. VI (47 pp.) is an article by W. NODDACK on *Photochemistry*, and includes the luminescence concomitant to certain chemical reactions.

The final chapter (135 pp.) is written by FRANK and JORDAN on the *Excitation of Quantum Jumps by Collision*, and is a slightly abridged version of their excellent book by the same title. This book will be reviewed in next month's Physical Review, and so to avoid duplication no attempt will be made to describe it here. It seems rather unfortunate that other portions of the volume might not also similarly be published separately in book form.

It is perhaps needless to say that the entire volume is attractively finished, free from misprints, and quite completely documented with references to the literature. Pp. x+782. Verlag Julius Springer, Berlin, 1926. Price 57 Reichsmarks; bound 59.70.

J. H. VAN VLECK

PROCEEDINGS
OF THE
AMERICAN PHYSICAL SOCIETY

MINUTES OF THE CHICAGO MEETING, NOVEMBER 26 AND 27, 1926.

The 141st meeting of the American Physical Society was held at the Ryerson Physical Laboratory, Chicago, Illinois, on November 26 and 27, 1926. The President of the Society, PROFESSOR DAYTON C. MILLER, presided. Morning and afternoon sessions were held with an attendance of about one hundred and fifty. The Saturday morning session was divided into two sections.

On Friday evening the Society held an informal dinner at the Quadrangle Club, attended by seventy-nine members and guests.

The regular meeting of the Council was held on Friday, November 26, 1926. The following were elected to membership: Arthur S. Adams, C. Leonard Albright, J. A. Bearden, E. R. Bell, Arthur A. Bliss, Ray W. Boydston, Gail P. Brewington, Townsend Brown, Francis X. Burda, Robert H. Canfield, Andrew Christy, F. Evelyn Colpitts, Elbert F. Cox, F. H. Crawford, Robert H. Dalton, L. H. Dawson, Raymond C. Dearle, Henry B. DeVore, S. R. Durand, V. E. Eaton, Willard H. Eller, Howard M. Elsey, LeRoy E. Emerich, Gerald W. Fox, H. H. Friend, A. P. Friesen, Metta C. Green, V. B. Hall, Gustaf W. Hammar, S. M. Hanley, Alfred E. Haussmann, Margaret Hays, S. W. Heimlich, Robert Holzer, N. C. Jameson, Francis A. Jenkins, Arthur J. M. Johnson, N. H. Johnson, L. W. Jones, F. M. Kannenstine, Harry R. Kiehl, Thomas J. Killian, Victor E. Legg, Harold M. Lewis, G. H. Liebel, Julius E. Lilienfeld, Ernest G. Linder, Arthur C. Lockerwitz, George A. Lyle, Brother C. F. X. Majella, Henry Margenau, Frank C. McDonald, Alfred W. Meyer, Henry Miller, Lewis B. Miller, J. W. Million, Jr., Franklin Mohr, Hans Muller, Morris Muskat, William G. Nash, L. F. Ollmann, Henry Otten, Jr., Linus Pauling, Carl Pfanstiehl, H. T. Plumb, Elizabeth Richards, Wesley M. Roberds, George I. Rock, R. Rollefson, T. A. Rouse, William Rule, E. O. Salant, James W. Sappenfield, G. C. Schleter, G. R. Sears, Raymond J. Seeger, C. Willard Sharp, Manne Siegbahn, J. Kenneth Smith, L. O. Sordahl, Leland J. Stacey, George A. Stinchcomb, Carrington H. Stone, Francis L. Talbot, Walter G. Traub, Hugh D. Ussery, Willy Uyterhoeven, G. D. Van Dyke, John A. Victoreen, Clifford

N. Wall, Lawrence A. Ware, M. Russell Wehr, Albert E. Whitford, Hugh B. Wilcox.

The regular scientific session consisted of fifty-seven papers (eight of which were read by title), abstracts of which are given on the following pages. An **Author Index** will be found at the end.

HAROLD W. WEBB, *Secretary.*

ABSTRACTS

1. Refraction of x-rays by method of total reflection. RICHARD L. DOAN, University of Chicago.—This is a continuation of the work described in a paper presented at the last Washington meeting of the Physical Society. Highly reflecting metallic surfaces of Ag, Cu, Au, Ni, and Fe, prepared by sputtering in vacuum onto an optical glass surface, were used as mirrors for the reflection of monochromatic x-rays obtained from copper and molybdenum water-cooled Coolidge tubes. Indices of refraction, as calculated from critical angle measurements, agree in general with theoretical values as given by the Drude-Lorentz dispersion formula, although two exceptions have been noted. The refraction of the line $CuK\alpha_1$ in Cu is particularly interesting because of the pronounced resonance effect due to the K-electrons. The theoretical value of the index of refraction calculated on the assumption of two K-electrons differs by about 20 per cent from the values obtained on the assumption of one or three electrons but agrees with the experimental determination to within two per cent. The expected departure from theory when an absorption limit is approached too closely has been observed in the cases of $CuK\beta$ refracted in Cu and $CuK\alpha_1$ in Ni. The refraction of $CuK\alpha_1$ in gold involves an effect due to the L-electrons and a theoretical calculation made on the basis of Stoner's assumed distribution of these electrons gives a value which agrees fairly well with experiment.

2. M series x-ray absorption spectra of osmium, iridium, and platinum. R. A. ROGERS, University of Iowa.—Using a metal x-ray tube and vacuum spectrometer of the Siegbahn type, the absorption spectra have been investigated from 3.5A to 7A. Spectrograms have been obtained showing five discontinuities for osmium at 6.194A (M_1), 5.975A (M_2), 5.027A (M_3), 4.412A (M_4), and 4.037A (M_5); four for iridium at 5.961A (M_1), 5.754A (M_2), 4.851A (M_3), and 4.270A (M_4); four for platinum at 5.736A (M_1), 5.541A (M_2), 4.674A (M_3), and 3.738A (M_5). Discontinuities corresponding to an M_5 level for iridium and an M_4 level for platinum were not obtained. The first two discontinuities, corresponding to M_1 and M_2 , for each element are displaced toward shorter wave-lengths by more than 0.1A from the positions predicted, from theoretical computations, by Sommerfeld and Bohr and Coster. The displacements are quite consistent with those reported by Zumstein for tungsten. The experimental values for the M_3 and M_4 discontinuities lie between the two sets of computed values for those levels. While the experimental values for M_5 are slightly lower than the computed ones, yet the deviation from those values is comparable to that of M_3 and M_4 . Two types of absorption discontinuities were found on the spectrograms—"white line" absorption and "limits" separating regions of unequal darkening. No evidence was found of a component on the short wave-length side of M_3 as was reported by Zumstein for tungsten.

3. The x-ray L absorption edges of the elements Sn to Ru inclusive. GEO. D. VAN DYKE and GEO. A. LINDSAY, University of Michigan.—The L absorption edges for the elements Sn (50), In (49), Cd (48), Ag (47), Pd (46), Rh (45), and Ru (44) have been photographed with the use of a Seigbahn vacuum spectrograph. Calcite was used as a

reflecting crystal. The absorbing screens for Sn, In, Cd, and Pd were rolled from the pure metal. The Ag absorption occurred in the film on the photographic plate. Rh and Ru were pulverized, mixed with collodion, and allowed to spread out in thin films. Since it has been found that the wave-length of the critical x-ray absorption limit depends upon the chemical combination of the element, and in many cases is accompanied by a series of absorption "lines" or fine structure on the short wave-length side of the principal edge, an investigation carried on with the pure element should yield energy values more characteristic of the substance than those obtained from compounds. A single white line on some of the plates is the only evidence of fine structure. Values of ν/R are calculated and compared with Coster's values for the same elements in compounds.

4. The intensity of reflection of x-rays by crystals and the Compton effect. G. E. M. JAUNCEY, Washington University.—In a recent paper by Bragg, Darwin and James (Phil. Mag. 1, 897, (1926)) a formula is given for the case of an ideally imperfect crystal, corrections being made for extinction and temperature. At high orders of reflection the experimental intensity becomes much less than the formula demands. It is suggested that a further correction factor is introduced by the Compton effect, it being supposed that only those electrons which are in orbital positions U such as to scatter unmodified rays take part in the crystalline reflection of x-rays. Jauncey's theory of the unmodified line gives the ratio of the numbers of electrons in the U and M positions (Phys. Rev. 27, 687(1926)). A calculation of the quantity F in the Bragg, Darwin and James formula can then be obtained from this ratio on the assumption that the electrons in the U position in the atom scatter as a whole.

5. A theory of the mechanism of crystal growth. WHEELER P. DAVEY, Pennsylvania State College.—There is considerable evidence that crystallization does not proceed uniformly along a plane surface but, instead, proceeds along a sort of three-dimensional lattice-work which is later filled in with crystalline material. For instance if a supersaturated solution of photographic hypo is crystallized, the three-dimensional lattice-work may be seen, simulating the crystal axes, with hypo solution in the interstices. This suggests that all "single crystals" grow in somewhat similar fashion. Evidence of such a lattice-work may be seen inside the contraction cavities of large-grain pure copper crystallized in dry oxygen-free H₂. The ends of a similar lattice-work were found at the end of a large single crystal of copper from which the molten metal had been suddenly removed. Evidences of the lattice-work were also found on the surface of copper cast in H₂ and in the surface skin surrounding single crystal copper. This means that the material which solidifies later in the meshes of the lattice-work is under tension. Thus all crystals are produced in a state of strain. This accounts satisfactorily for etching pits, the "solution cavities" of Honess, dendrite formation and other metallographic phenomena as well as the customary imperfections in crystal structure noted in x-ray work.

6. Solid solutions of chromium and nickel and of iron and nickel. F. C. BLAKE, JAMES LORD and A. E. FOCKE, Ohio State University.—Curves are given showing that chromium goes into the nickel lattice up to 63 percent chromium by weight the maximum amount of distortion being 2.8 percent. From 63 percent to 100 percent chromium by weight the nickel is in the face-centered chromium lattice, but this lattice being metastable at ordinary temperatures most of the chromium separates out as body-centered chromium. In the case of iron and nickel the iron distorts the nickel lattice up to 74 percent iron by weight, after which the nickel is in the face-centered iron lattice up to 100 percent iron by weight; but face-centered iron is stable only at high temperatures so most of the iron separates out at room temperature. In both cases miscibility is complete but there is overlapping between the regions of distorted face-centered nickel-chromium (or nickel-iron) and body-centered nickel-chromium (or nickel-iron). On

account of the small difference in lattice between isomorphs of chromium, nickel and iron, a degree of precision higher than that now in use must be attained before the methods of x-ray analysis can determine whether the phase that separates out contains both metals in the body-centered state.

7. The synthesis and disintegration of atoms as shown by an application of the Wilson cloud-track method. WILLIAM D. HARKINS and H. A. SHADDUCK.—In 1923, Harkins and Ryan (*J. Am. Chem. Soc.* 45, 2096) developed and applied on a large scale a modification of the Wilson Cloud-Track Method which was capable of indicating the most important features of the mechanism of the disintegration of a light atom under bombardment. By the use of their procedure both Blackett (*Proc. Roy. Soc.* 107, 349 (1925)) and the writers have obtained photographs which show that a fast α -particle may unite with a nitrogen nucleus on impact, and that a hydrogen nucleus is released. In 265,000 α -tracks of 8.6 cm range we have thus far found two disintegrations. In one of these the track of the H-particle is at an angle of 118° with that of the α -particle, and the range of the proton is 19.6 cm. That a proton is actually emitted is shown by the fact that kinetic energy is not conserved and the heavy nucleus gains 11% of the kinetic energy from the α -particle. Also the track of the proton is only one-tenth as bright as the other tracks, and its visible portion is three times longer than is possible for any heavier particle.

8. Polarization of $\lambda 2537$ of mercury. H. F. OLSON, University of Iowa.— $1S - 2p_1$ of mercury excited by plane polarized light shows 79% polarization both in the absence of any magnetic field and in the presence of a field parallel to the electric vector in agreement with recent results of Keussler. That such a field should produce no change in the polarization is in accord with Heisenberg's extension of the principle of spectroscopic stability. That the polarization is not complete might be interpreted as due to collisions but more probably is due to the fact that in very weak fields some of the fine components of 2537 have not the same Zeeman pattern as in strong fields. The polarization with other relative orientations of field and light vector and the variation of polarization with field intensity in weak fields may be interpreted successfully by means of a semi-classical model, with proper relative intensities parallel and perpendicular to the light vector, rotating after excitation with an angular velocity $\frac{1}{2}g(e/m)$ (H/c) and emitting a damped wave. From curves connecting depolarization, rotation of maximum of polarization, etc., with field intensity κ has been found to be $1.02(\pm .02) \cdot 10^7 \text{ sec}^{-1}$.

9. Polarization of light excited by electron impact. JOHN A. ELDREDGE, ALEXANDER ELLETT, and HARRY F. OLSON, University of Iowa.—Ellett, Foote and Mohler and also Skinner have observed the polarization of the mercury spectrum when excited by a well defined stream of slow moving electrons. The present experiment shows that the lines of the sharp subordinate series are in general weakly polarized; but those of the diffuse subordinate series quite strongly polarized (in agreement with Skinner). In this series the electric vector of the excited light is normal to the electron stream whenever $j = 0$ and parallel to the stream for lines involving a decrease of j . In the cases in which j increases the line is less strongly polarized and our results are not definite. As has been previously suggested we suppose the excited atoms with their j vector in or near the plane normal to the electron stream. Qualitatively the results for this series are in agreement with the concept (Rubinowicz) that the atom emits a plane polarized or circularly polarized light quanta according as j remains constant or changes by one. This simple theory for the polarization can not be correct, however, as it leads to parallel polarization never greater than 33%, as contrasted with 60% which has been found for some lines; it also falls down when applied to the somewhat weaker polarization of the other series.

10. Impact polarization and the spinning electron. A. ELLETT, University of Iowa.—The principle of conservation of angular momentum together with Heisenberg's exten-

sion of the principle of spectroscopic stability lead Foote, Mohler and the writer to predict for $\lambda 2537$ of mercury polarization with major electric vibration parallel to the exciting electron beam, contrary to fact. Eldridge, Olson and the writer have shown that in most cases lines of the mercury spectrum for which ΔR during the collision is ± 1 exhibit polarization of the type to be expected if the Zeeman levels for which $m = \pm 1$ are favored in excitation, whereas if ΔR in excitation is zero the assumption that the level $m = 0$ is favored leads to the correct conclusion. On the spinning electron hypothesis these results may be interpreted by saying that when R changes the spinning electron turns over during the collision and gives to the atom a unit of angular momentum parallel to the electron beam, and to the magnetic field which may be applied in this direction without changing the resulting polarization. Likewise $1s - 2p_1$ of sodium should show zero polarization and $2p_2 - 3d_2$ of thallium should show polarization, if the reorientation of the spinning valence electron relative to the orbital momentum is brought about by the colliding electron turning over. If this is not true, the latter should behave like D_2 of sodium.

11. Spectroscopic interpretation of the magneton numbers in the iron group. A. SOMMERFELD, University of Munich, and O. LAPORTE, University of Michigan.—For the spectroscopic interpretation of the measured magneton numbers for the ions of the first long period an average of the $j.g$ -values for the different levels of the polyfold ground-term must be taken. This was not necessary for the paramagnetism of the rare earths (Hund) since the separations $\Delta\nu$ are so large that only the lowest level needs to be considered. The exact formula for the magneton number (in Weiss-units) becomes:

$$\mu_W = 4.97 (\sum N_i j(j+1)g(j, l, s)^2 / (\sum N_i)^{\frac{1}{2}});$$

j, l, s are the quantum numbers of the level in question and N_i the weight: $(2j+1)$ exp. $(-hc\Delta\nu/kT)$. The terms which are assumed to represent the normal state of the ions are computed according to the Stoner Periodic System using the rules given by Pauli and Hund. If the lowest term is single (i.e., of S type), the magnetic moments computed in the old fashion and those according to this formula must furnish the exact measured value—this is indeed the case for Fe⁺⁺⁺ and Mn⁺⁺, the lowest term of which is 6S —whereas in general the observed values lie between the two curves drawn for $\Delta\nu = 0$ and $\Delta\nu = \infty$. The Boltzmann factor also causes a dependence of μ upon the temperature. The Heisenberg-Schroedinger quantum mechanics does not alter the above formula.

12. Fluorescence spectra in metallic vapours excited by the light in the mercury arc. J. C. McLENNAN, University of Toronto, and I. WALTERSTEIN, University of Chicago.—The fluorescence spectrum of iodine obtained by McLennan with iodine vapour excited by the light in the mercury arc, suggested an investigation into the effects of ultra-violet light on the vapours of other elements. Fluorescence spectra were obtained from the vapours of sulphur, selenium, tellurium, and bismuth at moderate temperatures by using a large quartz mercury lamp as source of excitation. The vapour of sulphur gave a set of bands extending over the range of the visible spectrum. Selenium at 325°C gave a fluorescent spectrum ranging from 2200A to 6500A while at 425°C it emitted a different spectrum consisting only of 9 very broad bands between 4178A and 4829A, and this latter spectrum itself disappeared at higher temperatures. The fluorescence spectrum of tellurium consisted of a set of regularly spaced bands in the visible region, and the relative intensities of the bands varied according to the pressure of the vapour. Bismuth emitted a band spectrum in the region 4400A to 4900A. It was found that the region of the mercury arc which excited the tellurium vapour to produce fluorescence radiation was between 2536A and 3655A.

13. Extreme ultra-violet spectra using large angles of incidence. J. BARTON HOAG, University of Chicago.—A vacuum spectrograph has been constructed using a concave

speculum grating of 215.3 cms radius having 591 lines per mm. The familiar Rowland mounting is used except the slit is placed close to the grating making the angle of incidence approximately 80°. Using carbon and magnesium electrodes, spectra have been obtained from 220A to 1700A. The scale varies from 3.54A per mm at 1600A to 2.26A per mm at 550A in the first order. Preliminary measurements give an accuracy of .04A.

14. Note on the auroral green line 5577. DAVID A. KEYS, McGill University.—In view of the recent important work of McLennan, Vegard and others on the origin on the auroral green line 5577, the light emitted from the electrical discharge in mixtures of (1) helium and oxygen and (2) argon and oxygen was investigated with a Hilger quartz spectograph of D type by the writer while a guest of the Nela Research Laboratory at the kind invitation of Dr. W. E. Forsythe. In a mixture of oxygen and argon (argon pressure = 40 mm, oxygen pressure = 8 mm) contained in a pyrex tube 8 mm internal diameter made in H-form, the line 5577 appeared very strongly. Tungsten electrodes were used, the current was 80 milliamps/cm² and potential 800 volts from a transformer. The oxygen soon combined with the tungsten forming a bluish deposit on the glass walls after which no trace of the line appeared. This result confirms that of McLennan, Ireton and Thompson (Nature, Sept. 25, 1926) and is further evidence that the line is primarily due to oxygen. Some evidence of the line in a mixture of helium and oxygen was also found.

15. Spectrum of Cu II. A. G. SHENSTONE, Princeton University.—The theoretically lowest terms of Cu II are $^1S(d^{10})$ and $^3D, ^1D(d^9s)$. Approximate separations are predictable from Cu I. They should combine with $(d^9p) ^3P, ^3D', ^3F, ^1P, ^1D', ^1F$ and these also with higher $^3D, ^1D(d^9, s)$. Such terms, except 1S , have now been found, accounting for all strong Cu II lines down to $\lambda 1944$. Terms are all inverted except 3F which is partially inverted. The three possible combinations of 1S should be about $\lambda 1400$ with separation of 5185 and 494 cm⁻¹. Other terms, probably from d^9d , have been found but not designated. Intensities are regular except for inter-system combinations. Zeeman patterns to $\lambda 1979$ give excellent confirmation except for $^3D_3'$ and 1F_3 which apparently share their g-sum, irregularly. Calculation of limits indicate, contrary to theory, that 3D_3 and 3D_2 converge to one limit and 3D_1 and 1D_2 to another. The separations $^3D_3 - ^3D_1$ for the two terms are identical with $^4eD_4 - ^4eD_1$ of Cu I. Calculated ionization potential of Cu II is approximately 17.8 volts from 3D_3 and 1.8 volts higher from 1S . Published analyses of spectra Ni I and Pd I contain $^3D, ^1D$ terms showing same peculiarities of separation and convergence as Cu II terms. Calculated I. P.'s are Ni I, 7.8 volts, Pd I, 8.5 volts.

16. The absorption spectrum of antimony vapor. R. V. ZUMSTEIN, National Research Fellow, University of Michigan.—Antimony vapor is polyatomic. By slowly admitting the vapor into a hot carbon tube at about 1400°C, the molecules of vapor were dissociated into atoms and the atomic absorption spectrum was studied. The experimental method was described in The Physical Review, May, 1926. The arc lines 2311.50, 2175.88, 2068.38 were strongly absorbed. 2023.86 and 2127.46 were also absorbed but with considerably less intensity. These results are in agreement with the analysis of the antimony arc spectrum by Ruark, Foote, Mohler and Chenault (B.S. Sc. Papers 19, 479, (1924)). All of the five absorption lines come from the $3d_2$ state, which is without doubt the normal state of the atom. The absorption of $\lambda 2311.50$ was previously observed by Narayan and Rao. (Phil. Mag. 50 648, (1925).)

17. Excitation of arc spectrum of nitrogen. R. A. WOLFE and O. S. DUFFENDACK, University of Michigan.—The arc spectrum of nitrogen was excited in an interrupted low voltage arc in a mixture of helium and nitrogen. The nitrogen arc lines were very strong in a limited region whereas in other regions helium lines or nitrogen bands strongly

predominated. The intensity of the nitrogen lines was such that the spectrum could be photographed on a contrast plate in two hours with a Hilger E 1 quartz spectrograph. This spectrograph with glass prism and lens was employed in the region 4000-8900A, where exposures of three hours sufficed. All but a few of the lines reported by Merton and Pilley were verified, and a considerable number of additional lines were found. A number of these agree with lines reported by Hardtke, not found by Merton and Pilley. Others of these fill vacant spaces in multiplets computed by Kiess for the quartet system. The strength of the nitrogen lines in this arc is undoubtedly due to a high degree of dissociation of the nitrogen by excited helium atoms present in large concentration. This is in accord with the theory of the low voltage arc and with K. T. Compton's explanation of the origin of the nitrogen arc lines in Merton and Pilley's discharge.

18. A compound interferometer for fine structure work. WILLIAM V. HOUSTON, National Research Fellow, California Institute of Technology.—The principal difficulty in the use of the Fabry-Perot interferometer to measure spectral fine structure is that when high resolution is used the successive orders usually overlap. This difficulty can be avoided by using two such interferometers in series. The dispersion of the interferometer is independent of the plate separation, while the distance between orders is inversely proportional to it. Thus an instrument with a small separation may be used as a preliminary filter to eliminate many of the orders in one of larger separation, without affecting the fine structure pattern. In this case the resolution is even greater than that due to the larger separation. To get the best results it is necessary to adjust the separations to the ratio of small whole numbers. This can be done by means of the fact, discovered by Perot and Fabry, that white light fringes appear when this condition is satisfied. The mathematical theory of this instrument has been worked out and an instrument is almost finished, which will be applied to the study of the Balmer lines and other fine structure problems. It promises to be especially valuable in the study of hyper-fine structure.

19. Some laboratory observations bearing on the spectra of comets. HARVEY B. LEMON, University of Chicago.—Among the most conspicuous bands in comet spectra are those of the Swan spectrum attributed in the past by some to a carbon molecule and by others to CH or $(CH)_2$. All spectra appearing in comets can be produced with a large excess of helium and low partial pressures of carbon compounds. If hydrogen also is present, revealed by the Balmer lines, the Swan spectrum is brilliantly developed in a Wood type tube, and this spectrum appears and fades simultaneously with the Balmer series. This is taken as direct evidence for the hydrocarbon origin of this spectrum, and also for the presence of hydrogen in comets. Sodium occasionally appears in cometary nuclei, always temporarily near perihelion. In Halley's comet Slipher found only D_2 , and in Brooks' comet Wright found D_2 three times D_1 in intensity. Usual laboratory excitation gives $D_2 : D_1 = 10 : 7$. In a thermionic tube with CO at 10^{-5} cm or less and a trace of Na as impurity, the D lines appear when the filament is heated to its maximum temperature. Their relative intensity is $D_2 : D_1 = 5$ to $25 : 1$, and the similarity between their appearance and the conditions of excitation to that in comets becomes striking.

20. The spectra of comets. N. T. BOBROVNIKOFF, University of Chicago. (Introduced by Harvey B. Lemon.)—All bands and lines observed in the cometary spectra can be attributed to: (1) Carbon and its compounds (the first positive (Swan), and the third negative groups, CO^+ , "high pressure" Fowler CO bands, C+H bands, line spectrum C^+ ; suspected:—Baldet-Johnson system and the Triplet system). (2) Nitrogen and its compounds (N neutral, line spectrum, N^{++} , and the first negative and third positive groups, the violet and red groups of CN; uncertain: N^+). (3) Hydrogen, the continuous molecular spectrum and probably the secondary spectrum. These spectra can be obtained in the laboratory in an excess of inert gases and with a partial pressure

of the emitter of the order 10^{-4} – 10^{-5} cm. For their production no disruptive discharge is necessary. The excitation potentials of these spectra do not exceed 24 volts. In the occasional appearance of sodium D lines, near distance to the sun is the chief though not only factor. Neutral helium is suspected in comets. The radiation pressure formula of Schwarzschild cannot be applied to the case of comets' tails which are of a gaseous nature. Einstein's modification of Planck's radiation formula may be applied.

21. Band spectrum, continuous emission, and continuous absorption of fluorine gas. HENRY G. GALE and GEORGE S. MONK, University of Chicago.—The band spectrum, consisting of ten bands between 5100 Å and 7200 Å has been photographed by long exposures with a concave grating spectrograph of 2.64 Å per mm dispersion. Sufficient detail has been obtained for an analysis of two bands and to show the general structure of two others. The zero points of the bands are given by $\nu = 17438.8 + (1104.9n' - 2.9n'^2) - (1071.5n'' - 9.9n''^2)$, yielding frequencies $\nu_0 = 19637.0, 18540.8, 17438.8, 16377.2, 15335.3, 14325.0$; having vibrational quantum numbers $n' n'' = 2, 0; 1, 0; 0, 0; 0, 1; 0, 2; 0, 3$ respectively. Analysis of the bands at $\nu_0 = 17438.8$ and $\nu_0 = 16377.2$, having the same initial vibration frequency, and satisfying the combination $R(m) - P(m)$, gives $2B = 3.8 \pm 0.4$, or, $J = 14.5 \times 10^{-40}$. A peculiarity of these bands is the increasing fuzziness of the lines from band to band toward the red. For experimental reasons the emitter is believed to be the F_2 molecule. In spectrograms obtained using a spark discharge in fluorine two continuous emission bands are shown at approximately 2800 Å and 2600 Å. Spectrograms showing the absorption of fluorine have been obtained, using columns of the gas, at atmospheric pressure, as short as 7 cm and as long as 3 m. Continuous absorption occurs to the violet of 4100 Å. No line absorption spectra were obtained.

22. Intensity relations and electronic states in spectra of diatomic molecules. ROBERT S. MULLIKEN, Washington Square College, New York University.—The correspondence principle predicts definite intensity relations for P , Q , and R band lines in molecules having a rotational energy term $F = B(j^2 - \sigma^2) + \dots$, provided σ is an electronic quantum number corresponding to a precession about the internuclear axis (along which the angular momentum $\sigma\hbar/2\pi$ is directed). Hönl and London have given equations, obtained with the help of the summation rule, for the three possible cases $\Delta\sigma = 0, \pm 1$. Let I represent intensity. Then for low values of j (rotational quantum number), the theory predicts $I_R > I_P$ (especially when σ is large) if σ decreases during emission, but $I_P > I_R$ if σ increases, and $I_Q = I_P + I_R$, approximately, in both cases. For $\Delta\sigma = 0$, the prediction is $I_P = I_R$, with I_Q small (vanishing with σ) and falling with increasing j . Various band spectra have recently been interpreted by the writer as corresponding to electronic transitions ${}^1S \rightarrow {}^1S$ (CuH type), ${}^1P \rightarrow {}^1S$ (AlH, He₂ "series" bands), ${}^1D \rightarrow {}^1P$ (He₂ λ5733), ${}^1S \rightarrow {}^1P$ (He₂ λ4546 and 6400, CO Angstrom), with $\sigma = 0$ for 1S , $\sigma = 1$ for 1P , and $\sigma = 2$ for 1D states. These interpretations, and the proviso mentioned above as to the nature of σ , are now found completely confirmed in a comparison of available intensity data with the predictions of the theory.

23. The beta bands of nitric oxide. FRANCIS A. JENKINS, HENRY A. BARTON, and ROBERT S. MULLIKEN, Harvard University and Washington Square College, New York University.—The NO_β bands have been photographed, using an active nitrogen source, in the second order of the 21-foot concave grating at Harvard University. Each band consists of two sub-bands H and L each composed of a P and an R branch of nearly equal intensity, and a very weak Q branch (much weaker in H than in L) whose intensity falls steadily from the first line. The otherwise continuous P - R series shows two missing lines in the H sub-band, four in the L sub-band. The quantum analysis discloses two distinct initial (H' and L') and two distinct final (H'' and L'') sets of rotational levels, all with integral quantum numbers. All the above relations are accounted for if the rotational terms are of the form $B(j^2 - \sigma^2) + \dots$, with $\sigma = \frac{1}{2}$ for

the H' and H'' levels, $\sigma = 1\frac{1}{2}$ for the L' and L'' levels, and $j = \sigma + \frac{1}{2}, \sigma + 1\frac{1}{2}, \sigma + 2\frac{1}{2}, \dots$; the intensities agree closely with those calculated from the appropriate Hönl and London equations (cf. preceding abstract). The bands evidently correspond to $^2P \rightarrow ^2P$ electronic transition. Preliminary values for the internuclear distance are $r_{H'} = 1.44$, $r_{L'} = 1.40$, $r_{H''} = 1.16$, $r_{L''} = 1.14$, all times 10^{-8} cm.; the r'' values refer to the normal state of NO.

24. Carbon monoxide band excitation potentials. ANN B. HEPBURN, University of Chicago.—By using a hot filament three element tube, in which the grid and filament were so arranged as to enclose a field free space about one mm from the filament, it was possible to make visual and photographic determinations of the excitation potentials of the 0,0 bands of the Angstrom, Comet Tail, First Negative Deslandres, and Balder-Johnson band systems of CO. A residual pressure of mercury vapor from the condensation pumps was present in the tube and was used as a means of correcting for the P.D. across the filament and contact e.m.f.'s in the tube. $\lambda 2537$ (4.9 volts) was used with the photographic observations and $\lambda 5461$ (7.7 volts) was used for the work in the visible. Computations made by Birge indicate that $\lambda\lambda 4511, 4880, 2190, 3794$ should be produced by electrons having a minimum velocity corresponding to 10.7, 16.7, 19.8, 19.8 volts respectively. The experiments performed confirm the computations within the limit of experimental error, namely, $\pm .1$ volt.

25. An investigation of some hydrocarbon bands. FRANK C. McDONALD, University of Chicago. (Introduced by Harvey B. Lemon.)—Two new bands, $\lambda 2264, \lambda 2367$, have been analyzed according to the quantum theory. These bands were found when methane was introduced into a Wood tube and excited by a condensed discharge. The same bands appeared when acetylene was mixed with helium and excited by a transformer discharge. Many more lines were observed on the methane plates than on the acetylene plates. These bands have been arranged in P and R branches with a single missing line. They have been shown to belong to the same system with a common initial state. The possibility of a CH ion as the carrier is considered. New plates with high dispersion of a band, $\lambda 3143$, originally reported by Fortrat, have been obtained. However, the structure of the band on these plates seemed to differ in several respects from that given by Fortrat. This band and a subsidiary band, $\lambda 3157$, were found when methane was allowed to flow through a Wood tube and subjected to a condensed discharge. A more complete analysis has been made than that previously given.

26. The titanium bands. R. T. BIRGE and A. CHRISTY, University of California.—Using chiefly previously published data, we have been able to arrange 28 of the well-known titanium bands (eight with a measurable second head) in one system, and to assign vibrational quantum numbers. The heads are given by

$$\nu = \frac{19,350.0}{19,340.0} \left\{ (833.1n' - 4.5n'^2) - (1003.5n'' - 4.5n''^2) - \dots \right\}$$

with an average residual of one cm^{-1} . The electronic energy change and the frequencies of vibration show a close correlation with the corresponding values for the aluminum bands which are now definitely known to be due to AlO. The distribution of intensity among both the vibrational and the rotational states is closely the same for the two molecules. A rough preliminary estimate of the moment of inertia shows a similar correlation. All these facts point very strongly to the conclusion that these titanium bands are due to TiO, and not to TiO₂, and this fact should be considered in astrophysical work on these bands, which form the dominant feature of M-type stars. Fine structure analysis of the 0-0, 1-0, and 0-1 bands, using new spectrograms taken especially for us by Dr. King, is now in progress.

27. The fine structure of three infra-red absorption bands of ammonia. G. A. STINCHCOMB and E. F. BARKER, University of Michigan.—Using a grating spectrometer with a rock salt fore-prism, the fine structure of the 1.98μ , 2.2μ and 3.0μ bands of ammonia was determined. The 3.0μ band has been previously resolved by B. J. Spence. This work checks the shape of the curve and the frequency differences, but differs somewhat in the values assigned to the wave-lengths, and furnishes a little more detail. The 1.98μ band consists of about 30 lines spaced with fair regularity throughout the entire band. Its center is marked neither by an absent line, nor by a single zero branch of great intensity like that at 3.0μ . The frequency difference between adjacent lines approximates 10.0 cm^{-1} . The 2.2μ band is extremely irregular making the location of the lines somewhat uncertain and yielding no obviously characteristic frequency difference. Here also no zero branch is apparent. While an accurate determination of the percentage of absorption was not considered of first importance, the growing interest in this phase of the problem has led us to employ unusual care, and it is believed that the percentage values assigned to the lines are fairly accurate.

28. Critical potentials of the spark lines of mercury. JOHN A. ELDREDGE, University of Iowa.—Block has classified as belonging to three groups 300 spark lines of mercury and Dejardin has found three threshold values for the exciting potentials. However the number of lines studied by Dejardin was small and it might be questioned whether all of the known spark lines did actually fall into these three groups. The intensities of 30 of the stronger spark lines have been measured as a function of voltage and three critical values found less than 150 volts, at 18, 24 and 57 volts respectively. The absolute values of such critical potentials is not certain as the values may be altered several volts by changing the current density.

29. Collisions of the second kind between zinc and mercury atoms. J. G. WINANS, University of Wisconsin.—The preliminary results are described in Nature 118, 46 (1926). Additional evidence has been obtained that mercury atoms in the $2P$ state are effective in collisions of the second kind with zinc atoms. The quartz tube containing zinc and mercury vapors was illuminated by nearly monochromatic light of $\lambda 1849$ ($1S-2P$) obtained by a focal isolation method from a hot mercury arc. The zinc sharp triplet ($2p_{1,2,3}-2s$) appeared very clearly in the secondary radiation and failed to appear when all wave-lengths shorter than 2100 were absorbed from the exciting light by a sheet of very thin glass. Similar results were obtained using the water cooled mercury arc and the aluminum spark as light sources. $\lambda 1849$ has been photographed through an air path of 90 cms. The zinc lines which appear when various light filters (chlorine, glass, and acetic acid) are placed in the path of the exciting light from a mercury arc, give evidence that some mercury atoms in the $3d$ state transfer their entire energy to zinc atoms in collisions of the second kind. A calculation on the basis of the kinetic theory shows that, under the conditions of this experiment, an excited mercury atom with an associated metastable state is probably about twice as effective in producing collisions of the second kind as one with no metastable state near it.

30. The resonance glow in a hydrogen discharge tube. ROGERS D. RUSK, Northwestern College.—At pressures of hydrogen below 0.2 mm and potentials higher than the minimum arcing potential a blue haze extends throughout the hot filament discharge tube. Systematic variations of gas pressure, discharge potential, filament current and anode distance have been made to determine the nature of the glow, which corresponds to the type-three discharge mentioned by Richardson and Tanaka (Roy. Soc. Proc. 106 A, 640, (1924)). For a fixed anode distance the appearance of the glow occurred at a constant potential for pressures below 0.2 mm at which pressure it became indistinguishable from the more common arc type of the glow. The intensity of the glow and its extent are functions of gas pressure, anode distance and potential. Weakness

of the Balmer lines and the effect of pressure change suggest a close relationship between the life of the excited molecule and its collision frequency.

31. The distribution of energy among electrons rebounding from helium atoms. A. L. HUGHES and L. W. JONES, Washington University.—A narrow beam of electrons of known velocity was directed into helium at various pressures below .01 mm. A pair of slits selected those electrons rebounding at 90 degrees ± 3 degrees, and their distribution of velocities was measured by the magnetic field method. The pressure used was sufficiently low to insure that the rebounding electrons had made but one collision. For electrons having energies ranging from 16 to 100 volts, it was found that the rebounding electrons had exactly the same energy as they had before collision. In particular, it was noted that there were no electrons rebounding at 90 degrees with a loss of energy corresponding to excitation (20 volts) or to ionization (25 volts).

32. Secondary electron emission from molybdenum. ALBERT W. HULL and J. M. HYATT, General Electric Co.—A special three-electrode tube was used, consisting of a short straight tungsten filament in the axis of a long cylindrical molybdenum grid and plate. The tube was thoroughly exhausted, a small amount of caesium introduced, the tube sealed off from the pump, and the plate bombarded by caesium positive ions at 600 volts for five hours. The tube was then immersed in liquid air and the plate heated by induction until the plate current showed no change with continued heating. Measurements of plate current were made, as a function of grid and plate voltage, from zero to 2000 volts. The fraction of the primary electrons which reached the plate was determined by removing the tube from liquid air, reversing the potentials, and measuring the positive ion currents from the filament to grid and plate. The number of secondary electrons per primary electron was thus calculated and found to increase from 0.45 at 20 volts to a maximum of 1.23 at 900 volts, decreasing to 1.04 at 2000 volts. These values were reproducible within 2% at different times and in different tubes:

33. Secondary electron emission produced by positive caesium ions. J. M. HYATT, Research Laboratory of the General Electric Company and Union College.—The source of the positive ions, a short tungsten filament maintained at about 1200°K in the presence of caesium vapor, was mounted on the axis of a long cylindrical molybdenum grid and plate. A potential of -600 volts was applied to the grid and potentials from +50 to -650 were applied to the plate. While the plate was between +50 and 0 only secondary electrons from the caesium covered grid reached it. When the plate potential was made negative it caught positive ions in addition to the secondary electrons. The plate current became constant at -50 volts and remained so until the plate potential reached that of the grid. At this point the plate current suddenly increased 4% due to the emission of secondary electrons from the plate. Further increase of the positive ion velocities was accompanied by a uniform increase of the secondary electron emission. Similar observations were made with the grid maintained at six lower potentials. Determinations made of the secondary electron emission from both grid and plate were in agreement and showed that the number of secondary electrons per positive ion striking the caesium covered surfaces increased uniformly from .02 at 200 volts to .11 at 600 volts.

34. The effect of an electric field on a radiating hydrogen atom. K. L. HERTEL, University of Chicago. (Introduced by A. J. Dempster.)—In a previous paper experiments were described in which hydrogen canal rays were allowed to pass into a very high vacuum, so that the natural decay of radiation could be observed and the changes in polarization produced by a transverse electric field during the radiation process. The experiments have been continued under improved conditions with various fields, and various velocities of the rays. In all cases the original polarization is suddenly reversed as soon as the field is applied so that the electrical component parallel to the field becomes

stronger. This change in polarization must take place in less than 2×10^{-9} seconds. In the uniform field the polarization of the radiation decreases gradually to zero or even reverses slightly. Measurements were made with three different velocities of the rays and showed that the time required for this gradual return of the polarization is about 4×10^{-8} seconds. Photographs were also made of the rays on emerging from the condenser. Here again there was an increase in the polarization of the light emitted the component parallel to the field again becoming stronger. This took place in the stray field at the end of the condenser and occurred farther out with strong fields than with weak.

35. Dependence of the free path of potassium ions in various gases on their velocity F. M. DURBIN, University of Chicago. (Introduced by A. J. Dempster.)—Potassium ions from a hot anode were accelerated through potential differences varying from 9 to 350 volts between an anode and a slit. The beam passing through the slit was bent into a semicircular path by a magnetic field so as to fall on a second slit. The number passing through this distance of 11 cm without neutralization or scattering out of the beam was observed by an electrometer with different gas pressures in the chamber. Keeping the current to the first slit constant, the intensity of the rays decreased exponentially as the pressure was increased. The mean free path may be deduced and a comparison with the kinetic theory free path gives the number of collisions made by the ions before being lost from the beam. In helium this number varied from 10 at 250 volts to 2.34 at 8.5 volts. Air, hydrogen, nitrogen, helium, oxygen and argon were studied, and in all cases the curves giving the dependence of the free path on the velocity showed an approach to a constant high value of the free path at the higher velocities, and a more or less rapid decrease to a value approximating the kinetic theory value at the lowest speeds.

36. Electrical properties and nature of active nitrogen. PHILIP A. CONSTANTINIDES, University of Chicago. (Introduced by A. J. Dempster.)—Glowing active nitrogen was drawn in succession through two sets of electrodes each consisting of two concentric cylinders. The ionization current in the second electrode remained constant despite the variation from 0 to 250 volts/cm in the field of the first electrode. This indicates that the ionization is produced by changes taking place after the passage of active nitrogen through the first electrode. Using electrodes of various areas, the negative charges were found to be proportional to the areas of the negative electrodes, which shows that the conductivity is due to photo-electrons emitted from the electrodes. The effect of various gases on the duration of afterglow has been examined, the most important result being that it is not affected by helium even when the helium is made ten times the density of the nitrogen. It was found that hydrogen and mercury molecules are not ionized by collisions with active nitrogen molecules, while indications are that iodine molecules are ionized. This suggests that the phenomena associated with active nitrogen may be due to a metastable state of the nitrogen molecule with energy between 9.4 and 10.4 volts.

37. On the nature of gaseous ions. HENRY A. ERIKSON, University of Minnesota.—When ionizing rays are passed through oxygen, nitrogen, hydrogen, carbon dioxide and argon, a positive ion and a negative ion are formed. These have all initially the same mobility in air. The value of this mobility in moderately dry air is 1.87 cm/sec per volt/cm. In a fraction of a second the initial positive ion changes into a final ion which has a mobility of 1.36. The negatives undergo no change. No greater mobility in air than 1.87 is observed. The value 1.87 is the mobility of the simplest singly charged body present.

The lack of dissociation, the known nature of the ionizing process, the results in the case of argon, the possible separation of the two groups of ions and the like mobility of the initial ions as well as the final ions, leads to the following conclusion that an electron

escapes from the molecule due to the action of the ionizing agent. The initial positive ion is thus formed. The electron set free soon attaches itself to a neutral molecule thus forming the negative ion. These are the two 1.87 bodies. The positive 1.87 body soon shares an electron with a neutral molecule thus forming the 1.36 two molecule body. The value 1.87 is thus a characteristic of a one-molecule ion and 1.36 a characteristic of a two-molecule ion.

38. The activity of monovalent ions. HANS MUELLER, Mass. Institute of Technology.—Debye's theory of strong electrolytes breaks down when applied to small ions because the approximation $\sinh \phi = \phi$ ($\phi = e\psi/KT$) is no longer justified. In this paper the differential equation $\Delta\phi = \sinh \phi$ is solved by extending analytically by an integration by steps Debye's solution $\phi = K e^{-r}/r$, correct for small values of ϕ . The activity-coefficients f are easily calculated with the following relation: $-kT \log f$ is the difference in the work to charge one ion in pure water and to charge it in an electrolyte with the concentration c in which all other ions already have their full charge. For small ions this calculation gives $f(c)$ curves which are below Debye's limiting curve for $a=0$. The curves almost coincide with those calculated by Bjerrum (Danske Videnskabernes Selskab. 8, 9, (1926)) assuming associated ions.

Concentration (mole/liter)	$-\log f(a=10^8 \text{ cm})$	Bjerrum's values
1	0.456	0.463
0.5	0.360	0.366
0.2	0.252	0.255
0.1	0.189	0.188
0.05	0.136	0.133
0.02	0.084	0.085

Hence Debye's theory fits the experimental results also for small ions without assuming partial association.

39. Piezoelectricity of crystal quartz. L. H. DAWSON, Naval Research Laboratory, Washington, D. C. (Introduced by E. O. Hulbert.)—Measurements with a quadrant electrometer of the piezoelectric charge in optically perfect crystal quartz have shown that the different specimens of quartz may produce charges of different magnitude. The piezoelectric charge appeared to be an integral effect over the surface since an exploration of the surface by an approximation to a point contact showed that charges varying in magnitude and sign may be produced on adjacent portions of the surface. The piezoelectric charge increased as the temperature was raised from room temperature to 60°C and decreased thereafter to 576°C where it disappears. The cooling curves show a lag. A relation between the pyro- and piezoelectric effects is pointed out. The facts established appear to be in accord with the theories of the imperfections of crystals and to agree with the views of Bragg and Gibbs in regard to the mechanism of the production of pyro- and piezoelectricity. The piezoelectric charges on surfaces variously oriented with respect to the optic axis showed a characteristic distribution hitherto unsuspected and not explainable by simple theory. This characteristic distribution lead to an accurate method for determining the direction of the electric axes of quartz.

40. An electronic theory of passivity. WILLIAM D. LANSING, University of Illinois. (Introduced by J. Kunz.)—Iron occupies a unique position in the middle of the first long period of the periodic table. Under normal conditions the electrons are probably distributed among the energy levels as 2,8,14,2. Under strong oxidizing conditions this may become 2,8,8,8, a structure analogous to krypton, and thus become passive, and non-magnetic as well. A method was developed for producing thin films of iron by cathode sputtering. These films were found to be passive. The work of Ingersoll and DeVinney on nickel would lead us to believe that these films were non-magnetic

also, but our magnetic measurements are not yet complete. The electrode potential of ordinary iron in 0.5 molal FeSO_4 was found to be +0.365 volts with respect to the hydrogen electrode, while passive iron in the same solution had an electrode potential of -0.508 volts. Thermodynamically, passive iron is the more stable, with a free energy change of 35700 cal. The electrode potential of sputtered iron in this solution ranged from 0.035 v. to -0.065 v., becoming more noble with time. This is explained by the supposition that the film is still too thick to be passive and non-magnetic all the way through.

41. A new electrophoretic mobility formula. MELVIN MOONEY, National Research Fellow, University of Chicago.—According to current theories of electrophoresis, the mobility of a particle should be independent of its size. However, the author has shown experimentally that with oil drops immersed in water there is a definite variation in mobility with the diameter of the drop. Therefore a new mobility formula has been developed, applicable to a rigid sphere in water containing a di-ionic electrolyte. The new theory takes into account the effect of ionic diffusion, and also the motion of the water, on the charge distribution in the electric double layer. The mobility formula is obtained in the form of an asymptotic power series, of which only the first two terms have been calculated. However, these are sufficient to give a theoretical value for the slope when mobility is plotted against $1/D$, D being the diameter of the sphere. This formula has been tested with experimental results obtained with oil drops in solutions of various electrolytes at concentrations of 10^{-1} to 10^{-5} normality. At .01 normal or higher concentrations the theory definitely fails. At lower concentrations there is rough agreement between theory and experiment. More precise mobility measurements are necessary for a more decisive test of the theory at low concentrations.

42. A determination of the dielectric constant of air by a discharge method. A. P. CARMAN and K. H. HUBBARD, University of Illinois.—Two air condenser systems, one containing the test condenser and the other the balancing condenser, are charged to equal opposite potentials and the opposite charges are mixed and discharged through a galvanometer. The two condenser systems are adjusted until the galvanometer deflection is zero. A special form of rotating commutator was devised for which the contact resistances are small and uniform. This commutator has three pairs of make and break contacts, two for charging and discharging the two condensers, and one pair connected so that a single battery is used to charge both condensers. The capacity of the test condenser is obtained in terms of readings on a condenser which forms part of the balancing condenser system. The ratio of the capacities of the test condenser with a vacuum and with air for dielectric is then obtained. The calibration for the readings is made with the apparatus in place, by simple changes of connections. Possible errors from time lag, thermal expansions and deformations from pressure changes are discussed. The average of twelve separate measurements gives 1.000594 for the dielectric constant of air at 0°C and 760 mm Hg. pressure. The twelve separate readings agree in the fifth decimal place.

43. Shielded oscillator for Hertzian waves. J. TYKOCINSKI-TYKOCINER, University of Illinois.—A thermionic tube is mounted at each end inside a brass cylinder in contact with the cold electrode. The grids of the tubes are connected by means of an insulated rod placed concentrically in the cylinder. The electromagnetic field of the oscillator is confined to the space inside the cylinder, where a standing wave is produced along its axis with a potential node in a plane dividing the length of the cylinder in two equal parts. The variation of frequency is produced by condensers mounted inside the cylinder. The cylinder is closed at each end by means of rotating shielding caps which serve as dials for the tuning mechanism. Measurements on antennae or Lecher wires were made undisturbed by the stray field of the oscillator, by connecting them with two points of

the rod, reached through holes made in the cylinder on both sides of the nodal plane. Standard 5 and 50 watt oscillating tubes were used. With an oscillator having a cylinder 100 cm long and 7.3 cm in diameter a frequency of 60×10^6 to 65×10^6 was produced. A shorter cylinder 66 cm long and 4.8 cm in diameter gave a frequency of 85×10^6 .

44. A principle governing the distribution of current in systems of linear conductors. FRANK WENNER, Bureau of Standards.—Reference is made to practically all the laws, theorems, principles and procedures generally considered to pertain to the distribution of direct current in systems of linear conductors. Consideration is then given to a principle which has been used but little and seems to be practically unknown. This principle is applicable to systems of linear conductors in which the currents are proportional to the impressed electromotive forces and may be stated as follows: The current in any branch is that which would result if all impressed electromotive forces were replaced by a single impressed electromotive force located in the particular branch and equal to the drop in potential which originally would have appeared across a break had the branch been opened. A proof of this principle is given and some of the advantages to be gained by its use are illustrated by the solution of a graded series of problems. In some of these the currents are direct and constant, in others the currents are alternating, and in one the currents are transient.

45. A new electrophoresis cell. MELVIN MOONEY, National Research Fellow, University of Chicago.—Endosmotic streaming along the walls of an electrophoresis cell is compensated by reverse streaming along the axis. To eliminate the resulting velocity gradient in the water, a new cell was designed consisting essentially of a complete loop or hydrodynamic circuit. The lower half of the loop is a long 0.7 mm capillary tube, with thin walls to permit microscopic observation of the colloidal particles within. The upper half, filled with distilled water, is a short 12 mm tube and therefore has a very small hydrodynamic resistance. Consequently the water moves through the capillary with uniform velocity over its cross-section, the compensating reverse flow taking place through the large tube. The advantages are: (1) the correction applied to the observed velocity of a colloidal particle to obtain its velocity with respect to the water is no longer subject to errors in locating the particle in the tube; (2) the endosmotic velocity of the water is generally opposite and approximately equal to the electrophoretic velocity. Consequently the arrangement is suitable for precise measurement of differences in mobility of different particles or of the same particle under different fields.

46. The magnetic susceptibility of rare earth metals. E. H. WILLIAMS, University of Illinois.—The magnetic susceptibilities of four rare earth metals, namely, cerium, lanthanum, praseodymium and yttrium, have been determined. In each case the value of the susceptibility depends on the intensity of the magnetic field, decreasing as the field is increased from 10 gauss to 4000 gauss. In this respect the magnetic susceptibility of the rare earth metals resembles very much the behavior of the permeability of iron. Owing to the low value of the susceptibilities, 20×10^{-6} to 50×10^{-6} dyne cm per gram, for the fields used, it is impossible with the methods available to fill in the gap for fields between 10 gauss and zero. This gap constitutes the most interesting part of the curve.

47. The magnetic moment of atomic hydrogen. T. E. PHIPPS and JOHN B. TAYLOR, University of Illinois. (Introduced by W. H. Rodebush.)—The magnetic moment of atomic hydrogen has been investigated by the atomic ray method introduced by Stern and Gerlach. Atomic hydrogen formed in a discharge tube by the method of R. W. Wood was first used. The ray was formed in a special all-glass slit system of three slits sealed to the discharge tube. The ray was detected by the reduction resulting on contact with a target coated with molybdenum trioxide. A sharply defined blue line against a white background was the result. In the magnetic field the ray was separated into two branch-

ing rays. There was also evidence of a central undeviated ray, which is believed to be due to molecular rather than atomic hydrogen. From a measurement of the deflection, the magnetic moment of the hydrogen atom was calculated to be one Bohr magneton, within the limits of experimental error. In addition, atomic hydrogen formed by the hot filament method of Langmuir was used. The increased velocity of the atoms in this case allowed less separation of the ray, but a deflection was distinctly recorded. Finally, the product formed on exposing a mixture of mercury vapor and hydrogen to ultra-violet light was investigated. This is believed by Cario and Franck, Taylor and others to be atomic hydrogen. Thus far attempts to form a ray which will reduce the target have been unsuccessful. The reasons for this are being investigated.

48. A preliminary report on the study of the emission spectra and surface tension alterations in experimental animal tumors. DONALD C. A. BUTTS, THOMAS E. HUFF, and FREDERICK PALMER, JR., Hahnemann Medical College, Philadelphia, Pa.—In view of the fact that analytical chemical methods of comparing normal and pathologic tissue have offered little vital information as to the obscure alterations in pathologic cell change, and to further substantiate findings of one of the writers, the authors have studied the physical, chemical, and physical-chemical nature of experimental animal tumors, with interesting results. Although the results do not as yet warrant a conclusive report, several findings are of physical interest, and promise to materially advance our knowledge of cancer causation and to open up a promising field for a scientific method of attack.

49. Fluorescence and chemiluminescence of cod-liver oil. JAY W. WOODROW and G. M. WISSINK, Iowa State College.—It has been shown that cod-liver oil will produce a developable image on a photographic emulsion and that this effect is much more pronounced if the oil has been previously exposed to ultra-violet light. At first this effect was thought to be due to an ultra-violet radiation but it was later explained as a direct chemical action analogous to the Russell Effect. We have found it possible to obtain a chemiluminescence of cod-liver oil by the oxidation of the heated vapor. The luminescence is of a bluish-green color but it is so faint that we have been unable as yet to obtain its spectrum. Kautsky and Neitzke have recently shown that the fluorescent and chemiluminescent spectra of all the substances they investigated have intensity maxima at the same wave-length. We have photographed the fluorescent spectrum of cod-liver oil illuminated by the light from a quartz mercury-vapor arc and find that it has a maximum intensity at a wave-length of about 5000A. The color of the fluorescent light as observed by the eye appears to be the same as that produced by chemiluminescence.

50. New measurements upon the light-sensitiveness of crystalline selenium. A. M. MACMAHON, University of Chicago.—A study is being made of the electrical conductivity of the element selenium, in crystalline form, with the purpose of expressing the light-sensitive property quantitatively in terms of reliable standards. As a preliminary report a three-parameter family of curves, showing the change in the electric current through a single, well-tested specimen as a function of the time, when the intensity and wave-length of the incident light and the applied potential difference are separately varied, is presented. These experimental results, relating the current, i , with the time of illumination, t , may all be fitted with surprising accuracy by a mathematical expression of the form,

$$i - i_0 = A(1 - e^{-at}) + B(1 - e^{-bt})$$

(Cf. Brown, Phys. Rev. 33, 1, (1911).) The numerical values of the constants A , a , B and b are deduced and plotted as functions of the parameters named above. The extension of these data should be fruitful in the development of a more adequate theory than exists at the present time for these phenomena.

51. The effect of a variation from the condition for achromatism in lenses. T. TOWNSEND SMITH, University of Nebraska.—It is well known that two thin lenses in contact will form an achromatic pair, if the focal lengths of the two are in the ratio of the dispersive power of the glasses. The focal length of such a combination is a minimum for some wave-length (λ_1), which depends upon the ratio of the focal lengths and which is near $550m\mu$, if the dispersive power be specified in terms of lines C and F. There seem to be no criteria available for judging of the goodness of the color correction in its dependence upon λ_1 . The present work is an attempt to get some information upon this question. With the aid of Hartmann's dispersion formula and on the assumption of a dense flint (Schott 0-103) diverging and a silicate crown (Schott 0-60) converging lens, the resultant brightness on the axis has been calculated for various values of the focal lengths and for various apertures, and from these values, graphically represented, an estimate may be made as to the goodness of the color correction in so far as it depends upon these variables.

52. On the theory of heats of fusion. N. RASHEVSKY, Westinghouse Research Laboratory, East Pittsburgh.—Plotting the potential energy ϕ of an aggregation of atoms against the atomic distance δ , we obtain a curve, having a minimum at $\delta = \delta_0$, (δ_0 = space-lattice econstant at absolute zero) and tending assymptotically to zero for $\delta = \infty$. At these two points we have $d\phi/d\delta = 0$. Between these points there is a point δ_1 , where $d^2\phi/d\delta^2 = 0$. As long as $\delta < \delta_1$, the deformation of the body causes a force to appear, which tends to restore the initial state, and which increases with increasing deformation. For $\delta > \delta_1$ the restoring force diminishes with increasing deformation. Hence there can be no question even about an approximate behaviour of the body as of an elastic one. This leads to the assumption, that when due to thermal agitation, the space-lattice constant reaches the value δ_1 , the body becomes liquid. The amount of work, necessary to increase δ from δ_0 to δ_1 is thus interpreted as the total heat of fusion. Using for ϕ the expression $\phi = A/\delta^3 - B/\delta^n$, and calculating A , B , and n from the compressibility and the thermoelastic constants according to Gruneisen, we may calculate with our assumption the heats of fusion. The values thus calculated for seven metals are in pretty good agreement with the experimental ones.

53. Theory of the specific heat of methane. JAKOB KUNZ, University of Illinois.—D. M. Dennison has recently given an analysis of the oscillations of methane based on the infra-red absorption bands. The results of this analysis and the quantum theory of radiation are used for the theoretical determination of the specific heat of methane. It is found in general that the theoretical values are a little higher than the experimental values (as function of the temperature).

54. Optimum conditions for music in rooms. F. R. WATSON, University of Illinois.—Musicians prefer rooms for playing that are reverberant, while listeners are better pleased with deadened rooms. A series of experiments was conducted to adjust these apparently contradictory conditions. After investigating a number of rooms of widely different volumes that varied in reverberant qualities, a final experiment gave the solution. A room adjusted for "perfect" conditions was found unsatisfactory for both playing and listening, but on transferring the absorbing material from the end of the room occupied by the players to the end used for listening, the conditions were regarded as very acceptable both for playing and listening. This experiment indicates the desirable conditions for concert halls, studios, broad-casting rooms, etc., and suggests suitable arrangements for various acoustic experiments.

55. The theory of the Herschel-Quincke tube. G. W. STEWART, University of Iowa.—The well-known explanation of the Herschel-Quincke interference tube is that there is elimination of the transmitted wave when the difference in path in the two

branches is an odd number of half wave-lengths. (This is a sound conducting tube branching into two parts of different lengths and reuniting, having a constant total area of cross-section at these two junctions.) This theory is incomplete. The ratio of the transmitted to the incident acoustic energy is

$$16 \sin^2(\alpha_2 + \alpha_3)/2 \times \cos^2(\alpha_2 - \alpha_3)/2 \times \{ [1 - 2 \cos(\alpha_2 + \alpha_3) + \cos(\alpha_2 - \alpha_3)]^2 + 4 \sin^2(\alpha_2 + \alpha_3) \}^{-1}$$

where α_2 and α_3 are the phase changes over the two branches of the tube. This ratio is zero not only when $\alpha_2 - \alpha_3 = (2n+1)\pi$ as stated above, but also when $\alpha_2 + \alpha_3 = 2n_1\pi$, provided $(\alpha_2 - \alpha_3) \neq 2n_2\pi$, n_1 and n_2 being independent integers. The result is a great increase in number of interference frequencies. This theory is verified by experiment.

56. A new instrument for measuring surface tension. F. E. POINDEXTER, University of Florida.—The downward pull on the stem of a hydrometer due to the surface tension of the liquid is used to measure this tension. The liquid wets both the inside and outside of the hydrometer stem, the sensitivity of the instrument depending, therefore, upon the wall thickness of the projecting stem and the density of the liquid, i.e. $T = \frac{1}{2}\rho S(r_2 - r_1)g$, where T = surface tension, ρ = density of the liquid, S = the length of the portion of the stem submerged by the pull of the surface tension, r_1 and r_2 are the inside and outside radii of the stem respectively, and g = acceleration of gravity. The $(r_2 - r_1)$ of the one used was .040 cm and $S = 3.57$ cm, giving the surface tension of water to be 69.97 dynes per cm at 27.5°C in good agreement with the value of 69.50 found by Ramsey and Shields by the capillary tube method.

57. Thermo-electric effect in single crystal zinc. ERNEST G. LINDER, University of Iowa. (Introduced by E. P. T. Tyndall.)—Data are presented on the thermal e. m. f. against copper of six single crystal wires of zinc, of which the orientations of the main crystallographic axis with respect to the wire axis, range from 11.4° to 90° . The temperature interval is from -182° to 475°C . From the data are calculated the thermo-electric power, Peltier coefficient, and difference of the Thomson coefficients for Zn_\perp against Zn_\parallel . The data also provide a test for the Voigt-Thomson law for the variation of the thermo-electric power with crystal orientation. The law¹ is verified for the low temperatures, but the deviations at the high temperatures (300° – 400°) are greater than the experimental errors are thought to be. The thermo-electric powers of liquid Zn against solid single crystal Zn of different orientations, and against polycrystalline Zn are given the value -7.89 m.v./deg. for $e_l - e_s$ for Zn_{poly} , having been found. A theoretical expression is derived for the thermo-electric power of polycrystalline zinc in terms of the principal thermo-electric powers of the component crystals.

AUTHOR INDEX

- Barker, E. F.—see Stinchcomb
- Barton, Henry A.—see Jenkins
- Birge, R. T. and A. Christy—No. 26
- Blake, F. C., James Lord and A. E. Focke—No. 6
- Bobrovnikoff, N. T.—No. 20
- Butts, Donald C. A., Thomas E. Huff and Frederick Palmer, Jr.—No. 48
- Carman, A. P. and K. H. Hubbard—No. 42
- Christy, A.—see Birge
- Constantinides, Philip A.—No. 36
- Davey, Wheeler P.—No. 5
- Dawson, L. H.—No. 39
- Doan, Richard L.—No. 1
- Duffendack, O. S.—see Wolfe
- Durbin, F. M.—No. 35
- Eldridge, John A.—No. 28
- , A. Ellett and Harry F. Olson—No. 9
- Ellett, A.—No. 10
- , see Eldridge
- Erikson, Henry A.—No. 37
- Focke, A. E.—see Blake
- Gale, Henry G. and George S. Monk—No. 21
- Harkins, William D. and H. A. Shadduck—No. 7
- Hertel, K. L.—No. 34

- Hepburn, Ann B.—No. 24
Hoag, J. Barton—No. 13
Houston, William V.—No. 18
Hubbard, K. H.—see Carman
Huff, Thomas E.—see Butts
Hughes, A. L. and L. W. Jones—No. 31
Hull, Albert W. and J. M. Hyatt—No. 32
Hyatt, J. M.—No. 33
———, see Hull
Jauncey, G. E. M.—No. 4
Jenkins, Francis A., Henry A. Barton and
 Robert S. Mulliken—No. 23
Jones, L. W.—see Hughes
Keys, David A.—No. 14
Kunz, Jacob—No. 53
Lansing, William D.—No. 40
Laporte, O.—see Sommerfeld
Lemon, Harvey B.—No. 19
Linder, Ernest G.—No. 57
Lindsay, Geo. A.—see Van Dyke
Lord, James—see Blake
MacMahon, A. M.—No. 50
McDonald, Frank C.—No. 25
McLennan, J. C. and I. Walerstein—
 No. 12
Monk, George S.—see Gale
Mooney, Melvin—Nos. 41 and 45
Mueller, Hans—No. 38
Mullikan, Robert S.—No. 22
——— see Jenkins
Olson, H. F.—No. 8
——— see Eldridge
Palmer, Frederick Jr.—see Butts
Phipps, T. E. and John B. Taylor—No. 47
Poindexter, F. E.—No. 56
Rashevsky, N.—No. 52
Rogers, R. A.—No. 2
Rusk, Rogers D.—No. 30
Shadduck, H. A.—see Harkins
Shenstone, A. G.—No. 15
Sommerfeld, A. and O. Laporte—No. 11
Smith, T. Townsend—No. 51
Stewart, G. W.—No. 55
Stinchcomb, G. A. and E. F. Barker—
 No. 27
Taylor, John B.—see Phipps
Tykocinski-Tykociner, J.—No. 43
Van Dyke, Geo. D. and Geo. A. Lindsay—
 No. 3
Walerstein, I.—see McLennan
Watson, F. R.—No. 54
Wenner, Frank—No. 44
Williams, E. H.—No. 46
Winans, J. G.—No. 29
Wissink, G. M.—see Woodrow
Wolfe, R. A. and O. S. Duffendack—
 No. 17
Woodrow, Jay W. and G. M. Wissink—
 No. 49
Zumstein, R. V.—No. 16

THE
PHYSICAL REVIEW

THE CRYSTAL STRUCTURE OF MAGNESIUM
PLATINOCYANIDE HEPTAHYDRATE

BY RICHARD M. BOZORTH AND F. E. HAWORTH

ABSTRACT

Positions of the Mg and Pt atoms in crystals of $MgPt(CN)_4 \cdot 7H_2O$. These have been definitely determined by means of x-ray oscillating-crystal photographs and Laue photographs, using the theory of space-groups. Because the other atoms are too light in comparison with the metal atoms, especially Pt, their positions could not be determined. The Pt atoms are located at 0 0 0 and $\frac{1}{2} \frac{1}{2} \frac{1}{2}$, the Mg atoms at 0 0 $\frac{1}{2}$ and $\frac{1}{2} \frac{1}{2} 0$, in a tetragonal unit of structure $14.6\text{A} \times 14.6\text{A} \times 3.13\text{A}$. Two units of structure are shown in the figure. The peculiar *optical properties* are believed to be associated with the unusual arrangement of the heavier atoms in widely spaced rows parallel to the tetragonal axis. In these rows Mg atoms alternate with Pt atoms, and the distance between any two adjacent atom-centers is 1.57A. The shortest distance between rows, however, is 10.3A, 6.6 times the distance between atoms in the same row. The *atomic radii* of Mg and Pt as determined by Bragg from other crystal data do not agree with the observed distance between these atoms, the calculated value being 2.7A, the observed distance 1.57A. The observed distance, however, is consistent with that calculated by the method of Davey, who assumes that the radius of an ionized atom differs much from the radius of the same atom un-ionized, and that the radii of Cs^+ and I^- are substantially equal in crystals of CsI.

INTRODUCTION

TETRAKONAL crystals of $MgPt(CN)_4 \cdot 7H_2O$ ¹ are of special interest because of their peculiar optical properties² and resultant beautiful appearance. They are red by transmitted light, but by reflected light the prism faces are a brilliant metallic green and the ends of the prism, perpendicular to the tetragonal axis, have a violet

¹ The water content is said to vary *continuously* from 8.1 H_2O to 6.8 H_2O , when exposed to dry air, the crystals being similar in this respect to the zeolites. See H. B. Buxhoeveden and G. Tammann, Zeit. anorg. Chem., 15, 319-327 (1897); and J. W. Mellor, Comprehensive Treatise of Inorganic and Theoretical Chemistry, Longmans Green and Co., 6, 575-576 (1925).

² R. W. Wood, Physical Optics, 2nd Ed., The Macmillan Co., New York, 560-561 (1919). For a bibliography of this and other platinocyanides, and their crystallography, see Gmelin-Kraut, Handbuch der Chemie, Carl Winter, Heidelberg, 5 .3, 867-868 (1915).

tinge. They exhibit strong dichroic fluorescence; rays polarized in the direction of the tetragonal axis are yellow, those polarized perpendicular to the axis are red. Other hydrated salts containing the platinocyanide ion fluoresce when exposed to ultra-violet light or radium, but with these salts the fluorescence does not appear to be polarized as it is in the magnesium salt. None of these other salts is known to be tetragonal, being either orthorhombic or monoclinic.

The crystals have been examined crystallographically by Lang,³ who observed the forms {100}, {001} and {111}, and found the axial ratio $c/a = 0.6103$.

The determination of the crystal structure was undertaken at the suggestion of H. E. Ives of these laboratories, in the hope that it might furnish some suggestion for an explanation of the optical behavior. The crystals were prepared by slow evaporation of an aqueous solution. X-ray data were obtained from oscillating-crystal photographs and Laue photographs.

THE UNIT OF STRUCTURE

Molybdenum K-radiation was reflected onto a photographic plate from (100)' and (001)' faces (primed crystallographic indices are those according to Lang³) of an oscillating crystal, using a calcite crystal for comparison. The sines of the grazing angles θ for reflection are given in Table I. The wave-length of the $K\alpha_1$ line is taken to be 0.7075 Å, and the grating space of calcite 3.029 Å.⁴

TABLE I
Oscillating-crystal data, using Mo $K\alpha_1$ radiation, $\lambda = 0.7075 \text{ \AA}$

Old	(<i>hkl</i>)	New	sin θ	Old	(<i>hkl</i>)	New	sin θ
(100)'	(110)		0.034 0.0686 0.1028 0.1369 0.1711 0.2054	(001)'	(001)		0.226

If that reflection from each face which occurs at the smallest angle is considered to be in the first order, the dimensions of the corresponding unit of structure are $10.3 \text{ \AA} \times 10.3 \text{ \AA} \times 1.57 \text{ \AA}$. However, when the content of this unit is calculated from the density, directly measured as 2.39 g/cm^3 , it is found to be only 1/2 molecule of $\text{MgPt}(\text{CN})_4 \cdot 7\text{H}_2\text{O}$.

³ V. v. Lang. Sitz. Ber. Akad. Wiss. Wien, 111.2a, 1161 (1902).

⁴ A. H. Compton, H. N. Peets and O. K. De Foe, Phys. Rev. (2) 25, 625-629 (1925).

Analysis of Laue photographs (tungsten target x-ray tube) taken with the beam perpendicular to the (001)' face and perpendicular to the (100)' face showed that the unit of structure must be enlarged to $14.6\text{A} \times 14.6\text{A} \times 3.13\text{A}$, containing two molecules. The faces originally designated (100)', (001)' and (111)' by the crystallographers now become (110), (001) and (041), respectively. Hereafter, all indices will be referred to the new unit just described, containing two molecules.

In analyzing the Laue photographs, spots were projected onto a gnomonic net, and the wave-lengths calculated according to the equation

$$n\lambda = 2d_{100} (h^2 + k^2 + l^2 a^2/c^2)^{-1/2} \sin \theta$$

where λ is the wave-length of the x-rays, $d_{100} = 14.6\text{A}$, $c/a = d_{001}/d_{100}$, $d_{001} = 3.13\text{A}$, and h , k and l are the indices of the reflecting plane. The smallest value of $n\lambda$ calculated for any spot was found to be 0.25A , a value consistent with the voltage across the tube, therefore reflections for which the value of $n\lambda$ lay between 0.25 and 0.50A were considered to be first order reflections only. For all planes which reflected in the first order, $h+k+l$ was an even number, consequently the structure is built on a body-centered lattice. Planes for which $h+k+l$ was odd were considered to reflect only in the second order when $n\lambda$ lay between 0.50 and 1.00A .

THE SPACE-GROUP AND THE ARRANGEMENT OF THE ATOMS

All types of forms, that is, forms whose indices represented all combinations of odd and even indices (including forms $\{001\}$, $\{0kl\}$, $\{hk0\}$, $\{h \cdot h \cdot 2p+1\}$ and $\{h \cdot h \cdot 4p\}$, where p is any integer) reflected in either the first or second order depending *only* on whether $h+k+l$ was an even or an odd number. Furthermore, the Laue photograph taken with the x-ray beam perpendicular to the (001) planes showed a tetragonal axis of symmetry and four reflection planes; and the photograph for which the beam was perpendicular to the (110) planes showed a digonal axis of symmetry and two reflecting planes. The only space-groups⁵ with which these data are consistent are D_{4h}^{17} , D_4^9 , C_4^9 , and $D_{2d}^{11} = V_d^{11}$. Since there is no evidence that the crystals do not possess all the symmetry which it is possible for a tetragonal crystal to possess, the correct space-group is probably D_{4h}^{17} .

⁵ W. T. Astbury and Kathleen Yardley, Phil. Trans. Roy. Soc. Lond., **224A** 221-257 (1924).

The arrangements⁶ predicted by all of these space-groups except C_{4v}^9 for two equivalent atoms in a unit of structure, are the same, namely:

$$(1) \ 0\ 0\ 0, \frac{1}{2}\ \frac{1}{2}\ \frac{1}{2} \quad (2) \ 0\ 0\ \frac{1}{2}, \frac{1}{2}\ \frac{1}{2}\ 0.$$

The atom-positions predicted by C_{4v}^9 are:

$$(3) \ 0\ 0\ u; \frac{1}{2}, \frac{1}{2}, \frac{1}{2} + u;$$

where u may have values between zero and unity. In either case the Mg and Pt atoms are placed in lines parallel to the tetragonal axis, and each line is composed of both kinds of atoms arranged alternately. If the values of u are put equal to 0 and $\frac{1}{2}$, the positions of the atoms according to (3) are those specified in (1) and (2). Although the x-ray diffraction data do not rule out arrangement (3) for values of u which do not differ by $\frac{1}{2}$, physical considerations make it very probable that the atoms lie in the unique positions. If they were not so placed these atoms would be grouped in pairs, each Mg atom, for example, being nearer to one of its neighboring Pt atoms than to any other Pt atom, and the shortest distance between the centers of a Mg and a Pt atom would be less than 1.57A, a distance already considerably smaller than that to be expected on the basis of Bragg's values of atomic radii,⁷ or of Wyckoff's more recent tabulation,⁸ although not surprisingly small according to Davey's hypothesis.⁹

The x-ray data are of course quite powerless to place the C, N, O or H atoms, since the reflecting powers of these atoms are much less than those of the Mg and Pt atoms. Possible arrangements for C and N atoms include those placing them at the corners of squares of undetermined sizes which lie in planes parallel to (001) planes and which have Pt atoms at their centers. Such an arrangement is similar to that of the Cl atoms around the Pt atoms in K_2PtCl_4 .¹⁰

Seven molecules of H_2O cannot be placed in a manner consistent with the apparent high symmetry. It is suggested as probable that the

⁶ R. W. G. Wyckoff, The Analytical Expression of the Results of the Theory of Space-Groups, Carnegie Institution of Washington Publication No. 318, 78-99 (1922).

⁷ W. L. Bragg, Phil. Mag. (6) 40, 169-189 (1920). The radius assigned to Mg is 1.42A. The radius of Pt is not given in this article but may be calculated from more recent data [Pt to Cl, 2.33A in K_2PtCl_4 , R. G. Dickinson, J. Am. Chem. Soc. 44, 2409 (1922)] using Bragg's radius for Cl, 1.05A. This gives for Pt the radius 1.28A. The distance Mg-Pt from these data is 2.7A, a value to be compared with 1.6A, the distance Mg-Pt here found by experiment in $MgPt(CN)_4 \cdot 7H_2O$.

⁸ R. W. G. Wyckoff, Proc. Nat. Acad. Sci., 9, 33-38 (1923).

⁹ W. P. Davey, Gen. Elect. Rev., 29, 274-287 (1926).

¹⁰ R. G. Dickinson, loc. cit. 7.

highest observed water content,¹ corresponding to $MgPt(CN)_4 \cdot 8H_2O$, is that characteristic of perfect crystals. The 16 oxygen atoms, and also the 32 hydrogen atoms, can then be placed in equivalent positions according to arrangements derived from the space-group D_{4h}^{17} , the only one of the possible space-groups listed above which will permit 32 atoms to be arranged in equivalent positions.

Data from one of the Laue photographs are given in Table II, where d/n and λ are expressed in Å, and I is the estimated photographic

TABLE II
Laue photographic data for $MgPt(CN)_4 \cdot 7H_2O$. W radiation
incident normally upon (110) planes

$n^*(hkl)$	d/n	I	λ	$n(hkl)$	d/n	I	λ
(341)	2.13	5	0.44	(7.12.1)	0.99	0.4	0.47
(451)	1.83	2	.33	(053)	.99	.5	.47
(561)	1.60	0.3	.25	2(351)	.97	.3	.37
(112)	1.56	4	.46	(163)	.96	.5	.45
(132)	1.49	3	.42	(273)	.93	.4	.42
2(340)	1.45	1	.42	(8.13.1)	.91	.3	.40
(352)	1.33	0.7	.34	(7.11.2)	.91	.2	.32
(790)	1.27	.6	.32	2(470)	.90	.2	.47
(691)	1.23	.8	.44	(383)	.89	.3	.38
(572)	1.15	.1	.25	(493)	.85	.2	.35
2(450)	1.13	.1	.25	2(461)	.85	.1	.28
2(241)	1.13	.3	.49	(9.14.1)	.84	.2	.34
(7.11.0)	1.11	.4	.48	(7.13.2)	.83	.3	.40
(7.10.1)	1.11	.4	.36	(334)	.77	.1	.34
(592)	1.05	.5	.42	(354)	.75	.1	.44
(123)	1.04	.3	.31	(174)	.73	.1	.42
(233)	1.01	.3	.50	(15.9.2)	.73	.05	.32
(8.11.1)	1.01	.3	.30	(194)	.71	.1	.39
(143)	1.00	.3	.50	(3.11.4)	.67	.1	.35

* $n=1$ unless otherwise stated.

intensity of the spot. In this table are included all planes having $d/n > 1.00\text{Å}$ which were inclined to the x-ray beam so that they could have reflected any wave-lengths between 0.25 and 0.50Å .

DISCUSSION OF THE RESULTS

(a) *Optical properties.* As mentioned in the introduction, the fluorescent light is different in character depending on whether the plane of the analyzer is set parallel to or perpendicular to the tetragonal axis. Although some such difference would be expected for any fluorescent tetragonal crystal, a difference as large as that found for $MgPt(CN)_4 \cdot 7H_2O$ is not ordinarily observed. The reason for the peculiar optical properties of this crystal appear to be closely associated with the relative positions of the Mg and Pt atoms in it. These

atoms are arranged in rows parallel to the tetragonal axis, the distance between atom-centers in any one row being 1.57 Å. The shortest distance between any two rows, however, is 10.3 Å, 6.6 times the distance between two atom-centers in the same row. This arrangement is illustrated, to scale, in Fig. 1. Vibrations of the metal atoms must therefore encounter much greater resistances in the axial direction than in directions perpendicular thereto. Even in the regions between the rows of Mg and Pt atoms where the fluorescent light may possibly originate, the components of the electric field parallel and perpendicular to the axis may be expected to differ greatly in magnitude, producing much different effects upon light polarized in these directions.

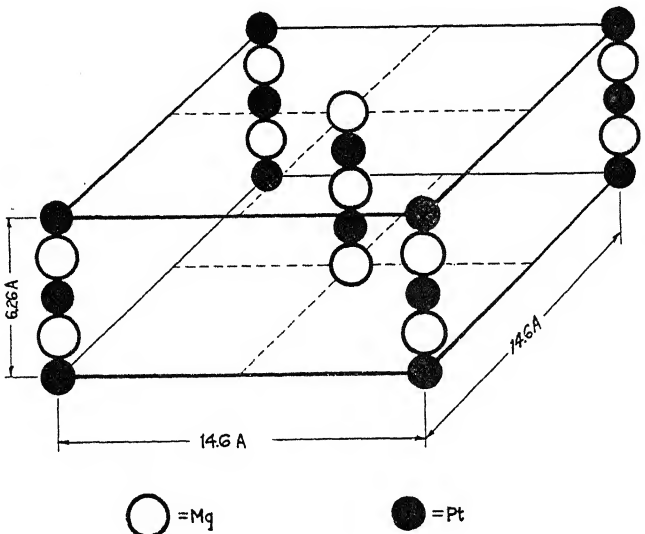


Fig. 1. Arrangement of magnesium platinum atoms in platinocyanide heptahydrate.

(b) *Atomic radii.* Since the original table of atomic radii in crystals proposed by Bragg⁷ and based upon the inter-atomic distances observed in FeS₂, Fe, CaCO₃, C (diamond), etc., other values have been suggested, based on different methods of allotting to each atom its proper fraction of the total distance between its center and that of its neighbor, the quantity directly determined by means of x-rays. Wyckoff⁸ has used the distances in CsCl₂I as a starting point, while Davey has assumed that the radii of Cs⁺ and I⁻ are equal in CsI, and has argued that ionized and un-ionized atoms have very different radii. Although it is to be expected that the radius of an atom will depend both upon the kind and upon the arrangement of the surround-

ing atoms, it nevertheless appears that when an atom has a fixed charge it behaves as if it had a "sphere of influence" which does not vary more than 10 percent if the surrounding atoms are not too different in the crystals compared. The radii proposed by Bragg and by Davey, however, differ from each other by much more than this amount, their values for the radius of the Cl^- ion being 1.05 and 1.59 Å, and for the K^+ ion 2.07 and 1.55 Å, respectively. The nature of this difference causes great discrepancies in the predicted distances between ions of like sign such as I^- to I^- , or Mg^{++} to Pt^{++} . Bragg's predicted distance between I^- ions is 2.80 Å, while the observed distance is 4.21 Å in CdI_2 ¹¹ and in SnI_4 .¹² The predicted distance between S^{--} ions in MoS_2 ¹³ is 2.05 Å, the observed distance 3.49 Å.

It may be argued that the radii of negative ions "in contact" with each other will be greater than their radii in contact with positive ions, for the similar charges might be expected to keep them farther apart. This same argument, however, would tend to increase the distance between Mg^{++} and Pt^{++} ions to a value much greater than 2.70 Å, the sum of the Bragg radii, while the distance here observed is only 1.57 Å. All these discrepancies noted above may be removed by assigning to Mg^{++} a radius 0.87 Å, consistent with Davey's ideas, and to Pt^{++} a radius 0.70 Å, consistent with the distance between Pt^{++} and Cl^- in K_2PtCl_4 ¹⁴ and with Davey's value for the radius of the Cl^- ion. The structure of $MgPt(CN)_4 \cdot 7H_2O$ accordingly lends support to Davey's method of calculating atomic radii and to the results already obtained by this method.

Since writing the above, the authors have read the paper by W. L. Bragg on "Interatomic Distances in Crystals,"¹⁴ in which he states that the radii given in his 1920 paper should be corrected by about 0.7 Å, the radii of the anions being increased and those of the cations decreased by this amount. This brings the radii into agreement with the values proposed by Wasastjerna¹⁵ in 1923, but they still differ by about 0.2 Å from those proposed by Davey. A set of values which is intermediate between these two, and therefore not very different from either of them, may be obtained from the four relations:



¹¹ R. M. Bozorth, J. Am. Chem. Soc., **44**, 2232-2236 (1922).

¹² R. G. Dickinson, J. Am. Chem. Soc., **45**, 958-962 (1923).

¹³ R. G. Dickinson and L. Pauling, J. Am. Chem. Soc. **45**, 1466-1471 (1923).

¹⁴ W. L. Bragg, Phil. Mag. (7) **2**, 258-266 (1926).

¹⁵ J. A. Wasastjerna, Soc. Sci. Fennica Comm. Phys.-Nat. **1**, No. 38, 1-25 (1923).

(obs. in K_2PtCl_4)¹⁰, $Mg^{++} + O^{--} = 2.10$ (obs. in MgO),¹⁶ and $Cl^- - O^{--} = 0.40$ (commonly accepted difference). Values so obtained are given in Table III.

TABLE III

Ion	Bragg (1920)	Wasastjerna (1923) Bragg (1926)	Davey (1926)	Calculated
Cl^-	1.05A	1.72A	1.59A	1.63A
O^{--}	0.65	1.32	>1.05	1.23
Mg^{++}	1.42	0.75	<1.05	0.87
Pt^{++}	(1.28)	—	—	0.70

Both Wasastjerna's values, and Davey's values as far as they go, are consistent with the observed distance between Mg^{++} and Pt^{++} in $MgPt(CN)_4 \cdot 7H_2O$, and the agreement with each seems good considering that the radius of the "sphere of influence" may be expected to change with the kind and arrangement of the surrounding atoms, and indeed the "radius" may be different in different directions especially in the case of atoms surrounded as are the Mg^{++} and Pt^{++} in $MgPt(CN)_4 \cdot 7H_2O$.

BELL TELEPHONE LABORATORIES, INC.,
September 15, 1926.

¹⁶ R. W. G. Wyckoff, Am. J. Sci. 10, 107 (1925).

SERIES SPECTRA OF BORON, CARBON, NITROGEN,
OXYGEN, AND FLUORINE

BY I. S. BOWEN

ABSTRACT

Practically all of the unidentified strong lines of boron, carbon, nitrogen, oxygen, and fluorine occurring in the extreme ultra-violet spectra of the vacuum spark have been classified as due to jumps between levels in B_I , C_I , C_{II} , N_{II} , N_{III} , O_{II} , O_{III} , O_{IV} , F_I , F_{II} , F_{III} , and F_{IV} . The levels thus found are correlated with those demanded by the Russell-Heisenberg-Pauli-Hund theory.

I. INTRODUCTION

IN previous articles by Professor Millikan and the author¹ the series spectra of one and two-valence-electron atoms of the elements in the first row of the periodic table have been traced. The present paper is an extension of the methods there used to the more complex atoms of this same group of elements.

Since the spectra of these elements are much more complex than those previously studied and as the Russell-Heisenberg-Pauli-Hund theory has shown, there is, in general, no direct connection between the type of the term, i. e. S , P , D , F , and the corresponding k value of the electrons involved, a further extension of the notation is necessary. The notation used throughout this paper is as follows: All terms arising from the normal state of the atom of any n electron system, i. e. that due to the configuration of $2s$ electrons and $(n-2)p$ electrons or in Russell's notation the s^2p^{n-2} configuration, are designated by a . Those terms due to the configuration formed when one of the s electrons is moved to a $2p$ orbit, i. e. the sp^{n-1} configuration are designated by b , while terms which have their origin in the p^n configuration, i. e. the arrangement attained when both of the s electrons are raised to $2p$ orbits, are indicated by c . When one of the p electrons is moved to an excited s orbit making an $s^2p^{n-3} \cdot s$ configuration, the terms thus formed are marked with k preceded by a numeral indicating the total quantum number of the orbit occupied by the excited electron. Likewise, when one of the p electrons is raised to an excited p or d orbit forming an $s^2p^{n-3} \cdot p$ or an $s^2p^{n-3} \cdot d$ configuration, the terms produced are designated by m and n respectively.

¹ Bowen and Millikan, Proc. Nat. Acad. Sci. **10**, 199 (1924).

Bowen and Millikan, Phys. Rev. **26**, 310 (1925); **28**, 256 (1926).

The maximum term multiplicity is indicated in the usual way by a small figure written above and at the left of the letter indicating the type of the term. In the tables where no ambiguity can arise as to

TABLE I
Series lines of B_I

Int.	λ I. A. Vac.	ν	$\Delta\nu$	Designation	Term Values	
1	1825.89	54767.8	15.9	$aP_1 - 3nD$	aP_1	67544.6
2	1826.42	54751.9		$aP_2 - 3nD$		67529.1
3	2089.59	47856.3	15.1	$aP_1 - bD$	bD	19688.1
3	2090.25	47841.2		$aP_2 - bD$		
	2497.53	40039.6	15.3	$aP_1 - 3kS$	$3kS$	27504.9
	2498.48	40024.3		$aP_2 - 3kS$		3nD
						12777.0

the multiplicity of the term, the indices are omitted. In the present notation primes are omitted as no longer necessary.

II. THREE-ELECTRON SYSTEMS

Since in atoms of this type one electron only is in an uncompleted group, the Hund theory predicts that the type of any term is the same as that of the orbit in which the excited electron finds itself, i. e. when the electron is in an s orbit it gives rise to a 2S term, when in a p orbit to a 2P term, etc. All of these terms belong to the doublet system. This, of course, is true only so long as the p electron alone is excited and the completed group of $2s$ electrons is left undisturbed. Jumps between terms thus formed by the excitation of the single p electron result in the regular doublet series of lines in these atoms. In C_{II} these series have been very completely analyzed by Fowler.² Table II includes only those of Fowler's lines for which much greater accuracy and resolution can now be obtained than were available at the time his article was written. For this reason the present table of C_{II} lines should be considered as supplementary to his. In the case of N_{III} Fowler³ has also identified the first term of the principal and of the second diffuse series, but was unable to obtain the lines corresponding to jumps of the electron to its normal position in the atom. The position of these resonance lines can be predicted with a considerable degree of accuracy by extrapolation from the corresponding

² A. Fowler, Proc. Roy. Soc. 105, 299 (1924).

³ A. Fowler, Series in Line Spectra, p. 165.

TABLE II
Series lines of C_{II}

Int.	λ I. A. Vac.	ν	$\Delta\nu$	Designation	Term	Values
		Doublets				
2	594.79	168127.	65.	aP_1-4nD	aP_1	196658.8
2	595.02	168062.		aP_2-4nD	aP_2	196595.0
5	687.053	145549.2	63.1	aP_1-3nD	bS	100164.9
5	687.351	145486.1		aP_2-3nD	bP_1	86033.9
5	858.088	116538.2	64.2	aP_1-3kS	bP_2	85992.3
6	858.561	116474.0		aP_2-3kS	bD	121727.4
7	903.620	110666.0		aP_1-bP_2		
8	903.960	110624.4	62.8	aP_1-bP_1		
8	904.133	110603.2	62.7	aP_2-bP_2		
7	904.472	110561.7		aP_2-bP_1		
6	1036.336	96493.8	63.7	aP_1-bS		
6	1037.021	96430.1		aP_2-bS		
2	1141.61	87595.6		$bD-4mP$		
10	1334.539	74932.2	65.4	aP_1-bD		
10	1335.705	74866.8		aP_2-bD		
2	1760.44	56804.0	13.2	$bD-3mP_2$		
1	1760.85	56790.8		$bD-3mP_1$		
		Quartets				
5	1009.870	99022.6	21.5	bP_1-cS		
6	1010.090	99001.1	28.6	bP_2-cS		
6	1010.382	98972.5		bP_3-cS		

lines of B_I and C_{II} using the method already applied to the identification of similar lines in C_{III}.¹ This method leads to the identification of the 452A and the 374A lines as given in Table III. Since the 374A line falls very close to a strong oxygen line, its wave-length may be somewhat in error.

The Hund theory further predicts that when one of the *s* electrons is removed to a $2p$ orbit the sp^2 configuration thus formed will give rise to a quartet 4P term and doublet 2S , 2P and 2D terms. If the second *s* electron is moved to a $2p$ position making a p^3 configuration,

then 4S , 2P and 2D terms will result. All of the doublet terms due to the sp^2 configuration should combine strongly with the normal doublet a^2p level of the s^2p configuration. Since all of the electrons in both

TABLE III
Series lines of N_{III}

Int.	λ I. A. Vac.	ν	$\Delta\nu$	Designation	Term Values	
Doublets						
1	374.31	267158.		$aP - 3nD$	aP_1	382225.8
1	451.91	221283.	161.	$aP_1 - 3kS$	aP_2	382051.4
1	452.24	221122.		$aP_2 - 3kS$	bS	251223.4
5	684.997	145986.0		$aP_1 - bP_2$	bP_1	236351.0
6	685.519	145874.9	175.1	$aP_1 - bP_1$	bP_2	236240.2
6	685.820	145810.9	174.5	$aP_2 - bP_2$	bD_2	281195.6
5	686.340	145700.4		$aP_2 - bP_1$	bD_3	281201.3
5	763.348	131001.8	173.1	$aP_1 - bS$	cP	151222.1
5	764.358	130828.7		$aP_2 - bS$	$3kS$	160936.1
2	772.903	129382.3	12.8	$bD_3 - cP$	$3mP_1$	136572.85
2	772.980	129369.5		$bD_2 - cP$	$3mP_2$	136536.82
7	989.803	101030.2	180.1	$aP_1 - bD$	$3nD_2$	115000.
7	991.571	100850.1		$aP_2 - bD$	$3nD_3$	114994.14
1	1006.03	99400.6		$bS - cP$		
3	1183.04	84528.2	108.0	$bP_1 - cP$		
3	1184.55	84420.2		$bP_2 - cP$		
	4098.48	24399.30		$3kS - 3mP_2$		
	4104.55	24363.22	36.08	$3kS - 3mP_1$		
	4635.46	21572.83		$3mP_1 - 3nD_2$		
	4641.94	21542.70	35.99	$3mP_2 - 3nD_3$		
	4643.21	21536.84	5.86	$3mP_2 - 3nD_2$		
Quartets						
3	771.545	129610.1	60.3	$bP_1 - cS$		
4	771.904	129549.8	80.5	$bP_2 - cS$		
4	772.384	129469.3		$bP_3 - cS$		

arrangements are in 2-total-quantum-number orbits, all lines due to combinations between them should obey the irregular doublet law.

In carbon, nitrogen, and oxygen⁴ Professor Millikan and the author have already identified a $p\bar{p}'$ group fulfilling these conditions. This group is evidently the combination between the a^2P and the b^2P levels. In C_{II} Fowler has found an x level which combines strongly with the low a^2P level to produce the strong lines at 1036A. This is unquestionably the b^2S term of the sp^2 configuration, since the lines connecting it with the 2P levels have, within experimental error, exactly the separation of the 2P levels. The strongest lines in the carbon spectrum are a pair at 1335A, which is shown by the data in the present paper, and also by some of Lang and Smith's data,⁵ to have a separation about 2 frequency units larger than that of the true a^2P separation as obtained from the a^2P-b^2P group at 904A. These lines are definitely due to C_{II}, for if we assume them to be due to a jump into the a^2P level then the levels from which this jump starts combining with the $3m^2P$ and the $4m^2P$ levels would give rise to lines at 1760A and 1141A. These lines are observed at almost exactly their calculated position, and the 1760A doublet which is the only one that can be resolved shows a separation about 2 frequency units larger than that of the $3m^2P$ levels involved. These considerations make it practically certain that this unidentified level is the b^2D term of the sp^2 configuration. Since all combinations with 2P terms show separations slightly larger than that of the 2P terms themselves it is evident that these b^2D terms are inverted.

TABLE IV
Irregular doublets, three-electron systems

Element	ν	$\Delta\nu$	ν	$\Delta\nu$
		aP_2-bS		aP_2-bP_1
C _{II}	96430.1	34398.6	110561.7	35138.7
N _{III}	130828.7	33152.3	145700.4	34392.6
O _{IV}	163981.		180093.	
		aP_2-bD		bP_3-cS
B _I	47841.2	27025.6		
C _{II}	74866.8	25983.3	98972.5	30496.8
N _{III}	100850.1	25699.3	129469.3	30313.7
O _{IV}	126549.4		159783.	

⁴ Bowen and Millikan, Phys. Rev. 26, 150 (1925).

⁵ Lang and Smith, J.O.S.A. & R.S.I. 12, 523 (1926).

The line due to the change from these b^2S and b^2P levels to the a^2P levels can be traced from C_{II} to O_{IV} while those due to the jump from b^2D to a^2P can be traced from B_I to O_{IV}. In each case, where accuracy of measurement is sufficient to detect it, this last pair shows a separation slightly larger than that of the other two. In all cases the lines due to these jumps follow the irregular doublet law as shown in Table IV.

That lines involving the b^2S and b^2P levels are missing in B_I, or at least are so weak that they cannot be obtained in high enough orders to be resolved, is probably due to the fact that these levels have negative term values, i. e. it requires more energy to produce these levels than it does to ionize the atom by removing the p electron.

In N_{III} and O_{IV} additional lines are observed which are obviously due to the combination between the b^2S , b^2P , and b^2D terms and the c^2P term of the p^3 configuration. That these lines are missing or very weak in C_{II} is probably due to the fact that the c^2P term involves an energy nearly equal to that of ionization of C_{II}.

In addition to the doublet lines already mentioned, we should expect the lines due to the combination between the quartet b^4P and the quartet c^4S term. Such a group of lines following the irregular doublet law (see Table IV) and having the relative separations characteristic of quartets, has been traced from C_{II} to O_{IV}. While no other lines involving the b^4P level can be located to check this identification, yet it seems certain since the variation of intensity of the lines in going from element to element is such as to indicate that they belong to a three-electron system. Further there is no place for such lines in the Hund scheme for either the two or four-electron systems.

The term values in C_{II} given in Table II are based on Fowler's value for the $3m^2P$ term, while those given in Tables I and III for B_I and N_{III} are based on that of the $3n^2D$ term which was assumed equal to 1/4 and 9/4 respectively of that of the corresponding term in C_{II}. This method gives results that are probably accurate to 1000 frequency units in B_I and 3000 or 4000 in N_{III}. Since it has not been possible to make any positive identification of the a^2P-3k^2S and a^2P-3n^2D lines in O_{IV} no term values are given in Table V. Methods similar to those used in identifying these lines in N_{III} seem to indicate that a^2P-3k^2S is the 279.7A line⁶ and a^2P-3n^2D is the 238.6A line. In any case the lines must fall very close to these positions. If we assume the identification of 238.6A is correct and further assume a value for $3n^2D$ 16/4 times as great as in C_{II} we get $a^2P = 623500$ fre-

⁶ Millikan and Bowen, Phys. Rev. 23, 1 (1924).

TABLE V
Series lines of O_{IV}

Int.	λ I. A. Vac.	ν	$\Delta\nu$	Designation
Doublets				
4	553.318	180728.		$aP_1 - bP_2$
5	554.066	180484.	388.	$aP_1 - bP_1$
5	554.507	180340.	391.	$aP_2 - bP_2$
4	555.270	180093.		$aP_2 - bP_1$
4	608.390	164368.	387.	$aP_1 - bS$
4	609.828	163981.		$aP_2 - bS$
1	616.93	162093.		$bD - cP$
6	787.716	126949.3	399.9	$aP_1 - bD$
6	790.205	126549.4		$aP_2 - bD$
1	802.21	124656.		$bS - cP$
2	921.27	108546.	240.	$bP_1 - cP$
3	923.31	108306.		$bP_2 - cP$
Quartets				
3	624.609	160100.	132.	$bP_1 - cS$
4	625.126	159968.	185.	$bP_2 - cS$
4	625.848	159783.		$bP_3 - cS$

quency units which cannot be an error by more than 1 percent regardless of whether the above identifications are correct or not.

III. FOUR-ELECTRON SYSTEMS

The Hund theory predicts that the different configurations of a four-electron system will be characterized by terms as follows:

$$\begin{aligned}
 s^2p^2 & \quad \longrightarrow \quad ^1S, ^1D, ^3P \\
 sp^3 & \quad \longrightarrow \quad ^1P, ^1D, ^3S, ^3P, ^3D, ^5S \\
 s^2p \cdot s & \quad \longrightarrow \quad ^1P, ^3P \\
 s^2p \cdot p & \quad \longrightarrow \quad ^1S, ^1P, ^1D, ^3S, ^3P, ^3D \\
 s^2p \cdot d & \quad \longrightarrow \quad ^1P, ^1D, ^1F, ^3P, ^3D, ^3F
 \end{aligned}$$

Fowler⁷ has already analyzed many of the lines in the spectra of N_{II}. His triplet terms should be correlated with those of the Hund

⁷ A. Fowler, Proc. Roy. Soc. 107, 31 (1925).

theory as follows: p_1, p_2, p_3 , are due to the $s^2p \cdot 3s$ configuration, d_1, d_2, d_3 , and p_1', p_2', p_3' to the $s^2p \cdot 3p$ configuration, d_1', d_2', d_3' , to the $s^2p \cdot 3d$ configuration, and p_1^2, p_2^2, p_3^2 to the $s^2p \cdot 4s$ configuration.

TABLE VI
Séries lines in C_I

Int.	λ I. A. Vac.	ν	$\Delta\nu$	Designation
3	1328.839	75253.7	Triplets	
4	1329.100	75238.9	14.6	$aP_0 - bP$
4	1329.583	75211.6	27.6	$aP_1 - bP$
3	1560.267	64091.6	16.1	$aP_0 - bD$
4	1560.660	64075.5	29.6	$aP_1 - bD$
5	1561.381	64045.9		$aP_2 - bD$
2	1656.27	60376.6		$aP_1 - 3kP_2$
3	1657.01	60349.7		$aP_{0,2} - 3kP_{1,2}$
2	1657.37	60336.6		$aP_1 - 3kP_1$
2	1657.92	60316.5		$aP_1 - 3kP_0$
2	1658.13	60308.9		$aP_2 - 3kP_1$

If this correlation is correct, then p_1, p_2, p_3 and p_1^2, p_2^2, p_3^2 are the first two members of a series of corresponding levels. Due to this fact one can obtain an estimate of the term values, with an error not greater than 1000 or 2000 frequency units, by making these two terms fit a Rydberg formula. Such a calculation indicates that Fowler's term values should be increased by 20300 frequency units. That this value is approximately correct is shown by the fact that it gives to his d' term a value just above 50000 which is similar to that of the terms due to the $s^2p^{n-3} \cdot d$ configuration of other singly ionized atoms of this group of elements.

From the triplet separations of Fowler's terms, lines connecting these terms with the normal 3P levels were identified and the term value of these levels determined as given in Table VII.

In addition to these lines which are produced when a p electron is excited, other very strong lines should be expected when one of the s electrons is displaced to a $2p$ orbit. As before all lines produced by the return of this electron should follow the irregular doublet law. Such groups of lines, all obeying the irregular doublet law, (see Table VIII)

TABLE VII
Series lines of N_{II}

Int.	λ I. A. Vac.	ν	$\Delta\nu$	Designation	Term Values*	
Triplets						
3	533.53	187431.		$aP_{0,1}-3nD_{1,2}(-d'_{2,3})$	aP_0	239373.3
3	533.71	187368.		$aP_2-3nD_{1,2,3}(-d'_{1,2,3})$	aP_1	239324.7
4	644.633	155127.0	48.8	aP_0-bS	aP_2	239241.6
5	644.836	155078.2	82.7	aP_1-bS	bS	84246.3
5	645.180	154995.5		aP_2-bS	bP_0	130150.0
2	671.027	149025.3		$aP_1-3kP_2(-p_1)$	$bP_{1,2}$	130155.3
3	671.397	148943.2		$aP_{0,2}-3kP_{1,2}(-p_{2,1})$	$bD_{1,2}$	147121.4
1	671.650	148887.1		$aP_1-3kP_1(-p_2)$	bD_3	147135.2
2	671.780	148858.3		$aP_1-3kP_0(-p_3)$		
2	672.026	148803.8		$aP_2-3kP_1(-p_2)$		
6	915.603	109217.6	42.9	aP_0-bP_1		
6	915.963	109174.7	6.5	aP_1-bP_0		
6	916.018	109168.2	81.0	$aP_1-bP_{1,2}$		
8	916.698	109087.2		$aP_2-bP_{1,2}$		
6	1083.983	92252.4	49.6	aP_0-bD_1		
7	1084.566	92202.8	82.7	$aP_1-bD_{1,2}$		
3	1085.540	92120.1	13.7	$aP_2-bD_{1,2}$		
8	1085.701	92106.4		aP_2-bD_3		
1	1275.06	78427.7		$bD_3-3mP_2(-p'_1)$		
1	1276.18	78358.9		$bD_{1,2}-3mP_1(-p'_2)$		
0	1276.74	78324.5		$bD_{1,2}-3mP_0(-p'_3)$		

*Assuming $3kP_2(p_1) = 90300$.

have been traced through the four-electron atoms of this row of the periodic system, with characteristics as follows:

a^3P-b^3S . This group appears as three sharp lines with no further structure. It does not appear in C_I for the same reason that a^2P-b^2S does not appear in B_I.

a^3P-b^3P . The separations of these lines are very similar to those of the preceding ones. The center component is double in two instances where it has been possible to obtain particularly good resolutions.

These separations are such as to indicate that $b^3P_1-b^3P_2$ is so small that it cannot be resolved while $b^3P_0-b^3P_1$ can just be separated with the highest resolution.

TABLE VIII
Irregular doublets, four-electron systems

	aP_2-bS		aP_2-bP		aP_2-bD_3	
	ν	$\Delta\nu$	ν	$\Delta\nu$	ν	$\Delta\nu$
C _I			75211.6		64045.9	
N _{II}	154995.5		109087.2	33875.6	92106.4	.28060.5
O _{III}	196781.	41785.5	142075.1	32987.9	119719.2	27612.8
F _{IV}	237699.	40918.	32551.9		27514.8	
			174627.		147234.	

a^3P-b^3D . In this group of lines the long wave-length component is double, the main line having a weak satellite on the short wavelength side. The separation of the extreme components is a little greater than in the preceding groups, thus indicating an inverted D term.

In O_{III} it has been possible to classify a few singlets by means of constant frequency differences occurring between certain lines.

In Table VII none of the lines of N_{II} identified by Fowler have been included. Many of the lines, however, involve levels classified by him. In such cases where his designation differs from the present one, his has been added in parenthesis.

No term values for C_I and O_{III} are given in Tables VI and IX since no sequence of corresponding levels has been found and no certain identification of the a^3P-3n^3D lines can be made. In C_I the a^3P-3n^3D lines should be found at about 1300A. It may be that a partially resolved group at 1277A should be identified as these lines. If this is correct and $3n^3D$ is assumed 1/4 of its value in N_{II} then a^3P has a value of 91300 which, regardless of the correctness of the identification of 1277A, can hardly be an error by more than 5 percent. Similarly the 374.3A and the 305.7A lines⁶ in oxygen are probably a^3P-3k^3P and a^3P-3n^3D respectively, which, if $3n^3D$ is 9/4 of its value in N_{II}, would give a value of $a^3P=443900$, which is probably correct to 2 percent.

TABLE IX
Series lines in O_{III}

Int.	λ I. A. Vac.	ν	$\Delta\nu$	Designation
		Singlets		
0	328.34	304562.	22919.	$aD - 3nP$
0	355.06	281643.		$aS - 3nP$
2	395.52	252832.	22899.	$aD - 3kP$
2	434.91	229933.		$aS - 3kP$
6	525.79	190190.	22916.	$aD - bP$
4	597.82	167274.		$aS - bP$
		Triplets		
4	507.384	197089.	116.	$aP_0 - bS$
5	507.684	196973.	192.	$aP_1 - bS$
6	508.180	196781.		$aP_2 - bS$
6	702.327	142383.8	99.3	$aP_0 - bP_1$
6	702.817	142284.5	16.3	$aP_1 - bP_0$
6	702.898	142268.2	193.1	$aP_1 - bP_{1,2}$
7	703.853	142075.1		$aP_2 - bP_{1,2}$
7	832.926	120058.7	117.4	$aP_0 - bD_1$
8	833.741	119941.3	194.3	$aP_1 - bD_{1,2}$
3	835.094	119747.0	27.8	$aP_2 - bD_{1,2}$
9	835.288	119719.2		$aP_2 - bD_3$

IV. FIVE-ELECTRON SYSTEMS

For atoms of this type the Hund theory predicts that the terms produced by the various electron configurations will be of the following types:

$$s^2p^3 \quad — \quad {}^4S, {}^2D, {}^2P$$

$$sp^4 \quad — \quad {}^4P, {}^2P, {}^2D, {}^2S$$

$$s^2p^2 \cdot s \quad — \quad {}^4P, {}^2P, {}^2D, {}^2S$$

$$s^2p^2 \cdot p \quad — \quad {}^4S, {}^4P, {}^4D, {}^2S, {}^2P, {}^2D, {}^2P, {}^2D, {}^2F, {}^2P$$

$$s^2p^2 \cdot d \quad — \quad {}^4P, {}^4D, {}^4F, {}^2P, {}^2D, {}^2F, {}^2S, {}^2P, {}^2D, {}^2F, {}^2G, {}^2D$$

Hopfield⁸ and Kiess⁹ have classified the lines of N_I while A. Fowler¹⁰ has classified many of the lines of O_{II} in the region between 2000A and 7000A, and R. H. Fowler and Hartree¹¹ have correlated the levels obtained by A. Fowler with those demanded by the Hund theory.

TABLE X
Series lines of F_{IV}

Int.	λ I. A. Vac.	ν	$\Delta\nu$	Designation
0	419.95	238124. Triplets	425.	$aP_{0,1}-bS$
0	420.70	237699.		aP_2-bS
2	570.63	175245.	224.	aP_0-bP
3	571.36	175021.	394.	aP_1-bP
4	572.65	174627.		aP_2-bP
4	676.06	147916.	243.	aP_0-bD
5	677.17	147673.	439.	aP_1-bD
5	679.19	147234.		aP_2-bD

In A. Fowler's list of levels there were no 4P terms that could be correlated with the 4P level due to the $s^2p^2 \cdot d$ configuration. For that reason R. H. Fowler and Hartree identified A. Fowler's x_3 term as this level but marked the correlation as doubtful. While this work was in progress, Professor H. N. Russell pointed out a group of strong lines in the violet that evidently were due to jumps from three levels to all of the quartet terms due to the $s^2p^2 \cdot p$ configuration. Since the term values of these new levels are very close to that of the other quartet terms arising from the $s^2p^2 \cdot d$ configuration it is obvious that they should replace x_3 in R. H. Fowler and Hartree's classification. With Professor Russell's permission his lines and the term values calculated from them are included in Table XI. Still another group of lines which represent combinations between a second triple level and the quartets of the $s^2p^2 \cdot p$ configuration has been found in the region near 2000A. The position and separations of these levels make their assignment as the 4P term of the $s^2p^2 \cdot 5s$ configuration very certain. Since Fowler has already identified the 4P terms due to the

⁸ Hopfield, Phys. Rev. 27, 801 (1926).

⁹ Kiess, J.O.S.A. & R.S.I. 11, 1 (1925).

¹⁰ A. Fowler, Proc. Roy. Soc. 110, 476 (1926).

¹¹ R. H. Fowler and Hartree, Proc. Roy. Soc. 111, 83 (1926).

TABLE XI
Series lines of O_{II}

Int.	λ I. A. Vac.	ν	$\Delta\nu$	Designation	Term Values
Doublets					
0	440.49	227020.		$aD - 3nP(-bp'')$	aP 242554.
1	441.93	226280.		$aD - 3nD(-cd')$	aD_2 256192. aD_3 256208.
0	470.30	212630.		$aP - 3nD(-cd')$	
2	481.53	207671.		$aD - 3n'D(-bd')$	bP_1 70262. bP_2 70430.
2	483.82	206688.		$aD - 3n'P(-ap'')$	bD 117029.
3	485.48	205982.		$aD - 3nF$	
2	515.47	193998.	57.	$aP - 3n'D_2(-bd'_2)$	
2	515.62	193941.		$aP - 3n'D_2(-bd'_2)$	
3	518.23	192965.		$aP - 3n'P(-ap'')$	
3	537.813	185938.	153.	$aD - bP_1$	
4	538.258	185785.		$aD - bP_2$	
3	580.409	172292.	168.	$aP - bP_1$	
4	580.975	172124.		$aP - bP_2$	
2	600.583	166505.		$aP - 3kD(-ad')$	
5	616.309	162256.	198.	$aD - 3kP_2(-2p_2)$	
5	617.064	162058.		$aD - 3kP_1(-2p_1)$	
6	644.159	155241.		$aP - 3kS(-as')$	
5	672.913	148608.	185.	$aP - 3kP_2(-2p_2)$	
5	673.752	148423.		$aP - 3kP_1(-2p_1)$	
7	718.495	139179.8	14.3	$aD_2 - bD$	
7	718.569	139165.5		$aD_2 - bD$	
6	796.665	125523.3		$aP - bD$	
Quartets					
2	430.06	232326.		$aS - 3nP$	Term Values*
3	539.067	185506.	157.	$aS - 3kP_3(-ap_3)$	aS 283366.
2	539.524	185349.		$aS - 3kP_2(-ap_2)$	bP_1 163282.8 bP_2 163364.9 bP_3 163528.3
1	539.837	185241.	108.	$aS - 3kP_1(-ap_1)$	
8	832.756	120083.2		$aS - bP_1$	
9	833.326	120001.1	82.1	$aS - bP_2$	$5kP_1$ 25665.5 $5kP_2$ 25561.3
10	834.462	119837.7		$aS - bP_3$	$5kP_3$ 25395.4

*Assuming $3kP_3(ap_3) = 97860$.

TABLE XI (*continued*)

Int.	λ I. A. Air	ν	$\Delta\nu$	Designation	Term Values	
0	1956.78	51087.7		$3mD_3 - 5kP_3(d_3 -)$	$3nP_1$	50756.79
1	1959.70	51011.6		$3mD_2 - 5kP_2(d_2 -)$	$3nP_2$	50823.28
3	1961.60	50962.2		$3mD_4 - 5kP_3(d_4 -)$	$3nP_3$	50896.37
2	1963.20	50920.6		$3mD_3 - 5kP_2(d_3 -)$		
0	1963.61	50910.0		$3mD_2 - 5kP_1(d_2 -)$		
2	2016.60	49572.4		$3mP_2 - 5kP_3(p'_2 -)$		
2	2020.44	49478.0		$3mP_3 - 5kP_3(p'_3 -)$		
1	2021.45	49453.3		$3mP_1 - 5kP_2(p'_1 -)$		
4	2182.72	45799.9		$3mS - 5kP_3(s_2 -)$		
2	2190.66	45634.0		$3mS - 5kP_2(s_2 -)$		
2	2195.70	45529.3		$3mS - 5kP_1(s_2 -)$		
1	3872.45	25816.15		$3mD_2 - 3nP_1(d_2 -)$		
2	3874.10	25805.16		$3mD_1 - 3nP_2(d_1 -)$		
1	3882.45	25749.66		$3mD_2 - 3nP_2(d_2 -)$		
2	3893.53	25677.05		$3mD_2 - 3nP_3(d_2 -)$		
1	3896.30	25658.13		$3mD_3 - 3nP_2(d_3 -)$		
4	3907.45	25584.92		$3mD_3 - 3nP_3(d_3 -)$		
4	4121.48	24256.31		$3mP_1 - 3nP_1(p'_1 -)$		
2	4129.34	24210.14		$3mP_2 - 3nP_1(p'_2 -)$		
6	4132.82	24189.74		$3mP_1 - 3nP_2(p'_1 -)$		
0	4140.74	24143.49		$3mP_2 - 3nP_2(p'_2 -)$		
7	4153.31	24070.42		$3mP_2 - 3nP_3(p'_2 -)$		
3	4156.54	24051.70		$3mP_3 - 3nP_2(p'_3 -)$		
4	4169.23	23978.50		$3mP_3 - 3nP_3(p'_3 -)$		
4	4890.93	20440.31		$3mS - 3nP_1(s_2 -)$		
5	4906.88	20373.87		$3mS - 3nP_2(s_2 -)$		
6	4924.60	20300.57		$3mS - 3nP_3(s_2 -)$		

$s^2p^2 \cdot 4s$ and $s^2p^2 \cdot 3s$ configurations, this gives a series of three consecutive terms from which it is possible to determine term values with an error of not greater than 30 or 40 frequency units. The progression of k^4P_1 terms was used for this purpose since they are based on the most stable state of the O^{++} ion. This calculation showed that all of Fowler's term values of quartet levels should be decreased by 2140 frequency units.

TABLE XII
Irregular doublets, five-electron systems

	$aS - bP_3$	
	ν	$\Delta\nu$
N_I	88169.4	
	88150.8	
	88106.7	
O_{II}	119837.7	31731.0
		32059.3
F_{III}	151897.	

The normal terms of both quartet and doublet systems were then obtained through the various combinations with the terms identified by Fowler and by Russell.

As before the lines due to changes from an sp^4 to an s^2p^3 configuration follow the irregular doublet law as seen in Table XII.

TABLE XIII
Series lines of F_{III}

Int.	λ I. A. Vac.	ν	$\Delta\nu$	Designation
2	429.49	232834.	357.	$aD - bP_1$
4	430.15	232477.		$aD - bP_2$
2	464.25	215401.	384.	$aP - bP_1$
2	465.08	215017.		$aP - bP_2$
7	567.70	176149.		$aD - bD$
4	630.17	158687.		$aP - bD$
Quartets				
7	656.10	152416.	177.	$aS - bP_1$
8	656.86	152239.	342.	$aS - bP_2$
8	658.34	151897.		$aS - bP_3$

In Table XI none of the lines identified by Fowler have been included, but where lines involve levels classified by him his designation in parenthesis has been placed after the regular designation. All of the wave-lengths of lines above 1900 \AA are taken from unclassified lines in Fowler's table of O_{II}.

TABLE XIV
Series lines of F_{II}

Int.	λ I. A. Vac.	ν	$\Delta\nu$	Designation
4	546.84	182869.	Triplets 344.	aP_2-3kS
3	547.87	182525.	150.	aP_1-3kS
2	548.32	182375.		aP_0-3kS
8	605.67	165106.		aP_2-bP_1
7	606.27	164943.		aP_1-bP_0
9	606.81	164796.		aP_2-bP_2
4	606.95	164758.		aP_1-bP_1
7	607.48	164614.		aP_0-bP_1
8	608.06	164457.		aP_1-bP_2

V. SIX- AND SEVEN-ELECTRON SYSTEMS

Of the six-electron systems of this group the O_I spectra has already been classified by others.¹² In F_{II} only two groups can be classified

TABLE XV
Series lines of F_I

Int.	λ I. A. Vac.	ν	$\Delta\nu$	Designation
4	806.92	123928.	Doublets 410.	aP_2-3nx
3	809.60	123518.		aP_1-3nx
5	951.81	105063.		aP_2-3kP_1
7	954.78	104736.	409.	aP_2-3kP_2
6	955.53	104654.	405.	aP_1-3kP_1
5	958.49	104331.		aP_1-3kP_2

¹² A. Fowler, Series in Line Spectra, p. 166.
Hopfield, Astrophys. J. 59, 114 (1924).

with certainty as shown in Table XIV. It is quite likely that the a^3P-3n^3D line can be identified as a rather weak partially resolved group at 472A. If this is correct and $3n^3D$ is assumed to have a value four times as great as in O_I, then a^3P is equal to 261300 with an error not larger than 5 percent.

In F_I only two groups have been identified in this region, while De Bruin¹³ has identified a third doublet $p\bar{p}'$ group in Carragan's data in the red. Since it involves a separation of 325.6 frequency units, doubtless should be identified as $3k^2P-3m^2P$. No term values can be determined with great accuracy, but if we assume $3nx$ equal to 13000 we obtain a^2P equal to 136900, a value which is probably correct to 1 or 2 percent.

NORMAN BRIDGE LABORATORY OF PHYSICS,
CALIFORNIA INSTITUTE OF TECHNOLOGY.
November 11, 1926.

¹³ De Bruin, K. Akad. Amsterdam Proc. 35, 751 (1926).

THE VELOCITY DISTRIBUTION OF ELECTRONS ISSUING FROM SMALL HOLES

BY ROBERT H. DALTON AND WARREN P. BAXTER

ABSTRACT

The velocity distribution of a beam of 50-volt electrons issuing from a hole 0.022 cm in diameter in a copper plate 0.02 cm thick has been measured. Seventy percent of the electrons were found to retain approximately their initial velocity. By coating the sides and edges of the hole with lampblack initial velocity. By coating the sides and edges of the hole with lampblack 95 % of the electrons were transmitted without appreciable energy loss. Similar results were obtained with grids of 100 mesh copper gauze.

INTRIBUTION.—Preliminary to the construction of a magnetic electron velocity filter, some experiments were undertaken to determine the effect of passage through small holes or fine-mesh gauzes on the velocity distribution of an electron beam. Lehman and Osgood¹ found that with velocities of the primary beam corresponding to from 200 to 1000 volts less than 1% of the electrons passing through a hole 0.19 mm in diameter in a copper plate 0.135 mm thick retain their initial velocity. Since in similar experiments with 50-volt electrons we

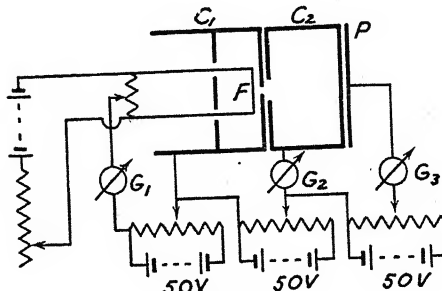


Fig. 1.

were able by using non-reflecting surfaces to get through more than 90% of the electrons with their initial velocity, it seems worth while to publish a brief description of our experiments.

Experimental arrangement. The apparatus is shown diagrammatically in Fig. 1. The source of electrons is a platinum filament *F* coated with calcium oxide operating on a potential-drop of 2 volts. Surrounding this is the cylindrical copper cage *C*₁, pierced by a hole 0.022 cm in diameter at a point opposite the center of the filament. The copper in

¹ Lehman and Osgood, Proc. Cambridge Phil. Soc. 22, 731 (1925).

the neighborhood of the hole is 0.02 cm thick, and the distance to the filament is about 0.1 cm. C_2 is a similar cage 2 cm long with a hole 0.5 cm in diameter in the end facing C_1 . The ends of the cages are discs which screw into place so that they may readily be replaced by grids, in which case the copper plate P is used to measure the current traversing the second of these. It is about 0.1 cm from C_2 . All the cages have an inner diameter of 3 cm. The cages, plate, and filament are mounted rigidly with respect to one another and are suspended with the axis of the cylinders parallel to the earth's magnetic field in a tube closed by a ground-glass stopper (set in sealing wax) and connected with a liquid-air trap, a McLeod gauge, and vacuum pumps. G_1 , G_2 , and G_3 are galvanometers measuring the total current, the current from C_2 , and the plate current, respectively.

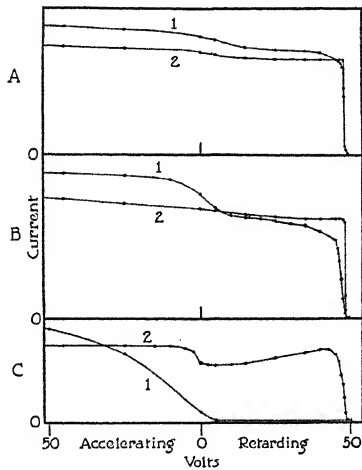


Fig. 2.

The general procedure was as follows. The apparatus was pumped out to a pressure of 10^{-4} to 10^{-5} mm, and the pumps were kept running during all the measurements. An accelerating potential of 50 volts was established between C_1 and the filament, and the temperature of the latter adjusted till a convenient emission resulted. The current through G_2 was then measured with various retarding potentials between C_1 and C_2 . When the end of C_2 was replaced by a grid, the plate-current was read on G_3 with various retarding potentials between C_2 and the plate.

Experimental results. The experimental curves are reproduced in Fig. 2. Curve A(1) was obtained with the hole 0.022 cm in diameter. The metal parts were baked out in vacuum at about 400° before

placing in the apparatus, but no attempt was made to reduce the surface layer of copper oxide. The current to cage C_2 is plotted against the retarding or accelerating potential between C_1 and C_2 . It is apparent from the curve that about 70% of the electrons (based on the current at zero volts) retain nearly their original velocity. To determine whether low velocity reflection and secondary emission were affecting the distribution, the end of C_1 was now coated with lampblack in a candle flame, since Gehrts² has shown that a lampblacked surface is a good absorber for electrons. Curve $A(2)$ shows the result obtained using the same total emission as for curve $A(1)$. About 95% of the electrons have their initial velocity. It is also interesting to note that the actual number of electrons retaining their initial velocity is nearly the same in the two cases, so apparently the only action of the soot is to remove from the beam all those electrons which strike even a glancing blow, thus preventing reflection and secondary emission, and eliminating the low-energy group previously present. Another distribution curve was taken after sooting C_1 and C_2 completely; but the curve was practically the same as $A(2)$, showing that C_2 was an efficient Faraday cage.

These are much better distributions than were obtained by Lehman and Osgood in the experiments above cited. The difference may be due to the higher voltage at which they worked, since it is known that the reflection of electrons from copper increases with the voltage up to 200–300 volts. The nature of the surface as determined by the previous treatment of the copper would also affect the reflection. In some earlier experiments where a crude apparatus was used, in which the metal parts were not baked out, we obtained curves somewhat similar to theirs, but after sooting the copper surfaces the results were as good as with the apparatus described above.

Since, in most of the experiments in electron impact work, the electrons traverse wire gauze grids, an experiment was tried to determine the effect of lampblack under these conditions. The hole in C_1 was replaced by a circular grid of 100 mesh copper gauze 0.5 cm in diameter, while the end of C_2 opposite the plate was replaced by a similar grid 2.5 cm in diameter. Curve $B(1)$ is a distribution curve of the current reaching C_2 in the absence of lampblack. In this case only about 60% of the electrons retained approximately their initial velocity, while the majority of these have suffered a small energy decrease. Curve $B(2)$ shows the distribution after the grids and cages had been

² Gehrts, Ann. d. Physik. 36, 995 (1911).

sooted. It is apparent that about 90% of the electrons have their initial velocity. The absolute magnitudes have no meaning, since the emission was much higher in the second case.

To demonstrate further the effect of carbon, distribution curves of the plate current were taken first without and then with lampblack. These are reproduced in curves *C*(1) and *C*(2), respectively, in which the plate current is plotted against the accelerating or retarding voltage between C_2 and *P*. *C*(1) is similar to curves obtained by Lawrence³ with a very short Faraday cage. *C*(2) shows a much better distribution, but it is poor compared to the curves above, which probably indicates that carbon is not a perfect absorbent. *C*(1) is plotted to a much smaller current scale than *C*(2), since the form of the curve and not the magnitude of the current is important.

The authors wish to express their thanks to Dr. G. Glockler for his help and advice; also to the Carnegie Institution of Washington for financial assistance received from a grant made to Prof. A. A. Noyes.

GATES CHEMICAL LABORATORY, CALIFORNIA INSTITUTE OF TECHNOLOGY,
PASADENA, CALIFORNIA,
October 29, 1926.

³ Lawrence, Proc. Nat. Acad. Sci. 12, 29 (1926).

PHOTOELECTRIC EMISSION AS A FUNCTION OF COMPOSITION IN SODIUM-POTASSIUM ALLOYS

BY HERBERT E. IVES AND G. R. STILWELL

ABSTRACT

The entire series of alloys of sodium and potassium have been investigated with respect to the relative values of the photoelectric currents produced by light polarized with the electric vector in and at right angles to the plane of incidence. The pure metals when molten exhibit values below three for the ratio of the two emissions; the alloys show *three maxima* at compositions approximately 20, 50, and 90 atomic percent of sodium, with values from 10 to 30 for the ratio; the minima between show low values approximating those for the pure metals. The maxima and minima of the ratio of emissions are due to complicated variations in magnitude of the two emissions compared.

ELSTER and Geitel discovered that the photoelectric emission from the liquid equimolecular alloy of sodium and potassium is greatly altered in amount when the plane of polarization of the (obliquely incident) light is varied.¹ They do not appear to have investigated alloys of other proportions than those of the equimolecular one. Pohl and Pringsheim,² who studied the photoelectric properties of this alloy, as well as of the pure alkali metals separately, worked under the belief that the high ratio of the emissions occurring when the light is polarized with the electric vector first in, then perpendicular to the plane of incidence (*selective* and *normal* effects) was a characteristic of the pure metals as well. Subsequent work³ has however shown that pure sodium and potassium, in the liquid form, do not exhibit (at least in the visible spectrum) the high ratio effect found in the equimolecular alloy. It becomes therefore of interest to learn how the photoelectric properties, particularly the ratio of emissions defined above, vary with the relative proportions of sodium and potassium in the alloy.

In order to investigate this question, we made up a series of photoelectric cells of the form shown in Fig. 1. These were simple spherical bulbs made of Pyrex glass and provided with electrodes. An auxiliary side bulb was attached, into which the alloy was introduced first, by distillation, and from which it was poured into the main bulb, — a procedure found advisable for removing any traces of floating impurity.

¹ Elster and Geitel, Ann. d. Physik LIII, p. 433 (1894).

² Pohl and Pringsheim, "Die Lichtelektrischen Erscheinungen" Vieweg (1914).

The alloys were prepared in the distilling system by the following method. Pure sodium and potassium were first distilled in vacuo separately into long pyrex tubes (of about 1 cm diameter). From these tubes, pieces were broken off as nearly as possible of the proper lengths to give the alloy desired. These pieces, after weighing, were introduced into a multiple bulb distilling system attached to the photoelectric cell. The alkali metals were then melted and completely distilled over in vacuo, following the general method and precautions described in earlier papers.³ After the distilling system was sealed off, the pieces of glass tube which had contained the alkali metals were weighed, and the difference in weight before and after gave the amounts

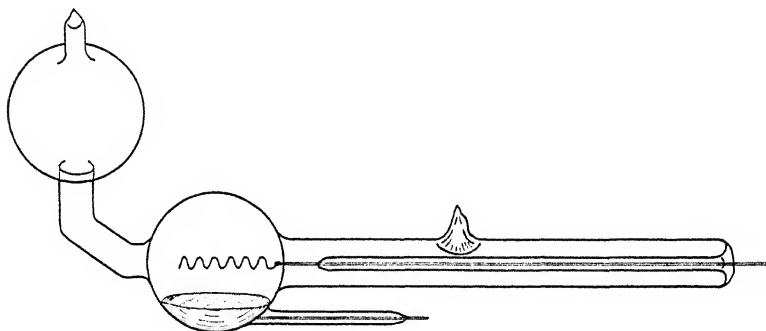


Fig. 1. Type of photoelectric cell used for studying emission characteristics of Na-K alloys.

of alkali metal. Some error is introduced through the crust of oxide which forms at the ends of the columns of alkali metal in the glass tubes. This error can be made relatively small by using tubes of generous length.

Photoelectric currents were excited by the total light of a helical-coil tungsten filament, incident at an angle of 60° after passing through a nicol prism and a lens which focussed an image of the filament on the alloy surface. The cells were operated with 120 volts of applied potential, and the currents were measured on a high-sensibility d'Arsonval galvanometer.

Before giving the results of the measurements it is desirable to discuss some details with regard to the alloys. First of all, it is of extreme importance that the two metals used be pure. The criterion for purity which we have found most useful is really an outcome of this study, and its statement here partially anticipates the conclusion from the

³ Ives and Johnsrud, *Astrophys. J.* LX, 4, p. 231 (Nov. 1924).

work. The criterion is this: *the ratio of emission defined above for illumination by light incident at 60°, shall be not more than 2 or 3 to 1* for the pure metals when liquid just above their melting points. A very small admixture of either metal with the other greatly increases this ratio. Also it appears probable that other materials than the alkali metals, when present as impurity, may raise the ratio. All our samples of sodium and potassium, after the preliminary distillation, and before being used for the preparation of alloys, were tested by this criterion in a trial cell. It was found that some of the

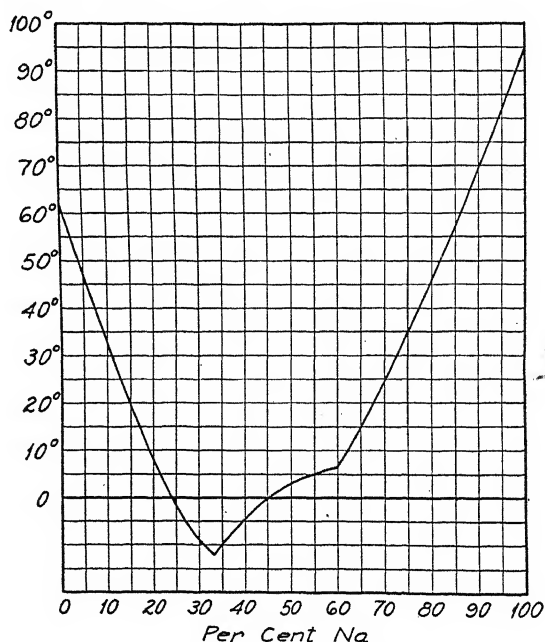


Fig. 2. Melting points of Na-K alloys.

"pure" sodium and potassium obtained from chemical-supply firms fails to meet this test. The greater part of our work has been done with metals from Mallinckrodt, which have uniformly given a low value for the ratio in question.

The physical properties of the Na-K series have already been rather thoroughly studied. The relationship between melting point and composition is given by Kurnakow and Puschin,⁴ whose results are shown in Fig. 2, here reproduced for reference. It will be noted that all alloys in the range from 15 to 70 atomic percent of sodium are liquid at room

⁴ Kurnakow and Puschin, Zeits. Anorg. Chem. 30, p. 109 (1902).

temperatures. Since for our purposes the surface must be specular, the alloys in this range are suitable for study at room temperature. The alloys outside this range were warmed just sufficiently to melt them. Through the middle of the range of alloys liquid at room temperatures the liquid appears perfectly homogeneous, not unlike mercury. The alloys on the borderline between the liquid and solid states at room temperatures frequently exhibit a surface structure apparently consisting of floating crystalline plates or of liquid pools separated by projecting thin crystal walls. These crystalline formations sometimes persist as the alloy is cooled, and can frequently be observed in pure slowly-cooled solid sodium and potassium, thus affording nearly specular surfaces suitable for optical measurement.

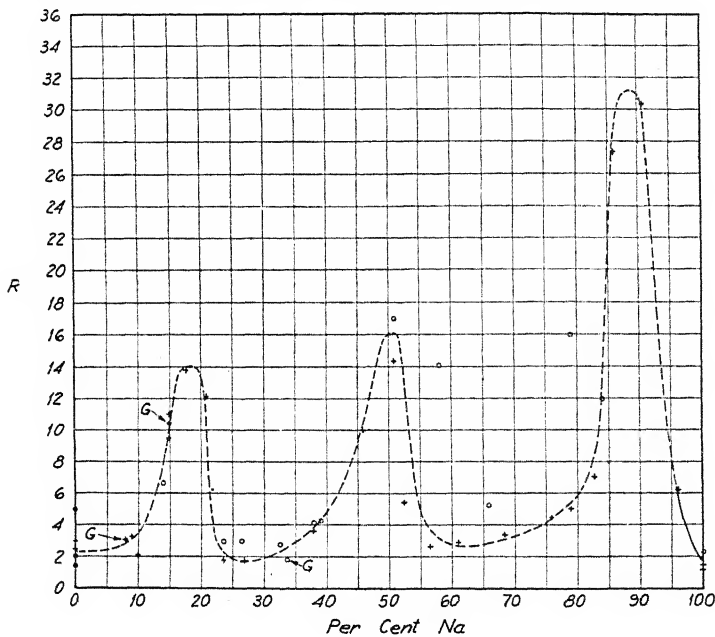


Fig. 3. Ratio of photoelectric emissions for excitation by obliquely incident light polarized in two directions ("selective" and "normal") as a function of atomic percentage of Na in Na-K alloy.

The first series of observations here reported are those made on approximately forty cells of the type of Fig. 1. The results are shown in Fig. 3, where the abscissas represent alloy compositions in atomic percent, the ordinates represent the ratio:

$$R = \frac{\text{emission with electric vector in the plane of incidence}}{\text{emission with electric vector perpendicular to the plane of incidence}}$$

The outstanding fact is the occurrence of *three maxima*, two close to the ends of the diagram, and one at the middle, corresponding to the equimolecular alloy. Every cell made up is represented in the figure, without regard to the fact that in the earlier cells the quantities of the two metals used were too small to enable us to ascertain the relative proportions as accurately as was later done, resulting in a greater scattering of results and consequent blunting of the maxima. The observations designated by crosses form the group made last, when the technique was most completely developed, and should be given the greatest weight. They indicate that the maxima are quite sharp. Several observations, marked *G*, were made on cells in which the vacuum was imperfect, as shown by the characteristic rapid increase

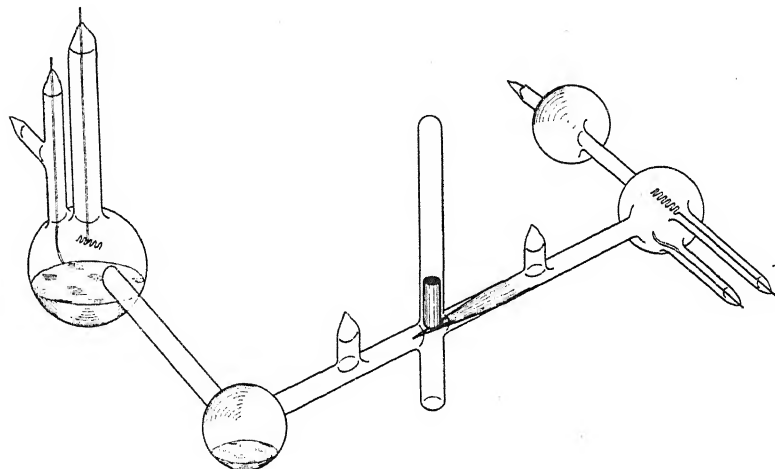


Fig. 4. Special cell used to study complete series of Na-K alloys by successive additions of K (from right-hand bulbs) to Na (in left-hand bulb).

of current with voltage, or by the occurrence of a glow discharge when tested with a spark coil. It will be noted that these cells fall in their proper places on the curve, indicating that the emission ratio R is not affected by the presence of gas.⁵

The data of Fig. 2 show merely the *ratios* of emissions. It is of interest to know how the two emissions in question vary individually.

⁵ Fleischer and Dember in Zeits. f. Tech. Phys. 3, 1926, p. 133, report experiments on potassium in which the emission characteristics of a sealed cell changed with time. The title of their article states that the photoelectric properties are studied with regard to their dependence on gas content. Actually no measurements were made of gas pressure nor was any evidence given that the gas content varied. In the light of our work, it appears to us more probable that the change occurring with time was in the crystalline structure of the surface.

This information cannot be deduced from the measurements on separate cells, each containing different alloys, because of differences in the total emission due to unavoidable variations of conditions occurring in their preparation. In order to determine the emissions in absolute measure, it appeared necessary to construct a cell in which the composition of the alloy could be altered progressively. For this purpose, a double cell was made, as shown in Fig. 4; the two sections were separated from each other by a thin cone-shaped glass diaphragm which could be broken by a falling slug of iron after the two cells had been separately filled with alkali metal and exhausted. Molten metal from one cell could then be allowed to flow by small increments into the other. In order to get an approximate measure of the proportions of the alkali metals present as the mixture proceeded, the bulb selected for the mixing chamber was calibrated beforehand by putting in known volumes of mercury and measuring the dimensions of the mercury pool with a cathetometer. If the meniscus of mercury were the same as that of the Na-K alloys this would afford a reasonably exact measure. Actually the alloys near the sodium end (which were the first produced, potassium being added to an initial small globule of sodium) differ in shape of meniscus quite markedly from mercury, so that the volume measurements were not very satisfactory near the sodium end of the series, and must be taken as merely approximate. (Were the experiment to be repeated, the alloy pool would be photographed in profile and plan, and the volume determined by area measurements of the photographs). The measurements however do show the progressive change in composition sufficiently for the immediate purpose.

The results of this experiment are shown in Figs. 5 and 6. Considering first the behavior of the ratios of emission under the two conditions of polarization (Fig. 5) it appears that the three maxima obtained with the forty individual cells are confirmed. The maxima are not however so sharp, the central maximum is doubled, and is relatively higher and wider, so that the neighboring minima are not so low as in the individual cells. These differences between the behavior of the alloys in separate cells and the progressive mixture are, we believe, to be ascribed to the fact that with the separate cells there was ample time for the alloys to attain equilibrium, while with the series in a single cell the measurements were made immediately after each mixture, and often only a few minutes elapsed before the next step of the series was undertaken.

Considering next the behavior of the two photoelectric currents separately (Fig. 6) we see that the maxima and minima of the ratio are associated with a very complicated course of the two constituent

emissions. Thus taking the "normal" current case " $E \perp$ " this exhibits a minimum at approximately 12 atomic percent Na, and a maximum at 25 atomic percent. The maxima and minima in the ratio at 18 and 30 atomic percent are almost entirely due to these variations in

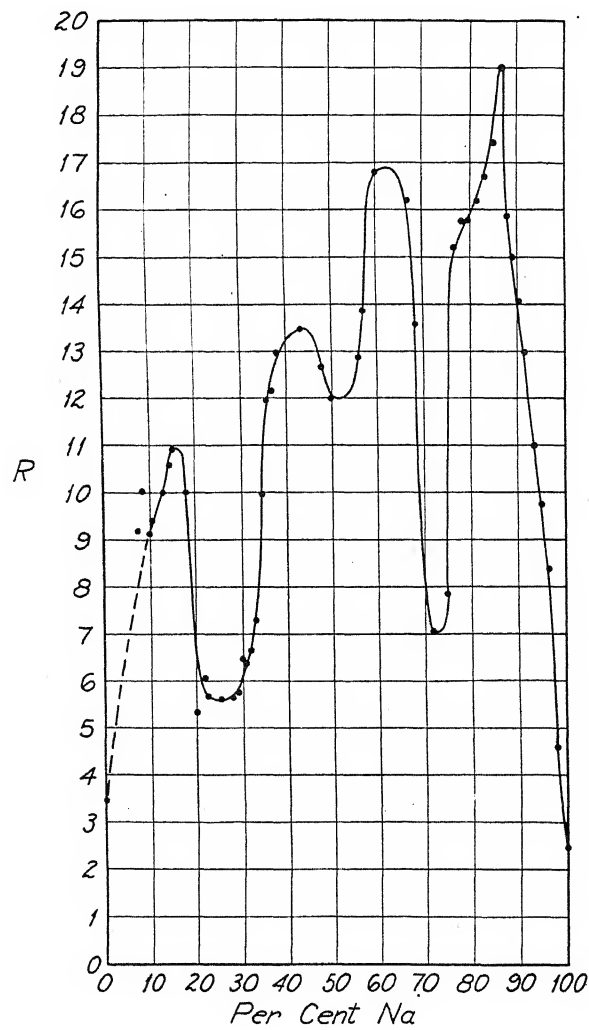


Fig. 5. Ratio of "selective" to "normal" emissions as obtained from series of alloys mixed in cell shown in Fig. 4.

the "normal" current, since the "selective" effect merely shows a practically uniform increase through this region. Toward the other end of the series however, the condition is reversed. While the "normal"

emission ($E \perp$) decreases slowly, the "selective" emission ($E \parallel$) interrupts its gradual rise by a sharp drop and subsequent rise, which accounts for the minimum in the ratio in the neighborhood of 70 atomic percent. It is evident from Fig. 6 that the phenomena are

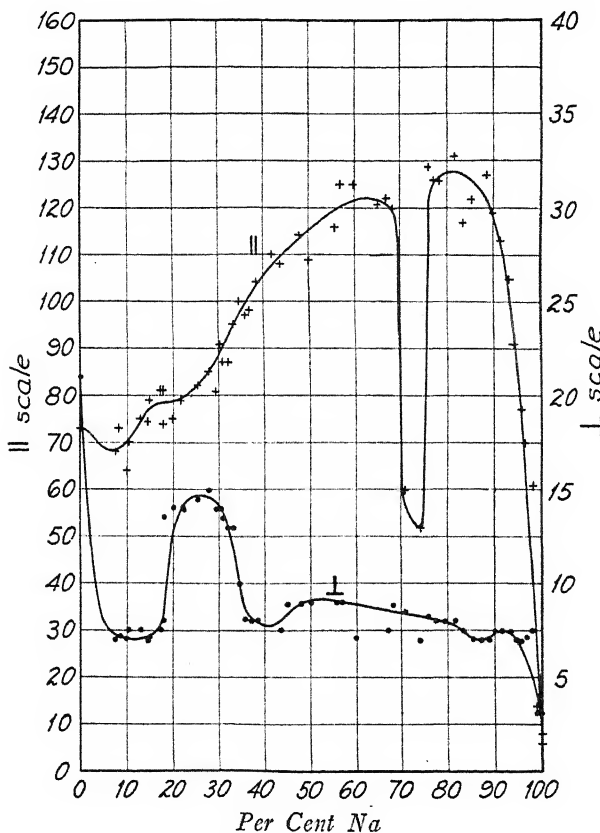


Fig. 6. Variation of "normal" (\perp) and "selective" (\parallel) emissions as function of Na-K composition, as obtained in cell shown in Figure 4.

quite complex; to obtain complete information, it will be necessary to study the emission with spectrally resolved light. This will be undertaken at an early date.

DISCUSSION

In previous papers, it has been suggested that the great difference in photoelectric emission which occurs in certain cases when the plane of polarization of the exciting light is varied, is to be attributed to a regular orientation of the surface atoms or molecules. The results

of the present study may be interpreted in the same way if we consider the sodium and potassium atoms as forming a series of atomic groups, as the relative proportions of the metals vary. Certain of these groups may be pictured as consisting of chains or other structures which will tend to become oriented in definite ways at the liquid surfaces, and to respond differently according to the direction of the electric vector with respect to the surface. The coincidence of the central maximum with the composition KNa, supposed to be a metallic compound, is suggestive. There appears however to be no other correlation with either integral atomic proportions, or with other physical properties as indicated by the melting point data. A possible working hypothesis is that the maxima close to the two ends of the series are to be ascribed to surface layers of unit atomic thickness of potassium or sodium. Further light may be obtained on these questions by studying the distribution of response through the spectrum.

In a previous study of a sodium-potassium alloy,³ support was found for the hypothesis of orientation of the surface atoms or molecules by the fact that the ratio of emissions was greatly reduced in value when the alloy was heated. This observation has been completely confirmed in the present work by numerous observations on alloys all through the series, which however need not be shown, since they are adequately represented by the data shown in the earlier paper. The evidence for the existence of orientations of atoms at the surface has been supplemented in the present work by the actual observation of crystalline planes on the surface of semi-molten alloys, as already mentioned. The selective-normal ratio of emissions from these crystalline surfaces is in all cases higher than from the same material when completely melted. Further evidence of the same sort is obtained from the observation that pure sodium may solidify with flat specular areas, and these, unlike the previously observed specular solid potassium,³ and unlike molten sodium, show relatively high ratios (7 to 8) for the selective-normal ratio. These high values rapidly drop as the temperature of the solid sodium is raised, approaching the molten value (2-3) continuously. The high ratios found in smooth solid sodium increase as the cell stands, suggesting an increasing crystalline character of the surface.

It may be noted that the conclusion drawn in an earlier paper³ that sodium-potassium alloy is the only one of the alkali metal alloys which has a high selective-normal ratio may be subject to revision in the light of the new results on Na-K alloy. It is possible that alloys

of the other alkali metals, in different proportions than those thus far studied will show high values for this ratio.⁶

We desire in conclusion to acknowledge our indebtedness to Mr. A. L. Johnsrud for his aid in the volume measurements used to determine the alloys compositions.

BELL TELEPHONE LABORATORIES, INCORPORATED

NEW YORK, N. Y.

October 11, 1926.

⁶ Another factor contributing to the occurrence of high ratios has been found since the work here described was completed. This is a failure of the proportionality between photoelectric current and illumination for the "normal" emission. This will be treated in a later paper.

THE SYMMETRICAL TOP IN THE UNDULATORY MECHANICS¹

BY R. DE L. KRONIG AND I. I. RABI

ABSTRACT

Schrödinger's method for determining the energy levels of an atomic system is applied to the case of the symmetrical top (moment of inertia about axis of symmetry C , the other one A). The energy values are found to be

$$W_{jn} = \frac{\hbar^2}{8\pi^2} \left[\frac{1}{A} j(j+1) + \left(\frac{1}{C} - \frac{1}{A} \right) n^2 \right]$$

in agreement with the result obtained by Dennison from the matrix mechanics. The quantum numbers j and n must be integers restricted by $0 \leq j, |n| \leq j$, while half-integral values are not permissible. The intensities of transitions are also calculated.

INTRODUCTION

THROUGH the important work of Schrödinger² the problem of finding the energy levels of an atomic system has been reduced to the determination of the characteristic values of a certain second order partial differential equation for a function U of the generalized coordinates, the so-called wave equation. It is the purpose of this paper to apply his procedure to the case of the symmetrical top, a mechanical system useful in the interpretation of molecular spectra. Dennison³ has obtained the energy values and intensities of this system in terms of three quantum numbers, j, n, m on the basis of the matrix mechanics. He has, however, only shown that his solution satisfies certain conditions following directly from the fundamental equations of the matrix mechanics without proving that all these equations are obeyed themselves, although a comparison with the amplitudes of the top in the classical theory made it probable that his results are entirely satisfactory. Moreover the question remained unsettled whether j and n had to be given integral or half integral values. For these reasons a treatment of the same problem by Schrödinger's method does not appear superfluous.

¹ See the preliminary note, Nature 118, 805 (1926). In a paper which came to our attention after this article was sent in for publication F. Reiche, (Zeit. f. Phys. 39, 444, 1926), also investigates the energy values of the symmetrical top by the same method and arrives at results identical with ours. He does not, however, treat the intensities, and therefore it was thought worth while to publish our results.

² E. Schrödinger—Ann. d. Phys. 79, 361, 489, 734, (1926).

³ D. Dennison—Phys. Rev. 28, 318, (1926).

THE WAVE EQUATION AND ITS SEPARATION

Schrödinger's wave equation states that

$$\Delta U + \frac{8\pi^2}{h^2} (W - V) U = 0, \quad (1)$$

where Δ denotes the gradient of the divergence in the non-Euclidean configurational space and $V(q^i)$ the potential energy of the system under consideration. The question to be answered is: For what values of the constant W do solutions U exist which are finite throughout the configurational space (and zero at infinity if the space extends to infinity)? These values W shall represent the energies of the stationary states.

To describe the motion of the symmetrical top we shall use Euler's angles θ, ϕ, ψ ; θ denoting the angle between the z -axis in space and the axis of symmetry z' of the top, ϕ and ψ the angles between the line of nodes (line of intersection between the x' - and x -axes respectively). The kinetic energy in terms of the generalized momenta is given by

$$2T = \frac{1}{A} p_\theta^2 + \left(\frac{\cos^2 \theta}{A \sin^2 \theta} + \frac{1}{C} \right) p_\phi^2 + \frac{1}{A \sin^2 \theta} p_\psi^2 - \frac{2 \cos \theta}{A \sin^2 \theta} p_\phi p_\psi,$$

A and C being the moments of inertia of the top about the x' - and z' -axes respectively. For our system the partial differential equation (1) for U becomes

$$\begin{aligned} \frac{\partial^2 U}{\partial \theta^2} + \frac{\cos \theta}{\sin \theta} \frac{\partial U}{\partial \theta} + \left(\frac{A}{C} + \frac{\cos^2 \theta}{\sin^2 \theta} \right) \frac{\partial^2 U}{\partial \phi^2} + \frac{1}{\sin^2 \theta} \frac{\partial^2 U}{\partial \psi^2} \\ - \frac{2 \cos \theta}{\sin^2 \theta} \frac{\partial^2 U}{\partial \phi \partial \psi} + \frac{8\pi^2 A W}{h^2} U = 0. \end{aligned} \quad (2)$$

This equation will be separated by the substitution

$$U = \Theta(\theta) \begin{cases} \sin(n\phi + m\psi) \\ \cos(n\phi + m\psi) \end{cases} \quad (3)$$

where $\Theta(\theta)$ is a function of θ alone. It is necessary that U returns to the same value if ϕ and ψ are increased by integral multiples of 2π , since then the mechanical system takes up the same position. This can only be accomplished by having the constants n and m equal to

integers. Substituting (3) in Eq. (2) gives an ordinary second order differential equation for Θ

$$\frac{d^2\Theta}{d\theta^2} + \frac{\cos\theta}{\sin\theta} \frac{d\Theta}{d\theta} - \frac{(m-n\cos\theta)^2}{\sin^2\theta} \Theta + \sigma\Theta = 0, \quad (4)$$

$$\sigma = \frac{8\pi^2 AW}{h^2} - \frac{A}{C} n^2. \quad (5)$$

DETERMINATION OF THE CHARACTERISTIC VALUES⁴

Eq. (4) can be transformed into the hypergeometric equation by a suitable change of variables. We shall introduce the following notation:

$$\begin{aligned} \lambda_1 & \left\{ \begin{array}{l} \frac{1}{2}(m+n) \\ -\frac{1}{2}(m+n) \end{array} \right. & \lambda_2 & \left\{ \begin{array}{l} \frac{1}{2}(m-n) \\ -\frac{1}{2}(m-n) \end{array} \right. & \lambda_3 & = \frac{1}{2} + \left(\frac{1}{4} + \sigma + n^2 \right)^{1/2} \\ \mu_1 & & \mu_2 & & \mu_3 & = \frac{1}{2} - \left(\frac{1}{4} + \sigma + n^2 \right)^{1/2} \end{aligned} \quad (6)$$

The brackets in the first two expressions mean that λ_1 and λ_2 shall be so chosen from the two quantities behind the bracket that $\lambda_1 \geq 0$, $\lambda_2 \geq 0$; e.g. if $(m+n) \geq 0$, $(m-n) \leq 0$, then $\lambda_1 = \frac{1}{2}(m+n)$, $\mu_1 = -\frac{1}{2}(m+n)$, $\lambda_2 = -\frac{1}{2}(m-n)$, $\mu_2 = \frac{1}{2}(m-n)$. Furthermore we introduce in Eq. (4) the new independent variable

$$x = \frac{1}{2}(\cos\theta + 1) \quad (7)$$

and the new dependent variable

$$X = x^{-\lambda_1}(x-1)^{-\lambda_2}\Theta. \quad (8)$$

Eq. (4) then takes the form of the hypergeometric equation

$$x(1-x)\frac{d^2X}{dx^2} + [\gamma - (\alpha + \beta + 1)x]\frac{dX}{dx} - \alpha\beta X = 0, \quad (9)$$

where

$$\alpha = \lambda_1 + \lambda_2 + \lambda_3, \quad \beta = \lambda_1 + \lambda_2 + \mu_3, \quad \gamma = 2\lambda_1 - 1. \quad (10)$$

From these and our choice of λ_1 and λ_2 it follows always that

$$\gamma - 1 = 2\lambda_1 \geq 0, \quad \alpha + \beta - \gamma = 2\lambda_2 \geq 0.$$

Moreover $\gamma - 1 = p$, where p is an integer ≥ 0 .

⁴ See L. Schlesinger—Differentialgleichungen, (Sammlung Schubert No. 13, Göschen 1900, Chapter 4.)

To the interval of our old variable θ from 0 to π there corresponds the interval from 0 to 1 of the new variable x . From Eq. (8) it follows that if Θ is to be finite in this interval including the limits, then (since λ_1 and $\lambda_2 \geq 0$) X must be regular inside this interval and at the limits must not become infinite of higher order than $x^{-\lambda_1}$ and $(x-1)^{-\lambda_2}$.

The solution of Eq. (9) is expressible in terms of hypergeometric series. We know that $\gamma - 1 = p$, where p is zero or a positive integer. We distinguish the following cases:

(a). If $p > 0$ and neither α nor β is equal to one of the numbers $1, \dots, p$; or if $p = 0$ and neither α nor β is equal to zero, then two independent particular solutions in the neighborhood of $x = 0$ are given by

$$X_1 = F(\alpha, \beta, \gamma, x),$$

$$X_2 = G(\alpha, \beta, \gamma, x) + F(\alpha, \beta, \gamma, x) \log x,$$

where

$$F(\alpha, \beta, \gamma, x) = 1 + \frac{\alpha \cdot \beta}{1 \cdot \gamma} x + \frac{\alpha(\alpha+1)\beta(\beta+1)}{1 \cdot 2\gamma(\gamma+1)} x^2 + \dots$$

is the hypergeometric series, and G is a series

$$G(\alpha, \beta, \gamma, x) = x^{1-\gamma} \sum c_k x^k, \quad c_0 \neq 0.$$

(b). If $p > 0$ and at least one of the quantities α or β is equal to one of the quantities $1, \dots, p$, then

$$X_1 = F(\alpha, \beta, \gamma, x),$$

$$X_2 = x^{1-\gamma} F(\alpha+1-\gamma, \beta+1-\gamma, 2-\gamma, x).$$

In the second series the zero factors in the numerators and denominators of the coefficients are to be omitted.

(c). If $p = 0$ and at least one of the quantities α and β is zero, then

$$X = \text{Const.}$$

will be a solution.

We see that there are no solutions Θ fulfilling the requirements of finiteness inside the interval unless at least one of the quantities α and β is zero or a negative integer. For if that is the case, the solution X_1 will have only a finite number of terms and hence be finite throughout the interval. However, if neither α nor β is a negative integer or zero, X_1 will become infinite for $x = 1$, since $F(\alpha, \beta, \gamma, x)$ diverges for $x = 1$ if, as in our case, the real part of $\gamma - \alpha - \beta \leq 0$, becoming infinite as $(1-x)^{\gamma-\alpha-\beta} = (1-x)^{-2\lambda_2}$ (or as $\log(1-x)$ if $\gamma - \alpha - \beta = 0$). The

solution X_2 on the other hand becomes infinite as $x^{1-\gamma} = x^{-2\lambda_1}$ (or as $\log x$ if $1-\gamma=0$).

From Eq. (6) and Eq. (10) it follows that if α and β are real, $\alpha \geq \beta$ so that for convergence β must be zero or a negative integer. That will only be the case if

$$\sigma = j(j+1) - n^2, \quad j = (\lambda_1 + \lambda_2), (\lambda_1 + \lambda_2 + 1), \dots, \quad (11)$$

as is easily seen from (6) and (10). Hence j must be a positive integer or zero since $\lambda_1 + \lambda_2$ is always a positive integer or zero. As a direct consequence of the condition expressed in Eq. (11),

$$j \geq \lambda_1 + \lambda_2,$$

we have

$$j \geq |n|, \quad j \geq |m|, \quad (12)$$

since, according to the definition (6) of λ_1 and λ_2 , $(\lambda_1 + \lambda_2)$ is always the larger of the two quantities $|n|$ and $|m|$.

Introducing our value σ into Eq. (5) we get for the energy levels

$$W_{jn} = \frac{\hbar^2}{8\pi^2} \left[\frac{1}{A} j(j+1) + \left(\frac{1}{C} - \frac{1}{A} \right) n^2 \right]$$

in harmony with Dennison's³ results, but with the additional information that j and n must be integers. The requirements (12) shows that for a given j and n there exist $2j+1$ values of m . This $(2j+1)$ -fold occurrence of the value W_{jn} among the characteristic value of the wave equation corresponds to the fact that the state (j, n) will divide into $(2j+1)$ levels under the action of an external field. The quantum number j determines the total moment of momentum, n the moment of momentum about the axis of symmetry.

CALCULATION OF INTENSITIES

As shown by Schrödinger² and Eckart⁵ the matrix elements of the coordinate q^i in the Born-Heisenberg mechanics are given by

$$q^i(k, l) = C_k C_l \int dv q^i U_k U_l, \quad (13)$$

where U_k and U_l are the characteristic functions belonging to the states k and l respectively, while dv is the element of volume of the

⁵ C. Eckart—Phys. Rev. 28, 711, (1926).

configurational space. The integration extends over the whole domain of the variables. C_k is defined by

$$C^2_k \int dv U^2_k = 1. \quad (14)$$

If in our problem we consider a radiating charge attached to the top such that its coordinates in the system of axes x' , y' , z' rigidly connected to the top are a , 0 , c , then its coordinates in space are given by

$$\begin{aligned} x &= c \sin \theta \sin \psi + a \cos \phi \cos \psi - a \cos \theta \sin \phi \sin \psi, \\ y &= -c \sin \theta \cos \psi + a \cos \phi \sin \psi + a \cos \theta \sin \phi \cos \psi, \\ z &= c \cos \theta + a \sin \theta \sin \phi. \end{aligned}$$

We have but to substitute these and our characteristic functions in Eqs. (13) and (14) and to evaluate the definite integrals.

As an example we shall take the coordinate z . For the matrix element corresponding to the transition $j, n, m-j', n', m'$ we find with the aid of Eq. (13)

$$\begin{aligned} z(j, n, m ; j', n', m') &= C_{inm} C_{j'n'm'} \int_0^\pi \int_0^{2\pi} \int_0^{2\pi} A(C)^{1/2} \sin \theta d\theta d\phi d\psi \\ &\cdot (c \cos \theta + a \sin \theta \sin \phi) \Theta(j, n, m, \theta) \Theta(j', n', m', \theta) \\ &\cdot \begin{cases} \sin(n\phi + m\psi) & \sin(n'\phi + m'\psi) \\ \cos(n\phi + m\psi) & \cos(n'\phi + m'\psi) \end{cases} \end{aligned}$$

the volume element dv in the non-Euclidean space being given by

$$dv = (g)^{1/2} d\theta d\phi d\psi = A(C)^{1/2} \sin \theta d\theta d\phi d\psi.$$

It is immediately evident that due to the integration over ϕ and ψ $z(j, n, m ; j', n', m')$ will be different from zero only when $n' = n$, $n' = n \pm 1$ and $m' = m$. These conditions correspond to the well-known selection rules for the radiation emitted by the top. It will be sufficient for the purpose of illustration to restrict ourselves now to the case $n' = n$. We then have

$$\begin{aligned} z(j, n, m ; j', n, m) &= 4\pi^2 c C_{inm} C_{j'n'm} A(C)^{1/2} \\ &\cdot \int_0^\pi d\theta \sin \theta \Theta(j, n, m, \theta) \Theta(j', n, m, \theta). \end{aligned} \quad (15)$$

For $C_{jn,m}$ we integrate over ϕ and ψ in Eq. (14) and obtain

$$4\pi^2 A(C)^{1/2} C_{jn,m}^2 \int_0^\pi d\theta \sin \theta \Theta^2(j, n, m, \theta) = 1 \quad (16)$$

and similarly for $C_{j'n'm'}$.

We now proceed with the evaluation of the integrals. Expressing Θ in terms of the hypergeometric series according to Eqs. (7) and (8) and writing

$$\beta = -\nu, \quad \alpha = \epsilon + \nu, \quad (17)$$

where ν is a positive integer or zero, we get for the first integral

$$\begin{aligned} I_1 &= \int_0^\pi d\theta \sin \theta \cos \theta \Theta(j, n, m, \theta) \Theta(j', n, m, \theta) \\ &= (-1)^{\epsilon-\gamma} \int_0^1 dx (1-2x) F(\epsilon + \nu, -\nu, \gamma, x) F(\epsilon + \nu', -\nu', \gamma', x) x^{\gamma-1} (1-x)^{\epsilon-\gamma}. \end{aligned}$$

Both ϵ and γ are the same in the two functions F , since they are given by

$$\epsilon = 2(\lambda_1 + \lambda_2) + \lambda_3 + \mu_3, \quad \gamma = 2\lambda_1 - 1$$

according to Eqs. (10) and (17), and are hence independent of j according to Eq. (6).

All integrals occurring in this and the remaining calculations can be reduced to the general form

$$\int_0^1 dx F(\epsilon + \nu, -\nu, \gamma, x) F(\epsilon' + \nu', -\nu', \gamma', x) x^{\gamma-1} (1-x)^{\epsilon-\gamma} \quad (18)$$

by means of the relation valid for any hypergeometric series

$$\begin{aligned} xF(\epsilon + \nu, -\nu, \gamma, x) &= \\ \frac{(\gamma-1)(\gamma-2)}{(\epsilon+\nu-1)(\nu+1)} [F(\epsilon + \nu - 1, -\nu - 1, \gamma - 1, x) &- F(\epsilon + \nu - 1, -\nu - 1, \gamma - 2, x)] \end{aligned}$$

Multiplying the differential equation (9) for $F(\epsilon + \nu, -\nu, \gamma, x)$, which in our new notation is

$$x(1-x)F'' + [\gamma - (\epsilon + 1)x]F' = -\nu(\nu + \epsilon)F, \quad (19)$$

by $x^{\gamma-1}(1-x)^{\epsilon-\gamma}$, it is seen that

$$-(\epsilon + \nu)\nu F x^{\gamma-1} (1-x)^{\epsilon-\gamma} = \frac{d}{dx} [F' x^\gamma (1-x)^{\epsilon-\gamma+1}]. \quad (20)$$

Substituting $F(\epsilon + \nu, -\nu, \gamma, x)$ from this relation in (18) and integrating by parts we get

$$\frac{1}{\nu(\epsilon + \nu)} \int_0^1 dx F'(\epsilon + \nu, -\nu, \gamma, x) F'(\epsilon + \nu', -\nu', \gamma', x) x^\gamma (1-x)^{\epsilon-\gamma+1}.$$

This procedure can be continued by differentiating Eq. (19) and getting a relation similar to Eq. (20) with F' and F'' instead of F and F' . Since the F 's are polynomials in x it is thus possible to reduce the integral (18) after a finite number of steps to the form

$$\text{const.} \int_0^1 dx \cdot x^p (1-x)^q = \frac{\text{const.} p! q!}{(p+q+1)!}.$$

In our example I_1 vanishes except when $\nu' = \nu \pm 1$, $\nu' = \nu$ or $j' = j \pm 1$, $j' = j$. This result represents the selection rule for j . If $\nu' = \nu$ i. e. $j' = j$, then

$$I_1 = \frac{2(-1)^{\epsilon-\gamma} \nu! [(\gamma-1)!]^2 (\epsilon+\nu-\gamma)! (\epsilon-1) (\epsilon-2\gamma+1)}{(\gamma+\nu-1)! (\epsilon+\nu-1)! (\epsilon+2\nu) (\epsilon+2\nu-1) (\epsilon+2\nu+1)}.$$

The integral in Eq. (16) is evaluated in the same fashion and gives

$$C_{j^2 nm} = - \frac{(-1)^{\epsilon-\gamma} (\gamma+\nu-1)! (\epsilon+\nu-1)! (\epsilon+2\nu)}{8\pi^2 A(C)^{1/2} \nu! [(\gamma-1)!]^2 (\epsilon+\nu-\gamma)!}.$$

Then from Eq. (18)

$$z(j, n, m; j, n, m) = - c \frac{(\epsilon-1)(\epsilon-2\gamma+1)}{(\epsilon+2\nu-1)(\epsilon+2\nu+1)} = c \frac{n m}{j(j+1)}.$$

This agrees with Dennison's³ expression, our notation j, n, m corresponding to his m, n, σ . In the same way the other intensities are computed. They too are found to agree with Dennison's values except that the quantities called by him $B_{m n-1 \sigma \mp 1}^{mn}$ and $B_{m-1 n-1 \sigma \mp 1}^{mn}$ must be

$$\left(B_{m n-1 \sigma \mp 1}^{mn} \right)^2 = \frac{(m \pm \sigma)(m \mp \sigma + 1)(m+n)(m-n+1)}{16m^2(m+1)^2},$$

$$\left(B_{m-1 n-1 \sigma \mp 1}^{mn} \right)^2 = \frac{(m \pm \sigma)(m \pm \sigma - 1)(m+n)(m+n-1)}{64m^2(m^2 - \frac{1}{4})},$$

a difference probably due to a misprint arising from the inversion of a \pm sign.

DEPARTMENT OF PHYSICS,
COLUMBIA UNIVERSITY,
November 4, 1926.

THE ENERGY OF THE CROSSED-ORBIT MODEL OF THE HYDROGEN MOLECULE

BY ELMER HUTCHISSON

ABSTRACT

Computations are made with the classical quantum theory to determine the energy of a model of the hydrogen molecule similar to the crossed-orbit model of the helium atom with the nucleus divided and separated into two parts. In the preliminary computations the repelling force between the diametrically opposed electrons is neglected, allowing the masses and the charges of the two electrons to be lumped together. This reduces the problem from one of four bodies to one of three bodies and the computations follow those made by Pauli on the H_2 ion except that the mass and charge of the electron are doubled. The effect of the interaction is then obtained in a manner similar to that used by Kramers for the helium atom. In this method terms with undetermined coefficients are introduced into the perturbing potential. The coefficients are then determined so as to reduce the square of the ratio of the perturbing force to the real force to a minimum. Applying this method to the crossed-orbit model of the hydrogen molecule, the energy of the normal state is found to be 45.2 volts. This value is much higher than that given by experiment (31.42 volts), so that it is necessary to conclude that according to the older quantum theory the model does not correspond with reality.

I. INTRODUCTION

THE hydrogen molecule consists of four bodies, two positively charged nuclei and two electrons. The dynamical problem of the determination of the energy of the stationary state of lowest energy cannot be solved completely unless certain assumptions are made. The highly symmetrical circle model proposed by Bohr¹ in 1913, must be discarded since it is unstable and since its energy values do not agree with experiment. Other models may be devised by analogy with the slightly simpler problems of three bodies, the hydrogen molecule ion and the neutral helium atom. The former problem has been investigated with great completeness independently by Pauli² and Niessen.³ All types of orbits have been considered. The orbits lying in a fixed plane containing the axis are not discussed in detail, partly because they are unstable and partly because the electrons come arbitrarily close to the nuclei. The other or spacial orbits fall into three classes, the orbits of the mid-plane, those symmetrical with respect to the mid-plane, and

¹ For details see—Sommerfeld—Atombau, Appendix 14.

² W. Pauli Jr., Ann. der Phys. **68**, 177 (1922).

³ K. F. Niessen, Doctor's Dissertation, Utrecht (1922); Ann. der Phys. **70**, 129 (1923).

those which are unsymmetrical. Those orbits which lie in the mid-plane (including the Bohr circular orbit) are unstable with respect to a small displacement perpendicular to the plane.⁴ The orbits of the symmetrical class are proved dynamically stable while the question is left unanswered for those inherently improbable orbits, the unsymmetrical class.

The orbit of smallest energy of the symmetrical class, which should represent the normal ionized hydrogen molecule, consists of a multiply periodic orbit on the surface of an ellipsoid of revolution. We can obtain an approximate idea of the path of the electron by imagining a sine wave wrapped around an ellipsoid of revolution which has the two nuclei as foci. The energy and constants of this orbit have been computed both by Pauli and by Niessen.

Considering the other three body problem, that of the neutral helium atom we find a larger variety of models has been proposed.⁵ In the crossed-orbit model of helium it is assumed that the orbits of the two electrons are of the same size and shape but inclined at approximately 120° to each other. The energy and dimensions of this model have been determined independently by J. H. Van Vleck⁶ and H. A. Kramers.⁷

Since in general we may obtain a model for the hydrogen molecule by splitting the helium nucleous into two parts and separating them, we would expect, as was suggested by M. Born⁸ in 1922, a hydrogen molecule model corresponding to the crossed-orbit model of helium. The orbits, neglecting the interaction of the electrons, would resemble those of the hydrogen molecule ion deduced by Pauli and Niessen and the perturbations due to the interaction of the electrons may be obtained in a manner similar to that used by Kramers for the helium atom. It is the purpose of this paper to make calculations for this crossed-orbit model of the hydrogen molecule.

II. INVESTIGATION OF THE MECHANICAL SYSTEM

In the crossed-orbit model the nuclei determine the axis giving the well known dumb-bell form usually associated with diatomic molecules. The electrons travel about this axis in orbits which intersect at about

⁴ In spite of this fact, H. C. Urey (Phys. Rev. 27, 216 (1926)) has recently made some computations with these orbits and obtains agreement with one interpretation of the work of Olson and Glockler but the results are not very convincing.

⁵ For complete discussion see J. H. Van Vleck, Quantum Principles and Line Spectra, Bull. N. R. C. No. 54, p. 86 (1926).

⁶ J. H. Van Vleck, Phil. Mag. 44, 842 (1922).

⁷ H. A. Kramers, Zeits. f. Physik. 13, 312 (1923).

⁸ M. Born, Die Naturwissenschaften 10, 677 (1922).

120°. For preliminary computations we may reduce our problem to one of three bodies by neglecting the repelling force of the two electrons. In this way the relative position of the electrons is immaterial and the two electrons may be lumped together into a body with two units of charge and mass. The mathematics needed in this case follows closely that used by Pauli in the H_2 ion with the exception that the mass and charge of the electron are doubled. In this section, we shall use both Z and Z' as the charge on the nuclei. In the preliminary work, $Z = Z' = 1$, so that the distinction is of no consequence.

The possibility of treating this system of two nuclei and one electron as conditionally periodic, depends essentially upon the fact that the nuclei may be considered stationary. This approximation is sufficient for our purpose since the mass of the electron is small compared to that of the nuclei and the contribution to the total energy due to motion of the nuclei is also small.

In the problem of two attracting centers, the variables of the Hamilton-Jacobi partial differential equation may be separated by means of elliptical coordinates. Let r_1 and r_2 represent the distances of the electron from the nuclei, $2c$ be the distance between the nuclei, ρ be the distance of the electron from the axis and ϕ be the azimuth about the axis. The elliptical coordinates are defined by

$$\lambda = (r_1 + r_2)/2c \quad \mu = (r_1 - r_2)/2c \quad (1)$$

The curves, $\lambda = \text{constant}$, form a family of confocal ellipses while those, for which $\mu = \text{constant}$, form confocal hyperbolas with the nuclei as foci. From the definition it follows that $\lambda \geq 1$ and $-1 \leq \mu \leq +1$. The distance from the axis is given by

$$\rho = c[(\lambda^2 - 1)(1 - \mu^2)]^{1/2} \quad \text{and} \quad z = c\lambda\mu \quad (2)$$

where z is the distance of the electron above the mid-plane. We may now write for the potential energy

$$E_{\text{Pot}} = -\frac{2Z'e^2}{r_1} - \frac{2Z'e^2}{r_2} + \frac{Z^2e^2}{2c} = -\frac{4Z'e^2}{c} \frac{\lambda}{(\lambda^2 - \mu^2)} + \frac{Z^2e^2}{2c} \quad (3)$$

and for the kinetic energy

$$E_{\text{Kin}} = m(z^2 + \dot{p}^2 + \rho^2\dot{\phi}^2). \quad (4)$$

We then obtain for the Hamiltonian function

$$H = \frac{1}{4c^2m(\lambda^2 - \mu^2)} \left[(\lambda^2 - 1)\dot{p}_\lambda^2 + (1 - \mu^2)\dot{p}_\mu^2 + \left(\frac{1}{\lambda^2 - 1} + \frac{1}{1 - \mu^2} \right) \dot{p}_\phi^2 \right] - \frac{4Z'e^2}{c} \frac{\lambda}{\lambda^2 - \mu^2} + \frac{Z^2e^2}{2c} = W \quad (5)$$

and we may let $W - (Z^2e^2/2c) = -\alpha_1/4c^2m$ thus defining α_1 . Since ϕ does not occur in the Hamiltonian function p_ϕ is a constant and we set $p_\phi = \alpha_3$ (ϕ = cyclic coordinate). We may now separate the variables in equation (5), giving

$$p_\lambda = [F(\lambda)\alpha_1]^{1/2}/(\lambda^2 - 1) \quad (6)$$

where

$$\begin{aligned} F(\lambda) = (-\lambda^2 + B\lambda + C)(\lambda^2 - 1) - A &= -\lambda^4 + B\lambda^3 \\ &\quad + (1 + C)\lambda^2 - B\lambda - (A + C). \end{aligned}$$

and

$$A = \alpha_2^2/\alpha_1 \quad B = 16e^2cmZ'/\alpha_1 \quad C = \alpha_2/\alpha_1. \quad (7)$$

Likewise

$$p_\mu = [G(\mu^2)\alpha_1]^{1/2}/(1 - \mu^2) \quad (8)$$

where

$$G(\mu^2) = (\mu^2 - C)(1 - \mu^2) - A = -\mu^4 + (1 + C)\mu^2 - (A + C).$$

Now

$$W = -\frac{\alpha_1}{4c^2m} + \frac{Z^2e^2}{2c} = -\frac{4c^2}{c} \frac{Z'}{B} + \frac{Z^2e^2}{2c} = -\frac{c^2}{2c} \left[\frac{8Z' - BZ^2}{B} \right]. \quad (9)$$

To quantize this motion we apply the Wilson-Sommerfeld rule that $\oint p_k dq_k = n_k h = J_k$. In our problem we have

$$J_1 = \oint p_\lambda d\lambda \quad J_2 = \oint p_\mu d\mu \quad J_3 = \int_0^{2\pi} p_\phi d\phi$$

and then

$$J_1 = n_1 h \quad J_2 = n_2 h \quad J_3 = n_3 h.$$

Another necessary condition is that for the equilibrium of the nuclei. We may state this condition thus—the forces acting on the nuclei must vanish when averaged over a period. In Pauli's paper it is proved that this condition is satisfied when the virial law for Coulomb forces is fulfilled. This relation states that $2E_{\text{kin}} = -E_{\text{pot}}$ on the time average or in other words

$$\overline{E_{\text{pot}}} = 2W \quad \text{since} \quad W = E_{\text{pot}} + E_{\text{kin}}. \quad (10)$$

In this paper we are interested primarily in the orbit of smallest energy. It is proved in Pauli's paper that the orbit of smallest energy is the orbit with the smallest quantum numbers. The smallest value of

the azimuthal quantum number n_3 is unity, since $n_3 = 0$ would give an orbit of the plane containing the axis, which has already been excluded. Likewise, n_2 the quantum number associated with the μ coordinate cannot equal zero for in this case we would have $\mu = \text{constant}$ which is impossible for the symmetrical class of orbits. The orbit of smallest energy has therefore the quantum numbers 0, 1, 1. In reality we are assuming that the quantum numbers are 0, $\frac{1}{2}$, $\frac{1}{2}$ for each electron since we have two electrons. The orbit of the electron is therefore a multiply periodic orbit on the surface of an ellipsoid of revolution generated when the ellipse $\lambda = \text{constant}$ is rotated about the axis. The setting of λ equal to a constant simplifies the Hamilton-Jacobi equation since $p_\lambda = 0$.

We must now obtain an expression for the time mean value of any quantity averaged over the orbit of the electron. Suppose we consider a quantity Q , the time mean value of this quantity is given by

$$\bar{Q} = \mathcal{J}Qdt/\mathcal{J}dt \quad (11)$$

where the integration is carried over a complete period.

Using the Hamilton canonical equations and from Eqs. (5) and (8), we obtain for the time mean value of any quantity

$$Q = \mathcal{J}Q(\lambda^2 - \mu^2)[G(\mu^2)]^{-1/2}d\mu/\mathcal{J}(\lambda^2 - \mu^2)[G(\mu^2)]^{-1/2}d\mu. \quad (12)$$

We can apply this equation to the nuclear equilibrium condition (10). From (3) it is clear that in our present case the potential energy is given by

$$E_{\text{pot}} = -\frac{4e^2}{c} \frac{\lambda}{\lambda^2 - \mu^2} + \frac{e^2}{2c}.$$

Making use of this equation and (9), Eq. (10) becomes

$$\frac{\lambda}{\lambda^2 - \mu^2} = \frac{1}{8} \left[\frac{16 - 2B}{B} + 1 \right] = \frac{16 - B}{8B}. \quad (13)$$

Applying the mean value equation (12) and remembering that λ is constant, we obtain as our equilibrium condition

$$\mathcal{J}[G(\mu^2)]^{-1/2}d\mu = [(16 - B)/8B\lambda]\mathcal{J}(\lambda^2 - \mu^2)[G(\mu^2)]^{-1/2}d\mu. \quad (14)$$

We now come to the consideration of the possible orbits. The type of multiply periodic orbit is determined by the roots of $[F(\lambda)]^{\frac{1}{2}}$ and $[G(\mu^2)]^{\frac{1}{2}}$. The values of these roots are discussed very completely by Pauli. From Eqs. (6) and (8) it is evident that at the libration limits

(where $\dot{p}_k = 0$) the values of these radicals must reduce to zero or in other words the libration limits are given by the real roots of these quantities. Since in our problem λ is constant we need only consider the roots of the biquadratic $[G(\mu^2)]^{\frac{1}{2}}$. For symmetrical orbits it is necessary for the electron to swing between plus and minus values of one root which we call $+(x_1)^{\frac{1}{2}}$ and $-(x_1)^{\frac{1}{2}}$. The other root, x_2 may be shown to be negative giving imaginary positions of the electrons. We may therefore write $[G(\mu^2)]^{\frac{1}{2}} = [(x_1 - \mu^2)(|x_2| + \mu^2)]^{\frac{1}{2}}$. It is possible by using special values of λ and μ to determine a relation between x_1 and x_2 and λ . This is determined in Pauli's paper and the same relation holds in our problem, that is

$$1 - x_1 = \frac{(\lambda^2 - 1)^2(\lambda^2 - |x_2|)}{(1 - |x_2|)\lambda^2(1 + \lambda^2) - (\lambda^2 - 1)^2|x_2|} \quad (15)$$

and the relations involving B and A are given by

$$A = (1 - x_1)(1 + |x_2|) \quad B = 2(\lambda^4 + x_1|x_2|)/\lambda(1 + \lambda^2). \quad (16)$$

From the equilibrium condition of the nucleus (14) we have the equation

$$\mathcal{J}[(x_1 - \mu^2)(|x_2| + \mu^2)]^{-1/2}d\mu = \\ [(16 - B)/8B\lambda]\mathcal{J}(\lambda^2 - \mu^2)[(x_1 - \mu^2)(|x_2| + \mu^2)]^{-1/2}d\mu. \quad (17)$$

The integrals occurring in this equation are elliptic and must be reduced to standard forms before computations may be made. This may be done by the substitution

$$\mu = -(x_1)^{1/2} \cos \phi \quad \text{and} \quad k^2 = x_1/(x_1 + |x_2|). \quad (18)$$

Using $K(k)$ and $E(k)$ to represent elliptic integrals of the first and second kind respectively, the equilibrium condition then reduces to (See Pauli's paper for details)

$$[(\lambda^2 + |x_2|) - 8B\lambda/(16 - B)]K(k) = (x_1 + |x_2|)E(k). \quad (19)$$

A second condition is given by $J_2/J_3 = 1$ and using (8) we obtain

$$2\pi J_2/J_3 = A^{-1/2}\mathcal{J}[(x_1 - \mu^2)(|x_2| + \mu^2)]^{1/2}(1 - \mu^2)^{-1}d\mu. \quad (20)$$

This may also be reduced to standard forms by the same substitution, giving finally,

$$\frac{\pi}{2} \left(\frac{J_2}{J_3} + 1 \right) = \frac{(x_1 + |x_2|)E(k) - (1 - x_1)|x_2|K(k)}{[(1 - x_1)(1 + |x_2|)(x_1 + |x_2|)]^{1/2}} \\ + F(\beta, k')E(k) - [F(\beta, k') - E(\beta, k')]K(k) \quad (21)$$

where $k'^2 = 1 - k^2$ and $\beta = 1 - x_1$.

In our problem we must determine the three constants, λ , x_1 , and $|x_2|$. We may do this now since we have three equations, (19), (21) and (15), involving only these constants. Since two of these equations are complicated transcendental equations the best method of attack is trial and error. In this case a value of λ was assumed and values of x_1 and $|x_2|$ corresponding to this value were found such that Eqs. (15) and (19) were satisfied. These values were substituted in (21) and a curve plotted for the variation of J_1/J_2 with λ . By interpolation and rechecking, satisfactory values were obtained. They are:

$$\lambda = 1.3753 \quad x_1 = .83389 \quad |x_2| = .37839.$$

From these values the nuclear separation and energy may be computed. We have

$$B = 2(\lambda^4 + x_1|x_2|)/\lambda(1+\lambda^2) = 1.9580$$

and

$$A = (1 - x_1)(1 + |x_2|) = .22896$$

and therefore from (7) we obtain

$$c/a_1 = n_3^2 \cdot (B/16A) = .53448.$$

From (9) we obtain

$$W = - (e^2/2c)[(8/B) - 1] = - 5.7735 Rh \quad (22)$$

where R is the Rydberg constant.

We have now computed the energy and constants of the dynamical problem of an electron of two units of charge and of mass moving under the attraction of two fixed nuclei with unit charges. The next part of the problem is to determine the effect of the interaction of the two electrons, which has been neglected in this section.

III. THE ENERGY TO A FIRST APPROXIMATION

In the preceding section we have neglected the repulsion due to the interaction of the two electrons. When the interaction was neglected the position of the electrons relative to each other was immaterial. Now, however, the relative position is very important and we must assign a position to them. It is assumed that the electrons are always diametrically opposed, that is, they are always 180° apart. From the symmetry of the model this is the only reasonable assumption that can be made.

To compute the interacting effect of the electrons, we turn to perturbation theory. An approximate value of the disturbance due to the electrons can be obtained by applying to the orbit obtained in the last

section, the theorem that the energy of the perturbed orbit is to a first approximation equal to the energy of the unperturbed orbit plus the perturbative potential averaged over the unperturbed orbit.⁹ Since the perturbing force amounts to about $\frac{1}{2}$ to $\frac{1}{6}$ of the real force we would not expect this approximation to hold very closely. Our theorem says

$$W = W_0 + \bar{V}_p. \quad (23)$$

In our case the perturbing potential is given by

$$V_p = e^2/2\rho = e^2/2c[(\lambda^2 - 1)(1 - \mu^2)]^{1/2}. \quad (24)$$

To average this over the unperturbed orbit we must use the mean value equation, (12). The denominator then occurring may be integrated by using the same substitution as for Eq. (17). The numerator after substitution consists of an integral involving a sixth power under a radical. The presence of the $(\lambda^2 - \mu^2)$ term combined with the radical makes it impossible to reduce the integral to standard elliptic forms by substitutions. The easiest way to integrate this expression is graphically.¹⁰ First, it is necessary to obtain values of the time, t , corresponding to successive values of μ , by integrating the equation for dt used in (12). We obtain after integrating

$$t = \frac{\lambda^2 + |x_2|}{(x_1 + |x_2|)^{1/2}} \int_{\cos^{-1} \alpha x^{-1/2}}^{\pi/2} (1 - k^2 \sin^2 \phi)^{-1/2} d\phi - \\ (x_1 + |x_2|)^{1/2} \int_{\cos^{-1} \alpha x^{-1/2}}^{\pi/2} (1 - k^2 \sin^2 \phi)^{1/2} d\phi$$

or

$$t = \frac{\lambda^2 + |x_2|}{(x_1 + |x_2|)^{1/2}} [\bar{K}(k) - F(k, \phi)] - (x_1 + |x_2|)^{1/2} [E(k) - E(k, \phi)]. \quad (25)$$

We may now plot values of $Q = (1 - \mu^2)^{-\frac{1}{2}}$ directly against time. This was done on a large scale and the area measured with a planimeter giving an accuracy of more than one part in one thousand. The graphical integration gives

$$\int_0^{x_1} (1 - \mu^2)^{-1/2} dt = 3.7857. \quad (26)$$

⁹ For complete discussion see J. H. Van Vleck, Quantum Principles and Line Spectra, Bulletin N. R. C. No. 48, p. 189 (1926).

¹⁰ It is not advisable to plot the integrand against μ because at the end points the integrand goes to infinity.

The perturbing potential may now be computed

$$\overline{V}_p = \frac{e^2}{2} \frac{\bar{l}}{\rho} = \frac{e^2}{2a_1} \frac{a_1}{c} \frac{3.7857}{(.94417)(2.86737)} = 2.1662Rh. \quad (27)$$

Making use of Eqs. (22), (23) and (27) the energy of the hydrogen molecule may be computed to a first approximation, thus

$$W = (-5.7735 + 2.6162)Rh = -3.1573Rh. \quad (28)$$

IV. APPLICATION OF KRAMERS' METHOD TO THE HYDROGEN MOLECULE

The approximation used in the preceding section is not sufficient for our purpose because the perturbing force is such a large fraction of the actual force. In the crossed-orbit helium problem the same difficulty is present with this first approximation since in that case the perturbing force at its maximum value amounts to 50% of the actual force. In order to decrease the ratio of these forces Kramers tries other methods. One method is to use $(Z-\alpha)$ as the nuclear charge in the unperturbed orbit and then balance this by considering $-\alpha e^2/r + e^2/4\rho$ as the perturbing potential. In this case r is the distance of the electron from the nucleus and α is suitably chosen to reduce the ratio of the forces as much as possible. These values must be multiplied by two for both electrons giving $e^2/2\rho$ as the interaction term of the electrons. Kramers finds however that, for helium, the ratio of the forces, under these potentials, is not materially reduced. He does find, though, that if he considers the electron to be under the influence of a potential of the form $-(Z-\alpha)e^2/r + C/\rho^2$ with a perturbing potential of the form $-\alpha e^2/r - C/\rho^2 + e^2/4\rho$, the ratio of the perturbing to the real force is greatly reduced. This method is especially advantageous in Kramers' problem because the motion under this new unperturbed potential is almost as simple as without the second term. The influence of this term is merely to decrease the angular velocity of the electron about the nucleus in a given ratio. The only change necessary in the equations of motion is that we replace p_ϕ by p_ϕ' keeping, however, as the quantum condition $p_\phi = h/2\pi$ for the two electrons.

Kramers' method of reducing the ratio of the perturbing to the real force can also be used advantageously for the computations on the crossed-orbit model of the hydrogen molecule. This may be easily seen from a consideration of the Hamiltonian function. In place of the original Hamiltonian function given by (5) we shall have (remem-

bering $p_\lambda = 0$) as the Hamiltonian function of the new unperturbed orbit

$$H_0 = \frac{1}{4c^2m(\lambda^2 - \mu^2)} \left[(1 - \mu^2)p_u^2 + \left(\frac{1}{(\lambda^2 - 1)} + \frac{1}{1 - \mu^2} \right) p_{\phi'}^2 \right] \quad (29)$$

$$- \frac{4Z'e^2}{c} \frac{\lambda}{(\lambda^2 - \mu^2)} + \frac{Z^2e^2}{2c} = W_0$$

where $Z' = (Z - \alpha)$ and $p_{\phi'}^2 = p_\phi^2 + 4m\beta e^2$. For the perturbing potential we shall have

$$\Delta E = - \frac{4\alpha e^2}{c} \frac{\lambda}{(\lambda^2 - \mu^2)} - \frac{\beta e^2}{c^2(\lambda^2 - 1)(1 - \mu^2)} + \frac{e^2}{2c[(\lambda^2 - 1)(1 - \mu^2)]^{1/2}} \quad (30)$$

This perturbing potential just balances the changes in the unperturbed orbit and includes the interaction term. Perhaps the nature of the perturbing potential will look more familiar in other coordinates. It becomes

$$\Delta E = - \frac{2\alpha e^2}{r_1} - \frac{2\alpha e^2}{r_2} - \frac{\beta c^2}{\rho^2} + \frac{e^2}{2\rho} \quad (31)$$

where r_1 , r_2 and ρ have the meaning given in Eq. (1). To apply this to a given problem α and β must be chosen so as to reduce the square of the ratio of the perturbing to the real force as much as possible.

The changes which occur in the original perturbed orbit due to the presence of the α and β terms in the new unperturbed motions may easily be given a physical interpretation. The introduction of $(Z - \alpha)$ changes the nuclear attraction. The replacement of the angular momentum p_ϕ by the new value $p_{\phi'}$ has the effect of decreasing the velocity of rotation by a given amount so that the repelling force of the electron is just balanced by the decrease in the centrifugal force. This method is not quite as simple to use in the case of the hydrogen molecule as it was in Kramers' case of the helium atom. In Kramers' case it was easy to derive an expression for the quantized energy of the new unperturbed motion in terms of the old motion. In this case it is necessary to obtain the energy of the unperturbed motion in the same tedious manner as was used in the original motion.

In order to apply the theorem relating to the average value of the perturbative potential accurately it is necessary that the time average of the square of the ratio of the perturbing to the real force be made as

small as possible. We use the relation $F = -\text{grad } (\Delta E)$ and obtain the result

$$M^2 = (\text{grad } \Delta E)^2 / (\text{Real Force})^2 = Z^{-2} \{ \alpha^2 - \mathcal{A}\alpha + \mathcal{B}\gamma^2 - \mathcal{C}\gamma + \mathcal{D}\alpha\gamma + \mathcal{E} \} \quad (32)$$

where $\gamma = \beta/c$ and

$$\begin{aligned} \mathcal{A} &= \frac{\lambda(\lambda^2 - \mu^2)(\lambda^2 + 3\mu^2)(1 - \mu^2)^{1/2}}{4(\lambda^2 - 1)^{1/2}(1 + 3\lambda^2)(1 - \mu^2)(b + \mu^2)} \\ \mathcal{B} &= \frac{(\lambda^2 - \mu^2)^4}{4(\lambda^2 - 1)^3(1 + 3\lambda^2)(1 - \mu^2)^3(b + \mu^2)} \\ \mathcal{C} &= \frac{(\lambda^2 - \mu^2)^4(1 - \mu^2)^{1/2}}{8(\lambda^2 - 1)^{5/2}(1 + 3\lambda^2)(1 - \mu^2)^3(b + \mu^2)} \\ \mathcal{D} &= \frac{\lambda(\lambda^2 - \mu^2)(\lambda^2 + 3\mu^2)}{(\lambda^2 - 1)(1 + 3\lambda^2)(1 - \mu^2)(b + \mu^2)} \\ \mathcal{E} &= \frac{(\lambda^2 - \mu^2)^4}{64(\lambda^2 - 1)^2(1 + 3\lambda^2)(1 - \mu^2)^2(b + \mu^2)}. \end{aligned}$$

In the above relations b has been written for $\lambda^2(\lambda^2 - 1)/(1 + 3\lambda^2)$.

It is now necessary to average each of the coefficients over the unperturbed orbit. To do this we substitute back in the mean value Eq. (12). The integrals arising from this substitution are very complicated and only some of them may be reduced to standard elliptic forms. The coefficients of α and γ after substitution in (12) consist of a sixth power under a radical similar to the numerator in (24) and one must resort to graphical integration. The integrals were all evaluated graphically and, where possible, the actual integration was also carried out. In the latter cases, the integrations all agreed closer than one part in one thousand. The graphical integration was carried out in the same manner as described for Eq. (24). After integration, Eq. (32) becomes:

$$\begin{aligned} M^2 = Z^{-2} \{ \alpha^2 - .60205\alpha + 3.2218\gamma^2 - 1.0673\gamma + 3.2714\alpha\gamma \\ + .09844 \} \end{aligned} \quad (33)$$

This expression is a minimum when $\alpha = .17750$ and $\gamma = .07551$. Substituting these back into M^2 and letting $Z = 1$ we find $M^2 = .00475$ which shows that we have reduced the time average of the square of the ratio of the perturbing to the real force to less than one part in 200. Also in the above equation if we take $\beta = 0$, then α becomes .30103 which gives .00783 as a minimum value of M^2 . We shall make calcu-

lations with each of these sets of coefficients and they should check within one part in one hundred. We now have the perturbation constants and are ready to compute the energy of the new unperturbed motion and the average perturbative potential.

In order to find the method which would work most accurately for the crossed-orbit model of the hydrogen molecule, preliminary computations were made using the Bohr circle model as an example. This model has the advantage that it may be easily solved accurately and the energy is known when the interaction of the electrons is included. The problem was to apply Kramers' method to this simple case and find the manner in which it applied most accurately. The different ways in which it was applied consisted in assuming different charges on the nuclei for different portions of the energy, in each case balancing them by means of the perturbative potential in such a manner that the final charge in each case would be Z alone. An example would be to consider the charge on the nuclei to be $(Z-\alpha)$ both for the equilibrium of the nuclei and for the equilibrium of the electrons. In this case a term $(2Z\alpha - \alpha^2)/2c$ must be included in the perturbative potential so that the final mutual potential energy of the nuclei is $Z^2e^2/2c$. However, it was found that for this simple case, an exact solution could be obtained when the nuclei were considered in equilibrium under the charge Z and the electrons were in equilibrium under the charge $(Z-\alpha)$. An exact solution is obtained because it is possible to reduce the ratio of the perturbing to the real force to zero.

Coming back to the crossed-orbit model, our new unperturbed motion has for its Hamiltonian function

$$H_0 = \frac{1}{4c^2m(\lambda^2 - \mu^2)} \left[(1 - \mu^2)p_u^2 + \left(\frac{1}{\lambda^2 - 1} + \frac{1}{1 - \mu^2} \right) p_{\phi'}'^2 \right] - \frac{4Z'e^2}{c} \frac{\lambda}{(\lambda^2 - \mu^2)} + \frac{Z^2e^2}{2c} \quad (34)$$

where

$$p_{\phi'}'^2 = p_{\phi}^2 + 4m\beta e^2 \quad \text{and} \quad Z' = Z - \alpha \quad (35)$$

In this case also we will consider the charge on the nucleus as Z when we are considering the equilibrium of the nuclei and as $(Z-\alpha)$ when we are considering the equilibrium of the electrons. We shall quantize the real angular momentum p_{ϕ} and not p_{ϕ}' which is the angular momentum of the false unperturbed orbit which we have set up. We may consider p_{ϕ}' as quantized directly if we use a false quantum

number n_3' . The value of this false quantum number may be determined from (35), since $\beta = \gamma c$ thus,

$$n_3'^2 = n_3^2 + (16m\gamma e^2 c \pi^2)/h^2 = n_3^2 + (4c\gamma/a_1) \quad (36)$$

where the radius of the one-quantum orbit of the hydrogen atom is given by $a_1 = h^2/4\pi^2 me^2$.

Using (7) we obtain for the new unperturbed motion

$$c/a_1 = n_3' [B/16A(Z - \alpha)] \quad (37)$$

The factor $(Z - \alpha)$ enters since this relation really comes from the equilibrium of the electrons. Replacing (37) in (36) we obtain

$$n_3'^2 = n_3^2 + [4\gamma n_3'^2 B/16A(Z - \alpha)] = n_3^2 + .19635 n_3'^2$$

in which the values of A and B are those given in (22) and the values of α and γ are those given in (33). This equation may now be solved for n_3' where $n_3 = 1$, we obtain $n_3' = 1.1155$ and $J_2/J_3 = .89647$.

Since, for the condition of equilibrium of the nuclei, the charge of $Z = 1$ is used on each nucleus, the Eq. (19) remains the same. Eq. (15), which involves only the roots of $G(\mu^2)$, clearly, will not change. Therefore to obtain the new values of λ , x_1 and $|x_2|$ we must again solve Eqs. (19), (21) and (15) with the single exception that J_2/J_3 is equal to .89647 instead of unity. This computation is not as difficult as the first since the curve between J_2/J_3 has already been plotted. The final values are obtained by trial and error as before. The new values are

$$\lambda = 1.4026 \quad x_1 = .81160 \quad |x_2| = .39852 \quad (38)$$

from which $B = 2.0152$ and $A = .26348$. The nuclear separation $2c$ is given by $2c/a_1 = 1.4460$ and the energy of our new unperturbed orbit is given by

$$W_0 = -\frac{e^2}{2c} \left[\frac{8(Z - \alpha)}{B} - 1 \right] = -3.1339 Rh. \quad (39)$$

It is now necessary to average the perturbative potential over this new unperturbed orbit. The perturbing potential as given in (30) becomes

$$\begin{aligned} \overline{\Delta E} = & -\frac{4\alpha e^2 \lambda}{c} \frac{1}{(\lambda^2 - \mu^2)^{-1}} - \frac{\beta e^2}{c^2} \frac{1}{[(\lambda^2 - 1)(1 - \mu^2)]^{-1}} \\ & + \frac{e^2}{2c} \frac{1}{[(\lambda^2 - 1)(1 - \mu^2)]^{-1/2}}. \end{aligned} \quad (40)$$

The average values are obtained by substitution in the time average Eq. (12).

By reducing the integrals, then occurring, to standard elliptic integrals of the 1st, 2nd and 3rd kind, we obtain as the average of the perturbative potential over the new unperturbed orbit

$$\overline{\Delta E} = [-1.7017 - .4017 + 1.8403]Rh = -.2631Rh. \quad (41)$$

The final value of the energy may now be computed. We obtain for this, combining (39) and (41)

$$W = W_0 + \overline{\Delta E} = [-3.1339 - .2631]Rh = -3.397Rh \\ = 45.2 \text{ volts.} \quad (42)$$

In order to furnish a check on this value of the energy we may next compute the energy and dimensions with the other set of constants $\beta=0$ and $\alpha=.30103$. In this computation n_3 is not changed. This means that the relative dimensions of the model are not changed but only the absolute values. Repeating the same steps as before we obtain as the final value of the energy

$$W = W_0 + \overline{\Delta E} = [-2.4274 - .9945]Rh = -3.4219Rh.$$

This value agrees with the value of the energy given in (42) as well as could be expected with the approximation used in this case (see Eq. 33) and it verifies the latter parts of the previous calculations.

V. COMPARISON WITH EXPERIMENT AND CONCLUSIONS

An experimental value of the energy of the hydrogen molecule may be determined from the heat of dissociation and the energy of two hydrogen atoms. The most recent determination is that of Witmer,¹¹ who obtained the heat of dissociation from spectral data. His most probable value is 4.34 volts or 100,100 cal/mol. This result is higher than the previous result of Langmuir,¹² who obtained 3.6 volts or 84,000 cal/mol., but it agrees with the earlier values of Isnardi¹³ and Wohl.¹⁴ Witmer's value corresponds to $(2 \times 13.54 + 4.34)$ 31.42 volts for the hydrogen molecule. The energy given above of 45.2 volts for the crossed orbit model is so much higher than experiment that the model cannot correspond with reality. This result is not very surprising since

¹¹ E. E. Witmer, Proc. Nat. Acad. Sci. **12**, 238 (1926).

¹² I. Langmuir, J. Amer. Chem. Soc. **37**, 417 (1915).

¹³ T. Isnardi, Zeits. f. Elektrochem. **21**, 405 (1915).

¹⁴ K. Wohl, Zeits. f. Elektrochem. **30**, 49 (1924).

the three body problems of the neutral helium atom and the hydrogen molecule ion do not agree with experiment. Furthermore the moment of inertia deduced from this model is 4.91×10^{41} gm cm, which is much larger than the value derived from specific heat data. This is another example of the deficiency of the older or classical quantum theory. It is hoped that the new matrix theory, which has been introduced since this work was started, will clear up the quantum theory problem of more than two bodies.*

The writer wishes to express his sincere appreciation to Professor J. H. Van Vleck for his interest and assistance throughout this work.

DEPARTMENT OF PHYSICS,
UNIVERSITY OF MINNESOTA,
August 15, 1926.

* Note added in Proof: Since the above was written a paper has come out by Alexandrov in Ann. der Physik 81, 603, (1926) treating the problem of the hydrogen molecule ion from the standpoint of the new wave mechanics. This paper indicates that the new mechanics gives a value of the energy in agreement with experiment.

THE ELECTRON AFFINITY OF HYDROGEN AND THE SECOND IONIZATION POTENTIAL OF LITHIUM

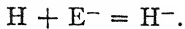
BY LINUS PAULING¹

ABSTRACT

On the assumptions that electrons in atoms and ions can be considered to be in hydrogen-like orbits under the influence of an effective nuclear charge $(Z-s)e$, and that the screening constant s is the same for ions with the same structure, there is calculated for the second ionization potential of lithium the value 76.2 v., and for the electron affinity of hydrogen atoms the value -1.85 k. cal./mol. These values are shown to lie within the range permitted by existing spectral and thermochemical data. With the use of the electron affinity of hydrogen it is shown that theoretically the hydride ion should be unstable in aqueous solution.

INTRODUCTION

THE electron affinity of hydrogen. Two recent attempts have been made to determine the electron affinity of hydrogen, E_H ; i. e., the amount of energy evolved by the reaction



In both cases use is made of thermochemical data; thus if all quantities but E_H are known, the following equation suffices for its determination:

$$E_H - D_H = Q_{MH} + S_M + I_M - U_{MH}.$$

Here D_H is the heat of dissociation of $\frac{1}{2}\text{H}_2$ to H, Q_{MH} is the heat of formation of crystalline MH from metallic M and $\frac{1}{2}\text{H}_2$, S_M is the molal heat of sublimation of M at low temperatures, I_M is the work of ionization of M, and U_{MH} is the molal crystal energy of MH. With the exception of U_{MH} the required energy quantities are known with considerable accuracy. The crystal energy may be calculated by the Born equations; for the sodium chloride structure, for example, we have

$$U_{MX} = 614 \cdot (1 - 1/n)(\rho/M)^{1/3},$$

in which ρ is the density, M the molecular weight (per MX), and n the repulsion exponent of the crystal. The value of n is in general found from the compressibility of the crystal; in the absence of any data for metal hydrides, however, n must be estimated, and the dis-

¹ Fellow of the John Simon Guggenheim Memorial Foundation.

crepant results of different workers arise from variations in its estimated value.

Joos and Hütting² contend that the replacement of another alkali metal ion by lithium ion should cause the same change in n as the replacement of a halogen ion by the hydride ion, H^- ; for in each case an ion whose outer shell contains eight electrons is replaced by one whose outer shell contains only two electrons. On using the corresponding value

$$n_{MH} \cong n_{LIX} \cong 6,$$

they obtain, with the use of data from sodium, potassium, rubidium, and caesium hydrides, the average result $E_H - D_H = -10$ k. cal./mol, which gives $E_H = 23$ k. cal./mol if D_H is taken as 33 k. cal./mol, or

$$E_H = 30 \text{ k. cal./mol} \quad (1)$$

if D_H is given the more generally accepted value 40 k. cal./mol.³

Kasarnowsky⁴ has criticized this procedure, and adopted another one. He states that the values of U for the lithium salts calculated by substituting $n=6$ in the Born formula, as was done by Joos and Hütting, are in considerable disagreement with the experimental values of that quantity, and concludes that this procedure should not be followed. Finding that in general U for a lithium salt is experimentally approximately equal to U for another alkali halide of the same structure and same molecular volume, he makes the assumption that this is true also for the alkali hydrides. From data for lithium, calcium, and barium hydrides, LiH , CaH_2 , and BaH_2 , chosen because of their relatively accurately known densities, he obtains (assuming calcium and barium hydrides to have the calcium fluoride structure) the value $-62+4$ k. cal./mol for $E_H - D_H$. The concordant value -59 k. cal./mol is obtained from sodium hydride, NaH , with the use of an estimated molecular volume. With $D_H = 40$ k. cal./mol, this gives

$$E_H = -22 \text{ k. cal./mol.} \quad (2)$$

Kasarnowsky states that the error in his calculations can hardly exceed ± 20 k. cal./mol, and that the electron affinity of hydrogen must hence be negative.

² G. Joos and G. Hütting, Zeits. f. Elektrochem. 32, 201 (1926); 32, 294 (1926).

³ The value $E_H = 37$ k. cal./mol was similarly obtained in an earlier computation, a slightly different value of n being used. See K. Fajans, Zeits. f. Elektrochem. 26, 493 (1920).

⁴ J. Kasarnowsky, Zeits. f. Physik 38, 12 (1926). See also Joos and Hütting, ibid., 39, 473 (1926).

In order to substantiate this very interesting result it is desirable to have an independent determination of the energy quantity E_H . This is especially true in view of the great uncertainty inherent in calculations of the crystal energies of hydrides. In both previous attempts it is assumed that the crystal energy of a hydride can be taken as equal to that of a lithium salt with the same molecular volume; the disagreement in results arising in a difference in the method of determining the crystal energies of the lithium salts, and in the choice of experimental data. It seems highly probable, however, that this fundamental assumption is in error. The repulsion exponent (i. e., the compressibility) of a salt containing the lithium ion, with two electrons contained within a radius of about 0.40A, would hardly be expected to be the same as that of a salt containing the hydride ion, with two electrons within the very large radius of about 1.5A.⁵ The hydride ion has far the most open structure of all known atoms and ions; and it is to be expected that this structure will have an appreciable influence on the repulsion exponent of hydride crystals.

The second ionization potential of lithium. The second ionization potential of lithium, the amount of work required in order to remove one further electron from the singly ionized lithium atom, Li^+ , in the normal state $1S$, has not been directly determined by the method of electron impact; nor has the term value $1S$ been found from the analysis of the lithium spark spectrum. Schüler⁶ has recently evaluated sixteen terms of par-lithium II, including $4S$, $5S$, $6S$, and $7S$. From a comparison of the values of the effective quantum number of these terms of lithium II with those of helium, he has, by a rather violent extrapolation, estimated for $1S$ the term value $648000 \pm 32000 \text{ cm}^{-1}$, corresponding to a second ionization potential for lithium of between 76 and 84 v. Werner⁷ has similarly obtained fifteen term values of par-lithium II, including $3S$, $4S$, and $5S$; his values and Schüler's being in good agreement. He likewise extrapolates to $1S$, for which he estimates the effective quantum number to lie between 0.85 and 0.90. This corresponds to a term value between 541000 and 606000 cm^{-1} , and a second ionization potential of lithium between 66.9 and 74.9 v.

It is evident that from spectroscopic data now available it can be concluded only that the second ionization potential of lithium is probably in the range between 67 and 84 v.*

⁵ See Note 9.

⁶ H. Schüler, Zeits. f. Physik 37, 568 (1926).

⁷ S. Werner, Nature 118, 154 (1926).

*See Note, p. 291.

THE ENERGY OF HELIUM-LIKE IONS

Since the early days of the quantum theory of spectra the x-ray term values have been explained by the assumption that the electron orbits are hydrogen-like, the nuclear charge Ze being diminished through the mutual screening effect of the electrons to the effective value $(Z-s)e$, in which s is called the screening constant.⁸ In ions with the same number of electrons and of similar structure, but with different atomic numbers, s is assumed constant. In the course of the application of this method of treatment to the polarizabilities, diamagnetic susceptibilities, and sizes of ions with rare gas structures, it was observed that it also allows the prediction of the energies of ions with the helium structure.

The energy of a hydrogen-like electron characterized by the total quantum number n and under the influence of the effective nuclear charge $Z_{\text{eff}}e$ is

$$-2\pi^2mc^4Z_{\text{eff}}^2/h^2n^2 = -13.54Z_{\text{eff}}^2/n^2 \text{ volts.}$$

In helium there are two equivalent electrons, each with $n=1$; the total energy of a helium-like atom or ion is, then,

$$W = -27.08(Z-s)^2 \text{ volts.} \quad (3)$$

Let us represent by I_1 and I_2 the work required to remove to infinity the first and the second electron, respectively. The removal of the first electron leaves the second under the influence of the entire nuclear charge Ze , and in the lowest orbit, with $n=1$; we accordingly have

$$I_2 = 13.54Z^2 \text{ volts.} \quad (4)$$

Since $I_1 + I_2 = -W$, the ionization potential I_1 is given by the equation

$$I_1 = 27.08(Z-s)^2 - 13.54Z^2 \text{ volts.} \quad (5)$$

The experimental value of I_1 for helium is 24.5 v., so that $W=78.7$ v. and $Z-s=1.705$. Assuming that this value of $s=0.295$ holds also for H^- , Li^+ , etc., the predicted energy values given in Table I are obtained. It is believed that these values are very close to the true ones; for the consideration of the more complicated problem of the term values of the K -level in heavier elements has shown that s undergoes only a slight change from element to element.

The value 76.2 v. for the second ionization potential of lithium is almost exactly in the middle of the entire range of probable values

⁸ See, for example, A. Sommerfeld, "Atombau," 4th Ed., pp. 454-461 and 546-551.

given by Schüler and Werner. Corresponding to it is the predicted term value 618000 cm^{-1} for $1S$ of lithium II. In addition the interpolated value 118700 cm^{-1} for $2S$ of lithium II may confidently be predicted; this does not differ greatly from Werner's extrapolated

TABLE I

	$Z-s$	$-W$	I_2	I_1
H ⁻	0.705	13.46 v.	13.54 v.	-0.08 v.
He	1.705	78.7	54.16	+24.5
Li ⁺	2.705	198.1	121.86	76.2
Be ⁺⁺	3.705	372	217	155
B ⁺⁺⁺	4.705	600	338	262

value 120000 cm^{-1} . The predicted values for these terms may be useful in the identification of observed lines in the lithium spark spectrum. No comparison with experiment can be made for Be⁺⁺, B⁺⁺⁺, etc.

The most interesting result of this calculation is the value of I_1 for H⁻, which is the electron affinity of hydrogen. Converting it into k. cal./mol, we obtain

$$E_H = -1.85 \text{ k. cal. / mol} \quad (6)$$

As the discussion in the introduction has shown, this is not in disagreement with the thermochemical data. Kasarnowsky's statement that the electron affinity of hydrogen atoms is negative is substantiated; but its value is much nearer zero than Kasarnowsky's values.⁹

The stability of the hydride ion in solution. As mentioned by Kasarnowsky, the negative value of the electron affinity of hydrogen illustrates well the part played in chemical reactions by crystal energy; for in hydride formation the crystal energy in effect not only dissociates the hydrogen molecules, volatilizes the metal, and ionizes its

⁹ The treatment of orbits as hydrogen-like permits the theoretical prediction of atomic radii, in order of magnitude at least. In the absence of a completely rational procedure, we may assume the atomic radius to be approximately equal to the distance from the nucleus at which the characteristic functions corresponding in the wave mechanics of Schrödinger to the hydrogen-like "orbits" in the atom become nearly zero. Schrödinger (Ann. d. Physik 79, 371 (1926)) has remarked that this distance is approximately equal to the major axis of the corresponding ellipse. We may then write

$$r = r_0 \cdot n^2/Z_{\text{eff}} = 1.064 n^2/Z_{\text{eff}} \text{ Angstroms}$$

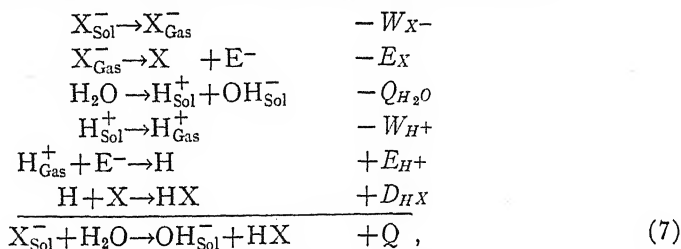
Using the values of $Z_{\text{eff.}} = Z-s$ given in Table I, we obtain

$$r = \begin{array}{ccccc} \text{H}^- & \text{He} & \text{Li}^+ & \text{Be}^{++} & \text{B}^{+++} \\ 1.510 & 0.625 & 0.394 & 0.287 & 0.226 \text{A.} \end{array}$$

These values are in reasonable agreement with the Li⁺-H⁻ distance in crystalline lithium hydride, 2.05A. (J. Bijvoet and A. Karssen, Proc. Amsterdam Acad. 25, 27 (1922)), and the less easily interpretable gas-kinetic radius of helium, 0.94A. (K. F. Herzfeld, Handbuch der Physik, Vol. 22, p. 436, (1926)).

atoms, but also does work in forming the unstable hydride ion from the atom and electron. In solution in a fused salt also the hydride ion might be stable, for the electrostatic energy against the surrounding oppositely charged ions would take the place of the crystal energy. The value found for the electron affinity of hydrogen shows, on the other hand, that the hydride ion in solution in water would react with the water molecules to form hydroxyl ions and gaseous hydrogen. To illustrate the use of the electron affinity in thermochemical calculations this instability in solution will be considered in detail.

The reaction of a univalent ion X^-_{Sol} in solution and a water molecule to form hydroxyl ion and HX may be written as follows:



$$\text{with } Q = D_{HX} + E_{H^+} - W_{H^+} - Q_{H_2O} - E_X - W_{X^-}. \quad (8)$$

Here W_{X^-} and W_{H^+} are the heats of hydration of the ions X^- and H^+ ; the significance of the other symbols is evident from their use. Of the energy quantities entering into Q , E_{H^+} is equal to 13.54 v., or 311 k. cal./mol; W_{H^+} to 249.6 k. cal./mol¹⁰; and Q_{H_2O} to 13.5 k. cal./mol; so that we have

$$Q = 47.9 + D_{HX} - W_{X^-} - E_X. \quad (9)$$

The values of Q for the hydride ion and the halide ions are given¹¹ in Table II.

TABLE II

	D_{HX}	W_{X^-}	E_X	Q
H^-	80	87*	-1.87	42.8 k. cal./mol
F^-	78.5 + D_F	87.0	$64 + D_F$	-26.6
Cl^-	89	70.1	88	-21.2
Br^-	75	66.2	80	-23.3
I^-	59	61.0	71	-25.1

*Assuming the radii of hydride and fluoride ions to be equal.

The entropy change during the reaction of Eq. (7) may be neglected, on account of the similarity of the original and final substances;

¹⁰ The heats of hydration are taken as the free energies of hydration given by T. J. Webb, Proc. Nat. Acad. Sci. 12, 524 (1926); the difference between energy and free energy is not great enough to matter in this calculation.

¹¹ D_{HX} from H. Senftleben and I. Rehren, Zeits. f. Physik 37, 529 (1926); W_{X^-} from Webb; E_X from E. v. Angerer and A. Müller, Phys. Zeits. 26, 643 (1925).

hence Q may be identified with the free energy change $-\Delta F = RT \ln K$, in which K is the equilibrium constant of the reaction. The large negative values of Q for the halide ions show that the ions are stable in solution, and do not hydrolyse. On the other hand, the large positive value for the hydride ion requires that it be unstable in solution; thus it is in equilibrium with 1 mol/liter of hydroxyl ion and with hydrogen at one atmosphere pressure only at a concentration of about 10^{-29} mol/liter.

MUNICH, OCTOBER 9, 1926.

Note added to proof. It is necessary to mention, moreover, that the new quantum mechanics leads to the result that the normal state of helium is not an extrapolation of the S series of orthohelium, but lies between the ortho-and parhelium series. See Heisenberg, Zeits. f. Physik. 39, 499 (1926).

MEASUREMENT OF INDEX OF REFRACTION OF GASES AT HIGHER TEMPERATURES

By E. W. CHENEY

ABSTRACT

The thermal coefficients of the indices of refraction of air, N₂, SO₂, NH₃, and CO₂.—For light of the visible spectrum these coefficients were not found to differ from the thermal coefficients of density change in the range 0–300°C. At 0°C, 760 mm the values of $(n - 1) 10^7$ for λ5852A, 6143A, and 6678A were found to be:

λ	Air	N ₂	NH ₃	CO ₂	SO ₂
5852A	2925	2985	3795	4485	6637
6143A	2919	2977	3785	4473	6615
6678A	2912	2969	3771	4465	6598

Incidentally the rate of expansion of quartz with temperature was found to be constant within the temperature interval 25–300°C, and to have an average value of expansion coefficient of $0.946(10)^{-6}$. A kilowatt neon Geissler tube is described.

A FABRY-PEROT interferometer was used to measure at higher than room temperatures the indices of refraction of several gases including some having polar molecules. It was hoped at the beginning of the experimental work that time would be had to extend the measurements into the infra-red. A recent article¹ gives very well the theory of the instrument and methods of use.

Apparatus. Fig. 1 will give an idea of the present experimental arrangement. It shows the optical system and an electric furnace encircling the Fabry-Perot interferometer. Light from a neon tube produced Haidinger interference fringes on the slit of the spectroscope. A camera photographed the fringes.

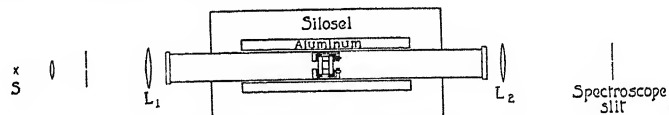


Fig. 1. Arrangement of apparatus.

The neon tube was constructed in the laboratory and furnished a particularly brilliant and satisfactory source for the interference work. The hard glass tube has large cylindrical electrodes, a narrow capillary about five inches long, and contains neon at a pressure of about 5 mm. The tube rests at two points in a water tank. (See Fig. 2.)

¹ W. H. J. Childs, J. Scientific Instruments 3, Nos. 4 and 5 (1926).

Rubber tubing containing mercury makes the requisite flexible and water-tight seals around the lead-in wires. The tube has operated continuously for hours, with an input of a kilowatt furnished by a 10,000-v., 3-kw transformer.

The circular interferometer mirrors were made by sputtering platinum over their central portions in order to have inert surfaces. They remained good after heating in the furnace provided the glass had been baked for some hours before the sputtering. The laboratory mechanician ground on a lathe three fused quartz posts, (from the Hanovia Chemical Co.) for the etalon. For the more accurate adjustment of lengths, I ground the posts by hand on a flat steel disc. For testing the lengths of the posts one of the interferometer mirrors was mounted

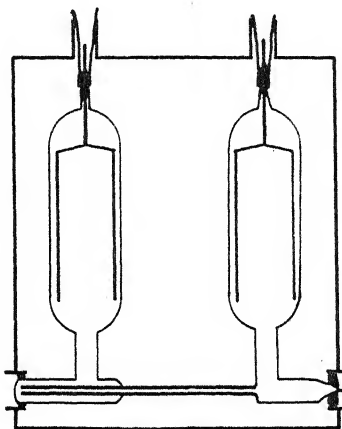


Fig. 2. The neon tube.

horizontally in a converging beam of mercury green light. The three quartz posts stood on this mirror. The second mirror, mounted in a light frame with levelling screws, rested on the quartz posts. By moving the top mirror a little with one or another of the levelling screws until the interference fringes appeared, it was easy to tell which quartz posts were longer. I ground the posts by hand until the Haidinger fringes showed the same order of interference over the whole of the mirrors when they were separated by the quartz posts. The mirrors and posts were then mounted in a steel cylinder about three inches long. Small coiled tungsten springs held the mirrors against the quartz posts. Steel springs were not satisfactory at higher temperatures, owing to variation in elasticity. The interferometer after adjustment was shoved to the center of a steel tube 35 inches long.

An electric furnace with a heating coil wound on a heavy cast aluminum cylinder to give uniform heat distribution surrounded 19 inches of the 35 inch steel tubing, which passed axially through the furnace. A can of Silosel insulated the furnace. This was mounted in a tank of water so that its heat capacity would reduce random temperature fluctuations. The water tank was mounted on screws so that the interferometer could be moved to bring the interference fringes accurately on the slit. Storage cells furnished the heating current and iron wire ballast lamps, kindly donated by the Edison Lamp Works of the General Electric Company, satisfactorily compensated for fall in voltage of the storage cells during long heating periods. With this arrangement the temperature in the furnace would remain constant to within 1/30 of a degree for hours. Changes in temperature of the interferometer due to the heat transference by the gases upon their entrance to the tube, however, caused trouble.

A copper-constantan thermocouple sealed in a glass tube projected through the casing of the interferometer until it was in the space between the interferometer plates. The thermocouple was heated for 50 hours at about 300°C, and then calibrated. A second calibration after 50 hours more of heating showed no change in the thermocouple. A potentiometer and a mirror galvanometer gave the electromotive force and could exhibit a change of 1/30°C in the temperature of the thermocouple. A Weston cell in a constant temperature bath served as a standard e.m.f.

Mercury in an inch bore manometer tube measured the gas pressure. Both surfaces of mercury could be raised and lowered simultaneously to prevent errors due to adhesion. A cathetometer which had been compared with a standard meter bar gave the heights of the mercury column and the readings were properly reduced to standard conditions.

A high grade photographic objective focussed the interference fringes upon the slit of the spectroscope. The rings were photographed on panchromatic plates and were measured with a traveling microscope reading to 1μ . The fractional order of interference at the center of the interference circles is equal to $A d^2 - p$, where d is the diameter of the p 'th ring from the center, and A is a constant for any one wave-length, i.e. $P/(d_{p-1}^2 - d_p^2)$, where P is the order of interference. A is determined from measurements on two ring diameters and an approximate value of P . The A 's are inversely proportional to the wave-lengths, so that A 's measured for different lengths may be reduced to the A for some particular wave-length. This was done for measurements made on many lines and the values averaged, to give as good values for the

various constants as could be obtained with more effort from the usual formula involving the focal length of the projecting lens. The fractional order of interference at the center of the interference circles was determined to the third decimal place.

Preparation of gases. N₂ came from a commercial cylinder and passed over hot copper for elimination of oxygen. The air and N₂ filtered through six feet of drying tubes containing CaCl₂ and P₂O₅ and further passed through a liquid air trap on their way to the apparatus.

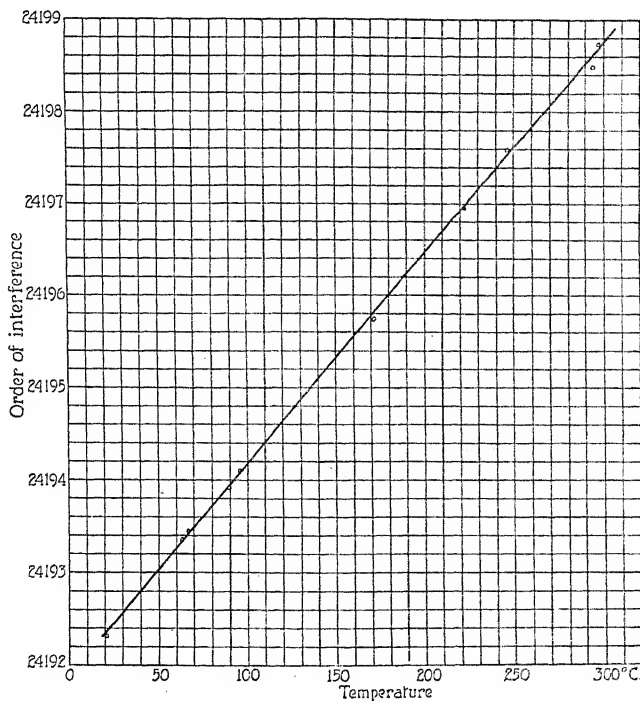


Fig. 3. The variation of the order of interference for vacuum with temperature.

HCl and marble in a Kipp generator furnished CO₂. This was dried by CaCl₂ and P₂O₅ and frozen in a liquid air trap. The middle portion of the sublimate was used each time.

The NH₃ came from a tank as a liquid. It boiled out of a Dewar flask equipped with an electric heating coil, and after passing over KOH, froze in the liquid air trap. The middle portion of the distillate was used.

The SO₂ came from a tank, was dried by passage through the drying tubes, and further purified by the usual freezing process.

Measurements. The index of refraction of a gas is given by dividing the order of interference with the gas between the plates by the order of interference with the interferometer evacuated. For the best results the pictures enabling these orders to be computed should be taken at precisely the same temperature. Unfortunately cooling by the admission of the gases made this procedure impossible. Although alterations in the interferometer with change in temperature were not quite continuous, the order of interference for the vacuum, at the same temperature as the gas under consideration, was obtained by interpolation from vacuum values at neighboring temperatures.

Fig. 3 shows the order of interference for a vacuum between the interferometer plates plotted against temperature. The order of interference at the lowest temperature plotted (21.4°C) is 24192.312.

TABLE I
Measured values of $(n-1) \times 10^6$ for various gases
Wave-length of light 5852 \AA . Values reduced to 760 mm pressure

Temp. °K	$(n-1) \times 10^6$	Temp. °K	$(n-1) \times 10^6$
Air			
294.5	270	445.1	180
338.3	236	508.1	153
363.1	221	567.5	148
Nitrogen			
244.5	276	446.1	185
338.7	239	497.0	157
365.6	222	569.3	144
Ammonia			
294.3	358	445.8	231
339.2	302	499.2	210
366.2	280	568.1	182
Carbon dioxide			
294.4	411	439.4	277
333.7	373	483.6	247
363.5	334	567.6	222
Sulfur dioxide			
294.3	612	434.4	418
335.1	537	481.2	371
360.1	499		

The expansion of the interferometer is shown to be moderately uniform. The slope of the line divided by the total order of interference, in Fig. 3, incidentally gives the average coefficient of expansion of quartz as 0.946×10^{-6} for the temperature interval 25°C - 300°C , a figure higher than given in the tables. An attempt was made to account for the divergence of this value with Randall's measurements²

² Randall, Phys. Rev. 30, 216 (1910).

on the thermal coefficient of expansion of quartz by taking account of change in length of the quartz posts due to change in tension of the tungsten springs. The required change in tension did not appear to be of a possible order of magnitude. Moreover, the rate of expansion of quartz with temperature is seen to be constant in the temperature interval 25°–300°C. This would seem to be in accord with expectation, but it disagrees with Randall's results. While the explanation of these discrepancies does not affect the discussion of the index of refraction of gases, it is still to be desired.

Table 1 summarizes the measurements on the indices of refraction at various temperatures. Measurements were made with pressures

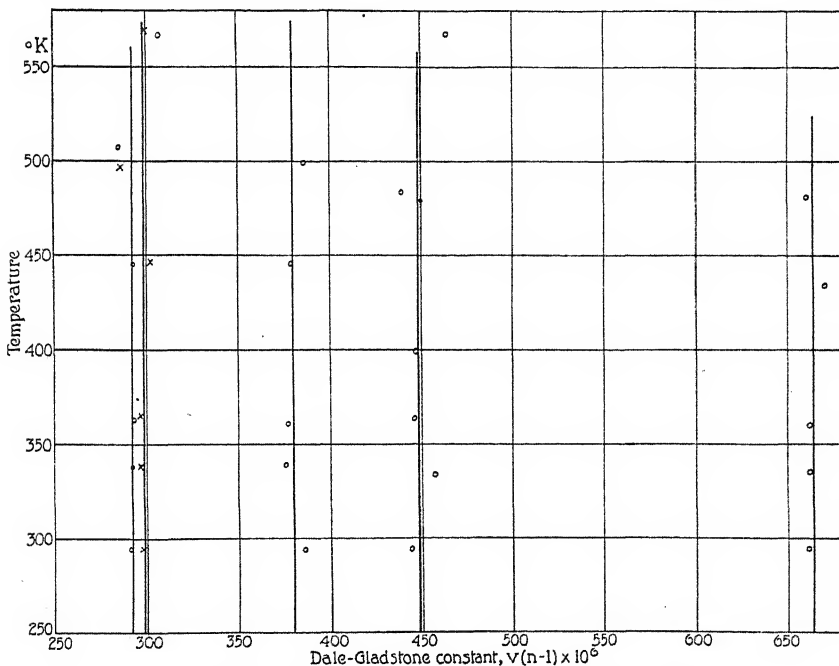


Fig. 4. The constant of the Dale-Gladstone law, $(n-1)v \times 10^6$, plotted against temperature for the gases air, N_2 , NH_3 , CO_2 , SO_2 .

close to 760 mm and the readings reduced to values at 760 mm by multiplying by the inverse ratios of the pressures. Corrections for compression of the quartz by the gas are not necessary. Column 3 gives the indices of refraction of the wave-length 5852.488A reduced to standard pressure.

The Dale-Gladstone law states that $(n-1)v = \text{constant}$ where v is the specific volume or is a number proportional to it. Fig. 4 shows $(n-1)v \times 10^6$ plotted against temperatures for the various gases.

The volume v for the imperfect gases was computed by van der Waal's equation, taking v at 0°C to be 1 cc. No departure from the linearity required by the Dale-Gladstone formula can be detected from these measurements, or in other words, the thermal coefficient of the index of refraction is the same as the density coefficient. The measurements up to 150°C show less irrationality than do the measurements at higher temperatures. The lines are drawn giving equal weight to the four measurements at the lower temperatures. The intersections of these lines with the line $T=273^{\circ}\text{K}$ give values of the indices of refraction of the various gases at 760 mm for 5852.488Å in good agreement with the accepted values for the D line. Similar lines were drawn for the wave-lengths 6143.062Å and 6678.276Å. Table II gives the values of $(n-1) \times 10^7$ at 0°C, 760 mm for the various gases and various wave-lengths.

TABLE II
Values for $(n-1) \times 10^7$ at 0°C, 760 mm pressure

Gas	$\lambda 5852\text{A}$	$\lambda 6143\text{A}$	$\lambda 6678\text{A}$
Air	2925	2919	2912
N ₂	2985	2977	2969
NH ₃	3795	3785	3771
CO ₂	4485	4473	4465
SO ₂	6637	6615	6598

Theory³ shows that in the infrared there may be a temperature coefficient of the index of refraction differing from the density coefficient for polar molecules, and measurements by Meggers and Peters⁴ indicate such a temperature coefficient near the ultra-violet absorption bands in air. It should be interesting to study the temperature coefficient of the index of refraction in these regions.

I wish to express here my thanks to Dr. K. T. Compton for his encouragement and advice.

PRINCETON UNIVERSITY,
September 2, 1926.

³ P. Debye Phys. Zeit. **13**, 97 (1912).

⁴ Meggers and Peters, Bulletin of the Bureau of Standards **14**, 371 (1917).

A DETERMINATION OF THE DIELECTRIC CONSTANT OF AIR BY A DISCHARGE METHOD

BY A. P. CARMAN AND K. H. HUBBARD

ABSTRACT

Two air condenser systems, one containing the test condenser and the other the balancing condenser, are charged to equal opposite potentials, the opposite charges are mixed and discharged through a galvanometer. The two condenser systems are adjusted until the galvanometer deflection is zero. A special form of rotating commutator was devised for which the contact resistances are small and uniform. This commutator has three pairs of make and break contacts, two for charging and discharging the two condensers, and one pair connected so that a single battery is used to charge both condensers. The capacity of the test condenser is obtained in terms of readings on a condenser which forms part of the balancing condenser system. The ratio of the capacities of the test condenser, with a vacuum and with air for dielectric is then obtained. The calibration for the readings is described. This calibration is made with the apparatus in place, by simple changes of connections. Possible errors from time lag, thermal expansions, and deformations from pressure changes are discussed. The average of thirteen separate measurements gives 1.000594 for the dielectric constant of air at 0°C and 760 mm Hg pressure. The thirteen separate readings agree in the second significant figure of the decimal part of the result.

THE first measurement of the dielectric constant of air was made in 1874 by Boltzmann.¹ He measured the change of potential for constant charge of an air condenser, when the air was exhausted. He obtained the value 1.000590 for the dielectric constant of air at 760 mm pressure and at 0°C. In 1877 Ayrton and Perry² determined the dielectric constant of air by comparing, with a quadrant electrometer, the potentials of condensers with and without air. Their value 1.00150 for the dielectric constant of air is generally considered in error. The next determination of the dielectric constant of air was made in 1885 by Klemencic,³ an assistant working in Boltzmann's laboratory. He obtained the change in capacity of a large air condenser when the air was exhausted, by measuring with a galvanometer the discharges of the condenser. The condenser was charged and discharged sixty-four times per second by a tuning fork commutator. He gives the value 1.000586 as the dielectric constant of air at standard pressure and temperature. Klemencic's individual values vary from 1.000718 to

¹ L. Boltzmann, Wien. Berichte 69, Part 2, 795 (1874).

² Gordon's Electricity and Magnetism, Vol. 1, p. 130.

³ I. Klemencic, Wien. Berichte Bd 91; also Rep. d. Physik, Bd. 21 (1885).

1.000478, and he rejects the last ten of his twenty values on account of irregularities. The average of his twenty values is 1.000599.

The next absolute determination of the dielectric constant of air seems to be that of Fritts,⁴ who compared the capacities of air condensers by the beats of a heterodyne circuit,⁵ recording the beats by an ingenious photographic method. He obtained the value 1.000540 for the dielectric constant of air. In the same year Zahn,⁶ also using a heterodyne method, got the value 1.000572.

In view of these variations in values obtained for the dielectric constant of air, and particularly because the methods using high fre-

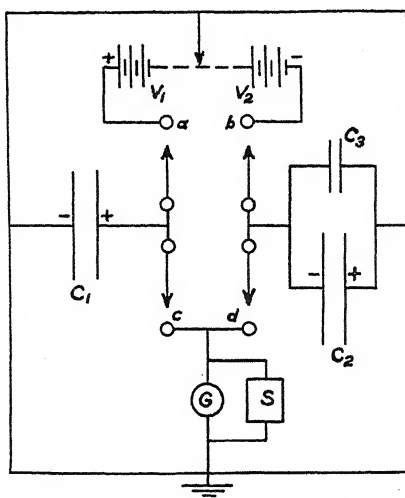


Fig. 1. Diagram of circuit previously used.

quency oscillations have given lower values than Boltzmann's and Klemencic's values, it was thought desirable to make a new determination by one or both of the older methods. This work began in 1923 directly after Fritts' determination in this laboratory. The method used consists in charging two nearly equal air condensers to opposite potentials, and then discharging the two condensers simultaneously through a sensitive galvanometer. The charging and discharging takes place numbers of times per second so that the galvanometer gives a steady deflection for the discharge. The object is to adjust the two opposite discharges until the galvanometer deflection is zero. The

⁴ E. C. Fritts, MS Doctor's thesis, Univ. of Ill. Library, Feb. 1923; Physical Review 23, 345 (1924).

⁵ Hyslop and Carman, Phys. Rev. 15, 243 (1920).

⁶ C. T. Zahn, Phys. Rev. 23, 781; 24, 401.

arrangement for this method as used by A. P. Carman and K. O. Smith⁷ in 1923, is shown in Fig. 1.

At first the well known commutator of Fleming and Clinton⁸ was used for the charging and discharging of the condensers, but the galvanometer deflections were so unsteady because of irregular contacts of the brushes of the commutator, that finally an entirely new commutator was devised and used with satisfaction in all this investigation. In the new commutator, contact is made by bringing a platinum-tipped rod end-on against a plate. The rod is connected with insulation bushings to a brass block which fits on an eccentric part of the commutator shaft. The rods are kept horizontal by suitable bearings, and are in pairs, one on the right side and the other on the left side of the eccentric block. The eccentricity in this particular instrument is 3 mm, so that the rods move backwards and forwards through 3 mm in a harmonic motion. The platinum plate is carried through a flat cushioning spring on an adjustable support, so that the end of the rod makes contact with the plate at the rod's maximum outward position. Thus when the contact on the right side is made, the contact on the left side is broken, and vice versa. In the final form of this commutator, as used in this investigation, there are four pairs of rods, so that four connections can be made (or broken) at the same time. It will be seen that in our final circuit, the third pair proved important in allowing the use of a single undivided battery. Various other improvements are found in the final form of this commutator not found in the form described in 1924.⁹

In the equation for the above arrangement of apparatus, it is assumed that the commutator speed and the voltages V_1 and V_2 are absolutely constant for the five or ten minutes of an experiment. Also, the galvanometer was found to vary more or less, unless the shunt was made too low for extreme sensitivity. These difficulties led to the development of a new circuit in which there is a single battery for the charging, and there are better conditions for the balance. The new arrangement has come gradually after many experiments from the first circuit. For the work on this development with the long careful tests and observations involved, credit is due to Mr. Hubbard who took up the investigation with the senior author for the last two years.

The essential parts of the final circuit are shown in Fig. 2. The charging battery of about 50 "B" storage cells is shown at V. The

⁷ MS of Master's thesis by K. O. Smith, Library of Univ. of Ill., June, 1923.

⁸ Fleming and Clinton, Proc. Phys. Soc. London, 18, 389 (1903).

⁹ A. P. Carman, J.O.S.A., 9, 175 (1924).

test-condenser C_B is built rigidly and is under a bell jar so that the gaseous dielectric can be exhausted. Its capacity is 0.04 mf. The balancing condenser C_N has approximately the same capacity as C_B . The variable condensers C_D and C_M are in parallel with C_B and C_N respectively and serve for final balancing. The commutator with three pairs of contact rods is indicated by the arrows. The commutator speed was about 1500 r.p.m. The key K_1 is at the start in position Q , so that contacts 6 and 7 are at the same potential. While contacts 5, 6, and 7 are closed, contacts 1, 2 and 3 are open, and vice versa. To insure mixing of the condenser charges, contacts 1 and 2 close just an instant before 3 closes. If the capacity of the test condenser is equal

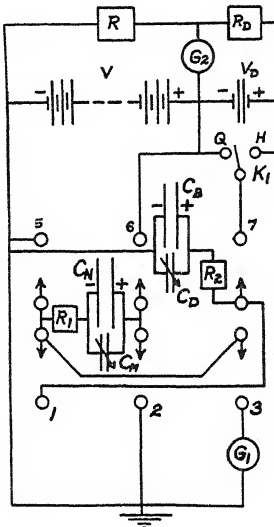


Fig. 2. The new circuit (simplified).

to that of the balancing condenser, there is zero charge remaining after the mixing and consequently no current through the galvanometer. The possible sensitivity can be calculated as follows. Suppose the test and balancing condensers are equal so that there is zero galvanometer current. Now change the capacity of $C_B + C_D$ by C , and the resulting current is I_g . Then $I_g = CVn$, where n is the commutator speed in r.p.s. The galvanometer deflection is $d = I_g/F = CVn/F$ where F is the figure of merit of the galvanometer. The sensitivity of the system to change of capacity is then $d/C = Vn/F$. The figure of merit of the galvanometer is about 10^{-10} amperes per mm deflection. We thus calculate the sensitivity, $d/C = 25$ mm galvanometer deflections for

1 mmf change. Let C_1 be the capacity of the test condenser C_B , and K_1 the dielectric constant for a low pressure, and C_2 and K_2 the corresponding capacity and dielectric constant of C_B at normal air pressure. If C_B is the capacity with perfect vacuum as the dielectric then $C_1 - C_2 = C_B(K_1 - K_2)$. Putting this in the above equation for sensitivity, we get $d/(K_1 - K_2) = C_B V n / F$. Using approximate values, we get $d/(K_1 - K_2)$ equal to 10^6 mm galvanometer deflections per unit change in K . That is, applied to the dielectric constant of air, a change from 1.000590 to 1.000591 should make a difference of one millimeter in the galvanometer deflection. The final results show that we approximate this calculated sensitivity in having variations only in the sixth decimal place.

It is seen directly that the circuit is sensitive to change of voltage. This makes it important to guard against stray induced e.m.f.'s. Thus it was found that for certain commutator speeds, the galvanometer was unsteady. This was traced to voltages induced from the field of the 60 cycle power circuit, these producing considerable galvanometer deflections if the commutator speed was $\frac{60}{2}$, $\frac{60}{3}$, $\frac{60}{4}$, or etc. r.p.s. These stray e.m.f.'s disappeared completely at suitable commutator speeds. The procedure for the calibration of the apparatus and the calculation of the dielectric constant is as follows:

I. With the key at Q , the condenser C_M is adjusted to give zero galvanometer deflection. The pressure of the gas in C_B is P_1 and its dielectric constant is K_1 . Then

$$C_B K_1 V + C_1 K_D V + C_s K_s V = 0 \quad (1)$$

where C_B and C_1 are the capacities of the condensers C_B and C_D for vacuum, and C_s is the algebraic sum of all other capacities in the circuit, and K_1 , K_D and K_s are dielectric constants of the respective dielectrics.

II. Change pressure of gas in C_B to P_2 with dielectric constant K_2 , and bring galvanometer deflection to zero by changing capacity of C_D to C_2 . Then

$$C_B K_2 V + C_2 K_D V + C_s K_s V = 0. \quad (2)$$

From Eqs. (1) and (2), we get

$$K_1 - K_2 = (C_2 - C_1) K_D / C_B \quad (3)$$

The calibration to determine $(C_2 - C_1)/C_B$ is carried out by adding the resistances R and R_D , the galvanometer G_2 , and the two opposing cells giving the resultant e.m.f. V_D .

(1) The key, is on position Q and the condensers are adjusted to zero galvanometer deflection

$$C_B K_B V + C_3 K_D V + C_L K_L V + C_{s1} K_{s1} V = 0 \quad (4)$$

where C_L is a part of the capacity $(C_N + C_M)$ (see step 3 below), and C_{s1} is the algebraic sum of all remaining capacities in the circuit. K_B , K_D , K_L and K_{s1} are dielectric constants.

(2) The key is turned to position H , and the galvanometer deflection is brought to zero by changing condenser C_D . Then

$$C_B K_B V' + C_4 K_D V' + C_L K_L V + C_{s2} K_{s2} V + C_{s3} K_{s3} V' + C_{s4} K_{s4} V_D = 0 \quad (5)$$

Here $V' = V + V_D$ and the meanings of the other terms are apparent.

(3) The key is placed at Q , and condenser C_B is disconnected, and capacity C_L of $(C_N + C_M)$ being also removed, the galvanometer deflection is zero. Then

$$C_5 K_D V + C_{s1} K_{s1} V = 0. \quad (6)$$

(4) The key is placed at H , and zero galvanometer deflection is produced by changing C_D . Then

$$C_6 K_D V' + C_{s2} K_{s2} V + C_{s3} K_{s3} V' + C_{s4} K_{s4} V_D = 0. \quad (7)$$

From Eqs. (4), (5), (6), (7), we get

$$C_B K_B (V' - V) + K_D [V'(C_4 - C_6) - V(C_3 - C_5)] = 0. \quad (8)$$

Substituting $V_D = V' - V$, we get

$$C_B = \frac{K_D [V'(C_4 - C_6) - V(C_3 - C_5)]}{-K_B V_D}. \quad (9)$$

In the above calibration, V and V' are assumed constant, and there were actually no variations of sufficient magnitude to cause appreciable error. If the resistances R and R_D are adjusted to give zero deflection of galvanometer G_2 , then R' , R and R_D , are proportional to V' , V and V_D , where $R' = R + R_D$. Introducing these proportional quantities into Eq. (8), we get

$$C_B = \frac{K_D}{K_B} \frac{R'(C_4 - C_6) - R(C_3 - C_5)}{-R_D} = \frac{K_D}{K_B} A; \quad (10)$$

where A is a constant determined by the calibration. Eq. (10) thus gives the capacity C_B in terms of capacity differences as observed on condenser C_D . By combining Eqs. (3) and (10) we get

$$(K_1 - K_2) = (C_2 - C_1) K_B / A. \quad (11)$$

If we use the same gas at the same pressure and temperature we have $K_B = K_1$, then

$$(K_1 - K_2)/K_1 = (C_2 - C_1)/A$$

or

$$K_2/K_1 = (C_1 - C_2 + A)/A. \quad (12)$$

The reduction to standard temperature and pressure is made on the assumption that the dielectric constant is proportional to the density of the gas, and hence directly proportional to the absolute temperature and inversely proportional to the pressure. We get the equation in the form

$$(K_0 - 1) = \frac{760T(C_2 - C_1)}{273(P_1 - P_2)[A - (C_2 - C_1)]} \quad (13)$$

where

$$A = \frac{R'(C_4 - C_6) - R(C_3 - C_5)}{-R_D}$$

as indicated in Eq. (10). We thus get an absolute determination of the dielectric constant of air by the above procedure. The calibration is made with all parts in place, by simply throwing a switch, and is indeed a part of the procedure each time.

In the above method, it is of course assumed that the insulation is "perfect" and this was found by repeated tests to be the case except on some days of very high humidity and consequent surface condensation. No measurements were made on such days. It is assumed that the charging and the discharging are complete in the time of the commutator contact. The inductance and resistance of the circuit were such that no error was caused by time lag. This was verified experimentally.

The importance of the test condenser is such that a brief description of it is desirable. This condenser is constructed of iron plates, each plate being five inches square and one-sixteenth of an inch thick. We will call the two armatures of the condenser, *A* and *B*. Armature *A* consists of fifty plates with forty-nine spaces, each space being three thirty-seconds of an inch wide. The *A* plates are held together by four quarter-inch steel rods or bolts which pass through holes in the corners of the plates. Iron washers of uniform thickness were carefully turned, and used on the rods between the plates, thus securing uniform spacing. The rods are threaded at the ends, and strong nuts are used to clamp the plates rigidly together. Armature *B* consists of forty-nine plates held together by rods, with spaces and nuts similar to those for *A*. The plates of *B* occupy the spaces between the plates of *A*, with small but safe air clearance. A common arrangement in an air condenser

of this kind is to have the diagonals of the plates of *A* at right angles to those of *B*. To get more effective use of the surfaces, we placed half of the *B* plates with their diagonals making an angle of 35° to the right of the diagonals of *A*, and the other half of the *B* plates making the same angle to the left. These *B* plates are clamped together on the rods by strong nuts in groups of two or three for rigidity and for uniform spacing. All rods are clamped to a thick plate of Pyrex glass, holes being bored through the glass and the rods are held firmly in place by nuts and washers on each side of the plate. This glass plate is at the top, so that the *B* plates are in fact suspended from the glass plate. The insulation between *A* and *B* was found "perfect" for our purpose. The *A* armature is joined to earth. The condenser and the glass plate are completely shielded by grounded sheet iron disks and cylinders. The only dielectric in the field, except the air, is the glass between the widely separated rods; and for a condenser of this size the correction for this dielectric is negligible.

The constancy of the capacities of "test" and the "balancing" condenser system is, of course, a fundamental requirement, and this was tested with great care. One annoying variation was finally eliminated by putting the comparison, as well as the test condenser, and the rotating commutator on separated supports, from which it was inferred that the mechanical vibrations introduced a small capacity change in the comparison condenser. The temperature effects on the capacities of the condensers proved troublesome until understood. The condensers are made of several materials, the thermal expansions and contractions, due to even a very moderate temperature change, introduce deformations which persist for a considerable time. The resulting change in capacity is shown by the creeping of the galvanometer deflections. This creep was fairly constant and so could be allowed for, but it was possible to find times and conditions when the creep was very small. A more fundamental difficulty was a capacity change which we ascribed to the displacement of the parts of the condenser by the pressure of the gaseous dielectric. Our test condenser as described above is very strongly built and all parts are of iron except a pyrex glass insulating plate. It was found that, if the gas in the condenser had been at normal pressure for several hours, and it was then evacuated, and allowed to return to normal pressure, there was a galvanometer deflection showing a small capacity change. After the first evacuation and return to normal pressure, the change in capacity was not observed until the condenser had again rested. This effect, though small, is difficult to evaluate. It is an effect equally important in all

methods of obtaining the absolute dielectric constant of a gas, and may exist in small condensers in the same ratio as in large condensers. The important adjusting condenser C_D is of the rotating wing type, and is very carefully built with heavy brass plates turned from cast brass. It has a circular scale and vernier, but the readings for the calibrations were made by means of a telescope and circular scale, a mirror being mounted on top of the rotor shaft of the condenser. The readings were kept in that part of the calibration curve which is a straight line. The bell jar over the test condenser was exhausted by a Hy-vac pump, and the admitted air was carefully dried by passing slowly through tubes containing phosphorus pentoxide. The temperatures were measured by means of sensitive thermocouples, two couples being inside of the bell jar, and one couple on the outside.

This method, as indicated, has been developed slowly after many tests and changes. The special form of commutator devised in the course of the work is satisfactory in making and breaking contact regularly in time and with small and constant resistance. The speed of the commutator can be varied easily through a wide range. Theoretically, changes in speed of the commutator are eliminated in the equation, but these changes in speed are so very small that no appreciable error enters from any secondary effect due to speed change. Speeds of about 1500 were used in the final measurements. The very difficult requirement of constancy in the ratio of potentials of two charging sources has been met by using a single battery for charging both condenser systems, so that variations of the voltage of the charging battery do not come in. The arrangement for calibrating the apparatus in place, by only connecting and disconnecting keys, also reduces possible errors.

Results: After many preliminary trials, the following final measurements were made when the temperature conditions were fairly satisfactory. Early morning hours were used in three of four runs to secure even temperatures. All measurements are included.

	Dielectric constant	Pressure change (mm Hg)
Morning, June 18, 1926	1.000598	732.4
2-6 A.M.	1.000597	730.9
	1.000593	732.9
	1.000595	734.4

Afternoon, June 18	1.000597	738.1
2-4 P.M.	1.000598	737.8
	1.000590	543.2
Morning, June 19	1.000594	731.9
2-4 A.M.	1.000592	730.1
	1.000591	544.3
	1.000592	548.7
Morning, June 27	1.000592	723.2
2-6 A.M.	1.000592	723.5

It will be noted that all of the thirteen separate measurements agree in the second significant figure of the decimal. The final average is 1.000594. Boltzmann's value of 1.000590 is in closer agreement with this value of 1.000594 than the more generally quoted value of 1.000586 of Klemencic. These values by static charge methods are larger than the values by oscillation methods obtained recently by Fritts and by Zahn.

PHYSICS LABORATORY,
UNIVERSITY OF ILLINOIS,
October, 1926.

THE MAGNETIC MOMENT OF THE HYDROGEN ATOM

BY T. E. PHIPPS AND J. B. TAYLOR

ABSTRACT

The magnetic moment of the hydrogen atom has been investigated by the atomic ray method introduced by Stern and Gerlach. Atomic hydrogen formed in a discharge tube by the method of R. W. Wood was first used. The ray was formed in a special all-glass slit system of three slits sealed to the discharge tube. The ray was detected by the reduction resulting on contact with a target coated with molybdenum trioxide. A sharply defined blue line against a white background was the result. In the magnetic field the ray was separated into two branching rays. There was also evidence of a central undeviated ray which is believed to be due to hydrogen active chemically but probably not in the atomic state. From a measurement of the deflection the magnetic moment of the hydrogen atom was calculated to be one Bohr magneton within the limits of experimental error. This result is of interest because of the questions raised by the new quantum mechanics of Heisenberg, Born, and Jordan, and by the spinning electron theory of Uhlenbeck and Goudsmit. Atomic hydrogen formed by the hot filament method of Langmuir was next used. The increased velocity of the atoms in this case resulted in less separation of the ray, but a deflection was distinctly recorded. Finally, the product formed on exposing a mixture of mercury vapor and hydrogen to ultra-violet light was investigated. This is believed by Cario and Franck, Taylor, and others to be atomic hydrogen. Thus far attempts to form a ray which will reduce the target have been unsuccessful. The reasons for this are being investigated.

THE magnetic moment of the hydrogen atom is of great interest since the hydrogen atom is the basis for the calculation of the unit of magnetic moment in Bohr's theory of the atom. Moreover, the magnetic properties of the hydrogen atom have recently become of unusual interest because of the questions raised by the new quantum mechanics of Heisenberg,¹ Born and Jordan,² and by the new theory of Uhlenbeck and Goudsmit,³ which gives the "spinning electron" a magnetic moment of its own. Born,⁴ in quoting an unpublished work by Pauli on the theory of the hydrogen atom, has stated that Pauli's theory contemplates a non-magnetic atom. This however does not take into account the theory of Uhlenbeck and Goudsmit, which if accepted will make necessary an addition to Pauli's theory. This state of upheaval in the theories makes direct experiment very desirable.

¹ W. Heisenberg, Zeits. f. Physik, 33, 879 (1925).

² M. Born and P. Jordan, Zeits. f. Physik, 34, 858 (1925).

M. Born, W. Heisenberg, and P. Jordan, Zeits. f. Physik, 35, 557 (1926).

³ Uhlenbeck and Goudsmit, Nature, 117, 264 (1926).

⁴ M. Born, "Problems of Atomic Dynamics," M. I. T., Cambridge, Mass., '26.

In this work the magnetic properties of the hydrogen atom have been investigated. The experimental method was that of atomic ray deflection introduced by Stern and Gerlach⁵ in their investigation of the magnetic moments of several of the metal atoms. Stern and Gerlach secured direct evidence of space quantization and orientation when their rays of atoms were divided into separate rays on passage through an inhomogeneous magnetic field. Silver, copper, and gold showed a magnetic separation which yielded a value of magnetic moment closely equal to the Bohr unit magneton. One of the authors⁶ verified the work of Stern and Gerlach on silver in a modified apparatus, and in addition found the alkali metals sodium and potassium to possess unit magnetic moments.

The equation relating the amount of deflection of the atomic ray to the magnetic moment of the atom is

$$\frac{1}{M} = \frac{1}{2s} \left(\frac{\partial H}{\partial s} \right)_0 \frac{l^2}{3.5RT} \left\{ 1 + \frac{l^2 M}{12 \times 3.5RT \times s} \left[\left(\frac{\partial H}{\partial s} \right)_i - \left(\frac{\partial H}{\partial s} \right)_0 \right] \right\}$$

Here s is the amount of deflection measured as shown later; M is the magnetic moment (gauss-cm per mol); l is the length of the pole pieces of the magnet, the distance the atomic ray must travel through the magnetic field; $(\partial H/\partial s)_0$ is the value of the inhomogeneity of the field at the point where the ray enters the field; $(\partial H/\partial s)_i$ is the corresponding inhomogeneity at the end of the field, after the deflection of the ray. This is not equal to $(\partial H/\partial s)_0$ since $(\partial H/\partial s)$ changes in value from point to point across the field between the pole pieces, being greatest next to the knife-edged pole piece. The values of $(\partial H/\partial s)$ are obtained for any distance of the ray from the knife edge by a preliminary mapping of the field. The $3.5 RT$ term comes from the expression which Stern⁷ found in his direct measure of the velocity of the silver atom. In the present work the hydrogen atom has been found to be magnetic and its magnetic moment has been calculated.

A. ATOMIC HYDROGEN FROM THE DISCHARGE TUBE

The discharge tube. Hydrogen was prepared by the electrolysis of barium hydroxide solution, dried when desired by passing through a liquid air trap, and admitted to the discharge tube through a regu-

⁵ O. Stern, Zeits. f. Physik, 7, 249 (1921).

W. Gerlach and O. Stern, Ann. d. Physik, 74, 673 (1924).

W. Gerlach, Ann. d. Physik, 76, 163 (1925).

⁶ J. B. Taylor, Phys. Rev., 28, 576 (1926).

⁷ O. Stern, Zeits. f. Physik, 2, 49 (1920).

lated leak. In most of the work with the discharge tube, the hydrogen was not dried, in accordance with the procedure of R. W. Wood.⁸ The discharge tube was similar to that used by Wood, Bonhoeffer⁹ and Copaux.¹⁰ It was made of 18 mm Pyrex tubing and had a total length of 3.5 meters. The electrodes were cylinders made from aluminum sheet and crimped to tungsten lead-out wires. The electrode tubes were bent over as shown in Fig. 1, to prevent small particles dislodged from the electrode surface from falling into the central portion of the discharge tube. Such metallic particles were undesirable since they catalyze the recombination of atomic to molecular hydrogen, as was shown by the change in color of the discharge in the vicinity of such

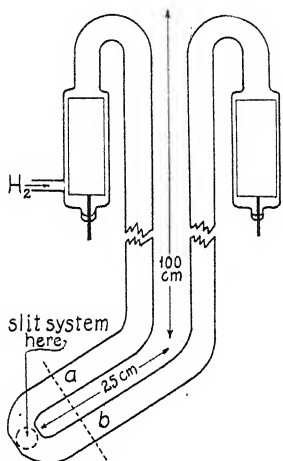


Fig. 1.

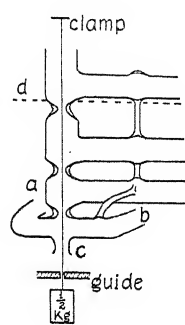


Fig. 1. The discharge tube.
 Fig. 2. Method of preparing the glass slit system.
 Fig. 3. Completed slit system, showing preliminary target.

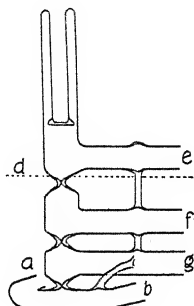


Fig. 3

particles from deep pink to white. These particles were seen to glow intensely in the discharge on account of the heat liberated on their surface. The tube was operated on a 1 kw transformer at 25000 volts. The pressure of undried hydrogen was 0.12 mm. Under these conditions a pure spectrum consisting of intense lines of the Balmer series against a black background was observed by means of a Zeiss pocket spectroscope. When the tube was first put into operation the complex secondary spectrum sometimes appeared in the background, but with

⁸ R. W. Wood, Phil. Mag. 42, 729 (1921).

⁹ K. F. Bonhoeffer, Zeits. f. Phys. Chem. 113, 199 (1924).

¹⁰ Copaux, Perperot, and Hocart, Bull. soc. chim. 37, 141 (1925).

prolonged operation of the tube this disappeared and pure Balmer series remained. This phenomenon was first described by R. W. Wood.

The slit system. To form the atoms present into a ray, an all-glass slit system was sealed to the central portion or foot of the discharge tube as indicated in Figs. 1, 2, and 3. When a metal slit system was sealed to the midpoint of the discharge tube, the discharge for an inch or more to each side was distinctly white. For this reason glass as a material for the slit system was preferred to metal.

Each of the three slits used was 0.075 mm wide and 3 mm long. They were constructed by placing a steel ribbon of these dimensions through a glass apparatus (Fig. 2), which had been constricted at three points. This ribbon was suspended from one end as shown, stretched taut by a weight on the other end, and adjusted to hang perfectly straight through a guide which permitted no twist. Then beginning at the top each constriction was heated in turn and the glass pinched with knife-edged tweezers on to the ribbon. Each pinch was followed by careful heating and annealing to relieve all strain in the system. This procedure gave the three slits the perfect alignment necessary for the formation of a sharply defined ray of atoms. Finally, after the three pinches had been made, the whole tube carrying the slits was given a prolonged annealing in a large air-free gas flame. When cooled to approximately 100°C it was then immersed in a hot bath of hydrochloric acid to dissolve out the steel ribbon. The glass rod supports shown between the side tubes (Figs. 2 and 3) served to keep the slit system rigid during and after the pinching treatment and yielded support to the fragile slits. These supports were not heated during the annealing. The system was sealed off at *c* (Fig. 2) and later made part of the discharge tube as shown in Fig. 1, by sealing on at *a* and *b*.

From each slit-chamber tubes led off through liquid air traps to separate high-speed mercury vapor pumps. This use of separate pumps maintained a progressively increasing vacuum in the system. In the discharge tube itself a pressure of 0.12 mm was produced through the leak valve from the hydrogen generator. The pump between the first and second slits then reduced this pressure to approximately 0.005 mm in the first chamber. On account of this reduced pressure, atoms leaving the discharge tube through the first slit and directed towards the second slit suffered only slight interference in their path. Then between the second and third slits another pump caused a reduction to less than 0.0001 mm. The increased free path in this chamber further favored the progress of the directed ray of atoms, and the third slit served to define the ray still more sharply. Stray hydrogen atoms may

have been removed also by recombination on the glass walls. This would aid in the production of a well-defined ray.

The target. This unidirectional ray entered the chamber above the third slit where it was received on a target of molybdenum trioxide (Fig. 3). The target was a ground fire-polished surface of glass which was coated with a very fine-grained deposit of molybdenum trioxide. The deposit was formed by holding the cold target intermittently in the smoke produced by igniting a piece of molybdenum sheet in a hot oxygen-gas flame. Very fine smoke particles resulted from the ignition. A surface when prepared properly showed no grain under a magnification of $26\times$ and was almost pure white, with a very slight yellow tinge. The image which the ray of atomic hydrogen formed on the target by reduction of the trioxide to a lower oxide, was a dark blue and was distinctly visible against the white background.

Assembly of the apparatus. In the preliminary tests without the magnetic field, the target was introduced as a re-entrant tube (Fig. 3, above the dotted line). The distance from the third slit to the target was 3 cm to reproduce the length of path required later in the magnetic measurement. With this preliminary apparatus the conditions for forming an image of the atomic ray were studied. When satisfactory conditions had been determined the upper portion was removed at d (Fig. 3) and the remaining slit system was cemented into the brass box (Fig. 4) containing the pole pieces.

This pole piece box had been used previously by one of the authors⁶ in the determination of the magnetic moments of the alkali metals, and it was modified only slightly to allow the replacement of the pair of metallic slits used in that investigation by the new glass slit system.

The slit system was held rigidly in a brass collar and plate with high melting de Khotinsky cement. Adjustment of the slit path to parallelism with the knife edge and to the desired distance from the knife edge was accomplished by motion of this plate, which was slotted about four screws set into the body of the box. When the slit path had been properly adjusted, the screws were tightened and all joints were made vacuum tight with a beeswax-resin mixture. The pole-piece box with its slit attachment was then clamped between the broad faces of the electromagnet,¹¹ and sealed to the discharge tube at a and b (Fig. 1), and to the vacuum pumps at e , f , and g (Fig. 5). The target consisted of a re-entrant glass tube of the form shown in Fig. 4. The preparation of the molybdenum trioxide surface has been described above. The

¹¹ The same electromagnet used in the previous investigation already mentioned.

target was sealed into the annular channel at the top of the pole-piece box with beeswax-resin mixture.

Fig. 5 shows the complete connections for a magnetic measurement with atomic hydrogen from the discharge tube. Pump No. 1 evacuated directly the first slit-chamber, and through stopcock *S* served to evacuate the discharge tube and connections to the hydrogen generator. Pump No. 2 evacuated the second slit-chamber and the pole-piece box. High range McLeod gauges were used to determine the vacuum conditions in the slit-chambers and pole-piece box.

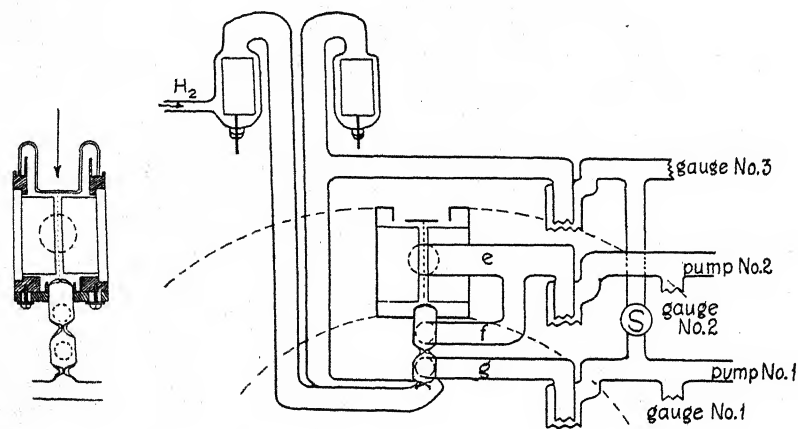


Fig. 4.

Fig. 5.

Fig. 4. Pole-piece box with slits and target attached.
Fig. 5. Diagrammatic sketch of complete connections. Dotted lines indicate position of electromagnet.

Procedure. With *S* open, a high vacuum of the order 10^{-6} mm or less was obtained in the entire system. *S* was then closed and the hydrogen leak regulated until an approximate pressure of 0.12 mm was obtained in the discharge tube, as recorded by McLeod Gauge No. 3. The discharge could not be maintained at pressures very much lower than this; while at higher pressures the ray became more diffuse, as was shown by a greater general reduction over the face of the target. For a run without magnetic field the discharge was then started. For a run with magnetic field the field was applied before the discharge was started. In the latter case, on account of the large heating effect caused by the magnetic field, it was found necessary to cool the foot of the discharge tube with running water. At the end of about twenty minutes a light line image caused by the ray could be seen distinctly by looking down on the target (as shown by the arrow in Fig. 4). It was

rather surprising that the image could be seen from the reverse side in this manner. This very desirable result was due doubtless to the extreme thinness of the molybdenum trioxide deposit and to the penetrating power of the ray of atomic hydrogen. At the end of approximately four hours the image appeared to have reached its maximum density. The target was then removed, the image was examined under the microscope, and measured with a micrometer eyepiece. Photomicrographs were then made of the image and of a comparison scale (0.1 mm divisions), by which means the micrometer measurements were confirmed.

Discussion of images. Fig. 6, I and II are photomicrographs $7\times$ of images secured without and with the magnetic field respectively. These photomicrographs were taken with light transmitted through the glass target and oxide coating. Separation into two lines is very distinct. A remarkable difference in the appearance of the image was noticed depending on whether it was viewed by transmitted or reflected light.

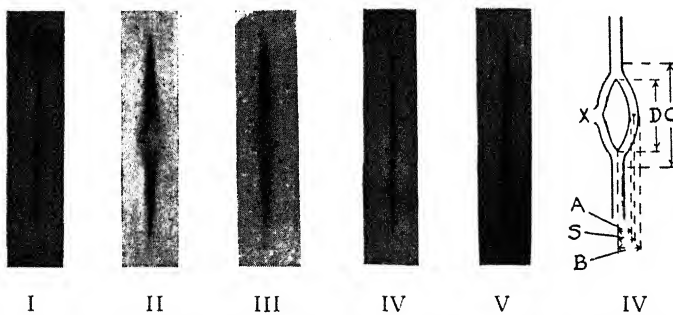


Fig. 6. I, II, III. Photomicrographs ($7\times$) of images secured with hydrogen discharge tube. I. Without field. II. With field, showing separation of ray. III. With field showing separation overshadowed by diffuse central ray.

IV, V. Images secured with atomic hydrogen from a hot filament. IV. Without field. V. With field, showing broadening secured with high velocity atoms.

VI. Diagrammatic sketch of II. $s=0.19$ mm, $c=2.2$ mm, $D=0.9$ mm, $A=0.08$ mm, $B=0.30$ mm.

Fig. 6, II shows clearly the two lines which were always most prominent by transmitted light. Fig. 6, III shows the entirely different appearance by reflected light. Here a central undeviated line with diffuse edges overshadows the deviated branches to such an extent that a casual observer might fail to notice them.

The following tentative explanation of this phenomenon is offered. The two branches seen in Fig. 6, II (transmitted light) are due to atomic hydrogen. The undeviated central line of III (reflected light) is due to hydrogen active chemically toward molybdenum trioxide, but probably not in the atomic state. The dissociation of molecules into atoms in the discharge is far from complete. Bonhoeffer⁹ estimates that 20 percent

only is dissociated under conditions similar to those of this experiment. The ray then consists in large part of hydrogen molecules. It is conceivable that high speed hydrogen molecules or excited molecules produced in the discharge might be active chemically but show no appreciable deviation in the magnetic field, thus accounting for the central undeviated line.

If this explanation is received as plausible, it remains to explain why the two branches (Fig. 6, II) ascribed to atomic hydrogen should be indistinct by reflected but very plain by transmitted light; whereas the undeviated line (Fig. 6, III) ascribed to molecular hydrogen should be far more distinct by reflected than by transmitted light. If it be assumed that atomic hydrogen penetrates the molybdenum trioxide coating to a greater depth than does molecular hydrogen, it is apparent that there will be much greater depth to an image formed by atomic hydrogen than to one formed by molecular hydrogen, and this depth of image will best appear when it is viewed by transmitted light, under which condition one observes the accumulated effect of reduction in all the layers. On the other hand, reduction due to molecules would be more superficial in character, and such an image would appear strong by reflected light, but would show very little opacity by transmitted light.

To test the idea that the central line might have been caused by high velocity hydrogen molecules, the hydrogen entering the lowest slit was heated to 400°C in the absence of a discharge. (The temperature of the discharge had previously been shown to be about 400°C. See below.) After 17 hours no image was visible on the target. This result shows that normal hydrogen molecules at the temperature of the discharge probably could not have caused the central line. It seems not unlikely that this undeviated line may have been due to excited hydrogen molecules from the discharge. The peculiar character of the central line as described above, and our present conception of the hydrogen atom seem to preclude the possibility that it was caused by atomic hydrogen.

The flattened cusp at the center of the left branch (Fig. 6, II) marked "X" in Fig. 6, VI, shows the position of the knife-edged pole piece. At this point the ray has actually been drawn against the knife edge by the greater inhomogeneity of the field at the edge. For this reason the more uniformly deflected right hand branch was chosen for the measurement of s . Fig. 6, VI is a diagram of II with dimensions. The distance s is the quantity used in the calculation of M , the magnetic moment.

Temperature of the discharge. Before a calculation of magnetic moment could be made, it was necessary to measure the temperature in the discharge tube. This temperature appears to be very uncertain on account of the violent electrical conditions existing in the discharge. To get an approximation of the temperature a glass-sheathed thermocouple (chromel-alumel, B. & S. No. 28) was sealed into the discharge tube and made to extend centrally down the entire length of the foot of the discharge tube (Fig. 1), a length of about 25 cm. The junction was not more than 3 cm distant from the point at which the slit system was sealed. A glass sheath was used in order to avoid to a large degree the false temperature effect which would have been observed with a

bare thermocouple on account of recombination of atomic hydrogen on its surface. The temperature recorded was about 390°C at the pressure (0.12 mm) used in the magnetic experiments.

Calculation of the magnetic moment. The data for the calculation of M , the magnetic moment of the hydrogen atom, are as follows. l , the pole piece length, 3 cm; the distance from the middle of the slits (i.e. of the ray) to the knife edge, 0.29 mm, corresponding to the value $(\partial H/\partial s)_0 = 140,600$ gauss/cm; $s = 0.19$ mm; $(\partial H/\partial s)_1 = 107,800$ gauss/cm; T the absolute temperature, 663°K. Upon substitution of these values into the equation given above, there results $M = 6050$ gauss-cm. This is 8 percent higher than 5600 gauss-cm, the magneton value calculated on the basis of Bohr's theory.

Errors. Should a high precision determination of the moment of the hydrogen atom be made, the following errors must be eliminated. (a) Errors in $(\partial H/\partial s)_0$ and $(\partial H/\partial s)_1$ may amount to 2 percent. (b) Three independent measurements of s by different observers from the same photomicrograph agreed within 2 percent. s cannot be measured with extreme accuracy at present since the deflected ray is slightly diffuse at its edges and is broader than the original ray. This "spreading" is a consequence of the Maxwellian distribution of velocities, i.e. the s for individual atoms is spread over a range of values. This can be remedied by producing a ray of single (or narrow-range) velocity atoms. Narrower slits would also reduce the uncertainty in the measurement of s by decreasing the width of the image of the deflected ray relative to the total splitting. The detection of the ray on targets of molybdenum trioxide was very satisfactory. The images formed were easily visible and permanent. (c) The temperature (velocity) error. There is an uncertainty of perhaps as much as 25° (approximately 4 percent) in the above value of the temperature of the discharge from the following causes. Slight fluctuations in pressure were unavoidable; and it was found that the temperature varied inversely as the pressure. Another uncertainty was the unknown extent to which the glass sheathing of the thermocouple catalyzed the recombination of the hydrogen atoms. This operated no doubt to make the observed temperature higher than the true temperature of the discharge. Since this factor was thought to be a very important one, 390°C probably represents a maximum value for the temperature of the discharge. Losses by conduction away from the thermocouple junction were minimized by leading the thermocouple wires through a considerable length of the discharge tube. For obvious reasons a metal radiation shield could not be introduced into the discharge, and consequently radiation losses

were uncertain and perhaps large. On account of the uncertainty of measuring the temperature of the discharge, a direct determination of the velocity of the atoms leaving the discharge tube (by a method similar to that used by Stern⁷ with silver atoms) will probably be the best way in the future of eliminating the temperature error.

The summation of errors in the above determination of the magnetic moment of the hydrogen atom may amount to 10 percent. Within experimental error then the hydrogen atom has been shown to have a magnetic moment equal to one Bohr magneton. This experimental result appears to be in harmony with Bohr's conclusions as to the magnetic properties of the hydrogen atom, and provides a condition that must be met by the newer quantum theories.

B. ATOMIC HYDROGEN FROM A HOT FILAMENT

Following the tests on atomic hydrogen made in a discharge tube, atomic hydrogen formed by the hot filament method of Langmuir¹² was investigated. The discharge tube was replaced by a simple glass chamber containing a tungsten filament spot-welded through nickel intermediate supports to tungsten lead-in wires (B. & S. No. 18). The filament consisted of 15 turns of 7 mil wire closely wound on a core of approximately 1 mm diameter. The filament was heated by a current of 2.5 amperes to a temperature estimated at 2800°C. It was placed within less than 1 mm of the first slit. Hydrogen was admitted as described for the discharge tube and the same pressure was used. To prevent possible poisoning and deterioration of the filament the hydrogen was first dried by passing it through a liquid air trap. The chamber was water-jacketed.

With all other conditions identical with those of Section A, an image on the molybdenum trioxide target was visible in about 40 minutes. However, as indicated in Plate 5, a splitting of the image did not appear. Because of the greatly increased velocity of the atoms formed on the glowing filament, the deflection of the ray in the magnetic field appeared only as a slight broadening. On account of the presence in the ray of extremely high velocity molecules, probably capable of reducing molybdenum trioxide, a heavy undeviated central line helps to overshadow the separation. Plate 4 shows the image in the absence of a magnetic field. With narrower slits the broadening might be resolved into a separation which would allow a calculation of the magnetic moment.

¹² I. Langmuir, *J. Am. Chem. Soc.*, **38**, 2221 (1916).

C. ACTIVE HYDROGEN BY THE MERCURY VAPOR, HYDROGEN, ULTRA-VIOLET LIGHT METHOD

Recently Cario and Franck,¹³ Taylor and Marshall,¹⁴ Bonhoeffer,¹⁵ and others have investigated the chemical reactions of the product formed on exposing a mixture of hydrogen and mercury vapor to ultra-violet light. The nature of the reactions obtained indicated the presence of atomic hydrogen. To conclude the present investigation, it was thought desirable to test the magnetic properties of active hydrogen produced by this method. The chamber containing the tungsten filament was replaced by a shorter chamber with a quartz end-plate and a reservoir of mercury. This chamber was heated to 45°C (the temperature employed in Cario and Franck's experiment), and exposed to the ultra-violet light from a water-cooled mercury arc. The quartz window of the arc was placed in contact with the quartz end-plate of the slit system. A pressure of hydrogen from 0.1 to 0.2 mm was maintained. The slit system and the rest of the apparatus were the same as in Sections A and B.

Preliminary trials in which re-entrant rods coated with molybdenum trioxide were sealed into the lower chamber resulted in almost instantaneous reduction of the white trioxide to the blue lower oxide. The test rods were then removed. After several runs with a slit system and target, one of which lasted for 43 hours, no trace of an image was secured on the target. This unexpected result led to a short investigation of the reasons for the failure to obtain a ray of the active product. A bare thermocouple (platinum, platinum-rhodium, B. & S. No. 36) was sealed into the reaction chamber in order to note any rise of temperature due to recombination of hydrogen atoms on its surface. No rise was noted. The same thermocouple sealed into a side tube leading from the discharge tube (Section A) and at 10 cm distance from the discharge showed a rise of temperature of more than 600°C. Furthermore a small amount of molybdenum trioxide introduced into the ultra-violet reaction chamber showed only slightly more than a surface reduction after an eight hour period of exposure. Boats of the trioxide similarly placed in side arms of the discharge tube showed reduction to a depth of a millimeter in a few minutes time.

The conclusion which may be drawn from the behavior of thermocouples, and from the chemical activity in the discharge tube and

¹³ Cario and Franck, Zeits. f. Physik 11, 161 (1922).

¹⁴ H. S. Taylor and A. L. Marshall, J. Phys. Chem. 29, 1140 (1925); J. Phys. Chem. 30, 34 (1926).

¹⁵ K. F. Bonhoeffer, Zeits. f. Phys. Chem. 119, 474 (1926).

the ultra-violet chamber respectively, is that atomic hydrogen if present in the latter case can be there in small amounts only. This may explain the failure to secure a detectable ray of atomic hydrogen in a reasonable length of time from the ultra-violet chamber. However, since our preliminary experiments with oxide coated rods showed that appreciable amounts of molybdenum trioxide were reduced by *some* active substance in the ultra-violet chamber, the failure to produce a beam may also be explained by the assumption that the active substance consisted not of atomic hydrogen but of short-lived excited hydrogen molecules¹⁶ or of mercury hydride.¹⁷ Either of these products might be expected to possess sufficient chemical activity to reduce molybdenum trioxide when first formed in the lower chamber, but might have too short a life to form a ray. This question is receiving further investigation.

In conclusion the writers wish to thank the Department of Physics for the use of the large Dubois magnet. They also wish to acknowledge the grant of funds from the Graduate School of the University of Illinois, which has made this research possible.

LABORATORY OF PHYSICAL CHEMISTRY,
UNIVERSITY OF ILLINOIS,
November 15, 1926.

¹⁶ E. K. Rideal and Hirst, *Nature*, **117**, 449 (1926).

¹⁷ K. T. Compton, *Phil. Mag.*, **48**, 360 (1924).

K. F. Bonhoeffer, *Zeits. f. Phys. Chem.*, **116**, 391 (1925).

THE MAGNETIC PROPERTIES OF EVAPORATED NICKEL AND IRON FILMS

R. L. EDWARDS

ABSTRACT

Coercive force, retentivity, and hysteresis loop forms for evaporated films of Ni and Fe.—Films of nickel and iron, produced by evaporation at low pressure, were studied with the object of verifying the reported existence of an abrupt change of coercive force at a critical thickness, and also to discover the cause of certain peculiar hysteresis loop forms. *Critical thickness* was found for iron films at approximately 50 m μ , in satisfactory agreement with Sorensen. At this thickness the coercive force changes abruptly from the high value of approximately 100 for thinner films. The observations were made upon films deposited on a base of aluminum foil, .0025 cm in thickness. The foil was heated previous to and during deposit. No such critical thickness was observed in nickel. Peculiar *hysteresis loops* were found. Nickel films unheated have very narrow loops, with magnetic induction nearly proportional to the field up to 139 gauss, where the induction is one-third to one-half that of the metal in bulk. Films heated previous to and during deposit give a magnetic induction at 139 gauss that is approximately three times as great, or like that of metal in bulk. But the retentivity and coercive force increase five-fold and become less like those of the metal in bulk. In similarly heated films of iron, these last two magnetic properties are also much greater than with metal in bulk. The peculiarities of the films are probably caused by the nature of the crystalline state. To what extent the phenomena depend upon the presence of the aluminum base is yet to be ascertained. The present view is that the presence of gas alters the crystal growth. On the whole the experiments seem to emphasize the importance of the influence of the crystalline state upon magnetic properties.

THE investigation of thin films of the ferromagnetic elements has disclosed two peculiar properties,—a very large change in magnetic induction at a fairly well defined critical thickness, and under certain conditions broad, nearly rectangular, hysteresis loops. The earlier work¹ done in this field was on films electrolytically deposited, and the above effects were attributed² to the influence of various occluded gases present, especially hydrogen. If, however, these properties are inherent in the metals themselves, the establishment of this fact is of importance in the theory of magnetism.

In order to test the magnetic as well as other properties of the ferromagnetic elements, deposited in the absence of contaminating influences,

¹ Seckelson, Ann. d. Physik **67**, 37 (1899). Maurain, Jour. d. Physique, **10**, 123 (1901); **1**, 90 (1902). Schild, Ann. d. Physik, **25**, 586 (1908); **1**, 151 (1902). Gans, Phys. Zeits. **12**, 911 (1911); and others.

² Kaufman and Meier, Phys. Zeits. **12**, 513 (1911).

this laboratory has been making a study of films produced by evaporation. Sorensen³ found some evidence of a thickness critical for coercive force in evaporated films of nickel at about $200 \text{ m}\mu$ and in iron at $55\text{m}\mu$. The coercive force changed abruptly to lower values as the thickness was increased.

The first purpose of the present investigation was to check these critical thicknesses. If they exist, are they independent of the various conditions accompanying deposition, such as the heat-treatment of the film, the emission velocity from the evaporating filament, and the residual gas pressure?

The apparatus used in this study was not essentially different from that used by Sorensen, to whose paper the reader is referred for details. The evaporation occurred in a horizontal cylindrical glass vessel, containing two film carriers, one below the hot filament and one above. An electric heater was placed under the lower one. The carriers moved back and forth perpendicularly to the filament and in a manner insuring a uniform deposit. Later observations by Mr. K. J. Miller have shown that the variation in film thickness does not exceed 5 percent except at the extreme edge of the film. As a base for the films, aluminum foil one mil in thickness was employed. The lower film is the hotter as the upper one is not only further from the heater, but it is also shielded from it by the lower foil. Temperatures of the lower foil were measured for various heating currents by means of a thermocouple. Temperatures at the upper position though not determined were in all cases much lower.

To reduce the initial magnetization observed by Sorensen in some of his films, brass parts were substituted for iron in the evaporation apparatus, but as noted later, this substitution failed to accomplish its purpose.

RESULTS FOR NICKEL

In order to determine the critical thickness of nickel, if such existed, a large number of films were deposited and tested. It was found that the thickness affected the magnetic properties only slightly if at all, but variations of the heat-treatment during deposition had very considerable effects. The films are therefore classified according to their heat-treatments.

The results are presented in Table I. Subsequent to nickel film No. 6 all films deposited in the lower position are listed under an odd number, those deposited above, under an even. The only films discarded were those which had oxidized, or those deposited during improper function-

³Sorensen, Phys. Rev. 24, 658 (1924).

ing of the evaporation apparatus. The graphs are plotted with ordinates 4π times the intensity of magnetization, rather than induction.

TABLE I

Nickel films having minimum heat treatment. δ is the film thickness in $m\mu$; β_{139} , the magnetic induction at 139 gauss; I_r , retentivity in percent; H_c , coercive force in gauss

Film No.	δ	β_{139}	I_r	H_c	Film No.	δ	β_{139}	I_r	H_c
8	23	1350	16	5	36	104	1940	26	24
2	39	1240	18	5	44	123	2100	32	32
5*	40	1330	30	11	13**	132	1680	31	35
40	67	2120	25	32	38	139	2100	28	29
14	75	1140	12	17	34	147	1520	12	10
32	77	2040	36	26	10	222	1300	25	28
20	90	1250	14	12	<i>Bulk nickel</i>				
22	96	1310	31	35	Annealed		4900	31	1.2
28	99	1430	32	35	Unannealed		3600	68	30

* 5 is an upper film.

**Heater not in action during deposition of 13.

Though most of the "unheated" films of Table I were subjected to the indirect heating effect of the heater in addition to that of the filament, the similarity of their loop forms would indicate that their temperatures did not differ widely. Films No. 34 and No. 10, Fig. 1, *a* and *b*, show the limits between which most of them lie. In Fig. 1, *c* is a hysteresis loop of a well-annealed specimen of the nickel wire (dimensional ratio 265) used for filaments, while *d* is a loop of an unannealed specimen of the same wire. All graphs of Fig. 1 are plotted on the same scale of magnetization and field strength.

The increasing retentivities and coercive forces with increasing thickness observed in Table I are probably due to the more prolonged heating which the thicker films necessarily received, since No. 34, $\delta=147$, for which the tube was water-cooled throughout, though a comparatively thick film, has the narrow form of loop shown by the thinner films. In those least heated, the coercive force and the area of the hysteresis loops are almost vanishingly small. In this respect they resemble well-annealed nickel. The dissimilar forms of their loops however make this similarity meaningless. The annealed bulk nickel is nearly saturated at a low field, while in the films, the magnetic induction is nearly proportional to the field up to the strongest fields that were available, yet at all points low compared with that of bulk metal.

All foils were heated in contact with a carbon lamp some twenty minutes before the pre-deposit weighing. Yet later work indicated that the occluded gas and water vapor still remaining on the foil largely affected

the magnetic properties of the film deposited thereon. To test this evidence, two films were deposited unheated on foils which had been heated

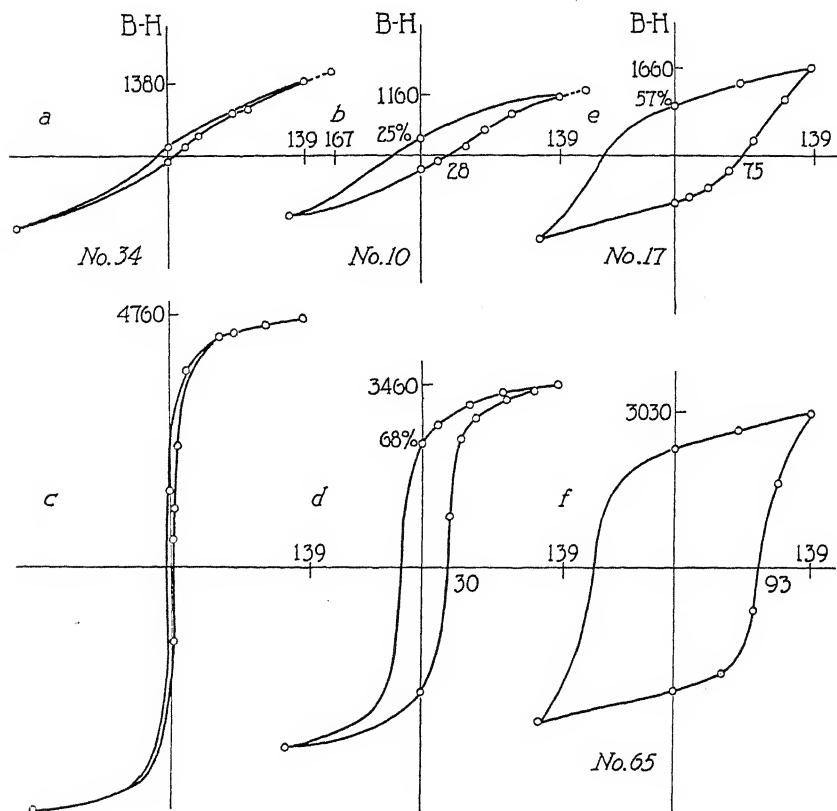


FIG. 1. Hysteresis curves for nickel films.

to 325° for forty minutes in the evaporation apparatus before depositing the films. The following results were obtained:

r	Film No.	δ	β_{139}	I_r	H_c
	72	83	2130	44	46.5
	71	161	2680	58	49

Changing the position of No. 72 in the evaporation apparatus during the interval between the heating and the evaporation process permitted its exposure to the atmosphere for several minutes and probably accounts for its lower induction, retentivity, and coercive force. Nevertheless both films show a decided increase in these properties over the films also deposited unheated but whose foils did not receive such a pre-deposit heat-

treatment. Their characteristics are very similar to those of the heated films of Table II following.

In order to determine the loss in weight of the foil due to extreme heating, two foils were heated to 325° for an hour in the evaporation apparatus and then reweighed. The loss in weight in neither case exceeded 0.05 mg, which corresponds to the weight of a nickel film of about 3m μ in thickness.

TABLE II

Nickel films heated during deposition, foils not previously baked. δ is the film thickness in m μ ; β_{139} and β_{167} , the magnetic induction at 139 and 167 gauss, respectively; I_r , retentivity in percent; H_c , coercive force in gauss

Film No.	δ	β_{139}	β_{167}	I_r	H_c	Film No.	δ	β_{139}	β_{167}	I_r	H_c
6	51	1700	1950	67	67	17	135	1800	2300	57	75
4	63	2300	2460	59	55	35	176	2550	2700	54	79
1	68	1740	1900	48	58	27	180	2430	2820	67	78
31	99	2510	3100	55	58	9	388	2160	2500	67	67
11	103	2010	2230	40	75						

Table II lists those films which were heated during deposition to a temperature of about 200°, but the foils of which were given no pre-deposit heating. Fig. 1 e shows the graph for a representative film of this group, No. 17, ($\delta=135$). There is no evidence of any critical thickness shown in this table.

Table III presents the data for the films whose foils were heated for forty minutes at 200° previous to deposition, as well as heated to the same temperature during deposition. These show a further large increase in coercive force and retentivity. Fig. 1 f is for film No. 65, ($\delta=257$), which

TABLE III

Films heated during deposition, foil previously well baked. δ is the film thickness in m μ ; β_{139} and β_{167} , the magnetic induction at 139 and 167 gauss, respectively; I_r , retentivity in percent; H_c , coercive force in gauss

Film No.	δ	β_{139}	β_{167}	I_r	H_c	Film No.	δ	β_{139}	β_{167}	I_r	H_c
51	50	1830	2800	59	81	73	179	2200	2650	80	96
63	63	1220	1900	72	104	53	182	2620	3100	75	87
47	76	2300	3600	81	99	69	183	2700	3200	76	96
67	78	1500	2100	58	87	87	219	2480	2850	70	88
41	94	2120	2800	72	104	59	224	2960	3350	73	84
45	97	2100	2680	62	94	43	230	2600	2780	67	81
39	104	2350	2850	65	104	37	244	3100	3500	78	93
61	107	1560	2200	69	104	65	257	3170	3520	78	93
21	123	2100	2600	71	104	77	259	2480	2950	68	89
15	161	2600	3000	76	83	55	276	2650	3000	74	78
81	168	2460	2820	71	90	89	304	2960	3300	75	89

may be taken as representative. These films were very hard both mechanically and magnetically. They were initially strongly magnetized, and the unsymmetrical hysteresis loops obtained for many would indicate

that demagnetization was imperfectly accomplished. No critical thickness is indicated.

Oxidation invariably accompanies deposition at temperatures of 300° with the tube exhausted no better than was feasible in this work. The magnetic effects are greatly reduced retentivity and coercive force,—the former by a fourth or fifth, the latter by a half. There is no decrease in the calculated magnetic induction, though a part of the weight of the film from which the magnetic induction is calculated is nickel oxide. The induction is low however compared with that of bulk metal.

The brass surfaces in the evaporation apparatus adsorbed much gas and prevented the attaining of vacua much better than .001 mm and when the tube was heated during the deposition of a film, rapidly rising pressures invariably occurred. When pressures reached about .005 mm, the evaporation and heating processes were interrupted to permit reduction of the pressure. The most serious result was in the unequal heat-treatments which different films, supposedly treated alike, received, and it is to these variations rather than to the pressure variations that the comparatively wide range of results for heated nickel films is probably due. Later test cases showed the magnetic characteristics to be practically independent of pressure up to at least .015 mm, that is, the magnetic properties of such films were certainly no less uniform.

After some of the nickel films used in this investigation had stood in air for six weeks, they showed a magnetic induction lowered by about ten percent. There was however no change in the retentivity or coercive force. The slow change in properties of nickel films was also observed by Peacock⁴ in his work on the Hall effect, and by Manning in his yet unpublished work on optical effects.

RESULTS FOR IRON

The brass parts introduced in the evaporation apparatus to reduce the initial magnetization, not only failed to accomplish their purpose with the nickel films, but also owing to adsorbed gases introduced serious difficulties in the pressure control. The brass parts were accordingly replaced with iron for the work on iron films. Pressures through this portion of the investigation were maintained at less than .001 mm.

Preliminary tests indicated a broadening of the hysteresis loops with increasing heat-treatment as was the case with nickel. But in order to test for the presence of a critical thickness, most of the iron films were given the same type of heat-treatment,—heating the foil to 200° for an hour and then depositing the film at the same temperature. As in the case

⁴ Peacock, Phys. Rev. 27, 474 (1926).

of nickel, the iron films of Table IV are listed in order of their thickness as calculated from their weighings. There is striking evidence of a critical thickness shown by this table. Typical hysteresis loops (No. 5 and No. 9) below and above the critical thickness are shown in Fig. 2, *a* and *b*.

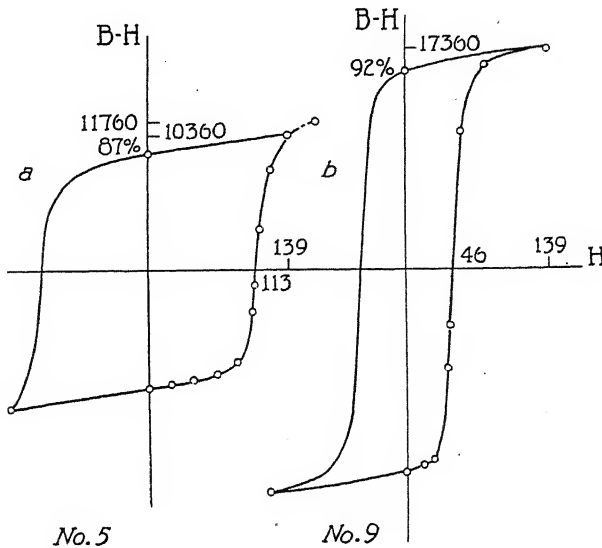


FIG. 2. Hysteresis curves for iron films.

The coercive forces of these films would indicate a thickness between 35 and 44 m μ as critical. However, the column of magnetic inductions

TABLE IV

Results for iron

δ is the film thickness in m μ ; β_{139} and β_{167} , the magnetic induction at 139 and 167 gauss, respectively; I_r , retentivity in percent; H_c , coercive force in gauss

Film No.	δ	β_{139}	β_{167}	I_r	H_c	Film No.	δ	β_{139}	β_{167}	I_r	H_c
45	22	15,450	16,100	88	89	9	68	17,500	17,800	92	46
5	28.4	10,500	11,900	87	113	35	69	17,000	17,400	90	45
29	30	13,800	16,600	89	110	15	69.5	16,300	16,400	92	43.5
19	34	8,600	10,200	77	99	43	71.5	16,300	16,600	92	39
49	35	15,300	16,200	93	95	11	79	15,400	16,000	90	46
39	44	19,250	19,600	91	49	3	85	18,100	18,200	90	35
41	54	16,000	16,600	90	52	7	141	15,200	15,400	83	23
21	54	16,100	16,200	91	48	Unannealed					
47	59	13,700	14,100	90	69	iron ^b		18,500	18,700	70	9

furnishes a valuable check on the correctness of the calculated thickness and indicates a slightly higher critical value. Film No. 39 is evidently of

^b Ewing, J. A., "Magnetic Induction in Iron and Other Metals."

a greater thickness than the value calculated from weighting. Taking $\beta_{189}=16,000$ as the average magnetic induction of films of near the same thickness from which to calculate the thickness of No. 39, we obtain $\delta_{39}=52$ instead of 44. Similarly calculating the thickness of No. 47, we obtain $\delta_{47}=50$ instead of 59 m μ , which would make 50 m μ appear as the best value of critical thickness. These corrections indicate that the error in the thickness determination may be as much as 15 percent. But Table IV gives unmistakable evidence of a thickness critical for coercive force, placing its value at approximately 50 m μ .

The iron filament shows a strong tendency to oxidize even at pressures of .001 mm. The maintenance of evaporation then requires a progressively increased heating current, and at much higher pressures evaporation may not be accomplished. The study of the effect, if any, of pressure variation on the magnetic properties of the iron films would obviously require the use of oxygen-free gas. This was not attempted.

According to Ewing⁵, the magnetic induction of bulk iron for the maximum fields used in this work should be about 18,700—(there is little difference in magnetic induction for annealed and unannealed iron at this field strength.) The magnetic induction obtained by the writer for evaporated iron films runs about 15 percent below this value. This does not agree with Sorensen's determinations which were of the order of 15 percent higher than that of bulk iron. The lower value would seem to be more in accord with the predictions of the Hall-effect in evaporated iron films^{4,6} in that the low value of field required to saturate the Hall e.m.f. implies that a smaller intensity of magnetization is possible in such films than in bulk metal. It is possible, however, that the difference in magnetic inductions in the two investigations is due to dissimilar heat-treatments.

SUMMARY OF RESULTS

This investigation of the magnetic properties of evaporated nickel and iron films was undertaken with the hope of determining the existence of a thickness critical for abrupt change in the coercive force, and of discovering the cause of certain peculiar hysteresis loop forms. Though difficulties arising from occluded gases may have prevented the appearance of a critical thickness in nickel, surprising consequences of various types of heat-treatment are revealed. Nickel films deposited unheated have very narrow hysteresis loops, remarkable in that the magnetic induction is nearly proportional to the field up to 139 gauss. The magnetic induction at this field is from a third to a half that of unannealed nickel in bulk. If, however, the occluded gases are driven out by a pre-deposit heating, the

⁵ Steinberg, Phys. Rev. 21, 22 (1923).

magnetic induction, retentivity and coercive force all increase very decidedly giving magnetic properties very similar to those obtained on heating only during the deposition of the film. But if these heat treatments are combined, a large further increase in these properties is obtained, in which case the films are very hard mechanically as well as magnetically, and though magnetic fields in the evaporation apparatus were neutralized as far as possible, these films were all initially rather strongly magnetized.

In iron there is observed a thickness of about $50 \text{ m}\mu$, which is critical for coercive force. This is approximately the value determined by Sorensen.⁴

The hysteresis loops for iron obtained in the two investigations both above and below the critical thickness are in agreement. Coercive forces and retentivities are numerically practically the same, but the present investigation gives values of magnetic induction which are about 30 percent lower than those of the earlier work.

DISCUSSION

There is a definite effect of heating the film, namely an abnormally large hysteresis loop, and, at large fields, a more nearly normal susceptibility. There is much evidence that these effects are in some way related to the crystal formation. That the deposition of a metallic film on a cold surface is amorphous was first stated by Langmuir.⁷ This theory has since had experimental verification with x-ray spectrograms⁸ and with the ultra-microscope⁹, while a post-deposit heating was found to induce a crystal growth. Ingersoll and DeVinney¹⁰ found that sputtered nickel films deposited at liquid air temperature were practically non-magnetic. After being heated, these films assumed their usual magnetic properties. Though in no case were the films of the present investigation deposited at a really low temperature, the magnetic induction of the least heated films is very small even in the strongest fields available, and there is reason to believe that if deposition had occurred at very low temperatures, the films might be non-magnetic. The temperature required to induce crystal growth during deposition, if this is the cause in the change in magnetic properties, is decidedly less than that required after deposition has occurred.

There are some extraneous influences present whose effects might be considered as masking the intrinsic properties of the metal. That the

⁷ Langmuir, Am. Chem. Soc. J. **38**, 2221 (1916).

⁸ Kahler, Phys. Rev. **18**, 210 (1921).

⁹ Reinders and Hamburger, K. Akad. Amsterdam Proc. **19**, 958 (1917).

¹⁰ Ingersoll and DeVinney, Phys. Rev. **26**, 86 (1925).

effect of a pre-deposit heating of the foil is due to driving off the gas can scarcely be questioned. The fact that a film deposited *unheated* on a foil, which has been *previously heated*, has magnetic characteristics very similar to those of a film produced on a foil which is heated *during deposition only*, might infer that heating the foil either before or during deposition merely drives off the gas. But heating the film during its deposition produces the same change and of a similar magnitude whether or not the gas has been initially baked out of the foil. In either case the loop forms become more rather than less abnormal. It is evident, then, that the peculiar hysteresis loops cannot be due to the presence of gas. On the contrary, it seems that the gas, directly or indirectly, interferes with the phenomena.

We have assumed that the aluminum foil base on which deposition occurs does not affect the magnetic properties of the film. There are, however, two possible ways in which its influence might be present. The projected particles from the filament may alloy with the aluminum of the base. Were this true, the magnetic properties of the film would show decided change with thickness as the comparatively slow velocity with which the molecules emerge from the filament could not penetrate a depth of several hundred molecules of the aluminum. A second possible influence of the base is its interference with magnetostriction. Though this would not seem great enough to be the cause of the peculiar phenomena, experiments are now being devised in this laboratory in which all influences of the base will be removed.

One other operation deserves notice. When the film with its aluminum foil base is rolled for insertion into the magnetic test apparatus, a compression of the film must occur. For a film of thickness $100 \text{ m}\mu$, on a foil of 1 mil thickness such as was used, rolled to a radius of curvature of 1 mm which is approximately the minimum, this compression would amount to about one percent. Furthermore one side of the film is compressed slightly (about one percent) more than the other. Though the compression is much more than the elastic limit of the metals employed, since all films are similarly treated in this respect, it would not cause the remarkable variation observed in the film properties. However annealing after the rolling process should be tried.

It is well known that hysteresis decreases with increasing crystal size of metal in bulk. These crystals are probably very large as compared with those of evaporated films. It has been suggested that the function which determines hysteresis may be of a type that vanishes for either very large or very small crystals. Jensen¹¹ regards hysteresis as largely deter-

¹¹ Jensen, J. Am. Inst. Elec. Eng. 43, 558 (1924).

mined by the amount of cementing material between the crystals which would ordinarily increase with decreasing size. It seems possible however that crystal strain or deformation may be a more important factor in determining hysteresis than mere crystal size. Perhaps perfect crystals are not formed by the evaporation process. The velocity of the particles on impinging may be too great for the molecular field properly to orient them. The observed film properties were not altered appreciably by changes in the velocity of emission, produced by variations of filament temperature. Welo and Baudisch¹² have produced crystals of magnetite by methods giving very different crystal sizes. Before they are annealed, their magnetic properties differ widely, but after annealing, even though crystal sizes remain dissimilar, their magnetic properties become similar. The necessity for annealing their crystals was probably occasioned by the rapidity of formation. It is possible that annealing the evaporated films would result in more nearly normal crystals.

McKeehan¹³ considers atomic magnetostriction as the prime cause of hysteresis, and in the experimental work on which his conclusions were based, this view would seem to be correct. It would be remarkable indeed if all hysteresis could be traced to this one cause. The evidence obtained by this study of thin films indicates that hysteresis is a crystalline rather than an atomic phenomenon.

In conclusion the writer wishes to express his appreciation to the members of the Department of Physics of the State University of Iowa for their assistance and interest, and especially to Professor G. W. Stewart under whose direction the work was carried on.

HALL OF PHYSICS,
UNIVERSITY OF IOWA,
July 10, 1926.

¹² Welo and Baudisch in a private communication.

¹³ McKeehan, Phys. Rev. 26, 274 (1925).

THE HALL EFFECT IN BISMUTH WITH SMALL MAGNETIC FIELDS

By C. W. HEAPS

ABSTRACT

The Hall coefficient for a bismuth plate of dimensions $0.011 \times 0.9 \times 2.0$ cm has been measured for magnetic fields ranging from 0.07 to 2.40 gauss. The average value of the Hall coefficient, R , in this range was 11.5, and variations of R due to change of field strength in this range were less than experimental errors. For larger fields the Hall coefficient of this specimen decreased from 13.5 for a field of 650 gauss to 5.9 for a field of 8600. It is concluded that for similar ranges of field the data reported by Palmer H. Craig are erroneous, probably because of insulation leakage or uncompensated thermomagnetic effects. A simple method of making very thin bismuth plates is described.

INTRODUCTION

IT IS a well known fact that the coefficient of the Hall effect for ordinary cast bismuth increases as the magnetic field is diminished.¹ Recently Palmer H. Craig has reported² surprisingly large values of this Hall coefficient when magnetic fields smaller than about 0.3 gauss were used, and he suggests that modifications will have to be made in the theory of the Hall effect in order to account for his results. There are already several other phenomena connected with the Hall effect which theories have not explained; the genuineness of this new phenomenon should therefore be very thoroughly established.

The writer on several occasions has measured very small electromotive forces produced by the Hall method and has experienced some difficulties because of insulation leakage in various parts of the circuit. This leakage, if it exists, will usually result in a specious magnification of the Hall constant. Another difficulty sometimes arises if thermo-electric currents have to be balanced out of the Hall circuit. The Joule heat of the primary current must be dissipated in the specimen, and it is very difficult to secure uniform temperature under these conditions. Convection currents and irregularities of structure of the specimen are apt to produce slight temperature differences, and these result in thermal e.m.f.'s when associated with contacts used for detecting the Hall e.m.f. Such thermal e.m.f.'s may be balanced out by the potentiometer when no magnetic field acts. Putting on the field, however, will destroy this balance, since the thermoelectromotive force of bismuth with respect to copper is altered by the presence of a field.

¹ Campbell, "Galvanomagnetic and Thermomagnetic Effects," p. 42.

² Craig, Phys. Rev. 27, 772 (1926).

The result might be an apparent exaggeration of the Hall e.m.f. To detect such an effect the primary current must be broken and the effect of a magnetic field on the potentiometer setting noted before there is time for equalization of temperature in the specimen.

To eliminate errors of this kind it is often sufficient to reverse the direction of the magnetic field and calculate the mean of the Hall e.m.f.'s for the two directions of field. The thermal effect is thus averaged out, since it does not reverse with the field while the Hall e.m.f. does.

Craig appears to have been very careful about mounting his specimen but does not mention any special precautions taken to keep his electrical circuits insulated from each other. Also, he states that "potentials due to Thomson and allied effects were accurately measured the instant the longitudinal current was broken,"—however, he apparently did not test for the effect of the field on these potentials. Furthermore, it does not appear in his paper that spurious temperature effects were averaged out by reversing the magnetic field.

Because of the possibility of these sources of error in Craig's work the writer has made some measurements of the Hall coefficient in weak magnetic fields and has not found the abnormal values reported by Craig.

APPARATUS

A thin plate of bismuth (listed by Eimer and Amend as c.p.) was made by the following method. A glass tube with one end drawn down slightly was clamped vertically and a bismuth rod inserted. The rod was prevented from slipping out of the bottom by the slight constriction there. About 10 cm below the end of the tube was placed a clean, horizontal glass plate. The lower end of the glass tube was now heated with a small flame till the bismuth melted and a single large drop was allowed to fall on the glass plate below. By a little practice in adjusting temperatures and distance of fall very thin, uniform, circular films of metal can be produced on the glass plate in this way.

The film chosen for experimentation was 0.011 cm thick, and was cut into a rectangular shape of dimensions 0.9×2.0 cm. Small arms of bismuth were left projecting from the sides of the specimen and the terminals for the Hall e.m.f. were soldered to the ends of these arms with Wood's metal. The leads for the primary current were soldered to strips of sheet copper which in turn were fixed with Wood's metal to the bismuth specimen.

Manipulation of the plate was not difficult because it was rather tightly adherent to the glass upon which it was formed. Hence, it was

possible by carefully scraping the edge of the plate to adjust the Hall electrodes so that they were quite accurately on an equipotential surface when the primary current flowed and there was no magnetic field.

For the sake of thermal insulation a thick coat of paraffin was put over the plate and over the junctions of all wires leading to it, and a layer of cotton was wrapped around the whole assembly. It was then mounted, with ebonite insulation, on a stand arranged with a graduated circle so that the specimen could be rotated about a horizontal axis in the plane of the plate and parallel to its length.

The Hall electrodes were connected through a potentiometer to a galvanometer of resistance 16.6 ohms and sensitivity 17.3 mm per microvolt. The primary current electrodes were connected through an ammeter and rheostat to a 6-volt storage cell. The galvanometer circuit and the primary current circuit were insulated from the earth and from each other by ebonite,—except, of course, where interconnection occurred in the bismuth plate.

When a primary current of 1.3 amperes was sent through the specimen it required about half an hour to secure constant temperature conditions. After that length of time the galvanometer reading remained quite constant, or drifted so slowly as not to interfere with observations.

For producing the magnetic field a pair of Helmholtz coils was used. Each coil had a radius of 10.2 cm and consisted of 5 turns of No. 24 enamelled wire on a carefully turned micarta form. The field for a given current was calculated from the dimensions of the coils. The effect of the earth's field was eliminated as in Craig's work, by setting the plane of the bismuth plate parallel to the earth's field.

Measurements were made as follows. The galvanometer readings were noted in quick succession for the field in one direction, for the field reversed, and for the field in the original direction. The reading for the reversed field was subtracted from the average of the first and third readings and the difference divided by two. The result gave the deflection due to the Hall effect for the field used, and errors due to slow drift of the galvanometer were eliminated. The corresponding e.m.f. was calculated from the known sensitivity of the instrument. This method is quick and accurate, and it gives the same result as the potentiometer method provided the potential drop in the specimen due to the galvanometer current is negligible compared with the Hall e.m.f.³

³ Heaps, Phys. Rev. 12, 346 (1918).

The potentiometer in the galvanometer circuit was used for balancing small thermal e.m.f.'s and for obtaining the sensitivity of the galvanometer.

The sensitiveness of the apparatus was such that turning the plate over so as to reverse the earth's field gave a deflection of 24 mm.

RESULTS

The table gives a set of results obtained for small magnetic fields.

TABLE I

The Hall coefficient for bismuth for small fields, with a primary current of 1.3 amps.

H (gauss) :	0.07	0.09	0.13	0.23	0.29	0.35	0.40	0.51	0.77	1.06	1.54	2.40
R :	11.4	11.3	11.0	11.3	11.3	11.8	11.5	11.7	11.9	11.6	11.6	11.7

Here H is the magnetic field strength and R is the Hall coefficient calculated in the usual way. Each value of R recorded above is the average of at least five values. These five values for any one field differed among themselves by about as much as the different values of R in the table. Apparently the change of R for a range of magnetic field from 2.4 to 0.07 gauss is no greater than the errors of the experiment. Craig found R increasing by a factor of more than 10 in this same range.

To test the effect of electric leaks one side of the potentiometer was connected by a wire to the slate bench on which the apparatus was disposed. Craig states that such a connection in his apparatus was found to increase stability, so presumably he used it in his work. It introduces a leak to ground in the galvanometer circuit. Another wire was next used to connect the enamelled iron tube of the rheostat in the primary current circuit to the floating side of the reversing switch in the circuit of the Helmholtz coils. No particular care had been taken to insulate these coils from the slate table top, and the 6-volt storage battery used for exciting the coils was standing directly on the tile floor supporting the table. This second wire thus served as a leak from the primary current circuit to ground, and the effectiveness of the leak was altered by closing the reversing switch.

With these leaks in operation and a current in the coils to give a field of 0.06 gauss, the galvanometer deflections were 4.1 and 2.0 cm, respectively, for the two settings of the reversing switch. The smaller of these deflections gives an apparent Hall coefficient about 17 times too large for this field. When larger magnetic fields were used the effect of these leaks was not so apparent because the deflections which they produced were in this case smaller than the deflections due to the Hall e.m.f.

The curve of Fig. 1 shows how the Hall coefficient of this particular specimen varies for strong magnetic fields. These fields were produced by a Weiss electromagnet with pole pieces 10 cm in diameter and 2.3 cm apart. The fields were measured with a bismuth spiral. There is no evidence of a rise in the curve as the field increases, though Craig found R increasing from 15 to 29 as the field increased from 1000 to 4220.

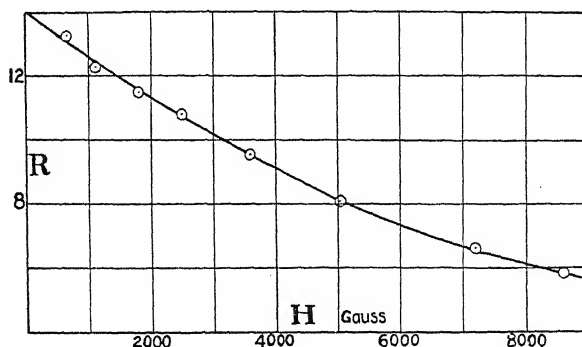


Fig. 1. Variation of the Hall coefficient, R , with the field strength, H .

The curve of Fig. 1 indicates a larger value of R for small fields than the data of Table I show. This apparent discrepancy is due to the fact that a primary current of only 0.2 amperes was used in getting the curve, while 1.3 amperes were used for the data of the table. The larger current heated the thin bismuth plate very perceptibly and the resulting rise of temperature diminished the Hall coefficient.⁴

CONCLUSIONS

For bismuth in the form of a crystal conglomerate the Hall coefficient diminishes in regular fashion as the magnetic field increases. There is no abnormal increase of the coefficient as the field becomes very small.

It appears probable that Craig's results are incorrect because of imperfect insulation of his apparatus. He states that the stability of his system was increased by grounding his potentiometer. There should, however, be no instability which could be corrected in this fashion unless leaks of variable resistance are present.

It is also possible that the lack of agreement of Craig's results with those reported in the present paper is due to his not having eliminated thermomagnetic effects.

THE RICE INSTITUTE,
HOUSTON, TEXAS,
October 18, 1926.

⁴ Campbell, "Galvanomagnetic and Thermomagnetic Effects," p. 49.

TEMPERATURE DISTRIBUTION ALONG A FILAMENT

By V. BUSH AND KING E. GOULD

ABSTRACT

A method has been developed for adapting a new integrating machine to the solution of: (1) the integral equation which applies to the distribution of thermionic emission along the central portion of a long filament in an evacuated vessel, the effect of the thermionic emission upon the filament temperature (by changing the heating current as well as by a direct cooling action) being considered; (2) the differential equation which applies to the temperature distribution near the end of a long filament from which the thermionic emission is negligible compared with the filament heating current; (3) The integro-differential equation which applies to the distribution of temperature and thermionic emission along an entire filament heated, in an evacuated vessel, by a direct current. This takes into account the effects of thermionic emission as well as cooling due to thermal conduction. All these solutions fully account for the variation of the following quantities with temperature, graphical relations being used throughout: (a) thermal conductivity; (b) thermionic emission; (c) resistivity; (d) radiation. The method has been applied to various typical cases of tungsten and thoriated tungsten filaments, and in those cases where an experimental check was possible it was found that the results were in good agreement with the measured quantities.

INTRODUCTION

THE differential equations which represent physical conditions along an incandescent filament heated by a direct current may be set up easily, and, with certain simplifying assumptions, solved by formal methods. Even with these simplifying assumptions, such solutions become very laborious, and when the empirically determined variations of the parameters are to be taken into account, such formal solutions become impossible.

There has been developed, in the Massachusetts Institute of Technology Electrical Engineering Research Laboratory, an integrating machine which may be adapted to the solution of numerous types of differential and integral equations, and the equations which apply to the incandescent filament are among these. The integral equation which applies to the part of an electrically heated, thermionically emitting filament over which the cooling due to the thermal conductivity of the filament is small may be solved directly upon this machine. Furthermore, by a method of successive approximations, the integro-differential equation which takes into account the thermionic current as well as cooling by thermal conduction to the filament supports may

be solved by means of this new device. In every case the actual resistivity, thermal conductivity, radiation emissivity, and thermionic emission, as functions of the temperature, are considered; graphical, rather than analytical relations being used throughout.

The object of this paper is to show the method of attack upon this filament problem, to present some of the typical results obtained, comparing them with measured quantities, and to bring together in a single check various empirically determined properties of tungsten and thoriated-tungsten filaments.

EQUATIONS WHICH EXPRESS PHYSICAL CONDITIONS

No cooling due to thermal conduction. Consider the central portion of a long filament heated by a direct current, and let the filament be emitting thermionically at such a rate that the total emission over the portion considered is great enough to affect the filament current, all emitted electrons being drawn from the wire to a neighboring plate by an electric field. The emission is sometimes comparable with the filament current in the case of thoriated-tungsten or oxide-coated filaments, or with filaments in alkali vapor. Let it be assumed that the cooling due to thermal conductivity is negligible over this part of the filament, as it will be if the filament is very long. The following identity applies to any element in this portion of the filament;

Electrical Input = Radiation output + Cooling due to thermionic emission. Or,

$$i^2 R_T = f(T) + \phi I \quad (1)$$

where i is the filament current, which is a function of the distance along the filament (considered throughout this paper as measured from the negative end of the portion of filament); R_T is the resistance of the filament per unit length, as a function of the absolute temperature, T ; $f(T)$ is the radiation per unit length of filament at the temperature T , and ϕI is the cooling per unit length of filament due to the thermionic emission, I , at the temperature T , ϕ being the work function for the filament material in equivalent volts.

If i_0 represents the filament current at the negative end of the portion of filament considered, then i is given by

$$i = i_0 - \int_0^x Idx \quad (2)$$

and thus Eq. (1) becomes

$$i_0 - [(f(T) + \phi I)/R_T]^{1/2} = \int_0^x Idx \quad (3)$$

which may be written in the form

$$\psi(T) = \int_0^x F(T) dx \quad (4)$$

Emission neglected. If the filament is such that the emission current is negligible compared with the filament current, then the filament current, i , remains constant along the wire, as is the case usually with pure tungsten filaments. In this case the cooling due to thermionic emission is usually entirely negligible. Taking the cooling due to thermal conductivity into account,

Electrical input = Radiation output + Conduction output, or

$$i^2 R_T = f(T) + \left[-K_T \frac{d^2 T}{dx^2} - \frac{d K_T}{dT} \left(\frac{d T}{dx} \right)^2 \right] \quad (5)$$

where K_T is the thermal conductivity of the filament per unit length, at the temperature T , x is the distance from a support, and the other symbols have the same meaning as before.

In one case (Fig. 7), the second conduction term in the square brackets of Eq. (5) was neglected. There is no loss of generality of the method in doing this, as a new temperature scale, T' , may be adopted with which the conduction output will be given by one term only, $[-K d^2 T' / dx^2]$, K in this case being constant. This will be demonstrated below. After making this substitution we may write

$$d^2 T' / dx^2 = (1/K) [f(T) - i^2 R_T] = \lambda(T) = \lambda'(T'). \quad (6)$$

Emission and thermal conductivity both accounted for. If the emission is sufficient, and enough of the emitted electrons are removed by an electric field, the filament current is appreciably affected. Assuming that all emitted electrons are removed, the equation which represents conditions along the filament is,

$$i^2 R_T = f(T) - K(d^2 T' / dx^2) + \phi I \quad (7)$$

the temperature scale which makes the thermal conductivity constant being adopted. x here represents the distance from the support at the negative end of the filament.

Eq. (7) may be written

$$\left[i_0 - \int_0^x I dx \right]^2 R_T = f(T) - K(d^2 T' / dx^2) + \phi I \quad (8)$$

or

$$(f(T) - K d^2 T' / dx^2 + \phi I) / R_T^{1/2} = \int_0^x I dx \quad (9)$$

Temperature scale to give constant thermal conductivity. In terms of degrees absolute, the conduction output per unit length of filament is given by the bracketed expression in Eq. (5). But in terms of the new temperature scale T' , this is assumed to be $[-Kd^2T'/dx^2]$ where K is an arbitrary constant. Thus

$$K_T(d^2T/dx^2) + (dK_T/dT)(dT/dx)^2 = K(d^2T'/dx^2) \quad (10)$$

This has the solution

$$T' = (1/K) \int_0^T K_T dT + K_0 \quad (11)$$

which gives the relation between T' and T , K_0 being a second arbitrary* constant. Any value of K and K_0 may be assumed; the final result in terms of T will be the same in any case.¹

SOLUTION OF EQUATIONS

In solving the differential and integral equations, the values of resistivity, thermal conductivity, and radiation intensity of tungsten, as functions of the temperature, were taken from a paper by Forsythe and Worthing,² while the thermionic emission from tungsten and thoriated tungsten, as a function of the temperature, and the work function for thorium were taken from a paper by Dushman.³ For lack of better knowledge, the thermal conductivity has been assumed constant up to 1000°K, and equal to its value at that temperature, the variation above this temperature being taken into account.

Eq. (5) may be solved directly upon the integrating machine, to give the thermionic emission per unit length, against distance from any given point on the filament. This solution, as has been noted, neglects all effects due to thermal conductivity. It is particularly fortunate that the emission can be directly determined, as it is the emission that is wanted, more often than not, in such a problem, and if the temperature distribution is desired it may readily and accurately be obtained from the emission curve.

Fig. 1 shows a typical result obtained by this method. This is drawn for a thoriated tungsten filament three mils in diameter carrying 0.976

¹ A description of the integrating machine and its use in evaluating such integrals as that of Eq. (11) will be found in the Jour. Frank. Inst. Jan. 1927. The adaptation of this machine to the solution of equations such as (5), and (8), is not included in that paper, but the authors of the present paper hope to publish an article on that subject in the near future.

² Forsythe and Worthing, Astrophys. J. 61, 147 (1925).

³ Dushman, Gen. Elec. Rev. March 1923.

amperes at the point from which the distance is measured (which is the negative end of the portion of filament considered), and it is assumed

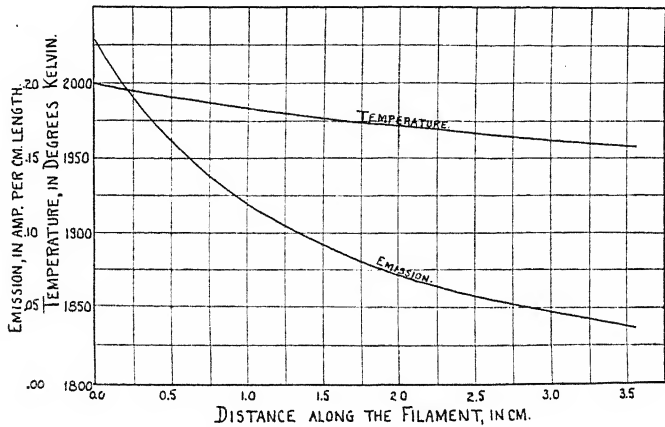


Fig. 1. Variation of temperature and thermionic emission along a thoriated tungsten filament, diam. 3 mils, current 0.976 amps.

that all emitted electrons are carried away to an adjacent plate by an electric field.

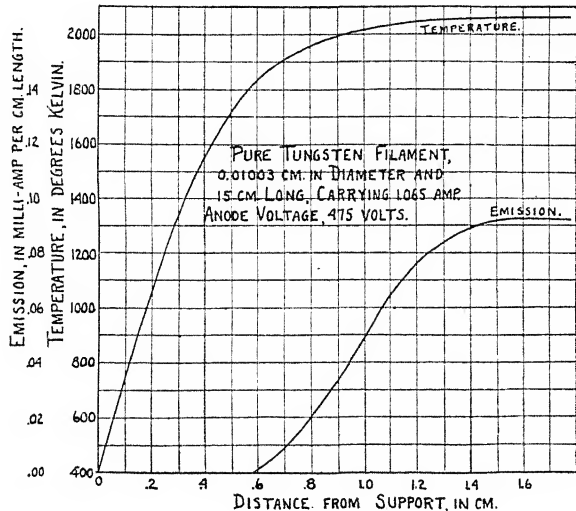


Fig. 2. Solution of Eq. (6) neglecting the cooling term.

Fig. 2 represents the solution of Eq. (6), using the absolute temperature scale, with a variable thermal conductivity, but neglecting the second cooling term. The boundary conditions were: at $x=0$, $T=$

400°K, and when $i^2R_T = f(T)$, $dT/dx = 0$. The latter assumption is equivalent to saying that the filament was so long that the temperature at the center became that of a similar filament infinitely long. This is practically the case. As the filament was of pure tungsten, the thermionic emission had virtually no effect upon the temperature distribution.

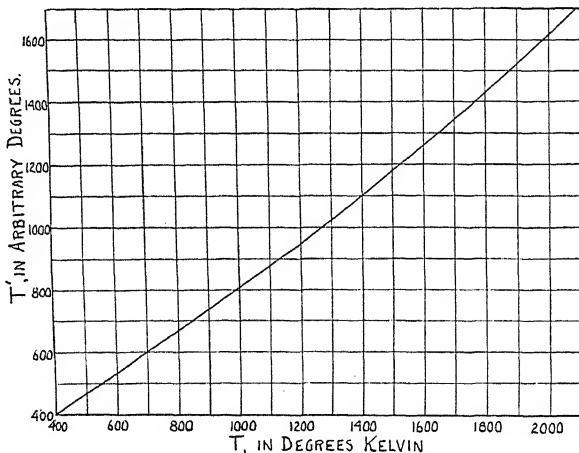


Fig. 3. Relation of the temperature scale T' for which the thermo-conductivity of tungsten is constant to the absolute temperature scale, T .

Fig. 3 shows the relation of the temperature scale T' , for which the thermal conductivity of tungsten is constant, and equal to 1.23 watts per cc per degree C, to the absolute temperature scale T , and represents a solution of Eq. (11). Fig. 3 was obtained by integrating, with the integrating machine, the thermal conductivity, K_T , plotted against the absolute temperature, K being chosen to give a convenient scale for T' , and K_0 being such as to make the two scales coincide at 400°, that is,

$$T' = (1/K) \int_{400}^T K_T dT + 400$$

Fig. 4 represents the solution of Eq. (8), using the temperature scale T' , for the filament of Fig. 2, under similar conditions. Thus Fig. 4 should give the correct temperature distribution, rather than Fig. 2, which is only an approximation. However, a comparison of Figs. 2 and 4 will show that the effect of neglecting the second cooling term is, in this case at least, very small indeed.

The data for the filament to which Figs. 2 and 4, as well as Fig. 5, apply were taken from a paper by Dushman, Rowe, Ewald, and Kidner⁴ (Tube 107-1). The calculated values check quite well with

⁴ Dushman, Rowe, Ewald and Kidner, Phys. Rev. March, 1925.

the measured quantities, as will be seen from the data in Table I. Fig. 5 is just the same as Fig. 4, except that it is drawn for a smaller filament current, and was determined as a further check of the method, and also of the data in the paper noted above.

TABLE I

Data for the filaments referred to in Figs. 2, 4 and 5.

The quantity f is the ratio of emission which would exist if the entire filament were at maximum temperature to the actual total emission.

	Fig. 2		Fig. 4		Fig. 5	
	Calc.	Meas.	Calc.	Meas.	Calc.	Meas.
Filament voltage (volts):	11.99	11.77	12.02	11.77	9.32	9.12
Maximum temperature ($^{\circ}$ K):	2070	2065	2070	2065	1900	1897
Total emission (m.a.):	1.21	1.15	1.21	1.15	.110	.1065
f :	1.147	1.143	1.147	1.143	1.18	1.167

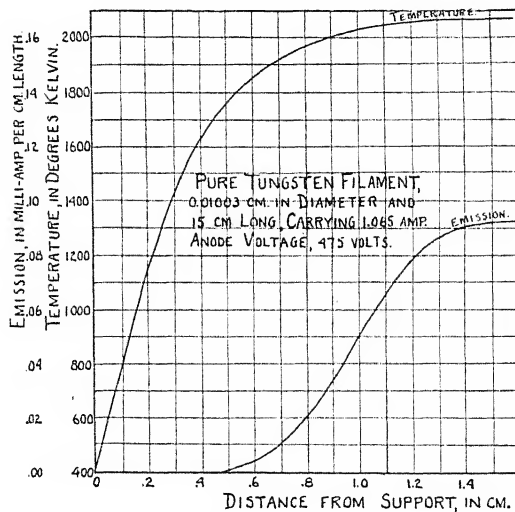


Fig. 4. Solution of Eq. (8) using the temperature scale, T' .

Fig. 6, which is drawn for a thoriated tungsten filament with zero potential gradient at the cathode (that is, with an electric field just great enough to remove all emitted electrons), represents the solution of Eq. (8), with the boundary conditions; when $x=0$, $T=400^{\circ}\text{K}$, when $x=\text{length of filament}$, $T=400^{\circ}\text{K}$, and the assumption that over the central part of the filament there was no cooling due to thermal conductivity. This cooling was found to be negligible in the actual case. It will be noted that the emission falls off very rapidly as the distance from the negative end of the filament increases, because of the drop in filament temperature produced by the decrease of filament current.

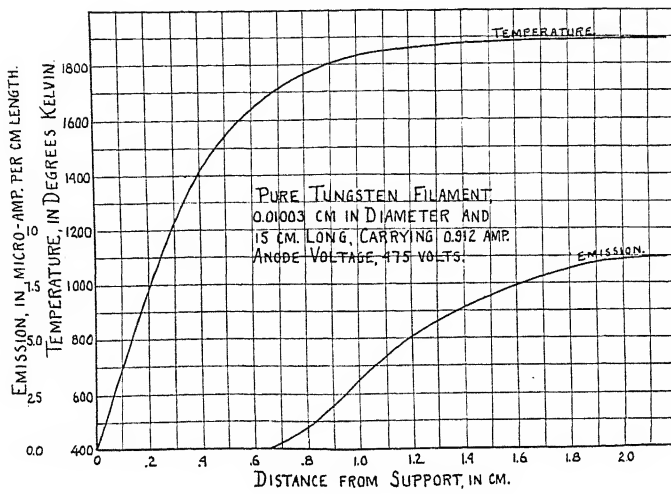


Fig. 5. Solution of Eq. (8) using the temperature scale, T' . The filament current is less than for Fig. 4.

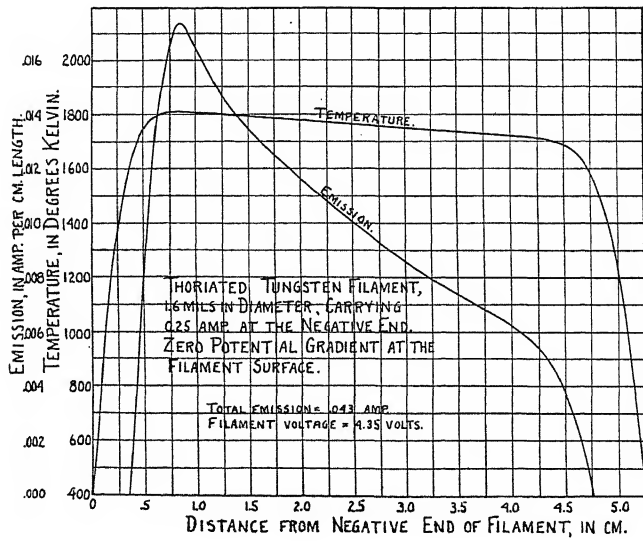


Fig. 6. Solution of Eq. (11) assuming the temperature to be 400°K at the ends of the filament.

Fig. 7 shows that the cooling due to thermionic emission from the thoriated tungsten filament is considerable, the error in maximum temperature which would result if this cooling term were neglected being about 125°K. Fig. 7 also gives some idea of the effect of other terms in Eq. (8), and shows the several steps in obtaining the temperature distribution of Fig. 6 from $x=0$ to the point where dT/dx is 0. First the filament current was assumed constant, and curve (4) was determined. The second cooling term was neglected here, but the effect

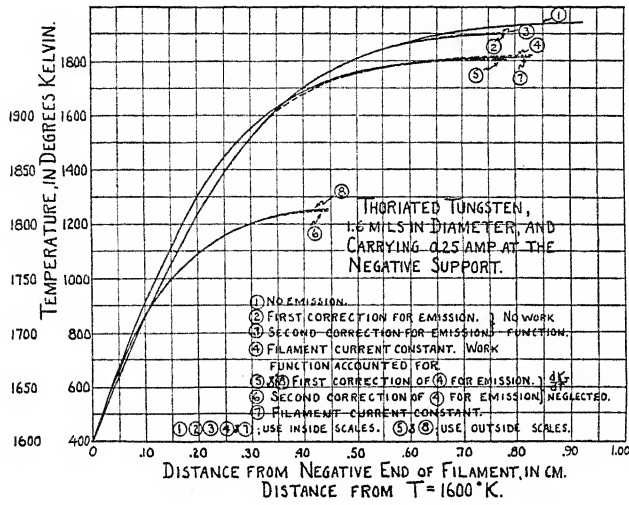


Fig. 7.

is very small, as a comparison of curves (7) and (4) will show. Then the value of $\int_0^x Idx$, as a function of x , was determined from curve (4), and placed in Eq. (8) which was solved, as before, for curve (5). Curve (6) was obtained from (5) in a similar manner, and as these last two were practically coincident, the maximum difference being about 2°K, the successive approximations were carried no further. The central portion of the emission curve of Fig. 6 represents the solution of Eq. (3), and the temperature distribution near the positive end of the filament was determined just as for the negative end.

A Fellowship from the Coffin Foundation made possible the pursuance of this work.

ELECTRICAL ENGINEERING RESEARCH LABORATORIES,
MASSACHUSETTS INSTITUTE OF TECHNOLOGY,
April, 1926.

BOOK REVIEWS

Handbuch der Physik. Edited by H. GEIGER UND KARL SCHEEL. Band I, *Geschichte der Physik. Vorlesungstechnik.*—The first 179 pages of this volume is a history of physics from antiquity down to the year 1895, from the pen of E. Hoppe of Göttingen. The history is prepared largely from original sources or from recent articles and monographs on special historic topics. It is rich in bibliographical references. That antiquarian research is bringing to light matters of interest to physicists is evident from the fact that Hoppe devotes three pages to Babylonian developments in arithmetic, astronomy and metrology. The author makes out a case in favor of a Babylonian "absolute system" of units. Time was measured by sun-dials and also by water clocks. The unit of weight (mine) was the amount of water escaping in a unit of time (sussu) from an opening at the bottom of a vessel kept full of water. Thus, it is suggested that the Babylonian yard, mine, sussu corresponded to our C G S-system. The author is quite free from national bias. Attributing the electric telegraph to Gauss and Weber, and failing to mention Joseph Henry whose Albany experiments came somewhat earlier, is only an oversight. The treatment of the history of the nineteenth century is necessarily condensed and is not without gaps. But all things considered, this outline history of physics deserves commendation.—Pp. 404. Julius Springer, Berlin, 1926. FLORIAN CAJORI

Anregung von Quantenspruengen durch Stoesse. J. FRANCK and P. JORDAN.—The experiments of Franck and Hertz in 1913 opened up a new field in experimental physics—the study of the dynamics of the interactions between electrons, atomic structures, and radiation. This study, in which the senior author of the present book has played a leading role, has been guided by the quantum theory of atomic structure which has recently been put in a powerful form by Heisenberg, Born and Jordan. The authorship of the present book therefore assures the reader of an unusually competent exposition of the experimental facts and of their theoretical interpretation.

The somewhat one-sided development of the subject is reflected in the book. The chapters dealing with the measurements of critical potentials and their relation to spectroscopic data show the very satisfactory completeness of our knowledge of the energy relations at impact, at least with atoms. On the other hand the chapters on the kinetics of the electron in gases, on the efficiency of excitation by electron impact, on ionization and excitation by positive ion impact indicate how very meagre is our knowledge of the momentum changes at impact, and the conditions, other than energetic, which determine whether or not a collision will result in an excitation of the atom structure. The last chapter contains a very interesting discussion of the possibilities of applying the method of impacts to the study of the elementary processes of chemical reactions.

The book is of great value not only for its complete, concise and logical presentation of the facts (the literature references are complete up to the first months of 1926) but also for the many stimulating suggestions of ways for the further development of the fascinating subjects under discussion.—Pp. viii + 312. 51 figs. Julius Springer, Berlin, 1926. JOHN T. TATE

Introduction to Contemporary Physics. KARL K. DARROW.—New as the science of subatomic physics is, the motives for its study are among our oldest forms of scientific interest, dating back at least to the time when fundamental questions of the origin and nature of the material universe were given the very different answers still accepted by the self-styled Fundamentalists. Modern answers to these fundamental questions differ from the ancient answers not merely in content, nor merely in emphasis on the descriptive rather than the historical aspects of the questions. The ancient authors wrote with a self-confidence most complete and contagious, and usually stated results without any discussion of evidence; the contemporary physicist, on the other hand, lacks

the self-confidence, and asks his readers, or such of them as can, to study the evidence and judge for themselves the validity of his answers. This demands of contemporary intelligent readers a willingness to study a great mass of experimental data, most of which would be quite uninteresting, not to say boresome, to the majority of them, were it not related to these fundamental questions. To an author of a book on contemporary physics, this situation presents a serious problem. Relating these dry data to the live questions means, practically, relating the data to theories, tentative answers to the questions. The problem is, to establish this relation without allowing it to give the theories a false air of authority. In the words of the author, "The only feasible procedure is to separate the data from the models, as far as is reasonably practicable; to choose a few theories for presentation, according to one's own fallible estimate of their serviceableness, elegance, or chance of long survival; and to advise the reader to discriminate between the facts of experience and the atom-models devised to copy them, and in dealing with these latter to distinguish their essential from their irrelevant features. This advice I have tried to give in the introductory pages, and at intervals elsewhere."

The author's execution of this procedure commands most hearty admiration. In his *Prolegomena*, the relation of theories to experimental data is discussed with a clarity and perspective giving invaluable guidance to the student venturing for the first time into serious exploration beyond the settled ground of classical physics. If, as is possible, the author's caution might lead the beginner to despair of getting answers to fundamental questions bearing a closer relation to reality—whatever that is—than is suggested by the word "model", such doubts are dispelled in the first two chapters, entitled "The Experimental Electron" and "The Experimental Atom", where the basic facts about these once-hypothetical particles are established. In the next chapter evidence is amassed, leading to the subdivision of electrons within the atom into three groups, those concerned in properties of atoms showing periodicity in the series of elements, those showing steady progression, and those showing neither; these groups are then identified as outer, inner, and nuclear groups. The positive electricity is next located, by reference to alpha-ray data, and the data from deflections of electrons by atoms is used to show the ambiguous character of the term "radius of an atom". The main features of the picture of the atom are thus derived from experimental evidence, with a minimum of reference to any theories.

When radiation is taken up, the spectacular history of the wave and quantum theories brings theoretical speculation into more prominence. Nevertheless, the existence of stationary states of electrons in atoms is deduced from experimental evidence before these states are described as orbits; and in the seven chapters devoted to them, the properties of these states are treated in the same way as far as appears practicable. The historical order of the theoretical and experimental work is not overlooked, but is discussed in such a way as to make it subordinate to this logical arrangement. This policy of maintaining so thoroughly the distinction between the established and the tentative aspects of the theories necessarily involves a good deal of repetition and extra work, on the part of the student, as well as the author, but it insures the student's flexibility of mind with regard to the tentative aspects—that is, with regard to a very large fraction of the subject—and after all, is not such a valuable result well worth a good deal of work?

While this book is obviously intended for students with sufficient interest and intelligence for real work, it does not presuppose a knowledge of physics beyond a two or three quarters college course, nor of mathematics beyond elementary calculus. This, of course, limits its scope somewhat. The correspondence principle, for example, gets very scanty recognition. But this limitation makes the book available not only for prospective physicists, but for chemists, biologists and others willing to work for a clear idea of the basis for the contemporary physicists' views of matter. From the reviewer's experience with many reports in independent reading by such students, it is evident that this book will prove extremely useful.

Among its valuable features, in addition to those mentioned above, is its excellent style. It makes evident to the reader that he must not be in the class for whom a current periodical abbreviates "Continued on next page" to "Just turn the page", but not to "Over"; nevertheless it is straightforward, clear and human. This last quality is especially noteworthy in a book on this subject, where each grade of readers requires its own proper medium between cold, plain, uniform, matter-of-fact statements, that can be read in a monotone, and the "popular", animated and animistic, Sunday-supplement style, that acquaints its readers with difficulties of the helium-atom problem through extensive case studies on bigamous households. In this book, matter-of-fact exposition of course fills most of the pages, but it is in a style far from cold or plain, and it is relieved by other material which, as in the Sunday supplement, is suitable for the class of readers for whom it is written. Thus facts lending themselves readily to quizzical expression are enlivened thereby, and on the philosophy of scientific theorizing, a topic at once fundamental, abstract, and easily lost in dullness, the vivacity of many of the comments on its psychological aspects helps the student to realize that the discovery of the laws of things so far removed from human experience is an intricate and fascinating human problem.—Pp. xxvi & 453. D. Van Nostrand Co., 1926. Price \$6.00.

D. L. WEBSTER

Magnetism and Atomic Structure. EDMUND C. STONER.—This book of 371 pages with 56 diagrams includes the most important advances in our knowledge of magnetism through the year 1925. It discusses magnetism in the light of the Bohr theory of atomic structure. It does not pretend to be exhaustive. However, the important facts and theories are presented concisely and lucidly. The style is clear and attractive. Experimental methods used in determining magnetic constants are described in sufficient detail. It is written by an investigator and an expert.

Some of the subjects treated are: The history of the subject, classical electromagnetic theory, quantum theory, the gyromagnetic effect, Gerlach and Stern experiments, the Zeeman effect, the Barkhausen effect, the assignment of electrons to orbits and interpretation of magneton numbers, the theory of Weiss, relation of magnetism to chemistry, and resonance radiation.

It is of particular interest to see Stoner's view on the reasons for the particular assignment of electrons to orbits which is due to him. To the reviewer, however, it would appear that the intensities of x-ray lines are not as conclusive proofs as the general consistency of the Goudsmit, Pauli, Heisenberg, Hund, Russell, Laporte spectroscopic developments which are also mentioned in the book.

The realization of the importance of the spinning electron came after the book was written. The gyromagnetic anomaly, g values, and the relativity doublet difficulty appear now in a new light, especially with the aid of the new mechanics. Similarly the subject of resonance radiation has received recent important contributions which could not be included. Among older papers it may be mentioned that Fermi and Rasetti have performed the same experiment as Breit and Ellett in a more thorough manner and quite independently.

Various interesting suggestions are made throughout the book. For example, it is suggested that Gaschler's experiments and the high magnetic field (10^{11} gauss) due to K electrons in U are connected with each other.—Pp. xiii + 371, 56 figs., Methuen and Co., London, 1926.

G. BREIT

Kolloidchemie. RAPHAEL ED. LIESEGANG.—This volume forms Volume VI of Wissenschaftliche Forschungsberichte, Naturwissenschaftliche Reihe, Edited by Dr. Raphael Ed. Liesegang. It is in reality a collection of notes and references to the colloid chemical literature which has appeared since 1914. The author states in the preface that the volume is not to be regarded as a textbook or as a handbook but rather as a "Sammelreferate". The book is divided into 24 sections or chapters including such

headings as synthesis, optics, viscosity, plasticity, capillarity, adsorption, contact catalysis, coagulation, sedimentation, electrical phenomena, Brownian movement, surface tension, etc., and some 800 literature citations are given.

Probably no other colloid chemist, given the task of selecting the most important contributions to the literature of colloid chemistry since 1914, would select the same group which has been selected by Liesegang. It is probably equally true that no two colloid chemists would select groups that closely approximated each other, consequently the reviewer cannot find fault with the selection of material. That is the prerogative of the author, and it is only natural that the selection should reflect his views. The reviewer, however, does not believe that the relatively few references to American and English literature as contrasted to the many citations to German literature is a fair index of the number of meritorious publications. Another valid criticism is the brief treatment of certain sections; for example, the "viscosity of protoplasm" is given 9 lines with 2 citations, both to German literature, and "plasticity" is given less than a page with only 4 references, all to German literature. How the author could overlook the contributions of Bingham in this field is beyond the comprehension of the reviewer.

The volume contains no tabular data or figures, and its value will be limited to the use which the physicist or chemist can make of it as a source of collected and annotated literature citations. It is well printed on good paper and appears relatively free from typographical errors; however, the dibenzoyl-l-leucine mentioned near the top of p. 131 should be di-benzoyl-l-cystine. It should be in all reference libraries.—Pp. xii + 176. Theodor Steinkopff, Dresden and Leipzig, 1926. Price 8.0 M unbound, 9.5 M bound.

ROSS AIKEN GORTNER

The Anatomy of Science. GILBERT N. LEWIS.—This book, which comprises the Silliman lectures at Yale for 1926, is ostensibly addressed to the intelligent layman, and presents to him an account of the contemporaneous attitude of scientific men toward our fundamental scientific notions. The chapter headings show the scope of the book: Methods of Science—Numbers; Space and Geometry; Time and Motion; Light and the Quantum; Probability and Entropy; The Non-Mathematical Sciences; Life—Body and Mind.

In spite of its ostensible address to the layman, the physicist will perhaps find even more of stimulation and interest here than the layman. Every physicist is becoming increasingly aware that one of the most important tasks both for him as an individual and for physics as a science is a reformulation of attitude toward fundamental concepts. The author has been known for his interest in fundamentals ever since he was one of the first in this country to accept the then new doctrine of relativity, and now his matured attitude toward these questions will be found of the greatest interest and stimulation, entirely irrespective of whether the reader agrees with his point of view in all respects. As may be judged from the chapter headings, the book examines more than the bases of physical science only, and will be found to contain, as the author says, "a singularly satisfying little philosophy".

The book makes charming reading; it is always entertaining and at times is touched with an imaginative insight truly poetical. It is good that physics has such a book. Pp. ix + 229, 8×5 inches. Yale University Press, New Haven, Conn., 1926. Price \$3.00.

P. W. BRIDGMAN

Les Equations de la Dynamique de L'Ether. HENRI EVRAUD.—This monograph contains two chapters and an appendix. The first chapter develops the mathematical technique of the tensor analysis and discusses affine and metrical geometrics. In the second chapter the dynamics of the ether are developed from a minimum principle and the resulting equations are shown to contain Lorentz's electrodynamics as well as Einstein's theory of gravitation.—Pp. 66. Librairie Scientifique Albert Blanchard, Paris, 1926.

LEIGH PAGE

PROCEEDINGS
OF THE
AMERICAN PHYSICAL SOCIETY

MINUTES OF THE PHILADELPHIA MEETING

DECEMBER 28, 29, 30, 1926

The twenty-eighth Annual Meeting (the 142nd regular meeting) of the American Physical Society was held at the University of Pennsylvania, Philadelphia, Pennsylvania, on Tuesday, Wednesday, and Thursday, December 28, 29, and 30. The presiding officer was Professor Dayton C. Miller, President of the Society. The average attendance was about three hundred.

The annual joint session with Section B was held on Tuesday afternoon, with Professor William Duane, Chairman of Section B, presiding. The retiring Vice-President, Professor H. M. Randall, opened the joint meeting with an address entitled "Infra-Red Spectroscopy." This was followed by an address by Professor W. F. G. Swann on "The New Quantum Dynamics," and discussion of this topic by Dr. G. Breit and Professor J. H. Van Vleck. The attendance at this session was about four hundred.

On Wednesday evening, December 28, there was a dinner for the members of the Society and of Section B and their friends at the Hotel Bartram, attended by two hundred and four persons.

Annual Business Meeting.—The regular annual business meeting of the American Physical Society was held on Wednesday morning, December 29, 1926, at eleven o'clock. A canvass of the ballots for officers resulted in the elections for the year 1927 as follows:

<i>For President;</i>	K. T. Compton
<i>For Vice-President;</i>	Henry G. Gale
<i>For Secretary;</i>	Harold W. Webb
<i>For Treasurer;</i>	George B. Pegram
<i>For Member of the Council,</i> <i>Three-year term;</i>	Raymond T. Birge
<i>For Members of the Council,</i> <i>Four-year term;</i>	{ Paul D. Foote G. W. Stewart
<i>For Members of the Board of</i> <i>Editors of the Physical</i> <i>Review, Three-year term;</i>	{ G. Breit P. W. Bridgman L. W. McKeehan

The Secretary reported that during the year there had been 154 elections to membership. The deaths of 6 members had been reported during the year, 34 had resigned and 21 had been dropped. The total membership, including those newly elected, was 512 Fellows and 1341 Members, making a total of 1853.

The Treasurer presented his financial report for the year 1926. The Managing Editor presented the financial report for the Physical Review for the year 1926. In his report of the condition of the Review he stated that it had shown a loss for the past year, and was probably facing losses in future years. The financial reports were ordered printed and distributed to the members.

To enable the Society to provide adequate support for the Physical Review in future years, the Treasurer, on behalf of the Council, introduced the following resolution: *Resolved: That Article I, Section 1, of the By-laws be amended to read "The annual dues of fellows shall be fourteen dollars and of members ten dollars, payable on the 1st of January," this amendment to take effect January 1, 1928.* This resolution was passed by 44 affirmative votes to 7 negative.

Meeting of the Council.—At the Meeting of the Council held on December 28, 1926, three persons were elected to Fellowship, three were transferred from Membership to Fellowship, and twenty-nine were elected to Membership. *Elected to Fellowship:* F. W. Goucher, Karl F. Herzfeld, Fritz Zwicky. *Transferred from Membership to Fellowship:* Hugh L. Dryden, Carl H. Eckart, Francis D. Murnaghan. *Elected to Membership:* William H. Abbott, Kenneth T. Bainbridge, Garnett F. Barnes, David G. Bourgin, Katherine Chamberlain, J. Davidson, Jr., Sophie W. Eldridge, C. W. Gartlein, Daniel E. Harnett, Marshall C. Harrington, Jos. E. Henderson, J. H. Hsu, Karl H. Hubbard, Carl Kenty, John J. Livingood, John B. Miles, Jr., L. W. Moench, P. M. Morse, Sister Mary S. Murray, Carl A. Pearson, R. J. M. Raven-Hart, C. M. Slack, Arthur P. Tanberg, W. Norris Tuttle, A. H. Wait, Harvey E. White, R. M. Williams, B. S. Woodmansee, W. Morris Young.

The regular program of the American Physical Society consisted of 77 papers, Numbers 1, 5, 11, 12, 17, 18, 19, 27, 43, 49, 50, 53, 66, 68, 70, and 73 being read by title. The abstracts of these papers are given in the following pages. An Author Index will be found at the end.

HAROLD W. WEBB,
Secretary.

ABSTRACTS

1. The absorption of beta-rays. J. A. GRAY and B. W. SARGENT, Queen's University.—An examination has been made of the absorption of the β -rays of radium E and uranium X in carbon, aluminum, copper, tin and lead. The former rays have the following approximate relative ranges (expressed in grams per cm^2), in these substances, viz., 62, 64, 71, 89 and 100. For the β -rays of uranium X, the corresponding numbers

are 78, 81, 82, 95 and 100. As the relative ratios of atomic weight to atomic number are 79, 82, 87, 94 and 100, the experiments indicate that the energy lost in an atom by the β -rays of uranium X is, on an average, proportional to the atomic number.

2. A new theory of the origin of the actinium series. T. R. WILKINS, University of Rochester.—It is suggested that the variation of the radii of pleochroic haloes in rocks of various geological ages can be explained if the actinium series is considered as coming from an isotope of uranium I (actino-uranium I) whose decay-constant is several times that of uranium I. These parent isotopes are assumed to have been in radioactive equilibrium originally but in geological time actino-uranium has largely disappeared and today forms but several percent of uranium. From a study of haloes, conclusions are drawn regarding the decay-constants of actino-uranium and the time since equilibrium. On the basis of such a theory, a considerable fraction of uranium lead would be due to actinium and the ages of rocks calculated either from lead or helium content will be in error—probably as much as 40% in the case of the oldest rocks.

3. Possible dependence of frequency of characteristic x-radiation on the temperature of the target. J. H. PURKS and C. M. SLACK, Columbia University.—Recent papers by H. S. Read (*Phys. Rev.* April and Nov. 1926) indicate that the absorption of x-rays depends upon the temperature of the absorber. This result has been interpreted as possibly due to a shift of the K absorption limit through about 11 volts. At the suggestion of Prof. Bergen Davis we have investigated a possible change of frequency of Mo $K\alpha$ with the temperature of the target. Water-cooled and standard Coolidge tubes were used. The energy was such as to make the target of the second tube white hot, the temperature being well over 1000°C , though it was not measured because of negative results. Narrow slits were used and narrow rocking curves obtained. Peaks could be located to 2 seconds of arc. The reflecting angle of calcite crystal for Mo $K\alpha$ is about 24000 seconds, hence there is no change of 1 part in 12000 due to temperature. If the K limit is shifted as Read's results indicate, it may be due to a destruction of the outer levels of the atom without any appreciable change in the (K-L) difference.

4. Investigation of metal films by x-ray analysis. KARL HOROVITZ, International Research Fellow, University of Chicago.—Using the focussing x-ray vacuum spectrograph described some time ago ("Science," Sept., 1926), a method was developed of investigating metallic films deposited on glass and other surfaces in a high vacuum by any kind of atomic rays. The metallic films are then analyzed directly where they are originally formed without changing the vacuum or contaminating the metals with gases. Deposits of potassium have been investigated at liquid air temperature. Very thin, coloured or black layers did not yield a diffraction pattern. Potassium mirrors about 0.15 mm thick gave a diffraction pattern corresponding to a body centered cubic lattice $a=5.15$. Other metals and different methods of forming the deposits are now being studied.

5. The polarizing angle for x-rays. C. S. BARRETT and J. A. BEARDEN, University of Chicago (Introduced by H. G. Gale).—The classical theory of x-ray scattering predicts 90° for the polarizing angle of scattering from either an electron at rest or an electron moving with the final velocity of the quantum process. Intermediate velocities, as postulated in the quantum theories of Jauncey, Compton and Woo, give a polarizing angle of less than 90° and dependent upon wave-length. Dirac (*Proc. Roy. Soc. A112*, 405 (1926)) predicts 90° on the basis of the new quantum dynamics. Previous experimental determinations of the angle have not been decisive. Using filtered radiation from a tungsten x-ray tube operated at 190,000 volts the polarization angle was measured by the ionization method. With wave-lengths of 0.215, 0.24, and 0.37A (as measured by absorption) the polarizing angle was found to be $90^{\circ} 30'$, $91^{\circ} 20'$ and $90^{\circ} 50'$ respect-

ively. Thus within the probable experimental error no shift from 90° or dependence on wave-length was observed. This is in agreement with the new quantum dynamics but not with the theories of Jauncey or Compton-Woo, which predict 83° 53' and 84° 10' respectively as the polarizing angle for 0.215A.

6. X-ray coloration of kunzite and hiddenite. P. L. BAYLEY, University of Rochester.—Absorption curves have been obtained from 2000 to 300 m μ for a pink sample of kunzite and a yellow green sample of hiddenite both before and after exposure to x-rays. The kunzite had only one weak wide absorption band at 540 m μ . The hiddenite had bands at 1670, 1000, 630, 438, 432, 378, and 368 m μ . After x-ray treatment, the hiddenite showed only a slight increase in absorption below 440 m μ . However, the x-rays colored the kunzite very similarly to the hiddenite but slightly more bluish green (as has been noted by others). Bands which were not present before radiation occurred at 910 and 625 m μ . The positions of maximum transmission were 730 and 540 m μ which were nearly identical with those of hiddenite. No trace of the hiddenite bands below 500 m μ could be found in the radiated kunzite. The fact that by x-radiation there can be produced in kunzite absorption in the region 1250 to 450 m μ which is so similar to that of hiddenite, would suggest that the green color in both materials is due to a similar physical cause. The methods of production need not have been similar.

7. X-ray diffraction measurements on some of the pure compounds concerned in the study of Portland cement. E. A. HARRINGTON, Bureau of Standards.—Using the powder photographic method of x-ray analysis the crystal symmetry, lattice constants, and densities of Al₂O₃, Fe₂O₃, Ca(OH)₂, 3CaO · Al₂O₃, and 5CaO · 3Al₂O₃ have been determined. The values found for CaO, CaCO₃, and SiO₂ are added to complete the list of cubic, hexagonal, and rhombohedral crystals of important compounds in Portland cement research.

8. The crystal structure of magnesium di-zincide. JAMES B. FRIAUF, Carnegie Institute of Technology.—Crystals of the intermetallic compound, MgZn₂, were prepared and the crystal structure was determined from x-ray data furnished by Laue and rotation photographs. The crystal was found to have hexagonal axes with $a = 5.15\text{ \AA}$ and $c = 8.48\text{ \AA}$. The unit cell contains four molecules. The effect of absorption in the crystal in determining the wave-length giving a maximum intensity of reflection in Laue photographs was used to confirm the dimensions of the unit cell. The atoms have the positions:

Zn: $u, \bar{u}, 1/4; 2\bar{u}, \bar{u}, 1/4; u, 2u, 1/4; \bar{u}, u, 3/4; 2u, u, 3/4; \bar{u}, 2\bar{u}, 3/4; 0, 0, 0; 0, 0, 1/2$
Mg: $1/3, 2/3, v; 1/3, 2/3, 1/2 - v; 2/3, 1/3, 1/2 + v; 2/3, 1/3, \bar{v}$.

Where $u = 0.830$ and $v = 0.062$. The magnesium atoms have very nearly the arrangement that has been proposed by Bragg for the oxygen atoms in ice. The least distance between two magnesium atoms is 3.15A, between two zinc atoms, 2.52A, and between a magnesium and a zinc atom, 3.02A.

9. The relative probabilities of the photo-electric emission of electrons from Ag and Au. F. K. RICHTMYER and L. S. TAYLOR, Cornell University.—Data previously reported by one of us (F. K. R., Phys. Rev. January, 1926) indicated that the ratio, R_L^K , of the number of $K+L+M+\dots$ photo-electrons to the number of $L+M+\dots$ photo-electrons decreases from about 7.5 in the case of Mo to about 5.1 in the case of Pb. These data were approximate and were not in agreement with any of the existing theories. The theories of J. J. Thomson and of de Broglie require values of R_L^K large than above and increasing more rapidly with *decrease* in atomic number. The theory of Kramers requires values of R_L^K of about 5.1 and *independent* of atomic number. More careful data has now been taken through the K absorption limit of Ag and Au,

using narrow slits (about 5 x-units wide). The magnitude of the discontinuity in the mass absorption coefficients through the limit is determined with a precision of one percent. But the value of R_L^K computed from this discontinuity depends entirely on the magnitude of the correction for scattering. If a mass scattering coefficient, σ/ρ , of 0.8 be assumed for both Ag and Au, the value of R_L^K is 6.4—*independent of atomic number as required by Kramers*, but larger than predicted by him. If the Thomson (classical) value of σ/ρ be assumed (*i.e.*, $\sigma/\rho = 0.2$), then R_L^K for Ag is 6.0 and for Au is 4.4. Values of R_L^K cannot be determined unambiguously until better data on scattering coefficients is available.

10. A possible relation between radiation and ionization potentials of iron. OTTO STUHLMAN, University of North Carolina.—The critical potentials of iron, found in recent investigations by Thomas, Chu and Richardson and by Chalkline claim to possess the following term values in common, $M_{II\text{ III}}$ at 54 volts, M_I at 93 volts and L_{III} at 706 volts. If we agree to retain the following (I) potentials, 11.1, 19.4, 41.2, 54.6, 103.5, 169.4, as determined by Thomas and new (I) potentials of 5.72, 7.29, 11.14, and a (R) potential at 8.14 volts, then all critical (R) potentials published can probably be attributed to multiple impact.

11. The 29 volt critical potential of hydrogen. ROGERS D. RUSK, North Central College.—Low voltage arc characteristics for varying anode distances and gas pressures have been measured in hydrogen using a special tube containing two hot filaments and two nickel anodes. Striking and breaking potentials of one arc were observed when the region of that arc was illuminated by the glow from the other arc in the same tube at pressures below 0.2 mm. With increasing intensity of illumination the arc could be struck with great regularity at potentials down to the minimum maintaining potential for any given filament current, anode distance and gas pressure, but never lower. The lowest maintaining potential for the type of glow observed was 29 volts and it is suggested that this represents primarily a molecular excitation level capable of sustaining intense cumulative ionization and having a critical excitation period of the order of 10^{-8} sec. as indicated by the quenching effect of pressure change.

12. Spectral intensity distribution in a hydrogen discharge. E.W.TSCHUDI, Winthrop College, Rock Hill, S. C.—A cold-cathode discharge tube has an auxiliary tube attached from which cathode rays are projected against the main cathode. A photo-electric cell, attached to a monochromatic illuminator, is used to measure relative intensity distribution of H_{γ} and H_{δ} , respectively, from the main cathode through the cathode dark space into the negative glow with and without excitation of the auxiliary tube. When the main cathode is bombarded by the electron stream the intensity of spectral illumination in the negative glow is increased by about 20 percent. This increase does not result from the mere addition of an illumination which appears when the auxiliary tube is alone excited to the illumination of the main discharge, but may be attributed to the production of soft x-rays in the gas which are capable of exciting the gas molecules.

13. Excitation of spectra by atomic hydrogen. F.L. MOHLER, Bureau of Standards.—Hydrogen from a Wood discharge tube flowed into a tube containing metal vapor and the spectrum emitted by the mixture was photographed. Observations of Bonhoeffer (Zeits. f. Phys. Chem., 116, 391 (1925)) with sodium and mercury are confirmed. Sodium and cadmium gave strong emission of their first resonance lines and no other lines or bands. Potassium showed the first resonance line faintly. Mercury gave the complete hydride band spectrum and also faint emission of the resonance line at 2537A. Caesium, magnesium, thallium and zinc gave no line or band spectra. The excitation energies of the observed lines and bands are, except for 2537 of mercury, less than 3.8 volts though

many lines of lower energy did not appear. There are two possible explanations of the radiation. The metal atom may be excited in a three body collision with two hydrogen atoms. In this case the entire energy of recombination of hydrogen, 4.38 volts, should be available for excitation. The second possibility is that first a hydride is formed and that this reacts with H to form H₂ and an excited metal atom. The available energy of excitation is the energy of recombination of H minus the energy of formation of the hydride. The second theory seems to offer the best explanation of the observations.

14. The absorption of ultra-violet light by organic vapors. ALPHEUS W. SMITH, CECIL E. BOORD AND C. S. PEASE, Ohio State University.—This paper gives a preliminary report of work being done on the absorption by organic vapors in the ultra-violet. An aluminum under-water spark served as a source of continuous radiation. The spectra were photographed by means of a Hilger E2 quartz spectrograph and the vapors were inserted between the source of light and the slit of the spectrograph in glass tubes with quartz ends. The intensities of the absorption lines were determined by a Moll microphotometer. The following vapors have been studied,—benzene, diethyl ether, methyl normal amyl ether, and ethylene chlorohydrin. In each case the absorption spectrum consists of four or more prominent bands which are resolved into a number of lines of varying intensities. The photographic records from the microphotometer show that these bands are very similar in structure. Each band consists of a very prominent line with neighboring lines of less intensity lying on the side of the longer wave lengths. The observed lines are broad and also shaded toward the longer wave lengths. They have the appearance of unresolved band spectra. The most prominent of these lines lie at approximately $\lambda = 2590\text{A}$, $\lambda = 2530\text{A}$, $\lambda = 2470\text{A}$ and $\lambda = 2420\text{A}$. The intensity of the absorption changes with the composition and structure of the compounds. The other characteristics of the bands remain essentially unchanged.

15. New series in the spectrum of fluorescent iodine. F. W. LOOMIS, New York University.—Several new series are found in Wood's spectra of fluorescent iodine and their constants (d and γ) are measured. From these, \bar{n} , the vibrational quantum number of the fluorescent molecule before excitation, (taking $n_0=0$ for simplicity) is calculated and in each case comes out nearly integral. Most of the series extend into the antistokes region as far as the order $p = -\bar{n}$. None of them extend further. Moreover the frequency of the origin of the band to which the resonance line of each series belongs, when calculated from d and the writer's values of the constants of the iodine absorption spectrum, agrees well, in every case, with the origin of a known band whose n'' is equal to the \bar{n} previously calculated for the series. These results confirm the reality of the series and yield values of n' and n'' for each doublet in it. A plot of (n', n'') for all the fluorescent doublets which have been identified, suggests that the intensity diagram would show a pattern having maxima along roughly hyperbolic curves, analogous to that found by Birge for the β bands of nitrogen. Several of the fluorescent series have the same n' but very different m'' 's. Comparison of their intensities suggests that relative probabilities of transition do not appreciably depend on m' .

16. On the infra-red spectrum of mercury. VLADIMIR P. LUBOVICH, University of Colorado.—In the paper by McLennan and Shaver an account was given of a photographic investigation of the mercury spectrum from $\lambda = 6908\text{A}$ to $\lambda = 11137\text{A}$. The spectrum was photographed in the first order of a diffraction grating, higher orders being cut off with Wratten filter No. 22. The present work seems to prove that due to a transparent filter and incorrectly measured wave-lengths, higher order lines were ascribed to the infra-red spectrum. The conclusion is reached partly through the analysis of McLennan and Shaver's work, partly by means of a new photographic study of the mercury spectrum with a prism instrument. The investigation also includes the measurement of wave-lengths up to $\lambda = 13670\text{A}$. Beyond this limit four more lines are detected, the last

one being in the neighborhood of $\lambda 27000\text{A}$. Nineteen lines are identified photographically apparently for the first time. Among the newly photographed lines the line $\lambda = 10141\text{A}$ was suggested by McLennan and Shaver to be a doublet. The present work verifies the original observation of Paschen that it is a single line. In view of the contradictory results of previous investigations regarding the absorption of $\lambda = 10141\text{A}$ by non-luminous mercury vapor the author reexamines this question with a result which confirms the conclusion of McLennan and Shaver that no absorption exists.

17. Absorption spectra in the extreme ultra-violet. J. J. HOPFIELD, University of California.—Absorption spectra of nitrogen, air, acetylene, and carbon monoxide have been obtained with widely varying pressure. They show selective absorption and a region of continuous absorption on the short wave-length side. This region again shows selective absorption and abounds in maxima and minima when low enough pressures are used. Acetylene shows band absorption beginning at $\lambda 2300$. At lower pressures maxima of absorption are found at $\lambda\lambda 1520, 1480, 1430$, and many other both narrow and wide bands to $\lambda 1000$. Nitrogen shows besides the bands already found by Sponer strong continuous absorption beginning at $\lambda 990$. Absorption occurs in the discharge tube also. The principal lines of the four ultra-violet series of N I are thus observed, and a group of lines $\lambda 1085$ due to ionized nitrogen. A few carbon lines were found when CO was used. These are probably the resonance lines of this element. The Cameron bands of CO are found in absorption and prove directly that these arise from the normal state. 0-0 to 0-4 are observed. Four or five bands of an apparently new system in CO begin with either $\lambda 1696.9$ or 1664.4 as the 0-0 band, and continue with $\lambda\lambda 1634.0, 1604.9$, and 1577.6 as consecutive members.

18. The ultra-violet band spectra of nitrogen. R. T. BIRGE AND J. J. HOPFIELD, University of California.—The ultra-violet nitrogen system previously analyzed by us (Nature 116, 15 (1925)) has been greatly extended to include 60 bands between $\lambda 1250$ and $\lambda 2025$. More accurate measurements prove that the assignment of this system to NO is unjustified. Moreover, it has now been found by Sponer (Nature, in press) in absorption in cold nitrogen. It is the resonance system of nitrogen, corresponding directly to the fourth positive group of CO. The other weaker progression found by Sponer in nitrogen, as we have since proved, is absorbed *only* in the discharge tube, and is in fact merely the usual absorption spectrum of CO. We have identified two other progressions of emission bands lying between $\lambda 1030$ and $\lambda 1520$. Both have the same lower electronic level as the above nitrogen system, and extend this level to $n = 18$. They locate two new electronic levels at $104,410 \text{ cm}^{-1}$ and $103,660 \text{ cm}^{-1}$. The four electronic levels associated with the ultra-violet nitrogen systems are probably singlet levels, while the four levels associated with the familiar nitrogen systems are triplet. Transitions between the two types of levels are not in general to be expected, from theoretical considerations, and none have as yet been found in nitrogen.

19. Infra-red absorption by the N-H bond; in aniline and alkyl anilines. JOSEPH W. ELLIS, University of California, Southern Branch.—The infra-red absorption spectra of aniline, five monoalkyl anilines and five dialkyl anilines have been recorded below 2.8μ by means of a self-registering quartz spectrograph. Prominent bands of absorption, occurring at 1.47μ and 1.04μ for aniline, appear with diminished intensity for monoalkyl anilines and disappear for the dialkyl anilines. A band at 2.8μ exhibiting changes, analogously to these two, has already been announced by F. K. Bell (J. Amer. Chem. Soc., 47, 2192, (1925)). The frequencies in mm^{-1} of these three bands are expressible by the parabolic formula, $\nu_n = 375.8n - 18.3n^2$, and are believed to constitute a non-harmonic series of vibrations characteristic of the N-H bond. The series is analogous to one already attributed by the author to vibrations of the C-H bond. Two other bands, apparently associated with the presence of the N-H bond, occur at 1.20μ and 2.00μ .

for aniline. The former is not detectable in the spectra of monoalkyl anilines because of overlapping bands, but the latter is shifted to 2.05μ . A quantum theory explanation is offered as to the origin of these bands on the basis of combinations of N-H and C-H frequencies.

20. A new method of determining the time of appearance as well as the time of duration of spectrum lines in spark discharges. J. W. BEAMS, National Research Fellow, and ERNEST O. LAWRENCE, National Research Fellow, Yale University.—Light segments a few centimeters in length obtained by a method described elsewhere (see previous abstract) emanating during various time intervals after the beginning of a spark discharge fall upon a very sensitive photo-electric cell. Plotting the observed photo-electric currents against the time intervals elapsing between the beginning of the spark and the production of the light segments, there are obtained curves having significant changes in slope. Abrupt increases in the photo-electric current determine the time of appearance of the various spectrum lines while decreases in the current indicate their disappearance. The above method is very reliable and gives the time of appearance of the spectrum lines with a high degree of precision.

21. The arc spectrum of germanium. C. W. GARTLEIN, Cornell University (Introduced by R. C. Gibbs).—The wave-lengths of the lines in the arc spectrum of germanium have been measured in the region above 1860\AA with an accuracy of at least 0.1\AA . From these measurements the relative energy levels have been worked out and the jumps corresponding to 56 lines have been identified. In the normal state the atom contains two (p) valence electrons which give rise to the lower levels 3P , 1D , 1S , with the 3P lying deepest, as is predicted by the theory of Hund. The next higher levels arise from the electron configurations (ps) and (pd). The energy levels have been correlated with the ultimate and persistent lines found by other investigators. The arc spectrum of Ge closely resembles the arc spectra of Si, Sn, and Pb.

22. Stages in the excitation of the spectrum of indium. JOHN G. FRAYNE, Antioch College, and C. W. JARVIS, Ohio Wesleyan University.—The indium metal was vaporized at a temperature of 650°C in an iron cylindrical anode within a quartz tube. Electrons from an oxide-coated Pt filament passed through a cylindrical grid into a force free space where they collided with the atoms of indium vapor. The spectrum was viewed end on through a transparent quartz window. At 3.3 volts the lines $2p_1 - 2s$ and $2p_2 - 2s$ appeared. At 4.2 volts the additional lines $2p_1 - 3d$ and $2p_2 - 3d$ appeared. At seven volts higher members of the series appeared. At 13.2 volts the spectrum became very intense and lines appeared in addition to the recognized series lines. At this potential a second electron may have been detached from the atom, assuming that ionization occurred at seven volts. At 23 volts many lines appeared in the visible and near ultra-violet but most of them have been recognized as air lines. Using voltages as high as 80 no other lines appeared. The lines from the $2p_1$ level were consistently stronger than those from the $2p_2$ level at temperatures ranging from 600° to 800°C . The latter level is considered to be the lowest and should give the strong lines of the spectrum.

23. On the spectra of boron. R. A. SAWYER, University of Michigan, and F. R. SMITH, Pennsylvania State College.—Spectra of boron in the region $\lambda\lambda 2300-5800$ were obtained by the "vacuum spark" method, using electrodes of boron, and boron and carbon. The vacuum spark chamber was made of glass and so designed that considerable adjustment of the spark-gap could be made without opening the spark-box. The lines were photographed with a two-prism glass spectrograph and a Hilger 2E quartz spectrograph. After checking for impurities about ninety new lines were ascribed to boron. Starting with the term values of B I, B II and B III given by Millikan and Bowen, about twenty-five of these lines have been classified in series.

24. Energy level studies on metallic vapors using a high temperature tungsten furnace. O. S. DUFFENDACK and J. G. BLACK, University of Michigan.—Following in general the method originated by Duffendack in 1922, an electrically heated tungsten cylinder is clamped horizontally between heavy water-cooled leads and enclosed in a large water-cooled copper cylinder provided with observation windows and containing pure hydrogen. An insulated U-shaped tungsten or molybdenum trough extends axially through the furnace and holds the material to be studied. Absorption studies on copper vapor yielded new absorption lines at 2618.37, 2824.39, 2882.81, 2961.19, 3010.87, 3194.09 and 5782.08 all originating in the metastable $^2D_{2,3}$ level in agreement with Shenstone's analysis, together with previously reported absorption lines and copper-hydride bands. The copper lines 3247, 3274, 5106, 5700, 5782 and several copper-hydride bands were obtained in emission. These five lines originate in the $^2P_{1,2}$ level. Experiments proved that this state was reached by absorption of resonance radiation rather than by thermal excitation. No absorption lines originated in this level. The metastable $^2D_{2,3}$ level from which absorption lines were observed is reached by thermal action. These experiments were made principally to test the furnace. It is being adapted for investigations of resonance radiations, critical potentials, and other properties of elements at high temperatures. It compares favorably with other furnaces and avoids difficulties due to oxidation and impurities.

25. On the Zeeman effect and the structure of the arc spectra of Cu and Rh. L. A. SOMMER, International Research Fellow, Harvard University (Introduced by E. A. Saunders).—Investigating the arc spectrum of Cu, Shenstone and the author are in agreement in the classification of the doublet term group 2P , $^2\bar{D}$, 2F which lies near the quartet term group 4P , $^4\bar{D}$, 4F , but reach different conclusions regarding the classification of the higher doublet term group 2P , $^2\bar{D}$, 2F , and especially the term-groups *with negative term-values*. The author uses chiefly his own measurements of the Zeeman effect for the assignment of the terms, while Shenstone bases his designations mainly on line intensities. A more general formulation of the selection rule for k for jumps of one or more electrons is proposed. While the first (alkali-like) term-system (doublet-terms) corresponds to atomic states in which the 4_1 electron rotates around the rest of the atom with its ten 3_3 electrons, the second system (doublet and quartet-terms) is due to states in which the outer electron rotates around an inner shell consisting of nine 3_3 and one 4_1 electron. One set of lines in the visible is associated with the simultaneous transition of two electrons. Of about 660 measured lines of the Cu-arc more than half are combinations within or between the two term-systems. From the series limits it is found that the removal of the 3_3 electron requires a potential 10.9 volts, while the 4_1 is bound with the well-known potential of 7.6 volts. In the Rh spectrum 50 percent of the lines measured in the arc are arranged in a definite term-system by means of the Zeeman effect data.

26. Absorption spectra of iron, cobalt and nickel. W. F. MEGGERS, Bureau of Standards, and F. M. WALTERS, JR., Carnegie Institute of Technology.—The under-water-spark absorption spectra, as well as the ordinary vapor absorptions, have been investigated by others, but not in sufficient detail in connection with the spectral structures for Fe, Co and Ni. Employing the apparatus and method described by Meggers and Laporte in the *Physical Review* for October, 1926, these spectra were reexamined throughout the visible and ultra-violet regions. Our spectrograms show 263 iron lines (2166 to 4404A), 340 cobalt lines (2137 to 4121A), and 225 nickel lines (2124 to 3858A) absorbed in the source. In each case, the majority of these are identical with the stronger lines of the arc-emission spectra, and practically all such lines are found to involve either the normal state or some low metastable state of the neutral atoms. The type of source used showed most of the metallic spark lines in emission but certain groups were present in absorption with low intensity. The latter involve the

lowest energy states of the ionized atoms. With the aid of these data on absorption the known spectral structures for neutral and for ionized Fe, Co and Ni have been confirmed, and many new levels have been established.

27. Spectra of the high-current vacuum arc. ARTHUR S. KING, Mount Wilson Observatory.—High-current arcs were used in a vacuum chamber at a pressure of about 5 mm of mercury, the arcs studied being those of iron, chromium, titanium magnesium, copper, and silicon, using electrodes of small diameter. The central vapor-stream of this arc, carrying 1500 amperes or more at 110 volts, is of intense brightness and shows a completeness of ionization usually obtainable only in high-potential sparks of very disruptive character. The spectrum is that of the ionized atom, lines of the second stage of ionization often appearing. The production of neutral-atom lines is evidently confined to the outer vapors of the vacuum arc, and only those arc lines which are little subject to broadening (usually low-temperature lines) retain sufficient density to register photographically. This arc is useful as a source of high excitation in a rarefied gas, operating without difficulty, and sufficiently bright to be photographed with high dispersion. The enhanced lines emitted, when of low energy-level in the ionized atom, usually show self-reversal, and in general the peculiarities of line-structure and the tendency to dissymmetry under high excitation are shown for enhanced lines in the same degree as the high-current arc in air shows these features for arc lines. These phenomena indicate the relative energy-levels and multiplet groupings of enhanced lines, also their degree of wave-length stability.

28. Some relations in the spectra of stripped atoms. R. C. GIBBS and H. E. WHITE, Cornell University.—Starting with the known values of the arc and spark spectra of one electron systems in all three of the long periods it has been found possible, by using the regular and irregular doublet laws as guides, to recognize the first pair of doublets in the principal series for stripped atoms as far as Mn_{VII} in the first long period, Zr_{IV} in the second long period, and Pr_V in the next period. The first pair of inverted diffuse doublets with satellite have also been located for Sc_{III}, Ti_{IV}, and V_V. These doublets possess very consistent frequency separations and the relative intensities of the lines are in agreement with the usual rule. Evidence is obtained indicating that in Sc_{III} we have the first instance, as originally predicted by Bohr, of a closer binding in a *d* orbit than in either a *p* or an *s* orbit. In fact, on the Moseley diagram the line for the 3*d* level crosses the lines for 4*p* and 4*s* levels in passing from K_I to Sc_{III}. The relative closeness of binding of the 3*d* orbit becomes even greater in the case of Ti_{IV} and V_V. The experimental data conforms very closely to both the regular and irregular doublet laws in the case of all first pairs of principal series doublets. Very consistent values for screening constants are obtained when the regular doublet law is applied to these doublets.

29. Two electron multiplets of the first and second long periods. H. E. WHITE and R. C. GIBBS, Cornell University.—Three characteristic multiplets arising from two valence electron systems of the first and second long periods of the periodic table have been found to follow very well the so-called regular and irregular doublet laws. These multiplets are of the type $^3D_{1,2,3} - ^3P_{0,1,2}$, $^3D_{1,2,3}$, $^3D'_{1,2,3}$, and $^3D_{1,2,3} - ^3F_{2,3,4}$, and have been extended in the first long period from Ca_I to Cr_V, and in the second long period from Sr_I to Cb_{IV}. The two electrons giving the above triplet levels are, in the initial state in 3*d* and 4*p* orbits while in the final state they occupy 3*d* and 4*s* orbits.

30. On metastable neon and argon. RICHARD RUDY, Research Laboratory, Nela Park.—The light from a Geissler tube (10 mm Hg, 100 mil-amp./cm²) was sent through the positive column of a second tube (15 cm long, .007 to .05 mil-amp. cm²). The absorption of 6402, one of the lines involving the metastable *s*₃ state, increased when the

pressure was lowered from 8 mm downwards and beyond the minimum discharge potential. This absorption had no influence upon the volt-ampere characteristic ($<1/2$ per cent), the metastable states being reestablished after emission (resonance). Strong absorption was also found in the negative glow. Increase of temperature at constant density increased the potential gradient for currents <1 millampere by shortening the so-called life of the metastable states in the same proportion as it reduces the absorption in neon or mercury. Argon added to neon did not seem to change the absorption as long as the discharge was chiefly maintained by neon. The next higher group of lines $s_5\ 3p_0$, $s_5\ 3p_1$ etc. in argon are not absorbed (<4 percent) under conditions where $s_5\ 2p_0$ shows 90 percent absorption.

31. Low pressure electric discharge in intense electric fields. C. DEL ROSARIO, Bartol Research Foundation and Yale University.—Attempts were made to pull electrons out of a cold fine filament by means of the intense electric field produced at its surface when it is made the inner member of a cylindrical condenser. Most of the experiments were done in high vacuum of the order of 10^{-8} mm Hg as measured with an ionization gauge. The fineness of the filaments used ($5 \times 10^{-4} - 10 \times 10^{-4}$ cm diameter) made it possible to obtain intense fields with smaller potential differences than those used by previous investigators. Different sizes of filaments were tried in order to dissect out the influence of the field and that of the potential difference on the current. Using a platinum-sputtered quartz filament, the platinum coating was torn off before electrons could be pulled out. With platinum filaments the field could be raised to 2×10^6 volts/cm without producing a current greater than 10^{-11} amp. The potential current curves of former observers could however be closely duplicated by admitting a little air into the apparatus. This fact together with the absence of any noticeable effect of the size of the filament on this curve suggests that the currents obtained by previous investigators may have been due to low pressure gas discharge.

32. A pseudo photographic effect of slow electrons. Jos. E. HENDERSON, Yale University (Introduced by W. F. G. Swann).—While using a magnetic spectrograph it was found that photographic plates subjected to a beam of slow moving electrons showed a dark line at the position calculated from the constants of the apparatus. This line was present on the plate even before development. In a further investigation 500 volt electrons were allowed to fall on different materials including glass, quartz, calcite, platinum, copper, nickel, silver, aluminum, zinc, lead and brass. The discoloration appeared on all of these. This discoloration seemed to be characteristic of the material being bombarded both as regards appearance and chemical behavior. The marking on the glass had a very metallic lustre but was readily attacked by strong alkalies. The line on the platinum was unattacked by the alkalies but was removed readily by aqua regia. The discoloration disappeared from the glass when it was heated above 450°C in air. From the nature of the apparatus it does not seem probable that a deposit could in any way be coming from the cathode. The apparatus employed gave an electron beam of comparatively high intensity, the current in the beam being several micro-amperes. Exposures of a few hours were necessary in order to get a good discoloration.

33. Quantum theory of the specific heat of hydrogen chloride. ELMER HUTCHISSON, University of Pittsburgh.—The new quantum mechanics indicates that the specific heat of simple dipole molecules like those of HCl may be calculated using half integer rotational and vibrational quantum numbers in the expression for the energy and using $p_m = 2m$ for the a priori probability (Cf. J. H. Van Vleck, Phys. Rev., Nov. 1926). Recently Hicks and Mitchell have computed the specific heat of HCl at various temperatures and its entropy using energy levels obtained from band spectra data but with

an a priori probability $p_m = 2m+1$. These values have been recomputed using the new quantum theory a priori probabilities. In this case it is found that the specific heat-temperature curve rises to a maximum above the classical value at about 12°K. There are not any experimental data at these low temperatures to confirm or contradict this maximum but at room temperatures the new specific heat curve agrees better with existing experimental values than that computed by Hicks and Mitchell.

34. A suggestion of an explanation of the long life of metastable atoms. G. BREIT, Carnegie Institution of Washington.—According to the recent theory of Schrödinger the term values of an atom are the characteristic values of E in his equation $[H, \psi] = E\psi$. The variable ψ when multiplied by its conjugate $\bar{\psi}$ gives the charge density. From this point of view the resultant electric moment of an atom due to the simultaneous presence of the states E_n, E_m is the element $q(nm)$ of the coordinate matrix q . The frequency of oscillation of the doublet is $\nu = 1/h(E_n - E_m)$. The above is Schrödinger's picture of radiation if $q(nm) = 0$. However, radiation may exist even in $q(nm) = 0$ corresponding to a coil aerial in radio for which the doublet also vanishes. Estimating the life of an atom on this basis, it is found to be of the order of almost a second. This is an agreement with the measurements [Dorgelo]. It is suggested, therefore, that the matrix mechanics represents only a first and rough approximation of the radiating properties of an atom and that Schrödinger's $\psi\bar{\psi}$ picture of electric charge density may be used to calculate radiation by means of classical formulas with retarded potentials even though matrix elements should vanish. A metastable atom is from this point of view analogous to a radio loop, while a non-metastable atom is analogous to an antenna.

35. Wave theory of the electron. W. P. ALLIS and H. MÜLLER, Massachusetts Institute of Technology.—The electron is considered as a wave of frequency $\nu = (mc^2 + eV)/h$ and wave number $\mu = c(m^2 - m_0^2)^{1/2}/h$ with which electricity is associated as energy is associated with an electromagnetic wave. Its group velocity $d\nu/d\mu$ is the velocity of the electron. The electricity is always "ether coupled." Uniform rectilinear motion or motion in certain orbits which are shorter than the wave-train are non-radiating. The quantum conditions are obtained as by de Broglie. The "quantum jump" is a continuous process in which charge gradually passes from the wave corresponding to the initial to that corresponding to the final state. During the process the waves form "groups" traveling with the velocity $\Delta\nu/\Delta\mu$ which obey the electromagnetic laws. In the Compton effect two plane waves form plane uniformly moving groups. The field must be zero on these groups. The scattered beam, superposed on the incident beam, is made to satisfy this condition and the conservation of energy and momentum relations result. In radiating hydrogenic atoms Δk groups move around the nucleus with the frequency $\Delta\nu/\Delta k$, and therefore radiate light of frequency $\Delta k \cdot \Delta\nu/\Delta k = \Delta W/h$. The indivisibility of the electron leads to the principle of selection.

36. The length of radiation quanta. ERNEST O. LAWRENCE, National Research Fellow, and J. W. BEAMS, National Research Fellow, Yale University.—Certain theoretical considerations of experimental facts lead to the conclusion that visible light quanta have lengths of the order of magnitude of 1 m. Closely allied to this conclusion, though quite independent of theory, is the length of time required for the photo-electric absorption of a light quantum by an electron, a time interval which has not been measured by experimental observation. By a refinement of a method previously described (J.O.S.A. & R.S.I., 13, 597 (1926)) we have succeeded in producing flashes of light of the order of magnitude of 10^{-10} sec. duration, i. e., pulses of radiation a few centimeters in length. The average intensity of these flashes was roughly from a hundred to a thousand times greater than that of a 10 ampere arc. This fact in conjunction with a photo-electric cell of great sensitivity has enabled us to measure the photo-electric effects produced by these short pulses of light. Our results show that the magnitude

of the photo-electric effect per unit incident energy is independent of the length of the light pulses, and therefore, that light quanta are less than 3 cms in length and electrons absorb radiation quanta photo-electrically in less than 10^{-10} sec.

37. Effect of a magnetic field on the dielectric constant. J. J. WEIGLE, University of Pittsburgh.—Assuming a molecule or atom possessing magnetic and electric moments perpendicular to each other the effect of a magnetic field on the dielectric constant has been calculated by the methods of the classical statistical dynamics. It is assumed that at high temperatures the classical theory leads to the same results as the new quantum dynamics. For the average electric moment in the direction of the electric field (perpendicular to the magnetic field) the expression obtained in the first approximation is $\mu^2 E / 3kT$ where μ is the electric moment, E the electric field intensity, k the Boltzmann's constant and T the absolute temperature. This expression is the same as that obtained if there were no magnetic field present and might explain the negative experimental results of L. Mott Smith and C. R. Daily (Phys. Rev. Nov., 1926). Thus it does not seem necessary to reject Langevin's theory of Paramagnetism as has been suggested (Huber Phys. Zeit. 27, 619 (1926)).

38. The quantization of the rotational energy of the polyatomic molecule by the new wave mechanics. ENOS E. WITMER, National Research Fellow, Harvard University.—For the purpose of quantizing the rotational energy the polyatomic molecule may be regarded as a rigid body with three principal moments of inertia, A_x , A_y , A_z . Assuming A_z to be the greatest or the least of these three quantities, let $a = \frac{1}{2}(1/A_z - 1/A_y)$, and $c = 1/A_z - \frac{1}{2}(1/A_x + 1/A_y)$. Then $a/c \leq 1$. The new wave mechanics gives the following formula for the energy, E , as a function of the quantum numbers:

$$E = (\hbar^2/8\pi^2) \{ m(m+1) \frac{1}{2}(1/A_z + 1/A_y) + n^2 c + \sum_{r=1}^{\infty} f_r(m, n) a^{2r} / (c^{2r} - 1) \},$$

where $f_1 = \frac{1}{8} [m^2(m+1)^2/(n^2 - 1) + 2m(m+1) - 3n^2]$.

The quantum numbers m and n are integers, and $n \leq m$. The process of solution apparently enables one to determine as many of the coefficients f_r as are desired. This formula is very similar to the one given by the classical quantum theory (cf. Witmer, Proc. Nat. Acad. Sci. October, 1926). The convergence of this series for values of a/c in the neighborhood of unity remains to be considered.

39. The significance and scope of the idea of frequency in physics. WM. S. FRANKLIN, Mass. Inst. of Technology.—Exponential (or periodic) solutions of the wave equation are essentially necessary when a bounded system is being considered; such solutions for extended media are merely simple and convenient. Periodic solutions for extended media are physically justifiable because wave disturbances generally originate in quasi-closed systems, and such solutions for extended media are useful because they are easily formulated mathematically and because the phenomena of dispersion, of interference and of diffraction are steady for periodic waves. The advent of the Bohr relation $W = \hbar\nu$ raised the idea of frequency to an exalted position which was extremely puzzling from the physical point of view, and the Bohr relation accentuated the non-critical use of the idea of frequency which was widely prevalent before Bohr's theory came forth. The Schrödinger wave mechanics brings us sharply back to the recognition of frequency as an ideal, because Schrödinger's mechanics is based on a generalized wave equation of which the only mathematically feasible solutions are exponential solutions and because Schrödinger attempts to formulate only those solutions which originate in closed or quasi-closed systems.

40. Influence of temperature on selenium photo-sensitivity. ROBERT J. PIERSOL, Westinghouse E. & M. Co., E. Pittsburgh.—Previous results on the influence of temperature on selenium have covered a range above 0°C. Various investigators have interpreted these data as either due to metallic conduction or due to electrolytic con-

duction. Experiment has shown that the dark current of a certain selenium cell decreases from 1×10^{-3} amperes at room temperature to less than 5×10^{-10} amperes at liquid air temperature, while the light current (due to one hundred foot candles intensity) decreases from 6×10^{-3} amperes to about 5×10^{-3} amperes with the decrease in temperature. This points to the fact that the dark current is entirely due to thermal conduction. Since H. E. Ives has shown that on cooling potassium from room temperature to liquid air temperature, due to increase in work function, the photo-electric current is decreased about 25 percent; it would appear that the light current in selenium is due to photo-electric conduction. As noted, a selenium cell at liquid air temperature gives a ratio of 1×10^7 between the current due to 100 foot-candles and the dark current, thereby forming the most sensitive photometric instrument known for the measurement of feeble light intensities.

41. Actino-electric effects in argentite. W. A. SCHNEIDER, Washington Square College, New York University.—Actino-electric effects are observed in argentite and it is shown that the seat of conversion of light into electronic energy occurs both at the contacts as well as at certain spots on the crystal. The effect is found to be absent if the crystal structure is destroyed. The actino-electric current-intensity curves show a peculiar secondary effect at certain intensities, varying for different samples, however. On investigation of the actino-electric e.m.f.'s with reference to varying times of exposure and constant times of recovery it is found that an exponential relation exists between them which can be represented by $i = ae^{-bt}$. The "b" however is not a constant but increases with time of recovery and is the determining factor in the dark current and photo-electric hysteresis of the crystal. It may be very intimately connected with the positive part of the primary photo-electric current as described by Gudden and Pohl.

42. Photo-electric emission as a function of composition in sodium-potassium alloys. HERBERT E. IVES and G. R. STILWELL, Bell Telephone Laboratories, Inc.—The entire series of alloys of sodium and potassium have been investigated with respect to the relative values of the photo-electric currents produced by light polarized with the electric vector in and at right angles to the plane of incidence. The pure metals when molten exhibit values below three for the ratio of the two emissions; the alloys show three maxima at compositions approximately 20, 50 and 90 atomic per cent of sodium, with values from 10 to 30 for the ratio; the minima between show low values approximating those for the pure metals. The maxima and minima of the ratio of emissions are due to complicated variations in magnitude of the two emissions compared.

43. Some properties of Geiger counters. R. D. BENNETT, National Research Fellow, Princeton University. (introduced by H. D. Smyth).—In the course of an investigation of the properties of Geiger counters they were found to be sensitive under certain conditions to ultra-violet light. The points used were of the sphere type and of platinum. Apparently the action comes about by the release of a photo-electron from the surface of the sphere-point. The maximum effective wavelength was about 2725A, corresponding to a work function of 4.54 volts, nearly that for platinum. Measurement of the photo-electric effect from a platinum surface in air at atmospheric pressure indicated that the number of pulses recorded was of the same order of magnitude as the number of photo-electrons released. A measurement of intensities across interference fringes in the ultra-violet gave variations similar to those recorded by other methods. Photo-electrons from the wall of the chamber, positive ions or electrons from a filament at about 300°, or ions blown in with gas, have proved sufficient to excite this type of counter. The number of pulses recorded depends markedly on the applied potential and may vary fivefold within the active range of any particular counter. Counters of this type have been made having less than one "stray" per half hour.

44. The life history of an adsorbed atom of caesium. J. A. BECKER, Bell Telephone Laboratories, Inc.—Previous work (Phys. Rev., August, 1926) indicated that when a caesium atom strikes a hot tungsten surface it may retain its valence electron, share it with the tungsten, or lose it completely. The adsorbed ions produce enormous changes in the thermionic and evaporation characteristics. A further analysis shows that the average life of an absorbed atom under equilibrium conditions is N/A , where N is the number of absorbed atoms and A the arrival rate. Both can be determined experimentally. When the filament is at 660°K and the arrival rate that corresponds to caesium at 20°C, the surface is completely covered and an atom stays on it for one second. For a temperature of 620°K, smaller arrival rate and complete covering the life is about one minute. At times "edges" separate the filament into two regions covered to about 1 percent and 15 percent. Several different experiments show that this edge must be about .03 centimeter wide. For part of this edge more caesium evaporates than arrives, and conversely. Hence atoms must move from one part of the edge to the other. Consequently the atoms must cover distances a million times their diameter.

45. Interpretation of data dealing with thermionic emission. W. R. HAM, Pennsylvania State College.—Equations for thermionic emission are of the form $i = AT^n e^{-b/T}$ the most commonly used values of n being $\frac{1}{2}$ or 2. The validity of this equation is determined by substituting values of i and T in the equation $\log i - n \log T + b/T = \log A$, and ascertaining whether a straight line is obtained when values of $\log i - n \log T$ are plotted against $1/T$. It is shown mathematically that a straight line may be obtained for all values of n from $-\infty$ to $+\infty$ including $n=0$ provided b is a suitable function of b_0 and T and therefore no improvement in accuracy of values of i and T or increase in their range can differentiate between various values of n . Hence to obtain a value of n experimentally, independent knowledge concerning A or b must be obtained. Using the value of b obtained calorimetrically by Davisson and Germer, together with their data for thermionic emission for tungsten, the equation $i = A e^{-b/T}$ is found to fit with great exactness. Values of b and A for certain other elements are computed on this basis. From a quantum standpoint according to Wien, a value $n=0$ demands that the concentration in metals of electrons available for thermionic emission at a particular T be relatively small.

46. Technique of the Dufour cathode ray oscillograph for the study of short time occurrences. G. F. HARRINGTON and A. M. OPSAHL, Westinghouse E. & M. Co., E. Pittsburgh (Introduced by C. E. Skinner).—In general, methods, circuits and procedure are set forth for using the Dufour plate-in-vacuum cathode ray oscillograph for studies of phenomena of such short time duration as to preclude the effective use of any other known oscillograph. Phenomena where such a method of analysis can be used to advantage are: dielectric breakdown in general, dielectric spark lag, characteristics of gaseous conduction, and behavior of electrical systems when subjected to surges. It is found that the time for the cathode beam to complete its path is so short that mechanical synchronizing devices are considered relatively unsatisfactory. Circuits are given for use in exciting the oscillograph, then initiating the transient condition to be recorded. It is also made possible to have voltage surges from the circuit being studied switch on the oscillograph and record themselves. The arrangement of apparatus is shown together with sufficient information so that it may be duplicated readily. Conditions and precautions are given for recording the coordinates that can be obtained conveniently with one cathode stream. These relations are: phase relations, voltage-time, current-time, voltage-current, voltage-current-time. The cathode ray oscillograph records these relationships accurately if proper care is taken with the circuits and checks and made to make certain that effects due only to the measuring circuits are eliminated.

47. A hot wire vacuum gauge. A. L. HUGHES and A. M. SKELLETT, Washington University, St. Louis.—A gauge was needed for following fairly rapid changes of pressure between .1 mm and .00001 mm. A 1-mil tungsten filament, 5 cms long, was mounted along the axis of a glass tube connected to the vacuum system. A current from a 4-volt storage battery was passed through the tungsten filament in series with an approximately equal and adjustable resistance R . With the highest attainable vacuum, the potential drop along the tungsten wire in the gauge was balanced against a 2-volt storage battery, using a galvanometer as an indicator, and varying R slightly to secure an exact balance. Using hydrogen to calibrate the gauge, it was found that the deviations from a balance were accurately proportional to the pressure over a range from .000007 mm to .28 mm. The lower limit can no doubt be decreased still further by taking special precautions to maintain constant conditions.

48. A new selective radiometer of molybdenite. W. W. COBLENTZ and C. W. HUGHES, Bureau of Standards.—Previous communications described samples of molybdenite having closely adjacent spots which generate positive and negative actino-electric current. Although practically no electric current is obtained on exposing the whole crystal to light either spot can be used as a radiometer. Recently discovered samples exhibit only one polarity, producing a large galvanometer deflection when the whole crystal is exposed to radiation of wave-lengths shorter than 1μ . In the darkened laboratory, connected with a d'Arsonval galvanometer, under a daylight illumination of 0.8 foot-candle the molybdenite crystal developed an e.m.f. equivalent to 1 f.c. = 3×10^{-6} volt. Connected with a high-resistance d'Arsonval galvanometer, deflections of 1.5 mm were observed in moonlight of only 0.008 f.c. Connecting the samples of molybdenite with a millivoltmeter, on exposure to the sun, under a normal illumination of 8,000 foot-candles, the deflection was 3 to 4×10^{-4} volt or 1 f.c. = 4×10^{-8} volt; i. e., increasing the illumination intensity 8,000-fold decreased the intrinsic sensitivity about 130-fold. In spite of this lack of proportionality for high intensities (preventable perhaps by exposing only the most sensitive spot) this device has applications as a selective radiometer, rivaling the gas-ionic photo-electric cell in quickness of action and requiring no external battery.

49. The absorption of radio waves in the upper atmosphere. E. O. HULBURT, Naval Research Laboratory, Washington, D. C.—The absorption of radio waves in the upper atmosphere, put to one side in the theory of Taylor and Hulbert because of its smallness, has been calculated on the assumption that it results from collisions between the electrons and molecules of the atmosphere. Formulas are derived for the dispersion and absorption of the variously polarized waves, and quantitative agreement is indicated with observed data of ranges and degradation of intensity with distance from the transmitter. It is pointed out that as these data become more extensive they may lead to more exact knowledge of the electronic and molecular pressures overhead.

50. Propagation of electromagnetic waves along co-axial cylindrical conductors separated by two dielectrics. N. H. FRANK, Massachusetts Institute of Technology.—A solution of the Maxwell equations for a harmonic electromagnetic wave propagating along co-axial cylindrical conductors separated by two dielectric media has been obtained. The velocity of phase propagation of this wave is given by

$$v^2 = (c^2/\epsilon_1\epsilon_2) (\epsilon_1 \ln(r_3/r_2) + \epsilon_2 \ln(r_2/r_1)) \div (\ln(r_3/r_2) + \ln(r_2/r_1))$$

if the conductors and dielectrics are considered perfect. c is the velocity of light in vacuum, r_1 , r_2 , r_3 the distances from the center of the cable to the outsides of the inner conductor, first dielectric, and second dielectric respectively. ϵ_1 and ϵ_2 are the dielectric constants of the first and second dielectrics respectively. An experimental investigation of this formula by an extension of a method employing the Lichtenberg figures (Phys.

Rev. 25, 865, (1925)) using ethyl alcohol, rubber and air as dielectrics and copper conductors showed that the above formula was satisfied within an experimental error of about 2 percent. Although the Lichtenberg figures are obtained by the use of an aperiodic pulse, the application of the above relation to this case can easily be justified, since the velocity given by the formula is also the velocity of propagation of the wave front even when the dielectrics and conductors are not perfect.

51. Subfundamental piezo-electric vibrations in quartz plates. J. R. HARRISON, Wesleyan University.—With a new type of piezo-electric crystal mounting, it has been found possible to obtain piezo-electric reactions of very much lower frequency than that of the transverse fundamental, first described by Cady (Proc. I. R. E. 10, 83 (1922)). The "transverse fundamental" is the frequency of the compressional wave in the direction of the largest dimension of the plate, both ends being free. The new mode of vibration is also different from any previously observed in that it is dependent to a large degree on more than one crystal dimension. The crystal mounting is so designed that the electric field is applied to two areas which are symmetrically disposed with respect to the longitudinal axis of the quartz plate, and the polarities in the quartz are in opposite directions. With the electric field applied in this manner, piezo-electric crystals operate successfully either as resonators or as oscillators at this subfundamental frequency. The luminous glow emitted by crystals when resonating in a low pressure chamber, lately described by Giebe and Scheibe (Elektrotech. Zeit. 13, 380), can also be observed at the subfundamental frequency, the luminosity presenting striking peculiarities which still await explanation.

52. Factors affecting the constancy of quartz piezo-electric oscillators. EARLE M. TERRY, University of Wisconsin.—A study has been made of the effect of mechanical stresses, temperature, and circuit constants upon the frequency of an oscillating plate of quartz connected in the usual way across the grid-filament elements of an electron tube, a tuned resonance circuit being placed in series with the plate. Frequency changes were measured by determining the change in pitch of the audio frequency beat note between this oscillator and a similar one furnishing a constant frequency. Various kinds of deformations were produced by resting the plate on a three point support and applying forces at a single point on its upper surface at different positions. For loads up to 500 grams the frequency change is of the order of one part in 500,000 per gram, the change being sometimes positive and sometimes negative, depending upon the type of deformation. The crystal was later placed in an enclosed chamber and subjected to air pressures of 20 atmospheres. The frequency decreased by approximately one part in 74,000 per atmosphere, the rate of change increasing somewhat with the pressure. A theoretical study has been made of four commonly used circuits in which the crystal is replaced by its electrical equivalent, as given by Cady, and an expression for the resultant frequency obtained, holding within the limits of experimental error.

53. Precise determination of frequency by means of piezoelectric oscillators. J. TYKOCINSKI-TYKOCINER, University of Illinois.—The oscillating current whose frequency is to be determined is inductively superimposed upon the oscillations of a piezoelectric oscillator. The plate current of the driving thermionic oscillating tube is compensated by a potentiometer arrangement so that the current variations can be observed by a microammeter. The relation between the plate current of the piezoelectric oscillator and the exciting frequency was investigated experimentally. The curves show a sharp current maximum and minimum with an intermediate steep line crossing the zero current abscissa. The point of intersection corresponds to resonance. If the exciting frequency equals exactly the fundamental frequency or a harmonic of the piezoelectric oscillator, no influence whatsoever is exerted upon the plate current. But a deviation

of 1.15 of the frequency measured (294100 per second) can still be detected when the quartz crystal is clamped between two electrodes. With the crystal free, frequency variations less than one in a million are detected by a violent vibration of the microammeter pointer. The plate current variation in the measured circuit is of a different character and less pronounced.

54. High pressure powder contact rectifier. J. E. LILIENFELD and C. H. THOMAS, Davy Electrical Corp.—This rectifier makes use of the known contact combination, aluminum to cupric sulphide. It has been realized that the pressure is of importance with respect to the rectification, and therefore with a certain available compressing force, a definite contact area has to be maintained. It appeared later that highly compressed CuS powder offers just enough flexibility at its surface to secure intimate contact with the metal provided sufficient pressure is being maintained. The rectifier consists of cells made from a limited area about 25 square mm against a thin layer of CuS which has been forced into non-polarizing nickel cups. A compression force of about one thousand pounds is supplied by an *helical* spring. The resistance of the cell decreases until a critical pressure is reached. Every rectifier of the present size will deliver 2.5 to 3 amperes d.c. at 2 volts and on a lower amperage, higher voltage up to $3\frac{1}{2}$ volts. A difference of the characteristics is noticeable between a pure resistance and an inductance load. Oscillograms of the current through a resistance load show complete and distortionless full wave rectification, while those of the current through a new filter circuit of inductances and resistances show suppression of the ripple to less than one percent of the total voltage.

55. A correlation between the power loss, dielectric constant and conductivity of various glasses. LOUISE S. McDOWELL and HILDA BEGEMAN, Wellesley College.—Values of power factor, dielectric constant and resistivity are given for six glasses of widely varying resistivity. In general the order of decreasing conductivity is found to be also the order of decreasing power factor and decreasing dielectric constant. Exceptions to this order are noted and an explanation of the correlation based on electron theory is proposed.

56. Mechanical forces between electric currents and saturated magnetic fields. VLADIMIR KARAPETOFF.—The general case considered is that of N independent electric circuits placed in a medium of variable permeability and subject to saturation, in parts or as a whole. The problem is to determine the component (in a given direction) of the mechanical force acting upon one of the electric circuits, upon a group of circuits, or upon a group of circuits with part of the magnetic medium rigidly attached to them. Use is made of the expression for the stored electromagnetic energy, W , of the system, assuming all the electric circuits to be first open and then closed one by one. Such a treatment necessitates a number of partial saturation curves, giving the linkages with the individual electric circuits when some of the other circuits are closed and the rest are open. A virtual displacement, δs , is then given to the part of the system under consideration, keeping the linkages or the currents constant, and the force, F , is determined from a comparison of the work done, $F \cdot \delta s$, and the change in the stored energy, δW . It is shown that the familiar reciprocal relationship for the mutual inductance, $M_{21} = M_{12}$, in a medium without saturation, can be generalized to a more involved integral expression for a saturated medium.

57. Thermal agitation of electricity in conductors. J. B. JOHNSON, Bell Telephone Laboratories, Inc.—Ordinary electric conductors are sources of random voltage fluctuations, as the result of thermal agitation of the electric charges in the conductor. The average effect of the fluctuations has been measured by means of a vacuum tube amplifier, where it manifests itself as a component of the phenomenon commonly called

"tube noise." A part of the "tube noise" arises in the first tube and other elements of the apparatus; the remainder in the input resistance, with a mean square voltage fluctuation $(V^2)_m$ which is proportional to the resistance R of that conductor. The ratio $(V^2)_m/R$, of the order of 10^{-18} watt at room temperature, is independent of the material and shape of the conductor, but is proportional to its absolute temperature. In the range of audio frequencies, at least, the noise contains all frequencies at equal amplitudes. The noise of an input resistance of only 5000 ohms may exceed that of the rest of the circuit, so that the limit of useful amplification is at times set by the thermal agitation of charges in the input resistance of the amplifier.

58. The electrical resistance of metals as a function of pressure. A. T. WATERMAN, Yale University.—Assuming that the effect of hydrostatic pressure on the electrical resistance of metals is solely due to the accompanying volume change, the author's expression for the electrical resistance $R = CT^a e^b/T$ has been shown (Phys. Rev. 25, 4, p. 585) to be in agreement with experimental data on the pressure effect, provided the rate of change of b with volume is constant. Theoretical development of the influence of pressure on resistance, involving the effect of pressure on the chemical equilibrium postulated between atoms, ions and electrons within the metal, indicates that the pressure coefficient of resistance $1/R dR/dp$ is given by $\frac{1}{2}C + (1/2RT)(dx/dp + \delta v)$, where C = compressibility, x = energy change involved in the assumed reaction liberating electrons within the metal, and δv = a possible volume change accompanying the reaction. x may be expressed as the difference between the mean potential energies of an electron in the bound and in the free states. On calculating the compressibility (assuming only electrostatic forces) in terms of these quantities it appears that the change in resistance with pressure is chiefly due to a change in the mean potential energy of the free electrons. Furthermore, for elements in the same column of the periodic table, the rate of change with volume of the mean potential energies of both the bound and the free electrons is in approximate linear relation to the atomic number.

59. Molecular fields. DAVID G. BOURGIN, Lehigh University.—The treatments of statistical problems arising in physics which are based on direct extension of formulae, which are rigorously true for small values of n , have usually proved extremely complicated and have been discarded in favor of the methods of statistical mechanics. The recent statistical researches of Pearson provide a basis for development of a direct method which does not suffer from the objection of awkwardness. The advantages of this direct method are the greater transparency of the calculations and the fact that the number of necessary approximations may often be cut down or made more plausible. In the particular problem of molecular force fields, assuming random angular distribution under no impressed forces, an expression has been derived for the probability that the resultant field lies between F and $F+dF$. This fundamental expression has been evaluated for the case of a gas using current approximations. Some of the overlapping results of Holtsmark and Gans for this case are confirmed.

60. A general theory of the electrical properties of surfaces of contact. RICHARD D. KLEEMAN, Union College.—In a previous paper (Phys. Rev. 20, 174–185 (1922)) the writer developed a theory of the e.m.f. associated with the part of a solution in contact with a metal plate. This theory is now extended to include the plate itself, and further generalized to apply to any two substances or mixtures in contact in any given state. The e.m.f. between two given points, one of which is situated in each substance, is expressed in terms of the coefficients of diffusion and the mobilities of the ions and molecules under the action of forces due to an asymmetrical distribution of matter and electricity, and externally applied electric fields. It is usually impossible to predict how these quantities vary from one part to another. But from the general nature of the

equations obtained the existence of a number of effects some of them still unknown can be predicted. A systematic experimental study of these effects is being undertaken.

61. Theory of cell with liquid junction. PAUL B. TAYLOR, University of Pennsylvania.—A simple integral is derived for the e.m.f. of the general cell with liquid junction in terms of transference numbers and molecular free energies. The transference numbers are made to depend upon the solution of a set of differential equations for the interdiffusion of two electrolytes each consisting of any possible mixture of ions. These equations involve the ionic mobilities and the molecular free energies, but not the free energies of the individual ions. It follows that the e.m.f. of a cell with liquid junction is not a function of ionic free energies and so can not possibly be manipulated to yield these quantities. Thus the values found in the literature purporting to measure hydrogen ion free energy, the so called Ph numbers, when based on such cells are quite unjustified. Henderson has given a formula, recently improved by Harned, for the p.d. of the liquid junction. This p.d. can not be found in terms of thermodynamic data (except at infinite dilution), but the formula modified to yield cell e.m.f. is a useful first approximation to a solution of the differential equations. A solution which may be considered a second order approximation has been derived.

62. The absolute zero of the externally controllable entropy and internal energy of a substance or mixture. R. D. KLEEMAN, Union College.—The internal energy of a substance or mixture may be divided into two parts, one of which is externally controllable, and therefore a function of temperature and volume, while the other part is not. The entropy may similarly be divided into two parts. It is shown that in thermodynamics we are only concerned with the controllable internal energy and entropy and that these quantities may have zero values. The temperature and volume corresponding to these zero values may be obtained by means of the theorem that the specific heat of a mixture kept at constant volume can only have positive values, which may be said to follow from our conceptions of temperature and heat content, and the postulate that the increase in pressure per unit increase in temperature at constant volume cannot be infinite, which will probably be readily admitted. It is then obtained that the controllable internal energy and entropy of a substance or mixture in the condensed state in contact with its vapour at the absolute zero of temperature have zero values. Formulae for the controllable internal energy, entropy, free energy and potential corresponding to any density and temperature may then readily be deduced.

63. On the dependence of ionic mobility on the nature of the medium. HENRY A. ERIKSON, University of Minnesota.—If air ions pass through air containing impurities such as carbon dioxide or water vapor, it is found that the mobility diminishes as more of the impurity is added. The conditions involved are such as to lead to the conclusion that the change is due to the change in the medium and not to a change in the ions.

64. Variation with state of the optical constants of caesium. J. B. NATHANSON, Carnegie Institute of Technology.—The optical constants of caesium were determined for the solid and liquid states, for wave lengths 5400, 5890, and 6410 Å. Observations were made at 23°C and 33°C, the melting point of caesium being 26°C. The glass cell containing the caesium mirror was warmed by means of a small electrical oven enclosing the mirror and containing suitable apertures for the incident and reflected light rays. The method of observation was that previously employed. (Phys. Rev. 25, 75 (1925).) The optical constants were computed by means of Drude's equations. When the metal changed from the solid to the liquid state, it was found that the angle of azimuth of restored plane polarization, as well as the phase difference between the components of the light vector parallel and perpendicular to the plane of incidence, changed very little, thus producing only slight changes in the values of the coefficient of absorption, k , the

index of refraction n , and the reflecting power R . For example, for $\lambda 5400\text{A}$ and solid caesium, $k=3.74$, $n=0.308$, and $R=0.595$, while for liquid caesium, the corresponding values are 3.66, 0.310, and 0.588.

65. An unusual magnetostrictive effect in Monel metal. S. R. WILLIAMS, Amherst College.—Magnetically, nickel is a most interesting metal. No less so are its alloys as permalloy, for instance, demonstrates. Monel metal, an alloy of nickel and copper, has also some very interesting magnetic properties. Among these is the fact that it loses its magnetic properties in the neighborhood of 100°C . The Joule magnetostrictive effect was studied in both hot and cold rolled rods of Monel metal. Some behaved like cobalt and others like nickel. The most interesting effect was, that if a magnetizing field of about 1000 gauss was left impressed on the Monel metal rod, it would continue to shorten, although the field was not varied, until the heat from the coil finally penetrated and the two effects worked against each other. This after effect in Monel metal is four to five times greater than the change in length due to varying the imposed magnetic field, whereas the after effect in nickel is only about $1/20$ of the main Joule effect. The biggest magnetostrictive effect in Monel metal is that due to time when a certain field is applied and maintained constant.

66. Magnetic susceptibility of single-crystal elements. C. NUSBAUM, Case School of Applied Science.—A modified form of the Terry torsion balance is being used for the determination of the magnetic susceptibility of a number of single-crystal metals along their respective crystallographic axes. The sample is mounted on a specially designed table and may be rotated in the magnetic field around any given axis. An investigation has been made on tellurium which has a three-fold axis of rotational symmetry. Curves show the variation of the susceptibility with the angle of rotation as the crystal is rotated around any of its axes. A similar study is also being made of the single crystals of Cd, Bi, Sb, Sn, and Zn.

67. The effect of wave-length on the differences in the lags of the Faraday effect behind the magnetic field for various liquids. FRED ALLISON, Alabama Polytechnic Institute.—Through the employment of a method by means of which two magnetic fields can be applied and removed simultaneously, it has recently been found by Beams and Allison that in various liquids there is a lag of the Faraday effect behind the magnetic field. This lag varies with different liquids and the differences in these lags for several liquids were determined with a precision of 0.4×10^{-9} sec. The present paper extends the work to an investigation of the differences in the lags of the Faraday effect for several liquids when different wave-lengths of light are used. The liquids studied were carbon bisulphide, carbon tetrachloride, chloroform, benzene and xylene, the wave-lengths being the spark lines Mg4481, Zn4912,24, Mg5173,83, Cd5338,78. It is found in every case that the differences in the time-lags of the Faraday effect behind the magnetic field are inversely proportional to the wave-lengths of light used. The extreme variations observed in these time-lag differences range from 0.3×10^{-9} sec. for the longer wave-lengths to 7.5×10^{-9} sec. for the shorter waves, depending upon the two liquids compared, the precision of an observation being 0.3×10^{-9} sec.

68. Relation of heat transmission to humidity in insulating materials. L. F. MILLER, University of Minnesota.—The hot and cold plate apparatus, with guard ring, taking twelve inch square samples was used, which seems best for preserving the moisture content acquired at the different humidities. Measurements were made at the same humidities to which the sample was exposed. To avoid short circuiting thermocouple due to wetting, enameled Advance (formerly Ideal) and copper wires were employed. Special apparatus was used to humidify the room and moisture content was measured by weighing. As checks, three different instruments measured the relative humidity, one

instrument being a continuous recorder. Materials investigated were: wood-pulp fibre, flax-fibre, cane-fibre and rag-paper felt, all approximately 1/2 inch thick. All thermocouples used were found to be reliable to $1/10^{\circ}\text{C}$. The temperature difference was not much over 10°C , which reduces the tendency of the moisture to move from hot side toward the cold side. Indication of results is that the heat transmission increases linearly as the moisture content. Up to 100 percent relative humidity there is an average increase in moisture content of about 15 percent by weight of dry sample weight and about a 15 percent increase in heat transmission for the four materials. At 100 percent relative humidity absorption is more rapid and moisture content much greater, with corresponding increase in thermal-conductivity.

69. Thermal expansion of graphite. PETER HIDNERT and W. T. SWEENEY, Bureau of Standards.—An investigation on the thermal expansion of longitudinal and transverse sections of artificial graphite (99.2 to 99.7 percent carbon) over various temperature ranges between room temperature and 600°C has recently been completed. The coefficients of expansion of graphite are low. For example, the coefficient of expansion of ordinary steel is about six times the coefficient of longitudinal sections of graphite and about four times the value for transverse sections between 20 and 100°C . The transverse samples expand considerably more than the longitudinal samples (approximately 45 percent). The coefficients of expansion increase with temperature. For both the longitudinal and transverse sections, the coefficients of expansion decrease slightly as the purity (carbon content) increases. The following table gives a resumé of average coefficients of expansion for various temperature ranges.

Section	<i>Average Coefficient of Expansion ($\times 10^6$) per Degree Centigrade</i>				
	20 to 100°C	20 to 200°C	20 to 300°C	20 to 400°C	20 to 500°C
Longitudinal	1.9	2.0	2.2	2.4	2.5
Transverse	2.9	3.0	3.2	3.5	3.7

70. Theory of the magnetic nature of gravity. CORNELIO L. SAGUI, Castelnuovo dei Sabbioni, Italy.—The only physical reality considered necessary is the electromagnetic field. A ray of light is considered as formed of a series of extremely small electrical resonators without ohmic resistance. In such a resonator a sine disturbance once started will go on without end. A transmitting medium for the energy is not considered necessary. The electromagnetic waves would consist of a sort of magnetic quanta moving to and fro. Matter would be built up similarly of electrical resonators, so that the gravitational force would be represented by the integral value of all the magnetic quanta of the elementary resonators moving to and fro about the body in a radial direction, at a distance which should be a function of the total number of resonators composing the body in question. Thus the gravitational field would not be infinite, but limited by the mass of the body itself. A ray of light going through a gravitational field of such a kind must modify its frequency within certain limits. A second modification of its frequency would result from the motion of the earth, in such a way that when the motion was in the same direction as that of the ray the frequency would become smaller.

71. Cosmic aspects of atmospheric electricity. LOUIS A. BAUER, Carnegie Institution of Washington.—There being at present no generally accepted theory to account for the origin and maintenance of the earth's negative electric charge, it is of peculiar interest to study the laws and modus operandi of the changes to which atmospheric electricity is subject during the day, year, and from year to year. These changes, which even on meteorologically-undisturbed days are on the order of the absolute values of the atmospheric elements themselves, show remarkable terrestrial and cosmical aspects; i.e., they are in general of the same character and sign at stations both in the northern and southern hemispheres. Recent world-wide observations give further confirmation

of these striking facts. A brief discussion is also given of the relation of the atmospheric-electric results to recent measurements of the ozone content of the atmosphere, of the sun's ultra-violet radiation, of radio-reception, and of solar activity.

72. Measurements of the variation of residual ionization in air with pressure at different altitudes. W. F. G. SWANN, Yale University.—Under the auspices of the Bartol Research Foundation, measurements of residual ionization were made, in an iron sphere, at Colorado Springs and at the summit of Pikes Peak, for pressures ranging from atmospheric up to 1000 lbs. per square inch. In one set of experiments the iron sphere one inch in thickness was shielded by about 2 inches of lead and in the other set it was unshielded. Corresponding observations were reproducible with an accuracy of about 2 percent. The mean apparent absorption coefficient α (the coefficient calculated for the case of a vertical radiation) was $5 \cdot 2 \times 10^{-4}$ per meter of air estimated at atmospheric pressure, and it was the same to within a few percent of its value from whatever corresponding parts of the pressure ionization curve it was calculated. The increase in ionization per atmosphere increase in pressure decreased with the pressure but became sensibly constant at the higher pressures. The absolute increase in ionization per cc per atmosphere increase in pressure at the highest pressures was 0.75 for the summit of Pikes Peak.

73. Radiometric measurements on the planet Mars, 1926. W. W. COBLENTZ and C. O. LAMPLAND, Bureau of Standards.—Measurements with vacuum thermocouples intercepting only 0.01 of the area of the planetary image confirm previous observations, showing: the southern (summer) hemisphere warmer than the northern hemisphere; the dark areas hotter than the adjacent bright areas; the forenoon side cooler than the afternoon side (exceptions; sunset clouds, or dark area on east limb irradiated an hour before sunrise). Temperature differences between the center of the disk and the limbs (and poles) appear smaller than previously observed; probably seasonal, which was a month after Martian summer solstice instead of a month before as obtained in 1924. Owing to clouds and the "limb light" of the Martian atmosphere, estimates of temperatures on east and west limbs are too low. Afternoon clouds seemed denser than morning clouds—not necessarily a general condition. The following tentative estimates of Martian surface temperatures are given; as viewed on the central meridian, the south polar region 10° to -10°C ; south temperature zone 20° to 25°C (clouds— 10°C); center of disk 20° to 30°C ; north temperature zone 0° to 20°C ; north polar region -25° to -40°C ; east limb (after being irradiated for an hour) -20°C , no phase -25°C , clouded -35°C ; west limb (terminator) 0°C , no phase -10°C , clouded -30°C .

74. On the effects of dust, smoke, and relative humidity upon the potential gradient and the positive and negative conductivities of the atmosphere. G. R. WAIT, Carnegie Institution of Washington.—A discussion is given of simultaneous observations of atmospheric electricity, dust-content, and relative humidity obtained at the Watheroo Magnetic Observatory, Western Australia.—The dust-content series (by Aitken's counter) during February to April, 1924, gives consistent results indicating that the potential gradient is approximately doubled for increase of dust-content from zero to 10,000 particles per cubic centimeter and thereafter a very slow increase with increased dust-content. Thus one is not justified in extrapolating, as has been done, values for dust-free air when the data are obtained only for high dust-contents. Both positive and negative conductivities decrease about half when the dust-content changes from zero to about 5,000 particles per cubic centimeter and decrease very slowly thereafter with increased dust-content. The ratio of positive to negative conductivity, as might be expected, increases with increasing dustiness. The more extensive simultaneous observations of the atmospheric-electric elements and relative humidity, using data taken only at times of low dust-content, show that these elements are similarly affected by an

increase in relative humidity, but to a lesser extent. The analysis shows that very few transformed large ions pass through the conductivity instruments without being recorded. The great importance of more observations of this kind in investigating the behavior of ions in air is pointed out.

75. Demonstration of an improved form of Rijke tube of high efficiency. A lecture experiment in acoustics. R. W. Wood, Johns Hopkins University.—By increasing the number of gauzes, a tube was constructed which continued sounding for two minutes or longer.

76. The direct comparison of the loudness of pure tones. B. A. KINGSBURY, Bell Telephone Laboratories, Inc.—The intensities of 11 pure tones necessary to make them as loud as certain fixed levels of a 700 cycle test tone were judged by 22 observers, 11 men and 11 women. Frequencies from 60 to 4000 cycles were used and intensities from the threshold of audibility to levels somewhat louder than ordinary conversation. It was found that if the amplitudes of pure tones are increased in equal ratios the loudness of low frequency tones increases much more rapidly than that of high frequency tones although for frequencies above 700 cycles the rate is nearly uniform. As a loudness unit the least perceptible increment of loudness of a 1000 cycle tone was employed. In absolute magnitude this varies from level to level, but in the ordinary range of loudness it becomes constant. The variability of the data from which the averages were computed was separated into a factor expressing dissimilarity of ears and another expressing errors of observers' judgment. There was no level at which the variances were a minimum. Dissimilarity of ears causes more variation than errors of observers' judgment.

77. Physical and biological effects of high-frequency sound waves of great intensity. R. W. Wood, Johns Hopkins University, and ALFRED L. LOOMIS, Tuxedo, N. Y.—This paper describes effects observed with sound-waves of 300,000 vibrations per second, obtained with a piezoelectric quartz plate driven by an electrical oscillator of 2 kilowatts output at 50,000 volts; thermic effects; elevation of the free surface of the liquid by the pressure of the waves; atomization of the surface with waves of great intensity; destruction of the red blood corpuscles in a living animal and other biological effects.

AUTHOR INDEX

- Allis, W. P. and H. Mueller—No. 35.
Allison, Fred—No. 67.
- Barrett, C. S. and J. A. Bearden—No. 33.
Bauer, Louis A.—No. 71.
Bayley, P. L.—No. 6.
Beams, J. W. and Earnest O. Lawrence—
No. 20.
Beams, J. W.—See Lawrence.
Bearden, J. A.—see Barrett.
Becker, J. A.—No. 44.
Begeman, Hilda—see McDowell.
Bennett, R. D.—No. 43.
Birge, R. T. and J. J. Hopfield—No. 8.
Black, J. G.—see Duffendack.
Boord, Cecil E.—see Smith.
Bourgin, David G.—No. 59.
Breit, G.—No. 34.
- Coblenz, W. W. and C. W. Hughes—
No. 48.
Coblenz, W. W. and C. O. Lampland—
No. 28.
del Rosario, C.—No. 31.
Duffendack, O. S. and J. G. Black—
No. 24.
- Ellis, Joseph W.—No. 19.
Erikson, Henry A.—No. 63.
- Frank, N. H.—No. 50.
Franklin, Wm. S.—No. 39.
Frayne, John G. and C. W. Jarvis—No. 22.
Friauf, James B.—No. 8.
- Gartlein, C. W.—No. 21.
Gibbs, R. C. and H. E. White—No. 28.

- Gibbs, R. C.—see White.
Gray, J. A. and B. W. Sargent—No. 1.
Ham, W. R.—No. 45.
Harrington, E. A.—No. 7.
Harrington, G. F. and A. M. Opsahl—
No. 46.
Harrison, J. R.—No. 51.
Henderson, Jos. E.—No. 61.
Hidnert, Peter and W. T. Sweeney—
No. 69.
Hopfield, J. J.—No. 17.
—see Birge.
Horovitz, Karl—No. 4.
Hughes, A. L. and A. M. Skellett—No. 47.
Hughes, C. W.—see Coblenz.
Hulburt, E. O.—No. 49.
Hutchisson, Elmer—No. 33.
Ives, Herbert E.—No. 42.
Jarvis, C. W.—see Frayne.
Johnson, J. B.—No. 57.
Karapetoff, Vladimir—No. 56.
King, Arthur S.—No. 27.
Kingsbury, B. A.—No. 76.
Kleeman, Richard D.—Nos. 60, 62.
Lampland, C. O.—see Coblenz.
Lawrence, Ernest O. and J. W. Beams—
No. 36.
Lawrence, Ernest O.—see Beams.
Lilienfeld, J. E. and C. H. Thomas—
No. 54.
Loomis, F. W.—No. 15.
Lubovich, Vladimir P.—No. 16.
McDowell, Louise S. and Hilda Begeman
—No. 55.
Meggers, W. F. and F. M. Walters—
No. 26.
Miller, L. F.—No. 68.
Mohler, F. L.—No. 13.
Mueller, H.—see Allis.
Nathanson, J. B.—No. 64.
Nusbaum, C.—No. 66.
Opsahl, A. M.—see Harrington, G. F.
Pease, C. S.—see Smith.
Piersol, Robert J.—No. 40.
Purks, J. H. and C. M. Slack—No. 3.
Richtmyer, F. K. and L. S. Taylor—No. 9.
Rudy, Richard—No. 30.
Rusk, Rogers D.—No. 11.
Sagui, Cornelio L.—No. 70.
Sargent, B. W.—see Gray.
Sawyer, R. A. and F. R. Smith—No. 23.
Schneider, W. A.—No. 41.
Skellett, A. M.—see Hughes, A. L.
Slack, C. M.—see Purks.
Smith, Alpheus W., Cecil E. Boord and
C. S. Pease—No. 14.
Smith, F. R.—see Sawyer.
Sommer, L. A.—No. 25.
Stilwell, G. R.—see Ives.
Stuhlman, Otto—No. 10.
Swann, W. F. G.—No. 72.
Sweeney, W. T.—see Hidnert.
Taylor, L. S.—see Richtmyer.
Taylor, Paul B.—No. 61.
Terry, Earle M.—No. 52.
Thomas, C. H.—see Lilienfeld.
Tschudi, E. W.—No. 12.
Tykocinski-Tykokiner, J.—No. 53.
Wait, G. R.—No. 74.
Walters, F. M. Jr.—see Meggers, W. F.
Waterman, A. T.—No. 58.
Weigle, J. J.—No. 37.
White, H. E. and R. C. Gibbs—No. 29.
White, H. E.—see Gibbs.
Wilkins, T. R.—No. 2.
Williams, S. R.—No. 65.
Witmer, Enos E.—No. 38.
Wood, R. W.—Nos 75, 77.

THE
PHYSICAL REVIEW

THE REFLECTION OF X-RAYS BY CRYSTALS AS
A PROBLEM IN THE REFLECTION OF RADIA-
TION BY PARALLEL PLANES

BY SAMUEL K. ALLISON

ABSTRACT

It is pointed out that the previous solutions of the problem of the reflection of radiation from parallel planes by Lamson and Gronwall are physically incorrect since the intensities, not the amplitudes, of contributions from individual planes, have been added. It is shown that a mathematical method due to Darwin leads to a solution identical mathematically with those of Lamson and Gronwall. Using this result, the intensity of reflection is evaluated for certain ranges of the constants directly related to the reflected and transmitted amplitudes due to a single plane.

THE problem of the reflection and transmission of radiation by a set of parallel, equidistant, reflecting planes has been treated by Darwin¹, Lamson², and recently, Gronwall³. The solution of this problem is at least of theoretical interest in the treatment of the intensity of reflection of x-rays by crystals, for if we adopt the Bragg picture of the reflection of x-rays by atomic planes, as contrasted with the space-lattice treatment of Laue, the reflection and transmission of a crystal sheet for an incident x-ray beam is essentially a problem of this type. The treatment of the problem of the reflection of x-rays by the methods used in the optics of isotropic media has been criticised by Ewald⁴, but recently Bragg, Darwin and James⁵, have pointed out that the methods used by Darwin give results almost identical with those of Ewald.

The treatments of the problem by Lamson and Gronwall, while excellent mathematically, are open to the fundamental objection that in computing the total reflection as a function of the amount reflected from each plane, the *intensities* from each plane have been added. Now in any practical case, and certainly in the crystalline reflection of x-rays, the

¹ Darwin, Phil. Mag. 27, 675 (1914).

² Lamson, Phys. Rev. 17, 624 (1921).

³ Gronwall, Phys. Rev. 27, 277 (1926).

⁴ Ewald, Zeits. f. Physik 30, 1 (1924); Ann d. Physik 54, 519 (1918).

⁵ Bragg, Darwin, and James, Phil. Mag. 1, 897 (1926).

waves in question are coherent, and instead of their intensities, their amplitudes should be added. Nevertheless it can be shown that a large part of the mathematical work laid down by these authors is useful in the physically correct solution of the problem. The mathematical treatment of Gronwall is complete and elegant; he has obtained a solution intended to give the amount of radiation reflected from an incident beam of unit intensity by an infinite number of parallel planes, and also to give the amounts reflected and transmitted by a finite number of planes. The solutions for a finite number of planes are exceedingly complicated when expressed in terms of the constants of one plane and will not be considered here. The principal purpose of this paper is to attempt to give an acceptable physical meaning to the mathematical results of Gronwall for the reflection from an infinite number of parallel planes.

Let us consider the incidence of a monochromatic, parallel (an obvious idealisation), beam of x-rays of unit amplitude upon the face of a perfect crystal at the proper angle for reflection according to the Bragg law. We will neglect the influence of the index of refraction, also the polarisation and temperature corrections etc. According to the Bragg picture we can consider the atoms reflecting the x-rays to be arranged in planes. Let R_1 be the amplitude reflected by a single plane, and let T_1 be the amplitude of the wave emerging from the lower side of the plane, that is, the transmitted amplitude. Let R_n be the amplitude of the total wave reflected by n planes (as it emerges above the crystal face) considering all possible internal multiple reflections, and T_n be the amplitude of the total wave transmitted by n planes. Then following the method of Gronwall it is easily shown that the following equations hold⁶.

$$R_{n+1} = R_n + T_n^2 R_1 / (1 - R_1 R_n) \quad (1)$$

$$T_{n+1} = T_n T_1 / (1 - R_1 R_n) \quad (2)$$

These are second order difference equations, and if R is the amplitude of reflection from an infinite number of planes, Gronwall has shown⁷ that they lead to the result.

⁶ These equations may be obtained from Eqs. (8) and (7) of Gronwall's paper by making the substitutions $t = T_1$, $r = R_1$, $R'_n = R_n - R_1$. The introduction of R' terms in Gronwall's treatment is unnecessary.

⁷ The radical in (3) comes in as the result of solving a quadratic equation, and Gronwall gives reasons for selecting the proper sign before the radical which are not valid for the case where amplitudes, and not intensities, are added. Nevertheless, an argument valid for the present treatment may be advanced which leads to the same selection of sign. Referring to Gronwall's paper, the quadratic to be solved is his Eq. (18). In carrying through the treatment in the notation of this article, we would let $\rho_n = 1 - R_1 R_n$; then Gronwall's (18) becomes

$$\rho + T_1^2 / \rho = \rho_1 + T_1^2$$

$$R = (1/2R_1)(1 - T_1^2 + R_1^2 - [(1 + T_1^2 - R_1^2)^2 - 4T_1^2]^{1/2}) \quad (3)$$

It is interesting to note that this same result was obtained with a slightly different method of approach by Darwin⁸, though it is not explicitly stated in his paper in exactly this form. With Darwin let t_n be the amplitude of the total transmitted wave above the $(n+1)$ st plane. Then t_0 is the amplitude of the incident beam. If r_n is the amplitude of the total reflected wave above the $(n+1)$ st plane, then r_0 is that of the reflected beam from an infinite number of planes. As before let R_1 and T_1 be the amplitudes of the waves reflected and transmitted by a single plane. Then it follows that

$$r_n = R_1 t_n + T_1 r_{n+1} \quad (4)$$

$$t_{n+1} = T_1 t_n + R_1 r_{n+1} \quad (5)$$

If we eliminate r from these equations, we obtain

$$T_1(t_{n-1} + t_{n+1}) = t_n(1 + T_1^2 - R_1^2) \quad (6)$$

Darwin now assumes a solution of the form

$$t_n = t_0 x^n \quad (7)$$

Solving for x after insertion in (6) gives

$$2T_1x = 1 + T_1^2 - R_1^2 \pm [(1 + T_1^2 - R_1^2)^2 - 4T_1^2]^{1/2} \quad (8)$$

in which it is easily shown⁹ that the negative sign alone gives a result of physical significance.

From (7) and Eqs. (4) and (5) we may also obtain

$$(r_0/t_0) = (1/2R_1)(2R_1^2 + 2T_1x - 2T_1^2) \quad (9)$$

and if we substitute the correct value of x from (8)

$$r_0/t_0 = (1/2R_1)(1 - T_1^2 + R_1^2 - [(1 + T_1^2 - R_1^2)^2 - 4T_1^2]^{1/2}) \quad (10)$$

This is the result of Gronwall and Lamson if we consider t_0 as unity. The method of Darwin thus involves only first order difference equations, but Gronwall's method seems more readily adaptable to the study of reflec-

Now the product of the roots of this equation (solved for ρ), is T_1^2 and if they are unequal, one is greater and one less than T_1 . But from our equation (2), the present ρ_n must be greater than T_1 or the amplitude of the transmitted beam would increase in the passage through the system. Thus the larger value of ρ is the physically significant one, as Gronwall concludes from other considerations.

⁸ Darwin, Phil. Mag. 27, 675, see p. 678 (1914).

⁹ From the form of the quadratic from which (8) is obtained it follows that the product of the two roots given in (8) must be unity. If they are unequal, only the one less than unity can have physical significance by (7).

tion and transmission by a finite number of planes. Thus we see that three different methods of approach lead to the same solution, as expressed in (3).

If we consider the expression (3) for the amplitude of the reflected beam, we see that for a certain range of R_1 and T_1 , namely $T_1 < 1 - R_1$. R will be imaginary. The physical significance of this is of course that there is a phase shift in reflection, and that

$$I = |R|^2 \quad (11)$$

where I is the intensity of the reflected beam.

Let us assume that the wave trains incident on, and reflected and transmitted by, a single plane, may be represented as follows.

$$y_i = e^{i\omega t} \quad (12)$$

$$y_r = b e^{i(\omega t + \delta)} \quad (13)$$

$$y_t = k e^{i\omega t} \quad (14)$$

Thus in (13) we assume a phase shift δ on reflection, but in (14) we neglect the shift in transmission. From these assumptions it follows that

$$R_1 = b e^{i\delta}, \quad T_1 = k \quad (15)$$

If we substitute these values in (3) and perform the operation indicated in (11) we should obtain an expression for the reflected intensity. Even with the simple assumptions (12), (13), (14), this expression becomes very complicated if the operations are carried out without auxiliary assumptions. We will first assume that δ is small so that $e^{i\delta} = 1 + i\delta$. We will also set $k = 1 - h$. Using these substitutions it follows, without neglecting any terms, that

$$\begin{aligned} [(1 - R_1^2 + T_1^2)^2 - 4T_1^2]^{\frac{1}{2}} &= [b^4 - 4b^2 + 2b^2 h(2 - h) \\ &\quad + h^2(2 - h)^2 - i\delta(8b^2 - 4b^4 - 4b^2 h(2 - h))]^{\frac{1}{2}}. \end{aligned} \quad (16)$$

If h and b are small, and terms of power higher than two may be neglected in comparison with $\pm(h^2 - b^2)$, this may be written

$$[(1 - R_1^2 + T_1^2)^2 - 4T_1^2]^{\frac{1}{2}} = 2[(h^2 - b^2) - 2b^2 i\delta]^{\frac{1}{2}} \quad (17)$$

We may express the result of taking the square root in (17) in two ways

$$\text{Case I } h > b \quad 2((h^2 - b^2)^{\frac{1}{2}} - b^2 i\delta(h^2 - b^2)^{-\frac{1}{2}}) \quad (18)$$

$$\text{Case II } h < b \quad 2(-b^2 \delta(b^2 - h^2)^{-\frac{1}{2}} + i(b^2 - h^2)^{\frac{1}{2}}) \quad (19)$$

In obtaining these expressions expansion by the binomial theorem was used, neglecting higher order terms.

If we treat first Case I, and insert (18) as the value of the radical in (3), we obtain, setting $k^2 = 1 - 2h$

$$R = (1/2b) \{ 2h + b^2 - 2(h^2 - b^2)^{\frac{1}{2}} + 2b^2\delta^2(h^2 - b^2)^{-\frac{1}{2}} \\ - i\delta(2h - b^2 - 2(h^2 - b^2)^{\frac{1}{2}} - 2b^2(h^2 - b^2)^{-\frac{1}{2}}) \} \quad (20)$$

Now if δ is small, the real part of R will be much greater than the imaginary part, and we obtain

$$I = (1/b^2)(h - (h^2 - b^2)^{\frac{1}{2}})^2 = (h/b - [(h^2/b^2) - 1]^{\frac{1}{2}})^2 \quad (21)$$

In Case II, we obtain for R

$$R = (1/2b) \{ 2h + b^2 + 2b^2\delta(b^2 - h^2)^{-\frac{1}{2}} - 2\delta(b^2 - h^2)^{\frac{1}{2}} \\ - i(2h\delta - b^2\delta + 2b^2\delta^2(b^2 - h^2)^{\frac{1}{2}} + 2(b^2 - h^2)^{\frac{1}{2}}) \} \quad (22)$$

Neglecting higher order terms, this gives

$$R = (1/2b)(2h - 2i(b^2 - h^2)^{\frac{1}{2}}) \text{ and } I = 1 \quad (23)$$

Thus in Case II the intensity of the reflected beam will differ from that of the incident only by very small quantities. This means practically 100% reflection under the ideal conditions postulated.

Neither of the results (22) or (23) are valid if h and b are so nearly equal that terms in their cubes and higher powers are not negligible in comparison with $\pm(h^2 - b^2)$. Nevertheless it is possible to evaluate I if $h = b$, thus obtaining a point in this region. It is easily shown that here the intensity of reflection, as in Case II, will differ from unity only by very small quantities.

Case II, $b > h$, is the most important, as at the wave-lengths ordinarily used, the crystals widely used in x-ray spectroscopy have $b > h$. The result of perfect reflection from a perfect crystal at the maximum of the "rocking curve" for this case has previously been obtained by Darwin and Ewald. The result of Case I, $b < h$, might possibly be of interest in the reflection of very soft x-rays from crystals containing heavy atoms.

The author gladly acknowledges discussions with G. Breit, O. Laporte and T. H. Gronwall on the subject matter of this paper.

DEPARTMENT OF PHYSICS,
UNIVERSITY OF CALIFORNIA, BERKELEY.
Sept. 11, 1926.

SPARK SPECTRUM OF COPPER (Cu II)

By A. G. SHENSTONE

ABSTRACT

Terms in the spectrum of Cu(II).—The spark spectrum of copper consists of (1) a low set of terms 3D and 1D from the structure (d^9s); (2) an intermediate set 3P , $^3D'$, 3F , 1P , $^1D'$, 1F (d^9p); (3) a high set 3D , 1D (d^9 , s); (4) probably a 1S (d^{10}), the lowest term and giving combinations outside the observed range. All of these terms except 1S have been identified by intensities of combinations and by Zeeman effects. They are all inverted except 3F which is only partially so; and the interval rule does not hold. The terms $^3D_3'$ and 1F_3 apparently share their g -sum and are otherwise not differentiable. The value of 1S can be found from arc spectrum limits to be about 22224 wave numbers lower than 3D_3 . The application of the combination principle makes possible the calculation of accurate wave numbers in the ultra-violet to $\lambda 1944$.

Comparison with corresponding terms in Ni(I) and Pd(I).—A comparison is made with corresponding terms in Ni(I) and Pd(I) and it is shown that the limits of the component term series in all three cases apparently do not agree with Hund's predictions. It is important that the difference $^3D_3 - ^3D_1$ in the three spectra is constant within the series to less than 1/10%; in the case of Cu(II), being apparently absolutely constant and equal to the difference $^4D_4 - ^4D_1$ of the arc spectrum.

An ionization potential for Cu(II) is calculated as about 20.5 volts.

IN AGREEMENT with the theory of the production of spectra developed by Hund¹ the author has shown in a recent paper² that the arc spectrum of copper consists of two parts; first, an ordinary doublet spectrum due to the atom in states in which all but one of the twenty-nine electrons are in closed groups of orbits; second, a quartet-doublet spectrum due to the atom in states in which nine of the last eleven electrons are in 3_3 orbits, one is in a 4_1 orbit and the last is in either a 4_1 or some less firmly bound condition. There are indications of a less completely developed third spectrum arising from structures in which only eight electrons remain in 3_3 orbits. The lowest terms of the first two types of spectra are $^1S(d^{10}s)$ and $^3D(d^9s^2)$. The brackets give, symbolically, the electron configurations, the letters denoting the k -values of the orbits, and the indices the numbers of electrons. Only the last eleven electrons are given, since the others remain in closed groups.

The two types of ion on which the two branches of the arc spectrum are built are (d^{10}) and (d^9s) which spectroscopically are terms of type 1S and 3D , 1D . The series of terms in the two branches of the arc

¹ Hund, Zeits. f. Physik, 33, 841 (1925).

² Shenstone, Phys. Rev. 28, 449 (1926).

spectrum will, therefore, have as limits the spark 1S and the various components of the terms 3D , 1D . We can, then, find approximately the difference $^1S - ^3D$ by calculating the limits of series of terms in the two parts of the arc spectrum. The limit of the 2S terms is taken as zero, according to the usual convention. There are two 4D terms (d^9s , s) available for the calculation of the limits of the second arc spectrum. The 4D_4 terms are the lowest and should converge to the spark 3D_3 . This limit falls at -22224 , indicating that the difference $^1S - ^3D_3 = 22224$, the 1S being the lower term. This value may be in error by perhaps 1500 units since only two series members are available for the calculation.

Combining with the low spark terms 1S and 3D , 1D there should be found a triad 3P , $^3D'$, 3F , 1P , $^1D'$, 1F due to the electron configuration d^9p . Such terms should also combine with higher series members of the sequence 3D , 1D , (d^9 , s). The comma between d and s is used to denote that the s -electron is in an excited level, for instance 5_1 , 6_1 , etc.

The spectrum of the copper arc in the ultra-violet contains many strong spark lines which can be distinguished with some difficulty by the ordinary arc-spark comparison method. If the arc is run from batteries and self-induction is avoided as far as possible, the spark lines become relatively weak and the distinction can be made more easily. The low-voltage arc³ in Cu vapor has also been used by the author for the separation of arc and spark lines.

A number of the ultra-violet spark lines have been observed by Stücklen⁴ in the under-water spark and wrongly placed as arc lines. From their appearance under the conditions of that experiment, there can be no doubt that they are among the most easily excited spark lines. They are all included in the following Table I which gives the combinations of the lowest 3D , 1D with the intermediate terms 3P , $^3D'$, 3F , 1P , $^1D'$, 1F . It will be noticed that all of the terms of Table I are inverted with the exception of the partially-inverted 3F , in agreement with the predictions of the Hund theory. The method of determining the designations of the terms and their magnitudes is given below.

The lowest term of this set is 3D_3 and it has been arbitrarily assigned the value zero, the remaining terms then all assuming positive values. The assignment is provisional only, awaiting the discovery of the exact difference $^1S - ^3D_3$ which would then be added to all of the terms.

The combinations of the intermediate set of terms of Table I with a higher 3D , 1D are given in Table II. These two sets include every copper spark line of the quartz region which is also emitted in the ordinary copper arc. A large number of the lines also appear in the spectrum of the low-voltage arc when the current density is large.

³ Shenstone, Phil. Mag. 49, 952 (1925).

⁴ Stücklen, Zeits. f. Physik 34, 562 (1925).

The lines of Table II lie, for the most part, in a spectral region in which greater accuracy of measurement is possible. The term differences have, therefore, been computed from that table. The actual values of terms above 3D_3 have then been computed by the use of the few lines of Table I which have been measured with reasonable accuracy by Mitra⁵ and by Wolfsohn.⁶ The wave numbers of lines calculated from Hasbach's⁷ and Eder's⁸ measurements diverge progressively from the values predicted by the combination principle. If these differences

TABLE I
Classification of certain ultra-violet spark lines of copper.

	a^3D_3 0.0	a^3D_2 918.5	a^3D_1 2069.7	a^1D_2 4335.7	
a^3P_2	44489.9 1497.9	44489.9 (W) (10)	43571.4 (W) (5) (8)	42420.6 (2) (5)	40154.3 (7) (2)
a^3P_1	45987.8 933.4		45069.3 (W) (10)	43918.1 (WM) (5)	41652.2
a^3P_0	46921.2			44852.4	
a^3F_4	46802.1 -283.0	46803.6 (4)			(6)
a^3F_3	46519.1 1420.2	46520.1 (3)	45601.3 (4)	(8)	42183.1 (0)
a^3F_2	47939.3	47941.2 (8)	47020.7 (M)	45870.4	43603.4 (9)
a^3D_3'	48912.5 652.4	48914.8 (1)	(8)	(3)	44576.8 (WM) (7)
a^3D_2'	49564.9 1608.4	49568.1	48648.9 (2)	47497.2 (7)	45229.4 (W) (4)
a^3D_1'	51173.3		50258.6 (6)	49106.3	46838.0 (6)
a^1F_3	49991.3	49995.0 (2)	49075.5 (2)	(5)	45655.5 (M) (5)
a^1D_2'	51424.3	51427.1	50509.4 (1)	49357.9 (1)	47090.2 (5)
a^1P_1	51667.1		50751.9	49600.8	47331.1 (M)

are plotted against wave-length, a curve is obtained which rises to a maximum of about $\Delta\nu = 3.8$ at $\lambda = 2000$ and thereafter falls with shorter wave-length. If the present analysis of the Cu spark spectrum is admitted as correct, then it is possible to calculate much more accurate wave-lengths than have been previously known in the region $\lambda 1944$ to $\lambda 2200$. The values given in Tables I and II are Hasbach's and Eder's; the values in the Table IV at the end of this paper are those calculated by the use of the combination principle. The frequencies given in Table IV have a probable error of about 0.4 units.

⁵ Mitra, Ann. d. physique 19, 315 (1923).

⁶ Wolfsohn, Ann. d. Physik 80, 415 (1926).

⁷ Hasbach, Zeits. f. Wiss. Phot. 13, 399 (1914).

⁸ Eder, Wien. Ber. 123 II a, 616 (1914).

The intensities given in Tables I and II are the author's visual estimates of the photographic intensities of the lines. In general, the combinations which do not involve a change in multiplicity are in excellent agreement with theoretical expectation, with one striking exception, the absence of the line $a^3D_2 - a^3D_3'$. Its intensity should be about 4; and, indeed, the corresponding line of Table II is present with

TABLE II
Classification of additional spark lines of copper.

	b^3D_3 86083.7	b^3D_2 86404.6	b^3D_1 88153.3	b^1D_2 88435.0
a^3P_2	44489.9 1497.9	41593.8 (5)	41914.7 (0) (5)	43945.1 (0)
a^3P_1	45987.8 933.4		40416.8 42165.5 (1)	42447.3
a^3P_0	46921.2		41232.1	
a^3F_4	46802.1 -283.0	39281.6 (4)	(8)	(0)
a^3F_3	46519.1 1420.2	39564.9 (0)	39885.5 (5)	41915.5 (1)
a^3F_2	47939.3	38145.2	38465.4	40213.9 40496.9
a^3D_3'	48912.5 652.4	37171.2 (1)	37492.1 (3) (7)	39521.4 (0)
a^3D_2'	49564.9 1608.4	36518.9	36839.7 (4)	38588.4 (6)
a^3D_1'	51173.3		35231.2	36980.2
a^1F_3	49991.3	36092.4 (1)	36413.4 (5) (0)	38443.7 (7)
a^1D_2'	51424.3	34659.5	34980.5 (5)	36729.0 (1)
a^1P_1	51667.1		34737.5	36486.9 36767.9

intensity 3. The intensities of the intersystem combination lines do not obey, even approximately, the usual qualitative rules. For instance, a^1D_2 combines with a^3P_2 much more strongly than with a^3P_1 . Moreover, the relative intensities of the intersystem lines of Tables I and II are entirely different. This seems quite anomalous.

ZEEMAN EFFECTS

Zeeman patterns of most of the lines included in Tables I and II have been measured. The magnet used produced a field of about 34000 gauss, and the lines were photographed in a Hilger E1 quartz spectrograph. In the region below $\lambda 2500$ the dispersion is great enough to give trustworthy measurements of Zeeman separations; but, in the

longer wave-lengths a rather large error may occur. The patterns, except in a few cases, are resolved only as triplets. In such cases the pattern predicted by the use of Landé's *g*-values has been reduced to a theoretical blend triplet by the following procedure. The intensities of the components of a complicated pattern follow a quadratic formula and in consequence the center of gravity will always be approximately 1/4 of the way from the strongest to the weakest component. For instance,

$${}^3D_3 - {}^3P_2 \text{ Z.E.} = (\bar{0}, 1, 2) \bar{6}, 7, 8, 9, 10 / 6 \sim (0) 7 / 6 \sim (0) 1.17.$$

I am indebted to Professor H. N. Russell for this useful suggestion.

The observed patterns and the calculated are both given in the wave-length Table IV at the end of this paper. The agreement is very good in the main and fixes without doubt the nature of the low 3D , 1D terms. In fact, all the lines of Table I show excellent agreement except those involving the terms a^3D_3' and a^1F_3 . These two terms certainly have *g*-values which are neither 1 nor 4/3, the theoretical values. The observed patterns are, however, consistent with the sharing of the *g*-sum 7/3 between the two terms, the *g* of a^3D_3' being approximately 1.1 and of a^1F_3 approximately 1.2. From relative intensities of combinations, these two terms are also interchangeable. It is, therefore, impossible to differentiate between them and the designations given rest solely on their positions relative to the other terms a^3D_2 and a^3D_1 . A parallel case occurs in the Cu arc spectrum, where a^4D_3' and a^2F_3 are apparently not differentiable.

The Zeeman patterns of the lines of Table II are satisfactory considering the smallness of the actual separations on the plates. They again show disagreement for the terms a^3D_3' and a^1F_3 discussed above. In Table IV the asterisks indicate those lines which involve the two terms in question.

There remain only comparatively weak lines of Cu(II) unclassified. A number of these are undoubtedly due to structures such as d^9d combining with d^9p . A number of individual levels have been found, but the lines are so weak and so poorly measured that in no case can the levels be classified with certainty. This material is therefore reserved for future publication.

The lowest term of the copper spark should be ${}^1S(d^{10})$. As has been pointed out above, it should lie about 22224 wave-numbers deeper than a^3D_3 . The possible combinations are contained in $d^9p \rightarrow d^{10}$ and reduce to the following three only, because of the *j*-selection principle. They should lie within 1500 wave-numbers of the following positions.

${}^1S - a^3P_1$	$\nu = 68212$	$\lambda = 1466$
${}^1S - a^3D_1$	$\nu = 73397$	$\lambda = 1363$
${}^1S - a^1P_1$	$\nu = 73891$	$\lambda = 1353$

Of these strong lines, the last should be the most intense.

One of the lowest states of the doubly ionized copper atom Cu III should be a 2D term which arises from the structure d^9 . The addition of an s -electron gives terms 3D , 1D (d^9s) which are undoubtedly the low terms of Table I and the high terms of Table II. The addition of a second s -electron yields terms 4D , 2D , $^2D(d^9s, s)$; or, when the two s -electrons both occupy 4_1 orbits (d^9s^2), a 2D alone. Such terms are the c^4D , e^4D and m^2D of the atomic spectrum. It can be shown⁹ that the series of component terms of $^4D(d^9s, s)$ should converge to different components of the spark 3D term. In particular, the series 4D_4 should converge to 3D_3 and 4D_1 to 3D_1 . In other words, the difference $^4D_4 - ^4D_1$ should approach, at any rate in higher series members, the difference $^3D_3 - ^3D_1$. The following table shows that in fact this difference $^4D_4 - ^4D_1$ is already in the first series member practically equal to $^3D_3 - ^3D_1$. The evidence is very strong that the same difference also persists into the spectrum Cu III where it should be $^2D_3 - ^2D_2(d^9)$.

Cu(I) $d^9s^2 \quad m^2D_3 - m^2D_2 = 2042.9$	Cu(II) $d^9s \quad a^3D_3 - a^3D_1 = 2069.7$
$d^9s, s \quad c^4D_4 - c^4D_1 = 2069.0$	$d^9s \quad b^3D_3 - b^3D_1 = 2069.6$
$d^9s, s \quad e^4D_4 - e^4D_1 = 2069.6$	Cu(III) $d^9 \quad ^2D_3 - ^2D_2 = 2069.6?$

The remarkable agreement of the separations in this case and of the similar terms in the spectra of Ni(I) and Pd(I) given below, is predicted by the theory recently outlined by Slater.¹⁰

The following approximate agreements of arc and spark separations are also significant. The arc terms belong to the group which arises from the structure $d^9s d$; the spark term is the lowest 3D .

Cu(I) $d^4G_6 - d^4G_5 = 848.1$	$d^4G_5 - d^4G_3 = 1220.0$
$d^4F_5 - d^4F_4 = 802.6$	$d^4F_4 - d^4F_2 = 1223.4$
$d^4D_4 - d^4D_3 = 798.8$	
$d^4P_3 - d^4P_2 = 749.0$	
Cu(II) $a^3D_3 - a^3D_2 = 918.5$	$a^3D_2 - a^3D_1 = 1151.2$

The 4G term used above is the alternative given in the author's paper² at the foot of page 459.

In addition to the above excellent agreement of separations, there is the fact that $^4G_4 - ^4G_3$, $^4F_3 - ^4F_2$, $^4P_2 - ^4P_1$ are all small, fulfilling the theoretical prediction that each of these pairs of terms should have a single limit. For bringing to my notice all the above agreements of separation and for the prediction from them of the spark intervals I am indebted to O. Laporte.

The spectra of Ni(I) and Pd(I) should be similar to that of Cu(II). Pd(I) does in fact possess two sets of terms corresponding in detail to the high and low 3D , 1D sets in Cu(II). The first set is as given by

⁹ Hund, Zeits. f. Physik 34, 296 (1925).

¹⁰ Slater, Phys. Rev. 28, 291 (1926).

TABLE III
Corresponding terms in spectra of Cu(II), Ni(I) and Pd(I). Series limits and ionization potentials.

<i>j</i>	Terms	Cu(II)		Ni(I)		Pd(I)	
		$\Delta\nu$	$\Delta\nu$ (sum)	$\Delta\nu$	$\Delta\nu$ (sum)	$\Delta\nu$	$\Delta\nu$ (sum)
3D (d^2s)	3 0.0	918.5	918.5	204.8	675.0	6564.0	1191.0
	2 918.5	1151.2	2069.7	879.8	833.3	7755.0	3529.9
1D	1 2069.7	2266.0	4335.7	1713.1	1696.8	10093.9	2338.9
	2 4335.7	3409.9		3409.9		11721.7	1627.8
3D (d^3, s)	3 86083.7	320.9	86404.6	42605.8	184.1	48304.2	215.3
	2 86404.6	1748.7	88153.3	42789.9	1506.3	49019.5	3532.1
1D	1 88153.3	281.7	88435.0	44112.1	1322.2	52356.3	3316.8
	2 88435.0	44262.5		44262.5	150.4	52487.7	151.4
Limits of	Cu(III) (d^9)			Ni(II) (d^9)		Pd(II) (d^9)	
3D	3 144388		2D_3	62944	2D_3	69106	2D_3
	2 144502	2069		63017	1505	69099	3533
1D	1 146457		2D_2	64449	2D_2	72639	2D_2
	2 146048			64247		72452	
Ionization potentials	17.8 volts			7.8 volts		8.5 volts	

McLennan and Smith¹¹; but, in the high set the 3D_2 and 1D_2 have been interchanged. In the above paper this set of levels is arranged so that 3D is partially inverted, though the intensity relations agree equally well with the present arrangement. Moreover, it is now brought into perfect accord with the similar terms in both Cu(II) and Ni(I). The two sets of 3D , 1D of Ni(I) are contained in Bechert and Sommer's¹² paper. They were picked as members of a series by Hund.¹

The corresponding terms of the three spectra are given opposite each other in Table III. The most striking similarity is found in the interval $^3D_3 - ^3D_1$. In Cu(II), this interval changes when we pass from the low 3D to the high 3D , by only 0.1 wave-numbers, a change which is quite within the experimental error. In Ni(I) the corresponding change is -2.0 and in Pd(I), +2.2 wave-numbers. The 3D_2 and 1D_2 terms are placed in relatively the same positions in all three spectra. The 3D intervals are all reversed from the 'normal' order, i.e., $^3D_3 - ^3D_2 < ^3D_2 - ^3D_1$.

The series of component levels of 3D and $^1D(d^9s)$ must converge to the two components of the term $^2D(d^9)$ of the next higher ion. It can be shown (Hund⁹) that the limits should be as follows: 3D_3 and 1D_2 converge to 2D_3 ; and 3D_2 and 3D_1 to 2D_2 .

At the foot of Table III are given the series limits calculated from the two sets of levels for each of the three spectra. The ionization potentials are obtained from the 3D_3 limits. In the case of Cu II the potential given is for the removal of the *s*-electron from the structure d^9s . The ionization from d^{10} to d^9 would require approximately 20.5 volts, the difference of 2.7 volts being calculated from the term difference $^1S - ^3D_3$.

It has been pointed out that the extreme separation of the 3D terms ($^3D_3 - ^3D_1$) is almost constant in each of the spectra. This fact, and the behavior of the extreme terms in analogous cases in other spectra, makes possible a reasonable certainty that the separation of the calculated limits for these levels will agree closely with the actual separation. For example, the analogous 4D terms in Cu(I) give almost exact agreement of calculated and experimental limit separations.

The calculation of limits from only two series members in such cases as 3D_2 and 1D_2 must necessarily give much less certain results, and conclusions drawn from such calculations must require confirmation. An extreme case is the series of ms^3P terms in lead.¹³ Nevertheless, there is a peculiarity of the calculated limits in these three spectra which is at least noteworthy. That is, the exact agreement of the calculated limits for the component series 3D_3 and 3D_2 ; and the only slightly less

¹¹ McLennan and Smith, Roy. Soc. Proc. 112A, 110 (1926).

¹² Bechert and Sommer, Ann. d. Physik 77, 351 (1925).

¹³ Gieseier and Grotrian, Zeits. f. Physik 39, 377 (1926).

TABLE IV
Wave-lengths and classification of spark lines of Cu.

λ	Auth.	Int.	ν	Comb.	Z. E. (obs.)	Z. E. (calc.) Blend
2884.38	H	1	34659.5	$a^1D_3' - b^3D_3$		
2877.89	H	5	34737.5	$a^1P_1 - b^3D_2$	(0) 1.19	(0) 1.25
2857.9	Ex	0	34980.5	$a^1D_2' - b^3D_2$		
2837.56	H	4	35231.2	$a^3D_1' - b^3D_2$	(0) 1.48	(0) 1.5
2769.85	H	6	36092.4	$a^1F_3 - b^3D_3$	(0) 1.22	(.84) 1.16*
2745.43	H	5	36413.4	$a^1F_3 - b^3D_2$	(0) 1.31	(0) .83*
2739.9	Ex	1	36486.9	$a^1P_1 - b^3D_1$		
2737.5	Ex	1	36518.9	$a^3D_2' - b^3D_3$		
2721.84	H	5	36729.0	$a^1D_2' - b^3D_1$	(0) 1.31	(0) 1.25
2718.96	H	6	36767.9	$a^1P_1 - b^3D_2$	(0) 1.04	(0) 1.00
2713.66	H	7	36839.7	$a^3D_2' - b^3D_2$	(0) 1.02	(0) 1.17
2703.34	H	6	36980.2	$a^3D_1' - b^3D_1$	(0) .47	(0) .50
2701.12	H	7	37010.7	$a^1D_2 - b^3D_2$	(0) 1.02	(0) 1.00
2689.46	H	7	37171.2	$a^3D_3' - b^3D_3$	(.57) 1.17	(0) 1.33*
2666.44	H	3	37492.1	$a^3D_3' - b^3D_2$	(0) .99	(0) 1.50*
2620.78	Ex	0	38145.2	$a^3F_2 - b^3D_3$		
2600.43	H	6	38443.7	$a^1F_3 - b^3D_2$	(0) 1.30	(0) 1.00*
2598.96	H	5	38465.4	$a^3F_2 - b^3D_2$	(.82) .89	(.87) .92
2590.68	H	4	38588.4	$a^3D_3' - b^3D_1$	(0) 1.40	(0) 1.50
2571.91	H	0	38870.0	$a^3D_2' - b^3D_2$		
2544.96	H	10	39281.6	$a^3F_4 - b^3D_3$	(0) 1.11	(0) 1.13
2529.48	H	6	39521.9	$a^3D_3' - b^3D_2$	(0) 1.03	(0) 1.66*
2526.73	H	4	39565.0	$a^3F_3 - b^3D_3$	(.67) 1.12	(.62) 1.21
2506.41	H	8	39885.5	$a^3F_3 - b^3D_2$	(0) .98	(0) 1.00
2489.64	H	7	40154.3	$a^1D_2 - a^3P_2$	(.86) 1.21	(.75) 1.25
2485.95	H	6	40213.9	$a^3F_2 - b^3D_1$	(0) .72	(0) .75

λ	Auth.	Int.	ν	Comb.	Z. E. (obs.)	Z. E. (calc.) Blend
2473.47	H	5	40416.8	$a^3P_1 - b^3D_2$	(0) .83	(0) 1.0
2468.58	H	1	40496.9	$a^3F_2 - b^1D_2$		
2424.56	H	1	41232.0	$a^3P_0 - b^3D_1$		
2403.47	H	4	41593.8	$a^3P_2 - b^3D_3$	(0) 1.08	(0) 1.17
2400.10	H	2	41652.2	$a^1D_2 - a^3P_1$	(0) .64	(0) .75
2385.06	H	0	41914.8	$a^3P_2 - b^3D_2$		
			5.5	$a^3F_3 - b^3D_2$		
2370.88	H	0	42165.5	$a^3P_1 - b^3D_1$		
2369.88	H	6	42183.3	$a^1D_2 - a^3F_3$		
2356.65	Calc	2	42420.2	$a^3D_1 - a^3P_2$	(0) 1.12	(0) 1.17
					(0, .9) 1.45, 2.49	(0, 2) 1, 3, 5
						2
2355.15	"	0	42447.2	$a^3P_1 - b^1D_2$		
2294.374	W	5	43571.4	$a^3D_2 - a^3P_2$	(.66) 1.37	(.59) 1.33
2292.68	Calc	0	43603.6	$a^1D_2 - a^3F_2$		
2276.261	W.M	5	43918.1	$a^3D_1 - a^3P_1$	(1.0) .48, 1.52	(2) 1, 3
2274.86	Calc	0	43945.1	$a^3P_2 - b^1D_2$		
2247.003	W	10	44489.9	$a^3D_3 - a^3P_2$	(0) 1.15	(0) 1.17
2242.621	W.M	9	44576.8	$a^1D_2 - a^3D_3'$	(0) 1.16	(0) 1.66*
2228.88	Calc	5	44851.5	$a^3D_1 - a^3P_0$	(0) .49	(0) .50
2218.107	M	8	45069.4	$a^3D_2 - a^3P_1$	(0) .86	(0) 1.00
2210.27	Calc	7	45229.2	$a^1D_2 - a^3D_2'$	(0) .96	(0) 1.04
2192.27	"	10	45600.6	$a^3D_2 - a^3F_3$	(0) .96	(0) 1.00
2189.631	M	6	45655.6	$a^1D_2 - a^1F_3$	(0) 1.50	(0) 1.00*
2179.41	Calc	8	45869.6	$a^3D_1 - a^3F_2$	(0) .80	(0) .75
2148.98	"	4	46519.1	$a^3D_3 - a^3F_3$	(.79) 1.16	(.63) 1.21
2135.98	"	10	46802.1	$a^3D_3 - a^3F_4$	(0) 1.08	(0) 1.12
2134.36	"	4	46837.6	$a^1D_2 - a^3D_1'$	(0) 1.11?	(0) 1.25

λ	Auth.	Int.	ν	Comb.	Z. E. (obs.)	Z. E. (calc.) Blend
2125.047	M	4	47020.8	$a^3D_2 - a^3F_2$	(.82) .89	(.88) .92
2122.98	Calc	5	47088.6	$a^3D_2 - a^1D_2'$	(0) 1.05	(0) 1.00
2112.09	"	5	47331.4	$a^1D_2 - a^1P_1$	(0) 1.02	(0) 1.00
2104.81	"	3	47495.0	$a^3D_1 - a^3D_2'$	(0) 1.34	(0) 1.5
2085.30	"	3	47939.3	$a^3D_3 - a^3F_2$	(0) 2.37†	(0) 2.0
2054.99	"	8	48646.4	$a^3D_2 - a^3D_2'$	(0) 1.09	(0) 1.17
2043.81	"	8	48912.5	$a^3D_3 - a^3D_3'$	(.60) 1.06	(0) 1.33*
2037.13	"	6	49072.8	$a^3D_2 - a^1F_3$	(0) 1.22	(0) .84*
2035.85	"	7	49103.6	$a^3D_1 - a^3D_1'$	(0) .48	(0) .50
2025.50	"	5	49354.6	$a^3D_1 - a^1D_2'$	(0) 1.29	(0) 1.25
2016.90	"	1	49564.9	$a^3D_3 - a^3D_2'$		
2015.58	"	1	49597.4	$a^3D_1 - a^1P_1$		
λ (Vac)						
2000.348	"	7	49991.3	$a^3D_2 - a^1F_3$	(0) 1.08	(.84) 1.16*
1989.860	"	2	50254.8	$a^3D_3 - a^3D_1'$		
1979.971	"	2	50505.8	$a^3D_2 - a^1D_2'$	(0) 1.01	(.25) 1.08
1970.497	"	0	50748.6	$a^3D_2 - a^1P_1$		
1944.606	"	2	51424.3	$a^3D_3 - a^1D_2'$		

† Outside of wide pattern.

* Lines involving a^3D_3' or a^1F_3 .

H—Hasbach, Kayser & Koenen. Vol. VII.

Ex—Exner and Haschek, " " "

M—Mitra, Ann. d. physique 19, 315 (1923).

W—Wolfsohn, Ann. d. physik 80, 415 (1926).

exact agreement for 3D_1 and 1D_2 , contrary to the theory. The following diagram compares the theoretical prediction and the apparent result.

Theoretical limits	Apparent limits
$^3D_3, ^1D_2 \rightarrow ^2D_3$	$^3D_3, ^3D_2 \rightarrow ^2D_3$
$^3D_2, ^3D_1 \rightarrow ^2D_2$	$^3D_1, ^1D_2 \rightarrow ^2D_2$

It is remarkable that the apparent limits of 3D_2 and 1D_2 are exactly reversed from their expected positions, i.e., the deviations from the theoretical positions are closely $\mp(^2D_3 - ^2D_2)$. In other words, there would be excellent agreement if the designations of 3D_2 and 1D_2 could be interchanged. This, however, is definitely prohibited by Zeeman effects and intensities of combinations in Cu II, and, therefore, by analogy, in the other spectra.

The same type of peculiarity of convergence is evident in the following case of the 4D terms of Cu(I). The limits of the extreme terms agree exactly with the experimental limits. The 4D_2 term, however, instead of converging with 4D_1 to 3D_1 diverges apparently to 3D_2 , as is evident from the separations given.

Limits	$\Delta\nu$	$\Delta\nu$
4D_4	22224—	
4D_3	22428	3D_3 —
4D_2	23123—	3D_2 —
4D_1	24293—	3D_1 —
	899	918
	1170	1151

Such peculiarities may be coincidence. They would then be merely evidence of the same disturbing forces in all three spectra. This would not be surprising, since the structures involved are the same. The discovery of higher series members should remove any doubt there may be in the interpretation of these points.

The author has the greatest pleasure in thanking Dr. H. N. Russell for his very important assistance in the preparation of this paper.

PALMER PHYSICAL LABORATORY,
PRINCETON, NEW JERSEY.
December 10, 1926.

ELECTRONIC STATES AND BAND SPECTRUM STRUCTURE IN DIATOMIC MOLECULES

III. INTENSITY RELATIONS

BY ROBERT S. MULLIKEN

ABSTRACT

The correspondence principle predicts definite intensity relations for P , Q and R band lines in molecules having a rotational energy term $F(j) = B(j^2 - \sigma^2) + \dots$, provided σ is an electronic quantum number correlated with a precession about the internuclear axis (along which the angular momentum $\sigma\hbar/2\pi$ is directed). Hönl and London have used the summation rule method to obtain exact equations for each of three possible cases $\Delta\sigma = 0, \pm 1$; these equations are recast here in more convenient form. According to recent work of Dennison, these equations very probably remain valid in the new quantum mechanics. Theoretical curves for the cases $\Delta\sigma = +1$ and -1 are given.

Various electronic emission bands have been interpreted by the writer as corresponding to electronic transitions ${}^1S \rightarrow {}^1S$ (CuH type), ${}^1P \rightarrow {}^1S$ (AlH, He₂ "series" bands), ${}^1D \rightarrow {}^1P$ (He₂ $\lambda 5733$), ${}^1S \rightarrow {}^1P$ (He₂ $\lambda 4546$, $\lambda 6400$, and CO Ångstrom bands), with $\sigma = 0$ for 1S , $\sigma = 1$ for 1P , and $\sigma = 2$ for 1D states. Comparison of the predictions of the above theory with the available intensity data on the bands mentioned, assuming in each case thermal equilibrium at a suitable (arbitrarily chosen) temperature, gives in every case qualitative agreement with the predicted distribution for that particular case; usually the agreement appears to be complete within the often comparatively large uncertainties of the data. Oscillation-rotation absorption bands corresponding to $\sigma' = \sigma'' = 0$ fall under the theory as a special case, and the data on these bands (in particular the quantitative data of Kemble and Bourgin on HCl) agree with the theory. Intensity relations in ${}^2S \rightarrow {}^2S$ (violet CN type) and ${}^2P \rightarrow {}^2S$ (ZnH type) transitions are briefly discussed; the intensity relations resemble those for ${}^1S \rightarrow {}^1S$ and ${}^1P \rightarrow {}^1S$ transitions, but no satisfactory theory is as yet available.

The close agreement between theory and experiment for spectra interpreted as due to transitions involving 1S , 1P , or 1D states seems to make conclusive the already strong evidence for these interpretations. Furthermore (in connection with the observed selection $\Delta\sigma = 0, \pm 1$) it shows that 1S , 1P , and 1D molecular states all belong to a class in which σ is an electronic quantum number correlated with a precession about the internuclear axis.

In ${}^1S \rightarrow {}^1P$, ${}^1P \rightarrow {}^1S$, and ${}^1D \rightarrow {}^1P$ transitions, there exist in practice (cf. II of this series) two rotational states (A and B) for each value of j . The agreements noted were obtained by disregarding the subdivision into A and B sub-states; the fact that agreement was obtained in this way shows incidentally that the a priori probabilities of A and B sub-states must be equal.

Another phenomenon not contemplated by the theory, but present in all the He₂ bands, is that alternate lines are missing in each branch. The cause of this is obscure, but the evidence for its existence is conclusive and so justifies the procedure, which is necessary to obtain the agreement described above between theory and experiment, of inserting in Eqs. (5)-(6) a factor zero for alternate lines in each branch.

INTRODUCTION

THE importance of a study of intensity relations among band lines has been emphasized by Kratzer¹ and by Kemble^{2,3}. Up to the present, however, practically nothing has been done to compare experiment with theory except in the case of bands composed of *P* and *R* branches only.

As a result of a study of evidence from missing lines, presence of *Q* branches, and systematic relations for odd and even molecules, the writer has recently concluded^{4,5,6,7} that many known band spectra involve rotational terms of the form $B(j^2 - \sigma^2) + \dots$. Band spectra also exist which involve terms of the form $B(j - \rho)^2 + \dots$, while there are others involving more complex forms. A study of observed intensity relations lends strong support, as will be shown in the present paper, to the conclusions just mentioned. For notation, etc., reference should be made to a previous paper.⁶

SURVEY OF WORK ON THE INTENSITY PROBLEM FOR BANDS CONTAINING A SINGLE *P* AND A SINGLE *R* BRANCH

Bands without Q branches. Experimentally, known bands consisting of *P* and *R* branches and without *Q* branches comprise (*a*) infrared oscillation-rotation bands with one *P* and one *R* branch, such bands ordinarily being observed in absorption (examples: CO and halogen halide bands), (*b*) electronic bands having one *P* and one *R* branch (examples, CuH, AgH, AuH, I₂ bands), and (*c*) electronic bands having two *P* and two *R* branches, but with the two branches of each kind usually forming a series of close doublets (examples, violet CN and analogous bands).

In the case of oscillation-rotation bands, the presence of a σ is, according to the correspondence principle, a necessary and sufficient condition for the presence of a *Q* branch;^{1,8} the presence or absence of a ρ appears to be immaterial from the standpoint of the correspondence principle. Hence for type (*a*) above, we may conclude that $\sigma = 0, \rho \geq 0$. (Throughout this article $\sigma h/2\pi$ and $\rho h/2\pi$ denote components of electronic angular momentum which are respectively parallel and perpendicular to the internuclear axis.) The correspondence principle then gives further information in regard to the expected intensities of the lines of the *P* and *R* branches (see below).

¹ A. Kratzer, Naturwiss. 27, 577 (1923); Ann. d. Physik 71, 72 (1923).

² E. C. Kemble, Proc. Nat. Acad. Sci. 10, 274 (1924); Phys. Rev. 25, 1 (1925).

³ E. C. Kemble, Zeits. f. Physik 35, 286 (1925).

⁴ R. S. Mulliken, Proc. Nat. Acad. Sci. 12, 144 (1926).

⁵ R. S. Mulliken, Proc. Nat. Acad. Sci. 12, 151 (1926).

⁶ R. S. Mulliken, Phys. Rev. 28, 481 (1926).

⁷ R. S. Mulliken, Phys. Rev. 28, 1202 (1926).

⁸ A. Sommerfeld, Atombau und Spektrallinien, 4th Edition, Chapter 9, (1924).

In the case of electronic bands, the presence of a σ is a sufficient condition for the presence of a Q branch, but not a necessary one⁹ unless or until restrictions are placed on the types of electronic motions which are assumed to be possible. The absence of a Q branch in types (b) and (c) is, however, satisfactory evidence that σ (i. e. σ' and σ'') is zero; but the correspondence principle gives no definite information in regard to the intensities of the P and R lines unless a molecular model is assumed.

Oscillation-rotation bands without a Q branch. By application of the correspondence principle to bands of type (a), using the device of hypothetical magnetic components to remove degeneracy, Kemble made it probable² that the intensities of the lines of both P and R branches should be given by the relation

$$I = ie^{-E_0/kT}, \text{ where } i = a \bar{p} \quad (1)$$

Here E_0 is the value of $F(j)$ for the initial molecular state, a is to a first approximation a constant (but see below), and \bar{p} is the mean of the a priori probabilities p of the initial and final rotational states. Experimental work of Kemble and Bourgin¹⁰ on the HCl absorption band at 3.46μ completely confirms Eq. (1), provided \bar{p} is assumed to have the values $2, 4, 6, \dots$ for successive lines of each branch, or what is the same thing, provided $p=1, 3, 5, \dots$ for the rotational states having $m=\frac{1}{2}, 1\frac{1}{2}, 2\frac{1}{2}, \dots$.

Fowler¹¹ and Dieke¹³ have shown that Eq. (1) can also be obtained for type (a) bands by a rather formal application of the summation rule, provided the succession of p values $1, 3, 5, \dots$ is used, as above; any other choice of p values gives a stepwise-advancing or alternating set of intensities.

Mensing,¹⁴ Fues,¹⁵ and Oppenheimer¹⁶ have shown that for oscillation-

⁹ H. A. Kramers and W. Pauli, Jr. Zeits. f. Physik 13, 351 (1923). For further discussion cf. ref. 6, p. 488.

¹⁰ E. C. Kemble and D. G. Bourgin, Nature, June 5, 1926.

¹¹ R. H. Fowler, Phil. Mag. 49, 1272 (1925). Fowler attempted to extend the application of the summation rule to the case of bands (including electronic bands) having Q branches. He concluded that the P and R branches (aside from the Boltzmann factor and variability in a) should always be equally intense here, as in bands of the simple $P-R$ type. Kemble then pointed out³ that this conclusion based on the summation rule is in conflict with the correspondence principle, according to which there are many cases where such equality of P and R branches is not to be expected. Finally, the work of Hönl and London¹² showed that Fowler's conclusion is incorrect, and that the results of the two methods are in harmony.

¹² H. Hönl and F. London, Zeits. f. Physik 33, 803 (1925).

¹³ G. H. Dieke, Zeits. f. Physik 33, 161 (1925).

¹⁴ L. Mensing, Zeits. f. Physik 36, 814 (1926).

¹⁵ E. Fues, Ann. der Physik 80, 367 (1926).

¹⁶ J. R. Oppenheimer, Proc. Camb. Phil. Soc. 23, Part 3, p. 327 (1926).

rotation bands, if $j_e=0$ (i. e. $\rho=\sigma=0$),¹⁷ the new quantum mechanics yields directly the relation $i=a\bar{p}$ of Eq. (1) and the p values 1, 3, 5, . . .¹⁸

In a systematic study of known band spectra^{6,7} the writer concluded that all known bands of types (a) and (b) are due to transitions in even molecules having $j'_e=j''_e=0$,¹⁷ and $F(j)=Bj^2+\dots$ with $j=m=\frac{1}{2}, \frac{1}{2}, 2\frac{1}{2}, \dots$. Such transitions were classified as ${}^1S \rightarrow {}^1S$ transitions, and it was shown that definite characteristics properties ($j_e=0$, diamagnetic behavior, single rotational states) may be attributed to 1S states, thus implying that such states correspond to a definite molecular model. It was further concluded that 1S states belong to a class of states for which $F(j)=Bm^2+\dots=B(j^2-\sigma^2)+\dots$, with $\sigma=0, 1, 2, \dots$ for ${}^1S, {}^1P, {}^1D, \dots$ states, and $j=\frac{1}{2}, 1\frac{1}{2}, 2\frac{1}{2}, \dots$ in all (with the condition $j \geq \sigma$).

With $j=m=\frac{1}{2}, 1\frac{1}{2}, 2\frac{1}{2}, \dots$ for 1S states, the results of the preceding paragraphs require $p=2j$, hence Eq. (1) takes the form

$$I = ie^{-E_0/kT}, \text{ with } i = 2aj \quad (2)$$

If $p=2j$ for 1S states, it is reasonable to expect the same relation for ${}^1P, {}^1D, \dots$ states, and in fact for all electronic states, of both odd and even molecules. According to the writer's conclusions,^{4,6} j has integral values for odd molecules but half-integral values for even molecules.¹⁸

Electronic bands of type (b). The summation rule method of Fowler and Dieke leads to the conclusion that Eq. (1) should hold for electronic bands of type (b) as well as for bands of type (a). The intensity data of Frerichs²⁰ on the CuH bands, which are of type (b), show that Eq. (1) is indeed applicable here, even to the extent of accounting for the observed superior intensity of the P branch (in emission bands $E_0=E'$ and the exponential factor in Eq. (1) favors the P branch, while in absorption bands $E_0=E''$ and this factor favors the R branch^{3,11,18}). The intensity relations in the analogous AgH and AuH bands appear to be of the same type. In the I_2 absorption bands, as Fowler has pointed out,¹¹ the approximately equal intensity of the two components

¹⁷ The assumption made by Kemble, Fowler, and Dieke, that a ρ may be present (other than a "secondary" ρ as discussed in ref. 7, p. 1206), is then probably unnecessary if not unjustified for bands of types (a) and (b).

¹⁸ The new quantum mechanics^{14,15,16,27} formulates the rotational energy in terms of a different set of j values than those used here. For the case $j_e=0$, the result is $F(j)=B(j+\frac{1}{2})^2+\dots$, with $j=0, 1, 2, \dots$, hence $p=2j+1$. Thus it is evident that the j values of the quantum mechanics are analogous to Sommerfeld j values (since $p=2j+1$), while the writer's j values (for which $p=2j$) are analogous to Lande J values. Since the writer has concluded^{4,6} that the correct j_e values for molecules are of the Sommerfeld type, it would then be logical to adopt the j values of the quantum mechanics. Largely in order to avoid confusion of notation as compared with earlier papers, the writer's j values will, however, be used here.

²⁰ R. Frerichs, Zeits. f. Physik 20, 170 (1923).

in each doublet (one P , one R line) in the "resonance spectrum," again shows the applicability of Eq. (1).

The necessary applicability of Eq. (1) to all bands of type (b) is not obvious from the correspondence principle (cf. the discussion in a preceding paragraph); such a definite result would seem to imply a particular molecular model. The solution of this difficulty probably is that precisely the model corresponding to Eq. (1) is required by nature. This idea is supported by the fact that all known bands of type (b) appear to be in agreement with Eq. (1). Again, although it is not obvious that restrictions as to model (except that $\sigma=0$ and the absence of a Q branch are assumed) are required in deriving Eq. (1) by the summation rule method, it should be noted that Eq. (1) can be obtained as a special case of a more general Eq. (4) given below which involves definite assumptions in respect to a model. From the evidence presented below in regard to bands where $\sigma \neq 0$, it is altogether probable that the model on which Eq. (4) is based is the correct one for all known bands obeying Eq. (1).

INTENSITY RELATIONS IN BANDS INVOLVING ROTATIONAL TERMS OF THE FORM $B(j^2 - \sigma^2)$: APPLICATION OF THE CORRESPONDENCE PRINCIPLE

Application of older form of correspondence principle. In order to apply the correspondence principle to the intensity relations in bands of the type here under consideration, it is necessary to know or to assume something about the nature of the quantity σ (for the cases here considered, $\rho=0$). It will be shown below that predicted and observed intensity relations for a number of band spectra are in agreement if we assume that σ is an *electronic quantum number* which is correlated with a *precession about the internuclear axis*. This assumption is also strongly supported by the fact that in observed bands, according to interpretations recently given by the writer,^{6,7} the selection rule $\Delta\sigma=0$ or ± 1 is observed.²¹ Furthermore, as Hund has recently shown,²² precisely such a precession and such a selection rule are to be expected from theoretical considerations. The relation of the results of the present and previous papers of this series to Hund's theory will be discussed in a separate paper.²³

²¹ Thus in ${}^1S \rightarrow {}^1S$ transitions (CuH bands etc.⁶), $\Delta\sigma=0$, while the CO Angstrom, AlH, and He₂ bands furnish examples of $\Delta\sigma=+1$ and $\Delta\sigma=-1$.

²² F. Hund, Zeits. f. Physik 36, 657 (1926).

²³ Strictly it is *not* σ itself, but the component σ_k of σ due to orbital electronic angular momentum, with which the precession here under discussion is correlated; σ itself is a resultant of σ_k and σ_s , where σ_s is the component along the internuclear axis of the resultant angular momentum s of electron spin; generally $\Delta\sigma_s=0$ so that $\Delta\sigma_k=\Delta\sigma$. In bands of the ZnH type (${}^2P_1 \rightarrow {}^2S$, ${}^2P_2 \rightarrow {}^2S$), however, $\Delta\sigma=\frac{1}{2}$ and $1\frac{1}{2}$, but $\Delta\sigma_k=1$, indicating that σ_k is more fundamental than σ , as also follows from Hund's theory. These points will be further discussed in a later paper.

For a precession of the type indicated, the predictions of the correspondence principle for the intensities of P , Q , and R branch lines are completely analogous to those for the transitions $\Delta j = +1$, 0, and -1 in a line spectrum multiplet. For any selected initial rotational state, if θ represents the angle between j and the figure axis (direction of σ), the intensities should then be given to a fair degree of approximation by the following proportions:²⁴

$$(a) \quad \sigma' - \sigma'' = \pm 1, i_P : i_Q : i_R = \frac{1}{2}(1 \mp \cos \theta)^2 : \sin^2 \theta : \frac{1}{2}(1 \pm \cos \theta)^2 \quad (3)$$

$$(b) \quad \sigma' - \sigma'' = 0, i_P : i_Q : i_R = \frac{1}{2} \sin^2 \theta : \cos^2 \theta : \frac{1}{2} \sin^2 \theta$$

In the necessary averaging of the intensity factors of Eq. (3) over the initial and final states, a linear average may be expected to give good results, as in the line spectrum case. Thus suppose $\sigma' = 1$, $\sigma'' = 0$, $j' = 2\frac{1}{2}$. Noting that $\cos \theta = \sigma/j$, one has $\sigma'/j' = 1/2\frac{1}{2}$, $\sigma''/j'' = 0$, and $i_P : i_Q : i_R = \frac{1}{2}[(1 - 1/2\frac{1}{2})^2 + 1] : [1 - (1/2\frac{1}{2})^2 + 1] : \frac{1}{2}[(1 + 1/2\frac{1}{2})^2 + 1] = 0.68 : 1.84 : 1.48$.

Nature of 1S states and relation to ${}^1S \rightarrow {}^1S$ bands. For the special case $\sigma' = \sigma'' = 0$, according to Eq. (3b), we have $\cos \theta = 0$ for all values of j , and $i_Q = 0$, $i_P = i_R$. This is in essential agreement with Eqs. (1) and (2).

The applicability of Eq. (2) to all known electronic bands corresponding to ${}^1S \rightarrow {}^1S$ transitions therefore no longer presents a difficulty but indicates that 1S molecular states belong to the class of σ -type states, σ being correlated with a precession about the internuclear axis. The fact that 1S molecular states combine spectroscopically with 1P states ($\sigma = 1$) supports this conclusion, which is furthermore in line with recent theoretical considerations of Hund.²²

Hönl and London's application of the summation rule. As shown by Hönl and London,¹² Eqs. (3a) and (3b) can be replaced by more exact equations (Eqs. 4-5-6 below) obtained by an application of the summation rule. Hönl and London's treatment depends on the existence of a close formal analogy between the transitions $\Delta j = 0, \pm 1$ in line spectrum multiplets and the transitions $\Delta j = 0, \pm 1$ (Q , R , P , branches) in band spectra, and between $\Delta k = 0, \pm 1$ in line spectra and $\Delta \sigma = 0, \pm 1$ in band spectra, and thus implicitly involves the assumption that σ is correlated with a precession about the internuclear axis as assumed above in connection with Eq. (3).

Hönl and London's equations should of course be applicable to odd as well as to even molecules, using appropriate j values in each case (Hönl and London do not consider this point at any length). The

²⁴ These equations are stated by Hönl and London.¹² The transitions $\Delta \sigma$ (or $\Delta \sigma_k$) = ± 1 or 0 correspond to $\Delta k = \pm 1$ or 0 in the line spectrum case.

equations involve the assumption $p=2j$, which may be expected to hold equally well for odd and even molecules.^{25,26}

Eq. (4) is applicable to vibration-rotation as well as to electronic bands; Eq. (2) is now seen to be merely the special case of Eq. (4) corresponding to $\sigma'=\sigma''=0$. Eqs. (5) and (6) are obviously applicable only to electronic bands.

In all cases the relation $I=ie^{-E_0/kT}$ of Eqs. (1) and (2) is applicable, but of course implies thermal equilibrium.

In Eqs. (4)-(6) as given below, Hönl and London's original equations have been considerably altered in form for the sake of convenience in application. In terms of the notation and assignment of j values here adopted, and expressed in terms of j (i. e., the mean of j' and j'') rather than of j' or j'' (for Q branches $j'=j''=j=j$), the equations are as follows:

For the case $\sigma'=\sigma''=\sigma$,

$$\left. \begin{aligned} i_P &= i_R = 2a(j^2 - \sigma^2)/j \\ i_Q &= 4aj\sigma^2/(j^2 - \frac{1}{4}) \end{aligned} \right\} \quad (4)$$

For the case $\sigma' - \sigma'' = +1$,

$$\left. \begin{aligned} i_P &= a(j - \sigma')(j - \sigma' + 1)/j \\ i_Q &= 2aj(j - \frac{1}{2} + \sigma')(j + \frac{1}{2} - \sigma')/(j^2 - \frac{1}{4}) \\ i_R &= a(j + \sigma')(j + \sigma' - 1)/j \end{aligned} \right\} \quad (5)$$

For the case $\sigma' - \sigma'' = -1$,

$$\left. \begin{aligned} i_P &= a(j + \sigma'')(j + \sigma'' - 1)/j \\ i_Q &= 2aj(j - \frac{1}{2} + \sigma'')(j + \frac{1}{2} - \sigma'')/(j^2 - \frac{1}{4}) \\ i_R &= a(j - \sigma'')(j - \sigma'' + 1)/j \end{aligned} \right\} \quad (6)$$

By applying the methods of the matrix mechanics to the closely allied case of the symmetrical rotator, Dennison²⁷ has obtained equations which are in complete agreement with those of Hönl and London, and there seems no reason to doubt that Eqs. (4)-(6) will remain valid, on the basis of the new quantum mechanics, for the diatomic molecule with $j_e=\sigma$.

²⁵ Hönl and London assume $p=2j+1$ (so that their j values are the same as those of the new quantum mechanics¹⁸), using, however, the designation m instead of j ; they also use m_0 where σ is here used. In the present notation and j numbering, Hönl and London's m would then be replaced by $j-\frac{1}{2}$. However, m as used by Hönl and London is neither m' nor m'' specifically, but represents whichever is the larger of the two ($m=m''=\bar{m}+\frac{1}{2}$ for P , $m=m'=m''=\bar{m}$ for Q , and $m=m'=\bar{m}+\frac{1}{2}$ for R branches). It will then be readily seen that the substitution $m=j$ is correct for both P and R branches, while for Q branches $m=j-\frac{1}{2}$, if the j values are to be those here adopted.

²⁶ In the analogous atomic case, the relation $p=2j+1$ holds for both even and odd molecules, the j values (Sommerfeld) being integral in the former and half-integral in the latter case.

²⁷ D. M. Dennison, Phys. Rev. 28, 329 (1926): Eq. (25). Dennison's m and n correspond to $j_0-\frac{1}{2}$ and σ_0 in the present notation. To get from Dennison's equations to Eqs. (4)-(6), the former must be multiplied by the factor $2j_0$, and also by certain constant factors 1, 2 or 4 (because Dennison's equations are amplitude equations).

*Comparison of results of old correspondence principle with those obtained by summation rule method.*¹¹ Since the summation rule method is supposed to involve nothing more than a refinement of the old correspondence principle, Eqs. (3) and (4)-(6) should be in asymptotic agreement for large quantum numbers. That this is the case can readily be verified. The agreement is in fact close even for small quantum numbers if we amplify and somewhat modify Eq. (3) by assuming $i = a\bar{p} = 2aj$ as in Eqs. (1) and (2), giving to a values proportional to the appropriate trigonometric functions of Eq. (3); Eq. (1) is then in agreement with Eq. (3b) for the special case $\sigma = 0$. Considering again the case $\sigma' = 1$, $\sigma'' = 0$, $j' = 2\frac{1}{2}$ as an example (cf. above, following Eq. 3) one now finds $i_P : i_Q : i_R = 2.04 : 4.60 : 2.96$, whereas Eq. (5) yields the ratio $2 : 5 : 3$.

Inaccuracy of Hönl and London equations for large j values. As shown by Kemble,² the factor a in Eq. (1) is not quite the same for the P and R branches in oscillation-rotation bands, and differs more and more as j increases. This difference is due to the variation in the moment of inertia as a result of the vibration of the molecule. The latter renders the rotation non-uniform, and affects the Fourier amplitudes which according to the correspondence principle govern the relative intensities of the P and R branches. This factor always tends to make the P branch more intense, thus assisting the Boltzmann factor in emission bands and opposing it in absorption bands. The effect of this factor remains present on the basis of the summation rule,²³ and in the new quantum mechanics.¹⁶

The existence of a similar effect in electronic bands seems likely, but the theory has not yet been developed. Other deviations from the relations predicted by Eq. (4)-(6) are to be expected in case of appreciable departure of the electronic angular momentum or its components from rigid orientation with respect to the internuclear axis. The experimental evidence bearing on the above points will be discussed below.

Form of theoretical intensity distribution for specific cases. Effect of Boltzmann factor. According to the preceding discussion, the relative intensities of the lines of a band are determined by the product of a factor i which represents a transition probability times an a priori probability $2j_0$, and a factor $e^{-E_0/kT}$, the Boltzmann factor. The factors $2j_0e^{-E_0/kT}$ assume thermal equilibrium for the initial states. This is to be expected in absorption bands, but not in emission bands as ordinarily excited. Nevertheless in practice the rotational energy distribution appears to be normally of a type corresponding well to thermal equilibrium at some specifiable "effective temperature"²⁹ which

²³ R. H. Fowler, Phil. Mag. 50, 1079 (1925).

²⁹ The vibrational energy distribution does not in general take a form corresponding to thermal equilibrium (cf. R. S. Mulliken, Phys. Rev. 26, 21-2 and 333 (1925)).

apparently approximates the actual temperature of the surroundings. The question has been examined especially by Birge,³⁰ in a quantitative study of intensity distribution in the violet cyanogen bands as emitted by various sources.

The types of intensity distribution to be expected for the cases $\Delta\sigma = \pm 1$ are best appreciated by an examination of the theoretical curves in Figs. 1-3 below. For these cases the *Q* branch is roughly twice as strong as the *P* or the *R* branch, while the two latter are roughly equal in intensity. These relations are asymptotically true for large quantum numbers, except for the effect of molecular vibration, and of the Boltzmann factor favoring the *P* branch. For small values of *j*, the relative intensities of the branches, especially of the *P* and *R* branches, depend markedly on the sign of $\Delta\sigma$ and the magnitude of σ .

It is of interest to note that, as between the *P* and *R* branches, the branch which has the larger number of missing lines⁶ is always the weaker after it begins. Thus for $\sigma' = 1, \sigma'' = 0$, the first *P* line has $(j' \rightarrow j'') = (1\frac{1}{2} \rightarrow 2\frac{1}{2})$, or $j = 2$, while the first *R* line has $(j' \rightarrow j'') = (1\frac{1}{2} \rightarrow \frac{1}{2})$, or $j = 1$; for the *P* branch the *i* factors of Eq. (5) have the values 1, 2, 3, . . . for $j = 2, 3, 4, \dots$, while for the *R* branch they are 2, 3, 4, . . . for $j = 1, 2, 3, \dots$. But for $\sigma' = 0, \sigma'' = 1$, the first *P* line has $j = 1$ and the first *R* line $j = 2$, and correspondingly the *i* factors for the two branches are interchanged (cf. Eq. 6) as compared with the previous case. For the case $\Delta\sigma = 0$, where the number of missing lines is the same in the *P* as in the *R* branch, the *i* values likewise are equal for any given value of *j*.

The case $\Delta\sigma = 0$ (Eqs. 1 and 4) is illustrated in the present paper only for $\sigma = 0$, where the *Q* branch vanishes. If $\sigma > 0$, a weak *Q* branch is to be expected, proportional to σ^2 in intensity (cf. Eq. 4); but in all cases the intensity should fall from the beginning, asymptotically approaching zero, for large *j* values, as compared with those of the *P* and *R* branches.

RELATION OF ROTATIONAL DOUBLING AND ALTERNATING INTENSITIES TO THE THEORY

Rotational doubling. In the development of Eqs. (3)-(6) it was assumed, partly explicitly, partly implicitly, that to each value of *j* there corresponds just one rotational state, and that *P*, *Q*, and *R* branches all involve the same sets of rotational states. But in practice, as shown in a previous paper,⁷ the rotational states are double (*A* and *B* sub-states) when $\sigma > 0$, and what is worse, the *P* and *R* branches involve *A* \rightarrow *A* and *B* \rightarrow *B* combinations, while the *Q* branches involve *A* \rightarrow *B* and *B* \rightarrow *A* combinations (cf. Fig. 1 and Eqs. 2 and 3 of ref. 7). Hence between *Q* branches on the one hand and *P* and *R*

³⁰ R. T. Birge, *Astrophys. J.* 55, 273 (1922).

branches on the other there is an independence which is neither anticipated nor explained by the correspondence principle as applied in the theory outlined above. For example, in a ${}^1P \rightarrow {}^1S$ electronic transition ($\sigma' = 1, \sigma'' = 0$), there is a Q branch involving exclusively initial rotational states of the A type, and a P and an R branch each involving exclusively B -type initial states; the final rotational states are of a single type, probably⁷ the B type. Similar anomalies occur in the case of ${}^1S \rightarrow {}^1P$, ${}^1D \rightarrow {}^1P$ and other transitions⁷ and doubtless in general for combinations of σ -type terms.

If, however, we deliberately overlook these phenomena, by lumping together in all cases the A and B states corresponding to any particular value of j , it is possible to make a comparison between experimental intensity data and the theory as given above. The procedure is justified by the results, as will be shown below, so that it seems permissible to regard the simple theory as an essentially correct first approximation to reality. The success of this method obviously implies an equality of the a factors of Eqs. (5), (6), or (7), for Q as compared with P and R branches, and so indicates equal a priori probabilities for rotational states of the A and B types.

Alternating intensities. Another phenomenon which is not capable of being accounted for by the simple theory is that of alternating intensities in band lines. In this connection reference should be made to a previous paper⁷ and to references given there. Formally, alternating intensities of the observed type can be reproduced, so far as is known from the data now available, if in Eqs. (4)-(6),—or other corresponding equations for rotational terms not of the σ type,—the factor a is permitted to have a value or set of values which differ in a constant ratio for alternate lines.³¹ The same ratio is applicable to P , Q and R branches, but in such a way that all lines having a common value of j' or j'' , rather than of j , are weakened or intensified. The alternation must therefore be a property of the *molecular states* involved, not of the transition probabilities. This is shown especially by the He_2 bands⁷ and the N_2^+ bands.

If, as in the He_2 bands, alternate lines are completely missing in each branch, the intensities of the remaining lines can be plotted against j on a single curve which should be of the same form as if every line were present, if the above-suggested assumption of a constant ratio factor (here zero) is correct. On this basis, as will be shown below, the theoretical and observed intensity curves are in fact in agreement.

As shown in a previous paper,⁷ the system of alternate missing levels in the He_2 molecule is such as to render impossible ${}^1S \rightarrow {}^1S$ and ${}^1P \rightarrow {}^1P$ transitions. This is a rather extreme example of the difficulties which

³¹ Cf. also fuller discussion by J. H. Van Vleck, Phys. Rev. 28, 980 (1926).

the phenomenon of alternating intensities presents, from the correspondence principle standpoint.

COMPARISON OF THEORY WITH EXPERIMENTAL EVIDENCE: BANDS INVOLVING SINGLET ELECTRONIC STATES

Singlet electronic states (1S , 1P , 1D , . . . , with $\sigma = 0, 1, 2, \dots$) are characteristic of even molecules. For these molecules the j values are half-integral.

Nature of available data. Comparatively little work has been done on the quantitative measurement of the intensities of band lines. Nevertheless there is a considerable mass of useful data, for the most part of two types (1) eye estimates of photographic blackening (2) measurements or curves of photographic density against wave-length. In the absence of disturbing factors (serious variations of plate sensitivity, etc. with wave-length; effects of impurities; unresolved doublets; lack of care to use a uniform scale in the case of eye estimates; etc., etc.), both these types of data, especially the second, are valuable in giving correctly the *order of intensity* of the lines in a band.

The value of such information can be seen from the following considerations. Suppose all the lines of a band (including lines on both the ascending and descending parts of the intensity curves) are arranged in order of intensity (a) according to theory (b) according to experimental data of the type mentioned. A little consideration will show that substantial agreement of the two modes of arrangement would constitute a verification of the theory falling not far short of being completely satisfactory, a chance agreement being exceedingly improbable.

With data of the type mentioned, the theoretical curves of absolute intensities and the experimental curves should usually differ mainly in the existence of a relative flattening of the latter for higher intensities: thus equalities and inequalities, but not intensity ratios, should be correctly reproduced.

Intensities in ${}^1S \rightarrow {}^1S$ transitions ($\sigma' = \sigma'' = 0$). The applicability of Eqs. (1) and (2) to bands involving ${}^1S \rightarrow {}^1S$ transitions has been discussed in the first section. Certain minor points remain to be considered. Although in the case of the HCl bands at 3.46μ the work of Kemble and Bourgin confirms the predicted greater intensity of the R branch in absorption, due to the Boltzmann factor, there are other infra-red absorption bands, as pointed out by Fowler,¹¹ in which the P branch appears to be the stronger. Aside from the possibility of experimental error, this may be ascribed (as Oppenheimer has intimated¹²) to a variation of the a factor of Eqs. (1) and (2) due to molecular vibration (cf. above, p. 398), in such a way as to favor the P branch, even to the extent of making it stronger than the R branch by overcoming the contrary effect of the Boltzmann factor.

The excess intensity of the *P* over the *R* branch in the CuH bands is considerably greater¹¹ than that predicted by the theory because of the effect of the Boltzmann factor alone. On the latter basis, the strongest *P* line should be about 7.5% more intense than the strongest *R* line, while according to Frerich's data,²⁰ the excess is about 27%, 13%, or 11%, in three different bands. It seems possible that the discrepancy is due to the effect of molecular vibration. Such an effect is especially likely here on account of the high temperature (about 3400°C, assuming Eq. 1),³² which causes the maximum intensity in each branch to lie at relatively high values of *j*.

Intensities in $^1P \rightarrow ^1S$ transitions ($\sigma' = 1, \sigma'' = 0$) in helium bands. The class of bands under discussion is represented, according to recent conclusions of the writer,^{7,33} by a large number of helium bands, the

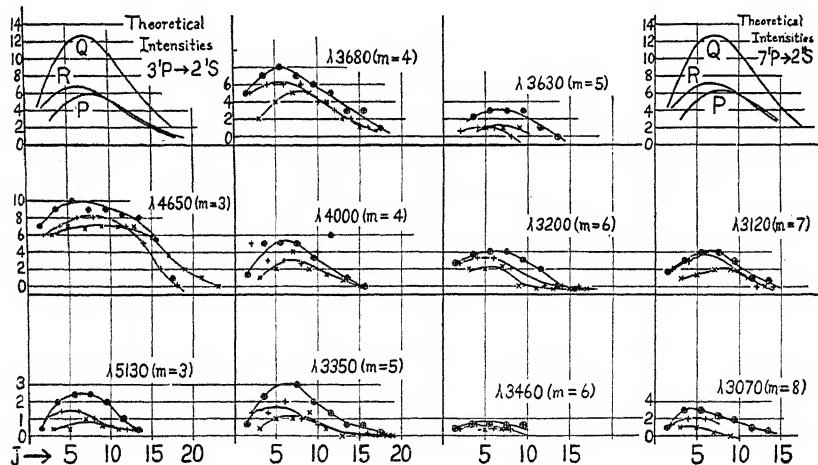


Fig. 1. Theoretical and observed intensities in $m \ 1P \rightarrow 2 \ ^1S$ helium bands of the "main" and "second" series. The theoretical intensities correspond to an assumed temperature of 700°C. The observed intensities for *P*, *Q*, and *R* branches, respectively, are denoted by X, \oplus , and +.

"series" bands of Fowler and Curtis and Long. Although only eye estimates of intensity are available, these exist for so many bands that a good comparison with theory is possible. Such a comparison is made in Fig. 1. Theoretical curves (the intensities are of course on an arbitrary scale) are given in Fig. 1 only for two extreme cases $3^1P \rightarrow 2^1S$ and $7^1P \rightarrow 2^1S$: these and other (intermediate) cases differ, —but only slightly,—in respect to the value of E_0 as a function of *j*, in the Boltz-

³² The distribution seems to be of the thermal equilibrium type. The assumption $T = 3640^\circ K$ gives $j = 14+$ for the strongest *P* line and $j = 14-$ for the strongest *R* line, in agreement with observation.

³³ R. S. Mulliken, Proc. Nat. Acad. Sci. 12, 158 (1926).

mann factor. The temperature of 700°C assumed for all cases gives good agreement with the experimental intensity curves.³⁴

The theoretical curves in Fig. 1 for the transition $3^1P \rightarrow 2^1S$ are based on the calculations given in Table I. Entirely analogous cal-

TABLE I

Calculation of theoretical intensities for helium band $\lambda 4650(3^1P \rightarrow 2^1S)$ transition, assuming $t=700^\circ\text{C}$ ($kT=679$). The absolute values of i and I are without significance here; the $I_{\text{obs.}}$ values, being eye estimates, are furthermore not directly proportional to true intensities. The values of E' and kT are in wave-number units.

P and R Branches

$j' - \frac{1}{2}$	E'	$e^{E'/kT}$	Designation*	i	$I_{\text{calc.}}$	$I_{\text{obs.}}$			Designation*	i	$I_{\text{calc.}}$	$I_{\text{obs.}}$	
							$\lambda 4650$	$\lambda 5130$					
2	37	1.06	$R'(1)$	3	2.82	6	1		$P(2)$	2	1.90	6	0
4	136	1.22	2	5	4.08	7	1+		3	4	3.27	7	0
6	292	1.54	3	7	4.55	8	1+		4	6	3.90	7-	1
8	503	2.10	4	9	4.30	8	1		5	8	3.83	7	1-
10	770	3.11	5	11	3.54	8	1-		6	10	3.22	7	0
12	1090	5.00	6	13	2.60	7	0		7	12	2.40	7	0
14	1464	8.65	7	15	1.73	5	-		8	14	1.62	6-	-
16	1889	16.1	8	17	1.06	2	-		9	16	0.99	4-	-
18	2365	33	9	19	0.58	1-	-		10	18	0.55	2	-
20											1		
22											0		

* In the notation of Curtis and Long.

Q Branch

Designation	$j' - \frac{1}{2}$	E'	$e^{E'/kT}$	i	$I_{\text{calc.}}$	$I_{\text{obs.}}$	$\lambda 4650$	$\lambda 5130$
$Q(1)$	1	9	1.01	3	2.96	7	0	
2	3	80	1.12	7	6.23	9	2	
3	5	208	1.36	11	8.12	10	2+	
4	7	391	1.78	15	8.43	9	2+	
5	9	631	2.54	19	7.49	9	2	
6	11	932	3.94	23	5.84	8+	1	
7	13	1272	6.5	27	4.15	8	0	
8	15	1677	11.8	31	2.60	6	-	
9	17	2141	23.5	35	1.49	1	-	

culations apply for $7^1P \rightarrow 2^1S$ and other transitions. The theoretical intensities ($I_{\text{calc.}}$) are calculated by means of the equation $I = ie^{-E'/kT}$ (for emission bands E_0 of Eq. 1 is E'). The E' values (in wave-number units) are from Curtis and Long's analysis of the $\lambda 4650$ ("main series") band.³⁵ The E' values are nearly the same for the "second series"

³⁴ The intensity estimates on the bands corresponding to the most excited electronic states were made on a different set of exposures than for the remaining bands and the $^1D \rightarrow ^1P$ and $^1S \rightarrow ^1P$ bands discussed below, so that a different value of T might have been anticipated; the change seems, however, to be within the errors of the data.

³⁵ The E' values are essentially those given in Table VII of Curtis and Long's paper (Proc. Roy. Soc. 108A, 513, 1925), except for an additive constant $-B\sigma^2$ (since $\sigma=1$, $-B\sigma^2=-B=-7$), due to the assumption here of the form $B(j^2-\sigma^2)$ in place of Bj^2 used by Curtis and Long.

bands as for the corresponding "main series", so that practically the same theoretical curves are applicable to both. The i values are as given by Eq. (5). The theoretical curves are obtained by plotting the calculated I values against j . Of course we are really dealing with a discontinuous function, so that the continuous curves are of significance only as an aid to the eye in appreciating the relation of the points through which they are drawn. Furthermore, in drawing the curves (both theoretical and experimental) the points corresponding to alternate j values (which strictly should be plotted with zero intensity) have been disregarded. This matter has been discussed in a previous section (p. 400).

A comparison of the theoretical and experimental curves on the above basis, bearing in mind the various possible causes of distortion and error in the experimental curves, indicates that the two are in essential agreement. Considering individual bands, the agreement is not always very good, but the deviations seem irregular, and most of them disappear if one replaces the individual curves in imagination by an average curve. Individual deviations may be only apparent and due to the crudeness of the method of recording intensities, or they may in some cases be due to perturbations (also, see below).

The agreement with theory may be described under the following headings:

(1) The Q branch is always the strongest, and, so far as can be seen from the data, may well actually be twice as strong as either of the other two branches, as predicted; the latter relation is indicated especially in the bands of low intensity, where the estimates of blackening are more nearly proportional to true intensity.

(2) The values of j for the *strongest line* in each branch are on the whole in the correct order $P > Q > R$, and differ by the correct amounts; these j_{\max} values are moreover practically the same in all the bands, showing that the same effective temperature applies to all.

(3) The R branch is always markedly stronger than the P branch for small j values (the first R line is approximately twice as strong as the first P line, although j is only two thirds as great), while for large j values the two branches are asymptotically about equal in intensity. The first R line is about equal in intensity to the first Q line.

In spite of the crudity of the intensity data, the experimental curves are thus unmistakably of the predicted type for $\sigma' = 1$, $\sigma'' = 0$, and equally unmistakably are different from the predicted types for any other pair of values of σ' and σ'' , even for the same value of $\Delta\sigma$ (cf. curve for $\sigma' = 2$, $\sigma'' = 1$, in Fig. 2). The agreement is all the more remarkable in view of the fact that alternate lines in each branch are missing, and in view of the existence of rotational doubling, since neither of these facts is anticipated by the theory. It is important

to note that the agreement would not exist if the j values had not been assigned on the assumption of alternate missing lines.

Taken together with the evidence previously given,⁷ the present results seem to constitute conclusive evidence in favor of the interpretation of the He_2 bands given in previous papers.^{33,7}

The fact that the agreement with theory is not disturbed by the circumstance that the Q lines arise from A rotational sub-states and the P and R lines from B sub-states indicates (among other things) that the two sub-states have equal a priori probabilities (cf. discussion above, p. 399).

There seem nevertheless to be certain systematic minor deviations from the theoretical curves. For the bands involving highly excited initial electronic states, there is a tendency toward more rapid decrease of intensity for high j values than the theory calls for. For the most excited states, there even seems to be a shift, for the line of maximum intensity in each branch, toward a lower value of j than predicted. These effects can probably be attributed to a marked instability of molecules having high j values, especially for the higher electronic states (such instability is also indicated by the setting in of a rapid diminution in the rate of growth of the spacing of the rotational energy levels). Due to this instability, such molecules are presumably reduced in numbers below the proportions corresponding to statistical equilibrium. The question of instability has been discussed by Curtis.³⁶

Other $^1P \rightarrow ^1S$ transitions: the AlH Bands. Primarily on the basis of missing lines, the known AlH band system has been classified⁷ as corresponding to a $^1P \rightarrow ^1S$ electron transition. The bands should therefore show intensity relations similar to those in the He_2 bands just discussed, but without the complication of alternate missing lines. According to Eriksson and Hulthén,³⁷ the Q branch is approximately twice as strong as the P or R branch, as it should be for a $^1P \rightarrow ^1S$ (or $^1S \rightarrow ^1P$) transition. The intensities (eye estimates) given by Eriksson and Hulthén give indications of the expected superior intensity of the R as compared with the P branch for low j values; the same is true of the data of Mörikofer³⁸ on the same bands (for "Form I" of the discharge).

A more definite confirmation of the predicted intensity relations is obtained by a study of a photometer curve of the $\lambda 4354$ ($n' \rightarrow n'' = 1 \rightarrow 1$) band as given by Eriksson and Hulthén. So far as can be seen, the intensities are in agreement with prediction (for thermal equilibrium at a fairly high temperature), but it does not seem worth while to make a detailed comparison, since there is much superposition of lines

³⁶ W. E. Curtis, Proc. Roy. Soc. 103A, 315 (1923).

³⁷ G. Eriksson and E. Hulthén, Zeits. f. Physik 34, 775 (1925). In regard to the intensity of the Q branch, cf. footnote on p. 777.

³⁸ W. Mörikofer, Dissertation Basel, 1925.

from different branches. The peaks corresponding to the first line of the *R* branch ($j=1$) and the second line of the *P* branch ($j=3$) are, however, fairly free from neighboring peaks,³⁹ and their intensities are seen to be roughly equal, in agreement with the theoretical prediction that $i=2$ for both (cf. Eq. 5). This, in connection with the evident superiority of intensity of the *Q* branch, is good evidence that the intensity relations are of the predicted type. The observed relations may be contrasted with those predicted for the case $\sigma'=\sigma''=0$, where the intensities of the lines mentioned should be in the ratio 1 : 3, and with those for $\sigma'=0$, $\sigma''=-1$, where the *R* line in question should be *absent*, and the *P* line should have $i=4$.

Intensity relations in $^1D \rightarrow ^1P$ transitions ($\sigma'=2$, $\sigma''=1$): the helium band $\lambda 5733$. In previous papers^{7,33} it was concluded that $\text{He}_2 \lambda 5733$ is the (only known) representative of a $^1D \rightarrow ^1P$ transition, with $\sigma'=2$, $\sigma''=1$. The intensity data in Table II below are eye estimates by Curtis.⁴⁰ The corresponding theoretical intensities are obtained in much the same way as for the $^1P \rightarrow ^1S$ transitions in He_2 , using the relation $I = ie^{-E'/kT}$, calculating the *i* values from Eq. (5), and assuming the same effective temperature (700°C) as in the previous case, since the photographs were made under the same conditions. In one respect the procedure is different, due to the fact that the $\lambda 5733$ band has six branches (two of each type), as compared with three for the bands previously discussed; this is due to the occurrence of rotational doubling for both 1D and 1P states.⁷ As in the $^1P \rightarrow ^1S$ bands, each branch has alternate lines completely missing. This, however, occurs in such a way that one *P*, one *Q* and one *R* line is present for each value of j' or j'' (above $j'_{\min.}$ or $j''_{\min.}$), and in Fig. 2 all these lines have been plotted in a continuous series for the experimental as well as for the theoretical curves. The theoretical intensities of course lie (nearly) on a continuous curve, since the theory makes no provision for rotational doubling, except in so far as this affects the value of $E'(j)$.⁴¹ The fact that the observed intensities also lie on smooth curves in spite of the fact that the intensities for alternate values of j correspond to different rotational sub-states, indicates that (as in the "series" bands) the two sub-states (*A* and *B*) are alike in respect to their a priori probabilities, etc. If the present discussion does not make these points clear, a study of Fig. 2 and Table II, in connection with the discussion of $\text{He}_2 \lambda 5733$ in ref. 7, should do so.

From Fig. 2 and Table II it is evident that the substitution of $\sigma'=2$ for $\sigma'=1$, without any change in $\Delta\sigma$, is enough to produce a very great

³⁹ In the notation of Eriksson and Hulthén, these lines are *R*(1) and *P*(4).

⁴⁰ W. E. Curtis, Proc. Roy. Soc. 101A, 38 (1922).

⁴¹ As a matter of fact, the values of $E'(j)$ fall into two sets which are sufficiently different so that the theoretical curve should not be quite smooth (cf. Table II); for convenience, however, a smooth curve has been drawn in Fig. 2.

TABLE II

Calculation of theoretical intensities for helium band $\lambda 5733$ ($3^1D \rightarrow 2^1P$ transition) assuming $t = 700^\circ\text{C}$

See note at top of Table I. The "Designations" are those given by Curtis,⁴⁰ and also used by Kratzer. For the experimental I data, see Fig. 2 or ref. 40. The E' values for $j' = 2\frac{1}{2}, 4\frac{1}{2}, 6\frac{1}{2}, \dots$ are $F'_A(j)$ values. These values were obtained as follows: (a) $E'(2\frac{1}{2})$ and $E'(3\frac{1}{2})$ were first calculated from $E \sim B(j^2 - \sigma^2) = B(j^2 - 4)$, using $B_A = B_B = 7.56$, $\sigma = 2$, as given in ref. 7; (b) then making use of the $\Delta_2 F'$ values given by Kratzer (Zeits. f. Physik 16, 353, 1923), the remaining E' values were obtained by suitable summation (by definition—see ref. 6, Eqs. 10, — $\Delta_2 F(j) = F(j+1) - F(j-1)$). E. g., $E'_A(4\frac{1}{2}) = E'_A(2\frac{1}{2}) + \Delta_2 F'_A(3\frac{1}{2})$; $E'_A(6\frac{1}{2}) = E'_A(4\frac{1}{2}) + \Delta_2 F'_A(5\frac{1}{2})$, etc., while $E'_B(5\frac{1}{2}) = E'_B(3\frac{1}{2}) + \Delta_2 F'_B(4\frac{1}{2})$, etc. The quantities here designated $\Delta_2 F'_A(3\frac{1}{2})$, $\Delta_2 F'_A(5\frac{1}{2}), \dots$, and $\Delta_2 F'_B(4\frac{1}{2}), \Delta_2 F'_B(6\frac{1}{2}), \dots$, are respectively identical with Kratzer's $\Delta F_2(1)$, $\Delta F_2(2), \dots$, and $\Delta F_1(2), \Delta F_1(3), \dots$ (cf. Kratzer's Table 6, p. 359). The E' values for $j' = 17\frac{1}{2}$ to $20\frac{1}{2}$ were estimated approximately by extrapolation.

$j' - \frac{1}{2}$	E'	$e - E'/kT$	Designation	i	I
2	17	1.03	$R'(1)$	6	5.85
3	62	1.10	$R(2)$	$6\frac{2}{3}$	6.09
4	122	1.19	$R'(2)$	$7\frac{1}{2}$	6.30
5	199	1.34	$R(3)$	$8\frac{2}{5}$	6.27
6	287	1.53	$R'(3)$	$9\frac{1}{3}$	6.10
7	395	1.79	$R(4)$	$10\frac{2}{7}$	5.75
8	510	2.12	$R'(4)$	$11\frac{1}{4}$	5.31
9	650	2.60	$R(5)$	$12\frac{2}{9}$	4.70
10	790	3.20	$R'(5)$	$13\frac{1}{5}$	4.13
11	963	4.14	$R(6)$	$14\frac{2}{11}$	3.43
12	1126	5.26	$R'(6)$	$15\frac{1}{6}$	2.88
13	1332	7.10	$R(7)$	$16\frac{2}{13}$	2.28
14	1516	9.3	$R'(7)$	$17\frac{1}{7}$	1.84
15	1756	13.2	$R(8)$	$18\frac{2}{15}$	1.37
16	1958	17.8	$R'(8)$	$19\frac{1}{8}$	1.07
17	(2232)	27.1			
18	(2449)	37			
19	(2755)	60			
20	(2987)	82			

$j' - \frac{1}{2}$	Designation	i	I	Designation	i	I
2	$Q_2(1)$	$3\frac{1}{3}$	3.25	$P(2)$	$2\frac{1}{3}$	0.65
3	$Q_1(1)$	$5\frac{5}{6}$	5.33	$P'(2)$	$1\frac{1}{2}$	1.37
4	$Q_2(2)$	$8\frac{1}{10}$	6.81	$P(3)$	$2\frac{2}{5}$	2.02
5	$Q_1(2)$	$10\frac{4}{15}$	7.66	$P'(3)$	$3\frac{1}{3}$	2.48
6	$Q_2(3)$	$12\frac{8}{21}$	8.09	$P(4)$	$4\frac{2}{7}$	2.80
7	$Q_1(3)$	$14\frac{13}{28}$	8.08	$P'(4)$	$5\frac{1}{4}$	2.94
8	$Q_2(4)$	$16\frac{19}{36}$	7.80	$P(5)$	$6\frac{2}{9}$	2.94
9	$Q_1(4)$	$18\frac{26}{45}$	7.15	$P'(5)$	$7\frac{1}{5}$	2.77
10	$Q_2(5)$	$20\frac{34}{55}$	6.44	$P(6)$	$8\frac{2}{11}$	2.56
11	$Q_1(5)$	$22\frac{43}{66}$	5.48	$P'(6)$	$9\frac{1}{6}$	2.22
12	$Q_2(6)$	$24\frac{53}{78}$	4.69	$P(7)$	$10\frac{2}{13}$	1.93
13	$Q_1(6)$	$26\frac{64}{91}$	3.76	$P'(7)$	$11\frac{1}{7}$	1.57
14	$Q_2(7)$	$28\frac{76}{105}$	3.09	$P(8)$	$12\frac{2}{15}$	1.31
15	$Q_1(7)$	$30\frac{89}{120}$	2.33	$P'(8)$	$13\frac{1}{8}$	0.99
16	$Q_2(8)$	$32\frac{103}{136}$	1.84	$P(9)$	$14\frac{2}{17}$	0.79
17	$Q_1(8)$	$34\frac{118}{153}$	1.28	$P'(9)$	$15\frac{1}{9}$	0.56
18				$P(10)$	$16\frac{2}{19}$	0.45
19				$P'(10)$	$17\frac{1}{10}$	0.29
20				$P(11)$	$18\frac{2}{21}$	0.22
				$P'(11)$		

change in the quantitative theoretical intensity relations. The *observed* intensities lie on curves which agree very closely in form (including the position of the line of maximum intensity) with the theoretical curves. The predicted very high intensity of the first few *R* lines and the corresponding very low intensity of the first *P* lines are verified. These agreements give powerful support to the interpretation of the band as having $\sigma' = 2$, $\sigma'' = 1$.

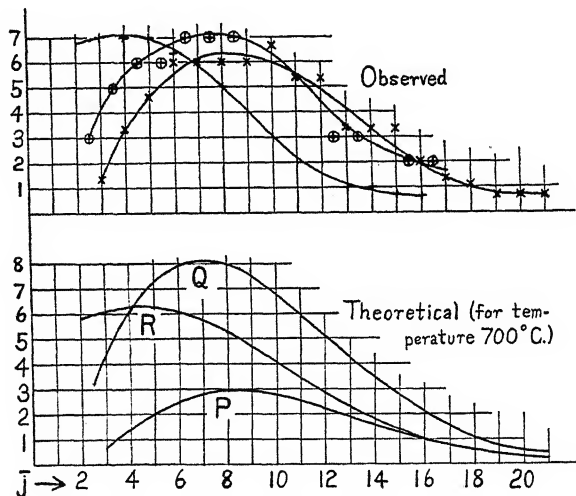


Fig. 2. Intensity relations in $\lambda 5733$ helium band ($3^1D \rightarrow 2^1P$). The "observed" points are Curtis's estimates,⁴⁰ except that for the *P* lines Curtis's estimates have been multiplied by $2/3$ (cf. text). Points where two or more lines are superposed have been omitted. Thus Q_1 (5), Q_2 (7), and R' (1) are all superposed (the calculated position of Q_2 (7) is 17467.85, in sufficiently good agreement with that of an observed line for which $\nu = 17467.30$). The previously unassigned line $\nu = 17471.64$ (int. 2) is evidently Q_3 (8). It is possible that Q_1 (8) is present and superposed on R' (2). It seems probable that the apparent abnormally high intensity of P' (5) is due to the superposition of a line not belonging to the band.

In certain respects the observed intensities of Fig. 2 and Table II seem to disagree with the theory: the *Q* branch as a whole is relatively too weak and the *P* branch is much too strong, in spite of the fact that in Fig. 2 Curtis's intensity estimates³⁸ for the *P* branch have been multiplied by a factor $2/3$ before plotting (partial justification for this procedure is obtained by an examination of the reproduction given by Curtis, in which the *P* branch appears relatively considerably weaker than Curtis's data indicate). It seems possible that the apparent high intensity of the *P* branch may be largely due to change of plate sensitivity with wave-length (the *P* branch extends from $\lambda 5821$ to $\lambda 5748$, the *Q* branch from $\lambda 5733$ to $\lambda 5716$, the *R* branch from $\lambda 5724$ to $\lambda 5646$,

and in this part of the spectrum rapid changes of plate sensitivity occur for some types of plates; Curtis does not state what type of plate he used). It also seems possible that a different intensity scale may have been (more or less unconsciously) used for the eye estimates in the different branches. The high intensity of the P branch might also be due partly to variability in the a factor of Eq. (5). Further experimental work is needed.

Intensity relations in $^1S \rightarrow ^1P$ transitions ($\sigma' = 0, \sigma'' = 1$): helium bands $\lambda 4546$ and $\lambda 6400$. The helium bands $\lambda 4546$ and $\lambda 6400$ correspond to transitions $4^1S \rightarrow 2^1P$ and $3^1S \rightarrow 2^1P$ ($\sigma' = 0, \sigma'' = 1$ in both cases), according to the conclusions of previous papers.^{7,33} Eye estimates of intensity⁴⁰ are available. In Table III these are compared with the theoretical

TABLE III

Intensities in helium bands $\lambda 4546$ and $\lambda 6400$ ($4^1S \rightarrow 2^1P$ and $3^1S \rightarrow 2^1P$ transitions), assuming $t = 700^\circ C$.

See note at head of Table I. The numbers under the headings R , Q , and P , are Curtis's designations⁴⁰ for the lines of the three branches.

$j' - \frac{1}{2}$	E'	$e^{E'/kT}$	R	i	$I_{\text{calc.}}$	$I_{\text{obs.}}$	$\lambda 4546$	$\lambda 6400$
1	16	1.02						
3	88	1.14	1	2	1.76	3	(8)	
5	218	1.38	2	4	2.90	3	8	
7	405	1.82	3	6	3.30	3	9	
9	648	2.60	4	8	3.08	3	10	
11	947	4.03	5	10	2.48	3	6	
13	1300	6.78	6	12	1.77	1	3	
15	(1707)	12.3						

$j - \frac{1}{2}$	Q	i	$I_{\text{calc.}}$	$I_{\text{obs.}}$	$\lambda 4546$	$\lambda 6400$	P'	i	$I_{\text{calc.}}$	$I_{\text{obs.}}$	$\lambda 4546$	$\lambda 6400$
1	1	3	2.93	3	10		1	3	2.93	4	10	
3	2	7	6.16	4	10		2	5	4.40	6	10	
5	3	11	7.99	6	10		3	7	5.08	6	10	
7	4	15	8.26	6	10		4	9	4.96	6	10	
9	5	19	7.30	6	10		5	11	4.23	6	10	
11	6	23	5.70	5	10		6	13	3.22	6	10	
13	7	27	3.98	4	8		7	15	2.21	3	—	
15	8	31	2.51	3	3		8	17	1.38	1		

intensities, assuming $t = 700^\circ C$ as for the other helium bands, but using Eq. (6) in calculating the i values. The predicted intensities are similar to those for $^1P \rightarrow ^1S$ transitions except that here the P branch should be stronger than the R branch throughout its course, but especially at the beginning.

The observational data are not very satisfactory. For $\lambda 6400$ the recorded intensities indicate that the plate was overexposed, no distinction being made between lines exceeding a certain intensity. However, in both $\lambda 6400$ and $\lambda 4546$ the predicted relatively low intensity of the

R branch is verified, and for $\lambda 4546$ the data on the *Q* branch indicate agreement with the theory.

In both bands, as in $\text{He}_2 \lambda 5733$, the recorded intensities of the *P* branch lines are greater, relatively to those of the *Q* branch, than one would expect from the theory. If these deviations are real, they might perhaps be ascribed to the effect of nuclear vibration (but $n' = n'' =$ only $\frac{1}{2}$, probably), or to a lack of rigid binding of σ (cf. above, p. 398). Further more careful intensity measurements will be needed before definite conclusions can be reached.

Even with the present data there can, however, be no doubt that the bands have an intensity distribution entirely different from those in $^1P \rightarrow ^1S$ and $^1D \rightarrow ^1P$ bands, and differing from these in at least qualitatively the correct way.

New data on helium bands: note added in proof. McLennan, Smith, and Lea have recently published intensity data on a number of helium bands at low temperatures (walls of discharge tube at 21°K. , 85°K. , and 300°K. in various runs).⁴² The data on the relative intensities of the *P* and *R* branches are in excellent agreement with the theory for the ($^1P \rightarrow ^1S$) bands $\lambda\lambda 4650, 5130, 3680, 4000, 3630$, and for the ($^1S \rightarrow ^1P$) bands $\lambda\lambda 4546$ and 6400 . In the latter case, the new data furnish a welcome supplement to those of Table III, although the absence of data on the *Q* branches is unfortunate. In the former case, the *Q* branches are more intense than the *P* and *R* branches, as expected, although apparently not twice as intense; however, it is not clear whether the data are supposed to be quantitative. The data for $\lambda 5733$ ($^1D \rightarrow ^1P$), on the *P* and *R* branches only, are in poorer agreement with the theory than are those of Curtis.—In respect to the values of j for the strongest line of each branch, a sample calculation indicates that the observed distributions correspond to the low temperatures used. But the branches fade out much too slowly with increasing j ; this probably means that a considerable fraction of the molecules were in a region of relatively high effective temperature.

Intensity relations in $^1S \rightarrow ^1P$ transitions: CO Angstrom bands. In a previous paper,⁶ the CO band system of Ångström and Thalen has been interpreted as due to an electron transition for which $\sigma' = 0, \sigma'' = 1$. Photographs of these bands were recently taken by the writer in the second order of the 21 foot concave grating at Harvard University. The bands were excited by a transformer discharge in CO_2 at low pressure. The photographs were taken in connection with a study of the Zeeman effect and were not intended for photometric work; it was found later that the exposures without field offered valuable material for the present work.

⁴² J. C. McLennan, H. G. Smith, and C. A. Lea, Proc. Roy. Soc. 113A, 183 (1926).

In order to obtain more accurate data than would be secured by eye comparisons, a photometer curve was run on the $\lambda 4835$ band ($n' = 0$, $n'' = 1$), with the kind assistance of Dr. H. A. Barton, using the micro-photometer at Princeton University. The galvanometer readings (proportional to intensity of light transmitted through the plate) for the center of each band line were then taken from the curve. Each such reading was then subtracted from the "fog" reading for a neighboring region between band lines. The results were plotted against j in Fig. 3,

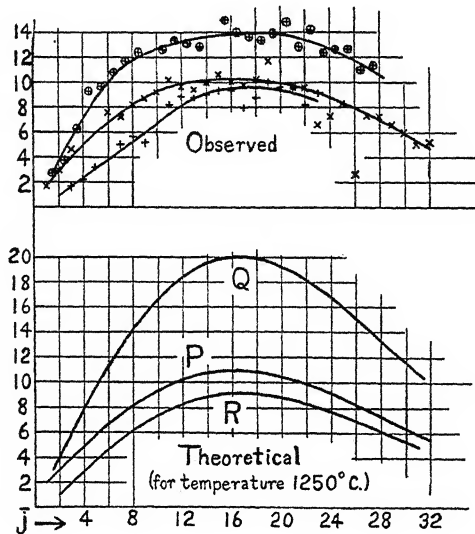


Fig. 3. Intensity relations in CO Angstrom and Thalen band ($^1S \rightarrow ^1P$) at $\lambda 4835$.

omitting, however, data on lines which were imperfectly resolved by the photometer. Results obtained in the above manner are similar in meaning to eye estimates, but more reliable.⁴³

Bearing in mind the nature of the data, the agreement between the theoretical and experimental curves as shown in Fig. 3 (assuming an effective temperature of 1250°C) is very satisfactory throughout the range of j values for which data were obtained. As predicted, the P branch is stronger than the R branch throughout its course, and much stronger at the beginning, while the Q branch is stronger than either the P or the R branch. As in other cases, however, the P branch seems to be slightly stronger than is predicted with the assumption that a in Eq. (6) is constant; as already discussed on p. 398, this effect may

⁴³ By making assumptions as to the characteristics of the plate, semi-quantitative intensity data might have been obtained, but this did not seem worth while at the time on account of the doubtfulness of the necessary assumptions.

perhaps be attributed to vibration of the molecule.⁴⁴ The extent of the agreement between theory and experiment can best be verified from the theoretical curves by picking out various pairs or sets of lines whose intensities should be equal, and comparing with the experimental curves. Examination of other CO bands of the same system disclosed similar intensity relations, but no detailed measurements were made.

INTENSITY RELATIONS IN BANDS INVOLVING DOUBLET AND HIGHER ELECTRONIC STATES

Eqs. (4)–(6) may be expected to hold in general for odd as well as for even molecules, for bands involving, in both the initial and final states, rotational terms of the form $B(j^2 - \sigma^2) + \dots$. Thus Eq. (4) should apply to ${}^2P_1 \rightarrow {}^2P_1$ and ${}^2P_2 \rightarrow {}^2P_2$ transitions; this is confirmed by experiment, as will be shown by Barton, Jenkins, and the writer in a later paper. Similarly in ${}^2D \rightarrow {}^2D$, ${}^3P \rightarrow {}^3P$ and other combinations, Eqs. (4)–(6) should hold.

When rotational terms of the form $B(j - \rho)^2 + \dots$ are involved in one or both electronic states, Eqs. (4)–(6) are inapplicable and it is not obvious what relations should take their place. Nevertheless, the observed intensity relations seem to be at least qualitatively in agreement with these equations. Thus for ${}^2S \rightarrow {}^2S$ transitions (violet CN band type, type (c) of the first section of this paper) the obvious structure and intensity relations are the same as for ${}^1S \rightarrow {}^1S$ (type b) transitions, except that each line is a doublet, due to the presence of a ρ with approximately the values $\pm \frac{1}{2}$. In ${}^2P_1 \rightarrow {}^2S$ and ${}^2P_2 \rightarrow {}^2S$ transitions ($j_e' = \sigma = \frac{1}{2}$ or $\frac{3}{2}$, $j_e'' = \rho = \pm \frac{1}{2}$), the intensity distributions in the various branches in known cases (ZnH, CdH, and HgH bands) shows a resemblance to those for other transitions such as ${}^1P \rightarrow {}^1S$ where σ decreases during emission.

The writer wishes to express his appreciation of the stimulating discussion and valuable criticism of Professor E. C. Kemble.

WASHINGTON SQUARE COLLEGE,
NEW YORK UNIVERSITY,
November 13, 1926.

⁴⁴ The anomalous intensity of the P line $j=26$ (perhaps also of other lines) is due to a perturbation; this line is also shifted a considerable distance from its expected position.

ROTATIONAL TERMS IN THE MgH BANDS

BY WILLIAM W. WATSON AND PHILIP RUDNICK

ABSTRACT

Rotational term data for the green MgH bands.—The values of the rotational terms for the vibrational states $1/2$, $3/2$, and $5/2$ in the green MgH bands are tabulated.

Analytical representation of the terms. The Kratzer, Kramers and Pauli formula is applied to the data with the following values giving the best fit: $i'_{\min} = \frac{1}{2}$, $i''_{\min} = \frac{1}{2}$, $\sigma' = \frac{1}{2}$, σ'' small ($< \frac{1}{2}$), ϵ' and ϵ'' small (≤ 0). The term $m=1$ exists, thereby making it impossible to let $j=m-1$. Other predicted electronic quantum numbers are shown to agree less well with the observed ΔF values.

I. INTRODUCTORY

IT IS the intent of this paper to supplement an earlier description of the MgH band spectrum¹ with a more complete tabulation and discussion of the rotational term values therein involved. These and similar data should come into critical reconsideration in the general program of correlation between band and series spectra which is being carried forward by such work as that of Mulliken,² Mecke,³ and in particular a recent theoretical paper by Hund.⁴

Wave-numbers for the first six branches in the band $\lambda 5211$, which are assigned the vibrational quantum numbers $n'=n''=\frac{1}{2}$,⁵ are given in Table I. Tables II and III give values of ΔF for initial and final electron levels (single and double primes) and for several vibrational levels. The values for the levels in which $n=\frac{1}{2}$ are most complete and will be used for further discussion. They are taken from the P and R branches alone because of the probable anomaly in the Q branches.⁶ Successive differences ($\Delta^2 F$ and $\Delta^3 F$) of ΔF are also tabulated for later convenience.

¹ Watson and Rudnick, *Astrophys. J.* **63**, 20 (1926).

² Mulliken, *Proc. Nat. Acad. Sci.* **12**, 144, 338 (1926). *Phys. Rev.* **28**, 481, 1202 (1926).

³ Mecke, *Zeits. f. Physik* **36**, 802 (1926).

⁴ Hund, *Zeits. f. Physik* **36**, 657 (1926).

⁵ In the authors' earlier paper this band was designated as the $(0, 0)$ band. For more recent evidence in favor of the use of half-integral vibrational quantum numbers, see Watson, *Nature*, **117**, 692 (1926).

⁶ For an explanation of the "combination defect" introduced by the Q branch see Mulliken, *Phys. Rev.* **28**, 1206 (1926).

TABLE I
Wave-numbers in the MgH band $\lambda 5211$, $n' = n'' = \frac{1}{2}$

<i>m</i>	$P_1(m)$	$P_2(m)$	$Q_1(m)$	$Q_2(m)$	$R_1(m)$	$R_2(m)$
1			19273.39		19287.93	
2	19261.74		75.96		301.26	
3	52.91		78.28		15.19	19318.70
4	43.83		81.07		29.88	33.14
5	35.03	19239.52	84.00	19287.64	45.06	48.13
6	26.98	30.50	87.93	90.68	60.90	63.53
7	19.39	22.40	92.47	94.79	77.23	79.69
8	12.98	15.26	97.45	99.68	94.21	96.50
9	06.39	08.86	303.31	305.24	411.85	414.03
10	01.04	03.28	09.75	11.53	30.20	32.26
11	196.39	198.54	16.74	18.70	49.06	51.03
12	92.52	94.70	24.56	(26.50)	68.55	70.50
13	89.36	91.38	33.20	34.84	88.57	90.38
14	86.93	89.36	42.28	43.86	509.18	510.95
15	85.20	87.66	52.12	53.67	30.58	32.27
16	84.91	—	62.64	64.18	52.01	53.96
17	84.91	—	73.79	75.25	74.37	76.11
18	85.69	87.66	85.71	87.19	97.05	98.89
19	87.66	89.36	98.22	99.67	620.34	622.16
20	90.04	91.83	411.36	412.82	44.05	45.83
21	93.37	95.17	25.21	26.53	68.33	69.68
22	97.40	99.28	39.67	41.08	92.92	94.75
23	202.27	204.18	54.74	56.11	718.11	719.95
24	07.98	09.82	70.50	71.84	43.62	45.44
25	14.40	16.33	86.74	88.10	69.61	71.52
26	21.61	23.60	503.66	505.02	96.02	98.03
27	29.74	31.62	21.11	22.48	822.84	824.64
28	38.50	40.44	39.35	40.55	49.97	51.76
29	48.14	50.02	57.83	59.21	77.40	79.27
30	58.49	60.39	77.25	78.57	905.12	907.35
31	69.70	71.57	97.05	98.31	33.40	35.06
32	81.72	83.57	617.20	618.58	61.67	63.53
33	94.79	96.33	38.13	39.49	90.49	92.35
34	307.98	309.75	59.53	60.91	20019.33	20021.20
35			81.46	82.81	48.58	50.41
36			703.89	705.24	77.94	79.75
37			26.75	28.12	107.83	109.66
38			50.00	51.36	37.46	39.23
39			73.89	75.31	67.26	68.99
40			98.03	99.66		

II. ANALYTICAL REPRESENTATION OF THE TERMS

It is instructive to inquire in just what measure the usual Kratzer, Kramers and Pauli term

$$F(m) = B[(j^2 - \sigma^2)^{1/2} - \epsilon]^2 + \dots \quad (1)$$

will satisfactorily represent the data of Table II. For convenience, ϵ is preceded by a negative sign, and allowed negative values to accord

with Kratzer's theory of narrow doublets. m is here used merely as a counting-number arising in the empirical ordering of the bandlines; j is the rotational quantum number. From (1) with satisfactory approximation,

$$\Delta F(m) = F(m+1) - F(m-1) = 4B(j-e) - 2B\epsilon\sigma^2/(j^2-1) \quad (2)$$

Succeeding differences may then be written:

$$\Delta^2 F(m) = \Delta F(m) - \Delta F(m-1) = 4B + 4B\epsilon\sigma^2/(j^3 + \dots) \quad (3)$$

$$\Delta^3 F(m) = \Delta^2 F(m) - \Delta^2 F(m-1) = -6B\epsilon\sigma^2/(j^4 + \dots) \quad (4)$$

The $\Delta^3 F$'s in Table II correspond to that in (4).

TABLE II
Term values for the lowest vibrational state, $n = \frac{1}{2}$

m	Initial State			Final State		
	$\Delta F'(m) = F'(m+1) - F'(m-1)$	Successive differences		$\Delta F''(m) = F''(m+1) - F''(m-1)$	Successive differences	
	$\Delta F'(m)$	$\Delta^2 F'(m)$	$\Delta^3 F'(m)$	$\Delta F''(m)$	$\Delta^2 F''(m)$	$\Delta^3 F''(m)$
a. Terms arising from the low-frequency doublet components						
2	39.30			35.02		
3	62.41	23.11		57.43	22.41	
4	86.10	.69	+.58	80.16	.73	+.32
5	110.00	.90	+.21	102.90	.74	+.01
6	133.97	.97	+.07	125.67	.77	+.03
7	57.94	.97	.00	48.32	.65	-.12
8	81.78	.84	-.13	70.84	.52	-.13
9	205.38	.60	-.24	93.45	22.61	+.09
10	29.21	.83	+.23	215.44	21.99	-.62
11	252.63	.42	-.41	237.85	22.41	+.42
12	76.14	.51	+.09	59.88	.03	-.38
13	99.24	.10	-.41	81.49	21.61	-.42
14	322.16	22.92	-.18	303.13	.64	+.03
15	44.89	.73	-.19	24.20	.07	-.57
16	367.09	.20	-.53	345.38	.18	+.11
17	89.40	.31	+.11	66.19	20.81	-.37
18	411.19	21.79	-.52	86.71	.52	-.29
19	32.67	.48	-.31	406.92	.21	-.31
20	53.98	.31	-.17	26.92	.00	-.21
21	474.96	20.98	-.33	446.58	19.66	-.34
22	95.52	.56	-.42	65.99	.41	-.25
23	515.84	.32	-.24	84.94	18.95	-.46
24	35.64	19.80	-.52	503.71	.77	-.18
25	55.21	.57	-.23	22.01	.30	-.47
b. Terms arising from the high-frequency doublet components						
4				79.18		
5	108.61			102.64	23.46	
6	133.03	24.42		125.73	.09	-.37
7	57.29	.26	-.16	48.27	22.54	-.55
8	81.24	23.95	-.31	70.83	.56	+.02
9	205.17	.93	-.02	93.22	.39	-.17
10	28.98	.81	-.12	215.49	.27	-.12

(These terms become identical with the above for large values of m)

First, it may be noted that the right member of (4) vanishes for large values of m , while the corresponding experimental values are definitely finite and negative. For low values of m , Δ^3F is positive for the low-frequency doublet components and negative for the high-frequency components. The two cases may be distinguished analyti-

TABLE III
*Term values for higher vibrational states
taken from the low-frequency doublet components*

m	Initial State $\Delta F'(m) = F'(m+1) - F'(m)$		Final State $\Delta F''(m) = F''(m+1) - F''(m)$	
	For the vibrational state $n=3/2$		For the vibrational state $n=5/2$	
	$\Delta F'(m)$	$\Delta F''(m)$	$\Delta F'(m)$	$\Delta F''(m)$
3	35.99	33.34	34.66	32.15
4	47.50	44.48	45.95	42.88
5	59.13	55.35	57.17	53.55
6	70.74	66.41	68.20	64.14
7	82.30	77.32	79.58	74.71
8	93.85	88.15	90.83	85.34
9	105.36	98.88	101.77	95.50
10	16.50	109.75	12.86	105.85
11	128.00	120.43	123.63	116.19
12	39.34	30.95	34.43	26.21
13	50.30	41.47	45.12	36.42
14	61.33	51.70	56.12	46.38
15	72.18	61.91	66.16	56.17
16	183.01	172.10	176.68	165.68
17	93.44	81.95	86.33	75.38
18	203.97	91.85	96.24	84.77
19	14.43	201.63	206.40	94.15
20	24.46	11.12		
21	234.47	220.42		
22	44.22	29.57		
23	53.99	38.68		
24	63.34	47.65		
25	72.29	55.92		

cally as having respectively negative and positive values for ϵ . This is the usual procedure, and is obviously indicated by the right member of (4). The sign of ϵ can be changed, however, only by a displacement⁷ of the values assigned to j . Consequently, if the two lines in a doublet are to be associated with terms having ϵ 's of opposite signs, those terms must also have different rotational quantum numbers.

Mulliken has suggested (ref. 2) that the emission of these bands is due to a transition $3^1S - 3^3P_1$ in the Mg atom, that $\epsilon' \cong \epsilon'' \cong \pm \frac{1}{2}$, $\sigma' \cong 1$, and $\sigma'' \cong 0$. Now on applying Eq. (2) to the observed ΔF 's of

⁷ Refer to (2). The right member of the equation depends upon j and ϵ principally through the difference $(j - \epsilon)$, and accordingly, in order to give ϵ any desired value, it is only necessary to let j differ from the counting-number m by a suitable constant.

Table II, one finds that the quantity $(j - \epsilon)$ has half-integral values in both initial and final states, and consequently if the ϵ 's equal $\frac{1}{2}$, both j' and j'' must have integral values. The following expressions of the form (1) with the customary fourth power term added must then represent numerically the terms of Table II for moderate values of m :

Low-frequency components:

$$F'(m) = 6.00[\{(m-1)^2 - 1\}^{1/2} + \frac{1}{2}]^2 - .000336 []^4 \quad (5a)$$

$$F''(m) = 5.70[\{(m-1)^2\}^{1/2} + \frac{1}{2}]^2 - .000332 []^4 \quad (5b)$$

High-frequency components:

$$F'(m) = 6.00[m^2 - 1]^{1/2} - \frac{1}{2}]^2 - .000336 []^4 \quad (5c)$$

$$F''(m) = 5.70[m - \frac{1}{2}]^2 - .000332 []^4 \quad (5d)$$

The values of B and ϵ , except for the arbitrary constant which may be introduced, are quite definitely determined by the experimental data; merely the order of magnitude is indicated for σ^2 . The coefficients of the fourth power terms were computed from the Kratzer formula⁸ $\omega_0 = (-4B^3/D)^{1/2}$ with the aid of the vibrational energy data for the bands.⁹ A comparison of the ΔF 's calculated from Eqs. (5a) and (5b) with the experimental values is given in Table IV. If you let $\epsilon = 0.55$, the calculated ΔF 's agree perfectly at $m = 5$, but then they are higher for lower m 's and lower for values of $m > 5$ than the observed values. It is to be concluded that the observed data for these bands cannot be accurately fitted to the Kramers and Pauli formula after the fashion of Eqs. (5). A much better fit is obtained with Eqs. (6) below.

As indicated in Table I, the term $m = 1$ is observed. We have re-examined our plates to verify this point and are quite certain that these two lines really are present. Granting that $m = 1$ exists, j could not be taken equal to $(m-1)$ as we have done above,¹⁰ without violating the necessary relation $j^2 \geq \sigma^2$. We therefore put j equal to $m - \frac{1}{2}$ and $m + \frac{1}{2}$ for the low and high frequency components respectively with the following results:

Low-frequency components:

$$F'(m) = 6.00[\{(m - \frac{1}{2})^2 - (\frac{1}{2})^2\}^{1/2} + 0.11]^2 - .000336 []^4 \quad (6a)$$

$$F''(m) = 5.70[\{(m - \frac{1}{2})^2 - (\frac{1}{2})^2\}^{1/2} + 0.02]^2 - .000332 []^4 \quad (6b)$$

High-frequency components:

$$F'(m) = 6.00[\{(m + \frac{1}{2})^2 - (\frac{1}{2})^2\}^{1/2} - 0.89]^2 - .000336 []^4 \quad (6c)$$

$$F''(m) = 5.70[\{(m + \frac{1}{2})^2 - (\frac{1}{2})^2\}^{1/2} - 0.98]^2 - .000332 []^4 \quad (6d)$$

These expressions yield ΔF 's which agree much better with the observed values than do those from Eqs. (5), as will be seen from the

⁸ Kratzer, Ann. d. Physik 71, 72 (1923).

⁹ W. W. Watson, Phys. Rev. 27, 801 (1926).

¹⁰ Kratzer (Zeits. f. Physik 23, 298 (1924)) lets $j = m - 1$ for the CH bands, but since he did not observe the lowest terms, he did not encounter this question.

comparison of the observed and calculated ΔF 's for values of m up to 10 given in Table IV. Eqs. (6) do not represent the data exactly for

TABLE IV
Comparison of values of $\Delta F'$ and $\Delta F''$ calculated from Eqs. (5a) and (6a) with observed values.

m	Calc. from (5a)	$\Delta F'(m)$ Calc. from (6a)	Obs.	Calc. from (5b)	$\Delta F''(m)$ Calc. from (6b)	Obs.
2		39.22	39.30	34.18	34.75	35.02
3	64.93	62.66	62.41	56.95	57.42	57.43
4	84.73	86.54	86.10	79.68	80.14	80.16
5	108.18	110.39	110.00	102.35	102.80	102.90
6	31.81	34.16	33.97	24.94	25.40	25.67
7	55.44	57.86	57.94	47.45	47.91	48.32
8	78.99	81.45	81.78	69.86	70.32	70.84
9	202.45	204.91	205.38	92.15	92.60	93.45

the highest values of m . The reason appears from the fact that the fourth power term in the energy expression yields values of $\Delta^3 F(m)$ which are linear in m , whereas the experimental values of Table II are practically independent of m for the higher terms, suggesting the presence of an appreciable third power term in the energy expression.

It seems probable, then, that for the MgH bands the j 's have half-integral values, the minimum values of both j' and j'' being $\frac{1}{2}$. The probable values of the electronic quantum numbers are $\sigma' = \frac{1}{2}$, $\sigma'' < \frac{1}{2}$ (very small, judging from the linear course of the ΔF 's), and $\epsilon' \approx \epsilon'' \approx 0$. This being the case, it is apparent that these bands resemble more the ZnH bands than they do the CH bands, and consequently they are not to be classed with the latter bands in the table of structure types.

THE UNIVERSITY OF CHICAGO (W.W.W.)
WASHINGTON, D. C. (P.R.)
November, 1926.

EXCITATION OF SPECTRA BY ATOMIC HYDROGEN

BY F. L. MOHLER

ABSTRACT

Spectroscopic excitation of Na, K, Cs, Mg, Cd, Zn, Hg, Tl vapors by atomic hydrogen.—Hydrogen from a Wood discharge tube flowed into a tube containing metal vapor and the spectrum emitted by the mixture was observed. Sodium and cadmium gave strong emission of their first resonance lines and no other lines. Potassium showed the first resonance doublet faintly. Mercury gave the complete hydride spectrum and faint emission of $\lambda 2537$. Caesium, magnesium, thallium and zinc gave no line spectra.

Theory of excitation of spectra by atomic hydrogen.—Two possibilities are suggested. A three body collision of two hydrogen atoms and a metal atom may result in recombination of the hydrogen and excitation of the metal atom. A metal hydride may first be formed and this in a two body collision with a hydrogen atom may react to give H_2 and an excited metal atom. The available energy of excitation is somewhat less in the second case.

INTRODUCTION

R. W. WOOD¹ has found that hydrogen may be almost completely dissociated when a powerful discharge is maintained in a long tube through which moist hydrogen is streamed. The high degree of dissociation is indicated by the fact that, in the middle portion of the tube, only the atomic lines (Balmer series) can be seen. If the gas is pumped off from near the center of the tube the atomic hydrogen may be drawn some distance from the discharge, for its life is of the order of 0.3 sec. under favorable conditions. Wood² and Bonhoeffer³ have studied many of the physical and chemical properties of atomic hydrogen by this means. Their results indicate that the successful operation of the discharge tube depends on the fact that the smooth clean surface of a glass tube exposed to water vapor or oxygen is unable to catalyse the recombination of hydrogen while almost any other solid surface is an effective catalytic agent.

Bonhoeffer⁴ has obtained some experimental results on spectra excited when other gases, particularly metal vapors, are mixed with the atomic hydrogen. The foreign substance is introduced at some distance from the discharge tube to avoid any question of electrical excitation and the spectrum is observed near the point where the gases mix. This is a very interesting case of chemical luminescence and in view of the fact that some of his results are quite unexpected it seemed

¹ Wood, Proc. Roy. Soc. 97, p. 455 (1920).

² Wood, Proc. Roy. Soc. 102, p. 1 (1923).

³ Bonhoeffer, Zeits. f. Phys. Chem. 113, p. 199 (1924); 119, p. 385 (1926).

⁴ Bonhoeffer, Zeits. f. Phys. Chem. 116, p. 391 (1925).

worth while both to repeat his experiments and to extend the method to other metals. Details of his results will be given in connection with the present observations.

EXPERIMENTAL PROCEDURE

Fig. 1 illustrates the experimental arrangement used. Hydrogen was supplied by an electrolytic generator kept in continuous operation with a current of one or two amperes. The gas passed through a long

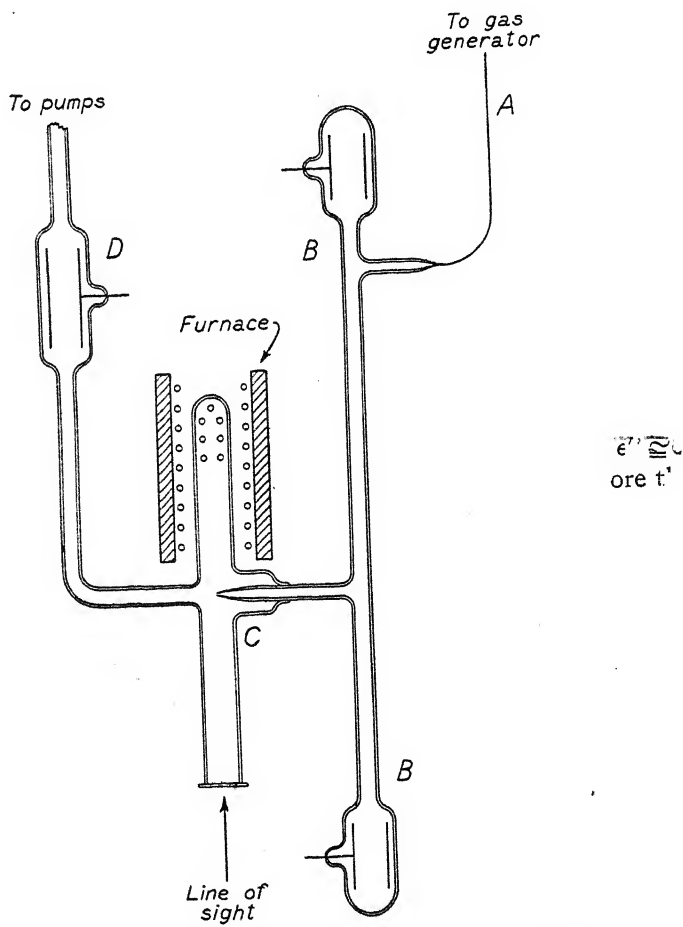


Fig. 1. Apparatus for excitation of metal vapor by atomic hydrogen.

capillary tube A into the discharge tube B, thence into the mixing chamber C, and from C was drawn off through a series of pumps. The discharge tube was about 150 cm long and 1.5 cm in diameter. The

mixing chamber was a tube about 2 cm in diameter into which the hydrogen flowed through a nozzle 1 mm in diameter at the tip. One end of this tube contained metal which could be heated by an electric furnace while the other end was closed by a quartz window through which the radiation could be observed.

The discharge was excited by a 5,000 volt transformer giving about 0.5 amps. in the secondary. The gas pressure was between 0.1 and 0.05 mm, corresponding to a gas flow of about 1,000 cc per second. Under these conditions there is no tendency for the discharge to pass into the tube between B and C nor for the vapor to diffuse into tube B. An auxiliary electrode D made it possible to draw a discharge through the mixing chamber when desired. Spectrum observations of this discharge gave useful information as to the composition of the gas mixture in C. Visual observations of the spectrum of the discharge in B indicated whether the operation of the tube was satisfactory. The metal in the mixing chamber was usually heated by an electric furnace to a temperature sufficient to give a vapor pressure comparable with the gas pressure, approximately 0.1 mm. Mercury however was heated enough by the atomic hydrogen to give a high vapor pressure.

In the first experiments with sodium, the mixing chamber was a simple cross with sodium in one arm and hydrogen passing through the two perpendicular arms. When the tube was first heated there was a brilliant yellow glow where the gases mixed but this soon faded. The trouble was that sodium or sodium compounds contaminated the tube between B and C so that rapid surface recombination took place. This was evidenced by the fact that dirty spots became very hot. The device shown in Fig. 1, with hydrogen entering through a small nozzle, reduced to a minimum the back diffusion of impurities and made it possible to maintain a bright glow for over twelve hours. Nevertheless contamination of the tubing is the most serious source of difficulty in these experiments. The mixing tube was cleaned after every run and the entire apparatus was frequently cleaned and sections of new tubing put in. Spectra were photographed with a Hilger E₂ quartz spectrograph.

OBSERVATIONS

Sodium. A diffuse yellow glow became conspicuous at about 200°C. This became much brighter and concentrated near the nozzle at higher temperature. The optimum temperature for long exposures was about 350°C. Both dicyanine stained plates and Speedway plates were used to secure maximum sensitivity to infra-red and ultra-violet lines, but exposures up to twelve hours showed only the D lines. Rough comparison exposures were made with a sodium flame and a discharge through the mixing chamber. The lines near 8190A and 3300A, if

present at all, were weaker relative to the D lines in the mixture than in the flame, enormously weaker than in the discharge. The results confirm Bonhoeffer's observations⁴ with additional evidence as to the infra-red region.

Potassium, rubidium and caesium. Bonhoeffer⁴ concluded that no visible lines of these metals were excited. With rubidium and caesium a blue light was observed over the surface of the metal, the spectrum being apparently continuous. In the present work, potassium heated to about 250°C was photographed with dicyanine stained plates and with unstained plates. A twelve hour exposure showed only the first doublet of the principal series 7665-99A, and this very faintly. Caesium when first exposed to the hydrogen, showed the surface fluorescence described by Bonhoeffer, but the effect was transient. A four hour exposure with a stained plate, and with caesium maintained at about 200°C, showed nothing.

Magnesium, heated to 600°C, showed no lines either visually or on a Speedway plate. I conclude that the resonance line $1^1S - 2^3P_1$ at 4571A was definitely absent. A transient green surface fluorescence was observed when magnesium in powder form was put in the tube.

Cadmium, heated to about 350°C, gave the resonance line $1^1S - 2^3P_1$ at 3261A in great intensity. A ten hour exposure showed the line much widened by over-exposure. No other lines or bands were seen.

Zinc was heated to about 440°C and a seven hour exposure showed nothing. The first resonance line is in this case at 3076A. Several check observations confirmed the fact that this line was absent under conditions which gave strong excitation of the cadmium resonance line.

Mercury. The spectrum excited in the presence of mercury vapor has been photographed by Bonhoeffer,⁴ who found the mercury hydride bands strongly excited and the resonance line at 2537A present but faint. My observations confirm this. The mercury is warmed by the stream of atomic hydrogen until rapid evaporation takes place, and then a violet glow is visible. A ten hour exposure showed nearly all the known mercury-hydride bands and 2537. The band spectrum which extends from 4520 to 3270A has been analyzed in detail⁵ and can safely be ascribed to a diatomic molecule HgH which is very unstable.

Thallium. Visual observation showed no luminosity when the metal was heated to 600°C which gives definite evidence of the absence of the green line $2^2P_2 - 2^2S$ at 5350A.

Water vapor. Water vapor is always present under the conditions of the experiment and the water band at 3064A, ascribed to OH, is emitted in the atomic hydrogen stream. The presence of metal vapor suppressed this afterglow.

⁵ Hulthén, Zeits. f. Physik. 32, p. 32 (1925).

Table I summarizes the spectrum observations and gives the excitation potentials of the observed lines and of other significant lines which seemed to be definitely absent. There would seem to be no simple correlation between the occurrence of the lines and their excita-

TABLE I
Spectra excited by atomic hydrogen.

Element	Wave-length	Series	Excit. Pot.	Intensity
Na	5890-6	$1S-2P$	2.1	strong
	8183-94	$2P-3D$	3.6	absent
	3302-3	$1S-3P$	3.7	absent
K	7665-99	$1S-2P$	1.6	weak
	4044-7	$1S-3P$	3.0	absent
Cs	All lines		1.4 to 3.9	absent
Mg	4571	$1^1S-2^3P_1$	2.7	absent
Cd	3261	$1^1S-2^3P_1$	3.8	strong
Zn	3076	$1^1S-2^3P_1$	4.0	absent
Hg	2537	$1^1S-2^3P_1$	4.9	weak
HgH	4520 to 3274	Bands	3.1 to 3.8	strong
Tl	5350	$2^2P_2-2^2S$		absent

tion voltage. With the exception of the mercury line at 2537A, all the observed lines and bands have excitation potentials less than 3.9 volts, though many lines with lower excitation potentials did not appear. The absence of hydride spectra, except in mercury, is also interesting, for zinc, cadmium and magnesium have hydride spectra quite similar to that of mercury.

INTERPRETATION OF RESULTS

The various experiments on the properties of hydrogen drawn from a Wood tube clearly indicate that atomic hydrogen is the active agent. The relatively long life of the atoms can be explained by assuming that two atoms cannot spontaneously recombine to form a molecule, and theoretical considerations support this assumption. The process of recombination is to be considered as a special case of changing from one vibration state to another and, in the normal electronic state, the vibration states of homopolar molecules are metastable.⁶ Hence two atoms cannot radiate away the energy of recombination, and some third body must be present to take up this energy. A possible explanation of spectrum excitation by atomic hydrogen is that a three body collision of two hydrogen atoms and a metal atom takes place in which part of the energy of recombination is expended in producing excitation of the metal atom. The process is the converse of the Franck and Cario experiment in which H₂ is dissociated by optically excited mercury vapor.⁷

⁶ Birge and Sponer, Phys. Rev. 28, p. 259 (1926).

⁷ Franck and Cario, Zeits. f. Physik. 11, p. 161 (1922).

Miss Sponer⁸ has explained the afterglow spectra of pure nitrogen and of mixtures of nitrogen and other gases on the assumption that active nitrogen is atomic nitrogen which recombines only by three body collisions. The energy of recombination, 11.5 volts, is sufficient to excite the complete arc spectra of all metal vapors though there is evidence that all lines do not appear in their normal intensity.⁹

The work of dissociation of hydrogen can be directly measured, though with difficulty, from the amount of dissociation at high temperature. Values so obtained range from 3.7 to 4.2 volts.^{10,11} A more certain value is derived from the band spectrum by assuming that the limiting value of the vibration energy of the normal electronic state is equivalent to the work of dissociation. Witmer¹² has derived a value 4.34 volts from one series in the Schumann region, and a more complete analysis of the H₂ spectrum by Dieke and Hopfield¹³ gives 4.38 volts.

The simplest assumption as to the excitation of other atoms by atomic hydrogen is that any atomic states of energy less than the energy of recombination can be excited in a three body collision. My results show that this is not the case. Thus in cadmium the state 2³P₁ of energy, 3.8 volts is strongly excited while in sodium the state 3³P of energy, 3.7 volts is not excited. The strong emission of the D lines shows that in this comparison there is no question of contamination of the tube suppressing radiation. Particular care was taken to maintain comparable conditions in the experiments with zinc and cadmium and it may be that zinc is not excited because the energy of recombination is insufficient. This would mean that it is less than 4 volts, a value definitely at variance with the band spectrum results. In view of the existence of an unknown factor preventing the excitation of some states, the evidence for a low value is not conclusive.

The excitation of the mercury hydride spectrum can be explained by assuming that first HgH is formed and that then the hydride is excited in a three body collision. The energy of recombination of HgH is very small (Hulthén⁵ estimates it at 0.37 volts on the basis of the observed vibration states) so that no visible radiation can result from its formation. Probably the reaction between Hg and H takes place at the liquid mercury surface. (Bonhoeffer).⁴ The hydrides of the other metals studied are also very unstable, and the energy involved in their formation cannot give atomic spectrum excitation. Possibly

⁸ Sponer, Zeits. f. Physik. 34, p. 622 (1925).

⁹ Ruark, Foote, Rudnick and Chenault, J.O.S.A. & R.S.I., 14, p. 17 (1927).

¹⁰ Langmuir, J. Amer. Chem. Soc., 38, p. 221, 1916.

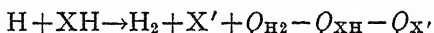
¹¹ Isnardi, Zeits. f. Elektro. Chem. 30, p. 405 (1915).

¹² Witmer, Proc. Nat. Acad. Sci. 12, p. 238 (1926).

¹³ Dieke and Hopfield, Zeits. f. Physik., in press.

the failure to observe hydride spectra except in mercury is explained by the fact that the higher temperatures and lower pressures employed prevented the existence of any appreciable concentration of these unstable compounds.

There is a possibility however that hydride formation plays an essential part in all the reactions. Suppose that first a metal hydride XH is formed (possibly at a solid or liquid surface) involving a heat of reaction Q_{XH} and that subsequently an atom of hydrogen reacts with XH to form H_2 and an excited atom X' of energy $Q_{X'}$.



This reaction will take place if $Q_{X'} < Q_{H_2} - Q_{XH}$. Q_{XH} is small yet the small difference will account for the nonappearance of lines near the threshold value. Occurrence of line emission will depend on the existence of the hydride as well as on the available energy. This hypothesis seems to account for the observations on line spectrum excitation but it does not offer a simple explanation of the HgH bands. Possibly the primary product is in this case HgH_2 , though chemical evidence as to the existence of such a compound is questionable.

Neither theory accounts for the excitation of the mercury line at 2537A. The energy required, 4.9 volts, is much more than the available energy from recombination and some multiple excitation process must be involved.

BUREAU OF STANDARDS,
December 20, 1926.

MULTIPLETS IN TWO ELECTRON SYSTEMS
OF THE FIRST LONG PERIOD*

By R. C. GIBBS AND H. E. WHITE

ABSTRACT

Wave-lengths and comparative positions of certain multiplets in the spectra of Ca_I, Sc_{II}, Ti_{III}, V_{IV}, Cr_V.—When an electron in a 4p orbit jumps to a 4s orbit in the presence of another valence electron in a 3d orbit, multiplets of the type $^3D_{1,2,3} - ^3P_{0,1,2}$; $^3D_{1,2,3} - ^3D'_{1,2,3}$; $^3D_{1,2,3} - ^3F_{2,3,4}$ appear. These multiplets for Ca_I, Sc_{II}, Ti_{III} have already been recognized by other investigators. The same multiplets for V_{IV} and Cr_V have now been found and the wave-lengths of the lines have been measured. The progressive shift in the relative positions of these multiplets in passing from element to element has been noted. The regular and irregular doublet laws have been found to hold fairly accurately for two electron systems when one of the electrons jumps between two orbits, p and s, having the same total quantum number.

ACCORDING to the new theory of space quantization a single valence-electron gives rise to a system of doublet levels. In the presence of another valence-electron, however, the doublet levels are replaced by singlet and triplet levels, except when both electrons are in s orbits having the same total quantum number. These triplet levels in general give rise to groups of lines called multiplets.

Ca_I, Sc_{II}, Ti_{III} etc., each contains two valence electrons and we should therefore expect to find such multiplets in their spectra and also that each of the three multiplets would have somewhat the same structure for all these atoms.

The Ca_I spectrum is known from the work of Russell and Saunders,¹ in which they find the lowest level to be a 1S_0 level. This 1S_0 level is the resultant of two similar (s) electrons in orbits of total quantum number 4, the normal state of the atom. When one of these (s) electrons is excited to a 3d orbit, the two electrons will then give rise to 1D_2 and $^3D_{1,2,3}$ levels. If the other (s) electron is now displaced to a 4p orbit, the two electrons, one in a 3d orbit and the other in a 4p orbit, will give rise to 1P_1 , $^1D'_2$, 1F_3 , $^3P_{0,1,2}$, $^3D'_{1,2,3}$, $^3F_{2,3,4}$ levels. When the electron in the 4p orbit returns to the lower 4s orbit there will result radiations corresponding to jumps from any one of the 1P_1 , $^1D'_2$, 1F_3 , $^3P_{0,1,2}$, $^3D'_{1,2,3}$, $^3F_{2,3,4}$ levels to any one of the 1D_2 or $^3D_{1,2,3}$ levels except those excluded by the selection principle ($\Delta j = 0, \pm 1$). The jumping

* The assistance of a grant to the first author from the Heckscher Research Foundation of Cornell University which enabled us to obtain the results described in this report is gratefully acknowledged.

¹ H. N. Russell and F. A. Saunders, *Astrophys. J.* 61, p. 38 (1925).

of one electron from the $4p$ orbit to the $4s$ orbit, the stationary state of the other valence electron in the $3d$ orbit remaining unchanged, will correspond exactly to the jumps in the one electron systems² except that here it is jumping in a field which is modified by the presence of another electron in a $3d$ orbit. This causes not only a shift in the radiated frequency but an increase in the number of lines radiated.

Scandium in the normal state contains three valence electrons, two of them are in s orbits and the other in a d orbit, the latter being more tightly bound than either of the (s) electrons. If now an electron be removed from the normal scandium atom it will probably be one of the (s) electrons which is ejected. The two remaining electrons should then give rise to 1D_2 and $^3D_{1,2,3}$ levels as the lowest state in the first spark spectrum of scandium, with the $^3D_{1,2,3}$ according to Hund,³

TABLE I
Titanium (III) triplets. (H. N. Russell).

		a^3D_3 361.69	(227.2)	a^3D_2 134.48	(134.5)	a^3D_1 000
$a^3D'_1$	39360.7	9	2564.17	1	2549.32	
			38999.0		39226.2	
$a^3D'_2$	39103.1	7	2581.21	8	2566.16	5
			38741.5		38968.7	39103.0
$a^3D'_3$	(166.9)			6	2577.22	7
	38936.2				38801.5	2568.29
a^3F_4	40095.4	10	2516.76			
			39733.7			
a^3F_3	(412.7)	2	2543.17	9	2528.56	
	39682.7		39320.9		39548.2	
a^3F_2	(324.7)	0	2564.36	2	2549.45	8
	39358.0		38996.0		39224.1	2540.78
a^3P_2	42959.8	8	2347.50	3	2335.05	0
			42598.5		42825.7	2327.75
a^3P_1	(85.3)			5	2339.73	1
	42874.5				42740.0	2332.39
a^3P_0	(5.9)					42874.5
	42880.4					3 2332.07 42880.4

² R. C. Gibbs and H. E. White, Proc. Nat. Acad. Sci. **12**, p. 448 (1926); **12**, p. 675 (1926).

³ Hund, Zeits. f. Physik **33**, p. 345 (1925).

lying deeper than the 1D_2 level. If now the (*s*) electron is displaced to a $4p$ orbit, and the (*s*) electron is indeed more free to move than the (*d*) electron, we again get 1P_1 , $^1D'_2$, 1F_3 , $^3P_{0,1,2}$, $^3D'_{1,2,3}$, $^3F_{2,3,4}$ levels.

Similarly, Ti_{III}, V_{IV} etc., will give these same types of levels when two, three, etc., valence electrons have been removed respectively, giving as before 1D_2 and $^3D_{1,2,3}$ as the lower levels, when one electron is in a $3d$ orbit and the other is in a $4s$ orbit, and 1P_1 , $^1D'_2$, 1F_3 , $^3P_{0,1,2}$, $^3D'_{1,2,3}$, $^3F_{2,3,4}$ levels when the (*s*) electron has been displaced to a $4p$ orbit.

TABLE II
Vanadium (IV) triplets.

		a^3D_3 600.4	(385.0)	a^3D_2 215.4	(215.4)	a^3D_1 000
$a^3D'_1$	50656.9	6 1997.74 50056.6		1 1982.49 50441.6		
	(424.6)					
$a^3D'_2$	50232.3	5 2014.83 49632.0		5 1999.32 50017.0		3 1990.75 50232.3
	(310.2)					
$a^3D'_3$	49922.1			2 2011.80 49706.7		4 2003.12 49922.1
a^3F_4	52171.4	6 1939.07 51571.1				
	(712.9)					
a^3F_3	51458.5	0 1966.25 50858.2		6 1951.48 51243.1		
	(519.5)					
a^3F_2	50939.0	0 1986.54 50338.8		1 1971.47 50723.6		6 1963.13 50939.0
a^3P_2	54797.2	8 1845.09 54197.9		6 1832.07 54583.1		4 1824.91 54797.2
	(83.2)					
a^3P_1	54880.4			5 1829.28 54666.3		1 1822.10 54881.7
	(140.8)					
a^3P_0	55021.2					4 1817.48 55021.2

The lines caused by transitions from the $^3P_{0,1,2}$, $^3D'_{1,2,3}$, $^3F_{2,3,4}$ states to the $^3D_{1,2,3}$ states are characteristic multiplets of which $^3D_{1,2,3} - ^3D'_{1,2,3}$ is the easiest to recognize by its somewhat symmetrical configuration. This multiplet is composed of seven lines, while the other two $^3D_{1,2,3} - ^3P_{0,1,2}$ and $^3D_{1,2,3} - ^3F_{2,3,4}$ are made up of six lines

each. These multiplets in Ca_I are given by Russell and Saunders¹ in the visible region of the spectrum, and those for Sc_{II} by Meggers⁴ in the ultra-violet region. Dr. Russell has very kindly put at our disposal his unpublished data of the corresponding multiplets of Ti_{III} . These three multiplets are given in Table I, with the relative term values of the levels, where the value of the 3D_1 level is taken as zero. The intensities of the Ti_{III} lines are taken from our own photographs of these multiplets. The first two multiplets of V_{IV} recorded in Table II occur at the threshold of the air absorption limit of the ordinary grating spectrograph. The other multiplet, $^3D_{1,2,3} - ^3P_{0,1,2}$ of V_{IV} as well as all three multiplets of Cr_{V} lie still deeper in the ultra-violet and were obtained from plates very kindly taken for us by Dr. I. S. Bowen of the California Institute of Technology using a vacuum spectrograph.

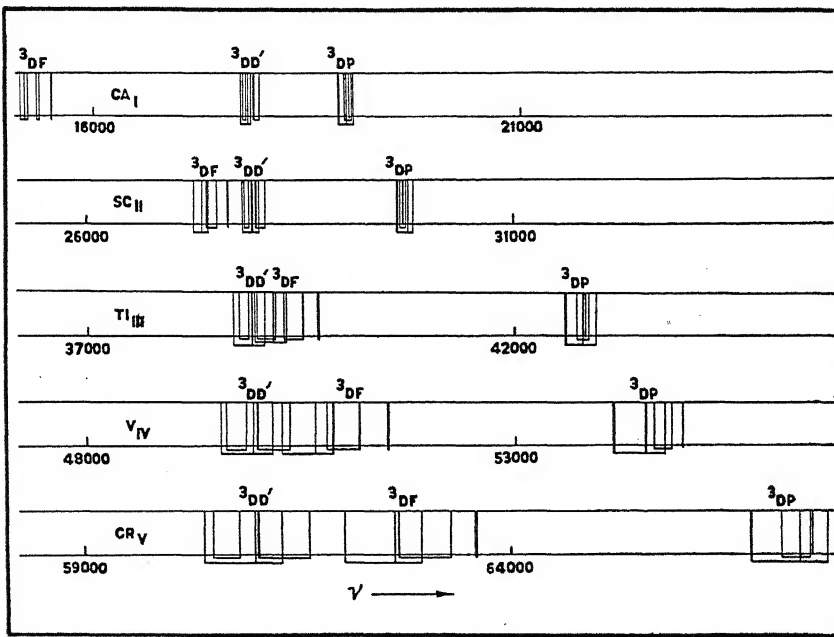


FIG. 1. Relative positions of multiplets.

Since we are here dealing with lines arising from an electron transition between orbits of the same total quantum number they would be expected to follow the irregular doublet law just as was found to be the case for the doublets of these elements² when their atoms contain only one valence electron. Fig. 1 is given for the purpose of showing the

⁴ Meggers, Journal Wash. Acad. Sci. 14, p. 419 (1924).

application of the irregular doublet law to each group of lines, i.e. the almost linear progression of ν with increasing atomic number, as well as the relative shifting of the 3DF and 3DP multiplets with respect to the $^3DD'$ multiplet. It may be seen that the 3DF and $^3DD'$ groups progress very regularly while the 3DP group shows small irregularities in going from element to element.

TABLE III
Chromium (V) triplets.

		a^3D_3 912.0	(596.7)	a^3D_2 315.3	(315.3)	a^3D_1 000
$a^3D'_1$	61943.6	6	1638.51	0	1622.64	
	(630.0)	61031.0		61628.0		
$a^3D'_2$	61313.6	2	1655.60	5	1639.40	1
	(488.2)	60401.0		60997.9		1630.96
$a^3D'_3$	60825.4			2	1652.63	4
				60509.5		1644.05
a^3F_4	64477.9	7	1573.16			
	(895.5)	63566.3				
a^3F_5	63582.4	1	1595.64	4	1580.62	
	(633.5)	62670.8		63266.3		
a^3F_2	62948.9	?	(1611.95)	2	1596.59	2
		62036.7		62633.5		1588.57
a^3P_1	67669.7	8	1497.97	5	1484.67	0
	(230.2)	66757.0		67355.0		1477.75
a^3P_1	67439.5			6	1489.75	3
	(51.4)			67125.3		1482.81
a^3P_0	67490.9				5	67439.5
					1481.68	
					67490.9	

The regular doublet law, derived by Sommerfeld⁵ from relativity considerations and by Heisenberg and Jordan⁶ from the new quantum mechanics of the spinning electron, shows not only that the value of $(\Delta\nu)^{1/4}$ should be a linear function of Z , but that $\Delta\lambda$ should remain nearly constant for increasing atomic number. These laws are found

⁵ Sommerfeld, Atombau, 4th German edition 1924, p. 144.

⁶ W. Heisenberg and P. Jordan, Zeits. f. Physik, 37, p. 276 (1926).

to hold even in these triplet systems except for possibly the Ca_I multiplets. The values given in Table IV show how beautifully these relations are fulfilled. Using the same constant in Sommerfeld's

TABLE IV

$$\begin{aligned} \text{Regular doublet law} \\ \Delta_1\lambda = (a^3D_3 - a^3D'_3) - (a^3D_2 - a^3D'_2) \\ \Delta_2\lambda = (a^3D_3 - a^3D'_3) - (a^3D_2 - a^3D'_2) \end{aligned}$$

Element	$\frac{\Delta\nu}{a^3D_3 - a^3D_2}$	$(\Delta\nu / .0456)^{1/4}$	s	$\Delta_1\lambda$	$\Delta_2\lambda$
Ca _I	21.9	4.681	15.32	6.63	12.43
Sc _{II}	109.97	7.008	13.99	13.98	17.95
Ti _{III}	227.2	8.400	13.60	14.85	17.04
V _{IV}	385.0	9.585	13.41	15.25	17.09
Cr _V	596.9	10.696	13.30	15.87	17.09

relativity formula as is used for doublets of the same period² the screening constants are found for every element to be larger, by a very nearly constant value, than they are for the corresponding one electron systems which is the effect to be expected from the addition of one more valence electron.

In these two electron systems it is found that the observed frequencies appear at very nearly the same region of the spectrum as do the corresponding doublets of the one electron systems in this same period.² This relation is shown in Table V using the $4^2S_1 - 4^2P_1$ line in the doublet

TABLE V
Shift due to the presence of a second valence electron.

	Doubles $4^2S_1 - 4^2P_1$		Triplets $a^3D_3 - a^3F_4$	Dif.
Ca _{II}	25191.6	Ca _I	15525.9	9665.7
Sc _{III}	36565.3	Sc _{II}	27663.6	8901.7
Ti _{IV}	47533.3	Ti _{III}	39733.7	7799.6
V _V	58249.9	V _{IV}	51571.4	6678.5
Cr _{VI}	68713.8	Cr _V	63566.3	5147.5

systems and the $a^3D_3 - a^3F_4$ line in the triplet systems. The consistently larger frequencies of the doublets as compared with those of the triplets suggests that this shift in frequency from one system to the other is caused by the screening effect of an additional electron, in this case an electron in a $3d$ orbit.

One of the irregular doublet laws requires that the value of $\Delta(\nu/R)^{1/2}$ be a constant for the corresponding term values of the stationary states between which a transition is taking place. The only term values known are those given by Russell and Saunders¹ for Ca_I. The term values used to obtain the Moseley diagram Fig. 2 are merely extrapolated

values computed from the known values of the first element Ca_I, the slope of the extrapolated curve for $(\nu/R)^{1/2}$ being so chosen as to yield a similar line for other levels when these other levels are obtained by adding or subtracting the observed frequencies of radiation from those of the extrapolated levels. Although these extrapolated term values may differ somewhat from their true values, yet the figure shows very well the way in which the different levels are changing in going from element to element, and when once started, serves as an aid in predicting the approximate positions of new lines.

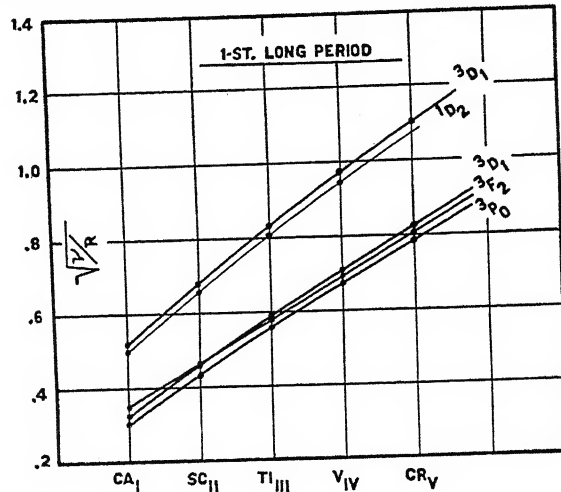


FIG. 2. Moseley diagram.

We have here been dealing with two valence electrons, the initial state of the atom having one electron in a $4p$ orbit and the other in a $3d$ orbit. The final state finds one electron in a $4s$ orbit and the other in a $3d$ orbit. It is interesting to note that this electron transition may take place in two ways, either one electron is jumping from a $4p$ to a $4s$ orbit, the $3d$ electron remaining fixed, or two electrons are jumping, one from a $4p$ orbit to a $3d$ orbit and the other from a $3d$ orbit to a $4s$ orbit. In the latter case one electron is changing by $k=1$ and the other by $k=2$ which is in accordance with the usual quantum conditions of two electron jumps.⁷ The sum of the total quantum numbers is the same in either of the above mentioned cases.

CORNELL UNIVERSITY,
November 10, 1926.

⁷ W. Heisenberg, Zeits. f. Physik, 32, 841 (1925).

ON ELECTRON SCATTERING IN HELIUM

By E. G. DYMOND

ABSTRACT

Velocity and angular distribution of electrons scattered by single collisions in helium.—An apparatus is described in which both the velocity and the angular distribution of electrons which have suffered single collisions in a gas are examined. It is found in helium that, for initial velocities of 100 volts and over, the principal energy loss is due to the excitation of the 2^1S state, corresponding to 20.5 volts. No loss corresponding to 19.7 volts is found for these velocities. For still higher velocities it seems probable that the energy interchange ceases to be quantized, and that the atom is capable of absorbing temporarily more energy than is required for excitation. The angular distribution of electrons which have lost 20.5 volts energy in colliding shows very marked maxima, the predominant one being in the forward direction. The bearing of the Schrödinger wave mechanics on this point is discussed.

THE problems of electron collisions have been in the past attacked from only two sides; that is by the determination of critical potentials and of the efficiency of excitation and ionization. The information which we may obtain from these sources, useful as it has been, is, especially in the case of efficiency of inelastic impact, very incomplete, and also is insufficient in itself to provide us with an idea of the mechanism of excitation or ionization. We need in addition to the energetic relations of collisions, those of momenta also. We must consequently trace the paths of the colliding bodies as well as determine the interchange of energy between them.

Because of the disparity in the masses of the atom and the electron it is only necessary to follow the latter. Little work has been done in this field. Davisson and Kunsman¹ have investigated the scattering of electrons by thin metal films and Langmuir² has found some surprising features in the scattering on excitation in a gas.

In view of the unexpected results obtained by these workers and of the great theoretical interest recently attached to these phenomena the work to be described here was undertaken in order to determine with some exactness the angular distribution of the electron paths about the initial direction after a collision has taken place, and also to investigate the energy losses in a region of velocity which has hitherto been difficult of access. A brief report on the scattering has already been published.³

¹ Davisson and Kunsman, Phys. Rev. 22, 242 (1923).

² Langmuir, Phys. Rev. 27, 806 (1926).

³ Dymond, Nature, p. 336, September 4, 1926.

EXPERIMENTAL ARRANGEMENTS

A magnetic deflection method was used to determine the velocity distribution. The apparatus is shown in side and end elevations in Fig. 1. The source of electrons was a short tungsten filament surrounded by a copper cylinder A, whose end was closed by two discs pierced with two slits S_1 . On the application of a field between cylinder and filament, this portion of the apparatus acted as an electron "gun." shooting out a narrow beam of electrons into the surrounding space. A glass tube supported the gun and received the leads from the filament and cylinder. This tube could be rotated about an axis BB, a ground sleeve C lubricated with rubber grease maintaining the airtightness of the whole. Immediately below the axis BB were two slits S_2 and S_3 .

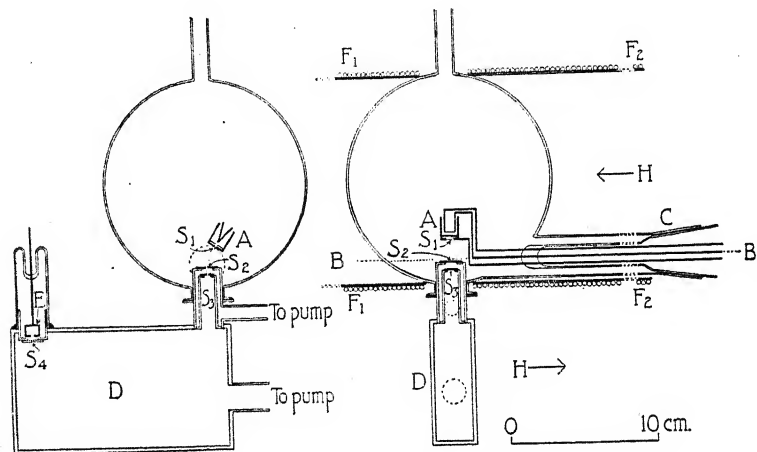


Fig. 1. Side and end elevations of apparatus.

It will be seen that these slits could select a group of electrons which had been scattered out of the main beam by collision with the gas anywhere along the line BB. By rotating the tube on which the gun is mounted the angle of scattering could be varied from 0° to 90° . By a suitable choice of gas pressures it was assured that electrons could pass through the slits S_2 and S_3 only after having made one collision.

After passing through S_3 the electrons were bent round in a magnetic field and received by the Faraday cylinder E through the slit S_4 . By a device not shown, the width of S_4 could be adjusted while the apparatus was evacuated, a thin copper diaphragm being employed to take up the motion of the slit and to maintain gas tightness. A wide slit enabled feeble effects to be observed, while a narrow slit was required to separate groups of electrons of small velocity difference. Differences of velocity of 1 in 1000 could readily be detected. The

slits S_1 were 0.5 mm broad and 0.5 mm deep; S_2 was 0.1 mm broad and 0.9 mm deep; S_3 was 0.1 mm broad and V-shaped. S_4 was also V-shaped and could be varied from 2 mm to zero. All slits were 5 mm long. Two independent diffusion pumps of large capacity pumped off the gas leaking through S_2 and S_3 and maintained a low pressure in the interior of the brass velocity analyzing chamber D . This was necessary to prevent further scattering in this region. The error in the angle of scattering, due to electrons which do not travel in the plane of the paper (Fig. 1, side elevation), was not more than 1° , given by the ratio of the length of the slits to the length of path within the chamber D .

It will be noted that the magnetic field producing the deflection must not extend into the part of the apparatus where the collisions under consideration take place. As the determination of the velocity was made by varying the magnetic field and thus bringing electrons of different speeds on to the slit S_4 , any field in the neighborhood of S_2 would by bending the primary electron stream vary the angle of scattering. A pair of coils in the Helmholtz arrangement (not shown) were used. They were sufficiently large to produce a sensibly uniform field over the whole of the apparatus; this field was compensated in the region comprising the gun A and slit S_2 , by a pair of solenoids F_1 and F_2 , carrying a fraction of the current through the main coils. The exact compensation was best effected by turning the gun to the vertical position, that is, corresponding to zero scattering angle, when there was no gas in the apparatus. The ratio of the currents through the two sets of coils was varied, until electrons were found to pass through the slit system and be received on E . The setting was found to be critical but did not require to be altered for different electron velocities, that is to say, for different magnetic fields. This method of compensation rendered the electron paths beneath the slits S_2 and S_3 far from circular, but as only comparative results for the velocities were required, this can raise no objection.

The helium, which was used throughout the research, was initially purified in a circulatory system by passing over heated copper oxide and charcoal cooled in liquid air. From the storage reservoir it could be passed into the apparatus through a fine capillary, passing again over cooled charcoal. Leaking through the slits S_2 and S_3 , it was pumped off into another reservoir, and after repurification could be used again. The continual flow of gas made for purity, and in spite of the presence of a wax joint, joining the brass chamber to the glass part of the apparatus, and of the lubricated sleeve C , no trace of impurity was evident in the gas, as tested by the method later to be described. The current arriving at the Faraday cylinder E was measured by a Compton electrometer. It was frequently necessary to use the instrument at a sensitivity of 25,000 mm per volt. Except

for a steady drift of zero no difficulty was experienced in working at this sensitivity, until the onset of hot weather. The climate of New Jersey was then found unsuitable for further work on such small effects.

DISCUSSION OF RESULTS

Due to the presence of three variables, the initial velocity of the primary beam, the velocity of the secondary scattered beam and the angle of scattering, the complete investigation is very lengthy and has not yet been made. It is felt however that the results already obtained may have sufficient interest to be reported now.

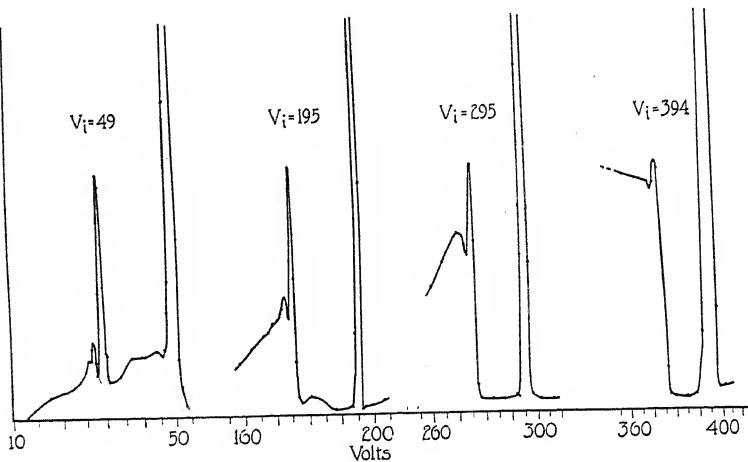


Fig. 2. Showing the relation of the number of electrons scattered by 5° , with their velocity for various initial velocities V_i .

We will first consider the velocity relations when the scattering angle is held constant. In the instances to be discussed, with one exception, this angle was 5° .

The results for a number of velocities, V_i , of the primary beam are collected in Fig. 2, where the ordinates represent the number of electrons scattered, and the abscissas are proportional to the magnetic field and consequently to the square root of the energy. The pressure of gas in all cases was 0.03 mm of mercury, except in those for which $V_i = 400$ volts, where it was 0.09 mm. Doubtless the broadening of the principal peak for those initial velocities was due to the higher gas pressure in the analyzing chamber D .

We notice in all cases two principal features, the presence of two peaks, one at a velocity equal to that of the primary beam, due to elastic reflection, and one some 20 volts lower, due to inelastic collisions which lead to excitation of the atom. The absence of any intermediate

peak speaks for the purity of the gas, if we except the run for $V_i = 50$, in which the liquid air surrounding the charcoal was low. There is also a smaller peak corresponding to large energy loss, constantly associated with the main one. The energy losses, calculated from the separation of the peaks is shown in Table I.

TABLE I
Energy losses of electrons in helium for various initial velocities V_i .

V_i	Energy losses (volts)		
49	19.7	20.7	22.6
97.6	—	20.8	23.2
196.	—	20.4	23.1
297.	—	20.4	24.2
395.	—	21.5	—
572.	—	22.0	—

For an initial velocity of 49 volts a slight hesitancy in the rise of the 20.7 volt peak may be interpreted as a loss of 19.7 volts energy. It is however very indistinct. It should correspond to the transfer $1^1S \rightarrow 2^3S$. The main peak is plainly due to the transfer $1^1S \rightarrow 2^1S$, which requires 20.55 volts. The mean value, determined from the first four rows is 20.58 volts. Lesser accuracy is to be expected for the higher initial velocities, as the loss of energy bears a smaller ratio to the initial energy.

The smaller peak is due to a complex of the higher states of helium, which are too close together to be resolved. Its behaviour is remarkable. With increase of initial velocity it gains in importance with respect to the 20.55 volt peak, and simultaneously broadens. By 400 volts initial velocity it forms a continuum which decreases very slowly with increasing energy loss and is perceptible to 200 volts.

It is possible that this continuum is due to ionization. As the electron ejected from the atom may have any velocity we should expect no sharp rise in the velocity distribution curve corresponding to a loss of 24.5 volts, a rise which in fact is never found. But if an electron loses say 200 volts in ionization, there should appear an electron of 175 volts energy, which has been ejected from the atom.

It seems that in fact there may be such an electron, if we look for it at scattering angles greater than 5° . Fig. 3 shows the scattering for an initial velocity of 340 volts and scattering angle 15° . A pronounced maximum at 50 volts has made its appearance, while the continuum afore mentioned rises to a maximum at about 290 volts. If we accept the view here given, there is a discrepancy of 25 volts in the expected positions of the two peaks. We can however form no complete picture of the processes involved without full knowledge of the behaviour of the curve shown in Fig. 3 for all angles. From the data already obtained

it appears that the maximum at 50 volts persists to large angles of scattering, while that in the neighborhood of 200 volts declines; the measurements are not yet sufficiently complete to show any periodic variation in intensity, as is the case with the peak due to excitation, to be discussed later.

It is difficult however to ascribe this continuum to ionization when we consider the relative intensities, for $V_i=50$ and $V_i=400$. For the lower velocity there is little or no evidence of any effect due to ionization, indicating that it is spread over a wide range of velocities. Now Compton and Van Voorhis⁴ have shown that the efficiency of ionization

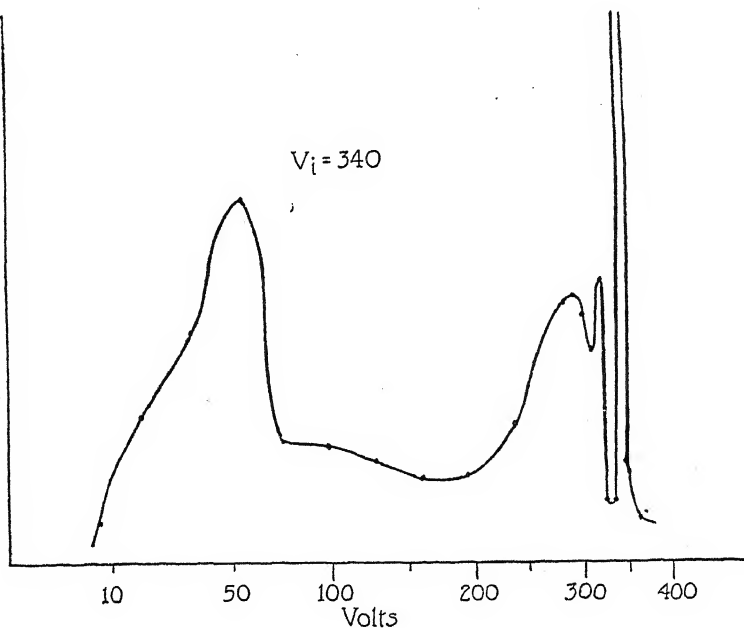


Fig. 3. Showing the number of electrons scattered by 15° for an initial velocity $V_i=340$.

in helium at 400 volts is only about twice its value at 50 volts. Further the continuum at the higher velocity does not begin at a point corresponding to an energy loss of 24.5 volts, but in the neighborhood of 22 volts.

Now for an electron whose speed is great compared with that of one of the orbital electrons of helium, the time of collision is short compared with the period of rotation in the orbit, or compared with the time required for quantization, if we speak in terms of the old quantum theory. No exact formulation of what this means when expressed in the new mechanics has been made, but a clue has been provided by

⁴ Compton and Van Voorhis, Phys. Rev. 27, 724 (1926).

Heisenberg,⁵ who has reintroduced the idea of atomic frequencies. It is not unreasonable to expect therefore that when the time of collision is short compared with these frequencies (Resonanz-schwingungen) the normal laws of energy transfer break down, and that we may here admit the possibility that an electron may lose more energy to the atom than is necessary to cause transfer from one stationary state to another. A stable state would quickly be assumed by radiating the excess of energy, presumably in continuous radiation.

The continuum extending for energy losses greater than 22 volts is precisely what we should expect on this view.

It will be seen that when the series of curves shown in Fig. 2 is complete for all angles, the determination of the excitation probabilities will be an easy matter. The ratio of the heights of the subsidiary peaks to that due to elastic collisions, when integrated over all angles will give the excitation probabilities of the respective states. Except to note the absence of excitation to the first orthohelium state, requiring 19.7 volts, at the higher velocities, we can as yet make no certain statement on this point.

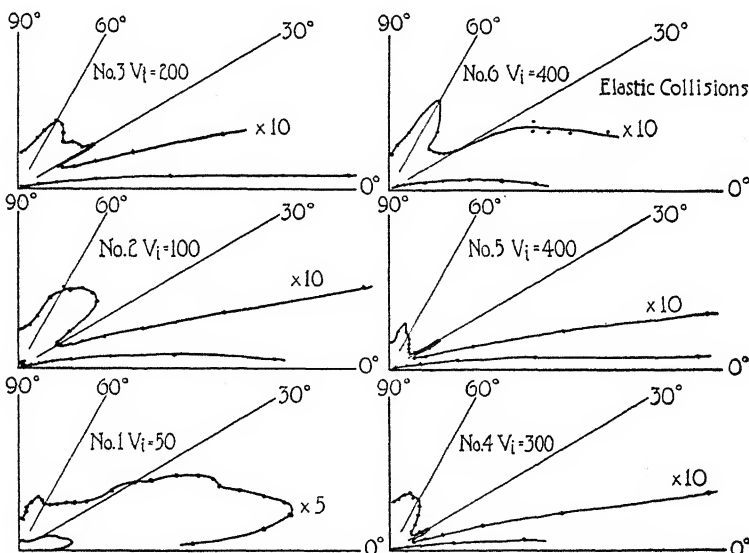


Fig. 4. Showing the number of electrons scattered at different angles for various initial velocities V_i . Nos. 1, 2, 3, 4 and 5 are for electrons which have lost 20.5 volts energy. No. 6 is for electrons which have lost no energy.

THE VARIATION OF SCATTERING WITH ANGLE

To determine the angular relations of the various types of collision it is only necessary to set the magnetic field to allow electrons with the

⁵ Heisenberg. Zeits. f. Physik 38, 411 (1926).

required energy loss to enter the Faraday cylinder and to rotate the electron gun A (Fig. 1).

A thorough investigation so far has only been undertaken for electrons losing 20.5 volts energy, that is to say, for those giving rise to the $1^1S \rightarrow 2^1S$ transition, for which $\Delta j=0$. Fig. 4 shows the mean results of several runs at each angle. The radius vectors are proportional to the number of electrons scattered per unit solid angle at the various angles. The curves shown in my letter to Nature³ are drawn from the same data, but represent the number scattered between two cones of semi-angles θ and $\theta+d\theta$. They differ from the curves here shown by a factor $\sin \theta$, which profoundly changes the relative intensities of the various maxima. It should be noted that Fig. 4 represents the original determinations, as of course the solid angle subtended by the slit S_2 at the point of impact is constant for all scattering angles.⁶ The curves are reduced to have a common area, except where a multiplying factor indicates otherwise.

The principal maximum is found to move to smaller angles with increasing initial velocity. Above 100 volts it is too near zero to measure, but the rise increases in steepness at the higher velocities. The concentration of nearly all the electrons, which have excited at high velocities, in the forward direction is the effect already noted by Langmuir.² It should be noticed that as in the transition of the helium atom considered there is no change in the angular momentum ($\Delta j=0$), the electron cannot pursue identical paths before and after collision, but one must be displaced parallel to the other (assuming that there is no deflection). For a collision in which $\Delta j=1$, there is a unique striking radius for which the electron may pursue a straight path, but in general the path after collision will also be displaced laterally.

In addition to the maximum considered, in which all but a small fraction of the electrons lie, another maximum is found at larger angles, which moves with increasing initial velocity of the electron in the opposite direction, that is to say to greater angles.

Further, for velocities greater than 200 volts, there appears a peak, remarkable for its sharpness, which does not alter its position but increases in intensity with increasing velocity. The positions of these various maxima are shown in Table II.

The last row of the table, and the top right hand curve of Fig. 4 (No. 6), show the data for a run where the scattering was due to elastic

⁶ Note added to proof. A correction must be applied to all the curves shown in Fig. 4, because of the fact that the small volume, in which the collisions considered take place, varies with the angle of scattering. The radius vectors must be multiplied by $\sin \theta$, and consequently the curves shown in the letter to Nature represent the true scattering per unit solid angle. Table II, showing the positions of the maxima, has had this correction included.

impact. The points are somewhat scattered owing to the difficulty of finding the top of an exceedingly sharp peak in the velocity distribution curve.

The scattering is of completely different character from that due to inelastic impacts. The principal maximum lies further out and is not

TABLE II
Positions of maxima in the angular scattering of electrons of various initial velocities V_i which have lost 20.5 volts energy.⁶

V_i		Positions of maxima	
48.9	24°	—	45° ? 70°
72.3	8	—	
97.5	5	—	50°
195.	<2.5	30°	59
294.	<2.5	30°	69
400.	<2.5	30°	70
400.	7	—	62

so intense relative to the rest of the curve. The fixed peak at 30° does not appear.

Any discussion of these results on the basis of the old quantum theory must inevitably lead to the same difficulties as appear in the explanation of the work of Davisson and Kunsman,¹ on the scattering of electrons in metal films. However Elsasser⁷ has shown that this class of phenomenon may be treated as a diffraction effect of the phase waves of De Broglie. More recently Born,⁸ on the basis of the Schrödinger wave mechanics, has shown that inelastic collisions should give rise to a periodic variation of scattering with angle, similar to a diffraction pattern. The theoretical side of the problem is however not yet sufficiently advanced to give detailed information on the phenomena to be expected, so that the results above reported cannot be said to substantiate the wave mechanics except in the most general way.

In conclusion I must express my deepest gratitude to Professor Karl T. Compton for extending to me the privilege of working in the Palmer Laboratory and for his constant interest and help, and also to the International Education Board for their support during my stay in Princeton.

PALMER PHYSICAL LABORATORY,
 PRINCETON UNIVERSITY,
 November, 1926.*

* Received December 24, 1926.

⁷ Elsasser, Die Naturwissenschaften 13, 711 (1925).

⁸ Born, Zeits. für Physik, 38, 803 (1926).

IONIZATION AND RESONANCE POTENTIALS IN GALLIUM AND INDIUM

BY CHARLES W. JARVIS

ABSTRACT

The critical potentials of gallium and indium have been experimentally determined by the method of inelastic impact. A simple three-electrode tube and the Hertz-differential tube as a simple three-electrode tube or as a four-electrode tube were used. Ionization was detected by the modified space charge method, by the Lenard method, and by the change in the gap resistance. The following critical potentials below ionization were observed: in gallium vapor 3.07 v. ($2p_2 - 2s$), 4.22 v. ($2p_2 - 3d_2$), 2.70 v. ($2p_1 - 2s$), 3.8 v. ($2p_1 - 3d$); in indium vapor 0.30 v. ($2p_2 - 2p_1$), 3.03 v. ($2p_2 - 2s$), 4.07 v. ($2p_2 - 3d_2$), 2.8 v. ($2p_1 - 2s$). Two ionization potentials were observed: in gallium vapor 5.8 and 13.2 v.; in indium vapor 6.3 and 14.1 v. The ionization potentials are judged to be accurate to 0.5 volts.

INTRODUCTION

THE importance of the exchange of energy between a colliding electron and atom or molecule and the relation of the energy exchanged in spectral excitation is well recognized. The results obtained by the method of electronic excitation have been analyzed with success on the basis of the quantum theory. Thus critical potentials are extremely valuable in establishing the orbital levels of the valence electron. The validity of the theory is further established by the step-wise excitation of lines or groups of lines of the arc series. The excitation of the single line 2537A in mercury at 4.9 volts is an outstanding example. Rather recently it has been recognized that an exchange of energy between a colliding electron and an atom or molecule may not be followed by a spectral process.¹ This exchange is not restricted by the selection principle whereas the absorption and emission of radiation is thus restricted. The interpretation of a critical potential for which there is no certain and definite emission or absorption line is as yet somewhat in doubt. Some of the critical potentials in mercury vapor reported by Franck and Einsporn² are in this category.

The present work was undertaken for the purpose (1) of getting an independent check on the work of Franck and Einsporn with mercury; (2) of determining the principal critical potentials in gallium and indium which have not been previously investigated by the method of

¹ Sommerfeld, Atomic Structure and Spectrum Lines, (Trans. by Brose) 3rd Ed., Ch. 6, 3, pp. 347.

² Franck and Einsporn, Zeits. f. Physik 2, pp. 18-19 (1920).

³ Mohler and Ruark, J. Op. Soc. Am. 7, pp. 819-830 (1923).

electronic impact. Mohler and Ruark³ have made some measurements with thallium of this group. They report that the potential corresponding to the transition $2p_2 - 2p_1$ masks all other higher resonance potentials.

APPARATUS AND METHOD

Three electrode tube. Preliminary work with mercury and most of the work with gallium and indium was done with this type of tube either in its simple form or as a modification of the Hertz differential tube by making proper electrical connections. Fig. 1 represents the three-electrode tube if we consider only these essential elements: filament F_2 , cylindrical grid A , and cylindrical plate B . The filament was platinum, oxide-coated. Electrons were accelerated through a relatively large distance to the cylindrical grid A by a potential V_A and were then retarded through a relatively short distance to a cylindrical electrode B by a retarding potential V_B . Galvanometers G_2 and G_1 were inserted to determine the partial current to B and the total current to A . The electrodes were constructed of nickel. In some of these tubes seals were made with De Khotinsky cement, and in others the seals were made by sealing tungsten wire directly into Pyrex glass. The method of applying the potentials to the electrodes was essentially that shown in Fig. 1 for the Hertz differential tube.

High vacua were produced with all types of tubes by means of a Jones' mercury vapor pump backed by a simple mercury vapor pump, in turn backed by a motor driven rotary oil pump. A mercury gauge was inserted between the Jones' high vacuum pump and the tube under investigation. A tube once baked and highly exhausted could be sealed by means of a trap gauge and communication subsequently established with the high vacuum pump while it was in operation at its highest efficiency. Except in case of accidental breakdown, air was never readmitted to the tube after initial exhaustion and baking. A liquid air trap was inserted between the gauge and tube in the case of gallium and indium.

The Hertz differential tube. (a) *Electrodes and filaments.* Fig. 1 shows the electrode arrangement together with the potentiometer scheme used in applying the potentials. An oxide-coated platinum filament F_1 was used as a source of electrons. This was placed very close to the gauze enclosing one end of the inner cylindrical box A . Electrons were accelerated into the box under various potentials, V_A . The electrons diffused out through the side of box A to the cylinder B (1) under zero retarding potential, (2) under a small retarding potential, V_B , usually 0.1 volt. A shielding electrode C was maintained at earth potential in order to reduce the effect of external stray potentials. The filament F_2 was used to determine ionization potentials by the

method of modified space charge. It was sometimes used as the source of electrons when the tube was used as a simple three-electrode tube. It was used as a collecting electrode for positive ions when the tube was used to detect ionization by the Lenard method. Its area would intercept little radiation, and therefore, the results should be little affected by the photoelectric effect.

The electrodes were all made of nickel, *B* and *C* from thin nickel sheet and *A* from nickel gauze of 100 or 150 mesh to the inch. The nickel electrodes were electrically welded to tungsten wires which were sealed directly into the Pyrex tube. The entire tube could be enclosed in a furnace for baking.

(b) *Detection of currents.* The galvanometer G_4 (Fig. 1) was used to determine the constancy of the potentiometer current and also for the

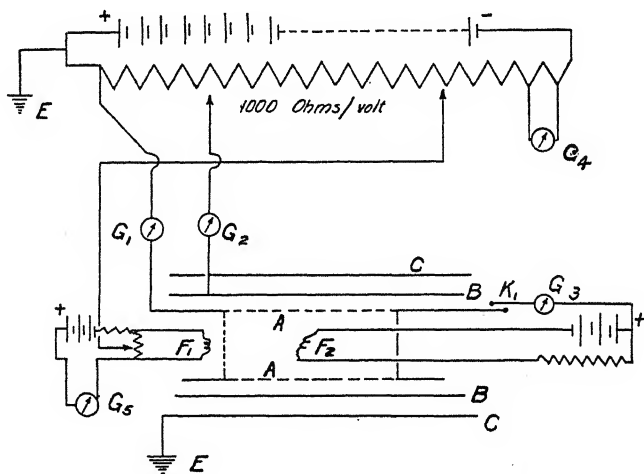


Fig. 1. Arrangement of filaments and electrodes and potentiometer scheme for applying potentials.

detection of ionization by the method of change in gap resistance. A reflecting galvanometer G_5 was inserted in the filament (F_1) circuit and a scale was arranged to receive a spot of light reflected from the mirror of this galvanometer. The scale was so placed as to be under the direct observation of the reader while data were being taken for resonance potentials. The current for F_1 was supplied by two high capacity batteries in parallel and was constant to 1 part in 2000 for several hours. This current was usually of the order of 1.5 amps. The currents as registered by galvanometers G_1 and G_2 were not accepted as trustworthy if there were any indication of a simultaneous change in the galvanometer G_5 . Many runs of 10 hours duration were obtained when the filament current was extremely steady and the temperature

of the tube constant to within 1° or 2°C. A moderately sensitive Thomson galvanometer G_1 was used to determine the total current from F_1 to box A , while the partial current from A to B was determined by means of a highly sensitive Broca galvanometer. These galvanometers were also used with the simple three-electrode tubes.

(c) *Method used for resonance data.* For a given value of V_A (the accelerating potential) the galvanometers G_1 and G_2 were read, (1) with V_B equal to zero volts (2) with V_B equal to 0.1 volts. The reading of G_2 with V_B equal to zero volts we call R_1 and the reading with V_B equal to 0.1 volt we call R_2 . Then $R_1 - R_2$ gives the value of the differential current corresponding to the potential V_A . Thus one point on the differential current-voltage curve is obtained. In most of the work the voltage V_A was increased in steps of 0.1 or 0.2 volts. In this way the data for the resonance curve as shown in Fig. 2D was obtained. In case it was desired to plot the total current curve the reading of galvanometer G_1 was used.

(d) *Method used for ionization data.* The data for the ionization curves shown in Figs. 2A and 2D, and 3F were obtained by the method of modified space charge. To obtain these curves the values of V_A were plotted against the current obtained from the readings of the galvanometer G_3 (Fig. 1). The connections were altered to obtain these data. The connection between G_2 and B was broken, B and A being connected externally, and the key K_1 closed to insert the galvanometer G_3 into the circuit between F_2 and A . Consideration of Fig. 1 will show that the filament F_2 is negative with respect to A . Consequently, electrons would be accelerated toward A and the current registered by G_3 and limited by space charge would remain constant for a constant current through F_2 and for all values of V_A below the ionization potential. This constancy is shown by the flat portions of the ionization curves. When V_A is made large enough that the electrons entering box A have sufficient energy to ionize, then a neutralization of part of the negative space charge in A takes place with the consequence of a sudden rise in the current as registered by the galvanometer G_3 . This sudden rise is interpreted as the ionization point. Of course the value of V_A at which this takes place needs correction.

In the Lenard method filament F_2 was maintained negative with respect to all other electrodes and the galvanometer G_2 was connected to it, the battery and galvanometer G_3 being disconnected from F_2 . In this method the initial rise in current to F_2 as registered by G_2 so connected was interpreted as the ionization point. (See Fig. 3, curve G, for indium.)

At the ionization point there is a change in the gap resistance between filament F_1 and the electrode A . Since this is a shunt on a part

of the potentiometer circuit, the current as registered by the galvanometer G_4 increases since the total resistance in series with the potentiometer battery has decreased. This increase in G_4 was found to be coincident with the sudden increase in G_3 due to the modification of the negative space charge in box A for mercury. Hence, considerable importance has been given to the modification of the gap resistance for the case of gallium and indium in which the other methods of determining the ionization potentials did not give as definite results as had been hoped for.

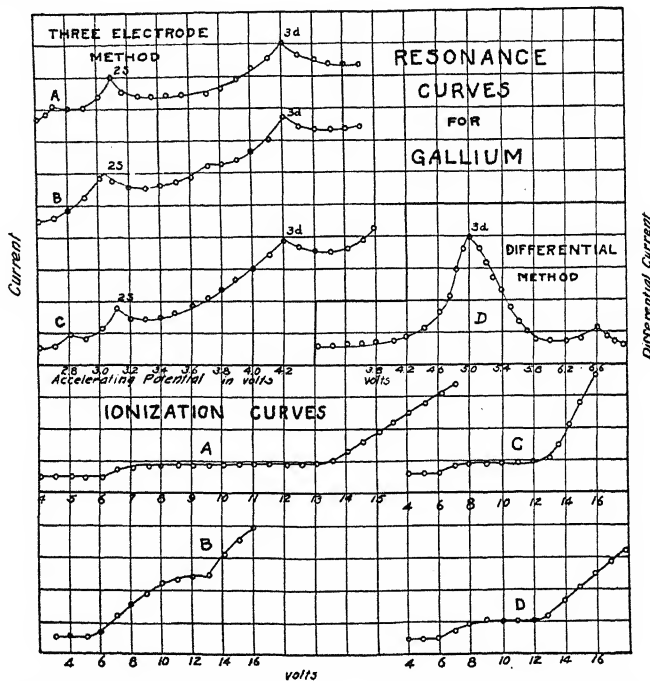


Fig. 2. Curves showing the principal critical potentials for gallium.

(e) *Criterion for properly baked tube.* When first exhausted the tubes did not show smooth current potential curves. Baking and pumping was continued until smooth electronic curves were obtained. The vapor to be studied was then admitted and resonance and ionization data secured.

RESULTS

(a) *Mercury.* (*Hertz-differential method.*) The results with this element were reported at the Washington meeting of the American Physical Society (1926), and are given in tabular form in an abstract in the *PHYSICAL REVIEW*.⁴ The results are in general agreement with

⁴ Jarvis, *Phys. Rev.* 27, pp. 808 (June 1926).

those of Franck and Einsporn, with the addition of several values below 4.68 volts. Work is being continued to determine, if possible, the meaning of the critical potentials found below 4.68 volts. Six such critical potentials have been found. It is thought they may be ascribed to the mercury molecule.

(b) *Gallium.* Typical results for gallium are shown in the various curves given in Fig. 2. Both the gallium and indium used were certified as 98.5 percent pure. Two different tubes were used with this element. Three resonance curves shown in the upper left hand portion of the figure were obtained from the Hertz differential type tube used as a simple three-electrode tube. They show transitions corresponding to the $2s$ and $3d$ levels very decidedly. The other resonance curve was obtained with the other tube used in the differential manner. It shows the transition to the $3d$ level as a pronounced peak. This curve gave but slight indication of the $2s$ level.

The results obtained for ionization are shown by the curves *A*, *B*, *C*, and *D* in the lower portion of Fig. 2. Curves *A* and *D* were obtained by the Lenard method, and *B* and *C* were obtained by the modified space charge method. Another curve not shown gave marked evidence of ionization at about 6 volts by the method of change in gap resistance. The curves shown have been corrected for filament drop and velocity distribution by an approximate method. These curves give evidence of a weak type ionization at about 6 volts and a stronger second type ionization at about 13 volts. No evidence was obtained indicating the transition $2p_2 - 2p_1$.

The results for gallium are summarized in Table I. One critical potential at 1.96 volts was found for which there is no corresponding spectral relation. No interpretation is offered for it.

TABLE I
Critical potentials in gallium.

No.	Critical potentials (volts) from different curves						Mean	Calc.	λ	Series
1	2.20	1.80	1.85	2.10	1.85		1.96		6300	?
2	2.70	2.70	2.60	2.80			2.70	2.96	4172*	$2p_1 - 2s$
3	3.10	3.00	3.00	3.05	3.15		3.07	3.06	4033*	$2p_2 - 2s$
4	4.20	4.20	4.52	4.25	4.25		4.22	4.29	2872	$2p_2 - 3d_2$
Ionization potentials (volts) from different curves.										Mean Calc
Type 1	5.5	5.8	5.5	6.3	6.0	5.8	6.4	5.5		5.80 5.97
Type 2**	13.0	13.8	12.5	12.8	13.0	13.6	14.0	13.2		13.2

*4172A and 4033A are "raies ultimes."

** New arc type of ionization.

(c) *Indium.* The various critical potentials found for indium are represented in the curves of Fig. 3. The intermediate portions of the

resonance curves *A* and *B* are omitted to facilitate plotting. The latter portions of these curves showing the $3d$ level have had the ordinates reduced in order to keep within the allotted space. Curve *A* was obtained with a slightly higher filament temperature than curve *B* and hence the correction is slightly different. Curves *A*, *B*, *C*, and *D* show critical potentials corresponding to transitions to the $2s$ and the $3d$ levels for indium as decided peaks. The retarding potential applied between electrodes *A* and *B* (Fig. 1) was kept constant at 2.5 volts

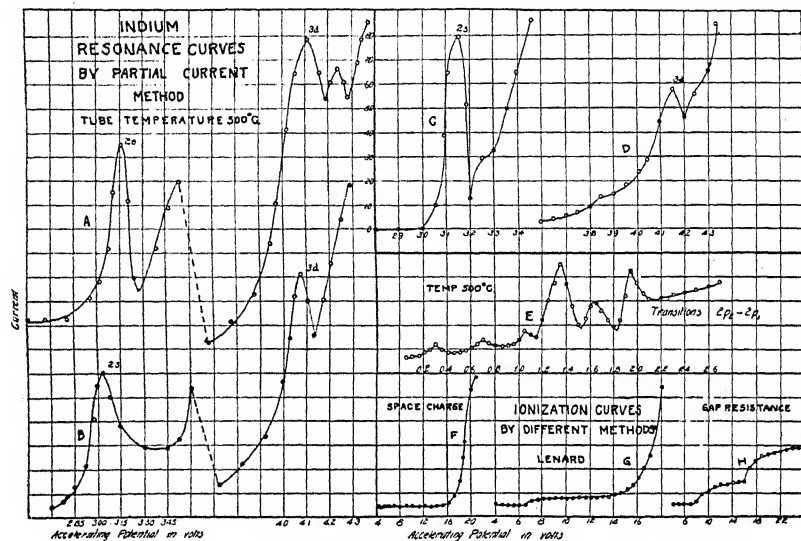


Fig. 3. Curves showing the principal critical potentials for indium.

while data were being taken for curves *A*, *B*, *C*, and *D*. The filament F_1 was shielded with a nickel shield, only the hottest portion being exposed to box *A*. Only a slight correction was necessary. The tube was equivalent to a four-electrode tube in which the two inner grids were at the same potential. Some of the curves show a double peak, the separation being 0.1 to 0.2 volts. This may be due to the transition $2p_2 - 2p_1$ of either gallium or indium. Curve *E* was obtained with a small retarding potential in order to bring out the transition $2p_2 - 2p_1$ whose theoretical value is 0.273 volts. The analysis of eight such curves is given in the upper portion of Table II. These results are obtained as differences between recurring peaks on the same curve. The results on ionization are shown by the three curves *F*, *G*, and *H* obtained by the modified space charge, the Lenard, and the gap resistance methods, respectively. Two types of ionization at 6 and 14 volts, approximately, are evident from these curves.

DISCUSSION OF RESULTS

(a) *Gallium and indium.* The curves give no evidence of the transition $2p_2 - 2p_1$ for gallium unless an occasional double peak with 0.1 to 0.2 volt separation could be so interpreted. Spectral considerations place these levels 0.102 volts apart, and it may be that they are too close together to be clearly distinguished by the method of inelastic impact. Foote and Mohler⁵ have found a series of recurring peaks at

TABLE II
Critical potentials in indium.

Transition	Curve No.	Potential (volts) of peaks					Mean	diff.
$2p_2 - 2p_1$	1	0.55	0.85	1.15	1.47	1.75	2.04	0.30
	2	.30	.70	1.06	1.35	1.65	1.93	.32
	3		.77	1.07		1.56	1.85	.26
	4		.60	.89	1.17			.28
	5		.60	.94	1.25	1.55		.32
	6	.34	.65	1.05	1.32	1.62		.32
	7		.65	.95	1.25	1.55		.30
	8	.30	.56	.88	1.15	1.40		.28
							Mean of means	0.297
							Calculated value	.273
Transition	Volt values from different curves							Mean
$2p_2 - 2s$	3.05	2.96	3.00	3.01	3.05	3.15	2.96	3.03
$2p_2 - 3d$	4.05	4.00	4.20	4.05	4.06	4.12	3.97	4.07
Ionization	Potentials of breaks					Mean (corr.)	Calc.	
Type 1	7.5	8.5	6.7	7.0		6.3 ± 0.5	5.76	
Type 2***	15.2	15.4	15.0	14.8		14.1 ± 0.5		

* Corresponding absorption line 4102A.

** Corresponding absorption line 3039A.

*** New arc type of ionization.

0.9 volt apart for thallium agreeing well with the series relation for the $2p_2 - 2p_1$ transition. The author's value of 0.297 volt is in fair agreement with 0.273 volts based on series relations for the transition $2p_2 - 2p_1$ in the case of indium. All curves for gallium show the transitions $2p_2 - 2s$ and $2p_2 - 3d_2$ and several (see curves A and C for resonance, Fig. 2) show the transition $2p_1 - 2s$. Grotrian⁶ and Frayne and Smith⁷ have shown that for gallium and indium the lines of the series $2p_1 - ms$ are absorption lines as well as those of the series $2p_2 - ms$. This work is in agreement with theirs but would indicate that the transition $2p_2 - ms$ is

⁵ Foote and Mohler, Phil. Mag. 37, pp. 35-50 (1919); also J.O.S.A. 7, pp. 819-830 (1923).

⁶ Grotrian, Zeits. f. Physik 18, pp. 169-192 (1923); also 12, pp. 218-231 (1922).

⁷ Frayne and Smith, Phys. Rev. 27, p. 23 (1926).

more probable than the transition $2p_1-ms$. Several curves for gallium (see curve *B*, Fig. 2) gave evidence of a critical potential at approximately 3.8 volts which corresponds to a wave-length of 3260A. This line is the first member of the series $2p_1-md$ and was found as an absorption line by Grotian⁶ and also by Frayne and Smith.⁷ With indium the transitions corresponding to the levels $2s$ and $3d$ came out consistently as well as the transition $2p_2-2p_1$. However, a few curves (not shown in Fig. 3) gave pronounced evidence of the transition $2p_1-2s$ and $2p_1-3d$. The results with both gallium and indium are in fair agreement with the spectral series arrangement. One value for gallium at 1.96 volts has not been reconciled with spectral data. With both gallium and indium the second type of ionization at 12 to 14 volts was found to give the more pronounced breaks in the potential curves. It is thought that the second valence electron is involved at this point. If this be true, then additional spectrum lines should appear at this voltage. Spectroscopic investigation of this point has been undertaken by Frayne and Jarvis⁸ for indium. Their results will appear in a later issue of the PHYSICAL REVIEW.

In conclusion the author expresses his gratitude to the Physics Department of Ohio State University where this work was done, and to Dr. Alpheus W. Smith under whose direction and sustaining influence this work was carried out.

OHIO WESLEYAN UNIVERSITY,
September 1, 1926.

⁸ Frayne and Jarvis, PHYS. REV., in press.

THE PHOTOELECTRIC PROPERTIES OF THOROUGHLY OUTGASSED PLATINUM¹

BY LEE A. DUBRIDGE

ABSTRACT

Effect of heat treatment on the photo-currents from Pt.—The total photoelectric emission from a strip of Pt foil excited by the full radiation from a quartz mercury arc was studied while the strip was put through an extended heat treatment in pressures as low as 10^{-8} mm Hg as read on an ionization gauge. Prolonged heating at $1200^{\circ}\text{--}1400^{\circ}\text{C}$ caused the photo-current to decrease to a final value which could not be further reduced by additional heating for as long as 300 hours at temperatures up to the melting point. The photo-current was found to increase spontaneously from the low values observed immediately after a heating interval to much higher values if the strip was allowed to remain at room temperature for a short time. After thorough outgassing of the strip and the tube however this "recovery" effect finally disappeared.

Effect of heat treatment on the long wave-length limit of Pt.—The long wave-length limit was determined by using filters of dilute acetic acid in a fluorite cell to cut out the shorter Hg lines. The threshold was found to shift during outgassing from above 2500 Å to a final steady value of 1958 ± 15 Å. This is at variance with Suhrmann's value of 2675 Å but is shown to be in agreement with the work of Tucker and Woodruff. Pressure readings taken with an ionization gauge of high sensitivity confirm the conclusions (a) that decreasing photo-currents are caused by the evolution of absorbed gases, (b) that increasing photo-currents (recovery effect) are due to the adsorption of gas by the cool Pt surface, and (c) that the final low values of the photo-emission are characteristic of the gas-free Pt. Heating an outgassed strip in air at 0.015 mm pressure caused the photo-currents to disappear; heating in hydrogen at the same pressure caused them to increase. They were brought back to values characteristic of the completely outgassed state in each case by heating for 30 sec. at a pressure of 10^{-6} mm.

Influence of temperature on the photo-emission from Pt.—The photoelectric effect of Pt is found to be independent of the temperature only in the region below 500°C . At higher temperatures up to 1200°C the photo-currents increase considerably with temperature and the threshold shifts slightly to the red. Several explanations of the effect were tested and are discussed, the conclusion being that it is a genuine temperature effect characteristic of the metal itself and due to the increase in the thermal energies of the "free" electrons which may become appreciable at the higher temperatures.

INTRODUCTION

IN SPITE of the large amount of recent research on the subject, the status of the problem of the photoelectric behavior of metals which have been thoroughly cleaned of occluded gases is still a rather un-

¹ A preliminary report of this work appeared in Proc. Nat. Acad. Sci. 12, 162 (1926).

certain one. Strange to say, however, the principal points of disagreement between various observers lie not so much in the experimental facts observed as in the conclusions drawn from them and in the explanations offered. In the case of platinum, for example, while there is general agreement as to the type of behavior observed when the photo-current excited by the radiation from a quartz mercury arc is studied as a function of the time for which the specimen has been outgassed by heating, there are still three questions at least upon which the experimenters in this field are divided, namely: (1) the old problem of whether the observed decrease in the photo-current with outgassing continues indefinitely, or whether it is possible to reach a limiting state characteristic of the cleaned metal itself; (2) the question as to which, if any, of the many observed values of the photoelectric threshold may be accepted as the true value characteristic of the platinum; (3) the problem of formulating a theory to explain the effects of gases and to account for the observed results. The experimental work to be described in the present paper was undertaken for the purpose of obtaining further evidence on all three of these questions. Reviews of previous work in this field have been given by other writers² and only a brief statement of the present status of each problem will be given here.

In regard to the first, Wiedmann and Hallwachs² and their students have been led to the view that the photoelectric effect is not an intrinsic property of the metal at all but that, as outgassing progressed, the photo-currents excited by the light ordinarily used would disappear, and the long wave-length limit would shift steadily further into the ultra-violet, reaching finally the region near 1200 Å where ionization of the gas atoms themselves begins. Other observers^{3,4,5} are inclined to the view that the platinum itself is the seat of the photo-currents and that the absorbed gases merely assist (or hinder) their escape; that it should be possible to reach a state where the photo-currents from the Pt itself are obtained and where the threshold, while it may be far in the ultra-violet, still has a value characteristic of the cleaned metal, unaffected by the presence of gases. Actually to reach such a state has proved to be a difficult task.

The second problem, that of the characteristic long wave-limit of Pt, is thus seen to be intimately connected with the first. Observed values of the threshold have been pushed steadily to shorter wave-lengths as more complete outgassing has been attained, and Tucker⁶ and

² See Wiedmann, *Jahrb. d. Radioakt. u. Elekt.* 19, 112 (1922). See also refs. 5, 6, 9.

³ Welo, *Phys. Rev.* 12, 251 (1918); *Phil. Mag.* 45, 593 (1923).

⁴ Piersol, *Phys. Rev.* 8, 238 (1916).

⁵ Woodruff, *Phys. Rev.* 26, 655 (1925).

⁶ Tucker, *Phys. Rev.* 22, 574 (1923).

Woodruff⁵ have reported specimens which were insensitive to the mercury arc radiation for a short time after long heating. Tucker concludes that this indicates a threshold below 1850A though Woodruff believes it may be as high as 2200A because of the observed weakness of the shorter lines in the spectrum. Suhrmann⁷ on the other hand reports a limiting value of 2675A after long heating. Obviously before acceptable final values of the threshold can be obtained, a stable limiting state of the specimen must be reached in which the photo-currents remain unchanged during further intense treatment. This condition has not heretofore been realized in the case of Pt, though Kazda⁸ seems to have attained an analogous condition in the case of flowing mercury.

The third problem—that of formulating a theory to account for the effects of gases—has also presented difficulties. The theory which has been most widely accepted as explaining the largest number of observed facts is that of Wiedmann and Hallwachs⁹ who assumed, (a) that the initial low sensitivity observed for a fresh platinum specimen is due to the presence on the surface of an adsorbed layer of electro-negative gases which tends to prevent the escape of electrons, this surface layer being quickly removed by the heat treatment giving rise to a large initial increase in the photo-current; (b) that in addition there are gases absorbed within the body of the metal itself which in some way aid in the ejection of electrons, and their gradual removal during heating causes the photo-current to decrease slowly and the threshold to shift into the violet. The implied consequence of this theory was that if all absorbed gases could be removed the photo-currents would disappear.

These assumptions have been confirmed in many respects by the experimental work of Sende and Simon,¹⁰ Suhrmann,¹¹ and Herrmann,¹² but Welo,³ Piersol⁴ and Woodruff⁵ have been led to the conclusion that they do not account for many observed facts. The latter observers regard the Pt as the seat of the photo-electrons and believe that occluded gases retard rather than assist in their emission. An attempt was made in the present work to obtain a more direct test between these viewpoints.

METHOD

Several experimental tubes of slightly different forms were used, a diagram of one of the later ones being shown in Fig. 1. The specimen

⁷ Suhrmann, Zeits. f. Physik 33, 63 (1925).

⁸ Kazda, Phys. Rev. 26, 643 (1925).

⁹ Wiedmann and Hallwachs, Verh. d. Deutsch. Phys. Ges. 16, 107 (1914).

¹⁰ Sende and Simon, Ann. d. Physik 65, 697 (1921).

¹¹ Suhrmann, Ann. d. Physik 67, 43 (1922); Zeits. f. Physik 13, 17 (1923).

¹² Herrmann, Ann. d. Physik 77, 503 (1925).

to be tested consisted in a strip of Pt foil, .01 mm thick, 2 mm wide and about 10 cm long, hung in the form of a loop inside the receiving cylinder *C* of nickel or molybdenum. The strip could be heated by a current from a 20 volt storage battery conducted in through the tungsten leads *T* to which the strip was spot-welded. Its temperature could be measured by means of an optical pyrometer focussed onto it through the thin window *W*. The true temperature was determined

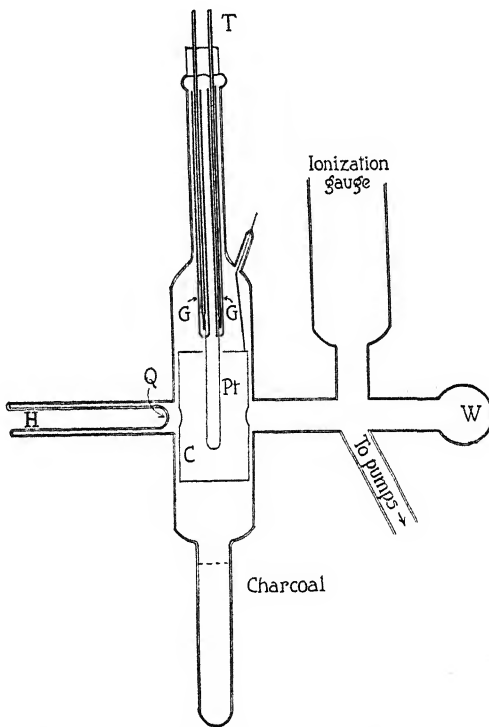


Fig. 1. Photo-electric tube. *Q*, quartz window; *W*, pyrometer window; *c*, collecting cylinder; *GG*, Pyrex tubes to shield tungsten leads, *T*.

from the observed black body temperature using data published by Mendenhall.¹³ Light from a Cooper-Hewitt Type Y, 110 volt quartz mercury arc, or from a metallic spark, could be focussed by means of a quartz lens through the quartz window *Q* onto the Pt. The window *Q* was sealed to the pyrex tube without the use of wax or cement by a graded quartz to pyrex seal. Since nearly all the runs were carried out at pressures below the range of measurement of the McLeod gauge these lower pressures were measured by a sensitive ionization gauge of the type described by Dushman and Found.¹⁴ The apparatus was

¹³ Mendenhall, J. Astroph. 33, 91 (1911).

¹⁴ Dushman and Found, Phys. Rev. 23, 734 (1924).

connected to the pumps without the use of wax or cement joints to avoid troubles arising from their use. Outgassing at 550°C was possible.

The photo-currents were measured by a Compton electrometer whose sensitivity was 5000 mm per volt. A resistance of 400 megohms shunted across the quadrants permitted the currents to be measured by the "steady deflection" method, the current sensitivity being 5×10^{-18} amp/mm.

In order to prevent scattered light from striking the tungsten supports *T*, or the upper parts of the strip which were not thoroughly outgassed, these were kept well above the top of the cylinder and were enclosed in small pyrex tubes *GG* which prevented light of shorter wave-lengths from reaching them and also prevented any electrons leaving them from reaching the cylinder. All of the observed currents then came from the lower parts of the strip which were heated to a uniform temperature.

To furnish to the strip if necessary more energy in the shorter wave-lengths, the region *H* could be converted into a hydrogen discharge tube by an obvious device. The hydrogen discharge is known to be rich in wave-lengths between 2200A and 1600A.

After an initial cleaning of the Pt, the entire apparatus was baked out at temperatures up to 550°C for periods varying from several hours to several days—or until the pressure with the tube hot had been reduced to 10^{-6} mm Hg or less. In some cases the Pt strip was glowed at a dull red heat during baking. After this treatment the photo-current was quite large, its actual value depending upon the time for which the treatment had been continued in each particular case. The Pt strip was then heated by an electric current for various intervals of time and at various temperatures, photo-current readings being taken intermittently during the process. The heating current through the strip was shut off while the photo-current was being measured. During the heating at higher temperatures the cylinder *C* could be rotated about a vertical axis by means of an external magnet to bring the holes in the cylinder out of line with the windows *Q* and *W* to prevent condensation of platinum on these windows.

THE TOTAL PHOTOELECTRIC CURRENT

Photo-current readings using the mercury arc as a source were taken on 15 different specimens of Pt, cut from foil obtained from three different sources, all of high purity. The strips were subjected to a variety of cleaning treatments before being introduced into the tube, and to many different forms of heat treatment after being sealed in. All, however, exhibited substantially the same form of final behavior of the total photo-current as a function of the time of heating, viz., in every case in which the heating was carried on for a sufficient length

of time the photo-current eventually reached a final limiting value, —not zero—which value could not be further reduced by heating of any kind.

Observations on three typical specimens have already been published¹ and those for a fourth are presented herewith (Fig. 2). This curve may be taken as typical of all the runs which were taken. The maxima in the curve at 22 hours and 50 hours of heating are characteristic of the irregularities which often appeared in the first part of the curves and seemed to be due to incidental pressure variations which were unavoidable during the initial stages of outgassing. Many of the curves

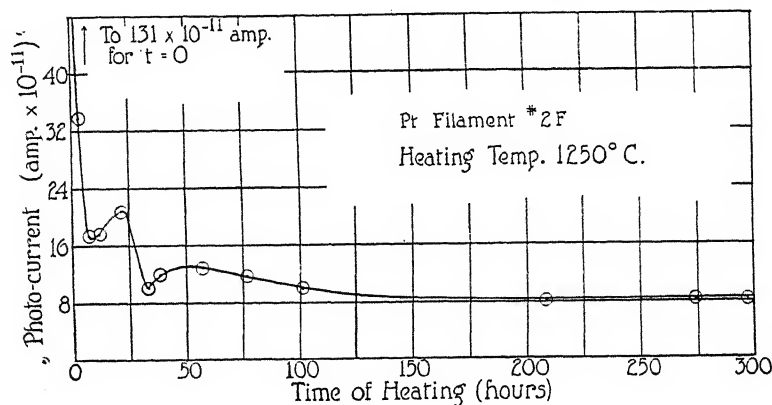


Fig. 2. Variations in the total photo-current during outgassing.

showed no irregularities at all, but in any case they all gradually disappeared as the heat treatment progressed, so that the photo-current approached a limiting value which was truly a stable one.

It should be emphasized that this limiting value is reached only after the heating has been carried on for long periods of time at temperatures higher than 1100°C and at pressures lower than 10^{-6} mm. While the actual number of hours of heating required varied considerably with the temperature and the pressure conditions, in no case was a true final value of the photo-current attained, even at the highest heating temperatures, in less than 10 hours of actual heating time. In most cases at moderate temperatures ($1200^{\circ}\text{--}1400^{\circ}\text{C}$) from 20 to 50 hours were required, while in some cases, as in Fig. 2, the limiting value was reached only after 150 hours of heating. Furthermore, the value of the photo-current observed in the final outgassed state was the same for all Pt specimens which were studied under the same set of incident light conditions.

Every effort was made to determine whether this final value of the photo-current could not be reduced by some type of further treatment.

Among the procedures which were tried were the following: (a) heating for still longer intervals of time at the higher temperatures, up to 1500°C; (b) "flashing" intermittently for intervals of a few seconds each at still higher temperatures, close to the fusion point (a procedure suggested as the most effective one by Herrmann¹²); (c) heating for long periods at temperatures at which considerable vaporization of the Pt took place, thus cleaning off the outer surface of the specimen; (d) heating in the immediate presence of a mass of charcoal cooled by liquid air the more rapidly to absorb the evolved gases; (e) heating the strip while the entire tube around it was lowered to liquid air temperatures by means of a copper jacket; (f) further reducing the pressures to as low as 10^{-8} mm by additional baking out and heating of all metal parts at the highest possible temperatures. All these methods were, however, equally ineffective in lowering the final value of the photo-current, though most of them when tried on a fresh specimen did cause it to reach its limiting value more quickly. A thoroughly cleaned specimen is thus still sensitive to the arc radiation.

A phenomenon reported by Woodruff and by Tucker and referred to as the "recovery" of the photo-emission was also studied in this connection. When the Pt strip is allowed to stand at room temperature for a short time immediately after a heating interval, the photo-current increases spontaneously up to a value which depends upon the previous heat treatment and the pressure and which may be only a few percent less than the maximum value observed during the initial stages of outgassing. It was found by the author, however, that this recovery becomes less rapid and the final value reached becomes steadily smaller as the outgassing progresses and the pressures in the tube become smaller. If the outgassing is carried on long enough that the pressures are reduced to below 10^{-7} mm the effect finally disappears entirely and the photo-currents observed immediately after heating remain constant for many hours. This phenomenon will be more fully discussed later in connection with the pressure effects which were found to accompany it. (See Fig. 3.)

THE LONG WAVE-LENGTH LIMIT

The variations of the long wave-length limit of Pt described in the previous paper¹ have been checked on other specimens, using as before light filters to cut out successively the shorter lines in the mercury spectrum,—a method used by Williamson.¹⁵ These experiments quite definitely place the photoelectric threshold for Pt cleaned by the process already described in the region between the mercury lines $\lambda 1943$ and $\lambda 1973$.

The filters used in these determinations consisted of weak solutions of acetic acid in distilled water, introduced into an absorption cell with

¹⁵ Williamson, Phys. Rev. 21, 107 (1923).

fluorite windows which was placed in the path of the incident light. The thickness of the fluid layer in the cell was 3.2 cm. Photographs taken with a Bausch and Lomb quartz spectrograph, using Schumann plates,¹⁶ showed that in the light transmitted by the empty cell the shorter mercury lines including $\lambda 1850$ were present with considerable strength. Distilled water in the cell served to cut out the 1850 line alone, leaving $\lambda 1943$ still quite strong. A solution formed by adding three drops of 36 percent acetic acid to 25 cc of water when placed in the cell cut out the 1943 line and all below, leaving 1973 still quite strong. Adding six drops of acetic acid to 25 cc of water gave a solution which cut out $\lambda 1973$. The longer wave-length lines were cut out using the solutions described by Williamson.¹⁵

When a fresh strip of Pt was tested after a long initial baking at about 500°C the photo-current could be reduced to zero only after all lines of the mercury spectrum up to and including $\lambda 2482$ had been cut out by filters. The threshold for such a specimen is thus in the neighborhood of 2500A. After long outgassing, however, and after the photo-current had reached its limiting value, it could be reduced to zero by the filter which cut out the 1943 line and all below it leaving $\lambda 1973$. It was not reduced to zero by cutting out $\lambda 1850$ alone leaving $\lambda 1943$. The threshold has thus been shifted to the region between 1943 and 1973A. Using an aluminum spark as a source the threshold was similarly found to lie between the Al lines $\lambda 1930$ and 1990. The photo-current was taken to be "zero" in the above observations only when no observable deflection of the electrometer was obtained even after its sensitivity had been increased up to its maximum value by increasing the potential on the needle. In every case a current as great as .05 percent of that produced by the total arc radiation could be easily observed. These results appear at first sight to be in conflict with those of Tucker⁶ and Woodruff,⁵ but there is a possibility, suggested by Woodruff, that in their work the radiation below about 2200A was too weak to be effective.

If we assume the photoelectric threshold for thoroughly outgassed Pt to be in the neighborhood of 1958A and make use of the quantum relation

$$h\nu_0 = \phi e,$$

we may calculate the work function ϕ for such a surface. The value so obtained is 6.3 volts. The commonly accepted value for the thermionic work function of Pt is 5 volts though this is probably not the value for a thoroughly outgassed surface. Langmuir¹⁷ reports a value

¹⁶ The author is indebted to Mr. H. R. Lillie of this laboratory who made up the numerous Schumann plates required.

¹⁷ Langmuir, Phys. Rev. 2, 452 (1913).

of 6.6 volts for a surface which had been subjected to special heat treatment, and Woodruff also found high values for his outgassed surfaces.

RELATION BETWEEN PHOTOELECTRIC CURRENTS AND SURFACE GAS-CONTENT

In order to obtain more exact information on the observed variations in the photoelectric emission as related to the corresponding changes in the gas-content of the specimen and the gas pressures in the tube, a close record was kept of the ionization gauge readings during the runs on several Pt strips. The first point of interest in connection with these readings was to determine how the amount of gas being given off by the specimen during heating varied as the outgassing progressed. The readings for a typical run are given in Table I. In this table are

TABLE I
Progressive changes in pressure and photo-current during heat treatment.

Time of heating	Temp. °C	Pressure ×10 ⁻⁷ mm Fil. cold	Pressure ×10 ⁻⁷ mm Fil. hot	Ratio	Photo-curr. ×10 ⁻¹ amp. Fil. cold
10 min.	1250°	5.2	120.0	23.1	84.0
3 hr.	"	4.0	14.0	3.5	26.0
19 "	"	3.2	7.3	2.3	21.0
39 "	"	2.2	4.0	1.82	12.0
107 "	"	0.8	1.2	1.50	8.6
296 "	"	0.25	0.25	1.00	8.5
320 "	1360°	0.10	0.10	1.00	8.5

recorded the steady pressures as read by the ionization gauge while the Pt strip was glowing and while it was at room temperature, at various stages during the heat treatment. The pumps were running continuously during all readings.

These readings were taken on the same specimen whose photoelectric behavior is recorded in Fig. 2. It is seen at once that initially the filament was so saturated with gas that bringing it to a temperature of 1250°C caused a 23-fold increase in the pressure in the tube. After 296 hours of heating, however, during which time the photo-current had reached its limiting value, there was no change in the pressure when the heating current through the strip was turned on, showing that the evolution of gas from the specimen had practically ceased. After the readings recorded in the table were taken the strip was heated irregularly at various temperatures up, finally, to the fusion point, over a period of several days while temperature variation runs were in progress. During this time the pressure and the photo-current remained practically unchanged at the final values given in the table. Evolution of gas from the Pt thus ceases only after extended periods of outgassing—and only after this evolution of gas has ceased are stable

values of the photo-current attained. These observations then confirm the view that occluded gases assist rather than hinder the escape of photo-electrons and that their gradual removal causes the photo-currents to decrease.

Further confirmation of this view was found in a more careful study of the "recovery" of the photo-current when the strip was allowed to stand at room temperature for a short time. It was found that after such a period of standing, switching on the heating current through the Pt strip released a large amount of gas from the strip causing an instantaneous increase in the pressure in the tube. In the curves of Fig. 3 the magnitude of this pressure increase is plotted as a function of the time for which the strip had been standing cool. After only 50 hours of outgassing (Curves I and II) if the strip was allowed to stand at room temperature for 10 minutes, turning on the heating cur-

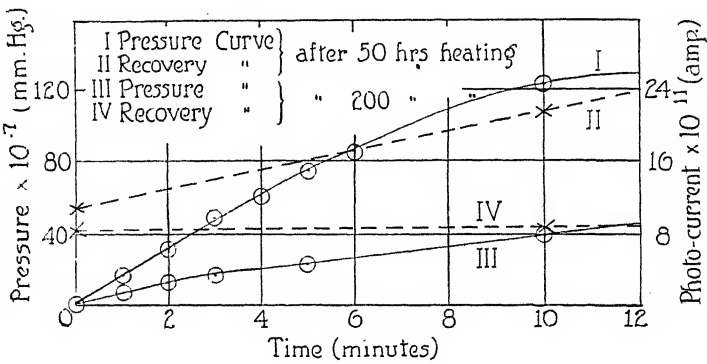


Fig. 3. Recovery of photo-current and accompanying pressure effects.

rent caused a sudden rise in the pressure from 2.0×10^{-7} mm to a peak value of 123×10^{-7} mm. During the same interval the photo-current nearly doubled its initial value. After 200 hours of outgassing (Curves III and IV) the pressure rise due to 10 minutes of standing was only from 1.2 to 40×10^{-7} mm and the rise in photo-current during this interval was only 4 percent. After 300 hours of heating (curves not shown) the rise in pressure as well as the increase in photo-current had practically ceased. The pressure rise caused by heating after a 10 minute interval at room temperature was only from 0.18 to 0.20×10^{-7} mm and after a two hour interval was only to 1.1×10^{-7} . The photo-current during the 10 minute interval now remained constant within the limits of observational error and in the two hour interval increased less than 8 percent.

These results point at once to the conclusion that the recovery of the photo-current is due to the formation on the cool Pt surface of a

gas layer which *increases* the photo-sensitivity of the metal. This layer evaporates at once when the strip is again heated, causing the instantaneous rise in pressure observed. When the Pt strip as well as the rest of the tube have been thoroughly cleaned of occluded gases this surface layer no longer forms and the recovery of the photo-current disappears. The fact that both these effects may be made to reappear by admitting a small amount of air into the tube indicates that the surface layer is formed by deposition on the cool Pt of residual gases in the tube. On the other hand the fact that the formation of the layer ceases only after the strip itself has been thoroughly outgassed might lead to the conclusion that the layer was formed on the surface by diffusion of gases from the interior of the metal. More data are needed to settle this point. In any case the above data on the formation of loosely bound surface layers seem to be in definite disagreement with the view advanced by Woodruff and Welo that the low final values of the photo-current are due to the presence of retarding layers, and in favor of the view that they are characteristic of the outgassed Pt itself. A Pt strip when most completely freed from gases is sensitive only to radiation of wave-length shorter than about 1958A.

If then the *final* low values of the emission are characteristic of the metal itself, the *initial* low values observed before any outgassing is begun must be due to a retarding layer formed on the specimen before it is introduced into the vacuum chamber. It seems probable that this may be a layer of oxide or adsorbed oxygen and nitrogen since it was found that heating the outgassed strip for 30 seconds in dry air at a pressure of 0.015 mm actually caused the photo-current to disappear. Heating again in vacuum brought the sensitivity back to the value characteristic of the outgassed metal. On the other hand heating the strip in hydrogen admitted through a palladium tube to a pressure of 0.015 mm caused a large increase in the photo-current, and it was again brought back to normal by short heating in vacuum. The high values of the photo-current which persist even after considerable outgassing are thus probably due to the presence of hydrogen, and possibly water vapor, which are notably hard to remove from the tube and which are readily absorbed by the Pt. Herrmann¹² and Suhrmann¹¹ have arrived at a similar conclusion, which also is consistent with data obtained by Welo.¹⁸

VARIATION OF THE PHOTO-CURRENT WITH TEMPERATURE

The temperature variation of the total photoelectric current previously reported¹ has been more carefully studied and its existence more firmly established. At temperatures between 1100°C (at which the thermionic emission is just perceptible) and 1250° (above which

¹⁸ Welo, Phil. Mag. (7) 2, 463 (1926).

the thermionic emission swamps the photoelectric current) the value of the photo-current was obtained by subtracting the electrometer reading obtained when the light from the arc was cut off from that obtained when the light was focussed on the specimen.

The results show that for thoroughly outgassed Pt the ordinarily assumed independence of the photoelectric effect of the temperature holds quite accurately for temperatures below about 500°C. Increasing the temperature of the specimen above this point however causes the photo-current to rise, slowly at first and then more rapidly, until at 1200° it is practically double its value at room temperature. Three explanations for such an effect may be offered, namely: (1) The variation might be due to the change with rise in temperature of the thickness or density of a surface gas layer; (2) it might be due primarily to the heating current through the strip rather than to the temperature, as suggested by the work of Shenstone¹⁹; (3) it may be a true temperature effect characteristic of the metal.

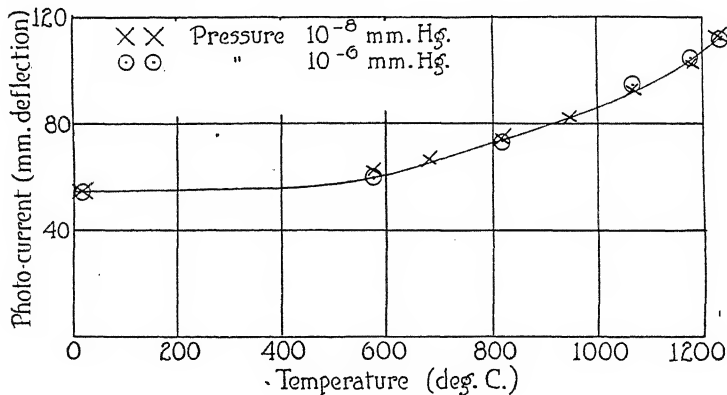


Fig. 4. Temperature variation of the photo-current.

To test the first possibility a large number of runs were taken on several specimens to determine whether the phenomenon exhibited the characteristics which would be expected of a gas effect. The results may be summarized as follows:

(a) The temperature variation described above is characteristic only of the thoroughly outgassed metal. During the earlier stages of outgassing the photo-current showed wide, irregular and non-reproducible changes with temperature, of the type obviously caused by the presence of gas. As the outgassing progressed the behavior gradually became more regular and ultimately settled down to the consistent type of variation shown in Fig. 4.

¹⁹ Shenstone, Phil. Mag. **41**, 916 (1921); **45**, 918 (1923).

(b) When this stage was reached the photo-current—temperature curves taken with temperatures increasing were coincident with those taken with decreasing temperatures,—a result which might not be expected of a phenomenon conditioned by gas-content.

(c) In the thoroughly outgassed state the ionization gauge showed no observable change in pressure in the tube when the temperature of the Pt strip was raised from 20° to 1250°C even when connection with the pumps had been broken by means of a mercury cut-off. The temperature variation thus cannot be due to evolution of gas from the specimen.

(d) The values of the photo-current at the various temperatures were independent of the residual gas pressure in the tube, as long as this was below 10^{-6} mm. In the curve of Fig. 4 the crosses and circles represent points taken with the tube pressure at 10^{-6} and 10^{-8} mm respectively. This result would also not be expected were the photo-currents being affected by the presence of a gas layer, since the characteristics of such a layer should depend upon the surrounding pressure.

It is considered that these results contain sufficient evidence to warrant discarding (1) as a possible explanation of the temperature variation.

That this variation is due primarily to the change in the current through the strip rather than to the temperature seems improbable since the variations of this type reported by Shenstone were very irregular in their nature, showing many time-lag effects when the current was on, and persisting for some time after the current which produced them had been shut off. The variation observed by the author showed none of these effects. Shenstone reported no results for Pt, but it seems evident from the results reported herein that the type of effect which he discovered does not exist for outgassed Pt.

We may then conclude that we are dealing with a true temperature variation of the photoelectric effect. It will be seen from the curve that the type of variation observed is not in disagreement with the results of previous observers who have reported the photoelectric current to be independent of the temperature, since previous observations were carried out in nearly every case at temperatures below about 600°C. It is only at higher temperatures that an appreciable variation is observed.

An increase in the photo-current with rise in temperature might be caused either (a) by an increase in the number of free electrons in the metal made available for ejection by the incident light, (b) by a decrease in the surface work function, or (c) by an increase in the thermal energy of the electrons. In the case of (b) or (c) the increase should be accompanied by a shift in the long-wave limit toward the red while no such shift would occur if the increase were produced by (a) alone.

To determine whether there was such a shift in the threshold, measurements were made of the ratio of the photo-current at 1200°C to that at 20°, *first* using the total radiation of the arc and *second*, when the 1850 line had been cut out by a filter. If these two ratios turned out to be equal this would have been evidence of no shift in the limit. It was found, however, that in the *first* case the ratio was approximately 2 : 1 while in the *second* it was nearly 4 : 1. In other words the change in the photo-current with temperature is greater for the longer wave-lengths (1850 cut out) than for the shorter (1850 included). There has thus been a shift in the threshold toward the red, though it still remained in the region between 1943 and 1973A. Koppius²⁰ also found evidence for a similar shift in the limit as the temperature was increased from 500° to 700°C. In view of this conclusion (a) must be eliminated as a complete explanation of the temperature variation and we are left to choose between (b) and (c).

Now the work function of a thoroughly cleaned metallic surface is presumably a constant characteristic of the metal itself and is theoretically nearly independent of temperature. Within the (relatively large) limits of error available in thermionic measurements the work function for clean metals is found to be constant over quite wide ranges of temperature. Nearly all the variations in work function (or contact potential) which occur under ordinary conditions can be traced directly to changes in surface contamination,—a factor which it was hoped had been eliminated in these experiments. Moreover any changes in contamination which might be expected to take place with increase in temperature would, in the light of the present results, cause the work function to increase rather than decrease.

We are thus led to conclude that the increase in the photo-current and shift in the threshold toward the red with rise in temperature are due to the increase in the thermal energies of the electrons within the metal. That these thermal energies become appreciable only at the higher temperatures is in line with the postulates of Hall's dual theory of metallic conduction²¹ and also with the conclusions to which Millikan and Eyring²² have been led by their experiments on pulling electrons from metals by intense electric fields. The latter agreement is of interest in its confirmation of the view that the electrons pulled from the metals in these experiments (the "free" or conduction electrons) are the same as those ejected photo-electrically. Moreover if the shift in the threshold is due to the thermal energies of electrons there should be a relation between this shift and the Thomson effect as pointed out

²⁰ Koppius, Phys. Rev. 18, 443 (1921).

²¹ Hall, Phys. Rev. 28, 392 (1926).

²² Millikan and Eyring, Phys. Rev. 27, 51 (1926).

by Nielsen,²³ and the specific heats of metals at high temperatures, as suggested by the work of Eastman, Williams and Young.²⁴

Now in the Einstein photoelectric equation as ordinarily written,

$$Ve = h\nu - h\nu_0$$

Ve represents the maximum energy with which the electrons emerge from the metal, $h\nu$ the energy they receive from the incident light, and $h\nu_0$ is usually assumed to be equal to ϕe , the energy lost by the electron in leaving the surface. Now if the electron through thermal collisions acquires the kinetic energy E_k in addition to the energy received from the incident light, the energy with which it should emerge from the metal is given by

$$Ve = h\nu + E_k - \phi e.$$

On comparison with the previous equation we may now set

$$h\nu_0 = \phi e - E_k,$$

an equation which has also been used by Nielsen.²³ Thus even though the work function ϕ remain constant, ν_0 may alter through a change in E_k in the sense that it will shift slightly to the red at the higher temperatures. As Nielsen has pointed out, the values of E_k will not be the same for all electrons but will be distributed according to Maxwell's law, so that at the higher temperatures the threshold should also show an appreciable lack of sharpness.

Suhrmann⁷ has obtained results which he interprets as indicating a shift in the limit toward the red between the absolute zero and room temperature, and also finds an apparent lack of sharpness in the threshold even at room temperature. He attributes both effects to thermal collisions suffered by a few of the electrons even at these lower temperatures. A more detailed study of the variation of the photo-electric threshold with temperature is now being undertaken by the author.

In conclusion the author wishes to express his appreciation to Prof. R. C. Williamson for numerous valuable suggestions and to Mr. A. B. Cardwell for his assistance during the latter part of the experimental work; and especially to acknowledge his very great indebtedness to Prof. C. E. Mendenhall under whose kindly supervision the above work was carried on.

LABORATORY OF PHYSICS,
UNIVERSITY OF WISCONSIN,
June 1926.*

²³ Nielsen, Phys. Rev. 25, 30 (1925).

²⁴ Eastman, Williams and Young, J. Am. Chem. Soc. 46, 1184 (1924).

* Received October 25, 1926.

THE EXCITATION OF FLUORESCENCE IN FLUORESCEIN

By E. H. KENNARD

ABSTRACT

Fluorescence in violation of Stokes' law, excited in an alcoholic solution of specially purified fluorescein, was compared by a photoelectric method with the reciprocal emission when fluorescent and exciting wave-lengths are interchanged. The following theoretical equation, recently proposed by the author, was found to be largely verified: $f_{yx}/f_{xy} = \lambda_x J_y / \lambda_y J_x$. Here f is the exciting power, i.e. $f_{yx} d\lambda_y$ is the emission of fluorescent energy from unit volume in the wave-length range $d\lambda_y$ when the fluorescing substance is illuminated with unit density of exciting radiation of wave-length λ_x , f_{xy} is the same thing with the wave-lengths interchanged, and J_x, J_y are the densities of black-body radiation for these two wave-lengths at the temperature of the fluorescing substance. A peculiar interest attaches to this equation because it contains no unknown constants.

Fluorescence, excitation and absorption curves for the same fluorescein were also determined with moderate accuracy. The fluorescence curves show a single maximum around 5240A but change shape as the exciting wave-length is varied. The excitation curve for fixed incident energy shows a maximum around 5000 for fluorescence at 5270; for other points in the fluorescence spectrum the maximum excitation occurs at shorter wave-lengths, e.g. at 4730 ± 80 A for fluorescence at 5009 or 5582. The curves suggest two superposed bands of different width but with almost coincident peaks. The maximum absorption occurs around 4750.

IN a recent paper¹ in the PHYSICAL REVIEW the writer obtained the following theoretical equation concerning the excitation of fluorescence:

$$\frac{f_{yx}}{f_{xy}} = \frac{\lambda_x J_y}{\lambda_y J_x}, \quad (1)$$

where f represents the spectral exciting power,² i.e. $f_{yx} d\lambda_y$ is the emission of fluorescent light per unit volume of wave-length between λ_y and $\lambda_y + d\lambda_y$ when the fluorescing substance is illuminated with a density unity of exciting radiation of wave-length λ_x , f_{xy} is the same thing with the wave-lengths interchanged, and J_x, J_y are the densities of black-body radiation at these two wave-lengths. This equation is remarkable

¹ E. H. Kennard, Phys. Rev. 28, 672 (1926).

² Note. The term "exciting power" is applied by Nichols and Merritt (Phys. Rev. 31, 381 (1910)) to the quantity f/a where a is the absorption. The usage adopted here seems to be a little more in harmony with the common use of the term "power", which usually refers to a determining factor that is directly and readily controlled and measured, such as the exciting intensity in the present case. Perhaps the ratio f/a might be called the "spectral efficiency" of excitation.

in that it contains no unknown constants whatever. If such an equation could be shown to hold for the fluorescence of liquid and solid substances, it should constitute a distinct step forward toward a theoretical understanding of these phenomena; in particular, it would give quantitative support to the familiar suggestion that the great breadth of the bands is due in some way to the energy of thermal agitation. The equation, in an older but substantially identical form, was found to agree with existing data on eosin and resorufin.³ The purpose of the present investigation was to test its validity on fluorescein, in which the shape of the fluorescence curve could not be assumed to be independent of the exciting wave-length.

The conclusion reached is that Eq. (1) is correct within the experimental errors as regards the implied variation of the anti-Stokes light with temperature, that it holds numerically wherever the anti-Stokes light is relatively bright, and at least approximates to the truth in all other cases tried.

I. APPARATUS

In order to measure the spectral exciting power for wave-lengths close together it is necessary to adopt the relatively unusual procedure of resolving both the exciting light and the fluorescence. This necessitates the measurement of very weak light. A visual spectrophotometer was first tried but was found inadequate, the light being about ten times too faint even when the slits were made regrettably wide. The next simplest method appeared to be photography; so a "spectrograph" was improvised on an old mirror-spectrometer base, with a large flint prism, and with good projection lenses mounted, along with the slits, in wooden boxes fastened tightly to the spectrometer arms. It was found, however, that sufficient blackening could be obtained only by many hours of exposure; so with reluctance the troublesome method of photo-electric photometry was substituted.

For this purpose an old Dolezalek electrometer was converted into a "Compton," the original description⁴ being followed except that the quadrants were made deeper. The instrument never worked really well; the worst of its irregularities finally ceased only when it was surrounded with a thick layer of cotton batting. The sensitivity was usually 10–15000 mm per volt at 250 cm. The photo-electric cell was one of the simplified Kunz type supplied by the Central Scientific Company; a special cell obtained from Professor Kunz himself was also tried but was not found much superior under the conditions of the experiment and was not used after being damaged by blue-glow discharges. Much time was lost in trying to compensate for a persistent

³ E. H. Kennard, Phys. Rev. 11, p. 37 (1918).

⁴ A. H. and K. T. Compton, Phys. Rev. 14, 85 (1919).

positive leak; for a high resistance, ionized air, alcohol, and India-ink lines on paper (K. T. Compton) were all tried but steadiness could not be obtained. Finally this drift was simply endured and in case of need partially compensated by allowing a little light to leak onto the cell from a lamp fed by a storage battery. The cell was mounted in an air-tight chamber, dried with P_2O_5 , immediately under the electrometer; the spectrograph slit was placed about 20 cm from it, to allow a little freedom for manipulation, but the light path was carefully screened. By means of B-batteries and dry cells a voltage varying from 225 to 229.5 volts was applied to the cell. As the voltage rose above 226.5 volts the sensitivity rapidly increased but large irregularities began to appear in the response to light, hence the higher voltages were avoided as much as possible. The rate-of-drift method was employed, but proportionality of deflection rate, corrected for dark drift, was relied upon only in subsidiary observations.

The exciting light was furnished by a new Hilger constant-deviation spectrometer illuminated by a 400-watt tungsten lamp, whose plane-spiral filament was turned almost edge-on and then focussed on the slit through large lenses. The current through the lamp was carefully held constant, and the combined system was calibrated as to transmitted energy with a Coblenz thermopile and galvanometer. Tests made later showed no detectable change in spectral distribution over the range here used even when the blackening was carried to the point where the lamp usually failed.

Spectral calibration of both instruments was made with lines from a hydrogen-helium tube and from mercury and iron arcs, a reference point being inserted in the exit slits. The slits were then adjusted to the desired width (from 40 to 78A), entrance and exit slits of each instrument being set about equally wide in terms of transmitted wavelength, and readings were taken of the first appearance and of the final disappearance of the green mercury line as the setting was altered; the mean of these two readings was taken as the setting at which this line was transmitted centrally through the slits, and from it a correction to the calibration curve was computed for use in making settings upon other wave-lengths. Half of the difference of the two readings was taken as the slit width.

Since the sensitiveness of the electrometer could not be depended upon to remain constant, all principal measurements were made by a substitution method. The light from a tungsten lamp behind a ground-glass screen was reflected by a right-angle prism upon a magnesium-oxide block which could be slipped at will in front of the spectrograph slit. The lamp ran on a track whose "zero" was found by measurement, the distance through the prism being divided by the refractive index. The lamp with its ground-glass was calibrated with a Lummer-Brodhun

contrast spectrophotometer against a tungsten lamp whose color temperature at 97.3 volts had been determined at the Bureau of Standards. The magnesium block was also verified to be non-selective over the same range of wave-lengths. The extreme range of intensities covered in the observations was 200 : 1. To reduce the brighter intensities a filter was interposed in the exciting beam; the filters used consisted of photographic films between glass plates, in ratio steps of 2. Three of the most used transmissions were determined directly with the spectrophotometer in comparison with carefully measured sector discs run at 40 R.P.S.; the transmission of the other filters at the same wave-lengths was then compared with these by an obvious substitution method, and relative transmissions of all filters at other wave-lengths were observed in reliance upon proportionality of intensity and slit width (carefully corrected for zero error). The filters were found to be uniform over their surfaces within the accuracy of observation but they varied somewhat with wave-length.

The entire optical system was amply screened against stray light, both outside and by means of diaphragms inside the instruments.

The material employed was a sample of fluorescein kindly furnished by Professor E. Merritt; it had been specially purified in the Cornell laboratory of chemistry and was said to test 100% pure by analysis. A concentrated mother solution in absolute alcohol was prepared and from this working solutions were made by heavy dilution with the same solvent, the concentration being adjusted so that brilliant fluorescence was obtained without excessive absorption in the spectral region under observation.

II. "ANTI-STOKES" OBSERVATIONS

Method of observation. For the principal observations designed to test Eq. (1), the intensity of the fluorescent light was increased by reflecting the exciting beam from a right-angle prism into the specimen and then taking the fluorescent light out backward, close to the prism, at an angle of 20–25° with the exciting beam. The paths of the two beams through the solution were thus made equal and the direct effect of absorption upon the result was eliminated; but absorption still had the disadvantageous effect of causing a much more rapid variation of intensity with wave-length than would occur with the beams at right angles. The specimen was contained in a glass tube about 18 mm in diameter and this was two-thirds enclosed on the sides by the upper end of a much thicker copper rod wound below with a heating coil, the exciting beam passing out through a slit in the copper in order to minimize scattered light, and a cylindrical lens of 7 mm focal length was inserted with the spectrograph slit and the useful part of the solution at conjugate foci. For the readings at room temperature a

thermometer was lashed to the rod near the tube (or at first merely placed over it on the tin screening). When the temperature was raised by means of the heating coil, a slender thermometer was passed down through a rubber cork into the top layer of the solution and a thick layer of wool was laid around the tube to check convection currents. In a subsequent test this thermometer was pushed down into the middle of the solution and then read 0.8° higher, so a correction of this amount was added to all "hot" readings. The temperature was easily held constant within half a degree.

To compare the reciprocal exciting powers for a chosen pair of wave-lengths, say λ_1 and $\lambda_2 > \lambda_1$, two similar half-sets of observations were taken, excitation being made at λ_2 in the first half-set and fluorescence observed at λ_1 these wave-lengths being then interchanged for the second half-set. The usual observational formula was $F D F F D C C D C C D C D F F D F$, F denoting a drift due to fluorescence, D a dark drift, and C a drift due to the comparison lamp, which was set to give about the same effect as the fluorescence. From each complete set of observations the observed ratio of the exciting powers, $R = f_{21}/f_{12}$, was calculated. Let F_1 , F_2 denote respectively the mean net rates of drift due to fluorescence in the two half-sets, L_1 , L_2 the means of the net drifts due to the comparison lamp each multiplied by the square of the distance from the magnesium block, B_1 , B_2 the relative spectral intensities of the comparison lamp at λ_1 and λ_2 , S_1 , and S_2 the relative intensities of the exciting beam at λ_1 and λ_2 , and t_1 , t_2 the transmissions of the filters used (usually none in the first half-set). Then

$$R = \frac{f_{21}}{f_{12}} = \frac{F_2 L_1 B_2 S_2 t_1}{F_1 L_2 B_1 S_1 t_2} \quad (2)$$

Theoretical values of R were then calculated from (1) with the assumption of Wien's law for J , so that

$$\frac{1}{R} = \frac{f_{12}}{f_{21}} = \frac{\lambda_2^6}{\lambda_1^6} e^{-\alpha(\lambda_2 - \lambda_1)} \quad (3)$$

where $\alpha = 1.435/T\lambda_1\lambda_2$, T being the temperature of the fluorescing substance. A large correction for slit-width is, however, necessitated by the rapid diminution of the anti-Stokes light with decreasing wave-length. Entrance and entrance slits being equal, the spectral transmission of either instrument is represented as a function of wave-length by an isosceles triangle whose base is twice the spectral slit-width, w , and can be written $k(1 - |\lambda - \lambda_0|/w)$, where λ_0 is the central wave-length and k is a constant. The amount of light issuing from the spectrograph when the central wave-length of excitation is λ_2 and the

spectrograph is set to transmit centrally a wave-length λ_1 will therefore be

$$F_{12} = k' \int_{\lambda_1 - \epsilon}^{\lambda_1 + \epsilon} \int_{\lambda_2 - \eta}^{\lambda_2 + \eta} f_{1'2'} S_2' \left(1 - \frac{|\lambda_1' - \lambda_1|}{\epsilon} \right) \left(1 - \frac{|\lambda_2' - \lambda_2|}{\eta} \right) d\lambda_2' d\lambda_1'$$

where $f_{1'2'}$, S_2' denote respectively the exciting power and the spectral intensity of the exciting beam for wave-lengths λ_1' and λ_2' , and ϵ , η are the respective slit widths of the two instruments. Putting $f_{1'2'} = f_{2'1'} \exp[-\alpha(\lambda_2' - \lambda_1')]$, in accordance with (3) but omitting the λ factors as inconsequential in the present connection, and then expanding f and S , we have

$$F_{12} = k' \int_{\lambda_1 - \epsilon}^{\lambda_1 + \epsilon} \int_{\lambda_2 - \eta}^{\lambda_2 + \eta} \left[f_{21} + (\lambda_1' - \lambda_1) \frac{\partial f_{21}}{\partial \lambda_1} + (\lambda_2' - \lambda_2) \frac{\partial f_{21}}{\partial \lambda_2} \right] \left[S_2 + (\lambda_2' - \lambda_2) \frac{\partial S_2}{\partial \lambda_2} \right] e^{-\alpha(\lambda_2' - \lambda_1')} \left(1 - \frac{|\lambda_1' - \lambda_1|}{\epsilon} \right) \left(1 - \frac{|\lambda_2' - \lambda_2|}{\eta} \right) d\lambda_2' d\lambda_1'. \quad (4)$$

If the wave-lengths are now interchanged on the two instruments, the issuing light becomes, with sufficient approximation,

$$F_{21} = k' \int_{\lambda_1 - \epsilon}^{\lambda_1 + \epsilon} \int_{\lambda_2 - \eta}^{\lambda_2 + \eta} f_{21} S_2 \left(1 - \frac{|\lambda_1' - \lambda_1|}{\epsilon} \right) \left(1 - \frac{|\lambda_2' - \lambda_2|}{\eta} \right) d\lambda_2' d\lambda_1' \\ = k' \epsilon \eta f_{21} S_2. \quad (5)$$

Carrying out the integration in (4) and then dividing (4) by (5), we find

$$\frac{F_{12}}{F_{21}} = \frac{1}{R} = e^{-\alpha(\lambda_2 - \lambda_1)} \frac{4}{\alpha^4 \epsilon^2 \eta^2} (\cosh \alpha \epsilon - 1)(\cosh \alpha \eta - 1) \\ \left[1 + \frac{1}{\alpha f_{21}} \frac{\partial f_{21}}{\partial \lambda_1} \left(\alpha \epsilon \coth \frac{\alpha \epsilon}{2} - 2 \right) - \left(\frac{1}{\alpha f_{21}} \frac{\partial f_{21}}{\partial \lambda_2} + \frac{1}{\alpha S_2} \frac{\partial S_2}{\partial \lambda_2} \right) \left(\alpha \eta \coth \frac{\alpha \eta}{2} - 2 \right) \right]. \quad (6)$$

The reciprocal of the right-hand member of (6), with the exponential factor omitted, was applied as a correction factor to the theoretical values of R . Approximate values of the derivatives of f_{21} as modified by absorption, which is obviously what is required in the formula, were obtained from subsidiary observations in which λ_1 and λ_2 were varied; in most of these, no allowance was made for the (moderate) spectral variation of sensitiveness of the observing system. The bracket in (6) containing these derivatives usually differed from unity by 1–3% (maximum, 10%) and the entire correction factor ranged from 0.86 to 0.95. Rough estimates indicated that the effect of higher derivatives of f was very small.

An attempt was made also to estimate another source of error, that due to light scattered inside the instruments. Such light will tend always to make the anti-Stokes light appear too strong and so to diminish the observed value of R , and it is particularly serious in these observations because of the relative faintness of the light under observation. Before taking any of the final data, the green light from a mercury lamp, isolated by absorbing glasses, was passed into the Hilger spectrometer and the amount of light issuing through the slit for various settings of the drum was determined photometrically in comparison with a direct beam from the lamp. Light from the spectrometer was then reflected into the spectrograph for a similar test upon that instrument, correction being now made for the scattering in the spectrometer. As an example, the light scattered through the slit when set 120A away from the entering wave-length came out about 0.00044 of the light transmitted without scattering, for both instruments; at 200A it was half as much. An approximate integration was then made, from the source calibration curve and from fluorescence and exciting power curves obtained in a separate rapid survey, to find the resulting error in R , this being done for only a few pairs of wave-lengths and interpolation being then employed for the others. The results ought to be correct at least within fifty percent.

A point clearly brought out by these calculations and not always properly appreciated is that the scattering in the observing instrument may for some settings be a more serious source of error than that in the exciting instrument because of the large amount of fluorescent light which is passing through and which is much stronger than the wave-length actually being observed.

The final results are given in Table I. λ_1 and λ_2 are the two wave-lengths for each set, I is a rough estimate of the intensity of the "anti-Stokes" light, R is the observed value of that quantity (anti-Stokes exciting power divided into the inverse power), ρ is the ratio of the theoretical value of R , corrected for slit width but not for scattering, to the observed value, and Sc is the estimated percent increase in ρ caused by scattered light. The same specimen was used throughout the first long series of observations at room temperature; for the series at a higher temperature, which followed, a fresh dilution was made from the mother solution with one drop of NaOH added, and fresh portions of this were taken at intervals; and the latter material was also used for the final five sets except that for the very last set six drops of NaOH were added to the specimen under observation. Other sets in considerable number were rejected because of some known or suspected error in the adjustments, but consistency in the policy as to rejections, independently of whether the theoretical equation was confirmed or not, has been preserved.

TABLE I
Results on the violation of Stokes' law

λ_1	λ_2	I	R	ρ	Sc	λ_1	λ_2	I	R	ρ	Sc
(Temperature, 20.0-24.4°)						(Temperature, 60.2-64.4°)					
5320-5469	8	8.23	1.02	12		5316-5469	11	4.67	1.53	9	
5265-5469	8	24.3	.89	13		5268-	9	11.6	1.20	9	
5219-5469	9	38.9	1.19	12		5176-5365	24	12.2	1.05	3	
5180-5469	6	83.6	1.12	13		5132-5316	37	11.0	1.11	2	
5176-5469	6	68.3	1.38	12		5132-5268	83	6.66	1.00	2	
5114-5469	3	290.	.90	14		5089-	51	13.3	.96	2	
5134-5269	54	7.37	1.08	2		5048-	25	23.7	1.02	3	
5091-5269	34	16.4	1.01	3		5009-	20	43.3	.96	4	
" "	33	16.2	1.08	3		4951-	7	92.	1.17	11	
5050-5269	17	29.3	1.13	4		4916-	4	115.	1.65	15	
" "	14	31.5	1.06	4		5048-5178	89	6.68	1.02	2	
5010-5269	9	57.0	1.16	6		5009-	47	10.8	1.13	3	
" "	8	55.8	1.25	6		4971-	24	19.8	1.15	5	
4976-5269	6	77.3	1.61	9		4936-	16	31.2	1.26	8	
5090-5200	60	6.45	.95	2		4898-	7	55.	1.33	10	
5050-5200	22	16.4	.77	4	(Temperature, 24-25°)						
5011-5200	24	14.8	1.67	13	5089-5268	19	15.5	1.14	3		
4976-5200	10	32.3	1.42	8	5048-5200	27	11.6	1.07	3		
4938-5200	4	113.	.82	12	5176-5364	11	17.8	1.03	3		
5011-5133	43	7.47	1.09	3	5177-5330	14	9.58	1.12	2		
4976-	26	13.2	1.18	5	" "	54	9.97	1.08	2		
4940-	11	25.7	1.14	7							

A glance at the results shows at once that the theoretical law expressed by Eq. (1) must at least come near to the truth. The discrepancies seem to be correlated chiefly with the intensity of the anti-Stokes light and not with either spectral position or temperature; a few of the largest were no doubt due to an undetected blunder in adjustment. In Table II the results are divided into three groups according to the intensity of the anti-Stokes fluorescence and mean values of ρ and of Sc are given for each group; the number of sets in the group is given in parentheses.

TABLE II
The data of Table I averaged by groups.

I	Cold			Hot		
	ρ	Sc		ρ	Sc	
25-60	(8)	1.067	2.6%	(6)	1.039	2.5%
12-24	(6)	1.15	3.3	(4)	1.104	5.0
3-11	(13)	1.15	10.	(5)	1.38	11.

Sources of error. The most serious source of error next to scattering undoubtedly lies in the spectral settings. An error of only one angstrom in the assumed difference in wave-length between the slits of the two instruments makes a difference of about 1.7% in the value of ρ . An accuracy of this order was striven for with more or less success in the calibrations, but it is doubtful whether subsequent settings are reliable

to this extent. The average deviation from their mean of the six electrometer readings ranged in different sets from 2 to 8%, so that the Accidental error in ρ would be at least several percent.

No correction is required for absorption, since the paths of exciting and of fluorescent light through the solution were equal and the total effect of absorption would therefore remain the same when the wave-lengths were interchanged. As a check, a very concentrated solution gave $R=13.81$ for the 5268-5089 ratio, whereas the same solution diluted to half and then to quarter strength gave $R=15.28, 15.20$. The strength usually employed lay between the last two. On the other hand, there does exist the possibility of a systematic error arising from the fact that the different wave-lengths coming from the source were not distributed spatially in quite the same manner in the solution; and an analogous inequality existed in regard to the fluorescent light. The resulting error is hard to estimate. In any case, it can hardly explain the systematic trend of the observed discrepancies, for it should be equivalent to a fixed shift in wave-length and so should produce the same percent of error in all ratios. Furthermore, a single set of readings taken later on the 5245-5090 ratio, under unfavorable conditions, with the exciting light taken out from a square cell at right angles to the exciting beam, gave $\rho=1.06$, in good agreement with the previous results.

Conclusion. In view of all these sources of error the conclusion seems justified that the first group of observations in Table II definitely support the theoretical equation given in (1) and the second group, $I=12$ to 24, are not inconsistent with it. A doubling of the allowance for scattered light would on the average pretty well cover all of the discrepancies; and it is a fact that a few imperfect tests with absorbing screens suggested considerably larger effects due to this cause. The third group of results are therefore not decisively inconsistent with (1) and show that this equation at least comes pretty near to the truth even when the anti-Stokes light is very weak.

The factor λ_x/λ_y in (1) is a characteristic contribution from quantum theory and its experimental verification would therefore be of particular interest. Here we can only say that the omission of this factor would make the observed agreement *worse* by 2-4%.

III. FLUORESCENCE, EXCITATION AND ABSORPTION CURVES

In August, with the photo-electric system working poorly, a rapid survey was made of the relative exciting powers for the solution of fluorescein that had been used in the "hot" observations. The material was put in a square cell and viewed near one corner at right angles to the exciting beam, a correction (0-20%) being made for absorption. The coefficient of absorption was determined with the spectropho-

tometer by the usual method of observing slit-widths first with the solution and then with pure alcohol in the cell and taking the logarithm of the ratio of these readings; the slit zero was found by measuring the known transmission of the 0.5 filter with extremely narrow slits. The smallest transmission through 2 cm of the solution came out about 10%. The spectrometer slit was not over 100A wide.

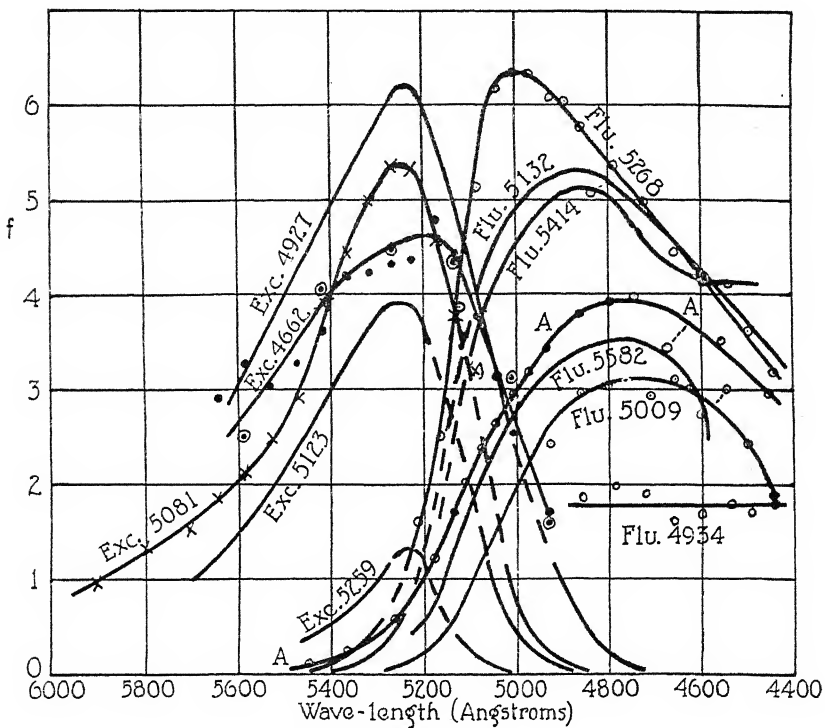


FIG. 1.

The results are shown in Fig. 1, curve *AA* giving the absorption on an arbitrary scale. The fluorescence curve was determined, using the comparison lamp, for excitation at 5081A (\times in the figure representing in part the means of several repetitions), and at 4662 (dots in the figure, the dots in circles denote values obtained from the excitation curves), also a few points at 4787. Excitation curves were then found, by simply varying the exciting wave-length and assuming proportionality of deflection rate and fluorescent energy, for fluorescence at 4934, 5009, 5132 (points not shown in figure), 5268 (more or less repeated), and 5132 and 5414 (points not shown). The scale factors of the various curves were assumed to be unknown and were adjusted so as to secure

the best harmony between all of the results. In this way there was obtained a set of numbers, some in duplicate, proportional to the true exciting power, f , for various pairs of wave-lengths; these are plotted twice over in the figure, first, as fluorescence curves (left) each giving the spectral intensity of fluorescence of various wave-lengths excited in unit volume by unit density of energy of a given wave-length, and, second, as excitation curves (right) each giving the spectral intensity of fluorescent emission from unit volume of a certain wave-length excited by unit energy density of various wave-lengths, all on the same arbitrary scale. Additional values calculated from Eq. (1) were used to extend each set of curves on one side beyond the region of direct observation.

Circumstances made it impossible to secure more than two electrometer readings on each point, with some checking back to guard against systematic change of conditions, consequently the observed parts of the curves may be in error by as much as 6% of the largest value of f shown (the upper parts of the curves marked "Exc. 5081" and "Fluo. 5268" being perhaps twice as accurate). Nevertheless the data seemed to possess at least temporary interest because they suffice to establish the following conclusions:

(1) The fluorescence curve is not constant in shape. Not only does it draw in its toes toward the violet as the exciting wave-length encroaches upon it, thus preserving the validity of Eq. (1), but the center also rises, until the exciting wave-length reaches 5000 \AA , after which the whole curve drops rapidly. This result is not necessarily in conflict with earlier data of Nichols and Merritt,⁵ who found no change of shape for a solution in water; their material was also doubtless less pure. Those authors found,⁶ however, for an alcoholic solution two maxima at 5340 and 5500, resp., with shoulders at 5240 and 5680, whereas here there is a single maximum at $5240 \pm 30\text{\AA}$. This difference may be due either to greater purity of the material used in the present investigation or to the fact that those authors appear to have excited with much shorter wave-lengths.

(2) The wave-length of maximum excitation shifts from $4730 \pm 80\text{\AA}$ for fluorescence at 5000 or at 5600 to $5000 \pm 40\text{\AA}$ for fluorescence at 5268.

(3) For a particular wave-length of fluorescence, excitation and absorption are obviously not (always) proportional. A rough integration yields the further result that the total fluorescence increases in relative strength, by a total amount of 28%, as the exciting wave-length rises from 4800 to 5100, after which it drops sharply; but too great reliance cannot be placed upon this result because the long-wave

⁵ Nichols and Merritt, Phys. Rev. 18, 403 (1904).

⁶ Nichols and Merritt, Phys. Rev. 32, 38 (1911).

part of the fluorescent spectrum is incompletely represented. Vavilov found⁷ total fluorescence and absorption to be proportional for an aqueous solution of fluorescein; but results similar to those described here were found by Valentiner and Rössiger.⁸

These results would all find qualitative explanation if there were in reality two fluorescence bands of invariable form with maxima close together, one being a broad band with a broad excitation curve having its maximum around 4730 and the other a narrower but stronger band with a narrow excitation curve at about 5000A.

A more thorough study of the exciting power in fluorescein would seem to be well worth while. Probably for this purpose the far greater rapidity of visual photometry as compared with the photo-electric method would amply compensate for the trouble of finding enough line sources or good screens so that spectral resolution of the source light could be avoided.

This investigation was made in the physical laboratory of Cornell University and was supported by a grant from the Heckscher Research Council. The assembling of apparatus and most of the observational work was done by Mr. L. S. Taylor, who acted as research assistant under the grant, and the author is deeply indebted to him for his skilful handling of the instruments and for his cheerful persistence in the face of difficulties. The author is also indebted to many of his colleagues in Cornell for innumerable courtesies during the progress of the work.

GÖTTINGEN,
November 15, 1926.

⁷ S. I. Vavilov, Phil. Mag. **43**, 307 (1922).

⁸ Valentiner and Rössiger, Zeits. f. Physik, **36**, 81 (1926).

A COMPOUND INTERFEROMETER FOR FINE STRUCTURE WORK

BY WILLIAM V. HOUSTON*

ABSTRACT

The overlapping of orders in a Fabry-Perot interferometer can be avoided by using two interferometers in series. The fundamental equation shows that the dispersion is independent of the plate separation, while the distance between orders is inversely proportional to it. Thus an instrument with a small separation may be used as a preliminary filter to eliminate some of the orders in one of larger separation. This will not affect the fine structure pattern, and the resolution will be even greater than that due to the larger separation. Such an instrument has been built and satisfies the predictions of the theory. A plate, taken with the green line of mercury, is shown to illustrate the effect of the preliminary interferometer.

AS AN instrument for studying spectral fine structure the Fabry-Perot interferometer has several advantages over other high resolution instruments. It has a uniform intensity distribution over the whole image;¹ it is free, if properly adjusted,² from the errors due to the overlapping of two members of a close doublet; and it can be used to measure absolute wave-lengths. Furthermore, the distance between orders, measured in frequency units, is independent of the wave-length, so that it is useful in the identification of spectral series. The outstanding difficulty, however, is that when the plates are separated far enough to give high resolution, the successive orders are so close together that the patterns overlap. It is to overcome this difficulty, without sacrificing the advantages, that this combination of two interferometers has been devised.

Light is transmitted through a Fabry-Perot interferometer with maximum intensity if it is incident at an angle θ such that $2d \cos \theta = n\lambda$, where d is the distance between the plates, λ is the wave-length, and n is an integer. Thus the distance between orders is given by

$$d(\cos \theta)/dn = \lambda/2d \quad (1)$$

and the dispersion by

$$d(\cos \theta)/d\lambda = n/2d = \cos \theta/\lambda \quad (2)$$

which is independent of d . The resolving power is proportional to the order of interference n , and hence to the separation d . Thus, to get a high resolving power it is necessary to use a large d . This brings the

* National Research Fellow in Physics.

¹ This is particularly true as contrasted with the echelon.

² W. V. Houston, *Astrophys. J.*, **64**, 81 (1926).

successive orders close together, and sometimes causes overlapping. But, if light is incident on the interferometer at an angle θ_0 corresponding to $n=n_0$, and no light is incident at the angle θ_1 corresponding to $n=n_0+1$, it is evident that no light can be transmitted at this angle. Thus this order will be missing from the transmitted pattern.

If an interferometer of small separation is used as a preliminary filter, it will transmit light to the second in certain directions only; but since the dispersion is independent of the separation, the fine structure pattern will be transmitted or destroyed as a whole. Thus if the separation of the second is twice that of the first, every other order will be transmitted, and the fine structure pattern will not be disturbed. Furthermore, the resolution will be even greater than with the second interferometer alone.

THE COMPLETE THEORY

Consider the four lightly silvered surfaces 1, 2, 3, and 4 in Fig. 1. Surfaces 1 and 2, and 3 and 4 are accurately parallel to each other,

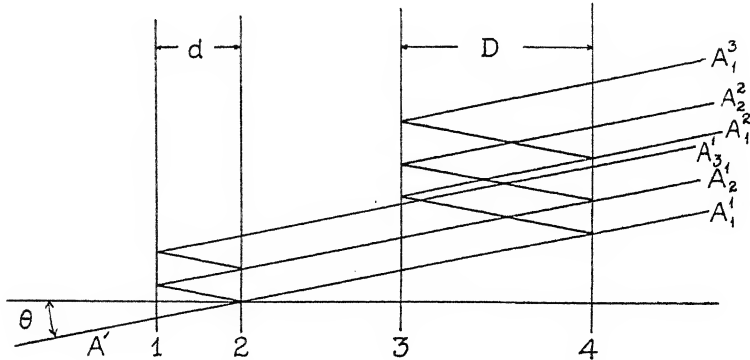


Fig. 1.

while 2 and 3 are inclined at just enough of an angle to prevent interference between them. This angle must be so small that the axes of the two instruments are practically together. Let A' be the incident amplitude, and A the resultant emerging amplitude. Let the amplitudes due to successive reflections be indicated by A_m^n where the subscript indicates reflections between the first surfaces, and the superscript indicates reflections between the second pair. Let R be the intensity coefficient of reflection and let $R=\rho^2$. We may neglect the absorption since it can be applied as a constant factor to the resultant intensity. From Fig. 1 it is evident that we have

$$\begin{aligned} A_1^1 &= A'(1-\rho^2)^2 & A_2^1 &= A_1^1 \rho^2 & A_3^1 &= A_1^1 \rho^4 \\ A_1^2 &= A_1^1 \rho^2 & A_2^2 &= A_1^1 \rho^4 & A_{m+1}^{n+1} &= A_1^1 \rho^{2(m+n)} \end{aligned}$$

Then the resultant amplitude is given by

$$A = A_1^1 \sum_{m=0}^{\infty} \sum_{n=0}^{\infty} \rho^{2(m+n)} \cos(wt - mb - nB) \quad (3)$$

where $B = 4\pi D \cos \theta / \lambda$ and $b = 4\pi d \cos \theta / \lambda$. Let $wt - mb = M$ and the summation becomes

$$\begin{aligned} A &= A_1^1 \sum_{m=0}^{\infty} R^m \sum_{n=0}^{\infty} R^n \cos(M - nB) \\ &= A_1^1 (1 - 2R \cos B + R^2)^{-1} \sum_{m=0}^{\infty} R^m [\cos(wt - mb) \\ &\quad - R \cos(wt - B - mb)] \end{aligned} \quad (4)$$

Carrying out the second summation and introducing a phase constant we have

$$A = A_1^1 (1 - 2R \cos B + R^2)^{-1/2} (1 - 2R \cos b + R^2)^{-1/2} \cos(wt + \psi). \quad (5)$$

Squaring this, the intensity is given by

$$I = (A_1^1)^2 / (1 - 2R \cos B + R^2)(1 - 2R \cos b + R^2) \quad (6)$$

Equation (6) is just the product of the corresponding equations for the two separate interferometers. This justifies the process, used in the qualitative theory, of considering the action of the second instrument on the light transmitted by the first, without reference to the interference processes in the first.

If the values of d and D are such that $2d \cos \theta = n\lambda$, and $2D \cos \theta = m\lambda$, both instruments will transmit a maximum at the angle θ . However, the next maxima of the two instruments will not coincide, in general, and so both will be greatly decreased in intensity. The next maxima that do coincide will be determined by the ratio of D to d . For example, if $d = D$ the pattern transmitted by the two will be the same as for one interferometer, but, as will be shown later, the maxima will be sharper. If $D = 2d$, the separation of orders is that due to the separation d , while the resolving power is that due to the separation D , i.e., only every other order of the second instrument is transmitted. If $D = 3d$, only every third order is transmitted. In all these cases the dispersion is the same so that computations of absolute wave-length and frequency difference can be carried out as with the simple instrument. This constitutes the principal advantage of the air interferometer over instruments in which the path difference is wholly or partly in glass.

To determine the resolving power we may assume that two fringes can be recognized as distinct if their maxima are separated by a distance equal to the width of one image where its intensity has dropped to one half its maximum value. The computations, of course, assume

two purely monochromatic lines of equal intensity. We then wish to find the value of B for which the intensity drops to $1/2$. In the case of a single interferometer we have

$$1 - 2R \cos B + R^2 = 2(1 - R)^2 \quad (7)$$

and hence

$$B = \cos^{-1}\{1 - (1 - R)^2/2R\} \quad (8)$$

The spectral range, or the difference in wave-length corresponding to the distance between orders, is given by the fundamental equation to be $\lambda^2/2D$. Hence

$$\lambda/\Delta\lambda = 2\pi D/\lambda \cos^{-1}\{1 - (1 - R)^2/2R\} \quad (9)$$

$2D/\lambda$ is the order of interference n so we have

$$\lambda/\Delta\lambda = \pi n / \cos^{-1}\{1 - (1 - R)^2/2R\} \quad (10)$$

For $R = 0.75$ this gives the resolving power as about $11n$.

For the two interferometers we have

$$(1 - 2R \cos B + R^2)(1 - 2R \cos b + R^2) = 2(1 - R)^4$$

or,

$$\cos B + \cos b - 2R(1 - \cos B)(1 - \cos b)/(1 - R)^2 = [4R - (1 - R)^2]/2R \quad (11)$$

B and b will both be small enough so that the cosines may be represented by the first two terms of their series so that we have

$$(1 + r^2)b^2 + Rr^2b^4/(1 - R)^2 = (1 - R)^2/R \quad (12)$$

where $r = D/d = B/b$. Here again we may neglect the fourth power of b , unless R is very large, so that

$$b = (1 - R)/(1 + r^2)^{1/2}R^{1/2} \quad (13)$$

Then we have

$$\Delta\lambda = \lambda^2(1 - R)/2\pi d(1 + r^2)^{1/2}R^{1/2}$$

or

$$\lambda/\Delta\lambda = n\pi R^{1/2}(1 + r^2)^{1/2}/(1 - R) \quad (14)$$

Thus the resolving power of the combination is equal to that of the smaller interferometer multiplied by $(1 + r^2)^{1/2}$. When $R = 0.75$ and $r = 1$ the resolving power is about $15n$.

Fig. 2 shows the shape and the separation of successive maxima when $D = 3d$ and $R = 0.75$. The two small maxima represent the remnants of the maxima cut out by the smaller instrument. These will be smaller as R increases, and also as they are farther from the principal maxima. This puts a limit to the value of r that can be used, since when r is large these spurious maxima will be closer to the principal ones and hence they will be stronger. When dealing with a fine structure in which the satellites are faint compared with the principal line, care must be taken not to mistake these maxima for satellites. If plates are taken with two different values of r , the true satellites can be

distinguished easily by the fact that their positions will be the same on both plates.

DESCRIPTION OF THE INSTRUMENT

An instrument of this kind has been built in the machine shop of this laboratory under the direction of Mr. Julius Pearson. An attachment was made for the interferometer previously built, so that the preliminary interferometer can be clamped to the frame of the other.

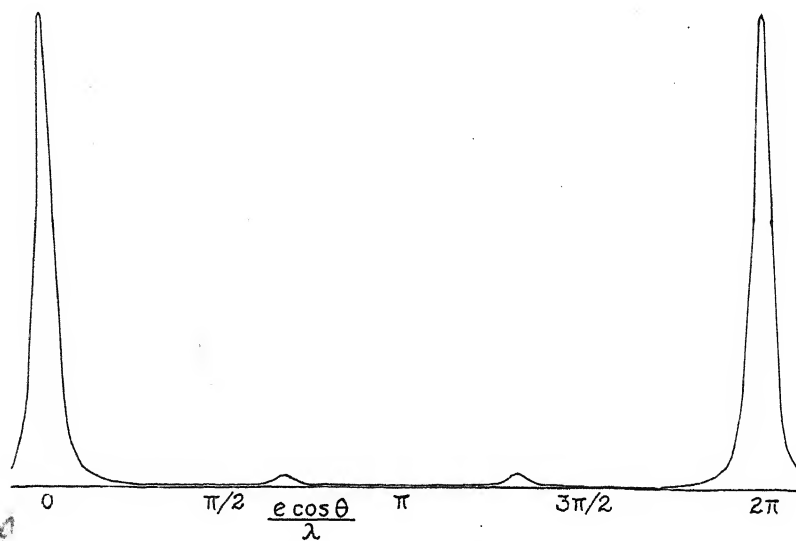


Fig. 2. Shape and separation of successive maxima when $D = 3d$ and $R = 0.75$.

This clamp carries a steel plate which can be rotated about two axes to set the optical axes of the two instruments together. This plate then carries one mirror which slides back and forth and can be fastened by set screws, and another which can be made parallel to the first. All the adjustments are made by screws working at the ends of levers which are held tightly against the screws by springs.

It has been found possible to make the necessary adjustments as follows. With the preliminary interferometer removed and the other set at about the separation to be used, the latter is adjusted until the plates are parallel. The other interferometer is then attached and its fringes are viewed from the side by means of a totally reflecting prism. In this way its plates can be made parallel. When the prism is removed the transmitted light shows the ring system of each interferometer as well as regions of brightness where the two systems coincide. If the axis of the preliminary interferometer is then adjusted until these regions of brightness are circles concentric with the other ring systems,

the instrument is in adjustment. To make one separation an integral multiple of the other the movable interferometer is opened or closed to make the circles of bright rings move toward the center. As the desired separation is approached these regions become wider until they cover the whole field. A white light source is then put in and the adjustment continued until the colored fringes appear. When the white central fringe appears the desired point has been reached. This phenomenon of white light fringes was first used by Perot and Fabry³ in the measurement of length.

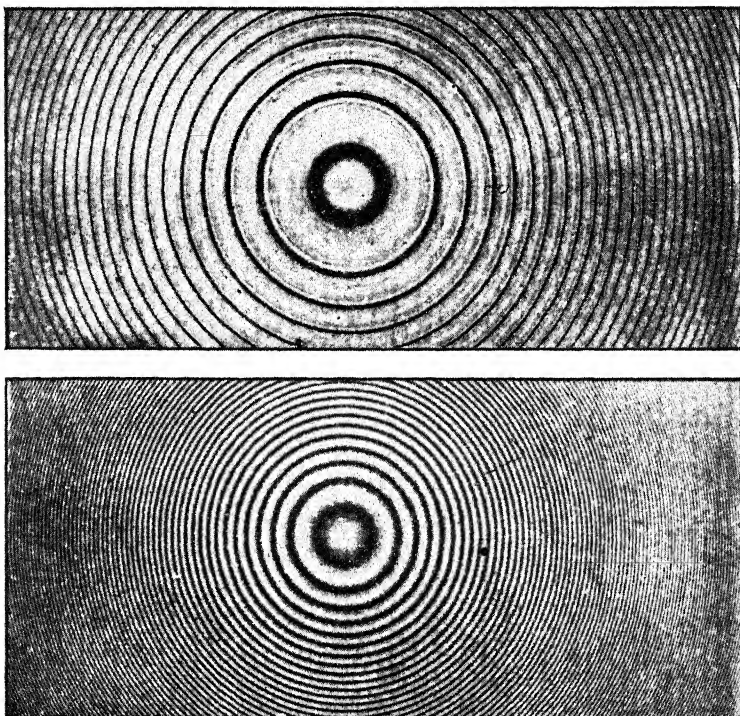


Fig. 3. Fringe system of the mercury line: above, through double interferometer; below, through the single interferometer.

A preliminary trial with rather inferior plane surfaces has given the plates reproduced in Fig. 3. The upper photograph shows the fringe system given by the green mercury line when one separation was about 3 mm and the other was about 9 mm. The lower photograph shows the same line through the 9 mm interferometer only. The overlapping of the fine structure patterns in this case causes the main line to appear fuzzy at the edges.

³ Perot and Fabry, Ann. chim. et phys. 7, 16 (1899).

Preparations are under way to apply this instrument to the study of the hydrogen doublets and to other fine structure problems. It should be valuable in the study of hyper-fine structure, such as that of mercury. The principal disadvantage is that a good deal of light is absorbed in passing through the four silver films, but this is characteristic of all high resolution instruments. On the other hand, this arrangement offers all the advantages of a fine grating in the direct measurement of fine structure, and is superior to the grating in resolving power and in the determination of absolute wave-lengths.

NORMAN BRIDGE LABORATORY OF PHYSICS,
CALIFORNIA INSTITUTE OF TECHNOLOGY,
November 15, 1926.

AN ABSOLUTE METHOD FOR MEASURING THE VELOCITY OF FLUIDS

BY H. E. HARTIG AND H. B. WILCOX

ABSTRACT

Trains of sound waves of a definite frequency, emitted by sound sources which are separated by a known distance, are sent up and down a pipe in which flows a stream of fluid whose velocity is required. Anti-nodes formed in the region between the sound sources undergo a shift the magnitude of which depends upon the velocity of the fluid. By using interrupted wave trains the effects of reflections at the ends of the pipe are eliminated. The meaning of the velocity measured by this method is considered when the flow of the fluid is turbulent. Experiments on air flow show that the anti-nodes are sharply defined, stationary with time, and occur on planes normal to the axis of the pipe. It is concluded that the average velocity as calculated from the sound shift method differs by a negligibly small amount from the average velocity obtained by dividing the total flow per second past a section, by the area of the section. A smoke cloud introduced into the air stream and timed over a known distance yields results which are compared with those obtained from the sound shift method.

HUGUENARD¹ has described an absolute method for measuring the flow of air through pipes. The method consists essentially in photographing a sound wave produced by one spark in moving air by the light of a second spark which follows at a known interval of time.

The method described in this article is based on the nodal shift occurring when a medium in which standing sound waves exist is set in motion.

I. DESCRIPTION AND THEORY OF METHOD

Consider a plane sound wave of frequency f , whose amplitude varies harmonically with time, originating at A and traveling in the positive x direction in a stationary medium; and a second plane wave of the same frequency and maximum amplitude originating at B and traveling in the negative x direction. Then stationary planes of zero pressure variation, or anti-nodes, are created. These anti-nodal planes are perpendicular to the x axis and are equally spaced one-half wave-length apart.

If now the medium moves in the positive x direction with velocity v the anti-nodes will shift in the direction of motion of the medium. The magnitude of the shift depends upon the distance between the sources at A and B , the velocity of propagation of sound in the stationary medium, and upon the velocity of the medium. In order to calculate the velocity of the medium it is sufficient to know the magnitude of the

¹ Huguenard, Comptes rendus 117: pp. 744-746 (Oct. 22, 1923).

shift, the distance between the sound sources, the velocity of propagation of sound in the stationary medium, and the form of the function which connects these quantities. This relation may be established as follows.

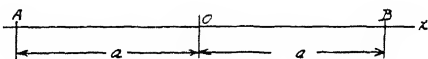


Fig. 1.

Let the origin be taken midway between the sources A and B which are separated by a distance $2a$ (Fig. 1). Then if ρ_1 be the increase in pressure at any point x at time t due to the wave originating at A , we have

$$\rho_1 = \rho_0 \sin 2\pi f(x+a)/[(V+v)-t]$$

where ρ_0 is the maximum pressure variation and V is the velocity of propagation of sound in the stationary medium. The pressure variation ρ_2 due to the wave which originates at B is given by a similar expression with appropriate changes in sign.

The total pressure variation at all points between $-a$ and a is

$$\rho_1 + \rho_2 = 2\rho_0 \sin \pi f \left(\frac{x+a}{V+v} + \frac{x-a}{V-v} \right) \cos \pi f \left(\frac{x+a}{V+v} - \frac{x-a}{V-v} - 2t \right).$$

The right hand member of this equation will be zero for all values of t provided that x lies between $-a$ and a , and satisfies the equation

$$\sin \pi f \left(\frac{x+a}{V+v} + \frac{x-a}{V-v} \right) = 0.$$

From this equation

$$x = \frac{n(V^2 - v^2)}{2fV} + \frac{av}{V}, \quad \pm n = 0, 1, 2, \dots$$

When v is zero the anti-nodes are located at points given by $X = nV/2f$.

The shift s in the position of the anti-nodes is, therefore,

$$s = av/V - n\lambda v^2/2V^2,$$

where λ is the wave-length in the stationary medium. When n is zero, that is for the anti-node at the origin, the velocity is given without approximation by $v = Vs/a$. If, however, observations are taken at points at which n is not zero and provided that v/V is small this equation gives results which are only slightly in error. If, moreover, observations of shift are taken upon a series of anti-nodes for which the algebraic sum of the n 's is zero, the number obtained by averaging these values will be equal to the shift corresponding to $n=0$.

To determine V , the velocity of sound, it is sufficient to measure the distance d between anti-nodes when the medium is at rest. Then $V = 2fd$, where the frequency f must be known.

Thus far it has been assumed that the fluid is flowing with constant velocity at every point in the pipe. In an actual case the flow is likely to be turbulent. It was shown by experiments on the flow of air in a pipe having an internal diameter of four inches that the anti-nodes were sharply defined on planes normal to the axis of the pipe and did not change position with time although the air flow was known to be turbulent. It is inferred from this result that the average axial component of the velocity at any instant is the same along any line of sufficient length and parallel to the axis, and that the average velocity at any instant along such a line does not change with time. The average velocity referred to is the velocity obtained by the sound shift method, and is defined by

$$v_1 = d / \int_0^d \frac{dx}{v_0 + \Delta v + V}$$

where V is the velocity of sound in the stationary medium and $v_0 + \Delta v$ is the instantaneous axial component of the velocity of the medium at any point, the integration being carried along the axis over a length d .

The average velocity necessary in calculating the volume of fluid flowing past a section of the pipe per second, is defined by

$$v_2 = (1/A)t \left[\iint_A (v_0 + \Delta v) dA \right] dt$$

where the double integral is extended over a normal section of the pipe.

When the velocity is a constant v_0 both of these definitions give v_0 as the average velocity. To compare v_1 and v_2 when $v_0 + \Delta v$ is not constant

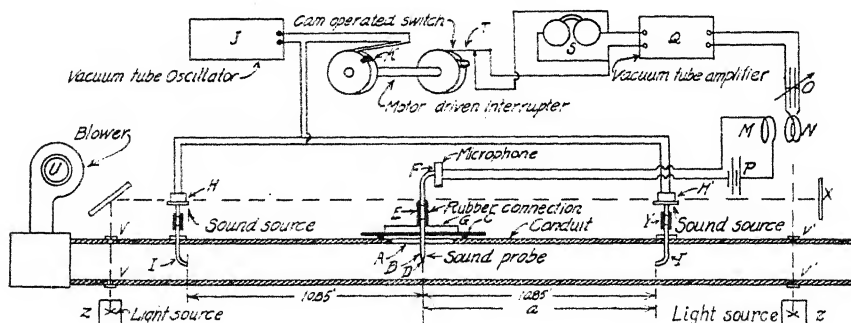


Fig. 2. Diagram of apparatus.

we shall make the following assumptions: (1) Along every line sufficiently long and parallel to the axis the instantaneous velocity of the medium is constant, $v_0 + \Delta v$ for one-half the length of the line, and $v_0 - \Delta v$ for the remaining half; (2) over every normal section of the pipe the velocity is constant, $v_0 + \Delta v$ for a time $t/2$, and $v_0 - \Delta v$ for an equal time.

Using the first assumption with the definition of v_1 we obtain $v_1 = v_0 - \Delta v^2/(v_0 + V)$. With the second assumption and the definition of v_2 we obtain $v_2 = v_0$.

With these rough approximations it appears that the two definitions give average values of velocity which differ by a small amount. In any event if Δv is small compared with v_0 the actual conditions approximate closely the ideal conditions for which the two definitions give identical results.

II. DESCRIPTION OF APPARATUS

The apparatus consists of a wrought iron pipe 4 inches in diameter and approximately 42 feet long, having a longitudinal slot A 18 inches long at the center. A sound probe B carried by a cover slide C projects through the slot to the center line of the pipe where it terminates in a narrow transverse slit D , the other end of the probe being connected by means of a short rubber tube E to the sound chamber of a microphone F . The slide C carries a pointer which allows its position to be read upon a fixed scale G graduated in hundredths of inches.

The sound sources are located at the quarter points of the pipe and consist of two telephone receivers H, H' which communicate by means of short rubber tubes with the bent tubes I . The sources are supplied with current by a Western Electric vacuum tube oscillator J . The current from the oscillator is established at regular intervals by an adjustable speed, motor-driven commutator K .

The battery P and the primary coil M which is inductively coupled with the coil N form a series circuit with the microphone F . The terminals of a tuned circuit consisting of the coil N and the variable condenser O , are connected to the input of an audio-frequency vacuum tube amplifier Q .

The listening receivers S are connected to the output of the amplifier. The receivers remain short circuited by the switch T except for a definite interval when the switch is opened by a cam on the shaft which drives the commutator K . The entire receiving apparatus was carefully shielded.

A current of air may be driven through the pipe by the motor-driven blower U .

The apparatus for the purpose of visually determining the fluid velocity consists of two light sources Z projecting beams of light through windows V, V' across the pipe, the light beams being directed by a mirror and lens system to an observing station X .

The operation of the apparatus is as follows: alternating current at a frequency of 2500 cycles per second operates sound sources H and H' at regular intervals of time which depend jointly upon the length of the contact segment of the commutator K and upon the adjustment

of its speed. In consequence of this current, the sound sources emit trains of waves of like frequency, which travel up and down the pipe. The amplitude of the two trains of waves is equalized by moving one or the other source in or out of the resonating connecting tubes Y , until the anti-nodes indicated at the receivers S are nearly perfect. A fine adjustment of amplitude is obtained by varying a resistance in circuit with one of the sources. The commutator K is used to avoid the superposition of waves set up by reflection at the ends of the pipe with the original waves, such combinations of original and reflected waves giving, as would be expected, anti-nodes of variable intensity and irregular spacing. Indeed, it was found that without commutation the anti-nodes shifted in an irregular manner when a current of air was passed through the pipe.

By changing the relative positions of the cam and short-circuiting switch it was observed that the time interval required for the disappearance of the musical character of a wave train corresponded to about one-half of a revolution of the cam shaft. The time allowed between listening to successive wave trains was approximately 0.4 sec.

On the same shaft with the commutator a cam operating a switch T renders the listening circuit inoperative except for the short time, about 0.02 sec. during which the undisturbed standing wave is being received by the probe B .

When a current of air is sent through the pipe the positions of the anti-nodes which were determined with the air at rest, are shifted in the direction of motion a distance s from which the average velocity of the air current is calculated as described.

III. VELOCITY BY THE SMOKE DRIFT METHOD

The results obtained by the sound shift method were compared with independent determinations of the air velocity made by introducing a smoke puff into the air current and measuring the time required for the smoke cloud to drift with the current over a measured distance. A single observer with a stop-watch took all observations of the time during a run. This was effected by passing a beam of light through windows V in the pipe near its beginning and by means of a mirror and a lens system directing the beam to a screen located close to the observer stationed at a similarly illuminated opening V' at the other end of the pipe.

It was found that the smoke cloud elongated in passing through the pipe and a greater time was required for the cloud to pass the downstream pair of windows than was required at the up-stream station.

The smoke drift method is similar to the color velocity method employed by Allen and Taylor² to determine the average velocity of

² Allen and Taylor, ASME Trans. 45, 285 (1923).

water flowing in a pipe. Colored solution is introduced into the pipe and the passage of the solution between observing stations is recorded. The velocity obtained by timing the center of the colored mass between stations was found equal to that obtained by measuring the discharge. In view of the experience of Allen and Taylor it appears reasonable to assume that the time to be taken in the smoke drift method is that required for the center of the cloud to traverse the distance between the stations.

The constancy of the average air velocity was checked by a vane type anemometer. The anemometer readings during a run agreed to within one percent.

IV. RESULTS

The results of two separate sets of determinations of the velocity of flow of air in a pipe are tabulated as follows:

	1st run	2nd run
Anti-node shift in cm (average of 5 readings)	$0.904 \pm .005$	$1.859 \pm .005$
Computed velocity in cm/sec	$94.2 \pm .6$	$193.5 \pm .6$
Velocity by smoke drift method (average of 18 readings)	95.4 ± 3.0	$195. \pm 4.5$

The velocity of sound in the pipe as determined from the average of five readings was 344.4 ± 0.6 meters per sec.

From their experience in conducting this investigation, the writers believe that the sound shift method will yield very accurate results in the measurement of the velocity of flow of gases in pipes, especially where a long straight column of the gas is available. Further work is being done in extending the sound shift method to the measurement of flow of water in pipes and open channels. Some preliminary work has been done to improve the accuracy of the smoke drift method by replacing the observer by an automatic recording device.

The writers wish to acknowledge the help and interest of Professors W. E. Brooke, F. W. Springer, F. B. Rowley and George W. Swenson of the Engineering College. We have also to thank Professor John T. Tate of the Physics Department, Messrs. H. S. Richardson and T. Adsem of the Northwestern Bell Telephone Company, and Mr. Ware for the loan of special apparatus.

Finally, we desire to express our appreciation to Dean Ora M. Leland of the College of Engineering for making funds available to procure needed equipment.

ENGINEERING LABORATORIES,
UNIVERSITY OF MINNESOTA,
September 10, 1926.

BOOK REVIEWS

Three Lectures on Atomic Physics. ARNOLD SOMMERFELD. Translated by HENRY L. BROSE.—This little book consists of three lectures delivered by Professor Sommerfeld at the University of London, and will be welcomed by theoretical physicists as being in a certain sense a supplement to his monumental "Atombau", for the lectures serve as an excellent summary of some of the most important recent developments in the quantum theory of line spectra. Naturally, in such a brief volume no attempt is made to discuss the mathematics of the new quantum dynamics, and instead more attention is given to some of their applications to spectroscopy. The first lecture includes the re-interpretation of the hydrogen and helium fine structure necessitated by recent theoretical developments and by refinements in experimental measurements of intensities. The second lecture is devoted to multiplet structures, including the quantum numbers proposed by Russell and Saunders, the definition of primed and unprimed spectral terms and their selection rules, and Pauli's principle of dissimilar quantum numbers. Simple, non-technical descriptions of this material have hitherto been rather scarce, and so Professor Sommerfeld's account is particularly welcome. The last lecture opens with the Smith-Stoner theory of the periodic table, and contains an interesting discussion of the nature of chemical linkage in tetrahedral crystal structures. The book is lucidly written, and not too technical. One cannot help but smile that the publisher should be so unfamiliar with Professor Sommerfeld's high standing in the world of atomic physics as to think it necessary to state in the blurb on the jacket that "Besides being an author himself, Professor Sommerfeld has annotated some of Einstein's writings on relativity!" E. P. Dutton and Co. 70 pp.

J. H. VAN VLECK

Crystalline Form and Chemical Constitution. A. E. H. TUTTON.—It is the purpose of this book to give a summary of Dr. Tutton's research on crystalline form which has extended over more than thirty years, and to show how the results of this research are related to the chemical constitution of the crystal and to the results of x-ray diffraction. The magnitude of the work which Dr. Tutton has done may be appreciated from the fact that he has made over 500 density determinations, has prepared more than 2,000 truly plane-faced section plates, and has measured over 45,000 crystal angles. His optical observations have been carried out for light from all parts of the spectrum for which the wave-lengths are accurately known. His work has meant the development of special instruments for grinding his crystals and for measuring their optical properties. These special instruments, together with his goniometers are described in some detail.

Dr. Tutton's work on isomorphism has completely confirmed Hatiy's principle that no two crystals of dissimilar chemical compositions have exactly the same interfacial angles. He points out the importance of isomorphism in locating atomic weights and gives a very good résumé of the knowledge of overgrowth and mixed crystals. Many of the illustrations and examples in this portion of the book are from the author's wealth of experience in such matters. There is an equally good review of optical activity with references to the work of Sir William Bragg and his associates.

The writer is unable to agree with the author's ideas in connection with ionized crystal structure given on page 29. For instance, in discussing sodium chloride and similar crystals the author states that "the structure appears as if it were of atoms and not of molecules, although, of course, the molecules are really there, as they were deposited from the saturated solution as such." If this were so, molten NaCl could not be electrolyzed. Physical chemists agree that the sodium and chlorine are present in the

solution as *ions*, not as *molecules* of NaCl. Otherwise, solutions of NaCl would not be conducting. Apparently the work of Debye has removed the last objection to this viewpoint. If we once assume the existence of ions in solutions of NaCl, it is very reasonable to assume that the sodium and chlorine are deposited upon the space lattice of the growing crystal as ions.

It is unfortunate that the book has a rather unwieldy sentence structure. A typical example is the following: (page 50) "For the measurement of crystal angles the No. 2A Fuess horizontal-circle goniometer (reading to half-minutes) was, and remains unbeaten for convenience and accuracy; and the No. 1A Fuess larger instrument, reading to seconds is the most efficient instrument for refractive index measurement by the best of all methods, that of the 60°-prism when cut to afford two of the three indices of these rhombic and monoclinic salts directly, one afforded by light vibrating parallel to the refracting edge and therefore to one of the three axes of the optical-ellipsoid, and the other corresponding to vibrations perpendicular to the edge and parallel to a second of the principal axes of the ellipsoid."

In spite of this, however, the book is a very valuable book and should be on the shelf of everyone who is working with crystal structure. xii+252 pp., 72 figs., Macmillan & Co. New York City, 1926. Price 3.60.

WHEELER P. DAVEY

Polarisations-Mikroskop, seine Anwendung in der Kolloidforschung und in der Farberei. HERMANN AMBRONN UND ALBERT FREY.—This is Volume Five of the series of monographs on the investigation of colloids which is being edited by Richard Zsigmondy. This book deals with the technique of the polarization-microscope, especially in regard to its use in the study of colloids. The first half gives an introduction to the theory of polarization and double refraction without the use of difficult mathematics. It takes up the manipulation and adjustment of the polarization-microscope and the uses of the various compensators and other accessories. The directions and explanations are very clearly written and illustrated by a number of well-chosen figures. The second half of the book is divided into two sections, dealing respectively with the phenomena of double refraction in dispersoid systems, and the optical methods for determining their sub-microscopic fine structure. The variation of double refraction of the colloids with the indices of refraction of various imbibed liquids is a method of investigation discussed in detail. A number of practical examples are used as illustrations. The book ends with a discussion of the theory of coloring with dyes and with chemical elements in suspension. The book is well written and will be of great value to anyone desiring an introduction into this field of investigation. Pp. vii+195, 48 figs. Akademische Verlagsgesellschaft m.b.H. Leipzig, 1926. RM 13.50 bound; 12.—unbound.

JOSEPH VALASEK

Galilei und sein Kampf für die copernicanische Lehre. EMIL WOHLWILL.—In recent time two investigators have devoted themselves to the intensive study of the life and times of Galileo, based upon documentary material of which much had not been previously available to historians. One of these investigators was Antonio Favaro who edited the great twenty-volume national edition of the works of Galileo, and prepared life-histories of friends and correspondents of Galileo. The other was Emil Wohlwill who devoted some forty years to Galilean questions. His first volume appeared in 1909; he died in 1912, and left behind an incomplete second volume which has been prepared for publication by Friederick Wohlwill, with the cooperation of several other German scholars. Emil Wohlwill made a new and critical examination of all source material, with the view of eliminating what to him seemed mythical in Viviani's life of Galileo. Though many readers may not accept all of Wohlwill's conclusions, his work on Galileo is worthy of most serious attention. In some instances, Wohlwill and Favaro differ—for instance,

on the authenticity of the narrative of the public experiments on falling bodies from the leaning tower of Pisa. Wohlwill argues from Galileo's manuscript, entitled *De Motu*, which consists of lecture notes prepared while in Pisa, that in his early years Galileo was still under the influence of Aristotelian ideas to such an extent that he could not possibly have taken the public stand against Aristotle as described by Viviani. After examining the *De Motu*, the present reviewer is not able to agree with Wohlwill on this point.

The official documents relating to Galileo and the inquisition became known in 1867. In the second volume, the treatment accorded Galileo by the Inquisition is discussed in great detail and with marked fairness.

Erster Band, 1909, pp. xx+646. Zweiter Band, aus dem Nachlass herausgegeben, 1926, pp. xii+435. Verlag von Leopold Voss, Leipzig.

FLORIAN CAJORI

Die Welt der Atome. ARTHUR HAAS.—This book consists of ten lectures delivered at the University of Vienna during the summer semester of 1926, the general topics of which are these: electrons, ions, alpha-particles, disintegration of nuclei, radiation, analysis of spectra, the Bohr-Sommerfeld atom-model, the Periodic Table, interpretation of stationary states, molecules, radioactivity, and speculations about transmutation of matter and energy.

With this condensed and undecorated style, the author succeeds in packing a remarkable amount of information into the book. His chief fault is the unquestioning presentation of the Bohr-Sommerfeld atom-model in its earliest form without the least intimation that it is tentative and may be transitory. In fact, two of his statements about the atom-model are already outmoded: the assignment of integer values to the azimuthal quantum-number for the permitted orbits in the model for the hydrogen atom, and the assertion that whenever an atom is in an *S* or *P* or *D* state its most loosely bound electron is in an orbit of azimuthal quantum-number 1 or 2 or 3. I have, however, found no mistakes of fact, except the statements that the spectra of the alkali metals contain singlet terms and that ninefold terms are known; possibly the latter of these is no longer a mistake. The intimation that the intensities of the various lines constituting a multiplet stand in integer ratios is much too strong. The reader should know that the assertion at the beginning of Chapter II ("the number of kinds of atoms is as great as the number of elements") is a false statement evidently made with full awareness and corrected seven pages further on ("the different kinds of atoms of an element are called isotopes"). There are other instances of this procedure; it would be dangerous therefore to stop reading in the middle of the book. Nevertheless, after all these objections are made, the richness and almost uniform reliability of the work still remain imposing. The illustrations are admirably chosen and reproduced. I can recommend the book, not indeed to the ordinary layman, but to the student of physics who is desirous of reviewing the knowledge which he has acquired or anticipating that which he expects.

to acquire from treatises which have not been so thoroughly divested of the mathematical processes. Pp. xii+130, 37 figs. Walter de Gruyter & Co., Berlin and Leipzig. Price 4.80 R.M.

KARL K. DARROW

Physico-Chemical Methods. JOSEPH REILLY, WILLIAM NORMAN RAE and THOMAS SHERLOCK WHEELER.—The authors have produced this manual primarily as an aid to the industrial chemist or investigator, but partly also for the advanced student. An impressive feature of the book is its wide scope. One finds all of the ordinary subjects discussed, and in addition many less usual, including for instance, nomography, the design and equipment of the laboratory, photography, the microscope, the photo-electric effect, and x-ray analysis. The appeal to the technical chemist is reflected in the appearance of such topics as the analytical distillation of butter fat. Exhaustive treatment of all the subjects discussed is manifestly impossible, yet those that, in the judgment of the authors, are most likely to be required, are fairly complete. In few cases is the treatment so perfunctory as to be of little value. On the other hand, trivial detail in text and figure is not always excluded. In appraisal of the book, there seem to be numerous minor criticisms of an adverse character possible, but few, if any, of major importance. Its good features seem greatly to outweigh the questionable ones. As to its usefulness to the workers it is designed to serve there can be no doubt. xi+735 pp., 453 figs., D. Van Nostrand Company, New York, 1926. Price 30s.

E. D. EASTMAN

Theory of vibrating systems and sound. IRVING B. CRANDALL.—This work is a text designed "to supplement rather than to replace the accepted treatises of sound". The supplementation is more than welcome. The author discusses many of the modern developments, such as problems of radiation, of transmission, and of architectural acoustics, but he gives fairly complete references to even a broader range of recent literature. The book has that freshness and forward outlook which might be expected from a research worker in the Bell Telephone Laboratories, where there are always consistently under way numerous and important investigations in acoustics. The student will find that the work is prepared in his interest. The text is clear and the problems add the opportunity of increasing one's comprehension.

The volume is limited to two hundred and sixty pages and consequently some of the recent fundamental contributions have necessarily been referred to with regrettable brevity. Most important among the omissions are the results of the investigations in the (author's own) Bell Telephone Laboratories. The title is intended to be specific and not to limit the meaning of "Sound," which correctly includes all mechanical vibrations. The value of the book for reference will be widely appreciated. x+260 pp., 24 diagrams, D. Van Nostrand Company, New York City, 1926. Price \$5.00.

G. W. STEWART

Thermodynamics (For Students of Chemistry). C. N. HINSHELWOOD, M.A.—The following quotation from the preface will indicate the author's point of view. "I have done what I can to make the fundamental ideas of thermodynamics as clear as possible and particularly to explain the methods by which the abstract general laws are brought to bear upon the actual problems of physics and chemistry A good deal of stress is laid, all through the book, on the interconnection between the law of thermodynamics and the kinetic theory I am out of sympathy with those who regard thermodynamics as a science based upon empirical laws independent of the actual nature of things. If it were not for the molecular kinetic nature of things there is no particular reason for believing that the laws of thermodynamics would be what they are."

In this little volume the author discusses in an interesting manner the first and second laws, the Gibbs-Helmholtz equation, entropy and other thermodynamic func-

tions, conditions of equilibrium, the phase rule, the problem of chemical combination and finally the relation between entropy and probability. Whenever it is possible, the subject under discussion is "explained" in terms of the molecular-kinetic theory of matter.

For two reasons, however, the reviewer feels inclined to doubt the usefulness of this book to a student beginning the study of thermodynamics. In the first place, such students are likely to have only a confused notion of the distinct roles played by laws and by theories in the development of their science, and this book will hardly serve to dissipate the confusion. In the second place, a student who wants to master the subject, must train himself by the application of thermodynamic equations to concrete problems. Now a remarkable feature of the book under review is the almost complete absence of numerical data of any kind. It contains no heats of reaction, no specific heats, no equilibrium constants, no activity coefficients.

Finally we may remark that in the few pages devoted to Nernst's Heat Theorem, the unwarranted assumption is made that specific heats of solids can be expressed by a few terms of a power series with the temperature as the variable. 185 pp., 11 diagrams. E. P. Dutton & Co. New York, 1926. Price \$1.80.

F. H. MACDOUGALL

Surface Equilibria of Biological and Organic Colloids. P. LECOMTE DU NOÜV.—The scope of this volume published in the American Chemical Society Monograph Series will be made clear by the following list of chapter headings: technique, drop of surface tension of a colloidal solution as a function of time, monomolecular layer of serum constituents, sodium oleate, egg albumin, characteristics of immune serum, influence of colloids on the crystallization of sodium chloride, surface equilibrium of complex colloidal solutions, interfacial tension, surface viscosity, general conclusions. This monograph is devoted almost exclusively to a description of the experimental work carried out by the author in the laboratories of the Rockefeller Institute and to an exposition of his theories and hypotheses. Workers in this field will find the volume very readable and stimulating. Since the experimental work reported in this volume consisted in measurements of surface tension by the ring method, using an apparatus designed by the author, one would expect a critical discussion of this particular procedure. This is however entirely lacking, the author being content with the theory of the ring method in its most naïve form. 212 pp. 74 figs. 24 plates. Chemical Catalog Co., Inc. New York, 1926.

F. H. MACDOUGALL

An Introduction to Surface Chemistry. E. K. RIDEAL.—In nine chapters, the author discusses the surface tension of liquids and of solutions, surface films of insoluble materials, liquid-liquid, gas-solid and liquid-solid interfaces, differences of potential at interfaces, conditions of stability in suspensions and emulsions, gels and hydrated colloids. While this volume contains a brief but excellent exposition of the facts and theories of what may be already called "classical" colloid chemistry, most readers will be interested chiefly in the chapters devoted to the properties and structures of surfaces.

In this connection, the author uses not only the resources of thermodynamics but also the theorems of kinetic theory and statistical mechanics in an admirable account of efforts to arrive at an intimate, molecular picture of surface layers and films. The reviewer is heartily in accord with the statement made by Dr. F. G. Donnan in his preface to this monograph that "every student and investigator of surface and colloid phenomena owes Dr. Rideal a warm debt of gratitude for his admirable survey and presentation of a great and rapidly advancing field of physico-chemical science." vi+336 pp. Cambridge University Press, 1926. Price 18s net.

F. H. MACDOUGALL

Beyond the Milky Way. GEORGE ELLERY HALE.—This very interesting book is divided into three chapters dealing respectively with the ancestry of the telescope, the measurement of heat from the stars, and observations on spiral nebulae beyond the Milky Way. It summarizes in popular style the most important of the recent astronomical observations and theories. Recent radiometric measurements on stars are presented with a discussion of their significance. The last chapter deals with the theory of "island universes," and includes a brief discussion of cosmic rays and their possible origin. It is a fascinating book to read, and contains many fine illustrations.—Pp. xv+105, 44 figs. Charles Scribner's Sons, New York, 1926. Price \$1.50.

JOSEPH VALASEK

Photometry. JOHN W. T. WALSH.—This is a very unusual book on this subject both in the choice of material and in its treatment. It does not contain details of planning lighting systems, or the uses of shades and reflectors, but deals rather with the measurement of illuminations, intensities of sources, and coefficients of transmission and reflection. Besides the usual photometric practice, the book contains a discussion of radiation theory, the eye and vision, spectro-photometry, physical photometry, and stellar photometry. At the end of each chapter is a very complete bibliography. This is valuable for anyone desiring to go more deeply into any of the subjects, for the author states that he has examined all journals on gas and electric engineering, illumination, physics, and general science, published in Great Britain, the United States, France, Germany, and Italy, from the first years of their publication. Under physical and stellar photometry are found discussions of the uses of photo-electric cells, thermopiles, bolometers, selenium cells, and photographic plates. Where these are incomplete, the excellent bibliography furnishes the key to further information. The material on standards of candle-power and standards of spectral distribution is also of great interest to those concerned with measurement of radiation. Although the book deals primarily with visible radiation, many of the physical spectro-photometric methods can obviously be extended to invisible radiation. There are a few mistakes; for example, the energy of photo-electrons is said to vary with the frequency of the light in a smaller ratio than " λ ." The errors are, however, of a minor character. The author has done a remarkable piece of work in bringing together this mass of information on photometric measurements. Many physicists, astronomers, and engineers will find much of value in this book. It is well written and contains many diagrams prepared with great care.—Pp. xxvii+505, 303 figures, D. Van Nostrand Company, New York, 1926. Price \$10.00.

JOSEPH VALASEK

THE
PHYSICAL REVIEW

THE CARBON ATOM MODEL AND THE STRUCTURE
OF DIAMOND

By R. B. LINDSAY

ABSTRACT

Electron orbits in the neutral carbon atom.—The atomic model of carbon used is assumed to have four 2_1 orbits. The dimensions of these orbits are computed by a method outlined in a previous paper using various assumptions as to screening, viz.: (a) spherical distribution of charge about the nucleus; (b) orientation in orbital planes with random phase relations; (c) orientation in orbital planes with definitely assigned phase relations. All the methods yield a value of the aphelion distance in the close vicinity of $2.00a_0$, where $a_0 = .532\text{A}$, agreeing well with the "radius" as obtained from the atomic volume, i.e. $2.06a_0$. The orbital energies, however, vary from $0.36 e^2/a_0$ to $0.76 e^2/a_0$ according to the screening assumption used, the largest value being obtained under hypothesis (c).

Approximate calculation of the lattice energy of diamond.—The atom models as computed under assumption (c) are distributed in the diamond lattice, and the field on any electron due to the rest of its own atom and to neighboring atoms is calculated as a function of the distance from the nucleus assuming that: (1) the orbital plane of the electron is oriented in a certain symmetrical way relative to the lines joining its nucleus to those of the neighboring atoms; (2) for a first approximation only the four nearest atoms need be considered as effective; (3) the effect of the electrons in the neighboring atoms is that of a time distribution of their charges in their orbital planes, disregarding definite phase relations such as have been assumed by previous writers. An approximate expression for the increase in energy of the electron due to the neighboring atoms is developed, and the calculation of the lattice energy per electron for various values of a , the lattice constant, is carried out. It is found that a has an upper limit of $3.00a_0$. In particular the lattice energy for $a = 2.74a_0$ comes out to be $0.55Rh$, and the corresponding heat of sublimation is 171 k. cal. per mol. The experimental value for a is $2.90a_0$ and for the heat of sublimation from 168 to 177 k. cal. per mol. The limitations of the method employed are emphasized.

INTRODUCTION

THE Bohr model of carbon consists of a nucleus with six positive charges surrounded by six electrons. Two of these electrons move in 1_1 orbits relatively near to the nucleus, while the original assumption of Bohr was that the four outer electrons move in 2_1 orbits whose planes are arranged in tetrahedral symmetry. This arrangement was suggested by the peculiar chemical behavior of carbon. Recent work by Fowler¹ on the spectrum of

¹ A. Fowler, Proc. Roy. Soc. A105, 299 (1924).

singly ionized carbon has seemed to cast doubt on this scheme. Fowler finds that the analysis of this spectrum points to the presence of a 2_2 orbit in ionized carbon. This might indicate in neutral carbon two 2_1 and two 2_2 orbits instead of the four 2_1 orbits previously assumed. The present writer is not yet sure that this is a necessary result of Fowler's work. Moreover there appear to be difficulties in fitting a 2_2 orbit of the energy required by Fowler's results in the field of the two 1_1 and two 2_1 orbits. These difficulties are not so great in the case of the possible two 2_2 orbits in neutral carbon; nevertheless simple preliminary calculations for such a model result in orbits too large to agree well with the dimensions of the neutral carbon atom as estimated from crystal structure and other sources. The writer hopes to discuss this matter fully in a later paper. In the present paper however, calculations on the orbits in the carbon atom and on the crystal structure of diamond will be carried out on the assumption that neutral carbon has four 2_1 orbits.

I. ORBITS IN THE CARBON ATOM MODEL

The first task in making any calculations on the carbon crystal structure is to estimate the orbits in the neutral carbon atom. The 1_1 orbits provide no difficulty for the electrons moving in them are so close to the nucleus that their influence on the other electrons of the same atom and on the electrons of other atoms may be accounted for merely by deducting two units from the charge on the nucleus. As a matter of fact, simple calculation based on assumptions made by the author in previous work² shows that the radius of the 1_1 orbits is about $0.2 a_0$, where a_0 is the radius of the smallest orbit in hydrogen and equals 0.532×10^{-8} cm.

The estimation of the 2_1 orbits may be carried out in a number of ways. First, we may use the general method suggested by the writer in previous work on the models of the alkali atoms² wherein the assumption is made that the screening on any given electron due to all the others is the same as that due to a spherical distribution in shells about the nucleus. This scheme takes no account of the possible existence of definite phase relations among electrons in the same group, and it also neglects the orientation of orbital planes. Moreover, it makes the effective nuclear charge on each electron at aphelion in a 2_1 orbit equal to one unit. Since the computation procedure using this method has been fully described in the papers of the writer above referred to, it will be unnecessary to discuss it further here. In what follows it is referred to as Method I.

A second method makes the assumption that there is orientation of orbital planes, and in particular that the planes of the four 2_1 orbits are arranged so as to be perpendicular respectively to the lines from the center to the vertices of a regular tetrahedron. The screening of a given electron due to the others in the same group is then assumed to be that of time distributions of the charges of the other electrons throughout their planes,

² R. B. Lindsay, Jour. Math. and Phys., Mass. Inst. of Tech. 3, 191 (1924). See also: Jour. Opt. Soc. of Amer., 11, 17 (1925).

thus still neglecting phase relations. Since this method is used in Part Two in the calculation of field values in the case of the diamond, it will be well to indicate it at some length here.

The problem here is to determine the average screening potential V^* at a point in one plane due to a time mean distribution of the charges of the other three electrons in their planes. The procedure will be first to compute the potential due to a circular ring of charge and then to integrate over all such rings from perihelion to aphelion.

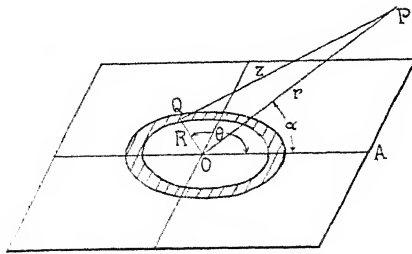


Fig. 1.

Consider the orbital plane shown in Fig. 1. Let O be the nucleus of the atom. It is desired to find the potential energy of an electron at P . If the charge per unit length of the ring is $q_0 e$ (e being the charge on the electron, or "unit" charge, as it has been called above), then

$$V_{R,R+dR}^* = e^2 q_0 \oint ds/z \quad (1)$$

$$= 2e^2 q_0 R \int_0^\pi (r^2 + R^2 - 2rR \cos\alpha \cos\theta)^{-1/2} d\theta \\ = 2e^2 q_0 R f(r, R) \quad (2)$$

where $f(r, R)$ is used to denote the integral. Now $q_0 = q/2\pi R$, where q is the total fraction of e which lies between R and $R+dR$. If the time spent by the electron between R and $R+dR$ is dt , and the total period of revolution of the electron is T , then $q = dt/T$. We therefore have

$$V_{R,R+dR}^* = (e^2 dt/\pi T) f(r, R)$$

and the potential energy of an electron at P due to the complete orbit will be

$$V^* = \int_{R(\min)}^{R(\max)} (e^2/\pi T) f(r, R) dt \quad (3)$$

Our next task is to evaluate $f(r, R)$. Making the substitution $2\psi = \pi - \theta$ and letting $b = (r^2 + R^2)/2rR \cos\alpha$, this reduces to the well known form

$$f(r, R) = (rR \cos\alpha)^{-1/2} \int_0^{\pi/2} 2[\frac{1}{2}(b+1)]^{-1/2} [1 - 2\sin^2\psi/(b+1)]^{-1/2} d\psi \\ = k K(rR \cos\alpha)^{-1/2} \quad (4)$$

where K is the complete elliptic integral of the first kind, and

$$k = [2/(b+1)]^{1/2}.$$

From the time equation of the orbit, derived by the Hamilton-Jacobi method, we have³

$$dt = mdR [2m(E - V) - k'^2 h^2 / 4\pi^2 R^2]^{-1/2} \quad (5)$$

where E and V denote respectively the total energy of the orbit and the potential energy of the electron at the distance R from the nucleus. The mass of the electron is indicated by m and k' is the azimuthal quantum number, h being Planck's constant. On substitution into the formula (3) we finally have for the screening potential at P :

$$V^* = \frac{(e^2/\pi a_0) \int_{R(\min)}^{R(\max)} Kk [Rr \cos \alpha / a_0^2]^{-1/2} [2(E - V) - k'^2 a_0^2 / R^2]^{-1/2} d(R/a_0)}{\int_{R(\min)}^{R(\max)} [2(E - V) - k'^2 a_0^2 / R^2]^{-1/2} d(R/a_0)} \quad (6)$$

where a_0 is as before the radius of the smallest orbit in hydrogen, which forms the natural unit of distance for this kind of calculation.

On introducing now the assumption of tetrahedral symmetry, it is clear that if the point P lies in any one of the other three orbital planes, the angle α in the expression for V^* may take on values from a certain minimum value $\alpha_0 \equiv \text{arc cos } (1/3)$ to a maximum value $\text{arc cos } 1$, depending on where P is taken in its orbital plane. The natural thing to do here, then, would be to take an average of V^* over this range of values. Actually it is found by computation to be accurate enough to consider this average as given by V^* for $\alpha = \text{arc cos } (0.8)$. Since this average will be the same for each of the other three electrons (because of the tetrahedral symmetry), to get the total screening potential at the point P , we need only multiply the value obtained in (6) by three.

In the calculation of V^* by (6) it is of course necessary to proceed by approximations, since the true orbit is not known to begin with. For this purpose it will be convenient to begin with an orbit which we have reason to believe is a first approximation to the true orbit, such as an elliptic orbit or better the orbit calculated according to Method I. For this orbit we know the value of the expression $[2(E - V) - k'^2 / (R/a_0)^2]^{1/2}$ as a function of R/a_0 , and hence the computation of V^* for any value of r can be carried out. From this we get a new V as a function of r and proceed to calculate the new orbit. Therefrom we can make a new time distribution leading to a new calculation of V^* and so get a second approximation. As was found in previous work of the writer,² this does not prove so tedious as might be imagined. The actual procedure in computing the orbit follows so closely the lines amply worked out by the author in the papers above referred to that it will be unnecessary to speak further of it here. In what follows

³ Loc. cit., see page 203 ff.

this second method of working out the orbit will be referred to as Method II.

A third possible method goes a step further and to the assumption of the orientation of the orbital planes in tetrahedral symmetry adds the hypothesis that the electrons move in their orbits in definite phases with respect to each other. It should at once be emphasized that this step involves the abandonment of the cubical symmetry characteristic of the previous methods, both as regards instantaneous and time average positions of the electrons. This introduces a further element of arbitrariness into the work which is justified only by the interest which has been aroused by the discussion of phase relation assumptions in atomic model calculations.⁴ There are a variety of hypotheses which may be made. Three particularly simple schemes suggest themselves, as follows. (I) The four electrons are at any instant all equidistant from the nucleus (i.e. they form a pulsating system). (II) The four electrons are grouped in two pairs, the electrons of each pair being equidistant from the nucleus at any instant and one pair being the other in phase by $T/2$ where T is the period of revolution. In this case there are two electrons at perihelion while the other two are at aphelion, etc. (III) The four electrons pass through perihelia at successive intervals of time equal to $T/4$. Of these schemes the first is extremely unlikely, as has been pointed out by the present writer in a previous paper.² Moreover, simple calculations based on it show that it would necessitate orbits which are far too large to fit reasonably any experimental data. The second and third plans are, however, worthy of consideration. In making calculations on any phase-relation scheme we can use two general methods of procedure, one of which is more arbitrary than the other.

In the first place we can suppose that each electron at any instant screens the others as a uniformly charged ring with radius equal to its distance from the nucleus at that instant. In this case, then, to calculate the screening potential on any electron due to the others at a given instant we determine from the assumed phase relation the position of the other electrons in their orbital planes at that instant and apply Eq. (2) above. This involves a knowledge of the time distribution of the charge on each electron orbit which is given by equation (5). On this plan the particular position of the orbit in its plane has no significance. The fact that the orbits rotate in their planes indicates that this is not a very arbitrary assumption. Calculations carried out under this plan using either of the two phase-relation hypotheses II and III will be referred to in what follows under A_1 and A_2 respectively.

Another way of applying the phase-relation assumptions will be to fix definitely not only the orientation of the orbital planes, but also the orientation of the orbits in their planes with respect to each other. This plan is

⁴ In this connection one of the Editors has kindly pointed out that the actual schemes which the author has devised for introducing phase relations (see discussion on page 502) are equivalent to; (1) an arrangement with twofold rotational symmetry about one of the original fourfold axes of the cube with no plane of symmetry and (2) an arrangement with twofold symmetry about one of the original fourfold axes of the cube with two planes of symmetry meeting at right angles in this axis and with no other symmetry.

arbitrary in that it affords wide room for choice. The fact, however, that in all this work we are retaining the basic assumption that each electron moves in an effectively central field of force helps to narrow the possibilities to some extent. In other words, it is desirable to arrange the orbits with respect to each other in such a way that the screening potential for any electron at a given distance r_0 from the nucleus is the same as that for any one of the other electrons when the latter is at distance r_0 from the nucleus. This acts to introduce a kind of symmetry into the orientation of the orbits. The writer has tried two modes of arrangement under this plan. In both of these the assumption is made that the four orbits are divided into pairs in such a way that the major axes⁵ of each pair lie in the plane formed by the normals through the nucleus to the planes of the orbits of that pair. The distinction between the two modes lies in the choice of angle between the major axes of a given pair. This angle can be either arc cos (1/3) or arc cos (-1/3). The former possibility is chosen in the first mode and the latter in the second mode. To make matters somewhat clearer, let us consider Fig. 2 in which O represents the nucleus and OA, OB, OC, OD represent the lines from the center to the vertices of a regular tetrahedron.

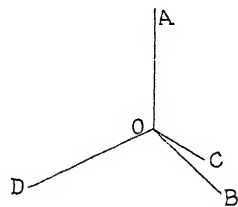


Fig. 2.

Then if we number the 2_1 electrons 1, 2, 3, 4, respectively, the orbital planes 1, 2, 3, 4 will be normal respectively to OA, OB, OC, OD . Table I indicates the specific arrangements corresponding to the first and second modes.

TABLE I
Arrangement of orbital planes in carbon atom.

Mode I				Mode II			
Major axis of orbit	Normal to	Lies in plane	Directed away from	Major axis of orbit	Normal to	Lies in plane	Directed
1	OA	AOD	OD	1	OA	AOB	as OB
2	OB	BOC	OC	2	OB	AOB	from OA
3	OC	BOC	OB	3	OC	COD	as OD
4	OD	AOD	OA	4	OD	COD	from OC

From the table it follows that in the first mode electron orbits 1, 4 and 2, 3 form pairs with angle between the major axes of the components of each

⁵ In the case of these orbits which are not real ellipses the major axis is defined as the line joining the nucleus and the electron when the latter is at aphelion, and its positive direction is away from the nucleus.

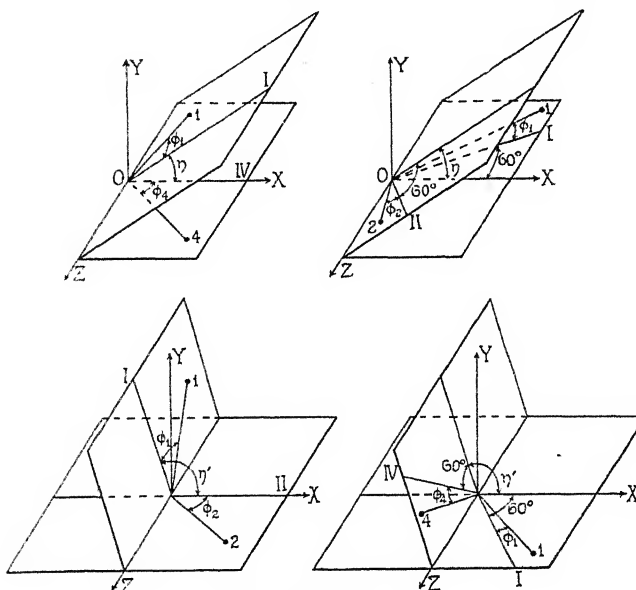
pair equal to $\text{arc cos } (1/3)$, while in the second mode electron orbits 1,2 and 3,4 form pairs with the corresponding angle equal to $\text{arc cos } (-1/3)$.

In applying each of these modes of arrangement it is necessary to develop formulas for the distance between any two electrons at any instant. From these the screening potential on an electron at a given distance from the nucleus can at once be calculated using the assumed phase relations. If we denote the polar coordinates of the four electrons in their orbital planes by $(r_1, \phi_1), (r_2, \phi_2), (r_3, \phi_3), (r_4, \phi_4)$ ⁶ and the distance from electron 1 to electron j at any instant as r_{1j} , we have

$$r_{1j}^2 = r_1^2 + r_j^2 - 2r_1r_j \cos(r_1, r_j) \quad (7)$$

where j takes the values 2, 3, 4 in rotation. To use this expression, it is necessary to have formulas for $\cos(r_1, r_j)$. These are developed by the use of the analytic geometry formula for the cosine of the angle between two lines, viz.

$$\cos(r_1, r_j) = \cos\alpha_1 \cos\alpha_j + \cos\beta_1 \cos\beta_j + \cos\gamma_1 \cos\gamma_j \quad (8)$$



Figs. 3A, 3B, 4A, 4B.

where $\alpha_1, \beta_1, \gamma_1$ are the direction angles of r_1 with respect to an appropriately chosen set of rectangular axes and $\alpha_j, \beta_j, \gamma_j$ are the corresponding angles for r_j . The following diagrams (Figures 3A, 3B, 4A, 4B) will serve to indicate the method chosen for the derivation of the values of $\cos(r_1, r_j)$, and will also make clear the cardinal features of each mode of arrangement. Figures 3A and 3B (top) refer to the first mode of arrangement and Figures 4A and 4B refer to the second. In each case $OI, OII, OIII, OIV$ represent the major axes

⁶ It is to be understood that the angle ϕ is in each case the angle made by the radius vector with the positive direction of the major axis.

of electrons 1, 2, 3, 4 respectively. The angles η and η' are $\text{arc cos}(1/3)$ and $\text{arc cos}(-1/3)$ respectively. In the first mode of arrangement it is unnecessary to provide a separate diagram for 03 because the symmetry enables us to deduce $\cos(r_1, r_3)$ from the expression for $\cos(r_1, r_2)$. A similar explanation holds in the case of the second mode. Applying formula (8) to these diagrams, we deduce the following expressions: For the first mode of arrangement

$$\begin{aligned}\cos(r_1, r_2) &= (1/3)\cos(60^\circ + \phi_1)\cos(60^\circ - \phi_2) - \sin(60^\circ + \phi_1)\sin(60^\circ - \phi_2) \\ \cos(r_1, r_3) &= (1/3)\cos(60^\circ - \phi_1)\cos(60^\circ - \phi_3) - \sin(60^\circ - \phi_1)\sin(60^\circ - \phi_3) \\ \cos(r_1, r_4) &= (1/3)\cos\phi_1\cos\phi_4 - \sin\phi_1\sin\phi_4\end{aligned}\quad (9)$$

For the second mode of arrangement

$$\begin{aligned}\cos(r_1, r_2) &= -(1/3)\cos\phi_1\cos\phi_2 - \sin\phi_1\sin\phi_2 \\ \cos(r_1, r_3) &= (1/3)\cos(60^\circ + \phi_1)\cos(60^\circ + \phi_3) - \sin(60^\circ + \phi_1)\sin(60^\circ + \phi_3) \\ \cos(r_1, r_4) &= -(1/3)\cos(60^\circ - \phi_1)\cos(60^\circ - \phi_4) + \sin(60^\circ - \phi_1)\sin(60^\circ - \phi_4)\end{aligned}\quad (10)$$

Calculations have been carried out using phase relation assumption III (page 501) with the two arrangements corresponding to (9) and (10). In what follows these will be referred to as B_2 and B_2' respectively. In making the calculations it has been assumed that electrons 2 and 3 are at $r_{T/4}$ (i.e. the distance from the nucleus corresponding to $t = T/4$) when electrons 1 and 4 are at perihelion and aphelion respectively; the sense of rotation for each orbit is taken to be counterclockwise to one looking inward toward O from A, B, C, D , respectively.⁷

In the case of any of the above specified methods of using definite phase relations, the fixation of the orbit after the determination of V as a function of r proceeds as in the previous cases. After V^* and therefrom V have been calculated from a first approximation to the orbit, a properly quantized orbit in this field is developed by the method of approximations above indicated. In what follows any plan involving the use of phase relations will be referred to under Method III with the appropriate subdivision indicating the special scheme under which the method is applied.

The results of the calculations based on the foregoing assumptions are presented in Table III which gives the values of the aphelial distances, orbital energies, and effective quantum numbers of the 2_1 orbits in neutral carbon according to the various methods used. The orbital energy is defined by the formula

$$E = -2\pi^2 N^{*2} e^4 m / h^2 n^{*2} \quad (11)$$

where e , m , and h have the usual significance, while N^* is the effective nuclear charge at aphelion and n^* is the effective quantum number.⁸ The values of E are given in multiples of e^2/a_0 .

⁷ For mode B_2' this is varied by having electrons 1 and 3 revolve counterclockwise while 2 and 4 revolve clockwise.

⁸ Loc. cit., see page 192.

TABLE III

	Method I	Method II	Method III			
r_{\max}/a_0	2.08	2.12	A_1	A_2	B_2	B_2'
E	-.36	-.49	-.40	-.50	-.69	-.76
n	1.17	1.28	1.22	1.23	1.32	1.41

In examining the results, it is interesting to note that the dimensions of the 2_1 orbit come out very nearly the same by all the methods, nor is there any systematic divergence. The actual values computed for r_{\max} agree rather well with the "radius" of the carbon atom as calculated from the atomic volume. For diamond this latter value is $2.06a_0$. The great divergences noted come in the energy values, the various ways of applying Method III yielding in general higher values than the simpler assumption of the first two methods. We might expect the model yielding the greatest numerical value for the energy and therefore being energetically more stable to be more nearly right. However, the arbitrary nature of the assumptions underlying plans B_2 and B_2' in particular makes it unwise to assume that these yield necessarily the most stable models. What we can be fairly sure of is the size and general time distribution for the 2_1 orbit, since these do not seem to depend very largely on the particular arrangement chosen.

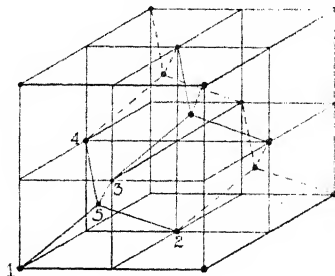


Fig. 5.

II. THE STRUCTURE OF DIAMOND

The crystal structure of diamond is well known to be the tetrahedral type indicated in Fig. 5. Each atom lies at the mid-point of a regular tetrahedron with four others at its vertices, the closest distance between neighboring atoms being designated by a , which has the experimental value 1.54A or $2.90a_0$.

The object of the present investigation is to replace the atoms in the diamond lattice by the models worked out in Part I, and with suitable simplifying assumptions to compute the lattice energy and the heat of sublimation. To carry this out it is necessary first to calculate the potential on any electron in a given atom due to the nucleus and the other electrons in the same atom as well as the nuclei and electrons in the neighboring atoms. For this calculation we must know not only the arrangement of the electron

system in a given atom but also the orientation of the system with respect to the neighboring systems. For the former we have a considerable range of choice, namely the various models worked out in Part I. It is essential, of course, to choose a model wherein the electrons move in definitely oriented orbital planes. As the basis of the present computations the writer has chosen arbitrarily plan B_2' under Method III. To see how the individual atoms are oriented with respect to each other, let us consider atom 5 in Fig. 5. The orbital planes of the 2_1 electrons in this atom are normal respectively to 51, 52, 53, 54, and we assume that the orbits are arranged in these planes according to plan B_2' above. Similarly the orbital planes of the electrons in atom 2 are normal respectively to 52, 53, 54, 51, since they are normal to lines parallel to these lines respectively. And so on in rotation for the others.

We shall not assume, however, definite orientation in their orbital planes of the orbits in atoms 1, 2, 3, 4, but shall consider the effect of the electrons in these atoms on any electron in atom 5 as that due to a time distribution of their charges in their orbital planes. In contrast to the work of other authors who have attacked the same or similar problems, notably Landé,⁹ we thus disregard any possible phase relations existing among the electrons

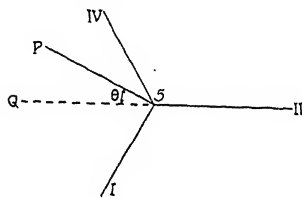


Fig. 6.

in different atoms. It is a matter of some interest, in the opinion of the present writer, to investigate the effect of disregarding such phase relations.

Because of the symmetry it will be necessary to compute V^* as a function of r for a single 2_1 electron in atom 5. For this we must then derive expressions for the distances from this electron to the nuclei of the other atoms and for the angles between these lines and the orbital planes of the electrons in the other atoms. The method of calculation of V^* and V is then identical with that described in full under Method II (pages 499 ff above). In other words we use formula (6), where α now takes a single definite value for each orbital plane considered, and r is replaced by u , the distance from the electron to the nucleus corresponding to that orbital plane. Since the calculation is designed to be only a first approximation it will be sufficient to consider only the four atoms nearest atom 5 in computing V^* . The determination of the distances u and the angles α is a problem in analytic geometry. Consulting for this purpose Fig. 6, let the plane of the paper represent the plane through 5 normal to the line 35, that is, be the plane of the orbit of the electron in atom 5 for which we are to compute V^* . Let 5I, 5II, 5IV, represent the projections on this plane of the lines (see Fig. 5) 51, 52, and 54. Then $r (= 5P)$

⁹ A. Landé, Zeits. f. Physik. 4, 410 (1921).

and $\theta (=P5Q)$ will be the polar coordinates of the electron considered. Remembering that the angle between each of the lines 51, 52, 54, and its projection is $\phi = \text{arc sin } (1/3)$, and denoting by u_1, u_2, u_3, u_4 , the distances from the electron to the nuclei of the four surrounding atoms, we find by application of formula (7):

$$\begin{aligned} u_1^2 &= r^2 + a^2 + 2ar \cos\phi \sin(\theta - 30^\circ) \\ u_2^2 &= r^2 + a^2 + 2ar \cos\phi \cos\theta \\ u_3^2 &= r^2 + a^2 \\ u_4^2 &= r^2 + a^2 - 2ar \cos\phi \sin(\theta + 30^\circ) \end{aligned} \quad (12)$$

If next we denote by α_{jk} the angle between the line u_j and the plane of the k th electron in atom j , we find that

$$\left. \begin{aligned} \sin\alpha_{11} &= -[a + r\cos\phi \sin(\theta - 30^\circ)]/u_1 \\ \sin\alpha_{12} &= [a/3 + r\cos\phi \sin(\theta + 30^\circ)]/u_1 \\ \sin\alpha_{13} &= a/3u_1 \\ \sin\alpha_{14} &= [a/3 - r\cos\phi \cos\theta]/u_1 \end{aligned} \right\} \quad (13A)$$

$$\left. \begin{aligned} \sin\alpha_{21} &= [a/3 + r\cos\phi \sin(\theta + 30^\circ)]/u_2 \\ \sin\alpha_{22} &= -[a + r\cos\phi \cos\theta]/u_2 \\ \sin\alpha_{23} &= a/3u_2 \\ \sin\alpha_{24} &= [a/3 - r\cos\phi \sin(\theta - 30^\circ)]/u_2 \end{aligned} \right\} \quad (13B)$$

$$\left. \begin{aligned} \sin\alpha_{31} &= [a/3 - r\cos\phi \sin(\theta - 30^\circ)]/u_3 \\ \sin\alpha_{32} &= [a/3 - r\cos\phi \cos\theta]/u_3 \\ \sin\alpha_{33} &= a/u_3 \\ \sin\alpha_{34} &= [a/3 + r\cos\phi \sin(\theta + 30^\circ)]/u_3 \end{aligned} \right\} \quad (13C)$$

$$\left. \begin{aligned} \sin\alpha_{41} &= [a/3 - r\cos\phi \cos\theta]/u_4 \\ \sin\alpha_{42} &= [a/3 - r\cos\phi \sin(\theta - 30^\circ)]/u_4 \\ \sin\alpha_{43} &= a/3u_4 \\ \sin\alpha_{44} &= [-a/3 + r\cos\phi \sin(\theta + 30^\circ)]/u_4 \end{aligned} \right\} \quad (13D)$$

The above formulas (13 A, B, C, D) are deduced by the application of the formula (8) to the diamond space lattice shown in Figure 5. To make this derivation somewhat clearer, Figure 7 illustrates diagrammatically the situation for the angles α_{3j} . The plane there represented is the plane normal to 53. The angles which $P3$ makes with the orbital planes of the electrons in atom 3 (viz. $\alpha_{31}, \alpha_{32}, \alpha_{33}, \alpha_{34}$) are complementary respectively to those¹⁰ which $P3$ makes with the normals to the orbital planes (viz. 31', 32', 35,

¹⁰ The smaller angles of course are chosen in each case.

34' respectively). Now 31', 32', 35, 34' are parallel respectively to 51, 52, 53, 54. We need therefore only use the method set forth in Part One (page 503) to deduce the equations (13C). The derivation of the others follows similarly.

The usual procedure at this point would be to assume a definite orbit as a first approximation; then, taking a definite value of a to begin with, to compute the values of V^* and V as functions of r . The fixation of the orbit would then follow the method outlined in Part One. Since, however, we are interested principally in the lattice energy, we can get a first approximation to this quantity without going through the above work. The method is as follows. The new 2_1 orbit, i.e. the orbit in the crystal lattice, will be

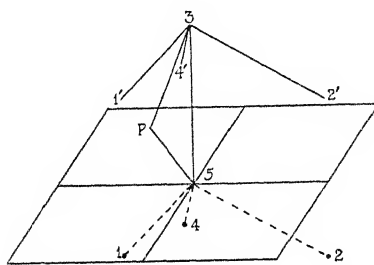


Fig. 7.

quantized with the same quantum number as the 2_1 orbit in the neutral atom. But V^* and V will be different functions of r and the orbital energy will be different. These facts are subsumed in the following equation.

$$\oint [2(E-V) + 2(\Delta E - \Delta V) - k'^2/r^2]^{1/2} dr = \oint [2(E-V) - k'^2/r^2]^{1/2} dr \quad (14)$$

where ΔE is the change in energy of the 2_1 orbit due to its presence in the lattice structure and ΔV is the change in V due to the same cause. The integration is taken from r_{\min} to r_{\max} and back again to r_{\min} . Expanding the radical on the left hand side, we have to a first approximation

$$\Delta E = \oint [2(E-V) - k'^2/r^2]^{-1/2} \Delta V dr / \oint [2(E-V) - k'^2/r^2]^{-1/2} dr \quad (15)$$

In (15) ΔV is, of course, a function of r which can be computed by the method outlined in the immediately preceding pages. The integration can then be carried out and a first approximation to ΔE obtained. It should be emphasized that in calculating (15) the values of $[2(E-V) - k'^2/r^2]^{1/2}$ used are those computed according to plan B_2' explained in Part I. These values will, of course, change slightly for changes in a , the lattice constant, but from the way the radical enters the formula, it is clear that this will not lead to material error.

The lattice energy per atom is given by¹¹ $\Phi = 4\Delta E$. The corresponding heat of sublimation per molecule which we may denote by H , is given by

¹¹ A. Landé, loc. cit., page 420.

$H = \Phi L / Q$ where L is the Avogadro number and Q the mechanical equivalent of heat. Here Φ is expressed in multiples of $e^2 / 2a_0 = Rh$, where R is the Rydberg number.

Table IV gives the calculated values of Φ and the corresponding heats of sublimation in k. cal. per mol for various values of a in the vicinity of the experimental value.

TABLE IV

a/a_0	3.0	2.9	2.8	2.74
Φ/Rh	.12	.23	.41	.55
H	38	71	126	171

From these results we may note in the first place that the values of H are of the right order of magnitude. Indeed, the experimental value of a is about $2.90a_0$ and the experimental value of H is about 170 k. cal. per mol. Unfortunately the curve giving H as a function of a does not show a maximum for a value of a in the vicinity of $2.90a_0$. In other words, the method chosen is incompetent to fix the equilibrium value of the lattice constant. That is due to the fact that it breaks down completely as a approaches values in the neighborhood of the aphelial distance of the 2_1 orbits in the carbon atom, viz. $2.0a_0$. Nevertheless it is clear that the method sets an upper limit to the value of a which is approximately $3.0a_0$. For values of a less than $2.5a_0$ the interpenetration of the orbits of the various atoms tends to render our average calculations meaningless, and it seems probable that it will be necessary to fall back to assuming definite phase relations among electron motions in the different atoms when such interpenetration takes place to a great extent.

SLOANE PHYSICS LABORATORY,
YALE UNIVERSITY,
August, 1926.

SERIES SPECTRA OF IONIZED PHOSPHORUS, P_{II}

By I. S. BOWEN

ABSTRACT

One hundred and ten of the strong lines of P_{II} have been classified as arising from various combinations between thirty-two terms of the triplet system. The observed terms are exactly those demanded by the Hund theory.

In previous papers¹ by Professor Millikan and the author the series spectra of one, two, and three-valence-electron atoms of phosphorus (P_{III}, P_{IV}, and P_V) have been analyzed. The present paper is an extension of the same methods, combined with the predictions of the Hund theory, to the analysis of the spectra arising from the four-electron atom of phosphorus, (P_{II}).

According to the Hund theory the various configurations of a four-electron system such as P_{II} should give rise to terms as shown in Table I.

TABLE I
Spectroscopic terms in a four-electron system, according to the Hund theory.

Configuration	Designation	Types of Terms
s^2p^2	<i>a</i>	$^3P, ^1S, ^1D$
sp^3	<i>b</i>	$^5S, ^5S, ^3P, ^3D, ^1P, ^1D$
$s^2p \cdot s$	<i>k</i>	$^3P, ^1P$
$s^2p \cdot p$	<i>m</i>	$^3S, ^3P, ^3D, ^1S, ^1P, ^1D$
$s^2p \cdot d$	<i>n</i>	$^3P, ^3D, ^3F, ^1P, ^1D, ^1F$

In Table II which gives the results of this analysis of P_{II} the terms arising from any configuration are designated by the letter appearing opposite it in the second column of Table I. In the case of terms due to the last three configurations of Table I the total quantum number of the excited electron is indicated in the usual way by a numeral preceding the designation of the term. Of course for P_{II} all electrons in the *a* and *b* configurations and all electrons except the excited one in the *k*, *m*, and *n* configurations are in three-total-quantum-number orbits.

While five terms arising from the $s^2p \cdot 4d$ configuration have been located, it has been impossible to determine the inner quantum numbers of these terms and consequently to sort them into components of the 3P , 3D , 3F terms that are demanded by the Hund theory for this configuration. This is because certain of the possible lines, the knowledge of whose presence or absence is necessary for the determination of the inner quantum number, so nearly coincide with other strong lines that they could not be detected, even if present. For this reason all of these terms have been indicated by an X.

¹ Bowen and Millikan, Phys. Rev. 25, p. 295, p. 591, p. 600 (1925).

TABLE II
Triplet series lines of P_{II}

Int.	λ I.A.Vac.	ν	Designation	Int.	λ I.A.Vac.	ν	Designation	Term Values
1	782.550	127787.4	aP_1-4nX_4	5	3473.86	28786.4	$3nP_5-4mP_2$	aP_0 160497.7
0	782.642	127772.3	aP_1-4nX_3	3	3479.73	28737.9	$3nP_1-4mP_1$	aP_1 160332.4
1	782.960	127720.4	aP_1-4nX_2	5	3503.99	28538.9	$3nP_5-4mP_1$	aP_2 160027.8
2	783.739	127593.5	aP_0-4nX_1	4	3519.60	28412.3	$3nP_1-4mP_0$	
0	784.464	127475.6	aP_2-4nX_4	4	3716.90	26904.1	$3nP_5-4mD_1$	
1	784.808	127419.7	aP_2-4nX_3	3	3762.87	26575.5	$3nP_5-4mD_2$	bP_1 50243.8
1	786.146	127202.8	aP_1-4nX_0	4	3769.76	26526.9	$3nP_1-4mD_3$	bP_2 50205.2
0	810.28	123414.1	aP_2-5kP_2	2	3787.76	26400.8	$3nP_5-4mD_1$	
			4	3794.67	26352.8	$3nP_1-4mD_1$		
			3	3796.16	26342.4	$3nP_5-4mD_1$		
1	906.996	110254.1	aP_2-bP_1	3	4034.81	24784.3	$4mD_1-4nX_4$	bD_1 56443.1
2	908.046	110126.6	aP_1-bP_1	3	4037.35	24768.7	$4mD_1-4nX_3$	bD_2 56394.7
2	908.356	110089.0	aP_1-bP_1	4	4063.22	24611.0	$4mD_2-4nX_4$	bD_3 56301.3
2	910.554	109823.3	aP_2-bP_2	4	4068.78	24595.5	$4mD_2-4nX_3$	
2	910.884	109783.5	aP_1-bP_1	5	4073.27	24550.3	$4mD_2-4nX_2$	
2	961.024	104055.7	aP_0-bD_1	5	4092.68	24433.9	$4mD_1-4nX_1$	
3	962.124	103936.7	aP_1-bD_2	4	4118.24	24282.2	$4mD_2-4nX_4$	$4kP_2$ 73900.0
3	962.568	103888.8	aP_1-bD_1	2	4121.93	24260.5	$4mD_2-4nX_3$	$4kP_1$ 73753.6
2	964.074	103726.5	aP_2-bD_3	6	4128.65	24221.0	$4mD_2-4nX_2$	$4kP_2$ 73372.9
3	964.932	103634.2	aP_1-bD_2	4	4131.93	24201.8	$4mD_1-4nX_3$	
3	965.400	103584.0	aP_1-bD_1	1	4403.19	22710.8	$4mP_0-4nX_4$	
4	1149.970	86958.8	aP_1-4kP_2	6	4415.52	22647.4	$4mP_1-4nX_4$	$5kP_2$ 37153.3
4	1152.825	86743.4	aP_0-4kP_1	5	4418.54	22631.9	$4mP_1-4nX_3$	$5kP_1$ 37042.0
5	1153.995	86655.5	aP_2-4kP_2	4	4427.18	22587.7	$4mP_1-4nX_2$	$5kP_2$ 36606.5
4	1155.020	86578.6	aP_1-4kP_1	6	4464.19	22400.5	$4mP_2-4nX_4$	
4	1156.985	86431.5	aP_1-4kP_0	4	4467.35	22384.6	$4mP_2-4nX_3$	
4	1159.105	86273.5	aP_2-4kP_1	6	4469.22	22375.3	$4mP_2-4nX_2$	
			8	4476.51	22338.8	$4mP_2-4nX_1$		
3	1301.865	76812.9	aP_0-3nP_1	4	4484.91	22297.0	$4mP_1-4nX_1$	$4mS$ 54496.2
3	1304.485	76658.6	aP_1-3nP_0	7	4532.04	22065.1	$4mP_2-4nX_0$	
2	1304.655	76648.6	aP_1-3nP_1	2	4535.07	22050.4	$4mP_2-4nX_1$	
2	1305.505	76598.7	aP_1-3nP_4	7	4556.08	21948.7	$4mS-4nX_4$	$4mP_0$ 55273.2
3	1309.890	76342.3	aP_2-3nP_1	7	4559.31	21933.1	$4mS-4nX_3$	$4mP_1$ 55195.1
4	1310.720	76293.9	aP_1-3nP_2	5	4629.99	21598.3	$4mS-4nX_2$	$4mP_2$ 54947.8
			6	4680.25	21366.4	$4mS-4nX_0$		
3	1532.49	65253.3	aP_0-3nD_1	0	4825.18	20724.6	$4mD_1-5kP_2$	
3	1535.86	65110.1	aP_1-3nD_2	4	4865.73	20551.9	$4mD_2-5kP_2$	$4mD_1$ 57332.0
2	1536.38	65088.1	aP_1-3nD_1	4	4928.53	20290.0	$4mD_1-5kP_1$	$4mD_2$ 57158.5
3	1542.29	64838.6	aP_2-3nD_3	7	4944.79	20223.3	$4mD_2-5kP_2$	$4mD_3$ 56829.8
2	1543.08	64805.5	aP_2-3nD_2	5	4955.70	20178.8	$4mD_1-5kP_0$	
1	2455.21	40729.7	$3nD_2-4mS$	7	4971.02	20116.6	$4mD_2-5kP_1$	
3	2482.71	40278.6	$3nD_2-4mP_2$	4	5153.63	19403.8	$4kP_0-4mS$	
5	2484.90	40243.1	$3nD_2-4mP_2$	6	5192.84	19257.3	$4kP_1-4mS$	$3nP_0$ 83674.7
3	2496.70	40052.9	$3nD_1-4mP_1$	9	5297.55	18876.7	$4kP_2-4mS$	$3nP_1$ 83685.5
4	2498.08	40030.7	$3nD_2-4mP_1$	8	5317.54	18805.7	$4kP_1-4mP_2$	$3nP_2$ 83733.9
4	2501.68	39973.1	$3nD_1-4mP_0$	9	5346.20	18704.9	$4kP_0-4mP_1$	
			8	5388.36	18558.5	$4kP_1-4mP_1$		
2	2604.49	38395.2	$3nD_2-4mD_3$	7	5411.15	18480.4	$4kP_1-4mP_0$	$3nD_1$ 95246.0
3	2606.79	38361.4	$3nD_2-4mD_2$	10	5427.42	18425.0	$4kP_2-4mP_2$	$3nD_2$ 95225.7
3	2625.54	38087.4	$3nD_1-4mD_2$	7	5501.23	18177.8	$4kP_1-4mP_1$	$3nD_3$ 95191.0
4	2626.94	38067.1	$3nD_2-4mD_1$	4	5379.60	18588.7	$4mP_1-5kP_2$	
2	2629.33	38032.5	$3nD_2-4mD_2$	8	5452.16	18341.4	$4mP_2-5kP_2$	
3	2637.56	37913.8	$3nD_1-4mD_1$	5	5485.06	18231.3	$4mP_1-5kP_1$	
2	2638.97	37893.6	$3nD_2-4mD_1$	6	5508.66	18153.2	$4mP_1-5kP_1$	
			6	5542.72	18041.7	$4mP_1-5kP_0$		
6	3420.21	29238.0	$3nP_2-4mS$	6	5584.88	17905.5	$4mP_2-5kP_1$	$4nX_0$ 33130.0
6	3425.84	29189.9	$3nP_1-4mS$	6	5589.80	17889.7	$4mS-5kP_2$	$4nX_1$ 32897.9
4	3427.16	29178.7	$3nP_0-4mS$	2	5729.27	17454.2	$4mS-5kP_1$	$4nX_2$ 32608.4
								$4nX_3$ 32563.0
								$4nX_4$ 32547.6

As in N_{II}^2 the lines arising from the jump from the sp^3 configuration to the s^2p^2 configuration are present but they are relatively much weaker than in that element, apparently because the term values of the sp^3 configuration lie much closer to the ionization energy of the atom in P_{II} than in N_{II} . The spectrum is also similar to that found by Fowler³ for Si_{I} . Just as in Si_{I} the $3nP$ term is inverted while all others are normal. In this respect the elements of the second row of the periodic table differ from the corresponding elements of the first row. For the lighter elements the $3nD$ term is normal while the bD and the bP terms are inverted.

From the table it is evident that all triplet lines which should be expected to appear strongly have been located. This is still another confirmation of the Hund theory and its great utility in the prediction of spectra.

In the table all wave-lengths above 2400\AA are taken from Geuter⁴ and corrected to I.A. Vac. The term values are determined by making the $4kP_0$ and the $5kP_0$ terms follow a Rydberg formula.

NORMAN BRIDGE LABORATORY OF PHYSICS,
CALIFORNIA INSTITUTE OF TECHNOLOGY.
JANUARY 14, 1927.

² Bowen, Phys. Rev. 29, 231 (1927).

³ Fowler, Phil. Trans. 225, p. 1 (1925).

⁴ Kayser, Handbuch der Spektroskopie, Vol. VI, p. 246.

THE DIFFUSION OF IMPRISONED RESONANCE RADIATION IN MERCURY VAPOR

BY MARK W. ZEMANSKY

ABSTRACT

The rate of diffusion of imprisoned resonance radiation in mercury vapor.—The imprisonment of resonance radiation in mercury vapor was studied by measuring the rate at which resonance radiation emerged from one face of a slab of vapor after the exciting light, incident upon the other face, was cut off. The radiation was found to fall off exponentially, and the exponential constant of decay was measured for vapor densities ranging from 0.77×10^{15} atoms per cc to 29×10^{15} atoms per cc, corresponding to temperatures ranging from 60°C to 130°C . Slabs of two different thicknesses were studied, one 1.95 cm, and the other 1.30 cm. It was found that for vapor densities lower than about 4×10^{15} atoms per cc, the exponential constant varied approximately inversely as the square of the thickness of the slab, in qualitative agreement with the theory of the diffusion of imprisoned radiation as worked out by Milne.

Extension of Milne's theory: broad exciting line; collisions of second kind.—In this region of vapor densities it was found also that the exponential constant decreased with the vapor density. The failure of Milne's results to give quantitative agreement with this result is discussed and it is suggested that this discrepancy is due to the fact that the exciting light in this experiment was a very broad spectral line, and that postulated by Milne of very narrow width. A rough method of extending Milne's theory to include the absorption and imprisonment of frequencies larger and smaller than the heart of the 2536.7 line is discussed, and it is shown that the experimental results can be explained on this basis. At higher vapor densities, the decay constant increased almost linearly with the number of absorbing atoms per cc. It is shown that this result is in accordance with the theory of imprisonment when extended to include impacts of the second kind. The probability of an impact of the second kind between a normal and an excited mercury atom is calculated from the experimental data and found to be approximately 9×10^{-4} .

INTRODUCTION

IT IS well known that the fluorescence excited in some solids and liquids persists for a short time after the excitation has been cut off. Wood,¹ and later, Gottling² and Wawilow³ studied the visible fluorescence excited in fluorescein, rhodamine, uranium glass, etc., and found that fluorescence persists after the cut-off of the exciting light for a time, which, in some cases, is as long as 10^{-2} secs.

Phillips⁴ investigated the visible fluorescence excited in mercury vapor, and showed that it was carried by a moving column of the vapor a considerable distance past the point of excitation. Since this fluorescence, consisting of a violet and a green band, depends upon the absorption of the

¹ R. W. Wood, Proc. Roy. Soc. A99, 362 (1921).

² P. F. Gottling, Phys. Rev. 22, 566 (1923).

³ S. J. Wawilow and W. L. Lewschin, Zeits. f. Physik. 35, 920 (1926).

⁴ F. S. Phillips, Proc. Roy. Soc. A89, 39 (1913).

mercury resonance line 2536.7 this experiment implies that mercury vapor is capable of holding resonance radiation in it for a short time. It does not determine, however, whether this is accomplished by metastable atoms or by repeated atomic absorptions and re-emissions, nor is it suitable to decide this question, since the origin of the visible fluorescent bands is so much in doubt.

The most direct experiment on persistent resonance fluorescence was made by Miss Hayner,⁵ who studied the actual resonance radiation emitted by mercury vapor after the excitation was cut off. Miss Hayner used a quartz mercury arc provided with a hot cathode so that it could be struck and cut off very rapidly by a commutator. Light from this arc was incident on one face of a small cylindrical quartz cell containing mercury vapor, and the rate at which the resonance radiation escaped from the other face, after the arc was cut off, was measured. She obtained the result that the resonance radiation fell off exponentially, with an exponential constant that was independent of the density of the vapor, and approximately inversely proportional to the thickness of the slab of vapor. She found also that the resonance radiation did not persist after the cut-off, if the absorption cell was sealed off after evacuation.

In 1912, Wood⁶ observed that resonance radiation excited in one portion of a mass of mercury vapor spread to other portions, and, by introducing a small quartz window, established the fact that this diffusion was not due to the movement of atoms. He concluded that the resonance radiation spread by repeated atomic absorptions and re-emissions. This idea was extended by K. T. Compton⁷ to explain certain peculiarities in the behavior of the arc. He suggested that resonance radiation becomes imprisoned within a mass of vapor because of the fact that a quantum of radiation is absorbed and re-emitted by many atoms before it finds its way out of the enclosing vessel. Calculations on the basis of this theory were made by Compton and by Webb⁸ who used the differential equation of diffusion to calculate the number of excited atoms in a mass of vapor and the rate at which radiation arrives at one boundary.

Recently this problem has received a more rigorous solution by Milne⁹ who used the Einstein radiation hypotheses to obtain the differential equation of the diffusion of imprisoned resonance radiation. Considering the vapor enclosed between two infinite planes, and monochromatic radiation incident upon one face, he obtained an exact expression for the radiation arriving at the other face after the exciting radiation was cut off. According to his result, the radiation should fall off exponentially with an exponential constant inversely proportional to: (1) The square of the number of absorbing atoms per cc; (2) The square of the thickness of the slab of vapor.

⁵ L. J. Hayner, Phys. Rev. 26, 364 (1925).

⁶ R. W. Wood, Phil. Mag. 23, 689 (1912).

⁷ K. T. Compton, Phys. Rev. 20, 283 (1922); Phil. Mag. 45, 752 (1923).

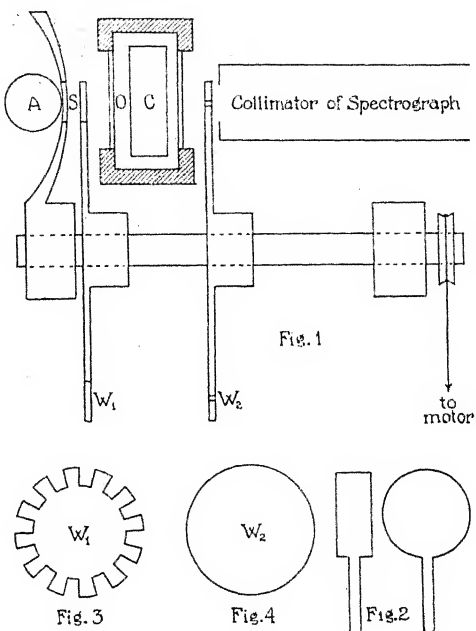
⁸ H. W. Webb, Phys. Rev. 24, 113 (1924).

⁹ E. A. Milne, Journ. Lon. Math. Soc. No. 1 (1926).

This result does not agree with Miss Hayner's experimental results, nor has it been possible to account for her results on the basis of any theory. Consequently it was thought worth while to repeat her experiment under better conditions. The following paper contains a description of such experiments and a theoretical discussion of the results.

METHOD AND APPARATUS

The method was essentially the same as that used by Miss Hayner. The total radiation from a water cooled, magnetically deflected quartz mercury arc A (see Fig. 1) passed through a horizontal slit S , 0.5 mm wide,



Figs. 1, 2, 3, 4

into a cylindrical cell C containing mercury vapor. The cell was of clear fused quartz with circular faces 5.1 cm in diameter, (see Fig. 2) which was baked out, evacuated and sealed off with a drop of mercury remaining in the stem. An electric oven O with quartz windows kept the faces and the stem of the cell at constant temperature. Between the oven and the slit there was a rotating wheel W_1 with twelve teeth. (see Fig. 3) The face of the wheel was very close to the slit and the edges of the teeth were parallel to the slit. This arrangement alternately transmitted the light and cut it off twelve times per revolution. Mounted on the same shaft as W_1 was a second wheel W_2 containing two sets of holes, (see Fig. 4) twelve holes in the outer set, and nine in the inner. The diameter of each hole was 0.3 mm. These holes acted as moving slits for a Hilger quartz spectrograph placed as is shown in Fig. 1, causing pairs of curved traces on the photographic

plate, each pair corresponding to one of the mercury arc lines. (see Fig. 5) The two wheels were so adjusted that, just as a tooth on W_1 was about to cover the slit S , a hole in W_2 presented itself in front of the collimator of the spectrograph. After a trace on the plate a few millimeters long (distance AB in Fig. 5) had been made, the tooth cut the exciting light off, and the persistent radiation produced a continuation of the trace (distance BC in Fig. 5). The small, rounded portion at the point B represents the interval of time required for the tooth to cover the breadth of the slit, usually about 10^{-5} secs.

The history of the radiation emitted from the cell after the exciting light was cut off was obtained by measuring the photographic density at different points along each trace; each point corresponding to a known interval of time after the cut-off. Density-time curves were plotted for both traces on the same graph. Since one trace was produced by twelve exposures per

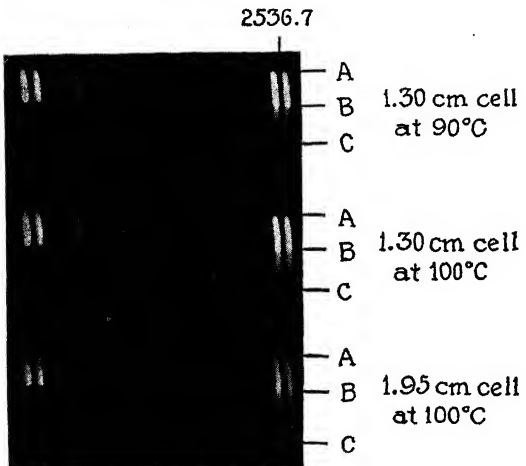


Fig. 5

revolution and the other by nine, corresponding densities represent exposure times in the ratio of 1 to 3/4. In order to determine the intensity relation between corresponding points on the two traces, two photographs were taken on the same plate, one with the usual spectrograph diaphragm, and one with a diaphragm which cut out 1/4 of the light. The trace representing full intensity and 3/4 time, was then compared with the trace representing 3/4 intensity and full time, and it was found that the two traces were identical when the photographic densities were between 0.4 and 0.8; that is, in the linear region of the curve of blackening of the plate. Thereafter, within these limits, the trace produced by nine exposures per revolution was used as a comparison trace representing 3/4 the intensity of the other trace.

On each plate three separate exposures were taken corresponding to three different sets of conditions. One of these was produced by the persistent radiation emerging from the 1.95 cm cell at 100°C. This pair of traces

was used as a standard of comparison and appears as the lowest pair of traces in Fig. 5. The trace representing full intensity is on the left. From these two traces the constant of contrast of the plate, γ , and the exponential constant, $1/T$, for the persistent radiation at 100°C were obtained in the following manner:

The two traces were placed in turn over the circular slit of the densitometer and the photographic densities of all points ten minutes of arc apart were measured. Translating angular distance into time, and plotting all values of photographic density that lay between 0.4 and 0.8 against the time, two curves were obtained, one for the full intensity trace and the other for the $3/4$ intensity trace. Each curve consisted of a rapidly decreasing portion, representing a small period during the cut-off of the exciting light, and a linear region representing the persistent radiation. The intersection of these two portions was taken as the instant of cut-off. Calling the density of this intersection point on the full intensity curve D , and the density of the corresponding point on the $3/4$ intensity curve D' , we have

$$\begin{aligned} D &= \gamma \log I + \text{const.} & (0.4 < D < 0.8) \\ D' &= \gamma \log \frac{3}{4}I + \text{const.} & " \end{aligned} \quad (1)$$

Whence

$$\gamma = (D - D') / \log_{10}(4/3) = (D - D') / 0.125$$

Now, let I be the intensity of the persistent radiation that gives rise to the full-intensity trace, t seconds after the cut-off of the exciting light. Then $I = I_0 e^{-t/T}$ where $1/T$ is the exponential constant to be measured. Combining this equation with Eq. (1) we obtain

$$D = -\gamma t / 2.30T + \text{const.}$$

which expresses the fact that the density-time curve is a straight line, when D is between 0.4 and 0.8 with a slope S equal to $\gamma / 2.30T$. The exponential constant for the persistent radiation at 100°C was then obtained from $1/T = 2.30S/\gamma$ and that corresponding to any other trace on the plate, from the relation $TS = T'S'$ where T' and S' refer to the second trace.

PROCEDURE AND RESULTS

Before exposing the plate, the stem of the cell which contained the drop of mercury was heated to the desired temperature, and the faces to a temperature about 5°C higher. In this way condensation of mercury on the faces of the cell was avoided. The wheels rotating so close to the oven which contained the cell caused a draft which tended to cool the oven, so that, at least three-quarters of an hour had to be allowed for the whole system to attain constancy. The temperature of the stem of the cell and the speed of the wheels remained constant within two percent during an exposure which lasted in most cases about one hour.

No difficulty was found at any time in obtaining imprisonment of resonance radiation in a sealed-off cell. It was evidently not necessary to have

freshly evaporating mercury present, since the liquid mercury remained in the stem of the cell throughout an exposure. Only that pair of traces corresponding to wave-length 2536.7 showed any trace on the plate *after* the cut-off of the exciting light. Although all the mercury arc lines were present in the exciting light, there was never any evidence of absorption and consequent re-emission of any wave-length other than 2536.7. It is, therefore, believed that whatever absorption of other wave-lengths occurred it played a negligible rôle in the imprisonment of the resonance radiation.

The exponential constant of decay of the persistent radiation from the 1.95 cm cell and the 1.30 cm cell at temperatures ranging from 60°C to 130°C (about a 30-fold increase in vapor density) was measured. The saturation vapor pressures of mercury at the temperatures employed were taken from Landolt and Börnstein's tables and the number of atoms per cc corresponding to the different vapor pressures calculated.

The results are presented in Table I. The first and second columns give temperatures and corresponding vapor densities respectively. The third

TABLE I

Rate of decay of resonance radiation emerging from a slab of mercury vapor after the exciting light, incident on other face, is cut off.
T is the time constant in the equation $I = I_0 e^{-t/T}$.

Temp. °C	No. of Atoms per cc $N \times 10^{-15}$	1.95 cm cell		1.30 cm cell	
		$(1/T) \times 10^{-3}$	$T \times 10^4$	$(1/T) \times 10^{-3}$	$T \times 10^4$
60	0.770	26.6	0.376		
70	1.40	14.2	0.704	28.1	0.356
80	2.50	8.81	1.13	19.3	0.518
90	4.40	7.07	1.41	12.1	0.827
100	7.26	6.89	1.45	9.47	1.06
110	11.8	7.72	1.30	9.00	1.11
120	18.8	9.64	1.04	10.6	0.944
130	29.0	13.2	0.757	13.5	0.740

and fourth columns give the corresponding values of the exponential constant $1/T$ and the time constant T for the cell 1.95 cms thick, and the fifth and sixth columns give the same quantities for the 1.30 cm cell. In Fig. 6 these results are plotted for both cells with the exponential constant as ordinate and the number of atoms per cc as abscissa.

DISCUSSION

In Fig. 6 it is seen that the curves for the two cells are of the same general character. At low vapor densities, the exponential constant of decay of the persistent radiation decreases very rapidly with increasing vapor density; and at high vapor densities, the exponential constant rises nearly linearly with the vapor density. That is, as the number of absorbing atoms increases, the resonance radiation remains imprisoned for a longer and longer time, until a maximum time is reached, after which, any increase in the number of absorbing atoms causes a diminution in the time of imprisonment of the radiation in the vapor.

Let us compare these results with those obtained by Milne. Assuming that one face of an infinite slab of vapor perpendicular to the x axis, is exposed to radiation of very narrow spectral width, and, neglecting molecular motion and impacts, Milne finds that the number of excited atoms per cc, n_2 , is given by the equation

$$\frac{\partial n_2}{\partial t} = \frac{1}{4\alpha^2 N^2 \tau} \frac{\partial^2}{\partial x^2} \left(n_2 + \tau \frac{\partial n_2}{\partial t} \right) \quad (2)$$

where τ represents the duration of the excited state produced by absorption of the radiation, N the number of atoms per cc, and α the atomic absorption

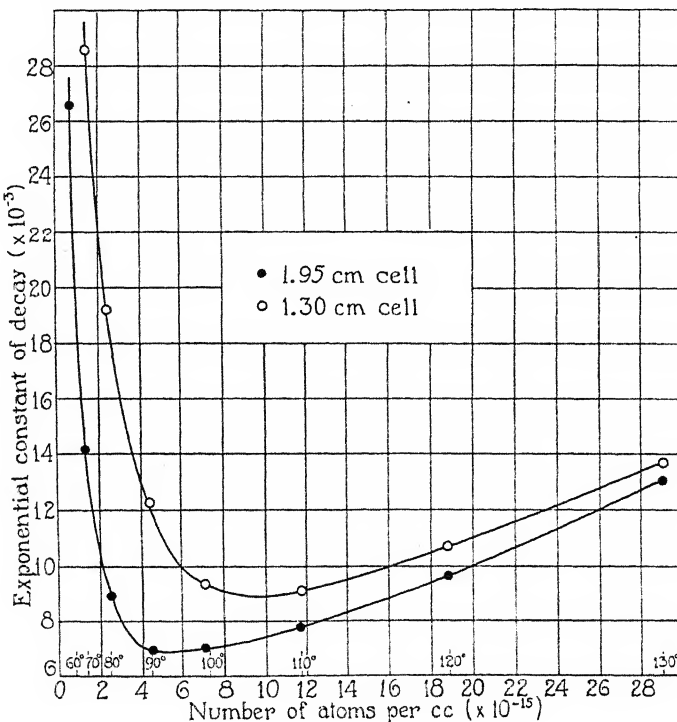


Fig. 6

coefficient for the exciting radiation. The solution of this equation yields the result that the radiation emerging from the far face of the slab after the exciting light, incident on the front face, is cut off, falls off exponentially, with a time constant T given by

$$T = \tau \left(1 + 4l^2 \alpha^2 N^2 / \pi^2 \right) \quad (3)$$

where l stands for the thickness of the slab. The duration of the 2^3P_1 state ($2p_2$ state, in the old notation), τ , for mercury is known to be 10^{-7} seconds.¹⁰

¹⁰ W. Wien, Ann. d. Physik. **73**, 483 (1914); Eldridge, Phys. Rev. **23**, 772 (1924); Phys. Rev. **24**, 234 (1924); Hanle, Zeits. f. Physik. **30**, 93 (1924); Turner, Phys. Rev. **23**, 464 (1924); Tolman, Phys. Rev. **23**, 693 (1924); Breit and Ellett, Phys. Rev. **25**, 888 (1925).

Malinowski¹¹ and Orthmann¹² measured the absorption coefficient of mercury vapor at a density of about 3×10^{13} atoms per cc for the radiation from a mercury resonance lamp at room temperature, and found a value of approximately 3. This gives for the atomic absorption coefficient a value of approximately 10^{-13} which can be regarded as reliable in order of magnitude at least.

Since, in this experiment, N , the number of atoms per cc, ranged from 0.77×10^{15} to 29×10^{15} and l was 1.95 cm for the thicker slab, and 1.30 cm for the thinner, $4l^2\alpha^2N^2/\pi^2 > 1$ and we can write Eq. (3) more simply

$$1/T = \pi^2/4\pi l^2\alpha^2 N^2 \quad (4)$$

which is the expression for the exponential constant that would result if, in the original differential equation, Eq. (2), the term $\partial^3 n_2 / \partial x^2 \partial t$ were neglected. Consequently in the region of vapor densities employed in this experiment we may neglect the last term in Eq. (2).

If now, we consider the left-hand part of the experimental curves in Fig. 6 for which $N < 4 \times 10^{15}$ atoms per cc, we see, at first, that the way in which $1/T$ varies with l is in good agreement with Eq. (4) which requires that $1/T$ be inversely proportional to l^2 . The ratio of the squares of the thicknesses of the two slabs is 2.2. At 70°C the inverse ratio of the exponential constants is 2.0, at 80°C it is 2.2 and at 90°C , 1.7.

A quantitative comparison, however, between Eq. (4) and the experimental values of the exponential constant for the thicker cell shows a large discrepancy. At 60°C for which $N = 0.77 \times 10^{15}$ atoms per cc, Eq. (4) gives $1/T = 1100$ as against the experimental value of 26600. At 70°C , Eq. (4) gives 330 whereas experiment yields 14200. At higher temperatures Eq. (4) gives values of $1/T$ that get rapidly smaller, approaching zero, whereas the experimental curve in Fig. 6 shows a minimum value for $1/T$ of about 7000 at 100°C and an almost linear increase for $1/T$ at higher temperatures.

This lack of agreement between theory and experiment leads us to seek an equation fitting the actual conditions of the experiment more closely than does that of Milne. There are certain obvious differences between the conditions assumed in Milne's development and those actually present in these tests. One of these can readily be disposed of as not materially affecting the quantity in question, $1/T$. The use of a cylindrical enclosure for the vapor instead of an infinite slab affects, for the most part, the functions which are coefficients of the exponential terms in the exact solution of the problem. A simple calculation shows that, for a cylindrical boundary the exponential constant is given by an expression the same as Eq. (4) except that instead of π^2 entering, we have approximately the value 14. This slight difference is unimportant.

Milne's equation does not take into account the gaseous diffusion of excited atoms under the concentration gradient which exists in the slab

¹¹ Malinowski, Ann. d. Physik. **44**, 935 (1914).

¹² Orthmann, Ann. d. Physik. **78**, 601 (1925).

during the steady state, and the effect of dissipative impacts (impacts of the second kind). This can be done in a manner indicated by Milne in a footnote in his paper, by replacing $\partial n_2/\partial t$ of his paper, which represents the rate at which excited atoms are being formed in a unit volume due to imprisonment, by $\partial n_2/\partial t - g\partial^2 n_2/\partial x^2 + kn_2$, where $g\partial^2 n_2/\partial x^2$ represents the rate at which excited atoms are forming due to gaseous diffusion, and kn_2 represents the rate at which excited atoms are disappearing through impacts of the second kind. From the kinetic theory of gases we have $g = c/3(2)^{1/2}\pi s^2 N$, where c is the root mean square velocity, s the distance between centers at impact, and N the number of atoms per cc; and $k = (2)^{1/2}\pi b s^2 c N$, where b is the probability that an impact between a normal mercury atom and an excited one is of the second kind.

The outstanding discrepancy between Milne's theory and the conditions actually present in this experiment, however, cannot be handled so easily, i.e. the effect of the absorption and imprisonment of frequencies larger and smaller than the heart of the 2536.7 line. There is no doubt that such absorption occurs, for it is known that the breadth of the absorption line at the temperatures studied is much larger than can be explained on the basis of the Doppler effect. The process of the diffusion of these frequencies comprising a broad absorption line must be very complicated, for we cannot consider that the imprisonment processes (repeated absorptions and re-emissions) of all the frequencies are independent of one another. Instead, we must take into account the fact that an atom that picks up a frequency corresponding to one part of the absorption line can re-emit a frequency corresponding to another part. Because of our ignorance of these changes of frequency we are not in a position to treat the effect of the broad absorption line rigorously, but since we are led to believe that the radiation composing the whole absorption line diffuses as a whole through the vapor, we may make the plausible assumption that the total radiation included in the broad absorption line obeys the same law of diffusion as that given by Eq. (2), except that, instead of α standing for an atomic constant (the atomic absorption coefficient), it represents a "mean or equivalent absorption coefficient" which is a function of the line breadth. Denoting by β the equivalent absorption coefficient and taking account of gaseous diffusion of excited atoms and impacts of the second kind between excited and normal atoms, we obtain the differential equation

$$\partial n_2/\partial t + kn_2 = (1/4\beta^2 N^2 \tau + g)\partial^2 n_2/\partial x^2$$

The solution of this equation gives the result that the radiation emerging from the far face of the slab of vapor after the exciting light incident on the front face is cut off, falls off exponentially with an exponential constant, $1/T$, given by

$$\frac{1}{T} = \frac{\pi^2}{4\tau l^2 \beta^2 N^2} + \frac{\pi c}{3(2)^{1/2} l^2 s^2 N} + (2)^{1/2} \pi b s^2 c N \quad (5)$$

The three terms of the right-hand member represent, in order, the effect of the imprisonment of the whole absorption line, the effect of gaseous diffusion, and the effect of impacts of the second kind.

The second term may be neglected completely, for numerical substitution shows it to be very small for the whole range of values of N . In the parts of the curves in Fig. 6 for which N is small, the third term may also be neglected. Comparison between experiment and the first term of Eq. (5) then, would serve only to determine the value of β as a function of N . Since the meaning of β in terms of physical constants of the vapor is not clear, the actual values of β are of no interest. It may be interesting, however to point out that if $1/\beta$ is taken as a linear function of N , good agreement is obtained between the form of the curves in Fig. 6 and the theoretical curves.

For large values of N the third term is of importance. This term, expressing the effect of impacts of the second kind, represents a linear relation between the exponential constant and N . Since the right-hand parts of the experimental curves in Fig. 6 show a distinct linear rise, we may regard this as strong indication that such impacts exist at these high vapor densities. There is abundant evidence for the existence of such collisions in mixtures of mercury vapor and inert gases, and the experiments of Wood and Kimura,¹³ and Goos and Meyer¹⁴ indicate that they are present also in pure mercury vapor. The experiments of Franck¹⁵ and his students indicate that the probability of such impacts between normal and excited mercury atoms is small, but do not yield a numerical estimate of this probability.

The results of this experiment can be used to calculate this probability, if we make the assumption that the rise of the exponential constant for large values of N is due solely to impacts of the second kind. For Eq. (5) gives as the slope of the straight line representing this rise $(2)^{1/2} \pi b s^2 c$ and Fig. 6 gives for this slope the value 3×10^{-13} from which b , the probability of an impact of the second kind between a normal and an excited mercury atom, can be calculated in terms of s the distance between centers at impact and c the root mean square velocity of the atoms. With s equal to 6.0×10^{-8} cm, and c equal to 2.2×10^4 cm/sec, b is found to be approximately 9×10^{-4} . That is, about one out of every thousand collisions between an excited mercury atom and a normal one is of the second kind. This does not contradict the result of Cario that every collision between an excited mercury atom and an air molecule is of the second kind, for, if an excited mercury atom pass on its excitation to a molecule of a foreign gas, the excited state of the mercury atom is destroyed; whereas if an excited mercury atom pass on its excitation to a normal mercury atom, there is merely a change in rôle and there still remains an excited mercury atom. Consequently, one would not expect every collision between an excited and a normal mercury atom to be dissipative. Cario's result shows clearly what effect we should expect a small amount of air to have in this experiment. Since the probability of

¹³ R. W. Wood and Kimura, Phil. Mag. 32, 329 (1916).

¹⁴ Goos and Meyer, Zeits. f. Phys. 35, 803 (1926).

¹⁵ J. Franck, "Anregung von Quantensprünge durch Stöße," p. 225.

a dissipative impact between an air molecule and an excited mercury atom is one thousand times the probability of such an impact in pure mercury vapor, air, at a pressure of .001 mm should have the same effect as mercury at a pressure of 1 mm. Consequently if there were air, at a pressure of .001 mm present in the cell at 100°C, instead of an exponential constant of 7000 we should expect a value of about 20000. This is approximately the value obtained by Miss Hayner for this temperature, and consequently it is suggested that the presence of a small quantity of air as an impurity liberated from the walls of the quartz absorption cell is a possible explanation of Miss Hayner's results. The failure of Miss Hayner to obtain persistent resonance radiation in a sealed-off absorption cell can be explained on the supposition that the cell was improperly evacuated and sealed off, so that, upon heating, the air pressure rose quickly to a value sufficient to increase the exponential constant to an unmeasureable value.

Further evidence that collisions of the second kind play an important rôle in the phenomenon of the diffusion of imprisoned resonance radiation is furnished by measurements of the opacity of the slab of mercury vapor. According to the simple theory of imprisonment neglecting impacts, the ratio of the incident to the transmitted light is

$$I_0/F_0 = 1 + l\alpha N$$

whereas, rough measurements show that the opacity of the slab for radiation from a cold resonance lamp increases much more rapidly with vapor density. Taking into account impacts of the second kind, the opacity is found to be

$$I_0/F_0 = \frac{1}{2}(\tau k)^{-1/2} \sinh 2l\alpha N(\tau k)^{1/2} + \cosh 2l\alpha N(\tau k)^{1/2}$$

which gives results in fair agreement with experiment.

In conclusion, I wish to express my indebtedness to Professor H. W. Webb, at whose suggestion and under whose guidance this work was done; and to Mr. L. J. Buttolph of the Cooper Hewitt Electric Company, I extend my sincere thanks for his kindness in placing at my disposal the mercury arc necessary for this work.

PHOENIX PHYSICAL LABORATORIES,
COLUMBIA UNIVERSITY,
December, 1926.

ON THE SURFACE HEAT OF CHARGING

BY LEWIS TONKS AND IRVING LANGMUIR

ABSTRACT

Calculation of the surface heat of charging for pure metals, for oxide coated metals and for monatomic films.—Two methods are pointed out for calculating the theoretically necessary reversible heat development or absorption accompanying the charging of the surface of a conductor. One method depends on a new relation $\eta_{s1} - \eta_{s2} = kT \ln (A_1/A_2) + \epsilon P_{21}$ between the surface heats, η_s , of the two surfaces, the A 's of electron emission equations of the type $i = AT^2 e^{-b/T}$ and the Peltier heat at the interface between the conductors. The other method consists of a comparison of the cooling effect of electron emission and the latent heat calculated from the temperature variation of emission. Experimental evidence points to $\eta_s = 0$ (nearly), $A = 60.2$ amps/cm² deg² (nearly) for all pure metals. Oxide coated filaments present a difficulty. For monatomic films the first method gives appreciable values of η_s and experimental data for use in the second method is lacking.

Stopping potentials of Na, K and Li yield further evidence that η_s is very small for all pure metals. The relation between surface heat of charging and certain assumptions fundamental to electron emission theory is discussed.

I. EXISTENCE OF A SURFACE HEAT OF CHARGING

THERE have long been grounds for believing that charging the surface of a conductor with electricity involves a reversible development of heat. By thermodynamical reasoning the quantity of heat may be estimated as of the order of the contact difference of potential times surface charge. Although by its smallness it has eluded experimental observation, such a surface heat of charging is required theoretically. By thermodynamical reasoning Kelvin showed that

$$dV_{21}/d \ln T = P_{21}' \quad (1)$$

where V_{21} is the contact difference of potential between two conductors, 1 and 2, T is the absolute temperature of the system, and P_{21}' is the heat absorbed by a unit of electricity in passing from the surface of 2 through the conductors and across the interface to the surface of 1. V_{21} is positive when the potential just outside of 1 is higher than that just outside of 2. P_{21}' has frequently been identified with the Peltier heat, P_{21} . With that interpretation, Eq. (1) fails experimentally even in order of magnitude.¹ Kelvin, himself, postulated a surface heat of charging to eliminate the discrepancy. Thus, denoting the heat absorbed when the surface of 1 is given an elementary positive charge by η_{s1} , Kelvin's relation becomes¹

$$dV_{21}/d \ln T = P_{21} + (\eta_{s2} - \eta_{s1})/\epsilon \quad (2)$$

where $\epsilon = -4.77 \times 10^{-10}$ e.s.u.

¹ Bridgman, Phys. Rev. 14, 306 (1919).

II. CALCULATION OF THE HEAT OF CHARGING FOR PURE METAL SURFACES

From Boltzmann's equation and the perfect gas laws Richardson first showed that

$$\epsilon V_{21} = kT \ln(i_2/i_1) \quad (3)$$

where k is the Boltzmann constant and i_2 and i_1 are the respective current densities of the emission from the surfaces of 2 and 1 under equilibrium conditions, that is, when all the electrons return to the surface. It seems most unlikely, however, that drawing off the whole emission current should appreciably affect the emission if we accept the electric image force point of view regarding the work function.² Eq. (3) gives an easy method for measuring the contact difference of potential, the direct measurement of which is difficult. This value of V_{21} may now be substituted in Eq. (2) giving

$$\frac{P_{21}}{T} + \frac{\eta_{s_2} - \eta_{s_1}}{\epsilon T} = \frac{k}{\epsilon} \frac{d}{dT} \left[T \ln \left(\frac{i_2}{i_1} \right) \right] \quad (4)$$

In many cases the electron emission data from a surface 1, can be accurately expressed by a law of the form

$$i_1 = A'_1 T^{\alpha_1} e^{-b_1/T} \quad (5)$$

where A'_1 and b_1 are constants determined by the data after the constant α_1 has been chosen. But there is quite a range in the values of this constant which fit the data well. Substituting Eq. (5) and a similar one for surface 2 in Eq. (4) we find

$$\frac{P_{21}}{T} + \frac{\eta_{s_2} - \eta_{s_1}}{\epsilon T} = \frac{k}{\epsilon} \left[\ln \frac{A'_2}{A'_1} + (\alpha_2 - \alpha_1)(1 + \ln T) \right] \quad (6)$$

The form of Eq. (4) shows that any law of the type of Eq. (5) which reproduces the value of i and its first derivative at any temperatures gives the correct value to the left member of Eq. (6) at those temperatures.

Now, since the choice of α_1 and α_2 is not critical in accurately representing the data over wide temperature ranges, and since in most cases a value of 2 for these constants fits the experimental results well and has some theoretical basis, we may take them each equal to 2 and thus get

$$\eta_{s_1} - \eta_{s_2} = kT \ln(A_1/A_2) + \epsilon P_{21} \quad (7)$$

where A_1 and A_2 are written for the case $\alpha_1 = \alpha_2 = 2$. To estimate the difference between the surface heats for two surfaces, the terms of the right member must be calculated roughly. We can do this for some pure metal surfaces. P_{21} can be found from thermoelectric data, but unfortunately such data are lacking for the well-known metallic emitters. There is, however, no reason to think that the Peltier heat is materially different from that for platinum against iridium for which data are available. Roughly extrapolating their thermoelectric power,³ dE/dT , to 2500°K, it is found that $dE/dT = P/T$

² W. Schottky, Jahrb. der Radioaktivität u. Elektronik, 12, 204 (1915).

³ Smithsonian Physical Tables, 6th Edit., Table 300.

$= 3 \times 10^{-5}$ volts/deg. giving P_{21} a value of 0.075 volt. The values of A for the pure surfaces of the metals tungsten, molybdenum, tantalum⁴ and thorium⁵ are known to within 15 to 50 percent and A_0 (60.2 amps/cm² deg²) is a possible value for each. Hence, for these metals, and perhaps for pure metals in general, we may put $1/1.5 < A_1/A_2 < 1.5$ so that $(kT/\epsilon) \ln (A_1/A_2) < (2500/11,600) \times 0.4 = 0.086$ volt in absolute value. It follows then that the absolute value of $\eta_{s1} - \eta_{s2}$ is less than 0.16 volt at 2500°K. It thus appears that the surface heats of charging of all pure metals do not differ from each other by more than a few percent of their work functions.

There is another method for evaluating η_s . Bridgman¹ has pointed out that three latent heats are involved in electron emission. First there is the latent heat of vaporization, η , which is absorbed when an electron evaporates from an isolated body into an electron atmosphere maintained at constant pressure. The body is left with the corresponding elementary positive charge. This quantity appears in the Clapeyron Equation (see below) applied to electron emission. Second, if everything is the same as above except that an electron flows into the body through a conductor when an electron evaporates, so that the surface charge remains constant during the process, then the latent heat of vaporization is denoted by η_p . This is the case in all electron emission experiments and η_p can be determined from the cooling effect of the electron emission. Third, if the body be simply given an elementary positive charge, the latent surface heat of charging, η_s , is absorbed from the surroundings.

It is easily seen that the second and third processes performed in succession are equivalent to the first, so that

$$\eta = \eta_p + \eta_s \quad (8)$$

and η_s can be found as the difference of η and η_p .

Since η_p applies to the evaporation of electrons under reversible conditions, and the cooling effect is always measured under irreversible conditions, these quantities are not identical. A simple analysis shows how they are related.

When an electron evaporates reversibly into an electron atmosphere maintained at constant pressure, there are three modes of heat absorption. First, there is the energy to free the electron at the temperature of the experiment which may be called η_{pT} . Second $3kT/2$ (on the average) is required to give the electron the proper kinetic energy and third kT is absorbed by a layer of the electron gas located roughly at the distance of the mean free path length from the emitting surface. This is the heat that is converted into the potential energy ρdv of expansion.

Under experimental conditions, however, the electrons do not evaporate reversibly, so the energy absorptions may be different. First, the smallness of the Schottky effect shows that η_{pT} is not changed appreciably when small

⁴ Dushman, Rowe, Ewald and Kidner, Phys. Rev. 25, 338 (1925).

⁵ C. Zwikker, Proc. Roy. Acad. Sci. Amst. 29, 792, (1926).

fields are used. Second, the kinetic energy carried away by each electron is $2kT$ (on the average). This is also true, of course, under reversible conditions, but then the faster electrons return to the surface more quickly leaving the average energy of those which remain in the space $3kT/2$. Third, the electrons evaporate into a space devoid of pressure so that no heat is absorbed in increasing the electron gas volume.

Thus it appears that the measured cooling effect is

$$\eta_c = \eta_{pT} + 2kT + 0$$

whereas the reversible cooling effect is

$$\eta_p = \eta_{pT} + 3kT/2 + kT$$

leading to

$$\eta_p = \eta_c + kT/2 \quad (9)$$

Then η can be found from the temperature variation of the electron emission. The relation is deducible directly from fundamental principles. Clapeyron's Equation applied to electron evaporation gives

$$\eta/kT^2 = d \ln p/dT$$

where p is the pressure of the electron gas. From kinetic theory $p/T^{1/2}$ is a constant independent of T . Making the indicated substitution and noting that $dT/T^2 = -d(1/T)$ we have, in terms of measurable quantities

$$\eta = -k \frac{d \ln (iT^{1/2})}{d(1/T)}.$$

Since, however, emission data are usually plotted in the form $\ln(i/T^2)$ against $1/T$ it is worth while to subtract the identity

$$(5/2)kT = -k d \ln T^{5/2}/d(1/T)$$

from this equation, obtaining⁶

$$\eta - (5/2kT) = -k d \ln (i/T^2)/d(1/T) \quad (10)$$

The derivative in the right member is recognized as the "constant" $-b$ of Eq. (5) where $\alpha=2$. It is to be emphasized, however, that the present derivation puts no requirement on that derivative. This derivation is independent of any assumption regarding the peculiar emitting properties of the surface and is valid whether or not Eq. (5) is valid. For convenience, and at the same time to distinguish between the derivative in Eq. (10) and b , we shall denote the derivative by $-b'$, so that

$$\eta = kb' + (5kT/2) \quad (11)$$

Now, combining Eqs. (9) and (11) in accordance with Eq. (10) we find

$$\eta_s = kb' - \eta_c + 2kT \quad (12)$$

⁶ The simplest procedure is to plot $\ln i$ against $1/T$; then Eq. (12) becomes $\eta_s = kb'' - \eta_c$ where b'' is the slope of that curve.

Davisson and Germer⁷ have measured both kb'/ϵ and η_s/ϵ for the same tungsten wire. They found the former to be -4.48 v. and the latter -4.91 v. For $T = 2270^\circ\text{K}$ $2kT/\epsilon = -0.391$ v., so that $-\eta_s/\epsilon = 4.48 - 4.91 + 0.39 = -0.04$ v. This value is less than the probable error of the measurements. Thus the surface heat of charging of tungsten is at most very small. We have already given the evidence that the surface heats for pure metals differ by amounts small compared to the work functions. It follows, therefore, that the surface heat of charging for all pure metals is probably but a small fraction of the work function.

III. THE HEAT OF CHARGING OF OTHER SURFACES

All the theoretical results obtained so far are directly applicable to surfaces bearing thin films of thorium, caesium, other alkali metals, etc., with the simplification that the Peltier heat can be eliminated if the junction of two metals be avoided by using the pure surface of the metal opposite the film-bearing surface. No measurements on the cooling effect of the evaporation of electrons from such a film are available so that only the difference of two surface heats can be calculated using Eq. (7). But in accordance with our conclusion regarding the magnitude of the surface heat of charging for pure metals we shall assume that for tungsten it is zero. Then, for a film, F , on tungsten Eq. (7) reduces to

$$\eta_{sF}/\epsilon = (k/\epsilon)T \ln (A_F/A_0) \quad (13)$$

This may be immediately applied to the following thermionic emission constants for the complete surface films listed with the results given in the

Type of surface	Mean temp. of observations	A	b	$-\eta_s/\epsilon$
Th on W ⁸	1500°K	3	30,500°	-0.39 v.
Ce on O on W ⁹	650°K	0.001	8,300°	-0.62 v.
O on W ⁹	1600°K	5×10^{11}	107,000°	+2.92 v.

last column. This contains the calculated surface heat in volts at the temperature given in column 2. The signs show that charging the surface positive is attended by the evolution of heat in the case of Th on W, for example, and by the absorption of heat in the case of O on W. The values for the surface heats calculated here are large enough to insure decisive results from cooling effect experiments performed on emitters of these types.

Another class of surfaces to be considered are those of the coated type. Here the coating is more than a surface, it constitutes a layer many molecules deep. Accordingly the cooling effect includes a Peltier heat, so that

$$\eta_c = \eta_{pT} + 2kT + \epsilon P_{pT} c \quad (14)$$

⁷ Davisson and Germer, Phys. Rev. 20, 300 (1922). For comparison with their notation $kb' = \phi_0$.

⁸ From data to be published shortly by S. Dushman. Values of A and b now published⁹ are 7 and 31,200 respectively, giving -0.28 v. for $-\eta_s/\epsilon$.

⁹ K. H. Kingdon, Phys. Rev. 24, 510 (1924).

Now

$$\eta_p = \eta_{pt} + (5kT/2)$$

as before, whence

$$\eta_p = \eta_c + (kT/2) - \epsilon P_{Pt} c$$

giving

$$\eta_s = \eta - \eta_p = kb' - \eta_c + 2kT + \epsilon P_{Pt} c \quad (15)$$

by use of Eq. (11). Experiments by Davisson and Germer¹⁰ show that $kb' - \eta_c + 2kT = 0$. Apparently, then, for the oxide coating

$$\eta_s c = \epsilon P_{Pt} c \quad (16)$$

This result leads to the expectation that $A_c = A_0$ within 3.7-fold where A_c is the A for the coated surface. For, taking surface 2 in Eq. (7) as pure tungsten and surface 1 as the oxide coating we have

$$\eta_s c - \eta_{sW} = kT \ln (A_c/A_w) + \epsilon (P_{WPt} + P_{Pt} c)$$

which, using Eq. (16), reduces to

$$kT \ln (A_c/A_w) = -\epsilon P_{WPt} - \eta_{sW} \quad (17)$$

From the Pt-Ir data again, dE/dT is 2×10^{-5} v./deg. at $1064^\circ K$, one of the standard temperatures used by Davisson and Germer. The Peltier term may therefore amount to $1064 \times 2 \times 10^{-5} = 0.02$ volt. Assuming η_{sW} to be proportional to temperature and to involve a possible error of 100 percent, it may still have a value of 0.04 volt at $1064^\circ K$. The result of the coated filament experiment expressed by Eq. (16) is probably good to 0.04 volt. Adding these possible discrepancies, multiplying by $\epsilon/kT = 11,600/1064$, taking the antilogarithm, and adding 25 percent to allow for the uncertainty in $A_w = A_0$ we obtain the factor 3.7 as noted above.

Estimating further that the error in determining A_c may amount to 70 percent we find finally, that

$$A_c (\text{meas.}) = A_0 \text{ within a factor of 6.3.} \quad (18)$$

Calculation from the experimental data readily gives $A_c (\text{meas.}) = 0.8$. Even 6.3 times this is 12 times too small. Here is a direct contradiction.

But an escape lies perhaps in supposing that only a small fraction of the filament surface is active. On the point of view that the coating is of porous structure and that the emission comes from patches where metal atoms predominate in the surface layer, that hypothesis is not unreasonable though not without difficulties. It would seem, however, that the active patches must be of such a size, that they are separated by distances greater than about 10^{-6} cm, the thickness of the region in which the electric image force is active in determining the escape of electrons. If the separation were less than this, thermodynamics would not recognize the surface as dis-

¹⁰ Davisson and Germer, Phys. Rev. 24, 666 (1924).

continuous, and the A calculated from the data would have to stand. This limitation fixes a lower limit to the average number of atoms in each patch.

The above difficulty leads to the question whether similar conclusions may have to be drawn for the monatomic surface films first discussed. It is known, however, that these films, when "complete", contain the proper number of atoms to cover the surface one deep. In these cases, then, such an explanation would be untenable and the difficulty if it should arise would be a serious one, indeed.

IV. STOPPING POTENTIALS AND THE HEAT OF CHARGING

Further light is thrown on the value of A for pure metals, and therefore on surface heats of charging by some stopping potential experiments of Millikan.¹¹ He cites the equation

$$-\epsilon V_{21} = h(\nu_{02} - \nu_{01}) - V_1 + V_2$$

where ν_0 is the threshold frequency for the emission of photoelectrons, V a stopping potential, and h Planck's constant. Experimentally he has found that the stopping potentials for clean surfaces of Na, K and Li in vacuum are identical. For these metals, then,

$$-\epsilon V_{21} = h(\nu_{02} - \nu_{01}) \quad (19)$$

Now assuming emission equations of the type $i = AT^2e^{-b/T}$ for substitution in Eq. (3), we have

$$\epsilon V_{21} = kT \ln(A_2/A_1) + k(b_1 - b_2); \quad (20)$$

It is reasonable to identify $h\nu_0$ with η_0 , η_0 being the value of η at 0°K. In accordance with conclusions 1 and 2 below, $\eta_0 = kb$. Substituting this and comparing with Eq. (19) we find

$$kT \ln(A_2/A_1) = 0$$

and

$$A_{Na} = A_K = A_{Li}$$

which is in accordance with the idea that $A = A_0$, nearly, for all pure metals, and that η_s is small.

V. THE HEAT OF CHARGING AND FUNDAMENTAL ASSUMPTIONS

The theoretical result expressed in Eq. (7) is quite in accord with certain conclusions of Bridgman¹² regarding, particularly, the significance of the value of A in the electron emission equation.

$$i = AT^2e^{-b/T}.$$

He denotes the specific heat of neutral atoms in the emitting surface which are associated with a single emitted electron by C_{pm} and the specific heat of the positively charged atoms left when the electron evaporates by C_{pp} . Summarizing his conclusions and writing ΔC for $C_{pm} - C_{pp}$, we have:

¹¹ Millikan, Phys. Rev. 18, 236 (1921).

¹² Bridgman, Phys. Rev. 27, 173 (1926).

(1) $A = A_0 = 60.2$ amps./cm² deg², Dushman's¹³ value, and $b = \eta_0/k$ if (a) the entropy of the positively charged atoms left when an electron evaporates is zero at 0°K and (b) $\Delta C = 0$.

(2) $A = A' \neq A_0$ and $b = \eta_0/k$ if (a) the entropy of the charged atoms is not zero at 0°K and (b) $\Delta C = 0$.

(3) A is a function of T and $b \neq \eta_0/k$ if $\Delta C \neq 0$.

(4) None of these possibilities is incompatible with the existence of a surface heat of charging since it is only necessary that

$$\Delta C = -\epsilon\sigma - Td(\eta_s/T)/dT \quad (21)$$

where σ is the specific heat of electricity in the metal. Let us confine ourselves to *first order effects* and consider the following practical cases (a) $A_1 = A_0$, the case of pure metal surfaces. We have shown in this case that $\eta_s = 0$ [Eq. (7) and conclusions from data on pure tungsten] so that $\Delta C = 0$ by Eq.(21). This case thus approximates to conclusion 1.

(b) $A_1 = A' \neq A_0$ but is constant, the case of surface films. Eq. (7) shows that η_s/T is a constant so that again $\Delta C = 0$. This case thus approximates to conclusion 2, but in addition our results show that a constant A which is not equal to A_0 , a charged surface entropy different from zero at 0°K, and a surface heat proportional to temperature are three aspects of one phenomenon.

It is noteworthy, perhaps, that so far as the writers are aware all surface films which maintain a constant structure have a constant value for A . On this basis we must exclude from consideration all experiments in which the emission is not reproducible or in which the surface film is subject to a rapidly established equilibrium which is variable with temperature. This happens, for instance, with adsorbed films of alkali metals on tungsten unless special precautions are taken.

RESEARCH LABORATORY
GENERAL ELECTRIC COMPANY.
JANUARY 3, 1927.

¹³ Dushman, Phys. Rev. 21, 623 (1923).

PIEZOELECTRICITY OF CRYSTAL QUARTZ

By L. H. DAWSON

ABSTRACT

Piezoelectricity of crystal quartz at constant temperature.—Experimental measurements with the quadrant electrometer of the distribution of the piezoelectric charge over the surface of a quartz crystal in a plane normal to the optic axis were found to vary in such a manner as to produce six regions of charge, three positive areas alternating with three negative. The areas had definite geometrical relations to the electric axes and therefore these facts yielded a new and accurate method of determining the directions of the electric axes in crystal quartz. In planes containing the optic axis there was a region of positive charge separated by a line in the direction of the optic axis from a region of negative charge.

Variation with temperature of the piezoelectric effect in quartz.—The piezoelectric effect increased by 20 percent from room temperature to 60°C and decreased thereafter, reaching zero at about 573°C. Cooling curves showed a lag.

Variability of the piezoelectric effect.—The piezoelectric charge produced on different specimens or on different areas of the same specimen, all specimens being optically perfect, varied from large positive values of charge to large negative values. In general, the surface of the crystal quartz produced piezoelectric charges of the same sign, but of varying magnitudes. The charge measured over the entire surface of a crystal appeared to be the average of the effects of the elementary areas. The specimens in the present experiments varied on the negative side of the crystal from 5.8×10^{-8} to 7.1×10^{-8} e.s.u./cm²×dyne, while on the positive side the variation was from 4.9×10^{-8} to 6.4×10^{-8} e.s.u./cm²×dyne. These numbers are not far from the accepted value of 6.3×10^{-8} e.s.u./cm²×dyne, of the "piezoelectric constant" of P. and J. Curie. Such variations are in keeping with recent x-ray investigations on the imperfections of crystals which indicate that crystals are mosaics of an elementary perfect struture.

INTRODUCTION

A N investigation perhaps more extensive than has been hitherto attempted of the piezoelectric effect in crystalline quartz is described in the following pages. The experiments have been greatly facilitated by exceptional opportunities existing in this laboratory for the selection and cutting of samples of quartz. The general laws of piezoelectric action, already well established, have been corroborated in full but in addition many new and unsuspected facts have been discovered. The theory of the piezoelectric effect available at present, although adequate for a description of the more general laws, is apparently incapable of coping successfully with the new phenomena. It appears that the formulation of a complete theory must await a more comprehensive understanding of the molecular structure of quartz. Further, the piezoelectric effect at various temperatures has been measured.

At the outset we may call to mind that a crystal of quartz is in the form of a hexagonal cylinder surmounted by a hexagonal pyramid; the faces of

the crystal, which may vary in length and breadth, lie at definite angles with each other. In Fig. 1, *JEGK*, *GDLK*, *DLMF*, *MNHF*, *HNIC* and *CIE* are the sides of the hexagonal cylinder, the angle between any two adjacent sides is 120° . The faces of the hexagonal pyramid *JKLMNIA* lie at an angle of $38^\circ 13'$ to the faces of the cylinder. The quartz crystal, a section of which is shown in Fig. 1, has four axes of symmetry namely, *AB*, *CD*, *EF* and *GH*. *AB* is called, in crystallographic terms, the trigonal axis, as there exists three symmetrical positions of the crystal as it is rotated about this axis. *AB* is also called the optic axis, because along this direction the crystal has unique optical properties. *CD*, *EF* and *GH* are digonal axes of symmetry, for there are only two positions of symmetry as the crystal is rotated around each of these axes. *CD*, *EF* and *GH* are known as the electric axes, since a pressure applied to the crystal parallel to these directions produces piezoelectric polarization in the same direction.

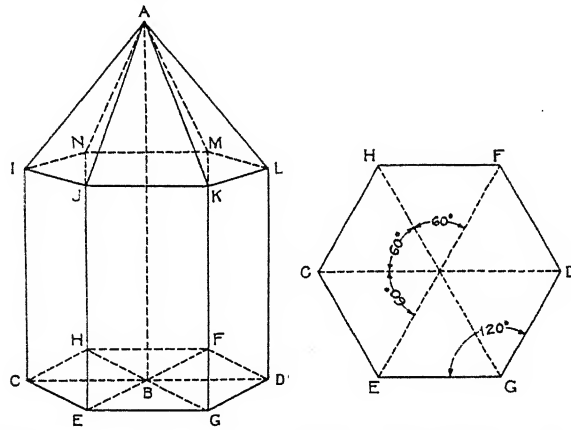


Fig. 1. A section of a quartz crystal showing the direction of the optic and electric axes.

No complete historical summary of the many researches on the piezoelectric phenomenon will be attempted here, but some of the more important papers may be mentioned. We pass over the early qualitative experiments of W. C. Roentgen¹ and direct attention to the more quantitative investigations of P. and J. Curie² in which were first brought out the laws governing the piezoelectric effect in quartz. Their studies made on a rectangular parallelopiped of quartz cut in such a manner that one of the electric axes was perpendicular to one of the faces, led them to conclude that a force applied along the electric axis produced a charge on the faces perpendicular to this axis that was directly proportional to the force, a positive charge accumulating on one of the faces and an equal negative charge on the opposite face. A reversal of the sign of the force produced a reversal of the charges. The magnitude *K* of the charge, was found to be 6.32×10^{-8} esu/dyne cm². This has been the accepted value. The present investigation shows that this

¹ Roentgen, Ann. d. Physik und Chemie, NF19-20, 513 (1883).

² P. and J. Curie, Comptes rendus 91, 294 (1880).

value is not a constant for all quartz but varies very materially for different specimens of optically perfect quartz. This is in keeping with the general ideas of crystal imperfections as discussed later.

W. Voigt³ has developed theoretical formulas for the piezoelectric charges in terms of the piezoelectric and elastic constants of the quartz. His formulas agreed with the experimental results of P. and J. Curies and from their piezoelectric constant he was able to deduce the various piezoelectric constants of the equations for quartz.

Recently W. Bragg⁴ and R. E. Gibbs⁵, from their x-ray studies of the molecular structure of crystal quartz have explained the piezo-electric effect as a distortion of the uniaxial nature of the crystal; while the production of pyroelectricity is due to the change of structure towards or away from hexagonal symmetry.

EXPERIMENTAL DETAILS

The apparatus shown in Fig. 2 consisted of a Compton electrometer *A* with a sensitivity of about 0.004 V/mm suitably shielded by an earthed brass cylinder *B*. The quartz *C*, under investigation, was placed upon the circular platform *D*. This platform was fixed in a horizontal position in such a manner that it could be rotated about the vertical axis *G* and the

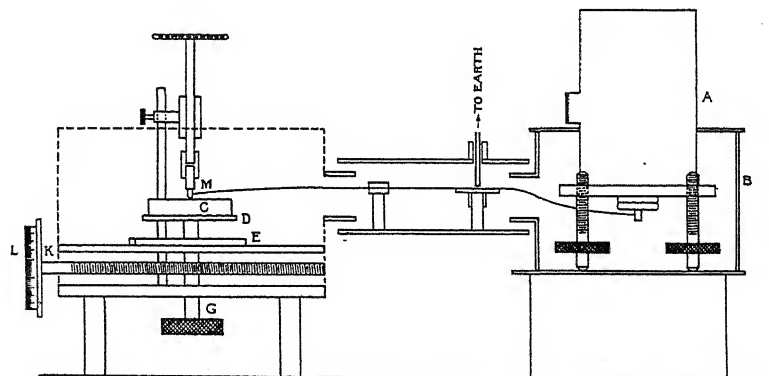


Fig. 2. Apparatus for the investigation of the piezoelectricity of quartz.

amount of rotation measured by the circular scale *E*. A longitudinal motion could be given the platform *D* by the screw *K* and measured by the divided head *L*. Thus any point of the quartz could be brought under the copper contact point *M*. The contact point was connected to the electrometer and insulated throughout by fused quartz. The apparatus was thoroughly shielded electrically and properly insulated switches were placed in the system. In some of the experiments, it was found desirable to apply or release the pressure on the quartz in a direction parallel to the plane of the

³ Voigt, Ann. d. Physik u. Chemie, NF55, 701 (1895).

⁴ Bragg and Gibbs, Proc. of Roy. Soc. A109, 405 (1926).

⁵ Gibbs, Proc. of Roy. Soc. A110, 443 (1926).

platform *D*. To accomplish this an instrument was designed in which a quick application or release of pressure to the contact point could be made by a suitably actuated cam.

In order to raise the quartz to any desired temperature an electric resistance furnace with a metal core was constructed which could be placed over the quartz and the core earthed, thus shielding effectually the quartz and contact point. To measure the temperature a calibrated chromel-nichrome thermocouple was inserted in the furnace with the quartz.

The capacity of the system which varied during the investigation from 34 m.m.f. to 41 m.m.f. was compared with the capacity of a standard condenser by the heterodyne beat method, the measurements being reliable to less than one percent.

PIEZOELECTRIC EFFECTS IN THE DIRECTION OF PRESSURE

Experiments were undertaken to determine the character of the distribution of charge over the surface upon which the pressure was applied. Specimens of optically perfect quartz were selected and cut in such a manner that the electric axis was normal to the large face of a parallelopiped $25 \times 28 \times 1$ mm. Each crystal was placed on table *D*, Fig. 2, and explored over the largest faces by releasing 1000 grams pressure from the contact point which had an area of about 0.1 mm^2 .

In general one side of the crystal would give positive deflections while the opposite side gave negative deflections. Small areas of negative charge were often found on the faces which gave positive deflections over most of the face; and corresponding areas of positive deflection were found on the negative face. Large deflections might occur at the center of the quartz or at the edge and the deflection for one crystal was often twice that of another crystal. There seemed to be no uniformity of results.

The question arose whether such a distribution was of permanent character. To answer this a crystal was subjected to a force of about 25 kilograms for 20 seconds and the surface explored and no change in the distribution could be observed. The same crystal was then raised to a temperature of approximately 600°C , thus transforming it to the Beta-quartz. After allowing it to return to the alpha-quartz state, the surface was again explored. Again no change was observed. Thus the distribution seems to be permanent.

To substantiate further the above results, a piece of quartz cut in the above manner and about $150 \times 100 \times 3$ mm was subjected to the exploring test and again the charge was found to vary over the surface. The piece was then cut into three parts and each part explored, but no change could be observed in the character of the distribution of the original charge. Each part was examined optically and observed to be free from twinning and other defects.

These variations in the piezoelectric charge are naturally to be attributed to imperfections in the quartz crystal, although these imperfections may be so minute as to escape detection by the usual examination with polarized

light. All that can be said is that the imperfections might be in the nature of small crystal fragments variously oriented in perhaps a random manner with respect to the large parent crystal, and that these little fragments are small in size, say less than 0.1 mm in their largest dimension. It may be pointed out further that these imperfections may be very small, indeed such as would result from a displacement of a small group of molecules. Recent developments in x-ray analysis of crystals lead to the idea that crystals are not perfectly formed as hitherto supposed^{6,7,8}, but are constituted of a mosaic of more elementary perfect structures, and that the axes of the more perfect crystals are not oriented in the same direction but may vary from a mean position. This explanation may account for the peculiar variation of the piezoelectric charge over the surface of quartz, although surface or volume strains may be contributing factors.

DISTRIBUTIONS OF CHARGE AROUND THE CYLINDRICAL SURFACE OF A CIRCULAR PIECE OF QUARTZ CUT PERPENDICULAR TO THE ELECTRIC AXIS

A cylindrical specimen of quartz 60 mm in diameter and 30 mm thick was cut from a rough piece of quartz free from flaws and twinning, in such a

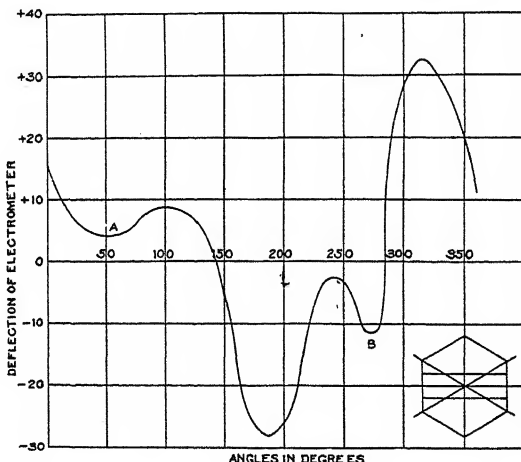


Fig. 3. Distribution of piezoelectric charge over the cylindrical surface of a crystal of quartz in which the plane containing the optic axis and the line perpendicular to one of the hexagonal sides of the crystal is parallel to the ends of the cylinder.

manner that an electric axis was normal to the ends of the cylinder and the optic axis parallel to the plane of the ends, the other electric axes being as shown in Fig. 3. An exploration of the distribution of the charge over the cylindrical surface was carried out by the application of a weight of 1000 gms directly to the exploring point which was placed perpendicular to the surface of the quartz. Care was taken to fasten the quartz cylinder concentrically on

⁶ W. L. Bragg, Darwin and James, Phil. Mag. 1, 897 (1926).

⁷ A. Muller, Nature, 121 (May 22, 1926).

⁸ Burgess, Nature, 116 (July 24, 1926).

table D, Fig. 2 and to have points of reference marked on it in such a manner that the data could always be referred back to the original specimen. The character of the distribution is shown in Fig. 3 where the abscissas are the angles of rotation of the quartz which were read every degree and the ordinates are electrometer deflections.

There appears to be one well defined region of positive charge and another of negative charge, the magnitude of the deflections of each being about equal, but the area of the positive region is larger than that of the negative.

One peculiarity which seems to be characteristic of the curve is the decrease of the curve to a minimum at *A* and then a rise to a maximum and finally a decrease to zero in the positive area and a similar phenomenon taking place in the region of point *B* in the negative area. It may be mentioned that the general characteristics of the curve always remained the same regardless of the method of holding the specimen to the plate.

DISTRIBUTION OF CHARGE AROUND THE SURFACE OF A CYLINDRICAL PIECE OF QUARTZ IN WHICH TWO ELECTRIC AXES LIE AT 60° TO THE END FACES

Next a cylindrical crystal of the same dimensions but cut as indicated in Fig. 4 was placed concentrically on table D. The results of a procedure

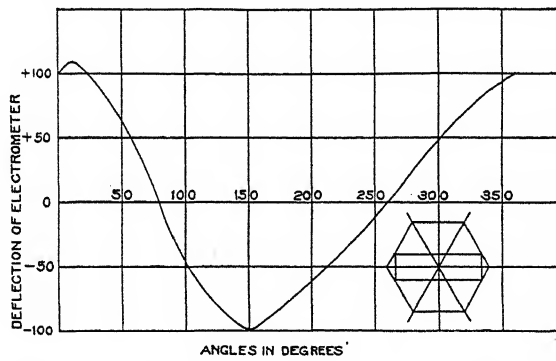


Fig. 4. Distribution of piezoelectric charge over the cylindrical surface of a crystal of quartz in which the plane containing the optic and an electric axis is parallel to the ends of the cylinder.

similar to the previous case is shown in Fig. 4 and it can be seen that there are two well defined regions, one of the positive charge and the other negative. The maximum deflections in both the positive and negative regions are of the same magnitude, but appear to occur about 150° apart and not 180° . The direction of the line dividing these areas lies more or less in the direction of the optic axis.

DISTRIBUTION OF CHARGE OVER THE CYLINDRICAL SURFACE OF A CRYSTAL IN WHICH THE OPTIC AXIS IS PERPENDICULAR TO THE ENDS OF THE CYLINDER

Finally, a crystal of the same dimensions as in the two previous cases was cut from a rough crystal in such a manner that the optic axis was normal to

the ends of the cylinder. The exploration of the cylindrical surface was carried out in a manner similar to the two preceding cases, and the character of distribution of the charge is shown in Fig. 5. There are three positive maxima and three negative and they occur accurately 60° apart and are the same magnitude and alternate in sign. There are six points where the charge becomes zero and they lie 60° apart.

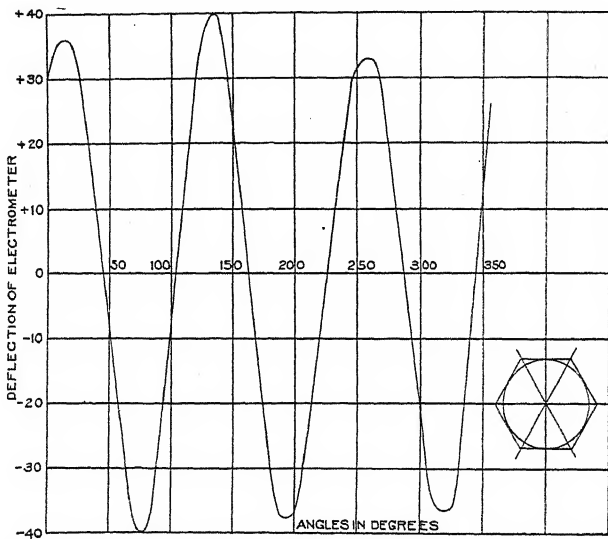


Fig. 5. Distribution of piezoelectric charge over the cylindrical surface of a quartz crystal in which the ends of the cylinder are parallel to the plane of the electric axes.

A METHOD FOR DETERMINING THE ELECTRIC AXES OF A SLAB OF QUARTZ CUT IN SUCH A MANNER THAT THE OPTIC AXIS IS PERPENDICULAR TO ITS PLANE

The above experiment serves as a new and precise method for determining the direction of the electric axes of a piece of quartz cut normal to the optic axis and in which there are no indications of the crystal form. The rough piece of quartz must first be examined for the optic axis and then cut into slabs of the desired thickness in which the optic axis is normal to the plane of the slab. The slab in which the directions of the electric axes are to be determined is placed on table *D* Fig. 2 and an exploration of a cylindrical surface, more or less parallel to the optic axis, is carried out and the points of either maximum or minimum deflection observed. In most cases the latter is preferable as being more accurately determined. In case two diametrically opposite points can be determined, it is only necessary to draw a line joining them, but in case of the absence of the opposite point the lines must be drawn in the direction of pressure. Now it must be remembered that the direction of production of zero charge lies normal to the electric axis of the piece; therefore it is only necessary to draw lines perpendicular to the observed lines to locate the electric axis.

In many cases that may arise it is impossible to find a surface on the quartz which will be nearly normal to the direction of pressure; then it is possible to produce such a surface by grinding a semi-cylindrical notch in the side of the quartz in such a manner that the generator of the semi-cylindrical surface is parallel to the optic axis. Thus placing the quartz on the table *D* in such a manner that the center of the notch coincides with the center of rotation of the table the exploring point can be brought in normal contact with this surface.

Many trials were made with this procedure both on samples of quartz in which faces were present and others in which faces were absent. In either case the electric axis could easily be determined within 2° .

MEASUREMENT OF THE MAGNITUDE OF THE PIEZOELECTRIC EFFECT

Samples of quartz $28 \times 25 \times 2$ mm and $28 \times 25 \times 1$ mm were cut with an electric axis normal to the 28×25 side and the two faces in contact with the electrodes parallel to each other within .025 mm. Forces of 50, 100, 200, 500, 1000 and 2000 grams were applied to each in the direction of the electric axis and in such a manner as to be equally distributed over the entire surface of the crystal. It was found after a few experiments that more consistent results could be obtained by sputtering the surfaces of the quartz in contact with the electrodes with platinum. Four samples of the results obtained are given in Table I and are representative of the results obtained in many trials on different crystals.

TABLE I

Crystal Number	Dimension in mm of surface in con- tact with electrodes	Charge (esu/cm ² dyne) $\times 10^8$	Date	Temp. °C
1 (a)	27×25	(-6.27±.23)	June 10	19.5
	27×11.5	(-6.37±.11)		24
	16×12	(-7.18±.16)		24
	11×8.5	(-6.89±.10)	" 28	24
	12×12	(-7.11±.16)	July 1	21
	11.5×12.5	(-6.43±.18)	" 1	21
2 (a)	27×25	(-6.05±.15)	June 11	19.5
	27×25	(-5.88±.12)		21
	27×25	(-6.16±.16)		19.5
	27×25	(-6.42±.30)	" 17	19.5
	27×25	(+4.94±.40)	" 17	19.2
	27×25	(+5.38±.04)	" 19	19.0
	27×25	(+5.47±.26)	" 21	19.0
3	27×25	(+4.99±.04)	June 28	24
4	27×25	(+6.41±.05)	June 28	24

Crystal number 1 was first explored by the point method and it was found that while each surface produced charges of like character there appeared to be a variation of 250 percent in the magnitude of the piezo-

electric charge. No regularity of distribution could be detected on any of the crystals.

The crystal was then subjected to test for the production of piezoelectric charge over the entire surface. The resulting charge is given in Table I, crystal I (a). The crystal was next cut into three pieces of unequal size and the piezoelectric charge of each measured with the resulting charge as given in (b), (c), (d), Table I. The largest of these three pieces was cut into two pieces and the charge determined (e) and (f), Table I. It can be seen that the charge produced varies very markedly among the separate pieces and that the charge for the whole piece is smaller than that for any one. No explanation of this peculiarity is available. To explain this phenomenon satisfactorily it will be necessary to investigate more samples of quartz; further work on this is in progress.

In order to show the accuracy with which the measurements could be repeated, crystal number 2 was measured on different days and under as nearly identical conditions as possible. Both the positive and negative faces were tested with the result that the charge on the positive face appeared to be uniformly smaller than that on the negative as is shown in crystal 2(a), (b), (c), (d), (e), (f), (g) of Table I. The results taken for the different days on the negative side of the quartz agree with each other within the limit of error that one would expect in this type of experiment, and the same may be said of the positive side.

As an example of the difference of charge produced on different samples of quartz, 3 and 4 of Table I are crystals cut from optically perfect material in as nearly the same manner as possible. They were subjected to test within a very few minutes of each other thus insuring as nearly identical conditions as possible, and it is seen from the table that they differ in charge by a large amount. This appears to be typical of the behaviour of quartz and is perhaps to be explained by the imperfections in crystal structure mentioned in an earlier paragraph.

TEMPERATURE COEFFICIENT OF THE PIEZOELECTRIC EFFECT OF QUARTZ

In the experiment on the variation of the piezoelectric effect with temperature, the specimen was placed on table *D*, Fig. 2 and the electric furnace placed over it. The apparatus was suitably shielded electrically and the temperature measured by a chromel-nichrome thermocouple. The charge was produced by lifting a 500 gm weight from the quartz. The temperature was varied by convenient intervals to a point well above 573°C, thus passing the transformation point of α -quartz to β -quartz. The apparatus was brought to the desired temperature and allowed to stand until temperature equilibrium conditions had been reached. Six readings were taken and the mean of the six was used as the recorded result. Two crystals from the different pieces of quartz were used.

The curves in Fig. 6 exhibit the results, where the abscissas are the temperatures of the quartz and the ordinates are electrometer deflections. The upper curves were taken with ascending and the lower with descending

temperatures. It is seen that the curves for both crystals are of the same character, starting from approximately the same value at room temperature and rising to a maximum at about 60°C. From the maximum the curves descend slowly until a temperature of about 300°C is attained. Beyond this point they descend rapidly, reaching low values in one case at a temperature of 440°C and in the other case at 480°C. Beyond these points the piezoelectric effect is extremely small and in the neighborhood of 550°C has practically disappeared.

Upon cooling no deflection of the electrometer could be detected until the apparatus had cooled down to 280°C, and then there appeared a very rapid rise to a maximum value at 60°C and from here to room temperature a decreasing charge was observed. The maximum reached on cooling was

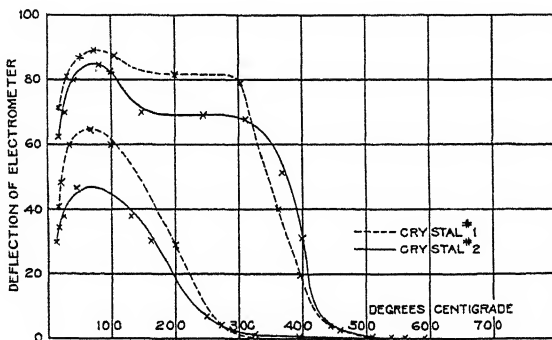


Fig. 6. Curves showing the effect of temperature on the piezoelectric effect in quartz.

approximately one half in one case and two thirds in the other of the maximum reached on heating, and the resulting piezoelectric effect at room temperature after cooling was about one half of the value of that before subjecting the crystal to heating. It was found that after the apparatus had remained untouched for 24 hours that both crystals had returned to their previous piezoelectric condition.

It was thought that the peculiarities of the curve might be due to the oxidation of the copper electrode, although this was very slight, but on substituting an aluminum rod for copper the same results were obtained.

The maximum in the curve has no evident explanation and was not expected. The lag in the piezoelectric effect however, is a phenomenon to perhaps be expected, since other effects of similar nature, for example in the moduli of elasticity, have been observed in the transformation of β -quartz to α -quartz.

I wish to express my thanks to Dr. E. O. Hulbert for suggesting the problem and for his keen interest and help in the work.

HEAT AND LIGHT DIVISION,
NAVAL RESEARCH LABORATORY,
September 10, 1926.

THE TRANSFORMATION PERIOD OF THE INITIAL POSITIVE AIR ION

BY LEILA M. VALASEK

ABSTRACT

Time constant of transformation from initial to final positive ion. Erikson has shown that when first formed in air at atmospheric pressure the positive ion has a mobility of 1.87 cm/sec. per volt/cm, but that it quickly changes over into an ion having a mobility of 1.36. By a method essentially the same as that used by Erikson, a quantitative study was made of the rate of transformation. It was found to be dependent on the humidity of the air. At a relative humidity of 32 percent, the half-value period was found to be 0.0132 sec.; at a relative humidity of 80 percent, it is 0.0354 sec.

IT HAS been shown that in the case of air and certain other gases the products of ionization consist of a negative ion, which retains its identity for a considerable time, and an "initial" positive ion, which is quickly transformed into a less mobile structure, the "final" positive ion.^{1,2} Rough estimates of the value of the time rate of the transformation of the initial positive ion have been given by Grumann² and by Tyndall and Grindley.³ The present research was undertaken for the purpose of making a more exact evaluation of this transformation constant.

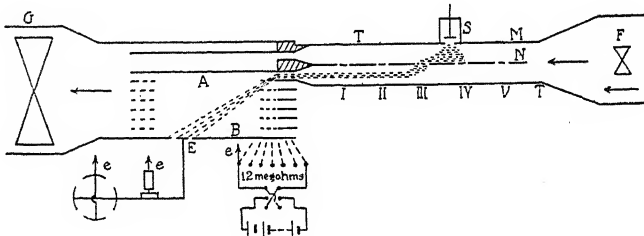


Fig. 1. Diagram of apparatus.

Measurements were made by means of an apparatus similar to that employed by Erikson.^{1,2} The ionic spectrum was obtained by passing a narrow stream of ionized air into the moving air between two plates, *A* and *B*, Fig. 1, between which was maintained a difference of potential. In the lower plate was a narrow insulated strip, *E*, connected to an electrometer. The ions, moving with the air stream in a horizontal direction and being deflected vertically by the electric field, were made to fall on *E* by proper adjustment of wind velocity and voltage. A curve showing the ionic mobility spectrum was obtained by plotting electrometer readings

¹ Erikson, Phys. Rev. 20, 117 (1922); 24, 622 (1924); 26, 465; 26, 625; 26, 629 (1925).

² Erikson, Phys. Rev. 24, 502 (1924).

³ Tyndall and Grindley, Proc. Roy. Soc. A110, 358 (1926).

against the voltage at constant wind velocity (See Fig. 2). The ions were formed in the upper half of the double tube T , Fig. 1, by alpha-rays from a polonium plate in the chamber S . Five windows were cut in the partition N dividing this tube, and S was placed so that ions entered the lower half of T through one of these windows, the others being, of course, closed. Between M and N a potential difference of 180 volts was maintained, to draw the positive ions vertically downward. Before obtaining the curves presented in this paper, a set of readings was taken at the air velocity used in this experiment, with a constant potential difference between A and B , in which the position of S was varied with respect to one of the windows. Then, in obtaining the curves of Fig. 2, the position of S with reference to a window was chosen to give the maximum possible current. It was found that with this arrangement about 97 percent of all the ions entering the lower half of the tube T were positive in charge. Hence, no correction was made for the loss of positive ions by recombination with negative ions in their passage into the measuring apparatus. Moreover, since the times

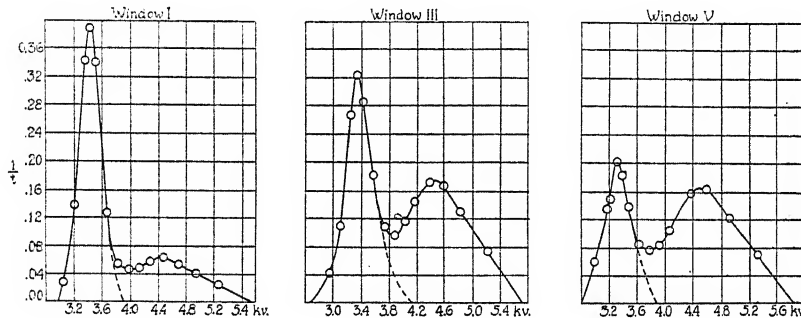


Fig. 2. Spectra of positive air ions of different ages.

here involved were very short, the number of positive ions lost by diffusion to the walls was considered negligible. To measure the current due to ions of different ages, a set of curves was obtained by placing S , successively, at each of the five windows. The relative ages of the ions from these windows were calculated from the wind velocity in T . To measure the latter, a small fan anemometer was placed at F , Fig. 1, and the velocity in T was deduced from its readings by a comparison of the cross-sectional areas of the two parts of the tube. The calibration of the anemometer was checked at the U. S. Bureau of Standards.

One may define λ , the time constant of the transformation, by the equation

$$dn/dt = -\lambda n. \quad (1)$$

Its integral is

$$n/n_0 = \exp(-\lambda t). \quad (2)$$

Here n_0 is the number of initial positive ions formed per second by the ionizing agent, and n is the number of these ions still unchanged after the

passage of a time t . Now, in Fig. 2 the ordinates are proportional to the number of ions reaching E per second. The area under the entire curve is accordingly proportional to the total number of positive ions entering the lower part of the tube T per second. Thus, the ratio n/n_0 can be taken as the ratio of the area under the first maximum of the curve to that under the entire curve. These areas were measured for all the curves with a planimeter.

In Fig. 3 are plotted as ordinates the values of $\log_{10} n/n_0$ obtained from the curves of Fig. 2. The relative "age" of the ions, plotted as abscissa in each case, is the time of passage of the ions from the window in question

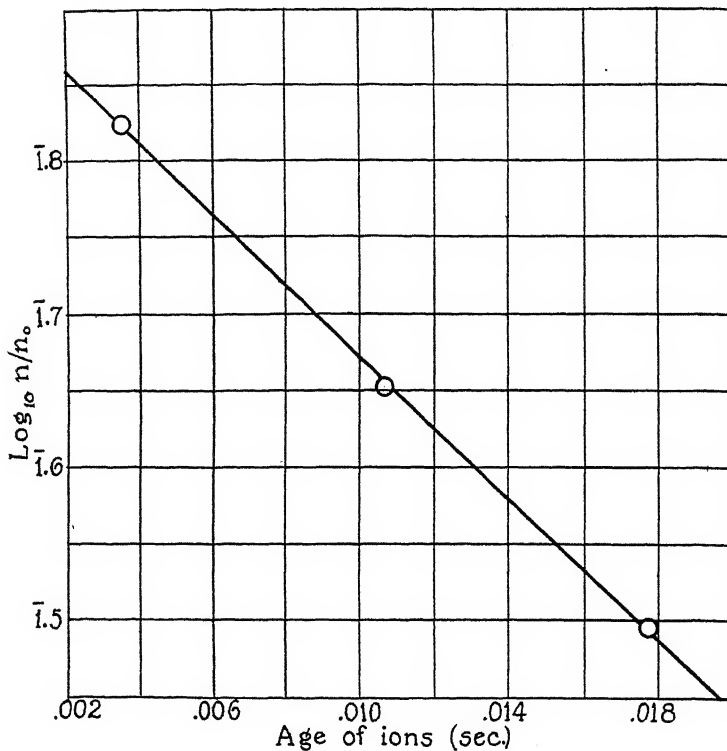


Fig. 3. Dependence of the logarithm of the relative number of initial positive ions on the age of the ions.

to a point 5 cm in front of window I. The actual time of passage to electrode E was not computed, since only the difference in times from the various windows is needed in determining λ .

In accordance with Eq. (2), λ is the product of $\log_e 10$ and the slope of the straight line of Fig. 3. The result of this calculation is

$$\lambda = 52.6 \text{ (sec.)}^{-1}$$

The half-value period is, accordingly,

$$\log_e 2/\lambda = 0.0132 \text{ sec.}$$

These curves were obtained at a humidity of about 32 percent.

It was found, however, that the value of λ is considerably affected by humidity conditions.³ At a relative humidity of 80 percent, for example, $\lambda = 19.6 \text{ (sec.)}^{-1}$, giving, as half-value period, 0.0354 sec. The values of the humidity here cited are those recorded at the U. S. Weather Bureau on the days on which the work was done. The windows of the room were kept open enough to assure that the humidity of the room was nearly the same as that outside. In the course of a set of readings, the humidity did not vary by more than 25 percent.

In seeking a conception of the mechanism of the humidity effect on the rate of transformation, it would seem natural to assume that the final ion has a greater tendency to load up with the water molecules than has the initial ion. For, if the curves were not carried to voltages high enough to include these heavy ions, the ratio n/n_0 would obviously be abnormally large. But this explanation can hardly be the correct one, for the results of this experiment do not in any way point to a successive decrease in the value of n_0 at the different windows. The data are, however, too meagre at present to point the way to a clear-cut picture of the action of the water molecules on those of the air.

The writer is indebted to Professor H. A. Erikson for his guidance in the course of this research. It was at his suggestion that the problem was undertaken.

PHYSICAL LABORATORY,
UNIVERSITY OF MINNESOTA,
November, 1926.

RESONANCE IN ALTERNATING CURRENTS CONTAINING A SINGLE HARMONIC

BY FREDERIC H. MILLER

ABSTRACT

Current-frequency relations in alternating current circuits as affected by harmonics.—*Series circuit.* The form of a current-frequency curve depends only upon the ratio $K = R^2 C/L$ (herein designated as the “resonance factor”), and the ratio a of the harmonic to the fundamental e.m.f. amplitude. Special cases are considered, particular attention being given to the third harmonic, and a method for plotting generalized current-frequency curves is outlined. As K increases, the value of a , below which the $I-f$ curve can have only one maximum, increases from zero to unity; for each harmonic n , there is a definite value of K given by $K_E = (n-1)^2(n^2+4n+1)/n(n^2+1)$, above which there can be only one peak to the curve no matter what the value of a . *Parallel circuit.* The current-frequency curve has only one minimum, regardless of the number of harmonics, but the position of the minimum point is dependent upon the number and amplitude of any harmonics present. A simple method of plotting generalized current-frequency curves is given, and the inductive and condensive currents briefly discussed. For each circuit, utilizing the relations obtained analytically, there is given an experimental method for determining the amplitudes of fundamental and harmonic in an e.m.f. wave.

THE phenomenon of resonance in a circuit having impressed upon it a sinusoidal e.m.f. is a familiar one, and full discussions of it have been presented by many writers. But the current-frequency relations as affected by the presence of harmonics in the voltage wave, although often met with in practice, are not so well known. It is the purpose of this paper to investigate some of these relations for the case in which one harmonic, of order n , is present in the applied e.m.f. Methods of analysis are here merely outlined, and the conclusions arrived at, stated.¹

The assumption is made that as the frequency varies, the ratio of the amplitudes of the two e.m.f. components remains a constant. The term “resonance” will be used in a broad sense, to denote the condition which obtains whenever the current becomes a maximum for the series circuit, or a minimum for the parallel circuit.

I. SERIES CIRCUIT

When a resistance R , a self-inductance L , and a capacitance C are connected in series, and an e.m.f. made up of the two components E_1 and E_n is impressed upon the circuit, the current is given by

$$I^2 = \frac{E_1^2}{R^2 + (L\omega - 1/C\omega)^2} + \frac{E_n^2}{R^2 + (nL\omega - 1/nC\omega)^2}, \quad (1)$$

¹ A complete formulation may be found in the writer's thesis having the same title, in the Cornell University Library.

where ω is the angular velocity, equal to 2π times the frequency f . Now when E_n is sufficiently large, the current-frequency curve will ordinarily have two maxima and one minimum, and will be similar in form to the upper curve ($a=1$) of Fig. 1. Hence by equating $dI/d\omega$ to zero, the angular velocities corresponding to the three points of zero slope will be represented by roots of the resulting equation. By taking the derivative in this manner, and employing the substitutions

$$K = R^2 C / L, \quad x = nLC\omega^2, \quad a = E_n / E_1,$$

there will be obtained the relation

$$\begin{aligned} & n^2(n^2 + a^2)x^6 + 2n^3(K - 2)(1 + a^2)x^5 + [n^2(K^2 - 4K - n^4 + 6) \\ & + (n^4K^2 - 4n^4K + 6n^4 - 1)a^2]x^4 - 2n(n^4 - 1)(K - 2)(1 - a^2)x^3 \\ & - [(n^4K^2 - 4n^4K + 6n^4 - 1) + n^2(K^2 - 4K - n^4 + 6)a^2]x^2 \\ & - 2n^3(K - 2)(1 + a^2)x - n^2(1 + n^2a^2) = 0. \end{aligned} \quad (2)$$

From this it is evident that the form of a current-frequency curve is dependent not only upon the relative amplitude of the harmonic e.m.f., but also upon the ratio $K = R^2 C / L$, which may therefore be designated as the "resonance factor". However, no change is produced in the curve when any of the three circuit constants are varied, provided this ratio K is preserved.

Physical considerations show that there may be no more than three positive roots of Eq. (2), and, depending upon the coefficients, there may be only one, two equal ones and a greater one, or three distinct positive roots. As a increases from zero to unity, these three conditions will successively prevail. When the value of a is such that two equal positive roots are obtained, K being given, then the $I-f$ curve will have a horizontal inflection point and one peak; this may be called the transition case.

From the symmetrical form of the above equation, it is seen that if $1/a$ be substituted for a , and $1/x$ for x , the equation will remain unchanged. It therefore follows that there are two values of a , one the reciprocal of the other, for each of K such that the current-frequency curve shall have a horizontal inflection point. In the ordinary case, when $a < 1$, the inflection point occurs to the left of the maximum, whereas if the reciprocal value $1/a$ be taken, the amplitude of the n th harmonic e.m.f. will exceed that of the fundamental, and the inflection point occurs to the right of the crest. The former case, a being less than unity, is the one usually met with in practice, and therefore of greater importance; this reciprocal relation has been indicated principally because of its value to the subsequent analysis.

Although it has not been found possible to express algebraically the function connecting K and a in the transition case, critical values of a for various values of K may be found by empirical methods, and, in addition, special cases falling under Eq. (2) may be treated by analytical methods.

By making the same substitutions in Eq. (1) as were employed in the development of (2), there is obtained

$$\frac{LI^2}{CE_1^2} = \frac{1}{x/n+K-2+n/x} + \frac{a^2}{nx+K-2+1/nx} . \quad (3)$$

This mode of expression allows for simpler calculation and plotting; furthermore, the current-frequency curves so drawn for various values of n and K will be perfectly general and may therefore be used in practice for all cases, no matter what the constants of the circuit may be. Such graphing consists in plotting $(I/E_1)(L/C)^{1/2}$ against $x^{1/2} = 2\pi f(nLC)^{1/2}$. Fig. 1 shows a typical current-frequency curve of this generalized form, n having been taken equal to 3, K to unity, and a taken as zero, lower critical value, and unity.

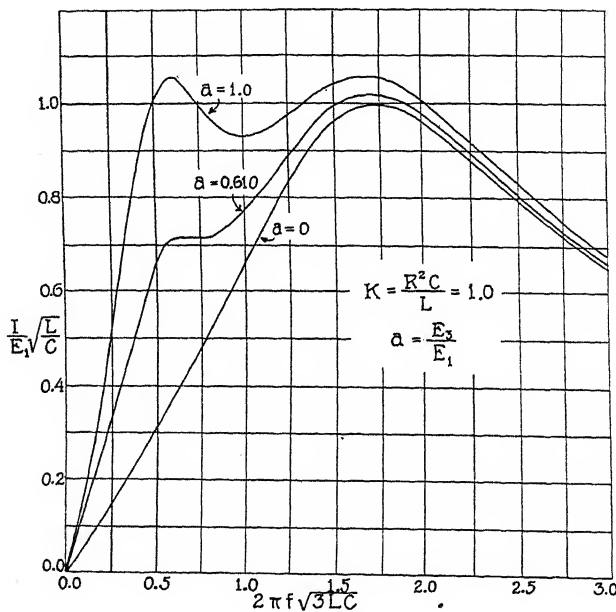


Fig. 1. Generalized current-frequency curves for the series circuit in which K is unity.

For the case of the third harmonic, curves have been drawn for a number of values of the resonance factor; these indicate several important characteristics. The depth of the trough obtained when $a = 1$ becomes less pronounced, and the three points of zero slope approach each other, as K is increased. The curves for the transition cases lie between the other two throughout the frequency range, and recede from the curve of $a = 0$ and approach that of $a = 1$ as the resonance factor becomes larger. Finally, a for the transition cases grows larger and larger as K increases.

In view of the latter statement, we should expect that since the reciprocal relation for a holds in the transition case, there would be a maximum value of the ratio $R^2 C / L$ beyond which there could be only one peak to the current-frequency curve regardless of the relative amplitude of E_n . That this is so is evidenced by the nest of $K - a$ curves shown in Fig. 2. For each value

of K up to the cusp-point of any particular curve considered, there are two reciprocal values of a ; and when the resonance factor is greater than that represented by the cusp-point, there can be no value of a yielding the transition case. Furthermore, if the values of K and a in any given case are such that the point having these values as coordinates lies within the area bounded by the proper curve and the a axis, there will be two maxima to the $I-f$ curve; if this point lies without that area, there will be but one maximum.

Turning now to a consideration of special cases, it will be at once noticed that when $K = 2$, Eq. (2) reduces to a cubic in x^2 , and by applying the condition for equal roots as given in the theory of equations to the resulting relation, the transition value of a is readily obtained. In particular, when

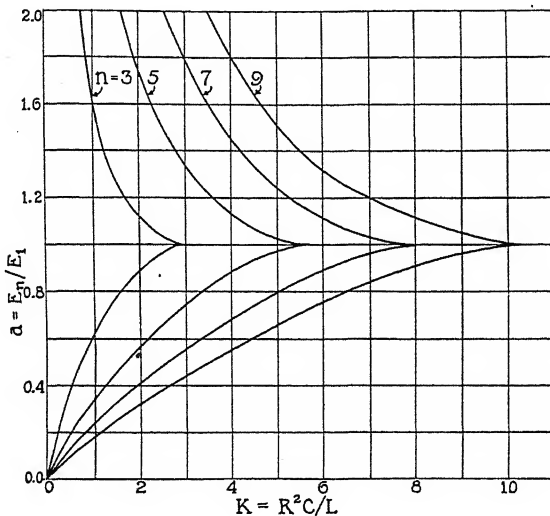


Fig. 2. Relation between K and a in transition cases for the series circuit. n = order of harmonic.

$n = 3$, the most common case arising in practice, we find for a the value 0.8893, or the reciprocal, 1.1245. Again, it is plain that when the resonance factor is zero, which occurs when there is no resistance, a must be zero (or infinite).

Thirdly, and most important of all, the exact limiting value of the resonance factor may also be determined. By putting $a = 1$ in Eq. (2), we get

$$\begin{aligned} &n^2(n^2+1)x^6 + 4n^3(K-2)x^5 + (n^2+1)(n^2K^2 - 4n^2K - n^4 + 7n^2 - 1)x^4 \\ &- (n^2+1)(n^2K^2 - 4n^2K - n^4 + 7n^2 - 1)x^2 - 4n^3(K-2)x - n^2(n^2+1) = 0. \quad (4) \end{aligned}$$

This equation has the roots ± 1 ; dividing through, therefore, by $(x^2 - 1)$, there is obtained after reduction a symmetrical fourth degree equation. Now since $a = 1/a$ in this case, we must have the double root $x = 1/x$; that is, x is unity. Hence substituting $x = 1$ in the fourth degree equation, it will be found that

$$K_E = (n-1)^2(n^2+4n+1)/n(n^2+1). \quad (5)$$

Thus, for all values of n , the resonance factor has a real and rational value when $a=1$ in the transition case. Fig. 3 shows the graph of Eq. (5); it is seen that there is approximately a linear relation between K and n , the resemblance to strict proportionality increasing as n becomes larger. It is particularly significant that the value of the resonance factor below which there may be two maxima to the $I-f$ curve increases as the order of the harmonic present increases.

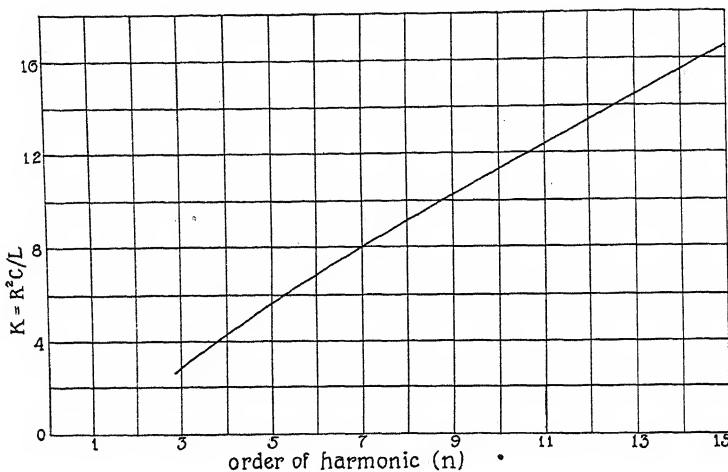


Fig. 3. Relation between K and n in transition cases for the series circuit.
 $K_B = (n-1)^2 (n^2+4n+1)/n(n^2+1)$.

By applying the test for turning points to Eq. (3), it will be found that when $a=1$ and K is less than the value given by (5), the current-frequency curve will always have its minimum at the frequency

$$f = 1/2\pi(nLC)^{1/2}. \quad (6)$$

The above relations are of theoretical interest alone, but in certain cases they may also be used in an experimental determination of the e.m.f. component amplitudes of a wave made up of the fundamental and the n th harmonic. Thus, if the variation in current as the frequency increases from a little below $f=1/2\pi n(LC)^{1/2}$ to a little above $f=1/2\pi(LC)^{1/2}$ is noted for a circuit whose resonance factor is small, and this process repeated for various values of K until the transition point is obtained, the magnitude of a may then be found from the proper $K-a$ curve; hence, if E is the measured voltage, the components will be given by $E_1=E/(1+a^2)^{1/2}$, and $E_n=aE_1$. Even when additional harmonics are present, provided they are small compared to the n th harmonic, the latter may be approximately determined by this method.

II. PARALLEL CIRCUIT

The line current in a parallel circuit consisting of the three branches R , L , and C , is in general given by²

$$I^2 = E^2 [g^2 + (\sigma/L\omega)^2 + (\delta C\omega)^2 - 2C/L], \quad (7)$$

where g is conductance, $1/R$; and σ and δ are the distortion factors

$$\sigma = \left(\frac{E_1^2 + (E_3/3)^2 + \dots + (E_n/n)^2}{E_1^2 + E_3^2 + \dots + E_n^2} \right)^{1/2}; \quad \delta = \left(\frac{E_1^2 + (3E_3)^2 + \dots + (nE_n)^2}{E_1^2 + E_3^2 + \dots + E_n^2} \right)^{1/2}.$$

Differentiating this equation with respect to ω , and setting the derivative equal to zero as before, there is found

$$\omega^2 = \sigma/\delta LC. \quad (8)$$

Thus, no matter what the number of harmonics, there will be only one minimum point to the current-frequency curve, but the resonant frequency

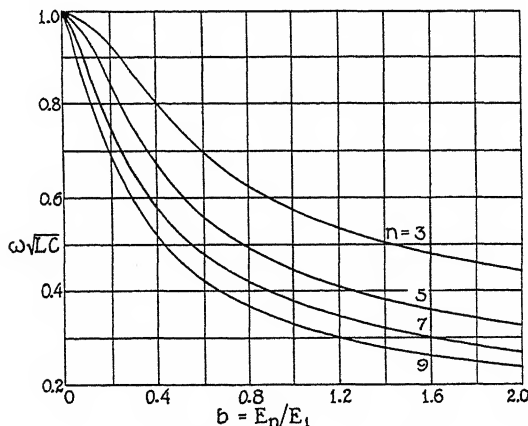


Fig. 4. Relation between b and $\omega(LC)^{1/2}$ for minimum current in the parallel circuit. n = order of harmonic.

depends upon both the orders of the existing harmonics and their voltage amplitudes. Now when only E_1 and E_n are present in the e.m.f. wave, (8) reduces to

$$\omega^2 = \frac{1}{nLC} \left(\frac{n^2 + b^2}{1 + n^2 b^2} \right)^{1/2}, \quad (8')$$

where $b = E_n/E_1$. Fig. 4 shows the relation between b and $\omega(LC)^{1/2}$ for various values of n . It is seen that for a given harmonic, the frequency at which minimum current is obtained becomes less as the ratio b of the ampli-

² For the derivation of this equation, see F. M. Mizushi, "An Analytical and Graphical Solution for Non-Sinusoidal Alternating Currents," Proceedings, A.I.E.E., June, 1915, pp. 1075-1086.

tudes increases. In addition, this frequency is less when n increases, b having some particular value.

Inserting the reduced distortion factors into Eq. (7), there is obtained for the current

$$I^2 = E^2 \left[g^2 + \frac{n^2 + b^2}{n^2(1+b^2)L^2\omega^2} + \frac{(1+n^2b^2)C^2\omega^2}{1+b^2} - 2C/L \right]. \quad (9)$$

Now the differential equations for the series and multiple circuits are of the same form, the only differences lying in the interchange of e and i , L and C , and R and g . Hence, substitutions similar to those employed for the series circuit may be made here; thus, when the expressions

$$K' = g^2L/C, \quad y = LC\omega^2, \quad \text{and} \quad b = E_n/E_1$$

are put into (9), the following simpler form is obtained:

$$LI^2/CE_1^2 = (K' - 2)(1+b^2) + (n^2+b^2)/n^2y + (1+n^2b^2)y. \quad (9')$$

It will be noticed that the compound constant K' is the reciprocal of the resonance factor K used for the series circuit.

Typical generalized current-frequency curves have been plotted from equation (9'), n having been taken as 3, K' as unity, and b equal to both zero and unity. These indicate that the presence of a third harmonic of large amplitude produces a greater effect as the frequency increases beyond the minimum point. Equation (9') also shows that the current at any given frequency becomes greater as K' increases.

The values of current flowing into the inductive and capacitive branches are given by

$$I_L = E\sigma/L\omega; \quad I_C = E\delta C\omega \quad (10)$$

respectively. When only the n th harmonic in addition to the fundamental is present, Eq. (10) may be expressed as

$$LI_L^2/CE_1^2 = (n^2+b^2)/n^2y; \quad LI_C^2/CE_1^2 = (1+n^2b^2)y. \quad (11)$$

These two quantities constitute two of the terms of equation (9'); hence a comparison between each of the branch currents and the line current may be readily made.

In all cases, σ and δ being constant, the inductance current varies inversely, and the condenser current directly, as the frequency. If, therefore, these two currents be plotted against frequency, the resulting curves will be rectangular hyperbolae and straight lines respectively. The slope of the straight lines increases as the number or order of the harmonics increases, so that the current at a given frequency is greater in magnitude. But there is very little difference in the graphs for the inductance current for various

wave forms; for example, if in Eq. (11) we take $b = 0$ in the one case, and $n = 3$ and $b = 1$ in another, the curves will have as equations

$$(I_L/E_1)(L/C)^{1/2} = 1/2\pi f(LC)^{1/2}; \quad (I_L/E_1)(L/C)^{1/2} = 1.054/2\pi f(LC)^{1/2}$$

By the use of curves similar to Fig. 4, the amplitudes of the fundamental and any harmonic may be determined experimentally, just as for the series circuit. Since there is in all cases only one minimum to the current-frequency curve for the parallel circuit, the method is here somewhat more readily applied; but on the other hand, the presence of a number of harmonics is not made so evident.

DEPARTMENT OF PHYSICS,
CORNELL UNIVERSITY,
January 20, 1927.

THERMO-ELECTRIC EFFECT IN SINGLE CRYSTAL ZINC

BY ERNEST G. LINDER

ABSTRACT

Thermal e.m.f., thermo-electric power, Peltier heat of single crystal Zn against Cu as functions of crystal orientation.—In continuation of previous work data are presented on the thermal e.m.f. against copper of six single crystal wires of zinc, of which the orientations of the main crystallographic (hexagonal) axis with respect to the wire axis, range from 11.4° to 90° . (The average deviation from the mean for these observations is 0.8° .) The temperature interval is from -182° to 475°C . The apparatus designed to enable measurements to be made above the melting point is described in detail.

Thermo-electric power, Peltier heat, and difference of Thomson coefficients for Zn_\perp against Zn_\parallel .—From the data are calculated the thermo-electric power, Peltier coefficient, and difference of the Thomson coefficients for Zn_\perp against Zn_\parallel . The data also provide a test for the Voigt-Thomson law for the variation of the thermo-electric power with crystal orientation. The law seems to be verified within the limits of experimental error for the low temperatures, but the deviations at the high temperatures (300° – 400°) are greater than the experimental errors are thought to be.

Thermal e.m.f. of liquid Zn against single crystal and polycrystalline Zn.—Further, the thermo-electric powers of liquid Zn against solid single crystal Zn of different orientations, and against polycrystalline Zn are given. The value $-7.89\mu\text{v. per deg. for } e_\perp - e_\parallel$ for Zn (polycrystalline) having been found. A theoretical discussion of the thermo-electric effect in polycrystalline substances having different properties along only two of the crystallographic axes, leads to the formula $\bar{\epsilon} = (1/3)(2e_\perp + e_\parallel)$, and indicates that such a polycrystalline metal wire should behave the same as a single crystal wire of orientation 54.5° , the experimental value found being between 65° and 70° . It appears from this formula that polycrystalline Zn may be considered as an alloy of two parts Zn_\perp and one part Zn_\parallel .

INTRODUCTION

IN 1925 the author published a preliminary account¹ of measurements which he was then making of the thermo-electric properties of single crystal zinc. Since that time papers have appeared by P. W. Bridgman² who investigated the thermo-electric properties of Sn, Bi, Cd, Sb, Te, and Zn, from 20 to 100°C for various ranges of orientations, and by Grüneisen and Goens,³ who made similar measurements on Zn and Cd from -253 to 100°C . The work which is described in this paper is a continuation of that previously reported. It consists of measurements with an improved apparatus of the thermo-electric properties of six Zn crystals, over an increased range of both orientation and temperature.

¹ E. G. Linder, Phys. Rev. 26, 486 (1925).

² P. W. Bridgman, Nat. Acad. Sci. Proc. 11, 608 (1925); Proc. Amer. Acad. Sci. 61, 101 (1926).

³ Grüneisen and Goens, Zeits. f. Physik. 37, 378 (1926).

GENERAL METHOD AND APPARATUS

Only in a few details was the general method of investigation different from that usually employed in thermo-electric research. The Zn crystals were prepared by a method similar to that devised by Czochralski,⁴ the apparatus shown in Fig. 1 being used. The electric furnace, *F*, contained the crucible of molten Zn from which the crystal was drawn. The square brass bar, *B*, ran vertically through the two guides, *C*, and was raised at the desired rate by a weight motor which wound up a steel wire, *K*, running over a pulley and fastened to the lower end of *B*. Another steel wire, *L*, ran to a counterbalance. The entire mechanism was mounted on a heavy wooden

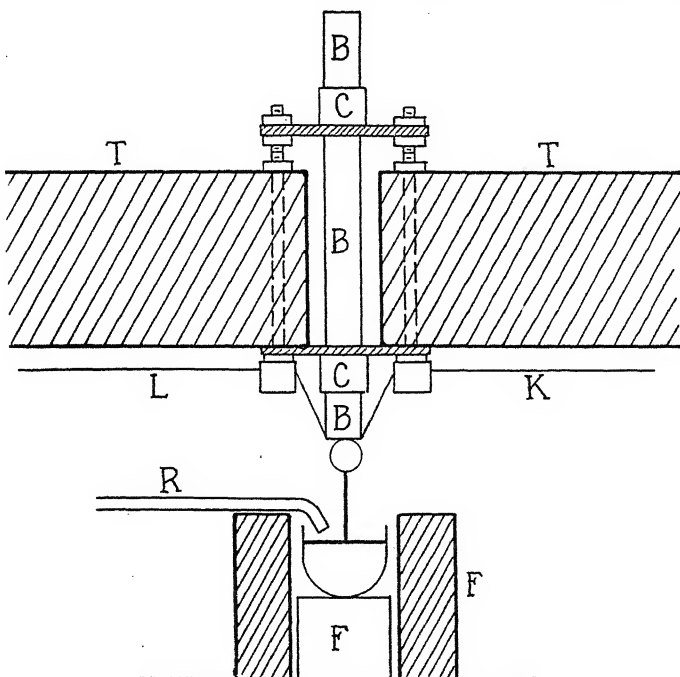


Fig. 1. Apparatus for production of crystals.

support, *T*. In order to regulate the rate of cooling of the crystal, an air current was directed against it through the tube *R*.

The thermal e.m.f. against Cu was measured for various temperature differences by keeping one junction at 0°C and varying the temperature of the other. The essential parts of the apparatus employed for this are shown diagrammatically in Fig. 2. The Zn single crystal, *Z*, was held in a vertical position, its lower end, the hot junction, being at *H*, and the upper end, or cold junction, at *C*. The entire crystal was snugly surrounded by a glass tube, the purpose of which was to protect the crystal and to support it after the temperature at *H* rose above the melting point. *H* was actually a hemispherical Cu block, which closed the lower end of the tube and into

⁴ Czochralski, Zeits. f. Phys. Chem. 92, 219 (1918).

which were fused three wires leading to the binding posts *A*, *B* and *C*. No solder was used to make the hot junction, the crystal being fused directly to the copper by pressing it against *H* while *H* was heated and a zinc chloride flux applied. It was found that the crystal structure was not thus destroyed, but maintained up to the surface of contact with the copper. Obviously solder would contaminate the junction, especially above its melting point, and further, this contamination would cause serious errors since the temperature gradient at *H* was usually very steep. This entire junction was surrounded by fire clay held in a crucible and heated by a bunsen burner. For temperatures lower than that of the room the crucible was removed and the junction immersed in, or placed at suitable heights above, the

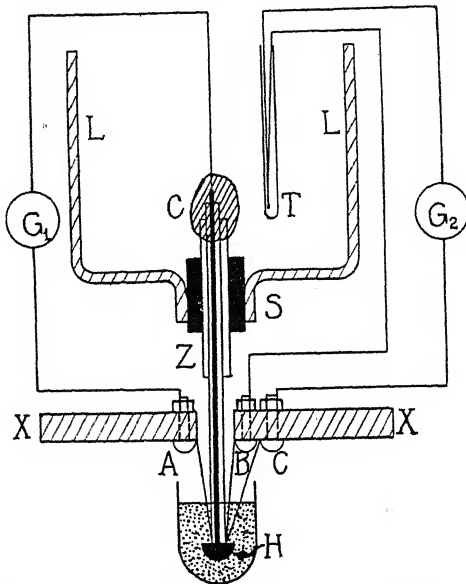


Fig. 2. Apparatus for measuring thermo-electric e.m.f.

surface of liquid oxygen. The wire leading to *A* was of Cu, and constituted the second element of the thermo-electric circuit, *AG₁CH*. *G₁*, a sensitive galvanometer in series with a high resistance, was calibrated in microvolts. The wires leading to *B* and *C* constituted elements of the Cu-Advance, temperature-measuring circuit, *BTG₂CH*. The asbestos board, *X*, served both as a support for *H* and as a shield between the flame and the ice container *L*. The crystal in its glass tube, passing into *L* through a second, larger tube in a rubber stopper, *S*, was soft soldered to the copper wire at *C*, and this junction, together with the ends of the two glass tubes surrounded with a wad of sealing wax.

This apparatus is different from that employed in the previous work, modifications being necessary in order to measure the e.m.f. above the melting point, and also because it was thought that possibly the previous method of sealing in the crystal had introduced some error.

RESULTS

I. Thermo-electromotive force, thermo-electric power and Peltier heat as functions of crystal orientation. The observed values of the thermal e.m.f. against Cu for each of the six single crystals are given in Table I, the e.m.f. being considered positive when it is directed from the hot to the cold junction through the Zn. The data are partially represented in the graphs of Fig. 3

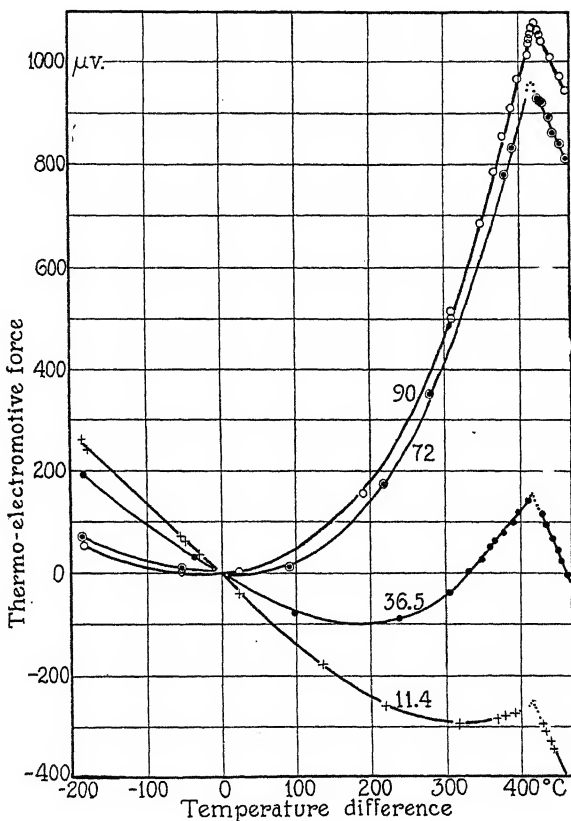


Fig. 3. E.m.f. vs temperature-difference for various orientations. Each curve is labeled with its orientation angle.

orientations 70° and 74° being omitted since their curves are very nearly coincident with that for 72° . The curves of Fig. 3 may be well represented between 0°C and the melting point by empirical equations of the type: $E = At + Bt^2 + Ct^3$, where E is the thermal e.m.f., t the temperature difference of the junctions, and A , B , C , constants characteristic of the individual curves. Bridgman² found that second degree equations represented his results for zinc, but this may be due to his more limited temperature range. Over the same range the writer's results can also be represented by second degree equations. Differentiation of such an equation with respect to t yields the thermo-electric power e .

TABLE I
Observed thermal e.m.f. of single crystal Zn against Cu.

$8, \theta = 11.4^\circ$ $t^\circ C$	$10, \theta = 36.5^\circ$ $t^\circ C$	$7, \theta = 70^\circ$ $t^\circ C$	$11, \theta = 72^\circ$ $t^\circ C$	$5, \theta = 74^\circ$ $t^\circ C$	$9, \theta = 90^\circ$ $t^\circ C$
$E_\mu V$	$E_\mu V$	$E_\mu V$	$E_\mu V$	$E_\mu V$	$E_\mu V$
-181	263	-180	192	-182	75
-174	242	-33	34	-179	-181
-52	74	99	-76	-68	53
-45	64	238	-88	-64	3
-28	39	304	-38	-42	2
25	-34	331	3	-32	157
136	-178	348	27	-26	515
219	-258	358	50	21	686
317	-292	368	63	56	504
368	-284	378	79	103	788
378	-278	389	96	194	856
389	-274	398	118	262	389
398	-267	409	140	317	910
409	-257	411	144	368	965
411	-255	413	148	378	1015
413	-253	415	149	389	1035
415	-257	417	148	409	411
417	-264	419	140	411	1045
419	-270	422	132	413	413
422	-280	423	125	415	1055
423	-284	428	114	417	415
425	-294	433	94	419	1045
430	-308	441	67	423	1013
435	-327	448	44	425	417
441	-343	455	21	430	419
455	-400	465	-5	432	1075
465	-436	474	-39	441	422
470	-455			452	1070
474	-461			465	890
				474	808

The only theory so far proposed to explain the thermo-electric properties of crystals is the thermodynamical one of Voigt⁵ and Thomson,⁶ according to which

$$e = e_{\parallel} \cos^2 \theta + e_{\perp} \sin^2 \theta = e_{\perp} + (e_{\parallel} - e_{\perp}) \cos^2 \theta \quad (1)$$

where θ is the angle between the hexagonal axis and the axis of the wire, e_{\parallel} and e_{\perp} are the thermo-electric powers parallel and perpendicular to the hexagonal axis, respectively.

The treatment of Voigt leads specifically to Eq. (1) above. Bridgman⁷ considers that Voigt's and Thomson's analyses have taken no account of either the internal or surface Peltier heat and that therefore Eq. (1), as derived by Voigt, cannot be expected to apply to an actual thermocouple. leaving aside the theoretical considerations underlying the derivation of the equation it is interesting to test it experimentally, considering it, for the moment, as purely empirical. Bridgman has made such a test for zinc and other metal crystals and arrives at the conclusion that the equation is not generally valid for the representation of the experimental facts. The

⁵ Voigt, Lehrbuch der Kristallphysik.

⁶ W. Thomson, Math. and Phys. Papers I, p. 232.

⁷ Reference 2, p. 128.

chief deviation is found in the case of the Peltier heat. This conclusion is based on the non-linear relation between specific resistance and a constant a' , which is shown to be proportional to the Peltier heat at 0°C .

The writer's own results have been applied to test the validity of Eq. (1) in a somewhat different fashion. It is evident from the equation that e plotted against $\cos^2 \theta$ should give a straight line. Such curves for various temperature differences are given in Fig. 4, (points plotted as circles) and, as is evident, the law appears to hold for the lower temperatures, but there seems to be a deviation for the 300° and 400° curves. That is deviation actually exists and is not due to experimental error is further indicated by the fact that the author's previous data¹ show the same type of variation. (e was not calculated in the previous paper but may be obtained from the

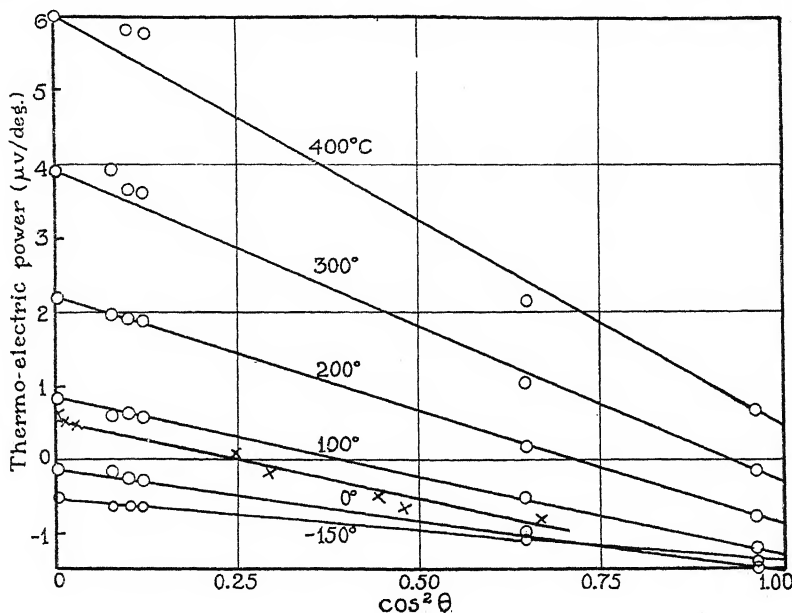


Fig. 4. Thermo-electric power against copper vs $\cos^2 \theta$ for various temperature differences.
Linder, O; Bridgman, X.

curves there given.) Neither can this be due to the variation of θ with the temperature since a simple calculation based on thermal expansion coefficients found by Grüneisen and Goens⁸ shows this to be considerably too small.

It should further be pointed out that if the usual thermodynamical relation for the Peltier heat, $\Pi = T dE/dt$, is assumed, then the curves of Fig. 4 also show how far Eq. (1) is valid to express the nature of the variation of Peltier heat with the orientation angle. Returning now to Bridgman's data, they may be reduced in a similar fashion. dE/dt is, in his notation, given by $a' + 2bt$, and expressions are given for calculating a' and b from the

⁸ Grüneisen and Goens, Zeits. f. Physik. 29, 141 (1924).

points plotted in his Fig. 4.⁹ The thermo-electric power thus computed for $t=60^\circ$ is plotted as crosses (\times) in Fig. 4 against $\cos^2\theta$. As is evident, a fairly good straight line results; what deviations exist are not systematic and may well be due to experimental error. In fact Bridgman's 46.5° curve¹⁰ is of doubtful validity since it differs considerably from its neighbors and resembles very much curves which the author has obtained from specimens which were not single crystals but consisted of two or three single crystals together. The same criticism may be made of his 80° or 83° curve. The other curves for the Peltier effect, which Bridgman gives are all nearly straight lines with the exception of the one for tin. Here, however, the experimental points are so scattered that it is uncertain whether the curve is straight. In view of the above it seems that the Voigt-Thomson symmetry relation is obeyed to a much closer degree than was concluded by Bridgman.

II. Relative Thermo-electric Properties of Zn_\perp and Zn_\parallel . Grüneisen and Goens³ have pointed out the desirability of obtaining the thermo-electric properties of a single metal. To do this they have expressed the various thermo-electric constants of one principal orientation, Zn_\perp (i.e., $\theta=90^\circ$) against the other, Zn_\parallel (i.e., $\theta=0^\circ$). The results described under Section I above may be presented in a similar fashion.

From the Voigt-Thomson law, Eq. (1), we get, by integration,

$$E = E_\parallel \cos^2 \theta + E_\perp \sin^2 \theta, \quad (2)$$

where E is the e.m.f., providing that θ is independent of the temperature difference, t , of the junctions. As has been mentioned above, this is very

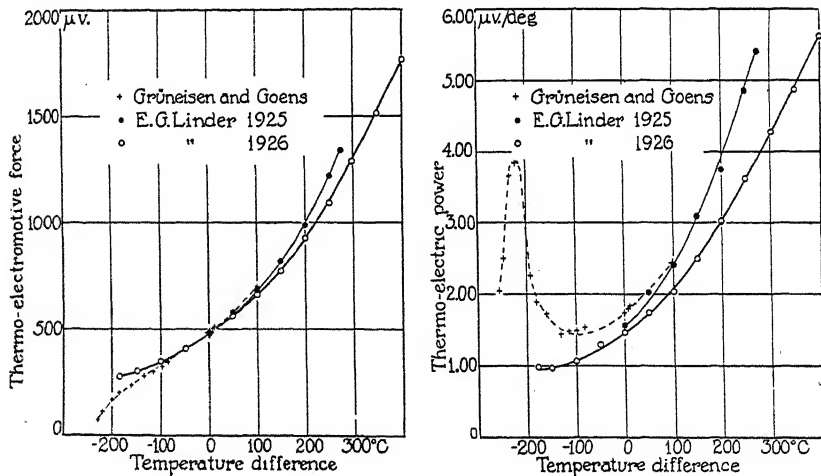


Fig. 5. Thermal e.m.f. for Zn_\perp against Zn_\parallel .

Fig. 6. Thermo-electric power for Zn_\perp against Zn_\parallel .

⁹ Reference 2. There is an error in Bridgman's Fig. 4, p. 116, since he has not plotted the angles between the crystal axis and the length of the rod as abscissas but their complements. He also has the sign of his Δ wrong according to its definition on p. 114.

¹⁰ Reference 2, Fig. 3, p. 115.

nearly true and will be assumed so. Hence, by introducing into Eq. (2) the observed values of E_{\perp} and E for 11.4° , the values of E_{\parallel} may be calculated. For the purpose of comparison we now introduce the value $E(0^{\circ}, -253^{\circ}) = 483.6 \mu\text{v.}$ (i.e., the e.m.f. with one junction at 0° and the other at -253°C) taken from the work of Grüneisen and Goens, and by use of the law of intermediate metals, get

$$E(t, -253^{\circ}) = E(0^{\circ}, -253^{\circ}) + E(t, 0^{\circ})$$

where all of the E 's are for Zn_{\perp} against Zn_{\parallel} . The values obtained in this manner together with those of Grüneisen and Goens are represented graphically in Fig. 5, and are tabulated in Table II. In this figure, and also in

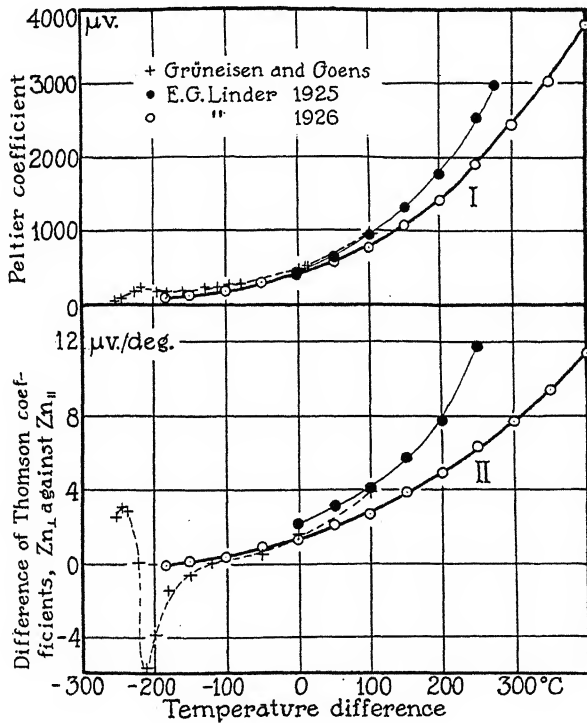


Fig. 7. I Peltier coefficient for Zn_{\perp} against Zn_{\parallel} . II differences of the Thomson coefficients for Zn_{\perp} against Zn_{\parallel} .

Figs. 6 and 7, are displayed the writer's earlier results, reduced in the same fashion, together with those of Grüneisen and Goens.

The thermo-electric power, $e = dE/dt$, can be obtained by measuring the slope of the tangents to the curve of Fig. 5. It is to be noted that dE/dt is independent of the additive constant, $E(0^{\circ}, -253^{\circ})$. The values of the thermo-electric power thus obtained are listed in Table II and graphed in Fig. 6.

According to Kelvin's thermodynamical theory, the Peltier coefficient is given by .

$$\Pi = Te,$$

where T is the absolute temperature of the junction. The values calculated according to this formula are given in Table II and curve I, of Fig. 7.

The difference of the Thomson coefficients, which, from the same theory, is given by

$$\sigma_{\perp} - \sigma_{\parallel} = T(de/dt),$$

TABLE II

Thermal e.m.f., thermo-electric power, Peltier heat and difference between Thomson coefficients for Zn₁ against Zn₂.

T	e	$E(t, -253^{\circ})$	e	II	$\sigma_{\perp} - \sigma_{\parallel}$
-182°C		275 μv	.99 $\mu\text{v}/\text{deg.}$	90 μv	-.11 $\mu\text{v}/\text{deg.}$
-150		304	.96	118	.10
-100		355	1.07	185	.37
-50		414	1.32	295	.92
0		484	1.47	402	1.39
50		564	1.77	572	2.18
100		661	2.05	765	2.69
150		771	2.53	1075	3.87
200		921	3.00	1420	4.87
250		1087	3.63	1900	6.33
300		1285	4.28	2450	7.67
350		1511	4.85	3025	9.45
400		1770	5.65	3800	11.40

can also be calculated by using values of de/dt obtained by measuring the slope of the tangents to the curve of Fig. 5. The data so obtained are given in Table II and curve II of Fig. 7.

III. Behavior at the melting point. Observers disagree as to whether there is a break in the thermo-electric power curve at the melting point. For zinc Darling and Grace¹¹ and also H. Pélabon¹² write that they observed no

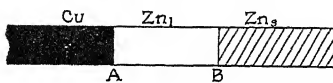


Fig. 8. Diagram of zinc crystal—copper junction above the melting point of zinc.

change, while, on the other hand, J. Koenigsberger¹³ observed one, and gives the experimental value $e_e - e_s = -10 \mu\text{v./degree}$, where e_e is the thermo-electric power of liquid Zn and e_s that of solid Zn. He also gives the theoretical values, $-5.6 \mu\text{v./deg.}$ from Bernoulli's formula¹⁴ and $-6.0 \mu\text{v./deg.}$ from Lorentz's formula.¹⁵ As may be seen from Fig. 3, the author found a distinct break at the melting point. The crystal structure—at least insofar as it determines the thermo-electromotive force—breaks down suddenly and not gradually as the temperature passes that point. Further, those parts of the curves above 419°C are approximately parallel, which is precisely what we should expect, for after the Zn crystal has melted we have the situation depicted in Fig. 8. The junction A , between the solid Cu and liquid

¹¹ Darling and Grace, Proc. Lond. Phys. Soc. 30, 14 (1917).

¹² H. Pélabon, Ann. d. physique, 13, 169 (1920).

¹³ J. Koenigsberger, Ann. d. Physik. 47, 563 (1915).

(homogeneous) Zn may vary in temperature from 419°C up, and the e.m.f., E_A , due to it, is the same for all crystals; on the other hand, the junction B , between liquid Zn and crystalline Zn, is always at the same temperature, i.e., 419°C, but the e.m.f. due to it, E_B , is different for crystals having different orientations. Thus E_B acts as an additive constant, and the total e.m.f., $E = E_A + E_B$, represents a family of parallel lines. The values of $e_l - e_s$ for different orientations, and values for two specimens of polycrystalline Zn are arranged in Table III. The average value, $-7.98 \mu\text{v}/\text{deg.}$,

TABLE III
Thermo-electric power of solid and liquid zinc at the melting point.

θ	e_s $\mu\text{v}/\text{deg.}$	e_l $\mu\text{v}/\text{deg.}$	$e_l - e_s$ $\mu\text{v}/\text{deg.}$
11.4	1.13	-3.61	-4.75
36.5	2.00	-3.20	-5.20
72	4.87	-3.58	-8.45
90	5.30	-3.23	-8.55
P. C. 1	4.25	-3.64	-7.89
P. C. 2	4.88	-3.18	-8.06

which the author obtained for Zn_{poly} , is in better agreement with the theoretical values than those of Koenigsberger mentioned above.

The principal sources of error in the measurements presented in the above three sections probably are: (1) the determination of the orientation¹; (2) the measurement of the temperature of the hot junction (a different copper-advance thermocouple and block, H , Fig. 2, were used in order to prevent contamination of the block due to diffusion into it by the liquid Zn, each being made, however, with wires from the same spools and in an identical manner); (3) impurity of the zinc. Merck "highly pure" zinc was employed.

IV. Effect in polycrystalline substances: As is well known, many so-called isotropic substances are, in reality, quasi-isotropic, i.e., random aggregates

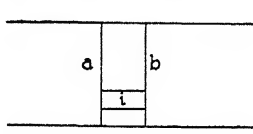


Fig. 9.

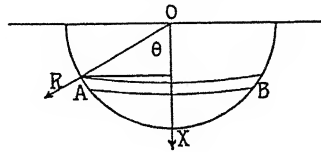


Fig. 10.

of small crystal particles. Since this is the case, it should be possible to express the properties of the aggregate in terms of the properties of its component single crystal parts. An attempt to do this in the case of the thermo-electric properties of polycrystalline metals has met with a fair degree of success.

Consider an arbitrary, cross-sectional element, ab , Fig. 9, of a polycrystalline conductor constituting one of the elements of a thermo-electric circuit. The two plane boundaries of ab , we shall assume to be equipotential surfaces. Let V be the potential difference between them. Let I_i , r_i and E_i be the

current, resistance and thermal e.m.f. of any one crystal in this element. Then, assuming that each crystal extends from a to b , we have, from Kirchoff's second law

$$V = I_i r_i + E_i.$$

Further, the total current I is given by

$$I = \sum_i p_i I_i = \sum_i p_i (V - E_i) / r_i, \quad (3)$$

where p_i is the concentration of crystals having the orientation θ_i . This may be found as follows: In Fig. 10 let OX represent the axis of the Zn wire, and OR the hexagonal axis of any crystal. It is evident that the probability of the hexagonal axis making an angle between θ_i and $\theta_i + d\theta$ with the wire axis is (area of strip AB_i)/ $2\pi r^2$ or $p_i = \sin \theta_i d\theta$. Now Eq. (3) holds for any value of I , hence put $I=0$, then,

$$V \sum_i p_i / \sigma_i = \sum_i p_i E_i / \sigma_i,$$

where σ_i is the specific resistance of any Zn crystal of orientation θ_i , and is given by

$$\sigma_i = \sigma_{\parallel} \cos^2 \theta_i + \sigma_{\perp} \sin^2 \theta_i. \quad ^5$$

Introducing the similar expression for E , Eq. (2), we have

$$\begin{aligned} V &= \frac{\int_0^{\pi/2} E_{\parallel} \cos^2 \theta + E_{\perp} \sin^2 \theta}{\int_0^{\pi/2} \frac{\sin \theta}{\sigma_{\parallel} \cos^2 \theta + \sigma_{\perp} \sin^2 \theta} d\theta} \sin \theta d\theta \\ &= E_{\perp} + (E_{\parallel} - E_{\perp}) / (4r) \end{aligned}$$

where $r = \sigma_{\parallel} / \sigma_{\perp}$. Assuming that $r = 1$, we have

$$V = \bar{E} = E_{\perp} + (1/3)(E_{\parallel} - E_{\perp}) \quad (4)$$

and by comparison with Eq. (2) it follows that $\cos^2 \theta = 1/3$; whence $\theta = 54.5^\circ$. In other words, a polycrystalline wire should give the same thermal e.m.f. as a single crystal wire having an orientation of 54.5° . The author found the experimental value of $65-70^\circ$ for Zn. The agreement is not good, but in view of the assumptions we could not expect it to be better.

Unfortunately, as far as the author is aware, there are no other data suitable for checking this result. The variation among the different available measurements on polycrystalline metals is so great that it appears that a reliable check can be obtained only when the polycrystalline and single crystal measurements are made by *identical* methods and on the *same* samples of metal. For this reason it seems that Bridgman's conclusion, based on experimental data, that the thermo-electric properties of the aggregate cannot be found by averaging the properties of the single crystals, is scarcely justified.

By differentiating Eq. (4) with respect to t , and rearranging, we have,

$$\bar{e} = (1/3)(2e_{\perp} + e_{\parallel}),$$

and this is identical with a type of formula which has been found to give the thermo-electric properties of alloys of mechanically mixed crystals of different metals,¹⁴ therefore it appears as if polycrystalline metal, might be considered as an alloy of three components having properties corresponding to the three crystallographic axes, respectively, (two parts Zn_{\perp} and one part Zn_{\parallel} in the present case).

It should be pointed out that we obtain the same result, if, instead of taking a cross-sectional element, we consider a long strip parallel to the axis of the wire. In this case, instead of assuming the electrical conductivities equal, we assume the thermal conductivities so, and hence the temperature difference across each crystal will, on the average, be the same, so that we get,

$$\bar{E} = \sum_i p_i E_i,$$

which leads to Eq. (4).

It may also be worthwhile to mention that expressions for the thermal and electrical conductivities of polycrystalline metals can be obtained by similar methods and that these formulas are identical with those which have been found to hold for alloys of mechanically mixed crystals.¹⁵

CONCLUSION

Obviously the present electron theories of thermo-electricity are inadequate for the explanation of this effect in crystals, since electron gas pressure or electron concentration, as ordinarily understood, are not vector quantities, i.e., their magnitude is not a function of direction in the crystal. If, however, we take into consideration the fact that the spacing of the atoms in the lattice is different for different directions, and that, therefore, the mean free path of the free electrons would vary with direction and in consequence the electron gas pressure, we have a possible explanation.

The author wishes to express his thanks to Professor E. P. T. Tyndall for his valuable suggestions and criticism.

PHYSICAL LABORATORY,
UNIVERSITY OF IOWA,
November, 1926.

¹⁴ A. L. Bernoulli, Jahrb. d. Radioakt. 9, 270 (1912).

¹⁵ W. Guertler, Jahrb. d. Radioakt. 5, 17 (1908).

MAGNETIC PERMEABILITY OF IRON AND MAGNETITE IN HIGH FREQUENCY ALTERNATING FIELDS

By G. R. WAIT

ABSTRACT

Relative values of the permeability of cast-iron filings, iron wires, and iron powder in high frequency magnetic fields.—Wwedensky and Theodortschik have found the magnetic permeability of iron, steel, and nickel in alternating fields to be abnormally large in certain frequency bands (at about 100 meters for iron) and nearly normal in other regions. The general appearance of the phenomenon suggested the existence, in the material, of resonators corresponding to these frequencies. The phenomenon has been observed also by Kralovec. Two experimental methods have been followed in the present investigation, one the resonance method and the other the heterodyne method. Both utilized, in principle, the measurement of the change in inductance of a coil due to the introduction of the sample of material into it. The wave-length ranges covered were from 80 to 1700 meters by the heterodyne method and from 50 to 160 by the resonance method. The heterodyne method was used in an improved form which eliminated drifts. The results are in disagreement with those of Wwedensky and Theodortschik and with those of Kralovec. No anomalous change in permeability was found at any frequency. The following errors, which may have misled previous investigators, were found in the course of the present work: (a) anomalous behavior of capacities in series when these are connected in tube circuits, an effect the nature of which is unknown but which is related in some way to the length of the connecting wires; (b) a general variation in the apparent permeability as measured by one coil, presumably due to effects of distributed capacity; (c) apparent anomalies when a number of coils are used without comparing the results at the same wave-length; (d) an apparent anomaly in the permeability, at a critical frequency, arising from the presence of a metal shield inside the coil; (e) an effect of drift in the heterodyne method.

The absolute value of the permeability of powdered magnetite.—The permeability of magnetite in powdered form has been measured by two fairly independent methods. The values decrease from about 1.532 at 132.2 meters to 1.401 at 85.8 meters. After due allowance is made for density of packing, these values compare favorably with the results obtained by a static method by Welo and Baudisch.

THE magnetic permeability of iron in oscillating magnetic fields of wave-lengths greater than 1000 meters, has been found to be approximately constant¹ and similar to that in stationary fields. For shorter wave-lengths, Wwedensky and Theodortschik,² using soft iron wires, determined the permeability between wave-lengths 54 and 705 meters and, using steel and nickel wires, between 50 and 500 meters. Their curve for iron wires, where μ , the permeability, is plotted against λ , the wave-length in meters, is shown in Fig. 1. This shows a sharp maximum of the permeability at about 100 meters, between two sharp minima. This apparently anomalous behavior of the

¹ R. Brown, J. Frank. Inst. 183, 41 (1917).

² B. Wwedensky and K. Theodortschik, Ann. d. Physik. 68, 463 (1922), and Phys. Zeits. 24, 216 (1923). -

permeability, at about 100 meters, was explained by the above workers as being due to the resonance of elementary magnets of which the iron is supposed to be composed, their frequency of oscillation being approximately 3×10^6 per second. J. Kralovec, making measurements on cast-iron filings,

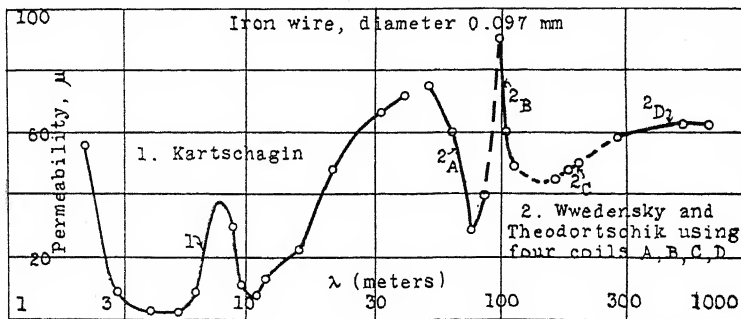


Fig. 1. Results by Kartschagin and by Wwedensky and Theodortschik.

found anomalies between 80 and 90 meters and again between 100 and 110 meters. Observations on magnetite failed to show similar critical changes in permeability. The fundamental importance of obtaining definite proof as to the existence of such oscillators has led to the present investigation.

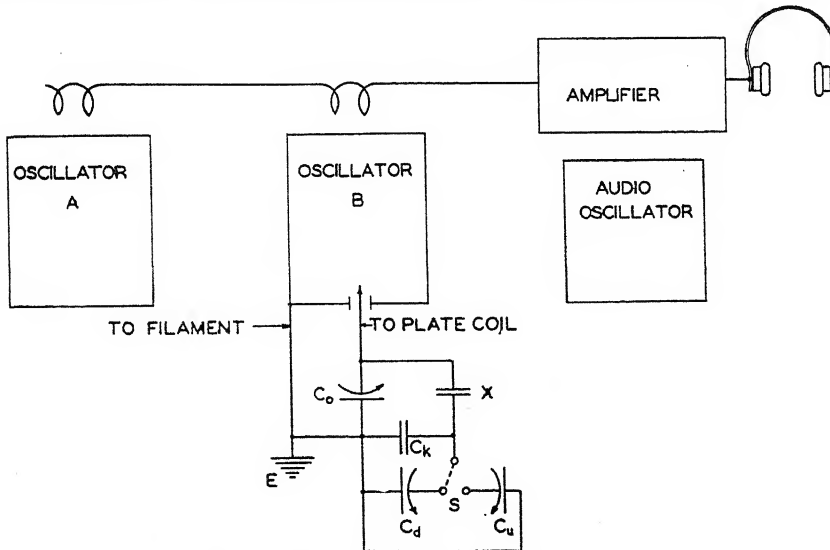


Fig. 2. Diagrammatic sketch of apparatus.

APPARATUS AND EXPERIMENTAL METHODS

Two of the four methods used by Wwedensky and Theodortschik were used in a modified form in the present investigation. In method I, two electron-tube oscillators, *A* and *B*, of Fig. 2 were tuned so as to give a small number of beats which were detected by means of an audio-frequency

amplifier. The two oscillators were coupled loosely; the coupling coils were connected to the "input" of a three-tube amplifying unit and the phones to the "output." The sample, upon being introduced into the coils of set *B*, changed the tuning of the two sets by changing the inductance of the coil. The sets were returned to the original pitch by compensating for the changed inductance by a corresponding change in the capacity *C* of the system of condensers shown. This change was affected by altering the setting of *C_o*, a variable air condenser in series with the coil. The capacity of the air condenser *X*, was kept constant at about 219 mmf. *C_k* is a mica condenser of about 5500 mmf. *C_u* and *C_d* are variable air condensers, each with a range of about 30 mmf to 900 mmf. *S* is a mercury switch which automatically substitutes *C_d* for *C_u* when the sample is introduced quickly into the coil by a lever system. A rigid iron structure provides for exact centering of the sample in the coil and prevents movement of the sample in any direction after introduction. Sets *A* and *B* are shielded electrically by brass boxes. The amplifying unit and also all "A" and "B" storage batteries are in wooden boxes covered with sheet iron. All exterior electrical connections are properly shielded. In some of the work a tin-foil shield was introduced into coil "B" to shield the sample. A set of six pairs of oscillating coils of properly selected inductances, wound on bakelite tubing, gave considerable overlapping of wave-lengths. The total range of wave-lengths extended from about 80 meters to 1,700 meters. Table 1 gives particulars regarding each coil.

TABLE I

Particulars of coils used.

Coil No.	1	2	3'	3	4	5
Length (cm)	5.0	5.0	5.0	5.0	5.0	7.5
Diameter (cm)	8.8	8.8	8.8	8.8	8.8	8.8
No. of turns	7	10	14	26	51	76
Obs. inductance (micro-henries)	5.1	9.5	16.4	58	208	373

To measure the wave-lengths used, an auxiliary oscillator was set at resonance with sets *A* and *B* so as to leave unaltered the tuning that had been obtained between them. Then by means of a calibrated wave-meter the frequencies of the auxiliary oscillator were determined.

The selection and arrangement of capacities shown in Fig. 2 as *X*, *C_k*, and *C_u* (or *C_d*) acted as an extremely fine adjustment of capacity of condenser *C_o*. The curve connecting ΔC_d and ΔC is almost a straight line, and a change of nearly 900 mmf is required in ΔC_d to produce a change of 1 mmf in ΔC .

In practice, the sample was removed from the coil, sets *A* and *B* were tuned to a convenient pitch, and the audio-frequency amplifier was tuned to a pitch giving a very small number of beats. Upon introducing the sample into the oscillating coil of set *B*, retuning was effected by condenser *C_d*. Some drift was frequently present when it was necessary to remove and reintroduce the sample several times and to make appropriate readjustments of *C_d* for each determination of ΔC_d . The drift was kept to a minimum by

frequent charging of the storage batteries and replacing from time to time of the oscillating tubes (*UV* 199).

In method II, a resonating circuit was set at resonance with an oscillator. Upon introducing a sample into the coil of the resonating set, resonance could again be obtained by compensating for the changed inductance by a corresponding change in the capacity of the circuit. Detection was made by a thermocouple and galvanometer, a low and a high sensitivity galvanometer being used for magnetic fields of high and low intensity respectively.

Belz³ showed that for a substance with cross-sectional area A' and length l' , volume $V' = A'l'$, with sufficiently small susceptibility k , introduced into an oscillating coil of cross-sectional area A and length l , volume $V = Al$, if the inductance, L , of the coil is altered by an amount ΔL , then, neglecting effects arising from eddy-currents, demagnetization, end effects of the sample, and an alteration in the magnitude of the field due to the presence of the interior shield,

$$(V/V')(\Delta C/C) = (V/V)(\Delta L/L) = 4\pi k$$

where C is the capacity of the system and ΔC the change in capacity necessary to compensate for the change in inductance. Wwedensky and Theodortschik applied this formulae to their results to get a quantity termed "apparent permeability." In their case, since their sample was longer than their coil, the ratio V/V' reduced to the corresponding ratio of areas. In the present paper, to make proper comparison with their results easier, the quantity $\Delta C_d/(C_0 + K_n)$ has been plotted against λ , the wave-length in meters, where the expression $(C_0 + K_n)$ represents the total capacity and ΔC_d that necessary to compensate for the change in inductance of the coil due to the introduction of the sample. This procedure is sufficient to show any apparent changes in the relative values of permeability.

RESULTS BY THE BEAT METHOD

Iron filings as a sample. In preliminary work an apparently anomalous behavior for iron filings was obtained for particular settings of condenser C_0 , in general similar for the various oscillating coils used. Tests showed that this could not be attributed to a faulty calibration of C_0 , nor to the resonance of portions of the circuit having long lead-in wires with the main part of the circuit. The magnitude of the anomaly did not appear to depend upon the amount of iron used as a sample, and consequently could not be a permeability effect. Tests with experimental shields showed the cause of the anomaly was connected with eddy-currents set up in the shield altering the inductance of the oscillating set over the band of frequencies where the anomaly appeared.

In the definitive experiments the region of wave-lengths from about 99 to 1700 meters was covered, using iron filings as a sample. The same sample was not used throughout this range, as was the case later with the iron powder in insulating wax, consequently the results have not been given in

* M. H. Belz. Proc. Cambridge Phil. Soc. **21**, 52 (1922); Phil. Mag. **44**, 479 (1922).

graphs. However, in all the tests with these samples, after remedying the difficulty produced by the interior shield, no change in permeability at apparently critical frequency occurred.

Iron powder as a sample. For iron powder embedded in insulating wax, and formed into a sphere, relative permeability curves are shown in Fig. 3 for wave-lengths 84 to 1300 meters. Aside from small irregularities, the curves are smooth. In the region of 85 to 95 meters, there are irregularities amounting to about three percent of the value of ordinate. This is greater than can be ascribed to experimental error. This variation always occurred to some extent in the preliminary work, and was always of the same form regardless of the sample used. Various tests applied definitely proved that this was not due to eddy-currents set up in the sample nor to a change in its permeability.

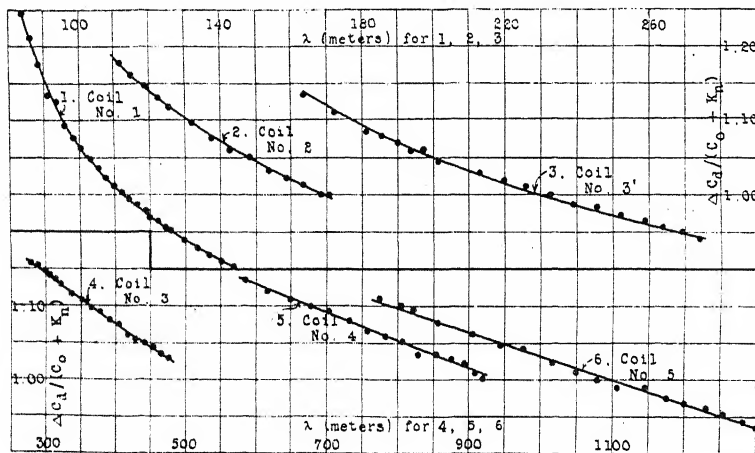


Fig. 3. Results for iron powder embedded in insulating wax, made into spherical form, for wave-lengths 84 to 1300 meters.

In Fig. 4 are presented curves for iron powder and iron wires showing the usual depression at 91.3 meters. When, however, the inductance in series with condenser C_d is increased, the depression gives way to a small maximum. When the inductance is added both to condensers C_u and C_d , the irregularity at this point disappears. This together with considerable additional evidence (a fuller discussion of which is prohibited on account of the lack of space) indicate that this irregularity is due to resonance between certain parts of the circuit.

A regular run with iron powder as a sample, made after shortening the connections between condensers X and C_x gives a curve (curve 6, Fig. 4) that is free from any resonance phenomenon, and is approximately horizontal. Data for curve 5 of Fig. 4 were obtained after replacing the connections as before. It will be seen that the resonance phenomenon has reappeared. It may be well to point out that the value of condenser C_k was different for these two curves from that for all previous curves; this has altered the

absolute values involved in these curves. All the above evidence points to the fact that the phenomenon shown between 85 and 95 meters is due to the resonance of one part of the circuit with another, and has nothing to do with

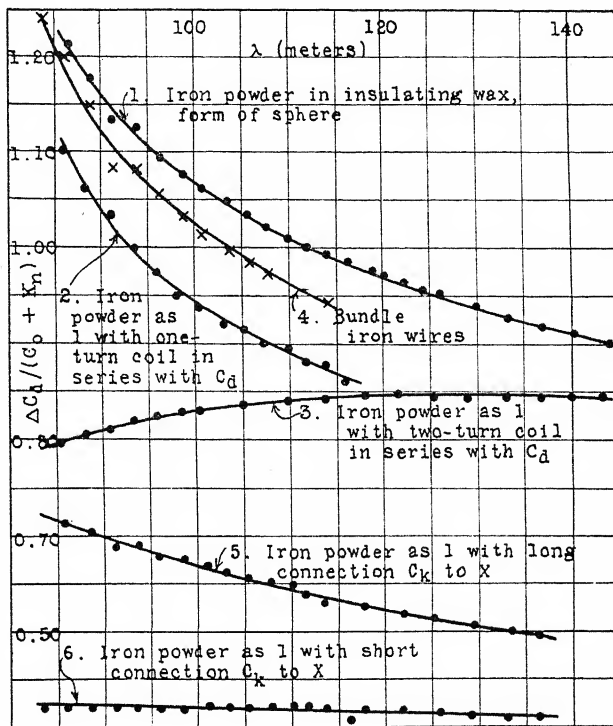


Fig. 4. Tests on iron powder and wires showing apparent irregularities due to particular circuit connections.

the resonance of the elementary magnets of the sample. A sample set of observations and computations is shown in Table 2.

TABLE II

Sample set of observations and computed values of approximate permeability μ , for a bundle of 24 iron wires 24 cm long, 0.0127 cm in diameter each, using oscillating coil No. 1.

$$C = X^2 C_d / (C_u + C_k + X) \quad (C_d = C_u + C_k + X) \\ A, \text{ cross-sectional area of oscillating coil, } = 60.85 \text{ cm}^2 \\ A', \text{ cross-sectional area of sample, } = 0.0121 \text{ cm}^2$$

Div	C_o mmf	C_d mmf	ΔC_d mmf	C_u mmf	ΔC mmf	μ	λ meters
5	44.5	93.3	510.1	508.7	1018.8	0.580	83.7
10	65.5	91.8	501.9	516.6	1018.5	0.590	82.1
15	91.2	89.8	491.0	527.1	1018.1	0.603	7.92
20	117.2	89.7	490.5	527.2	1017.7	0.603	7.53
25	142.8	84.8	464.4	552.9	1017.3	0.636	7.52
30	168.5	82.0	449.6	567.4	1017.0	0.654	7.36
35	194.5	79.1	434.1	582.4	1016.5	0.673	7.24
40	220.0	76.2	418.4	597.8	1016.2	0.692	7.13
45	246.0	73.0	401.2	614.6	1015.8	0.714	7.04
50	272.0	70.0	385.0	630.4	1015.4	0.734	6.99
55	298.0	67.0	369.4	645.6	1015.0	0.747	6.81
70	376.0	57.0	312.2	696.6	1008.8	0.821	6.68

Magnetite in a powdered condition in insulating wax. Results for powdered magnetite in insulating wax formed into a sphere, are shown by curve 1 in Fig. 5. It will be seen that the slope of the curve is large, the difference between the maximum and minimum values of ordinate amounting to about 27 percent of the smallest value. Now, using the same data to compute the permeability (designated as method A), by means of the equation $\mu = (V/V')(\Delta C/C) + 1$, curve 7 of Fig. 5 is obtained. The slope of the latter curve is very small compared with that of the former. The difference between the maximum and minimum values of ordinate in this case is less than 5 percent

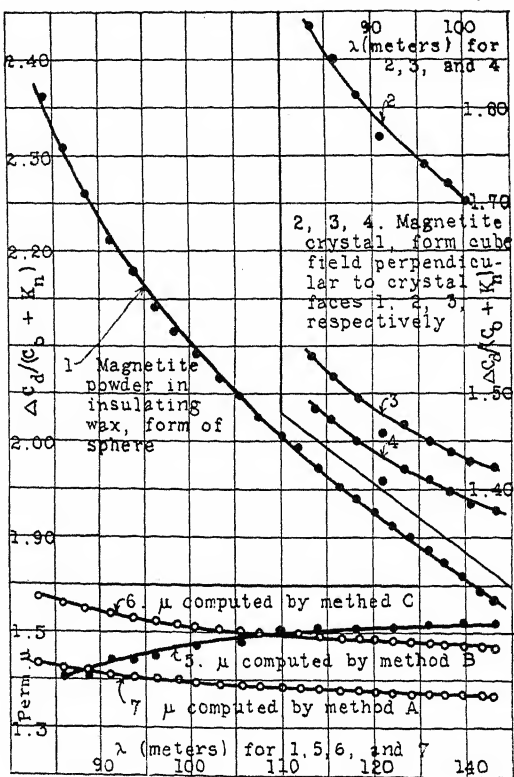


Fig. 5. Results for magnetite powder and magnetite crystal.

of the smallest value. Similarly, if the permeability (obtained as for curve 7, Fig. 5) had been used as the ordinate in curves of Fig. 3 their slopes would have been somewhat smaller. The difference in ordinates at overlapping wave-lengths for any two curves would under these circumstances have been less; however, each curve would still require an appreciable correction-factor in order to produce superposition throughout the overlap. It is probable that the failure of Wwedensky and Theodortschik to consider this possibility has led to an error in their results. This is particularly evident

in the region (see Fig. 1 for wave-lengths between 90 and 100 meters) where the greatest change in permeability appears to have occurred, and which was explained by them on the basis of resonance of elementary magnets.

A crystal of magnetite was sawed perpendicular to its crystal axes so as to form a cube, 0.8 cm on a side. The results using this as a sample are shown in curves 2, 3, and 4 of Fig. 5. It will be seen that the value of the former quantity depends upon the direction of magnetization with respect to the axes of the crystal. The value of the ordinates for curve 2 are about 22 percent greater than those for curve 3, whereas those for curve 4 are about 3 percent less than those for curve 3. Calculating the permeabilities by means of the equation $\mu = (V/V') (\Delta C/C) + 1$ (which is permissible for relative values only) one finds that the permeability perpendicular to face 2 is less than that perpendicular to face 1 by 1.8 percent and greater than that perpendicular to face 3 by 0.26 percent. As a check, the relative permeabilities along the three different axes of the cube were determined by a static method at the Bureau of Standards by Mr. R. L. Sanford and his staff to whom thanks are due for this as well as for other courtesies extended. The permeability perpendicular to face 1 was found at field strengths 20 and 50 gauss, respectively, to be 2.2 and 3.4 percent greater than that perpendicular to face 2. No difference in permeability perpendicular to faces 2 and 3 could be detected by this method. The results by the two methods are thus in very good agreement, particularly so since the field strengths in the interior of the oscillating coil (calculated from a knowledge of the current flowing through the coil and the number of turns per centimeter) was always smaller than 20 gauss.

Curves 2, 3, and 4 of Fig. 5, show the usual depression of about 1.5 percent at about 91 meters, which becomes less than 0.15 percent using the equation $\mu = (V/V') (\Delta C/C) + 1$. This then is a very small variation but, small as it is, its presence has been successfully explained on the basis of the resonance of one part of the circuit with another. This again brings out the extreme sensitiveness of the method used in these measurements, and indicates how small any variation in permeability must be if it has escaped detection.

Absolute value of permeability of magnetite in a powdered condition. A magnetite crystal was powdered and the powder then worked into soft insulating wax. Observations were made with this as a sample, first in the form of a sphere and then as a flat sheet perpendicular to the magnetic field. In case of a sphere, for static conditions, the demagnetizing field is equal to $4\pi I_1/3$, consequently, $H_1 = H' - 4\pi I_1/3$, where I_1 is the intensity of magnetization, H' is the magnetizing field with the sample absent, and H_1 the actual field inside the sample. Substituting I_1/k for the value of H_1 , and μ for $(1+4\pi k)$ in the above equation and solving for I_1 , then $I_1 = 3kH'/(2+\mu)$, where k is the susceptibility of the material in question. In the case of a sheet perpendicular to the field, $H_2 = H' - 4\pi I_2$, and one obtains in a similar way, $I_2 = kH'/\mu$. If the ratio $I_1/I_2 = r$, then $\mu = 2r/(3-r)$. Now r may be taken as being equal to the ratio of ΔC_d for sphere and sheet, which

can be obtained for various wave-lengths. This then, gives a method (designated *B*) of determining the absolute value of permeability in which the demagnetizing effect of the sample has been eliminated. In Fig. 5, curve 5 shows the value of the permeability obtained by this method for wave-lengths 85.8 to 132.2 meters. It will be seen that the values decrease from about 1.532 for the greatest wave-length to about 1.401 for the shortest wave-length.

The following circumstances all tend to make the observed value of the permeability lower than its true value (some of the effects are the most pronounced at shorter wave-lengths and possibly may account for the observed decrease with wave-length):

1. Because the eddy-current effect is larger in the sphere than in the slab, the ratio of ΔC for the sphere and slab is reduced. The reductions are relatively greater for the shorter wave-lengths since the eddy-current effect increases with frequency.

2. The mean field strength for the slab is greater than for the sphere since the periphery of the slab is nearer the coil than is the surface of the sphere.

3. The decrease in the field strength of the coil with decreasing wave-length will cause the observed values of the permeability to fall off at the shorter wave-lengths.

4. Because of the finite thickness of the slab, the values of ΔC obtained for this case are too large for all values of the wave-length.

Welo and Baudisch⁴ recently determined, by a static method, the permeability of chemically prepared powdered magnetite. Since the permeability of a powder depends upon its density of packing,⁵ a direct comparison between the results of their work and the present can be made only after each has been reduced to conditions of similar packing. Each of the results may be reduced to a permeability of the material in solid form by means of formulas developed in the paper⁵ by Dr. Breit. The final results, however, will depend upon the assumptions made regarding conditions and state of the powder. For instance, Dr. Breit has treated the following cases: (*a*) a space lattice of spheres; (*b*) a space lattice of spherical holes; (*c*) laminary structure of powder the direction of the laminae being distributed statistically.

For an approximate determination of permeability under condition (*a*) the equation $(\mu - 1)/(\mu + 2) = q [(\mu_0 - 1)/(\mu_0 + 2)]$ may be used, where μ is the permeability of powdered form, μ_0 is the true permeability in solid form and q is the ratio of volume occupied by the solid material to the volume occupied by solid material and holes. From the results of Welo and Baudisch, μ is taken as equal to 2.1 (which is only approximate, since it was not measured for such low field strengths as was used in the present case). The value of q is taken as equal to 0.254 (which also is only approximate since the density of packing, where it varied from 1.32 grams per cm^3 , was reduced to

⁴ L. A. Welo and O. Baudisch, Phil. Mag., 50, 399 (1925).

⁵ G. Breit, Amsterdam Proc. Akad. Wet. 25, 293 (1922).

results for this density by a method only approximately correct, and since the density of the solid material is assumed to be equal to 5.2 grams per cm^3). The value of μ_o comes out negative for this case, which indicates that the conditions specified under (a) cannot be true here. Turning now to the results of the present investigation, the value of μ is taken equal to 1.521 and q by assuming that the density of the solid is equal to 5.2 grams per cm^3 , equal to 0.229, from which we get μ_o equal to 6.5. For the case of (b) the equation as given, may be rewritten into a more convenient form for use, for instance,

$$\mu_0 = (1/4) \{ 1 + (\mu - 1)(2 + 3p/q) + ([1 + (\mu - 1)(2 + 3p/q)]^2 + 8\mu)^{1/2} \}$$

where $p = (1 - q)$. By means of this equation, from the results of Welo and Baudisch we get μ_o equal to 6.6 and from the present data it comes out equal to 3.9. For the case of (c), the equation as given may be rewritten in the form,

$$\mu_0 = -3 + (3p/q)(\mu - 1) + \{ 9[1 - p/q](\mu - 1)]^2 + 24(p/q)(\mu - 1) + 1 \}^{1/2}$$

Calculating μ_o from the results of Welo and Baudisch, we find it equal to 7.0 and from the present results equal to 4.0. In view of the fact that the sample used by Welo and Baudisch had the greater density of packing, it would seem that cases (b) and (c) might more appropriately be applied to their results than to the present ones, and that case (a) might more appropriately be applied to the latter. One can see from these comparisons that μ_o obtained by the static method and that obtained for an oscillating magnetic field are in approximate agreement, perhaps as closely as the difference in conditions and the uncertainty of assumptions should warrant one to expect.

A second method (designated C) of determining the absolute value of permeability, while retaining certain defects that have been eliminated by the previous method, may also be considered. This method makes use of a simple calculation for the change in the inductance of a solenoid of finite length due to the introduction into its center of a sphere of permeability μ . It neglects the effect of eddy-currents and of the inhomogeneity of the field.

By definition, the change in the inductance of a coil brought about by the introduction of the sphere is equal to the change in flux through the coil produced by the sphere, provided a unit current is flowing through the coil. The unit current causes a certain field H in the region into which the sphere is put. Under the influence of this field the sphere is magnetized so as to have a magnetic moment $r^3[(\mu - 1)/(\mu + 2)]H$. As long as the sphere is small, the field H is sufficiently homogeneous to cause a uniform magnetization of the sphere. Under these circumstances, it is equivalent to a doublet. The flux through the coil due to the doublet may, for convenience, be thought of as produced by a small turn of wire enclosing an area S , carrying a current J and placed in the same position as the sphere. The area S must be perpendicular to H and the product SJ must be equal to $r^3[(\mu - 1)/(\mu + 2)]H$ so

as to make the equivalent shell of S have the same moment as the sphere. The flux through S due to a unit current in the big coil is SH and, therefore, on account of the reciprocity of mutual induction the flux through the big coil due to a current J in the single turn is $SJ \cdot H$. This is the required change in induction $\Delta L = SJH = r^3 [(\mu - 1)/(\mu + 2)] H^2$.

If the coil is a solenoid of length $2b$, radius a , with n turns per unit length, $H = 4\pi n b / (b^2 + a^2)^{1/2}$. Also the inductance, with the sphere removed is $L_0 = 8\pi^2 a^2 n^2 b \cdot K$, where K is Nagaoka's correction factor. Hence

$$\frac{\Delta L}{L_0} = \frac{[4\pi r^3/3] [3(\mu - 1)/(\mu + 2)] [b^2/(b^2 + a^2)]}{2\pi a^2 b K} = -\frac{\Delta C}{C}$$

(The development of this equation is due to Dr. G. Breit.)

The above equation may now be applied to the case of the sphere of wax containing the magnetite powder, where $r = 0.906$ cm. For the oscillating coil used, $a = 4.4$ cm, $b = 2.5$ cm, $K = 0.5562$, therefore $(\mu - 1)/(\mu + 2) = 602.9(-\Delta C/C)$. The values of μ computed by means of this formula have been plotted in curve 6 of Fig. 5. The values of the permeability obtained by means of the equation $\mu = (V/V') (\Delta C/C) + 1$ have been plotted in curve 7 of Fig. 5. If due allowance be made, as explained before, for the various factors that tend to lower the value of the permeability of curve 5 at the shorter wave-lengths, there is fair agreement between the values given in curves 5 and 6. The values represented by curve 7 could hardly be expected to give a closer agreement with the other two curves since several factors are operating to effect both its slope and its absolute value.

RESULTS BY RESONANCE METHOD

Iron filings, iron powder, and iron wires as samples. Results by this method have been obtained on iron filings, coarse and fine, in and out of paraffin, iron powder, and iron wires. The bundle of wires used as a sample was packed into a glass tube having a diameter of 0.8 cm and 10.5 cm long, each wire being on the average about 0.002 cm in diameter. The other samples were packed into glass tubes having diameters between 1.2 and 1.3 cm and lengths between 10 and 11 cm. In the case of the fine and the coarse filings in paraffin, two different field strengths were used, namely, 0.05 and 0.6 gauss respectively, and for the other cases 0.6 gauss only. The strength of the field was kept constant by varying the coupling between the oscillating and the resonating circuits, thereby keeping the deflection of the detecting galvanometer constant.

In the early part of the work, considerable difficulty was experienced with apparent variations in permeability, which were not always reproducible. Later results, however, showed that this was only an apparent variation and was in reality due entirely to instrumental causes. The region where the apparently large variation in permeability appeared in the results of Wwedensky and Theodortschik² has been covered by this method, yet

there appeared to be no critical variation in permeability with frequency within this range.

DISCUSSION OF RESULTS

Comparison of the present results with those obtained by previous investigators. The methods and results of Wwedensky and Theodortschik², hereafter referred to as W. and T., have been critically examined in an effort to find an explanation of discrepancies that exist between this work and theirs. It will be well to point out a few things, which in the opinion of the writer may have seriously affected the results of the previous investigations.

1. A serious drift occurred in the work of W. and T., which affected what they called their zero-reading (corresponding to the reading of C_u in the present investigation), amounting sometimes to as much as 13 percent of their total compensating capacity. This necessarily must have affected the accuracy of their results if the drift was not uniform, and if the time of reading the condenser with the sample in was not midway between the times of the two zero-readings. The methods in the present investigation greatly reduced, if they did not entirely eliminate, the possibility of drift. Two separate condensers were used, one when the sample was "out," and the other when it was "in," making it unnecessary to consume time in reading the compensating condenser until the sample was "out." A lever system permitted introduction of the sample in less than a second, and at the same time substitution of one condenser for the other. Thus adjustments with sample "in" and "out" were made within few seconds at most and any drift, was found negligibly small in actual practice.

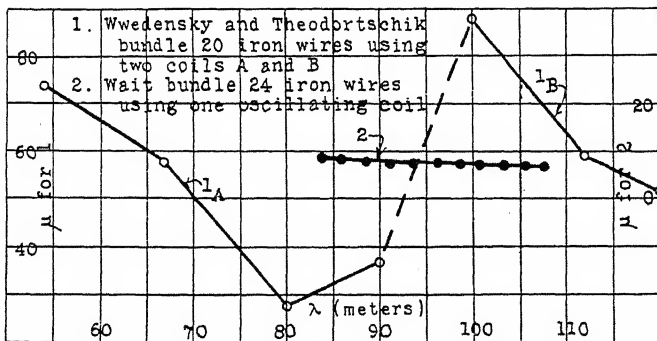


Fig. 6. Comparison of results on iron wires by Wwedensky and Theodortschik, and by Wait.

2. Fig. 6 gives the results of W. and T., the sample being a bundle of soft iron wires used in two different oscillating coils and shows the resonance band ascribed by W. and T. to the resonance of the elementary magnets of which the iron was supposed to consist. Fig. 6 gives also the results of the present investigation, the sample being a bundle of soft iron wires

of a similar diameter to those used by the other workers and like theirs having a length much greater than that of the coil, using, however, only one oscillating coil. W. and T. connected points, as shown by the dotted portion of their curve, obtained by different coils, a procedure which the writer's results show is not justified as correction-factors are required to refer data obtained with different coils to a standard coil.

The author wishes to express his indebtedness to the Director and staff of the Department of Terrestrial Magnetism, and particularly to Dr. G. Breit for valuable advice and assistance, to Mr. J. A. Fleming for continued interest, to Mr. C. Huff and assistants for help in designing and constructing apparatus, and to Mr. J. B. Goldsmith for assistance in the construction of graphs.

CARNEGIE INSTITUTION OF WASHINGTON,
DEPARTMENT TERRESTRIAL MAGNETISM,
October, 1926.

PHENOMENA DEPENDING ON THE CHANGE OF ELASTIC FREQUENCIES IN SOLID BODIES WITH PRESSURE

By F. ZWICKY*

ABSTRACT

Shift with pressure of the residual rays of a crystal.—Born's theory of the constituent forces in heteropolar crystals is adopted. As a new conclusion of this theory a formula for the shift of frequencies of residual rays with pressure is deduced. The shift corresponding to a pressure of 10,000 atm. amounts approximately to 7μ in the case of NaCl (residual rays at 50μ).

Effect of pressure on the electrical conductivity of metals.—Qualitative conclusions are drawn with respect to the dependence of elastic frequencies on pressure in any crystal. This leads to a rational explanation (suggested at first by Grüneisen) for the effect of pressure on the specific electric conductivity of metals, this conductivity being in general increased by pressure. The relation of our results to those obtained by Grüneisen and Bridgman previously in a quite different way, is discussed.

1. INTRODUCTION

THIS investigation was at first concerned with the problem of determining the shift of frequency of residual rays with pressure. It dealt naturally with heteropolar substances only, as only crystals built up by ions show selective frequencies in the far infra-red. From the results, however, it could be seen that it is possible to draw some important conclusions with regard to the conductivity of metals.

We first give the derivation for the change of frequency ν of residual rays with pressure P . The actual computation will be carried through only for the simple case of a cubic lattice of the type NaCl. The extension of the calculations to more complicated types of crystals would not involve any particular difficulties. Cases in which different tensions are applied in different directions of the crystal could also be calculated in the same way as described in this paper.

From the work of Born, Kossel and others it is known, that the cohesive forces in heteropolar chemical compounds are mainly of electrostatic origin, resulting from the electric field produced by the different ions. This theory has proved to possess a considerable range of validity, as lattice constants, compressibilities, elastic constants, frequencies of residual rays and heats of sublimation can be calculated from it. The results of such computations are in good agreement with the experimental data. The only very serious discrepancy between the theory and the facts seemed to appear between the calculated values of the breaking stress and the observed ones. The theoretical breaking stress, as deduced by the author,¹ was 400 times greater than

* Research Fellow in Physics, International Education Board.

the measured values known at that time. But also in this case the theory was proven to be right by the careful investigations of A. Joffé and his school.² Joffé showed that in all the previous experiments much too low values for the breaking stress had been found because of imperfect surfaces of the crystals used (tiny cracks). Eliminating this source of error Joffé found values for the breaking stress approaching very nearly those predicted by the calculations.

Born's theory was extended by different investigators,³ who have taken into account the deformability of the ions in an electric field. In addition to this the repulsion forces were taken more exactly into consideration. These are necessary to secure the stability of the lattices. No real explanation has yet been found as to their true origin. A satisfactory treatment, however, of all the phenomena mentioned above could be given by assuming these forces to be inversely proportional to some high power of the mutual distance r_{ik} of two ions i and k . The two particles then, carrying charges e_i and e_k respectively, possess the mutual potential energy

$$\epsilon_{ik} = e_i e_k / r_{ik} + A_{ik} / r_{ik}^{p_{ik}} \quad (1)$$

The constants A_{ik} and p_{ik} are to be determined. Three points of view have been adopted with regard to these constants. At first, attempts were made by Born and Landé to deduce the exact values for them in a rational way, with the help of atomic models. But no consistent results could be obtained because of lack of knowledge of the fundamental quantum laws governing the mutual interaction of two atomic systems.

The second procedure consists in the deduction of A and p from the behaviour of gas atoms similar to the ions in question. From viscosity measurements in argon, for instance, the repelling force acting between two argon atoms can be determined.⁴ A slight extrapolation permits one to apply the same law of force for the interaction of two Cl^- ions or of two K^+ ions, because of the fact that these ions have very similar electronic structure to the neutral A-atom. In this way the different properties of the alkali-halide crystals could be deduced.

The third method was originally applied by Born,⁵ who used the experimental data of the lattice constant and of the compressibility to determine A_{ik} and p_{ik} in every special case. The other properties of the crystals may then be calculated with the help of the A and p thus obtained. We choose this simple point of view as our starting point.

¹ F. Zwicky, Physik. Zeits. 24, 131 (1923).

² A. Joffé and M. Lewitzki, Zeits. f. Physik, 35, 442 (1926).

³ See for instance M. Born, Die Atomtheorie des festen Zustandes, Enzyklopädie der math. Wissenschaften, Vol. V₃, Heft 4. All references made in our paper to previous work on heteropolar crystals may be found summarized in this book.

⁴ J. E. Lennard-Jones, Proc. Royal Soc. London, 109, 584 (1925).

J. E. Lennard-Jones and P. A. Taylor, Proc. Royal Soc., 109, 476 (1925).

⁵ Ref. 3, p. 733.

Assuming for the mutual potential energy of two ions the expression (1) we get for the energy contained in a crystal of the type NaCl the amount (per ion).⁶

$$\epsilon = \sum_k \epsilon_{ik} = -13.9e^2/a^4 + \alpha' A/a^p \quad (2)$$

a = lattice constant, α' = some function of p .⁶ The sum has to be taken over all the particles surrounding the ion i . For numerical computations see Ref. 3.

The condition necessary for the equilibrium of the crystal is

$$(\partial\epsilon/\partial a)_{a=a_0} = 0 \quad (3)$$

or

$$1.74e^2 - \alpha A/a_0^{p-1} = 0 \quad (4)$$

which means a relation between A and p , provided that the lattice constant a_0 is taken from the experiments.

Deducing on the same basis a formula for the compressibility and comparing it with the observed data, Born was able to determine A and p separately. It is found that p is approximately equal to 8 or 9. For different crystals one finds slightly different values varying from 7.5 to 9.5. Numerical computations then give α for different values of p as in the following table.

TABLE I

p	7.5	8	8.5	9
α	4850	7200	10380	15200

2. RESIDUAL RAYS

It has been shown by previous authors⁷ that the origin of the selective absorption and reflection of radiation in the far infra-red by heteropolar crystals is connected with the oscillations which the positively charged part of the lattice is able to perform relative to the negatively charged part. These oscillations will indeed be excited by incoming electromagnetic radiation, as the electromagnetic field connected with this radiation will force the charges of different sign in opposite directions. Resonance occurs when the incoming and the elastic oscillations have approximately the same frequency. It is easy to show that crystals of the NaCl type possess only one characteristic oscillation of the kind mentioned. Our task is to calculate its frequency in the case of uniformly applied external pressure. For this purpose we have to determine the force which is necessary to hold the positive and the negative partial lattices in relative displacement $\xi^+ - \xi^- = \xi$ (see Fig. 1.). We will obtain this force by deriving first the change in potential energy $\Delta\epsilon$ of a particle due to the displacement ξ .

The effect of the displaced electric charges may be obtained by making use of the expression for the Lorentz force in a polarized isotropic medium.

⁶ A_{ik} and p_{ik} in (1) are really dependent on the individual ions i and k . It has been shown however that the effect produced by their differences is a very small one and can be neglected in the first approximation.

⁷ Ref. 3, p. 740.

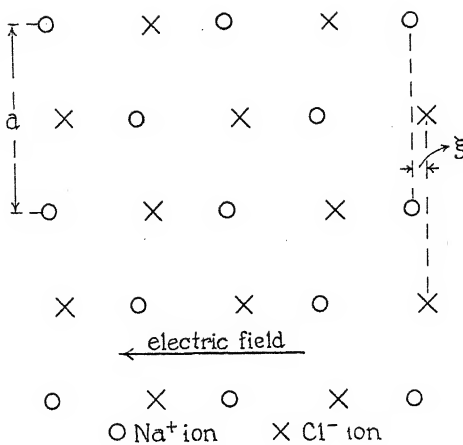


Fig. 1

The electric polarization or the moment per unit volume M being in our case equal to

$$M = \frac{1}{2} Ne\xi \quad (5)$$

(N = number of ions per cm^3)

The force per ion, due to the polarization is

$$4\pi e M / 3 = 2\pi N e^2 \xi / 3 \quad (6)$$

For the work necessary to produce a displacement $\delta\xi$ we then get

$$\delta\epsilon^- = -2\pi N e^2 \xi \delta\xi / 3 \quad (7)$$

By integration we obtain

$$\Delta\epsilon^- = -\pi N e^2 \xi^2 / 3 \quad (8)$$

$\Delta\epsilon^-$ is a negative quantity as can easily be seen. We transform our formula by making use of the fact that there are eight particles contained in the elementary volume a^3 .

$$\Delta\epsilon^- = -\pi N a^3 e^2 \xi^2 / 3 a^3 = -8\pi e^2 \xi^2 / 3 a^3 \quad (9)$$

The member $\Delta\epsilon^+$ originating from the repelling forces is obtained by adding the contributions of all the single ions surrounding the one considered. As a result,

$$\Delta\epsilon^+ = \beta A \xi^2 / a^{p+2} \quad (10)$$

where

$$\beta = 4p(p-1)[2^p + 4(2/3^{1/2})^p / 9 + 4(2/5^{1/2})^p / 5 + \dots]$$

Numerical values of β for some values of p are reproduced in table II.

TABLE II

p	7.5	8	8.5	9	9.5
β	35600	57700	92800	148000	235000

The whole energy due to the displacement ξ of the lattices is therefore

$$\Delta\epsilon = \Delta\epsilon^- + \Delta\epsilon^+ = (-8.4e^2/a^3 + \beta A/a^{p+2})\xi^2 \quad (11)$$

From this we get the force K per ion by differentiation

$$K = \partial(\Delta\epsilon)/\partial\xi = 2[-8.4e^2/a^3 + \beta A/a^{p+2}]\xi = f\xi \quad (12)$$

Now the equations of motion for the two different ions are

$$\begin{aligned} m^+ d^2\xi^+ / dt^2 &= f(\xi^- - \xi^+) = -f\xi \\ m^- d^2\xi^- / dt^2 &= f(\xi^+ - \xi^-) = f\xi \end{aligned} \quad (13)$$

Combining these equations we obtain

$$d^2\xi / dt^2 = -f\xi(m^+ + m^-) / m^+m^- \quad (14)$$

The harmonic oscillations representing the solution of this equation are characterized by the frequency

$$\nu = [f(m^+ + m^-)/m^+m^-]^{1/2}/2\pi \quad (15)$$

Denoting this frequency by ν_0 in case no external pressure is applied we have

$$\nu_0 = [(-8.4e^2/a_0^3 + \beta A a_0^{p+2})(m^+ + m^-)/2m^+m^-]^{1/2}/\pi \quad (16)$$

Making use of the relation (4) this may be written as

$$\nu_0 = [(-8.4 + 1.74\beta/\alpha)e^2(m^+ + m^-)/2m^+m^-a_0^3]^{1/2}/\pi \quad (17)$$

Application of external pressure changes the lattice constant from a_0 to $a_0 + \delta$, where δ is to be considered as a small quantity in all practical cases. Developing to the first order in δ we obtain

$$\nu = \nu_0(1 - \gamma\delta/a_0) \quad (18)$$

where

$$\gamma = [3 \cdot 8.4 - 1.74\beta/\alpha(p+2)]/2(-8.4 + 1.74\beta/\alpha)$$

Evaluating γ numerically the following table can be established

TABLE III				
p	7.5	8	8.5	9
γ	11.2	10.5	9.9	9.5

From this it may be concluded that the frequency changes relatively much more rapidly with pressure P than does the lattice constant. Expressing δ with the help of the volume-compressibility κ we get

$$\begin{aligned} \delta &= -\kappa a_0 P / 3 \\ \nu &= \nu_0(1 + \gamma\kappa P / 3) \end{aligned} \quad (19)$$

As an application we shall give the actual figures in the case of rock salt. For NaCl the compressibility found in the experiment is (P measured in Kg per cm²)

$$\kappa = 4.14 \cdot 10^{-6}$$

So to a pressure of 10000 atm. there would correspond the following frequency (for p the value 8 is used as given by Born's calculations)

$$\nu = \nu_0(1 + 0.145)$$

This means a displacement of the selective absorption line from $\lambda = 50\mu$ to $\lambda = 43.6\mu$. Pressures of this order can be realized experimentally either directly in some mechanical way (Bridgman) or by some indirect method, as for instance by electrolysis of the crystals. Joffé⁸ has shown that extremely high pressures can be reached in this latter way because of the enormous forces the space charges in the lattice exert on each other. So the possibility exists of checking our formula experimentally. As I hear through the kindness of Professor Joffé, measurements of this kind are going on in the Polytechnical Institute at Leningrad. The results thus obtained will be of some importance for the theory of crystals because they supply a new means of getting more information about the nature of the repelling forces. These are not yet very well known.

3. RESISTANCE OF METALS UNDER PRESSURE

The specific electric resistance of metals in general decreases with pressure. This has been shown especially by Bridgman⁹ in a long series of beautiful experiments. Now this fact presents considerable difficulty to the classical theories of metallic conduction. In fact we can deduce from these theories an approximate relation of the following type

$$1/\rho \propto N_e \Lambda$$

where $\rho = 1/\sigma$ is the specific resistance, N_e the number of free electrons per cm^3 and Λ the mean free path for these electrons. Now Λ , being inversely proportional to the number of atoms N_a per cm^3 , ρ will be roughly independent of the pressure in case we assume that N_e increases in the same way as N_a . More rigorous calculations show that the resistance should increase under all circumstances with pressure, which is in strict contradiction with the facts. Now there has been advanced an explanation of this fact by Grüneisen.¹⁰ The underlying idea is essentially this. The mean free path of electrons in the metal is not independent of temperature for the reason that the thermal oscillations of the atoms disturb their motion.¹¹ This may be thought to happen in the following way. In the space lattice of the metal the electrons of long path, moving approximately parallel to one of the lattice planes, contribute most to the conductivity. Now these electrons are more and more disturbed in their motion as the atoms are more and more displaced by the thermal agitation. The mean free path will then be approximately

$$\Lambda \propto 1/d^2$$

⁸ My information is taken from Joffé's lectures at the Calif. Inst. of Technology, 1925.

⁹ See for instance P. W. Bridgman, American Acad. of Arts and Sciences. Several papers in 1922-1925.

¹⁰ E. Grüneisen, Verh. d. D. Phys. Ges. 15, 186 (1913). I am indebted for this reference to the Editors of the PHYSICAL REVIEW.

where d is now the mean amplitude of the atom in its thermal agitation. From this standpoint we have the possibility of accounting for the experimental variation of conductivity with temperature¹² without being in contradiction with the facts of specific heat and the pulling of electrons from cold wires (electric field currents).¹³ Furthermore the increase of specific conductivity with pressure can easily be explained on this basis without making use of any artificial assumptions. Indeed the amplitudes of the atoms in their motion of thermal agitation are determined by the strength of the elastic force (f dynes per cm displacement are pulling the atoms back to their average positions). Now this elastic force can be compared with that mentioned above in the case of heteropolar crystals. We then make use of the results obtained in Section 2, and assume that they are approximately right for homopolar crystals also, i.e. that they have the same dependence on pressure as far as the magnitude is concerned. This could be justified indeed in a general way by merely making use of the fact that the repelling forces vanish much more rapidly with increasing distance of the particles under consideration than the attractive forces, which will be nearly always the case. If then d be the average maximum displacement of an atom we shall have for high temperatures this relation

$$fd^2 = 3kT \quad (k = 1.37 \times 10^{-16} \text{ erg})$$

Denoting with f , d and f_0 , d_0 the elastic constant and the amplitude of the atom in the compressed and in the natural state of the crystal respectively, then

$$\begin{aligned} d^2/d_0^2 &= f_0/f = v_0^2/v^2 = (1 - 2\gamma\kappa P/3) \\ \sigma \propto \Lambda &\propto 1/d^2 \propto (1 + 2\gamma\kappa P/3) \\ \sigma &= \sigma_0(1 + 2\gamma\kappa P/3) \end{aligned} \quad (20)$$

Thus from this point of view the increase of specific electrical conductivity σ with pressure is explained as follows. Since the elastic bonds of the atoms in the crystal increase in strength very rapidly with pressure, it is seen that the areas covered by the atoms in their thermal agitation decrease with pressure much more rapidly than the whole volume under consideration. For this reason the free space between the atoms (counted per cm^2) increases with pressure, so as to allow the conductivity electrons to move on longer mean free paths than before.

Experimentally it is found that

$$\sigma = \sigma_0(1 + cP) \quad (21)$$

¹¹ This conception has been adopted by different theories of metallic conduction. See for instance R. Seeliger, Enzyklopädie d. math. Wissenschaften, Teubner 1922, Vol. V₂, Heft 5, p. 870.

¹² Assuming Λ constant, the classical theory gave $\sigma \propto T^{-\frac{1}{2}}$ instead of $\sigma \propto T^{-1}$.

¹³ R. A. Millikan and C. F. Eyring, Phys. Rev. 27, 51 (1926).

So that for a lattice of the type NaCl, comparing (20 with 21) we should predict the following relation between the pressure coefficient c of electric conductivity and the compressibility κ

$$c = 2\gamma/3\kappa \sim 7\kappa \quad (22)$$

Now for metals we shall not have exactly the same molecular forces acting as in NaCl. Still our formula should give the right order of magnitude for the coefficient c , since its derivation is based essentially only on the fact that the repelling forces, compared with the attractive forces, decrease very rapidly with distance. Some experimental data obtained by Bridgman are collected just at random in Table IV, to show that our conclusion is right.¹⁴

	TABLE IV						
	Fe	Co	Rh	Pd	Ir	Pt	Au
$c \times 10^7$	24.2	9.3	17.4	19.6	13.5	19.5	33.3
$\kappa \times 10^7$	5.87	5.39	3.72	5.2	2.7	3.6	4.8
c/κ	4.1	1.7	4.65	3.75	5	5.4	6.9

There are also some metals, as for instance Bi, Sb, Ca, Li and Sr which behave abnormally. Their specific resistance increases with pressure. Evidently such a treatment as that suggested in this paper cannot be complete. It does not take into account such individual properties of the different metals as the dependence of number of free electrons on pressure, the forces acting on electrons in the interior of the crystals, etc.

In Grüneisen's original paper the change of elastic frequency with pressure has been computed in a quite different way from ours. He makes use of the quantum theory of equation of state of solid bodies (Debye, Grüneisen). Grüneisen's method is mainly a phenomenological one. This involves the necessity of making some general assumptions as to the behavior of solid bodies with temperature. It is, however, interesting to see that the results thus obtained check in the order of magnitude with those obtained in this paper in a more direct way. This is a justification of Grüneisen's assumptions.

Bridgman¹⁵ in his gap theory of metallic conduction also deduces the effect of pressure on conductivity by making use of the fact that the elastic frequencies decrease with pressure. His final formula for the change of conductivity is essentially the same as we have used it. His underlying picture, however, is quite different from that given above insofar as the electrons do not move freely through the spaces between the atoms. They on the contrary do not meet any resistance in moving through the atoms. It appears, however, to the writer that this theory is based too much on an overestimation of the size of the atoms in a crystal. Bridgman indeed considers them in general to be in direct mutual contact at the absolute zero point. Now most of the known evidence seems to indicate that there are large free spacings between the atoms. Such evidence is for instance

¹⁴ P. W. Bridgman, Proc. Amer. Acad. of Arts and Sciences, Vol. 59, No. 5, p. 114.

¹⁵ P. W. Bridgman, Phys. Rev. 9, 269 (1917); 17, 161 (1921); 19, 114 (1922).

furnished by the direct determination of atomic radii in crystals by investigation with x-rays. Scherrer and Debye¹⁶ find for instance in the case of diamond that the diameter of a C-atom (volume actually covered by the revolving electrons) amounts only to one-fourth of the mutual distance of the atoms. A second method of determining the gaps consists in direct comparison of diameters known from the kinetic theory with measured lattice constants. This gives in the case of alkali-halides dimensions of the gaps comparable with the dimensions of the constituting ions. Very strong evidence in favor of large gaps seems furthermore to be indicated by the fact that large amounts of matter may be transported through crystals without disturbing the lattice (electrolysis through crystals). The fact that constituent atoms may be extracted from crystals (mica for instance) without destroying the crystals, points also in the same direction.

It would be of very great importance if some conclusive evidence could be found with regard to the question whether slow electrons pass through atoms in approximately straight lines or not. Many physicists seem to consider, for instance, Ramsauer's well known results on behavior of slow moving electrons in certain gases as such evidence.¹⁷ The writer¹⁸ has tried to show, however, that even from the standpoint of classical dynamics it is not necessary to draw this conclusion. It would be, however, of extreme interest for the modern development of the quantum theory if this question could be settled definitely by some new experiments.

As another phenomenon connected with the change of elastic frequencies with pressure we may mention the specific heat of solid bodies. It is obvious that from the point of view of the quantum theory this change will affect the characteristic temperature Θ (Debye). Increase of ν means a higher value for Θ . The abnormal behavior (drop of specific heat) should be found then at higher temperatures in case external pressure is applied.

NORMAN BRIDGE LABORATORY OF PHYSICS,
CALIFORNIA INSTITUTE OF TECHNOLOGY,
January 18, 1927.

¹⁶ P. Scherrer and P. Debye, Physik. Zeits., Vol. 19, p. 474 (1918).

¹⁷ C. Ramsauer, Ann. d. Physik. Vol. 64, p. 513, 1921. "Slow" electrons means that their energy is less or about equal to the resonance energy of the deflecting atoms. The free electrons moving in the electric field in the metal will probably be such. Ramsauer's result is, that for several atoms as A, Kr, and Xe the effective area in their interaction with slow electrons is much smaller than the area given by the kinetic theory of gases. Electrons with their initial line of motion pointing towards the atom may in this case continue their path without being deflected appreciably by the atoms.

¹⁸ F. Zwicky, Phys. Zeits. 24, 171 (1923).

A DIRECT COMPARISON OF THE LOUDNESS OF PURE TONES

By B. A. KINGSBURY

ABSTRACT

The loudness of pure tones of frequencies 60 to 4000 cycles and for intensities from the threshold to 90 T.U. above the 700 cycle threshold.—The loudness of eleven pure tones was studied by adjusting the voltage applied to a telephone receiver to make these tones as loud as certain fixed levels of a 700 cycle tone. The average results of 22 observers, 11 men and 11 women, were arranged as contour lines of equal loudness through the normal auditory sensation area in terms of r.m.s. pressure in ear canal as a function of frequency. Frequencies from 60 to 4000 cycles were used and intensities from threshold of audibility to 90 T.U. above the 700 cycle threshold. It was found that if the amplitudes of pure tones are increased in equal ratios the loudness of low frequency tones increases much more rapidly than that of high frequency tones. For frequencies above 700 cycles the rate is nearly uniform.

A loudness unit.—As a loudness unit the least perceptible increment of loudness of a 1000 cycle tone was employed. In absolute magnitude this varies from level to level, but in the ordinary range of loudness it becomes constant. This unit takes into account the subjective character of loudness.

Sources of variation in data on loudness.—The variability of the data from which the averages were computed was separated into a factor expressing dissimilarity of ears and another expressing errors of observers' judgment. There was no level at which the variances were a minimum. Dissimilarity of ears causes more variation than errors of observers' judgment. The variances showed no significant sex difference.

THE purpose of this paper is to give data on the relative loudness of pure tones as judged by a group of eleven men and eleven women whose average threshold of audibility approximated former measurements. Since most ears probably can perceive nearly the same minimum amounts of sound energy and recognize about equal changes in pitch and intensity, measurements made by the above group should apply to the hypothetical average normal ear.

In Fig. 1 are shown the usual curves for the threshold of feeling and audition expressed in 20 times the common logarithm of the r.m.s. pressure on the ear drum (dynes per square centimeter) as a function of frequency. The pressure is that which would be produced in the ear canal if the walls and drums were rigid. The difference between any two ordinates is then the ratio of the pressures in transmission units (T.U.). This is the common unit for expressing amplitude ratios in telephony and at the same time takes into account the logarithmic relation between sensation and stimulus. The lower of the curves is the average threshold of audibility for the above group.

Let us imagine that the r.m.s. pressure of a test tone at the threshold of audibility is increased until it comes up to a level P . If one listens first to this tone and then to a tone of frequency f_1 , he can tell which appears

the louder and by adjusting the level of the tone f_1 , he can make the two appear equally loud. By comparing several tones with a test tone in this way a contour line of equal loudness through the region of audition may be determined. For instance, P_1 , P_2 , P_3 , etc. are points which were experimentally determined for one of these contours. In the work to be described 700 cycles was made the test tone, while the frequencies compared with it were distributed at approximately equal logarithmic intervals through the more important range of audition. This seemed the best way to secure results applicable in general to pure tones with measurements at a minimum number of frequencies.

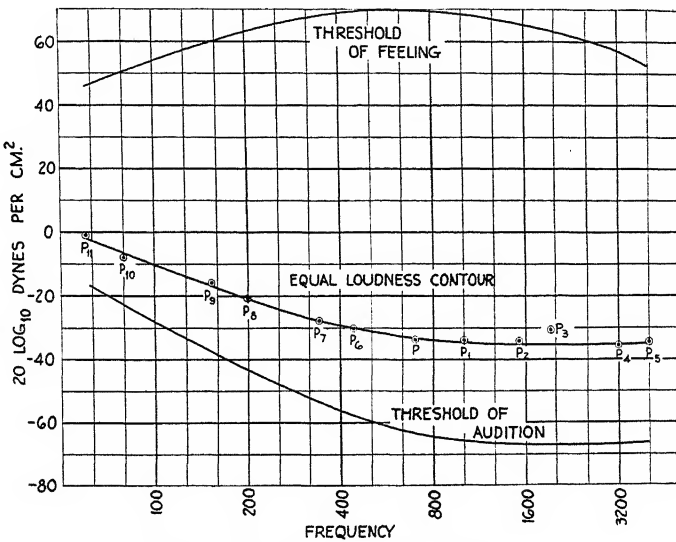


Fig. 1. Normal auditory sensation area.

In order to cover most of the intensities of ordinary sounds contours of equal loudness 10 T. U. apart at 700 cycles were selected up to levels somewhat above that of ordinary conversation. The 10 T. U. interval means that the amplitude of the sound wave for the 700 cycle tone at any contour was 3.16 times its value at the contour below this. There is no necessity for smaller intervals because a few fairly widely spaced contours should show quite definitely how the loudness of pure tones varies with level and frequency.

A schematic diagram of the apparatus used in the tests is shown in Fig. 2. It will be noted that the set-up consists of two symmetrical systems, which we have labelled *A* and *B*. The test tone was always furnished by the *A* oscillator. The filters in each case attenuated the first harmonic of the tone used about 75 transmission units. The thermocouples and galvanometers shown were used to measure the input currents of the attenuators. The resistance network attenuators which are calibrated to read the attenuation in transmission units could be readily connected by a switch to a special iron-clamped high impedance receiver.

The outline of the procedure in making tone balances was as follows: The *A* attenuator was placed in such a position that the observer could not see the dial; the dial of the *B* attenuator was covered with a cardboard screen, which prevented the observer from seeing the position of the pointer while making the adjustment. The 700 cycle test tone was set up on the *A* system and the frequency being compared with this on the *B* system. First three independent settings of the *A* threshold were made, then three for the *B* threshold. Next the experimenter set the *A* attenuator at one of the selected comparison levels and allowed the observer to adjust the *B* attenuator until when listening alternately to the two tones they seemed equally loud. The attenuator settings and the deflections of the meters

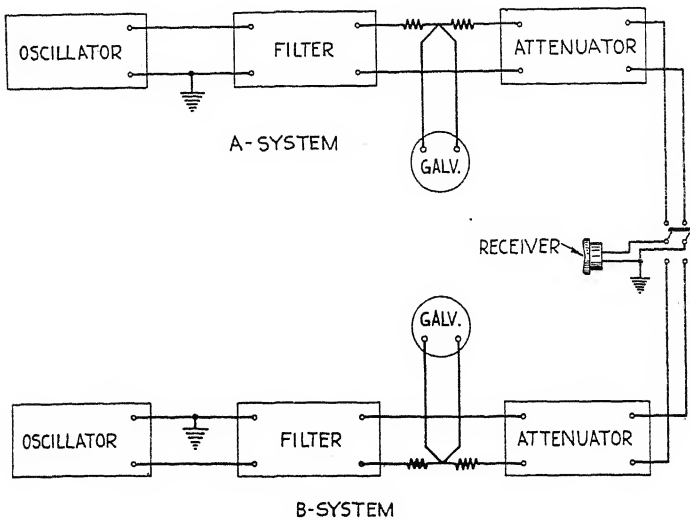


Fig. 2. Schematic diagram of apparatus.

were recorded for both systems. This process was repeated for the other fixed levels of the *A* tone, until three independent determinations had been made for each level. The order of taking the fixed levels of the *A* tone was made as random as possible and two successive determinations were seldom made at the same level. When the comparison of the two frequencies was finished, the *A* and *B* thresholds were once more secured.

From a calibration and check of the receiver and the input attenuator voltage, attenuator settings were reduced to the r.m.s. pressure in the ear canal in T.U. above or below one dyne/cm². It was found that r.m.s. pressures at the average *threshold of audibility* for this group coincided very closely with the values which represent the best estimates¹ for normal ears. Hence this threshold curve is taken as a datum from which all the other points on the diagram are to be reckoned.

¹ H. Fletcher, Useful Numerical Constants of Speech and Hearing, The Bell System Technical Journal, Vol. IV, No. 3, pp. 375, July, 1925.

In Fig. 1 were given the curves for the thresholds of feeling and audition. In Fig. 3, the data from loudness comparisons are plotted in a similar fashion

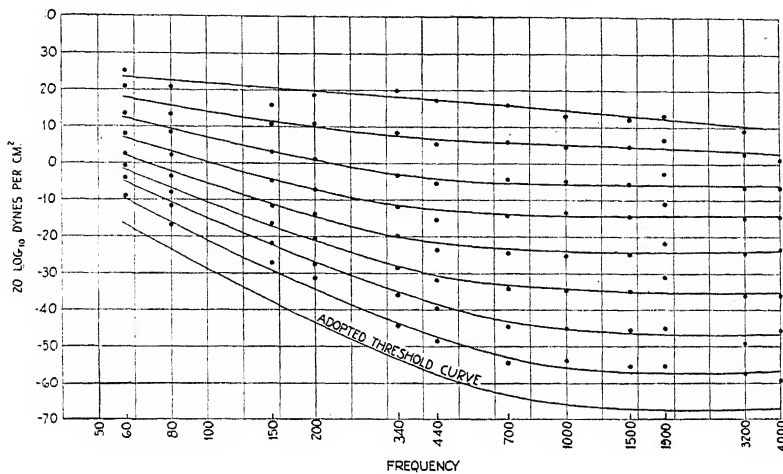


Fig. 3. Contour lines of equal loudness.

to demonstrate contour lines of equal loudness, the lowest curve being the threshold curve of audition.

These data may also be stated very conveniently in terms of *sensation level*, defined by the equation

$$S = 20 \log_{10}(P/P_0)$$

where P is the r.m.s. pressure of the sound wave and P_0 the minimum audible pressure for the average normal ear. That is, to get the sensation

TABLE I
SENSATION LEVEL (T. U.)
Each column represents $20 \log_{10} P/P_0$ of equally loud tones
Threshold of audibility adopted for these data (P_0 in dynes/cm²).

Frequency:	60	80	150	200	340	440	700	1000	1500	1900	3200	4000
$20 \log_{10} P_0$:	-16.5	-23.0	-37.0	-43.6	-53.5	-57.5	-63.4	-65.5	-67.0	-67.4	-67.6	-67.5

Frequency	Thres	Sensation level ($20 \log_{10} P/P_0$)										
60	0	8.4	12.5	15.7	19.2	24.8	29.9	37.3	41.9			
80	0	6.6	11.4	14.9	19.6	25.1	31.7	36.1	43.9			
150	0	9.9	15.2	20.8	25.6	32.5	39.7	47.8	52.9			
200	0	12.7	16.4	23.2	29.9	36.5	44.8	54.4	62.2			
340	0	9.4	18.0	25.1	33.8	41.7	50.7	61.6	73.5			
440	0	9.3	17.7	25.7	33.8	42.2	52.5	62.9	75.3	83.4		
700	0	9.3	19.3	29.3	39.3	49.3	59.3	69.3	79.3	89.3		
1000	0	11.7	20.7	31.1	40.7	52.1	60.9	69.8	78.5	86.8		
1500	0	11.6†	21.4	32.5	42.5	52.5	61.7	71.3	79.2	85.0		
1900	0	11.9†	22.4	36.3	45.7	56.7	65.0	73.7	80.2‡			
3200	0	9.9	18.5	31.6	43.1	52.8	61.1	70.0	77.0			
4000	0	8.0	22.1	31.6	44.0	53.2	61.1	68.9				
Loudness*	0	8.5	20.3	39.0	60.0	83.5	107.0	130.0	151.5	172.0		

* See 1000 cycle curve, Fig. 7.

† Average of 57 observations.

‡ Average of 63 observations.

level of any point in Fig. 3, it is merely necessary to notice how many T.U. the amplitude of the tone must be reduced to reach the threshold of audibility. In Table I, the data of Fig. 3 are expressed in terms of sensation level.

It has generally been assumed that loudness is a function both of the amplitude and frequency of the pressure wave, but the form of the function is not definitely known. The arbitrary levels of the 700 cycle tone had been chosen 10 T.U. apart, and loudness contours determined on this basis. At the level where the contours are closest together, the change in loudness for the same number of T.U. is greatest. The average interval between the contours was computed at each level, by adding together the intervals for each frequency and dividing by the number of frequencies. The first interval from the threshold was omitted since it was an irregular interval. The average interval between contours for each frequency was also computed. In Fig. 4 these data are plotted first with interval as a function of frequency and

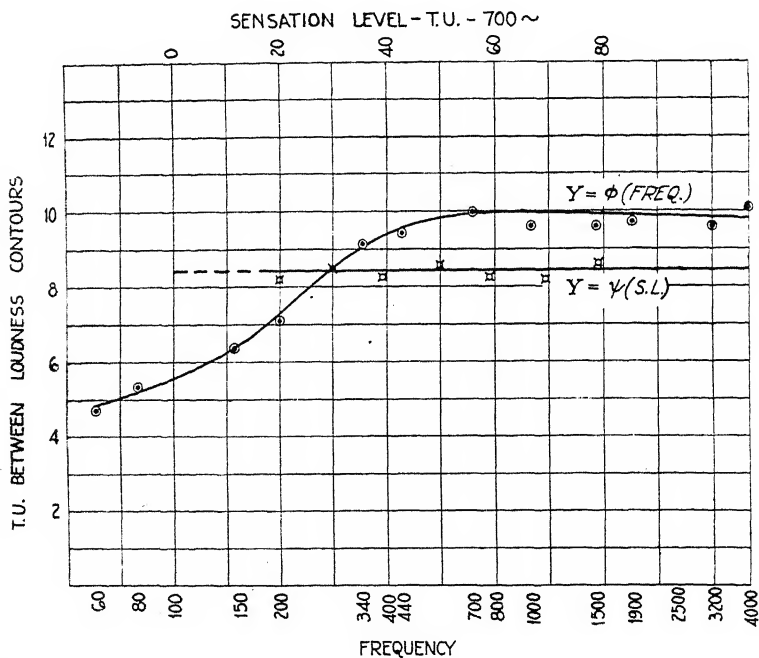


Fig. 4. Effect of sensation level and frequency upon sensation level increment between contours.

then with interval as a function of the sensation level of the 700 cycle tone. From these two curves it would appear that the interval between contours is about the same number of T.U. for all sensation levels, but that the loudness of low frequency tones increases much more rapidly than that of high frequency tones.

It seems desirable now to turn to another aspect of these results which should occupy a place of major interest in all hearing studies. This is the variation in observations which arises from the variability of an observer's judgment and the differences between ears. The usual procedure in reducing

data has been to take the arithmetic average of a number of observations and compute the standard deviation. In this case, because of the seemingly large importance of this variation, it appeared desirable to give it more careful treatment.

A particular value in Table I is the average of 66 observations, three of which were made by each of twenty-two observers. The deviation between any determination of an observer and his average can be readily calculated. The sum of the squares of these 66 deviations divided by 44 yields a quantity β which expresses the variance in observers' judgment. If X is an individual observation and \bar{X}_p , the average for that person this may be written: (Appendix I)

$$\Sigma(X - \bar{X}_p)^2 / 44 = \beta$$

These variances, one for each value in Table I are included in Table II.

TABLE II
Variances of data averaged for values of Table I in (T. U.)²

		20 log ₁₀ P_{700} :												
		-63.4 -63.4 -54.1 -44.1 -34.1 -24.1 -14.1 -4.1 +5.9 15.9												
		Frequency Thres _A		Thres _B										
60	$\alpha:$	29.9	54.3	35.4	34.9	33.4	34.2	50.7	67.5	59.1	27.0			
	$\beta:$	3.9	4.8	5.3	6.5	11.0	5.5	12.6	8.6	12.1	9.9			
80	$\alpha:$	23.4	24.8	20.1	26.5	21.4	28.3	37.4	36.8	21.5	17.8			
	$\beta:$	4.1	8.3	4.8	8.5	8.8	17.6	14.2	13.4	15.6	10.1			
150	$\alpha:$	30.1	56.9	34.2	34.0	34.0	39.7	47.8	71.8	109.9	80.4			
	$\beta:$	4.3	16.8	8.7	8.7	9.5	10.2	8.3	9.8	12.1	10.1			
200	$\alpha:$	32.6	36.7	11.4	40.7	27.0	33.7	34.8	64.5	67.4	26.2			
	$\beta:$	3.3	8.0	8.3	7.3	11.7	12.6	13.0	18.3	11.1	14.1			
340	$\alpha:$	30.3	34.5	22.2	13.7	24.0	29.9	42.4	52.1	64.5	24.4			
	$\beta:$	3.4	6.7	15.8	8.9	9.3	16.4	17.1	25.7	19.4	18.1			
440	$\alpha:$	31.7	54.3	21.8	22.6	31.0	38.9	43.8	48.9	41.5	31.3			
	$\beta:$	3.3	9.5	11.0	10.5	20.1	7.9	12.6	14.7	14.5	8.5			
700	$\alpha:$ *					1.1	0.2	2.0	1.1	.5	.8			
	$\beta:$					2.2	1.4	1.6	3.	3.6	1.4			
1000	$\alpha:$	30.3	42.9		27.5	21.2	22.2	15.7	13.2	16.4	17.9			
	$\beta:$	2.9	3.2		18.6	22.1	28.7	13.1	10.2	11.5	7.5			
1500	$\alpha:$	49.1	44.8		59.3	38.9	55.2	48.0	46.8	34.3	31.5			
	$\beta:$	3.2	2.8		14.4	26.2	17.7	16.6	13.0	4.7	4.2			
1900	$\alpha:$	30.6	70.0		97.4	48.1	56.1	53.8	43.0	36.6				
	$\beta:$	2.9	7.0		11.4	27.5	28.0	16.8	11.6	10.8				
3200	$\alpha:$	29.2	60.5		81.4	83.6	28.7	50.0	46.5	37.5	34.7			
	$\beta:$	3.7	3.3		36.3	22.3	29.4	33.6	16.5	11.3	12.1			
4000	$\alpha:$	18.7	100.8		96.0	71.9	73.1	44.3	51.6	25.4				
	$\beta:$	2.5	5.2		26.8	27.4	31.2	24.4	12.5	8.9				

* From the observations of 20 observers comparing 700 cycles with 700 cycles.

In all this work, measurements were made to the nearest T.U. and arithmetic averages and variances computed to the nearest 0.1 T.U.

The other factor which contributes to variation is the variance between ears. Let us call this variance α . A particular value in Table I is the arithmetic average of 22 averages, each of which is the arithmetic average of an observer's three settings. Let the general average be \bar{X} . Then we can make the following equation define α and β : (Appendix I)

$$3\sum(\bar{X}_p - \bar{X})^2/21 = 3\alpha + \beta$$

Since the value of β is known, α can be computed. The values are also given in Table II.

The standard deviation of the observations whose average is an individual entry in Table I is defined by the relation: (Appendix I)

$$S.D. = (0.97\alpha + \beta)^{1/2}$$

If Z equals the ratio of the error of the average to the observed standard deviation, it is a function only of the number of observations. Choosing

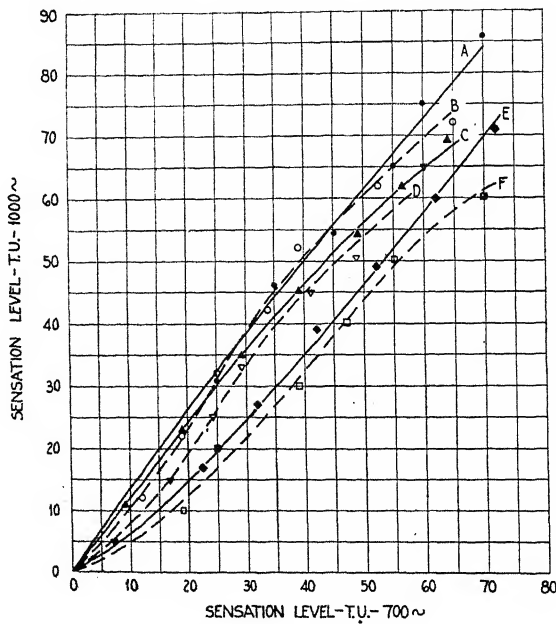


Fig. 5. Comparison of loudness balance methods.

the 95 percent error, a value in Table I will vary more than Z times its standard deviation only five times in a hundred, and another average outside of these limits would very likely be from another population of measurements. Z has in our case a value² of 0.25, and an entry in Table I is therefore determined to 1.5 or 2 T.U.

² W. A. Shewhart, Correction of data for errors of averages obtained from small samples, Bell System Technical Journal, V, No. 2, pp. 314, April, 1926.

All the experimental work up to this point had been carried on by making the levels of the *A* tone fixed and allowing the observer to adjust the *B* tone. In Fig. 5 are shown three pairs of representative comparisons, where each pair of curves *A* and *B*, *C* and *D*, *E* and *F* were made by the same individual. Every point shown is the average of 3 observations. *A*, *C* and *E* were made by fixing the level of the *A* tone as already described. For *B*, *D*, and *F*, the experimenter set the *B* tone and the observer adjusted the *A* tone for equal loudness. The results check rather closely; in fact two successive comparisons by the same method would not be more alike. The two comparisons were made about three months apart. It therefore seems reasonable in loudness comparisons to set the test tone at arbitrary levels.

In order to show conclusively that all points on a given contour represent equally loud tones, an additional simple check can be applied. If two *B* tones are compared directly will the result be the same as when each is compared with the *A* tone? To test this a direct comparison of 200 cycles and 3200 cycles was made by eleven male observers using 200 cycles as the *A* tone with fixed levels. Plotted in terms of $20 \log_{10}$ (volts on receiver) the results of the two methods are shown in Fig. 6. The direct comparison is

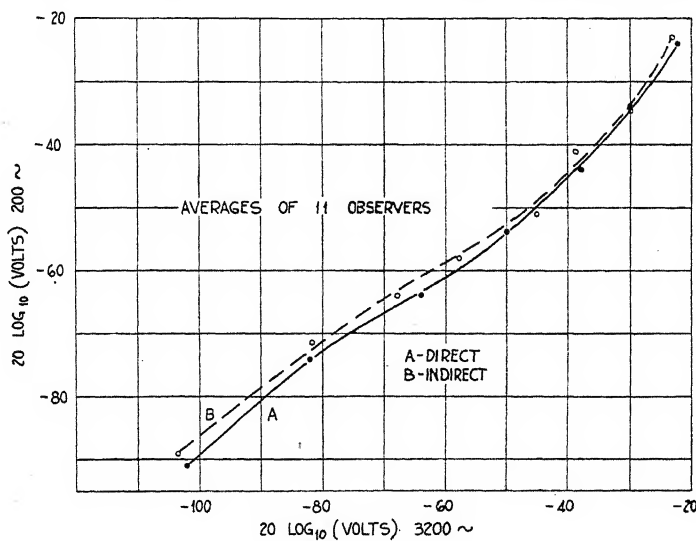


Fig. 6. Direct and indirect loudness comparisons.

the more accurate, since in the indirect comparison, variances are involved twice. In view of the values of α and β already given, the two curves do not appear significantly different.

DISCUSSION OF THE NATURE OF LOUDNESS

Since loudness is a subjective matter, it is rather difficult to determine what should be made the unit of loudness.³ Of course, any arbitrary scale

³ J. C. Steinberg, The Loudness of a Sound and Its Physical Stimulus, PHYS. REV., Second Series, Vol. 26, No. 4, pp. 507-523, October, 1925.

of loudness may be used provided that sounds which are equally loud have equal numbers on the scale and that loudness numbers vary progressively as we go from fainter to louder tones, but a system which recognizes some of the characteristics of loudness arising from the physical characteristics of audition would be preferable. Fig. 4 seems to show that in the ordinary range of hearing loudness is linear with sensation level if the Weber-Fechner Law holds. In light the unit of brightness has been made the least perceptible increment of brightness. Knudsen⁴ has data for several pure tones which show the relation between the Fechner ratio $\Delta E/E$ and the r.m.s. pressure in dynes per cm^2 in the ear canal. This ratio, "intensity sensibility of the ear" expresses the ratio of the smallest perceptible difference in the energy of a tone to its total energy. At 1000 cycles from these data, we were able to plot a curve in which the Fechner ratio was a function of the 1000 cycle sensation level. This curve was then extrapolated to the threshold on the assumption that there the ratio was unity.⁵ By making this ratio for the

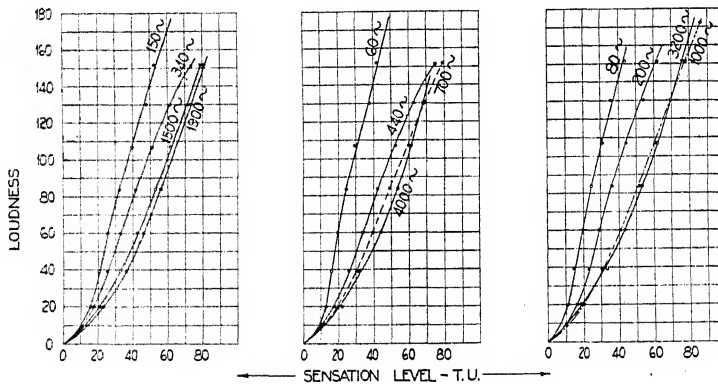


Fig. 7. Loudness of single frequency tones at various sensation levels.

1000 cycle tone our unit of loudness and calling the threshold of audibility zero loudness, it was possible to integrate from the above curve, a curve with the loudness of the 1000 cycle tone as ordinate and its sensation level as abscissa. That is, a 1000 cycle note just perceptibly above the 1000 cycle threshold has loudness unity; if it was just perceptibly louder than this its loudness is two and so on. This curve is marked 1000 cycles in Fig. 7.

The next step was to apply this unit to the data of Table I. Loudness numbers corresponding to the 1000 cycle sensation level given in this table were read from the 1000 cycle loudness curve. Each column in the table represented sounds which were equally loud in the ordinary sense, and the "loudness numbers" read from the 1000 cycle curve applied by the above definition to the other frequencies as well. Loudness for each frequency is thus numerically defined at several sensation levels. The remaining curves

⁴ V. O. Knudsen, Sensibility of the Ear to Small Differences of Intensity and Frequency, *Phys. Rev.*, Second Series, Vol. 21, pp. 84-103, January, 1923.

⁵ P. G. Nutting, The Complete Form of Fechner's Law, *Bulletin of the Bureau of Standards*, Vol. 3, No. 1, 1907.

of Fig. 7 were drawn up on this basis. A unit of loudness somewhat better for our purpose would have been the least perceptible increment of loudness of a 700 cycle tone compared with its sensation level, but data for such a unit are not available and there is reason to suspect that a curve of this kind between loudness and sensation level is much the same for 700 and 1000 cycles. Moreover, the unit used has been given a very definite quantitative value which makes it possible to compare it with any other unit. (Appendix II)

THE VARIABILITY OF THE DATA

An inspection of Table II fails to show any level of loudness where the similarity of ears is a maximum for all frequencies. In general the variances are smaller when the tones being compared are more nearly of the same frequency. Since α is usually greater than β , errors of judgment cause less variation than dissimilarity of ears. The differences in the values of α and β for the 700 cycle threshold are not significant. The statistical development on which these quantities rest makes them entirely independent quantities. If β is averaged for level, that is if the values in each column are added and the sum divided by the number in the column, it will be found that β reaches a maximum at about 40 T.U. above the 700 cycle threshold. The variance of judgment also varies with frequency being progressively smaller as we go from higher to lower frequencies. This makes it seem that the sensibility of the ear must be greater at low frequencies, which is equivalent to saying that the loudness sensation level curves will be steeper there.

The variability of ears does not seem to be correlated with frequency although it is somewhat less at the 1000 cycle comparison than elsewhere. The average α of equally loud tones below 700 cycles seems gradually to increase as loudness increases, while the average for equally loud tones above 700 cycles gradually decreases. In other words, at low frequency comparisons, ears are more alike for rather faint tones, while in the comparison of higher frequencies they are more alike at louder levels. This variability of ears is more nearly the same for all frequencies at about 40 T.U. above the 700 cycle threshold, but the error of judgment is here a maximum. It is therefore doubtful whether there is any best level for loudness comparisons. Practice seems to lower the 700 cycle threshold since it becomes lower in the same order as the balances were made. However, it appears probable that this effect is connected with other factors.

At 1900 cycles separate variances were computed from the observations made by the men and the women but no definite trend was found which would suggest sex differences in hearing.

CONCLUSION

When the amplitudes of single frequency tones are increased by equal ratios, high frequency tones increase in loudness more slowly than do low frequency tones. However, for frequencies above 700 cycles, the idea that tones are equally loud when they are an equal number of T.U. above the threshold is a very good approximation.

The study of the goodness of fit of regression lines which relate the sensation levels of equally loud tones may be made the subject of a later paper. An interpretation of such lines would be very much facilitated by a study of sensibility of the ear to intensity changes of pure tones because it is logical to suppose that in terms of this discrimination loudness matches are made.

APPENDIX I

In order to make the statistical analysis on which this paper rests easily available to the reader, a brief résumé⁶ of the method is included here.

If in a group of measurements two factors cause variation an analysis of variance offers a good method of treatment. Let X be an individual measurement, \bar{X}_p average of each class (determinations of each individual), \bar{X} arithmetic average of all X 's, k the number in each class and N' number of classes (observers). It can be shown that the following equation is true:

$$\sum_{1}^{kN'} (X - \bar{X})^2 = k \sum_{1}^{N'} (\bar{X}_p - \bar{X})^2 + \sum_{1}^{kN'} (X - \bar{X}_p)^2 \quad (1)$$

Let β represent the variance within classes. Here there are $N' (k-1)$ degrees of freedom, and we may write:

$$\sum_{1}^{kN'} (X - \bar{X}_p)^2 = N'(k-1)\beta \quad (2)$$

As twenty-two observers each making three observations were employed in determining the average values of Table I, we have, in this case, to put $k=3 \dots N'=22$.

The mean of the observations in each class is affected by the variance β divided by k as there are k observations in each class, and also by a variance α related to the difference between classes. As there are here $(N'-1)$ degrees of freedom, we write:

$$\sum_{1}^{N'} (\bar{X}_p - \bar{X})^2 = (N'-1)(\alpha + \beta/k) \quad (3)$$

where again for the special case of this paper $N'=22$ and $k=3$.

From (2) and (3) the value of α and β may be readily secured. It is only necessary to compute two of the three terms in Eq. (1). The usual procedure is to solve Eq. (1) for the summation on the left of Eq. (2) after evaluating the other two summations.

The standard deviation of our measurements from the general mean can be easily calculated from the above equations. The standard deviation is defined as:

$$(SD)^2 = \sum_{1}^{kN'} (X - \bar{X})^2 / (kN' - 1) \quad (4)$$

⁶ R. A. Fisher, Statistical Methods for Research Workers, 1925.

By the use of (1), (2) and (3) this reduces to:

$$(SD)^2 = [1 - (k-1)/(kN'-1)]\alpha + \beta \\ = .97\alpha + \beta \quad (N' = 22, k = 3) \quad (5)$$

We define Z by the relation

$$Z = (\bar{X} - m)/(SD) \quad (6)$$

where m is the true mean of all observations.² Z then is a function of the number of observations made and its value for any particular error may be determined from statistical tables. When this has been done, $(\bar{X} - m)$ can be computed.

APPENDIX II

The primary effort in this paper has been to discuss the loudness of pure tones in a simple experimental fashion without much regard to formulas of loudness. The least perceptible increment in the energy of a 1000 cycle tone was made the unit of loudness in the consideration of the pure tone

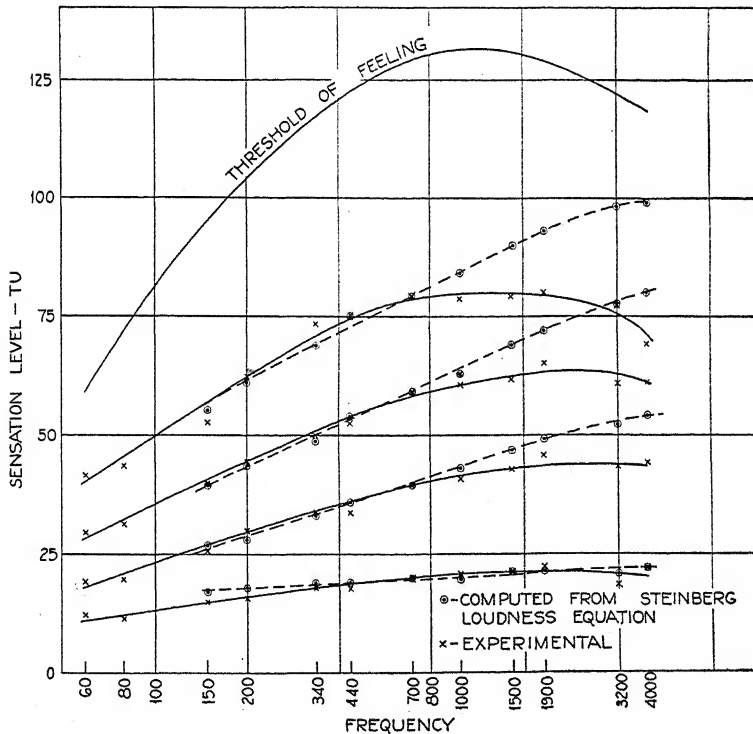


Fig. 8. Sensation levels of equally loud tones.

data because of its simplicity and direct application. However, this procedure did not justify the neglect of other methods of treating the data. Dr. J. C. Steinberg has developed a formula³ for loudness with the primary purpose of computing the loudness of complex sounds when the frequency

spectrum is known. This method involves essentially the summation of the loudness of the various frequency components. It can be applied readily to the loudness of pure tones. The formula employs two factors, first a weight factor which depends on the sensation level of the sound and its frequency, secondly a root factor which depends only on the sensation level of the sound. Using the values of the weight and root factors given by Dr. Steinberg, the sensation levels of tones of the frequencies studied as loud as 700 cycles at 19.3, 39.3, 59.3, and 79.3 T.U. respectively above its threshold value were determined. The results of these computations and the experimental results of this study are shown in Fig. 8 as curves for the sensation levels of equally loud tones. Computations were not made at 60 and 80 cycles because these weight factors were not stated. The procedure employed makes the computed and experimental values for the sensation levels of the 700 cycle tone coincide. For the lower frequency tones the computed values fit the experimental data rather well. If the values of the root factor are considered known and independent of frequency, weight factors may be computed on the basis of the pure tone data in this report.

The justification of this formula as well as any other which attempts to express loudness, must be substantiated both by the study of pure tone loudness and the Fechner ratio. The accuracy with which weight factors calculated from these pure tone data fit measurements on complex sounds has not yet been determined.

BELL TELEPHONE LABORATORIES, INCORPORATED
December 1, 1926.

BOOK REVIEWS

Allgemeine Grundlagen der Quantenstatistik und Quantentheorie. ADOLF SMEKAL. This treatise is published both as a part of the Encyclopädie der Mathematischen Wissenschaften and as a separate volume. It is divided into three main sections, dealing respectively with the principles of classical and quantum statistics, the general foundations of quantum dynamics, and the application of the contents of the first two parts to particular problems of quantum statistics. The discussion in the first part centers on such topics as the ergodic and quasi-ergodic hypotheses, the structure of the phase space, the assignment of a priori probabilities, and adiabatic invariants, with frequent references to the older article in the Encyclopädie by P. and T. Ehrenfest. The application of the classical theory to gases, solids, heat radiation, and problems of fluctuations is taken up next, due consideration being given to the recent work of Fowler and Darwin. It is shown how the empirical facts regarding specific heats and heat radiation are incompatible with a continuous weight function and lead to the notion of a discrete structure of the phase space. The statistics for such a space is then investigated, as well as the radiation law which it leads to in conjunction with Einstein's assumptions about the processes of emission and absorption. After thus having shown the necessity of a modification in the classical view of atoms and molecules, the author proceeds with a very complete account of the basis of the older quantum theory—the Rutherford-Bohr atomic model, the correspondence principle for multiple periodic systems, the theory of perturbations, impacts, and optical phenomena (absorption, dispersion, scattering, and diffraction), with applications fully mentioned but not discussed at great length. Unfortunately, and quite without the author's fault, this part of the book is not up to date, because our knowledge of atomic phenomena has advanced by leaps and bounds since the time the article went to press (August, 1925). The undulatory mechanics of de Broglie and Schrödinger, the matrix formulation of atomic dynamics introduced by Born and Heisenberg, as well as the numerous applications of these developments to individual problems will therefore not be found in the book. Nevertheless, this second part retains a distinct value, as the reader is furnished with a profound discussion of the principal difficulties in the way of a satisfactory description of atomic phenomena and especially of the dual nature of radiation. In addition the very complete bibliography should be useful to any atomic specialist.

The last part falls into three sections; the specific heat of gases, dissociation equilibria in gases and chemical constants, and the statistics of impact phenomena. It is greatly to be regretted that Einstein's theory of the degeneration of gases evidently was published too late to be given more than a brief mention in some footnotes. For the same reason the remarkable connection between this theory, de Broglie's waves of phase, and Pauli's equivalence principle for spectra could not be taken up.

The volume should prove valuable, particularly as a work of reference, and it is to be hoped that Professor Smekal some day will undertake to write a new edition, with the recent advances treated in the same thorough and critical spirit which pervades the present pages. Pp. vi+362. B. G. Teubner, Leipzig, 1926. Price, bound, R.M. 16.00.

R. DE L. KRONIG

Abhandlungen zur Wellenmechanik. E. SCHRÖDINGER.—This book of 169 pages of text with a preface of 9 pages contains reprints of six papers by the author. All the papers are on wave-mechanics. They represent the origin and the most important developments of the subject. The fundamental thought is remarkably keen and simple. It is roughly as follows: Since classical mechanics can be thought of as geometrical optics in a properly chosen

medium (Hamilton), it is supposed that *true* mechanics is wave optics in the same medium. Stationary states of atoms are thought of as stationary oscillations of the medium. This is the first step towards doing away with the cabalistic nature of quantum conditions and forms a most fundamental advance. Even though Schrödinger's way should not prove to be the best and ultimately accepted one, the very fact that it has been conceived gives one hope of understanding physics in terms of fundamental principles and ideas rather than complicated restricting conditions.

The results of the theory have proved to be identical with those of the theory of matrices. The formal identity of the two is very elegantly presented in the fourth paper of the series. The first two papers show the evolution of the idea with applications to the hydrogen atom, the oscillator, the rotator, band spectra. The third paper discusses the transition from microscopic to macroscopic phenomena. The fifth paper develops the theory of perturbations and applies it to the Stark effect of the hydrogen atom. It also gives absolute intensities in the hydrogen spectrum. The sixth paper introduces modifications in the wave equation required for non-conservative systems, gives an interpretation of the charge density in terms of the wave parameter, eliminates thereby a part of the radiation difficulty, discusses dispersion, and gives the wave equation for relativity and for magnetic fields.

The series of papers is preceded by a short introduction expounding concisely and clearly the fundamental idea, stating what the theory is capable of doing and where it fails. The whole is written in a very lucid and attractive style. Pp. ix+169, 12 figures, 1927: 8°, Leipzig, Johann Ambrosius Barth. Price, unbound, R.M. 5.70; bound, R.M. 7.50.

G. BREIT

Outline of Physical Chemistry. GEORGE SENTER. Fourteenth Edition. The fact that this book has reached its fourteenth edition may be considered to be ample evidence that teachers and students of chemistry, especially in Great Britain, regard it as a highly successful introductory treatment of physical chemistry. To the student beginning the study of this branch of chemistry, this book should prove to be an excellent and stimulating guide. The reviewer is glad to recommend it heartily.

There are two points which seem to merit adverse criticism. On page 246, it is stated that in the electrolysis of sodium sulfate sodium ions and sulfate ions give up their charges to the electrodes and then react with water liberating hydrogen and oxygen. This view is in conflict with that expressed on page 399 where discussing a similar problem it is stated that "the gases are products of the primary decomposition of water." Again, on page 286 the author declares: "The reason why the law of mass action does not apply to strong electrolytes has not been satisfactorily elucidated." This is certainly a remarkable statement by a physical chemist in view of the fact that the paper by Debye and Hückel dealing with strong electrolytes appeared nearly four years ago. The reviewer does not necessarily object to the exclusion of the theory of Debye and Hückel from an elementary presentation of the theories of electrolytic solutions. He does object strongly to such a misstatement as is found in the sentence just quoted. Pp. 419, 46 figs. D. Van Nostrand Company, New York, 1927. Price \$3.00.

F. H. MACDOUGALL

Das Element Hafnium. GEORG v. HEVESY. This monograph reviews the present state of our knowledge of the chemical and physical properties of the element hafnium. It is written by one of the discoverers of the element and one to whom we owe much of our information concerning it. After a brief description of the discovery of the element (the priority dispute is not discussed) the author details various methods for separating hafnium from zirconium. Following this is a statement of the properties of the element, its atomic weight, crystal structure, x-ray and optical spectra (with wave-length tables). The compounds discussed are the oxide, the double fluorides, the oxychloride, the phosphate and the acetylacetone derivative. There are chapters on the analytical chemistry of hafnium and on its occurrence and abundance in the earth's crust. The last chapter is devoted to an interesting discussion of the reasons for

the striking similarity between hafnium and zirconium. The book will form a valuable addition to the library of the chemist and the physicist. Pp. 49, 23 figs. Julius Springer, Berlin, 1927. Unbound, price Reichsmark 3.60.

JOHN T. TATE

Lehrbuch der Physik, MÜLLER-POUILLET, 11 Auflage, Zweiter Band, Lehre von der Strahlenden Energie (Optik), Erste Hälfte. Edited by O. LUMMER in collaboration with H. ERGELET, F. JÜTTNER, A. KÖNIG, M. v. ROHR, and E. SCHRÖDINGER.—As indicated by the first half of the volume on optics, the eleventh edition of this well known text is being thoroughly revised and brought up to date. The principal revisions are mentioned in this review. In the first chapter there is a new treatment of the history of the conception of the ether, dealing with the changes brought about by the development of the electromagnetic theory, and later, of the special, and finally, of the general theory of relativity. New material on the propagation of light in moving media, on the Doppler effect, and the aberration of light, is introduced. There are two new chapters on the optical properties of glasses and other materials, and on their dependence on chemical composition. The chapters dealing with the eye and vision have been enlarged from 72 pages in the tenth edition to 167 in the present. The improvement here is noteworthy. The chapter on interference is nearly doubled in length by the introduction of material chiefly on interference spectroscopy. The chapter concerning images of objects which are not self luminous, which includes Abbe's theory of the microscope image, has been extended to three times its former length. In this revision, the subject of ultra-microscopy receives special emphasis. There has been, in fact, a decided improvement in this text. If the second half of this volume, which was not available to the reviewer, is as thoroughly revised in the light of modern knowledge as this half has been, the work will be most valuable for general reference or as a text in the field of optics. Pp. xviii+928; 654 figs.+VII plates. Friedr. Vieweg & Sohn, Braunschweig, 1926. Price 50 M. unbound, 54 M. bound.

JOSEPH VALASEK

L'Energie Rayonnante, Tableaux Synoptiques de l'échelle des Longueurs d'Onde et des principales caractéristiques du rayonnement électro-magnétique avec un résumé des théories actuelles. A. FORESTIER.—This book contains tables of wave-lengths, together with formulas and constants having to do with radiation. Theories of radiation are summarized and various formulas for black body and spectral line radiation and for x-rays are given, with recent values of the constants appearing in them. The wave-length tables are historical in that they contain names and dates with most of the numerical data. The methods of investigation are also briefly summarized. The tables include wave-lengths from 30,000 meters to 0.0189 A. U. Cosmic rays are omitted. The recent work on joining the infra-red and Hertzian radiations and on gamma rays is summarized at the end of the book instead of being incorporated in the tables. Otherwise the selection and arrangement of material is very good. This volume will serve as a useful reference book for data on radiation.—Pp. 76. Librairie Scientifique Albert Blanchard. Paris, 1926. Price 20 f.

JOSEPH VALASEK

PROCEEDINGS
OF THE
AMERICAN PHYSICAL SOCIETY

MINUTES OF THE NEW YORK MEETING, FEBRUARY 25-26, 1927.
JOINT MEETING WITH THE OPTICAL SOCIETY OF AMERICA.

The 143rd regular meeting of the American Physical Society was held in New York City in the new Physics Laboratories of Columbia University on Friday and Saturday, February 25 and 26, as a joint meeting with the Optical Society of America. The presiding officers were Karl T. Compton, President of the American Physical Society, and W. E. Forsythe, President of the Optical Society of America. The attendance was about 300 persons.

On Friday morning there was a general session of the Optical Society. The program of the Optical Society on Friday afternoon consisted of two invited papers, the first by Professor F. K. Richtmyer of Cornell University on "The Extension of the Classical Laws of Optics into the X-ray Region of the Spectrum," and the second by Professor R. W. Wood of Johns Hopkins University on "The Experimental Control of the Radiating States of Optically Excited Atoms."

The sessions of the Physical Society were held on Saturday morning and afternoon. Each session was divided into two sections.

On Saturday the members of the two societies were the guests of Columbia University at a complimentary luncheon served in the Physics Laboratories.

Special Business Meeting. A special business meeting of the American Physical Society was held at the end of the afternoon session on Saturday. Article I of the By-Laws was amended by adding a section as follows:

"5. The Council shall, however, have power, by a special vote in each case, to honor a member or fellow by placing him on a retired list with no dues, provided such a member or fellow is not less than 65 years of age, and has retired from active service in his professorial or other corresponding position. A member or fellow going on the retired list will waive the receipt of the journals from the Society."

At the regular meeting of the Council held on Saturday, February 26, 1927, twenty-four were elected to membership: Boyd W. Bartlett, J. G. Black, Ralph B. Blackman, C. J. Calbick, Preston B. Carwile, Frank W. Constant, Edgar D. Doyle, Theodore Dreier, Samuel O. Grimm, Newton S. Herod, Raynor C. Johnson, Nicolas de Kolossowsky, F. W. Lancaster,

Donald P. LeGalley, Bernard Lewis, Sunao Nakamura, Saburo Numakura, George F. Taylor, H. L. Van Velzer, George B. Welch, E. J. Workman, Bernard L. Worsnop, Ziro Yamauti, William A. Zinzow.

The titles and abstracts of papers presented before the Optical Society of America will be found in the Proceedings of that Society, published in the *Journal of the Optical Society of America and Review of Scientific Instruments*.

The abstracts of the forty-seven papers presented before the American Physical Society are given in the following pages. An Author Index will be found at the end.

HAROLD W. WEBB, *Secretary.*

ABSTRACTS

1. The intensity of scattered x-rays and the Compton effect. G. E. M. JAUNCEY, Washington University.—Williams (*Phil. Mag.*, 2, 657, (1926)) and Jauncey (*Phys. Rev.*, 29, 206, (1927)) have shown that the experimental intensity of x-rays reflected by crystals can only be calculated on theoretical grounds on the assumption that it is only the electrons in the U state (*Phys. Rev.*, 27, 687, (1926)) which take part in the Bragg reflection. In the present paper it is assumed that all the electrons in the U state in a given atom cooperate in the unmodified scattering. This requires that the unmodified scattering per atom varies as F^2 and the modified scattering as $(Z - F)$, where F is the atomic structure factor as calculated by Williams and Jauncey and Z is the atomic number. The ratio of the scattering in a given direction to the Thomson scattering in the same direction is then approximately (so long as $F > 1$) given by $(F^2 + Z - F)/Z$. Calculated and experimental values, the latter in parentheses, follow for $\lambda = 0.41 \text{ \AA}$ scattered by copper: 40° , 4.1 (4.8); 60° , 2.58 (2.5); 80° , 1.88 (2.14); 100° , 1.42 (1.45); 120° , 1.25; 180° , 1.12.

2. The measurement of x-rays used for therapy. HARRY CLARKE, Rockefeller Institute.—If it is desired to measure the dose at a well-defined point, a very small ionization-chamber must be used, and the current will then be so small that it must be measured by means of an electroscope or an electrometer. For accuracy of measurement, as well as for convenience, the meter has to be mounted rigidly at some distance from the tube. On the other hand, the chamber should be movable for convenience in use. The proper design of a conductor to connect the chamber with the meter has, heretofore, presented a difficult problem. The conductor must be well-insulated, and protected against both electrostatic induction and leakage due to ionization; it must also be flexible. The writer's apparatus consists of two separate units. The portable unit consists of a small chamber connected with a condenser; the fixed unit is an electroscope with a calibrated variable condenser. The chamber unit is connected with the electroscope for charging; it may then be taken to any part of the laboratory for exposure to the rays. After exposure, it is returned to the electroscope for measurement of the quantity of electricity lost.

3. Reflection of soft x-rays. ELIZABETH R. LAIRD, Mount Holyoke College.—The experiments on the reflection of soft x-rays reported earlier (*Phys. Rev.* 27, 510, (1927)) have been repeated for copper, with slight changes in the apparatus, and the results confirmed; showing an absence of regular reflection at angles much above 5° at 950 volts and its presence at 340 volts. Also, at the lower voltage a fraction of the radiation is transmitted through fluorite, and the fluorite fluoresces; at the higher voltage the fluorite is quite opaque and does not fluoresce. It is inferred that the radiation at 950 volts does not include all that present at 340 volts. It is suggested that this may explain the different results obtained by Dauvillier

with the crystal reflection method using higher voltages and those of the critical potential method. A glass reflector with partially ground surface was used to show that the ground surface did not reflect.

NOTE: It has been found that glass reflects at large angles at 950 volts as at 340 volts. The phenomenon interpreted as a fluorescence of fluorite has not appeared on a later series of plates.

4. Further test of the theories of absorption of x-rays. F. K. RICHTMYER and L. S. TAYLOR, Cornell University.—At the Philadelphia meeting we reported measurements of the K discontinuity of Ag and Au in an attempt to decide between Kramer's theory of absorption and that of De Broglie. The uncertainty of the values of the mass scattering coefficients of Ag and Au made it impossible to decide between the two theories. The present measurements on Mo(42), Ag(47) and Sn(50) were made with the hope that the scattering coefficients for these three elements would not be far different and that the two theories might be thus tested. Assuming a reasonable value for σ/ρ , the data for the ratio of K absorption to L absorption are in better agreement with De Broglie's theory. But Kramer's theory gives a better value for the absolute magnitude of K absorption at the K limit.

5. The general radiation from a very thin target. WILLIAM DUANE, Harvard University.—Electrons, traveling horizontally with substantially the same velocity, pass through a hole in a block of iron. At its center, they meet the column of mercury moving downward in a mercury vapor pump. The mercury column acts as a very thin target, which continually renews itself. The radiation coming from the impacts of the electrons against the mercury column can be examined through suitable openings. Pin-hole camera photographs taken when the mercury pump is not running indicate some radiation coming from the interior walls of the apparatus. Such photographs taken with the mercury pump running show, in addition to the above, radiation coming from the space in which the electrons hit the mercury column. Measurements by means of an ionization chamber on the absorption of this radiation by aluminium indicate that it is not quite homogeneous, but much more nearly so than the radiation coming from a solid target. The average, or effective wave-length of the radiation is slightly longer than the short wave-length limit of the spectrum calculated from the constant (storage battery) voltage applied. Experiments with x-ray spectrometers on the distribution of energy in the spectrum are in progress.

6. An analysis of the arc and spark spectra of scandium. HENRY NORRIS RUSSELL, Princeton University, and WILLIAM F. MEGGERS, Bureau of Standards.—New measures of the arc spectrum (in which practically all the enhanced lines appear) have led to the classification of 337 lines of Sc I and 131 of Sc II leaving only a few weak lines outstanding. The spark spectrum is relatively simple. The lowest terms are 3D , 1D , arising from the electron configuration $3d\cdot 4s$. Next come $^3F'$, $^3P'$, 1S , 1D , 1G from $3d\cdot 3d$. All these terms combine with 3P , 3D , 3F , 1P , 1D , 1F from $3d\cdot 4p$; and these again with 3S , $^3P'$, 3D , $^3F'$, 3G , 1D , from $3d\cdot 4d$, and 3D , 1D from $3d\cdot 5s$. The last are in series with the lowest terms, and indicate an ionization potential of 12.8 volts. A 3P term arising from $4s\cdot 4p$ and a $^3P'$ from $4p\cdot 4p$ are also present. The arc spectrum is much more complex. The lowest term is $^2D(3d\cdot 4s\cdot 4s)$; then 4F , 2F , 2D , 2G , 4P ($3d\cdot 3d\cdot 4s$). The configurations $3d\cdot 4s\cdot 4p$ and $3d\cdot 3d\cdot 4p$ give numerous "middle" terms combining with these. Higher terms have been identified as arising from $3d\cdot 4s\cdot 5s$; $3d\cdot 3d\cdot 5s$; $3d\cdot 3d\cdot 3d$; $3d\cdot 4s\cdot 4d$, and $3d\cdot 4p\cdot 4p$. The first two of these belong to series and give the ionization potential 6.7 volts for the neutral atom. There are strong intercombinations between the doublets and quartets in the red, and weak ones in the ultra-violet. All details of the structure of both arc and spark spectra are in complete agreement with Hund's theory.

7. Multiplets in the spectra of vanadium (III). R. C. GIBBS and H. E. WHITE, Cornell University.—Using the regular and irregular doublet rules as guides, it has been found possible,

from the corresponding known multiplets in Sc_I and Ti_{III}, to identify the triad of multiplets of V_{III} designated as $^4F_{2,3,4,5} - ^4G_{3,4,5,6}$; $^4F_{2,3,4,5} - ^4F'_{2,3,4,5}$; and $^4F_{2,3,4,5} - ^4D_{1,2,3,4}$. For these multiplets the initial state is given by one 4p electron and two 3d electrons. In the final state the 4p electron has shifted to a 4s orbit. The separations of the $^4F_{2,3,4,5}$ levels are found to be in the ratio 2.50:3.52:4.50, in very close agreement with Landé's interval rule which for these levels gives 2.5:3.5:4.5. The relative intensities of the lines in these multiplets conform to the usual rule. A comparison of the data for one, two, and three electron systems of Sc, Ti, and V shows that the addition of first one and then a second d electron causes not only an increase in the multiplicity but also successive shifts in the radiated lines toward the longer wavelengths by very nearly the same frequency interval. It has also been found possible to identify the $^4F_{2,3,4,5} - ^4F'_{2,3,4,5}$ multiplet of Cr_{IV}.

8. A quantitative test of Hund's theory of doublet bands of the OH type. E. C. KEMBLE and F. A. JENKINS, Harvard University.—According to Hund (Zeits. f. Phys. 36, 657, (1926)) multiple electronic levels in molecules are due to different orientations of the electron spin vector relative to the internuclear axis. At low nuclear speeds the component of the spin vector parallel to the nuclear axis is quantized while at high speeds the component parallel to the resultant angular momentum is quantized. The consequent distortion of the molecule gives rise to bands in which each branch is composed of doublets or triplets with a maximum separation at the origin. In the case of doublets the effect of the distortion on the rotational term formula has been carried through quantitatively by one of the authors (Kemble) and the resulting equations have been tested on the data for NO beta bands by the other (Jenkins). The two levels involved have equal moments of inertia but different values of B in the empirical formula $E/h = A + Bj^2 + Cj^3 + \dots$. The observations confirm the theory and in particular check the following formula for $B : B = (1 \mp z)^2 h / 8\pi^2 I \pm z^2 \Delta_0$ where Δ_0 = term difference for doublet at zero rotation and $z = h / (8\pi^2 I \Delta_0 - 2h \pm 2k)$. The upper sign in each case goes with the lower level of the pair.

9. Vibrational levels in the blue-green band system of sodium. F. W. LOOMIS, New York University.—The lines in Wood's magnetic rotation spectrum of sodium vapor may, according to Kemble's theory of the Zeeman effect in band spectra, be considered as approximately representing band origins. Most of those in the blue-green region have been arranged into a band system and their frequencies formulated, in terms of the (integral) vibrational quantum numbers n' and n'' , which can, by comparison with the fluorescent series, be unambiguously assigned, as follows:

$$\nu = 20301.7 + (124.13n' - 0.84n'^2) - (158.5n'' - 0.73n'^{1/2} - 0.0027n''^2).$$

The location of the n'' levels makes it possible to plot the fluorescent series in the manner used with iodine and to identify approximately the bands to which the fluorescent lines belong. Moreover, when n' and n'' are plotted for all the rotation lines identified, a wide open parabola-like figure appears, of a type which Condon (Phys. Rev. 28, 1182 (1926)) has accounted for in terms of an hypothesis of Franck. This explains the effect on the fluorescent spectrum of varying the frequency of the exciting light, as reported by Wood (e. g. Physical Optics, Frontispiece, Fig. 8); since the separate patches in the blue and yellow which result from stimulation with blue light correspond to the two arms of the parabola, and the single green patch due to green stimulation corresponds to the vertex.

10. Equations for thermionic emission. W. R. HAM, Pennsylvania State College.—It has recently been shown that an equation of the form $i = A \epsilon^{-b_0/T}$ applies as well as any other to experimental data on thermionic and photoelectric emission. The derivation of this equation from Richardson's general equation is now discussed. The value for ϕ assumed is $\phi = \phi_0 - \frac{1}{2}KT - \int_0^x (dv/dx)dx$ where ϕ_0 is independent of T , K is the Boltzmann constant, and dv/dx the potential gradient in the space very near the surface of the thermionic emitter. The experimental and theoretical reasons for the assumption are stated. On substituting this

expression for ϕ in the general equation not only the first equation mentioned appears but also an equation $i = i_0 \exp[(ef_0^x (dv/dx)dx)/KT]$, which may be used to explain lack of saturation observed in thermionic currents as the applied PD is increased indefinitely. A discussion of the upper limit X of the integral appearing in this last equation follows and it appears that assuming sufficient experimental confirmation of the equation, a variable value of the dielectric constant is indicated in the work function region and this in turn implies that the electrons in this region are still in their atomic orbits.

11. Evidence for collisions of the second kind in the rare gases. GAYLORD P. HARNWELL, Princeton University.—A positive ray apparatus was used to investigate the products of ionization by electron impact in mixtures of helium, neon, and argon. The variation with pressure of the ratio of the two types of positive ions present was investigated in detail for three cases.

Case 1. A mixture of half helium and half neon was investigated. The ratio He/Ne was found to decrease regularly between .03 mm and .15 mm. At .03 mm the mean free path is approximately equal to the dimensions of the apparatus. Case 2. A mixture of half neon and half argon was investigated throughout the same pressure range. The ratio Ne/A decreased regularly between .05 mm and .15 mm, but this decrease was less rapid than in Case 1. Case 3. This mixture was half helium and half argon, and the pressure range was as above. The ratio He/A remained constant within experimental error, but as this mixture is least suited to analysis in a positive ray apparatus this result is the least conclusive. The observed effects are best explained by a type of collision of the second kind equivalent to ionization by positive ions. To account for the results obtained an electron must be transferred from an atom to an ion at a certain fraction of the collisions between an atom and an ion of lower ionizing potential.

12. Critical potentials of iron. RICHARD HAMER and S. SINGH, University of Pittsburgh.—The critical potentials of iron were investigated up to 132 volts. A long quartz tube enclosing two electrodes consisting of a central iron rod and a concentric iron cylinder was heated externally. Changes in potential could be made in practically equal or alternately large and small steps. Equal ones facilitated the plotting of differential curves. Alternate large and small steps facilitated observing differential deflections at desired potentials. Applied potentials were measured with a potentiometer. Repeatedly occurring breaks in the current potential curves were taken to indicate critical potentials. Many were checked by the differential methods. Those found are 3.7, 7.15, 11.2, 16.3, 19.4, 24.5, 29.0, 33.9, 38.8, 42.1, 45.7, 48.4, 51.4, 54.8, 61.6, 72.7, 89.6, 103.1, 111.6, 125.8 volts. Thomas and Compton did not find 38.8 and 45.7. Expect 72.7 and 89.6, all check with the observations of Thomas, usually within 0.3 volt. No marked break was, however, observed by us at 82.7. Possibly our 89.6 is an average effect corresponding to his 82.7 and 94.8. The method is being developed to differentiate multiple and fine structure potentials.

13. The ionization in HCl vapor. HENRY A. BARTON, National Research Fellow, Harvard University.—A mass spectrograph was used to study ionization in HCl vapor at low pressures, the resolving power being sufficiently good to distinguish between $(\text{HCl})^+$ and Cl^+ and to separate the isotopes. The results show that in pure HCl the primary type of ion formed by electron impact is $(\text{HCl})^+$. This is true from the ionizing potential of 13.8 volts to at least 75 volts. Cl^- ions were likewise observed but chiefly from near the filament where no electrons of more than three or four volts energy were available. Probably the HCl was dissociated at the filament, the Cl atoms then picking up electrons by virtue of their electron affinity. Further evidence of such dissociation was furnished by the observation of H_2^+ , H^+ , and Cl^- ions from impact. These ions were most prominent shortly after evacuation suggesting that water vapor from the walls aided in the dissociation. Detection of $(\text{H}_2\text{O})^+$ ions then confirmed the presence of water vapor. After some days the only ions at low pressures were $(\text{HCl})^+$ and Cl^- , the latter probably not from impact. Thus the results are contrary to the previously held assumption that H^+ and Cl^- are the products of electron impact in HCl.

14. Ultra-ionization potentials of mercury. ERNEST O. LAWRENCE, National Research Fellow, Yale University.—By a method of magnetic analysis of the bombarding electrons it has recently been shown that there are a succession of distinct types of inelastic impacts in mercury vapor above the ionization potential. (Phys. Rev. 28, 947 (1926)). Earlier measurements of the ionization of mercury by electron streams possessing Maxwellian velocity distributions by many investigators failed to bring out these critical potentials, although it seems that they should have been observed in a qualitative manner. The apparent discrepancy has been eliminated for the present investigation has shown that the ultra-ionization potentials are observable when using Maxwellian velocity distributions in the electron streams providing sufficient care is taken to insure constancy of conditions and the ionization is observed at intervals of 0.1 volt.

15. Ionization of mercury vapor by $\lambda 2537$. PAUL D. FOOTE, Bureau of Standards.—Measurements of the photoelectric effect in Hg vapor were made by the method employed for caesium vapor. (Phys. Rev. 27, 37 (1926)). Although the data were confined to a vapor pressure range and ratios of amplified photo-current to initial thermionic current, which were less than the corresponding values in caesium at which occur departures from the linear relation between photo-current and illumination, the relation for Hg vapor between illumination I and photo-current Δi was of the form $\Delta i = A I^2 / (1 + BI)^2$ where A and B are constants for a given vapor pressure. This law holds accurately in the range investigated, 25° to 60°C. Admixture of nitrogen greatly increases the effect while small amounts of hydrogen reduce the current rapidly to zero, as has been found by Houtermans. The above law approaches the relation $\Delta i = A I^2$ for small intensities, as found by Rouse and Giddings, showing that two separate excited atoms (since only the core of $\lambda 2537$ is effective) are involved in the ionization process. The increase by nitrogen shows that the metastable state 2^3P_0 plays a role. Hydrogen at a pressure of 0.0002 mm reduces the current to half its initial value. Since the quenching of 2^3P_1 by hydrogen, as observed in resonance radiation, is inappreciable for such small pressures the concentration of the 2^3P_0 atoms exceeds by a large factor that of the 2^3P_1 atoms. The complete mechanism of the ionization process is considered in some detail.

16. The striated discharge in hydrogen and helium. JOHN ZELENY, Yale University.—The striated discharge between cold electrodes in hydrogen exhibits the remarkable property that the distance between the striae for constant current in the tube passes through a sharp minimum as the pressure is increased, and at a higher pressure passes through a maximum. The pressures at which these reversals occur and the magnitudes of the changes are dependent on the current through the tube and on some other factors. At pressures near that at which the minimum stria distance is observed, the Faraday dark space, which covers about 2 cm of length in most of the pressure region indicated, contracts and one or more striae leave the head of the positive column and move up to and surround the cathode. The stria distance in helium was measured between pressures of 2.7 mm and 9.7 mm, and for these two pressures was found to be 11.3 mm and 6.0 mm, respectively, with 6 m.a. current. Measurements made in argon, oxygen, and air under the same conditions are also given, but the range of pressures in which measurable striae was observed is much more limited.

17. Pressures in discharge tubes, Part I,—Long slim tubes. W. H. CREW and E. O. HULBURT, Naval Research Laboratory, Washington, D. C.—The pressure changes in a discharge tube 3 m long, diameter 10 mm, due to uncondensed discharges were measured by a striation gauge. The striation gauge consisted of a second discharge tube (joined to the first) excited by direct current calibrated so that the shift of the striations of the positive column with pressure was known. With helium the temperature increment above the temperature, with no discharge, about 300°K, calculated from the pressures, were, respectively, 4°, 13° and 21°C for 200, 600 and 1000 watts in the long tube. With wet hydrogen the pressure increments, corrected for temperature, gave for γ , the concentration of hydrogen atoms (i.e., the number of

atoms divided by the number of atoms plus molecules) values which increased rapidly with the power to about 400 watts, being thereafter appreciably constant; the values of γ for 150 watts in the tube decreased from about 70 to 50 percent as the pressure decreased from 0.6 to 0.15 mm of Hg. With dry hydrogen and with oxygen γ was less, with nitrogen γ was close to zero. Complete curves were obtained with air, CO₂ and CO. Observations were also made with condensed discharges.

18. Movements of striae in discharge tubes under varying pressures. L. H. DAWSON, Naval Research Laboratory, Washington, D. C.—The striae of the positive column of a discharge tube move along the tube when the pressure of the gas in the tube is varied. The curves of this motion have been obtained as a function of the pressure, the distance apart of the electrodes, the diameter of the tube and the density of the current for wet and dry hydrogen, helium, nitrogen, air, carbon monoxide and carbon dioxide. The pressures, measured by a McLeod gauge, ranged from 0.6 to 0.05 mm of mercury. With these curves the discharge tube may be used as a sensitive and quickly responding pressure gauge. The motion of the striations increased with the diameter of the tube being roughly ten times greater in tubes 30 mm in diameter than in tubes 16 mm in diameter. For tubes in which the distance between the electrodes was less than the maximum distance of motion of the striae, as the pressure was diminished the positive column marched into the anode without distortion and vanished.

19. The constancy of the flashing period of a neon glow-lamp. ELIAS KLEIN, Lehigh University.—The comparison of a neon-lamp frequency (operated on d.c.) with that of a standard clock is accomplished by the pendulum which cuts off a light-beam incident upon a photo-electric cell connected with the grid of a vacuum tube. The neon lamp is placed directly in the plate circuit, or in a separate circuit which is coupled to the plate circuit, of the vacuum tube. The period of the lamp is adjusted by capacitance and resistance associated with the lamp. Periodically, the pendulum admits light to the cell, the grid becomes negative and the space-current is reduced to zero thereby suppressing one or more lamp-flashes. While the cell is inoperative the lamp-frequency is again that which is characteristic of the circuit. Therefore, one pendulum cycle marks two clock-intervals during which the lamp completes a number of flashes. If the lamp-period is constant, each interval shows exactly the same number of flashes. Preliminary observations indicate the lamp-period constancy to a fair degree of precision. Replacing the pendulum by a tuning-fork-shutter yields similiar results. This is also a methods for subdividing intervals of time.

20. An absolute ionization vacuum gauge. THOMAS H. JOHNSON, Yale University.—The inconvenience of calibration has been eliminated in this new simply constructed gauge. The electrodes, which consist of a fine, straight incandescent filament between and parallel to two plane plates, are maintained at potentials which give a uniform electric field over the electron paths. The gauge constant, k , defined as the ratio of the pressure to the number of ions per electron, is obtained by means of the relation $k = V_+/(a \int_0^\infty P(\nu) d\nu)$ where a is the distance and V_+ the potential between the filament and the positive plate, and $P(\nu)$ is the ionization probability per centimeter at unit pressure expressed as a function of the electron energy. (See Compton and VanVoorhis, Phys. Rev. 27, 724, (1926)). This method of obtaining the gauge constant assumes that all of the positive ions go to the negative plate. Ionization due to secondary electrons is neglected. Furthermore the effect of space charge on the electron paths and the potential distribution along the paths is not considered. However, measurements in mercury vapor in equilibrium with liquid mercury at 0°C, corrected for thermal effusion, show that the calculated constant is very nearly correct if V_+ is greater than 75 volts.

21. Post-arc conductivity and metastable states in mercury. M. L. POOL, University of Chicago (Introduced by A. J. Dempster).—For pressures from 0.3 to 10 mm current—potential curves have been obtained which suggest that around the collecting electrodes

there exist negative and positive space charge sheaths. Residual positive ions may, depending upon the size of the collecting electrodes, be made to persist as long as 1/10 sec. Galvanometric current—low potential curves have been obtained which can be explained by the diffusion of electrons from a region of high electron and positive ion concentration near the cathode. Cathode ray oscilloscope curves which show (even in the presence of air, He, H₂, CO₂, or A) a critical potential of about +3.2 volts can be accounted for by the same assumptions. No convincing evidence of a long lived (1/20 sec.) metastable state has been found. The apparent long lived states deduced from absorption of certain spectral lines may be due to the continuous formation of metastable states of very short life as the positive ions recombine. Impurities may thus have a large influence on these short lived atoms while not, however, altering the slow process of their formation.

22. Excitation of mercury vapor by positive ions. ERNEST J. JONES, University of Minnesota.—Saturated mercury vapor at 90°C was bombarded with positive potassium ions from the source developed by Kunsman. The resulting radiation from a field free space was photographed by a quartz spectrograph. At 160 volts accelerating potential only the 2537 line appeared after six hours exposure, with an average ion current of 1.5×10^{-5} amperes. At 640 volts and four hours exposure with an ion current of 2×10^{-5} amperes the following lines were obtained; 2537 (1S-2p₂), 3126 (2p₂-3d₂), 3132 (2p₂-3d₈), 3650 (2p₁-3d₁), 4046 (2p₃-2s), 4358 (2p₂-2s). At 1200 volts and under the same conditions the above lines were again photographed. No new lines appeared. At the latter potential the intensity of lines originating from levels higher than the 2p₂ was increased roughly 100% relative to that of the 2537 line. Comparison with the spectra excited by the electrons shows; (1) that the efficiency of excitation by positive ions is far less than by electrons; (2) that it increases with velocity at least up to 1200 volts; (3) that up to 1200 volts the probability of excitation to the 2p₂ level is greater than to higher levels; (4) that up to 1200 volts the excitation to levels higher than the 3d_{1,2,3} is not observed with a four hour exposure and current of 2×10^{-5} amp.

23. Velocity selector for atomic rays. J. TYKOCINSKI-TYKOCINER, University of Illinois.—An atomic ray on its way towards a target is directed through two vibrating slits suspended in a magnetic field at a distance D apart. The vibrations are controlled by a piezoelectric oscillator. The emerging ray contains selected velocities. For small ratios of the width w of the slits to its amplitude a , the selected velocities are determined by $v_n = 2Df/n$, where f is the frequency of the vibration and $n = 0, 1, 2, 3, \dots$ etc. For larger w/a ratios velocity bands may be obtained each embracing a range

$$v'_n - v''_n = 2Df[1/(n-w/2\pi a) - 1/(n+w/2\pi a)]$$

When used in connection with Gerlach and Stern magnetic moment analyzer, spectrum-like images should be obtained consisting of n pairs of sharply defined lines each showing a deflection

$$S_n = [(Ml^2n^2/8mD^2f^2)(\partial H/\partial S)_0] [\frac{1}{2} + \{1/12 + (\partial H/\partial S)_I/\frac{1}{6}(\partial H/\partial S)_0\}^{1/2}]$$

and a thickness

$$d_n = (\partial H/\partial S) (\frac{1}{2} + K) Ml^2nw/4mD^2f^2\pi a$$

The value for the magnetic moment M may be determined from either of these relations. For a selector, which is in the course of construction, the following data have been computed for rays of atomic hydrogen at 500°K ($f = 9000$ and $n = 2$): $v_n = 1800$ m/sec; $S_n = 1.5$ mm and $d_n = 0.095$ mm.

24. Inelastic collisions in ionized gas mixtures. GAYLORD P. HARNWELL, Princeton University.—The variation with pressure of the ionization by electron impact in mixtures of the rare gases with hydrogen and nitrogen was studied using a positive ray apparatus. All the results described refer to mixtures of the gases concerned in equal proportions. Mixtures of hydrogen with helium, neon, and argon were investigated in turn. In each case the number of rare gas ions decreased rapidly after a pressure of about .05 mm was reached. At this

pressure the mean free path was approximately equal to the dimensions of the apparatus. H_2 decreased slightly with pressure but less rapidly than when the rare gas was not present. H_1 and H_3 increased, the latter very rapidly except in the case of the neon mixture where the increase was less marked. In mixtures of nitrogen and the rare gases the same type of effect was observed. At higher pressures the rare gas ions decreased at approximately the same rate as the N_2 ions. The N_1 ions increased, being present in slightly greater numbers when the rare gases were present than when they were not. These results definitely support the other evidence for the existence of a type of collision of the second kind resulting in ionizations by positive ions.

25. Note on "pendulum" orbits in atomic models. R. B. LINDSAY, Yale University.—"Pendulum" or straight line orbits in an atom are usually ruled out as physically impossible since they apparently involve collision of the electron with the nucleus. Nevertheless their value in fixing energy levels was suggested a few years ago by J. W. Nicholson, who sought to show that in the simple two body problem such orbits are possible with quantized energy values of the same form as those of the circular and elliptic orbits (viz., $W = -2\pi^2 Ne^2 m_0 / n^2 \hbar^2$). Unfortunately in his quantum condition he used the rest mass m_0 throughout instead of the varying mass m . Correction of this error shows that his result is invalid without some modification of his premises. The present writer has been able to obtain quantized "pendulum" orbits with energies equal to the Balmer terms by the assumption that in addition to the inverse square force of attraction between nucleus and electron there is an inverse cube (or higher power) force of repulsion of such a character that it is effective only in the close vicinity of the nucleus, i. e. at a distance of the order of magnitude of 10^{-12} to 10^{-13} cm. It is believed that the result may be of interest in view of the possible utility of straight line orbits in atomic models with more than one electron.

26. Magnetic moments of iron in complex salts. L. A. WELO and O. BAUDISCH, Rockefeller Institute for Medical Research.—Although the moment of iron is 29 magnetons (Weiss) in the ferric ion and about 26 in the ferrous ion, it is known that the moment is nearly zero in the ferrocyanides, the pentacarboynl and the nitroprusside and that it is about 10 magnetons in the ferricyanides. The moment in the ferricyanides is probably the same as in the divalent copper ion. Possibly still other moments in iron may be found, and these may correspond to the ions of other transition elements. With this in view we have made a preliminary survey of 45 rare salts obtained from Professor Weinland of Würzburg. Twenty eight salts have the normal moment of simple ferric salts. Seven are hex-acetates of the type $[Fe_3(CH_3COO)_6(OH_2)]Cl$ and form a well defined group in which each iron atom has the same moment as the nickel ion with 16 magnetons. A hexa-benzoate $[Fe_3(C_6H_5COO)_6(OH)]ClO_4 \cdot C_6H_5COO$ also falls within this group corresponding to nickel. Two complex glycolates ($CH_2O \cdot COO$) apparently correspond to the chromium ion with 19 magnetons. No correspondences are noted in remaining salts. It was assumed that the salts obey the simple Curie law. Experiments to test this question are under way.

27. A system of structures for atomic nuclei. WARREN W. NICHOLAS, National Research Fellow, Cornell University.—First, a neutron structure is assumed (proton inside electron) which may offer a simple basis for the "packing effect." Second, the known series of isotopes is discussed with reference to the postulate that evolution of light elements was from complex to simple, the nuclei losing units smaller than the α -particle. Third, a geometrical structure for the atomic nucleus (protons and neutrons on alternate cube corners in a cubic lattice) is assumed which shows some main features in common with the known nuclear series. Fourth, a specific structure is proposed for the nucleus of sulphur 32 which can be followed through consecutive disintegrations, thereby accounting for the known isotopes from sulphur 32 to helium 4. Several of the disintegrations seem rather arbitrary, but some of the results, especially concerning the symmetry of the abundant nuclei, are suggestive. The above theory

may be tested by (1) further experiments on artificial disintegration, and by (2) precision determination of isotope masses.

28. On the condition of validity of macromechanics. M. S. VALLARTA, Massachusetts Institute of Technology.—The problem considered in this paper is: Assuming the associated wave of de Broglie and Schrödinger, under what conditions do the trajectories orthogonal to the equiphase surfaces of the wave (i. e., the rays) coincide with the mechanical paths determined by the classical Hamilton principle? If $\alpha(xyz)$ is the amplitude of the associated wave, sufficient conditions are shown to be: (a) α satisfies Laplace's equation, i. e. there are no inhomogeneities in the "medium" where the wave propagates; (b) the frequency of the associated wave is infinite, i. e. Planck's constant vanishes. The necessary and sufficient condition is that the equiphase surfaces determined from the wave equation coincide with the (classical) surfaces of constant action. De Broglie's condition for the validity of macromechanics (*Journal de Physique*, **7**, 321, (1926)) is then examined and applications to the hydrogen atom are given. The Sommerfeld-Wilson quantum conditions and their generalization by Wentzel (*Zs. für Physik*, **38**, 518, (1926)) are studied in the light of the above criteria, and it is shown that an azimuthal quantum condition always has a meaning, not however a radial quantum condition.

29. A general proof of the Langevin-Debye formula and the susceptibilities of O₂ and NO. J. H. VAN VLECK, University of Minnesota.—Using the new quantum mechanics, the formula $\alpha + N\mu^2/3kT$ given by Langevin and Debye for magnetic and dielectric susceptibilities respectively is derived without specializing the model further than to assume that the precession frequencies of the moment vector are small compared to kT/h . These precessions may be due to temperature rotation, coupling of spin magnetic moment relative to axis of figure, etc. Thus the Debye formula for dielectric constants is applicable even to asymmetrical polyatomic molecules. Previous explanations of the paramagnetic susceptibilities of gaseous molecules involved the unreasonable assumption of a magnetic moment freely quantized relative to the magnetic field, but now it can be quantized either with reference to the figure or temperature rotation axis (Hund's couplings of types a and b). Quantitative results agreeing with experiment to within about 1% are obtained assuming ³S normal levels in O₂ and Mulliken's suggestion of ³P states separated by 122 cm⁻¹ in NO. In NO the calculations include corrections for the fact that the contribution of the spin moment is somewhat diminished by its precession frequency (122 cm⁻¹) being comparable to kT/h , while the orbital moment precesses so fast that only its axial component $\sigma_k=1$ is effective.

30. On the calculation of changes of functions involving factorials as applied to entropy calculations. MORTON MASRUS, Worcester Polytechnic Institute.—In entropy calculations in connection with the kinetic theory of gases or the quantum theory the changes in functions depending on factorials have hitherto been calculated by a method depending on the replacement of factorials by continuous functions and differentiation. This method is neither simple nor logically satisfying. A new method of calculation is shown which depends on the direct evaluation, by simple well known processes, of

$$\Delta F = F(x + \Delta x, y + \Delta y, \dots) - F(x, y, \dots)$$

where F is a function involving the factorials of x, y, \dots , and where x, y, \dots and $x + \Delta x, y + \Delta y, \dots$ are taken as integers. The details of this method are illustrated by the treatment of two examples:

$$F_1 = \log \{ [(n+p-1)!] / [(n-1)!p!] \}$$

and

$$F_2 = \log \{ [n!] / [n_0! n_1! n_2! \dots n_p!] \}$$

In F_1 the change in F_1 produced by some change Δp is found, and in F_2 the condition for making F_2 a maximum, subject to the additional restrictions that $\sum n_i = n$ and $\sum (in_i) = p$ is derived.

31. Properties of substances and mixtures in the condensed state at the absolute zero of temperature. R. D. KLEEMAN, Union College.—With the theoretical researches previously communicated to the Physical Society (Philadelphia meeting) as basis, a number of properties of a substance or mixture in the condensed state at the absolute zero of temperature have been deduced. The most important of these are: $c_v = 0$, $(\delta c_v / \delta T)_v = 0$, $(\delta^n c_v / \delta v^n)T = 0$, $c_p = 0$, $(\delta c_p / \delta T)_p = 0$, $c = 0$, $dc/dT = 0$, $(\delta p / \delta T)_v = 0$, $(\delta^2 p / \delta T^2)_v = 0$, $d\dot{p}/dT = 0$, $d^2\dot{p}/dT^2 = 0$, $(\delta v / \delta T)_p = 0$, $(\delta^2 v / \delta T^2)_p = 0$, $dv/dT = 0$, $d^2v/dT^2 = 0$, where \dot{p} denotes pressure, v volume, T absolute temperature, and c_v , c_p , c , the specific heats at constant volume, constant pressure, and under vapor pressure, respectively. The total differential coefficients refer to a substance or mixture under the pressure of its vapor. In the paper quoted it was shown directly that $c_v = 0$, a result which is included in Nernst's Theorem. It is now shown that also $c_p = 0$ and $c = 0$, and that the specific heat possesses also the important properties expressed by $(\delta c_v / \delta T)_v = 0$, $(\delta c_p / \delta T)_p = 0$, and $dc/dT = 0$.

32. On the surface heat of charging. LEWIS TONKS and IRVING LANGMUIR, General Electric Co.—Two methods are available for calculating the theoretically necessary reversible heat development, or absorption accompanying the charging of the surface of a conductor. One method depends on a new relation $\eta_{s1} - \eta_{s2} = kT \ln(A_1/A_2) + eP_2$ between the surface heats, η_s , of the two surfaces, the A 's of electron emission equations of the type $i = AT^2e^{-b/T}$ and the Peltier heat at the interface between the conductors. The other method consists of a comparison of the cooling effect of electron emission and the latent heat calculated from the temperature variation of emission. Experimental evidence points to $\eta_s = 0$ (nearly), $A = 60.2$ amps/cm² deg² (nearly) for all pure metals. Published cooling effect measurements on an oxide coated filament give $\eta_s = 0$ whereas the value of A gives η_s not equal to zero. This leads to no contradiction if only part of the surface is emitting electrons. For monatomic films cooling effect measurements are lacking but the values of A give both positive and negative surface heats of charging.

33. Thermal agitation in conductors. H. NYQUIST, American Telephone and Telegraph Company.—At the December, 1926, meeting of the American Physical Society, J. B. Johnson reported the discovery and measurement of an e.m.f. due to the thermal agitation in conductors. The present paper outlines a theoretical derivation of this effect. A non-dissipative transmission line is brought into thermodynamic equilibrium with conductors of a definite temperature. The line is then isolated and its energy investigated statistically. The resultant formula is $E_\nu^2 d\nu = 4kT R d\nu$ for the r.m.s. e.m.f. E_ν contributed in a frequency range one cycle wide by a network whose resistance component at the frequency ν is R . T and k are the absolute temperature and the Boltzmann constant. Experimental data are available for the audible range and there the agreement between the formula and the data is good. It will be observed that neither the charge nor mass nor any other property of the carrier of electricity enters the formula explicitly. They enter indirectly through R . The formula above is based on the equipartition law. If the quantum distribution law is used the expression becomes

$$E_\nu^2 d\nu = [4h\nu R / (e^{h\nu/kT} - 1)] d\nu.$$

The two expressions are indistinguishable in the range of the measurements.

34. Temperature variations in wires heated by alternating current. L. SMEDE, Westinghouse Elec. and Mfg. Co., East Pittsburgh.—Corbino, in 1910 and 1911, gave a solution of the problem of the temperature variation of a wire heated by alternating current. In this solution it is assumed that the temperature variation is small compared to the average temperature of the wire. Certain terms are neglected in order to simplify the solution, which seem too large to neglect. In the present paper it is assumed that, for small temperature variations, the radiation is proportional to the first power of the absolute temperature, and that the resistance remains constant. On these assumptions an equation is derived which gives the same temperature variation as derived by Corbino.

35. The potential of photoactive cells containing fluorescent electrolytes. H. W. RUSSELL, Cornell University.—The variation of the potential of a photoactive cell containing a fluorescent electrolyte with time of illumination has long been a subject of dispute. Goldmann in particular, having noted that the potential approached a maximum which was independent of the intensity of the exciting light, arrived at a potential-time law on a theory involving the Hallwachs photo-electric effect. Measurements on cells with sputtered platinum electrodes containing Rhodamin B in absolute alcohol have been made. The potential has been measured with a string electrometer of small capacity and short period. Goldmann's limiting potential was not found. The magnitude of the effect does not vary with the frequency of the exciting light in accord with the true photo-electric effect, yellow light being more effective than blue light of the same intensity. A theory has been developed on the assumption that the exciting light causes a permanent chemical change in the electrolyte. Diffusion plays an important part in the potential-time relation. This theory predicts the shape of the potential-time curve and its variation with the intensity of the exciting light.

36. Optical absorption and photo-electric conductivity of sulphur crystals. B. KURREL-MEYER, Harvard University.—The optical absorption and photo-electric conductivity of single crystals of rhombic sulphur have been measured over the visible spectrum. The absorption is complete in the violet, but is relatively low from 500 to 650 m μ . The photo-electric conductivity is measurable between 400 and 650 m μ ; its maximum, referred to unit incident energy, lies at 470 m μ . There is strict proportionality between photocurrent and light intensity and between photocurrent and electric intensity throughout the ranges used. If there is a saturation value of the electric intensity it probably lies above 30,000 volts per cm, and is therefore very much higher than the saturation electric intensity in the diamond and in zincblende. This fact may be connected with the relative magnitudes of the refractive indices. The conductivity referred to unit absorbed light energy does not seem to obey the linear relation demanded by the quantum mechanism usually assumed for its production.

37. The periodicity of photo-electric thresholds. GEORGE B. WELSH, Cornell University.—Considering the photo-electric threshold as a measure of the energy taken from the incident radiation in order to detach one of the outer electrons from its atom, the elements having the most loosely bound electrons should permit detachment with the expenditure of minimum amounts of energy. Using the present available data, the curve showing the relation between photo-electric thresholds and atomic numbers exhibits a certain periodicity with strong maxima for the alkali metals and decreasing values as one proceeds towards the more electro-negative elements. The curve also shows minor peaks for Cu and Ag, but none for Au, where it might have been expected. When the widely varying conditions of observation are considered the amount of agreement is surprisingly good. A new measurement for the threshold of Ge (2590 Å) and a tentative one for Be are included; both of these assume their expected positions on the curve.

38. Tests of a New Selective Radiometer of Molybdenite. W. W. COBLENTZ, Bureau of Standards.—The radiometers were lamina of molybdenite having a resistance of about 40,000 ohms, and spots of only one actinoelectric polarity. A 10-ohm Thomson galvanometer was used. Focusing an artificial star (pinhole in front of a flat incandescent tungsten filament) on a vacuum stellar thermocouple (non-selective) gave a deflection of 232 cm; and 45 cm on the molybdenite receiver. The latter deflection would be increased about 60-fold (2500 cm) by using a high-resistance galvanometer. Measurements by Coblenz and Stetson at Benkoelen, Sumatra, Jan. 1, 1926, using a high resistance d'Arsonval gave a deflection of 2 mm in moonlight of 0.008 foot candle normal intensity. This could be magnified by using a lens or mirror. Settings on the star Vega (mag. 0.14) by Coblenz and Lampland, Oct. 1926, using the 42-inch Lowell reflector and a 5-ohm Thomson galvanometer gave deflections of 4 to 5 mm. With an electrometer or a suitable galvanometer the deflection would have been increased about 100-

fold (40 to 50 cm) which is 10 times that observed with a stellar thermocouple. A patient examination of molybdenite from various sources may reveal samples even more sensitive than those just described.

39. Thermal conductivity of fused quartz as a function of temperature. HERMAN E. SEEMANN, Cornell University.—Preliminary measurements of the thermal conductivity of a specimen of clear fused quartz indicate that this property increases linearly with the temperature, within experimental error, from .0026 cal./cm. deg. sec. at -25°C to .0064 cal./cm. deg. sec. at 950°C. The specimen was in the form of a hollow cylinder, closed at one end with a hemispherical cap. Energy to maintain a steady temperature gradient was supplied by means of an electrically heated filament mounted axially inside the specimen. Thermal contact with the specimen was made with mercury inside and outside at the lower temperatures and with the tin-lead eutectic at the higher temperatures. Inside and outside temperatures were obtained with thermocouples. A guard ring scheme was used to prevent heat loss or gain at the open end of the cylinder and correction was made for the heat flow through the hemispherical end cap.

40. Thermal expansion of beryllium. PETER HIDNERT and W. T. SWEENEY, Bureau of Standards.—Data on the linear thermal expansion of beryllium between -120 and +700°C have recently been obtained. The rod investigated was prepared by the Beryllium Corporation of America, and was found to have a density of 1.835 grams per cubic centimeter at 20°C. The coefficient of expansion increases rapidly with temperature. The coefficients or rates of expansion at -110 and +650°C are 5×10^{-6} and 20×10^{-6} respectively. Beryllium expands considerably less than the other elements of sub-group II B (Mg, Zn, Cd and Hg). Average coefficients of expansion for various temperature ranges are given in the following table.

Temperature Range: °C	Coefficient of Expansion $\times 10^6$	Temperature Range: °C	Coefficient of Expansion $\times 10^6$
-100 to - 50	7.0	20 to 300	14.0
-120 " + 20	8.1	20 " 400	14.8
- 50 " 20	9.8	20 " 500	15.5
+ 20 " 100	12.3	20 " 600	16.1
20 " 200	13.3	20 " 700	16.8

41. Internal friction in solids. A. L. KIMBALL and D. E. LOVELL, General Electric Co.—The internal friction of seventeen different solids is studied by a method previously described before this society (Phys. Rev. 25, 899 (1925)). By this method it was found that in every case the dissipative forces were the same whatever the speed of deformation, contrary to the assumption of many investigators that the forces are greater the more rapid the deformation. A simple approximate law of internal friction in solids which in general best fits the facts is $F = \xi f_m^2$ where F = frictional loss per unit volume per cycle of stress at a point in the solid f_m = maximum value of the stress amplitude at that point during a stress cycle. ξ = proportionality factor which may be called the internal friction constant. Values of ξ are tabulated for a number of different solids.

42. The nodal lines of bells. ARTHUR TABER JONES, Smith College.—Two systems of nodal lines are generally recognized for bells: A system of circles parallel to the mouth, and a system of vertical meridians. In the present work the number and position of these lines are checked for the lower modes of vibration and are determined for higher modes than those for which they have previously been known. The work was done as part of another investigation on the ten bells of the Harkness Memorial Chime at Yale University. The method was similar to that described in the Physical Review, 16, 247 (1920). On all of the Harkness bells the first ten partials have respectively the following numbers of nodal meridians: 4, 4, 6, 6, 8, 8, 10, 8, 10, 12. The nodal circles are more difficult to determine. For the first seven partials

the numbers of nodal circles are: 0, 1, 0, 1, 1, 2, 2. The nodal circle for the second partial lies about 1/3 of the way up the bell, and for the fourth and fifth partials the corresponding fractions are about 1/6 and 1/2. Surfaces of minimum intensity in the air close to the bells spread away from the metal in different directions for different partials.

43. Determination of the surface area of adsorbers. KARL HOROVITZ, International Research Fellow, Rockefeller Institute.—It is known that certain fatty acids or their compounds form mono-molecular layers covering the available surfaces (Langmuir, Harkins, a.o.). Extensive experiments on surface tension of sodium oleate solutions under various conditions (DuNouy) lead to the conclusion that sodium oleate is also adsorbed in a mono-molecular layer at the interface of two phases. Assuming that this mono-molecular layer of sodium oleate is formed on every adsorber it is possible in an exceedingly simple manner to determine the surface area of the adsorber from the quantity of sodium oleate adsorbed and the known dimensions of the sodium oleate molecule. The adsorption of the sodium oleate was determined from the change in the static values for the surface tension of the sodium oleate solutions at different concentrations, using the ring method (DuNouy tensiometer). The surface of different charcoals determined by this method was found to be of the order of magnitude of some 100 per sq. m.g. charcoal, the comparative surface areas for charcoals of different origins being in good agreement with the determination by other methods and other investigators.

44. A type of oscillation hysteresis. LAURISTON TAYLOR, Cornell University (Introduced by E. Merritt).—A simple triode oscillator was modified by placing a high resistance (.5-1.0 meg) shunted by a capacity of $1/10\mu f$, in series with the grid. The circuit then oscillates intermittently, the period during which oscillation occurs being called a zule. Over a wide region the zule frequency F is found to obey a simple relation to the constants of the circuit, i. e., $F = A \exp [(L_2 - kC_2)/2L_1]$, where A and k are constants. At the borders of these regions F is extremely sensitive to very small changes in L_2 and C_2 . A theory is given for the zule formation showing how they are related to the state of depression of the grid potential. Their finite length is due to a type of oscillation hysteresis, where oscillation ceases at one value of E_g and is resumed at a higher value. At the end of a zule, the mean of E_g is equal to the dynamic cut-off potential, and at the start of the next zule is several volts higher, increasing exponentially between these values. The variations of E_g were later studied by means of a synchronized oscilloscope, and all points of the theory were checked. Oscillation within the main circuit showed the same formation except that the potential between zules was constant.

45. A shear mode of crystal vibration. W. G. Cady, Wesleyan University.—In the various applications of piezo-electric quartz plates, it has until recently been customary to cut the plates with their faces perpendicular to an electric axis. The vibrations of such plates are then longitudinal, *i. e.*, stationary waves of compression and rarefaction. Various observers have recently found that plates cut *parallel* to the electric and optic axes (*i.e.*, parallel to a natural prismatic face of the crystal) are good piezo-electric oscillators, but hitherto no explanation has been offered. According to Voigt's theory of piezo-electricity, an electric field perpendicular to the electric and optic axes causes a shearing stress about the optic axis. Hence the deformation of a plate cut as indicated, when in a field normal to its surface, is a shearing strain, and under an alternating impressed field vibrations are to be expected, whose resonant frequency is determined by the shear-inertia of the plate and by the elastic force of restitution. Computed and observed values of the natural frequency are in satisfactory agreement.

46. Theory and application of low frequency piezo-electric vibrations in quartz plates. J. R. HARRISON, Wesleyan University.—Further study of the phenomena described at the December meeting (Phys. Rev. 29, p. 366, 1927) indicates that the observed frequencies of vibration are sufficiently in accord with those calculated from the formula for flexural vibrations to make it fairly certain that the vibrations are of this type. In general, agreement between

theory and observation is best for relatively long plates as would be expected. With relatively long rods the second mode of vibration having three nodes has also been observed. These facts are illustrated by numerical data and curves. An empirical formula has been derived which fits the observed data better than the theoretical equation for flexural vibrations. A plate $30 \times 10 \times 1$ mm vibrating at 60 kc was placed in the circuit of a type UX-210 tube as a power oscillator. The observed output power was about $\frac{1}{2}$ watt, which considering the low frequency compares favorably with the output from a high frequency quartz oscillators.

47. Theory of the magnetic nature of gravity and the Balmer series. CORNELIO L. SAGUI, Castelnuovo dei Sabbioni, Italy.—In a preceding paper dealing with a corpuscular conception of energy the equation $(x^2+x)/2 = y$ was found for the variation of the gravitational potential of physical nature, at least for an atomic space. The geometrical variation due to the Newtonian law is here not considered. With the same equation the Balmer lines are now studied and a physical meaning found for doublets, triplets and other groups of this kind. The Stark effect is also considered. The radiation of energy is also investigated and it is supposed to be due to a magnetic depression on the front of the traveling ray. Suggestion is given as to the astronomical verification of such a fact.

AUTHOR INDEX

- Barton, Henry A.—No. 13
- Baudisch, O.—see Welo
- Cady, W. G.—No. 45
- Clarke, Harry—No. 2
- Coblentz, W. W.—No. 38
- Crew, W. H. and E. O. Hulbert—No. 17
- Dawson, L. H.—No. 18.
- Duane, William—No. 5
- Foote, Paul D.—No. 15
- Gibbs, R. C. and H. E. White—No. 7.
- Ham, W. R.—No. 10
- Hamer, Richard and S. Singh—No. 12
- Harnwell, Gaylord P.—Nos. 11, 24
- Harrison, J. R.—No. 46
- Hidnert, Peter and W. T. Sweeney—No. 40
- Horovitz, Karl—No. 43
- Hulbert, E. O.—see Crew
- Jauncey, G. E. M.—No. 1
- Jenkins, F. A.—see Kemble.
- Johnson, Thomas H.—No. 20
- Jones, Arthur Tabor—No. 42
- Jones, Ernest J.—No. 22
- Kemble, E. C. and F. A. Jenkins—No. 8
- Kimball, A. L. and D. E. Lovell—No. 41
- Kleeman, R. D.—No. 31
- Klein, Elias—No. 19
- Kurrelmeyer, B.—No. 36
- Laird, Elizabeth R.—No. 3
- Langmuir, Irving—see Tonks
- Lawrence, Ernest O.—No. 14
- Lindsay, R. B.—No. 25
- Loomis, F. W.—No. 9
- Lovell, D. E.—see Kimball
- Masius, Morton,—No. 30
- Meggers, William F.—see Russell
- Nicholas, Warren W.—No. 27
- Nyquist, H.—No. 33
- Pool, M. L.—No. 21
- Richtmyer, F. K. and L. S. Taylor—No. 4
- Russell, Henry Norris, and William F. Meggers—No. 6
- Russel, H. W.—No. 35
- Sagui, Cornelio L.—No. 47
- Seemann, Herman E.—No. 39
- Singh, S.—see Hamer
- Smede, L.—No. 34
- Sweeney, W. T.—see Hidnert
- Taylor, Lauriston—No. 44
- Taylor, L. S.—see Richtmyer
- Tonks, Lewi, and Irving Langmuir—No. 32
- Tykocinski-Tykociner, J.—No. 23
- Vallarta, M. S.—No. 28
- Van Vleck, J. H.—No. 29
- Welch, George B.—No. 37
- Welo, L. A. and O. Baudisch—No. 26
- White, H. E.—see Gibbs
- Zeleny, John—No. 16

THE
PHYSICAL REVIEW

X-RAY ISOCHROMATS OF COPPER TAKEN IN DIFFERENT
DIRECTIONS RELATIVE TO THE CATHODE STREAM

By WARREN W. NICHOLAS

ABSTRACT

Variation with potential of the intensity of monochromatic x-rays of wavelengths 0.823 to 0.247 \AA for directions making angles of 36°, 90° and 144° with the cathode stream.—X-ray isochromats of copper were taken in three different directions relative to the cathode stream, for a target face making an angle of 25° with the cathode stream. Corrections were made for stray radiation in the neighborhood of the measured beam, for radiation due to secondary hits of cathode electrons which had been reflected backward from the focal spot at large angles, and for absorption in the target. It is established that, within experimental error, an isochromat of frequency ν varies linearly with the potential from potentials about $(5/4) H\nu$ to $2H\nu$, where $H\nu$ is the quantum voltage for excitation of frequency ν . The linear portions of the graphs were extrapolated to find the intercept on the intensity axis at $H\nu$. This intercept depended on $H\nu$, and also on θ , the angle between the measured x-rays and the cathode stream. For $\theta=90^\circ$ the intercepts varied between 0.062 I' (for $H\nu=50$ kv.) and 0.085 I' (for $H\nu=15$ kv.) with an average of 0.072 I' ; for $\theta=36^\circ$ the respective values were 0.076 I' , 0.096 I' , 0.086 I' ; for $\theta=144^\circ$, -0.035 I' , 0.010 I' , -0.017 I' . I' is the intensity of the isochromat at $2H\nu$. Values of $H\nu$ used were 15, 20, 30, 40, 50 kv. The intercept decreased, in general, for increasing $H\nu$, but for $\theta=36^\circ$ and $\theta=90^\circ$ the change was within the experimental error of $\pm 0.01 I'$.

Energy distribution in the x-ray continuous spectrum from a thick target.—Kulenkampff's formula for the energy distribution in the x-ray continuous spectrum for $\theta=90^\circ$ does not hold in detail for the higher voltages and different target face inclination used in the present work. Assuming total energy in the continuous spectrum proportional to the square of the voltage on the tube, and assuming suitable modifications of this law, for the forward and backward angles, from Sommerfeld's space distribution of energy as a function of cathode ray velocity, it is shown that the spectrum for the forward angle contains relatively more high frequency rays than the spectrum at 90°, and the spectrum at the backward angle contains relatively more low frequency rays.

Energy distribution in the x-ray continuous spectrum from a thin target.—On similar assumptions as to total energy, the spectra which would have been obtained from a very thin foil of copper are derived from the isochromats by Webster's method. The thin target spectra on a frequency scale, for $\theta=90^\circ$, are horizontal except for a sharp rise in intensity as ν approaches ν_0 , the high frequency limit. For $\theta=36^\circ$ the energy is approximately directly proportional to ν except for the region near ν_0 , where there is again the sharp increase. For $\theta=144^\circ$ the energy is approximately inversely proportional to ν except near ν_0 where there is a decrease for high voltages.

Theories by Kramers and Wentzel for $\theta=90^\circ$ are in fair agreement with the experiments as to thick target spectra, but if certain assumptions made in this paper are correct, Kramers' predicted thin target spectra are much more nearly in accord with the facts than are Wentzel's.

I. INTRODUCTION

PREVIOUS work on x-ray radiation in different directions relative to the cathode stream consists either of measurements of total intensity or of comparisons of the ionization spectrum at forward and backward angles. Inasmuch as a reduction of ionization spectrum measurements to energy spectra is very difficult with our present knowledge, such measurements should be supplemented by others in which these reductions do not occur.

To eliminate these reductions, one may use the isochromat method (measuring ionization at a given wave-length as a function of voltage applied to the tube, for constant current). Since ionization is directly proportional to energy, for a given frequency, and since no errors are involved for which suitable correction cannot be made, the isochromat is of the same form as though energy were directly measured. Although a family of isochromats does not determine the energy distribution in the spectrum without some additional knowledge (such as total energy in the spectrum as a function of voltage), nevertheless the isochromats themselves will often distinguish between a correct and an incorrect theory, and are a very valuable guide in the formulation of a new theory.

II. APPARATUS

The x-ray tube was of the Coolidge type, water cooled. The copper target face was inclined at an angle of 25° to the direction of the beam of cathode rays (see Fig. 1). Two parallel iron wires extended from the top of the anode approximately in a plane perpendicular to the cathode stream and in such a position that the cathode stream went between them. This was to prevent deflection of the cathode ray electrons by the electrostatic field near the target.

The anode was outgassed by cathode ray bombardment during evacuation. Toward the end of the outgassing process, small brilliant spots kept flashing up at the focal spot, and these flashes seemed to be simultaneous with abrupt gas discharges which were occurring at the same time. When the isochromats were being taken, an area of about a square millimeter at the focal spot was extremely bright for high currents. Unfortunately the surface of the target was roughened in the process of outgassing, so that not much value can be attached to the penetration measurements.

The focal spot was about seven millimeters broad, and this made necessary some special precautions about the position of the tube. The tube was provided with a lateral adjustment reading to a tenth of a millimeter, and the total radiation from the focal spot was plotted by moving the tube across narrow slits lined with the crystal table axis. The centroid of this graph was then found, and the tube set so that this centroid was lined with the slits. The position of the centroid shifted slightly with voltage and current, but any error in wave-length due either to the initial setting (re-adjusted for each isochromat) or to shift, or to both, must have been less than one x-unit. For an isochromat, the slit near the tube was widened so that the only slit limiting the beam was the one near the crystal. This is important on

account of the variation of the focal spot with voltage and current. Special tests were made to assure that the wires attached to the anode did not limit the beam. To insure definite conditions with regard to polarization, the cathode stream was kept always in the plane of the slits.

The generating plant, the electrostatic voltmeter, and the milliammeter were the same as described by Webster and Hennings,¹ and the calibrations

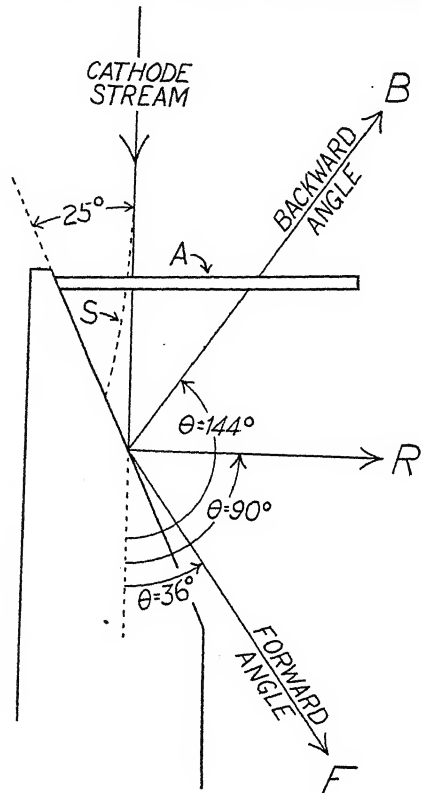


Fig. 1. Schematic diagram of anticathode showing directions of cathode stream and measured x-rays. The cathode stream passed between two wires *A*, which modified the electrostatic field near the anticathode so as to keep the cathode rays from being deflected into some such path as *S*. The continuous x-ray spectra were compared for directions *F*, *R*, and *B*.

and ionization readings were made in the same way. The spectrometer was of the Bragg type, but with a modification² which made possible the reading of wave-lengths directly on a micrometer screw. The Compton electrometer was calibrated by an ionization method, keeping the voltage on the tube constant and varying the current.

III. CORRECTIONS

The isochromats required corrections of three different types, to be discussed in this section. First, the stray radiation in the neighborhood of the

¹ D. L. Webster and A. E. Hennings, Phys. Rev. 21, pp. 301-325 (1923).

² W. W. Nicholas, J.O.S.A. & R.S.I. 14, p. 61 (January, 1927).

beam reflected from the crystal was evaluated by plotting it for different positions of the ionization chamber and interpolating to the position for the reflected beam. This radiation was probably due chiefly to diffuse scattering from the crystal.³ This correction averaged about two percent at the top of the isochromat.

The second correction was for a radiation produced over the whole surface of the target; it is thought to have been due to electrons which had been reflected from the focal spot at large enough backward angles to hit the target face a second time. Curves of the intensity of this radiation at a given wave-length as a function of voltage applied to the tube will be called "secondary isochromats." These secondary isochromats were determined by supporting a piece of lead so as to cut off the radiation from the focal spot and widening the slit nearest the tube in order to measure the radiation from the rest of the target face. They appeared to be linear, from about $(3/2)H\nu$ to $2H\nu$, where $H\nu^4$ is the quantum voltage for production of rays of frequency ν . The extrapolation of the linear portion always gave a negative intensity intercept at $H\nu$. This intercept was always a considerable fraction (1/4 to 2/3) of the intensity of the secondary isochromat at $2H\nu$. At $H\nu$ the secondary isochromats were tangential to the voltage axis. The actual correction was estimated on the assumption that the secondary isochromat radiation was produced uniformly over the target face. The amount of the correction was about three percent at $2H\nu$.

Third is the correction for absorption in the target. The swiftly moving electrons which make up the cathode stream will penetrate into the target, most of them suffering deflections but some of them going in fairly straight lines, and losing energy because of their impacts with the atoms of the target. A few of them will radiate x-rays somewhere along their path, but at any point they cannot radiate a frequency greater than that corresponding to the energy with which they reach the point, according to the Einstein relation. For instance, the maximum frequency of the spectrum must be produced very near the surface of the target, before the electrons have lost appreciable velocity. There will be a maximum depth at which any other frequency may be produced, corresponding to the maximum depth to which a cathode ray can penetrate and still retain enough of its original velocity to be capable of radiating this frequency. But rays of this frequency may be produced at any depth between zero and this maximum, so that in general there will be a depth distribution. The direction in which the absorption of the target for the x-rays is least will be, of course, the direction of the normal to the surface of the target. However, restricting ourselves to directions in the plane perpendicular to the cathode stream, the direction of least absorption will be the direction R (Fig. 1), the absorption increasing as the direction of observation makes greater angles with R , until the angle 90° is reached, when there is infinite absorption.

³ For a more complete discussion, see the paper by Webster and Hennings, reference 1.

⁴ H is equal to h/e , where h is Planck's constant, and e is the charge on the electron, as follows from Einstein's relation $Ve = h\nu$.

Now it is entirely possible that the fully corrected radiation for the direction R differs from that for directions perpendicular to the cathode stream but not in the plane of the paper, because, although there is symmetry about the cathode stream, there is not symmetry about the normal to the target face. For instance, one may easily imagine that the rays are slightly polarized in a direction normal to the face of the target. But as P. A. Ross⁵ has recently shown, polarization in the continuous spectrum is appreciable only near the high frequency limit, and errors in this region will affect the present results very little.

Accordingly, the correction for absorption in the target was made on the assumption that the fully corrected isochromats are dependent only on the angle θ (angle between cathode stream and measured x-rays) and independent of the angle ϕ (specifying angular position of the tube about the cathode stream as axis, and measured from the position of least target absorption,

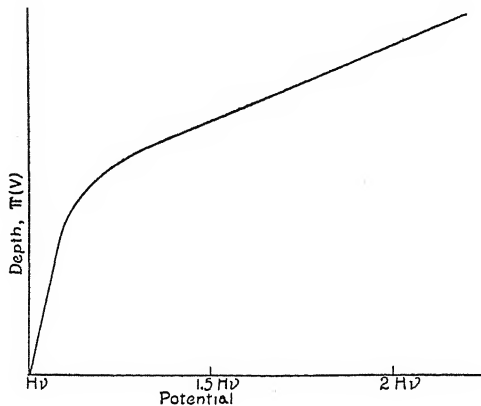


Fig. 2. Relative mean depth of production of rays of frequency ν as a function of voltage on the tube (after Webster and Hennings). $H\nu$ is the excitation potential for frequency ν .

the direction R , Fig. 1). Let $I=f(V)$ represent the fully corrected isochromat of wave-length λ and excitation voltage $H\nu$, for $\theta=90^\circ$. Assume that at a given voltage all the rays of wave-length λ may be considered as having been produced at some definite depth p , measured perpendicular to the face of the target, and let p vary with voltage according to the function $\Pi(V)$ shown in Fig. 2. (The curve of Fig. 2 was obtained by Webster and Hennings¹ for molybdenum at the K absorption limit wave-length and a target face inclination of about 55° . The scale of ordinates is omitted here). For the present target face inclination of 25° the depth measured along the path of the x-rays for $\theta=90^\circ$ and $\phi=0^\circ$ will be $x=p/\cos 25^\circ=1.10p$. If ϕ is increased, this effective depth increases; values of ϕ were actually used corresponding to effective depths x , $2.5x$, and $5x$. The measured isochromats of wave-length λ for effective depth rx should then be represented by

$$I_{rx}=f(V)e^{-\mu rx}=f(V)e^{-1.10\mu r\Pi(V)}$$

⁵ P. A. Ross, Phys. Rev. 28, 425 (1926), abstract.

where e is the base of natural logarithms, and μ is the absorption coefficient of copper for wave-length λ . If each ordinate is then divided by the ordinate in the same isochromat at $V = V_1$, the ratio, which will be called I'_{rx} , should be given by

$$I'_{rx} = \frac{f(V)}{f(V_1)} e^{1.10\mu r [\Pi(V_1) - \Pi(V)]}$$

The purpose of this last step is to reduce different isochromats to comparable scales. V_1 was chosen at about two-thirds of the way up the isochromat, where the relative intensity was considered most certain both on account of having a fairly large value and on account of the possibility of comparing it with points on either side.

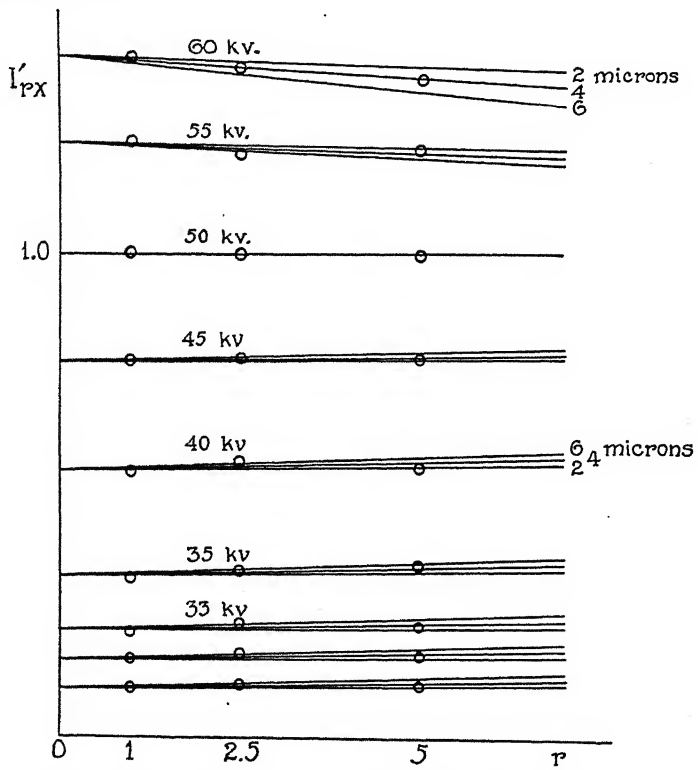


Fig. 3. Illustrating method for determination of the mean depth of production of x-rays in the anticathode.

Experimental values of I'_{rx} can be obtained directly from the data, and their dependence on r may then be compared with this expression as in Fig. 3 (the circles indicate experimental values). According to the formula the points corresponding to a definite voltage ought to lie on an exponential curve. Now the experimental results (compare Fig. 3) show that the slope of the curve must be very small in the vicinity of $r = 1$ to 5; this indicates that in reality the coefficient by which r is multiplied in the exponent is very small.

Accordingly, in the region to be considered, the curvature of the exponential line must be inappreciable. This accounts for the fact that the results of Fig. 3 seem to be fairly well represented by straight lines. Therefore the values for $r=0$ (corresponding to no target absorption) were obtained by extrapolating by means of straight graphs. The deviations from the predicted linearity, which were almost always of the kind shown in Fig. 3 (indicating too much absorption for $r=2.5$), are probably due chiefly to the roughness of the target face.

The graphs of I'_{rx} against r for the 30 kv isochromats are shown in Fig. 3. The families of lines correspond to mean depths of production at 60 kv of 2.0, 4.0, and 6.0 microns respectively. Similar families of lines were drawn for each set of isochromats. The depths selected, however, were not those which best fit the curves for that particular isochromat, but rather which lined up best with the curve of depths at $2H\nu$ for all the isochromats. The curve which was finally selected is shown in Fig. 4. In this connection it is worth noting

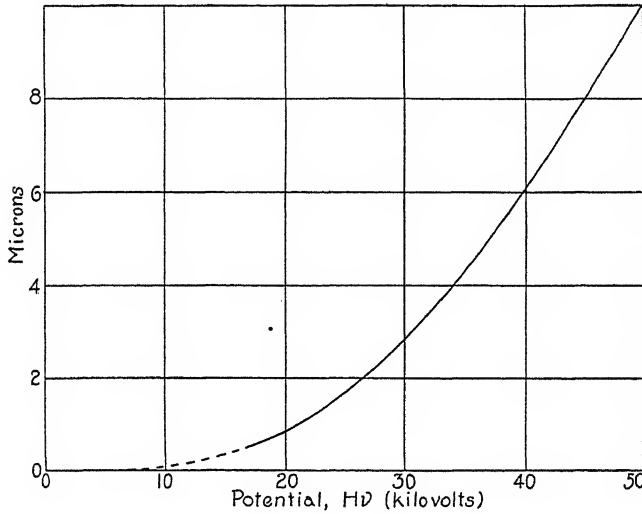


Fig. 4. Mean depth of production of rays of frequency ν at $2H\nu$.

that the values of r used in the corrections were nearly 1 for the backward angle and 5 for the forward angle. For this reason the values of I'_{rx} for $r=2.5$ were given very little weight in the selection of the mean depths for $2H\nu$. From Figs. 2 and 4 all the later absorption corrections could be made on the assumption that ρ is independent of the direction of observation of the x-rays. Absorption coefficients were calculated from a formula given by Richtmyer.⁶

IV. RESULTS

In Figs. 5, 6, and 7 are shown the fully corrected isochromats for $\theta=90^\circ$, $\theta=36^\circ$, and $\theta=144^\circ$, reduced to the same intensity at $2H\nu$. The forward angle, 36° , and the backward angle, 144° , were selected supplementary so as

⁶ F. K. Richtmyer, Phys. Rev. 27, 1 (1926).

to have polarization the same. For a copper target, the face of which is inclined at 25° to the cathode stream, and for the voltage range here investigated, it seems to be established that:

(1) An isochromat of frequency ν is linear, within experimental error, from about $(5/4)H\nu$ to $2H\nu$, where $H\nu$ is the quantum voltage for excitation of frequency ν .

(2) The linear portions of the graphs were extrapolated to find the intercepts on the intensity axis at $H\nu$. These intercepts, for $\theta = 90^\circ$, are within the limits of $+0.073I' \pm 0.02I'$, where I' is the intensity of the isochromat at twice the excitation voltage. The variation of the intercepts with $H\nu$ for $\theta = 90^\circ$ is within experimental error.

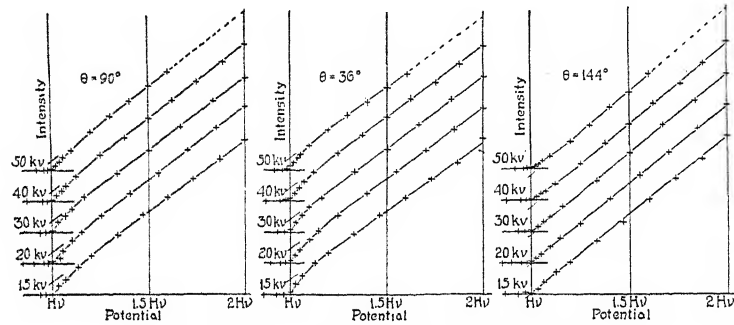


Fig. 5. Isochromats for $\theta = 90^\circ$ reduced to equal intensities at $2H\nu$. θ is the angle between cathode stream and measured x-rays.

Fig. 6. Isochromats for $\theta = 36^\circ$ reduced to equal intensities at $2H\nu$.

Fig. 7. Isochromats for $\theta = 144^\circ$ reduced to equal intensities at $2H\nu$.

(3) The intercepts for $\theta = 36^\circ$ were greater than those at 90° by about $0.01I'$, but this amount is not outside the limits of error. These intercepts were likewise independent of $H\nu$.

(4) The intercepts for $\theta = 144^\circ$ show a variation with voltage which is outside the experimental error, the intercept decreasing for increasing $H\nu$. The difference between these intercepts and the ones for $\theta = 90^\circ$ and $\theta = 36^\circ$ is well outside the limits of error, especially at high voltages, where the intercepts for $\theta = 144^\circ$ have a negative value.

A table of values for the intercept, obtained from the graphs, is shown below. The experimental error is about $\pm 0.01I'$. If anything, the results for $\theta = 36^\circ$ are less reliable than the others on account of the larger correction necessary for absorption in the target.

TABLE I

Quantum voltage of isochromat (kilovolts)	$\theta = 36^\circ$	$\theta = 90^\circ$	$\theta = 144^\circ$
15	+0.096 I'	+0.085 I'	+0.010 I'
20	+0.093 "	+0.075 "	0 "
30	+0.077 "	+0.072 "	-0.018 "
40	+0.086 "	+0.065 "	-0.040 "
50	+0.076 "	+0.062 "	-0.035 "

V. DISCUSSION

i. Empirical formulas for spectra at 90°. Kulenkampff⁷ has proposed the formula⁸

$$I_\nu = C \{ Z(\nu_0 - \nu) + Z^2 b \} \quad (1)$$

to express the results of his work on the continuous spectrum at voltages from 7 to 12 kilovolts for an angle of 90° between cathode stream and measured x-rays. I_ν is the intensity on a frequency scale at frequency ν , C is a constant, Z is the atomic number of the metal of the anticathode, ν_0 is the high frequency limit of the spectrum, dependent, of course, on the applied voltage, and b is approximately equal to 0.0025 when ν is measured in units 10^{18} sec⁻¹. This formula would give, for copper, isochromats whose intercepts (see above) are very approximately $0.01 ZI' / V_0$, where V_0 is the excitation voltage of the isochromat. The present work, and also the work of Webster and Hennings on molybdenum,¹ indicates very definitely that this formula for the intercepts cannot be correct at the higher voltages. On the other hand, the condition that the isochromat intercept shall be nearly constant (as indicated by the isochromat work) is approximated by the formula

$$J_\nu = C \{ Z(\nu_0 - \nu) + b' Z^2 \nu_0 \} \quad (2)$$

Putting $b' = 0.0019$ to give the isochromat intercepts for copper as low a value as allowable (0.05 I') from the present experiments, the spectrum intercepts coincide with those of formula (1) for 5400 volts, but are 2.2 too big at 12,000 volts.

It may be that some more general formula is required which will approximate (1) at low voltages and (2) at high voltages, but it is perhaps more likely that several dissimilarities in experimental conditions are responsible for the disagreement. For instance, in Kulenkampff's experiments the cathode stream was perpendicular to the crystal table axis, while in the present work the two were parallel. The former arrangement would cause a loss of intensity due to the reflection of polarized rays from the crystal, but since the spectrum is strongly polarized only near the high frequency limit,⁵ the factor should be negligible. A more promising source of explanation is the following extension of an idea of Kramers⁹ to explain the discrepancy between his theory and Kulenkampff's experiments. Kramers' theory predicted that the second term on the right hand side of formula (1) should be zero, and Kramers offered the suggestion that since many of the electrons of the cathode stream suffer large deflections on entering the target, some will be deflected out of the target with fairly high speed and in such a manner that they do not return to the focal spot and therefore are lost, in so far as concerns the radiation

⁷ H. Kulenkampff, Ann. der Physik, 69, 548 (1922).

⁸ A formula based on Webster's formula for isochromats (Phys. Rev. 9, p. 220, 1917) would represent much more closely the actual shape of the spectra near the high frequency limit, but for the present discussion of the magnitude of the intercepts, Kulenkampff's simpler formula is adequate.

⁹ H. A. Kramers, Phil. Mag. 46, 869 (1923).

actually measured. The form of the secondary isochromats of the present work suggests that the explanation may be well founded. These deflections vary with the atomic number of the metal of the anticathode, and it would be surprising if the number and speeds of the electrons lost did not depend on the angle between target face and cathode stream (90° in Kulenkampff's experiments; 25° here).¹⁰ More detailed discussion of the point must, however, await further experiment.

ii. Thick target spectra in different directions. As noted above, a family of isochromats does not determine the energy distribution in the spectrum without some additional knowledge, such as total energy in the spectrum as a function of voltage. It is very likely that this total energy will not be the same function of voltage for forward angles as it is for backward angles, and still different for 90° . As a basis for an approximation to these laws, the usually accepted law that the total energy is proportional to the square of the voltage¹¹ was assumed for 90° , and modifications for forward and backward angles were estimated from Sommerfeld's curves¹² of spatial distribution of energy as a function of cathode ray velocity. The estimated modifications of the V^2 law were: Total energy = aV^3 for $\theta = 36^\circ$, and total energy = $bV^{1.3}$ for $\theta = 144^\circ$, where θ is the angle between cathode stream and measured x-rays, and a and b are constants.¹³

For an approximation to the spectrum energy distribution from a thick target, it will be assumed that the isochromats are linear, with zero intensity intercept at V_0 , i.e. that they can be represented by the formula

$$I(V, \nu) = k(\nu)(V - V_0)$$

where $I(V, \nu)$ is the energy at frequency ν in a range $d\nu$, for applied voltage V , and V_0 is the quantum voltage for frequency ν . If $k(\nu)$ can be represented by $c\nu^n$, where c is a constant, the exponent n can be readily found by use of the total energy law

$$\int_{\nu=0}^{\nu=\nu_0} I(V, \nu) d\nu = A V^{2+\epsilon}$$

where A is a constant. It turns out, following Webster's analysis,¹⁴ that $\epsilon = n$, and the equation becomes

$$I(V, \nu) = c\nu^\epsilon(V - V_0)$$

Thus when $\epsilon = 0$ (spectrum at 90° , see above) the spectra on a frequency scale are represented by straight lines passing through the high frequency limit, and the lines for different voltages are parallel. When ϵ is equal to 1.0,

¹⁰ It is partly for this reason that the correction equivalent to the present secondary isochromat correction cannot be readily estimated for Kulenkampff's work.

¹¹ See Siegbahn, Spektroskopie der Rontgenstrahlen, p. 201.

¹² See Sommerfeld, Atombau und Spektrallinien, 4th Ed. p. 37.

¹³ It should be emphasized that there is no direct experimental evidence for these assumptions in their present form. But the general form of Sommerfeld's space distribution of energy for steady voltages has been confirmed by Loebe (Ann. d. Phys. **44**, 1033, 1914) and others.

¹⁴ D. L. Webster, Proc. Nat. Acad. **5**, 163 (1919).

corresponding to the forward angle of the present work, the spectra are curved concave downward, and have relatively more energy in the high frequencies than the straight line distribution has. For ϵ equal to -0.7 the spectra are curved concave upward, and have relatively more energy in the low frequencies.¹⁵ A consideration of the fact that actually the isochromat intercepts are greater, algebraically, for forward than for backward angles, leads to even greater asymmetry in the spectra.

iii. Thin target spectra in different directions. The difference in the isochromats for the various directions is perhaps most strikingly brought out by a consideration of the spectra that would have been obtained from an exceedingly thin foil of copper. A method for obtaining thin target spectra, involving the Thomson-Whiddington penetration law, and the total energy law, together with isochromat data has been given by Webster and Hennings.¹

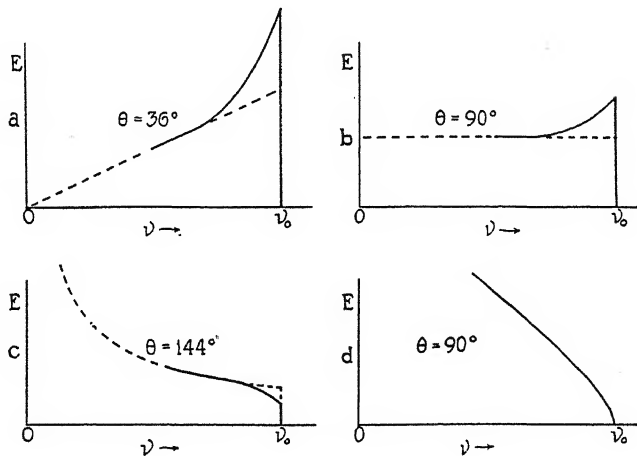


Fig. 8. Energy distribution in thin target spectra. E is the energy on arbitrary scales, θ is the angle between the cathode stream and measured x-rays, ν_0 is the high frequency limit. Curves a, b, c were derived from the isochromats and an assumed total intensity law for the various directions. Curve d is predicted by Wentzel's theory. Curve b, dotted portion, is predicted by Kramers' theory.

From this analysis the energy distribution in the thin target spectrum is given by

$$(b/2V_0)D_V I(V, \nu)$$

where the only quantity not previously defined is b , the coefficient of the Thomson-Whiddington law in the form $V_s^2 = V^2 - bs$. For the simplified case of linear isochromats, this may be written

$$(b/2V_0)k(\nu)D_V(V - V_0) = (c/2V_0)k(\nu)$$

where c is a constant. Taking the formerly determined values for $k(\nu)$, it is obvious that the thin target spectra on arbitrary intensity scales are of the forms indicated by the dotted lines in Fig. 8. If, now, account is taken of the

¹⁵ Compare Wagner's spectra in different directions J. d. Rad. Elek. 16, 212 (Dec. 1919).

marked deviation from linearity of the isochromats in the region near the quantum voltage, the thin target spectra are modified as shown approximately by the full lines of Fig. 8, a, b, c.

iv. *Comparison with theories for spectra at 90°.* A theory of the x-ray continuous spectrum proposed by Wentzel¹⁶ predicted that for $\theta=90^\circ$ the spectrum from a thin target should resemble approximately the graph (d) of Fig. 8. Wentzel assumed that the quantum spectrum can be derived from the classical spectrum (emitted by an electron describing a hyperbolic orbit about the nucleus) by a continuous compression of the classical spectrum energy toward lower frequencies, an infinite frequency in the classical spectrum corresponding to the high frequency limit of the quantum spectrum. This is analogous to the method of deriving the quantum line spectrum (e.g. Balmer's series) from the classical spectrum from an electron in an elliptical orbit (fundamental frequency with harmonics). A theory proposed by Kramers⁹ proceeded differently, Kramers' method of treatment being simply to chop off the classical spectrum at the high frequency limit given by the Einstein relation, and assume that the frequencies higher than this limit correspond to transitions to stationary states (which practically do not occur). His thin target spectra resembled the dotted portion of Fig. 8b. Both theories agree fairly well with experimental results on thick target spectra in spite of the striking disagreement for thin target spectra. This is due to wholly different methods of treating the loss of velocity of the cathode rays on penetrating the target. Kramers assumed that practically all the electrons are slowed up gradually within the target according to the Thomson-Whiddington law. (The efficiency of production of x-rays is so low that comparatively very few electrons will suffer any sudden losses of energy by radiation). Wentzel, on the other hand, followed Lenard in assuming that a large part of the electrons suffer absorption before they have penetrated far enough to have lost much velocity according to the Thomson-Whiddington law.

It is of very great theoretical importance to determine which of these two fundamentally different forms of the Correspondence Principle is more nearly correct. Now the present thin target spectra were derived from the isochromats on the assumption that practically all of the electrons are slowed up gradually within the target (i.e. that Lenard's absorptions are inappreciable). But on the other hand, if Lenard's absorptions had been assumed to be of chief importance, the derived thin target spectra at 90° would have resembled Wentzel's. Evidently then, one cannot, on the basis of the present work, discriminate between the two theories without a knowledge of what actually happens to the cathode rays on entering the target.

Kulenkampff¹⁷ has recently discussed these absorptions for the passage through air of electrons having an initial velocity corresponding to voltages in the neighborhood of 10 kv. This was in connection with experimental work on the total ionization in air produced by photoelectrons which had been

¹⁶ Gregor Wentzel, Zeits. f. Physik, 27, 257 (1924).

¹⁷ H. Kulenkampff, Ann. der Physik, 80. 3. p. 261, June 2, 1926.

ejected by x-rays of known energy. It appears that for these conditions Lenard's absorptions are extremely rare. If it could be concluded from this that the absorptions are also negligible in the present work, then the continuous compression theory of Wentzel could be said quite definitely to be wrong. It is scarcely permissible, however, to carry over the results for low voltages and gaseous media to high voltages and solid media.¹⁸ Nevertheless, it is difficult to understand what becomes of the energy of the electron in these atomic absorptions, considering the conservation of energy and the conservation of momentum together with the fact that the probability of production of an x-ray is extremely small.

v. *Comparison with theories for spectra in different directions.* As to the isochromats in the different directions relative to the cathode stream, neither Kramers' nor Wentzel's theory is developed to such an extent as to allow ready comparison of experiment with theory. It may be pointed out simply that the present results are in qualitative agreement with what would be expected if these theories were modified in some such way as that developed by Sommerfeld (see above) to account, by means of classical electrodynamics, for the early work in this field. It should be strongly emphasized that although considerations such as are elaborated in the first part of this discussion make it difficult to interpret theoretically the absolute magnitude of the intercepts of the present work, the difference between the intercepts for various angles between cathode stream and measured x-rays is not to be explained in this manner.

This work was done at Stanford University. I wish to thank Professor D. L. Webster, under whose guidance the work was completed, for his very generous help and advice. This paper has been revised and extended since the author became a National Research Fellow at Cornell University; I am grateful for having had the opportunity to discuss the paper with Professor H. A. Lorentz and Professor F. K. Richtmyer.

CORNELL UNIVERSITY,
December 14, 1926.

¹⁸ See also two papers by P. Lenard, Ann. d. Physik, 80, pp. 1-32 (May 18, 1926).

THE POLARIZATION FACTOR IN X-RAY REFLECTION

BY PAUL KIRKPATRICK

ABSTRACT

The polarization factor for the reflection of polarized x-ray radiation. An x-ray beam consisting of a multiplicity of superposed polarized radiations with non-coincident planes of polarization will exhibit the same scattering distribution in a plane normal to the beam as will a beam consisting of two plane polarized components, suitably intense, whose planes of polarization are mutually perpendicular. The customary polarization factor $\frac{1}{2}(1+\cos^2 2\theta)$ does not apply to reflection of polarized radiation and should be replaced by

$$\frac{\sin^2 \alpha + P \cos^2 \alpha + (P \sin^2 \alpha + \cos^2 \alpha) \cos^2 2\theta}{1+P}$$

In this quantity P is the primary polarization ratio and α is an angle defining the orientation of the tube with respect to the plane of reflection. For the orientation most often employed the new polarization factor reduces to $(P + \cos^2 2\theta)/(1+P)$. Radiation from a tube so oriented that α is 45° will be reflected with the same intensity as an equally intense unpolarized radiation, the polarization factor assuming the familiar form $\frac{1}{2}(1+\cos^2 2\theta)$. This orientation is recommended for future investigations, since it necessitates no knowledge of the primary polarization. A *new method for measuring the polarization of homogeneous x-rays* is presented.

INTRODUCTION

THE so-called polarization factor which appears in formulas expressing the intensity of x-rays reflected from crystals was first developed by Sir J. J. Thomson,¹ and serves to account for the decrease of intensity which the change in direction incurs. The factor expresses the proportional reduction of intensity involved in this process, and is written $\frac{1}{2}(1+\cos^2 2\theta)$. The factor may also be written $(\frac{1}{2} + \frac{1}{2}\cos^2 2\theta)$, thus exhibiting the fact that the intensity of the deviated portion of one-half of the incident (unpolarized) radiation is constant with the angle of deviation, while the intensity of the deviated portion of the other half varies as $\cos^2 2\theta$. The electric vectorial components of that half of the incident radiation which gives rise to the constant deviated portion lie in a direction at right angles to the plane of reflection while the components of the half which gives rise to the variable portion lie in the plane of reflection.

Although the polarization factor was designed to apply only to an unpolarized incident beam, those who have made use of it have not always been mindful of this limitation. Indeed the writer has not been able to discover a single case in the literature of crystal reflection where this restriction has been recognized, though the polarization factor has entered into the numerical computations of numerous papers.² The continuous spectral

¹ Thomson, Conduction of Electricity Through Gases.

² A. H. Compton, Phys. Rev. 7, 658 (1916); Bragg, James, and Bosanquet, Phil. Mag. 41, 308 (1921), and later papers; Harris, Bates, and MacInnes, Phys. Rev. 28, 235 (1926). These papers are representative of a much larger number which might be cited.

radiation from primary x-ray sources is never unpolarized, and Bishop's³ results indicate that the characteristic radiations may not be assumed to be free from polarization either. It is desirable to develop a polarization factor which shall apply to reflection of x-radiation initially partially or completely polarized.

AN EQUIVALENCE THEOREM

As a preliminary step it will be well to simplify our method of representing the beam emitted from the x-ray tube. The beam as actually emitted is complex, and must be supposed to be constituted of a large number of elementary emissions having their planes of polarization oriented in many different directions. It will now be shown that this beam scatters identically with a much simpler beam, consisting of two components polarized in mutually perpendicular planes. It is well known that the predominant direction

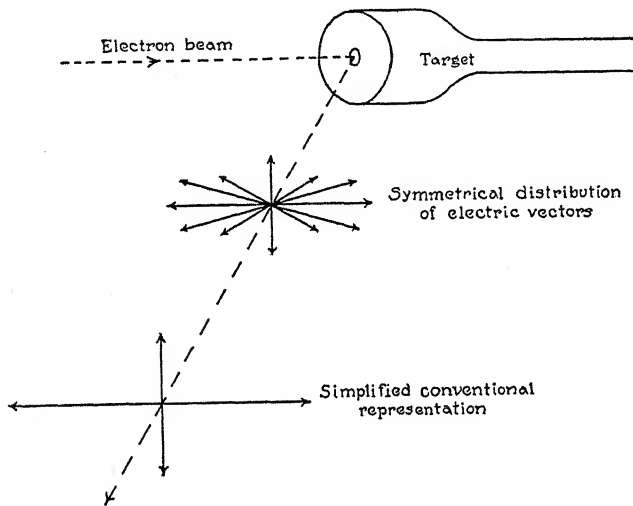


Fig. 1. Complex x-ray beam made up of a multiplicity of independent emissions. The electric vectors of the separate emissions are symmetrically disposed with respect to their prevailing direction, and in the present consideration may be replaced by two mutually perpendicular vectors.

of the electric vectors of the real beam lies in a plane containing the cathode stream. The symmetrical scattering of the beam on either side of this direction shows furthermore that the distribution of the planes of polarization of all the wave trains is a statistically symmetrical one with respect to the favored direction. The state of affairs is conventionally depicted in Fig. 1, where for every electric vector of amplitude E and inclination δ to the predominant direction there is represented also a similar electric vector symmetrically inclined upon the other side of the predominant direction. Fig. 1 also shows an equivalent system of two mutually perpendicular vectors, which will be shown to be a permissible substitution.

³ Bishop, Phys. Rev. 28, 625 (1926).

When such a beam is incident upon a scattering body of low atomic number the intensity of radiation scattered in any direction perpendicular to the beam is proportional to the sum of the squares of the amplitude components perpendicular to that direction. If the intensities of radiation thus scattered in the directions of minimum and of maximum scattering be compared experimentally, as has frequently been done, a ratio is obtained which characterizes the state of polarization of the beam as a whole, and which may be expressed

$$P = \frac{\sum (E \sin \delta)^2}{\sum (E \cos \delta)^2} \quad (1)$$

Eq. (1) may also be stated in two other forms which will presently be found useful. They are

$$\Sigma (E^2 \cos^2 \delta) = \Sigma E^2 / (P+1) \quad \text{and} \quad \Sigma (E^2 \sin^2 \delta) = \Sigma E^2 / (1+1/P) \quad (2)$$

Consider now the intensities of radiation scattered in two other mutually perpendicular directions, also normal to the direction of propagation of the beam. One of these directions of scattering, *A*, makes an angle ϵ with the

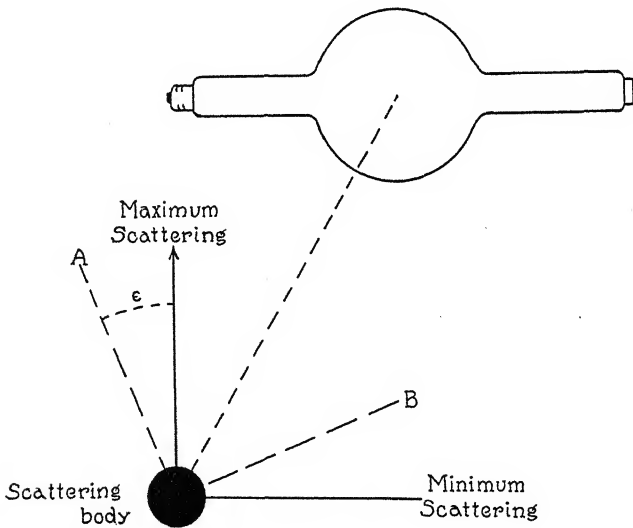


Fig. 2. X-ray scattering in a plane normal to the direction of propagation.

direction of maximum scattering. The ratio of the intensity of radiation thus scattered in the direction of *B* to that scattered in the direction of *A*, Fig. 2, may be formulated thus.

$$R = \frac{\sum (E \sin [\delta - \epsilon])^2 + \sum (E \sin [\delta + \epsilon])^2}{\sum (E \cos [\delta - \epsilon])^2 + \sum (E \cos [\delta + \epsilon])^2} \quad (3)$$

The double summations in numerator and denominator are necessary to take care of both members of the symmetrical pairs of electric vectors.

Upon expansion and simplification of Eq. (3) there is obtained

$$R = \frac{\cos^2\epsilon \sum E^2 \sin^2\delta + \sin^2\epsilon \sum E^2 \cos^2\delta}{\cos^2\epsilon \sum E^2 \cos^2\delta + \sin^2\epsilon \sum E^2 \sin^2\delta} \quad (4)$$

Substituting from Eq. (2) this becomes

$$R = \frac{P \cos^2\epsilon + \sin^2\epsilon}{\cos^2\epsilon + P \sin^2\epsilon} \quad (5)$$

It is apparent from this result that R is a function simply of P and ϵ , and does not require any special distribution of the individual δ 's. It is therefore permissible as far as R is concerned to assume any desired distribution for the planes of the elementary emissions. The simplest and most convenient assumption is that the emitted beam is made up of two plane polarized components with their electric vectors mutually perpendicular, the direction of one of them being parallel to the cathode stream. The relative amplitudes of these components may be chosen so as to give any value of P which a complex real beam might possess. Since the real beam may be replaced by the duplex beam without affecting R it may be concluded that any real beam will exhibit the same scattering distribution in a plane normal to the beam as will a beam consisting of two plane polarized components, suitably intense, whose planes of polarization are mutually perpendicular.

GENERALIZATION OF THE POLARIZATION FACTOR

In the beam of x-rays incident upon the reflecting crystal we need consider only such portion as is of the proper wave-length for reflection at the existing grazing angle, θ . Let this portion be regarded as consisting of two superposed plane polarized beams of the kind just discussed. The amplitudes may be designated by L and T , the greater one being L . The magnitudes of these amplitudes are governed by the requirements that $T^2 + L^2 = \text{total intensity}$, and $(T/L)^2 = P$.

For simple visualization let it be supposed that the plane of reflection is horizontal and that the x-ray tube is capable of rotation about the incident beam as axis. The orientation of the tube at any time may be specified by the angle α , between the plane of reflection and a plane defined by the incident beam and the cathode stream. Resolving the amplitudes T and L horizontally and vertically we have as vertical components $L \sin \alpha$ and $T \cos \alpha$, and as horizontal components $T \sin \alpha$ and $L \cos \alpha$. The reflected intensity due to the vertical components is constant with the angle of deviation, so that the intensity of this reflection portion is proportional to $(L \sin \alpha)^2 + (T \cos \alpha)^2$. The reflected intensity due to the horizontal components varies as $\cos^2 2\theta$, so that the intensity of this portion is proportional to $[(T \sin \alpha)^2 + (L \cos \alpha)^2] \cos^2 2\theta$. We therefore have

$$\text{Polarization factor} = \frac{\sin^2\alpha + P \cos^2\alpha + (P \sin^2\alpha + \cos^2\alpha) \cos^2 2\theta}{1 + P} \quad (6)$$

DISCUSSION

When the incident radiation is unpolarized P has the value unity, and Eq. (6) assumes the familiar form $\frac{1}{2}(1+\cos^2 2\theta)$. The tube orientation most often employed is probably that defined by $\alpha=0$. Investigators seldom if ever state the values of α employed in their work, but the diagrams accompanying all of the papers cited in footnote 2, indicate that the zero value was used in these cases. For this orientation we have

$$\text{Polarization factor } (\alpha=0) = (P + \cos^2 2\theta) / (1 + P)$$

Uncertainty as to the correct values of P makes it impossible to apply exact corrections to work done in the past. A computation based upon values regarded as plausible has shown however that some of the numerical results given in the papers cited should be modified by as much as ten percent.

Lacking precise information as to the values of P it is by all means desirable that future investigations involving comparisons between theoretical and observed intensities of reflection should be carried out with the x-ray tube oriented so that $\alpha=45^\circ$, that is, with the plane determined by the cathode stream and the incident ray inclined at an angle of 45° with the plane of reflection. In this case the right member of Eq. (6) becomes $\frac{1}{2}(1+\cos^2 2\theta)$, and P need not be known. Radiation received from a tube thus inclined will be reflected with the same intensity as unpolarized radiation, regardless of what its actual state of polarization may be.

The determination of P for x-rays of different wave-length and different conditions of excitation has been attempted by the writer⁴ and by Ross,⁵ using methods in which the intensity of radiation scattered by non-crystalline solids was measured. The results contained in the present paper furnish us with a simple and apparently superior method for the determination of this quantity. Let x-rays be reflected from a crystal with the x-ray tube in the $\alpha=0$ position, and again with the tube in the $\alpha=90^\circ$ position. Measure the intensities of reflection by an ionization method and call their ratio K . Then K is the ratio of the polarization factors for the two positions, and it follows quite simply that for the wave-length reflected

$$P = \frac{K - \cos^2 2\theta}{1 - K \cos^2 2\theta}$$

Determinations by this method are now in preparation.

DEPARTMENT OF PHYSICS,
UNIVERSITY OF HAWAII,
HONOLULU, T.H.,
February 10, 1927.

⁴ Kirkpatrick, Phys. Rev. 22, 226 (1923).

⁵ Ross, Bull. Am. Phys. Soc. Vol. 1, No. 10.

ELECTRONIC STATES AND BAND SPECTRUM STRUCTURE IN
DIATOMIC MOLECULES. IV. HUND'S THEORY; SECOND
POSITIVE NITROGEN AND SWAN BANDS;
ALTERNATING INTENSITIES

By ROBERT S. MULLIKEN

ABSTRACT

After a brief review of Hund's theory of molecular electronic states and band spectra, and a discussion of intensity relations and selection principles in terms of the correspondence principle, it is shown that practically all the available evidence, as embodied in previous papers of this series and elsewhere, is in agreement with the theory. The occurrence of p -type S terms and σ -type P and D terms is explained by the theory, as also the existence of p -type and σ -type doubling. Selection rules and other relations in $^2P \rightarrow ^2S$ and $^2S \rightarrow ^2P$ transitions (including, in agreement with Mecke and Hulthén, the CH, OH, MgH, and CaH bands) are discussed. Hund's interpretation of the second positive nitrogen bands as a $^3P \rightarrow ^3P$ transition is further developed, and extended to the Swan bands; the apparent absence of Q branches, and other intensity relations in these bands, are explained; the rotational doubling in these bands (accompanied by alternating intensities) is interpreted as σ -type doubling. It is shown that the alternating intensities or alternate missing lines in the He₂, N₂, Swan, and N₂⁺ bands can all be accounted for formally by the postulate that they are due to alternate (partially or completely) suppressed levels such that the suppressed values of $(j_k - \sigma_k)$ are always as follows: B rotational sub-states, $(j - \frac{1}{2} - \sigma_k) = 0, 2, 4, \dots$; A sub-states, $1, 3, 5, \dots$; here σ_k is the part of σ which is due to the orbital angular momentum of the electron, and j_k is the resultant of σ_k and the quantity m which measures the nuclear angular momentum in quantum units.—Finally, the questions of term-notation and -formulation, j values for odd and even molecules, etc., are considered. The NH β bands ($^3P \rightarrow ^3S$) are briefly discussed.

Introduction—Review of Hund's Theory. In a very important paper,¹ Hund has discussed from a theoretical standpoint the question of the nature of molecular electronic states, by a consideration of the orders of magnitude of the various electrical and magnetic interactions to be expected in a system composed of electrons and two nuclei.

Hund assumes that, as in atomic spectra, each electron (in particular, the r 'th electron) has orbital angular momentum corresponding to the (azimuthal) quantum number k , and in addition, a half-quantum ($s = \frac{1}{2}$) of spin angular momentum; the resultant of all the k_r 's is denoted k , and that of the s_r 's is denoted s .

Hund shows that in ordinary cases we may expect k to execute an essentially uniform precession about the internuclear axis, because of the strong axial field which must result (superposed on a central field) from the presence of two nuclei. The corresponding quantum number σ_k represents the component of k along the internuclear axis, and should be subject to the selection rule $\Delta\sigma_k = 0$ or ± 1 (for justification, cf. following section).

¹ F. Hund, Zeits. f. Physik, 36, 657 (1926). The notation used here is different from Hund's; his l , i , and p correspond to k , σ , and j as used here.

By analogy with atomic spectra, Hund assumes that the electric field of the nuclei has no effect on s , but that s tends to interact magnetically, as in the atomic case, with k . Since k should ordinarily precess rapidly about the internuclear axis, only the component along this axis, namely σ_k , is effective in orienting s . If the interaction between σ_k and s is sufficiently intense (case *a*), s is quantized with respect to the internuclear axis, about which it precesses; the corresponding quantum number may be designated σ_s . By analogy to the rule $\Delta m_s = 0$ (m = magnetic quantum number) in the Paschen-Back effect in atoms, Hund concludes that σ_s should be subject to the rule $\Delta \sigma_s = 0$. Since $\sigma = \sigma_k + \sigma_s$, it follows from the selection rules for σ_k and for σ_s that the rule $\Delta \sigma = 0$ or ± 1 should hold.

Hund shows that with a given value of σ_k , the various possible orientations of s in case (*a*) should give rise to a multiple electron level having (usually²) the same number of components as for a multiple atomic level possessing values of k and s equal to those of σ_k and s in the present case. Unlike the atomic multiplet, however, the components should all be equally spaced, but the spacing should be of the same order of magnitude as for a similar multiplet in an atom.

If the interaction between s and σ_k is small (case *b*), the torque which causes s to follow the motion of the internuclear axis may become inadequate as the rate of nuclear rotation increases. A gradual transition should then occur with increasing j , to a condition in which s is oriented and quantized with respect to j_k (j = resultant of j_k and s), j_k being the resultant of m and σ_k (here $\sigma_k = \sigma$). The expected selection rules in the extreme case are $\Delta \sigma_k = 0$ or ± 1 , $\Delta j_k = 0, \pm 1$, and $\Delta j = 0, \pm 1$.

Hund also discusses the question of fine structure. For additional details, reference should be made to Hund's paper, and to the excellent discussion by Kemble.³ In a brief review of the empirical data, Hund presented evidence of good agreement with his theory. One of the main objects of the present paper is to give a more complete discussion of the evidence, including that recently obtained by the writer and given in previous papers of this series and elsewhere.^{4,5,6,7}

Selection rules and intensity relations. The question of selection rules and intensity relations has been treated only briefly by Hund. For an understanding of the experimentally observed relations in terms of the theory, and of the connection of the Hönl and London-Dennison intensity equations

² Unlike the atomic case, the full number of components corresponding to the multiplicity should always be developed with the P terms; e.g. a 4P term would have four components ($\sigma_k = 1, \sigma_s = \pm \frac{1}{2}, \pm \frac{3}{2}$), instead of three as in the atomic case.

³ E. C. Kemble, Bulletin of National Research Council Subcommittee on Molecular Spectra, pp. 326-331 and 345-6 (1927).

⁴ R. S. Mulliken, Proc. Nat. Acad. Sci. **12**, 151 (1926).

⁵ R. S. Mulliken, Phys. Rev. **28**, 481 (1926).

⁶ R. S. Mulliken, Phys. Rev. **28**, 1202 (1926).

⁷ R. S. Mulliken, Phys. Rev. **29**, 391 (1927).

with Hund's molecular model, a somewhat more detailed consideration is needed. This can be given in terms of the correspondence principle.⁸

Let us begin with a particular harmonic component of frequency α ,—corresponding to a particular change in the total and azimuthal or other quantum numbers of the electron, and in the nuclear vibrational quantum number,⁹—in the Fourier analysis of the motion of the emitting electron, this harmonic component being taken with reference to a system of axes precessing with the electron orbit about the internuclear axis and of course also following the latter axis in its precession about the axis of total angular momentum. (Strictly, because of the slight perturbation of the orbital motion by the spin s , α should be considered as split into a group of components $\alpha \pm \tau\omega_s$, where ω_s is the frequency of precession of s about the internuclear axis; but, corresponding to the selection rule $\Delta\sigma_s = 0$, the amplitudes of all the components having $\tau > 0$ may be considered negligible). If now we transform to a set of axes fixed in the molecule, one of these being the internuclear or σ axis, the previous harmonic component α yields in general only three components (in so far as the precession of k about σ is uniform) of frequencies α (linear component along σ) and $\alpha \pm \omega_\sigma$ (right- and left-handed circular components about σ). Here ω_σ is the frequency of precession of k about the σ axis, and corresponds to the quantum number σ_k . The three components thus respectively correspond to the transitions $\Delta\sigma_k = 0$ and ± 1 . For brevity these three frequencies will be called β^0 , β^+ , and β^- . The question of the relative amplitudes of these three components need not concern us here.

Now let us consider any one of the above components β , and let us suppose that we are dealing with Hund's case (a). Transforming to a set of axes fixed in space, one axis being in the direction of j , we obtain in general three new components, namely a linear component, of frequency β , along j , corresponding to $\Delta j = 0$ (Q branch), and two circular components, of frequencies $\beta \pm \omega_j$, corresponding to $\Delta j = \pm 1$ (R and P branches); ω_j is the frequency of precession of σ about j . The relative amplitudes of these components can be expressed as trigonometric functions of the angle θ whose cosine is σ/j ; this is true even if σ differs from σ_k because of the presence of σ_s . The appropriate functions (cf. ref. 7, Eq. 3; the functions given in Eq. 3 are proportional to radiation intensities) are identical in form with those for $\Delta j = 0$, ± 1 in a line spectrum multiplet, since the Fourier components corresponding to $\Delta\sigma_k = 0$, ± 1 are identical in form and type (referred to the σ axis) with those (referred to the k axis) associated with $\Delta k = 0$, ± 1 in the atomic case; in the latter case $\cos \theta = (j^2 + k^2 - s^2)/2jk$. (We are here neglecting the effect of molecular vibration,—first pointed out by Kemble; for refs. cf. ref. 7. This alters the amplitude factors somewhat, in the molecu-

⁸ For a detailed discussion of the methods of the correspondence principle, cf. E. Buchwald, "Das Korrespondenzprinzip," F. Vieweg & Sohn, Braunschweig (1923); J. H. Van Vleck, Nat. Res. Council Bulletin No. 54, "Quantum Principles and Line Spectra," Chapter IX (1926); M. Born, "Atommechanik," especially pp. 118–121 (J. Springer, Berlin, 1925).

⁹ Cf. A. Kratzer, Naturwiss. 27, 577 (1933); W. Lenz, Zeits. f. Physik, 25, 299 (1924); . Condon, Phys. Rev. 28, 1182 (1926).

lar case.) The identity just stated formed the starting point of Hönl and London's derivations of their equations. In a previous paper⁷ it was stated that Hönl and London's three cases (Eqs. 4, 5, 6 of ref. 7) should correspond primarily to $\Delta\sigma_k=0, \pm 1$ rather than to $\Delta\sigma=0, \pm 1$; the reasons for this statement will now be evident from the discussion given above.

In Hund's case (b), starting with any one of the three harmonic components β , we first transform to a set of axes, one of which is along j_k , and which precess with j_k about j . This gives three components of frequencies β and $\beta \pm \omega_{jk}$, which for brevity may be denoted γ^0, γ^+ , and γ^- , corresponding to transitions $\Delta j_k=0, \pm 1$. The relative intensities are then given in the same form as before (Eq. 3 of ref. 7); but here $\cos \theta = \sigma_k/j_k$. The next step, using any one of the components γ , is to transform to axes which are fixed in space and one of which is parallel to j . The precession of j_k and s about their resultant j is completely analogous to the precession of k and s about their resultant j in the line spectrum case. Hence the relative intensities for the three components of frequencies $\gamma, \gamma \pm \omega_j$, corresponding to $\Delta j=0, \pm 1$, are again given by Eq. (3) of ref. 7, if here θ is the angle (usually small) between the vectors j_k and j , and if $\sigma' - \sigma''$ in Eq. (3) is replaced by $j_k' - j_k''$. By examination of Eqs. (3) it can be seen that if $\cos \theta = 1$, all the intensities vanish except those for which $\Delta j = \Delta j_k$; while if $\cos \theta$ is very near 1, as is necessarily the case in practise, except for small values of j_k or large values of s , the remaining intensities are very small. Except for certain weak series, a rule $\Delta j_s=0$ (where $j_s=j-j_k$) should be obeyed in the case of *doublet* terms, where $j=j_k \pm \frac{1}{2}$.

From the preceding we may conclude that in Hund's case (b) the intensity distributions in P , Q , and R branches (neglecting weak satellite lines where $\Delta j \neq \Delta j_k$) should fall under the same types as in case (a), each type being characteristic of a particular combination of values (initial and final) of σ_k and j_k , in the same way as of the σ and j values in case (a). Exact equations analogous to the Hönl and London equations will be given for case (b) in a subsequent paper. For transition cases between (a) and (b), it is not yet obvious what the intensity relations should be.

Singlet electronic states. The writer has shown that the band spectra of various molecules containing an even number of electrons are naturally classified as corresponding to transitions between singlet electronic states (${}^1S, {}^1P, {}^1D, \dots$) with $\rho \sim 0$ for all and $\sigma=0, 1, 2, \dots$. The following types of transitions are known (cf ref. 6, Table II): ${}^1S \rightarrow {}^1S$, ${}^1S \rightarrow {}^1P$, ${}^1P \rightarrow {}^1S$, and ${}^1D \rightarrow {}^1P$. These indicate a selection rule $\Delta\sigma=0, \pm 1$. For the case $\sigma=0$, the rotational states are single, for $\sigma>0$, they are double (" σ -type doubling"),^{5,6} the two rotational states having equal a priori probability.⁷ All these relations are in agreement with Hund's theory if we identify 1S , 1P , and 1D states in the sense here used with the three cases $\sigma_k=0, 1$, and 2 (all with $\sigma_s=s=0$) in Hund's theory. The selection rules $\Delta\sigma_k=0, \pm 1$, $\Delta\sigma_s=0$ are obeyed, and the occurrence of single rotational states for $\sigma=0$ and double rotational states for $\sigma>0$ is also in agreement with Hund's predictions. That σ_k (here equal to σ) is really an electronic quantum number

corresponding in general to a precession about the internuclear axis, is supported by the agreement of observed intensity relations,⁷ in bands of the types mentioned, with those predicted on the assumption that σ_k is such a quantum number. To be sure, the evidence in the cases cited gives no ground for decision as to whether it is $\Delta\sigma$ or $\Delta\sigma_k$ which governs the intensities. In many transitions^{4,6} of the type $^2P_{1,2} \rightarrow ^2S$ and $^2S \rightarrow ^2P_{1,2}$, however, we have $\Delta\sigma_k = \pm 1$, but $\Delta\sigma = \pm \frac{1}{2}$ or $\pm 1\frac{1}{2}$, giving evidence that σ_k , not σ , is the real quantum number.

Doublet electronic states. Band spectra corresponding to transitions between doublet electronic states are now known for a number of molecules containing an odd number of electrons. While in singlet states Hund's cases (a) and (b) are not distinguishable, since $s=0$, the two cases should in general be distinct in doublet states, if we suppose that the latter are characterized by $s=\frac{1}{2}$.

For 2S states we then expect $\sigma_k=0$ and $j_k=m$ (Hund's case b here becomes identical with his case d). Since there is no torque to orient s in the σ direction, it might seem that s could orient itself freely in any direction (or with respect to an external magnetic field). But the observed structure of the ZnH and similar bands of a $^2P \rightarrow ^2S$ type shows that the usual selection rule $\Delta j=0, \pm 1$ is observed, and that $\rho=\pm \frac{1}{2}$ for 2S states; also $\sigma=0$ as expected. The definite orientation of s as ρ in 2S states is attributed by Kemble⁸ to an interaction between s and a small magnetic field, parallel to m , developed by the molecule as a result of its rotation. The slight energy difference (ρ -type doubling⁵) which exists, for a given value of m , between F_1 states ($\rho=+\frac{1}{2}$) and F_2 states ($\rho=-\frac{1}{2}$) is also ascribed by Kemble to this field. The observed existence of just two energy levels for each value of j is in agreement with Hund's theory.

In $^2S \rightarrow ^2S$ transitions,^{5,6,10} the observed transitions ($F_1 \rightarrow F_1$ and $F_2 \rightarrow F_2$) are apparently limited to those in which ρ does not change sign, i.e. in which s does not reverse itself. This limitation $\Delta j_s=0$ is in agreement with the theory (cf above under "selection rules" . . .) for transitions between doublet states which fall under case (b). The theory however predicts the existence of additional weak lines, and in particular accounts for the hitherto unexplained (ref. 5, p. 506) apparent existence (ref. 5, p. 489; ref. 10) of an F_2 state with $j=0$; a more detailed discussion of the relation of theory to experiment for $^2S \rightarrow ^2S$ bands will be given in a later paper.

For 2P states, Hund's theory predicts $\sigma_k=1$, with $s=\pm\sigma_s=\frac{1}{2}$ in case (a), giving $\sigma=1\frac{1}{2}$ or $\frac{1}{2}$; in case (b), $\sigma_k=1$, $s=\frac{1}{2}=\pm j_s$. For many molecules (NO β bands,¹¹ ZnH and other bands listed under $^2P \rightarrow ^2S$ and $^2S \rightarrow ^2P$ in Table II of ref. 6), typical 2P states approximating case (a) actually occur, having a double electron level with $\sigma=\frac{1}{2}$ (2P_1) and $\sigma=1\frac{1}{2}$ (2P_2).

The existence of combinations $^2S \rightarrow ^2S$, $^2P_1, 2 \rightarrow ^2S$, $^2S \rightarrow ^2P_{1,2}$, and $^2P_1 \rightarrow ^2P_1$ and $^2P_2 \rightarrow ^2P_2$ (cf ref. 11, NO β bands), indicates that the selection rule

¹⁰ E. Hulthén, Phys. Rev. 29, 97 (1927); CaH bands, $^2P \rightarrow ^2S$ and $^2S \rightarrow ^2S$ types.

¹¹ F. A. Jenkins, H. A. Barton, and R. S. Mulliken, Phys. Rev. 29, 211A (1927), and forthcoming detailed articles; Nature, 119, 118 (1927).

$\Delta\sigma_k = 0$, ± 1 is obeyed, while the complete absence of the combinations ${}^2P_1 \rightarrow {}^2P_2$ and ${}^2P_2 \rightarrow {}^2P_1$ in the NO β bands gives striking evidence in support of Hund's rule $\Delta\sigma_s = 0$. The intensity relations¹¹ in the NO β bands also agree with the theory for case (a).

In ${}^2P \rightarrow {}^2S$ and ${}^2S \rightarrow {}^2P$ transitions involving case (a) 2P states, neither of the rules $\Delta\sigma_s = 0$ and $\Delta j_s = 0$ can be observed, since 2S states always fall under case (b). Actually in the ZnH, CdH, and HgH bands,⁴ we have $+\sigma_s \rightarrow \pm\rho$ in ${}^2P_2 \rightarrow {}^2S$ and $-\sigma_s \rightarrow \pm\rho$ in ${}^2P_1 \rightarrow {}^2S$,¹² giving altogether four P , four Q , and four R branches.

In addition to the more obvious examples of ${}^2P \rightarrow {}^2S$ and ${}^2S \rightarrow {}^2P$ transitions, there are several band spectra (CH, OH, MgH, etc.), briefly considered in previous papers,^{5,6} which may now likewise be classified as ${}^2P \rightarrow {}^2S$ (MgH) and ${}^2S \rightarrow {}^2P$ (CH $\lambda 3900$, OH), if one supposes with Mecke¹³ that the electronic doublet separation (${}^2P_1 - {}^2P_2$) shrinks rapidly with increasing j . As Hund has shown, this last feature finds a natural explanation in the transition from case (a) to case (b) of his theory. In this transition $\pm\sigma_s$ should go over, for normal multiplets, according to Kemble (private communication; cf. ref. 26), into $\mp j_s$, resulting in a decreasing electronic energy separation, and in terms of the Kramers and Pauli formula, giving a variable σ and ρ (cf. Eqs. 1 and 2 below).

Kratzer's interpretation of the CH bands, recently advocated in slightly modified form by the writer,⁵ involves, for the final state of the molecule, a constant $\sigma(\sigma = 1)$ and $\rho(\rho = \pm \frac{1}{2})$. For very large values of j this is obviously in harmony with Hund's case (b) as above discussed, for a 2P state. The excellent agreement of the experimental data with Kratzer's interpretation for small as well as large values of j must now probably be considered fortuitous (in agreement with Mecke and Birge, and contrary to earlier contentions of the writer⁵) in view of the strength of Hund's theory.

Hulthén has recently concluded¹⁰ that certain CaH bands should be classified, like the MgH bands, as ${}^2P \rightarrow {}^2S$. These differ from the HgH type bands in that the 2P_2 states combine only with the 2S states having $\rho = -\frac{1}{2}$, and the 2P_1 states only with $\rho = +\frac{1}{2}$, so that there are altogether only two P , two Q , and two R branches. Since in case (b) we expect (for normal doublets, $j_s = -\frac{1}{2}$ for 2P_2 states and $+\frac{1}{2}$ for 2P_1 states, this would indicate that the predicted rule $\Delta j_s = 0$ (see above under "selection rules . . .") is effective here as in ${}^2S \rightarrow {}^2S$ transitions. The 2P_1 and 2P_2 states both show Q "combination defects" which may be ascribed to σ -type doubling¹⁴ combined with Q "crossing-over,"¹⁵ just as in ${}^1P \rightarrow {}^1S$ transitions (cf. ref. 6, p. 1205, Eq. (1a), and Fig. 1). In CH $\lambda 3900$ there are six branches which follow similar selection rules to the CaH bands. The same is true of the OH

¹² There are of course two rotational sub-states, for each of the cases $+\sigma_s$ and $-\sigma_s$; in each case one of these combines with $+j_s$, the other with $-j_s$ (cf. ref. 6, Eq. 8A.)

¹³ R. Mecke, Zeits. f. Physik, 36, 795 (1926).

¹⁴ The σ -type doubling appears to be about equally great, in case (b), for 2P_1 and 2P_2 states, judging by the CH and OH bands; in CH (according to Kratzer's analysis) this doubling can be represented by using a double value of B .

¹⁵ R. Mecke, Phys. Zeit., 26, 227 (1925).

bands, except that there are additional weak branches (satellite series). In these CH and OH bands, or at least in OH, $j_s = +\frac{1}{2}$ for the 2P_2 states and $-\frac{1}{2}$ for 2P_1 , and the 2P doublet is inverted (cf. later paper), but the $\Delta j_s = 0$ rule still holds (for the six strong branches). In $\text{CH}\lambda 4300$ there are twelve branches, but, as will be shown in a later paper, these bands are due to a $^2D \rightarrow ^2P$ transition. A detailed comparative study of structure and intensity relations for the whole group of $^2P \rightarrow ^2S$ and $^2S \rightarrow ^2P$ transitions will be given in a later paper.

In agreement with Hund's theory, there are in all known 2P states four rotational states for each value of j except for $j=1$. In case (a), this results from σ -type doubling^{15a} in each of the electronic states 2P_1 and 2P_2 . In case (b), σ_k gives σ -type doubling,¹⁴ and on this is superposed $\pm s$ doubling; for large values of j , the latter goes over into ρ -type doubling, since then $j_s \sim \rho$; furthermore, the σ -type part of the doubling here shows the same properties (cf. above, CaH , $\text{CH}\lambda 3900$, OH) as for typical σ -type states (e.g. 1P states).⁶

Triplet electronic states: interpretation of second positive nitrogen and Swan bands. We now come to the question of band spectra due to combinations of triplet electronic states. For a 3P state, $\sigma_k = 1, s = 1; ^3P_0, ^3P_1$, and 3P_2 correspond in Hund's case (a) to $\sigma_s = -1, 0$, and $+1$, respectively, in case (b) to $j_s = \pm 1, 0, \mp 1$. Hund gives a theoretical diagram (Fig. 4) for a $^3P \rightarrow ^3P$ transition, and on p. 671-2 makes it probable that the second positive nitrogen bands^{16,17,18} are an example of this type corresponding for low values of j to case (a) and for high values to case (b). The fact that (aside from rotational doubling) only three P and three R branches are known in each band is accounted for by the selection principle $\Delta \sigma_s = 0$, or $\Delta j_k = \Delta j$, limiting the intense transitions to $^3P_0 \rightarrow ^3P_0$, $^3P_1 \rightarrow ^3P_1$, and $^3P_2 \rightarrow ^3P_2$.

For small j values, if case (a) holds, the molecular term values should have the form

$$F = F(n) + F(\sigma) + B(j^2 - \sigma^2) + \dots \quad (1)$$

Here $F(n)$ is the vibrational term, and $F(\sigma)$ is the electronic term which according to Hund's theory should have three equally spaced values cor-

^{15a} The splitting of the rotational levels into two is apparently much more pronounced in 2P_1 than in 2P_2 states in case (a), (ZnH , CdH , HgH , NO, refs. 4, 11); in fact the experimental evidence for any rotational splitting at all in 2P_2 states here is confined to certain perturbed lines in the HgH bands (cf. ref. 4, bottom p. 156, and refs. there given).

¹⁶ E. Hulthén and G. Johansson, Arkiv f. Mat., Astron. och Fysik, **18**, No. 28 (1924); Zeits. f. Physik, **26**, 308 (1924). The designations $\alpha, \beta, \gamma, a, b, c$, are respectively equivalent to $P_3, P_2, P_1, R_3, R_2, R_1$ in the notation of Lindau and Mecke. When used with numerical subscripts, e.g. a_3 , the subscript is the value of the quantum designation m ; the following relations hold:^{18a} P_1, R_1 , branches, $j'' = (m + \frac{1}{2}) + 1$; P_2, R_2 branches, $j'' = (m + \frac{1}{2})$; $P_3, R_3, j'' = (m + \frac{1}{2}) - 1$; thus $(m + \frac{1}{2})$ is the same as j_k'' (for values of j sufficiently large so that j_k has a meaning).

¹⁷ P. Zeit, Zeit. Wiss. Photog. **21**, 1 (1921); R. Mecke and P. Lindau, Phys. Zeits., **25**, 277 (1924); P. Lindau, Zeits. f. Physik, **26**, 343; **30**, 187 (1924). Lindau's m values are the same as Hulthén and Johansson's, for the R branch, but one unit lower for the P branch.

¹⁸ R. Mecke, Zeits. f. Physik, **28**, 261 (1924); Phys. Zeits., **25**, 1 (1924).

responding to $\sigma = 0, 1$, and 2 . For large j values, where case (b) is approximated, the relation is¹

$$F = F(n) + F(j, j - j_k) + B(j_k^2 - \sigma_k^2) + \dots \quad (2)$$

The three values of $F(j, j - j_k)$ should be closer together than those of $F(\sigma)$ in case (a), increasingly so with increasing j (cf. Hund's Fig. 3). The arrangement of the band lines and the relation between the j and j_k values for case (b) are shown in Fig. 1.

Several features will now be considered which have been discussed only very briefly or not at all by Hund. Since N_2 is an even molecule, the j values should (in the writer's numbering) be half-integral. That this is

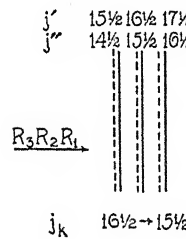


Fig. 1a

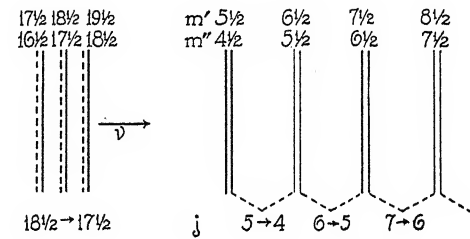


Fig. 1b

Fig. 1a corresponds roughly to the arrangement of the lines (missing lines are dotted) in the R branches of the Swan bands.^{18a} The arrangement is similar in the second positive nitrogen bands, except that (1) the dotted components are present but weak, (2) the doublets are unresolved in the R_3 branches and nearly so in R_2 (in regard to the relative positions of the two components in P_2 and R_2 cf. R. Mecke, ref. 16, p. 271, footnote), (3) R_1 , R_2 , and R_3 are more widely separated for a given value of j_k . The relative position of the strong and weak doublet components in relation to the j values is correct as given, for N_2 , but has not been definitely determined for the Swan bands. Fig. 1a is also applicable to the P branches (P_1 , P_2 , P_3) if the values of j' and j'_k given are reduced by two units.^{18a} Fig. 1b shows schematically the arrangement of the strong and weak lines in the R branches in the N_2^+ bands, as given by Fassbender.²²

true is shown by an examination of the $\Delta_2 F'$ and $\Delta_2 F''$ values for small values of j ; these^{14,15} are of the expected form $\Delta_2 F = 4BT$ with approximately half-integral T values, which shows (cf. ref. 5, p. 491) that the j values are half-integral if Eq. (1) is applicable.

The question of missing lines has been discussed by Hund. The theoretical values of j'' for the first line in each branch are readily specified, noting^{18a} that $\sigma = 0$ for P_3 and R_3 , 1 for P_2 and R_2 , 2 for P_1 and R_1 , and assigning to j_{min} in each case the first half-integral value in excess of σ . In Table I the predicted first lines are compared with those observed. The apparent presence of P_1'' ($2\frac{1}{2}$) is rather disconcerting. The apparent absence of R_1' ($2\frac{1}{2}$) is less strange, since this component of R_1 ($2\frac{1}{2}$) would be weak due to

^{18a} It is possible that the assignment of σ values, and the relation of j to j_k , for the $P_1 R_1$ and $P_3 R_3$ branches, should be interchanged in ref. 16, Table I, and Figs. 1a and 2b. Presumably $+\sigma_s$ (3P_1 in case a) goes over into $-j_s$ of case b, and $-\sigma_s$ (3P_0) into $+j_s$, for normal triplets, and the reverse for inverted triplets. The relation $(m + \frac{1}{2}) = j_k''$ of ref. 16 is reliable.

the alternating intensity phenomenon (see below). On the whole the results are not very satisfactory, but the experimental difficulties in determining the presence or absence of weak lines in a crowded region are great.

TABLE I
Values of $j'' - \frac{1}{2}$ for first recorded line of each branch

Band	P_1'	P_1''	P_2	P_3	R_1'	R_1''	R_2	R_3
$\lambda 3371$	3	2	2	1	3	2	2	1
3577	3	2	1	1	3	2	(1)	2
3805	(3)	2	(2)	1	(3)	2	1	0
3536	3	2	(3)	(3)	(3)	(2)	2	1
3755			2	1			(2)	1
3998				1				0
3710			4	1			4	0
3942			4	(1)	3	3	2	(1)
Theory	3	3	2	1	2	2	1	0

Notes. The data for the first five bands are from Hulthén and Johansson,¹⁶ and Zeit,¹⁷ for the last three, also the presence of $R_3(1)$ in $\lambda 3536$, the data are according to Lindau.¹⁷ Values in parentheses are uncertain due to superposition.

Closely analogous to the second positive nitrogen bands, as pointed out by Heurlinger, are the Swan (probably C_2 or perhaps C_2H_2) bands,^{19,20} which can therefore probably also be classified as $^3P \rightarrow ^3P$. The triplet separations in these bands are smaller than in the N_2 bands, indicating that Hund's case (b) is approached even for rather small j values.

The apparent absence of Q branches in the second positive nitrogen and the Swan bands can be explained by a consideration of the intensity equation of Hönl and London and Dennison for the case $\sigma' = \sigma''$ (cf. ref. 7, Eq. (4)). As in the $NO\beta$ bands,¹¹ only very short weak Q branches are to be expected (none at all in the case $^3P_0 \rightarrow ^3P_0$), whose presence would probably not be noticed without special search.^{21,22} Also, corresponding P and R branches should be approximately equal in intensity;²¹ so far as can be seen from the available data,¹⁶ this relation is fulfilled. Since according to Hund's theory 3P_0 , 3P_1 , and 3P_2 states have equal a priori probability for a given value of j , we should furthermore expect $P_1 (= P_1' + P_1'')$ in Table I) = $P_2 = P_3 = R_1$ ($= R_1' + R_2''$) = $R_2 = R_3$, approximately. This appears to be not in conflict with the data^{16,20} (but cf. Lindau, ref. 17, p. 351).

The rotational doubling in the N_2 and Swan bands is presumably σ -type doubling of the type specified by Eq. (2) of ref. 6.²³ In the Swan bands, the doubling is accompanied by alternate missing lines¹⁹ apparently of the same type as in the $^1D \rightarrow ^1P$ band of He_2 (cf. p. 1208-10 of ref. 6; and cf.

¹⁹ T. Heurlinger, Dissertation Lund, 1918; R. Komp, Zeits. Wiss. Photog., 10, 123 (1912); etc.

²⁰ R. Forrat, Ann. de physique 3, 350 (1915); Swan band $\lambda 5165$. R. C. Johnson, Phil. Trans. Roy. Soc. London, 226A, 157 (1927): comprehensive summary and large amount of new data.

²¹ The Hönl and London equations are of course directly applicable only for case (a), but may be expected to be at least qualitatively applicable here, especially for low values of j .

²² Certain additional series in the second positive nitrogen bands have been reported by Konen (cf. Heurlinger, ref. 19, p. 55), but are probably due to impurities (cf. ref. 16).

²³ Mecke earlier interpreted this doubling in the N_2 bands as ρ -type doubling.¹⁸

Fig. 1a of the present paper with Fig. 3 of ref. 6). This is true for all three P branches and all three R branches; also, the magnitude of the doublet separations is nearly the same in all three branches of each kind.

Fig. 1a shows how the strong and weak doublet components depend on j and j_k in the Swan bands.^{18a} It is without doubt significant that the relative positions of the strong and weak components are the same for all three members of a triplet (P_1, P_2, P_3 or R_1, R_2, R_3), hence are determined by j_k , not by j . For large values of j the P_2 and P_3 (eventually also the P_1) branches draw together (similarly with the R branches), and the scale of the multiplicity due to the three orientations of s becomes finer than that of the σ -type doubling. The tendency seems to be toward a coalescence of P_1, P_2, P_3 and R_1, R_2, R_3 each into a single series of alternate-missing-line *doublets* (of the $\text{He}_2 \ ^1D \rightarrow ^1P$ type) whose spacing and intensities are a function of j_k , and are presumably characteristic of σ_k .

The existence of rotational doubling for all three of the electronic states 3P_0 , 3P_1 , and 3P_2 (in spite of the fact that,—for low values of j ,— σ is zero for 3P_0 , just as for 1S , where rotational doubling is absent) is in agreement with Hund's theory, and gives the latter further support.

In the N_2 bands, there is an obvious doubling, accompanied by alternating relative intensities of the two components (P_1' and P_1'' ; and R_1' and R_2''), only in the P_1 and R_1 branches; here the doublet separation is approximately constant ($\Delta\nu \sim 0.24$),^{16,17} suggesting that it is mainly "electronic" in origin (cf. ref. 6, bottom of p. 1206). In the P_2 and R_2 branches, the existence of doubling coupled with alternating intensities is made evident by a displacement of the lines alternately to left and right, together with slight diffuseness in certain lines.¹⁷ In the P_3 and R_3 branches, the lines form a single series without alternating intensities, but by analogy with the Swan bands, there is no doubt a latent doubling as demanded by the theory; the existence of two series, related in intensity like those in the P_1 and R_1 branches, but superposed, would account for the observed apparently uniform non-alternating series, while with a truly single series any alternation would necessarily be evident.

The NH bands: note added in proof.—The NH bands recently analyzed by Hulthén and Nakamura (Nature, Feb. 12, 1927) and classed by them^{23a} as $^3P \rightarrow ^1S$ are in all probability $^3P \rightarrow ^3S$. The strong Q branches show $\Delta\sigma_k \neq 0$. The existence of Q combination defects and of three, rather than six, P (and Q , and R) branches show that an S electronic state is involved. (The $P'Q'R'$ branches evidently belong to a second band, as Hulthén and Nakamura point out). The final states in fact show a narrow triplet separation increasing linearly with j , as expected for 3S (case b). The initial states, showing wide triplets getting narrower with increasing j , must then be 3P .

A generalization concerning alternate suppressed rotational levels. Alternate weakened or suppressed lines in the N_2 and Swan bands, as in the He_2 bands (ref. 6, Fig. 2), are presumably due to a partial or complete suppression of alternate *rotational levels*. In the case of He_2 , it has been shown⁶ that the

^{23a} The classification $^3P \rightarrow ^1S$ was a misprint for $^3P \rightarrow ^3S$, the writer has since learned from Dr. Hulthén.

observed relations can be explained in terms of a system of missing levels which is characteristic for each type (1S , 1P , or 1D) of electronic state; the suppression of a level is a function only of j and of σ ; or, since $s=0$ and $\sigma=\sigma_k$ here, we may say that it is a function of j_k and σ_k . We may say further that, for each of the two types of rotational sub-states in He_2 , the suppressed values of $(j_k - \sigma_k)$ are characteristic and independent of σ_k and of the total quantum number of the excited electron, and are as follows (cf. ref. 6, Fig. 2): B sub-states, $(j_k - \frac{1}{2} - \sigma_k) = 0, 2, 4, \dots$; A sub-states, $1, 3, 5, \dots$; note that for $\sigma_k = 0$, only B sub-states occur.⁶

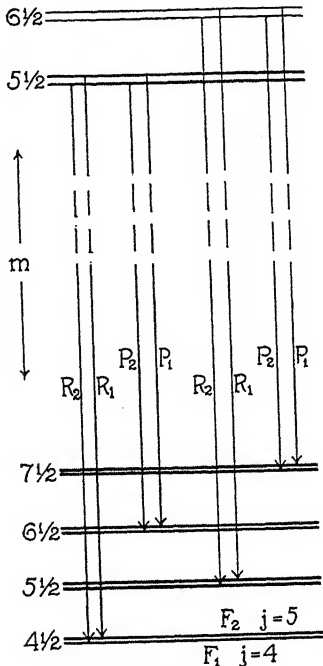


Fig. 2a

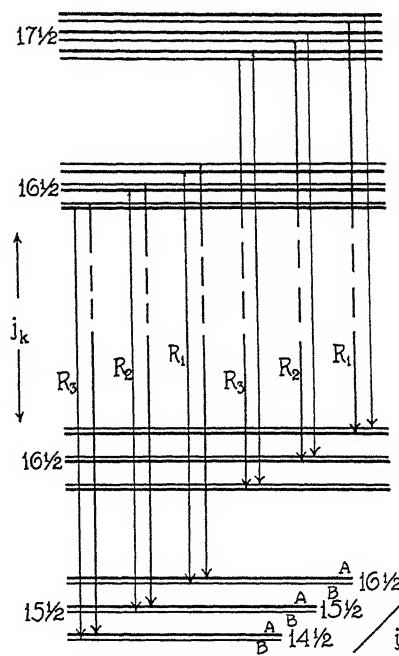


Fig. 2b

Fig. 2. Possible scheme of rotational energy levels and transitions, (a) for the negative nitrogen (N_2^+) bands, (b) for the Swan and second positive nitrogen bands; in (b) the three values of $j(j_k - 1, j_k, and $j_k + 1)$ for each value of j_k belong to 3P_0 , 3P_1 , and 3P_2 levels, respectively.^{18a} The spacings and intensities are not to scale. The relative position of the F_1 and F_2 levels in (a) and of the A and B levels in (b) is not certain; the same is true in (b) of the relative magnitude and order of the 3P_0 , 3P_1 , and 3P_2 levels and of the A and B rotational levels, in initial and final states. In (b), if suitable additional rotational levels are used, P branch transitions can be drawn, similar to the R transitions, with no "crossing over"; Q branch transitions should be very weak and involve crossing over ($A \rightarrow B$ and $B \rightarrow A$), according to Eq. (2) of ref. 6.$

Since there seems to be no reason why the scheme of alternate partially or wholly suppressed levels as a function of j_k and σ_k should differ from one homopolar molecule to another, it is reasonable to postulate that the statement just made for He_2 holds exactly for all homopolar molecules. The data on the N_2 and Swan bands are evidently compatible with this postulate, since the missing or weakened lines are a function of j_k (not of j), hence, we may say (σ_k being the same for all three 3P states), of $(j_k - \sigma_k)$. In the

N_2^+ bands ($^2S \rightarrow ^2S$ transition) the two branches (P and R) are each composed of alternately strong and weak doublets;²⁴ here again (Fig. 1b) weakness or strength is determined by j_k , or $j_k - \sigma_k$, not by j .

In the case of He_2 , the absence of observed combinations, such as $^1P \rightarrow ^1P$ and $^1S \rightarrow ^1S$, between like electronic states was attributed⁶ to a complete suppression of alternate rotational levels in both initial and final states. The occurrence of the combinations $^3P_0 \rightarrow ^3P_0$, etc. in the Swan and N_2 bands, and $^2S \rightarrow ^2S$ in the N_2^+ bands, then indicates that suppression occurs for one only of the two electronic states (Swan bands) or is only partial (N_2 and N_2^+ bands); partial suppression might be present in either or both of the two states.

A possible arrangement of the rotational levels for the N_2 and Swan bands is shown in Fig. 2b, and for the N_2^+ bands in Fig. 2a. In Fig. 2b the three levels corresponding to 3P_0 , 3P_1 , and 3P_2 are drawn equidistant in accordance with Hund's theory, and in agreement with the observed approximately equal spacing of the triplets formed by $R_1R_2R_3$ or $P_1P_2P_3$. The latter might, however, have arisen from a suitable non-equidistant arrangement of 3P_0 , 3P_1 , and 3P_2 in initial and final states. It is also uncertain whether the three levels are more widely spaced in the initial or in the final states, and whether in each case 3P_2 is the highest level as in a normal multiplet or the lowest as in an inverted multiplet.^{18a} The relative magnitude etc. of the rotational doubling in the initial and final states is also uncertain, since the doubling observed in the band-lines represents a difference of two term-doublings. These uncertainties can probably be removed only by the analysis of band systems having terms in common with the bands here under discussion.

General remarks on term-notation, term-formulation, j values, etc. Hund's theory gives no explanation of the phenomenon of alternating intensities in band lines.^{24a} Also it does not obviously account for the precise nature and selection rules which are observed in σ -type doubling, although it does predict correctly the presence or absence of such doubling. But at every point where the theory as so far developed is specific, all the experimental evidence appears to be in agreement with it.

The question of a systematic difference between the j numbering of even and odd molecules was not considered by Hund. In terms of the new quantum mechanics, the rotational energy for a σ -type term is given by $E^m = B[j(j+1) - \sigma^2] + \dots$ ²⁵ If this formulation is adopted, the experimental evidence^{4,5,6,7,11} shows definitely that $j(j=\sigma, \sigma+1, \sigma+2, \dots)$ is

²⁴ M. Fassbender, Zeits. f. Physik, 30, 73 (1924); R. Mecke, ref. 18.

^{24a} W. Heisenberg has recently presented a very interesting theory of alternating intensities (Zeits. f. Physik, Spring, 1927) in terms of the wave mechanics.

²⁵ This equation, obtained for the symmetrical rotator by D. M. Dennison (Phys. Rev., 28, 318, 1926), Kronig and Rabi (Nature, 118, 805 (1926), Phys. Rev. 29, 262, 1927), and by F. Reiche (Zeits. f. Physik, 39, 444, 1926), is doubtless also applicable here. Dennison does not decide between integral and half-integral j values, but Kronig and Rabi conclude that only integral values are allowable. This conclusion may well hold when σ corresponds to nuclear rotational energy, but in view of the experimental facts, evidently does not hold when σ is an electronic quantum number and when s is present with a half-integral value.

integral for even molecules and half-integral for odd molecules (the j values in the above formulation are all $\frac{1}{2}$ unit less than those used by the writer in previous papers). The same j values also hold in ρ -type terms, and doubtless in general.

In terms of Hund's theory, it is now apparent that the Kramers and Pauli rotational energy term $F(j) = Bm^2 + \dots = 2B[(j^2 - \sigma^2)^{1/2} - \rho]^2 \dots$, while formally capable of accounting for observed relations, is inappropriate physically, and should be replaced in Hund's cases (a) and (b) by Eqs. (1) and (2) above; in transition cases, the relation is more complicated. The variable electronic term in Eq. (2), which must also be present in transition cases, probably gives contributions²⁶ involving all powers of j . The contribution to the quadratic term probably accounts for the frequently rather large differences^{4,11} between the apparent B values for the components of a 2P or other multiple level; hitherto these have been interpreted as due to (unaccountably large) differences in moments of inertia, but recent work of Kemble and Jenkins²⁶ indicates that they can be accounted for quantitatively in terms of Hund's theory, with a single moment of inertia. The electronic contribution to the linear term in j also probably accounts in part (not wholly, since secondary ρ 's occur even for singlet electronic states) for the frequent occurrence of apparent "secondary ρ 's," whose existence is equivalent to the occurrence of a linear term in j ; also, cf. Kemble, ref. 3, pp. 345-7.

The "effective rotational quantum number" T , defined in previous papers⁵ as $j - \rho$, retains its meaning in Hund's case (a) (where $\rho = 0$, $T = j$). In case (b), T might best be redefined as $T = j_k$; in the special case of 2S states (where $j = j_k + \rho$, $\rho = \pm \frac{1}{2}$), this coincides with the previous definition. For transition cases between (a) and (b), the appropriate definition of T is not evident. When cases (a) and (b) are approximated, Eqs. 8E, 13, 14, and 15 of ref. 5, after dropping the terms in $\rho\sigma^2$, remain valid, in terms of T , for $F(j)$, $\Delta_1 F(j)$, $\Delta_2 F(j)$, and ν .

In terms of Hund's theory, it is evident that the notation 1S , 1P , 2P , etc., as used in previous papers of this series, is far from identical in meaning with that for the line spectrum case. According to the theory, the molecular quantities s , σ_k , and σ in case (a) play the same part in molecular multiplets as do s , k , and j (Sommerfeld's j_s , j_a , and j) in ordinary atomic multiplets (but cf. ref. 2). The most notable difference is the distinction required between k and σ_k in the molecular case. Practically there is at present little evidence on which to base this distinction. Probably σ_k is identical with k in many or perhaps even in most of the familiar band spectra. When it becomes possible to determine both k and σ_k , such a notation as e.g. ${}^2P_1^D$ might be introduced to describe the case $k = 2$, $\sigma_k = 1$, $s = \frac{1}{2}$, $\sigma_s = -\frac{1}{2}$. In the meantime, the continued use of the simple designations 2P_1 , 1S , etc. would seem to be both appropriate and convenient for the empirical classification of molecular electronic terms.

WASHINGTON SQUARE COLLEGE,
NEW YORK UNIVERSITY,
February 12, 1927.

²⁶ E. C. Kemble and F. A. Jenkins, Bull. Am. Phys. Soc. 2, No. 1, Abstr. No. 9 (Feb. 12, 1927).

SCREENING CONSTANTS FROM OPTICAL DATA

By O. LAPORTE

ABSTRACT

Grotian identified the relativistic doublets which correspond to the ionization of an n_2 shell in the spectra of the rare gases. Similarly the doublets which belong to the n_3 shells are found in the spectra of 29 Cu, 45 Rh, and 79 Au. The different relative stability of the n_3 electrons as compared with the $(n+1)_1$ electrons is clearly noticeable in every one of the three long periods. The screening constants are in good agreement with those computed from x-ray data, even in cases where the "optical" screening constant is obtained from elements the outer shell of which is not yet complete.

THE similarity of the energy diagrams of the x-ray spectra and of the optical alkali-spectra was first pointed out by W. Grotian¹ in 1922. It led Landé² to a complete identification of the x-ray terms as doublet terms according to the following diagram:

TABLE I

K_{11}	L_{11}	L_{21}	L_{22}	M_{11}	M_{21}	M_{22}	M_{32}	M_{33}
1^2S	2^2S	2^2P_1	2^2P_2	3^2S	3^2P_1	3^2P_2	3^2D_2	3^2D_3

in which the relativistic doublets appear as analogues of the magnetic complex structure, whereas the screening doublets seem to be caused by differences of the azimuthal quantum number. This analogy was used also by Sommerfeld³ to compute intensities of x-ray line groups and by Wentzel⁴ to predict the fine structure of the so-called x-ray spark lines. The complex structure of the x-ray energy diagram was finally made clear by the Russell-Hund theory of complicated spectra. It proved that on account of Pauli's⁵ exclusion principle, when ionizing a shell of N electrons z times, the same energy states and quantum numbers appear as in an atom with z valence electrons. In other words: incomplete shells of z or $N-z$ electrons show the same terms, if N is the "Besetzungszahl" (2, 6, 10, 14, etc.). Since Kossel we are accustomed to regard the x-ray levels as the stationary states of a simply ionized shell and hence must expect doublet terms of similar structure as for the alkalis. We thus arrive at an explanation of Table I.

But with the help of the Bohr-Stoner theory of the periodic system we can also predict the elements where these x-ray terms must appear on the surface of the atom and will be noticeable as optical doublet terms. The ionized K -shell will give a 1^2S term for the normal state of He^+ and H and

¹ W. Grotian, Zeits. f. Physik, 8, 116 (1922). See especially footnote No. 3 on page 117.

² A. Landé, Zeits. f. Physik 16, 391 (1923).

³ A. Sommerfeld, Ann. d. Physik 76, 284, (1925).

⁴ G. Wentzel, Zeits f. Physik 31, 445, (1925).

⁵ W. Pauli, Zeits. f. Physik 31, 765 (1925).

similarly we obtain a 2S term as lowest term of the alkaline-earth ions or the neutral alkali atoms. When ionizing the complete L shell at 10Ne , the electrons will arrange themselves so as to yield a 2^2P term as lowest term of Ne^+ or of 9F . In the same way we will get 3^2P , $4^2P \dots$ terms as the normal states of the ions of 18A , $36\text{Kr}, \dots$ or of the neutral atoms of 17Cl , $35\text{Br} \dots$ respectively. Applying the same reasoning likewise to the higher subgroups we must expect 2D terms with total quantum-number 3, 4, 5 at the end of the iron, palladium and platinum groups and finally a 4^2F term at the end of the rare earth group. Unfortunately the end of these shells is not so marked in the periodic table as the completions of the shells with azimuthal quantum number $k=1$ and 2; a more detailed discussion will be necessary to select the right elements, where one has to look for the x-ray terms in the optical region.

The above-mentioned appearance of the relativistic L -doublet in the spectrum of Ne^+ was first pointed out by Grotrian.⁶ As is well known he identified it with the two series limits which Paschen⁷ had found in the arc spectrum of Ne. Grotrian was also able to show, that the numerical value of Paschen's frequency difference agreed approximately with the separation computed with the Sommerfeld formula for relativistic doublets:

$$\frac{\Delta\nu}{R} = \frac{\alpha^2(Z-s)^4}{n^3j(j-1)} \quad (1)$$

if one inserts $Z=10$, $n=2$ and $j=2$. One can formulate this result as follows: substituting on the left side of this equation Paschen's empirical frequency difference for Ne and solving for the screening constant s , we obtain a value which is in close agreement with the value used for the representation of the relativistic doublets of the elements from $Z=13$ to $Z=92$. In his recent analysis of the arc spectrum of argon Meissner⁸ found, that, in strict analogy to neon, the terms converge toward two limits which he identified as M_{21} and M_{22} . From this doublet separation Grotrian⁹ computed the screening constants of this relativistic M doublet and compared it with that obtained from the x-ray spectra of the elements $Z=37$ to $Z=92$.

This latter note of Grotrian's suggested to me to try the same with the relativistic doublets appearing at the end of the three long periods, namely, the iron, palladium and platinum groups. The doublets in question are in the x-ray notation $M_{32}M_{33}$, $N_{32}N_{33}$, and $O_{32}O_{33}$; from the optical viewpoint they must appear respectively as 3^2D , 4^2D and 5^2D terms. As was mentioned before, the difficulty arises that the end of these n_3 shells is not so clearly noticeable—the “rare gas” at the end of these periods is evidently missing—the reason being that in each of the three shells two types of orbits furnish the lower terms.¹⁰ In a shell made up of n_2 or p electrons (e.g. B—Ne,

⁶ W. Grotrian, Zeits f. Physik **8**, 116, (1922).

⁷ F. Paschen, Ann. d. Physik **60**, 405 (1919); **63**, 201 (1920).

⁸ K. W. Meissner, Zeits. f. Physik **39**, 172 (1926).

⁹ W. Grotrian, Zeits. f. Physik **40**, 10 (1926).

¹⁰ For the following compare the author's paper on the complex spectra in Jour. Opt. Soc. Amer. **13**, 1 (1926).

Al—A, Ga—Kr etc.) the lowest terms arise from configurations with p electrons only (e.g. 2P of all from one p , 3P in Si from two p or (p^2) 4S in P from (p^3) etc.) On the other hand the lowest terms of an element in the iron group may arise from both 4_1 and 3_3 and similarly for the next periods from 5_1 and 4_3 electrons. In Professor Russell's notation we may summarize the results of the spectral classifications with the statement that in the long periods the low energy states of atoms or ions with z valence electrons are configurations of the types $(d^{z-2}s^2)$ $(d^{z-1}s)$ and (d^z) . Which of the three configurations will be so low as to furnish prominent combinations varies strongly for different elements and periods and cannot be predicted theoretically. Several empirical rules have been given to represent the facts,¹¹ the most obvious of them being that in higher spark spectra the influence of the s electrons will become smaller and terms of type (d^z) will prevail. As a consequence of Pauli's exclusion principle a shell of n_3 electrons becomes complete with the tenth electron. The problem therefore is to find 2D terms arising from a configuration of type (d^9) .

In order to find the doublet $M_{32}M_{33}$ in the first long period it seems reasonable to look for the term $^2D(d^9)$ in the arc spectrum of 27 Co. According to Bechert and Catalan,¹² however, the stable configurations of Co are of type (d^7s^2) and (d^8s) , whereas configuration (d^9) seems to be very unstable. Another possibility of finding the term $^2D(d^9)$ would be in the spark spectrum of Ni. So far as we know no data on NiII have been published.¹³ But we can find our relativistic doublet in the arc spectrum of the following element 29 Cu, which has recently been investigated by Shenstone and others.¹⁴ Besides the normal state of Cu, $^2S(d^{10}s)$, there exists an inverted metastable term which was identified by Shenstone to be $^2D(d^9s^2)$. Its separation equals 2043 cm^{-1} . We shall use this term for the computation of the screening constant. The presence of two 4_1 electrons, i.e., of the complete N_{11} shell has no influence: using the configuration (d^9s^2) for our purpose we only approach and approximate the conditions under which x-ray spectra are observed.

In the second long period the d electrons (4_3) have gained so much in stability that terms of type (d^z) —without any 5_1 electrons—occur even in arc spectra. About a year ago the writer¹⁵ identified a 2D term as the sought-for $N_{32}N_{33}$ doublet in the arc spectrum of rhodium. Its separation is $\Delta\nu = 2348 \text{ cm}^{-1}$. Also a 2D term was found by McLennan and Smith¹⁶ in the spark spectrum of palladium. This term, too, gives the right order of magnitude for the

¹¹ O. Laporte, Zeits. f. Physik, 39, 123 (1926). Compare also the somewhat different viewpoint of L. A. Sommer, Zeits. f. Physik, 37, 1 (1926).

¹² K. Bechert and M. A. Catalan, Zeits. f. Physik, 32, 336 (1925).

¹³ The term $^2D(d^9)$ probably corresponds to the normal state of Ni^+ . Comp. O. Laporte, Zeits. f. Physik, 39, 123 (1926).

¹⁴ A. G. Shenstone, Phys. Rev. 28, 449 (1926), C. S. Beals, Proc. Roy. Soc. A111 (1926); L. A. Sommer, Zeits. f. Physik, 39, 711 (1926).

¹⁵ O. Laporte, Journ. Opt. Soc. Amer., 13, 1 (1926). See especially p. 22.

¹⁶ J. C. McLennan and H. G. Smith, Proc. Roy. Soc. A112, 110 (1926).

screening constant. The separation given by McLennan and Smith is 3512 cm^{-1} .

As to the relative stability of d and s electrons, the third long period resembles the first period toward its end. It is, therefore, improbable that the $^2D(d^9)$ term will be found among the lower metastable terms of the arc spectrum of iridium ($Z=77$).¹⁷ As was pointed out by Grimm and Sommerfeld,¹⁸ the arc spectrum of gold resembles that of copper in the fact that s and d electrons are about equally stable, whereas in silver the s electrons exceed by far the d electrons in stability. Consequently one must expect a low metastable 2D term belonging to the configuration (d^9s^2), which, indeed, was recently published by McLennan and McLay¹⁹ in their second revised paper on Au. The separation of this term is 12274 cm^{-1} .

In Table II the screening constants s computed from the optical data²⁰ are compared with those of the x-ray spectra. Substituting the numerical values for R and α , and solving Eq. (1) for s , we have the formula:

$$s = Z - \left(\frac{n^3 j(j-1)}{5.83} \Delta\nu \right)^{1/4} \quad (2)$$

which was used for the calculation of the s values.

At the top of the table the quantum numbers and the optical notation are given, on the left side the x-ray notation. The numbers in italics are the

TABLE II
Comparison of the screening constants computed from optical data with those of x-ray spectra.

Optical notation Sommerfeld's Indices Bohr's Indices	2P 21–22 II–III	2D 32–33 IV–V	2F 43–44 VI–VII
L	$Z=17$ – 92 : 3.50 9 F : 3.21 10 Ne : 3.20		
M	$Z=37$ – 92 : 8.5 17 Cl : 7.50 18 A : 7.29	$Z=41$ – 92 : 13.0 29 Cu : 13.60 ²¹	
N	$Z=53$ – 92 : 17.0 35 Br : 18.13	$Z=51$ – 92 : 24.4 45 Rh : 25.17 46 Pd : 24.07	$Z=81$ – 92 : 34 71 Lu : ?
O	— 53 I : 29.10	— 79 Au : 45.55	

¹⁷ The tentative identification of two levels in the iridium spectrum as 2D by W. F. Meggers and O. Laporte (Phys. Rev. 28, 642, 1926, *vide p. 660*) must probably be given up, since the $\Delta\nu$ of this term is much too small to be of the right order of magnitude.

¹⁸ H. G. Grimm and A. Sommerfeld, Zeits. f. Physik, 36, 36 (1926).

¹⁹ J. C. McLennan and A. B. McLay, Proc. Roy. Soc. A112, 95 (1926).

²⁰ For the sake of completeness we include the screening constants computed from the data given by Turner, (Phys. Rev. 27, 397, 1926) for Cl, Br, I, and by Bowen (Phys. Rev. 29, 231, 1927) for the spectrum of F.

²¹ Note added to proof: The fact that the 2D term of Cu gives an s in agreement with that obtained from x-ray data has already been noted by A. G. Shenstone (Nature 116, 467, 1925).

screening constants as obtained from the relativistic x-ray doublets, whereas underneath the optical screening constants are given together with the elements from whose spectrum they were obtained.

In general the agreement is rather good. The large fluctuation of the s values for $N_{32}N_{33}$ in the spectra of Rh and Pd is remarkable.²² The largest deviation which is also discussed at length by Grotrian⁹ occurs for the $M_{21}M_{22}$ doublet in A and Cl. Grotrian explains this disagreement as due to the incompleteness of the M shell at A. Since the x-ray screening constant is obtained from elements with atomic number 37 and larger, where the entire M shell is completed, we should expect a smaller s for elements with atomic number smaller than 29 (Cu). But we see from Table II that this cannot be true; for we would have to expect a still larger deviation $s_{\text{x-ray}} - s_{\text{opt.}}$ for the doublet $N_{21}N_{22}$, a somewhat smaller one for $N_{32}N_{33}$ and good agreement for all the doublets which are last in their shells ($L_{21}L_{22}$, $M_{32}M_{33}$, $N_{43}N_{44}$). On the contrary we find $s_{\text{opt.}} > s_{\text{x-ray}}$ for $N_{21}N_{22}$ and fair agreement for $N_{32}N_{33}$ although the whole N shell does not become complete until after the rare earths ($Z > 71$). We consequently arrive at the conclusion that the value of the screening constant of a Stoner sub-group is independent of the presence of the sub-groups with higher azimuthal quantum k and that the relatively large positive and negative deviation of the optical and x-ray values are apparently due to irregular local disturbances.

Unfortunately the s value for $N_{43}N_{44}$ cannot yet be obtained from optical data, since the spectra at the end of the rare earth group have not been investigated. With the (very inaccurate) value 34 from x-ray data we obtain for the terms $^2F(f^{13})$, $^2F(f^{13}s^2)$ and also $^3F(f^{13}s)$ which we have to expect among the low metastable terms of 70 Yb, a separation of about 13,000 wave number units.

On the other hand we are able to predict screening constants for the O doublets.²³ Attempts are being made at this laboratory to separate the O_{21} and O_{22} levels for the heaviest elements.

DEPARTMENT OF PHYSICS
UNIVERSITY OF MICHIGAN,
February 25, 1927.

²² Compare the similar fluctuations of the s of the L -doublet near $Z=26$, which were pointed out by D. M. Bose, Phys. Rev. 27, 521 (1926).

²³ A. Sommerfeld (Journ. Opt. Soc. 7, 503, 1923) shows that the screening constants with the exception of that of the L -doublet, are integer multiples of 4.2. The two new values of the O -screening constants are also respectively 7 and 10 times this constant.

MULTIPLETS IN THREE ELECTRON SYSTEMS OF THE FIRST LONG PERIOD

By R. C. GIBBS AND H. E. WHITE

ABSTRACT

Wave-lengths and relative positions of multiplets in the spectra of Sc (I), Ti (II), V (III), and Cr (IV).—Using the regular and irregular doublet laws as guides, it has been found possible, from the corresponding known multiplets in Sc (I) and Ti (II), to identify the triad of multiplets of V (III) designated as $^4F_{2,3,4,5} - ^4G_{3,4,5,6}$; $^4F_{2,3,4,5} - ^4F'_{2,3,4,5}$; and $^4F_{2,3,4,5} - ^4D_{1,2,3,4}$. For these multiplets the initial state is given by one $4p$ electron and two $3d$ electrons. In the final state the $4p$ electron has shifted to a $4s$ orbit. The separations of the $^4F_{2,3,4,5}$ levels are found to be in the ratio 2.50:3.52:4.50, in very close agreement with Landé's interval rule. The relative intensities of the lines in these multiplets conform to the usual rule. A comparison of the data for one, two, and three electron systems of Sc, Ti, and V shows that the addition of first one and then a second d electron causes not only an increase in the multiplicity but also successive shifts in the radiated lines toward the longer wave-lengths by very nearly the same frequency interval. It has also been found possible to identify the $^4F_{2,3,4,5} - ^4F'_{2,3,4,5}$ multiplet of Cr (IV).

IT HAS been shown¹ that for the one electron systems of the first long period from K(I) to Mn(VII) the first lines of the principal series follow very closely the regular and irregular doublet laws. Each of these lines results from an electron in a $4p$ orbit jumping into a $4s$ orbit. Similarly for two electron systems of this same period from Ca(I) to Cr(V), we have been able to show that when one of the electrons in a $4p$ orbit jumps to a $4s$ orbit in the presence of an electron in a $3d$ orbit a triad of multiplets of the type $^3D_{1,2,3} - ^3P_{0,1,2}$, $^3D_{1,2,3} - ^3D'_{1,2,3}$, and $^3D_{1,2,3} - ^3F_{2,3,4}$, also follow the regular and irregular doublet laws.²

In the three electron systems Sc(I), Ti(II), and V(III), three multiplets forming a triad of the type $^4F_{2,3,4,5} - ^4D_{1,2,3,4}$; $^4F_{2,3,4,5} - ^4F'_{2,3,4,5}$; and $^4F_{2,3,4,5} - ^4G_{3,4,5,6}$, have been identified which obey these same laws. For these multiplets the initial state is given by one $4p$ electron and two $3d$ electrons. The final state finds one electron in a $4s$ orbit and the other two in $3d$ orbits. This transition may have taken place in two ways either by a one electron jump, $4p$ to $4s$, or by a two electron jump, $4p$ to $3d$ and $3d$ to $4s$. If the two electron jump takes place one electron has changed by $\Delta k = 1$, and the other by $\Delta k = 2$.

In either case the sums of the total quantum numbers for the initial and final states are equal, which is the necessary requirement that the resultant spectral lines follow the doublet laws.

Multiplets in the arc spectrum of scandium have been identified by Catalan.³ He reports three multiplets of the type $^4F_{2,3,4,5} - ^4D_{1,2,3,4}$, $^4F_{2,3,4,5}$

¹ R. C. Gibbs and H. E. White, Nat. Acad. Sci. Proc. 12, 448 (1926).

² R. C. Gibbs and H. E. White, Phys. Rev. 29, 426 (1927).

³ Catalan, Ann. de Soc. Esp. Fis. Y Quim. p. 466 (Nov., 1923).

$-^4F'_{2,3,4,5}$, and $^4F_{2,3,4,5} - ^4G_{3,4,5,6}$, in the region of 5000A.U. The intensities, wave-lengths, and frequencies of the lines in these multiplets as well as the relative term values are given in Table I. In Ti(II) a similar triad of the

TABLE I

Multiplet Triad in Sc(I) (Catalan)

 $d^2p \rightarrow d^2s$

		4F_6	4F_4	4F_3	4F_2
		157.3 (67.1)	90.2 (52.5)	37.7 (37.7)	000
4G_6	17783.3	200 5671.83 17626.1			
4G_5	17669.7	(113.6) 15 5708.63 17512.5	150 5686.83 17579.6		
4G_4	17576.1	(93.6) 2 5739.21 17418.9	15 5717.29 17486.0	100 5700.18 17538.4	
4G_3	17502.9	(73.2) 1 5741.34 17412.7	15 5724.08 17465.2	100 5711.75 17502.9	
$^4F'_6$	19830.7	125 5081.57 19673.5	10 5064.32 19740.5		
$^4F'_4$	19755.4	(75.3) 20 5101.08 19598.2	90 5083.70 19665.3	40 5070.21 19717.6	
$^4F'_3$	19695.8	(59.6) 40 5099.20 19605.5	60 5085.53 19658.2	10 5075.81 19695.8	
$^4F'_2$	19652.5	(43.3) 30 5096.72 19615.0	30 5086.99 19652.5	50 5086.99 19652.5	
4D_4	21231.5	40 4743.80 21074.3	8 4728.77 21141.2	0 4717.03 21193.9	
4D_3	21176.9	(54.6) 30 4741.02 21086.6	10 4729.21 21139.3	0 4720.77 21177.1	
4D_2	21139.3	(37.6) 18 4737.65 21101.7	10 4729.21 21139.3		
4D_1	21117.5	(21.8) 15 4734.10 21117.5			

same type in the region of 3000A.U. has been reported by Russell,⁴ and by Meggers, Kiess, and Walters.⁵ Their results are shown in Table II together with the relative values of the $^4F_{2,3,4,5}$, $^4D_{1,2,3,4}$, $^4F'_{2,3,4,5}$, and $^4G_{3,4,5,6}$ terms

⁴ H. N. Russell, *Astrophys. Jour.* 61, 254 (1925).⁵ Meggers, Kiess and Walters, *J.O.S.A.* 9, 364 (Oct., 1924).

where the 4F_2 term, which is the lowest level of the normal state of the ionized atom, is taken as zero. Applying the irregular doublet law, i.e. a

TABLE II

Multiplet Triad in Ti(II)^{4,5}

		$d^2p \rightarrow d^2s$			
		4F_5	4F_4	4F_3	4F_2
		393.3 (167.7)	225.6 (131.5)	94.1 (94.1)	000
4G_6	30240.6	40 3349.41 29847.4			
	272.5	15 3380.28 29574.9	40 3361.22 29742.6		
	233.6	4 3407.20 29341.3	15 3387.83 29509.0	30 3372.80 29640.4	
4G_5	29968.1				
	190.0		5 3409.80 29318.9	15 3394.57 29450.4	40 3383.76 29544.5
4G_4	29734.5				
	154.8				
	122.1				
4G_3	29544.5				
	187.4	60 3234.52 30907.6	15 3217.04 31075.5		
	154.8	20 3254.23 30720.4	50 3236.57 30888.0	15 3222.82 31019.8	
$^4F'_5$	31300.9				
	122.1				
	95.6				
$^4F'_4$	31113.5				
	70.1				
	69.1				
$^4F'_3$	30958.7				
	69.1				
	45.6				
$^4F'_2$	30836.6				
	45.6				
	27.1				
4D_4	32767.3	60 3088.03 32373.9	30 3072.10 32541.7	?	
	27.1				
	20.1				
4D_3	32698.2				
	20.1				
	15.6				
4D_2	32602.6				
	15.6				
	10.1				
4D_1	32532.5				
	10.1				

linear extrapolation of ν from each multiplet in Sc(I) and Ti(II), the corresponding multiplets were looked for in the spark spectrum of vanadium in the vicinity of 2500A.U. Three very strong multiplets have been identified in this part of the spark spectrum, the details for which are given in Table III. The wave-lengths in Tables I and II are given in I.A.(air) while those in

Table III are in I.A.(vac). Assuming the regular doublet law to hold an extrapolation from the values of the ${}^4F_{2,3,4,5}$ separations for Sc(I), and Ti(II) enabled us to predict the ${}^4F_{2,3,4,5}$ separations for V(III) to be about

TABLE III

Multiplet Triad in V(III)
 $d^2p \rightarrow d^2s$

		4F_5	4F_4	4F_3	4F_2
		705.1 (301.7)	403.4 (235.8)	167.6 (167.6)	000
4G_6	42867.6	200 2371.76 42162.8			
4G_5	42364.5	(503.1) 75 2400.40 41659.7	150 2383.18 41960.7		
4G_4	41933.5	(431.0) 2 2425.51 41228.4	80 2407.90 41530.0	125 2394.27 41766.4	
4G_3	41581.9	(351.6) 2 2428.43 41178.8	40 2414.62 41414.4	100 2404.89 41581.9	
${}^4F'_5$	43603.2	100 2331.09 42898.4	50 2314.81 43200.1		
${}^4F'_4$	43277.4	(325.8) 30 2348.94 42572.4	75 2332.39 42874.5	40 2319.65 43109.9	
${}^4F'_3$	42996.4	(281.0) 30 2347.78 42593.4	75 2334.87 42829.0	40 2325.78 42996.3	
${}^4F'_2$	42775.1	(221.3) 30 2347.00 42607.6	75 2337.80 42775.1		
4D_4	45479.2	70 2233.46 44773.6	25 2218.49 45075.7	2 2206.96 45311.2	
4D_3	45519.1	(39.9) 40 2216.55 45115.2	20 2205.00 45311.5	2 2196.88 45519.1	
4D_2	45251.4	(267.7) 30 2218.09 45083.8	8 2209.88 45251.4		
4D_1	45064.5	(186.9) 30 2219.04 45064.5			

$\Delta\nu = 172, 246$, and 310 . These separations are found to be $\Delta\nu = 167.6, 235.8$, and 301.7 which is in very close agreement with the predicted values. According to Lande's interval rule these separations should have values in the ratio $2.5:3.5:4.5$. The observed separations are in the ratio $2.50:3.52:4.50$.

Owing to insufficient data on chromium in the extreme ultra-violet we have as yet been able to identify with certainty only the $^4F_{2,3,4,5} - ^4F'_{2,3,4,5}$ multiplet and several lines of the $^4F_{2,3,4,5} - ^4G_{3,4,5,6}$ multiplet.

The linear progression in frequency of each of the above multiplets with the atomic number, is brought out most clearly in Fig. 1 for the first three

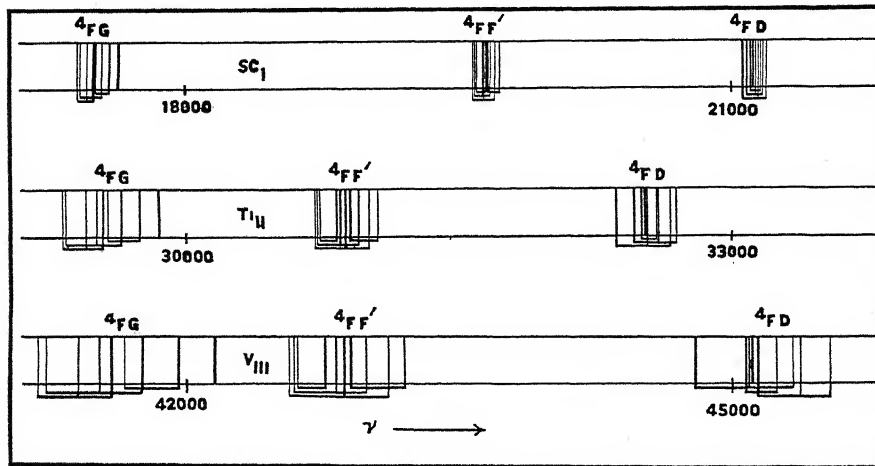


Fig. 1. Three electron systems of the first long period.

elements. It may be seen that by displacing the frequencies of each group of lines to the left by $\Delta\nu = 12,000$ with respect to the spectral groups of the element just preceding it, corresponding multiplets are seen to lie very nearly one below the other. In this way the small departures from the irregular doublet law appear to be magnified.

The increasing frequency separations of the $^4F_{2,3,4,5}$ levels, as may be seen in Fig. 1 follows directly from the regular doublet law which requires that $\Delta\nu = K(Z-s)$.⁴ This law although derived for doublet separations is found to apply also to multiplet terms.² The screening constants as computed from the above relation are given in Table IV. If Fig. 1 had been

TABLE IV
Regular doublet laws

	$\Delta\nu$ $^4F_5 - ^4F_4$	$(\Delta\nu / .0456)^{1/4}$	s	$\Delta_1\lambda$ $(^4F_5 F'_5 - ^4F_4 F'_4)$	$\Delta_2\lambda$ $(^4F_5 F'_5 - ^4F_5 F'_4)$
Sc(I)	67.1	6.193	14.807	17.25	19.51
Ti(II)	167.7	7.787	14.213	17.48	19.71
V(III)	301.7	9.018	13.982	16.28	17.85

plotted to a scale of wave-lengths in place of frequencies, the corresponding $^4F_{2,3,4,5}$ separations would have been almost the same for each multiplet in all three elements. This is also a consequence of the regular doublet law. This constancy of $\Delta\lambda$ between corresponding lines in each of these multiplets

is quite remarkable. Examples of this are given in the last two columns of Table IV. There are in a few cases departures from this rule just as there are occasional departures from the interval rule as given by Landé for term separations.

Starting with the one electron system of any of the elements given in Table V, it is seen that the screening effect due to the addition of first one

TABLE V
Screening effect of d electrons.

Doublets $\frac{p \rightarrow s}{4^2S_1 - 4^2P_2}$	Triplets $\frac{dp \rightarrow ds}{a^3D_3 - a^3F_4}$	Quartets $\frac{d^2p \rightarrow d^2s}{a^4F_5 - a^4G_6}$
Sc(III) 37039 .6	(9376.0)	Sc(II) 27663 .6
(11311.2)		(10037.5)
(12070.1)		(12221.3)
Ti(IV) 48350 .8	(8617.1)	Ti(III) 39733 .7
(9886.3)		(12315.4)
(11837.7)		(12181.5)
V(V) 59514 .4	(7943.0)	V(IV) 51571 .4
(9408.6)		(12181.5)
(11994.9)		(12181.5)
Cr(VI) 70535 .3	(6969.0)	Cr(V) 63566 .3
(10778.0)		(12181.5)

and then a second d electron is to shift the spectral lines toward the longer wave-lengths by very nearly the same frequency interval, while at the same time the multiplicity is increased. The uniformity of this shift is more strikingly brought out in Fig. 2 where in passing downward along any of the light diagonals there is a successive addition of d electrons with a simultaneous decrease in effective core charge. Fig. 2 also serves to bring out the nearly linear displacement of multiplets when successive d electrons are added keeping the effective core charge nearly constant i.e. upward along the heavy diagonals. The irregular doublet law which holds here for iso-electronic systems, is illustrated by the almost equal intervals along the verticals. To show this screening effect, we have taken the strongest line in each electron system as representing the position in the spectrum of that system of lines. In the one electron systems the $4^2S_1 - 4^2P_2$ line is the strongest line of the doublet since k and j are changing in the same direction. For the two electron systems the strongest line of all three multiplets is the line $^3D_3 - ^3F_4$. Similarly for the three electron systems the line $^4F_5 - ^4G_6$ is the strongest.

It is interesting to note that in general the jump from the multiple level having the largest k value into a common lower multiple level gives the strongest lines in the triad of multiplets; the intensities of the other multiplets following in an order corresponding to their relative k values. In each multiplet the stronger lines appear where k and j are changing in the

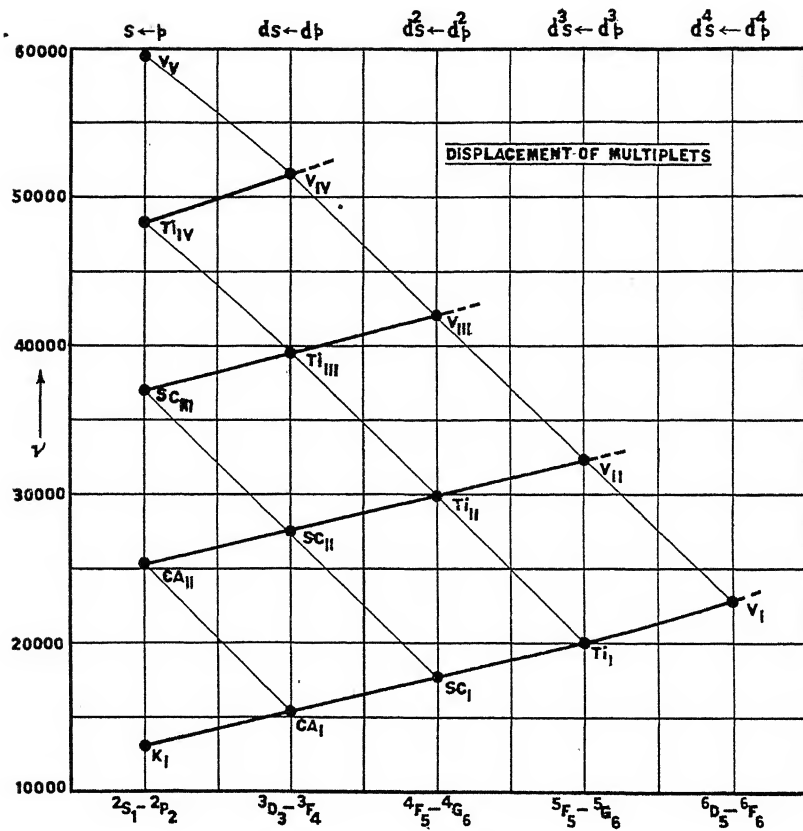


Fig. 2. Up heavy diagonals: successive addition of d electrons with constant core charge. Down light diagonals: successive addition of d electrons with simultaneous decrease in core charge. Up verticals: iso-electronic systems with successive increase in core charge.

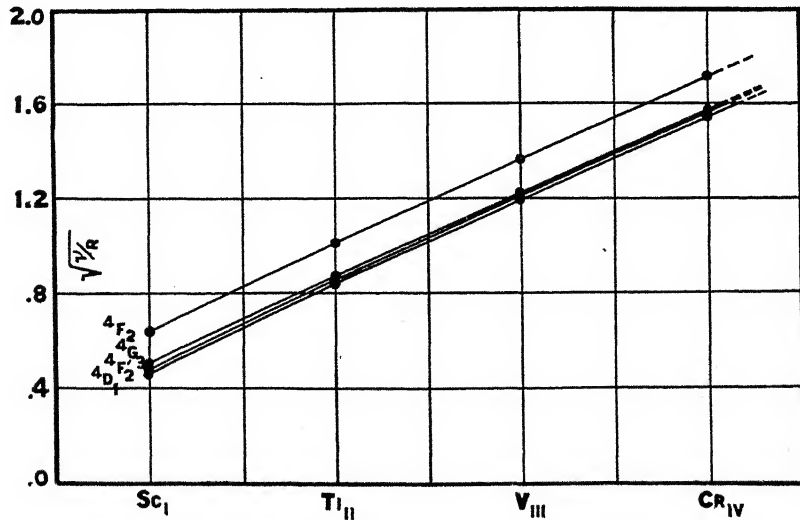


Fig. 3. Moseley diagram.

same direction. Of these stronger lines, which in Tables I, II and III are on the diagonals of each multiplet, the strongest line occurs for the transition involving the largest j values. From these intensity rules then it may be deduced that for a given electron configuration the most stable state occurs when the orbital axes and also the spin axes of all the valence electrons are as nearly as possible in the same direction. Furthermore when an electron transition takes place the most probable transition will be such that these axes retain as nearly as possible the same relative directions. The exceptions to this rule are probably accounted for, by ones inability to measure accurately the relative intensities of lines taken from different photographic plates, or from the failure of photography in general to record true relative intensities.

The lines on the Moseley diagram, Fig. 3, being parallel are a direct consequence of the irregular doublet law which requires $\Delta(\nu/R)^{1/2} = \text{constant}$, where ν is given in cm^{-1} . The values of $(\nu/R)^{1/2}$ were obtained by an extrapolation from terms already known in K(I), Ca(II), and Ca(I), Sc(II). It may here be pointed out that the regular and irregular doublet laws give an effective method of attack in the classification of spectra arising from higher states of ionization in iso-electronic systems of successive elements in any one Period.

CORNELL UNIVERSITY
January 27, 1927.

THE ABSORPTION SPECTRA OF Ga, In, Mn, Cr, Ni and Co IN UNDER-WATER SPARKS

BY ALPHEUS W. SMITH AND MORRIS MUSKAT

ABSTRACT

The absorption of gallium, indium, manganese, chromium, nickel and cobalt has been studied in under-water spark spectra. Many new lines, not previously found in absorption spectra, have been located. The results confirm and extend the observations on the absorption of these elements in the vapor state. For indium and gallium they confirm the conclusion that the normal state of the atom is the $2p$ state and for manganese, the conclusion that the ground level of the valence electron is the $1s$ septet level. For chromium, nickel and cobalt they afford a verification of the assignment of lines and arrangement of terms with respect to the ground level as given by Catalan and Gieseler for chromium, by Bechert and Sommer for nickel and by Catalan and Bechert for cobalt.

INTRODUCTION

A STUDY of the line absorption spectra of the different elements has become important in view of the information which it affords concerning atomic structure, especially the normal state of the last valence electron of the neutral atom. One of the principal methods of obtaining line absorption spectra of metals consists in observing the spectra which are emitted from oscillatory discharges passed between two metallic electrodes, immersed in water. Under these conditions, if oscillatory discharges of sufficiently high frequency are used, the spectrum of the metal consists of a continuous background on which the arc lines appear as reversed lines. Since it is the arc lines which are absorbed by the neutral atom, the lines which are reversed in the under-water spark give the same kind of information with respect to the neutral atom as is obtained by observing the absorption produced by a vapor of the metal in its normal state. Hence this method of obtaining absorption spectra of metals offers a means of extending and verifying results obtained by passing light through the normal vapor of the metal.

The absorption spectra of a large number of metals have previously been examined in under-water sparks. Finger¹ made the first important study of such spectra for seventeen metals. L. and E. Bloch² made similar observations on many of the same metals studied by Finger and extended the observations to some additional metals. Hulbert³ also made similar observations on many metals studied both by Finger and L. and E. Bloch and on some additional metals but the results are not interpreted in terms of spectral series. Buffam and Ireton⁴ and Clark and Cohen⁵ continued this work, extending it to

¹ Finger, Zeits. f. wiss. Photo., 7, 329 and 369 (1909).

² L. and E. Bloch, C. R. 174, 1456 (1922). Jour. de Phys. et Rad. (3), 6, 308 (1922).

³ Hulbert, Phys. Rev. (2), 24, 129 (1924).

⁴ Buffam and Ireton, Roy. Soc. Can. Trans. (3), 19, 113 (1925).

⁵ Clark and Cohen, Roy. Soc. Can. Trans. (3), 20, 1 (1926).

shorter wave-lengths and adding some elements not previously studied. The work of Clark and Cohen is devoted to the palladium-platinum group of metals.

The series relationships which have been recently worked out for a number of elements give a new meaning to such observations on line absorption. The recent work of Sur⁶ on iron, and of Stucklen⁷ on copper and cadmium suggests the importance of a more intensive study of some of the elements previously examined in order to obtain information concerning the correctness of the present assignment of the lines in spectral series and the arrangement of energy levels in the atom.

EXPERIMENTAL METHOD

The arrangement of the apparatus (Fig. 1) was similar to that used by Hulbert.³ The condenser *C* was charged by means of a 20 kv 2.5 kw Thor-darson transformer and then discharged through an auxilliary spark gap *S*

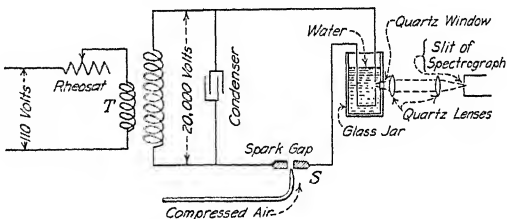


Fig. 1. Diagram of apparatus.

and the under-water spark in series. To insure an abrupt discharge compressed air was forced between the terminals of the auxilliary spark gap *S*. The primary of the transformer was connected to the 60-cycle, 110-volt-mains. The electrodes of the under-water spark were made of the metal whose absorption spectrum was being examined. Radiation from the under-water spark passed directly through the quartz window in the side of the glass jar and then through two quartz lenses by means of which it was brought to a focus on the slit of a Fery quartz spectrograph. The spectrum thus obtained was essentially continuous except for the absorption lines which belong to the arc spectrum of the metal from which the electrodes were made. Absorption lines due to the water were also observed and it is possible that a few absorption lines which do not belong to the arc spectrum of the metal may have been present.

For the ultra-violet region of the spectrum between about 2400 Å and 2100 Å distilled water was used in the jar. By refilling the jar with fresh distilled water several times during a single exposure it was possible under favorable conditions to photograph the spectrum as far as 2100 Å. For the region of the spectrum between the visible and about 2400 Å ordinary tap water was circulated rapidly through the jar. Care was taken to vary the

⁶ Sur, Phil. Mag. (7), 1, 433 (1926).

⁷ Stucklen, ZS. f. Phys., 30, 24 (1924); 34, 8 (1925).

conditions of excitation by varying the inductance and capacity to bring out the maximum number of absorption lines. The times of exposure ranged from a few seconds for the visible portions of the spectrum to several minutes for the extreme ultra-violet.

The wave-lengths of the absorption lines were determined by comparison with the wave-lengths of the emission lines in the spectrum of the copper arc which was always photographed on the same film as the absorption spectrum of the metal in the under-water spark. The distances of the absorption lines from each other and from the known lines in the emission spectrum of copper were measured with a travelling microscope and the unknown wave-lengths calculated in the usual manner. It was possible thus to identify the absorption lines with certainty.

EXPERIMENTAL RESULTS

Indium. The absorption of indium in the normal vapor is known from the work of Grotrian,⁸ Rao⁹ and Frayne and Smith.¹⁰ Its absorption has not been previously studied in the spectra of under-water sparks. The observed wave-lengths for which absorption occurs in the under-water spark are recorded in Table I. It is noticed that those lines are found which are to be

TABLE I
Absorption spectrum of indium.

$\nu = 2p_2 - ms$			$\nu = 2p_2 - md$			$\nu = 2p_1 - ms$			$\nu = 2p_1 - md_{1,2}$		
λ	m	Notes	λ	m	Notes	λ	m	Notes	λ	m	Notes
4101.72	2	1,2,3	3039.34	3	1,2,3	4511.27	2	1,2,3	3258.52*	3	1,2,3
2753.87	3	1,2,3	2560.16	4	1,2,3	2932.60	3	1,2,3	56.03*	3	1,2
2460.06	4	1,2,3	2389.56	5	1,2,3	2601.75	4	1,3	2713.95	4	1,2,3
						2468.01	5	1,3	10.28	4	1,2
						2399.25	6	1,3	2522.99*	5	1,2,3
									2521.36*	5	1,2
									2430.7	6	1,3
									29.68	6	1,4
									2379.66†	7	

* Lines unresolved but both seem to be present

² Rao in vapor

† New lines

³ Frayne and Smith in vapor

¹ Grotrian in vapor

⁴ Not found by authors in under-water spark.

expected from the series relationship and from previous observations on the absorption of light by the normal metallic vapor. A number of lines which have been previously observed as absorption lines in the vapor of indium were not found. These lines are with two exceptions in the far ultra-violet where the intensity of the spectrum from the under-water spark is too small for satisfactory observations. Besides these recorded lines two unclassified lines (λ 2957.02 and λ 2836.90) were observed. The recorded wave-lengths are those used by Fowler.¹¹

⁸ Grotrian, ZS. f. Phys., 12, 218 (1922).

⁹ Rao, Phys. Soc. Lond. Proc., 37, 259 (1924).

¹⁰ Frayne and Smith, Phys. Rev. (2), 27, 23 (1926).

¹¹ Fowler, Report on Series in Line Spectra, pp. 158-9.

Gallium. Because of the low melting point of gallium it was necessary to use it in the form of a gallium-tin alloy. The absorption spectrum of tin was first examined in the under-water spark. Then the absorption spectrum of the alloy of gallium and tin was studied. By the elimination of the absorption lines of tin from the spectrum of the alloy, the identification of the absorption lines of gallium was made possible. The absorption of the normal vapor of gallium is known from the work of Grotrian⁸ and Frayne and Smith.¹⁰ Table II shows the results. The recorded wave-lengths of gallium are those given by Klein.¹² For the shorter wave-lengths where the intensity of the under-water spectrum is small some wave-lengths previously observed as

TABLE II
Absorption spectrum of gallium

$\nu = 2p_2 - ms$ λ m Notes	$\nu = 2p_2 - md$ λ m Notes	$\nu = 2p_1 - ms$ λ m Notes	$\nu = 2p_1 - md_{1,2}$ λ m Notes
4032.98 2 1,2	2874.24 3 1,2	4172.06 2 1,2	2944.18* 3 1,2
2659.87 3 2	2450.08 4 2	2819.66 3 2	43.7* 3 1
2371.33 4 2	2294.20 5 2	2418.70 4 2	2500.71 4 2
2255.03 5 2	18.04 6 2	2297.87 5 2,3	2338.60 5 2
		36.10 6 2,3	2259.23 6 2,3

* Lines unresolved but both seem to be present ² Frayne and Smith in vapor

¹ Grotrian in vapor

³ Not found by authors in underwater spark.

absorption lines in the vapor were not located. This failure as in the similar case of indium is to be attributed to the faintness of the lines in that region of the spectrum. Except for this difference these observations confirm those made on absorption in the vapor.

Manganese. The electrodes were made of commercially pure manganese ground to suitable dimensions. The emission spectrum of manganese is known from the work of Catalan¹³ and Fuchs.¹⁴ In Table III these wave-

TABLE III
Absorption spectrum of manganese.

λ	Combination	Notes	λ	Combination	Notes
4032.49	$1^6S_3 - 1^6P_2$	1,2	2605.70	$1^7S_3 - 1^7P_2$	†
33.07	$1^6S_3 - 1^6P_3$	1,2	2593.72	$1^7S_3 - 1^7P_3$	†
30.76	$1^6S_3 - 1^6P_4$	1,2	2576.80	$1^7S_3 - 1^7P_4$	†
2801.08	$1^6S_3 - 2^6P_2$	1,2	2221.80	$1^6S_3 - 3^6P_2$	1
2798.27	$1^6S_3 - 2^6P_3$	1,2	13.80	$1^6S_3 - 3^6P_3$	1
2794.82	$1^6S_3 - 2^6P_4$	1,2	08.73	$1^6S_3 - 3^6P_4$	1

† New lines

¹ Zumstein in vapor

² Grotrian in vapor

lengths have been recorded out to two decimal places. The notation of the series classification has been modified to conform to modern usage. Table III

¹² Klein, *Astrophys. Jour.* 56, 373 (1922).

¹³ Catalan, *Phil. Trans. A*, 223, 127 (1922).

¹⁴ Fuchs, *ZS. f. wissenschaft. Phot.* 14, 263 (1914).

shows a comparison of the absorption of manganese in the under-water spark and its absorption in the vapor phase. Both Grotian¹⁵ and Zumstein¹⁶ have studied the line absorption of manganese in the vapor state. No previous observations on the absorption spectrum of manganese in under-water sparks are available. Grotian observed absorption at six wave-lengths as indicated in Table III. Zumstein found a large number of additional absorption lines but for the sake of brevity only a few of these have been included in Table III. Many of them have wave-lengths which are too short to come within the region of these observations.

It will be seen from Table III that the three prominent triplets which Zumstein found to be absorbed in the vapor are also absorbed in the under-water spark. In addition to these triplets there is found the triplet $^{17}S_3 - 1^7P_{2,3,4}$, which both Catalan and Back¹⁷ have attributed to singly ionized manganese. According to de Gramont¹⁸ these lines are *raies ultimes* in the spark spectrum of manganese. If these lines are correctly attributed to the singly ionized atom of manganese, they are the only absorption lines found in these observations on under-water absorption spectra which did not arise from the neutral atom. Stucklen⁷ seems to have found absorption by singly ionized cadmium in a under-water spark.

On account of the brittleness of the manganese the under-water spark did not behave as well as it did in the case of the other metals. This fact doubtless accounts for the failure to observe as many absorption lines for manganese in the under-water spark as were observed by Zumstein in the vapor.

Chromium. The wave-lengths in Table IV are from papers on the arc spectrum of chromium by Catalan¹⁹ and Gieseler.²⁰ The series combinations are taken either directly from Gieseler or when the multiplets are given only by Catalan his notation is changed to that of Gieseler in which the superscript at the left of the letter gives the multiplicity of the term and the subscript at the right of the letter gives the inner quantum number. The absorption of chromium vapor has been studied by Gieseler and Grotian²¹ and by Zumstein.²² Observations on the absorption spectra in the underwater sparks are available from the work of Finger¹ and Hulbert.³ Two prominent triplets have been found in the vapor and in the under-water spark. A third triplet further removed toward the ultra-violet was observed by Zumstein in chromium vapor. It is found here in the under-water spark spectrum. A large number of new absorption lines are also found. They are in agreement with the series combination given by Gieseler and Catalan. Besides these lines a number of unclassified lines were observed. These were distributed throughout the spectrum.

¹⁵ Grotian, ZS. f. Phys., **18**, 169 (1923).

¹⁶ Zumstein, Phys. Rev. (2), **26**, 765 (1925).

¹⁷ Back, ZS. f. Phys., **15**, 206 (1923).

¹⁸ de Gramont, C.R. **171**, 1106 (1920).

¹⁹ Catalan, Anales de Fisica Y Quimica, **21**, 84 (1923).

²⁰ Gieseler, ZS. f. Phys., **22**, 228 (1924).

²¹ Grotian and Gieseler, ZS. f. Phys., **22**, 245 (1924).

²² Zumstein, Phys. Rev. (2), **27**, 562 (1926).

TABLE IV
Absorption spectrum of chromium

λ	Combination	λ	Combination	λ	Combination	λ	Combination
4964.92	$4^5S_2 - 4a^5P_2$	3853.19	$4^5D_4 - 4b^5P_3$	3013.72	$4^5D_1 - 5a^5P_2$	2690.26	$4^5D_3 - 6^5F_2$
4829.36	—	31.03	$4^5D_3 - 4b^5P_2$	13.04	$4^5D_0 - 5a^5P_1$	84.72	$4^5D_4 - 6^5F_5$
4652.17	$4^5D_2 - 4a^5P_1$	22.08	$4^5D_3 - 4b^5P_3$	2996.58	$4^5D_2 - 2(\text{II})^5D_j$	84.31	$4^5D_2 - 6^5F_2$
51.30	$4^5D_2 - 4a^5P_1$	14.62	$4^5D_2 - 4b^5P_1$	95.79	$4^5S_1 - 5a^5P_1$	82.52	$4^5D_3 - 6a^5P_3$
26.19	$4^5D_1 - 4a^5P_1$	06.70	$4^5D_2 - 4b^5P_2$	94.07	$4^5S_1 - 5a^5P_2$	80.74	$4^5D_3 - 6^5F_4$
13.37	$4^5D_0 - 4a^5P_1$	3615.65	—	91.90	$4^5D_1 - 1(\text{II})^5D_j$	78.15	$4^5D_2 - 6^5F_3$
00.75	$4^5D_2 - 4a^5P_1$	05.33*	$4^7S_3 - 4a^7P_2$	88.67	$4^5S_2 - 5a^5P_3$	71.07	$4^5D_2 - 6a^5P_1$
4591.40	$4^5D_1 - 4a^5P_2$	3593.48*	$4^7S_3 - 4a^7P_3$	85.99	$4^5D_3 - 4(\text{II})^5D_j$	70.52	$4^5D_2 - 6a^5P_2$
80.06	$4^5S_2 - 4a^5P_1$	78.69*	$4^7S_3 - 4a^7P_4$	85.86	$4^5D_2 - 3(\text{II})^5D_j$	69.38	$4^5D_2 - 6a^5P_3$
65.53	—	10.53	—	80.79	$4^5D_0 - 2(\text{II})^5D_j$	62.78	$4^5D_1 - 6a^5P_1$
46.04	$4^5S_1 - 4a^5P_2$	3494.96	—	75.48	$4^5D_1 - 3(\text{II})^5D_j$	62.21	$4^5D_1 - 6a^5P_2$
14.53	—	81.30	—	71.11	$4^5D_2 - 4(\text{II})^5D_j$	58.52	$4^5D_0 - 6a^5P_1$
4496.86	$4^5S_1 - 4a^5P_3$	60.43	—	67.64	$4^5D_3 - 5(\text{II})^5D_j$	38.90	—
29.45	$4^5D_4 - 4^5F_1$	3266.55	$4^5D_4 - 5^5P_j$	11.14	$4^5D_4 - 4(\text{III})^5D_j$	18.28	—
4391.76	$4^5D_3 - 4^5F_2$	44.14	$4^5D_3 - 5^5D_j$	10.90	$4^5D_4 - 5(\text{III})^5D_j$	2591.86	$4^5D_4 - n^5P_i$
84.98	$4^5D_4 - 4^5F_4$	3065.07	—	05.49	$4^5D_1 - 1(\text{III})^5D_j$	77.66	$4^5D_3 - n^5P_i$
73.27	$4^5D_2 - 4^5F_1$	53.88	$4^5D_4 - 5a^5P_2$	2899.21	$4^5D_1 - 2(\text{III})^5D_j$	71.76	$4^5D_3 - n^5P_i$
71.28	$4^5D_3 - 4^5F_3$	37.05	$4^5D_4 - 5^5F_4$	93.26	$4^5D_3 - 4(\text{III})^5D_j$	66.55	$4^5D_1 - n^5P_i$
51.78	$4^5D_4 - 4^5F_5$	34.19	$4^5D_3 - 5a^5P_3$	89.26	$4^5D_4 - 5(\text{III})^5D_j$	60.71	$4^5D_2 - n^5P_i$
44.51	$4^5D_5 - 4^5F_4$	30.25	$4^5D_3 - 5^5F_3$	86.99	$4^5D_1 - 3(\text{III})^5D_j$	57.14	$4^5D_3 - n^5P_1$
39.72	$4^5D_6 - 4^5F_1$	29.17	$4^5D_2 - 5a^5P_1$	79.27	$4^5D_2 - 4(\text{III})^5D_j$	53.05	$4^5D_1 - n^5P_i$
37.56	$4^5D_1 - 4^5F_2$	24.36	$4^5D_2 - 5a^5P_2$	71.64	$4^5D_3 - 5(\text{III})^5D_j$	49.51	$4^5D_1 - n^5P_i$
4289.73*	$4^7S_3 - 4^7P_2$	21.57	$4^5D_4 - 5^5F_5$	2780.69	$4^5D_1 - nb^5P_3$	45.63	$4^5D_0 - n^5P_1$
74.80*	$4^7S_3 - 4^7P_2$	20.67	$4^5D_1 - 5^5F_1$	69.91	$4^5D_3 - nb^5P_2$	44.71	$4^5S_1 - nc^5P_i$
54.34	$4^7S_1 - 4^7P_4$	18.83	$4^5D_2 - 5a^5P_3$	66.54	—	38.97	$4^5S_1 - nc^5P_i$
3991.12	—	18.50	$4^5D_1 - 5a^5P_1$	64.35	$4^5D_2 - nb^5P_3$	35.27	$4^5S_2 - nc^5P_i$
33.91	—	15.20	$4^5D_0 - 5a^5F_1$	61.75	$4^5D_2 - nb^5P_1$	2366.85†	$4^7S_3 - 5^7P_2$
41.59	$4^5D_4 - 4(\text{I})^5D_j$	14.93	$4^5D_2 - 5^5F_2$	57.10	$4^5D_2 - nb^5P_2$	65.16†	$4^7S_3 - 5^7P_3$
28.64	$4^5D_4 - 3(\text{I})^5D_j$	14.77	$4^5D_1 - 5^5F_2$	52.87	$4^5D_1 - nb^5P_1$	64.74†	$4^7S_3 - 5^7P_4$
				48.29	$4^5D_1 - nb^5P_2$		

Bracketed lines are unresolved but both seem to be present.

* Observed by Hulbert in under-water spark, by Finger in under-water spark, Gieseiler and Grotrian in vapor, by Zumstein in vapor.

† Observed by Zumstein in vapor.

Nickel. Finger¹ as well as Buffam and Ireton⁴ has studied the under-water absorption spectrum of nickel. Angerer and Joos²³ have made observations on the line absorption of his element in the vapor phase. Table V shows the absorption lines observed in this investigation. The wave-lengths are those used by Bechert and Sommer²⁴ in their analysis of the nickel spectrum. It is to be noted that many new lines have been observed. These lines as well as those which have been previously observed are in agreement

²³ Angerer and Joos, Ann. d. Phys. 74, 743 (1924).

²⁴ Bechert and Sommer, Ann. d. Phys. 77, 351 and 537 (1925).

TABLE V
Absorption spectrum of nickel.

λ	Notes										
4466.54*	†	3571.87	1	3369.58	3	3057.65	1,2	2437.82*	†	2321.96	†
4202.33*	†	66.37	1,2	66.16	1	54.32	1,2	34.43	†	21.39	†
4074.89	†	61.75	†	65.77	1	50.83	1,2	24.03	†	20.03	†
10.14*	†	27.99	†	61.56	1	45.01	†	23.33	†	17.16	3
3973.55	†	24.54	1,2,3	22.32	1	37.94	1,2	21.33	†	13.98	3
72.16	†	23.44	†	20.26	1	31.87	1	19.31	†	12.34	2,3
3858.28	1	19.78	1	15.67	1,2	19.15	1	12.67	2	10.96	3
32.87	†	15.06	1,3	3282.70	†	12.01	1,2	10.68*	†	07.35	†
31.69	†	13.95	†	71.12	†	03.63	1,2	06.82*	†	06.45*	†
07.14	1	10.34	1	48.43	1	02.49	1,2	01.85	†	01.57	†
3793.60	†	07.70	†	43.06	1	2994.46	1	2396.39	2	00.77	†
92.33	†	00.85	1	34.66	1	92.60	1	94.50*	2	2298.23*	†
83.52	†	3492.97	1,2,3	32.95	1,2	84.13	1	93.12	†	96.54*	2
75.56	†	83.78	1	25.03	1	81.65	1	87.56	2	93.11	†
72.52	†	72.55	1	21.66	1	43.92	1	86.59	†	89.98	†
36.81	†	69.48	1	3197.12	1	14.01	1	84.40	†	88.39	†
22.48	†	61.66	1,2,3	95.58	†	07.46	†	76.02	†	87.32	†
3693.93	†	58.47	1,3	59.52	†	2865.51	†	69.22*	†	74.65	†
88.41	†	52.89	1,3	45.71	{	34.55	†	65.68	†	71.94	†
74.11	†	46.26	1,3	45.12	{	21.30	†	62.06	2	67.55	†
70.42	†	37.28	1	34.11	1,2	2798.65	†	60.64	†	61.41	†
64.09	†	33.57	1,3	29.31	†	46.75	†	58.87	†	59.45*	†
61.94	†	23.71	1	16.84*	†	2561.43	†	56.87	†	58.13	2
3649.63*	†	14.77	1,3	14.13	1	53.38	†	55.06	†	53.97*	†
34.94	†	13.94	{ 1	05.47	1	47.42	†	48.74	†	53.55	2
24.73	†	13.48	{ 1	01.88	{ 1,2	24.22	†	47.53	3	51.47	†
19.39	1	09.48	†	01.56	{ 1,4	2489.51	†	46.64	†	47.31*	2
12.73	1	3392.99	1,2	3099.12	1	84.04	†	45.55	†	13.29*	†
10.45	1	91.05	1	97.12	1	76.88	†	38.50	†	11.16*	2
09.31	1	85.34*	†	87.06*	1	72.24	†	37.49	3	06.80*	†
02.28	†	80.89	{ 1	80.76	{ 1,2	66.97	†	34.57*	2	01.55*	2
3597.70	1	80.58	{ 1	75.85*	†	54.00	†	31.70	3	2191.04*	2
87.93	†	74.23	1	66.43*	†	50.48	†	2326.43*	†	84.70*	2
77.21	†	71.99	1	64.63	†	41.83	†	25.80	{ 2,3	84.42*	†
										75.22*	2

Bracketed lines are unresolved but both seem to be present.

* Not classified by Bechert and Sommer. † New lines. 1. Finger in under-water spark. 2. Buffam and Ireton in under-water spark. 3. Angerer and Joos in vapor.

with the analysis of the spectrum as given by Bechert and Sommer. In addition to these classified lines a number of unclassified lines were found.

Cobalt. Table VI gives the results for cobalt together with the series classification as given by Catalan and Bechert.²⁵ The wave-lengths are

²⁵ Catalan and Bechert, ZS. f. Phys., 32, 336 (1925).

those given by Dhein.²⁶ They are recorded only to two decimal places. Observations on the absorption spectrum of cobalt in under-water sparks have been previously made by Finger,¹ and also by Buffam and Ireton.⁴ Both Angerer and Joos and Sur and Majumdar²⁷ have examined the absorption of this element in the vapor state. Except for minor departures the results of the present investigation confirm the earlier observations

TABLE VI
Absorption spectrum of cobalt.

λ	Notes	λ	Notes	λ	Notes	λ	Notes	λ	Notes	λ	Notes
4339.64*	†	05.37	†	33.04	1,2,4	62.20	†	2572.24*	2	65.04	3
20.37*	†	02.08	1,4	31.58	1	3061.83	1,4	67.33	†	2363.53*	2
03.24	†	3594.87	1,4	17.80	†	54.72		59.41*	2	58.21	†
4285.79	†	87.19	1,2	17.16	1	54.14	†	55.06	†	55.50	3
68.03	†	85.16	1,4	15.53	1	48.89	1,4	53.35	2	54.83*	4
52.30	†	84.80	4	14.74	†	44.01	1,2,3,4	53.00		53.43	3
34.00	†	79.03*	†	12.64	1,2,3,4	42.48	†	44.25	3,4	50.78*	2
4190.71	4	75.36	†	12.34	1,4	34.43	2,4	41.95*	2	46.58*	†
50.44	†	74.96		3409.18	1,4	17.55	2	38.78	†	46.18	3
21.33	1,2	69.38	†	05.12	1,2,3,4	13.60	†	35.93	3	45.05*	3
10.54	†	64.96	1,4	02.07*	†	05.77*	2	28.98	3,4	44.29	†
4092.40	†	60.90	1,4	3395.38	1,2,4	00.55	†	25.57*	2	35.98	3
76.13	4	58.78	†	90.80*	†	2989.60	1	21.40	3	29.15*	†
45.40	†	52.72	†	88.18	†	87.17	1,2,4	17.81	†	24.80*	†
20.90	†	50.60	†	85.23	1,4	29.52*	2	11.03	2	23.18	3
3997.91	2,4	42.98	†	83.92*	†	11.56	†	06.92*	†	21.26*	†
95.31	1,4	33.36	1,4	77.06*	†	2895.48*	†	00.51	2	19.27	†
87.12	†	29.82	1,3,4	70.33	2	86.45	†	2495.56	†	15.95*	†
65.24		29.04	1,4	67.11	†	50.96	2	76.64		13.71*	†
65.02		26.86	1,3,4	54.39	1,2,4	42.39*	4	76.43		11.65	2,3
57.94	†	23.44	1,4	46.94*	†	34.43*	†	73.92	†	09.03	†
52.92	†	21.74		34.15	1,4	33.93*	4	70.28*	†	04.22	†
35.97	†	21.57	1,4	33.39	†	20.00	†	67.71	†	2299.73*	†
33.92	2	20.09	1,4	25.24*	†	14.98	4	64.21*	†	96.25*	†
22.76	†	18.35	1,2,4	19.48*	†	11.53*	2	60.81	†	95.30*	3
3894.98	1,4	13.48	1,4	18.40*	†	2803.78	2	41.04*	†	93.05*	3
94.09	1	12.64	1,4	07.15*	†	2796.24	†	2439.03	3	2292.05*	†
3885.28		10.42	1,2,3,4	79.25*	†	74.96	†	36.77	3	90.35	†
84.61	†	09.84	1,4	65.35		64.19	†	32.20	3	88.84*	†
3873.96	1,4	06.32	1,3,4	64.84	†	52.07*	†	27.00*	†	87.86	3
73.12	1,4	02.62	1	49.99	4	45.11*	†	24.98	3,4	86.25*	2,3
45.47	1,2,4	02.28	1,2,3,4	47.18*	1,2,4	15.99*	†	23.63*	2	83.09*	†

²⁶ Dhein, ZS. wiss. Photo., 19, 289 (1920).

²⁷ Sur and Majumdar, Phil. Mag. (7), 1, 451 (1926).

TABLE VI (continued)

λ	Notes	λ	Notes	λ	Notes	λ	Notes	λ	Notes
42.06	1,4	3496.69	1	43.84*	†	05.86*	†	22.57*	2
41.46	†	95.69	1,4	37.03	†	2695.58	†	19.13*	†
11.07	†	91.32	1,4	3186.35	†	94.68*	2	15.32	3
08.11	†	90.74	4	74.91	†..	85.34	2	14.47	3
01.23*	†	89.41	1,4	59.66	4	80.11*	†	12.88*	3
3745.50	4	85.71*	†	58.77	4	75.99	2	11.65	3
04.06	2	83.42	1,4	54.79*	2	63.53*	4	08.74*	†
3693.48	†	76.37*	2	49.30	†	50.27	2,4	07.27	3,4
		93.12	1,3,4	47.06	4	48.65	2	02.12	3
90.72*	†	65.80	1,2,3,4	39.94	2	46.42	†	2396.24*	†
77.98	†	62.81	1,4	37.33	4	29.98*	2	91.99	3
56.97	†	60.73	†	21.56	2,4	23.45	†	89.58*	†
52.54	†	55.24	1	21.41	2,4	22.43	†	84.89	3
47.66	4	53.51	1,2,3,4	03.99	†	22.25	†	83.45*	2
31.34	1,4	49.44	1,3,4	86.78	†	2590.61*	†	80.52	3
27.81	4	49.17	1,4	82.61	2	80.84*	2	78.62*	†
24.96	4	43.65	1,4	72.35	1,4	78.93*	†	73.40*	†
18.01	†	42.92	1,2	71.95	†	74.36	2,4	71.76*	†
15.39*	†	36.97*	†	64.38	2,4			71.40*	†
									2181.12*

Bracketed lines not clearly resolved, though both seem to be present.

* Not classified by Catalan and Bechert. † New lines. 1. Finger in under-water spark. 2. Buffam and Ireton in under-water spark. 3. Angerer and Joos in vapor. 4. Sur and Majundar in vapor.

whether the absorption was obtained by means of the under-water spark or by means of the vapor of the metal. However, many lines not previously reported have been located and a more adequate confirmation of the series classification of Catalan and Bechert has thus been obtained. A number of new unclassified lines was observed and the presence of other unclassified lines confirmed.

DISCUSSION OF RESULTS

Indium and Gallium. The absorption lines found in the under-water spark spectra of indium and gallium confirm the results obtained from a study of the absorption by vapors of indium and gallium and in agreement with these results indicate that the normal state of the valence electron in both of these atoms is the $2p$ state.

Manganese. The three prominent triplets characteristic of the absorption of manganese vapor have been found in the under-water spark spectrum of this element. The fact that all these triplets originate from the $1s$ sextet level, shows that this term represents the normal state of the valence electron. A fourth triplet, ordinarily attributed to singly ionized manganese, has also been located.

Chromium. A large number of absorption lines not previously reported have been located in the under-water spark spectrum of chromium. These

lines give a rather complete verification of the arrangement of the energy levels in the chromium atom, above the ground $4S$ septet level. Not only were the three triplets arising from this term absorbed, but also almost all the classified multiplets whose final levels on emission, the quintet $4S$ and $4D$ terms, lie nearest the $4S$ septet level. The fact that the multiplets $4S$ originating from the $4S$ and $4D$ levels were absorbed, and those from other terms, such as the P -terms, were not absorbed, must be interpreted as showing the correctness of the assignment of the $4S$ and $4D$ levels as the next lowest to the $4^7 S$ level.

Nickel. In both nickel and cobalt more than a hundred lines were found which have not previously been observed in absorption. In each of these metals there is a group of terms relatively near the lowest or ground term. In nickel, according to the classification and notation of Bechert and Sommer the ground triplet term f_4^1 is followed successively by the triplet terms \bar{d}_3^1 , \bar{d}_2^1 , f_3^1 , \bar{d}_1^1 and f_2^1 and the singlet \bar{D}_2^1 which is separated by 0.4 volt from the term f_4^1 . Since the singlet term \bar{D}_2^2 which immediately follows the \bar{D}_2^1 term is separated by 1.6 volts from the f_4^1 term, it would be expected that in the under-water spark the absorption lines would start from the f^1 , \bar{d}^1 , and \bar{D}_2^1 levels. The absorption lines as recorded in Table V start from these levels. Furthermore this table includes nearly all the lines of appreciable intensity which, according to the classification of Bechert and Sommer, originate from these levels. Hence these results seem to strongly confirm their assignment of terms and levels for nickel.

Cobalt. In cobalt above the ground term f_5^1 there are, in the notation of Bechert and Sommer, successively the quartet terms f_4^1 , f_3^1 , f_2^1 , f_5^2 , f_4^2 , f_3^2 and f_2^2 and the doublet terms F_4^1 and F_3^1 . The greatest separation to these terms from the ground level f_5^1 is about one volt but the p_8^1 term which is immediately above the F_3^1 term is separated by about 1.6 volts from the f_5^1 term. Hence the absorption lines to be expected on the basis of this classification should start from the f^1 or the F^1 levels. Because of the much greater separation of the p^1 levels from the f^1 levels, the lines which start from the p^1 levels are not to be expected. Almost every line of appreciable intensity Table VI corresponding to an initial level of f_4^1 , f_3^1 , f_2^1 , f_5^2 , f_4^2 , f_3^2 and f_2^2 has actually been observed as an absorption line in the under-water spark. This fact gives a verification of the correctness of the term assignment of these lines and the arrangement of terms with respect to the ground level as given by Catlan and Bechert.

MENDENHALL LABORATORY,
OHIO STATE UNIVERSITY.

NOTE. Since the above was written a paper by Majumdar on the absorption spectrum of nickel appeared in *Zeit. f. Physik*, 39, 562 (1926). On the basis of about one-half as many lines as are recorded in Table V, he concludes that there is not sufficient data available to determine the ground level of the nickel atom. At the Annual Meeting of the American Physical Society, Dec. 28-30, 1926, Meggers and Walters reported on the absorption spectra of iron, nickel and cobalt in under-water sparks. (*Phys. Rev.* (2) 29, 358, 1927.)

STAGES IN THE EXCITATION OF THE SPECTRUM OF INDIUM

BY JOHN G. FRAYNE AND CHARLES W. JARVIS

ABSTRACT

The indium metal was vaporized at a temperature of 650°C in an iron cylindrical anode within a quartz tube. Electrons from an oxide-coated Pt filament passed through a helical grid into a force-free space where they collided with the atoms of indium vapor. The spectrum was viewed end-on through a transparent quartz window. At 3.3 volts the lines $2p_1 - 2s$ and $2p_2 - 2s$ appeared. At 4.2 volts the additional lines $2p_1 - 3d$ and $2p_2 - 3d$ appeared. At seven volts higher members of the series and several unclassified lines were present on the plates. At 13.2 volts the spectrum became very strong and the line 2306A appeared in addition to the recognized series lines. It is possible that the second arc spectrum was excited at this potential. The resonance lines were found to be less intense than the corresponding lines due to the metastable atoms.

INTRODUCTION

THE element indium is one of four members of the aluminum sub-group of Group III in the Periodic Table. The arc spectra of this group are characterised by series of well defined doublets and by the absence of the principal series found in the alkalis and alkali earths. Comparatively little research has been done on the spectra of this group. Mohler and Ruark¹ have studied the excitation by stages of the arc spectrum of thallium. Absorption spectra studies for thallium, indium and gallium have been made by Grotrian,² and also by Frayne and Smith.³ Electrical resonance and ionization measurements on indium and gallium vapors have been made by Jarvis.⁴ The indium used in this investigation was obtained from Mr. F. G. McCutcheon, Bartlesville, Oklahoma. Although some impurities were present it was found quite satisfactory at the temperatures employed.

EXPERIMENTAL PROCEDURE

On account of the high boiling point of indium it is necessary to heat the metal to a temperature of 650–700°C before the vapor pressure is sufficient to show any spectral lines on a photographic plate when bombarded with fourteen volt electrons for a period of five or six hours. This necessitated the use of quartz or porcelain tubing. In Fig. 1, *D* is a transparent quartz tube with an optically plane quartz window *E*. *A* is a cylindrical iron anode to which the nickel grid helix *B* is welded. The open end of the quartz tube was fitted with an iron cap *C* which was sealed vacuum tight with de Khotinsky cement and water cooled. The filament leads were brought out through a glass tube *H* which was cemented to the metal cap *C*. The indium metal

¹ Mohler and Ruark, J.O.S.A. 7, 819 (1923).

² Grotrian, Zeits. f. Physik, 12, 218 (1922) and 18, 169 (1923).

³ Frayne and Smith, Phys. Rev. 27, 23 (1926).

⁴ Jarvis, Phys. Rev. 29, 442 (1927).

was placed in the anode *A* and heat was applied by the electric furnace *F*. As the temperature was raised the indium metal tended to deposit on the quartz window and cloud it. This difficulty was overcome by placing the window in the hottest portion of the furnace. With this arrangement the tube could be operated for about ten days before any deposition was noticed.

The indium vapor proved to be very active chemically at 700°C. It combined with fine filaments of tungsten, molybdenum or platinum and with

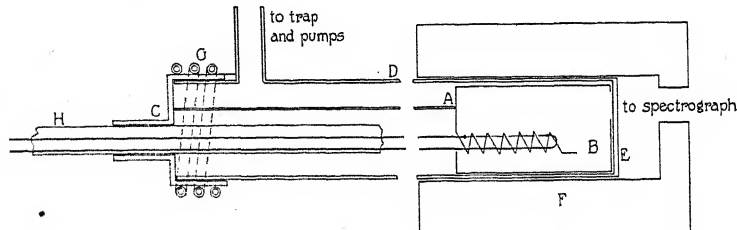


Fig. 1.

fine platinum strip. A 15 mil platinum oxide coated filament was found satisfactory, usually lasting about 120 hours. Electrons from this filament were accelerated through the nickel helix *B* into the force-free space between grid and anode where they collided with the atoms of the indium vapor. The resulting emission of spectral lines was viewed ~~electron~~, ⁱⁿ through the opening in the anode. A Hilger E3 quartz spectograph ^{were} used throughout.

EXPERIMENTAL RESULTS

The spectrum lines appearing at different anode voltages are given in Table I. It will be noticed that the first resonance line $2p_1 - 2s$ and the

TABLE I
Indium spectrum produced by electronic excitation.

Notation	3.3 v.	4.2 v.	6.9 v.	13.2 v.
$2p_1 - 2s$	4511.31 <i>A</i>	4511.31	4511.31	4511.31
$2p_2 - 2s$	4101.76	4101.76	4101.76	4101.76
$2p_1 - 3d$		3258.56	3258.56	3258.56
		3039.35	†3051.19	3051.19
$2p_2 - 3d$			3039.35	3039.35
			*2957.01	2957.01
$2p_1 - 3s$			2932.63	2932.63
			‡2858.30	2858.30
			*2836.91	2836.91
$2p_2 - 3s$			*2775.35	2775.35
$2p_1 - 4d$			2753.88	2753.88
$2p_1 - 4s$				2710.26
$2p_2 - 4d$				2601.75
$2p_1 - 5d$				2560.15
				2523.08
				‡*2306.07

* Listed as unclassified lines in the arc by Uhler and Tanch.

† Listed as an arc line by Kayser and Runge.

‡ Listed as a spark line by Exner and Haschek.

line of the metastable atom $2p_1 - 2s$ appear at the lowest voltage. The emission current was 0.3 m.a. and the time of exposure was 40 hours. At 4.2 volts the corresponding pair of lines resulting from transitions to the $3d$ level appeared in addition to the previous two lines. The current at this potential was about 0.6 m.a. and the exposure was for 24 hours. At 6.9 volts some higher members of the series appeared as well as several unclassified arc lines. Four of the latter are listed by Uhler and Tanch as arc lines. The line 3051A is given as a spark line by Exner and Haschek. The current at this potential was about 1.5 m.a. and the exposure lasted 14 hours. At 13.2 volts the arc became very brilliant the whole space between grid and anode being filled with a bluish-violet color. Up to this point the illumination was too weak to be observed by the eye. An exposure of three hours was found sufficient at this potential. A strong unclassified line 2306A appeared there. Several lines in the visible and near ultra-violet appeared here also, but they have been all traced to oxygen and other gaseous impurities.

DISCUSSION

It was found that the intensity of the lines $2p_1 - 2s$ and $2p_1 - 3d$ were consistently stronger than $2p_2 - 2s$ and $2p_2 - 3d$. This was especially notable at the lower voltages. Mohler and Ruark¹ found a similar occurrence with thallium lines and attributed it to the fact that the resonance radiation was partially absorbed in the cool vapor above the furnace. Here, however, there was no column of cool vapor in the path of the light. Further, Frayne and Smith³ have shown that at this temperature the $2p_1 - 2s$ is just as prominently absorbed as the $2p_2 - 2s$ line. This seems to indicate the return of atoms from the $2s$ or $3d$ levels to the $2p_1$ is more probable than to the $2p_2$ level. However, the work of Jarvis⁴ by electrical method used for determination of resonance potentials indicated sharper and stronger current voltage breaks for the transition $2p_2 - 2s$. Since absorption spectra show that many indium atoms are in the metastable state at 700°C the valence electron may be ejected directly from the $2p_1$ directly to the $2s$ level. If all of these should return to the $2p_1$ in addition to others ejected to the $2s$ from the $2p_2$ state one can see that the $2p_1 - 2s$ line might be much more intense than the corresponding resonance line.

The entire arc spectrum should appear at 6.9 volts. It was found that several unclassified lines appeared at this potential. It is difficult to believe that these lines belong to the so-called second arc spectrum, being produced by multiple excitation. The small electron current, 1.4 m.a., makes this rather improbable. If these are bona fide arc lines the energy level diagram for indium must be much more complicated than one representing only the well known p , s and d levels. All attempts to prove these to be combination lines have been futile.

At 13.2 volts there was evidence of strong ionization. The electron current increased very rapidly at this stage and the glow in the tube was very noticeable. It is possible that two electrons were removed at this potential and the resulting spectrum might be considered as a second arc. Undoubtedly

many lines in these spectrum must lie in the far ultra-violet and, of course, could not be observed with an ordinary spectrograph. It is quite possible that the line 2306A may correspond to the 1855A line in the Aluminum spectrum.

ANTIOCH COLLEGE,
YELLOW SPRINGS, O. (J.G.F.)
OHIO WESLEYAN UNIVERSITY,
DELaware, O. (C.W.J.)
February 1, 1927.

SECONDARY RADIATION AND POLARIZATION OF RESONANCE RADIATION IN CADMIUM

By WALTER A. MACNAIR

Secondary radiation in cadmium vapor containing mercury as an impurity.—Attention is called to the points of difference between the conditions under which the two types of optically excited spectra of mercury vapor appear, namely resonance radiation and fluorescence. In the present experiments it is noted that when a bulb containing cadmium with a slight impurity of mercury is illuminated by light of 2288A wave-length the secondary radiation contains the mercury line 2536.7A in addition to the cadmium lines 2288A and 3261A provided the metal is distilling. As soon as the vapor is stagnant, however, only the cadmium 2288A line appears. The suggestion is made that the phenomenon is due to the presence in the distilling vapor of unstable HgCd molecules. In such a molecule the Cd atom may absorb the 2288A radiation and subsequently in the breakdown of the molecule may excite the Hg atom by a collision of the second kind.

Polarization of the cadmium resonance, radiation in zero magnetic field.—The polarization of the cadmium resonance radiation (3261A) in zero magnetic field under certain conditions was found to be 35 percent. In order to explain this value by the kinetic theory, one must assign effective radii to the colliding atoms which are thirty times the radii effective in ordinary collisions.

HERE are two types of emissions from optically excited mercury vapor: the first appropriately termed "resonance radiation" by Professor R. W. Wood; the second, a bluish-green fluorescence. The names of Hartley, Wood, Steubing, Phillips, Van der Lingen and Wood, and Terenin¹ are associated with the study of the latter type. Van der Lingen and Wood concluded from one of these experiments, "However we interpret the results of the experiment, the fact is definitely established that only freshly formed mercury vapor is capable of exhibiting fluorescence." Professor Wood's explanation of the phenomenon, that is, that more diatomic molecules are evaporated into the vapor during active distillation than when the system is in equilibrium, has explained all the observations made up to the present time, although Pringsheim says that the explanation can hardly be brought into accord with thermodynamics.²

A similar phenomenon takes place in cadmium as shown by Terenin³ who found that cadmium vapor at 150°C illuminated with radiation of 2288A emitted this radiation alone only when the vapor was in the stagnant condition and that when weak distillation of the cadmium was induced by cooling a spot on the tube the vapor emitted not only $\lambda 2288$ but also $\lambda 3261$. A source which is not good for exciting resonance radiation, that is, a source

¹ Hartley, Proc. Roy. Soc. **76**, 428 (1905); Wood, Phil. Mag. **18**, 240 (1909); Steubing, Phys. Zeits. **10**, 787 (1909); Phillips, Proc. Roy. Soc. **89**, 39 (1914); Van der Lingen and Wood, Astrophys. Jour. **54**, 149 (1921); Terenin, Zeits. f. Physik, **31**, 26 (1925).

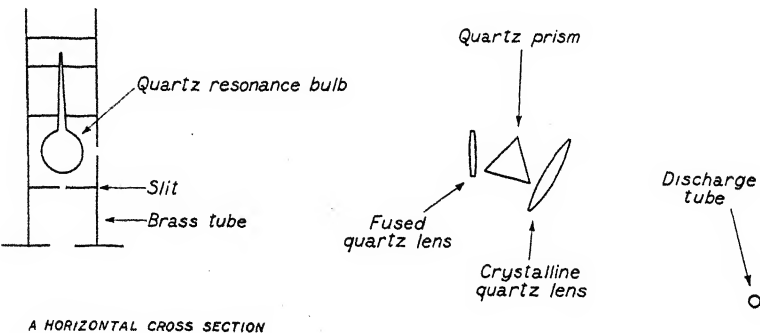
² Pringsheim, Fluorescenz und Phosphorescenz, p. 81.

³ Terenin, Reference 1.

in which the 2288 line is partially reversed, may be used to excite the distilling vapor in the above manner. The explanation given is similar to Professor R. W. Wood's explanation for the fluorescence in mercury vapor, which we have referred to. It is that diatomic molecules are evaporated from the surface of the metal during distillation in sufficient quantity to absorb an appreciable amount of radiation of 2288A wave-length. Some of these molecules then split apart after which one atom is in an excited state ready to emit $\lambda 3261$ and the other one is in the normal state. These cadmium molecules are known to be very loosely bound and unstable which results in the fact that the molecular absorption bands surround the atomic absorption lines, thus permitting the light outside of the center of the 2288 line to be effective in the above experiment.

The fact that the 3261 line does not appear in the secondary radiation of stagnant vapor illuminated with light of 2288A wave-length under the conditions of the experiment mentioned above means, of course, that collisions of the second kind are too few to excite normal atoms to the $2P$ state. At 200°C the effect of such collisions is apparent.

During some observations preliminary to work on the polarization of resonance radiation in cadmium, another peculiarity of distilling vapor as



A HORIZONTAL CROSS SECTION

Fig. 1. Arrangement of apparatus.

contrasted with stagnant vapor was observed. Several variations of the disposition of apparatus described hereafter were actually used from time to time, but Fig. 1 shows an appropriate set-up which is the one that was finally employed. The source of light, which excited the secondary radiation in the bulb, consisted of a straight Pyrex discharge tube having large aluminum foil electrodes at the ends and a quartz capillary in the middle. Hydrogen was streamed through the tube at 0.04 mm mercury pressure, sweeping out the cadmium vapor which was distilled over from a side tube by placing the central portion of the tube in a furnace heated to about 200°C . The discharge tube was driven by a large 7000 volt transformer carrying about 15 amperes at 110 volts through the primary. Such a source of light is suitable for exciting resonance radiation. The quartz lenses focused the images of the discharge in the capillary on the brass tube, and with the aid of a fluorescing screen any desired wave length could be passed through the

opening in the side of the tube and into the quartz bulb. The secondary radiation in the vapor was observed at right angles to the primary beam and through the slit indicated, which served as the slit for the analyzing spectroscope. The temperature of the bulb and stem were read by thermometers placed in contact with the quartz, the former being kept thirty or forty degrees above the latter by heating the brass tube underneath the bulb with a Bunsen burner.

The quartz bulb containing the cadmium remained evacuated on the vacuum system several days before it was sealed off and used.

A characteristic observation results when the bulb containing a little cadmium having a slight impurity of mercury is heated to 170°C and the stem kept at 140°C. If the bulb is now illuminated with light of 2288A wavelength, the secondary radiation consists of 2288A, 3261A, and 2536 (Hg, $1S - 2^3P_1$) as long as the metal is distilling from the bulb into the cooler stem, but just as soon as it has all left the bulb then only light of 2288A appears in the secondary radiation. The same thing has been observed with the bulb at 120°C and the stem somewhat cooler.

The appearance of the mercury line may be due to, (1) scattered $\lambda 2536$ light from the source which contained mercury as an impurity, (2) collisions of the second kind between excited cadmium atoms or molecules and normal mercury atoms or molecules, (3) the evaporation from the metallic surface of HgCd molecules by a process outlined hereafter. Precautions were taken to prevent any light of 2536A entering the bulb.

The possibility that the appearance of the mercury line in the secondary resonance radiation can be explained by collisions seems to be excluded immediately because the pressure of the stagnant vapor in which the mercury line is not apparent is comparable with that of the distilling vapor in which it does appear. It must be stated, however, that since the bulb and stem were not in temperature equilibrium there may be some doubt as to the relative vapor pressures during and after distillation. Another possibility would occur if the Hg₂ molecules and the Cd₂ molecules evaporated from the surface have very large effective radii in collision.

If one assumes that loosely bound unstable molecules, made up of one mercury atom and one cadmium atom, are evaporated from the metal surface, the transfer of energy may be accounted for in the following manner. The molecule absorbs a quantum of energy of 2288A radiation and stores it by an electron jump in the cadmium atom; then in the breakdown of the molecule the disturbance in the mercury atom due to its partner, the excited cadmium atom, is comparable to a collision of the second kind which results in a normal cadmium atom and an excited mercury atom, plus a certain amount of kinetic energy.

There is independent evidence that HgCd molecules are formed when there is mercury present with the cadmium and that these molecules are capable of absorbing energy from the radiation of a cadmium arc. The absorption of pure and mercury contaminated cadmium vapor, under conditions which did not prevent distillation, has been studied by Wood and

Guthrie⁴ who found decided differences in the absorption in the two cases. The most striking difference occurs exactly in the region in which we are most interested, namely, near 2288A. Pure cadmium vapor in a quartz bulb which is heated slowly, first reverses the 2288 line of a cadmium spark source in the center, the absorption line spreading with heating into a band symmetrical about the line. If mercury is present, however, the emission line of the source first reverses on the long wave length side and the absorption band spreads on the long wave length side with the rise in temperature of the bulb to 2307A before the 2288A line entirely disappears.

The mercury impurity was present in the cadmium in very small quantity and very intimately associated with it. The bulb had to be heated to 100°C before enough mercury vapor was present to show 2536A resonance radiation when excited by the unreversed 2536 line.

The quartz prism used as a dispersing piece between the source of light and resonance bulb, gave two images of the quartz capillary for each wavelength appearing in the discharge, one polarized horizontally and one vertically, separated sufficiently so that either one or the other could be focused on the opening in the side of the brass tube. Focusing the vertically polarized (electric vector vertical) 3261A beam so that it illuminated the stagnant vapor in the bulb which was at 252°C, the stem being at 212°C and photographing the cone of resonance radiation through a quartz Wollaston prism with pairs of varying relative exposure times until the weaker image in the longer exposure was of density equal to the stronger image in the shorter exposure it turned out that the resonance radiation was 35 percent polarized in a vertical direction when the bulb was in zero magnetic field. (The earth's field was neutralized to 0.02 gauss by a Hemhotz coil.) Under these conditions a spectroscopic analysis of the resonance radiation revealed, of course, secondary radiation of 3261A only.

It is generally assumed in accordance with Heisenberg's theory that mercury 2536 ($1S - 2^3P_1$) resonance radiation excited in a bulb in zero magnetic field by 100 percent polarized light would be 100 percent polarized except for interatomic disturbances. If cadmium is in this case like mercury, and there is no reason to believe otherwise, then we must account for observing only 35 instead of 100 percent polarization on the basis of collisions where a collision is produced by a normal atom coming near enough to an excited atom to disturb its orientation so that the emitted light has a random plane of polarization.

From kinetic theory we may write the following formula⁵

$$\sigma^2 = 160 \times 10^{-23} (mT)^{1/2} / t\beta$$

where σ is the sum of the effective radii of the colliding atoms, t the average time between collisions, β the pressure in millimeters mercury, m the atomic weight, and T the absolute temperature. Under the conditions of our

⁴ Wood and Guthrie, *Astrophys. Jour.*, **29**, 211 (1909).

⁵ See Datta, *Zeits. f. Physik*, **37**, 625 (1926); Schutz, *Zeits. f. Physik*, **34**, 260 (1925); Stuart, *Zeits. f. Physik*, **32**, 262 (1925).

experiment, p^6 is 5.5×10^{-4} , m is 112, and T is 525. If t were equal to the average life time of the excited atom, then 50 percent of the excited atoms would engage in a collision before returning to the normal state, but we observe that 65 percent have engaged in effective collisions so that the average time between collisions must be somewhat smaller than the life time of the excited state, not greatly, however, as an approximate calculation for this case gives the value of the former to be about 85 percent of the latter, so that for the purpose of our approximate calculation of σ we may take t to be 1×10^{-7} . This gives σ equal to 3×10^{-8} cms. The kinetic theory value of the radius of normal mercury atoms is 1.75×10^{-8} cms and the effective radius of 2^3P_1 mercury atoms when colliding with foreign gases is 5.9×10^{-8} cms⁷ so that σ for mercury on kinetic theory is 7.6×10^{-8} cms. We would expect σ calculated for collisions between normal and 2^3P_1 cadmium to be slightly greater, or about 1×10^{-7} cms. Depolarization influences are felt thirty times farther away, however, as shown by the fact that to account for the present polarization observed, σ must be taken thirty times the above value.

Other cases of large effective radii have been observed. By comparing the percent of polarization of D_2 resonance radiation in sodium vapor at 10^{-6} mms pressure excited by polarized light with the percent predicted by the Heisenberg theory Datta⁸ concludes that the effective radii of the colliding atoms are of the order of magnitude of 10^{-4} centimeters or about a thousand times the kinetic theory value.

By illuminating mercury vapor at various pressures in a magnetic field (fields of 2,000 to 18,000 gauss were used) with light of 2536A wave-length polarized with the electric vector parallel to the magnetic field and comparing the intensity of the part of the radiation polarized parallel to the magnetic field with the part polarized perpendicular to it. Schütz⁹ calculates that normal mercury atoms and mercury atoms in the 2^3P_1 state collide 66 times as often as is given by a kinetic theory formula similar to the one given above using the data for the radii of normal and excited mercury atoms quoted above. If such a formula is to give the observed average time between collisions, we must consider the sum of the radii of the colliding atoms to be $(66)^{1/2}$ or 8 times the kinetic theory value.

On the other hand, if the effect of a foreign gas present in the resonance bulb is studied in the same manner, it turns out that the kinetic theory value for the time between collisions is nearly correct. From the work of Wood and Mohler¹⁰ on the emission of both D lines by sodium vapor excited by one of them Schütz estimates that collisions, causing a transfer of energy, occur 50 times as often as one would expect on kinetic theory, or in other words, the sum of the effective radii of the colliding atoms is $(50)^{1/2}$ or 7 times the normal kinetic theory value.

⁶ Edgerton, Phil. Mag. 33, 33 (1917).

⁷ Stuart, reference 5.

⁸ Datta, reference 5.

⁹ Schütz, reference 5.

¹⁰ Wood and Mohler, Phil. Mag. 27, 456 (1919).

The radii of atoms, which are effective in collisions, depends on what the result of the collision is to be. The largest effective radii are observed in cases which result in reorienting the atoms, that is in cases of depolarizing influences of neighboring atoms. Where there is a transfer of energy from one atom to another which is almost but not quite in resonance lesser effective radii are observed and cases of totally dissimilar atoms colliding result in still lesser effective radii.

The experimental work described here was carried on at The Johns Hopkins University during the spring of 1925, and I am indebted to Prof. R. W. Wood for his invaluable suggestions given from time to time. I was not satisfied with the interpretation of the results at that time so publication has been withheld until now.

January 10, 1927.

IONIZATION BY COLLISIONS OF THE SECOND KIND IN THE RARE GASES

BY GAYLORD P. HARNWELL

ABSTRACT

A positive ray apparatus was used to investigate the products of ionization by electron impact in mixtures of helium, neon, and argon. The variation with pressure of the ratio of the two types of positive ions present was investigated in detail for three cases. Case 1: A mixture of half helium and half neon was investigated up to 0.15 mm pressure. The ratio He^+/Ne^+ was found to decrease regularly between 0.03 mm and 0.15 mm. At 0.03 mm the mean free path is approximately equal to the dimensions of the apparatus. The suggested reaction is: $\text{Ne} + \text{He}^+ \rightarrow \text{Ne}^+ + \text{He}$. Case 2: A mixture of half neon and half argon was investigated throughout the same pressure range. The ratio Ne^+/A^+ decreased regularly between 0.05 mm and 0.15 mm, but this decrease was less rapid than that of the ratio in Case 1. The suggested reaction is: $\text{A} + \text{Ne}^+ \rightarrow \text{A}^+ + \text{Ne}$. Case 3: This mixture was half helium and half argon, and the pressure range was the same as in the first two cases. The ratio He^+/A^+ remained constant within the limits of experimental error. Case 3a: A mixture of 15 percent helium and 85 percent argon was also investigated as there were theoretical grounds for believing that the rate of variation of He^+/A^+ with pressure would be greater in such mixture. In that case the ratio He^+/A^+ was found to decrease slightly. The suggested reaction is: $\text{A} + \text{He}^+ \rightarrow \text{A}^+ + \text{He}$.

The observed effects are best explained by a type of collision of the second kind which is equivalent to ionization by positive ions. To account for the results obtained an electron must be transferred from an atom to an ion at a certain fraction of the collisions between an atom and an ion of higher ionizing potential. The results obtained at low pressures corroborated the values for the probability of ionization in these gases obtained by K. T. Compton and C. C. Van Voorhis.

IN CONSIDERING certain experiments of Lind and Bardwell,¹ Professor K. T. Compton suggested the possibility of ionization by positive ions of high ionizing potential, probably as the result of collisions of the second kind. The present research was prompted by the belief that such a process might play an important rôle in many of the phenomena of ionization in gases and that it might be investigated by the modification of Dempster's positive ray apparatus used by H. D. Smyth² and Hogness and Lunn.³ The rare gases were selected for the first experiments, as they are monatomic and have well known ionizing potentials, and consequently the results obtained from them would probably be the most easily interpreted. It was well known that the intensities of the peaks in a positive ray apparatus fell off rapidly at high pressures because of collisions of the ions with the atoms or molecules of the gas and subsequent deflection or neutralization. Hence it was thought that secondary effects of the type looked for would be expected to appear in the region just before the peaks were extinguished by

¹ Lind and Bardwell, Science, Dec. 25, 1925, Vol. LXII, page 593.

² H. D. Smyth, Phys. Rev., 25, 452 (April, 1925).

³ Hogness and Lunn, Phys. Rev., 26, 786 (Dec., 1925).

the increased pressure. These effects would probably be intimately connected with the ionizing potentials of the two gases present. For they presumably represent the tenacity with which an electron is held in the atomic structure. If an ionized helium atom collided with a neutral neon atom it is conceivable that, because of the intensities of the fields involved, an electron would be transferred from the neon atom to the helium ion. The resulting bodies would then be a helium atom and a neon ion. The reverse of this process would not occur as the electron would then be originally attached to that atom which had the greater affinity for it. There would be no way of detecting any effects which might take place during the collision of an atom with an ion of its own kind. Hence the result which would be observed, in case collisions of the above kind took place, would be that the number of neon ions would be increased at the expense of the number of helium ions. The same reasoning would lead to the conclusion that argon ions would be produced at the expense of neon ions in mixtures of those two gases. Effects corresponding to the above were observed under various conditions, but the probability of the transfer occurring was not found to bear any simple relation to the ionizing potentials of the gases. While this investigation was in progress Hogness and Lunn⁴ published the results of certain experiments they had conducted with argon and nitrous oxide during which they had incidentally observed effects of the same nature as those contained in this paper.

APPARATUS AND PROCEDURE

The apparatus used is shown in Fig. 1. It is essentially the same as that used by Smyth² with only minor alterations. Chamber *A*, the high pressure region in which the ionization occurred, was quite heavily shielded as was also the path between that and chamber *B* where the magnetic deflection took place. The shielding was thought necessary as rather large magnetic fields were used during some parts of the investigation and it was desired that the effect of changes in the field should be negligible except in chamber *B*. The distance between the slit, *S*₁, maintaining the pressure difference and the collimating slit, *S*₂, was made as small as was consistent with good evacuation from the upper outlet. The filament was placed very close to the first gauze, *G*₁, in order that the chance of a collision between an electron and an atom in that region might be reduced to a minimum. The filament itself was placed inside a tube the lower end of which supported *G*₁ and *G*₂. The tube was solid above *G*₁, but there were openings between *G*₁ and *G*₂. It was found convenient to have two gauzes during part of the work to investigate and interpret certain effects which were met. The filament was of tungsten. The width of *S*₁ was about 0.05 mm, that of *S*₂ was about five times as great. The gases to be used were mixed and stored in a system in which the pressure could be varied between convenient limits, and were then admitted to chamber *A* through capillary leaks. A McLeod gauge was situated as close to chamber *A* as possible. The evacuating system consisted of two single stage diffusion pumps backed by a double stage and an

⁴ Hogness and Lunn, Phys. Rev., 28, 849, abstract (1926).

oil pump. The large metal-to-glass seal was made by grinding the parts together and covering the joint with both DeKhotinsky and Picein cements. This joint proved quite satisfactory under the fluctuation in temperature to which it was subjected. It was found necessary to wind a cooling coil around the outside of chamber *A* which contained the filament.

As the apparatus could not be baked out it had to stand under vacuum for a day or two before the nitrogen, oxygen, water vapor, etc. adsorbed

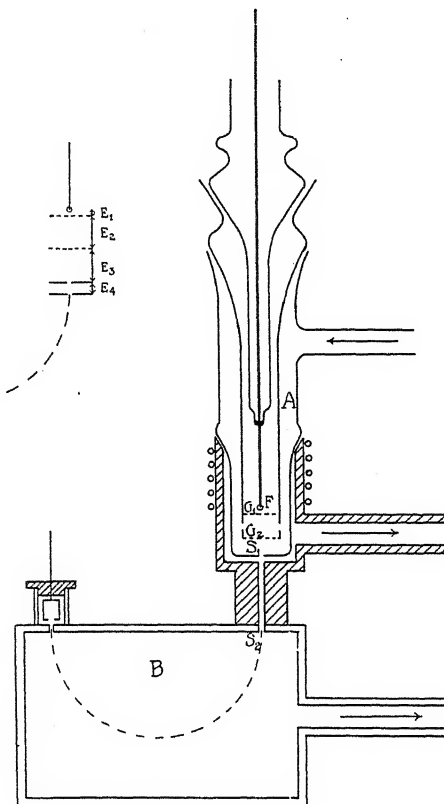


Fig. 1. Diagram of apparatus.

on the walls were reduced to a negligible quantity. Then after preliminary runs in hydrogen the behavior of pure helium was investigated under various conditions. At the high pressures used the amount of ionization was found to vary nearly linearly with the emission. In the final procedure the variable was the pressure and every change in pressure necessitated a slight change in the filament current in order to keep the emission constant. The fluctuation of the emission from one run to the next was very slight but sufficient to account for the greater part of the irregularity of the curves obtained. As E_1 , the accelerating voltage for the electrons, was increased the ions began to appear very soon after the critical potential was passed, but the

amount of ionization did not rise very rapidly at first and the values of E_1 used during the work were in the neighborhood of twice the critical potentials. E_2 and E_3 the accelerating voltages for the positive ions were kept of the order of five volts in the final measurements as it was found that larger values introduced complicating effects which will be discussed later. The curves that follow are not strictly comparable as it was necessary to change the magnetic field for different gases and it was found, as will be mentioned later, that the ionization as measured by the electrometer was not independent of the magnetic field used.

The variation of the area under the peak with pressure was investigated and the results for helium, neon, and argon are given in Fig. 2. As would be expected the forms of the curves when the ordinates are multiplied by the proper constant are approximately the same. The constant probably depends on the value of E_1 used and the ionizing potential of the gas. The means of several runs were taken and the discrepancies could be accounted

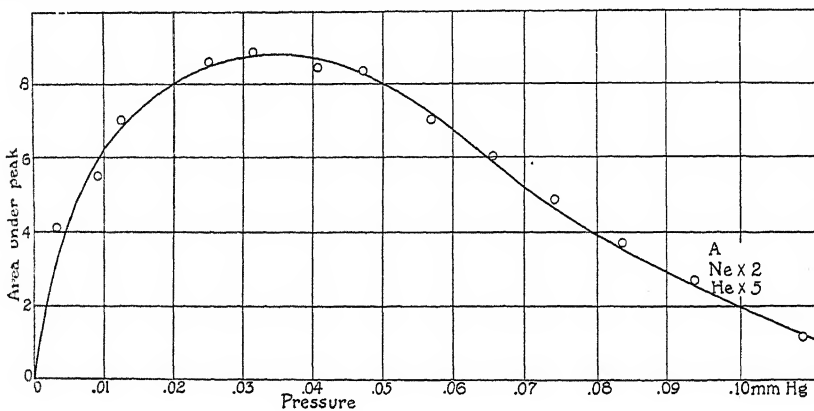


Fig. 2. Variation with pressure of the area under the peaks of positive ray analysis curves in A, He, and Ne.

for by the inevitable slight variations of voltages and filament emission. The abscissas are the pressures and the ordinates are measured in arbitrary units. A maximum of ionization occurs when the pressure is between three and four hundredths of a millimeter. The decrease in ionization after that point is presumably due to collisions with gas atoms resulting in deflection or neutralization, and it is therefore in that region that any secondary effects should be expected.

Several procedures were tried, such as taking runs at constant total pressure with varying mixtures of helium and neon, or with a constant partial pressure of one of the gases and varying the partial pressure of the other. These experiments showed in a qualitative way that some such an effect as the one looked for was actually taking place but they did not lend themselves to accuracy of measurement or ease of interpretation. The procedure finally adopted, as least equivocal and best adapted to the particular investigation, was to admit the gases in known and nearly equal proportions

and to vary the total pressure. The secondary effects would not be expected to occur below three hundredths of a millimeter pressure and should come more into evidence as higher pressures were reached. In this method the only variable was the pressure and it was susceptible of quite accurate measurement.

RESULTS

The first attempts were made using potentials for E_2 and E_3 in the neighborhood of fifteen or twenty volts. It was found that under these conditions the effects were complicated by having all the peaks double. The duality of the peaks was found to vary only with the potentials E_2 and E_3 . If these potentials were large the peaks were widely separated and as they were decreased the peaks became indistinguishable when E_2 plus E_3 was in the neighborhood of twenty volts. If E_3 was small and its direction reversed the extraneous peak was very much reduced. This and other evidence of a similar nature pointed to the theory that the second peak was produced by photoelectrons emitted from G_2 and S_1 and accelerated upward towards G_1 . This effect was eliminated by reducing E_2 and E_3 till their sum was well below the ionizing potential of any gas used. This still left the currents measured by the electrometer of a convenient order of magnitude. Other sources of slight error or irregularity were investigated and their effects reduced as much as possible.

The gases were thoroughly mixed in the reservoir by a method of contraction and expansion and also allowed to stand for some time after mixing before the runs were taken. Furthermore the possibility of a change in the ratio of the gases on passing through the capillary leaks into chamber A was considered. That is, it was thought that there might be a differential effect between the capillary method of pressure limitation and the slit method at S_1 in favor of one of the gases. This effect was investigated and found not to exist within the limits of experimental error. Any error due to minor irregularities in the mixture was greatly reduced by taking the mean of a series of observations. All the results were converted into the form of ratios and hence were independent of the fact that there is probably not an exact correlation between the area under the peaks and the number of ions present. However, the variation in size and shape of a peak with the magnetic field as a source of error will have to be mentioned again in the case of helium and argon.

By far the largest and most serious possibility of error is due to stray ionization present in chamber B . The electrometer was adjusted so that its natural drift when the filament was not glowing was extremely small. But as soon as ions were produced in A the drift increased. It is very probable that a small fraction of the ions entering B instead of continuing in a circular path are scattered from the beam. Some of these ions enter the Faraday cylinder and cause a deflection of the electrometer. This effect is more marked at low values of E_4 . And the possibility of error in that region was further enhanced by slight traces of N_2 and H_2O which could not be completely

eliminated. For equal areas of peaks the height as measured by the current to the electrometer varies to a first approximation as E_4 , so that the total error due to these effects became more serious with a gas of high atomic weight such as argon. Or more particularly when the discrepancy between the atomic weights of the two gases used was large. For if the atomic weights were not widely different the difficulty could be overcome by increasing the magnetic field and hence the corresponding value of E_4 for the peaks which would decrease the error due to scattered ionization. This will have to be mentioned again in the case of argon and helium.

The first gases used were helium and neon. The result in the case of a mixture of fifty percent of each (by volume) is shown in Fig. 3. The pressures plotted are the total pressures, the partial pressure of each gas being half of

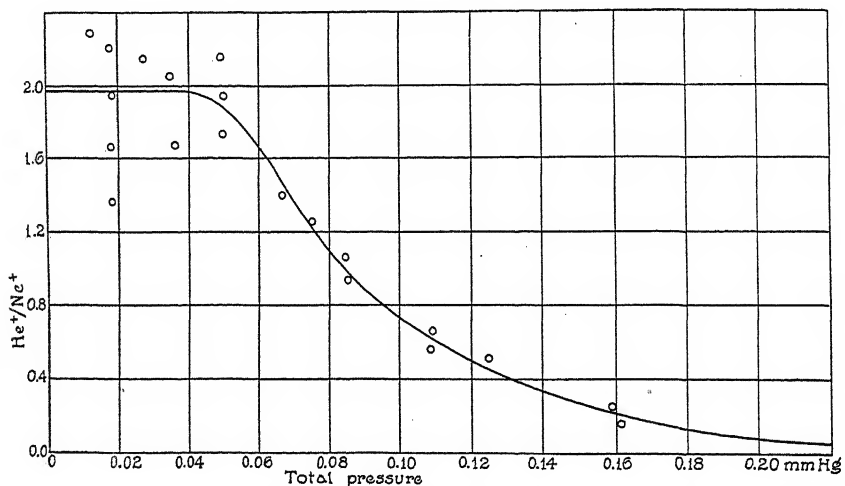


Fig. 3. Ratio of He^+ to Ne^+ for various pressures of a 50 percent mixture of He and Ne.

the pressure shown. The ordinates represent the ratio of the helium ions to the neon ions, as obtained by taking the areas under the peaks representing the two gases. E_1 was fifty volts and E_2 and E_3 were five volts apiece. The emission from the filament was maintained as nearly as possible at one milliampere. In this case the most convenient magnetic field to use with the available limits for E_4 was about 1700 gauss. In the region of pressure below five hundredths of a millimeter the ratio fluctuated rather widely. There seems to be no really adequate explanation for this. The most probable cause is that more difficulty was experienced in keeping the filament emission at a constant value in this region. The mean, however, remained practically constant. After the pressure passed five hundredths of a millimeter, approximately, the ratio dropped showing a predominance of neon ions. This is about the pressure judging from Fig. 2 at which any secondary effects should become noticeable. This is also the point at which the effect should occur from a more direct point of view. The distance between G_1 and S_1 was approximately two centimeters, and the pressure at which effects due to

collisions should become evident would be that at which the mean free path was of about this length. This should occur in these gases at about five hundredths of a millimeter. From this point the curve drops in a fairly regular fashion, and apparently approaches a lower value asymptotically. In the case of helium and neon the final value, if one exists, seems to be a very low one. It is probably closely related to the process of exchange of an electron from an atom to an ion outlined above. The difference between the original and final value of the ratio may even be a measure of the probability of the transfer occurring. It was not possible to carry these observations much above fifteen hundredths of a millimeter as the peaks had become very small by the time that pressure was reached. Also, for the same reason, the observations were less accurate as the drift of the electrometer due to scattered ionization had become a very appreciable fraction of the area of the peak. That was allowed for but it could not be done with great accuracy.

The next mixture used was that of neon and argon. In some ways this was a more favorable mixture to work with in a positive ray apparatus than

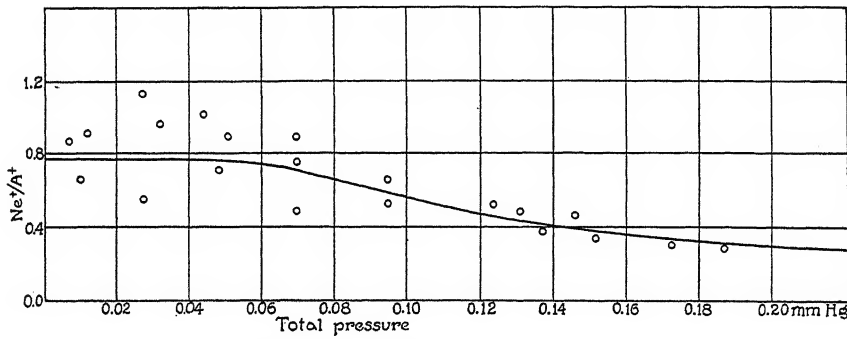


Fig. 4. Ratio of Ne^+ to A^+ for various pressures of a 50 percent mixture of Ne and A.

the previous one for the ratio of the atomic weights is 5:9 instead of 1:5. The reason that the value of this ratio effects the accuracy was mentioned above. Also the ionizing potentials are slightly lower, and the difference between them is about twice that in the previous case. The results for this mixture are shown in Fig. 4. As before the abscissas represent the total pressures and the mixture contained equal proportions of each gas. The ordinates are again the ratios of the areas under the peaks, but they are not strictly comparable to the ordinates in Fig. 3 for the magnetic field was about 3000 gauss in this case and the ionization as measured by the electrometer was not independent of the magnetic field. This curve shows the general characteristics of Fig. 3. The values of the ratio at lower pressures fluctuate rather widely as before. The most distinctive feature is that the change in the ratio of the ions with pressure is very much less than in the case of helium and neon. It also looks as if the slope approaches zero at higher pressures, but the evidence for this is not very conclusive.

The third mixture investigated was that composed of half helium and half argon. The conditions under which these observations were taken were as nearly as possible those of the previous runs. E_1 was fifty volts, E_2 and E_3 were five volts apiece, and the emission was kept at one milliampere. The magnetic field first used was about 2000 gauss. Approximately the same range of pressures was covered and with the same procedure, but within the limits of error no departure from the original value of the ratio of helium to argon was observed. However, the results were less convincing than in the two previous cases for the fluctuation in the actual areas of the peaks at constant pressure was considerably larger. This was due to the particular gases used for they were the least satisfactory ones to investigate by this method, the ratio of the atomic weights in this case being 1:9. Hence the argon appeared at a comparatively low value of E_4 and had a broad low peak much less susceptible to accurate measurement than the helium one. The particular difficulty, of course, was due to the electrometer drift caused by the scattered ionization in the argon region. Attempts were made to find a more satisfactory method of procedure. The most promising one was to investigate the behavior of one of the peaks, in this case the argon one, with

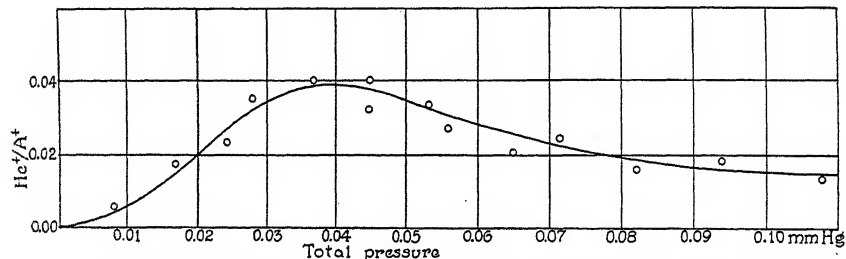


Fig. 5. Ratio of He^+ to A^+ for various pressures of a mixture of 15 percent He-85 percent A.

variation in the magnetic field and consequent variation in E_4 at different pressures. This was done and curves were obtained relating the peak area to the value of E_4 at which it was obtained. These were found to depend slightly on the pressure. With these data the two peaks of helium and argon could be measured at different magnetic fields such that the E_4 values at which they appeared were of the same order. By this means the area under the argon peak could be measured more accurately and its value extrapolated back to the value which it would have if measured at the same magnetic field as that used in obtaining the helium peak. This method yielded more consistent results and was presumably of greater accuracy. However, no change in the ratio of the peaks, within the limits of error, could be observed as the pressure was varied.

From simple kinetic theory considerations it can be seen that if this effect takes place as assumed, the rate of variation of the ratios: $\text{He}^+/(He^++\text{A}^+)$ and $\text{A}^+/(He^++\text{A}^+)$, with pressure should be greatest when the ratio of helium to argon is small. Acting on these considerations a mixture of 15% helium and 85% argon was investigated. The conditions

were almost the same as in the other experiments and the results are shown in Fig. 5. The ratio increases to a maximum at about .03 mm as would be expected from consideration of the partial pressure of the gases. After that point the ratio decreases slightly tending to show that the argon ions are being increased at the expense of the helium ions. Further evidence that this effect is taking place is given by the shapes and positions of the peaks. As the pressure increases beyond about .03 mm the He peak decreases in area but remains of the same shape and in approximately the same place. The argon peak decreases slightly but also broadens out and extends to higher values of E_4 showing that the region of production of argon ions is moving from G_1 toward S_1 . The evidence thus indicates that the process observed in the other mixtures occurs in a mixture of helium and argon though it is much less probable.

DISCUSSION

The outstanding result of these experiments is that this type of ionization by positive ions apparently does occur. Further experiments have been made with mixtures of the rare gases and gases whose molecules are diatomic. These results will form the subject of a later paper, but they tend to confirm the evidence contained in this one. If this effect occurs at a certain fraction of the collisions in any mixture of ionized gases it should have an important bearing on almost all discharge tube phenomena. A rough estimate of the probability of this electron transfer can be made from the slopes of the curves but the data are as yet insufficient to justify the publication of a numerical value.

The shapes of the curves in Figs. 3 and 4 further suggest that the probability of the transfer of an electron from an atom to an ion is not connected in a simple way with the electron affinities of the two gases involved. In fact, it even seems that though a difference in ionizing potential is necessary to cause such a transfer, yet the smaller this difference the more likely such a transfer is to occur. For the difference in ionizing potential between neon and argon is twice that between helium and neon. If this is so, and it is a result consistent with those of other experiments on collisions of the second kind, it accounts for the smallness of the effect in the case of helium and argon. For in this case the difference in ionizing potential is three times that in the case of helium and neon. These remarks apparently also apply to diatomic gases.

It should also be mentioned that the possibility of explaining the observed effect on the basis of a limiting speed for electrons in a mixed gas was considered. At sufficiently high pressures inelastic impacts would prevent the electrons from gaining sufficient energy to ionize the gas with the higher ionizing potential. However, such a situation could only exist when the length of the electron mean free path was of the order of the distance from the filament to G_1 , which from the constants of the apparatus would occur at a pressure of about 1.5 mm. This is very much higher than any pressure used.

Finally it might be mentioned that the mean values obtained for these ratios below three hundredths of a millimeter are in fairly good agreement with the values obtained by Compton and Van Voorhis⁵ for the probability of ionization in these gases. It was mentioned above that the area under the peak is probably not an accurate measure of the ionization in chamber *A* and also that the peak area varied with the values of magnetic field and E_4 used to obtain it. The points on the curves given here all represent runs in which the magnetic field was kept constant and the value of E_4 was varied. The behavior of peak area with magnetic field was investigated and from these results Figs. 3 and 4 can be replotted in such a way that the points represent runs in which E_4 is kept constant and the magnetic field varied. If this is done the shapes of the curves remain the same but the actual values of the ordinates are slightly different. And the ratios at low pressures when these ordinates are used are in quite good agreement with the same ratios calculated from the Compton and Van Voorhis results at the appropriate E_1 .

My thanks are particularly due to Professor K. T. Compton and Professor H. D. Smyth for the suggestion of the present investigation and for their invaluable assistance and helpful interpretations during the work.

PALMER PHYSICAL LABORATORY
PRINCETON, NEW JERSEY
February 5, 1927

titu.
ne E_4
; the

⁵ Compton and Van Voorhis, Phys. Rev., 27, 724 (June, 1926).

CHANGES IN THE PHOTO-ELECTRIC THRESHOLD OF MERCURY

By HUGH K. DUNN

ABSTRACT

Photo-electric threshold for the clean surface.—C. B. Kazda has found the photo-electric threshold of a mercury surface cleansed of impurities by means of a constant overflow. In the present work his value of 2735A for the threshold of clean mercury is checked.

Changes in photo-electric threshold of Hg. that take place in a high vacuum.—When the surface flow is allowed to stop in a high vacuum, some impurity attacks the surface, quickly raising the threshold to 2850A. If liquid air is not used, this impurity is present in larger amounts and attacks the running surface. Indications are that a surface film is formed and maintained in spite of the flow when liquid air is not used, or requires two hours or more for removal if liquid air is used. This impurity can not be one of the gases with extremely low melting points. It is not water, but may be a component of the stopcock grease. When the surface is left standing several days in a high vacuum, its threshold falls to 2680A. If liquid air is not used, the standing surface has a limit of 2560A. All of these values are closely reproducible.

Indirect effect of hydrogen on the photo-electric threshold of Hg.—Pure hydrogen in contact with the surface does not change the photo-electric behavior. When the mercury is condensed in the presence of hydrogen, some of the gas is dissolved in the metal. This does not change the characteristic threshold of the mercury. It does, however, have the effect of greatly impeding the action of other impurities that form on the surface. This is indicated by the fact that over two hours is required for the change from the threshold of 2735A for the clean surface to the maximum of 2580A, as compared with 13 minutes for this change when hydrogen is not present.

THE photo-electric threshold for mercury has been found by Kazda¹ at 2735A. He was able to eliminate all effects of impurities by making his measurements on a flowing surface. This was probably the first time that a clean surface of metal had been used in photo-electric experiments, with any degree of certainty, and it was thus possible for him to demonstrate that a metal does possess a definitely characteristic threshold. At the same time, the clean surface offers the best possible starting point for an investigation of the effect of impurities on the threshold. It was for the latter purpose that the work reported in the present paper was undertaken.

APPARATUS AND METHOD

The experimental arrangement was, in the main, just as it was used by Kazda. The reader is referred to his paper for a diagram of the apparatus and a more detailed account of the experimental method. Briefly, the surface flow was realized by operating a mercury still and allowing the condensed mercury to overflow from a cup inside the photo-electric cell. The source of light was a quartz mercury arc, and a monochromatic illuminator was

¹ C. B. Kazda, Phys. Rev. 26, 643 (1925).

arranged to direct light of any desired wave-length onto the mercury surface. The relative intensities of the lines of the arc were measured by means of a delicate thermopile, in vacuum. The photo-electric effect of any given wave-length was measured by a quadrant electrometer by the usual rate of deflection method. The photo-electric effect per unit intensity was then plotted as a function of the wave-length, and the intercept with the wavelength axis gave the threshold, with an uncertainty of not more than $\pm 10\text{\AA}$. When it was desired to follow rapid changes in the sensitivity the rate of deflection method was too slow. In such cases a constant deflection method was used, the quadrants connected to the photo-cell being shunted to the ground by a radioactive leak.

THE THRESHOLD FOR THE FLOWING SURFACE

The value found by Kazda for the long wave-length limit of the flowing surface of mercury was 2735 \AA . In more than a dozen determinations in the present work, this limit was always found between 2735 \AA and 2750 \AA . It

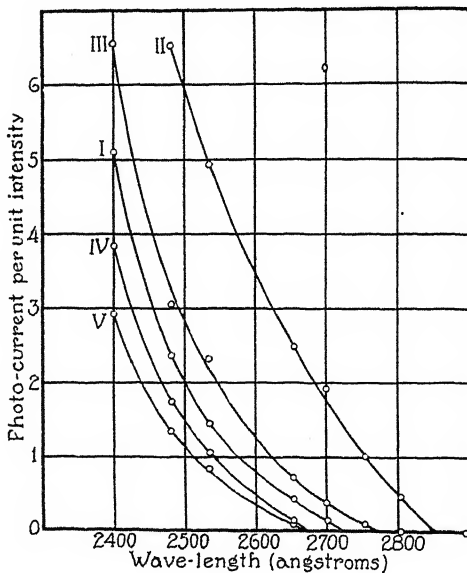


Fig. 1. Change of threshold of mercury. I. Curve for flowing surface. II. 13 minutes after turning off still. III. 18 hours after turning off still. IV. 66 hours after turning off still. V. 114 hours after turning off still.

must be noted too, that the higher values were obtained under less favorable conditions, i. e. less prolonged pumping and running of the still since the last contamination of the surface. A curve for the clean surface is shown at I, Fig. 1.

STATIONARY SURFACE IN HIGH VACUUM

Curve I, Fig. 3, shows the changes that take place in the sensitivity to the line 2653 \AA , when the clean surface is exposed to a vacuum of the order

of 10^{-6} mm of mercury. Before this experiment was started the surface had been flowing for some time and showed the normal threshold of 2735A. The sensitivity was constant. At the time marked zero the still was turned off. The surface flow immediately slowed down, and in about ten minutes stopped altogether. As may be seen from the curve, the sensitivity to 2653A rose to a maximum of about five times that when running, about 13 minutes being required for the rise. The sensitivity then began to decrease, rather rapidly for about 40 minutes, then more slowly. This slow fall continued over several days.

Fig. 1 shows the threshold curves for the changing surface. Curve I is for the flowing surface, and gives 2735A for the threshold. Curve II is for the highest point reached after stopping the flow, i. e. about 13 minutes after turning off the still. The limit given is 2850A. Curve III was taken after 18 hours of standing, the limit having now fallen to 2770A. Curve IV was taken after 66 hours, and V after 114 hours. Both show a threshold of about 2680A, indicating that a constant value has been reached. It is to be noted that the threshold first rises some 115A above that for clean mercury, but eventually drops to 55A below that value. It should be explained that curve II was not taken all in one run, as were the others, for the reason that the surface does not remain in the most sensitive condition long enough for a threshold curve to be taken. It was obtained by successively running curves like I, Fig. 3, for the different lines of the arc, the highest point of each being used for plotting the point of II, Fig. 1, for that wave-length.

From a study of these results it would seem that there are at least two stages to the process of contamination of the surface. This might be attributed to two different impurities, one acting very quickly and raising the threshold, the other lowering it, but acting much more slowly. It is more likely that one agent is responsible for both phenomena, a single layer of molecules assisting the release of electrons, but greater thicknesses tending to stop the slower electrons and thus lower the threshold. This is in accord with the results of Becker² on the thermionic work function of platinum covered with caesium.

CONTAMINATION BY REMOVAL OF LIQUID AIR

Marked changes in the long wave-length limit and sensitivity took place when the liquid air was removed from the trap connected with the apparatus. When this was done with a surface that had been standing for some time in a high vacuum, a drop in the threshold occurred. For example, the surface had been standing in a high vacuum for 46 hours, and showed a threshold of 2785A. With the pumps running continuously, the liquid air was removed. An immediate drop in the sensitivity to the 2653 line was noticed, and after two hours time it had fallen to zero. A threshold curve then showed the limit to be 2570A. This curve is shown at I, Fig. 2. After 20 hours curve II was taken. The limit had remained practically the same, falling perhaps to 2560A. The sensitivity, however, especially for $\lambda = 2400\text{A}$,

² J. A. Becker, Phys. Rev. 28, 341 (1926).

had decreased considerably. This value of 2560A was obtained repeatedly, and may then be taken as characteristic of standing mercury contaminated by something that is released when the liquid air is removed. After curve II was taken, the liquid air was replaced, and after 22 hours the threshold was found to have risen to 2600A, the surface not having been disturbed meanwhile. This was repeated on another occasion, the limit 2600A being observed after the liquid air had been replaced for 56 hours.

On one occasion a slight rise in sensitivity was first observed when the liquid air was removed. The surface had been standing for only a few hours, and had the limit 2830A. The deflection for $\lambda = 2653\text{A}$ was 253 mm. When

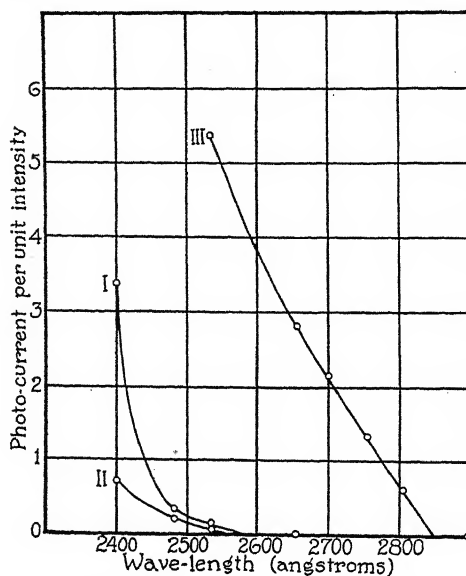


Fig. 2. Effect of removal of liquid air on the threshold. I and II. Curves for standing surface. III. Curve for flowing surface.

the liquid air was removed it rose in six minutes to 272 mm, then proceeded to drop in the usual manner. The threshold reached the value 2560A in two hours time.

When the liquid air was removed while the surface was running, nothing happened until the trap reached such a temperature that the frost began to disappear from its outside. Then, however, a sharp rise in sensitivity was noticed, while the threshold rose from the usual 2735A to the value 2850A. The curve is shown at III, Fig. 2. The rate of flow was increased until the surface was too turbulent to permit consistent results, but no change in this value was obtained. After the liquid air was replaced, several hours of pumping and running the still were required to bring the threshold back to normal. Repetition of the experiment gave identical results.

It thus appears that there is some impurity that can attack even the flowing surface if present in large enough concentrations. Furthermore, it seems probable that this is the same impurity that causes the highest

sensitivity of the surface standing in a high vacuum, since the same threshold, 2850A, was observed in both cases. When liquid air is used, the concentration of this impurity is not high enough to permit its attacking the flowing surface.

While the highest values reached by the threshold are identical, there is a difference in the lowest values reached by the standing surface, with and without liquid air. In the former case, there is a definite tendency to stop at 2680A, while in the latter case the limit falls to 2560A.

The impurity responsible for the threshold of 2850A would seem to be something whose vapor pressure increases rapidly in the neighborhood of 0°C. To test whether or not it is water vapor, a side tube containing a little water was sealed to the apparatus between the liquid air trap and the photocell, and immersed in liquid air. Liquid air was also kept on the regular trap. The apparatus was exhausted and the mercury surface brought to its normal running behavior. The 2653 line gave a deflection of 178 mm. The liquid air around the water was then replaced by brine at -20°C. The deflection began to fall very slowly, reaching 125 mm after 2½ hours. The brine was then removed, and the fall was more rapid, the deflection going to 92 mm in about 14 minutes. The liquid air was replaced, and the deflection rose in 9 minutes to 174 mm, close to its former value. At no point was any rise in sensitivity noted due to the release of the water, in spite of the fact that the brine was used to insure a very slow release at first. This result is not necessarily inconsistent with that of Kazda, who found that small amounts of water vapor cause a rise in the threshold of a standing mercury surface, for here the experiment was made with a flowing surface.

Since stopcocks were used as a part of the apparatus, it is evident that vapor from the stopcock grease must have been condensed in the liquid air trap. A side tube containing a small quantity of the grease was sealed to the apparatus, and treated in the same manner as the water had been (except that brine was not used). With pumps running and surface flowing, the liquid air was removed from the grease, while that on the regular trap was kept in position. This time the rise in sensitivity and threshold was observed, the latter reaching and holding the value 2850A quite exactly. While these tests are not entirely conclusive, it is very probable that some component of the grease is responsible for many of the changes observed.

HYDROGEN IN CONTACT WITH THE SURFACE

Extensive tests were made with hydrogen in contact with the mercury surface. The hydrogen was purified, and admitted to the apparatus at pressures ranging from 10^{-4} to 10^{-1} mm, and tests were made both with the standing surface and with the surface flowing at various rates. Observations were also made of the changes taking place when the surface flow was allowed to stop. In all cases the behavior was exactly as when the hydrogen was not present, with the exception that when the pressure exceeded 10^{-3} mm a slight decrease in the photo-current was noticed. This was undoubtedly a space, not a surface, effect, for it was roughly proportional to the pressure, and the same effect was observed when air was used instead of hydrogen.

We must conclude that pure hydrogen does not modify the surface in a way that affects the photo-electric behavior.

HYDROGEN PRESENT IN THE STILL

Suhrmann³ has proposed a theory that in an electron emission of any kind from a metal, a gas dissolved in the metal has the effect of increasing the emission, while an adsorbed layer of gas on the surface decreases the emission. An experiment was devised to test this theory, and, while it failed to confirm the theory, an interesting effect was discovered.

The apparatus had been constructed in such a manner that the still was connected with the photo-cell only by two small tubes. One of these contained the condensed mercury flowing to the cell, the other contained the overflow from the cell, running back to the bottom of the still. Since both tubes were full of mercury, a pressure of several centimeters could be

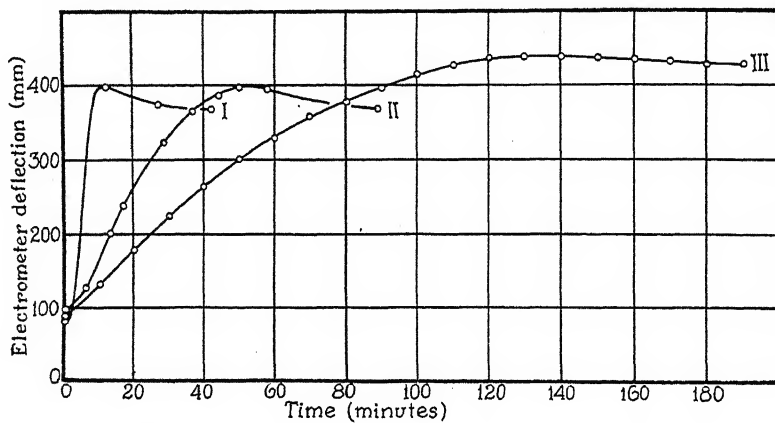


Fig. 3. Rise of sensitivity after stopping surface flow. I. Curve taken in high vacuum. II and III. Taken with hydrogen in the still.

maintained in the still without affecting the pressure in the cell. The two parts of the apparatus were connected to the same pumps, but could be separately closed off by means of large mercury-sealed stopcocks. A separate liquid air trap was provided for each branch. It was then possible to admit hydrogen to the still, while a high vacuum was maintained in the photo-cell.

With the still running, hydrogen was admitted to it, to a pressure of 8 mm. It was thought probable that some of the hydrogen would dissolve in the condensing mercury, and flow with it through the small tube to the photo-cell. An increase in emission would then occur if Suhrmann were right. No such increase in emission was observed, although the electrometer deflection was carefully watched for more than two hours, during which time the small tube leading to the cell must have emptied many times. No change in the sensitivity or threshold of the flowing surface occurred.

³ R. Suhrmann, Zeits. f. Tech. Physik, 4, 304 (1923).

When, however, the still was turned off and the surface flow allowed to stop, *the time required for the rise to maximum sensitivity was 49 minutes.* Two days previous, this time had been 12 minutes. In the year preceding and the two months following the experiment described here, this time of rise was observed under high vacuum conditions some 27 times, and always found to lie between 11 and 20 minutes. The 20-minute rise had been observed on only one occasion, the most common value being 13 minutes. The 49-minute rise was then a radical departure in behavior. It is shown in curve II, Fig. 3, where it may be compared with I, taken without hydrogen present. It is noticed that the highest sensitivity is practically the same, the only difference being the introduction of a time factor.

Curve I, Fig. 4, is the threshold curve for the flowing surface, either with or without hydrogen present in the still. Curve II was taken when the highest

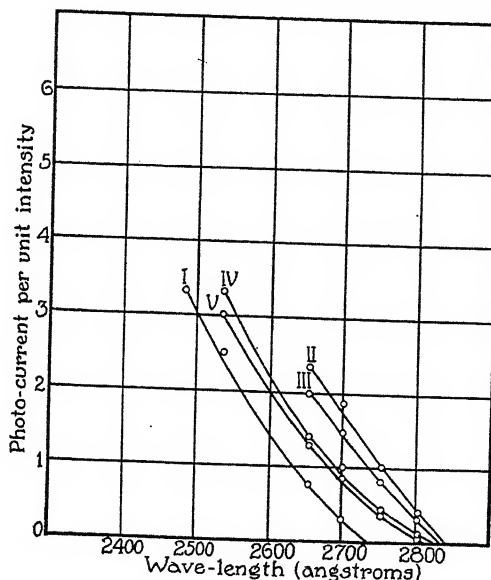


Fig. 4. Change of threshold with hydrogen in the still. I. Curve for flowing surface. II. 50 minutes after turning off still. III. 14 hours after turning off still. IV. 85 hours after turning off still. V. 110 hours after turning off still.

sensitivity had been reached, 50 minutes after turning off the still. The threshold shown is 2850A, the same as that reached when hydrogen is not present. The surface was then left standing, and curves III, IV, and V were taken after 14, 85, and 110 hours, respectively. If these are compared with the curves of Fig. 1, obtained similarly but without hydrogen present in the still, it is seen that the rate of fall of the threshold is now much less.

After curve V of Fig. 4 had been taken, the still was again started, the hydrogen being allowed to remain. After two hours of running, the normal threshold of 2735A was obtained. The time of rise after turning off the still was 44 minutes. The next day a repetition of the experiment gave 84

minutes, while three days later 124 minutes was required. This last result is shown in curve III, Fig. 3. In all cases the threshold reached the maximum of 2850A.

The hydrogen was then pumped from the still, the pumping being continued for several days and the still operated at the same time, in order to free the mercury from hydrogen as completely as possible. The time of rise was then found to be 20 minutes. Two weeks later it had fallen to 14 minutes. A second admission of hydrogen to the still increased the time again to 122 minutes, checking the former result.

From this behavior we may draw three conclusions: first, hydrogen does dissolve appreciably in the mercury and flow with it to the photo-cell; second, this dissolved hydrogen does not change the threshold of the clean running surface; third, the action of some other impurity is greatly impeded by the presence of the hydrogen. The explanation of this third result would seem to be that the hydrogen evaporates from the mercury surface and diffuses away from it, resulting in a lowering of the pressure of the other impurity in that vicinity.

The possibility of such an indirect effect of hydrogen, and perhaps of some other gases, should be considered in connection with many other photo-electric experiments. For example, Dümpelmann and Hein⁴ have found that the photo-electric sensitivity of a metal plate is increased when either hydrogen or oxygen is generated electrolytically on the other side of the plate. It is probable that this is due, not to any direct effect of the gas upon the photo-electric properties of the metal, but rather to the driving away, by the gas diffusing through the plate, of some other impurity that has been holding down the sensitivity.

In conclusion, I wish to express my warmest thanks to Professor R. A. Millikan for his direction of the work here reported.

NORMAN BRIDGE LABORATORY OF PHYSICS.
CALIFORNIA INSTITUTE OF TECHNOLOGY.
September 30, 1926.

⁴ R. Dümpelmann and W. Hein, Zeits. f. Physik, 22, 368 (1924).

ON ATOMIC PROPERTIES WHICH MAKE
AN ELEMENT A METAL

BY K. F. HERZFELD

ABSTRACT

A criterion for determining when an element will show metallic conductivity.— From the dielectric constant of a gas or from its refractive index, extrapolated to long wave-lengths, the molar refractivity R can be calculated. In the solid or liquid state we have $(n^2 - 1)/(n^2 + 2) = Rd/M$. The left side cannot be larger than 1. If the right side becomes larger than 1, the dispersion electron is set free and the body then has metallic conductivity. The necessary and sufficient condition for metallic conductivity is therefore $R > M/d$. The prediction is verified in the case of metals for which the refractive index is known or for which it can be calculated. It is shown that the condition is probably satisfied in the case of metals for which the refractive index cannot be calculated with certainty. The conductivity of sodium dissolved in liquid ammonia is discussed.

FOR a transparent body the refractivity, $(n^2 - 1)/(n^2 + 2)$, is proportional to the density. That $(n^2 - 1)$ does not vary proportionally with d is explained as follows. The polarization of a medium under the influence of an external electric force increases not only directly with increase in the number of molecules in unit volume, but also because of the presence of other polarized molecules near the one in question. These give rise to a force helping the external field, the so-called Lorentz-Lorenz force.

If p is the electric moment of a molecule and N the number of molecules per cm^3 , the polarization of 1 cm^3 will be

$$P = Np$$

The polarization of a molecule under the action of an electric force E is proportional to the force, thus $p = rE$ and we have for higher densities the equation

$$p = r(E + 4\pi P/3) \quad (1)$$

where the second term in the parenthesis is the Lorentz-Lorenz force. Writing N_L for the number of molecules in the mole, M for the molar weight and R for the molar refractivity, we have

$$4\pi Nr = 4\pi N_L rd/M = 3Rd/M.$$

Since $4\pi P/E = n^2 - 1$, we get

$$n^2 - 1 = 3R \frac{d}{M} \left(1 + \frac{n^2 - 1}{3} \right) \quad (2)$$

or

$$(n^2 - 1)/(n^2 + 2) = Rd/M \quad (3)$$

As an example of the constancy of R we may recall that R for carbon disulfide vapor is 0.2805, while for the liquid it is 0.2898. The slight deviation of 3 percent between these two figures has to be explained by a real change in the molecule, a "deformation."¹ Of course the particular factor $\frac{1}{3}$ in Eq. (1) is valid only in isotropic or cubic substances.

Now it is quite clear that the value of the left side of Eq. (3) cannot be larger than 1. What happens, then, if we start with a substance of large refractive index in the gaseous state and compress it, increasing the value of Rd/M until it reaches 1? We may answer this question by considering the equation of motion of the dispersion electrons in the molecule according to the classical theory. In a single molecule this equation would be

$$m\ddot{p} + 4\pi^2 m v_0^2 \dot{p} = e^2 f E$$

where v_0 is the characteristic frequency in the free molecule and therefore a measure of the force holding the electron in the molecule; f is the number of dispersion electrons.

For higher densities the above equation must be replaced by

$$m\ddot{p} + 4\pi^2 m v_0^2 \dot{p} = e^2 f (E + 4\pi P/3) = e^2 f (E + 4\pi N p/3)$$

or

$$m\ddot{p} + 4\pi^2 m v_0^2 (1 - Ne^2 f / 3\pi m v_0^2) \dot{p} = e^2 f E \quad (4)$$

Now we have

$$Ne^2 f / 3\pi m v_0^2 = Rd/M \quad (5)$$

R being taken for infinitely long waves of incident light. Therefore the characteristic frequency of the electrons in the molecule is diminished to the value

$$v_0(1 - Rd/M)^{1/2}$$

If Rd/M is equal to 1 the resultant force on the electron vanishes; the electron is set free.*

We conclude that the necessary and sufficient condition for a substance to have metallic conduction in the liquid or solid state is the following; It must have such a high value of R (which can be found by measuring the index of refraction in the vapor state for infinitely long wave-lengths) that

$$R > M/d \quad (6)$$

if the density of the solid or liquid state is inserted. This applies only if the vapor is monatomic, the solid nearly cubic or the liquid also monatomic.

¹ K. Fajans and G. Joos, Zeits. f. Physik 23, 1 (1924).

* If we have a thin gas with N molecules, each with one isotropically bound electron the system has $3N$ equal natural frequencies. Increase of the density increases the coupling, and this splits up the coincidence. We calculate the three equal lowest frequencies for which alone Equation 1 holds (homogeneous polarization). This mode of vibration is the only one excited by light waves.

TABLE I

Values of R and of M/d for certain elements.

The refractive index n is for the vapor at 0°C and 1 atm. The data for Na were taken from Wood's² paper, for the rare gases from the compilation of Herzfeld and Wolf,³ the rest from Cuthbertson's⁴ measurements.

Element	n	R	M/d (cm ³)	Element	n	R	M/d (cm ³)
Na	1.0041	61	23.6	He	1.0000347	0.518	27.4
Zn	1.00096	14.6	9.2	A	1.000278	4.15	27.8
Cd	1.00134	20.0	13	Kr	1.000418	6.25	38.4
Hg	1.00092	13.74	14.61 (liq.) 14.22 (sol.)	X	1.000682	10.2	37.3
S ₂	1.00100	16.42	31	P ₂	1.00120	17.9	26.6 (metal) 34 (white)
Se ₂	1.00153	22.84	33 (metal) 37 (glass)	As ₂	1.00155	23.1	26.2
Te ₂	1.00237	35.4	40.8				

How well this condition is satisfied is seen by referring to Table I in which are presented the calculated values of R and of M/d for a number of substances whose refractive indices in the gaseous state are known. Of these elements, four are metals with monatomic vapor, Na, Zn, Cd, and Hg. Of these only Na is cubic but we expect no large deviation on account of this fact. For Na, Zn and Cd the relation (6) is fulfilled. For solid Hg Rd/M is 0.965 and the metallic state, which demands that this quantity be greater than 1, can be accounted for by a real change in R , a "deformation" as in the case of CS₂. For liquid Hg the calculated value is 0.94 and the metallic state could be accounted for by a formation of molecules Hg₂, if the distance of the two atoms in the molecule were about $\frac{3}{4}$ of the apparent average distance.

For the rare gases in Table I R is less than M/d as we should expect since they are non-metallic. For the remaining elements listed in the table, which have diatomic molecules, the formula cannot be applied rigorously. If we assume that it can be applied the non-metallic nature would follow from the results. It is gratifying to note that Rd/M has the highest value for Te and As (0.87 and 0.88).

There are no other direct measurements for R except for the gases H₂, O₂, etc., for which it is well known that the value of Rd/M for the condensed state is less than 1. In other gases we could calculate R from the formula

$$R = \sum Ne^2 f / 3\pi mv_i^2 \quad (7)$$

if we knew the electron number f for each absorption line. This number determines the strength of the absorption line.

² R. W. Wood, Phil. Mag. **8**, 293 (1904). The density was calculated with the ratio of fringe shifts at 496 and 644°C, and the absolute value at 500°C given by Zisch, Zeits. f. Physik **8**, 137 (1922). This value was checked by theoretical calculation according to Eq. (5).

³ K. F. Herzfeld and K. L. Wolf, Ann. d. Physik **76**, 71 (1925).

⁴ C. Cuthbertson and E. P. Metcalf, Proc Roy. Soc. A80, 411 (1908); Phil. Trans. **207**, 135 (1906).

For Na it has been shown that the index of refraction of the vapor can be fairly well calculated by taking $f=1$ for both resonance lines (D lines) together and neglecting the others.⁵ We shall now assume the same to be true for the other alkali metals and for copper, silver and gold. The results of the calculations are presented in Table II and are interesting in the following respect. It may be suggested that the non-metallic character of an element is determined by its large energy of ionization, or in other words by the force which holds the electron in place, or by ν_0^2 . While this is true in general, the real determining factor is the ratio of this force to the density fd/M of the dispersion electrons in space. For example, the silver atom with a shell of 18 electrons⁶ holds its dispersion electron much more strongly than do the atoms of the alkali metals. If it had, in the solid state, the large molar volume of potassium (44.7) it would *not* be a metal. It is a metal in spite of the low value of R only because of its low molar volume. On the other hand if the rare gas xenon, with $R=10.2$, had in the solid state the low molar volume of copper, 7.1, it would be a metal.

TABLE II

	Li	Na	K	Rb	Cu	Ag	Au
Resonance line	λ : 6708	5890	7664	7800	3247	3280	2427
	R : 81.5	62.7	107	110	18.95	19.4	10.7
	M/d : 13	23.6	44.7	55.8	7.1	10.2	10.2

For other metals the calculation cannot be made with any certainty. We give in Table III after the symbol of the element the wave-length of the resonance line used,⁷ then the value of R calculated with only one electron contributing to the strength of the line and neglecting other lines, then the molar volume M/d , the minimum f necessary to make the element a metal if no other line contributes, and finally the total number of electrons in the last n_k group. It must be remarked that Kuhn⁸ found for the line 2768 in Tl a value for f of only 0.24, while for the other strong line, 3775, (which for $f=1$ would alone give R a value of 25.7) he found a value for f of but 0.1. With these values for f the two lines together would result in a value for R of but 5.58. So long as we do not know more of the absolute intensities of the absorption lines we cannot give decisive data for the metals listed in Table III.

In this connection we may remark that the condensation of carbon atoms to diamond must result in a marked change in the electron orbits, for otherwise, with the small molar volume of diamond (3.4) and with $f=2$, the diamond would be a metal even if the resonance line had a wave-length as short as 970A.

⁵ Chr. Fuchtbauer and W. Hofmann, Ann. d. Physik 43, 96 (1914). R. Ladenburg and R. Minkowski, Zeits. f. Physik 6, 153 (1921).

⁶ H. G. Grimm, Zeits. f. Phys. Chem. 98, 359 (1921).

⁷ Taken from H. N. Russell, Astrophys. J. 61, 223 (1925).

⁸ W. Kuhn, die Naturwiss. 13, 725 (1925).

TABLE III

Values of R and of M/d for certain metals.
R is calculated from Eq. (7) assuming $f=1$ for the single resonance line given in the second column.

Element	λ	$R(f=1)$	M/d	$f(\text{min})$	Electron number in last group
Be	2348	10.0	5.2	0.52	2
Mg	2852	14.7	14.1	0.96	2
Ca	4226	32.0	25.9	0.81	2
Sr	4607	38.4	34.5	0.90	2
Ba	5535	55.4	36	0.65	2
B	2498	11.3	4.5	0.4	1
Al	3961	29.3	10	0.34	1
Ga	4033	29.3	11.8	0.40	1
In	3256	19.1	16.1	0.84	1
Tl	2768	13.8	17.2	1.25	1
Pb	2833	14.5	18.25	1.26	2
Ti	3998	29.0	10.7	0.37	4
V	3841	26.6	9.28	0.35	5
Cr	4254	32.7	7.76	0.24	6
Mo	3902	27.6	10.65	0.39	6
Mn	4030	30.0	7.4	0.25	7
Fe	3720	25.9	7.1	0.27	8
Co	3465	21.6	6.8	0.31	9
Ni	2320	9.7	6.7	0.69	10
As	2349	10	13.1	1.31	3
Sb	2311	9.75	18.5	1.9	3
Bi	3067	17.0	21.5	1.27	3

It is well known that according to Kraus⁹ sodium dissolved in liquid ammonia is a conductor. If the molar conductivity is plotted against concentration it shows first for increasing concentration a decrease, as usual in electrolytes. But above 1 mole in 20 liters there is a slight increase and above 1 mole in 900 cm³ there is a strong increase in conductivity with concentration. From considerations similar to those already mentioned we should expect that in ammonia the valence electrons are set free by mutual action of neighboring sodium atoms at concentrations above 1 mole in 500 cm³, while for lower concentrations the conductivity would be due only to the action of ammonia on the sodium.

JOHNS HOPKINS UNIVERSITY
 PHYSICAL LABORATORY
 February 26, 1927.

⁹ C. A. Kraus, Jour. Am. Chem. Soc. 43, 749 (1921).

THE ABSORPTION OF RADIO WAVES IN THE UPPER ATMOSPHERE*

By E. O. HULBURT

ABSTRACT

Recent measurements have shown that radio waves below 150 meters fall off in intensity faster than required by an inverse square law for distances up to 1000 miles. This points to absorption of the wave by the medium, in this case the upper atmosphere. The absorption of the waves variously polarized is calculated on the assumption that it results from collisions between the electrons and molecules of the atmosphere. With reasonable average values of the electronic and molecular densities the amplitude A of the wave λ cms at a distance x cms is $A = \alpha x^{-1} \exp(-11.8 \times 10^{-16} \lambda^2 x)$, theoretically valid for waves from 16 to 160 meters to distances of 1000 miles. This agrees well enough with the scant range and intensity data, and it is pointed out that an extension of these data may lead to more exact knowledge of the overhead electronic and molecular pressures. From the absorption curves interesting possibilities appear of polarization of waves in the broadcast band 200-600 meters.

IN RECENT papers^{1,2} a quantitative theory of the manner in which radio waves pass over the earth has been developed. The waves are shown to reach distant points on the surface of the earth by passage through the outlying regions of the earth's atmosphere being refracted downward by the electrons of those regions. From the simple fact that radio waves, particularly of wave-length below 90 meters, are transmitted successfully with relatively small amounts of power to distances as great as half-way around the earth, it was assumed that the attenuation of the waves in the upper atmospheric strata was slight. As a matter of fact absorption of energy from the wave by the atmosphere was put aside entirely, but the calculations were made in such a way as to be undisturbed by a small absorption which of course exists. In the present paper the influence of absorption is considered with the result that certain facts about the ranges of the waves of the radio spectrum begin to be more clearly understood.

The optical properties of the upper reaches of the atmosphere are assumed to depend upon the molecules, ions and electrons which exist there. The magnetic field of the earth has an important influence which is recognized in the formulas. The electrons contribute largely to the dispersion of the electromagnetic waves, the molecules and ions only a secondary part in so far as they interfere with the electrons. All, however, contribute to the absorption, for we shall assume that the most important cause of the absorption of energy from the wave arises from collisions between the electrons and molecules. The effect of collision is to transfer a portion of the energy which the electron has received from the waves to the molecule and produce the

* Published by permission of the Navy Department.

¹ Taylor and Hulbert, Phys. Rev. 27, 189 (1926).

² Hulbert, Journal of the Frank. Inst. 201, 597 (1926).

disorderly motion called heat. The ions may justifiably be treated as molecules, for the effect of their charges on the dispersion and absorption is negligible (see reference 2, page 610). With these assumptions the general formulas for the dispersion and absorption are all available in treatises on magneto-optics, for example Lorentz³, and therefore for the special formulas developed here we need only record a few of the more essential steps. If an electron of mass m experiences f collisions per second with the molecules, it has been shown⁴ that this may be expressed as a frictional force gv on the electron, where v is the velocity of the electron and g is given by

$$g = 2mf. \quad (1)$$

In this formula the collisions are regarded as inelastic; this is a true absorption of energy. Other types of collisions may occur, such as elastic ones which cause scattering of the energy, etc. A more extended treatment may therefore be expected to modify (1). The change will probably not be great and for the present, at any rate, we shall be content to use (1) as it stands.

In writing down the equations of motion of the electron we assume no restoring force due to the medium and no effect of the electrons of each other. Let E_x and ξ be the X components of the electric force and the displacement of the electron, respectively, and η , ζ , E_y and E_z the Y and Z components of the quantities. N is the number of electrons per unit volume, e and m are the electronic charge and mass. The earth's magnetic field H is in the direction of the axis of Z . In c.g.s. electromagnetic units the equations of motion of the electron are

$$\left. \begin{aligned} m\ddot{\xi} &= eE_x - g\dot{\xi} + He\dot{\eta}, \\ m\ddot{\eta} &= eE_y - g\dot{\eta} - He\dot{\xi}, \\ m\ddot{\zeta} &= eE_z - g\dot{\zeta} \end{aligned} \right\} \quad (2)$$

The exact solutions of (2) are extremely cumbersome. The solutions become much simpler, however, if (following Lorentz) the approximation is adopted that the absorption is small in the space of a wave-length; fortunately this approximation is entirely acceptable in the case of the radio waves.

For incident plane waves advancing in the direction of H the approximate solution of (2) yields two circularly polarized components of refractive indices μ and absorption coefficients κ given by

$$\mu^2 = 1 - \frac{C\lambda^2(1-\lambda/\lambda_0)}{(1-\lambda/\lambda_0)^2 + G^2\lambda^2}, \quad (3)$$

$$\kappa = \pi CG / [(1/\lambda - 1/\lambda_0)^2 + G^2], \quad (4)$$

³ H. A. Lorentz, "The Theory of Electrons," Chap. IV (1916).

⁴ Lorentz, Loc. cit., p. 309 or more recently, Houston, Phil. Mag. 2, 512 (1926).

and

$$\mu^2 = 1 - \frac{C\lambda^2(1+\lambda/\lambda_0)}{(1+\lambda/\lambda_0)^2 + G^2\lambda^2}, \quad (5)$$

$$\kappa = \pi CG / [(1/\lambda + 1/\lambda_0)^2 + G^2], \quad (6)$$

where

$$C = Ne^2/\pi m, \quad \lambda_0 = 2\pi cm/He, \quad G = g/2\pi cm = f/\pi c \quad [\text{From (1)}], \quad (7)$$

c being the velocity of light in vacuum. With the value 0.5 gauss for H , λ_0 from (7) comes out to be 214 meters. The absorption coefficient κ is defined by the relation

$$A = A_0 e^{-\kappa x} \quad (8)$$

where A_0 is the initial amplitude of the wave and A the amplitude after traversing x cms of the medium.

For incident plane waves advancing normally to the magnetic field the solution of the equations of motion yields two plane polarized components, respectively parallel and perpendicular to H , of refractive indices μ and absorption coefficients κ given by

$$\mu^2 = 1 - \frac{C\lambda^2}{1 + G^2\lambda^2}, \quad (9)$$

$$\kappa = \pi CG / (1/\lambda^2 + G^2), \quad (10)$$

and

$$\mu^2 = \frac{(A^2 + B^2)^{1/2} + A}{2Q}, \quad (11)$$

$$\kappa^2 = \frac{2\pi^2}{\lambda^2} \frac{(A^2 + B^2)^{1/2} - A}{Q}, \quad (12)$$

where

$$A = pq + rs, \quad B = ps - rq, \quad Q = q^2 + s^2; \quad p = (1 + \alpha)^2 - \gamma^2 - \beta^2,$$

$$r = 2\beta(1 + \alpha), \quad q = \alpha(1 + \alpha) - \gamma^2 - \beta^2, \quad s = \beta(1 + 2\alpha);$$

$$\alpha = -1/C\lambda^2, \quad \beta = CG/\lambda, \quad \gamma = 1/C\lambda\lambda_0.$$

Expression (10) is an approximation based on small absorption, just as was the case in (3) and (4); it refers to the component with electric vector along H , and therefore to propagation in the absence of the magnetic field. Expression (12), however, which refers to the electric vector normal to H , is exact; the approximation of small absorption did not lead to much simplification. For no absorption, $g = G = \kappa = 0$, and the four formulas for μ , (3), (5), (9) and (11), reduce respectively to the formulas (2), (3), (5) and (6) of the earlier paper.¹

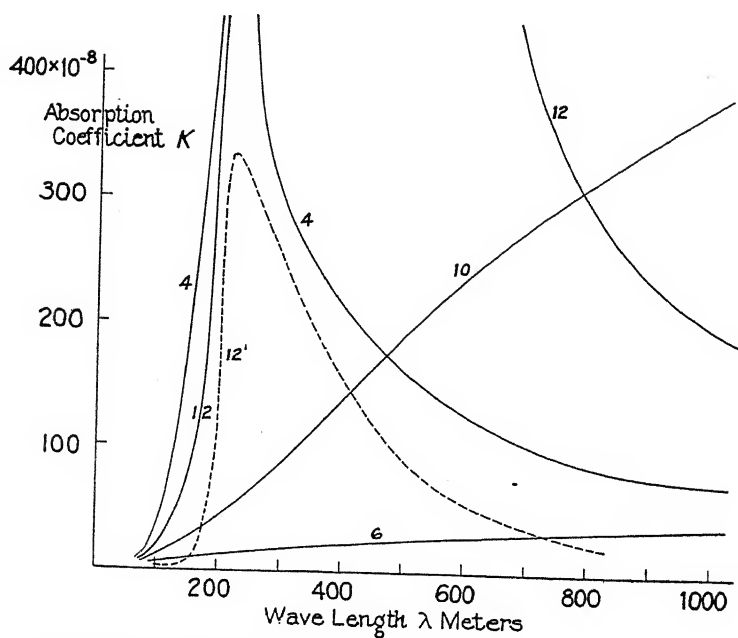


Fig. 1. Absorption coefficients of the upper atmosphere as a function of the wave-length for rays in and perpendicular to the earth's magnetic field, from equations (4), (6), (10) and (12). Curve 12' is curve 12 with ordinates reduced ten times.

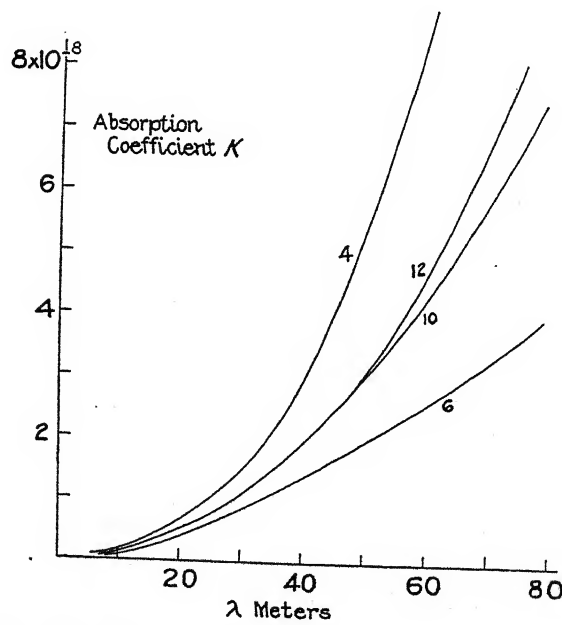


Fig. 2. The short wave portion of Figure 1 on a larger scale.

To bring out the general character of the absorption, κ from formulas (4), (6), (10) and (12) is plotted in curves 4, 6, 10, and 12, Fig. 1, respectively with $\lambda_0 = 214$ meters, $C = 2.5 \times 10^{-11}$ or $N = 280$ electrons per cc, and with $G = 1.5 \times 10^{-6}$. Curve 12 rises to such high values as to be off the page, so that it has been drawn again in curve 12', Fig. 1, on the same abscissas, but with ordinates ten times reduced. Since we shall be interested in the curves in the region of shorter waves below 100 meters, the respective formulas for κ have been plotted on a larger scale in the curves 4, 6, 10, and 12 of Fig. 2.

EXPERIMENTAL DATA

A program of measurements of the electric field A of the received wave at various distances from the transmitter for the shorter waves, below 200 meters, has recently been entered upon by Heising, Schelleng and Southworth.⁵ We choose a portion of their data for wave-lengths 44 and 66 meters under full daylight conditions; these are plotted respectively in curves 1 and 2, Fig. 3, in which the ordinates are the field strengths A in arbitrary

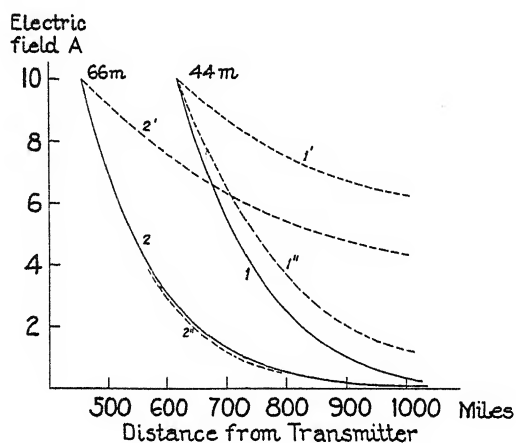


Fig. 3. The electric field as a function of the distance from the transmitter for a 44 and a 66 meter wave; curves 1 and 2 observed, curves 1' and 2' calculated by the inverse distance law, curves 1'' and 2'' calculated from (15).

units and the abscissas are the distances from the transmitter in miles. The curves do not claim great accuracy, their smoothness in the drawing really gives a wrong impression of the precision. They represent averages of field strengths which fluctuated over wide limits from day to day. Qualitative observations of the strengths of signals with waves below 100 meters have been recorded by Prescott,⁶ these are, however, unsuited to quantitative calculations. We shall have use for Taylor's⁷ ranges of transmission. These ranges in miles, under full daylight, averaged throughout a year for uniform

⁵ Heising, Schelleng and Southworth, Proc. Inst. Rad. Eng. 14, 613 (1926).

⁶ Prescott, "QST" 10, 9 (1926).

⁷ Taylor, Proc. Inst. Rad. Eng. 13, 677 (1925).

transmitting conditions, i.e. five kilowatts in a normal transmitting antenna, are plotted in curve 1, Fig. 4 as ordinates against the wave-lengths as absciss-

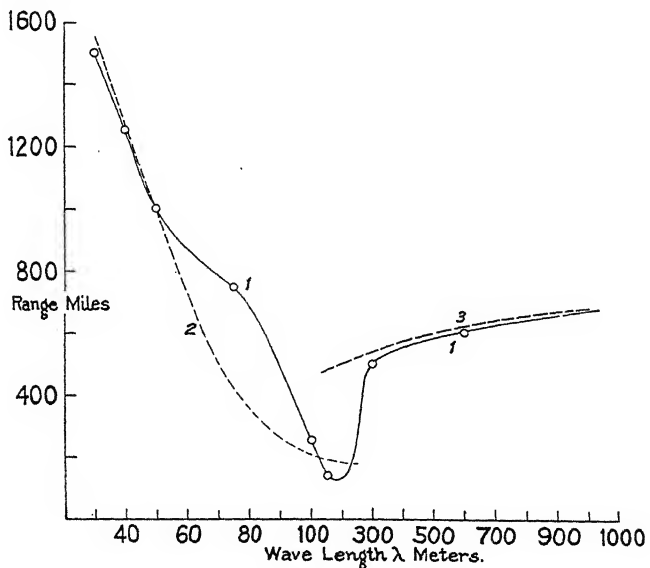


Fig. 4. The average daylight ranges, for uniform transmitting conditions, as a function of the wave-length; curve 1 observed, curves 2 and 3 calculated from (15) and (14) respectively.

sas. For the sake of clearness the scale of the abscissas for waves below 100 meters is ten times that for waves above 100 meters.

APPLICATION OF THE FORMULAS

Before entering upon a discussion of the experimental data in the light of the theoretical formulas, it is well to fix ideas by referring to Fig. 5, which shows the ray path ace of a 66 meter wave, and afe of a 44 meter wave, from

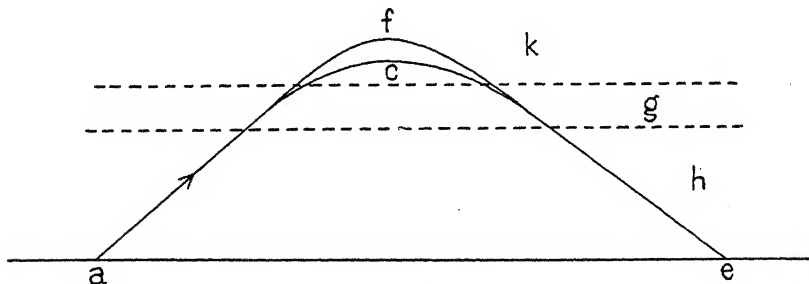


Fig. 5. Refraction of rays in the electronic regions g and k .

the transmitter a to the receiver e . In the region h of the atmosphere there are no electrons and the rays are straight. In the region g , marked off from h by a dotted line in Fig. 5 there are a considerable number of electrons and air molecules; it is here that the absorption may be supposed to

occur. Above this there is a region k of greater electronic density, but of lower molecular density, so that the absorption is again slight. The electronic density increases with the height reaching a value of the order of 10^5 at about 100 miles above the earth (an average for daylight over a year¹). In the regions g and k the rays bend over and return to the earth, and as seen from the refraction formulas (3), (5), (9) and (11) the 66 meter path is below the 44 meter ray. There is evidence² that the electron density sets in rapidly above h so that the curved portions of the ray paths are relatively short compared to the whole length of the path, and therefore the paths of a 44 and a 66 meter wave, for example, will not differ greatly.

We may now turn to the data of curves 1 and 2, Fig. 3, which have been chosen for numerical discussion for particular reasons. These curves give the electric fields of the 44 and 66 meter waves at distances from 600 to 1000 miles from the transmitter. At these distances the direct ground wave was absent so that the field strengths were due to rays refracted downwards from the upper atmosphere. Furthermore, multiple reflections and focussing of the rays by the electronic regions are probably of small influence here, so that for a given wave-length and state of polarization a single ray from the transmitter to a receiver may be assumed. The transmitter is considered to deliver its rays impartially in all directions to perhaps 30° above the horizontal. We shall further assume that the length of the ray path may be roughly calculated as if the ray travelled in a straight line to a height of 100 miles and there experienced sharp reflection. Thus, the ray path distance x is related to d , the great circle distance to the transmitter, by the equation, $x = (d^2 + 4h^2)^{1/2}$, h being 100 miles, and for $d > 400$ miles, $x = d$, approximately. If the electric field of the wave diminished inversely with the distance (i.e. the energy inversely with the square of the distance) the field strength would be shown in curves 1' and 2' of Fig. 3. In short, the observed field strengths fall off much more rapidly with the distance than the inverse first power; this too for the case, purposely selected, in which one might expect the inverse first power law to hold full sway. Evidently an additional cause of energy degradation is at work, and we take this to be the absorption of energy from the wave by the atmosphere.

We then write

$$A = A_0(x_0/x)e^{-\kappa(x-x_0)}, \quad (13)$$

where A and A_0 are the field strengths at ray path distances x and x_0 , respectively, and κ is the absorption coefficient defined in (8).

For the moment we must leave the ray picture of Fig. 5, to return to it later, and assume that the optical properties of the atmosphere are constant along the entire path of the ray. The absorption coefficient κ may then be calculated for $\lambda 66$ meters by substituting in (13) the coordinates of the ends of curve 2, Fig. 3, and comes out to be 5×10^{-8} . With this value of κ the curve 2'' was calculated corresponding to the observed curve 2; it is seen that the two curves are in close agreement. We might now determine κ for $\lambda 44$

¹ Breit and Tuve, Phys. Rev. 28, 554 (1926).

meters from curve 1, Fig. 3, in a similar manner, and then by substituting the respective values of κ for $\lambda 44$ and $\lambda 66$ meters in, say, formula (10) obtain two equations in the two unknowns C and G , and thereby determine C and G . Unfortunately such a procedure yields meaningless values for C and G , merely because the data of curves 1 and 3, Fig. 3, are not sufficiently accurate. It seems therefore best to proceed by making a frank assumption, namely, that throughout the course of the ray the average number of molecules per cc is 5×10^{14} ; this pressure corresponds to a height above the earth of about 50 miles.⁹ With a value -50°C for the temperature the number of collisions f which an electron makes per second with the molecules is calculated from classical kinetic theory to be 1.4×10^6 . From (1) and (7) this gives $G = 1.5 \times 10^{-5}$. Referring only to the state of polarization represented by (10) we introduce the value of G into (10) together with $\kappa = 5 \times 10^{-8}$ for $\lambda 66$ meters, and find $C = 2.5 \times 10^{-11}$ and 280 for the electronic density N . With the constants thus determined κ is calculated from (10) to be 2.29×10^{-8} for $\lambda 44$ meters, and the intensity degradation curve for this wave-length corresponding to the observed curve 1, Fig. 3, is calculated. This is given in curve 1'', Fig. 3, and is seen to agree with curve 1 within the error of observation.

It is of interest to see what can be done with the range curve 1 of Fig. 4, which gives the ranges reached by the various waves. We take this to mean the distance at which the wave amplitude is a constant small value, i.e. the value just detectable. (It will be appreciated that this is exactly the case of the intensity distribution curves of spectrum lines or bands derived from neutral wedge spectra.) Thus A in (13) is a constant, and (13) can therefore be used to calculate the ranges x or d , (x being the ray path distance and d the great circle distance) for values of λ by using the κ corresponding to each λ determined from (10) with the constants $C = 2.5 \times 10^{-11}$ and $G = 1.5 \times 10^{-5}$ given in the preceding paragraph. The quantity x_0 being entirely arbitrary is taken to be small with respect to x so that it disappears from the exponent in (13). The calculated range curve, made to pass through one observed point, i.e. 1000 miles for $\lambda 50$ meters, is given in the dotted curve 2 of Fig. 4 and agrees with the observed curve within the error of experiment for the waves from 16 to 150 meters. For waves longer than 200 meters the calculated ranges are below the observed values, as indeed is to be expected, since for these wave-lengths the ground wave is predominant at the shorter distances and the overhead ray is relatively feeble.

At first sight the fair agreement which has been reached between theory and experiment might appear meaningless. So many simplifying assumptions have been made that the theoretical picture might seem to have but little resemblance to reality. The considerations which follow, however, indicate the agreement to be genuine and to offer strong support of the theoretical ideas. The foregoing calculations are valid, within limits, for the general case of random polarization, in spite of the fact that they have been based on the absorption formula (10) which refers to a ray polarized in a particular

⁹ Humphreys, "Physics of the Air," 1920.

way. For, an exactly similar calculation with each of the other types of polarization represented by (4), (6), and (12) yields agreement with the experimental curves of Fig. 3 and 4 similar to that obtained with (10). This comes about because the values of κ from one of the curves of Fig. 2 are roughly proportional to those from any of the other curves. We have assumed that the rays pass through a homogeneous medium composed of, for example, 5×10^{14} molecules and 280 electrons in each cc, these numbers giving the desired values for the absorption. However, because of the approximately linear relation between κ , N and the molecular density we may keep the absorption values undisturbed and at the same time suppose that the absorption exists only in a certain fractional part of the ray path (the electrons having a density greater than 280, of course). Thus we return to the more exact conception of the ray paths sketched in Fig. 5, in which the absorption occurs only in the region g . The numbers 5×10^{14} and 280 are therefore to be regarded as properly chosen equivalent average values over the ray path.

The values of the molecular and of the electronic density are of course in no wise fixed by the foregoing calculations. The one has been a proper guess and the other has been calculated from it; when regarded as average values over the ray path the numbers are perhaps reasonable. With the experimental radio data at present this is about all that can be done. As these data improve and become more numerous we may hope that they may be fitted into a general scheme which in the end will depict the electronic and molecular pressures at all heights above the earth to which we may direct a radio ray so that it will return. We may take this occasion to mention that throughout this and the earlier papers^{1,2} we have been at pains as far as possible to draw conclusions as to the electrons, etc., of the upper atmosphere from the radio wave phenomena only. With the idea, wise or unwise, that these inferences may be entirely independent of, and therefore worthy of comparison with, similar inferences from other fields of experiment^{10,11}. Meanwhile others^{12,13} have been attacking the converse problem of calculating the ionization by means of the absorption of radiation, or in other ways, and from this to derive the facts of radio. However, we prefer to regard the radio waves as a means, and a fruitful one, of plumbing the outer depths just as the earthquake waves of seismology serve to search the earth beneath.

From the present viewpoint two programs, rather prosaic perhaps, of experimental measurements suggest themselves, namely, measurements of average field intensities of waves below 200 meters and observations of the polarizations of waves, say, 100 to 1000 meters, throughout distances to 2000 miles or more from the transmitter. The first is an extension of the curves of Fig. 3 and the work of Austin,¹⁴ the second is touched upon,

¹⁰ Chapman, Roy. Meteor. Soc., Quarterly Journal 52, 225 (1926).

¹¹ Bendorf, Phys. Zeitschrift 27, 686 (1926).

¹² Rice and Baker, Journ. Amer. Inst. Elect. Eng. 45, 535 (1926).

¹³ Lassen, Zeits. f. Hochfrequenztechnik, 28, 109 and 139 (1926); Elias, ibid., 27, 66 (1926).

¹⁴ Austin, Bull. Bur. Stand. 7, 317 (1911).

although slightly, in the experiments of Picard,¹⁵ of Smith-Rose and Barfield,¹⁶ and of Appleton.¹⁷ One must however, refrain from being too sanguine of the success of such programs. An experimental analysis of the received wave to discover its state of polarization is not simple. The ground causes complicating effects and the state undoubtedly varies more or less rapidly with the time. Particularly in the broadcast range of wave-lengths from 200 to 600 meters a glance at the absorption curves of Fig. 1 and the refraction curves (readily plotted from (3), (5), (9), and (11).) indicates a rather bewildering array of possible states of polarization. Apparently one might simplify things by dealing with east-west or north-south propagation, particularly at the equator where the earth's magnetic field is horizontal, or at the magnetic poles where it is vertical.

A discussion of the amplitudes of radio waves as a function of the distance from the transmitter is hardly complete without reference to the experimental measurements of Austin¹⁴ on waves longer than 300 meters. These, for daylight conditions, are expressed in condensed form by the Austin-Cohen formula, which may be written

$$A = (aA_0/d)e^{-bd/\lambda^s}, \quad (14)$$

where a , b and s are constants and d is the great circle distance to the transmitter. If the curves of Fig. 3 are calculated from (14) values much too low are found, as indeed is to be expected since (14) is not valid for the shorter waves. Using (14), with Austin's values for b and s , to calculate the range curve of Fig. 4 we obtain the dotted curve 3, which agrees very well with the observations at the longer wave-lengths. This merely means that Taylor's independent measurements were consistent with those of Austin. Formulas (13) and (14), although somewhat similar, should not be confused; they supplement each other. (13) gives the theoretical received amplitude due to a single overhead ray, for waves below 150 meters, whereas (14) gives the actual received amplitude, which in the general case may be due to several overhead rays and a ground ray, for waves longer than 300 meters. The complete theoretical amplitude degradation formula embracing all wave-lengths will perhaps be similar in form to these. Even now for practical purposes formula (13) with the value of κ from (10) may be used to calculate the relative amplitudes of the shorter waves at various distances from the transmitter under full daylight conditions. We obtain to a sufficiently close approximation,

$$A = (\alpha/x)e^{-\pi CG\lambda^2 x} = (\alpha/x)e^{-11.8 \times 10^{-10} \lambda^2 x}, \quad (15)$$

where α is a constant and λ and x are in cms, x being the ray path distance. (15) is valid for wave-lengths from 16 to 150 meters to distances of 1000 miles from the transmitter, and therefore covers as great a range of frequencies and distances as the Austin-Cohen formula. Because of the direct ground wave

¹⁵ Picard, Proc. Inst. Rad. Eng. 14, 205 (1926).

¹⁶ Smith-Rose and Barfield, Proc. Roy. Soc. 110A, 580 (1926).

¹⁷ Appleton, Proc. Roy. Soc. 109A, 621 (1926).

the formula does not hold too near the transmitter, for 75 meters waves within, say, 100 miles, and for longer waves within longer distances. The ground wave, however, can be calculated from the Sommerfeld formula.¹⁸ Expression (15) of course is not true at great distances. For instance, in the case of a 30 meter wave it gives at 5000 miles from the transmitter 10^{-7} , and at 3000 miles 10^{-4} , of the energy at 1000 miles, and qualitative experience indicates that the signal strengths are usually greater than these numbers. At great distances the showering down of energy from the upper atmosphere, or, in other words, the contribution of many possible ray paths, is sufficient to overshadow an inverse square law of energy attenuation further weakened by exponential absorption.

NAVAL RESEARCH LABORATORY,
WASHINGTON, D. C.,
January 7, 1927.

¹⁸ Sommerfeld, Ann. d. Phys. 28, 665 (1909).

ELECTRICAL MEASUREMENTS AT RADIO FREQUENCIES

By S. L. BROWN AND M. Y. COLBY

ABSTRACT

Methods of measuring resistance, inductance, capacity, and impedance at radio frequencies.—Resistance, inductance, capacity, and impedance are measured at radio frequencies with the aid of a vacuum tube voltmeter. The experiments described and the data presented illustrate methods of measurement at radio frequencies that are comparable to the corresponding measurements at low frequencies with regard to both simplicity and accuracy. The results indicate that the resistance of a circuit may be measured with an accuracy of one percent at a frequency of several million cycles per second when the value of the resistance is of the order of 0.01 ohm. Much lower values can be measured with a reasonable degree of accuracy. The calculated value of the high frequency resistance of No. 22 copper wire differs from the measured value by less than one percent. The inductance of a portion of a circuit may be measured by a voltmeter-ammeter method with an accuracy of one percent, even though the value of the inductance be only a small fraction of a micro-henry. The calculated values of the inductance of either a circular coil of one turn or two parallel wires forming a return circuit agree with the measured values. Capacities of the same order of magnitude as the smallest readable variation of the variable standard condenser which is used to tune the circuit may be very quickly and easily determined. The measured and the calculated values of the capacity of two parallel wires are in very close agreement. Certain rolled plate types of telephone condensers have sufficient internal inductance to cause them to resonate at low radio frequencies.

The methods of making many radio frequency measurements have been improved: (a) By using such a low resistance circuit that the coupling to the source of power could be made very loose. The coefficient of coupling was frequently as low as 1×10^{-6} . (b) By using a negligible amount of power from the oscillator, with the result that the e.m.f. induced in the tuned circuit remained constant. The power drawn seldom exceeded 2×10^{-5} watts. (c) By employing a sensitive and accurate voltmeter that is independent of frequency. Voltage changes of 0.2 millivolts could be detected by this instrument.

THE problem of simplifying many measurements at radio frequencies was undertaken by the authors nearly two years ago, after the development of a sensitive vacuum tube voltmeter¹ which is reliable for all frequencies, including the higher radio frequencies. The accurate measurement of such fundamental quantities as resistance, inductance, capacity, and impedance at radio frequencies may be facilitated by the use of this instrument. When the quantities to be measured are small, a sensitive vacuum tube voltmeter may be advantageously used in reducing the difficulties encountered in making these measurements, and an accuracy comparable to that obtained in low frequency measurements can be obtained. The experiments described in this paper were designed to illustrate the advantages that are gained by adapting this voltmeter to radio frequency measurements.

¹ M. Y. Colby, Jour. Sci. Instruments III, 342 (1926).

MEASUREMENT OF A SMALL RESISTANCE

The resistance of an oscillating circuit having very low resistance may be readily determined by a slight modification of the resistance variation method. A diagram of the circuit, the resistance of which is measured, is shown in Fig. 1. The inductance L was made of one turn of No. 0000 copper

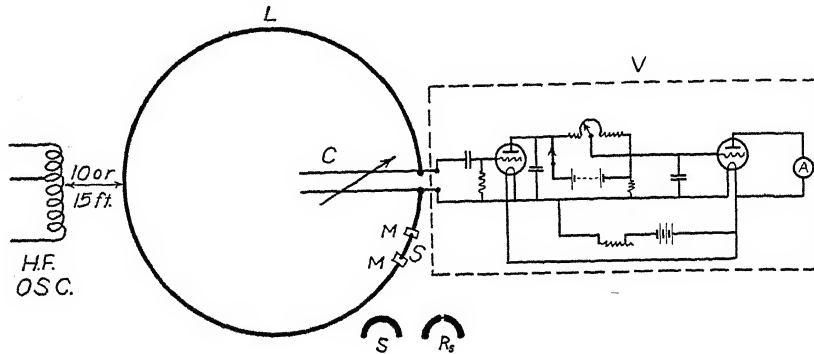


Fig. 1. Diagram of circuit for measuring high frequency resistance.

wire of one foot radius and the condenser C was a low-loss variable air condenser of the Bureau of Standards type. This circuit was very loosely coupled to an oscillator and was then tuned to resonance with it. The e.m.f. E_0 across the terminals of the condenser was measured by the vacuum tube voltmeter V . The short-circuit S was next removed and the standard resistance R_s substituted. The new value of e.m.f. E_x across the condenser was observed, and the resistance R_x of the circuit was calculated from the relation,

$$R_x = \frac{R_s}{E_0/E_x - 1}.$$

The values of R_x were always checked by using two standard resistances of different values. Values of the resistance of the circuit shown in Fig. 1, determined by this method, are given in Table I for several different frequencies.

TABLE I
High frequency resistance of a low resistance circuit

λ	C	R_s	E_0	E_x	R_x
119 m.	3885 $\mu\text{uf.}$.0626 ohms	.372 v.	.151 v.	.0428 ohms
119	3885	.0253	.360	.226	.0427
102	2866	.0626	.385	.166	.0476
102	2866	.0253	.383	.250	.0476
82	1827	.0626	.354	.171	.0585
82	1827	.0253	.368	.258	.0592
58	949	.0626	.368	.214	.0870
58	949	.0253	.370	.286	.0864
43	513	.0626	.350	.240	.1365
43	513	.0253	.394	.333	.1380

The short-circuit S was made of about two inches of No. 0000 copper wire, bent so as to fit into the mercury cups MM . The standard resistance R_s was an exact duplicate of the short circuit S , except that about one-eighth of an inch of the large copper wire was cut out and replaced by an equal length of manganin wire of small enough cross section that the skin effect was negligible. The use of this type of short-circuit and standard resistance insures a constant coefficient of coupling by making it unnecessary to change the shape, size, position, or configuration of the circuit when inserting or removing the standard resistance.

When the resistance of a circuit is very low, this plan of measurement, in terms of the e.m.f. across the reactance of the tuned circuit, is obviously superior to the usual plan, which involves the determination of the resonant current by means of an ammeter included in the tuned circuit. The chief advantage of this modification of the resistance variation method of measuring resistances over that usually practiced is that the resistance of the measuring instrument is not included in the resistance to be measured. In the case described here, the resistance of the circuit is so small that it might easily be concealed in the error of measurement if it is increased by the amount of the ammeter resistance.

To illustrate how a small resistance may be measured at radio frequencies, the circuit of Fig. 1 was employed. A length of approximately 1.5 inches of No. 22 copper wire was used. Short pieces of No. 0000 copper wire were soldered to its ends for making contact in the mercury cups MM . The circuit LC was very loosely coupled to an oscillator by placing the axis of the oscillator coil nearly at right angles to that of L and at a distance of 10 or 15 feet from L . The circuit was then tuned to resonance with the oscillator, and readings of the voltmeter V were taken with S , R_s , and the unknown resistance R_x , respectively, in the circuit. Calling the corresponding electromotive forces E_0 , E_s and E_x ,

$$R_x = R_s \frac{E_0/E_x - 1}{E_0/E_s - 1}.$$

The results obtained by this method are listed in Table II.

TABLE II
Resistance of a short piece of No. 22 copper wire at a frequency
of 3,000,000 cycles per second.

Trial	E_0	E_x	E_s	R_s	R_x
1	.339	.281	.221	.0253	.0098
2	.341	.282	.224	.0253	.0102
3	.369	.305	.240	.0253	.0099

D. C. resistance of R_x measured by bridge .00231 ohms
Diameter measured with micrometer calipers .062 cm
Wave length measured with wave meter 100 meters
 R_x calculated by Bureau of Standards formula² .0100 ohms
 R_x observed, (average) .00997 ohms.

² Bureau of Standards Circular No. 74.

Using a circuit similar to that shown in Fig. 1, the high frequency resistance of a fixed condenser of large capacity was determined. A low resistance coil having the proper inductance to cause the circuit to resonate at the desired frequency was used for L . The resistance of the circuit consisting of the coil L and the variable air condenser C was measured by the method previously described. The high capacity fixed condenser was then inserted in series with L and C , and the resistance of the circuit again measured; the resistance of the fixed condenser was, then, the difference between the two values thus obtained. This method is accurate when the capacity of the fixed condenser is large enough in comparison with that of the variable condenser C so that it is unnecessary to change the setting of C materially in order to retune the circuit after introducing the fixed condenser. Typical results of this measurement are shown in Table III.

TABLE III
High frequency resistance of fixed condensers.

Type of Condenser	Wave Length	Resistance of circuit before inserting condenser	Resistance of circuit after inserting condenser	Resistance of condenser
1 microfarad high voltage paper condenser	645 m. 405	0.213 ohms 0.358	0.295 ohms 0.465	0.082 ohms 0.107
.36 microfarad paper telephone condenser (Figure 6)	645 500 405	0.213 0.28 0.36	3.36 4.08 4.48	3.15 3.80 4.12

MEASUREMENT OF A SMALL INDUCTANCE

The value of a small inductance of negligible resistance may be determined by sending a measured current of known frequency through it and measuring the electromotive force across its terminals with the vacuum tube voltmeter. Thus the measurement of a small inductance at radio frequencies is reduced to the simple voltmeter-ammeter method.

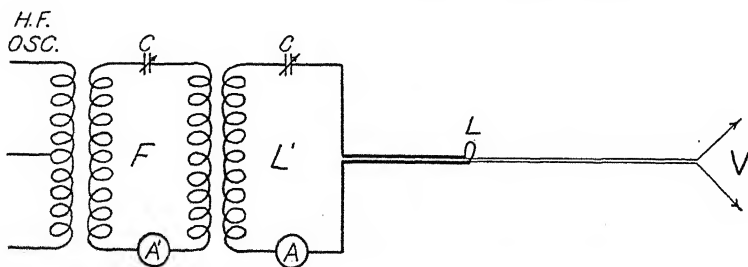


Fig. 2. Diagram of circuit for measuring the inductance of a small loop.

The inductance L of Fig. 2, consisting of a small circular coil of one turn, made of No. 14 copper wire, was connected in series with a coupling

coil L' , a tuning condenser C , and an ammeter A . This circuit was coupled to the high frequency oscillator through the intermediate tuned circuit F , which was used to filter out any harmonics that might be present in the oscillator circuit. The result of a typical measurement is given in Table IV.

TABLE IV

Measurement of a small inductance

Diameter of coil	3.70 cm.
Diameter of wire	.163 cm.
Ammeter reading	103 m. a.
Voltmeter reading	204 m. v.
Wave-length (by wavemeter)	710 meters
$L (=E/I\omega)$.0749 μ h.
L calculated from dimensions ^a	.0753 μ h.

The diagram of Fig. 3 shows two No. 10 copper wires WW 1645 cm long, stretched parallel to one another and spaced 10 cm apart. These wires were connected in series with an inductance coil L , a tuning condenser C , and an ammeter A . This circuit was coupled with a high frequency oscillator through the intermediate tuned circuit F . The e.m.f. across a measured

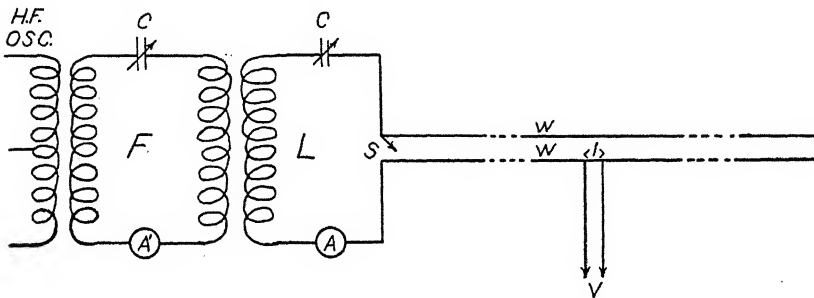


Fig. 3. Diagram of circuit for measuring the inductance of a short section of a straight wire.

length of one of the wires was measured by the voltmeter V , while the current through it was indicated by the ammeter A . The wave-length was determined by means of a wave meter. A few typical measurements by this method are shown in (a), Table V.

The total inductance of the wires WW was then determined in the following manner. With the switch S open, the circuit was tuned to resonance, the ammeter and voltmeter both serving to indicate resonance, and the capacity C_1 of the condenser C was observed. This was repeated with the switch S closed. If we represent the new condenser reading by C_2 , and the total inductance of the wires by ΔL , then,

$$\Delta L = \left[\frac{\lambda}{1.884} \right]^2 \frac{C_2 - C_1}{C_1 C_2} \quad (1)$$

The value obtained by this method is shown in (b), Table V. The length, diameter, and spacing of the wires were carefully measured and the induc-

^a Bureau of Standards Circular No. 74

tance calculated from these dimensions. The value thus obtained is shown in (c), Table V.

TABLE V

(a) *Measurement of a small inductance*

<i>l</i>	<i>I</i>	<i>E</i>	Inductance of <i>l</i>	Inductance per cm.
5 cm.	1 amp.	0.090 volts	0.0487 μ h.	0.0097 μ h.
10	1	0.172	0.0932	0.0093
15	1	0.260	0.141	0.0094
20	1	0.344	0.186	0.0093
Average inductance per cm. = 0.0094 μ h.				

(b) $C_2 = 2202 \mu\text{uf}$; $C_1 = 1784 \mu\text{uf}$; $\lambda = 1020$ meters.

ΔL (from Eq. 1.) = 31.2 μ h. Total length of wires = 3310 cm. Inductance per cm = 0.0094 μ h.

(c) Length of rectangle = 1645 cm; Width of rectangle = 10 cm; Diameter for wire = 0.234 cm.

ΔL (calculated from dimensions) = 29.7 μ h. Inductance per cm = 0.0090 μ h.

MEASUREMENT OF A SMALL CAPACITY

The circuit shown in Fig. 4 may be used to determine capacities of the order of 1 μuf . The condenser *C* is a low-loss variable air condenser capable of being read to 0.02 μuf . The inductance *L* is made of large copper tubing. Thus, the circuit, having a very low resistance, may be very accurately tuned to resonance with the aid of the voltmeter *V*. Two wires *WW* about 125 cm long were connected to the terminals of the condenser and rigidly

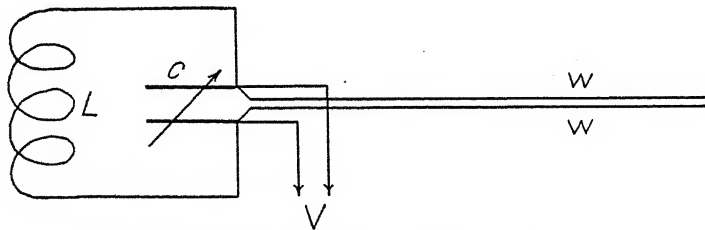


Fig. 4. Diagram of circuit for measuring a small capacity.

fixed parallel to one another. The circuit, very loosely coupled to an oscillator, was very accurately tuned to resonance, and the condenser read. A measured length of the wires was cut off, the circuit retuned, and the condenser again read. The capacity of the wires cut off was given, of course, by the difference of the condenser readings. The diameter of the wires and their distance apart were measured with micrometer calipers, and the capacity of the pieces cut off was calculated.⁴ The results of these measurements are shown in Table VI.

⁴ Bureau of Standards Circular No. 74.

TABLE VI

Measurement of capacity of two parallel wires. Wave length 143 meters; diameter of wires 0.203 cm; distance between wires (center to center) 0.447 cm.

Length of wire cut off	Observed capacity	Calculated capacity
4.4 cm.	0.85 μuf	0.83 μuf
5.8	1.10	1.09
10.2	1.95	1.91
29.5	5.51	5.53
49.9	10.35	10.38

Measurements of the capacity between the elements of vacuum tubes and the capacity of the socket terminals were made by this same method; and the results are shown in Table VII.

TABLE VII

Measurements of the capacity of vacuum tubes and sockets.

Type of tube	Filament to Plate capacity	Filament to Grid capacity	Grid to Plate capacity
201 A tube and socket	9.25 μuf .	8.5 μuf .	11.25 μuf .
Socket only	1.75	1.75	1.75
WD-11 tube and socket	5.00	5.00	3.60
Socket only	0.50.	0.50	0.25

MEASUREMENT OF THE IMPEDANCE OF A CONDENSER

The impedance of a paper telephone condenser was measured over a wide range of frequencies. The telephone condenser C (Fig. 5) was connected

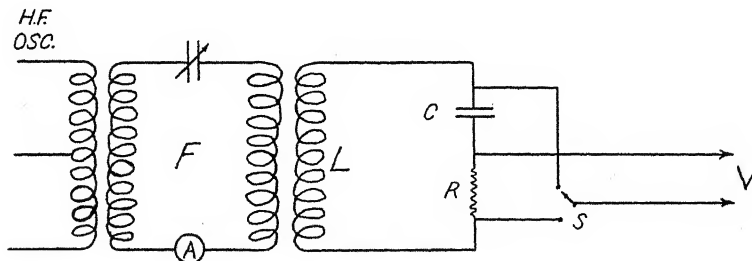


Fig. 5. Diagram for measuring the impedance of a fixed condenser at radio frequencies.

in series with a non-inductive standard resistance R and a coupling coil L . This circuit was coupled to an oscillator through the intermediate tuned circuit F . The voltmeter V was read with the switch S in positions 1 and 2,

respectively. Calling the corresponding electromotive forces E_c and E_R , the impedance Z , of the condenser C , is given by the relation,

$$Z = E_c/I, \text{ where } I = E_R/R.$$

The construction of the condenser used is shown in Fig. 6, and the curves of Fig. 7 show impedance plotted against frequency for the three

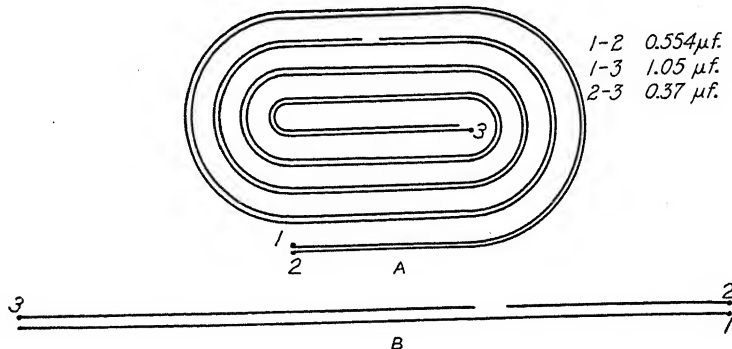


Fig. 6. Diagram showing the construction of the telephone condenser.

different sets of terminals corresponding to three different values of capacity. Table VIII shows data from which the curves were plotted. It will be noted

TABLE VIII
Impedance of paper telephone condensers.

Condenser	λ	E_c	I	Z
1.05 μf	2520 m.	0.332 v.	0.05 amp.	6.64 ohms
	4080	.146	.05	2.92
	4700	.118	.05	2.36
	5600	.0915	.05	1.83
	5975	.0880	.05	1.76
	6200	.0890	.05	1.78
	7200	.110	.05	2.20
	8000	.136	.05	2.72
	10000	.132	.03	4.40
0.37 μf	2000	.350	.05	7.00
	2860	.200	.05	4.00
	3000	.184	.05	3.68
	3100	.162	.05	3.24
	3300	.142	.05	2.84
	3400	.137	.05	2.74
	3500	.134	.05	2.68
	3550	.132	.05	2.64
	3600	.134	.05	2.68
	3750	.140	.05	2.80
	3850	.143	.05	2.86
	4100	.157	.05	3.14
	5150	.238	.05	4.68
0.554 μf	1000	.121	.100	1.21
	1800	.101	.05	2.02
	3150	.170	.05	3.40
	4120	.228	.05	4.56
	5070	.280	.05	5.60
	5975	.325	.05	6.50

that in two of the cases shown the inductance within the condenser was sufficient to cause the condenser to resonate at the frequency shown; whereas, in the third case, the curve shows no indication of resonance. An inspection of the diagram showing the construction of the condenser (Fig. 6) will suffice to make clear the reason for this difference.

The impedance of a variable standard air condenser of the Bureau of Standards type was measured at various settings by this method. The

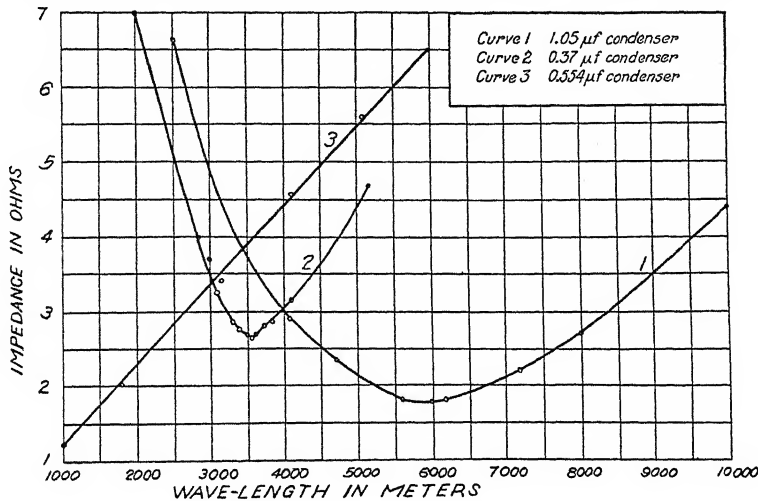


Fig. 7. Impedance curves for telephone condensers.

wave-length was determined by a wavemeter, and the corresponding values of capacity of the condenser were calculated from the measured values of its impedance. The results of this measurement are given in Table IX.

TABLE IX
Calibration of variable standard air condenser.
 $\omega = 2\pi f = 8.73 \times 10^5$

Condenser Setting	I	E_c	$C \left(= \frac{I}{E\omega} \right)$	C (taken from Bureau of Standards calibration)
180	0.750 m.a.	0.218 v.	3940 μuf	3928 μuf .
175	.692	.205	3860	3866
170	.715	.218	3758	3760
160	.693	.223	3555	3542
150	.668	.228	3352	3324
140	.642	.237	3105	3107
130	.614	.242	2905	2890
120	.590	.248	2728	2673
110	.700	.328	2445	2455
100	.627	.319	2255	2236

The curve of Fig. 8 shows capacity plotted against setting, the crosses indicating values obtained by this method while the circles represent values taken from the calibration furnished by the Bureau of Standards.

It is believed that the methods described here will be found to have many applications in high frequency measurements. This paper will be followed

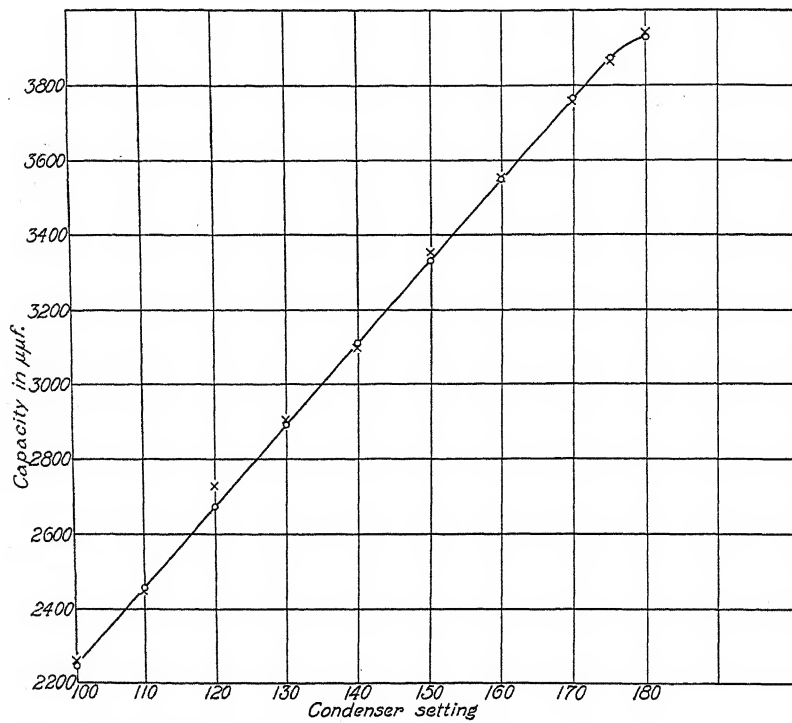


Fig. 8. Capacity of a standard condenser as determined from its measured impedance.

by one in which measurements of the resistance of low-loss variable air condensers are described. It will be shown that the resistance of the condenser in a low resistance circuit may be isolated.

HIGH FREQUENCY LABORATORY,
DEPARTMENT OF PHYSICS,
UNIVERSITY OF TEXAS.
February 15, 1927.

ON DIELECTRIC CONSTANTS AND MAGNETIC
SUSCEPTIBILITIES IN THE NEW QUANTUM
MECHANICS*

PART I.

A GENERAL PROOF OF THE LANGEVIN-DEBYE FORMULA

By J. H. VAN VLECK

ABSTRACT

In contradistinction to the old quantum theory, the new quantum mechanics yields very generally the Langevin and Debye formulas $\chi = N\alpha + N\mu^2/3kT$ for the magnetic and dielectric susceptibilities respectively. It is believed that our proof is considerably more comprehensive than previous ones, for it assumes only that the atom or molecule has a "permanent" vector moment of constant magnitude μ whose precession frequencies are small compared to kT/\hbar . There is no limit to the allowable number of superposed precessions. There can, for instance, be simultaneous precessions due to internal spins of the electron and to "temperature rotation" of the nuclei. The presence of other simultaneous external fields in addition to the applied electric or magnetic field introduces no difficulty. Besides the effect due to the permanent moment, there is the term $N\alpha$ which arises from "high frequency" matrix elements associated with transitions from normal to excited states. This term is proved independent of the temperature. The susceptibility formula contains the factor 1/3 in the temperature term as generally as in the classical theory because of the high spectroscopic stability characteristic of the new quantum mechanics. It is shown that the mean squares of the x , y , and z components of a vector are equal in the new quantum dynamics just as in the classical theory, the only difference being that in the new quantum theory we take the average by summing over a discrete distribution of quantum-allowed orientations instead of by integrating over a uniform continuous distribution.

1. INTRODUCTION.

THE present paper is part I of a series of articles on magnetic and dielectric susceptibilities in the new quantum mechanics, and contains the main elements of the mathematical theory. Part II will discuss the application to dielectric constants, especially in relation to previous work by other authors with particular models. Part III will deal with applications to magnetism, including the paramagnetism of O₂ and NO.

The main purpose of part I is to give a very general derivation, also some critical discussion, of the Langevin-Debye formula

$$\chi = N \left(\alpha + \frac{\mu^2}{3kT} \right). \quad (1)$$

Here χ is the susceptibility, N is the number of atoms or molecules per unit volume, k is the gas constant, and α is a constant independent of the absolute

* Presented at the New York meeting of the American Physical Society, Feb. 1927.

temperature T . We shall suppose the susceptibility χ to be either magnetic or electric, not because of any deep physical resemblance of the magnetic and electric polarizations, but simply because it is well known that they can both be calculated by quite similar mathematical procedures, so that we shall treat them together wherever possible. Thus $1+4\pi\chi$ will denote the dielectric constant or magnetic permeability, and μ the permanent electric or permanent magnetic moment of the molecule, depending on whether we are dealing with electric or magnetic polarization. The interpretation of the constant α is somewhat different in the two cases; in the electric one α is the "induced moment" due to elastic polarization of the atom or molecule by the impressed field, while in the magnetic case α is usually negative and represents the induced diamagnetic moment, although we shall see in part III that the magnetic α is occasionally positive due to the quadratic Zeeman effect associated with multiplet structures. Thus in magnetism α is usually small, and so ordinarily omitted. Historically, Eq. (1) was first applied to magnetism, as in 1905 Langevin¹ published his famous paper, and it was not until 1912 that Debye² extended the formula to dielectric constants by assuming that there could be a "permanent" as well as "induced" electric moment in polar molecules.

Our derivation of (1) will be based on the new quantum mechanics. There is, however, an interesting analogy with the classical theory, as it will be shown in part II that the same result could be obtained classically if we averaged continuously over all possible orientations of the moment and precession vectors relative to each other and to the field instead of summing over the discrete quantum states. It must be regarded as one of the triumphs of the new quantum mechanics that it will give the Langevin or Debye formulas very generally, whereas the old quantum theory replaced the factor $\frac{1}{3}$ in (1) by a constant C whose numerical value depended rather chaotically on the type of model employed, whether whole or half quanta were used, whether there was "weak" or "strong" spacial quantization, etc.³ This replacement of $\frac{1}{3}$ by C caused an unreasonable discrepancy with the classical theory at high temperatures, and in some instances the constant C even had the wrong sign.⁴ All these vicissitudes in C are avoided in the new mechanics, which gives the factor $\frac{1}{3}$ quite as generally as the classical theory. This

¹ P. Langevin, Journal de Physique, (4), 4, 678 (1905); Annales de Chim. et Phys. (8), 5, 70 (1905).

² P. Debye, Phys. Zeits. 13, 97 (1912). See also his excellent compendium on electric and magnetic polarizations in vol. VI of the Handbuch der Radiologie. The temperature effect due to permanent dipoles was also suggested later independently by J. J. Thomson, Phil. Mag. 27, 757 (1914).

³ Cf. W. Pauli, Jr., Zeits. f. Physik, 6, 319 (1921); L. Pauling, Phys. Rev. 27, 568 (1926).

⁴ Pauling³ shows that C would be negative in molecules of the HCl type if we use the a-priori probability $2m$ indicated by the recent band spectrum intensity measurements of Bourgin and Kemble. He therefore uses a probability $2m+1$ and finds C to be about 14 times the classical value $1/3$, but in a later paper⁴ shows that C would even then become negative in the formula for the dielectric constant on applying a magnetic field at right angles to the electric field. Needless to say, such a behavior is not found experimentally.

has already been shown by several writers⁵ for special models, and the present paper may be regarded as extending the result to the general case. In our opinion the general proof is usually quite as simple as the specialized ones with particular models, since the algebra of writing out and summing the various matrix elements is avoided, and there is the great advantage that it is unnecessary to know the precise form or values of these elements.

At this point it may be remarked that most of the classical derivations of (1) appear rather inadequate. The literature, to be sure, is full of purported "generalized Langevin theories,"⁶ but these for the most part are based on rather unsatisfactory physical premises, such as rigid magnetons, steady molecular currents, etc. The usual elementary derivation of the Langevin formula omits even the kinetic energy of rotation. Fortunately the calculations of Alexandrow⁷ and van Leeuwen⁸ show that the inclusion of this energy occasions no particular difficulty in symmetrical diatomic molecules. Miss van Leeuwen replaces an electron orbit by a current, but unlike most writers, she does not overlook the gyroscopic effect arising from the angular momentum concomitant to magnetic moment. No computations, however, appear to have previously been published which allow for the high degree of dissymmetry characteristic of the general polyatomic molecule, or for the precessions caused by internal spins⁹ of the electrons which are an important factor in magnetism. Thus the following treatment not only substitutes the new quantum for the classical viewpoint, but also gives increased generality. Yet it must be understood that we shall calculate only the terms in the susceptibility which are independent of the field strength. These are the only terms ordinarily of consequence in dielectric or in para- (or dia-) magnetic media, but the present paper does not pretend to treat ferromagnetism or saturation phenomena in which higher powers of the field F must be considered. Hence we have written Langevin's formula in its asymptotic form (1) valid for small (i.e. ordinary) values of the field rather than giving his more complete expression which contains the effect of all powers of $\mu F/kT$. We suppose throughout for simplicity that the effective average field on the atom is F rather than the more rigorous expression $F+4\pi P/3$. This amounts to assuming the polarization so small that the Clausius-Mosotti constant $(\epsilon-1)/(\epsilon+2)N$ reduces to $(\epsilon-1)/3N$; if this condition is not met there is no trouble, as we would simply have to replace χ in (1) by $3\chi/(3+4\pi\chi)$.

⁵ L. Mensing and W. Pauli, Jr., Phys. Zeits. 27, 509 (1926); J. H. Van Vleck, Nature, 118, 226 (1926); R. d. L. Kronig, Proc. Nat. Acad. 12, 488, 608 (1926); C. Manneback, Phys. Zeits. 27, 563 (1926); P. Debye and C. Manneback, Nature, 119, 83 (1927); L. Pauling, Phys. Rev. 29, 145 (1927).

⁶ For references see "Theories of Magnetism," Bull. Nat. Research Coun. no. 18; also van Leeuwen.⁸

⁷ W. Alexandrow, Phys. Zeits. 22, 258 (1921).

⁸ van Leeuwen, Leyden Thesis; summary in J. de Physique, (6), 2, 361 (1921).

⁹ We assume the reader to be familiar with the Uhlenbeck-Goudsmit spinning electron, die Naturwissenschaften 13, 953 (1925); Nature 117, p. 264 (1926).

2. THE FUNDAMENTAL ASSUMPTIONS

In order to derive the second term of (1) we find it necessary to assume only that the atom or molecule has a "permanent" moment vector whose precession frequencies are small compared to kT . Another way of saying the same thing is that the various component normal states have a vector moment of common magnitude μ , and have an energy spacing small compared to the equipartition allowance kT . A more precise explanation of these conditions is given in the following paragraphs.

The stationary states of many atoms and molecules are so spaced that at ordinary temperatures there is a fairly sharp delineation between normal and excited states. The excited states we define as having energies of excitation which are large in comparison with kT , and so they may be considered as virtually unoccupied in making the calculations. The normal states generally are a family of "component" energy levels whose separation is usually smaller than or comparable with kT . This splitting into components ordinarily results from the mutual precessions of the various constituent angular momentum vectors of the atom or molecule and from the precession of their resultant about some direction fixed in space. Thus the excited states are usually characterized by different electronic or possibly vibrational quantum numbers from the normal, whereas the component normal levels result from giving the molecules different amounts of "temperature rotation," different orientations relative to the external fields, or from allowing the spin axis of the electron to assume different orientations relative to the rest of the system.

It is clear that the magnetic or electric moment of the atom or molecule is a vector matrix M . We follow Born's procedure of writing matrices in bold-face type. Certain elements of the matrix M will be identified with transitions between normal and excited states, and will be shown in section 3 to contribute only to the constant term $N\alpha$ in (1) which is independent of the temperature; even without proof this seems fairly obvious from the fact that excited states have by definition energies large compared with kT . Hence to calculate the second or "temperature" term of (1) we replace M by a matrix \mathbf{y} formed from M by dropping the high frequency elements of M associated with transitions to excited states. This replacement of M by \mathbf{y} corresponds to the well-known separation of the "secular" from the high frequency variations in perturbation theory, and means that in computing the temperature effect the moment matrix may be considered to involve just the family of normal states rather than the more complicated aggregate of both normal and excited states. We suppose, moreover, that the atom (or molecule) has a moment of "definite" or "permanent" magnitude μ . This is not at all a drastic assumption, as it is involved in all permanent dipole theories, and without it the expression μ in (1) would have no meaning. This means that the magnitude $\mu = (\mu_x^2 + \mu_y^2 + \mu_z^2)^{1/2}$ of the vector matrix \mathbf{y} is constant with respect to the time and the same for the various normal states. Hence $|\mathbf{y}|$ is a diagonal matrix whose elements are all equal and in the terminology of Dirac it may be called a "c-number," which is the moment μ entering in Eq. (1). The vector \mathbf{y} will be constant in magnitude but usually

not in direction. The components u_x , u_y , u_z will, to be sure, involve no high frequency elements, as the latter have been eliminated in forming \mathbf{u} from \mathbf{M} , but these components will in general vary with the time due to the existence of "low frequency elements" which correspond to transitions between the different levels constituting the normal states and which arise usually from precessions of the various types cited in the preceding paragraph. In order to obtain the Langevin formula (1) it is essential simply that these "low frequencies" be small in comparison with kT/h , which is equivalent to saying that transitions between the various normal states involve energy changes of magnitude much less than kT .

In the above and elsewhere we use the terms, "direction of a vector," "precession," etc., rather freely, as a vector matrix clearly cannot be assigned the same simple geometrical interpretation as an ordinary directed segment. We mean, of course, simply the quantities in the Born-Heisenberg matrix theory which "correspond" to the precessions, directions, etc., of classical mechanics. In particular the precession frequencies mean the spectroscopic frequencies emitted or absorbed in transitions between various component levels whose separation is caused by the quantum analog of a classical precession effect. Throughout the present paper, and also in parts II and III, we use the language of the matrix rather than wave form of the new quantum mechanics, but the same results follow equally well with the wave viewpoint, in virtue of the general formal identity¹⁰ of the wave and matrix formulations for closed ("abgeschlossen") atomic systems. In fact we could even obtain the Langevin formula by going to the opposite extreme from the matrix aspect, and employing the "field" theory of Schrödinger, Madelung, and Gordon,¹¹ in which the electric charges are spread through space with a continuous density proportional to $|\psi|^2$, where ψ is the well-known Schrödinger wave-function. The identity of the results regarding susceptibilities ensues since Schrödinger¹⁰ has shown that the field theory gives the same electrical moment as the matrix viewpoint (neglecting relativity corrections), while Fermi¹² has proved it gives the same magnetic moment,¹³ utilizing the definition of the velocity of flow given by Schrödinger and others.¹⁴

¹⁰ E. Schrödinger, Ann. der Physik, 79, 734 (1926); C. Eckhart, Phys. Rev. 28, 711 (1926).

¹¹ E. Schrödinger, Ann. der Physik, 81, 109 (1926) 82, 257, 265 (1927); E. Madelung, Naturwissenschaften, 14, 1004 (1926); Zeits. f. Physik, 40, 322 (1926); W. Gordon, *ibid.*, 40, 117 (1926).

¹² Fermi, Nature, 118, 876 (1926).

¹³ It must be remarked, however, that calculations similar to Fermi's establish the similarity of results for the part of the paramagnetism arising from orbital angular momentum, and do not indicate just how to treat the "spin" phenomenon, as Fermi assumes the normal ratio of magnetic moment to angular momentum holds throughout. A further complication is that diamagnetism involves the velocity of light to the power $1/c^2$ rather than $1/c$, and the ordinary technique does not furnish a correlation to $1/c^2$, as the magnetic modifications in the definition of momenta, etc., would have to be considered, so that there is a bare possibility of a discrepancy. It seems, however, highly improbable that any successful theory will give different susceptibilities than those calculated by the matrix method.

¹⁴ For references see note 11.

The basic assumptions may be summarized in the words "permanence of moment" and "slowness of precession." The great generality arises from the fact that it is not necessary to specify the exact form of the precession, or the numerical formulas for the frequencies and amplitudes. The phrase "slowness of precession" must not be construed too literally, for the low frequency elements could result equally well from slow oscillations or other types of motion than precessions. We use the term "precession" for the sake of concreteness and because precessions are much the most common cause of low frequency components; "temperature rotation" of the nuclei about the center of gravity, for instance, can be considered as simply a precession about the invariable axis. It is also to be understood that besides the "low frequency elements" there are generally high frequency terms which are responsible for the constant term $N\alpha$ in (1). The essential requirement, of course, is that the "high" and "low" frequencies be always respectively large and small compared to kT/h . An important feature is that there is no limit to the number of precessions which can be superposed. Nevertheless, even our hypotheses are not sufficiently general in some instances. In the first place, in the case of dielectric constants, the centrifugal expansion of the molecule will violate the assumption of a "permanent electric moment," as the stretching will slightly increase the dipole moment in the higher quantum states, so that the diagonal elements of the matrix $[\mathbf{u}]$ are no longer equal. Fortunately this expansion effect is small, as band spectra show that the variation of moment of inertia with rotation rarely exceeds six per cent even in the more elastic excited states.¹⁵ A more important restriction is imposed by the requirement that the elements in the moment matrix \mathbf{M} are all of the "high" or "low" frequency type. Actually Laporte and Sommerfeld¹⁶ find that in atoms of the first long period of the Mendeleeff table the internal spins of the electron lead to precessions in the magnetic moment of what we may term the "medium" frequency type; i.e., precessions whose frequencies are of the same order of magnitude as kT/h . We shall find it necessary to treat the magnetism of NO by a special calculation in part III because the spacing of its spin doublet is about $.6kT/h$. Also the variable vibrational specific heats of certain molecules indicate that the energies of excitation of their nuclear vibrations are comparable with kT . Undoubtedly because of its secular character the magnetic moment does not have any terms of appreciable amplitude involving the vibrational frequencies. The electric moment will contain such terms, but fortunately their temperature effect will be very subordinate since the amplitude of nuclear vibration is usually small compared to the equilibrium nuclear spacing, and also since the polarization of a linear oscillator, which represents the nuclear vibrations to a first approximation, is independent of the temperature.¹⁷

¹⁵ Cf. R. T. Birge, *Nature*, 116, 783 (1925).

¹⁶ Laporte and Sommerfeld, *Zeits. f. Physik*, 40, 333 (1926).

¹⁷ This independence of the temperature for the polarization due to a linear oscillator is proved with the classical theory by P. Debye, *Handbuch der Radiologie*, Vol. VI, p. 613, and a simple calculation shows that it also holds in the new quantum mechanics.

3. PROOF

Let us suppose for simplicity that we are dealing with electric rather than magnetic polarization. The slight adaptations in the proof necessary to the magnetic case will be given in part III. Before application of the field F the electrical moment \mathbf{M} will be a matrix whose typical element may be denoted by

$$M_z(njm; n'j'm')e^{2\pi i\nu(njm; n'j'm')}$$

We have here taken the z -component, but there are, of course, similar formulas for the x and y components. For brevity we throughout omit commas from the arguments, and write $(njm; n'j'm')$ for $(n, j, m; n', j', m')$, etc. Following the conventional notation, such an element is associated with a transition from a state specified by indices n, j, m to one by n', j', m' . We shall let the first of the three indices be identified with quantum numbers (e.g. "electronic" and "vibrational") which have an effect on the energy large compared to kT , so that one particular value of this index gives states of especially low energy. This value will be denoted by n and yields the normal levels of the atom or molecule. The second index j or j' corresponds to quantum numbers (e.g. "inner," "rotational," "spin") whose effect on the energy is comparable with or smaller than kT . We do not, however, include in the second index the "axial" (also called "equatorial" or "magnetic") quantum number which specifies the spacial orientation by quantizing angular momentum about some fixed direction in space. Instead the third index m or m' is to be considered as representing the axial quantum number. Thus the various component levels of the normal state correspond to fixed n but different values of j and m , whereas the excited states have an index n' different from n . It is clearly to be understood that *each index, except the third, in general symbolizes more than one quantum number*; i. e., represents a multiple rather than single array. Hence we designate n, j, m as "indices" rather than quantum numbers. Our proof is thus by no means confined to systems with three quantum numbers or degrees of freedom.

Let us suppose an electric field F is applied in the z -direction. The susceptibility is the quotient of polarization by field strength, or $N\bar{M}_z^{(F)}/F$, where N is the number of molecules (or atoms) per unit volume, and $\bar{M}_z^{(F)}$ is the average value of the z -component of the electrical moment per molecule. This average, of course, differs from the time mean¹⁸ $M_z^{(F)}(njm; njm)$ for individual molecules, as the latter will be distributed among the different components of the normal levels. To get $\bar{M}_z^{(F)}$ we must average over these components with each assigned the probability required by the Boltzmann distribution formula. Hence it is apparent that

¹⁸ The time mean value in a non-degenerate system is a diagonal term of a matrix, and hence specified by an element in which the second trio of indices is the same as the first. In defining this time mean it is, of course, supposed that the molecule always remains in the same state. Thus the time mean is over a period long compared to the periods of the spectral lines but short compared to the duration of a stationary state. Heisenberg's statistics of fluctuations (Zeits. f. Physik, 40, 501, 1926) shows that (2) is still applicable even if we allow for a molecule changing states.

$$\chi = \frac{N}{F} \frac{\sum_{i,m} M_z^{(F)}(n jm; n jm) e^{-W(njm)/kT}}{\sum_{i,m} e^{-W(njm)/kT}}, \quad (2)$$

where W as usual denotes the energy. We suppose the system non-degenerate,¹⁹ so that all states have the same statistical weight; i.e. the same factor g in the Boltzmann expression $g e^{-W/kT}$.

Because of "induced polarization," the time mean $M_z^{(F)}(n jm; n jm)$ of the electrical moment in the field F is not the same as this mean $M_z(n jm; n jm)$ before application of F . We shall throughout use the superscript ^(F) to distinguish values in the field from those in its absence. It is clearly to be understood that all amplitudes, frequencies, and energies without this superscript relate to the case $F=0$. Now $M^{(F)}$ is easily calculated in terms of M by the perturbation methods of Born, Heisenberg, and Jordan,²⁰ or of Schroedinger.²¹ These writers show that²²

$$M_z^{(F)}(n jm; n jm) = M_z(n jm; n jm) - \frac{2F}{\hbar} \sum'_{n' j' m'} \frac{|M_z(n jm; n' j' m')|^2}{\nu(n jm; n' j' m')} . \quad (3)$$

This is, of course, the same result as given by extrapolation of the Kramers dispersion formula to infinitely long impressed wave-lengths. The sum over n' , j' , m' includes all excited and normal states except the given state n, j, m . This exclusion of the one term $n', j', m' = n, j, m$ is indicated by the prime inside the summation sign, and this interpretation of the prime is to be understood throughout the article. As usual ν denotes the frequency emitted (or absorbed) in the transition between two states when $F=0$. Eq. (3) is utilized by all the various writers⁵ who have calculated dielectric constants for particular models. It gives the polarization to terms of the first order in F , as this degree of approximation is necessary to get the ordinary susceptibility effects (cf. section 1).

Now the energy in the field is to first powers in F

$$W^{(F)}(n jm) = W(n jm) - F M_z(n jm; n jm). \quad (4)$$

This follows by well-known perturbation formulas of the new quantum mechanics,²⁰ which show that here just as in the old quantum theory the perturbed energy is to a first approximation the energy $W(n jm)$ in the absence of F augmented by the perturbative potential (here $-FM_z$) averaged over the unperturbed motion.

¹⁹ In case the system is degenerate, we may imagine the degeneracy removed by introducing a sufficient number of hypothetical supplementary infinitesimal internal forces. This is legitimate, as Eq. (25) of section 4 shows that the result is invariant of the manner in which the degeneracy is removed. There can be no spacial degeneracy, for the field F provides an axis for quantization if not already present when $F=0$.

²⁰ Born, Heisenberg, and Jordan, Zeits. f. Physik, 35, 567 (1927).

²¹ E. Schrödinger, Ann. der Physik, 81, 109 (1926).

²² Expressions of the type form $|M_z(n jm; n' j' m')|^2$ occurring in Eq. (3) etc. may also be written as the product $M_z(n jm; n' j' m') M_z(n' j' m'; n jm)$; for as the moment matrix is Hermitian, $M_z(n' j' m'; n jm)$ is the conjugate of $M_z(n jm; n' j' m')$, and the product of any complex number and its conjugate is the square of its absolute value. This other method of writing is that used by Born, Heisenberg, and Jordan.²⁰

We now expand the exponentials in (2) as power series in F by means of (4). When we do this and substitute (3) in (2) we find

$$\begin{aligned} \chi = & \frac{N}{F} \frac{\sum_{i,m} M_z(njm; njm) e^{-W(njm)/kT}}{\sum_{i,m} e^{-W(F)(njm)/kT}} \\ & + (B/kT) \sum_{i,m} |M_z(njm; njm)|^2 e^{-W(njm)/kT} \\ & - \frac{2B}{h} \sum'_{i,m,n',i',m'} \frac{|M_z(njm; n'j'm')|^2 e^{-W(njm)/kT}}{v(njm; n'j'm')} . \end{aligned} \quad (5)$$

Here we have discarded terms in F , F^2 , . . . , as we are interested in calculating only the constant part of the susceptibility. We have written $|M_z(njm; njm)|^2$ for $M_z(njm; njm)^2$ which is legitimate since diagonal elements are real. Also we have introduced the abbreviation

$$B = \frac{N}{\sum_{i,m} e^{-W(njm)/kT}} . \quad (6)$$

We must now suppose that the first line of (5) vanishes. (For this reason we have not bothered to expand the exponentials in the denominator of this line.) This involves no essential loss of generality,²³ for if it did not we would have a "permanent" or "residual" polarization even in the absence of the field.²⁴ Clearly the numerator of the first line of (5) vanishes by symmetry if the only external field is the applied electric field F , for in the absence of all fields there can be no preference between directions parallel and anti-parallel to F , and hence no moment along F ; another way of saying the same thing is that in the absence of all fields states with positive and negative values of the axial quantum number are equally probable. In solids there is, of course, the possibility of directed²⁵ inter-molecular fields, which might give the body a residual polarization when $F=0$, but such effects are not ordinarily found experimentally except in ferromagnetic media or in crystalline dielectrics, both of which are beyond the scope of the present article.

Separation of high and low frequency terms. Eq. (5) is a perfectly general expression for the susceptibility which does not require the hypotheses of "slowness of precession" or "permanent dipole moment" presented in section 2. For further simplification, however, these postulates must be introduced, and so we now proceed to make the separation into "low" and "high" frequency terms. In order to make connection with the notation employed in section 2, we write $\mu(jm; j'm')$ for the low frequency elements $M_z(njm; nj'm')$. Eq. (5), with first line omitted, then becomes

²³ Debye also notes (Phys. Zeits. 27, 67, 1926) in a calculation with the old quantum theory that the vanishing of an expression similar to the first line of (5) involves no essential loss of generality.

²⁴ The first line of (5) will not vanish if there is a "magneto-electric directive effect", to be explained in part II, but this effect is apparently never found experimentally.

²⁵ Random inter-molecular fields give no trouble, as with them the first line of (5) vanishes on the average by symmetry.

$$\begin{aligned} \chi = & (B/kT) \sum_{j,m} |\mu_z(jm; jm)|^2 e^{-W(njm)/kT} \\ & - \frac{2B}{h} \sum'_{j,m,j',m'} \frac{|\mu_z(jm; j'm')|^2 e^{-W(njm)/kT}}{\nu(njm; nj'm')} \\ & - \frac{2B}{h} \sum_{j,m,n',j',m', (n' \neq n)} \frac{|M_z(njm; n'j'm')|^2}{\nu(njm; n'j'm')} e^{-W(njm)/kT}. \end{aligned} \quad (7)$$

Here the first two and the third lines represent respectively the "low" and "high" frequency terms, as the third line involves only terms associated with transitions to the excited states $n' \neq n$.

The terms in the summation in the second line of (7) may be grouped together in pairs P_{12} of the form

$$\begin{aligned} P_{12} = & - \frac{2B}{h} \left\{ \frac{|\mu_z(j_1m_1; j_2m_2)|^2}{\nu(nj_1m_1; nj_2m_2)} e^{-W(nj_1m_1)/kT} \right. \\ & \left. + \frac{|\mu_z(j_2m_2; j_1m_1)|^2}{\nu(nj_2m_2; nj_1m_1)} e^{-W(nj_2m_2)/kT} \right\}. \end{aligned} \quad (8)$$

Now $\mu_z(j_2m_2; j_1m_1)$ is the conjugate of $\mu_z(j_1m_1; j_2m_2)$ and so has the same absolute magnitude. Also $\nu(nj_2m_2; nj_1m_1) = -\nu(nj_1m_1; nj_2m_2)$, and by the Bohr frequency condition $W(nj_2m_2) = W(nj_1m_1) - h\nu(nj_1m_1; nj_2m_2)$. Under the hypothesis of "slowness of precession," fully explained in section 2, we may develop the second exponential in (8) as a power series in the ratio $s = h\nu(nj_1m_1; nj_2m_2)/kT$. Then (8) becomes

$$P_{12} = -2(B/skT) |\mu_z(j_1m_1; j_2m_2)|^2 e^{-W(nj_1m_1)/kT} [1 - 1 - s - \frac{1}{2}s^2 - \frac{1}{6}s^3 - \dots] \quad (9)$$

If we neglect terms of the order s^3 within the bracketed factor this is the same as

$$(10) \quad P_{12} = (B/kT) \{ |\mu_z(j_1m_1; j_2m_2)|^2 e^{-W(nj_1m_1)/kT} + |\mu_z(j_2m_2; j_1m_1)|^2 e^{-W(nj_2m_2)/kT} \}$$

Now if the influence of orientation, i.e., of the axial quantum number, on the "unperturbed" energy $W(njm)$ is small compared to kT , we may replace $W(njm)/kT$ by an expression $W(nj)/kT$ independent of the index m . This approximation is usually one which is fulfilled with a high degree of precision. In the first place the ordinary case is that in which the molecule is subject to no external field except F , and then the unperturbed energy (i.e., the energy in the absence of F) is independent of orientation, so that the index m has absolutely no effect on W . To allow for the possibility of simultaneous electric and magnetic fields, or weak inter-molecular fields in liquids and solids, we admit the more general assumption that $W(njm) - W(nj)$ is not identically zero but small compared to kT .²⁶ Also it is clear that the

²⁶ It is to be noted that though we suppose $W(njm) - W(nj)$ and $h\nu(njm; nj'm')$ both numerically small compared to kT , we have not assumed that $W(njm) - W(nj'm')$ is negligible relative to kT . The latter assumption would be much more stringent, for usually there are selection principles which require that certain quantum numbers change only by zero or one unit, at least in the transitions of appreciable amplitude. In case the quantum numbers

"high" frequencies $\nu(njm; n'j'm')$ ($n' \neq n$) are affected but little by the indices j, m, j', m' , as the separations between components of the normal states or of the excited states are small compared to the interval between the normal and excited states. Hence in the third line or "high frequency part" of (7) we may without appreciable error replace $\nu(njm; n'j'm')$ by a number $\nu(n; n')$ independent of the indices j, m, j', m' .

If we use the simplifications given in the preceding paragraph, and substitute (10) for (8), Eq. (7) reduces to

$$\chi = (B/kT) \sum_{j,m,j',m'} |\mu_z(jm; j'm')|^2 e^{-W(nj)/kT} - \frac{2B}{h} \sum_{j,m,n',j',m'(n' \neq n)} \frac{|M_z(njm; n'j'm')|^2}{\nu(n; n')} e^{-W(nj)/kT}, \quad (11)$$

where now the first sum includes the diagonal elements $n', j', m' = n, j, m$.

It will be proved in section 4 that in virtue of the high degree of spectroscopic stability characteristic of the new quantum mechanics, an expression of the form

$$\sum_{m,m'} |A_z(njm; n'j'm')|^2$$

is invariant of the direction of the axis of spacial quantization and equals

$$\frac{1}{3} \sum_{m,m'} |A(njm; n'j'm')|^2.$$

Here $A(njm; n'j'm')$ denotes an element of the scalar magnitude $|A| = (\mathbf{A}_x^2 + \mathbf{A}_y^2 + \mathbf{A}_z^2)^{1/2}$ of a vector matrix \mathbf{A} whose z -component has elements of the form $A_z(njm; n'j'm')$. This consequence of spectroscopic stability is perhaps the most interesting and vital feature of the entire proof, as it underlies the general occurrence of the factor $\frac{1}{3}$ in the temperature term of the Langevin-Debye formula. On taking $A = M$ ($n' \neq n$) and $A = \mu$ ($n' = n$) (this is only a difference in notation) Eq. (11) becomes by the above

$$\chi = (B/3kT) \sum_{j,m,j',m'} |\mu(jm; j'm')|^2 e^{-W(nj)/kT} - \frac{2B}{3h} \sum_{j,m,n',j',m'(n' \neq n)} \frac{|M(njm; n'j'm')|^2}{\nu(n; n')} e^{-W(nj)/kT} \quad (12)$$

associated with the index j can assume a wide range of values, this means that $\hbar\nu(njm; n'j'm')$ is considerably smaller in magnitude than the general expression of the form $W(njm) - W(n'j'm')$ for then the selection principle requires that $\hbar\nu(njm; n'j'm')$ equal the difference of two adjacent, or nearly adjacent components of the normal levels rather than of two comparatively widely separated such levels.

This fact explains why we can apply our proof of the Langevin-Debye formula to molecules having "temperature rotation" even though by giving the molecule sufficient quanta of rotation the ratio $s = \hbar\nu(njm; n'j'm')/kT$ may be made as large as we please. For the numerical magnitude of the exponent in the Boltzmann distribution factor $e^{-W(nj)/kT}$ increases much more rapidly than s . (One varies approximately as the square, the other as the first power of the rotational quantum number.) Hence terms for which s is comparable with unity will have such a small exponential factor or probability that they can be disregarded. This will be discussed more fully in part II, where a calculation will be made of the error due to neglecting higher powers of s in (9).

Simplification of low frequency elements. From the rules for matrix multiplication it follows that

$$\sum_{j',m'} |\mu(jm; j'm')|^2 \quad (13)$$

is a diagonal element $\mu^2(jm; jm)$ of the matrix \mathbf{y}^2 , which is the square of the absolute magnitude of the secular moment vector matrix \mathbf{y} formed from \mathbf{M} by deleting the high frequency elements (cf. p. 730). Now in consequence of the hypothesis of a "permanent dipole moment," fully explained in section 2, the magnitude of \mathbf{y}^2 is independent of the time and the same for all the component levels constituting the normal state. Hence $\mu^2(jm; jm)$ is a number μ^2 independent of j and m , so that the expression (13) reduces to μ^2 and the low frequency part (first line) of (12) now becomes

$$(B/3kT)\mu^2 \sum_{j,m} e^{-W(nj)/kT}. \quad (14)$$

Now we have already supposed on p. 736 that $W(njm)$ can be replaced by $W(nj)$ in the exponential factors, so that the denominator of (6) is identical with the sum²⁷ in (14). Hence by (6) Eq. (14) is simply $N\mu^2/3kT$, which is the "temperature part" of the Langevin-Debye formula.

Invariance of high frequency part of χ . The high frequency terms, represented by the second line of (12), are not included in the ordinary calculations of molecular susceptibilities or dielectric constants, and instead it is usually taken for granted, perhaps by analogy with a classical linear oscillator,¹⁷ that their net effect is invariant of the temperature. The warrant for this seems to the author by no means so obvious but what it is repaying to actually demonstrate that the total contribution of the high frequency elements is independent of T . The analysis has, of course, been somewhat lengthened by their inclusion but gains considerably in completeness. The demonstration is an easy consequence of the "sum-rules" for intensities applied to absorption rather than emission, for it is the essence of these rules that an expression²⁸ of the form

$$\sum_{j',m'} |M(njm; n'j'm')|^2 \quad (15)$$

is independent of the indices j and m , provided the spacing of components is small compared to the frequency of the line itself; i.e., provided $\nu(njm; n'j'm')$ can be replaced by $\nu(n; n')$ as already assumed on p. 737. The sum-rules were first established on semi-empirical grounds, but the work of

²⁷ The double sum in (14) may also be written as the single summation $\sum_i p_i e^{-W(nj)/kT}$ where p_i is the number of quantum-allowed orientations for the state j ; i.e., the number of permissible values for the axial quantum number. The expression p_i would be the a-priori probability if the spacial degree of freedom were neglected and the system consequently treated as degenerate. Ordinarily $p_i - 1$ equals twice the maximum value of the axial quantum number, as positive and negative values of this number are equally probable.

²⁸ As usually stated, the sum-rules relate to the invariance of intensity, and intensity is proportional to the fourth power of the frequency as well as to the resultant amplitude M^2 which represents the combined effects of the x , y , and z components. However, we have seen that $\nu(njm; n'j'm')$ can without sensible error be replaced by an expression $\nu(n; n')$ independent of j, m, j', m' , and so the independence of the intensity-sums of j and m also implies the independence of (15) of j and m .

Born, Heisenberg, and Jordan,²⁹ and of Dirac³⁰ shows that they are required by the new quantum mechanics.³¹ The ordinary sum-rule for Zeeman components shows that $\sum_{m'} |M(njm; n'j'm')|^2$ is independent of m , and this taken in conjunction with the sum-rule for "multiplet" components³² (or band spectrum components) shows that (15) is independent of both j and m , at least provided j is associated with the one type of precession ordinarily identified with the inner (or rotational) quantum number. Actually we have already stated that the index j may correspond to several quantum numbers and hence represent the effect of several superposed precessions; e.g. simultaneous precessions resulting from internal spins of the electrons and from "temperature rotation." However, Dirac notes on p. 298 of his paper³⁰ that there is no difficulty extending the proof of the intensity rules to systems which are composed of any number of parts and which so contain any number of precessions, provided the parts are coupled together by "secular" forces which do not distort the motion and instead give rise only to pure precession. This result is also obvious from the correspondence principle inasmuch as the sum-rule is the quantum analog of the fact that classically the intensity of radiation is not appreciably affected by slow precessions which do not sensibly alter the sizes and shapes of the orbits. It must, however, be emphasized that the validity of the sum-rule requires that the coupling responsible for the separation of the normal levels into components must result in "pure precession" without distortion. This rules out centrifugal expansion and similar effects, but we have already seen at the close of section 2 that their effect is only subordinate.

From what has been said in the preceding paragraph we may replace (15) by an expression $|M(n; n')|^2$ independent of j and m , and so the second line of (12) reduces to

$$-\frac{2B}{3h} \sum_{n'(n' \neq n)} \left\{ \frac{|M(n; n')|^2}{v(n; n')} \sum_{i,m} e^{-W(n_i)/kT} \right\} \quad (16)$$

²⁹ Born, Heisenberg, and Jordan, Zeits. f. Physik, 35, 605 (1926).

³⁰ P.A.M. Dirac, Proc. Roy. Soc. 111A, 281 (1926).

³¹ Born, Heisenberg, and Jordan deduce the formulas proposed by Goudsmit and Kronig and by Hönl for the relative intensities of Zeeman components. Dirac gives the rather more difficult derivation of the formulas advanced by Kronig, Russell, Sommerfeld and Hönl for intensities in multiplets. These various formulas are more comprehensive than but necessarily include the corresponding sum-rules for Zeeman and multiplet components.

³² The ordinary statement of the sum-rule for the inner quantum number is essentially that the sum

$$\sum_{m'j'm} |M(njm; n'j'm')|^2 \quad (A)$$

is proportional to the a-priori probability p_j (cf. ²⁷) of the state j , assuming momentarily that j corresponds to the inner quantum number. Eq. (A) contains sums over m and m' inasmuch as the Zeeman components are supposed unresolved in the ordinary multiplet rule. The sum-rule for the magnetic quantum number shows that all the components of the state j contribute equally in the sum over m in (A). As there are p_j such components, the factor p_j thus cancels out if we do not sum over m in (A), thus making (15) invariant of both j and m .

The double sum in this equation is the same as the denominator of (6) inasmuch as on p. 736 we made the approximation $W(njm) = W(nj)$. Thus (16) becomes an expression

$$N\alpha = -\frac{2N}{3h} \sum_{n' (n' \neq n)} \frac{|M(n; n')|^2}{v(n; n')} \quad (17)$$

which is independent of T . This is the desired result, and (17) constitutes the "constant" part $N\alpha$ of the Langevin-Debye formula. The right-hand side of (17) does not involve the index m , or the direction of the axis of quantization,³³ and so the choice of this axis cannot influence $N\alpha$. It is clear that $N\alpha$ is positive since the $v(n; n')$ are negative or "absorption" frequencies.

Combination of the simplifications affected in the high and low frequency parts yields the complete Langevin-Debye formula $\chi = N\alpha + (Nu^2/3kT)$.

Special case that F is the only external field. It is to be noted that the proof has nowhere assumed that the axis of spacial quantization is the same as the axis of the applied field F . Ordinarily, however, F is considered to be the only external field, and then these two axes will coincide. When this is the case there will be no external influences when $F=0$, and hence there will be no secular precessions about the axis of quantization before application of F . This means that the third index will have no influence on the energy in the absence of F and consequently that all frequencies of the form $v(njm; njm')$ will vanish, as the absence of the superscript ^(F) (cf. p. 734) means the frequencies are to be measured with $F=0$. Nevertheless there will be no trouble with zero denominators in Eqs. (3), (5), (7), (8), as the matrices M_z or y_z will contain no elements in which $m' \neq m$ since the z -component clearly cannot involve the frequency of precession about the z -axis, which is the direction of F . Thus in Eqs. (3), (5), (7), (11) the summation over m' may be replaced by the substitution $m' = m$.

4. THE FUNDAMENTAL SPECTROSCOPIC STABILITY RELATION.

We have already mentioned that the high spectroscopic stability characteristic of the new quantum mechanics is the cardinal principle underlying the continued validity of the Langevin-Debye formula. We shall not attempt a precise definition of the term "spectroscopic stability."³⁴ It means roughly that the effect of orientation or of degeneracy in general is no greater than in the classical theory, and this usually implies that summing over a discrete succession of quantum-allowed orientations gives the same result as a classical average over a continuous distribution. In calculations of susceptibilities, and also in many other problems, the principle of spectroscopic

³³ It is obvious from the mode of definition that $M(n; n')$ cannot depend on the direction of the axis of quantization. Otherwise the total intensity of a spectral line, i.e., the x , y , and z effects combined, would depend on the direction of this axis, which is absurd.

³⁴ For references on spectroscopic stability and some discussion of its important application to the polarization of resonance radiation see J. H. Van Vleck, "Quantum Principles and Line Spectra," Bull. Nat. Research Council, no. 54, p. 171 ff.

stability may be regarded as embodied mathematically in the statement that the double sum

$$\sum_{l,l'} |f(sl; s'l')|^2 \quad (18)$$

is uniquely determined even in a degenerate system, and has a value invariant of the manner in which the degenerate degrees of freedom are quantized. Here $f(sl; s'l')$ denotes an amplitude element of any "quantentheoretische Grösse," i.e., of any matrix f which can be regarded as a function of the coordinates and momenta. We suppose the indices l and l' to correspond to a quantum number l whose value has no influence on the energy, while s and s' represent the effect of all other quantum numbers. The summation with respect to l extends over all the components of a family of states s whose energies ("Eigenwerte") coincide due to degeneracy. The interpretation of the sum over l' is similar. Thus the summation embraces all the various transitions which are possible between two "multiple" energy levels each composed of a number of equal-valued components. A simple physical illustration is summing over all the Zeeman components of a given spectral line in a vanishingly small magnetic field. The invariance of an expression similar to (18) has already been established by Born, Heisenberg, and Jordan³⁵ for the special case that only one of the systems of energy levels is multiple. This simplification would require that l (or else l') assume only one value in (18). The invariance of the more general expression (18) was mentioned without proof in a preceding paper by the writer,³⁶ and he is informed that the more general result has also been obtained independently by Born (unpublished). In the work of Born, Heisenberg, and Jordan, and of Born, it is supposed that f is a coordinate or momentum matrix, but this appears to be a needless specialization.

Proof. The demonstration is very similar to that given by Born, Heisenberg, and Jordan for the special case that one of the systems of levels s or s' is single, and we assume the reader has at least a superficial familiarity with their procedure³⁷ for quantizing the perturbations of a degenerate system. Let S be the "transformation matrix" associated with the passage from one mode of quantization of the degenerate system to another. The function S will generate a contact transformation from the original variables $p_1^0, \dots, p_n^0, q_1^0, \dots, q_n^0$ to a set of new variables $p_1, \dots, p_n, q_1, \dots, q_n$ by means of the connecting relations

$$p_k = Sp_k^0 S^{-1}, \quad q_k = Sq_k^0 S^{-1}.$$

If the system is made non-degenerate by applying an external field, the secular perturbations are calculated and quantized by finding the particular contact transformation which will reduce the perturbed energy to a diagonal matrix, but this fact is of no immediate consequence. Born, Heisenberg, and Jordan show³⁸ that in general

³⁵ Born, Heisenberg, and Jordan, Zeits. f. Physik, 35, 590 (1926).

³⁶ J. H. Van Vleck, Proc. Nat. Acad., 12, 662 (1926).

³⁷ Born, Heisenberg, and Jordan, Zeits. f. Physik, 35, 577-590 (1926).

³⁸ Ibid., p. 574.

$$f = S f^0 S^{-1} \quad (19)$$

where f^0 is the same function of the p^0 's and q^0 's that f is of the p 's and q 's, so that

$$f = f(p_1, \dots, p_n; q_1, \dots, q_n) \quad f^0 = f(p_1^0, \dots, p_n^0; q_1^0, \dots, q_n^0).$$

Now we suppose S to be a "secular" transformation matrix associated only with the ambiguity arising from the degeneracy, and hence $S(sl; s'l')$ will vanish unless $s=s'$. This means simply that in the language of section 3, S possesses no "high frequency elements," and in fact contains only elements associated with zero frequencies representing transitions between component states of coincident energy. Therefore by the rules for matrix multiplication an element of (19) may be written

$$f(sl; s'l') = \sum_{l'', l'''} S(sl; sl'') f^0(sl''; s'l''') S^*(s'l'; s'l'''). \quad (20)$$

Here we have made use of the fact³⁹ that in virtue of the orthogonality properties S^{-1} equals \tilde{S}^* , where S^* denotes the conjugate of S , and \tilde{S} the transposed matrix formed from S by interchanging rows and columns, so that $\tilde{S}^*(s'l'; s'l''') = S^*(s'l'''; s'l')$.

From (20) it is seen that

$$\sum_{l, l'} f(sl; s'l') f^*(sl; s'l') = \sum_{l, l', l'', l''', l^{iv}, l^v} \{ f^0(sl''; s'l''') f^{0*}(sl^{iv}; s'l^v) \\ S(sl; sl'') S^*(sl; sl^{iv}) S^*(s'l', s'l''') S(s'l'; s'l^v) \} \quad (21)$$

where we write l^{iv} for l'''' , etc. Now the orthogonality relations³⁹ give

$$\sum_l S(sl; sl'') S^*(sl; sl^{iv}) = \delta(l'', l^{iv}) \quad (22)$$

where

$$\delta(l'', l'') = 1, \quad \delta(l'', l^{iv}) = 0, \quad l'' \neq l^{iv} \quad (23)$$

There are also, of course, equations similar to (22) and (23) in which s, l, l'', l^{iv} are replaced by s', l', l', l''' respectively. Thus (21) becomes

$$\sum_{l, l'} f(sl; s'l') f^*(sl; s'l') = \sum_{l'', l'''} f^0(sl''; s'l''') f^{0*}(sl''; s'l'''). \quad (24)$$

Now on the right-hand side we may replace l'', l''' by l, l' for this is only a change in the notation for the variable of summation. Also the product of a complex number and its conjugate equals the square of its absolute magnitude. Therefore (24) may be written

$$\sum_{l, l'} |f(sl; s'l')|^2 = \sum_{l, l'} |f^0(sl; s'l')|^2. \quad (25)$$

This is the desired result, for it shows that an expression of the form (18) has the same value before and after the transformation, and is thus invariant of the mode of quantization.

It is noted that the expression (18) is invariant even when $s=s'$, for there is nothing in the above demonstration which requires $s \neq s'$. With $s=s'$ the summation in (18) or (25) extends over the various transitions within a multiple level rather than over those between two multiple levels.

³⁹ Ibid., p. 584, Eq. (11).

Application to spacial degeneracy. The most important application of (18) or (25) in calculating susceptibilities is to the case where the degeneracy arises from the absence of an external field, so that one direction in space is as good as another. Then the various values of the indices l and l' correspond to different values of the axial (often called "equatorial" or "magnetic") quantum number belonging to a system of "multiple" levels whose components differ from each other only in that they represent different "quantum-allowed" orientations relative to the axis of quantization. The contact transformation of the type considered above then simply involves a rotation of the coordinate axes, and means that the direction of spacial quantization is shifted from one direction in space to another. Now clearly if A is any vector, the double sum (18) has by symmetry the same value whether we take f equal to any one of the three components A_x , A_y , A_z provided we average (18) over all possible directions for the axis of quantization, for after the average there is no preference between the x , y , and z directions without external fields. But we have proved an expression of the form (18) invariant of the axis of quantization, and hence the average over all directions for this axis is unnecessary. Thus (18) always has the same values with f equal to A_x , A_y , or A_z regardless of the choice of the axis of quantization. Hence, since $A^2 = A_x^2 + A_y^2 + A_z^2$, it follows that

$$\sum_{l,l'} |A_x(sl; s'l')|^2 = \frac{1}{3} \sum_{l,l'} |A(sl; s'l')|^2 \quad (26)$$

with analogous equations involving A_y and A_z . This is the same result as was quoted on p. 737, section 3, except for a slight difference in notation. We there used the three-index notation $A(njm; n'j'm')$ instead of $A(sl; s'l')$ in order to permit further classification of the families of energy levels. The two indices n and j together correspond to s , and m to l .

The proof given above assumes complete spacial degeneracy, which means that the molecule should be subject to no external forces, and in section 3 we applied (26) to the "unperturbed motion" executed when the applied electric field F is zero. In section 3, however, we admitted the possibility of other simultaneous external fields independent of F (e.g., a "crossed" magnetic field), so that there was not necessarily spacial degeneracy and freedom from external influence when $F=0$. We can, nevertheless, still apply (26) to such cases if the result of these other external fields is only to introduce precessions or secular motions corresponding to frequencies of the form $\nu(sl; s'l')$, without any "high frequency perturbations" of the type $(sl; s'l')$, $s' \neq s$. For then the effect of these external fields is given by a "secular" contact transformation of the type considered above, which will leave invariant the values of expressions similar to the left-hand side of (26). Actually an external field will in general alter to some extent the amplitudes of terms of the type $(sl; s'l')$ ($s' \neq s$), but these "non-secular" perturbations will in general distort the amplitudes only to a low degree, as this is a well-known result in dynamics. Hence it is a good approximation to apply (26) even when the unperturbed motion corresponding to $F=0$ is itself a motion in some other external field. The usual case, of course, is

where F is the only external field, and then (26) holds rigorously for the unperturbed motion.

Illustrations of (26). An example or two will perhaps make the results obtained above more concrete. If A be a unit vector matrix, then A_z may be regarded as the cosine of the angle between this vector and some fixed direction in space chosen as the x -axis. Eq. (26) shows that the mean value of the square of the cosine of this angle is one-third when we average over all the various allowed orientations relative to the axis of quantization (not necessarily the x -direction). This is the same value as results by symmetry in the classical theory when we average over a uniform continuous distribution of orientations. This agreement is the underlying reason why the susceptibility formula (1) contains the factor $\frac{1}{3}$ quite as generally in the new quantum mechanics as in the classical theory.

Another simple illustration of (26) is furnished by the theory of diamagnetism. It can be shown that the diamagnetic susceptibility is proportional to $x^2 + y^2$ if the magnetic field is applied in the z -direction. Now by the rules for matrix multiplication the average value of x^2 for the state s is

$$\sum_{l,s',l'} |x(sl; s'l')|^2 / p_s \quad (27)$$

where s' is to be summed over all possible states, including $s' = s$, and where p_s is the number of l -components belonging to the multiple state s . In other words p_s is the a-priori probability of the state s , or, what is essentially the same thing, the number of values assumed by its axial quantum number. Now (27) is simply an expression of the form (18) summed over s' , and there are, of course, similar expressions for the y and z components. Hence by (26) the average values of x^2 , y^2 , and z^2 are equal, and since $r^2 = x^2 + y^2 + z^2$, we can take $x^2 + y^2 = \frac{2}{3}r^2$, just as in the classical theory. This has an important experimental application, as it shows that the diamagnetic susceptibility per molecule should not vary with pressure (see ref.³⁶)

DEPARTMENT OF PHYSICS,
UNIVERSITY OF MINNESOTA,
February 28, 1927.

BOOK REVIEWS

Die Verwendung der Röntgenstrahlen in Chemie und Technik. HERMAN MARK. (Bd. XIV des Handbuch der angewandten und physikalischen Chemie herausgegeben von G. BREDIG.)—The author of this installment of one of the current hand-books has himself contributed much to the application of x-rays in research. The task which he sets himself is to present in one volume everything that the user of x-rays for other than medical purposes needs to know. He has come so near to complete success that his treatise deserves very careful consideration.

The first section (101 pages) deals with the production of x-rays. It contains rather too long and too elementary an account of the electrical engineering problems which may arise, and too much space is devoted to obsolete devices. On the other hand, the practical notes on the construction and use of gas-discharge tubes and electron-discharge tubes with demountable parts will probably save the novice—who is frequently in the author's thoughts—a good deal more than the cost of the whole volume. The American reader, however, will not give quite as much weight as his German contemporary to arguments against ready-made (technische) tubes, and other rather high-priced pieces of apparatus, partly because the cost of the experimenter's time is relatively more important here than in Germany.

The second section (104 pages) deals with the properties of x-rays. A good deal of this section is obvious padding. Flagrant examples are found in the tables of ν/R and $(\nu/R)^{1/2}$ and in Table 28, which gives data on K and L absorption edges for the light elements. Incidentally, the value of R given (pp. 128 and 447) is not the value (109737 cm^{-1}) used in the tables. Figs. 136 and 141 are meaningless as printed without any clue as to the abscissae. Tables 32, 37b and 38 have suffered similarly by amputation of footnotes. There are a good many misprints and many of the values quoted correctly are now obsolete. The Spectroscopy of X-Rays, by Manne Siegbahn, Oxford Univ. Press (1925), and the recent review by A. E. Lindh, *Phys. ZS.* 28 24–62, 93–125 (1927), should be consulted in preference.

The third section (232 pages) is very much the best. The subject matter here is crystal structure and its analysis. The description of crystals, lattices and space-groups is based on books by Niggli and Wyckoff and is both full and clear. In Tables 52 and 52a (42 pp.), which belong in this section though printed as an appendix, an effort has been made to give by single entry all that can be written down concerning the symmetry and the coordinates of equivalent points in the 230 possible space-groups. This has required, among other things, a copying of Wyckoff's tables of coordinates. The success achieved in this monumental labor is only fair. No complete checking has been attempted but in about two-thirds of Table 52 and the associated part of Table 52a more than thirty errors have been found, any one of which might seriously delay an uncritical user. The coordinates (Table 52a) are so crowded together that the chance for mistakes in reading is considerable; space wasted in Table 52—"Koordinantenfangspunkt" appears at full length more than a hundred times—would here have been appreciated. The advantage of single entry is partly counterbalanced by the necessity of consulting non-adjacent pages. Table 46 is inconsistent with Table 52 from which it should be derivable. In spite of the faults noted the tables in this section will find frequent use.

In the analysis of crystal structure by x-ray methods the various procedures are well explained and their advantages and draw-backs are fairly put. Examples of each are presented in such detail that a beginner in the art will find most of his questions anticipated and can proceed to actual analyses with confidence. Such thoroughness as the author insists upon, involving in most cases the use of several different methods, would save the scientific public from many largely speculative "determinations" of crystal structure. The discussion of intensity in interference patterns of all sorts is especially good.

In the fourth section (12 pages) the reader meets with disappointment. Here the questions dealt with concern the sizes and orientations of the crystals in polycrystalline aggregates, in-

cluding colloids. The author has had so much to do with the second of the questions in researches on plastically deformed metals that one looks with confidence for a masterly account of the rather special artifices here necessary. He finds instead only a few generalities and the excuse that the book is already too long to permit the inclusion of more. As already hinted, the earlier sections might better have been slashed to make room here. Radiography is even more completely crowded out.

A series of notes and references (27 pages) and a subject index (10 pages) complete the treatise. The references are adequate but not very carefully checked, especially as to the spelling of proper names. The illustrations throughout the book are generally good but often differ enough from the text to make it clear that the cuts were not all available for comparison when proof was read. The scale of reproduction is erratic, some unimportant sketches (e.g. Fig. 81) being too large—one is put in twice!—and some important ones (e.g. Fig. 74), too small. There is, in Section I, a tendency to use trade catalog cuts and patent drawings which are not very informative. Some figures contain absurd mistakes (e.g. Figs. 134 and 252). The paper is of good quality, the type is rather too thin and too much crowded together to make for easy reading. Large octavo. Pp. xiii+528, 328 figs. J. A. Barth, Leipzig. Price, cloth bd. Rm 50.00 (\$12.00).

L. W. MCKEEHAN

Applied X-rays. GEORGE L. CLARK.—This book professes to be propaganda in favor of a wider use of x-rays, and as such it is excellent. It contains at least a brief mention of every known application, and enough detail in regard to every application not exclusively medical so that the reader can decide for himself whether x-rays are likely to be of service in any given case. No one responsible for improvements in an industry dealing largely with solid or semi-solid materials can fail, while reading it, to be impressed with the opportunities which x-ray methods offer him in the way of analysis, inspection and control. The style, which is emphatic, and the choice for detailed discussion of matters with which the author is personally familiar, conform well to the purpose intended. The mathematical knowledge required of the reader is not greater than can properly be expected, but sections here and there will prove difficult to one not familiar with the nomenclature of organic chemistry. Just these parts will most richly repay study by physicists. The long chapter on colloidal and amorphous structure in particular, describes experimental studies which are hardly, if at all, known to those whose interest in x-rays has been based on physics. There are, in this chapter and elsewhere, brief references to the author's own unfinished investigations and to finished work concerning which publication has until now been withheld. These notes and some practical advice in regard to experimental details make the book a primary as well as a secondary source of information which must be consulted by investigators.

There is urgent need for haste in the preparation of a book on x-rays, parts of which are sure to be out of date before they are printed. This explains, but does not excuse, the principal faults of the present volume. Of these the worst are carelessly worded statements, ambiguous or contrary to fact. For example, Kirchner's results on nickel steel are just the opposite of those credited to him (p. 172). Several errors creep in where the avoidance of explicit mathematics has forced the use of circumlocutions. References to periodical literature are too often defective in regard to volume number, page number or year of publication. Typical crystal structures (esp. pp. 145-6) have suffered from mistakes in copying or typesetting.

The author states (p. 175) that the diffraction rings characteristic of liquids are explicable only by transient lattice-structures or equivalent regularities in the arrangement of molecules. It has, however, been proven several times—most lately by F. Zernike and J. A. Prins, *ZS. f. Phys.* **41** 184-194 (1927)—that the mere existence in a liquid of a lower limit to the distance between molecule-centers is enough to explain the observed effects.

The paper, type, illustrations, index and binding are good. Large octavo. Pp. xiii+255, 99 figs. McGraw-Hill Book Company, New York City, Price \$4.00. L. W. MCKEEHAN

Practical Colloid Chemistry. WOLFGANG OSTWALD with P. WOLSKI AND A. KUHN. Translated by I. NEWTON KUGLEMASS and THEODORE K. CLEVELAND.—This book is a translation of the fourth edition of Dr. Ostwald's laboratory manual for students of colloid

chemistry. It is divided into ten chapters each one of which deals with an important phase of the subject. The ten chapters are entitled: I. Preparation of Colloidal Solutions; II. Diffusion, Dialysis, Ultrafiltration; III. Surface Tension and Viscosity; IV. Optical Properties; V. Electrical Properties; VI. Experiments with Gels; VII. Adsorption; VIII. Coagulation, Peptization and Related Phenomena; IX. Commercial Colloids and Other Material for Demonstration Purposes; X. Dispersoid Analysis. One hundred and eighty three experiments are listed in the first eight chapters. As these chapter headings indicate the student, performing these experiments, proceeds from a study of the methods for the preparation of colloids to their purification and then to a study of their properties. Each chapter begins with an explanation of the phenomena to be studied. The experiments themselves are for the most part very well chosen. In some instances however the directions are rather brief and not sufficiently specific. The translators should have used a little more care as there are some grammatical errors and the construction of some of the sentences is rather Teutonic. The book should be of considerable value as a laboratory guide to students entering the field of colloid chemistry. Pp. xvi+191. 22 figs. E. P. Dutton & Co. Price \$2.25.

L. H. REYERSON

Investigations on the Theory of the Brownian Movement. ALBERT EINSTEIN. Edited with notes by R. FÜRTH. Translated by A. D. COWPER. This volume contains five of the principal papers contributed by Einstein on the theory of the Brownian movement to the *Annalen der Physik* and the *Zeitschrift für Elektrochemie* during the period 1905 to 1911. The author has developed from first principles a mathematical theory of the movement and osmotic pressure of small suspended particles in a liquid and of their influence on the viscosity, etc., of the liquid, leading up to a determination of molecular dimensions. In the fifth paper is given a brief but comprehensive elementary theory of the Brownian movement. An appendix of notes by Dr. Fürth with corrections, later references, and some expansions of the original texts, is added. The work will serve as an admirable introduction to the study of osmotic pressure. The difficult task of the translator has not been particularly well done. The involved sentence structure of the original texts is often retained and makes anything but smooth reading. The typography, while adequate, is not distinguished, particularly in the mathematical forms. Pp. vii+124, 4 figs. E. P. Dutton, 1927. Price \$1.75.

JOHN T. TATE

Treatise on Thermodynamics. MAX PLANCK. Translated by ALEXANDER OGG.—This is the third English edition, a translation of the seventh German edition, of Planck's classic. Its appearance is particularly welcome because the previous English editions have been out of date for twenty years or more. The principal addition to be found in the present volume is, of course, the chapter on the Nernst heat theorem. There is also included a discussion of Ghosh's theory of the lowering of the freezing point of strong electrolytes and of Debye's equation of state for solids which contains the explanation of the variation of the specific heat with temperature as well as Grüneisen's law for the coefficient of thermal expansion. It is unfortunate that Debye and Hückel's theory of electrolytic dissociation could not have been included. The numerical data have been thoroughly revised and brought up to date. Commendation is due the translator for the faithfulness and skill with which he has done his work. The book is attractively printed and serviceably bound. Pp. iv+297, 5 figs. Longmans Green and Co., 1927. Price \$5.00.

JOHN T. TATE

PROCEEDINGS
OF THE
AMERICAN PHYSICAL SOCIETY

MINUTES OF THE LOS ANGELES MEETING, MARCH 5, 1927.

The 144th meeting of the American Physical Society was held in Los Angeles, California, at Berkeley Hall, University of California at Los Angeles.

The presiding officer was Professor S. J. Barnett. The attendance was about 40.

The program consisted of 31 papers, of which abstracts are given in the following pages. An AUTHOR INDEX will be found at the end.

D. L. WEBSTER,
Local Secretary for the Pacific Coast

ABSTRACTS

1. The reflection of x-rays by crystals as a problem in the reflection of radiation by parallel planes. SAMUEL K. ALLISON, University of California.—It is pointed out that the previous solutions of the problem of the reflection of radiation by parallel planes by Lamson and Gronwall are physically incorrect since the intensities, not the amplitudes, of contributions from individual planes, have been added. It is shown that a mathematical method due to Darwin leads to a solution identical mathematically with those of Lamson and Gronwall. Using this result, the intensity of reflection is evaluated for certain ranges of the constants directly related to the reflected and transmitted amplitudes due to a single plane.

2. A study of the infra-red solar spectrum with the interferometer. HAROLD D. BABCOCK, Mount Wilson Observatory.—*Solar wave-lengths in the infra-red.*—The solar spectrum in the interval $\lambda 6869-8980$ has been photographed on plates sensitized with *neocyanine* through interferometers crossed with a concave grating. Of the 507 lines measured, 176 are of solar origin; most of the remainder are probably lines of terrestrial water vapor. The *wave-lengths* were measured in terms of oxygen band lines due to terrestrial absorption and are expressed on the *neon scale*. *Identification of solar lines.*—The measurements have been used for a revision of the identification of solar lines, but refined laboratory wave-lengths are much needed for further work. The more prominent solar lines still awaiting identification are listed. *Differences between solar and terrestrial wave-lengths.*—In the absence of precise laboratory data for vacuum spectra in the infra-red, the new solar wave-lengths are compared with interferometer measurements on the spectrum of a short iron arc at atmospheric pressure. This brings out clearly the correlation of multiplet grouping, excitation potential and behavior under increased excitation with the combined influence of pressure displacement and pole effect. The data, though not definitive, are consistent with the gravitational displacement predicted by Einstein.

3. Fine structure of the Balmer lines of hydrogen. NORTON A. KENT, LUCIEN B. TAYLOR and HAZEL PEARSON, Boston University.—Using two optical trains (1) two crossed Lummer plates, the larger of resolving power 670,000, and (2) an echelon of resolving power 660,000, with a vacuum tube cooled with liquid air, the writers have determined the wave-length difference between the two well known components, λ' and λ'' ($\lambda' > \lambda''$) of $H\alpha$, $H\beta$ and $H\gamma$.

The doublet separations are shown in the table together with those given by Houston, which latter are in our estimation, the most reliable thus far obtained.

Current density	Houston 250	Kent, Taylor and Pearson 25	13 ma./sq. cm
$\Delta\lambda$ for H α	0.1358	0.1370	0.1391 Angstroms
$\Delta\lambda$ for H β	.0782	.0791	—
$\Delta\lambda$ for H γ	.0665	.0666	—

Our values are higher but this is not to be wondered at, because of the different current densities employed. A very reliable Lummer plate spectrogram, taken at 13 milliamperes per sq. cm, yields 0.1391 for H α , which is in harmony with such a current change. Microphotometer curves of *enlargements* of the original Lummer plate negatives reveal another component in λ' , unresolved but unquestionably present, in H α , H β and H γ . Hansen noticed assymmetries here in H α and H β . Further these are indications of another component in λ'' . The *magnitudes* of these six new components all agree well with the theoretical magnitudes on the spinning electron theory: their *positions* are in all cases too far toward the red—an effect probably due to the photographic processes involved.

4. The fine structure of the helium arc spectrum. WILLIAM V. HOUSTON, National Research Fellow, California Institute of Technology.—By means of the compound Fabry-Perot interferometer it has been possible to show that both the sharp series line 7065 and the diffuse series line 5876 of the orthohelium spectrum are triple. Under conditions which made reversal very improbable the strong component was shown to consist of two lines with intensity ratio about 5:3. This, with the weak component, makes a triplet of normal intensity ratios, and confirms the theoretical expectation that the helium spectrum should consist of singlets and triplets. The 2³P level is inverted with separations 0.992 cm⁻¹ and 0.071 cm⁻¹. This is in good agreement with the quantitative theory of Heisenberg. The D levels can be estimated from the 5876 line to be partly inverted. This experimental verification of the theoretical expectation removes the helium spectrum from its anomalous position among the spectra of the elements.

5. Series spectra of ionized phosphorus, P_{II}. I. S. BOWEN, California Institute of Technology.—One hundred and ten of the strong lines of P_{II} have been classified as arising from various combinations between thirty-two terms of the triplet system. The observed terms include nearly all the terms of the triplet system that are predicted by the Russell-Heisenberg-Pauli-Hund theory for the s²p², sp³, s²p·4s, s²p·5s, s²p·4p, s²p·3d, and s²p·4d configurations. The lowest level is the 3P₀ term of the s²p² configuration. This term has a value corresponding to an ionization potential of 19.82 volts.

6. Relationships in the spectra of the elements of the first row of the periodic table. R. A. MILLIKAN and I. S. BOWEN, California Institute of Technology.—Practically all of the strong ultra-violet lines that can be emitted by the atoms of the first row of the periodic table in all stages of ionization of the valence electrons have now been obtained and a general statement of the relationships between the frequencies of these lines has been formulated. These relationships are presented most simply and compactly in a new graph here given which depicts the generalized form of the Moseley law in the field of optics. Similarly a table of the ionization potentials of the atoms of the first row in all stages of ionization is here presented. Furthermore the predictions of the Russell-Heisenberg-Pauli-Hund theory as to the structure of spectra in general have been completely verified in the case of these light elements.

7. Interferometer Measurements on the Balmer Series. WILLIAM V. HOUSTON, National Research Fellow, California Institute of Technology.—The compound Fabry-Perot interferometer, with a resolving power of about one million, shows an unmistakable asymmetry of the short wave-length component of H α . Graphical analysis of a microphotometer curve indicates the presence of a component about 0.12 cm⁻¹ from the principal one, with about one sixth its

intensity. The presence of this component is the principal difference between the prediction of the spinning electron theory and that of the purely relativity theory. The observed intensity agrees well with that predicted by Sommerfeld and Unsöld. The intensity relations predicted by Sommerfeld and Unsöld make it possible to compute the position of each of the five components from the observed positions of the two centers of gravity. With the interferometer wave-lengths of the first three lines of the Balmer series R_H is found to be $109677.67 \pm .01$. Thus the accuracy of e/m , determined spectroscopically, is governed by the accuracy of R_{He} . From a mean of the values of Paschen and of Leo on He 4686, e/m is found to be 1.769, and it seems improbable that it can be below 1.765. This does not agree with the Zeeman effect measurements by Babcock, so that further work will be done with the interferometer to improve the value of R_{He} .

8. New infra-red absorption bands in methane. JOSEPH W. ELLIS, University of California, Southern Branch.—A recording infra-red spectrograph was employed to examine the absorption spectrum below 2.8μ of an 87.5 cm cell of pure methane. Five new absorption bands were found at 1.15μ , 1.37μ , [1.66μ , 1.72μ], and 1.80μ . Those at 1.66μ and 1.72μ are assumed to be the partially resolved first harmonic of the well-known fundamental at 3.33μ , while the 1.15μ maximum is interpreted as its unresolved second harmonic. The deviation from a true harmonic relationship is consistent with theory. The 1.37 and 1.80μ bands are doubtless the $(\nu_3' + \nu_4)$ and $(\nu_1 + \nu_4)$ combination bands, where ν_3' , ν_4 and ν_1 are the frequencies of the 1.69 , 7.67 and 2.37μ bands respectively. The latter two values, as well as that at 3.33μ , are from measurements by Cooley (*Astrophys. J.*, **62**, 73 (1925).), and the notation is consistent with his. The theoretical values of the above two combination bands are 1.38 and 1.80μ respectively. The degree of complexity recorded by Cooley in the 2.35μ region is also observed in this investigation. As a result of a check on the previous calibration of the instrument the wavelength values recorded in this abstract are slightly inconsistent with all values previously published by the writer. This correction will be more fully discussed elsewhere.

9. On King's classical theory of atomic structure. BORIS PODOLSKY, California Institute of Technology.—An analysis of King's paper (*A Classical Theory of Atomic Structure and Radiation*, Mercury Press, Montreal) shows that King assumes all electrons spinning with the same angular velocity. In motion the electron experiences a Lorentz-Fitzgerald contraction which is supposed to cause a precession. By assuming that the frequency of precession must equal the frequency of incident radiation in the case of photo-electric phenomena, and to an integral multiple of the orbital frequency in the case of radiation King obtains a picture of the quantum mechanism. There are, however, grave objections against this ingenious hypothesis. It is shown in the present paper that (a) the electron could not have a precession and absorb energy without changing the frequency of precession, (b) the electron cannot have a precession, (c) the picture is undesirable, for the precession of the electron (due to causes other than those discussed by King) has found its place in explaining the normal doublets and triplets, i. e. small changes of frequency and not the whole effect.

10. The magnetic dipole in Schroedinger's theory.—PAUL S. EPSTEIN.—Let us consider an electron moving in the field of a fixed nucleus to which a magnetic dipole of fixed direction is attached. It is known that in Bohr's theory this mechanism leads to the same energy levels as a spinning electron in the field of a simple nucleus, provided that we choose the moment of dipole as one half of the moment which a spinning electron would have. The calculations for this case have been carried out from the point of view of Schroedinger's undulatory mechanics and the final formulas are exactly those anticipated by Goudsmit and Uhlenbeck for the spinning electron.

11. Striking potentials of metallic arcs in vacuo. S.H. ANDERSON, University of Washington, —Simmon's theory of the minimum striking potential of metallic arcs in vacuo (*Phil. Mag.* **46**, pp. 816-819, 1923) has been tested with electrodes of magnesium and of aluminum. The electrodes were sealed into Pyrex glass bulbs (with one electrode adjustable by an electromagnet

outside) so that a high vacuum could be produced and maintained. With pressures of 10^{-4} bars, 1 bar and 10 bars, respectively, a persisting arc could *not* be struck with either kind of electrodes when potentials as high as 150 volts were applied. With a pressure of 100 bars of air, persisting arcs were struck with both the magnesium and aluminum electrodes. For magnesium the applied potential difference was 45 volts. While burning, the potential difference was 26 volts and the current 4 amperes. For aluminum the applied potential difference was 88 volts. While burning, the potential difference was 36 volts and current 3.1 amperes. It appears that the striking potential is dependent upon a gaseous atmosphere as well as the nature of the electrodes.

12. Mobilities of ions in hydrogen gas mixtures and the constitution of the ion. LEONARD B. LOEB, University of California.—Recent measurements of mobilities in HCl-air mixtures indicated that there was an increased concentration of HCl gas in the neighborhood of the ion, the effect being greatest for the negative ion. Experiments in mixtures of hydrogen with ether, and hydrogen with NH₃, have given the following new facts. Small amounts of ether *lower* the mobility of the *positive ion* in H₂ *abnormally* while the effect on the negative ion can be calculated from the law of mixtures. *Minute traces* of NH₃ in H₂ *increase* the mobility of the *positive ion to nearly that of the negative ion*. Further additions of NH₃ *lower* both positive and negative mobilities in H₂ faster than the law of mixtures demands, but not as fast as earlier experiments in air—NH₃ mixtures led one to believe. In a mixture of NH₃, ether, and H₂ the effect on the positive ions was to be calculated from the observed combined effects of what the ether alone produced added to what the NH₃ would have produced on a normal positive ion in H₂ without the increase due to NH₃ alone. These results can only be explained on the assumption that the ionized positive molecule or atom adds to itself at least one more molecule to make a positive ion. This conclusion is in accord with a similar conclusion recently drawn by Erikson on the basis of other evidence.

13. The effect of added gases on ammonia decomposition by optically excited mercury vapor. A. C. G. MITCHELL and R. G. DICKINSON, California Institute of Technology.—Ammonia decomposition has previously been shown to be sensitized to the mercury line 2537A by the presence of mercury vapor. In the present work the effect of added hydrogen, nitrogen, and argon on the rate of this decomposition has been studied, and the results correlated with the quenching of fluorescence of mercury vapor by these gases. It was found that with an ammonia pressure of 3 mm, a hydrogen pressure of about 0.1 mm suppressed the rate of decomposition by 50 percent; at lower ammonia pressures even less hydrogen was required. From the results of experiments at different ammonia and hydrogen pressures, the ratio of the efficiency of activation of ammonia by excited mercury, to the efficiency of de-activation of excited mercury by hydrogen has been estimated to be about 4×10^{-2} . On the other hand, several tenths of a millimeter of either argon or nitrogen were found to be without effect, as would be anticipated from the results of fluorescence experiments.

14. Direction of photo-electric emission. D. H. LOUGHRISE, California Institute of Technology.—Cloud expansion photographs of the photo-electrons produced in hydrogen, air, and argon by means of the K α radiation of Mo show that the most probable direction of emission is the same for all three gases, and forms an angle of about 70° with the x-ray beam. These angles have been measured by means of a stereoscopic comparator specially built for the purpose. The total number of tracks measured is 443. Distribution curves plotted with number of tracks starting at a given angle with the x-ray beam against the angle show a narrower peak for hydrogen than for the argon. This qualitatively supports the view that the distribution is due to secondary scattering by the electrons in the atoms through which the photo-electron passes and that the initial direction of emission may be constant for a definite wave-length and depend only on the radiation.

15. The velocity and number of the photo-electrons ejected by x-rays as a function of the angle of emission. E. C. WATSON, California Institute of Technology.—Magnetic spectra of the electrons ejected by x-rays from thin metallic films at angles ranging from 0° to 180° with

the direction of the x-ray beam have been obtained by the method of Robinson, de Broglie, and Whiddington. To the degree of accuracy of the measurements (0.5 percent) the maximum velocity of ejection is exactly the same in all directions. With thin foils of the heavier elements the numbers of electrons leaving the foil with this maximum velocity in the various directions is approximately the same. With foils of the very light elements, or with sputtered films so thin that Wentzel's criterion for single nuclear scattering holds, the number of electrons leaving the foil is greatest in a direction a little forward of perpendicular to the direction of the x-ray beam. The number of electrons leaving in other directions can be calculated by means of the theory of scattering, if the assumption is made that all the electrons start out from the atom in the same direction.

16. Spacial distribution of the photo-electrons ejected by x-rays. E. C. WATSON, California Institute of Technology.—The experiments of Wilson, Auger, Bothe, Bubb, Loughridge, and Kirchner have shown that the most probable direction of the photo-electron tracks in a gas traversed by x-rays is nearly the direction of the electric vector of the incident wave, but with an appreciable forward component. There is, however, a very considerable variation in the direction of the tracks. Theories to account for this apparent emission from the atom over a wide range of angles instead of in a definite direction have been proposed by Bothe, Bubb, Auger and Perrin, and Wentzel. It can be shown, however, that scattering must be present in all the experiments in sufficient amount to account for the distribution in direction, and the theory of scattering leads to a distribution function which fits the facts much better than any of the more elaborate theories. Consequently the fact that the photo-electron tracks do not have one definite direction does not constitute evidence for orbital velocities inside the atom.

17. The Shadowgraph Method as applied to a Study of the Electric Spark. HARVEY A. ZINSZER, Indiana University.—The method employed was essentially that devised by Foley and Souder (Phys. Rev. 25, 373, 1912.) Instantaneous shadowgrams having an exposure of the order of three microseconds were obtained. Introducing low values of inductance between the influence machine and the retarding capacity showed an improvement in the method of controlling the retardation of the illuminating spark; a micrometer auxiliary gap located outside the dark box and in parallel with the object gap both permitted the photographing of very early sparks and considerably improved the detail of all shadowgrams whether of early or late sparks. The diffusion of metallic vapor into the spark gap as proved spectroscopically was verified by instantaneous photography. Photographic life histories of various types of spark discharges were obtained and a theory of the phenomena involved in the condensed electric spark discharge was subsequently proposed.

18. Some remarks on the formation of negative ions. A. P. ALEXEIEVSKY, University of California (introduced by L. B. Loeb).—When an electron approaches a molecule of a gas, the molecule is polarized and the electron is attracted toward the molecule. The force of attraction is probably given approximately by Langevin's expression $f = (D - 1)e^2/2\pi r^5 N = K/r^5$ where D is the dielectric constant of the gas, N the number of molecules in 1 cc of gas, e the charge of the electron, and r the distance between the electron and the center of the molecule. An electron which has "attached" itself to a molecule is probably moving in an orbit a part of which lies inside the molecular core and the remainder outside it. Assuming that the electron cannot move inside the core all the time it is shown that all possible periodic orbits must lie inside a circle of radius $r = (Km)^{1/2}/p$ where m is the mass and p the angular momentum of the electron. Assuming that the least amount of angular momentum an electron can have is one Bohr unit it is found that for a given gas all periodic orbits must lie within the circle of radius $R = 2\pi(Km)^{1/2}/h$ where h is Planck's constant. It turns out that for helium and argon R is less than the radius of the core, while in gases with large dielectric constant R is considerably greater than the probable radius of the core.

19. Factors influencing thermionic emission. A. KEITH BREWER (National Research Fellow), California Institute of Technology.—The thermionic emission from gold has been determined in the presence of various gases at atmospheric pressure. Both the positive and

negative currents follow the Richardson equation, although there is no semblance of saturation. A distinct proportionality exists between the difference in the values of b , (Δb), for the positive and for the negative emission, and for the corresponding differences in the values of T , (ΔT). Again, when an emitter, such as iron, is slowly oxidized over, there is a gradual increase in the values of b and T for the positive emission which is concomitant with a corresponding decrease for the negative emission. When the value of b is the same for ions of each sign T is likewise the same. The relationship between Δb and ΔT is accounted for by the presence of an intrinsic force, possessing the properties of a resultant field, existing at the surface. The changes in T and b accompanying the oxidation of a surface is doubtless due to the presence of the negative oxygen ions of the oxide neutralizing the positive intrinsic field, and upon high oxidation, actually giving rise to a resultant negative field.

20. Remark on the theory of the Trouton and Noble experiment. PAUL S. EPSTEIN.—The physical cause why this experiment must be negative in the theory of relativity can be stated as follows: the torque acting on the moving condenser is compensated by the fact that the longitudinal and transverse masses of the condenser are not equal but stand in the ratio $1-v^2/c^2$ (v velocity of the condenser, c of light). To obtain the components of the acceleration the longitudinal and transverse ponderomotive forces on each plate must be divided by the corresponding masses. The resultant acceleration passes through the center of gravity of the system and so does not produce any rotation. It is usually overlooked, that in the absolute theory also we must distinguish between longitudinal and transverse mass, since the nuclei have an electric constitution. For instance, if we imagine them as rigid electrified spheres the ratio is, according to Abraham's theory, $1-4v^2/5c^2$. In this case we still have a compensation of $4/5$ of the torque and the effect is five times smaller than that expected under the assumption, usually made, that the whole of the torque can be observed. R. Tomaschek (Ann. d. Physik 78 p. 743, 1925) and C.T. Chase (Phys. Rev. 28, p. 378, 1926) give the maximum velocity that could remain undiscovered by them as 4 km/sec. Our remark would bring it to $4(5)^{1/2}$ km/sec = 9 km/sec, so that their results are hardly fit to check Miller's contentions.

21. Measurement of wave-length in water. ARTHUR W. NYE, University of Southern California.—A transmission grating was submerged in a trough of water and mounted on the stage of a spectrometer in the usual position. A window behind the grating allowed parallel light to enter at right angles to the window and grating. The diffracted first and second order spectra were received by the telescope as usual, except that the front surface of the objective was in water. A watertight flexible rubber connection was provided so that the front of the objective could remain in water, but allow the telescope to be swung freely to observe the spectral lines. The usual equation then applied but the wave-lengths as calculated were the lengths in water. The inverse ratio of these to the accepted values in air should give the air-water index of refraction. The results showed that the index of refraction differed not more than 0.0025 from the accepted values, at any point. Several prominent lines of Hg and Na were used, ranging from about 4000 Å to 6500 Å.

22. End corrections of pipes as a function of frequency. FLOYD C. OSTENSON and S. H. ANDERSON, University of Washington.—The correction due to the reflection of sound waves from the open end of a brass pipe has been measured by the usual method of finding two or more resonant lengths. Points of resonance were located using as a detector a telephone connected to a galvanometer through a thermionic tube as a rectifier. With a tube 10 cm in diameter there is a small constant increase in the end correction with increasing frequencies from 128 v.p.s. to 832 v.p.s., beyond which the increase becomes very rapid. With a tube 7.62 cm in diameter there is a maximum in the end correction at 640 v.p.s. beyond which there is a decrease.

23. The measurement of sound-absorption in a room. V. O. KNUDSEN, University of California, Southern Branch.—The differential equation for the status of sound energy in a room yields two useful relations for determining a , the sound-absorption of a room. These

relations are (1), $a = 4E/vI_{\max}$, for steady state; and (2), $I = I_{\max}e^{-avt}/4V$, for decay. (E =rate of emission of source, v =velocity of sound, I =average energy density, V =volume of room.) The usual method, developed by Sabine, makes use of (2), measuring the time t for a known diminution of intensity I . The advantages and limitations of this method, and also of two other possible methods, one involving the measurement of the average value of I_{\max} , and another involving measurements of oscillograms of the decay of sound, are discussed. With suitable instruments, the measurement of I_{\max} seems to be the most satisfactory method for determining a . Preliminary experiments and results are described which indicate that a , determined from (1) by intensity measurements, agrees within 2% of the value obtained from reverberation measurements. The frequency of the sound-source used varies periodically from 408 d.v. to 629 d.v. This shifts the interference pattern sufficiently to give approximately an average intensity of sound at any point in the room not too near the source.

24. Change of elastic frequencies in solid bodies with pressure. F. ZWICKY, California Institute of Technology.—The general theory for the constituent forces in heteropolar crystals has been developed by Born and other investigators. As a new conclusion of this theory a formula for the shift of frequency of residual rays with pressure is deduced. The shift corresponding to a pressure of 10,000 atm. amounts approximately to 7μ in the case of NaCl (residual rays at 50μ). Qualitative conclusions may be drawn with respect to the dependence of elastic frequencies on pressure in any crystal. Combining these results with a suggestion made first by Grueneisen, a rational explanation can be given for the effect of pressure on the specific electric conductivity of metals, this conductivity being in general increased with pressure. The relation of our results on conductivity to those obtained previously by Grueneisen and Bridgman in a quite different way, is discussed.

25. Effect of oil in storage on lightning discharge. ROYAL W. SORENSEN, California Institute of Technology.—As a part of a large laboratory program to determine means of protection against direct hits or induced sparks in oil reservoirs as produced by cloud charges or lightning strokes, a number of tests were made to determine the ability of oil to hold an electric charge or to influence the direction of discharge between electrodes on one of which oil is placed. These experiments show that as soon as oil is placed in an electric field circulation begins. Because of this oil does not act as a solid dielectric. That is, local charges cannot accumulate at spots on an oil surface. This point was proven by placing pans containing oil in a strong electric field produced by high-potential direct current. Charges could be detected on the surface of the oil only while the field was maintained between pan and an electrode above the oil. No charges were found after the source of energy was disconnected. Also, charged electroscopes when placed in contact with the surface of the oil will readily discharge. Other tests with the oil pan positive and the electrode above the pan negative also show that oil on a positive terminal does not influence spark discharge as does solid dielectrics placed near the positive terminal.

26. On the electrostatics of the thunderstorm. A. W. SIMON, California Institute of Technology.—The electrostatic phenomena of the thunderstorm are analyzed in somewhat greater detail than has been done before. The action of the storm cloud is shown to be analogous to the generation of charges and potentials by rubbing together two dissimilar substances, i. e., the fundamental experiment of frictional electricity. The generation of potentials and electric stresses by precipitation of charged rain and by the induction of charges at the earth's surface are discussed. It is shown that the "impulsive rush" lightning discharge of Lodge is electrostatically impossible. A relation between the change of gradient in an area, the polarity of the charged rain falling in the area, and the polarity of the overhead cloud is developed. Approximate numerical relations between gradients, charges, and potentials are deduced. Applications of the results to lightning protection are made.

27. Vacuum switch. H. E. MENDENHALL, California Institute of Technology.—Previous experiments on denuding metals of gases by various kinds of treatment have shown that arcing between contact points became continuously more and more difficult with further denudation, and suggested the possibility of interrupting large currents at high potentials in a

practically perfect vacuum without appreciable arcing. Experimental tests have now been carried up to the point where about 1000 amperes alternating current have been successfully interrupted at about 45,000 volts with practically no arcing. This report contains the details of these experiments.

28. Measuring the evaporation from a body of water. BURT and PAUL RICHARDSON, California Institute of Technology.—The method developed at this Institute by Cummings (*Phys. Rev.*, 25, 721, 1925; *Jour. Electr.*, 46, 491) and Bowen (*Phys. Rev.*, 27, 779, 1926) for measuring the evaporation from a body of water was employed under dissimilar circumstances in Pasadena and at Fort Collins, Colorado, to obtain results which show the relative importance of each factor in the evaporation equation of Cummings and Bowen: $I = S + LE(1+R) + U$, where I is the radiant energy integrated over any time interval, or more specifically, the solar and sky radiation in calories per sq. cm. corrected for reflection and back radiation. S is the heat energy represented by change in temperature of the water. LE is the latent heat represented by the evaporation during the same interval, L being the latent heat of evaporation, R represents the ratio of heat losses by convection and by evaporation, while U represents a relatively small correction for other losses.

29. Motion of an airship in a variable horizontal wind. H. BATEMAN, California Institute of Technology.—In the well known method of aerial navigation by dead reckoning the analysis is very simple when there is no wind or when the wind is uniform in velocity and direction. In the case of a variable wind the problem is complicated and so much is unknown that few results of importance can be expected. The problem is, however, mathematically interesting. Taking the case in which the wind blows in one direction and assuming that the propeller thrust depends linearly on the relative velocity, the problem reduces to a boundary problem for a certain type of linear differential equation of the second order. A solution of the problem is obtained for a case in which the wind drops steadily from one velocity to another.

30. A vertical seismometer. SINCLAIR SMITH, Mount Wilson Observatory.—An investigation of the properties of a flat spring when bent into a bow by two opposing collinear forces showed that over a limited range, the ratio of the total force to the force per unit extension becomes large. This property was made use of in the construction of a small vertical seismometer. Using a spring 12 cm long in a modified Galitzin form of instrument having a steady mass of 100 g. a period of 12 seconds was obtained. This instrument, however, differs from the Galitzin form in that it has a much larger range of stability and does not require such critical adjustments.

31. The Michelson-Gale earth-tide experiment repeated in Pasadena, California. W. T. WHITNEY, California Institute of Technology.—In this experiment, repeated in Pasadena under the direction of Dr. A. A. Michelson, a continuous record of the small tides in a north-south pipe and an east-west pipe, half filled with water, was obtained for the year 1924. A reduction of the observed pipe tides for the principal or semi-diurnal lunar tide, indicates clearly the loading due to the oceanic tides and a comparison of the relative phases of the pipe tides, the theoretical earth tide and the estimated phase of the ocean loading, indicates that the tilting in Pasadena due to the ocean load is approximately 2.5 times as great as that due to the earth tide proper. These results are obtained from a study of the north-south pipe tides only. The behavior of the east-west pipe tides seems anomalous and the controlling factors have not yet been isolated. It seems reasonable to suppose, however, that the local geologic configurations of fault planes and mountain blocks contributes in some manner to these irregularities. A small progressive tilt of this region is suspected though local conditions prevent a definite conclusion at this time.

AUTHOR INDEX

- Alexeievsky, A. P.—No. 18
Allison, Samuel K.—No. 1
Anderson, S. H.—No. 11
———see Ostenson
Babcock, Harold D.—No. 2
Bateman, H.—No. 29
Bowen, I. S.—No. 5
———see Millikan
Brewer, A. Keith—No. 19
Dickinson, R. G.—see Mitchell
Ellis, Joseph W.—No. 8
Epstein, Paul S.—Nos. 10 and 20
Houston, William V.—Nos. 4 and 7
Kent, Norton A., Lucien B. Taylor and Hazel
Pearson—No. 3
Knudsen, V. O.—No. 23
Loeb, Leonard B.—No. 12
Loughridge, D. H.—No. 14
Mendenhall, H. E.—No. 27
Millikan, R. A. and I. S. Bowen—No. 6
Mitchell, A. C. G. and R. G. Dickinson—
No. 13
Nye, Arthur W.—No. 21
Ostenson, Floyd C. and S. H. Anderson—
No. 22
Pearson, Hazel—see Kent
Podolsky, Boris—No. 9
Richardson, Burt and Paul—No. 28
Simon, A. W.—No. 26
Smith, Sinclair—No. 30
Sorensen, Royal W.—No. 25
Taylor, Lucien B.—see Kent
Watson, E. C.—Nos. 15 and 16
Whitney, W. T.—No. 31
Zinszer, Harvey A.—No. 17
Zwickly, F.—No. 24

THE
PHYSICAL REVIEW

THEORY OF THE INTENSITY OF SCATTERED X-RAYS

BY G. E. M. JAUNCEY

ABSTRACT

The writer's theory of the unmodified line in the Compton Effect (Phys. Rev., 25, 314, 1925) has recently been extended by Williams (Phil. Mag. 2, 657, 1926) and the writer (Phys. Rev., 29, 206, 1927) to the case of reflection of x-rays by crystals. Both these writers assume that it is only the U electrons (i.e. the electrons associated with unmodified scattering, see Phys. Rev., 26, 433, 1925) which take part in crystal reflection. In the present paper it is supposed that the U electrons in a given atom scatter coherently and also according to the classical theory, so that, if N_U is the number of U electrons in the atom, the intensity of the x-rays scattered in a given direction is N_U^2 times the intensity scattered by a single free electron in the same direction according to Thomson's theory. In previous papers it has been assumed that the intensity of unmodified scattering is proportional to N_U . Now, however, because of the above assumptions, it is proportional to N_U^2 . In modified scattering it is assumed that the S electrons (i.e. the electrons associated with modified scattering) scatter incoherently and according to the quantum theories of Compton, Jauncey and Breit. The modified scattering, as in previous papers, is, therefore, proportional to N_S , the number of S electrons in the atom. Formulas are obtained for the energy of the total (i.e. unmodified plus modified) scattering coefficient and for the ratio of the modified to the total scattering coefficient in terms of the angle of scattering, the primary wave-length and the critical absorption wave-lengths of the scatterer. The theory seems to work equally well for heavy as for light elements and explains the phenomenon of excess scattering.

It is also pointed out that Williams has made a small error in his correction for the interference of x-rays scattered by the U electrons in atoms in the same crystal plane. Rectifying this error, an excellent agreement between theory and the experimental atomic structure factors as found by Havighurst (Phys. Rev., 28, 869, 1926) for rock salt is obtained.

1. INTRODUCTION

ACCORDING to Thomson's theory¹ of the scattering of x-rays, the linear scattering coefficient per unit solid angle in a direction ϕ with the primary rays is given by

$$s_0 = (NZ\rho/W) \cdot (e^4/m^2c^4) \cdot (1 + \cos^2\phi)/2 \quad (1)$$

where N is Avogadro's number, Z the atomic number of the scatterer, ρ its density, W its atomic weight and e , m and c the charge and mass of the electron and the velocity of light respectively. Eq. (1) agrees fairly well with

¹ J. J. Thomson, Conduction of Electricity through Gases, 2nd Ed., p. 325.

experiment for moderately soft x-rays scattered by light elements at angles greater than 60° . When gamma rays, however, are scattered the experimental value of the scattering coefficient, which we shall denote by s , is more nearly given by

$$s = s_0 / (1 + \alpha \text{ vers } \phi)^3 \quad (2)$$

as observed by Compton.² In Eq. (2) $\alpha = h/mc\lambda$, where λ is the wave-length of the primary x-rays. Eq. (2) has been derived on theoretical grounds by Compton, Jauncey and Breit.³ However, for $\lambda = 0.545\text{\AA}$ scattered by rock salt, Jauncey and May⁴ have found for values of ϕ greater than 90° that s is between the value given by the right side of Eq. (2) and the Thomson value, s_0 . For angles less than 90° s becomes greater than s_0 , which phenomenon is known as excess scattering. This excess scattering was first observed by Crowther⁵ and Barkla and Ayers⁶ in the case of scattering by light elements. Later, Barkla and Dunlop⁷ observed excess scattering when x-rays are scattered by heavy elements at 90° , while still more recently Jauncey and Coven⁸ have observed this phenomenon for $\lambda = 0.41\text{\AA}$ scattered by copper at 110° .

Jauncey's theory of the unmodified line in the Compton effect^{9,10,11} supposes that unmodified scattering takes place from one set of electrons in an atom while modified scattering takes place from a second set of electrons. The electrons of the first set are said to be in the *U* state, while those in the second set are said to be in the *S* state. For brevity we shall hereafter refer to the electrons associated with the unshifted and shifted lines as the *U* and *S* electrons. Jauncey's theory gives the ratio of the number of *U* electrons of a given type (*K*, *L*, *M*, etc.) to the total number of the same type when these electrons are moving in circular orbits as¹²

$$\frac{N_U}{N_U + N_S} \equiv y = 0.5 - \frac{\psi}{2(2T)^{1/2}} + \frac{V}{4\psi(2T)^{1/2}} \quad (3)$$

and

$$\psi = (h/mc\lambda) \sin \frac{1}{2}\phi, \quad (4)$$

where $mc^2 V$ is the ionization energy of each electron and $mc^2 T$ is the kinetic energy of each electron in its Bohr orbit. Since y has different values for

² A. H. Compton, Phil. Mag. **41**, 749 (1921) and Phys. Rev. **21**, 483 (1923).

³ A. H. Compton, X-Rays and Electrons, p. 305.

⁴ Jauncey and May, Phys. Rev. **23**, 128 (1924).

⁵ J. A. Crowther, Proc. Camb. Phil. Soc. **16**, 112 (1910).

⁶ Barkla and Ayers, Phil. Mag. **21**, 275 (1911).

⁷ Barkla and Dunlop, Phil. Mag. **31**, 222 (1916).

⁸ Jauncey and Coven, Phys. Rev. **28**, 426 (1926).

⁹ G. E. M. Jauncey, Phys. Rev. **25**, 314 (1925).

¹⁰ G. E. M. Jauncey, Phys. Rev. **25**, 723 (1925).

¹¹ Jauncey and DeFoe, Phys. Rev. **26**, 433 (1925).

¹² Eq. (3) is in the form given by Nuttall and Williams in Phil. Mag. **1**, 1217 (1926). Previously the writer has used a formula where $T = V$ which is approximately the case.

the different types (K , L , M , etc.) of electrons, the different y 's are distinguished by the subscripts K , L , etc. If n_K , n_L , etc., are the numbers of K , L , etc., electrons per atom, then the average value of y , which we shall denote by \bar{y} , is

$$\bar{y} = \frac{n_K y_K + n_L y_L + \dots}{n_K + n_L + \dots} \quad (5)$$

Jauncey has also considered the case of scattering by electrons in elliptic orbits¹⁰ and has obtained a more complicated formula than Eq. (3). The y 's for elliptic orbits, such as the L_1 orbits, are supposed inserted in Eq. (5). If now it is assumed that the intensity of x-rays scattered in the direction ϕ by a U electron is the same as that scattered by an S electron, then Eq. (5) gives the ratio of the unmodified scattering coefficient s_1 to the total scattering coefficient $(s_1 + s_2)$, so that $s_2/(s_1 + s_2) = 1 - \bar{y}$.

Woo¹³ and DeFoe¹⁴ have tested this point experimentally and find for x-rays of various wave-lengths scattered by various elements that the experimental value of $s_2/(s_1 + s_2)$ is always considerably less than $(1 - \bar{y})$. On the other hand Jauncey's theory of the unmodified line requires that when x-rays are passed through a gas in a Wilson cloud apparatus, the ratio of the number of recoil electron tracks to the number of photoelectron tracks should be $(1 - \bar{y})\sigma/\tau$ where σ is the spherical scattering coefficient and τ the true absorption coefficient. Nuttall and Williams have found good experimental agreement with this prediction.

Summing up, we may say that the evidence is that Jauncey's theory of the unmodified line agrees well with experiment for those cases where the ratio of the numbers of U electrons to the number of the S electrons is concerned; while for those cases where the ratio of the intensities of the modified and unmodified rays is concerned the agreement is only qualitative and not quantitative. An attempt to explain this latter discrepancy and to rectify it is the purpose of this paper.

2. INTENSITY OF X-RAYS REFLECTED BY CRYSTALS

The hint as to the explanation of this discrepancy appears in a recent paper by Williams.¹⁵ Williams and independently, but later, the writer¹⁶ have shown that it is necessary to take the Compton effect into account in order to explain the variation of the intensity of x-rays regularly reflected (not diffusely scattered) by crystals. Both Williams and Jauncey calculate the atomic structure factor F on the assumption that it is only the U electrons which take part in crystalline reflection. On this account therefore the effective number of electrons per atom in crystalline reflection is $\bar{y}Z$. However, as Compton,¹⁷ Hartree¹⁸ and others have shown, there is partial inter-

¹³ Y. H. Woo, Phys. Rev. 27, 119 (1926).

¹⁴ O. K. DeFoe, Phys. Rev. 27, 675 (1926).

¹⁵ E. J. Williams, Phil. Mag. 2, 657 (1926).

¹⁶ G. E. M. Jauncey, Phys. Rev. 29, 206 (1927).

¹⁷ A. H. Compton, Phys. Rev. 9, 29 (1917).

¹⁸ D. R. Hartree, Phil. Mag. 50, 289 (1925).

ference between the wavelets scattered (in crystalline reflection) from different electrons in the same atom. For instance Compton¹⁷ has shown that if we consider only those electrons which are moving in circular orbits of radius a , the ratio of the average amplitude of the wavelet scattered by each electron in an atom to the amplitude of the wavelet scattered by a single free electron is

$$H = (\sin \xi) / \xi \quad (6)$$

where

$$\xi = (4\pi a \sin \frac{1}{2}\phi) / \lambda \quad (7)$$

Hartree¹⁸ has also obtained a formula for the case where the electrons are moving in elliptic orbits and he gives tables of values of H for various values of ξ . Williams then obtains the atomic structure factor F thus:

$$F = n_K y_K H_K + n_L y_L H_L + \dots \quad (8)$$

the subscripts K , L , etc., referring to the K , L , etc., orbits. Eq. (8), however, is only justified if, when we consider circular orbits of a given radius, the U electrons can be in any position in the orbit and the orbit can be oriented in any direction. However, on reference to Jauncey's paper on the unmodified line,¹⁰ it is seen that the U electrons are restricted to a certain area on the sphere of radius a . From Fig. 1 of this paper¹⁰ it follows that the interference factor is only given by H when y is unity. As y approaches zero the interference factor approaches unity. Hence the writer has calculated the interference factor from the following approximate formula:

$$H' = 1 - y(1 - H) \quad (9)$$

where H is given by Hartree's tables. This formula satisfies the conditions that $H' = 1$ when $y = 0$ and $H' = H$ when $y = 1$. The formula for the structure factor F is therefore given by

$$F = n_K y_K H'_K + n_L y_L H'_L + \dots \quad (10)$$

Hartree¹⁸ gives a formula for calculating the radius a of any circular orbit. From this value of the radius it is possible to calculate mc^2T , the kinetic energy of the electron in the orbit, by equating the moment of momentum to $kh/2\pi$ where k is the azimuthal quantum number. In this way values of T in Eq. (3) are calculated for circular orbits. For elliptic orbits T is calculated on the basis of a circular orbit of total quantum number equal to that of the elliptic orbit and then the method for calculating y for elliptic orbits according to a previous paper¹⁹ is applied. However, these methods of calculating T are not applied to the outermost orbits. For these orbits it is considered best to take $T = V$ where V is given by the ionization potential.

Havighurst²⁰ has recently obtained experimental F values for rock salt from the intensities of different orders of reflection of $MoK\alpha$ x-rays. Havighurst's values, however, contain the Debye temperature factor. Using the

¹⁹ G. E. M. Jauncey, Phys. Rev. **27**, 687 (1926).

²⁰ R. J. Havighurst, Phys. Rev. **28**, 869 (1926).

temperature factor given by Bragg, Darwin and James²¹ and inserting the wave-length used by Havighurst, values of F without the temperature effect have been obtained and are shown in the third column of Table I. The theoretical values as calculated from Eq. (10) are shown in the fourth column. The agreement between the third and fourth columns is good.

TABLE I
F-values for rock salt.

$\sin \frac{1}{2}\phi$	Experiment Including Temperature	Experiment Excluding Temperature	Theory
0.126	20.80	21.6	19.0
0.252	11.60	13.5	12.0
0.378	6.69	9.46	8.2
0.504	3.54	6.30	6.7

In Eq. (10) the distribution of electrons according to Stoner²² is used, while the values of V in Eq. (3) are obtained from the National Research Council Bulletins written by Duane and by Compton and Mohler.

3. INTENSITY OF X-RAYS SCATTERED BY AMORPHOUS SUBSTANCES

Since in crystalline reflection the U electrons in an atom scatter coherently, it is now assumed that the U electrons in an atom of an amorphous substance also scatter coherently. On the other hand an amorphous substance is distinguished from a crystal by the fact that the atoms of the amorphous substance scatter incoherently while the atoms of a crystal scatter coherently. Let p_v be the probability that the number of U electrons in an atom is v , where v is a whole number. Assuming that the wavelets scattered by these U electrons are in phase, the amplitude scattered by each of these atoms is v times the amplitude scattered by a single free electron so that the intensity scattered by each of these atoms is v^2 times the intensity scattered by a free electron. Adding the intensities scattered by the atoms with 1, 2, . . . , U electrons in the atom, the unmodified scattering coefficient s_1 is given by²³

$$s_1 = s_0(1^2 p_1 + 2^2 p_2 + 3^2 p_3 + \dots + Z^2 p_Z)/Z \quad (12)$$

It is further assumed in this theory that the S electrons in an atom scatter incoherently so that for these electrons Z in Eq. (2) is replaced by the number

²¹ Bragg, Darwin and James, Phil. Mag. **1**, 897 (1926).

²² E. C. Stoner, Phil. Mag. **48**, 719 (1924).

²³ In crystalline reflection it is only necessary to know the average number of U electrons per atom since the amplitudes due to all the U electrons in the crystal are added. On this account the formula for the intensity of reflected x-rays (see Bragg, James and Darwin²¹) from an ideally imperfect crystal contains a factor $N^2 F^2$ where N is the number of molecules per unit volume and F is the atomic structure factor. In other words the factor is $(NF)^2$ so that it is correct to take the average value of F . However, in scattering by amorphous substances, since we have assumed no coherence between the wavelets scattered by different atoms, the intensity contains a factor $N\bar{F}^2$, where \bar{F} is the root mean square of the atomic structure factor and therefore in this case it is not correct to take the arithmetical average of F as is done in crystalline reflection. In a paper read by the author at the New York Meeting of the Physical Society in 1927 the author used the arithmetical average and therefore the formula given in the abstract of that paper is only approximately correct.

of S electrons per atom. Hence s_2 the modified scattering coefficient is given by

$$s_2 = (1 - \bar{y})s_0 / (1 + \alpha \text{ vers } \phi)^3, \quad (13)$$

where \bar{y} is given by Eq. (5). From Eqs. (12) and (13), both $(s_1 + s_2)$ and $s_2 / (s_1 + s_2)$ can be obtained and compared with experiment.

The problem now reduces to finding an expression for p , in terms of the y 's (as given by Eq. (3)) and also an expression for the summation, $1^2 p_1 + 2^2 p_2 + \dots$. Let us consider the case of a sack containing black and white balls such that the probability of drawing a white ball is y . Let us suppose that all the balls in the sack are emptied into baskets each of which contains, say, four balls. What are the probabilities that a basket will contain 1, 2, 3 or 4 white balls? The probability p_4 that a given basket will contain 4 white balls is y^4 . Now let the probability of drawing a black ball out of the original sack be z so that $y+z=1$, then the probability of 1 black ball followed by 3 white balls being drawn is y^3z . However, in filling the baskets it matters not in what order the balls are drawn and, since all the drawings, $BWWW$, $WBWW$, $WWBW$, and $WWWB$, are equally likely, the chance p_3 of a basket containing 3 white balls and 1 black ball is $4y^3z$. It is easily seen that p_2 , p_1 and p_0 are given by $6y^2z^2$, $4yz^3$, and z^4 respectively. The p 's are therefore given by the terms in the expansion of the binomial $(y+z)^4$, the subscripts of the p 's being equal to the exponents of the y 's. It is easily seen that for baskets containing n balls each, the probabilities p_n , p_{n-1} , \dots are given by the respective terms of $(y+z)^n$. Next consider the case of two sacks, the probability of drawing a white ball from the first sack being y_1 and from the second sack y_2 . Now let us take n_1 balls out of the first sack and n_2 out of the second sack and put the (n_1+n_2) balls in one basket. The probability p , that the basket will contain v white balls is easily seen to be the sum of those terms in the expansion of $(y_1+z_1)^{n_1} \cdot (y_2+z_2)^{n_2}$ in which the sum of the exponents of the y 's is v . The argument can obviously be applied to any number of sacks.

Let us return to the case of one sack and baskets containing 4 balls and denote the summation $1^2 p_1 + 2^2 p_2 + \dots$ by S , then

$$S = 4y(y+z)^2(4y+z) \quad (14)$$

But $y+z=1$ so that

$$S = 4y(3y+1) = 4y+4 \cdot 3y^2 \quad (15)$$

The general formula for a basket containing n balls is

$$S = ny + n(n-1)y^2 \quad (16)$$

For the case of several sacks it can easily be shown that

$$\begin{aligned} S = & n_1 y_1 + n_2 y_2 + \dots \\ & + n_1(n_1-1)y_1^2 + n_2(n_2-1)y_2^2 + \dots \\ & + 2n_1n_2y_1y_2 + 2n_1n_3y_1y_3 + \dots \end{aligned} \quad (17)$$

If we replace the subscripts 1, 2, 3, etc., by K, L, M and give the n 's and y 's the same meanings as in Eq. (5), the unmodified coefficient is then given by

$$s_1 = s_0 S/Z \quad (18)$$

4. COMPARISON WITH EXPERIMENT

Jauncey and Coven⁸ have measured the total scattering coefficient $(s_1 + s_2)$ for $\lambda = 0.41\text{A}$ scattered by copper at various angles, their results being shown in the second column of Table II. In the third column are shown the theoretical values calculated according to Eqs. (12), (13) and (18). Stoner's distribution of $2K, 2L_I, 6L_{III}, 2M_I, 6M_{III}, 10M_V$ and $1N_I$ electrons is used.

TABLE II
Scattering from copper: Wave-length 0.41A.

Scattering Angle, ϕ	Experiment $(s_1 + s_2)/s_0$	Theory $(s_1 + s_2)/s_0$
40°	4.8	4.00
50	3.5	3.11
60	2.5	2.55
70	2.37	2.25
80	2.14	1.90
90	1.49	1.62
100	1.45	1.47
110	1.52(?)	1.36
150		1.11
180		1.04

It is seen that there is fair agreement between the second and third columns. The experimental value at 110° is doubtful.

In Table III the experimental values of $s_2/(s_1 + s_2)$ as determined by Woo¹³ and DeFoe¹⁴ are given in the third column, while the theoretical values are given in the fourth column.

TABLE III
Ratio of unmodified to total scattering.

Element, wave-length and experimenter	Angle	Experiment $s_2/(s_1 + s_2)$	Theory $s_2/(s_1 + s_2)$	$1 - \bar{\gamma}$
Aluminum $\lambda = .71\text{A}$	90	0.48	0.62	.80
	105	.53	.67	.83
	120	.59	.73	.86
Woo.	135	.68	.79	.88
	150	.71	.81	.89
Copper $\lambda = .41\text{A}$	90	.55	.43	.82
	100	.63	.47	.84
	130	.84(?)	.55	.87
DeFoe				

The fifth column gives the ratio $s_2/(s_1 + s_2)$ as calculated theoretically in a previous paper.¹⁰ It is seen that the theory of the present paper gives values which approach closer to the experimental values than those calculated according to the method of the previous paper.

5. DISCUSSION

A formula for the total scattering coefficient ($s_1 + s_2$) has been obtained which agrees fairly well with the experimental results for copper (see Table II). The theory therefore seems to explain the phenomenon of excess scattering. However, the formulas for s_1 and s_2 as derived in Section 3 depend on the assumption that the wavelets scattered by the U electrons in an atom are in phase. Due to small differences of the paths of rays scattered by the various U electrons in the same atom this assumption is not quite true. A correction for partial interference should therefore be added. The interference factors calculated by Hartree¹⁸ apply only to the case where the electrons are associated with crystal planes, and so cannot be used in the case of scattering by electrons in an amorphous substance. A correction might be made by using the methods of Debye²⁴ and Glocker and Kaupp²⁵ but this would complicate Eq. (12) by multiplying each term on the right side by an interference factor and so make impossible the derivation of the simple formula given in Eq. (18). The correction has therefore been omitted. The effect of the correction would be to diminish slightly the theoretical values in Table II and to increase slightly these values in Table III.

On the whole considering the evidence of Tables I, II, and III (DeFoe's values in Table III not being as reliable as Woo's values), it may be inferred that the experimental number of U electrons per atom is somewhat greater than that given by Eq. (5). From this it follows that the values calculated from Eq. (3) are somewhat too small. Since from Eq. (3) the conditions of wave-length and angle for which the unmodified line disappears¹⁹ are given, it must be that the wave-length is smaller or the angle greater than the wave-length and angle given by Eq. (3) when the unmodified line disappears. An indication that this is so experimentally is given by the experiments of Woo²⁶ and Jauncey and Boyd.²⁷

However, in spite of these small discrepancies, the writer believes that the theory as developed in this paper correlates surprisingly well the phenomena of the intensity of crystal reflection, the intensity of x-rays scattered by amorphous substances of high and low atomic numbers, the ratio of the energies of the modified and unmodified lines in the Compton Effect, and the conditions under which the unmodified line disappears.

WASHINGTON UNIVERSITY,
ST. LOUIS, MISSOURI,
February 14, 1927.

²⁴ P. Debye, Ann. d. Physik, **46**, 809 (1915).

²⁵ Glocker and Kaupp, Ann. d. Physik **64**, 541 (1921); see also Compton, X-rays and Electrons, p. 75.

²⁶ Y. H. Woo, Phys. Rev. **28**, 426 (1926).

²⁷ Jauncey and Boyd, Phys. Rev. **28**, 620 (1926).

EFFECT OF CHEMICAL COMBINATION ON X-RAY ABSORPTION

By W. B. MOREHOUSE

ABSTRACT

The x-ray absorption by aqueous solutions was measured before and after chemical reaction, employing a differential null method similar to that described by Becker (Phys. Rev. 20, 134, 1922). The direct and zirconium filtered beam from a water-cooled molybdenum Coolidge tube, operating at 30 kv peak, were used. Cells having equal compartments were used, so that the same elements were in the beam before and after combination.

Measurements were made on the following reactions:

- (A) $KI + I_2 + 2Na_2S_2O_3 \rightarrow KI + 2NaI + Na_2S_4O_6$.
- (B) $K_2Cr_2O_7 + 12KI + 14HCl \rightarrow 8KCl + 2CrCl_3 + 3I_2 + 6KI + 7H_2O$
- (C) $NaOH + HCl \rightarrow NaCl + H_2O$.
- (D) $KOH + HCl \rightarrow KCl + H_2O$.
- (E) I_2 in 70 percent alcohol $+ 2Na_2S_2O_3 \rightarrow 2NaI + Na_2S_4O_6$.

Corrections having been made for changes in density the results indicate: Reaction (A); the mass absorption coefficient for the solution after reaction for direct beam approximately 0.24 percent less than before reaction; for filtered beam 0.36 percent less; Reaction (B); direct beam; 0.25 percent greater; Reaction (C); direct beam; no appreciable change; Reaction (D); direct and filtered; no appreciable change; Reaction (E); direct beam; 0.36 percent less. The results indicate that the mass absorption coefficient for an element depends upon its valence or state of chemical combination. Since iodine, sulphur and chromium are the only elements changing valence and since computations from known absorption coefficients show that the absorption by the iodine in the beam is several times that by either the sulphur or the chromium, it seems probable that the absorption by iodine in the free state is greater than its absorption in the combined state.

INTRODUCTION

BENOIST,¹ from the result of his measurements on x-ray absorption, first stated that the x-ray absorption coefficient for an element is the same whether the element is in the free state or combined chemically with other elements. In fact one finds the same statement made in various books on x-rays.²

Several investigators³ have measured the x-ray absorption by chemical compounds and, assuming the above law, have computed the absorption coefficients of the elements present in the compounds. A critical comparison of the results obtained by these experimenters, as pointed out by Taylor³, indicates that the absorption coefficient for an element may depend upon

¹ Benoist, Journal de physique; 10, 658, (1901).

² W. H. and W. L. Bragg, X-rays and Crystal Structure, 4th ed., p. 41. de Broglie, Les Rayons X, 1922 ed., p. 48. Kaye; X-rays, 4th ed., p. 125. Ledoux, Lebard et Danvillier, La Physique des Rayons X, p. 135.

³ Auren, Phil. Mag. 33, 471 (1917); Phil. Mag. 37, 135, (1919); Phil. Mag. 41, 733, (1921); Taylor, Phys. Rev. 20, 709, (1922).

its state of chemical combination with other elements. Further, Bergengren,⁴ Lindh,⁵ and other investigators⁶ recently have shown that for the light elements the wave-length of the absorption limits and of certain emission lines does depend upon the valence of the element. Absorption coefficients for any wave-length must certainly be closely related to emission spectra and absorption limits. Accordingly this investigation was undertaken to study the effect of valence or chemical combination on x-ray absorption.

The absorption by two solutions placed in an x-ray beam was measured. They were then allowed to react chemically and the change in absorption after reaction was measured. Corrections were, of course, made for changes in density. An effect due to chemical combination has been found and measured but no quantitative claim is made for the present results. Further experiments should be performed to determine the value of the effect for different wave-lengths.

EXPERIMENTAL PROCEDURE

For measuring the relative absorption before and after chemical reaction a differential null method⁷ was employed. By means of two slit systems

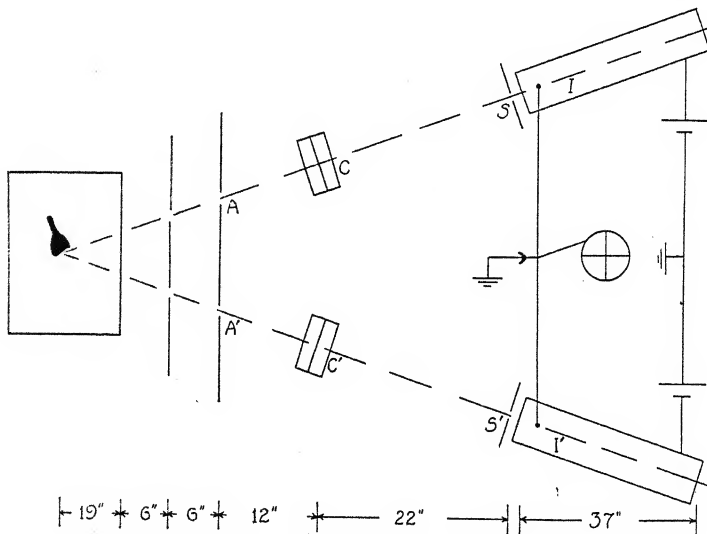


Fig. 1. Diagram of apparatus.

two x-ray beams A and A' from a molybdenum target of a water-cooled Coolidge tube were made to enter two ionization chambers I and I' respectively. These beams if unabsorbed would pass directly through the

⁴ Bergengren, C. R. 171, 624 (1920).

⁵ Lindh, C. R.; 172, 1175 (1921); Fysisk, Tidskr.; 20, 132 (1922); C. R.; 175, 25 (1922); Arkiv. f. Matem. Astr. o. Fys.; 18, 12 (1924).

⁶ Tandberg, Arkiv. f. Matem., Astr. o. Fys. 18, 1 (1924). Chamberlain, Phys. Rev.; 25, 525 (1925).

⁷ Becker, Phys. Rev. 20, 134 (1922). Read, Phys. Rev. 27, 373 (1926).

chambers without hitting their walls or the central rods. The projected area of the beam on the back end of ionization chamber I' was approximately 1.5 sq. in. (10 cm^2) at a distance of approximately 9 feet (2.75 m.) from the target. Methyl bromide was placed in the chambers to increase the absorption of the x-rays. The chambers were connected together by rubber tubing so the pressures would equalize. The outside of one chamber was charged positive and the other equally negative. In front of chamber I' was a fixed slit S' 1 in. (2.54 cm) square and in front of chamber I an adjustable slit S easily adjustable to one forty thousandth of an inch. The insulated central rods in the ionization chambers were connected together and to a Compton electrometer. A balance was readily obtained when the electrometer showed no rate of drift. The apparatus was very sensitive and a change in balance of one part in ten thousand, measured in terms of the adjustable slit, could readily be detected.

Equal volumes of the solutions before reaction were placed in a cell C' having two equal compartments separated by either a removable or a fixed partition. In the case of the removable partition the solutions were allowed to react chemically by removing the partition and replacing it after the reaction was completed. In the case of the fixed partition the solutions were poured together into a beaker and after complete reaction the mixture was replaced in the cell. This cell C' was placed in the path of beam A' . Another cell C containing similar solutions was placed in the path of beam A to reduce to a minimum the relative changes in intensity of the two beams due to slight unavoidable fluctuations in the operation of the x-ray tube.

The exact procedure in getting the measurements was as follows. The empty cell C' was placed in beam A' . Then the cell C' plus solutions was placed in beam A' . Next the similar cell C and solutions were placed in beam A . Finally the solutions in beam A' were allowed to react. For each case the slit opening S_0 , S , S_1 and S_2 necessary for a balance was obtained.

The cells employed were made from bakelite. Each compartment was 3/8 in. (1 cm) wide. The sides and partition were of bakelite 1/16 in. (1.6 mm) thick. Other cells were used which had the sides and partition of aluminum 0.020 in. (0.5 mm) thick covered with bakelite lacquer, and of hard rubber 1/16 in. thick. Measurements with any cell gave the same results.

The change in balance caused by the reaction may be due to either a change in the absorption coefficient of the solutions or to a change in density or both. Therefore it was necessary that the densities of the solutions before and after reaction be known accurately. For this purpose a Westphal balance was used.

The positions of the solutions relative to the direction of the beam were interchanged to be sure that the effect was not due to scattering caused by the different positions of the elements before and after reaction. This would also eliminate any error due to the compartments not being equal.

A source of alternating current for operating the x-ray tube was obtained by running a rotary converter from a Terrill regulated D. C. generator. Four 100 ampere-hour 6 volt storage batteries were soldered together giving a 12 volt source for the filament. Sufficient time was always allowed for the batteries to approach a constant discharge rate, after which the tube electron current decreased very steadily and at a very slow rate. In all cases the voltage across the tube was 30 K.V. peak.

Measurements were taken using the unfiltered direct beam from the tube. Later an approximately monochromatic beam was obtained by filtering the direct beam through zirconium filters.

All records and computations were made in terms of the adjustable slit width and the density of the solutions before and after reaction.

FORMULAS

It can readily be shown that for a simple homogeneous mechanical mixture of several elements which are absorbing monochromatic x-rays.

$$\mu = \frac{\mu_a \rho_a + \mu_b \rho_b + \mu_c \rho_c + \dots}{\rho_a + \rho_b + \dots + \rho_m + \rho_n + \dots} \quad (1)$$

where μ is the mass absorption coefficient of the mixture, μ_a , μ_b , etc., are the mass absorption coefficients and ρ_a , ρ_b , etc., are the partial densities in gm per cc for each element present in the mixture. The density of the mixture is equal to the sum of the partial densities. Also it can be shown that for solutions not too concentrated the energy absorbed by a given thickness of the solution is directly proportional to the density.

In the present experiment the rate at which energy I enters the chambers is directly proportional to the slit opening S . (over at least a small range of openings.) i.e.

$$I = KS \quad (2)$$

When no substances are in beam A , if S_0 is the slit opening necessary to effect a balance with the box only in beam A' , and S the slit opening with the box plus solutions in the same beam then

$$S = S_0 e^{-[\mu_1 \rho_1 x_1 + \mu_2 \rho_2 x_2]} \quad (3)$$

where μ_1 and μ_2 are the mass absorption coefficients given by Eq. (1), ρ_1 and ρ_2 the density, x_1 and x_2 the thickness of solutions (1) and (2) respectively.

Assuming (1) that the solutions are at the same level in each compartment and (2) that there is no change in either the density or the absorption coefficient it can readily be shown that the transmission after reaction will be the same as before and

$$S = S_0 e^{-\mu \rho' x} \quad (4)$$

where μ is given by Eq. (1), $\rho' = (\rho_1 + \rho_2)/2$, and $x = x_1 + x_2$.

In general a change in density due to the reaction will occur and also there may be a change in μ . This will necessarily cause a change in the

transmission and from Eq. (4) a relation between the change in transmission as measured by the change in slit opening, the change in μ , and the change in density can readily be obtained by differentiating and dividing, remembering that x and S_0 are constant.

$$\frac{dS}{S \cdot 2.303 \log_{10} S/S_0} = \frac{d\mu}{\mu} + \frac{dp}{\rho'} \quad (5)$$

dS is the change in slit opening necessary to regain a balance after reaction. $d\rho$ is equal to the difference between the measured density ρ after reaction and ρ' .

The only effect of a change in temperature due to the reaction will be to produce a change in density for Read⁸ has shown that the effect of temperature on the absorption coefficient is less than one percent for changes in temperature of 500°C.

The following will show that when a heterogeneous x-ray beam of definite intensity passes through several different materials the amount of energy absorbed is independent of the order in which the materials are placed and if they are mixed it is independent of the order in which the molecules are arranged. The amount of energy absorbed will, however, depend upon the ratio of the intensities of the various wave-lengths present in the beam.

Consider an x-ray beam, composed of two wave-lengths λ_1 and λ_2 of energy $I_{0\lambda_1}$ and $I_{0\lambda_2}$ respectively, which passes through two substances *A* and *B*. Let a_1 and a_2 , b_1 and b_2 be the absorption constants for substances *A* and *B* corresponding to wave-lengths λ_1 and λ_2 respectively. Let I_1 and I_2 be the energy corresponding to wave-lengths λ_1 and λ_2 which gets through the substances. Then

$$I_1 = I_{0\lambda_1}(1 - a_1)(1 - b_1) \quad (6)$$

$$I_2 = I_{0\lambda_2}(1 - a_2)(1 - b_2) \quad (7)$$

and the energy of the emerging beam is given by

$$I_1 + I_2 = I_{0\lambda_1}(1 - a_1)(1 - b_1) + I_{0\lambda_2}(1 - a_2)(1 - b_2) \quad (8)$$

Equations (6) and (7) are independent of the order in which the beam encounters the molecules of the substances and therefore the energy transmitted which is given by Eq. (8) must be independent of the order in which the beam encounters the molecules of the substances.

The energy absorbed by the substances is given by

$$(I_{0\lambda_1} + I_{0\lambda_2}) - (I_1 + I_2) = (I_{0\lambda_1} + I_{0\lambda_2}) - [I_{0\lambda_1}(1 - a_1)(1 - b_1) + I_{0\lambda_2}(1 - a_2)(1 - b_2)] \\ = I_{0\lambda_1}(a_1 + b_1 - a_1 b_1) + I_{0\lambda_2}(a_2 + b_2 - a_2 b_2) \quad (9)$$

The average absorption constant for the substances is given by

$$\bar{X} = \frac{(I_{0\lambda_1} + I_{0\lambda_2}) - (I_1 + I_2)}{I_{0\lambda_1} + I_{0\lambda_2}} \quad (10)$$

⁸ Read, Phys. Rev. 27, 373, 1926.

Therefore

$$\bar{X} = \frac{I_{0\lambda_1}(a_1 + b_1 - a_1 b_1) + I_{0\lambda_2}(a_2 + b_2 - a_2 b_2)}{I_{0\lambda_1} + I_{0\lambda_2}} \quad (11)$$

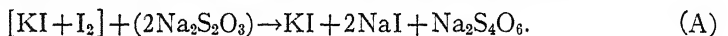
Equation (11) shows that the average absorption constant \bar{X} depends on the ratio of the energy in each wave-length to the total energy in the beam and is only constant provided these ratios are constant. This argument may be extended to include any number of wave-lengths and any number of substances.

Therefore the absorption of heterogeneous x-rays by materials depends upon the energy in the various wave-lengths to the total energy in the beam, and therefore will depend upon the x-ray tube, the voltage applied to the tube, and upon the manner in which the x-rays are filtered.

For a constant ratio between the energy in the various wave-lengths of the x-ray beam the change in the mass absorption coefficient of the solutions due to the chemical reaction can be computed from Eq. (5).

SOLUTIONS STUDIED AND EXPERIMENTAL RESULTS

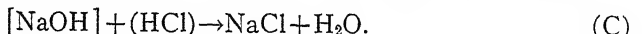
The following reactions were studied using dilute solutions,



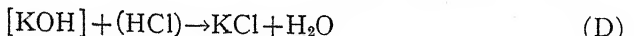
12.7 grams of iodine were dissolved in 1000 cc of a solution of potassium iodide which contained 25 grams of KI per liter. The solution of sodium thiosulphate contained 25 grams $Na_2S_2O_3 \cdot 5H_2O$ per liter. Equal volumes reacted.



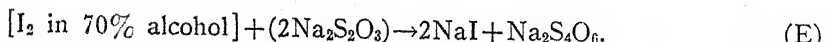
The solution of potassium dichromate contained 5 grams $K_2Cr_2O_7$ per liter. The solution of potassium iodide contained approximately 40 grams KI per liter and the solution of HCl contained 10 grams HCl per liter. The reaction was the equivalent of equal volumes of these solutions reacting.



The solution of sodium hydroxide contained 28 gms NaOH per liter. The solution of HCl contained 26 gms HCl per liter. Equal volumes reacted.



The solution of potassium hydroxide contained 28 grams KOH per liter and the solution of HCl contained 18 grams HCl per liter. Equal volumes reacted.



12.7 grams of iodine was dissolved in 70% solution of alcohol making a liter of solution. The solution of sodium thiosulphate contained 25 grams of $Na_2S_2O_3 \cdot 5H_2O$ per liter. Equal volumes were used.

In each case the substances in square brackets were initially in one compartment of the cell and the substances in round brackets in the other compartment.

SAMPLE OF CALCULATIONS

The following is a complete sample set of data and computations on Reaction A.

Voltage across tube: 30 kv peak.

X-ray tube electron current: 10.4 milliamperes.

Sensitivity of electrometer: 2000 mm per volt.

Volume of each solution used: 160 cc.

S_0 :	1.2494"	1.2495"	1.2500"	Average	1.2496
S :	0.1720	0.1717	0.1717		0.1718
S_1 :	0.9881	0.9883	0.9885	0.9882	0.9883
S_2 :	0.9950	0.9953	0.9953	0.9954	0.9952

S_1 is the slit opening with similar solutions in both beam *A* and *B* before reaction and S_2 is the slit opening after the solutions in beam *A* have reacted.

Density of $[I_2 + KI] = \rho_1 = 1.0266$ gm per cc.

Density of $(Na_2S_2O_8) = \rho_2 = 1.0124$ gm per cc.

Density of solution after reaction $= \rho = 1.0182$ gm per cc.

$$\rho' = (\rho_1 + \rho_2)/2 = 1.0195 \text{ gm per cc.}$$

$$d\rho = \rho' - \rho = -0.0013 \text{ gm per cc.}$$

$$dS = S_1 - S_2 = -0.0069''.$$

$$\frac{dS}{2.303 S_1 \log_{10}(S/S_0)} = \frac{d\mu}{\mu} + \frac{dp}{p}$$

$$d\mu/\mu = -0.0022.$$

$$\text{Change in } \mu = -0.22\%.$$

TABLE I

Values of the change in absorption coefficient resulting from chemical reaction. The last line in the table gives the average percent change in μ for each type of reaction studied. In case 1 the x-ray beam passed through the substance in square brackets first, and in case 2 it passed through the substances in round brackets first.

Reaction A Unfiltered beams (percent)		Reaction A Zirconium filtered beams (percent)		Reaction B Unfiltered beams (percent)		Reaction C Unfiltered beams (percent)		Reaction D Unfiltered beams (percent)		Reaction D Zirconium filtered beams (percent)		Reaction E Unfiltered beams (percent)	
1	2	1	2	1	2	1	2	1	2	1	2	1	2
- .36	- .17	- .22	- .33	+ .27	+ .15	+ .21	- .13	- .06	+ .19	- .02	+ .09	- .40	- .23
- .29	- .23	- .18	- .19	.45	.20	.18	- .00	- .05	.00	+ .09	.09	- .35	- .31
- .30	- .42	- .64	- .41	.31	.32	.18	- .09	- .16	.04	- .18	.20	- .36	- .23
- .35	- .22	- .33	- .18	.21	.21	.14	- .05	- .09	.05	- .06	.13	- .31	- .23
- .22	- .31	- .59	- .27	.20	.22	.12	- .18	- .13	.07	+ .05	- .06	- .36	- .29
- .21	- .40	- .25	- .23	.18	.21	.11	- .20	- .17	.01	- .10	+ .15	- .28	- .34
- .10	- .15	- .44	- .24	.48	.35	.12	- .12					- .24	- .38
- .27	- .21	- .43	- .76	.33	.31							- .35	- .54
- .08	- .20		- .35	.32	.31							- .53	- .54
- .23	- .16			.22	.25							- .54	- .50
	- .14			.21	.25								
				.12	.23								
				.12	.16								
				.17	.17								
- .24	- .24	- .33	- .38	+ .26	+ .24	+ .15	- .11	- .11	+ .06	- .04	+ .10	- .37	- .34
$\pm .03$	$\pm .03$	$\pm .04$	$\pm .04$	$\pm .03$	$\pm .02$	$\pm .02$	$\pm .02$	$\pm .02$	$\pm .02$	$\pm .03$	$\pm .03$	$\pm .02$	$\pm .03$
$-(.24 \pm .03)$		$-(.36 \pm .04)$		$+(.25 \pm .03)$		$+(.02 \pm .02)$		$-(.03 \pm .02)$		$+(.03 \pm .03)$		$-(.36 \pm .03)$	

In reaction (A) and (E) the iodine changes its valence from 0 to -1 and the valence of the sulphur increases positively. In reaction (B) the iodine changes its valence from -1 to 0 and chromium from 6 to 3. In reaction (A) the amount of iodine per sq. cm in the beam before and after reaction was .032 gms of which .013 gms changed its valence. In reaction (B) the amount of iodine per sq. cm in the beam before and after reaction was .031 gms of which .013 gms changed its valence. In reaction (E) the amount of iodine per sq. cm in the beam before and after reaction was .013 gms and all of it changed its valence.

In reactions (C) and (D) the valence of all elements in the beam is the same after reaction as before. For these determinations a cell with a removable partition was used and the compartments were not exactly equal. Equal volumes were used and the solutions were not at the same level which explains why the effect is positive for one case and negative for the other. The average of the results being practically zero (at least within experimental error) indicates that probably the effect due to the reaction is approximately zero.

The results in general indicate that the mass absorption coefficient for an element depends upon its valence and is therefore different for different states of chemical combination. Computations from known absorption coefficients show that the absorption by the iodine in the beam was several times (approximately 15 times) that due to either the sulphur or the chromium, which indicates that probably the measured effect is practically all due to the iodine. This is also indicated by the results for reaction (E) where all the iodine changed its valence.

The larger effect from reaction (A) when using the filtered beam may indicate that the effect is different for different wave-lengths of x-rays, or it may be caused by the change in the ratio of the intensities of the various wave-lengths present in the beam as indicated by Eq. (11). The filtered x-rays when using a zirconium filter are at best only approximately monochromatic.

THEORETICAL EXPLANATION OF RESULTS AND A COMPARISON WITH THE RESULTS OF EXPERIMENTS INDICATING A DEPENDENCE OF THE WAVE-LENGTH OF ABSORPTION LIMITS AND EMISSION SPECTRA UPON VALENCE.

Experimental results⁹ show that on the short wave-length side of the K absorption limit the atomic absorption coefficient can be represented by the following approximate formula

$$T_a = CN^4\lambda^3. \quad (1)$$

where T_a is the atomic absorption coefficient; C is a constant; N is the atomic number; and λ is the wave length of the x-rays. On the long wave-length side of the limit the formula has practically the same form excepting the exponents may be slightly different, and C is different.

⁹ Richtmyer, Phys. Rev. 17, 264 (1921); Richtmyer & Warburton, Phys. Rev. 21, 721 (1923).

For the K absorption limit, Moseley's law may be written in the form

$$\lambda_K = K_1/(N - b)^2 \quad (2)$$

where λ_K is the wave length of the absorption limit, K_1 is a constant, N is the atomic number, and b is the screening constant.

If Eq. (2) be combined with Eq. (1) there results¹⁰

$$T_a' = C' N^4 / (N - b)^6 \quad (3)$$

where T_a' is the atomic absorption coefficient just at the short wave-length side of the absorption limit.

Differentiating Eq. (3) with respect to T_a' and b there results

$$dT_a' / T_a' = 6db / (N - b) \quad (4)$$

which at once indicates that if the screening constant increases the value of T_a' increases, and vice versa.

The results of several experimenters^{4,5,6} show that in general the absorption limit comes at a shorter wave length when the element is in the combined state than when it is in the free state, also that the wave length is different when the element is combined under different valences. Usually the higher the valence the shorter the wave length. On the basis of Moseley's law, equation (2), this must mean that the value of the screening constant, when the element is in the combined state, is less than when the element is in the free state since the atomic number of the element is certainly the same whether the element is free or combined.

Experimental results¹¹ also show that the wave length of the emission lines depends upon the valence of the element. The wave length is longest when the element is in the free state and appears to decrease as the valence increases in the combined state. This again, on the basis of Moseley's law, must mean that the screening constant when the element is in the free state is greater than when it is in the combined state.

By comparing these results with equation (4), it becomes apparent that at the absorption limit the absorption coefficient for an element when in the combined state must be less than when it is in the free state. It seems reasonable to think that the same may be true at any wave length which would explain qualitatively at least, the present results and show that they are in accord with the experiments^{4,5,6,11} mentioned above.

CRITICISM OF EXPERIMENT AND RESULT

For the work described the balance method is good. However the intensities of the two beams were not exactly the same and changes would necessarily cause errors in the observations. These changes were reduced to a minimum by having similar solutions in each beam. The accuracy of taking slit readings was about 2×10^{-4} in. and of taking density measurements about 2×10^{-4} gm per cc.

¹⁰ Richtmyer, Phys. Rev. 27, 1 (1926).

¹¹ Ray, Phil. Mag. 49, 168 (1925); 50, 505, (1925).

An obvious suggestion might be that the effect was due to a difference in the scattering before and after reaction, but since the measured effect was the same no matter which solution the beam passed through first it seems very probable that it was not due to a difference in scattering. It is very difficult to say whether the effect was caused by the short or long wave lengths present in the beam.

CONCLUSIONS

The results appear to indicate that the x-ray absorption by an element depends upon its valence and therefore upon its state of chemical combination. In the case of Iodine they seem to indicate that its absorption may be greater in the free state than in the combined state.

It gives me great pleasure to thank Professor F. K. Richtmyer for his many valuable suggestions and his keen interest during the progress of this experiment. He suggested the study.

ROCKEFELLER HALL,
CORNELL UNIVERSITY.
June, 1926.*

* Received February 23, 1927—EDITOR.

THE HEAT ENERGY OF X-RAYS

By ROY KEGERREIS

ABSTRACT

Efficiency of a tungsten-target Coolidge x-ray tube operated at peak voltages from 100 to 200 kv.—The efficiency of x-ray production was experimentally determined for voltages between one and two hundred kilovolts. The high voltage energy input into the x-ray tube was measured by means of an absorption calorimeter. The intensity of the x-rays was measured by means of the temperature rise of a lead absorption cup arranged so that the effects due to scattering and fluorescence of the x-rays as well as effects due to external temperature conditions were eliminated. Elaborate precautions were also taken to suppress electrostatic and electromagnetic induced effects from the high voltage circuits. The efficiency was found to be proportional to the peak voltage. The factor of proportionality was 0.0032 when the efficiency is expressed in percent and the peak voltage in kilovolts.

I. INTRODUCTION

THE purpose of the present investigation is to extend our knowledge of the efficiency of x-ray production to the region of high voltage x-rays, 100–200 kv. The general problem of the efficiency of x-ray production has been examined by others, notably by Weeks¹ in 1917, in whose paper an excellent summary of the work prior to that date is given. Since then Ulrey² and Kuhlenkampff³ have also examined the problem. However, the two latter writers used an ionization method to determine the energy of the x-rays. Boos⁴ has shown that the ionization is not strictly proportional to the energy absorbed when different wave-lengths are compared. A more reliable method is to measure the heating effect as was done by Weeks. The most recent work on the heat energy of x-rays is by Terrill⁵ who has extended the measurements to x-rays excited by a potential of 100 kv. Since much of present day therapeutic work is done with x-rays from a tube excited at 100 to 200 kv it is worth while to extend the measurements to x-rays of such penetrability.

II. METHOD AND APPARATUS

In measuring the energy of x-rays care must be taken that none of the energy of the primary beam disappears in any form other than in heat energy absorbed in the calorimeter. This is done by causing the x-rays to pass into a deep cylindrical lead cup. Under these conditions the reflected, scattered and fluorescent x-rays as well as the beta-rays produced by the

¹ Paul T. Weeks, Phys. Rev. 10, 564 (June, 1917).

² Clayton T. Ulrey, Phys. Rev. 11, 408 (1918).

³ Helmuth Kulenkampff, Ann. d. Physik, 69, 548 (June 9, 1922).

⁴ B. Boos, Zeits. f. Physik 10, 1 (1922).

⁵ H. M. Terrill, Phys. Rev. 28, 431, (September, 1926).

primary x-rays are finally absorbed in the lead cup. A diagram of the calorimeter is presented in Fig. 1. The cup was made of lead 1.6 mm thick; such a thickness of lead will absorb at least 99 percent of the x-rays. The x-rays entered the cup through a circular aperture in a lead shield above the absorbing cup. The diameter of the aperture was 4.92 cm. The solid angle subtended by the aperture at the focal spot of the target of the x-ray tube was 0.000622. Four copper coaxial cups surrounded the lead absorbing cup in order to shield it from external temperature changes. Temperature measuring coils and rheostat heating coils are wound on these cups so that their temperatures might be determined and controlled. The resistance of

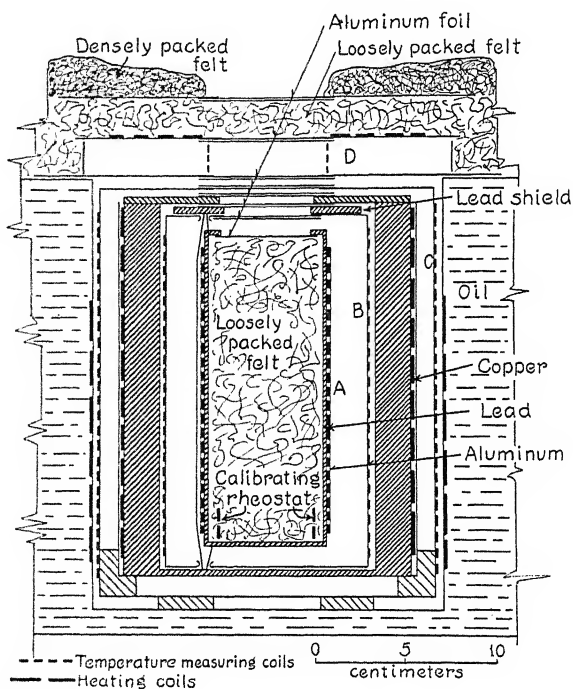


Fig. 1. Diagram of the calorimeter.

each of the temperature measuring coils was about 107 ohms. The outermost cup *C* formed the inner wall of an oil bath which contained about six gallons of transil oil. It was necessary to have a window in the cover of each cup in order to allow the x-rays to enter without undue absorption. All windows were covered with a double thickness of aluminum foil (0.0025 cm thick) with one sheet of the thin paper (1.7 milligrams per sq. cm) between them. The pieces of aluminum foil were closely clamped to the covers of the cups so as to insure good thermal contact. One of the intermediate cups was made with the top and bottom three millimeters thick, the cylindrical walls were double and the intervening space was filled with water. The conductivity and heat capacity were accordingly rather large. The surfaces

of all the cups were polished by buffing. The case which contained the system of cups was covered with two thicknesses of hair felt, one inch thick as shown in Fig. 1.

The entire success of the experiment depends on the maintenance of reproducible temperatures in and about the coaxial cups. The thermal conditions must be constant for all runs. It would be ideal to have exact temperature equilibrium throughout the system of coaxial cups but such a condition is exceedingly difficult to attain because of the very long time required for the heat transfers to take place. It was accordingly decided to set up exactly the same small temperature differences between the various parts at the start of each run. The temperatures of the inner parts were held slightly higher than that of their surroundings. All the parts of the apparatus were maintained at a constant temperature throughout a run except the three inner cups; the absorbing cup warmed up because of the absorption of the x-rays and the two cups immediately exterior to it were warmed by manually controlled heating currents through resistance coils. The conditions were thus nearly but not exactly those of thermal equilibrium.

A small coil (70.70 ohms resistance) which was wound with wire of negligible temperature coefficient of resistance was permanently placed in the bottom of the absorbing cup for calibrating purposes. Heating currents were sent through this coil for one minute out of each five while a calibration was being made.

A Snook Special x-ray machine was used as a source of high voltage. This machine gives a pulsating direct current of 120 pulses per second. As is well known this pulsating current causes static and leakage effects on any other electrical circuits which may be near. Much shielding and non-inductive winding of all coils was employed to minimize these effects but the total elimination of such influences from the results was accomplished only by operating the x-ray tube during an initial period of from one to four hours while equilibrium for constant temperature was being set up, with the residual of all the disturbing influences present. An actual measurement of the heat energy in x-rays was begun by removing a thick lead cover from the orifice in the bottom of the lead-lined box containing the x-ray tube, thus permitting the x-rays to enter the absorbing cup. No changes in the connections were made in the high voltage or Wheatstone bridge circuits when this piece of lead was removed. Constant electrical conditions during the initial period as well as during the run itself were thus unquestionably assured.

The target of the x-ray tube was of tungsten and during the part of the experiment in which the heating effect of the x-rays was being determined the tube was operated in an air space, in a box lined with lead one-fourth inch thick. Electric fans caused currents of air to circulate through the box and over the container of the absorbing cup and about the room generally. Three barriers of thin aluminum foil (0.0025 cm thick) were placed between the target and the box which contained the lead absorbing cup. During a particular run the peak voltage remained constant and was measured by

means of a sphere gap in air. The current through the tube was maintained at 4 milliamperes during all runs.

The intensity of the beam of x-rays was corrected for the absorption which takes place in the glass of the x-ray tube. The absorption was determined from measurements taken with an ionization chamber and a gold leaf electroscope of rays which had passed through a second x-ray tube of the same type. The square root of the fraction of the x-rays transmitted through the two thicknesses of the glass gives the fraction transmitted through one thickness. No correction was made for the absorption by the various thicknesses of aluminum foil. It is a negligible factor in the work since the total thickness is less than 0.05 cm. The absorption by the 40 cm of air which was between the x-ray tube bulb and the absorbing cup was also neglected.

It has been pointed out by Weeks that the high voltage current in an x-ray tube does not follow a sine curve and that therefore the power input cannot be calculated directly from voltmeter and ammeter readings. Weeks determined the power input by measuring the heat produced in the x-ray tube by the bombardment of the target by electrons from the filament. This method was used in the present investigation. The power input was not measured at the same time as the heating effect of the x-rays. Instead a separate experiment was devised to measure the power input when the x-ray tube was operated at each one of a set of different peak voltages and a current of 4 milliamperes. This was accomplished by immersing the x-ray tube in a tank containing 45 gallons of oil. The tank was made of wood lined with $\frac{1}{8}$ inch (3.2 mm) lead. The outside of the tank was covered with two layers of hair felt one inch thick. During a run the oil in the tank was kept stirred. The temperature rise per hour for a given voltage on the tube was determined by a mercury in glass thermometer. Correction was made for the heat produced by the filament current by running the filament with no production of x-rays. A curve was then plotted between the temperature rise per hour produced by the bombardment of the target with electrons and the peak voltage. Next a heating coil was placed in the oil and a curve plotted of the temperature rise per hour of the oil tank and the watts input. From these two curves it was possible to determine the relation between the power input into the tube and the peak voltage, the current always being kept at 4 milliamperes.

III. EXPERIMENTAL RESULTS

Typical curves for the heating effect of the x-rays are shown in Fig. 2a. The horizontal portions of the curves (Fig. 2a) represent readings before the x-rays were allowed to enter the absorbing cup, while the sloping portions represent readings when the x-rays were entering the cup. The slope of the rising part of each curve gives a measure of the power absorbed. The slope is expressed in increase in resistance in ohms per hour. The watts computed from the calibration curve of the lead absorbing cup (Fig. 2b)

are a measure of the intensity of the x-rays which pass into the absorbing cup. The actual x-ray energy emitted by the focal spot into the absorbing cup is secured by correcting the value for the absorption in the glass of the

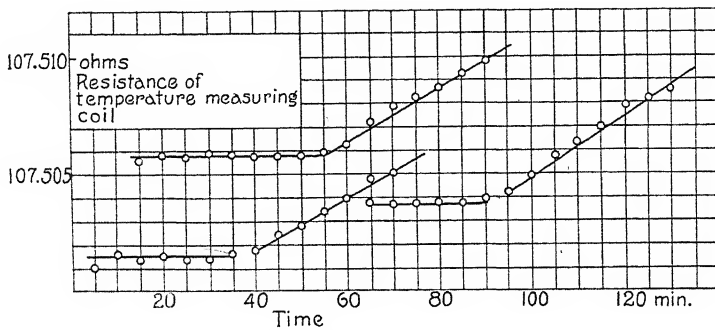


Fig. 2a. Showing the increase in temperature of the calorimeter after the x-rays are allowed to enter.

x-ray tube and also for the shape of the curve for angular distribution of intensity. The total x-ray emission is then secured by multiplying this corrected value by the ratio between the total solid angle about the target

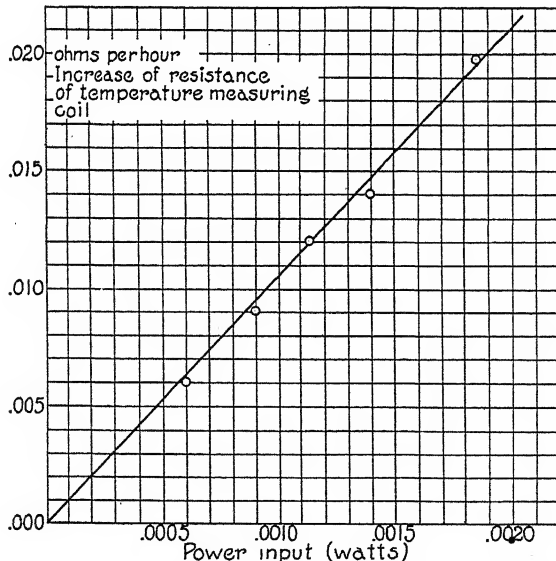


Fig. 2b. Calibration curve for the lead absorbing cup, showing the relation between the power input and the rate of increase in temperature.

and that subtended by the aperture above the absorbing cup. The final results are presented in Table I and in Fig. 3.

In Fig. 3 a curve is plotted between the figures in the third column and the square of the peak voltage. It will be seen that the points fall approxi-

TABLE I

Peak kv.	High voltage input (watts)	Power of x-rays in unit solid angle (watts)	Heat energy of x-rays.		
			Column 3 Column 2	Efficiency $\times 2\pi$	Column 4 $\times 4\pi$
98.5	270	0.0796	0.000295	0.18%	0.37%
124.5	335	.101	302	.19	.38
143.3	383	.137	359	.22	.45
161.9	425	.175	413	.26	.52
178.8	462	.203	440	.27	.55
196.3	499	.222	445	.28	.56

mately on a straight line, showing that the x-ray output varies nearly as the square of the applied voltage. Comparing the above figure for the efficiency at 98.5 kv with that obtained by Terrill at 100 kv it is seen that the two results are in fairly good agreement. The fifth column gives the ratio of

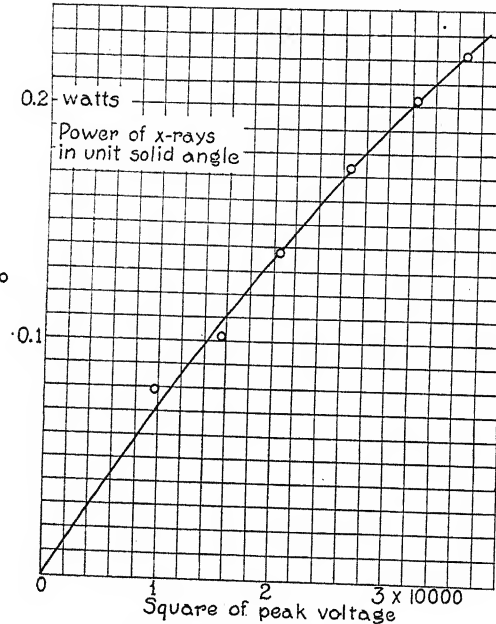


Fig. 3. Variation of the power of the x-rays with the square of the peak voltage.

output to input supposing the intensity to be uniform over the hemisphere exposed to radiation. This is an approximation to the energy actually radiated as x-rays from the tube. The next column gives the preceding multiplied by 2. These are the efficiencies when the x-ray energy absorbed by the target is included in the output. The figures in column 3 are for radiation in the direction of maximum intensity which was only one percent higher than the intensity in a direction perpendicular to the axis of the tube and at an angle of 45° to the target.

It has been shown that the x-ray output varies nearly as the square of the applied voltage. Such a conclusion is also arrived at by Brainin,⁶ Ulrey² and Kulenkampff³ who used entirely different methods of measurement.

The values of the efficiency would be considerably increased if the very soft x-rays, which are completely absorbed by the glass of the x-ray tube and the air, were taken into account. (It is to be pointed out that the corrections which were made for the absorption in the walls of the tube apply only to those rays which are transmitted.) The efficiencies that have been found are based on a uniform intensity throughout the total solid angle which surrounds the target. Such an efficiency may be approached in apparatus as a limiting case.

The experiments upon which this report is based were performed in the Physics Laboratory of the University of Michigan.

Chicago, Illinois
December 11, 1927

⁶ C. S. Brainin, Phys. Rev. 10, 461 (June, 1917).

ON THE CALCULATION OF THE SPECTROSCOPIC TERMS
DERIVED FROM EQUIVALENT ELECTRONS

BY HENRY NORRIS RUSSELL

ABSTRACT

The calculation of the spectroscopic terms which result from an atomic configuration containing several equivalent electrons, in which Pauli's restriction is operative, can be made very simply by the extension of a notation due to Breit. The results are in agreement with those previously given by Hund for p and d electrons and those of Gibbs, Wilber and White for f electrons. Some minor alterations in notation are suggested.

IT IS now well established that the spectroscopic terms belonging to an atom in a given state of ionization depend upon the combined influence of all the electrons outside the complete "shells." When these electrons are unlike (differing in either their total or azimuthal quantum numbers) the determination of the terms produced by any configuration is very simple; but when they are equivalent in these respects, the restriction stated by Pauli becomes operative, according to which no two electrons in the same atom can have the same values for all four of the quantum numbers which define their state. The following method permits a rapid analysis of the effects of this limitation.

The notation is substantially that of Hund's book.¹ The *state of a single electron* in an atom is completely defined by five quantum numbers, s , l , n , m_s and m_l . Of these, s defines the "spin" and is always $\frac{1}{2}$ (in the usual units of $h/2\pi$), l is less by a unit than Bohr's azimuthal quantum number, and n is equal to Bohr's total quantum number. The quantities m_s and m_l are magnetic quantum numbers, giving the orientations of the spin-axis and the orbit plane in a (hypothetical) magnetic field strong enough to break down all couplings between individual orbital or spin vectors; m_s has the value $\pm \frac{1}{2}$, while m_l runs from l to $-l$ by steps of a unit. Pauli's restriction then demands that no two electrons in the same atom have the same values of n , l , m_s and m_l . The small letters, s , p , d , f , . . . , are used to describe electrons for which $l=0, 1, 2, 3, \dots$; so that, for example, $2s$, $4p$, $3d$, have exactly the same meanings as Bohr's 2_1 , 4_2 , 3_3 .

States of an atom (which correspond to the separate magnetic levels into which a component of a multiple term is divided) may be defined by the numbers S , L , m_s and m_L .² Of these, S represents the vector sum of the s 's

¹ Hund, Linienspektra und periodisches System der Elemente. Berlin, 1927. (Julius Springer).

² Hund uses l for the electron and L for the atom; but if both are to be used as subscripts, as is described here, the capital letter appears preferable. The use of s (and S) to denote both spin-vectors and orbits (or terms) is not likely to lead to any misunderstanding, and it is not worth while to change the notation already adopted by several active workers to avoid this formal objection.

and defines the multiplicity, being $0, \frac{1}{2}, 1, \dots$, for singlets, doublets, triplets, \dots ; L is the vector sum of the l 's and is $0, 1, 2, 3, \dots$, for S, P, D, F, \dots terms. The magnetic quantum numbers, as ordinarily defined, are in weak fields $m = m_L + m_S$, and in strong fields $m' = m_L + 2m_S$.

When only one electron is active (as in Na I, Ca II, etc), the quantities denoted by small and large letters become identical. In this case a total quantum number n can be assigned to the atomic state. When more than one electron is active, no such assignment is possible, and a complete description of the situation demands the specification of n and l for each electron. For example, the lowest energy-state of Ti I is $(3d)^2 (4s)^2, ^3F_2$; two of the four active electrons being in $3d$ orbits, and the other two in $4s$ orbits.

m_S	2	1	0	-1	-2
1	3	2	1	0	-1
0	2	1	0	-1	-2
-1	1	0	-1	-2	-3
	j = 1	2	3		

Fig. 1. Relation between m_S , m_L and the inner quantum number j , for a regular 3D term.

The relation first stated by Pauli, between m_S , m_L and the inner quantum number j ³ has been simply expressed graphically by Breit.⁴ The values of m_L are written above the top of a rectangle, those of m_S at the left, and the magnetic levels which unite into a single component of the term in the absence of an external field, are then obtained by dividing the rectangle into L-shaped strips, as shown by the dotted lines in Fig. 1, which corresponds to a 3D term ($S=1, L=2$). The three "runs" of m from 3 to -3, 2 to -2 and 1 to -1 correspond respectively

m_S	3	2	1	0	-1	-2	-3	
$\frac{1}{2}$	$\frac{7}{2}$	$\frac{5}{2}$	$\frac{3}{2}$	$\frac{1}{2}$	$-\frac{1}{2}$	$-\frac{3}{2}$	$-\frac{5}{2}$	$j = \frac{7}{2}$
$-\frac{1}{2}$	$\frac{5}{2}$	$\frac{3}{2}$	$\frac{1}{2}$	$-\frac{1}{2}$	$-\frac{3}{2}$	$-\frac{5}{2}$	$-\frac{7}{2}$	$j = \frac{5}{2}$

Fig. 2. Relation between m_S , m_L and the inner quantum number j , for an inverted 3F term.

to the components $^3D_3, ^3D_2, ^3D_1$. The maximum numerical value of m in each "run" gives the inner quantum number of the component, in Sommerfeld's notation.

The arrangement here given holds good in general for "regular" terms. For inverted terms, the strips are inverted as shown in Fig. 2, representing a

³ j is not written as a capital (a) to avoid confusion with Landé's usage, (b) because inner quantum numbers have a meaning only for atomic states, and not for the separate electron-orbits.

⁴ Breit, Phys. Rev. 28, 334 (1926).

2F term. The same arrangement may be obtained by keeping the strips as before but changing the sign of each individual m_s and m_l .

When two unlike electrons occur in an atom, the values of L and S resulting from the combination of their individual values of l and s may be derived by the aid of Sommerfeld's form of the vector-model, or as Breit has shown, by the graphical process just illustrated. For example, Fig. 1 represents the combination of a p -electron ($l=1$) and a d -electron ($l=2$) provided that the outer vertical and horizontal rows are supposed now to represent the two sets of values of m_l , and the quantities inside the rectangle the values of m_L which are obtained by adding the others in all possible combinations. Dividing them into strips as before we obtain runs of m_L from 3 to -3 , 2 to -2 and 1 to -1 , which give $L=3, 2, 1$, or D, P, S , terms. If additional electrons (not equivalent to any previously considered) are to be added, the values of m_L for each term of this first resultant are to be combined independently with those of m_l for the new electron.

The s -vectors are similarly treated; thus Fig. 2 represents the addition of an additional electron ($s=\frac{1}{2}$) to a configuration giving a sextet term $S=3$, the new runs of m_s being from $7/2$ to $-7/2$ and $5/2$ to $-5/2$, and the new terms septets and quintets.

So long as the electrons are all dissimilar there is no restriction on these combinations. Any pair of values of m_L, m_l may be added to give a new m_L and any other pair of values of m_s, m_s to give a new m_S . It is therefore sufficient to consider the combinations of the two separately; and terms of any given type (S, P, D) will appear in both the multiplicities produced by adding the new electron.

But when the electrons are equivalent in their total and azimuthal quantum numbers, Pauli's restriction operates. All cases in which both m_l and m_s are the same for a pair of electrons must be excluded, and, what is more, cases obtainable from one another by a mere permutation of the order in which the electrons are counted correspond to the same atomic configuration, and give exactly the same energy-level.

How this works may best be seen by an illustration. In the case of two equivalent p -electrons, the diagram for m_L is as follows.

	1	0	-1
1	[2]	1	0
0	1	[0]	-1
-1	0	-1	[-2]

When $m_s=0$, the individual values of m_s must be $+\frac{1}{2}$ and $-\frac{1}{2}$. The two electrons are dissimilar in this respect, and hence the combination of the m_l 's is unrestricted, giving runs of m_L , 2 to -2 , 1 to -1 and 0. But when $m_s=1$ (or -1) the two m_s 's are alike, and the m_l 's are restricted. The values of m_L on the diagonal, which are bracketed above must now be excluded, and the values below the diagonal become mere duplicates of those above. All that remains of m_L is the run 1 to -1 .

Collecting these results we have,

$m_S = 1$	$m_L =$	$ 1 \text{ to } -1 $	
0	$ 2 \text{ to } -2, $	$ 1 \text{ to } -1, $	0
-1		$ 1 \text{ to } -1 $	
			1S
	1D	$^3P'$	

We have evidently here exactly the sets of values of m_S and m_L which are required to form the terms indicated at the bottom.

In order to distinguish between primed and unprimed terms a very simple rule which is now being followed by several investigators may be deduced from Heisenberg's statement that, in any electron transition which gives rise to radiation, one electron changes its azimuthal quantum number by one unit, while at the same time one other may change by two. If then we assign to the various types of orbits 0, 1, 2, 3, for s , p , d , f , electrons respectively (which are Hund's values of l) it is evident that the sum of the l 's, in any transition, must change from odd to even, or vice versa. This gives us two groups of terms,—even terms (l sums even); S , P' , D , F' , G , etc.: odd terms (l sums odd): S' , P , D' , F , G' , etc.—which may be distinguished by the fact that the odd terms have an odd number of p and f electrons, taken together, in the configuration. If primed terms are defined in this way, a notation is obtained which is consistent with the accepted notation for the sodium, calcium and aluminum groups, and which may be applied without ambiguity to all cases.

In the case of three p -electrons, the sum $m_S = \pm 3/2$ may be obtained only when all three of the values of m_s are alike. The three values of m_l must then all be different; that is, they must be 1, 0 and -1, and $m_L = 0$. The sum $m_S = \frac{1}{2}$ is obtained when two of the m_s 's are $\frac{1}{2}$ and the other $-\frac{1}{2}$. The first two give the run 1 to -1 for m_L . Since the third electron is dissimilar (having a different value of m_s) this run combines freely with the m_l of the third electron, giving runs from M_L of 2 to -2, 1 to -1 and 0. The case where $m_s = -\frac{1}{2}$ is exactly similar.

We thus find the array

$m_S = \pm \frac{3}{2}$	$m_L =$	0
$\pm \frac{1}{2}$	$= 2 \text{ to } -2, \quad 1 \text{ to } -1, \quad 0$	
	$^2D'$	2P

Beyond this point we need not go, for, as is well known, a complete shell of six p -electrons must have $m_S = 0$, $m_L = 0$, giving a 1S term. A shell of five electrons gives the same values as a single electron, and one of four the same as one of two, except that the sign of each individual m_S and m_L is changed, whence it follows that the terms are the same as those previously calculated, but are inverted.

The advantages of the present method of calculation are more apparent in the case of equivalent d-electrons. When discussing it, we will, for brevity, write (4) to denote the "run" 4 to -4, etc. The free combination of any two

runs (m) and (n) (where we may suppose $m \geq n$), then gives a set of runs ($m+n$), ($m+n-1$), and so on to ($m-n$).

For two d-electrons, we have the diagram

	2	1	0	-1	-2
2	[4]	3	2	1	0
1	3	[2]	1	0	-1
0	2	1	[0]	-1	-2
-1	1	0	-1	[-2]	-3
-2	0	-1	-2	-3	[-4]

When $m_s=0$ combination is unrestricted, but when $m_s=\pm 1$ the diagonal values must be rejected and the quantities below the diagonal are duplicates of those above, so that we have simply the runs (3) and (1). Our array then becomes

$m_s = \pm 1$	$m_L =$	(3)	(1)	
0	= (4)	(3) (2)	(1)	(0)
		1G	$^3F'$	1D

We may next note that, with five d -electrons and $m_s = \pm 5/2$, all the m_s 's are of the same sign and m_L must necessarily be 0. With four electrons and $m_s = \pm 2$, only one of the five possible values of m_L is lacking in any set, so then m_L has the run (2) as in the case of a single electron. Finally, for three electrons, and $m_s = \pm 3/2$, two are lacking, and m_L has the runs (3) and (1).

Very little further calculation is now necessary. For three electrons and $m_s = \frac{1}{2}$, we have two with $m_s = +\frac{1}{2}$, giving runs (3) and (1), and one with $m_s = -\frac{1}{2}$, giving the run (2). These runs combine without restriction, giving, in the first case, runs of (1), (2), (3), (4) and (5), and in the second (1), (2) and (3). Here we have

$m_s = \pm \frac{3}{2}$	$m_L = (1) (2) (3) (4) (5) (1) (2) (3)$
$\pm \frac{1}{2}$	(1)
	$^2P' \quad ^2D \quad ^4F' \quad ^2G \quad ^2H' \quad ^4P' \quad ^2D \quad ^2F'$

For four electrons, $m_s = \pm 1$ can be obtained from three electrons from which m_s has one sign and $m_L = (3)$ or (1), and one of the other sign, giving the same combinations as before, while when $m_s = 0$, $m_s = +\frac{1}{2}$ for two and $-\frac{1}{2}$ for the other two, giving runs of (3) and (1) to be combined freely with another (3) and (1).

In writing the resulting array, we may record simply the number of runs of m_L of each length found for any given value of m_s , as is done below. The number of terms of the highest multiplicity and of any given sort (S, P, D) is then equal to the number of runs listed under the corresponding value of m_L and in the row headed by the highest value of m_s . The numbers of terms of any lower multiplicity are found by subtracting, from the numbers in the

row headed by the corresponding value of m_s , the numbers in the row next above these.

The results for four and five equivalent d-electrons are shown in Table I. In the latter case, $m_s = \pm 5/2$ gives the single run (0), $m_s = \pm 3/2$ the resultant of runs of (2) for the four similar electrons, and (2) for the other one and $m_s = \pm 1/2$ that of (1) and (3) for the group of three electrons and (1) and (3) again for the group of two.

TABLE I

The array for four and five equivalent d electrons.

	m_L	(0)	(1)	(2)	(3)	(4)	(5)	(6)
Four electrons	$m_s = \pm 2$							
	± 1		2	2	2	1		
	0	2	2	4	3	3	1	1
Five	$m_s = \pm 5/2$	1						
	$\pm 3/2$	1	1	1	1	1		
	$\pm 1/2$	2	2	4	3	3	1	1
Terms	S	P'	D	F'	G	H'	I	
	Quintets			1				
	Triplets		2	1	2	1	1	
Four electrons	Singlets	2		2	1	2		1
	Sextets	1						
	Quartets	1	1	1	1	1		
Five electrons	Doublets	1	1	3	2	2	1	1

Our analysis is now complete. The resulting terms may be arranged in the form shown in Table II.

TABLE II

Resulting terms for equivalent d electrons

d^{10}	1S						
d, d^9	2D						
d^2, d^8	$^3P', ^3F'$	1S	1D	1G			
d^3, d^7	$^4P', ^4F'$	2D	$^2P', ^2D, ^2F', ^2G, ^2H'$				
d^4, d^6	5D	$^3P', ^3F'; ^3P, ^3D, ^3F, ^3G, ^3H'$		$^1S, ^1D, ^1F, ^1G, ^1I$			
d^8	6S	$^4P', ^4F'; ^4D$	4G	$^2D, ^2P', ^2D, ^2F, ^2G, ^2H', ^2S, ^2D, ^2F, ^2G, ^2I$			

This is identical, in content, with Hund's table⁵ but brings out the noteworthy regularities in arrangement in a somewhat different manner. The terms of lowest energy level are found in the second column and the other terms of practical importance in the third.

The case of equivalent f electrons demands a little more reckoning. Two such electrons may be treated in the same fashion as two d-electrons, giving

$m_s = \pm 1$	$m_L =$	(1)	(3)	(5)		
0	= (0)	(1)	(2)	(3)	(4)	(5) (6)
		1S	$^3P'$	1D	$^3F'$	1G
					$^3H'$	1I

⁵ Hund, *Linienspektra*, p. 119. The table in his original paper, lacks a 3G term for d^4 and a 1S for d^6 .

With three electrons, and $m_s = \pm 3/2$, the actual cases must once more be counted, and care must be taken not to count the same combination twice. This may be assured by combining the first two electrons as above and adding a third only when its value of m_L is less than for either of the other two. In this way each permutation will evidently be counted once and only once.

For the two electrons the exhibit of the permissible values of m_l and m_L forms a triangle, as follows.

$m_l=2$	1	0	-1	-2	-3	
$m_L=5$	4	3	2	1	0	3
	3	2	1	0	-1	2
		1	0	-1	-2	1
			-1	-2	-3	0
				-3	-4	-1
					-5	-2

We may begin by combining $M_L=5$ in the first column of the triangle with the values of m_l in subsequent columns and in the outer row above, then the values $M_L=4, 3, 2$, in the next column with the numbers in the *following* columns of the outer row and so on. Thus we get the series of numbers

$$\begin{array}{ccccccccc} 6, & 5, & 4, & 3, & 2; & 4, & 3, & 2, & 1; & 2, & 1, & 0; & 0, & -1; & -2 \\ & & & & & 3, & 2, & 1, & 0; & 1, & 0, & -1; & -1, & -2; & -3 \\ & & & & & & & & & 0, & -1, & -2; & -2, & -3; & -4 \\ & & & & & & & & & & & & -3, & -4; & -5 \\ & & & & & & & & & & & & & & & -6 \end{array}$$

which may be immediately rearranged into the runs (6), (4), (3), (2), (0).

For $m_s = \pm \frac{1}{2}$ we have two electrons with m_s of like sign, giving the runs (1), (3), (5), and one of opposite sign with the run (3). The final array may then be written as follows.

m_L	(0)	(1)	(2)	(3)	(4)	(5)	(6)	(7)	(8)
$m_s = \pm \frac{3}{2}$	1		1	1	1		1		
$= \pm \frac{1}{2}$	1	1	3	3	3	2	2	1	1
Terms	S'	P	D'	F	G'	H	I'	K	L'
Quartets	1	-	1	1	1		1		
Doublets	1	2	2	2	2	2	1	1	1

The remaining computations are now straightforward. Four electrons with m_s alike give again the runs (0), (2), (3), (4), (6), five give (1), (3), (5), six give (3) and seven give (0).

The results were worked out independently by Messrs. Gibbs, Wilber and White, and may be found in their paper, (which immediately follows this).

(By mutual agreement, the theory has been presented by one author, and the numerical results, so far as they are new, by the others.)

A word may be said about the notation of the terms corresponding to high values of L . The letter J has been omitted by Hund in accordance with German usage. P and S are preoccupied. The list of letters then becomes

$L =$	0	1	2	3	4	5	6	7	8	9	10
	S	P	D	F	G	H	I	K	L	M	N
$L =$	11	12	13	14	15	16	17	18	19	20	
	O	Q	R	T	U	V	W	X	Y	Z	

Even this extension is barely adequate to include what may be anticipated among the rare earths. The highest multiplicity to be expected is 11, which, as Hund points out⁶ should occur in Gd only, and give a term ^{11}F arising from the configuration f^7d^2s , which must be either the normal state or a very low metastable one. The highest value of L among the "middle terms" with one excited electron should occur in the same spectrum, arising from the configuration $(4f)^7(5d)^2(6p)$, which should give a term for which $m_L = 16$, of type 4V . Similar terms originating in the configuration f^6d^2p or f^8d^2p should occur in Eu and Tb. Still greater values of L could be reached in highly excited states; for example the configuration $(4f)^7(5f)(5d)(6d)(6p)$ representing an atom of Tb with three excited electrons, should give a maximum value $L = 20$, and a term which would demand the notation 6Z .

Among the multitude of levels given by this configuration would also be some derived from the 8S term of origin f^7 , which would be of multiplicity 12, and all types from ^{12}S to ^{12}L . These terms however would be very unlikely to give lines strong enough to be observable.

In conclusion, reference may be made to the beautiful manner in which Breit's graphical process⁴ solves the problem of the limits of series in complex atoms, and shows which components of a given term in the arc spectrum (for example) go to given components of the limiting term in the spark spectrum. The results are naturally in accordance with those given by Hund in Fig. 34 at the end of his book.

PRINCETON UNIVERSITY,
OBSERVATORY,
April 4, 1927.

⁶ Hund, *Linienspektra*, p. 177.

TERMS ARISING FROM SIMILAR AND DISSIMILAR ELECTRONS

By R. C. GIBBS, D. T. WILBER AND H. E. WHITE

ABSTRACT

Following the scheme of Hund¹ for similar s , p and d electrons the terms arising from similar f electrons have been worked out and tabulated. Tables have also been prepared for one and two electrons, where in the latter case these electrons are dissimilar i.e. have either different total or different azimuthal quantum numbers, and also for three electrons two of which are similar. These tables along with those for similar s , p and d electrons are found not only to be of frequent use but also to bring out certain rules that may be applied in determining spectral terms arising from any electron configuration.

MODERN spectroscopy depends to such a large extent upon the theoretical considerations of space quantization of the electrons in uncompleted shells of the atom that it seemed desirable to tabulate in compact form the terms arising from some of the more frequent electron configurations. Following the arrangement of tables given by Hund¹ for similar s , p and d electrons it has been possible to work out and tabulate the terms arising from one to fourteen f electrons. According to ideas put forward by Landé,² Pauli,³ and others the terms arising from any electron configuration are obtained from all possible combinations of the magnetic quantum numbers m_a and m_s , but Pauli³ has shown that for similar electrons certain special configurations must be excluded, i.e. two electrons cannot occupy the same orbit at the same time.

TABLE I

Similar s electrons.

(2)	$s-^2S$
(1)	s^2-^1S

Using the notation as proposed by Russell and Saunders⁴ and now being widely used, tables have been formulated for some of the more frequently occurring configurations. An electron is denoted by a small letter while

TABLE II

Similar p electrons.

(6)	p^1-	2P			
(15)	p^2-^1S		1D	$^3P'$	
(20)	p^3-	2P	$^2D'$		$^4S'$
(15)	p^4-^1S		1D	$^3P'$	
(6)	p^5-	2P			
(1)	p^6-^1S				

¹ Hund, Zeits. f. Physik 33, 345 (1925); 34, 353 (1925).

² Landé, Phys. Zeits. 22, 417 (1921); Zeits. f. Physik 17, 292 (1923).

³ Pauli, Zeits. f. Physik 16, 161 (1923); 31, 765 (1925).

⁴ H. N. Russell and F. A. Saunders, Astrophys. Jour. 61, 40 (1925).

capital letters are always used for terms. A dot before any small letter signifies that the electron has a different total quantum number than the one preceding it.

TABLE III

Similar d electrons.

(10)	$d^1 -$	$^2(D)$	
(45)	$d^2 - 1(SDG)$	$^3(P'F')$	
(120)	$d^3 -$	$^2(D)$	$^2(P'DF'GH')$
(210)	$d^4 - 1(SDG)$	$^3(P'F')$	$^1(SDF'GI)$
(252)	$d^5 -$	$^2(D)$	$^2(P'DF'GH')$
(210)	$d^6 - 1(SDG)$	$^3(P'F')$	$^4(P'F')$
(120)	$d^7 -$	$^2(D)$	$^3(P'DF'GH')$
(45)	$d^8 - 1(SDG)$	$^3(P'F')$	$^2(SDF'GI)$
(10)	$d^9 -$	$^2(D)$	$^5(D)$
(1)	$d^{10} - 1(S)$		$^4(DG) \quad ^6(S)$

The tables given here for similar electrons have all been checked by the combination formula for p things taken q at a time where p is the number of

TABLE IV

Similar f electrons.

(14)	$f^1 -$	$^2(F)$	
(91)	$f^2 - 1(SDGI)$		$^3(P'F'H')$
(364)	$f^3 - 2(PD'FG'III'KL')$		$^4(S'D'FG'I)$
(1001)	$f^4 - 1(SDF'GH'IK'LN)$	$^3(P'DF'GH'IK'LM')$	$^5(SDF'GI)$
(2002)	$f^5 - 2(PD'FG'III'KL'MN'O)$	$^4(S'DP'FG'HI'KL'M)$	$^6(PFH)$
(3003)	$f^6 - 1(SPD'FG'II'KL'MN'NO)$	$^3(P'DF'GH'IK'LM'NO)$	$^5(SP'DF'GH'IK'L) \quad ^7(F')$
(3432)	$f^7 - 2(S'PD'FG'II'KL'MN'OO')$	$^4(S'PD'FG'II'KL'MN')$	$^6(PD'FG'II') \quad ^8(S')$
(3003)	$f^8 - 1(SPD'FG'II'KL'MN'NO)$	$^3(P'DF'GH'IK'LM'NO)$	$^5(SP'DF'GH'IK'L) \quad ^7(F')$
(2002)	$f^9 - 2(PD'FG'II'KL'MN'O)$	$^4(S'PD'FG'II'KL'M)$	$^6(PFH)$
(1001)	$f^{10} - 1(SDF'GH'IK'LN)$	$^3(P'DF'GH'IK'LM')$	$^5(SDF'GI)$
(364)	$f^{11} - 2(PD'FG'II'KL')$		$^4(S'D'FG'I)$
(91)	$f^{12} - 1(SDGI)$		$^3(P'F'H')$
(14)	$f^{13} - 2(F)$		
(1)	$f^{14} - 1(S)$		

states a given electron may occupy and q the total number of electrons in consideration. This check on the terms shows that in the table given by

TABLE V

<i>One electron systems</i>	<i>Two electron systems</i>	
$s \rightarrow ^2S$	$s.s \rightarrow ^1S$	3S
$p \rightarrow ^2P$	$\begin{bmatrix} p.s \rightarrow ^1P \\ p.p \rightarrow 1(SP'D) \end{bmatrix}$	3P
$d \rightarrow ^2D$	$\begin{bmatrix} d.s \rightarrow ^1(D) \\ d.p \rightarrow 1(P'D'F) \\ d.d \rightarrow 1(SP'D F'G) \end{bmatrix}$	$^3(P'D'F)$
$f \rightarrow ^2F$	$\begin{bmatrix} f.s \rightarrow ^1(F) \\ f.p \rightarrow 1(P'D'F'G) \\ f.d \rightarrow 1(P'D'F'G'H) \\ f.f \rightarrow 1(SP'D F'G H'I) \end{bmatrix}$	$^3(F)$

TABLE VI
Three electrons. (Two similar).

$s^2 s - 2(S)$	$^2(D)$	$^2(P')$	$^4(P')$
$p^2 p - 2(P)$	$^2(PD'F)$	$^2(S'PD')$	$^4(S'PD')$
$p^2 d - 2(D)$	$^2(SP'DFG)$	$^2(P'DF')$	$^4(P'DF')$
$d^2 f - 2(F)$	$^2(PD'FGH)$	$^2(D'FG)$	$^4(D'FG)$
$s^2 f - 2(F)$			$^4(P)$
$p^2 s - 2(S)$		$^2(F')$	$^4(F')$
$p^2 p - 2(P)$		$^2(S'PD)$	$^4(S'PD)$
$p^2 d - 2(D)$		$^2(P'DF)$	$^4(P'DF)$
$p^2 f - 2(F)$		$^2(S'PD)$	$^4(S'PD)$
$d^2 s - 2(S)$		$^2(P'DF)$	$^4(P'DF)$
$d^2 p - 2(P)$	$^2(PD'F)$	$^2(P'DF)$	$^4(P'DF)$
$d^2 d - 2(D)$	$^2(SP'DFGH)$	$^2(P'DFGH)$	$^4(P'DFGH)$
$d^2 f - 2(F)$	$^2(PD'FGH)$	$^2(S'PD'FGH)$	$^4(S'PD'FGH)$
$f^2 s - 2(S)$	$^2(PD'FGH)$	$^2(F')$	$^4(F')$
$f^2 p - 2(P)$	$^2(PD'F)$	$^2(P'DF)$	$^4(P'DF)$
$f^2 d - 2(D)$	$^2(SP'DFGH)$	$^2(P'DFGH)$	$^4(P'DFGH)$
$f^2 f - 2(F)$	$^2(PD'FGH)$	$^2(S'PD'FGH)$	$^4(S'PD'FGH)$
		$^2(D'FGH)$	$^4(D'FGH)$
		$^2(GHIK)$	$^4(GHIK)$
		$^2(HI'K)$	$^4(HI'K)$
		$^2(GHI'I)$	$^4(GHI'I)$
		$^2(FGHI)$	$^4(FGHI)$
		$^2(DFGHI)$	$^4(DFGHI)$
		$^2(FGHI'K)$	$^4(FGHI'K)$
		$^2(DFGHI'K)$	$^4(DFGHI'K)$
		$^2(FGHI'KL)$	$^4(FGHI'KL)$
		$^2(DFGHI'KL)$	$^4(DFGHI'KL)$

Hund¹ for similar "d" electrons two terms are missing, namely a 3G term arising from d^4 electrons and a 2S term from d^5 electrons. In the tables for similar electrons we have indicated, in parentheses, before each electron configuration the total number of possible combinations of p (= number of possible values of $m_a \times$ number of possible values of m_s) things taken q (= total number of electrons in consideration) at a time. The terms for similar f electrons from one to fourteen have been worked out and checked in this same way. These have been arranged as given in Table IV. We originally arranged the terms from f electrons according to the scheme used by Hund¹ for similar p and d electrons and found a high degree of symmetry throughout the table, but owing to the length of such a table a more compact form has been given here. The multiplicity of all terms included in the parentheses is indicated by the superscript in front of the parenthesis. Where several identical terms appear, for any given electron configuration, we have indicated the total number of such terms by small arabic numerals placed directly below the term, for example 4D means that there are three 4D terms. Where there is but one such term to be represented this numeral has been omitted.

From the terms arising from dissimilar electrons, Table V, the simple rules for determining all the terms arising from the addition of another electron to any one given term may be inferred. From these rules the terms corresponding to any electron configuration can be elaborated. This we have done in Table VI for

the case of three electrons, two similar and one different. The electron configurations given in the above tables include nearly all of the cases that are of primary importance. It may here be pointed out that there is a striking similarity between the terms as given in Table VI and the table of inner quantum numbers as given by Russell and Saunders.⁴

If our present idea is correct for the rare earth group of elements a *d* electron must be added to the configurations in Table IV to obtain the ground terms of the arc spectra of the corresponding rare earths since in lanthanum a *5d* valence electron has been added. Furthermore when one of the rare earth atoms is excited the most probable electron to be excited will be an *s* electron from the already completed *6s* shell. This means that to the terms in Table IV we must add not only a *d* electron but also two dissimilar *s* electrons. It may be seen that the rare earth spectra are likely to be extremely rich in raes-ultimes.

CORNELL UNIVERSITY,
February 15, 1927.

Note added with proof, April 26, 1927. After this paper was submitted for publication we learned from Dr. H. N. Russell that he had independently worked out the terms arising from similar *f* electrons and that his results check with ours exactly. By mutual arrangement he has given in the preceding paper a detailed explanation of the principles and rules underlying the formation of these tables. The simple rule used by us to distinguish between primed and unprimed terms is given by him on page 785. The 3G and 2S terms which we have referred to above as missing in Hund's original paper are included in his book, "Linien Spectren und Periodisches System der Elemente" a copy of which we have just seen.

LINE INTENSITIES IN THE HYDROGEN CHLORIDE FUNDAMENTAL BAND¹

BY D. G. BOURGIN

ABSTRACT

Absorption intensities in the lines of the HCl fundamental band for tube-lengths from 0.0998 to 2.97 cm.—The transmission of columns of HCl 0.0998, 0.169, 0.248, 0.54, 0.996, and 2.97 cm long in the region of its fundamental vibration-rotation band at 3.5μ was measured with a bismuth-silver vacuum thermopile. The light was resolved by a quartz spectrometer. The curves give indirect evidence of the isotopic doubling and yield fairly accurate absolute and relative values of the intensities of the absorption lines. The values given are checked by several independent methods of calculation. The results confirm the predicted asymmetry in the intensities of corresponding lines in the *P* and *R* branches as suggested by Kemble's theory, the summation rule, and the new formulation of the quantum theory, and, further, verify the quantitative predictions of these theories when the statistical weights are suitably chosen. The particular choice favored by the data is the selection $p_M = 1, 3, 5, \dots$, if the lines are assumed to be singlets (and $p_M = 2, 4, 6, \dots$, if the lines are assumed to be spectroscopic doublets on the presumption that the summation rule is valid for this case). The lines are apparently narrower and deeper than heretofore supposed, and it is demonstrated that the exponential law of transmission is not applicable to the transmission curves even after these have been corrected by the usual slit-width correction formulas.

Einstein probability-of-transition coefficients.—The calculated values of the Einstein probability-of-transition coefficients are $B_{0,1} = 5.1 \times 10^{15}$ for the first line of the positive branch and $A_{0,1} = 58$ for the first line of the negative branch. These values are in harmony with estimates based on the correspondence principle.

Variation of the molecular moment with nuclear displacement.—The most plausible value of the variation of the molecular moment with nuclear displacement as determined for the region of the equilibrium position is 0.828×10^{-10} e.s.u. The combination of the measurements of this paper with Zahn's data on the dielectric constant of HCl yields more reasonable results when the calculations are made in accordance with the new quantum theory or classical theory than when the older forms of the quantum theory are used.

INTRODUCTION

THE recent and more precise developments of the quantum theory have focussed attention on the intensities of spectral lines in emission and absorption. Although the pioneer experiments at Utrecht and elsewhere have afforded intensity data for atomic systems, it appears that no corresponding quantitative work from this point of view has been done in the molecular field. The experimental part of this paper presents the results of an investigation of the absorption lines of HCl in the region of its fundamental band in the infra-red at 3.5μ .

¹ E. C. Kemble and D. G. Bourgin, Nature 117, 789 (1926); D. G. Bourgin and E. C. Kemble, Phys. Rev. 27, 802 (1926).

In accordance with general usage, the term absorption intensity of a line M is taken to mean the integral of the absorption coefficient taken over the absorption line and is written

$$\alpha_M = \int_M \mu(\nu) d\nu \quad (1)$$

where $\mu(\nu)$ is the absorption coefficient expressed as a function of the frequency. The subscript M takes on negative values for the P branch of the band and particularizes the M th line counting from the missing central component.

Absorption curves for the HCl fundamental band have been obtained for long tube-lengths by several experimenters.² The most accurate results are those of Imes³ and of Brinsmade and Kemble⁴ whose researches were carried out primarily to determine the positions, rather than the intensities, of the lines. In all published spectroscopic investigations²⁻⁸ of the fundamental absorption region of HCl, the measurements have been obtained for a single long gas-column. The unpublished thesis of Brinsmade and the recent indirect evidence adduced by Kemble⁹ indicate the possibility that the exponential law is inapplicable to the observed measurements. This conclusion is directly confirmed by the experiments reported in this paper. Hence it is not possible to estimate either the absorption coefficient for a particular frequency or the integrated value of the coefficient from data on a single tube-length.

For the case of the simple vibration-rotation bands under which the fundamental band of HCl is to be classified the following theoretical formula has recently been proposed by Kemble⁹

$$\alpha_M = (c/\nu^3) \bar{p}_M e^{-W_M/kT} \quad (2)$$

where ν is the frequency associated with the transition giving rise to the line, the exponential factor is the Boltzman factor taken for the initial state and \bar{p}_M denotes the arithmetic mean of the a priori probabilities involved in the transition. Kemble's derivation of Eq. (2) is based on a splitting up of the stationary states of the molecule by a hypothetical weak magnetic field and the assumption that the sum of the intensities of the simple Zeeman components passes continuously into the intensity of the band line as the strength of the magnetic field approaches zero.

The measurements of the intensities of lines in atomic spectra have suggested the empirical, so-called "summation rule."¹⁰ The rule has since

² Burmeister, Verh. d. D. Phys. Ges. **15**, 589 (1913).

³ E. S. Imes, Astrophys. J. **1**, 251 (1919).

⁴ J. Brinsmade and E. C. Kemble, Proc. Nat. Acad. Sci. **3**, 420 (1917).

⁵ E. von Bahr, Verh. d. D. Phys. Ges. **21**, 115 (1913).

⁶ Colby and Meyers, Astrophys. J. **53**, 300 (1921).

⁷ Colby, Meyers and Bronk, Astrophys. J. **57**, 7 (1923). (The last two papers give only the positions of the absorption maxima and not the entire absorption curve.)

⁸ G. Becker, Zeits. f. Physik **34**, 255 (1925).

⁹ E. C. Kemble, Phys. Rev. **25**, 1 (1925).

¹⁰ N. Burger and H. B. Dorgelo, Zeits. f. Physik **23**, 258 (1924).

been justified on theoretical grounds.^{11,12} Its extension to band spectra leads to an expression of the same general form as Eq. (2) except that the form of the frequency factor is left undetermined. Also the analogue, on the basis of the summation rule, of the probability factor in Eq. (2) takes on a different set of values for an arbitrary choice of statistical weights from that taken on by the term occurring in Eq. (2).

The new quantum theory introduced by Heisenberg and Born suggests that the intensity of the Zeeman component correlated with the transition $m \rightarrow m \pm 1$ and $r \rightarrow r \pm 1$, where m and r are the rotational and spatial quantum numbers respectively, is proportional^{13,14} to $(m \pm r)(m \pm r - 1)/(m^2 - \frac{1}{4})$. The intensity for the transition $m \rightarrow m \pm 1$, $r \rightarrow r$ varies as $(m^2 - r^2)/(m^2 - \frac{1}{4})$. It may be shown that a summation over all allowed values of r and application of the Kemble, Heisenberg postulate of the continuity of intensities^{9,11} leads to a linear dependence on the rotational quantum number in harmony with (2).

The experimental verification of Eq. (2) and the resolution of the ambiguity^{9,12,15} as regards the exact variation of the probability factor (and therefore the proper choice of weight factors) are important consequences of the present work.

The procedure adopted for evaluating the integrated absorption coefficients consisted in obtaining the absorption curves for six different absorbing columns varying in length from 0.0988 cm to 2.97 cm. Curves were drawn of the areas under the absorption lines plotted against tube-length. The gas columns were sufficiently short to permit of reasonably accurate extrapolation of these curves to zero tube-length. The initial slopes of these extrapolated curves, as will appear later, yield the desired absolute integrated absorption coefficients.

EXPERIMENTAL WORK

The HCl gas was obtained by dropping concentrated sulphuric acid on constant boiling HCl solution. Five Emmerling absorption towers were used to purify the gas and every precaution was taken to avoid its contamination.

The infra-red spectrometer was the quartz prism instrument constructed by Brinsmade and used by Brinsmade and Kemble. A variety of modifications in the details of the apparatus gave increased sensitivity and steadiness. It was of the Wadsworth¹⁶ constant deviation type as modified by Gorton.¹⁷ Fig. 1 shows a diagram of the optical system. The instrument

¹¹ W. Heisenberg, Zeits. f. Physik 31, 617 (1925).

¹² R. H. Fowler, Phil. Mag. 50, 1079 (1925).

¹³ D. M. Dennison, Phys. Rev. 28, 318 (1926).

¹⁴ I. Tamm, Zeits. f. Physik 37, 685 (1926). Dr. Tamm seems to infer incorrectly that neglecting the Boltzman factor the band intensities are practically independent of the rotational quantum numbers and follow the Maxwell-Boltzman distribution law.

¹⁵ G. H. Dieke, Zeits. f. Physik 33, 161 (1925).

¹⁶ Wadsworth, Phil. Mag. 38, 137 (1894).

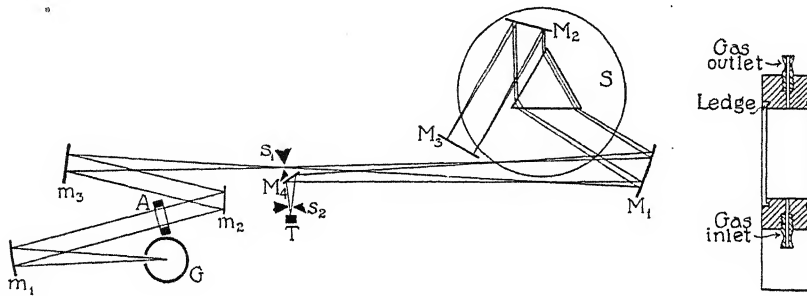
¹⁷ Gorton, Phys. Rev. 7, 66 (1916).

was provided with a 60° quartz prism having faces 5.1 cm high and 4.3 cm wide. The focal length of the concave mirror M_1 was 50 cm. The extreme spectral range falling on the thermopile slit was computed to be 126A, with both slit widths set at 0.3 mm.

The receiving instrument was a twenty junction bismuth silver vacuum thermopile constructed by Coblenz. Every effort was made to rid the thermopile case of occluded gas by long continued pumping.

The galvanometer was a Weston gravity controlled d'Arsonval type of instrument. The sensitivity was usually adjusted to a value between 2×10^{-8} and 8×10^{-9} volts per mm at a meter's scale distance.

A Nernst glower actuated by a steady alternating current was used as a light source. Direct current from storage batteries was used to run a



Figs. 1 and 2. Optical plan of set-up. G , Nernst glower; m_1 and m_3 , concave mirrors; m_2 , M_3 , M_4 , fixed plane mirrors; M_2 , plane rotating mirror; M_1 , collimating mirror; s_1 , entrance slit; s_2 , thermopile slit; T , thermopile; A , absorption chamber.

high-frequency motor-generator loaned to the writer by Professor G. W. Pierce. The usual variation in mean square current over a period of three or four hours was less than 0.005 amp.

The first absorption tube consisted of two brass frames between which cylinders of various lengths could be fitted. All the absorption tubes were fitted with quartz windows about 2 mm thick. The three shortest tubes (Fig. 2) were specially designed to permit an accurate measurement of the length of the absorbing column. The tubes were made of brass and an annular depression was cut around each window ledge. The windows were sealed in place by means of a ring of de Khotinsky cement placed on this depression. By this method it was possible to keep the window ledges perfectly clean so that the length of the tube could be measured by micrometering the distance between the ledges with the quartz plates removed.

The necessary data were (1) the transmission, T_1 , of the tube itself free from gas, and (2) the transmission, T_B , of the gas-filled tube. In terms of these transmissions the gas absorption is

$$1 - T_1/T_B \quad (3)$$

The tube transmission will be referred to as the "base-line," the precise determination of which presented a rather difficult problem. A difference

of the order of 0.5 percent was found for the variation in transmission of a 65 cm tube when filled with room air and when evacuated. Therefore, for the tube-lengths used in this research, the transmission of the air-filled tube could be used as the base-line. The stumbling block was the removal of all trace of gas from the absorption chamber since merely blowing or sucking air through was ineffective.

Four distinct methods of obtaining data to fix the base-line were followed and will be distinguished by the letters (a), (b), (c) and (d). For the 0.96 cm and 2.97 cm tubes, the procedure (a) was the following: Preliminary to the first run on either tube the two window frames, with the windows already attached, were mounted a distance apart equal to their separation with the particular brass cylinder to be used in the run and about eight base points were obtained in the region to be covered. The windows were purposely not treated to remove adsorbed gas since it was essential that the condition of the surfaces be the same as when the cylinder was in place and the tube filled with gas. This adsorption was quite apparent for, even after the exposure of the quartz windows to the air for a half-day, slight warming was sufficient to liberate enough gas to give off the sharp characteristic odor of HCl. The base-line having been determined, the glower the mirror and the stops which secured proper alignment were not varied till the run had been completed. The whole band could generally be covered in two runs (or three runs at most), therefore, for the second run the base-points were determined at the end of the run. This method of fixing the base-curve solved the problem of minimizing the inaccuracies due to the presence of occluded gas on the windows.

Method (a) was inapplicable to the shorter tubes which were constructed of a single brass plate. For two of the four runs on the 0.169 cm tube, the base-line was determined before and checked after the run, by evacuating the tube. This was method (b). For the other two runs and for the runs on the 0.248 cm tube and the run on the 0.0988 cm tube covering the negative branch, the procedure (c) was to determine the base-points for the positions of minimum absorption as these low absorption points were reached during the course of the experiment, a large capacity piston pump being used to take out most of the gas and the exhaustion then improved by cutting out this pumping unit and replacing it with a Cenco "Hyvac" oil pump. This method reduced the inaccuracies introduced by progressive variations during the course of the run and in the event of some sudden change limited the possibility of error to one line instead of casting suspicion on all the values of the run. In the case of the run on the positive branch with the 0.0988 cm tube, readings were taken at each point with the tube alternately evacuated and filled with gas. In this method (d) the tube was not moved at all and the true transmission was immediately given as the ratio of the successive readings when the tube was filled with gas and when it was pumped down. If the gas could be completely removed in a conveniently short time this method would be the most satisfactory inasmuch as it eliminates the intermediate step of obtaining the values of the glower

emission. The method is most successful when the volume to be evacuated is a minimum, which explains its use for the shortest tube-length. Because of possible unforeseen complications in the way of window-adsorption effects, it seemed advisable to limit the use of this plan to the one tube-length and test its value by the plausibility of the results obtained as compared with those for the other tube-lengths.

The spectrometer settings were read on a revolution counter and dial. In general, the interval used was about one dial revolution (the absorption peaks were about six turns apart near the center of the band) except in the neighborhood of the maxima where sometimes quarter revolutions were used.

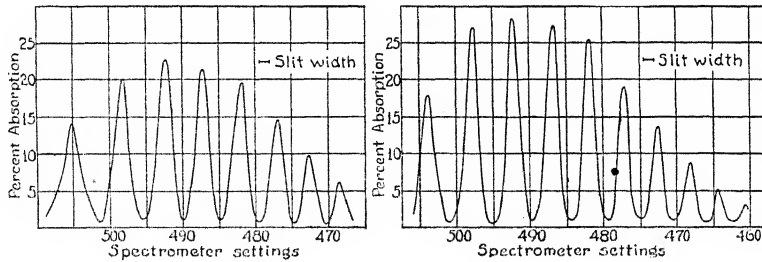
In calculating the absorption from the experimentally determined diminution in light intensity, it was assumed that the effects of selective scattering and selective reflection at the quartz-gas interface were negligible. As the curves of total absorption (area under peak) plotted as a function of the tube-length extrapolate naturally to the value zero for zero tube-length, it hardly seems possible that there could have been any appreciable selective reflection. The writer has no definite check on the assumption that scattering may be neglected, but since the selective scattering should be proportional to the absorption it is not likely that it could effect, markedly, the apparent relative absorption intensities of the different lines.

THEORY OF THE CALCULATIONS

The general plan for obtaining the integrated absorption coefficients has already been suggested in the introduction and it has been pointed out that the procedure involved the determination of the area under each absorption line for several tube-lengths. On denoting these areas, when measured in frequency units, by the symbol $A_M(x)$ it is possible to write

$$A_M(x) = \int_M [(T_B - T(x))/T_B] d\nu \quad (4)$$

where T_B is the base-line transmission and $T(x)$ is the transmission of the gas-filled tube of length x . Strictly speaking the absorption curve for a



Figs. 3A and 3B. Characteristic absorption curves taken with 0.169 cm and 0.248 cm tubes. *R* branch.

given line extends from $\nu=0$ to $\nu=\infty$ but the estimates were made on the assumption that the true area was closely approximated by the area under

the experimental curves, uncorrected for slit width, included between two successive minima separating the line in question from its neighbors (cf Figs. 3A and 3B).

With regard to the neglect of the overlapping of adjacent lines, it may be pointed out that (a) adjacent lines do not differ greatly in intensity and the overlapping of lines of equal intensity clearly leads to no error, (b) in the region where the intensities might be considered as changing comparatively rapidly the net gain from the more intense neighbor is, in general, very nearly balanced by the net loss to the less intense adjacent line, and (c) for the very short tube-lengths employed in these experiments, the intensity in the region between absorption lines is quite small.

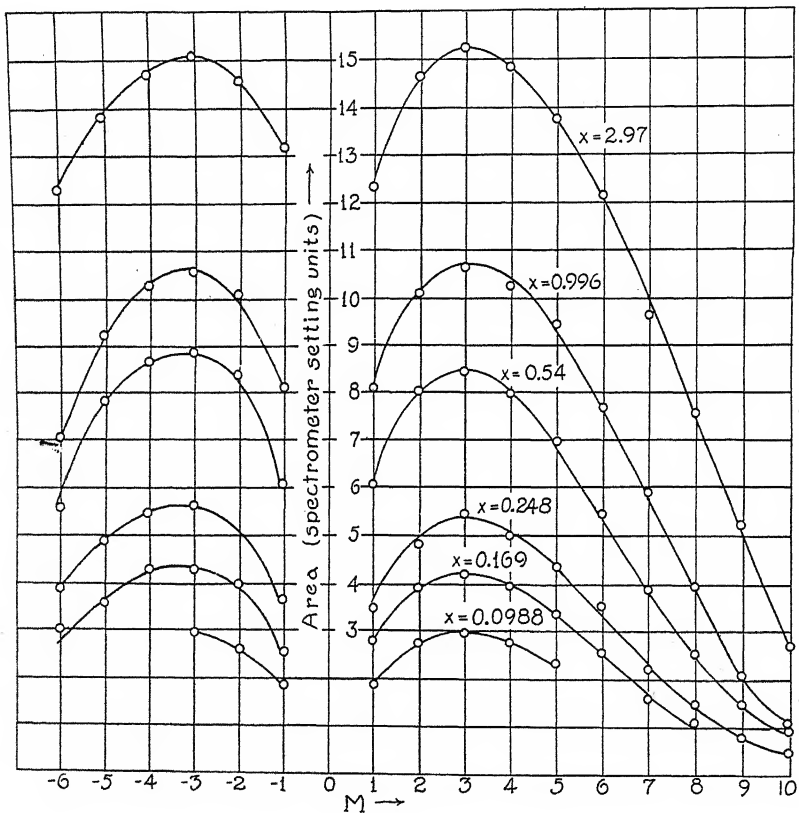


Fig. 3C. Smoothing curves.

The areas under the various absorption maxima were measured from the original curves without correcting for slit width. Clearly, since the area under any line regardless of slit width gives the fractional amount of light abstracted from a beam whose intensity is independent of frequency, the areas should not be affected by variations in the slit width which do not lead to serious overlapping.

For estimating the areas under the absorption curves large scale plots similar to Figs. 3A and 3B were used. A sufficient number of points were available for the lines, usually about seven or eight at least, to indicate the general appearance though, of course, there was some latitude in defining their shapes. For most of the tube-lengths several sets of overlapping data were available and the absorption data used in the calculations are the averages of these for each tube-length.

In the adaptation of the measured areas to the calculations a preliminary smoothing process was resorted to in order to reduce the inaccuracy in the individual lines. The smoothing was effected by drawing the best curve through the correlated points in a plot of line-number against line-area (Fig. 3C). In all the calculations based on direct application of the "five-term polynomial" method and in all methods involving use of the data for the line $M=3$ a second smoothing occurred in the choice of the most plausible curve through the points in the plots of area against tube-length of which Fig. 4 is the type.

TABLE I
Smoothed areas in frequency units.

<i>M</i>	2.97 cm	.996 cm	.54 cm	.248 cm	.169 cm	.0988 cm
1	1.178	.767	.574	.346	.265	.175
2	1.423	.979	.777	.484	.379	.262
3	1.526	1.071		.536	.415	.292
4	1.536	1.063	.826	.526	.401	.284
5	1.405	.986	.726	.455	.348	.236
6	1.317	.825	.581	.359	.270	
7	1.078	.643	.424	.257	.186	
8	.848	.433	.284	.166	.108	
9	.605	.287	.167	.088		
10	.329	.124	.103	.0509		
-1	1.172	.737	.559	.328	.238	.166
-2	1.285	.884	.731	.449	.345	.232
-3	1.285	.900	.754	.478	.374	.253
-4	1.225	.853	.717	.454	.345	
-5	1.103	.744	.623	.393	.292	
-6	.956	.551	.470	.300	.210	

The original areas were in units of percent and spectrometer settings. To change to a frequency standard two independent methods were employed to estimate $\Delta\nu/\Delta\theta$ where θ refers to the dial settings and ν to the frequency. In the first method this ratio was calculated from the prism-angle and the known dispersion curve of quartz. In the second method the values of $\Delta\theta$ for successive absorption maxima as determined from the experimental plots similar to Figs. 3A and 3B and the corresponding values of $\Delta\nu$ as given by Colby and Meyers,⁶ were plotted against line number M . The ratios of the values of the ordinates of the two curves for any value of M is the correlated value of $\Delta\nu/\Delta\theta$. The agreement of the two sets of values was quite good for the positive branch, although there was a slight departure for the negative branch. The mean of the two estimates was used in the calculation.

The primary purpose of the experiments was to determine the values of α_M for the various lines. It may immediately be shown that if we plot the area under an absorption line as a function of the tube-length x , α_M should be the slope of the curve at $x=0$. Thus, from the fundamental relation between the absorption coefficient and the intensity $I(\nu)$

$$dI(\nu) = -\mu(\nu)I(\nu)d\nu \quad (5)$$

we obtain

$$A_M(x) = \int_M (1 - e^{-\mu(\nu)x})d\nu \quad (6)$$

which gives immediately

$$(dA_M/dx)_{x=0} = \alpha_M = \int_M \mu(\nu)d\nu \quad (7)$$

The evaluation of the initial slopes of the various graphs of area against tube-length required by Eq. (6) is somewhat complicated by the large curvature near the origin. Several methods of attack were employed in the attempt to get as accurate a solution of the problem as possible.

The first of these methods consisted in fitting the five-term polynomial formula

$$A_M(x) = \omega^{(1)}x + \omega^{(2)}x^2 + \dots + \omega^{(5)}x^5 \quad (8)$$

to the data. This method is inaccurate since it accentuates the influence of the shorter tube-lengths in that a very small error in the area for the shortest tube produces a large error in the calculated value of $\omega^{(1)}$ or α_M .

A method which eliminates this difficulty is most easily explained if we start from the crude assumption that the absorption coefficient curves ($\mu(\nu)$ plotted against ν) for the various lines have the same shape so that by suitable change in the scale of ordinates any curve could be superposed on any other. This assumption is expressed by

$$\mu_M(\nu) = K_M F[\nu - (\nu_0)_M] \quad (9)$$

where $(\nu_0)_M$ is the frequency of the center of the M th line. If it were true, $A_M(x)$ would be a function of the product $K_M x$ or, what comes to the same thing, of $\alpha_M x$. Then if we consider two points corresponding to the same ordinate A on curves for different lines, this product must be the same for both. In other words for two such points

$$x_{M'}/x_M = \alpha_M/\alpha_{M'} \quad (10)$$

Hence the ratio of the integrated absorption coefficients for any two values of M could be determined by plotting curves of area against tube-length like the one of Fig. 4, and comparing the abscissas of any two points with equal ordinates.

This method of procedure leads, in practice, to values of $\alpha_M/\alpha_{M'}$, which vary with the ordinate (area) for which they are calculated, showing that

the lines are not exactly the same in shape. This is to be expected since HCl is a mixture of the constituents HCl_{35} and HCl_{37} so that each absorption line is an isotopic doublet. The separation of the doublet components depends on the rotational quantum numbers¹⁸ and therefore varies with M .

The variation of $x_{M'}/x_M$ with the corresponding ordinate A is not rapid for small values of A , however, and since

$$\lim_{A \rightarrow 0} \frac{x_{M'}}{x_M} = \lim_{x_M \rightarrow 0} \frac{x_{M'}}{x_M} = \frac{\alpha_M}{\alpha_{M'}} \quad (10.1)$$

it follows that the extrapolation of the $x_{M'}/x_M$ values to zero A (or zero x_M) gives an accurate method of evaluating the *relative* absorption coefficients.

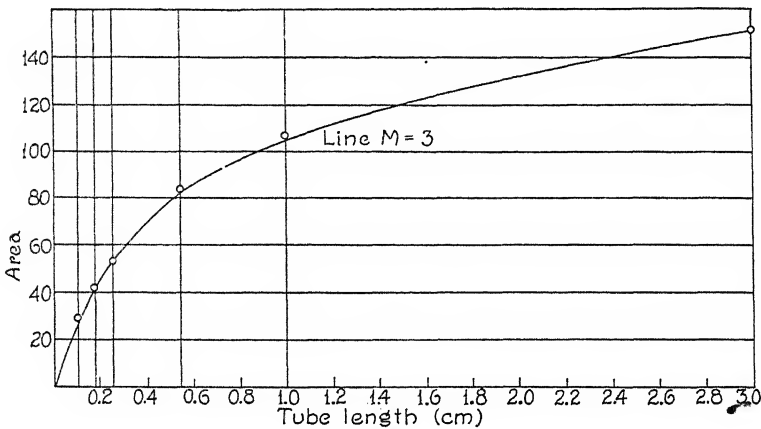


Fig. 4. Curve showing the variation of line area with tube-length.

In applying this method the line $M = 3$ was arbitrarily selected as a standard of comparison and an accurate curve was drawn through the points defined by corresponding values of smoothed area and tube-length (Fig. 4). For any other absorption line M each area obtained from a run using a gas column of length x_M was used to determine a value x_3 for which the ordinate of the standard curve was equal to the area in question. Then the values of the ratio x_3/x_M were plotted against x_M for each absorption line. These lines would have been straight lines, with ordinates equal to the relative absorption coefficients desired, if the shapes of all the lines had been the same. It is evident from Fig. 5 that the extrapolation to the axis of ordinates is a fairly safe one.

In view of the appreciable experimental errors, it is desirable to have some theoretical guide for drawing "best curves" for x_3/x_M . Such a guide will be suggested by the following analysis. The absorption coefficient may be written

$$\mu(\nu) = \mu'(\nu - \nu_1) + \mu''(\nu - \nu_2) \quad (11)$$

¹⁸ R. S. Mulliken, Phys. Rev. 25, 119 (1925).

where $\mu'(\nu - \nu_1)$ and $\mu''(\nu - \nu_2)$ are the respective contributions of each isotope and ν_1 and ν_2 are the frequencies of the absorption maxima for the corresponding isotopes. It will be brought out that the form of the absorption curves is determined by the magnitude of the terms

$$\int_M \mu(\nu)^n d\nu = \int_0^\infty \{ \mu'(\nu - \nu_1) + \mu''(\nu - \nu_2) \}^n d\nu \quad (11.1)$$

The expansion of $A_M(x)$ leads to the series

$$A_M(x) = \mu_M^{(1)} x - \mu_M^{(2)} x^2 / 2! + \mu_M^{(3)} x^3 / 3! \dots \quad (12)$$

where

$$\mu_M^{(j)} = \int_M [\mu_M(\nu)]^j d\nu$$

Let us make the assumption expressed in Eq. (9), then substituting $x' = xK_M/K_3$ in Eq. (12) gives for the expansion of A_M in terms of x'

$$A_M(x') = \mu_M^{(1)} K_3 x' / K_M - \mu_M^{(2)} \{ K_3 x' \}^2 / K_M^2 2! + \mu_M^{(3)} \{ K_3 x' \}^3 / K_M^3 3! \quad (12.1)$$

If the assumption made about the factorization of the absorption coefficient into a term dependent on the quantum numbers and another independent of the line were true (vide Eq. 9) it is seen that the coefficients of the various powers of the primed variables in Eq. (12.1) would be identical with those in the expression of $A_3(x)$ in powers of x . Actually, from the fact that $\partial[\mu'(\nu - \nu_1)]/\partial\nu$ (or $\partial[\mu''(\nu - \nu_2)]/\partial\nu$) is of one sign from 0 to ν_1 (or ν_2) and from ν_1 (or ν_2) to ∞ and the knowledge that $\mu'(\nu - \nu_1), \mu''(\nu - \nu_2) > 0$ it may be shown analytically or made evident graphically, that the integral $\int_0^\infty [\mu(\nu)]^n d\nu$ for $n > 1$ steadily diminishes on increase of the isotope separation. An equivalent statement is that for lines for which $(\Delta\nu)_M > (\Delta\nu)_3$, where $\Delta\nu$ is the isotope separation, the following inequality holds

$$\mu_M^{(j)} \{ K_3 / K_M \}^j < \mu_3^j \quad (9.1)$$

The sign of the inequality is reversed if $(\Delta\nu)_3 > (\Delta\nu)_M$.

(12) Inverting the series gives

$$x = a_M^{(1)} A_M + a_M^{(2)} A_M^2 + \dots + a_M^{(j)} A_M^j + \dots \quad (12.2)$$

Eq. (12.2) may be employed to yield the rigorous value of the ratio x_3/x_M . Thus

$$x_3/x_M = \frac{a_3^{(1)} A + a_3^{(2)} A^2 + \dots}{a_M^{(1)} A + a_M^{(2)} A^2 + \dots}$$

where x_3 and x_M are the values of x correlated with a given value of $A(x)$ (the subscript M or 3 would have no significance here) for the line $M=3$ and for the M th line respectively. Expanding the ratio in powers of A and then replacing A by its expansion in terms of x_3 or x_M yields

$$\begin{aligned}
 x_3/x_M &= \frac{a_3^{(1)}}{a_M^{(1)}} \left\{ 1 + \mu_3^{(1)} x_3 \left(\frac{a_3^{(2)}}{a_3^{(1)}} - \frac{a_M^{(2)}}{a_M^{(1)}} \right) + (\{\mu_3^{(1)}\}^2 - \mu_3^{(2)}) x_3^2 \right. \\
 &\quad \left. \left[\left\{ \frac{a_3^{(3)}}{a_3^{(1)}} - \frac{a_M^{(3)}}{a_M^{(1)}} \right\} - \frac{a_M^{(2)}}{a_M^{(1)}} \right] + \dots \right. \\
 &= \frac{a_3^{(1)}}{a_M^{(1)}} \left\{ 1 + \mu_M^{(1)} x_M \left(\frac{a_3^{(2)}}{a_3^{(1)}} - \frac{a_M^{(2)}}{a_M^{(1)}} \right) + (\{\mu_M^{(1)}\}^2 - \mu_M^{(2)}) x_M^2 \right. \\
 &\quad \left. \left[\dots - \frac{a_M^{(2)}}{a_M^{(1)}} \right] + \dots \right.
 \end{aligned}$$

where the $\mu_3^{(j)}$, $\mu_M^{(j)}$ coefficients occur in Eq. (12) and it is evident that

$$\lim_{x_M \rightarrow 0} x_3/x_M = \lim_{x_B \rightarrow 0} x_3/x_M = a_3^{(1)}/a_M^{(1)} = \mu_M^{(1)}/\mu_3^{(1)}$$

The coefficients $a_3^{(j)}$ and $a_M^{(j)}$ of the inverted series (12.2) are such functions of $\{\mu_M^{(j)}\}$ that if the distinction were dropped between $\{\mu_M^{(1)}\}_i$ and $\mu_M^{(j)}$ the ratio $a_M^{(j)}/a_M^{(1)}$ would reduce to unity. (For instance $a_M^{(1)} = 1/\mu_M^{(1)}$, $a_M^{(2)} = -\mu_M^{(2)}/\{\mu_M^{(1)}\}^3$).

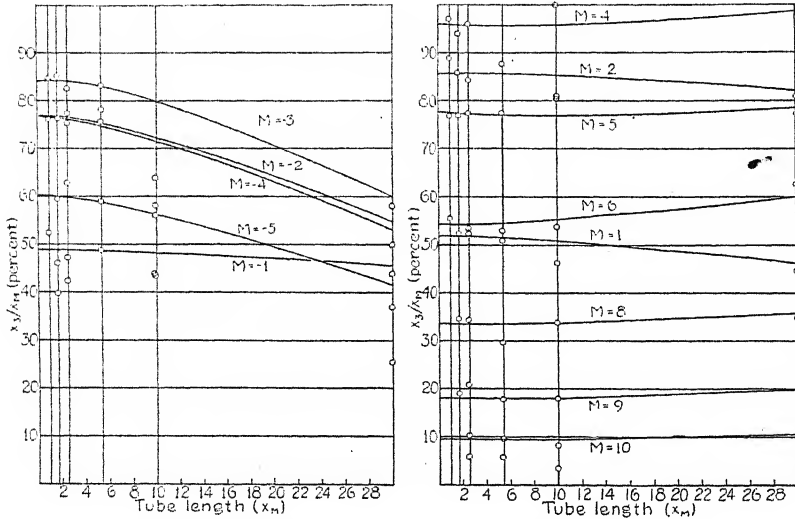


Fig. 5. Extrapolation plots for the "ratio" method.

It is, therefore, easily understood that the assumption of Eq. (9) would lead to the equality of the ratios $a_M^{(j)}/a_M^{(1)}$ and $a_3^{(j)}/a_3^{(1)}$ and this would carry with it the vanishing of all the terms in powers of the variable in Eq. (13). The isotope doubling disturbs the equality of $a_M^{(j)}/a_M^{(1)}$ and $a_3^{(j)}/a_3^{(1)}$ and the inequality of Eq. (9.1) points to the conclusion that the x_3/x_M vs x_M curves should be concave upwards for $3 < M$ and concave downward for $M < 3$, (at least initially.)

Although the rotational isotope separation is essentially a quadratic function of the quantum numbers, the resultant of the vibrational and rotational isotope separations may be considered as varying very nearly linearly in the region of the band center. Bearing this in mind, it is clear that since the values of A for the lines $M=7, 8, 9, 10$ were quite small for all the tube-lengths used the influence of the higher order terms in Eq. (13) would not be expected to be pronounced, but in the case of the negative branch where the areas are larger for lines equally far removed from the line $M=3$, the curvature should be more noticeable.

To determine the value of x_3 correlated with a given area, it was necessary to approximate the curve of area against tube-length for the line $M=3$ with some care. Two methods in particular were used for this purpose. One of these is discussed in some detail under the heading of Method III; the other, which will be referred to as Method II, utilized formula (8) to locate points corresponding to tube-lengths 0.01 cm, 0.02 cm, etc.

TABLE II
Interpolated values of areas.

x_3 (cm)	Method II $A(x)/12.28 \times 10^{-12}$	x_3 (cm)	Method III $A(x)/12.28 \times 10^{-12}$	x_3 (cm)	Method IV $A(x)/12.28 \times 10^{-12}$
0.01	0.3697	0.0323	1.103	0.01	0.37
0.02	0.716	0.0645	2.001	0.1	2.9
0.04	1.346	0.129	3.42	0.2	4.67
0.08	2.276	0.323	6.25		
		0.645	8.95	1.0	1.065
		1.29	12.2	2.0	13.5

Method III proceeds as follows: since the value of $\int_M (1 - \exp(-\mu(\nu)x))d\nu$ is only slightly affected by changes in the functional form of $\mu(\nu)$, whose influence is perceptible only when the integrand is quite small, one is prompted to use as a simple approximation

$$\mu(\nu) = \frac{a_M}{(\nu - \nu_1)^2 + b_M^2} \quad (14)$$

where a_M and b_M are certain characteristic constants. Therefore

$$A_M(x) = \int_{-\infty}^{+\infty} (1 - e^{-a_M x / (\nu^2 + b_M^2)}) d\nu$$

On defining n and Z as $a_M x / b_M^2$ and ν / b_M respectively, the last integral may be exhibited as

$$A_M(n) = 2b_M \left\{ \int_0^n (1 - e^{-n/(Z^2+1)}) dZ + \int_n^\infty (1 - e^{-n/(Z^2+1)}) dZ \right\}$$

The transformation $y = 1/Z$ applied to the second integral of the above makes it possible to write

$$A_M(n) = 2b_M \left\{ \int_0^c (1 - e^{-n/(z^2+1)}) dz + \int_{1/c}^0 (1 - e^{-v^2 n / (v^2+1)}) dy / y^2 \right\} \quad (15)$$

The integrals were evaluated graphically by finding the areas under the integrand curves for $n = 0.5, 1, 2, 5, 10, 25$. The constant c was taken as 20 (so that an approximation which replaced the second integral by n/c would have been only one percent out of the way).

The resulting plot of A_M against n was very similar to the curve of area as a function of tube-length except for the matter of scale. It was not difficult to apply a process of trial and error to establish values of n and b which secured a good fit of the theoretical A, n curve and the experimental A, x curve. The procedure consisted in studying the ratios of the two ordinates of the A, x curve, for ratios of the x 's equal to that between an arbitrary pair of n values and noting when this ordinate ratio was equal to the corresponding ordinate ratio of the A, n curve.

The constants $a_3 = 1.67 \times 10^{21}$ and $b_3 = 1.04 \times 10^{10}$ were evaluated from the relations $2b_3 = A_3(x)/A_3(n)$ and $a_3 = b_3^2 n / x_3$. The integrated absorption coefficient for the line $M = 3$ is

$$\alpha_3 = \int \mu_3(\nu - \nu_0) d\nu = \pi a_3 / b_3 \quad (16)$$

This is the only absolute absorption coefficient calculated in this way. The deviation of the extrapolation curve obtained by this method from that suggested by the terminated power series expansion method (Method II) was slight and in the expected¹⁹ direction in that the slope at the origin of the former curve was the greater.²⁰

RELIABILITY OF THE RESULTS

The principal sources of inaccuracy in the results given in this paper arise from: (a) experimental uncertainty in taking readings; (b) errors in the base-lines; (c) the cumulative effect of errors which separately may be very small (i.e. use of an inaccurate effective tube-length for the calculations, non-uniformity of the Nernst glower emissivity, uncertainty regarding $\Delta\nu/\Delta\theta$, errors in plotting the data and measuring the areas, etc.); (d) uncertainty regarding the possible effect of selective reflection at the windows of the chamber; (e) errors inherent in the methods employed for calculating the integrated absorption coefficients.

A consideration of the average number of readings and the accuracy of each makes it plausible to assume an accuracy of 0.75 percent for points of the base-line and transmission curves. For gauging the effect of an error of this magnitude on the precision of the measured line areas, it is suggestive

¹⁹ Since the alternating power series was terminated at a positive term and therefore would be expected to give too high values of ω^1 .

²⁰ A fourth method of calculation depended on the assumption of a step like variation for $\mu(v)$. The analysis is somewhat involved and is therefore omitted although the value of α_3 calculated in this way is included in Table II.

to treat the absorption line as being of a triangular shape and height k . Considering T_B to be sensibly constant over the line allows us to write

$$\frac{\delta A_M}{A_M} = \frac{\delta T_B}{T_B} \left\{ \frac{T_B}{T_B - k} \right\} \quad (17)$$

which reduces to (constant) $\times \delta T_B / T_B$ when it is realized that k/T_B is independent of T_B . Similarly the effect of inaccuracy in the transmission curve may be written

$$\delta A_M / A_M = \delta T^{(x)} / [T^{(x)} - k] \quad (17.1)$$

These formulas show the importance of using as high values for the base-line transmission as possible. On applying the Fresnel formula for the unavoidable reflection loss at each of the four reflecting surfaces of the two quartz windows, it turns out that in this work the value of the base-line transmission actually attained was only two percent or three percent less than that theoretically possible for infinitely thin windows.

The applications of expressions (17) and (17.1) suggest errors of the order of magnitude of 1 to 8 percent, the lesser values being correlated with the more intense lines in the R branch and the higher values with the weaker lines in this branch and the farther lines in the P branch.

One gauge of the effect due to the non-systematic causes enumerated under (c) would be the difference between the original and the smoothed areas as indicated in Fig. 3C. The smoothing curves are, however, somewhat arbitrary and the fact that the differences are very slight is not to be accepted too easily as a proof of the reliability of the results. However, it is not probable that the error is over 3 or 4 percent for the more accurate lines to 8 or 9 percent in the case of poorer measurements—the correlation being the same as for errors of type (b). The relative values are probably more accurate.

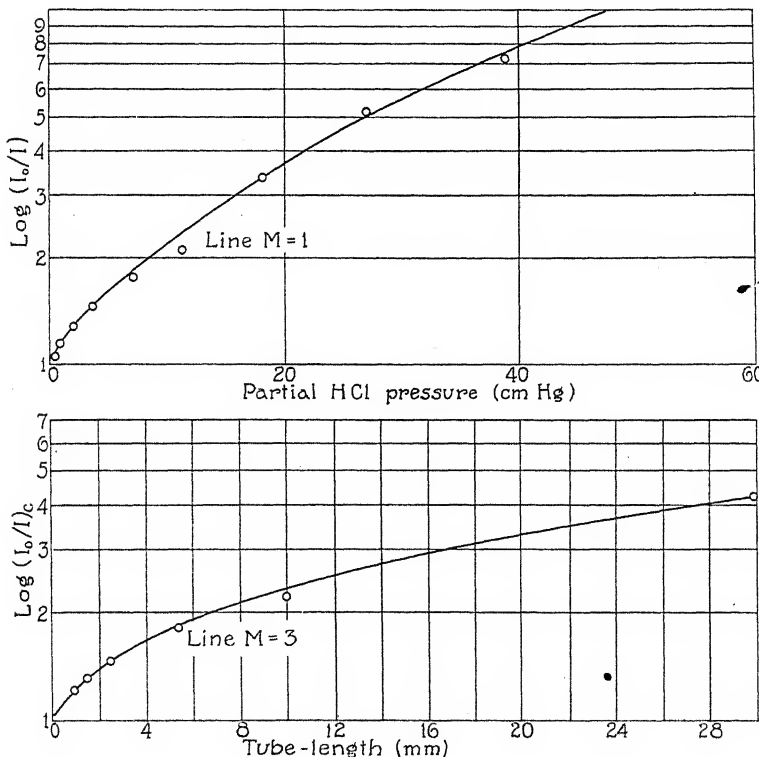
In using Method I an analysis of the error introduced in the final absolute values of the absorption coefficients by the estimated inaccuracies in the areas, indicates that the precision limits are about 15 percent for the stronger lines in the positive branch to about 25 percent for the weaker lines and the lines in the negative branch. The ratio methods are much more reliable especially for the relative values. It appears that a fair estimate for these methods would fix the reliability as being about 10 to 20 percent.

Both the mean square deviation of the calculated points from the best curves in Figs. 3A and 3B and the apparent close check between theory and experiment, to be pointed out later, suggests that the actual accuracy attained is better than these estimates would indicate. The close agreement in the estimates of the absolute value of α_3 as obtained from the four methods of calculating described above lends weight to the reliability of the values of α_M given in Table III.

DISCUSSION OF RESULTS

Before entering upon a study of the application of the experimental values of the integrated absorption coefficients to the primary theoretical problem of absorption intensities, it is worth while to remark some important general consequences of the data obtained in this research.

Width of spectral lines and failure of exponential law. One of the striking results is the unexpected magnitude of the absorption for short gas columns as compared with that to be expected from the application of the exponential law to the data for long tube-lengths. The failure of the exponential law for the line $M=3$ is shown by Fig. 6A. The ordinates are the quantities $\log_{10} (I_0/I)_c$, where $(I)_c$ is the apparent intensity of the transmitted light after correction for slit width by the Paschen-Runge²¹ formula and the tube-lengths are the abscissas. If the exponential law were obeyed the points in Fig. 6A would lie on a straight line through the point $\log (I_0/I) = 1$, $x = 0$. The decided curvature is proof that the exponential law is not valid in the region of maximum absorption.



Figs. 6A and 6B. Test of exponential law.

The law fails also when the partial pressure is varied instead of the tube-length, as indicated in Fig. 6B. No slit width correction was applied for

²¹ F. Paschen, Ann. d. Physik 60, 661 (1897).

this case but it is fairly clear that such a small correction would not affect the conclusion.

The apparent failure of the exponential law is due, no doubt, to the fact that the resolving power of the spectrometer with the slit widths used was not sufficient to give the true shape of the absorption curve even when the slit width correction is applied.

The lines are narrower and 'deeper' than they seem. In fact, we can calculate the equivalent half-breadth of the line $M=3$ from the approximating function used in Method III. From Eq. (14) it is readily seen that the half-breadth is $2b_3$. The numerical value is about²² 2.1×10^{10} frequency units. This is quite small in comparison with the spacing of the lines, which is about 54×10^{10} frequency units in the neighborhood of the line $M=3$. This is the half-breadth of a single line having the same A, x curves as the actual line $M=3$. Since the theoretical separation of the isotopic components is 6.78×10^{10} frequency units, it is clear that the actual half-breadth of the individual components, as calculated by this method, must be less than the equivalent half-breadth of the pair. Moreover, the variation in the isotopic separation with M should have a noticeable effect on the shape of the A, x graphs, as is proved by the curvature of the ratio plots of Figs. 3A and B.

The half-breadth given above is about one-fourth of the lower limit assigned by G. Becker⁸ on the basis of his study of the effect of pressure on the HCl band, and about one-fifth of the estimate given by Tolman.²³

The nature of the absorption curves may be interpreted as follows: Since the absorption lines appear to be really very sharp and quite intense at the center, most of the initial absorption is due to the center of the line and in the case of the strong lines, radiation of frequency corresponding to peak absorption is almost completely absorbed in less than one cm of gas path. For the long tubes the increase in absorption with tube-length is from the less intense absorbing region on either side of the maximum.

The relative intensities of the lines. An immediate conclusion to be drawn from the tabulated values of the integrated absorption coefficients (Table III) is that the intensities in the positive branch are higher than those in the negative branch as required by Eq. (2). Although the single published absorption curve of Brinsmade and Kemble is in agreement with this result the most frequently quoted experimental data (i.e. those of Imes) seemed to belie this prediction of theory.²⁴

²² This estimate depends somewhat on the line shape assumed. A subsequent paper will consider the effect, on the calculated values, of modifications in the supposed line shape and will give the results for the isotopic doublet structure.

²³ R. Tolman, Phys. Rev. 23, 693 (1924).

²⁴ Not only are corresponding maxima of Imes' absorption curves distinctly higher for the lines in the negative branch but the intensity estimates derived from these curves by Tolman²³ also emphasize the negative branch. The fact that $\Delta\nu/\Delta\theta$, for a grating decreases with ν indicates one explanation for the appearance of Imes' curves.

Fig. 7 shows a comparison of the experimental results with the formula of Eq. (2). The theoretical points yielded by the two sets of weights $p_M = 1, 3, 5, 7, \dots$, and $p_M = 2, 4, 6, \dots$, are both indicated. For the

TABLE III

Tabulated values of the integrated absorption coefficients.

M	Method I $\alpha_M = 46.6 \times 10^{10}$		Method III 50.2×10^{10}		Method IV 51.6×10^{10}
	α_M/α_3	Ratio Methods	α_M/α_3	Theoretical Values ($p_j = 1, 3, 5$)	$\alpha_M \times 10^{10}$ Best Values
	Method I			($p_j = 2, 4, 6$)	
1	0.552	0.518	0.474	0.606	25.4
2	0.883	0.857	0.853	0.895	42.
3		1.00	1.00	1.00	49.
4	0.976	0.959	0.961	0.926	47.
5	0.829	0.774	0.782	0.737	37.9
6	0.537	0.542	0.555	0.515	26.8
7	0.310	0.333	0.345	0.316	16.3
8	0.192	0.185	0.189	0.172	9.07
9	0.0847	0.091	0.092	0.083	4.6
10	0.081	0.047	0.040	0.036	2.35
-1	0.479	0.486	0.444	0.570	23.8
-2	0.781	0.764	0.736	0.789	37.5
-3	0.877	0.841	0.840	0.840	41.3
-4	0.79	0.768	0.736	0.731	37.6
-5	0.66	0.604	0.584	0.550	29.7
-6	0.51	0.347	0.389	0.333	21.5

latter sequence only the points calculated from Kemble's theory are plotted since obviously the experimental intensity variations are non-alternating.²⁵ The agreement is best for the choice of weights²⁶ $p_M = 1, 3, 5, \dots$.

The choice of statistical weights may be further tested in two other ways. On the assumption that the general form of Eq. (2) has already been corroborated by the comparison plots of Fig. 7 it appears that the ratio of α_M to the corresponding Boltzmann factor $e^{-W_M/kT}$ should yield a quantity proportional to \bar{p}_M . The multiplicative factor $|M|/M$ is used in the plot of this ratio against line number (Fig. 8) in order to obtain negative values of this ratio for the lines of the P branch.

The curve obtained is practically a straight line indicating that \bar{p}_M is a linear function of M as expected. The slight curvature is to be ascribed to the influence of the frequency term. A most important characteristic of the curve is that it practically passes through the origin so that \bar{p}_M must be proportional to M . This definitely excludes the series of values $p_M = 2, 4, 6, \dots$.

For the vibration-rotation bands the summation rule leads to the same type of intensity variation for the choice of weights $p_M = 1, 3, 5, \dots$, as.

²⁵ Discussion under summation rule.

²⁶ The new quantum theory by admitting the state $m=0$ and integral rotational quantum numbers seems to require this choice also.

does Kemble's theory. For other choices however it may easily be verified¹⁵ that alternating intensities are prescribed.²⁷

Absolute intensities and transition probabilities. The absolute values of the absorption coefficients are given in Table II. Method I was used to yield absolute values of the coefficients for all lines in the positive branch, while

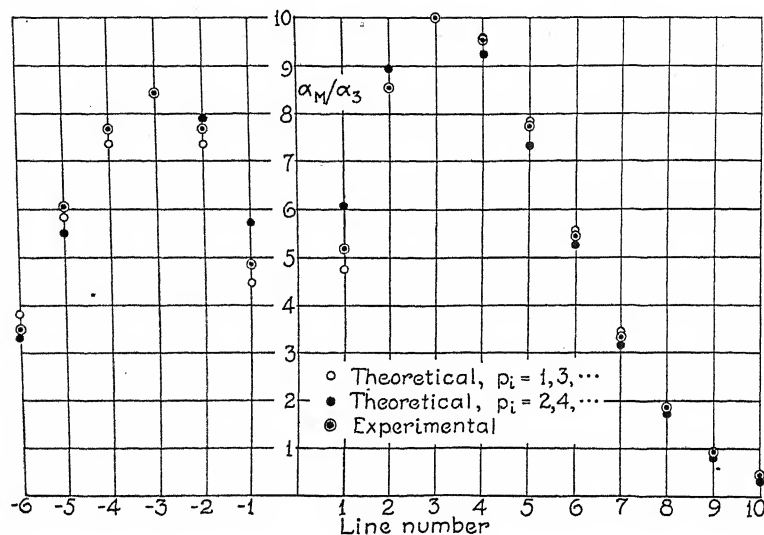


Fig. 7. Comparison of theory and experiment.

the other methods were used for the calculation of the single value for the line $M=3$. The best values of the absolute intensities,²⁸ namely those in the last column of the table were obtained by using the average value of α_3 as given by the methods listed in conjunction with the relative values derived from the ratio plots.

An important application of the data concerns itself with the Einstein probability-of-transition coefficients. It has often been shown that the integrated coefficient of absorption may be expressed in the form

$$\alpha_M = h\nu_M N_i B_{if}/c \quad (18)$$

where the subscripts i and f refer to the initial and final states, B_{if} is the Einstein coefficient of forced transition, ν_M is the frequency associated with

²⁷ If the HCl lines are unresolved doublets and not singlets as ordinarily supposed, it may be shown that the summation rule replaces \bar{p}_M by the sum $\bar{p}_M + \bar{p}_{M+1}$. The experimental data are therefore also in keeping with the assumption of a doublet line structure with the statistical weight series $\bar{p}_M = 2, 4, 6, \dots$, since the summation rule predicts the set of \bar{p}_M values $\bar{p}_M = 2, 2, 4, 4, \dots$ with this choice of \bar{p}_M . Mulliken's work on the correlation of the number of electrons in the molecule and the type of spectroscopic multiplet emitted (or absorbed) suggests a singlet structure in the HCl band spectrum.

²⁸ Tolman's estimates²⁹ are based on Imes' curves for a single tube length and are quite out of accord with the present results.

the transition $i \rightarrow f$ and N_i is the number of molecules in the state i . On evaluating N_i there is obtained after inverting formula (18)

$$B_{i,f} = \frac{\alpha_M c e^{W_i/kT} 8\pi I k T}{\nu_M \bar{p}_i N h} \quad (19)$$

The well known relation between the coefficients of forced and spontaneous transitions may be written

$$A_{f,i} = \frac{8\pi \hbar v^3 \bar{p}_i B_{i,f}}{c^3 \bar{p}_f} \quad (20)$$

where $A_{f,i}$ is the coefficient of spontaneous transition and the other terms have the meanings attached previously. On combining Eq. (19) and Eq. (20) there results the following expression for calculating $A_{f,i}$ from the data.

$$A_{f,i} = \frac{(8\pi \nu_{i,f})^2 e^{W_i/kT} k I T \alpha_M}{c^2 \bar{p}_f N h^2}$$

Reference to Eq. (2) shows that neglecting frequency terms, $B_{i,f}$ and $A_{i,f}$ vary as \bar{p}_M/\bar{p}_i . The salient features of the dependence of the coefficients on line number are (a) the comparatively slight difference in value of the coefficients for various lines, (b) the identity of the limiting values of the two types of coefficients for the P and R branches. Conclusion (b) is subject to modification because of neglected frequency terms. $B_{i,f}$ is expected to vary with the inverse 4th power of the frequency and $A_{f,i}$ with the inverse first power.

The values²⁹ $B_{0,1} = 5.12 \times 10^{15}$ and $A_{0,1} = 58$, associated with the lines $M = 1$ and $M = -1$ respectively, were calculated from formulas (19) and (20.1). The value of $A_{0,1}$ (and the values of $A_{f,i}$ which may readily be calculated from it) are about ten times those of Tolman;²³ however even the values given here are rather smaller than might at first be expected. The low values appear to have given Professor Tolman³⁰ some concern at the time but are really bona fide and in harmony with the predictions of the correspondence principle, as will appear incidentally in the following discussion of the effective ionic charge.

Since the absolute intensities of the lines are determined by the variation in the electric moment which accompanies the vibration, the amplitude of the electric moment variation can be determined from the absolute absorption coefficients.

²⁹ The subscripts on the Einstein coefficients refer to the rotational quantum numbers for the states involved.

³⁰ The wide range of values of $A_{f,i}$; obtained by Tolman is due to his erroneous values for α_M . Several of his conclusions are therefore to be modified and certain of his laws may obviously be made more precise in view of the substantiation of eq. (2).

The electric moment denoted by $\bar{p}(r)$ differs in value from the product of the nuclear separation and the charge on an electron because of the distortion of the Cl ion's symmetrical electronic configuration due to the presence of the H nucleus. The immediate object of this part of the paper will be to correlate the disturbing effect of the H ion with the distance apart of the nuclei. The calculation will first be carried through on the basis of the older form of quantum theory and as a first step the correspondence principle value for A_{01} is written³¹

$$A_{01} = \frac{16\pi^4\nu_{01}^3}{3hc^3} \bar{R}_{01}^2 \frac{\bar{p}_M}{\bar{p}_m} \quad (21)$$

where \bar{R}_{01}^2 is a certain mean square value of the Fourier series component of the variable electric moment $\bar{p}(r)$ associated with the transition giving rise to the line $M=-1$.

It may easily be shown that A_{01} is practically equal to the coefficient of spontaneous transition for a linear oscillator and that the effect of the rotational motion is very slight in modifying the value of R as calculated for the vibrational motion alone.

Practically all the usual methods of taking the average of R_{01}^2 for the linear oscillator as required in Eq. (21) lead to nearly the result

$$\bar{R}_{01}^2 = \frac{1}{2} R_{n=1}^2 \quad (22)$$

$$\text{or } = R_{n=1}^2 \quad (22.1)$$

where the assumption made for (22) is that the zero vibrational state is the initial state whereas the calculation for (22.1) supposes that the state $n=\frac{1}{2}$

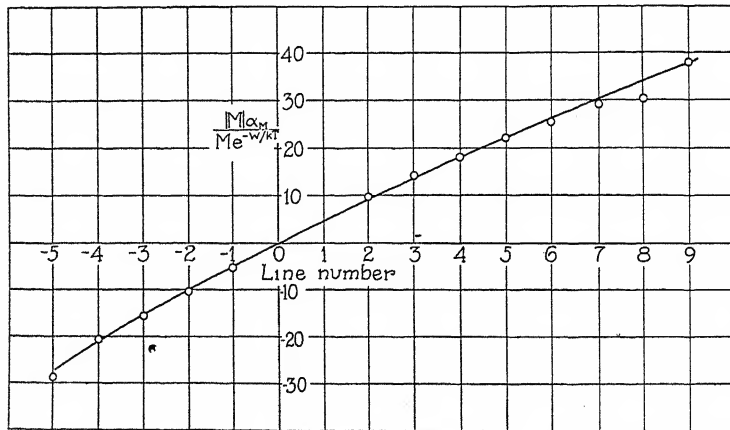


Fig. 8. Test of statistical weight choices.

is the lowest. The new formulation of the quantum theory leads to the relation $\bar{R}_{01}^2 = R_{n=1}^2$.

³¹ Cf. p. 811 for the presence of the factor $\bar{p}_M/\bar{p}_m = 2$.

The analysis of the line spacing and position in the HCl bands yields the value³³ $r_0 = 1.28 \times 10^{-8}$ cm for the equilibrium separation of³² the nuclei and $\delta = 0.12r_0$ for the amplitude of vibration about the equilibrium position for one quantum of vibrational energy.

Neglecting the contribution of harmonic terms the value of $R_{n=1}$ is $(dp/dr)_{r=r_0}\delta$. The simultaneous solution of Eqs. (21) and (22) leads to an expression for $(dp(r)/dr)_{r=r_0}$ in terms of known constants. On defining the "effective charge" as $q = p(r)/r$ one may write $(dp/dr)_{r=r_0}$ as $q_0 + (dq/dr)_{r=r_0} r_0$.

Zahn's³³ data for the dielectric constant of HCl yields values of $p(r)$ when substituted into expressions correlating the value of the dielectric constant and electric moment. The assumption that all the dipoles are similar and oriented at random leads to the Debye³⁴ formula. Pauli³⁵ and Pauling³⁶ have treated the problem on the assumption of a space quantization assuming integral and half integral rotational quantum numbers respectively. The new quantum theory reproduces the values of the constants occurring in the classical Debye formula.

At ordinary temperatures nearly all the molecules are in the lowest vibrational state. The Debye equation, or the modifications mentioned, when applied to Zahn's data yield the value $\bar{p}(r) = q_0 r_0$ even if one half quantum of vibrational energy is assumed for the lowest state. It is therefore possible to estimate $(dq/dr)_{r=r_0}$ by combining Zahn's value of $q_0 r_0$ with $(dp(r)/dr)_{r=r_0}$ as calculated in this paper. Table IV contains the values of q_0 and $(dq/dr)_{r=r_0}$ calculated on the basis of the several theoretical variants mentioned.

TABLE IV

Calculation of q_0 and $(dq/dr)_{r=r_0}$

Entries under the headings N or I are calculated under the assumption of half integral vibrational quantum numbers for the first and integral values for the last.

	Classical and new quantum theory		Pauli theory		Pauling theory	
Apparent charge q_0 (Calculated from C. T. Zahn's data)		0.818×10^{-10}		$.300 \times 10^{-10}$		$.261 \times 10^{-10}$
$(dp(r)/dr)_{r=r_0} \times 10^{10}$	N	I	N	I	N	I
$(dq(r)/dr)_{r=r_0} \times 10^2$	0.828	1.17	0.828	1.17	0.828	1.17
$q_0/r_0 \times 10^2$	0.008	0.196	0.414	0.679	0.442	0.71
	0.646	0.646	0.237	0.237	0.206	0.206

With the exception of the classical theory estimates and those depending on the new quantum theory it appears that the ratio $(dq/dr)_{r=r_0}:q_0/r_0$ is greater than 1 (Table IV). If the older form of the quantum theory be adhered to, the inference would be that somewhere near the origin the effective

³² E. C. Kemble, Jour. Opt. Soc. **12**, 1 (1926).

³³ C. T. Zahn, Phys. Rev. **4**, 400 (1924).

³⁴ P. Debye, Phys. Zeits. **13**, 97 (1912).

³⁵ W. Pauli, Zeits. f. Physik **6**, 139 (1921).

³⁶ L. Pauling, Proc. Nat. Acad. Sci. **12**, 32 (1926).

charge vs. nuclear separation curve is convex to the nuclear separation axis³⁷ or from another point of view that the formal continuation of the $q(r), r$ curve past the equilibrium point would intersect the $r=0$ axis below the $q(r)=0$ line. Consideration of simple models would suggest a positive value for the ordinate of the intersection point. The results seem, therefore, to be in harmony with the new rather than with the old quantum theory.³⁸

The writer wishes to thank Professor Lyman, Professor Pierce and Professor Chaffee for their kindness in placing the facilities of the Jefferson and Cruft Laboratories at his disposal and also to note his appreciation of the helpful advice of members of the Harvard faculty of Physics and Professor Bennett of Lehigh University. He is under special obligations to Professor Kemble who interested him in this subject and contributed many valuable suggestions.

JEFFERSON PHYSICAL LABORATORY,
HARVARD UNIVERSITY.
September 21, 1926.

Note added in proof, April 21, 1927.—In the interim since this paper was presented for publication the emphasis in modern physics has changed somewhat; so that references to the new quantum theory are to be interpreted in terms of 'wave' rather than 'matrix' bases. None of the conclusions of this paper are modified by this change in point of view.

³⁷ Since $q(r) = 0$ for $r = 0$.

³⁸ The results are in keeping also with the classical theory or with the assumption that the space orientation predicted by the older quantum theories is incomplete for small fields because of the disturbing influence of molecular collision though the last interpretation is not too plausible.

RELATIVE INTENSITIES OF SOME LINES IN THE MERCURY SPECTRUM

By JOSEPH VALASEK

ABSTRACT

Intensities of the most intense spectrum lines associated with transitions to and from the $2p_2$ state in mercury were measured by means of a photographic method. The spectrum of the vapor was excited by electron impact above the ionization potential. Variations in the line intensities due to changes in the accelerating potentials and vapor pressures were observed. At 22°C and with 50 volt electrons, there were about 1.7×10^{12} quanta of $\lambda 2537$ radiation emitted per cubic centimeter per second for a current density of 4.75×10^{15} electrons per square centimeter per second. From the intensities of the other lines relative to $\lambda 2537$, it was found that there are apparently more transitions to $2p_2$ than down from $2p_2$, as given by measurements of the radiation. This made it impossible to determine the probability of excitation of resonance from the intensities of the spectrum lines. A comparison is made between the relative intensities in the experimental tube and in a commercial arc.

THIS work was undertaken for the purpose of obtaining a measurement of the intensities of some of the lines in the mercury spectrum, using different electron speeds and vapor pressures. Lines associated with transitions to and from the $2p_2$ state were chosen with the original intention of obtaining a measure of the excitation of this state. A summary of the technique of line intensity measurements has lately been given by Dorgelo,¹ while the theory of the intensities of spectral lines has been recently discussed by Bartels.² In the latter paper it is shown how the intensities of emission lines depend on both the distribution of the various Einstein probabilities of emission and the relative probabilities of excitation of the various states from without the atom. This makes the intensity relations of emission lines difficult to interpret theoretically until one of these sets of probability coefficients is known. However, as suggested by Bartels, one might expect that the probability of excitation of the first resonance level could be obtained by measuring the intensities of lines emitted by transitions to and from this state and comparing the number of transitions to the resonance level with the number obtained from the intensity of the resonance line.

A diagram showing the disposition of the more essential parts in the tube used is given in Fig. 1. The grid G was close to the filament F , so that most of the collisions took place in the space between the grid and the plate P , which were kept at the same potential. The source of electrons was an oxide coating on a platinum surface which was heated by a tungsten filament. The latter was insulated from the platinum except at one end where they

¹ Dorgelo, Phys. Zeits., 26, 756, (1925).

² Bartels, Zeits. f. Physik 37, 35 (1926).

were connected together. Various accelerating potentials were applied between the platinum sheath and the grid by means of a potentiometer device. The grid and the plate were coated with soot to reduce the number of secondary electrons. The plate current was kept constant at 5 milliamperes throughout the series of observations recorded here. An electric heater wound around the tube made it possible to vary the pressure of the mercury contained inside. The radiation was transmitted to the spectrograph by a re-entrant quartz window Q , 1.28 cm in diameter, and sufficiently off the axis of the cylinder to be out of line with the filament. The window darkened because of a sputtered deposit as the tube was operated, but this effect was corrected for by repeating some of the exposures after a definite interval of time. A sooted nickel surface B , 3.2 cm behind the quartz window, served

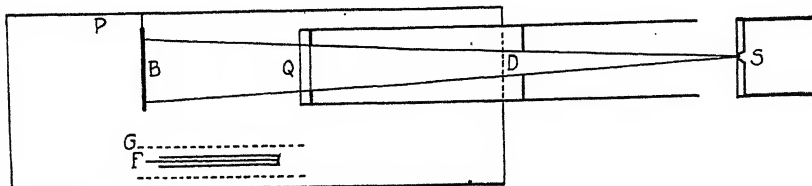


Fig. 1. Diagram of the experimental tube.

as a background. A diaphragm D kept the light reflected from the cylindrical surface from reaching the slit of the spectrograph at S . Since it has been found by R. W. Wood, that mercury vapor even at room temperature absorbs $\lambda 2537$ quite strongly, the room and spectrograph were ventilated, but this did not seem to produce any appreciable change in the results.

Since most of the lines were in the ultra-violet, the intensities of the spectrum lines were measured by a photographic method. The photographic density of each line was measured with a Moll (thermoelectric) microphotometer. The density is defined as the common logarithm of the ratio of the intensity of the light transmitted by an unblackened portion of the plate adjacent to the line, to the intensity of the light transmitted by the blackened portion. In making the exposures, the slit of the spectrograph was made wide enough so that the center of each line was blackened uniformly over a width greater than that of the microphotometer beam. A series of four or five exposures was made for each voltage and temperature. These were for two different times of exposure (either ten and one hundred seconds, or one hundred and one thousand seconds), with and without blackened calibrated wire screens interposed. The transmission factors of the screens used were measured photometrically and also with a Hilger selenium cell. It was assumed that their transmissions were non-selective over the range used.

The relation of the photographic density, D , to the common logarithm of the intensity, $\log I$, is given by the familiar Hurter-Driffield curve, which is straight over a fairly wide range of densities. The straight line is defined by

means of its slope, called the contrast, γ , and the intercept on the log intensity axis which is called the log inertia. The reciprocal of the inertia is called the speed, σ . We have then:

$$\log I = D/\gamma - \log \sigma$$

This formula applies only to the straight region of the characteristic curve, and it is simplest to discard all readings that are too light or too dense to be included in this region. For dim lines, a longer exposure must be given and a different pair of values of γ and σ must be used. Harrison³ has published values of γ and σ for a number of emulsions for exposures of ten seconds, and for wave-lengths between 4360 and 2144A. From these it is easy empirically to obtain values of these constants for other times of exposure by the use of the calibrated wire screens. Thus no assumption is made regarding the validity of the reciprocity law or of Schwartzchild's law. However, it is best not to rely on these published values too much, for variations may occur in development or in the emulsion itself. Of the two constants, it is the more important to know the value of gamma accurately and it is, fortunately, easy to measure gamma for each plate by the use of a few calibrated wire screens. To obtain $\log \sigma$, on the other hand, is not so easy for its measurement necessitates a set of standard spectrum lines of known intensities. However, if the variation of $\log \sigma$ with wave-length is known, a slight error in its value introduces an error of the same percentage in all the measurements. This will not affect the relative intensities. In calculating the results here presented, Harrison's values of $\log \sigma$ for ten seconds exposure were used, but the values of gamma and $\log \sigma$ for other times of exposure were independently determined for each plate. The plates were developed for five minutes at 21°C in the following developer:

Distilled water	2300	grams	Hydrochinon	12.9	grams
Elon	3.2	"	Potassium bromide	1.84	"
Sodium sulphite	48.7	"	Sodium carbonate	69.0	"

When used, the developer was diluted with three volumes of distilled water to one of developer. The stock solution will keep for several months when kept in a well stoppered bottle.

From the intensities of the lines, one can immediately find how many quanta of each frequency strike the plate per unit area per second. From the light losses in the instrument and the areas of the images and of the slit, one can calculate how many quanta enter the spectrograph per second. Assuming that the fraction of the total number of emissions entering the slit is proportional to the solid angle subtended by the slit, and knowing the portion of the glow which will be within the angular aperture of the instrument, one can calculate the average number of transitions of each kind per cubic centimeter of glow. The factor for converting intensities in quanta per square centimeter of photographic plate to the number of emissions per cubic centimeter of the glow was found to be 2.2×10^3 .

³ Harrison, J.O.S.A. & R.S.I., 11, 341, (1925).

The relative number of transitions per cubic centimeter per second as compared with the number for $\lambda 2537$ is plotted in Figs. 2(a) and 2(b) against, respectively, the temperature of the vapor and the accelerating voltage.

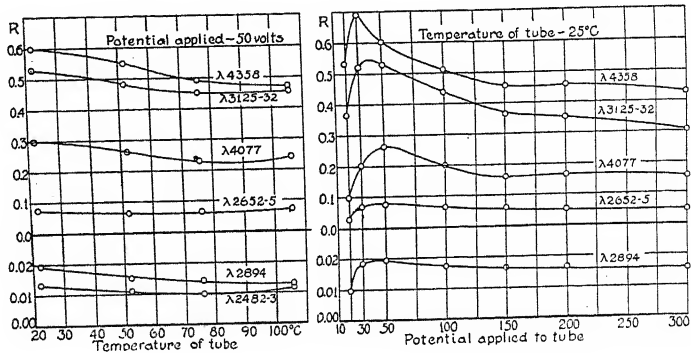


Fig. 2. Numbers of emissions relative to the number for $\lambda 2537$, (a) Variation with temperature of the vapor; (b) Variation with accelerating potential.

There are no marked changes in the intensities of the lines relative to $\lambda 2537$ under the conditions of these experiments except at the lower voltages.

The intensity of $\lambda 2537$ is plotted in Fig. 3 against the same variables. These curves are, of course, not as accurate as those of relative intensities; still they will serve to give the order of magnitude of the intensities and the

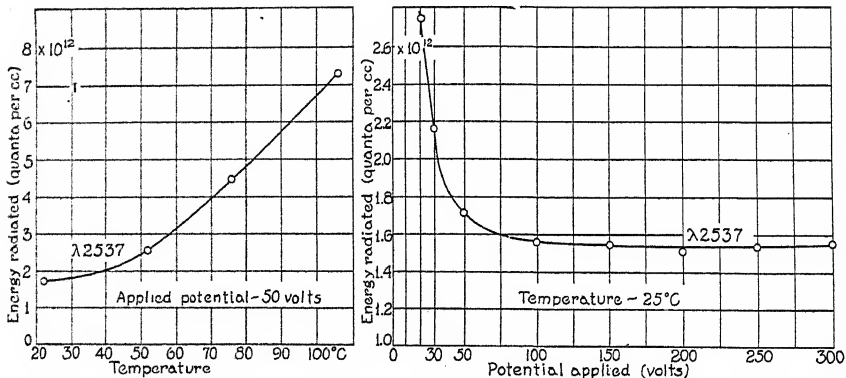


Fig. 3. Number of emissions per cubic centimeter for $\lambda 2537$, (a) Variation with temperature of the vapor; (b) Variation with accelerating potential.

manner of variation with voltage and temperature. These changes are of the general nature that one would expect. The average current density through the region of the glow photographed was 4.75×10^{15} electrons per square centimeter per second, as measured by a cage having a cross-section equal to that of the glow.

The intensities of the same lines emitted by a commercial "Lab-arc" were also measured. The relative intensities are entirely different from those

in the experimental tube. Table I gives a comparison of these two spectra in terms of the relative number of emissions compared to the number for $\lambda 2537$.

TABLE I
Comparison of relative number of emissions.

Wave-length	Notation	"Lab-arc"	Exper. Tube 50v.
4358	$2p_2 - 2s$	8.9	0.60
4078	$2p_2 - 2S$	0.76	0.30
3126-32 sum	$2p_2 - 3Dd_{23}$	3.61	0.53
2894	$2p_2 - 3s$	0.11	0.02
2652-5 sum	$2p_2 - 4Dd_{23}$	0.91	0.07
2537	$1S - 2p_2$	1.00	1.00
2482-3 sum	$2p_2 - 5Dd_{23}$	0.21	0.01

The data show that there are apparently more transitions to $2p_2$ than from it, at least when one considers only the transitions giving rise to radiation. Therefore it is not possible with either type of source to determine the "external excitation" probability of the $2p_2$ state by taking the difference between the number of transitions from that state and the number to that state as suggested by Bartels. Apparently there are many radiationless transfers down from $2p_2$. The very high current densities in the lab-arc would then be expected to enhance the subordinate series lines as compared with the resonance line.

UNIVERSITY OF MINNESOTA
DEPARTMENT OF PHYSICS
March, 1927.

PROBABILITY OF IONIZATION OF MERCURY VAPOR BY
ELECTRON IMPACT

By T. J. JONES*

ABSTRACT

Electrons from a hot filament were projected into an ionization chamber A containing mercury vapor, and were prevented from scattering by a magnetic field of 400 gauss parallel to the electron beam. The positive ions produced in a definite length of A were collected on a plate electrode while the primary electrons after passing through A were collected by a special form of Faraday cylinder. The resulting curve for N , the number of positive charges produced in 1 cm path by an electron moving through the vapor at 1 mm pressure as a function of the electron energy in volts is given. This curve, in good agreement with that obtained by Compton and Van Voorhis for mercury vapor, shows a maximum value of 20.5 at 90 volts. The values of P , the average number of positive charges formed at an impact, were then calculated from N by the relation $P = N\lambda$ where λ is the electronic mean free path. Assuming the kinetic theory value for λ the curve for P shows a maximum value of 0.35 at 90 volts, agreeing well with the value 0.32 at 100 volts calculated similarly by Compton and Van Voorhis. However, when the values of λ obtained by direct experiment are employed, the curve for P shows no indication of reaching a maximum. At 400 volts, P has a value of about 1 and the curve indicates values greater than 1 at higher voltages. Since the probability of ionization at an impact cannot be greater than unity, the assumptions made in evaluating this quantity have been examined more closely.

Such consideration indicates that the assumption that only singly charged ions are produced at an impact is invalid—a view that is supported by the experiments of Smyth. If, as seems reasonable from his experiments, it is assumed that at 400 volts doubly charged and singly charged ions are produced in equal amounts; the present results show that at this voltage the probability of ionization at an impact is about 0.6 while the probabilities of formation of double ions and of single ions are both about 0.3. These results indicate that the values of the probability of ionization at an impact, obtained by former workers for other gases, may also require modification because of the possible formation of multiple ions.

THE probability of ionization in gases by electron impact, as a function of the energy of the impacting electrons, has been examined by a number of investigators^{1,2,3} and it has been shown that the probability of an electron's ionizing an atom is not constant but rises from zero when the electron has less than the ionizing energy, to a maximum value when it has some energy higher than the ionizing energy. In all the gases investigated, this maximum value of the probability is less than 0.5 and occurs when the electron energy is equivalent to about 200 volts.

* Commonwealth Fellow.

¹ Hughes and Klein, Phys. Rev. 23 pp. 111, 450, (1924).

² W. P. Jesse, Phys. Rev. 26, p. 208, (1925).

³ K. T. Compton and C. C. Van Voorhis, Phys. Rev. 26, p. 436, (1925) and 27, p. 724 (1926).

K. T. Compton and C. C. Van Voorhis³ included mercury vapor among the gases examined by them, and found that in this case the probability of ionization at a collision had a maximum value of 0.31 when the electron energy was 100 volts. The subject was deemed of sufficient importance to merit further study by a different experimental method. This paper contains an account of such an investigation on mercury vapor.

EXPERIMENTAL ARRANGEMENT AND PROCEDURE

The experimental arrangement differed considerably from that of Compton and Van Voorhis. The general method employed was to project a stream of approximately stream of electrons of approximately homogeneous velocity along the axis of a tube into a region devoid of strong electric fields and to collect the electrons and the ions produced by them on a system of electrodes. The electron stream was prevented from scattering by a magnetic field applied parallel to the axis of the tube. Compton and Van Voorhis found that when they tried to use a magnetic field in this way the ratio of the positive ion current I_+ to the electron current I_- was very irregular, being affected by small variations in the magnetic field. As they failed to eliminate or to account for these variations they abandoned the use of the magnetic field. During the course of the present work this effect of the magnetic field was experienced, but after a number of preliminary trials with different experimental arrangements the trouble was found to be due to secondary electrons and was eliminated.

The apparatus employed together with the electrical connections used in making the measurements are shown in Fig. 1. The filament F , consisted of a small loop of tungsten wire just projecting through a small hole (diameter

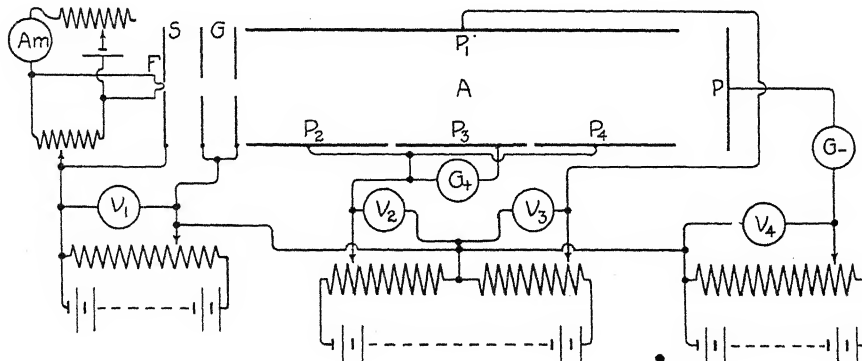


Fig. 1. Diagrammatic sketch of the tube and electrical connections.

2 mm) in the earthed plate S . The middle point of the filament was also earthed by connecting the two ends to a high resistance and earthing an intermediate point. This arrangement served to maintain an almost uniform field V_a between F and the grids G . Electrons from F were accelerated by V_1 through two holes (diameter 4 mm) in the grids into the space A . The

positive ions formed in the region were then collected on the electrodes P_2 , P_3 , P_4 , by applying an electric field between them and P_1 . P_2 , P_3 , and P_4 were separated by thin glass rings. Only the ions formed in the space directly above P_3 are collected on P_3 and pass through the galvanometer G_+ which was used to measure the positive ion current. One reason for adopting this "guard ring" system for the collecting plates was because the holes in the grids G , allowed the accelerating field V_1 to penetrate into the ionization chamber A so that some of the electrons that had passed through the holes would travel some distance in A before attaining their full velocity. Also with this arrangement the positive ions which are measured are produced in a distance traversed by the electrons equal to the length of P_3 , i.e. in a region of definite length.

The plates P_2 , P_3 , P_4 were each 3 cm long and it is reasonable to assume that when the electrons were travelling in the region directly above P_3 they had their full velocity corresponding to V_1 . The plate P served to catch the electrons after they had passed through the ionization chamber. Surrounding the electrode system and insulated from it was a copper sheath connected to G which served to eliminate extraneous surface potentials.

All the metal parts, with the exception of the filament, were of copper and were baked out in a small electric furnace at 450°C. At the same time, all the accessible parts were bombarded with an intense electron stream of 1000 volts velocity. The pressure of the mercury vapor was, throughout the experiment, that corresponding to the temperature of the vapor trap between the pumps and the tube. This trap was kept surrounded by melting ice so that the pressure of the vapor in the tube was 0.0002 mm.⁴ At such a low pressure it was unnecessary to consider any ionization due to multiple collisions.

The temperature inside the ionization chamber was determined in some of the preliminary experiments by placing a thermometer inside the tube, and was found to be about 70°C. This was taken as the temperature in A throughout the various observations.

The experimental procedure was to measure the positive ion current I_+ and the electron current I_- (by noting G_+ and G_-) as V_1 was increased from zero to 400 volts. The electric field between the collecting plates was meanwhile adjusted so that all the ions formed in A were collected. The magnetic field was also of sufficient strength (usually about 300 gauss) to prevent electrons scattered in the gas from reaching the ion collector. The ratio I_+/I_- gives the number of positive charges produced by each electron in traversing a path 3 cm long in the vapor at a pressure of 0.0002 mm and a temperature of 70°C.

Errors. In the experiments there are several possible sources of error. The main difficulty was that experienced in collecting the electrons after they had passed through the ionization chamber. When a beam of electrons impinges on a metal surface secondary electrons are emitted from that surface. For a given metal the number of these secondary electrons is a func-

⁴ A. Smith and A. W. C. Menzies, Ann. d. Physique 33, 979 (1910).

tion of the velocity with which the primary electrons strike the surface and at the higher-voltages may exceed the number of the primaries. Farnsworth⁵ has shown that for copper an appreciable fraction of the secondary electrons have velocities equal to those of the primary electrons. The type of electron collector usually employed is a Faraday cylinder of suitable dimensions. Such a collector was tried without success in the preliminary experiments. A little consideration however, shows that when a magnetic field prevents the electrons from being scattered appreciably, the Faraday cylinder is no longer a complete absorber of electrons.

The arrangement shown in Fig. 1 was tried and it was found that if a suitable electric field V_4 was applied between the ion-collectors and the plate P the number of secondary electrons from P was reduced considerably. For a certain range of values of this field the values of N were almost independent of the strength of the field and this was regarded as an indication that the secondary emission from P under these conditions was small. A further improvement in the arrangement for collecting the electrons was effected by replacing the plate P by a cylinder 14 cm long, closed at one end and having at the other end a hole just large enough to admit the electron stream. Within the cylinder the electrons passed between two copper plates maintained at a potential difference of about 1000 volts. With this arrangement the values of N were quite independent of the strength of the field between the plates when this exceeded a certain value. This could only mean that the cylinder was behaving as a complete absorber of the incoming electrons. The results given in the curves were obtained with this form of collector.

In order to ensure that all the ions formed in A were collected it was found necessary to maintain a potential difference as large as 4 volts between the collecting electrodes. This field could not appreciably affect the motion of the primary electrons as its direction was everywhere perpendicular to that motion. The potentials of the collecting electrodes were always varied in such a way that the potential along the axis of the ionization chamber was the same as that of the accelerating grids, i.e. V_1 .

Charging of the collecting electrodes by photo-electric action arising from the incidence of radiation excited in the mercury vapor was prevented by the magnetic field.

The velocity distribution of the primary electrons was not determined but it is reasonable to assume that nearly all of the electrons had velocities close to the velocity corresponding to V_a .

Slow electrons in the primary beam are usually secondary electrons coming from those metal parts, such as grid-wires, which are struck by the primary electrons. The present arrangement of the accelerating grids and the use of the magnetic field enable the electrons to enter A without having struck any metal parts on their way.

⁵ Farnsworth, Phys. Rev. 25, 41 (1925).

EXPERIMENTAL RESULTS AND DISCUSSION

The results of the observations are presented in the curves of Figs. 2 and 3. In order to be able to compare them directly with those of Compton and Van Voorhis the ratio I_+/I_- was divided by the pressure in mm and by the length of the electron path in cm. This gives the number of positive charges N which would be produced by each electron in traversing a path 1 cm long in mercury vapor at 1 mm pressure. If one were at liberty to assume, as

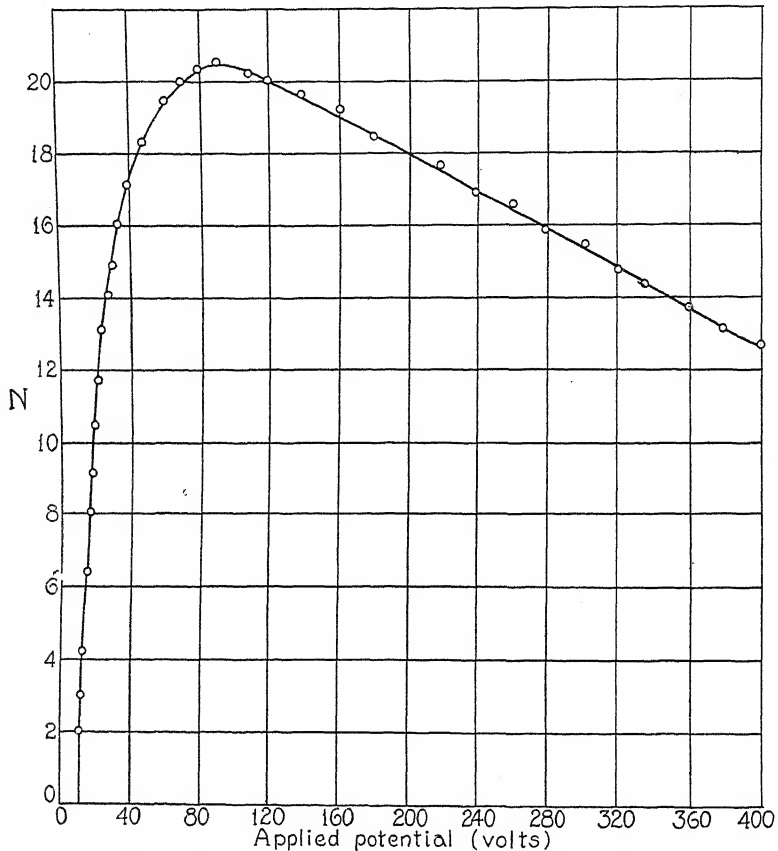


Fig. 2. Curve showing the variation with potential of the number of unit positive charges formed by each electron in traversing one centimeter path in mercury vapor at 1 mm pressure.

has tacitly been done by all other investigators in this field, that the positive ions are all singly charged, N would be equal to the number of positive ions formed by each electron under the above conditions. That the assumption is not justified, particularly at the higher electron velocities, is shown by the observations of Smyth⁶ on the formation of multiple ions in mercury vapor and is made further apparent by an analysis of the results of the present experiment. Fig. 2 gives the values obtained for N as a function of the

⁶ Smyth, Roy. Soc. Proc. A102, 283 (1922).

electron energy in volts. It is seen that N has a maximum value of 20.5 at 90 volts. This value for which N is a maximum together with the voltage at which it occurs agree very well with the values obtained by Compton and Van Voorhis, viz. 21.3 at 100 volts. The temperature of the chamber A was, in their case, 51°C and the difference between that temperature and the temperature in the present experiment is sufficient to account for almost all the difference in the value of the maximum N . After passing its maximum value the curve in Fig. 2 drops almost linearly and more rapidly than in the curve obtained by Compton and Van Voorhis.

If the values of N are divided by the number of collisions n , made in 1 cm. path by an electron moving through the vapor at 1 mm pressure, the average number P , of positive charges formed per electron impact, is obtained. If the ions were all singly charged P would be the probability of ionization at an impact. The number of collisions, n , is evidently the reciprocal of the electronic mean free path λ , so that $P = N\lambda$. The precise significance of P depends upon the choice of values for λ . If the kinetic theory value of λ is taken, P represents the average number of positive charges formed by each electron when the apsidal distance of its path from the center of an atom is less than the kinetic theory value of the radius of the atom. Compton and Van Voorhis assumed the kinetic theory value of λ in calculating P . The kinetic theory value of λ is $4\sqrt{2}$ times that of the mean free path of the gas molecules and for mercury vapor at a pressure of 1 mm, and at 70°C is 0.0174 cm. The values of P shown in curve 1, Fig. 3, were obtained by multiplying the values of N in Fig. 2 by this kinetic theory values of λ . P is seen to have a maximum value of 0.35 at 90 volts which compares well with the maximum value of 0.32 at 100 volts obtained by Compton and Van Voorhis.

If one takes for λ the values obtained experimentally by Brode⁷ and Maxwell,⁸ P would represent the average number of positive charges formed by each electron which is deflected appreciably from its rectilinear path. Curve 2, Fig. 3, gives the values of P obtained when Maxwell's values of λ are used. P continues to increase up to the highest voltages and shows no sign of approaching a maximum. At 400 volts P has the value 1 and the curve indicates that at still higher voltages P would have values greater than 1. Brode's values of λ are much greater than those of Maxwell; at 100 volts his value of λ is more than three times as great as the value obtained by Maxwell at that voltage. This would make P greater than 1 even at 100 volts. Maxwell, however, has shown that Brode's values are certainly too large.

Under the assumption that the ions are all singly charged, values of P greater than unity would be meaningless and would throw suspicion on the values of λ used in the calculations. In their determinations of the electronic mean free paths in mercury vapor, Maxwell and Brode consider a collision as a deflection of the electron through an angle greater than

⁷ Brode, Roy. Soc. Proc. A109, 397 (1925).

⁸ Maxwell, Proc. Nat. Ac. Sci. 12, 509 (1926).

some arbitrary critical angle, whereas in experiments on ionization a collision would be more completely defined as a process in which the colliding electron is deflected from its path or loses energy (possibly without appreciable deflection). Thus the values of λ obtained by these workers may not be appropriate for the evaluation of P . More appropriate values would

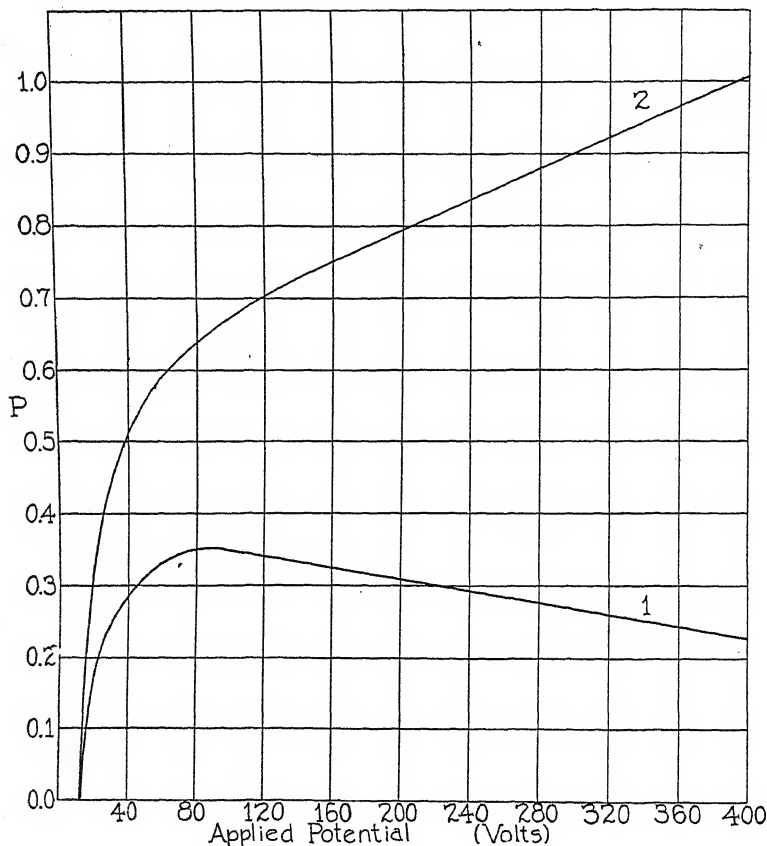


Fig. 3. Curve 1 shows the average number of unit positive charges formed by each electron in traversing a distance equal to the kinetic theory value of its mean free path. Curve 2, shows the average number of unit positive charges formed by each electron in traversing a distance equal to the mean free path as determined by Maxwell.

be those obtained by the method of Ramsauer⁹ in which either a deflection or a loss in energy or both is counted as an impact. Unfortunately no measurements by this method have been made for mercury vapor. However, mean free paths which have been obtained by both methods on the same gas indicate that, in the range of velocities used in the present experiment, there is no appreciable difference between them. In other words the chance that an electron loses energy without appreciable deflection is small.

⁹ Ramsauer, Jahrb. Rad. u. Elek. 19, 345 (1923).

It may also be pointed out that if the values of λ in nitrogen and in argon obtained by Brode,¹⁰ using the Ramsauer method, are used to calculate P from the values of N obtained for these gases by Compton and Van Voorhis, P at 325 volts for both argon and nitrogen is about 1.8.

It is therefore probable that the abnormal values of P cannot be accounted for on mean free paths considerations alone. It remains to consider N , the factor other than λ used in calculating P . In regarding P as the probability of ionization at an impact we have assumed that all the ions are singly charged. This assumption, as we have seen, leads to meaningless values of P and consequently we are forced to give up the assumption that all the ions are singly charged.

H. D. Smyth⁶ has investigated the formation of multiple ions in mercury vapor. His results show that double ions begin to be formed when the impacting electrons have energies corresponding to 20 volts. At the higher voltages (up to 300 volts) the curves show as many double ions as single and it is believed that the majority of these double ions were produced by single impact. Evidence was also obtained of the formation of triple ions.

If, in the present experiment, it be assumed that only single and double ions are produced and that at the higher voltages these are produced in equal amounts, it is readily seen that the number of positive ions formed by an electron at these voltages would be two-thirds of the corresponding values of N shown in Fig. 2., and the values of the probabilities of ionization in Fig. 3, would be correspondingly decreased. These reduced values of the probability would then be regarded as giving the sum of the probabilities of the formation of single and of double ions, so that at 400 volts the probability of formation of single ions would be about 0.3. It is also probable that the values of P obtained by previous workers for gases other than mercury vapor may also require modification in view of the possible formation of multiple ions. It seems best to postpone any further discussion or speculation suggested by these results until further data are available both on the nature of the collision between electron and atom and also on the formation of multiple ions.

It is a pleasure to acknowledge my indebtedness to Professor John T. Tate who suggested the problem together with the general method of attacking it, and also rendered valuable assistance in overcoming some of the difficulties encountered. The work has been done while the author was a Commonwealth Fellow.

PHYSICS LABORATORY,
UNIVERSITY OF MINNESOTA,
March 30, 1927.

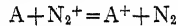
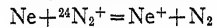
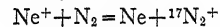
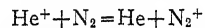
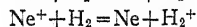
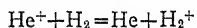
¹⁰ Brode, Phys. Rev. 25, 5 (1925).

IONIZATION BY COLLISIONS OF THE SECOND KIND IN
MIXTURES OF HYDROGEN AND NITROGEN
WITH THE RARE GASES

BY GAYLORD P. HARNWELL

ABSTRACT

The effect of the presence of a rare gas in ionized hydrogen and nitrogen was studied by means of a positive ray analysis of the products of ionization. The variation with pressure of the types of ions found was investigated in some detail for both hydrogen and nitrogen in the presence separately of helium, neon and argon. In all of the mixtures studied the evidence tends to support the view that a type of collision of the second kind takes place at which an atom is ionized by colliding with an ion of an atom of higher ionizing potential. Thus at high pressures corresponding to a large number of collisions the equilibrium is displaced in favor of the atom of lower ionizing potential. The following equations can be predicted from a knowledge of the ionizing potentials and they are all supported by the experimental evidence obtained:



Where ${}^{17}\text{N}_2^+$ and ${}^{24}\text{N}_2^+$ represent respectively the nitrogen ions produced at the expense of seventeen and twenty-four volts.

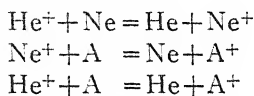
The situation for nitrogen is seen to be more complicated than that for hydrogen. In the latter case the evidence shows that the equations listed above are in the order of increasing probability. This tends to support the view that the probability of the transfer's occurring is an inverse function of the difference in ionizing potentials. The phenomena can not be interpreted as accurately in the case of nitrogen. However, the formation of ${}^{24}\text{N}_2^+$ by Ne^+ (24.5) was found to be the most probable of all the processes occurring in nitrogen and the results obtained with the other rare gases as far as they can be interpreted are also in accord with this view.

THE work forming the substance of this paper is a continuation of an investigation undertaken to detect any evidence for ionization at collisions of the second kind in mixtures of the rare gases.¹ A very short résumé of the previous results and the mechanism suggested to account for them will serve as an introduction to the rather more complicated situations found to exist in mixtures of the rare gases with hydrogen and nitrogen. The positive ray apparatus was the same as that used in the previous experiments. It was described in detail in the paper cited, so here it will be necessary only to outline the method of investigation employed.

In a partially ionized mixture of two monatomic gases there will be three general types of collisions taking place: atoms will collide with atoms, atoms will collide with ions, and ions will collide with ions. The second type of collision may be divided into two classes: an ion may collide with an atom

¹ Gaylord P. Harnwell, Phys. Rev. 29, 683 (May 1927).

of higher ionizing potential, or an ion may collide with an atom of lower ionizing potential. In the latter case the ion has a greater electron affinity than the atom and there may be a certain probability of an electron being transferred from the atom of small electron affinity to the ion of the atom of large electron affinity. As this interchange would not be reversible the effect of a large number of collisions would be to increase the number of ions of lower ionizing potential at the expense of those of higher ionizing potential. As the number of collisions would be proportional to the pressure, if a curve representing the ratio of the ion of higher ionizing potential to the ion of lower ionizing potential were plotted against the pressure it should commence to drop at a pressure at which the mean free path of an ion was comparable to the dimensions of the apparatus and continue to fall as higher pressures were reached. Also the slope of the curve should be a measure of the probability of the electron transfer outlined above. Mixtures of helium and neon, neon and argon, and of helium and argon were investigated for evidence of this effect and the following equations, given in the order of their probability, account for the results obtained:



Considering these equations from the point of view of the ionizing potentials of the gases it will be seen that the interchange is most probable in the case of helium and neon where the discrepancy between the ionizing potentials is least and least probable in the case of helium and argon whose ionizing potentials are the most widely separated. This is of particular interest by analogy with the thermodynamic argument developed by Klein and Rosseland² for collisions of the second kind between atoms and electrons where it is shown that the probability of an energy transfer is greatest when the energy to be transferred is least. The argument as there given is not absolutely conclusive nor is it strictly applicable to the present conditions but it is of interest in the light of the above results. One further point should be mentioned, namely that the probabilities of ionization of these rare gases as deduced from the experimental curves were in good agreement with the values obtained by K. T. Compton and C. C. Van Voorhis.³

As has been mentioned the apparatus was described in detail in a previous paper.¹ The ions were produced by the usual method of electron bombardment in a region whose pressure could be varied and then drawn into a region of very low pressure and analyzed by a magnetic field. The ion stream was detected by an electrometer and the current taken as a measure of the number of ions of that particular mass emerging from the high pressure region. The analyzing runs were made by varying the accelerating voltage (E_4) for the positive ions. The areas under the peaks obtained by such a run, and plotted on a mass scale ($1/E_4$), were taken as representing the number

² O. Klein and S. Rosseland, Zeits. f. Physik 4, 46 (1921); also Franck, Anregung von Quantensprüngen durch Stöße, Page 210 et seq.

³ Compton and Van Voorhis, Phys. Rev. 27, 74 (June 1926).

of ions of the particular type present in the high pressure region. The variation of this quantity with the pressure existing in the ionizing chamber, as measured by a McLeod Gauge as close to the apparatus as possible, was the relation investigated. As the pressure was increased the area under a peak, when a pure rare gas was in the chamber, increased up to a certain pressure due to the actual increase in the number of ions produced and then decreased showing that some of the ions produced were being scattered from the beam before they could emerge from the high pressure region. Consequently at high pressures the ions reaching the electrometer were mainly those produced near the slit which separated the high from the low pressure regions. At sufficiently high pressures the electrons were not able to ionize close enough to the slit so that any of the positive ions could be drawn out and the area under the peak reduced to zero.

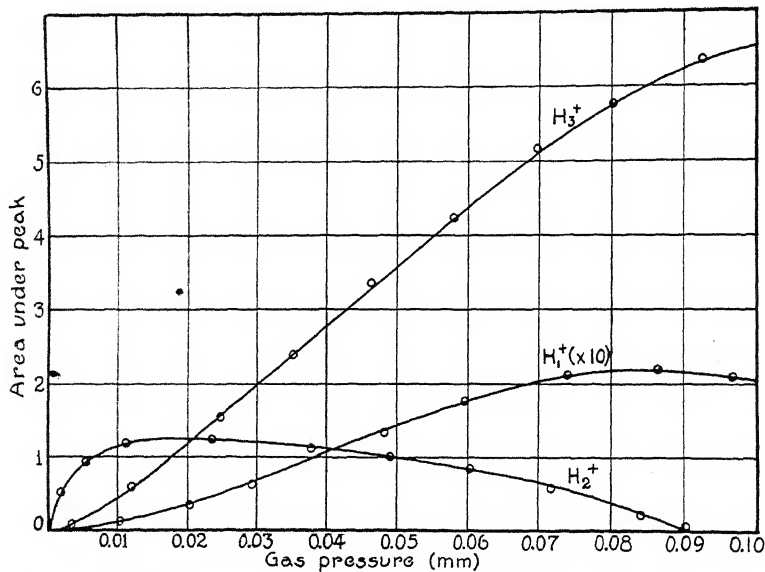


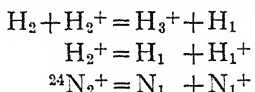
Fig. 1. Effect of pressure on the nature of the positive ion in hydrogen.

In dealing with a diatomic gas the observed phenomena become more complicated as can be seen from Figs. 1 and 2. It is quite well established from the work of H. D. Smyth⁴ and of Hogness and Lunn⁵ in hydrogen and nitrogen that the primary product of ionization is the molecular ion and that such ions as N_1^+ and H_3^+ are formed as a result of a secondary process. Any ionized hydrogen molecule apparently can dissociate, but the case is slightly different for nitrogen. Hogness and Lunn⁵ have shown that two types of N_2^+ exist one having been produced at the expense of twenty-four volts of energy and the other at the expense of seventeen. The former $^{24}N_2^+$ is capable of dissociating into N_1^+ but the latter, $^{17}N_2^+$, is not. Also there

⁴ H. D. Smith, Phys. Rev. 25, 452 (April 1925).

⁵ Hogness and Lunn, Phys. Rev. 26, 44 (1925); 26, 786 (1925).

is very good evidence for believing that H_3^+ is a secondary and not a tertiary product, that is, that the majority of it is produced directly from H_2^+ , and not by way of H_1^+ . The above reactions are represented by these equations:



These equations are well illustrated by Figs. 1 and 2. The primary product would be expected to predominate at low pressures where collisions are very infrequent and to behave in that region very much like a rare gas peak. This is what is observed, the primary product rising sharply from the origin. However, as soon as the pressure reaches a value such that an appreciable number of the ions collide before emerging from the high pressure region the character of the phenomena changes. It no longer resembles the

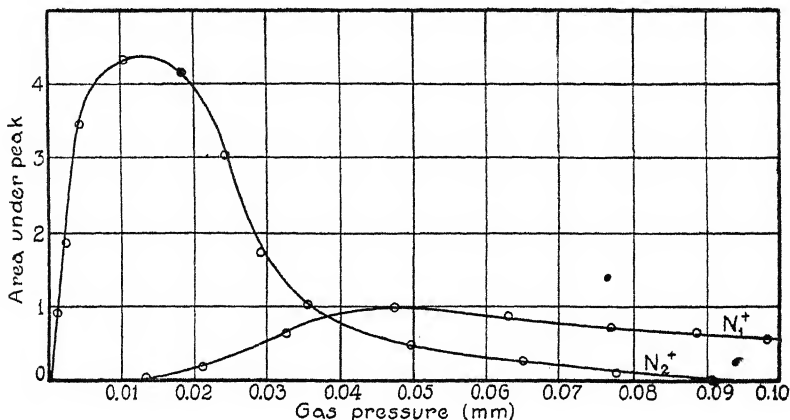


Fig. 2. Effect of pressure on the nature of the positive ion in nitrogen.

rare gas case for the secondary products appear in large quantities and the primary products drop very rapidly. At sufficiently high pressures the primary product entirely disappears though the secondary products are still present. This means that the primary product is only formed in the region so far removed from the slit from which the ions are drawn that it can not reach it without making several collisions at each of which it is likely to be deflected or dissociated. The secondary products on the other hand are formed nearer the slit at one of these collisions and continue toward the slit. There is less chance of their being deflected from the beam, and they are more stable so that there is also less chance of their being dissociated. These phenomena are very evident in both hydrogen and nitrogen. There are two secondary products in hydrogen, H_1^+ and H_3^+ , the latter greatly predominated under the conditions which existed in the ionization chamber. The accelerating potential for the ionizing electrons was well above twenty-four volts so in the case of nitrogen N_1^+ is present. When the electrons had only had twenty volts of energy the N_2^+ peak behaved exactly as a rare gas peak and no N_1^+ was observed.

In obtaining the curves of Figs. 1 and 2 and in all that follow the ionizing electrons have fallen through fifty volts, the field drawing the positive ions out of the high pressure region is four volts per centimeter, and the length of this region is about two and a half centimeters. The abscissas in all but Figs. 7, 8 and 9 represent total pressure, and in curves representing the characteristics of mixtures the observed pressure has been multiplied by

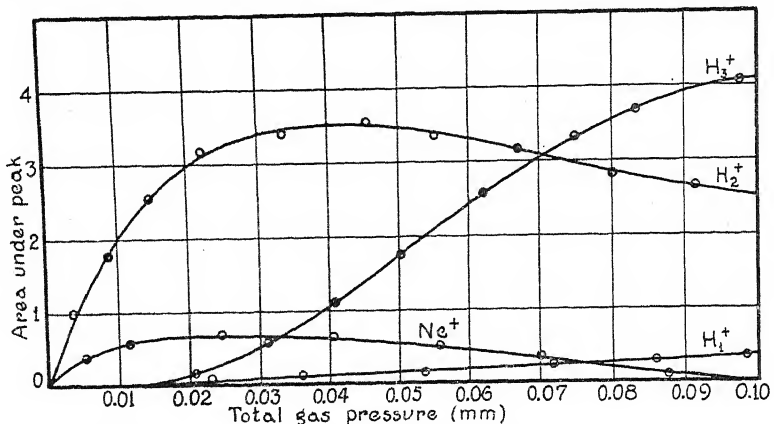


Fig. 3. Effect of pressure on the nature of the positive ion in mixtures of hydrogen and neon.

the ratio of the mean free path in the pure diatomic gas to the mean free path in the mixture so that the abscissae are directly proportional to the number of collisions and the curves are comparable with one another. Also all results refer to mixtures in which the two constituents are present in equal proportions unless otherwise stated.

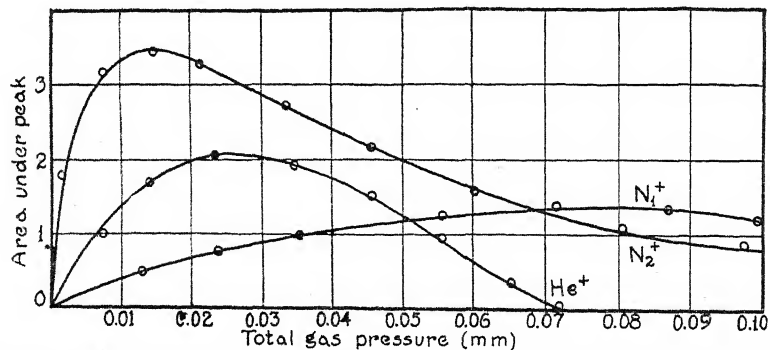


Fig. 4. Effect of pressure on the nature of the positive ion in mixtures of nitrogen and helium.

Figs. 3, 4, 5, and 6 represent the results obtained with mixtures of hydrogen and neon, nitrogen and helium, nitrogen and neon, and nitrogen and argon. The curves obtained with hydrogen and helium and with hydrogen and argon are not reproduced here as the same general phenomena are observed in the analogous curves with nitrogen. The ordinates of all these curves as directly calculated from the experimental data represent the

amount of the particular ion that is drawn out of the region of high pressure in the ionization chamber. In the cases of the curves representing the rare gases in the mixtures these ordinates have been too large to be represented on these diagrams. Hence they have been reduced in such a proportion that they bear the same ratio to the ordinates of the primary product of ionization

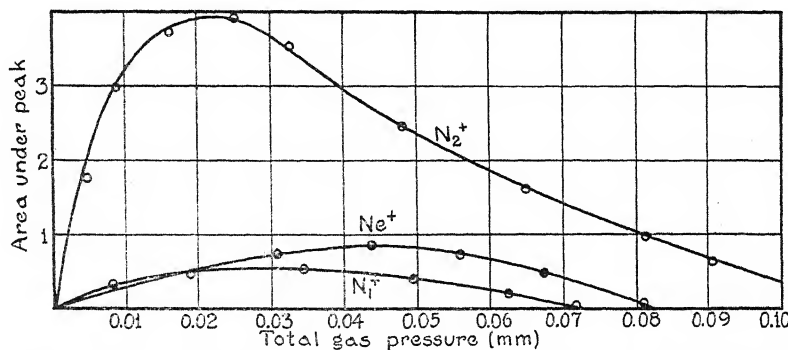


Fig. 5. Effect of pressure on the nature of the positive ion in mixtures of nitrogen and neon.

in the diatomic gas at low pressures as the probabilities of ionization of the two gases as given by the work of Compton and Van Voorhis.³ The justification for this procedure is that the ordinates of the curves obtained in mixtures of the rare gases with one another were about in proportion to their probabilities of ionization, at low pressures. And the curves obtained by plotting the value of the electrometer current do not represent the ions produced

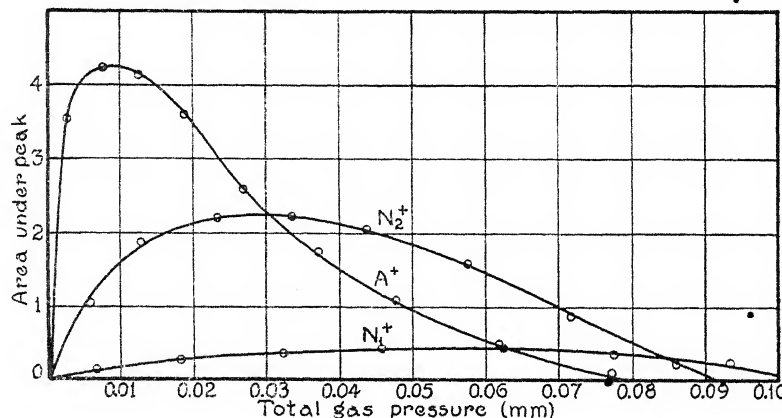


Fig. 6. Effect of pressure on the nature of the positive ion in mixtures of nitrogen and argon.

but only those which pass through the high pressure region. Hence the natural assumption is that the monatomic and diatomic ions are produced in the proportions found by Compton and Van Voorhis but that the probability of a monatomic ion passing through the high pressure region and remaining in the beam so that it will be recorded by the electrometer is

greater than for a diatomic ion. There is other evidence that this is the correct explanation, particularly that obtained from the position of the maximum of the rare gas curve, for the shape of the curve is a function of the probability of ionization and also of the probability of deflection or neutralization. From a consideration of the shapes of these curves in hydrogen and nitrogen it can be seen that the probability of deflection is less in hydrogen than in nitrogen, as would be expected. However, in the following analysis of these curves the rare gas curves are less important than the curves representing the primary and secondary products of ionization in the diatomic gas.

The ionization potentials of the gases used are approximately as follows:

$$\text{He} = 24.5 \text{ volts}$$

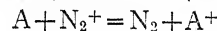
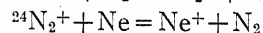
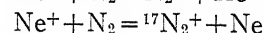
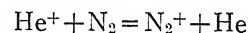
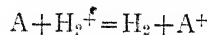
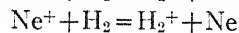
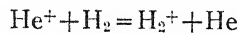
$$\text{Ne} = 21.5$$

$$A = 15$$

$$\text{H}_2 = 16 \text{ volts}$$

$$\text{N}_2 = 17 \text{ and } 24$$

And if the interchange of an electron at a collision between an atom and an ion is completely determined by the electron affinities or ionizing potentials involved it would be expected that the processes taking place would be represented by the following equations; where N_2^+ represents both types of ion:



Where the type of N_2 ion is not specified either one can be considered as obeying the equation. Also, if the relation that the probability of a transfer is inversely proportional to the amount of energy in excess of that transferred is found to be as applicable in the case of diatomic as in the case of purely monatomic mixtures, it would be expected that the hydrogen equations as listed are in the order of increasing probability. The nitrogen equations represent a more complicated case and it is a little difficult to know just how the probabilities should run except that the first equation should be the most probable, on these simple assumptions, as the difference in ionizing potentials for ${}^{24}\text{N}_2$ and Ne is only of the order of half a volt.

The phenomena observed in the mixtures containing hydrogen will be considered first and for the purpose of simplifying the discussion a slightly different method of plotting will be employed. The abscissas again represent the pressure, in this case the partial pressure of hydrogen, and the values are corrected for the difference of free path in the various mixtures so that they are really proportional to the number of collisions. The ordinates represent the value of the ratio $\text{H}_2^+/\text{H}_3^+$, this is the ratio of the primary to the secondary product of ionization. The ratio $\text{H}_2^+/\text{H}_1^+ + \text{H}_3^+$ could be used, but H_1^+ was present in such small quantities that the difference between these two ratios would be inside the limit of accuracy of the experiment. It brings out in a very convenient way the processes taking place, for the only difference in the conditions under which the curves shown in Fig. 7 are obtained is in

the type of collision possible to the two members of the ratio, that is whether the hydrogen can collide just with hydrogen or also with helium, neon, or argon. There will not be the possibility of the formation of H_3^+ at a rare gas collision for it can only be formed at a collision with another H_2 particle, hence the increased value of the ratio at high pressures in the mixtures will represent the secondary production of H_2^+ .

The curve marked 1 in Fig. 7 represents this ratio under normal conditions when only hydrogen is present. The curve drops from a very high

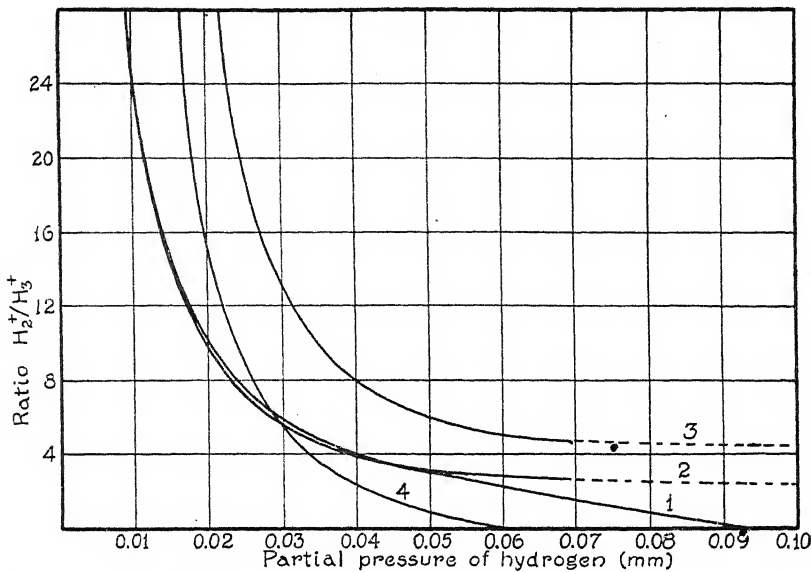
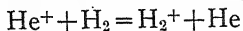


Fig. 7. Ratio of H_2^+/H_3^+ as a function of the partial pressure of hydrogen. Curve 1, in pure hydrogen; curve 2, in the presence of helium; curve 3, in the presence of neon; curve 4, in the presence of argon.

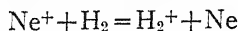
value at low pressures to zero at about nine hundredths of a millimeter. The reason that H_2^+ disappears is, as we have seen, that at that pressure the electrons from the filament are no longer able to ionize the hydrogen close enough to the low pressure region so that an appreciable amount of the ionized product can be drawn out without having suffered any collisions. H_3^+ being the secondary product and capable of surviving many collisions does not even reach its maximum value till after the H_2^+ has completely disappeared.

The curve marked 2 represents the variation of this ratio with pressure when helium is present in the ionization chamber. The character of this curve is quite different for pressures above five hundredths of a millimeter. Above that pressure as far as experimental points could be obtained the ratio H_2^+/H_3^+ remains practically constant. The interpretation of this is that H_2^+ is being produced near enough to the slit so that it can emerge from the high pressure region without having been dissociated. As we have seen, electrons are not able to do this, hence these hydrogen ions must have been

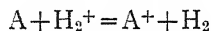
produced by collisions with helium ions. There is the alternative possibility that they may have been produced by collisions with excited helium atoms. In the present apparatus the two possibilities can not be distinguished. However, as the life of an ion would be much longer than that of an excited atom the first explanation is much the more likely. The process occurring can be represented by the equation:



The curve marked 3 represents the behavior of the ratio in the presence of neon. It is evident that the effect of neon is very similar to that of helium. The fact that this curve does not coincide with curves 1 and 2 at low pressures probably has little significance. It would be amply accounted for if the probability of deflection of an ion depended on the type of particle with which it collided. This is certainly very probable and it has not been previously allowed for. The chief difference between curves 2 and 3 is that the high pressure value of the ratio is considerably greater in the latter case. That is more H_2^+ is produced in neon than in helium for the same number of collisions. The equation would be similar to the helium one:



The curve marked 4 represents the behavior of the ratio in the presence of argon. The shape of this curve differs greatly from that of the two preceding ones. It would appear that a reverse phenomenon is taking place. The two possibilities to account for a change in the ratio are: that H_3^+ is created at a collision with an argon particle or that H_2^+ is destroyed. The former is obviously impossible directly and probably may be entirely neglected. The latter is exactly what would be predicted by the argon hydrogen equation:



It is difficult to form an accurate idea of the probabilities of electron interchanges between hydrogen and the rare gases from Fig. 7. However, the ordinates of curves 2 and 3 at high pressures tend to show that the process associated with 3 is the more probable. The hydrogen curves analogous to Figs. 4 and 5, which are not reproduced here, bring this out much more clearly and also tend to show that the process associated with 4 is the most probable of all. This is exactly what would have been expected by analogy with the rare gas mixtures¹ as can be seen by referring to the ionizing potentials given above.

Fig. 8 gives the analogous curves for nitrogen. The ordinates represent the values of the ratio $\text{N}_2^+/\text{N}_1^+$, and the abscissas are the partial pressures of nitrogen. These curves are very similar to those in Fig. 7 except that curve 3 representing the ratio in the presence of neon is missing. By referring to Fig. 5 it can be seen that the ratio has an infinite value in that pressure range where the other curves are of the most interest. The neon case will be discussed separately. In this case also the fact that the curves do not coincide at low pressures is probably not of great significance due to the considerations mentioned while discussing Fig. 7.

The curve marked 1 representing the ratio in pure nitrogen is very similar to the analogous curve in the case of hydrogen. Its behavior is almost identical throughout the entire pressure range. In this case also of course the ordinates represent the ratio of primary to secondary product, but the type of secondary product concerned is very dissimilar and Figs. 1 and 2 bear little resemblance to one another, hence it is rather remarkable that curves 1 in Figs. 7 and 8 should be so very much alike.

Curve 2 represents the ratio in the presence of helium. It is apparent that its behavior is very similar to the analogous curve in the case of hydrogen. The only differences are that the slope decreases more rapidly in the low pressure region of the curve and that the values of the ordinates approached almost asymptotically at high pressures are considerably greater

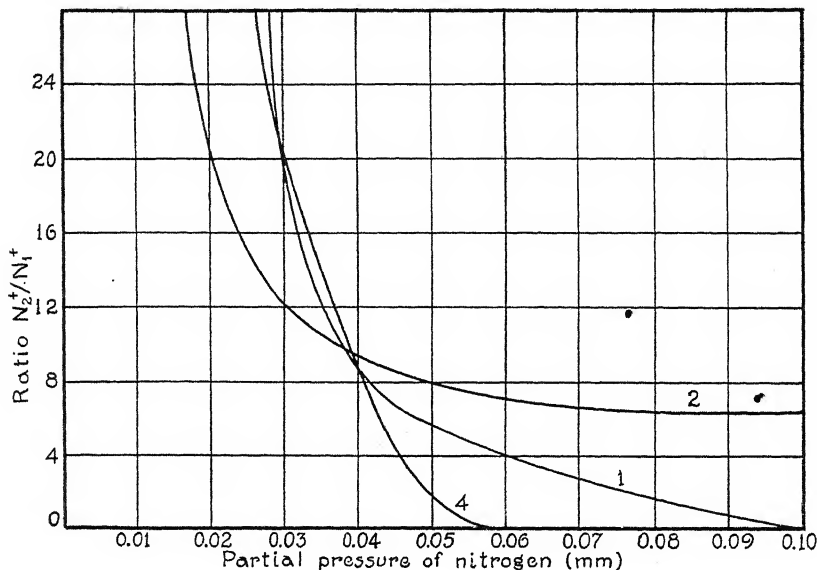
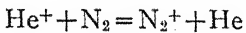


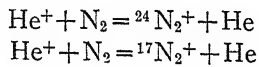
Fig. 8. Ratio of N_2^+ / N_1^+ as a function of the partial pressure of nitrogen. Curve 1, in pure nitrogen; curve 2, in the presence of helium; curve 4, in the presence of argon.

than those of curve 2 in Fig. 7. These differences are such as to be most easily accounted for by assuming a larger value for the probability of ionization of a nitrogen molecule when it collides with a helium ion than for the probability of ionization of a hydrogen molecule at a similar collision. This is in a general way what would be predicted from the ionizing potentials if it is true that the transfer is more likely when the energy to be transferred is smaller. The difference, however, should be very small for $^{17}N_2^+$ but very large for $^{24}N_2^+$. The equation representing the transfer would be analogous to the hydrogen one:



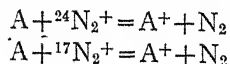
The phenomena, however, are rather more complicated in the case of nitrogen. In the first place the secondary product entering into the radio

plotted in Fig. 7 can not be increased at collisions between H_2^+ and the rare gas particles. This is not true in the case of nitrogen. For N_1^+ can be formed at any collision of $^{24}N_2^+$, if indeed a collision is necessary at all. In the second place two types of primary product are possible in the case of nitrogen, namely: $^{24}N_2^+$ and $^{17}N_2^+$. The former can dissociate at a collision, or possibly spontaneously, into N_1^+ . However, without more accurate knowledge of the probability of formation of the two types of primary product and of the probability of dissociation of $^{24}N_2^+$ only qualitative interpretations of the data that have been obtained are possible. The quantity of N_1^+ observed is probably a measure of the amount of $^{24}N_2^+$ present but the details of the dissociation such as the necessary conditions and probability of occurrence are not known. Hence the curves in Fig. 8 represent a more complicated situation than those in Fig. 7, and the main interest in this method of plotting is in the possibility of comparison between the two figures. Considering curve 2 of Fig. 8 in more detail it is seen that the numerator of the ratio can be increased by an increase in either primary product but that the production of one of these also automatically increases the denominator, hence it would be difficult without accurate knowledge of the probabilities involved to predict the form curve 2 would take. More information is given, however, by Fig. 4, which represents the variation of the ions with pressure in a mixture of nitrogen and helium. From this figure it can be seen that both N_1^+ and N_2^+ exist in larger quantities at high pressures than in pure nitrogen. This is what would be expected if they are produced at collisions with helium ions. The fact that a large amount of N_1^+ is observed at high pressures is very significant for it shows that a very large proportion of the nitrogen ions produced by the helium ions are of the type $^{24}N_2^+$. This is interesting from at least two points of view. In the first place it definitely places this ionization potential of nitrogen below the ionization potential of helium. In the second place it shows that the first of the following equations is much more probable than the second:



This is of interest from the point of view of the energy interchange occurring.

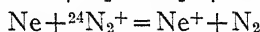
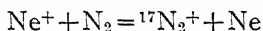
Curve 4 in Fig. 8 representing the variation of the ratio with pressure in the presence of argon is of some interest by comparison with the analogous curve in Fig. 7. The forms of the two curves are very similar, the outstanding difference being that the decrease is more rapid for the nitrogen ratio. This is exactly what would be expected from the foregoing considerations. N_2^+ would be decreased in accordance with the equations:



The latter being by far the more probable. Also N_1^+ would be increased by the collisions between $^{24}N_2^+$ and A^+ and also probably at a certain number of collisions with neutral argon; in fact, the validity of the first equation is rather doubtful. It is difficult to obtain much more information from Fig. 6.

However, it can be seen by a comparison of Figs. 2 and 6 that the rate of decrease of N_2^+ is much more rapid at high pressures when argon is present (all pressures given are total pressures) than in pure nitrogen. This is less true for N_1^+ . If of any significance at all this may be taken as supporting the second rather than the first equation just given.

Fig. 5 represents the results obtained in a mixture of nitrogen and neon. The most striking difference between it and Figs. 4 and 6 is seen to be the behavior of the N_1^+ ion. The secondary product of ionization actually disappears before the primary one. This has not been true in any of the preceding mixtures. The cause of this is probably contained in the equations:



According to these equations the only N_2^+ ion formed by a collision of the second kind with a neon ion is the type of ion not capable of dissociation. Hence at high pressures the only ions produced near enough to the analyzing chamber to be able to emerge from the high pressure region and be detected are N_2^+ ions. This was not true in the case of the helium mixture for in that case the $^{24}N_2^+$ was produced in large quantities and it could dissociate giving N_1^+ . In addition to this effect the presence of neon according to the second equation tends to decrease N_1^+ by decreasing $^{24}N_2^+$. These are exactly the phenomena which are observed. The N_1^+ ion decreases more rapidly than in any other mixture and disappears at a comparatively low pressure. On the other hand the N_2^+ ion is apparently little effected by the presence of

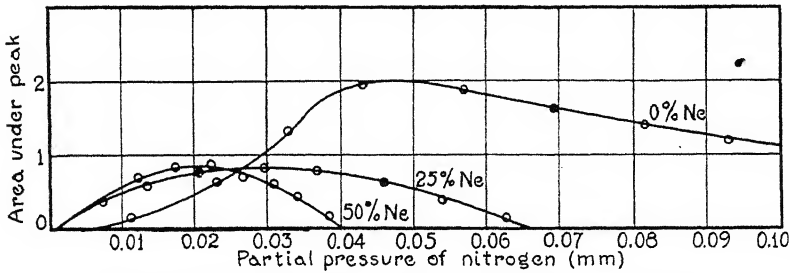
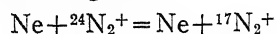


Fig. 9. Effect of mixtures of neon on the number of N_1^+ ions.

neon. Making the proper change in abscissae N_2^+ behaves much as it does in pure nitrogen. The effect of neon is about half way between that of helium and that of argon. This is just what would be expected from the equations for N_2^+ is increased at one type of collision and decreased at the other. Little can be said of the relative probabilities of these processes except that they must be of the same order of magnitude and probably roughly equal. From a consideration of Figs. 4, 5, and 6 it can be seen that by far the most probable of these ionizing processes that we have been considering is the production of $^{24}N_2^+$ by He^+ . The difference in ionizing potentials in that case is of the order of half a volt.

Fig. 9 has been included to show the very striking way in which N_1^+ decreases in the presence of neon. The ordinates represent the area of the

N_1^+ peak and the abscissa are the partial pressures of the nitrogen. N_1^+ is greatly decreased in the presence of 25 percent neon and still further when the neon is increased to 50 percent. This is exactly the result predicted by the second equation. If a sufficient number of collisions occurred the two equations could be considered together:



Thus it can be seen that the equilibrium at high pressures would be displaced greatly in favor of the stable form of N_2^+ . It might also be mentioned that the N_1 ionizing potential though not known accurately is certainly below that of Ne and reactions involving N_1 may be completely neglected.

CONCLUSIONS

From the detailed and rather complicated analysis of the experimental results two main conclusions become evident. The first is that at a certain number of collisions between an atomic or a molecular ion and an atom or ion of lower ionizing potential an electron transfer will occur. In all the mixtures of gases that have been studied so far no exception to this has been observed. The processes expected to occur at a collision can be predicted from a knowledge of the ionizing potentials of the atoms or molecules involved. Secondly the probability that a given transfer will occur appears to be an inverse function of the difference between the ionizing potentials involved. By far the most probable transfers seem to be those in which the ionizing potentials of the two gases concerned are nearly equal. When there is a large amount of excess energy the probability of the process occurring is very much smaller.

In conclusion I want to express my deep gratitude to Professor K. T. Compton and Professor H. D. Smyth for their interest and helpful suggestions during this work.

PALMER PHYSICAL LABORATORY,
PRINCETON, NEW JERSEY,
March 24, 1927.

THE NUMBER OF RADIATING ATOMS IN A HYDROGEN DISCHARGE TUBE*

By W. H. CREW AND E. O. HULBURT

ABSTRACT

About 90% of the energy radiated from a long hydrogen tube filled with moist hydrogen at a pressure of 0.54 mm of mercury and absorbing 400 watts was found to be carried by the first three lines of the Balmer series. From the measured values of this energy and of the relative intensities of $H\alpha$, $H\beta$ and $H\gamma$, the number of quanta of these lines emitted per atom per second was calculated to be 2.84, 0.43 and 0.10, respectively.

A GLASS hydrogen discharge tube may be arranged to emit the Balmer lines of hydrogen in great purity, their total energy being much greater than that of the other spectral radiations, such as the infra-red atomic lines, the spectrum of the molecules and the continuous spectrum. If the entire energy radiated from the tube in all directions is measured, if the number of atoms in the discharge tube is known, and if the relative intensities of each of the Balmer lines is known, the average number of quanta of each Balmer radiation emitted by each atom per second may be calculated. Experiments based on these ideas are described in the following pages. It has been found, for example, that in the case of $H\alpha$ under, let us say, normal discharge conditions this number is of unit order.

Apparatus. The discharge tube consisted of a straight tube of Pyrex glass 79 cm in length and of internal diameter 9 mm, with long side tubes leading to bulbs containing the electrodes, to a pressure gauge, to the pumps and to the hydrogen. The tube was excited by a 1 KW, 30 KV, 25 cycle transformer, the electrical energy in the tube being taken to be the product of the current and voltage.

Calibration of the thermopile. The radiation from the tube was measured by a thermopile and Paschen galvanometer, the thermopile being diaphragmed so that only about 2mm^2 were exposed to the radiation. An energy calibration was effected by observing the deflection caused by the radiation from a calibrated ribbon filament tungsten lamp. We are indebted to Dr. H. T. Wensel of the Bureau of Standards, who kindly loaned us the lamp and furnished its calibration, i.e. the temperature-current curve. With the filament at 2560° Kelvin and diaphragmed so that an area 0.12 cm^2 was exposed, the galvanometer deflection caused by the radiation, emitted normally from the surface, falling on the thermopile a meter away was 66 mm. A calculation of the spectral energy curve of the tungsten, by means of the black body formula and the emissive powers^{1,2} of tungsten,

* Published by permission of the Navy Department.

¹ Worthing, Phys. Rev. 10, 377 (1917).

² Weniger and Pfund, Phys. Rev. 14, 477 (1919).

showed that 65 watts/cm² were emitted normally, and that 99% of this was in the spectral region of transparency of the glass bulb, 0.32 to 3 μ . The glass bulb thus caused a loss of 9%, 1% being due to absorption and 8% to reflection. At a meter's distance the flux of energy was

$$0.91 \times 65 \times 0.12 \times 10^7 \div 10^4 = 7.10 \times 10^3 \text{ ergs/cm}^2.$$

This produced a deflection of 66 mm. Therefore 1 mm meant an energy flux of 108 ergs/cm².

Total energy from the hydrogen tube. With moist hydrogen in the tube at a pressure of 0.54 mm of mercury excited with 400 watts (66 milliamperes \times 7 kilovolts) the Balmer lines were intense, fourteen of them appearing on plates taken in five minutes with the large quartz spectrograph. Other lines and the continuous hydrogen spectrum of course were also on the plates, but with relatively feeble intensity. In addition there are certain infra-red lines from atomic hydrogen of wave-length below 3 μ which may come through the glass, i.e. the entire Paschen series and a portion of the Brackett and Pfund series. The entire intensity I_B of these infra-red lines was compared with the intensity I_R of all the Balmer lines by means of a Corning "Heat Transmitting" glass filter. Measurements showed that this filter transmitted 83% of the energy from 1.4 to 2.7 μ and was opaque below 0.7 μ . With the thermocouple at the side of the tube, the unscreened radiation produced a galvanometer deflection of 86 mm and when screened by the filter a deflection of 3 mm. Therefore

$$I_B/I_R = 86 \times 0.83/3 - 1 = 22.8.$$

This number was not very accurate, depending as it did on a 3 mm deflection, but sufficed to show that about 95% of the radiation from the tube was carried by the Balmer lines, the weak molecular lines, the continuous spectrum, etc.

A 43 mm deflection was observed with the thermopile 5 cm away from the side of the tube, (the excitation being always 400 watts and pressure 0.54 mm of mercury), and at other distances up to 15 cm the deflections were proportional inversely to the distance. The total energy E_s ergs/sec radiated from the side of the tube was, therefore,

$$E_s = 2 \times 5 \times \pi \times 79 \times 43 \times 108 = 1.153 \times 10^7 \text{ ergs/sec.}$$

Radiation from the end of the tube produced a deflection of 122 mm which remained constant when the thermopile was moved from 2 to 5 cm from the end of the tube. The total energy E_e radiated from the two ends of the tube was, then,

$$E_e = 2\pi \times 0.45^2 \times 122 \times 108 = 0.00168 \times 10^7 \text{ ergs/sec.}$$

The entire energy E radiated from the tube was, neglecting the end effects of E_s ,

$$E = E_s + E_e = 1.155 \times 10^7 \text{ ergs/sec.}$$

The efficiency of the tube. The total length of the hydrogen tube was 300 cm. When the tube was absorbing 400 watts, a section 79 cm long absorbed 105 watts and radiated 1.155 watts. Therefore the efficiency of the tube as a radiator of Balmer energy was about 0.9%.

Relative energy from the side and end of the tube. The small amount of energy delivered from the ends of the tube compared with that from the side deserves a few remarks. The measurements showed that $E_s/E_e = 685$. An exact theoretical derivation of this ratio would be tedious. It is evident, however, that the radiation from elements of the tube remote from the ends does not get out to the ends in full amount mainly because it escapes through the glass walls of the tube when the angle of incidence is not too close to grazing; it also suffers absorption on its way along the tube. For example, only 60% of the energy of rays striking the walls at a grazing angle of 10° is reflected (60% being the average of the reflecting powers 72 and 48%, for the electric vector parallel and normal, respectively, to the surface, as calculated from Fresnel's equations, taking the refractive index of the glass to be 1.5). Therefore after a few reflections practically all the energy of these rays has passed out to the side. It is only when the grazing angle becomes less than 3° that the average reflecting power is above 80% and that the light proceeds along the tube without much loss. For a grazing angle of 3° the calculated ratio E_s/E_e was greater than 400. If the absorption of energy along the tube were taken into account (there are no exact data yet for the absorption) E_e would be decreased and the number 400 increased, and we might expect satisfactory theoretical agreement with the observed number 685. Silvering the external walls of the tube would increase E_e ; this effect was demonstrated qualitatively by Merton and Johnson.³ In the present instance we surrounded the tube throughout its length by mercury, and obtained a galvanometer deflection of 180 with the thermopile at the end of the tube, whereas without the mercury the deflection was 122.

Relative intensities of H α , H β , and H γ . The relative intensities of the first three lines of the Balmer series were obtained by a spectrophotometric comparison with the spectrum of the calibrated tungsten lamp. When the discharge tube was filled with moist hydrogen at a pressure of 0.54 mm of mercury and was absorbing 400 watts, the relative intensities of the Balmer lines in the radiations from the side and the end of the tube were; side, H α :H β :H γ = 1.00:0.207:0.054; end, H α :H β :H γ = 1.00:0.40:0.08. These values and those of other observers show some variance. Although this is perhaps to be ascribed to widely differing experimental conditions, the question of the Balmer intensities can hardly be regarded as a settled one. For example Merton and Nicholson⁴ found that in a small capillary tube H α :H β :H γ as 1.00:0.264:0.183, and Nutting and Tugman⁵ 1.00:0.315:0.0055. In the electrodeless discharge in hydrogen Schlesinger⁶ observed that H α :H γ = 1.00:0.06.

The fact that the intensity of H α compared to the other lines is relatively less from the end of the tube than from the side is of course to be ascribed to absorption in the luminous hydrogen. It would follow that in the radiation from the end of the tube only the layers near the end are effective con-

³ Merton and Johnson, Phil. Mag. 46, 448 (1923).

⁴ Merton and Nicholson, Phil. Trans. 217 (1917).

⁵ Nutting and Tugman, Bull. Bur. Stand. 7, 49 (1911).

⁶ Schlesinger, Zeits. f. Phys. 39, 215 (1926).

tributors of $H\alpha$, whereas for $H\beta$ and $H\gamma$ the more remote layers are effective as well. A pretty demonstration of this is obtained by gazing into the tube through a red glass which transmits only $H\alpha$; in this case one sees hardly more than 50 cms into the tube. With a blue screen opaque to $H\alpha$ and transparent to $H\beta$ and $H\gamma$ the far end of the tube 80 cms away is quite distinct. The experiment is exactly in the manner of the spectroheliograph for seeing into the sun.

The number of quanta emitted per atom. In accordance with the foregoing measurements 90% of the energy delivered by the tube was carried by the first three Balmer lines, 5% by the infra-red lines, and the remaining 5% by the higher members of the Balmer series, the molecular lines, the continuous spectrum, etc. Then with $H\alpha:H\beta:H\gamma = 1.00:0.207:0.054$, and with $E = 1.155 \times 10^7$, the total energy each second emitted from the tube in the form of $H\alpha$ comes out to be 8.24×10^6 ergs; this amounts to 2.75×10^{18} quanta of $H\alpha$. We have shown in another investigation⁷ that the hydrogen under the conditions of the present experiment was almost entirely atomic. Therefore the $H\alpha$ energy was emitted by 9.65×10^{17} atoms (the pressure in

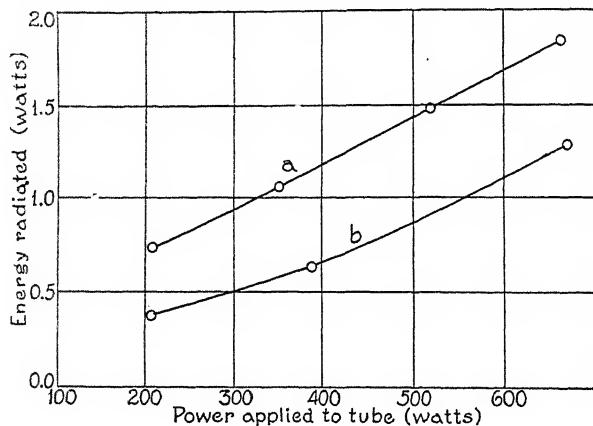


Fig. 1. Total radiation E as a function of the power for constant pressures 0.47 and 0.72 mm of mercury, curves *a* and *b*, respectively.

the discharge tube being 0.54 mm of mercury), and on the average each atom in the tube emitted 2.84 quanta of $H\alpha$ per second. Similarly, the average numbers of $H\beta$ and $H\gamma$ quanta per atom per second were 0.43 and 0.10 respectively.

Pfund⁸ has found that the total intensity of the Lyman series from much the same sort of hydrogen discharge as that of the present experiment was 8.8 times that of the Balmer, Paschen and Brackett series all added together. We may then conclude that the order of magnitude of the number of Lyman quanta emitted per atom per second was about 10.

Variation of the radiated energy with the power and pressure in the tube. The manner in which the total energy E varied with the power and pressure

⁷ "Pressures in Discharge Tubes," to be published soon.

⁸ Pfund, Journ. Optical Soc. Amer. 12, 467 (1926).

in the tube is shown in the curves of Figs. 1 and 2, the curves *a* and *b*, Fig. 1, which are for constant pressures of 0.47 and 0.72 mm of mercury, respectively, and the curve of Fig. 2 for a constant power of 400 watts. The full line portion of this curve was obtained by pumping the pressure down in steps and observing the galvanometer deflection with the tube lighted at each step. Towards the end of such a procedure at the lower pressures the tube became whitish and no longer glowed with the crimson radiance characteristic of a pure Balmer spectrum. This was due, it was supposed, to the burning off of the water vapor from the walls of the tube, thereby permitting them to catalyze the atoms to the molecular state. If the curve was repeated each point being obtained by refilling the tube with fresh moist hydrogen and then

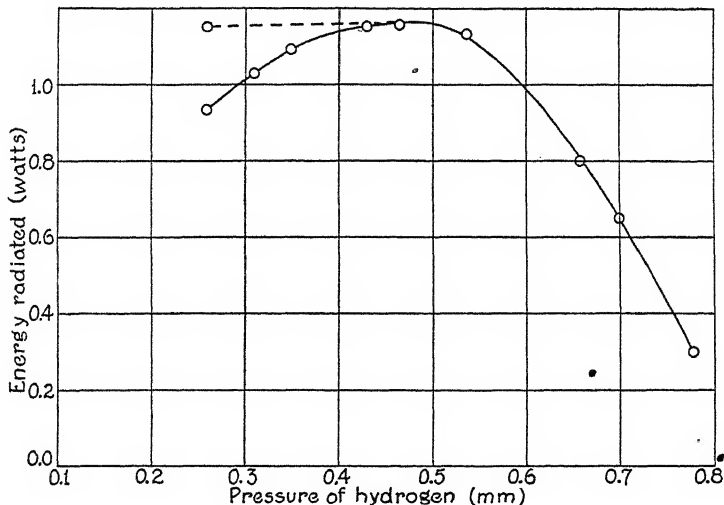


Fig. 2. Total radiation E as a function of the pressure for constant power of 400 watts.

pumping down to the desired pressure, the dotted branch of the curve of Fig. 2 was obtained, the curve for pressures above 0.45 being unchanged. In Fig. 1 for powers above 300 watts the hydrogen was practically all atomic, and the number of quanta emitted per atom was therefore proportional to E . From the highest point of curve *a*, Fig. 1, with 665 watts in the tube, each atom emits 5.2 quanta of $H\alpha$ per second. If we suppose that the time during which the atom remains in the excited state is 10^{-8} seconds, it is seen that the atoms of hydrogen, even under rather violent discharge conditions, are on the average in an unexcited state a relatively large part of the time.

In conclusion, we may remark that the present method is by no means restricted to the hydrogen lines, although, to be sure, these are comparatively easy to isolate spectroscopically, but is directly applicable to the determination of the number of quanta emitted per atom, or molecule, of any spectral line.

NAVAL RESEARCH LABORATORY,
WASHINGTON, D. C.,
February 17, 1927.

A STUDY OF THE POLARIZATION OF THE LIGHT FROM HYDROGEN CANAL RAYS

By K. L. HERTEL

ABSTRACT

Polarization of light from hydrogen canal rays and its rate of decay.—Light from hydrogen canal rays (principally H β) was found to be partially polarized, with the electric vector of the stronger component in the direction of motion of the particles. The amount of this polarization varied over a considerable range: the maximum polarization observed was about 10 percent. Measurements of the polarization at different positions along the canal ray bundle show that the polarization dies away more rapidly than does the intensity. Its half-value time is about one-third that for the intensity.

Effect of a transverse electric field on the polarization of light from hydrogen canal rays.—When an electric field at right angles both to the canal ray bundle and to the direction of observation is applied to the canal rays the polarization changes rapidly (in less than 10^{-9} sec.) at the points of entry to and exit from the field. The change is in the same direction at both entry and exit and is such that the component of the electric vector perpendicular to the direction of motion is increased relative to the parallel component. The change increases with the strength of the field up to 300 or 500 volts per cm after which the increase is small. In a weak uniform field (less than 200 volts per cm) the polarization appears to die out at about the same rate as with no field. In stronger uniform fields there is a tendency for the light to become polarized with the stronger component of the electric vector in the direction of motion. There is some evidence of periodicity in the polarization as the particles pass through a uniform field.

WHILE studying the effect of an electric field upon the radiating atom, Stark¹ observed qualitatively that the light from the canal rays of hydrogen was partially polarized. In 1915 Stark and Luneland² studied this polarization quantitatively, and found that the light from the moving particles was polarized, while that from the particles at rest was not polarized. They expressed the polarization as the ratio of the component vibrating in the direction of motion to that vibrating at right angles to it, and this ratio varied from 1.20 to 1.35 for the series lines of hydrogen. If these canal rays are allowed to pass through a small hole in the cathode and into a chamber where the pressure is maintained as low as possible, the intensity of the bundle dies out with distance from the hole. This rate of dying out has been studied by Wien³ and Dempster.⁴

It would be expected from the observations of Stark and Luneland that the light from the bundle entering the high vacuum chamber used by Wien

¹ Stark, Verh. d. D. Phys. Ges. 8, 104 (1908); J. Stark u. H. Kirschbaum Ann. d. Physik 43, 1002 (1914).

² Stark and Luneland, Ann. d. Physik 46, 68 (1915).

³ Wien, ibid. 60, 597, 1919; ibid., 66, 230, (1921); ibid., 73, 483, (1923).

⁴ Dempster, Phys. Rev., 15, 138, (1920); Astro. Jour., 57, 193, (1923).

and Dempster would be partially polarized. Rupp⁵ recently observed qualitatively that this light was partially polarized, showing that the polarization observed by Stark and Luneland persisted. The problem attacked in this series of experiments was a study in more detail of the polarization of the light from this bundle in high vacuum. It is to be noted that in this high vacuum chamber the particles are neutral, excited, moving with a high velocity, and disturbed very little by collisions with other particles. If now, these particles are subjected to an electric field or a magnetic field and an orientation is produced, it might be expected that the polarization would be changed, and since the particles have a high velocity, a "history" of the effect could be obtained by observing the polarization at various points along the path of the particles. The results of the experiments discussed here show that the light from the hydrogen canal rays at low pressure is partially polarized, and that this polarization dies out with distance from the cathode. They show further that polarization effects are produced by electric fields at right angles to the motion of the particles.

EXPERIMENTAL

The method used in producing the hydrogen canal rays in high vacuum was similar to that used by Wien and Dempster. Purified hydrogen was allowed to flow from a reservoir, through a capillary tube and liquid air trap into the discharge tube. Rectified current was sent through the discharge tube to produce the canal rays, which then passed through a small hole (0.48 mm diam.) in the cathode into the observation chamber. Here the bundle was photographed through a calcite crystal and the two images measured on a microphotometer. The gas that passed through the hole with the canal rays was pumped out by a rapidly acting pump, and in this way the pressure was kept low in the observation chamber.

The hydrogen was taken from a commercial steel tank and purified by slowly passing it through activated charcoal immersed in liquid air. The gas was then stored in a reservoir and introduced into the discharge tube as needed. In order to adjust the pressure in the discharge tube, it was necessary to adjust the rate of inflow of the gas. This was accomplished by using a capillary tube 20 cm long, having a bore of 0.5 mm, and inserting in the bore a glass rod slightly tapered and a little smaller than the bore. The glass rod was made by drawing down larger rod until the proper size was obtained. The piece of iron *F*, Fig. 1, was fastened to the large end of the glass rod so that it could be moved by means of a magnet from the outside. By adjusting the glass rod the resistance to the flow of gas could be changed to give any discharge-tube pressure desired. Using a reservoir pressure of 25 cm of mercury, the pressure in the discharge tube was changed from 0.14 mm to 0.07 mm of mercury when the rod was moved 8 cm.

As shown in Fig. 1, the discharge tube *D* was separated from the observation chamber *O* by the cathode (Fig. 2) resting on the ground joint *G*. The discharge tube proper was 55 cm long and 2.3 cm in diameter. Two different

⁵ Rupp, Ann. d. Physik 99, 1 (1926).

observation chambers were used in these experiments. The first was a cylindrical tube of Pyrex glass about 4.4 cm in diameter and the bundle observed through the cylindrical wall of the tube. The second observation chamber (*O*, Fig. 1) was designed to reduce to a minimum any polarization that might be introduced by the glass wall. It had a large tube extending in the direction of the camera and a good piece of plate glass fastened to the end of it with wax. The calcite crystal *C* which had been recently polished was properly oriented and cemented to this plate with Canada balsam, thus leaving only one reflecting face to introduce polarization. The lens of the camera was placed near the calcite crystal and the glass plate, so that any polarization introduced by strains in the glass plate would not be localized in the image.

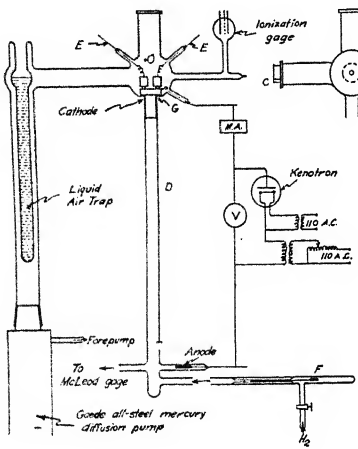


Fig. 1. Diagram of apparatus.

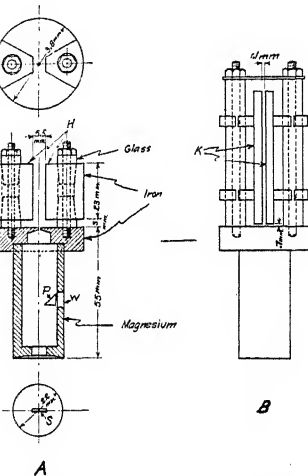


Fig. 2. Diagrams of cathodes.

The pressure in the discharge tube was measured by a MacLeod gage and in the observation chamber it was measured by an ionization gage which had been calibrated with the MacLeod gage. The current for the discharge tube was furnished by an alternating current transformer, rectified with one kenotron, and thus giving only one-half of the cycle. The current was measured by the direct current milli-ammeter M.A. and the voltage across the tube measured by the Braun voltmeter *V*.

The cathodes used in these experiments are shown in Fig. 2. The lower part, which extended down into the discharge tube, was made of magnesium to eliminate sputtering. *P* was a totally reflecting prism which reflected the light from the slit *S* through the opening *W* into the slit of a spectroscope for observing the Doppler effect. This magnesium cup was fastened to the cathode proper which in turn rested on the ground joint. In the center of the cathode was a hole 0.48 mm in diameter which allowed the canal rays to pass into the observation chamber. Cathode "A" was used to apply either a magnetic or an electric field to the bundle, the poles *H* acting either

as magnetic poles or as condenser plates. When a magnetic field was used the magnet was placed just outside the walls of the tube. On cathode "B" the condenser plates were made adjustable and set close together and near the cathode as shown in Fig. 2. The condenser plates were joined to the leads *E* (Fig. 1) which were in turn connected to a potentiometer for applying the field. Care was always taken to adjust the potential so that the potential of the cathode (which was grounded) was midway between that of the two plates *K*.

It was necessary in these experiments to keep the pressure in the observation chamber as low as possible in order that the number of collisions of the moving particles with the "rest" gas be reduced to a minimum. This was accomplished by connecting a Gaede all-steel mercury diffusion pump to the observation chamber with large tubing and using the special liquid air trap shown in Fig. 1. The total distance from the cathode to the mouth of the pump was about one meter. In this way the ratio of the pressures on the two sides of the cathode could be maintained up to 330 to 1. With wax joints in the system, this ratio was reduced a little.

METHOD OF PHOTOMETRY

The luminous bundle was studied by photographing it at right angles both to the direction of motion of the particles, and to the direction of the field. The photographs were taken with an ordinary camera through a calcite crystal 1 cm thick. The crystal was oriented so that one image was produced by the light vibrating in the direction of motion of the particles, while the other was produced by the light vibrating at right angles to it. A 0.7 mm slit made of bakelite was placed 8 mm in front of the bundle and parallel to it, to prevent the two images from overlapping as the bundle became diffuse. The images were about 0.5 mm apart on the photographic plate, and the blackening could be easily measured with a microphotometer. Beyond the bundle another piece of roughened bakelite was placed so that no light could be reflected through the slit into the camera. Cramer Hi Speed plates were used and developed with Cramer Contrast Developer. Exposure times of 10 to 20 minutes were found to give the right density to be used on the microphotometer. The microphotometer was of the thermopile type, having a Coblenz thermopile and a Leeds and Northrup high sensitivity galvanometer.

In order to convert the microphotometer readings into relative intensities a series of intensity spots were placed on every photographic plate and a calibration curve made for each plate. The intensity spots were formed on the plate by allowing light from a uniformly illuminated screen to pass through holes of various sizes and to fall on the plate 7 cm away. There was a velvet lined tube leading from each hole to the plate so that the light falling upon any one part of the plate came through only one hole. The relative intensity with which the plate was illuminated at any one point was directly proportional to the area of the hole through which the light passed, and from the relative areas of the holes the corresponding relative intensities were

determined. A gas-filled tungsten light was used to illuminate the screen after it was found by test to give the same density curve as the light from the region just in front of the cathode. In the microphotometer the slit of the instrument was vertical and was adjusted to less than half the width of the image of the bundle which was also placed vertical. The plate was placed on a horizontal slit 0.6 mm wide, so that only 0.6 mm of the image was measured at a time. This represented from 0.9 to 1.1 mm of the bundle since the reduction of the camera was 1.5 to 1.85 times. In measuring a plate, the intensity spots were first placed over the horizontal slit and moved horizontally past the instrument; in this way the average deflection for each intensity spot was obtained. The two images of the bundle to be measured were then placed across the slit and the deflection for the maximum density of each image was observed. These data were taken at 1 mm intervals along the length of the image. The deflections for the intensities giving the calibration curve for the plate, and from this calibration curve the deflections for the image were changed into relative intensities. Using this method of photometry, the images and comparison are placed on the same plate, exposed for the same length of time to the same quality of light, and developed in the same developer at the same time. Also the microphotometer readings of the two images were taken as near the same time as practical. In this way the photographic plate with the microphotometer acted as a medium for comparing intensities, and consequently the accuracy depended primarily upon the uniformity of both the photographic plate and the microphotometer measurements.

DATA AND RESULTS

The data in Figs. 3 and 4 were taken with the cylindrical observation chamber and the cathode "A" (Fig. 2), and for the data in Figs. 5, 6 and 7 the observation chamber shown in Fig. 1 with cathode "B" were used. The set of curves shown in each figure was made from the data taken from one photographic plate. I_p was the intensity of the light whose electric vector was vibrating parallel to the direction of motion of the particles, and I_n the intensity of light whose electric vector was vibrating at right angles to this. The ratio I_p/I_n was plotted against the distance along the bundle. Several plates were discarded because of their non-uniformity.

In Fig. 3 A, the solid line shows the dying out of the partial polarization with distance from the opening in the cathode, and the broken line shows the dying out of the total intensity. It is seen that the partial polarization decreases at a faster rate than the intensity itself and becomes practically zero by the time the total intensity has reached half value. The remaining curves of Fig. 3 show the effects of various electric fields upon the polarization. The notation "field applied" show the distance over which the field was applied and is the 23 mm distance of cathode "A" Fig. 2. The polarization of the light as the particles are entering the observation chamber is approximately the same as with no field, but this changes quite rapidly as the particles enter the field, the light becoming polarized in

the opposite direction by the time the particles are in the uniform field. In this uniform field the polarization dies out at about the same rate as

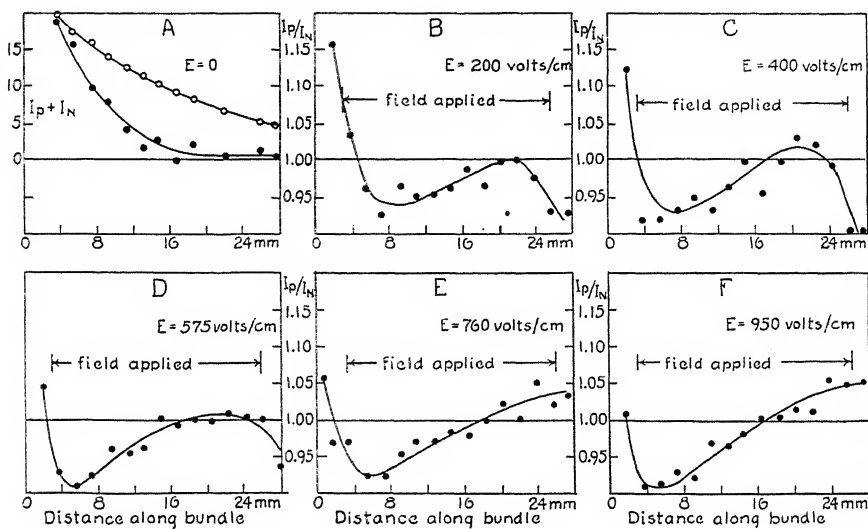


Fig. 3. Showing the variation of intensity and state of polarization of the light along the canal ray bundle. $P = 0.097$ mm, $p = 0.00029$ mm, $V = 5000$ volts, $I = 9.0$ m.a., $S = 5.4 \times 10^7$ cm/sec.

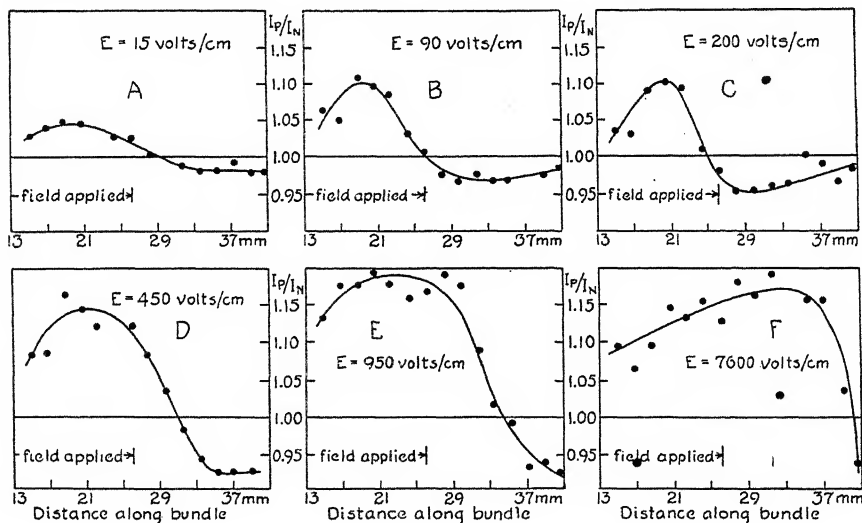


Fig. 4. Showing the variation of the state of polarization of the light along the canal ray bundle. $P = 0.100$ mm, $p = 0.00030$ mm, $V = 4200$ volts, $I = 9.5$ m.a.

with no field at all, and in the stronger fields I_p again becomes greater than I_n . When the particles pass out of this uniform field another change in the

polarization takes place. This change is similar to the change that occurred as the particles entered the field, and I_p again becomes the stronger. It is

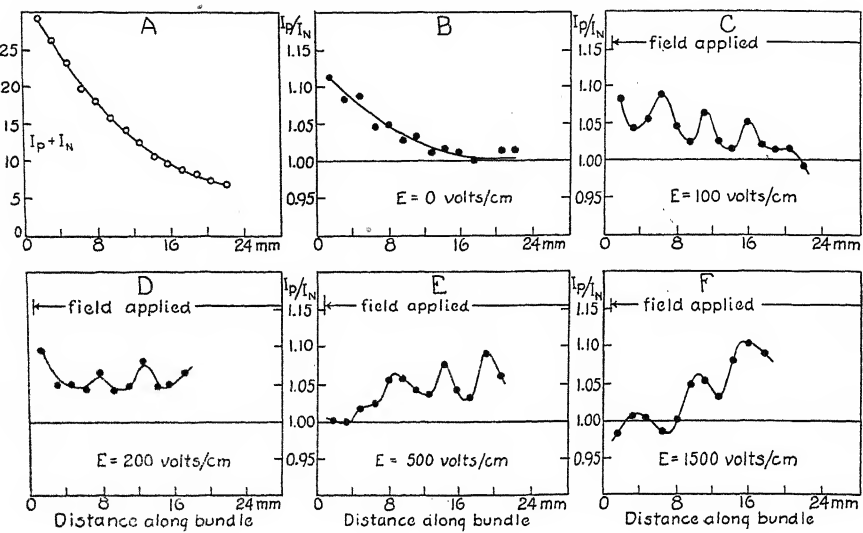


Fig. 5. Showing the variation of intensity and state of polarization of the light along the canal ray bundle. $P=0.080$ mm, $p=0.00034$ mm, $V=6300$ volts, $I=8.0$ m.a., $S=4.1 \cdot 10^7$ cm/sec.

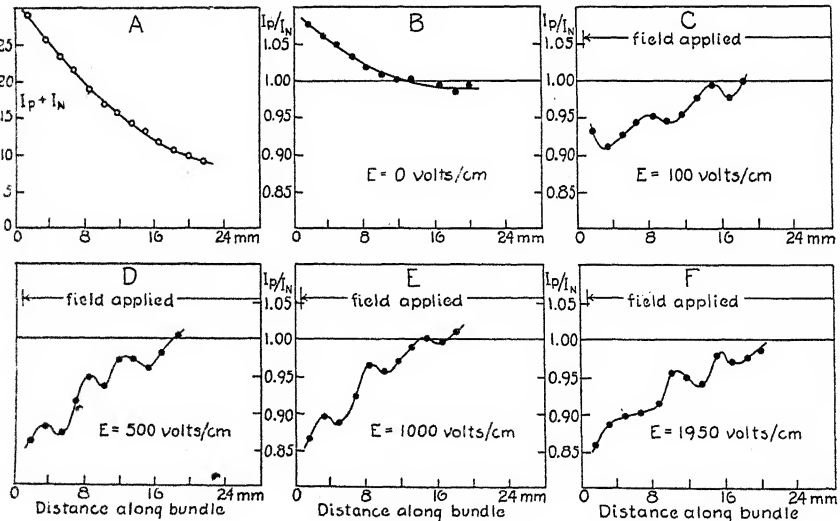


Fig. 6. Showing the variation of intensity and state of polarization of the light along the canal ray bundle. $P=0.0925$ mm, $p=0.00034$ mm, $V=6000$ volts, $I=9.5$ m.a., $S=5.2 \cdot 10^7$ cm/sec.

seen that as the field was increased this last change took place later and later, and in the last two curves (E and F) it did not occur at all. In a similar

way the change that took place as the particles entered the field seemed to occur a little earlier with the stronger fields.

In order to confirm the conclusion that a sudden change in the polarization occurred as the particles passed out of the field, a series of photographs were taken of this region of the bundle. The results obtained are shown in Fig. 4 with the field varied from 15 to 7,600 volts per cm. In every case a change occurred, and in general the change occurred later for stronger fields. For the field of 7,600 volts per cm the change took place about 1 cm beyond the end of the condenser plates. In the two curves *B* and *C* of Fig. 4 there is evidence that after this sudden change took place in the polarization, the polarization once more decreased.

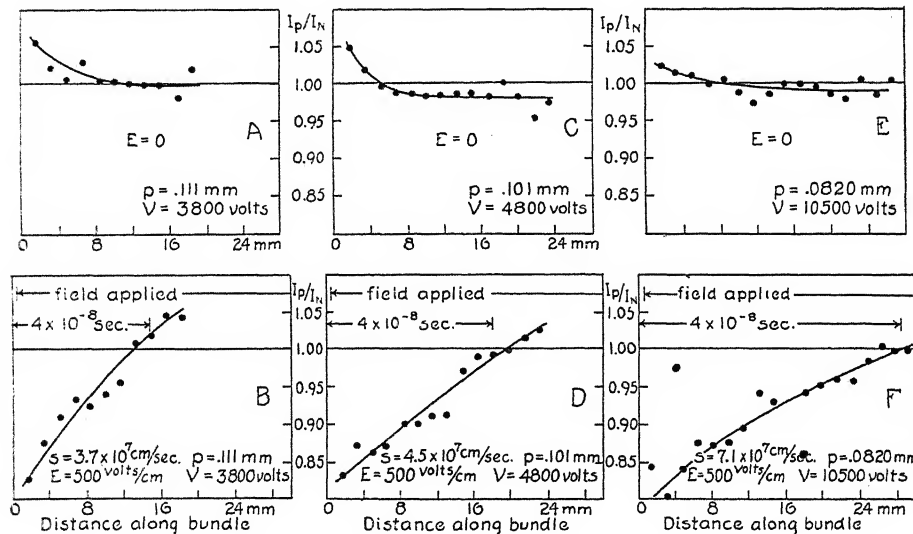


Fig. 7. Showing the variation of the state of polarization of the light along the canal ray bundle for various pressures and potentials in the main discharge tube. $\rho = 0.00035 \text{ mm}$, $I = 8.5 \text{ m.a.}$

The data shown in Figs. 5, 6 and 7 were taken with cathode "*B*" and the observation chamber shown in Fig. 1. The dying out of the polarization is shown in curve *B* of Fig. 5 with no field applied, and *A* is the total intensity curve of the data from *B*. The total intensity was taken as the sum $I_p + I_n$. A smooth curve through the points in *B* gives some idea of the accuracy of the data. If a smooth curve had been drawn through the points in *C* it is plainly seen that the points would be much farther from the curve than in *B*. It is for this reason that a curve was drawn directly through the observed points. When this was done the curve took on the appearance of a "wave" with a certain regularity. In the same way the rest of the curves were drawn directly through the observed points. In the case of *F* another "wave" appears but with a longer wave-length than *C*, and starting in the opposite phase. The curve *E* suggests a combination of two waves, and

when *C* and *F* are combined, with the phase in both of them reversed, a curve almost identical with that of *E* results. The curves in Fig. 6 are drawn just as those in Fig. 5, *A* being the total intensity curve of *B*, and *B* being the polarization curve with no field. Similarly the rest of the curves represent the polarization with various electric fields. If the wave-lengths of *C* in Figs. 5 and 6 are converted into periods of time, 5 *C* gives a period of 1.2×10^{-8} seconds, and Fig. 6 *C* gives 1.3×10^{-8} seconds, the field being 100 volts per cm in both cases. From these data there seems to be some evidence for a periodicity in the polarization in a uniform field, yet the effect is too near the limit of accuracy of the experiment to make the evidence conclusive.

In Fig. 7 the electric field was kept at 500 volts per cm and the pressure in the discharge tube varied to give particles of different velocities. It was found that in the case of the slow moving particles the polarization decreased to zero in a shorter distance than for the faster particles. Since the velocity of the particles was known in each case, the time required for the polarization to reach zero could be calculated. It was found to be about 4×10^{-8} seconds in each case. In these curves the change of polarization produced as the particles entered the field had evidently all taken place before the curves started. This means that the change took place in less than 2×10^{-9} seconds.

When the various photographic plates were compared it was found that the initial polarization appearing in the bundle was not the same for the various plates. No definite reason can be given for this, but it may be due to the presence of small amounts of some impurity like mercury, for it is known that the presence of mercury changes the character of the hydrogen canal rays. The amount of polarization produced as the particles entered an electric field depended upon the strength of the field, increasing rather rapidly with the field until 300 to 500 volts per cm was reached, but after this the increase was small. The amount of polarization introduced also seemed to be independent of the velocity of the particle or the amount of initial polarization.

The bundle was also subjected to a small magnetic field but there was no effect that could be detected.

In conclusion the writer wishes to thank Dr. A. J. Dempster, who suggested the problem, for his interest and helpful suggestions during the investigations.

RYERSON PHYSICAL LABORATORY,
UNIVERSITY OF CHICAGO,
March 3, 1927.

ELECTRON EMISSION FROM THORIATED TUNGSTEN

BY S. DUSHMAN AND JESSIE W. EWALD

ABSTRACT

Constants of the electron emission from a monatomic layer of thorium on tungsten at temperatures from 1000° to 2000°K .—The electron emission for a monatomic layer of thorium on tungsten is best represented for zero field strength by the relation $I = 3T^2e^{-50,500/T}$, where I is expressed in amps/cm². The emission was measured for different states of activation of the filament. If we let θ be the fraction of surface covered with thorium, then for $\theta < 0.95$ (approximately) $\log A_\theta$ varies linearly with b_θ where the emission for the given surface is represented by $I = A_\theta T^2 e^{-b_\theta/T}$. It is also pointed out that the emission for a monatomic film of thorium on tungsten is greater than that observed for metallic thorium.

INTRODUCTORY REMARKS

AS SHOWN in a previous paper¹ the emission data for tungsten and tantalum are in satisfactory agreement with the equation

$$I = AT^2e^{-b_0/T} \quad (1)$$

where A has the value 60.2 amp./cm² degree². The emission data for molybdenum were not in as good agreement, owing largely to the use of a temperature scale which more recent work has shown to be in error.²

Some observations by K. H. Kingdon³ and further experiments by the writers led to the conclusion that in the case of the emission from monatomic layers, Eq. (1) no longer holds true, at least the constant A has a value different from 60.2. It therefore seemed important to obtain data as accurate as possible on the emission for one such case—that of thoriated tungsten.

As shown by I. Langmuir,⁴ the emission from tungsten containing thoria is due to a monatomic layer of thorium on the surface, the thorium atoms being obtained by reduction at high temperatures of some of the thoria throughout the metal and the subsequent diffusion of the thorium atoms to the surface.

EXPERIMENTAL METHOD

In general, most of the emission data obtained by the writers and their associates have been secured with tubes similar to that described in the paper on the emission from tungsten, molybdenum and tantalum, that is the cathode was in the form of a V-shaped filament (total length 10 to 15 cm) and the anode consisted of a calcium deposit on the walls of the tube, as

¹ S. Dushman, H. N. Rowe, Jessie Ewald and C. A. Kidner, Phys. Rev. 25, 338 (1925).

² A recalculation of the electron emission data for this metal on the basis of Worthing's published data for the radiant emissivity (Phys. Rev. 28, 190, 1926) leads to the values $A = 60.2$, $b_0 = 51,300$, which are also in agreement with results obtained by C. Zwicker.

³ K. H. Kingdon, Phys. Rev. 24, 510 (1924).

⁴ I. Langmuir, Phys. Rev. 22, 357 (1923).

shown in Fig. 1 of the above mentioned paper.¹ Some of the data mentioned in the latter part of this paper were taken with such tubes. For the purpose of reference, we will designate such tubes as type A.

However, the most accurate data were obtained on tubes (Type B) in which, instead of a V-shaped filament, a straight filament was used along the axis of the tube, with a molybdenum spring at one end to prevent bowing. Fine tungsten wires were welded onto the leads at each end of the filament and these were used to measure the voltage drop along the filament. The calcium deposit on the wall was obtained from two tungsten spirals (one at each end of the tube) containing calcium wire. A charcoal tube, which was immersed in liquid air during the measurements, was also sealed onto one end of the tube. Whether this extra precaution was really necessary is questionable, as more recent work, carried out since the observations recorded here were made, has shown that the residual oxygen pressure obtained with calcium or magnesium deposited on glass is *much lower* than that obtainable with charcoal in liquid air. However, it is certain that by adopting both these methods of cleaning up residual gases the vacuum attained was so good that the emission from an activated filament remained constant over a long period, and there was no difficulty in obtaining reproducible results.

TEMPERATURE SCALE

The temperature scale for tungsten used is that worked out by Dr. H. A. Jones of this laboratory.⁵

The potential-difference (V) along the filament and the current (A) were measured on precision instruments. A first approximation to the correct temperature was obtained by calculating the value of the function A' ($=A/d^{3/2}$, where d is the diameter). The value of V was then corrected for end-loss effect in the manner indicated in a subsequent section and the corrected value of W' ($=W/ld$ where W is the corrected value of the power input and l is the length) calculated. The corresponding value of T was then obtained from a large scale plot of W' versus T .

Occasional checks on the temperatures calculated in this manner were obtained by direct pyrometry of vacuum lamps made up with the same wire as the filaments in the tubes used for electron emission measurements and aged in the same manner.

The diameter of the wire used was, of course, determined by weighing a long length of it and assuming the density to be 19.35.

LEAD-LOSS CORRECTION

As the filament is cooled near the leads, it is obvious that the potential difference along the filament, watts radiated, or electrons emitted, are less for a given current than they would be if the whole length of filament between leads were at the same temperature. The ratio between the value of the emission (or watts radiated, etc.) calculated for the latter case and that

⁵ H. A. Jones, Phys. Rev. 28, 202 (1926). See also Forsythe and Worthing, Astrophys. J. 61, 126 (1925).

actually observed is designated as the correction factor, f . It is evident that for a given length of filament, the lower the temperature, the greater the value of f ; also that f must increase as the length of filament is decreased. In the case of emission data from thoriated tungsten, the range of temperatures used is much lower (1000–1600°K) than that for tungsten (1500–2300°K). Hence lead-loss corrections are much more important in this work than in the case of the other metals previously investigated.

The values of f were calculated by means of the relations derived by I. Langmuir.⁶ Let H denote any function of the temperature, such as power radiated, luminosity, or electron emission, and let L denote *half the length* of filament between two leads. Also let ΔL_H denote the effective shortening due to cooling at one lead. Then:

$$f = \frac{L}{L - \Delta L_H} = \frac{L dV/dL}{(L - \Delta L_H) dV/dL} = \frac{V + dV}{V + \Delta V - \Delta V_H} \quad (2)$$

where V is *one half* the total potential difference along the filament, ΔV is the correction for voltage drop (due to one lead), ΔV_H is the correction (in volts) for loss in value of H (due to one lead).

For lead-loss correction of potential drop in volts, the relation used was

$$\Delta V = .00013(T - 400) \quad (3)$$

The value of ΔV_H is a complicated function of b_0 and the temperature. In the following table are given the values of ΔV_H used for the case of a surface completely covered with thorium.

$T:$	1000	1200	1400	1600
$\Delta V_H:$	0.415	0.49	0.56	0.625

A method which suggested itself for eliminating the uncertainty in the value of the lead-loss correction consisted in *comparing measurements* on two different lengths of the same wire. This method was also used and the results obtained, as shown in a subsequent section, are in agreement with those obtained on the individual filaments after correcting for the effect of leads.

In the case of partly activated surfaces, b_0 is greater than for the fully activated condition and the value of ΔV_H is also different. In the present paper the values of this correction were obtained from the curves shown in Fig. 11 in the General Electric Review paper by the writers.⁷

CORRECTION FOR ANODE VOLTAGE

As pointed out in a previous paper by the writers,⁸ the observed emission has to be corrected not only for cooling effect of leads, but also for the effect of anode voltage. Schottky has derived the following relation for calculating

⁶ I. Langmuir, Trans. Far. Soc. 17, Part 3 (1921). See also S. Dushman and Jessie Ewald, Gen. Elec. Rev. 26, 154 (1923). A more complete discussion of the method of deriving these formulas will appear in the near future in a paper by I. Langmuir and S. Dushman.

⁷ It is to be noted that in this paper the values of ΔV_H are wrongly given as for *two* leads; whereas they should apply to only *one* lead.

the emission at zero field strength (i_0) in terms of the emission, i_V , at field strength dV/dx

$$\log_{10} i_V = \log_{10} i_0 + 4.39(dV/dx)^{1/2}/2.30T \quad (4)$$

(It is assumed that the space currents are much below those corresponding to space charge,—a condition which was fulfilled in all cases.)

Schottky actually showed the validity of this relation for anode voltages up to 5000 for conditions in which the maximum value of dV/dx was considerably greater than those existing in the tubes used in the present investigations. More recent work by Mr. N. B. Reynolds in this laboratory has shown that Eq. (4) is also applicable to thoriated tungsten filaments for field strengths which are many times greater than those worked with in the present investigation.

According to this equation the values of i_0 for a given tube are obtained by plotting $\log i_V$ against $V^{1/2}$ at constant temperature. From the values of $\Delta \log i / \Delta V^{1/2}$ obtained for different temperatures an average value of $T \Delta \log i / \Delta V^{1/2}$ was derived and this was then used to calculate the value of i_0 at each temperature.

EMISSION DATA FOR FULLY ACTIVATED SURFACES

The most accurate data were obtained from measurements with two tubes, K-363 and K-364, which were made up with axially located filaments and special voltage leads, as described in a previous section. The tungsten wire used contained approximately 1.8 percent ThO₂, and had a diameter of 0.00876 cm.

Tube	Filament Length	Area
364	15.94 cm	0.438 cm ²
363	8.05	0.221

$$L_1 - L_2 = 7.89 \quad S_1 - S_2 = 0.217$$

While exhausting the tubes on the condensation pump, they were baked out for 2 hours at slightly above 360°C, in order to remove all gases from the

TABLE I
Data for determination of temperature scale.

Filament current (amp.)	P. D. along filament (volts)		$V_1 - V_2$ 7.89	Corrected P. D. along filament (volts)		W'	T
	K363	K364		K363	K364		
0.25	0.792	1.73	0.119	0.96	1.90	3.40	1109
.30	1.085	2.34	.160	1.285	2.55	5.47	1209
.35	1.421	3.025	.203	1.635	3.24	8.10	1300
.40	1.796	3.769	.250	2.01	3.99	11.40	1385
.45	2.203	4.587	.302	2.43	4.82	15.50	1469
.50	2.642	5.454	.356	2.87	5.68	20.30	1545
.55	3.105	6.387	.416	3.35	6.63	26.10	1621
.60	3.610	7.372	.476	3.83	7.60	32.62	1695
.80	5.886	11.854	.757	6.10	12.09	69.20	1942
1.00	8.637	17.250	1.091	8.79	17.42	125.0	2220

TABLE II
Emission data for calculating the thermionic constants of thoriated tungsten filaments.

Emission data K-364					K-363	Difference in emission		
T	i_0	f	$\log_{10} I + 6$	f(obs)	i_0	Δi_0	$\log_{10} I + 6$	$(I/T^2) + 12$
1109	1.17×10^{-6}	1.93	0.713	1.80	1.31×10^{-7}	1.04×10^{-6}	0.679	0.589
1151	3.18	1.77	1.109	1.63	6.24	2.56	1.072	.950
1209	1.40×10^{-5}	1.63	1.717	1.55	3.29×10^{-6}	1.07×10^{-5}	1.692	1.527
1244	3.17	1.56	2.052	1.50	8.34	2.34	2.033	1.843
1300	1.09×10^{-4}	1.48	2.565	1.52	2.67×10^{-5}	8.23	2.579	2.351
1336	1.94	1.44	2.805	1.36	6.27	1.31×10^{-4}	2.780	2.528
1385	5.38	1.39	3.232	1.42	1.59×10^{-4}	3.79	3.240	2.957
1421	9.46	1.36	3.467	1.36	3.08	6.38	3.468	3.163
1469	2.09×10^{-3}	1.32	3.800	1.32	7.23	1.37×10^{-3}	3.800	3.466
1500	3.32	1.30	3.993	1.24	1.29×10^{-3}	2.03	3.971	3.619
1545	7.14	1.28	4.319	1.29	2.54	4.60	4.326	3.948

glass walls and from the charcoal; the filaments were then flashed at about 2400°K for a couple of minutes and the calcium evaporated onto the walls. The exhaust was continued for a few minutes and the tubes sealed off.

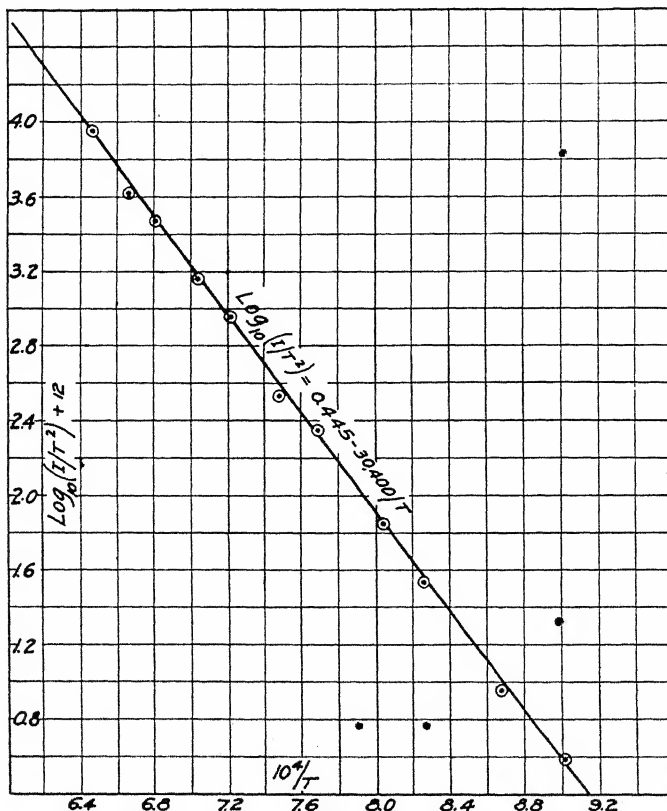


Fig. 1. Values of $\log (I/T^2)$ plotted against $10^4/T$. Tube K363.

Before taking data, the filaments were aged for 3 hours at 2400°K and then flashed for 1.5 minutes at 2900°K to reduce thoria. They were then activated at 2100°K or lower to a maximum emission, using 1500°K as testing temperature.

The data for the determination of temperature scale are given in Table I, while Table II gives the emission data used for calculating the thermionic constants. Under i_0 are given the emission data (after correcting for anode voltage), and in the case of K-364 there are also given the values of f used in calculating $\log I$ for each value of T . The differences between the values of i_0 at constant T for the two filaments are tabulated under Δi_0 and the last two columns give the corresponding values of $\log I$ and $\log (I/T^2)$.

From these values of $\log I$ and the values of i_0 observed for K-364 values of the correction factor for the latter filament were calculated. These are given under f (obs.).

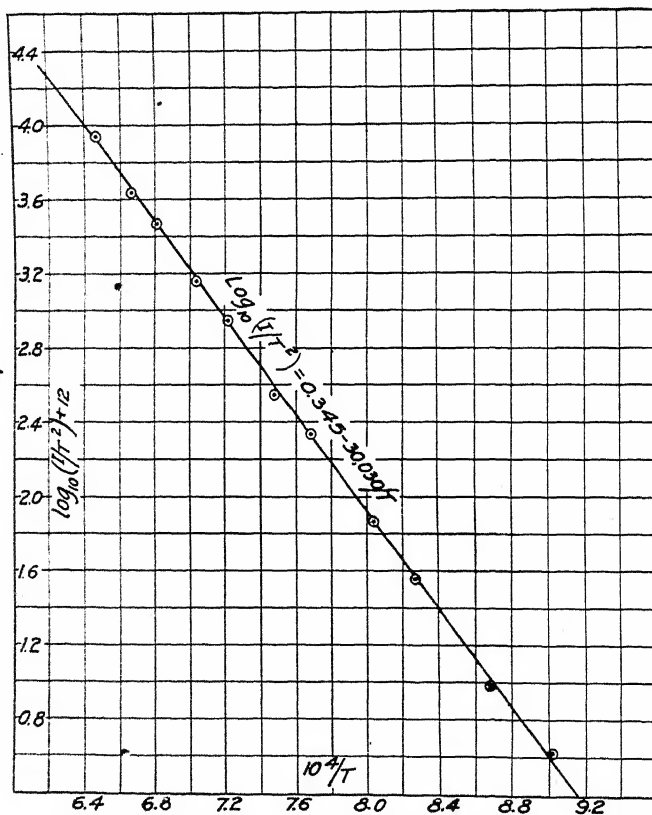


Fig. 2. Values of $\log (I/T^2)$ plotted against $10^4/T$. Tube K364.

Fig. 1 shows a plot of the values of $\log (I/T^2)$ given in the last column of Table II. Using the method of least squares these data give the values

$$A = 2.85 \text{ amps}/(\text{cm}^2\text{deg.}^2); b_0 = 30,400 \text{ (deg. K).}$$

Fig. 2 shows a similar plot of the data obtained for K-364. The resulting values are:

$$A = 2.21, \quad b_0 = 30,030.$$

While the values of A and b_0 calculated for each set of data are slightly different, it is evident from the data given in Table II as well as the plots in the two figures, that the emission data are practically identical.

SOURCES OF ERROR

The possible sources of error involved in an accurate determination of the thermionic constants for an electron emitter such as a monatomic film of thorium on tungsten are even more numerous than those involved in measurements with pure metals. In the following section these are discussed briefly.

Incomplete activation. In order to obtain a completely covered film, special care must be taken to activate the filament for a long period at as low a temperature as possible. The exact procedure differs not only with the diameter of the filament, but also with the content of thoria and other factors which depend upon the previous metallurgical history of the wire. As will be shown in a subsequent section, a surface which is only 99 percent covered gives an emission which is approximately 90 percent of that of a fully covered film.

Positive ion bombardment. Even an extremely low pressure of residual gas (10^{-6} mm of Hg or less) will cause a considerable decrease in emission owing to bombardment by positive ions, and as shown by Kingdon, this effect increases rapidly with anode voltage. This was avoided in the present investigation by using calcium volatilized on the glass.

Temperature scale. This is undoubtedly the greatest source of error in all emission measurements. As it was impracticable to pyrometer the filaments *in situ*, the temperatures were calculated from the corrected power input or from the values of $V'A'^{1/3}$. However, for the same radiation intensity, different filaments may vary in temperature by as much as one percent from the average values given in the tables of characteristics, depending not only on the aging schedule, but also on the nature of the wire.

Now since

$$dI/I = (2 + b_0/T)dT/T$$

it is evident that a one percent change in temperature at $T=1000$ causes a 30 percent change (approximately) in emission. Thus it is quite possible, especially at lower temperatures, to obtain a variation in emission at apparently the same temperature of as much as 30 percent.

End loss correction. The data for K-363 illustrate well the cooling effect of leads on short filaments. The values of f calculated for this case ranged from 1.75 at $T=1545$ to 2.12 at 1421 and to much greater values at lower temperatures. Consequently no accurate calculations could be made on the basis of the data for this tube alone. However, an inspection of Table II

shows that when the data for K-364 and K-363 were combined, values of $\log I$ were obtained which were in good agreement with those obtained with K-364 alone, after introducing a correction for end loss. The agreement between values of f (obs), calculated in the manner discussed in a previous section, and values of f as actually used, is satisfactory, as it is within the limits of error of temperature determination.

Obviously the correction for end losses could be avoided by a construction of tube involving the guard ring principle. Data obtained on such a tube (No. 204) are given in Table III. The filament used had a diameter of 0.0103 cm and a total length of 19.65 cm. The length of the central portion on which emission data were taken was 10.3 cm. The anode consisted of three separated magnesium deposits on the glass wall.

TABLE III

Data obtained with tube in which end corrections were made unnecessary by the use of guard rings.

T	$\log (I/T^2) + 12$	$10^3/T$	I	T (calc)
1155	.9368	.8658	1.15×10^{-5}	1148
1216	1.4998	.8224	4.67	1208
1276	2.0150	.7836	1.69×10^{-4}	1266
1335	2.4579	.7491	5.12	1323
1385	2.8600	.7219	1.39×10^{-3}	1378
1453	3.3077	.6882	4.29	1447
1515	3.7100	.6601	1.18×10^{-2}	1511
1612	4.2738	.6204	4.88	1615

The fourth column gives the values of I (after correcting for Schottky effect) as calculated from the emission measurements on the central portion of the filament, while the second column gives corresponding values of $\log (I/T^2)$. The values of the thermionic constants obtained from the plot were $A = 6.2$; $b_0 = 31,600$.

Comparing emission data as observed at corresponding temperatures, on this tube and on K-363, it is found that the latter are slightly higher. The last column of Table III gives values of T which would correspond to the observed values of I if we assume the thermionic constants $A = 3$, $b_0 = 30,500$, which, as will be pointed out below, we believe to correspond to maximum emission data.

The difference between the values of T (calc) and values given in the first column is within the limits of experimental error, especially at the lower temperatures.

THERMIONIC CONSTANTS FOR FULLY ACTIVATED SURFACE

While observations have been made on a number of other tubes, the writers believe that the data obtained on K-364 and K-363 are the most accurate, since they correspond to maximum emission observed at any temperature. Taking into consideration the different possible sources of error, these results are best represented by the thermionic constants

$$A = 3.0; b_0 = 30,500.$$

Table IV gives emission data calculated for the range $T = 1000$ to $T = 2000^\circ\text{K}$. It is necessary to observe in this connection that owing to evapora-

tion of thorium, the actually observed emission tends to be less than that given in the table at temperatures above 1800°K approximately. The third column in this table gives the efficiency of emission in amperes per watt—a property which is of extreme importance in the practical utilization of such

TABLE IV

Emission data for a thoriated tungsten filament calculated for the range 1000° to 2000°K.

<i>T</i> (°K)	<i>I</i> (amp/cm ²)	<i>I/W</i> (amp/watt)	$d \ln I / d \ln T$
1000	1.73×10^{-7}	2.86×10^{-7}	32.5
1100	3.31×10^{-6}	3.21×10^{-6}	29.7
1200	3.95×10^{-5}	2.37×10^{-5}	27.4
1300	3.27×10^{-4}	1.27×10^{-4}	25.5
1400	2.03×10^{-3}	5.28×10^{-4}	23.8
1500	1.00×10^{-2}	1.811×10^{-3}	22.3
1600	4.06×10^{-2}	5.22×10^{-3}	21.1
1700	1.40×10^{-1}	1.29×10^{-2}	20.0
1800	0.428	3.03×10^{-2}	19.0
1900	1.164	6.28×10^{-2}	18.
2000	2.864	1.20×10^{-1}	17.3

filaments. The last column gives the value of the exponent *n* in the approximate equation

$$I = A T^n, \text{ where obviously } n = 2 + b_0/T.$$

The emission data actually obtained with different sizes of wire and in various types of tubes may vary from the values given in Table XI by as much as 25 percent, owing to experimental errors, such as those mentioned in previous paragraphs.

The following table (V) gives a comparison between emission data as observed on various tubes and values calculated from the observed power input in accordance with data given in Table IV. In all cases, corrections were made for lead losses and Schottky effect.

TABLE V

Comparison of emission data observed with values calculated from data of Table IV.

Tube No.	<i>T</i>	<i>I</i> (obs.)	<i>I</i> (calc.)
202	1450	3.2×10^{-3}	4.3×10^{-3}
	1650	5.25×10^{-2}	7.2×10^{-2}
	1212	4.8×10^{-5}	5.0×10^{-5}
	1352	7.7×10^{-4}	8.5×10^{-4}
	1473	7.6×10^{-3}	6.5×10^{-3}
161	1030	3.3×10^{-7}	4.5×10^{-7}
	1100	2.6×10^{-6}	3.3×10^{-6}
	1190	2.7×10^{-5}	3.0×10^{-5}
	1290	2.3×10^{-4}	2.6×10^{-4}
	1403	1.9×10^{-3}	2.0×10^{-3}
	1528	1.9×10^{-2}	1.6×10^{-2}

In each of these tubes the wire used was approximately 0.010 cm in diameter, but differed in thoria content and also in regard to other manufacturing details. The agreement between *I* (obs.) and *I* (calc.) is within the limits of experimental error in practically all the cases.

The following data (Table VI) were obtained with a thoriated wire 0.00403 cm diam. (1.59 mil) such as used in construction of commercial UX-201A tubes. The tubes used for this experiment were exhausted in the same manner as commercial 201A tubes. The filaments ($l=4.45$ cm) were mounted in the axis of a 0.5 inch diameter cylinder (about 1.5 inches long). The temperature was calculated from the observed power input (after correcting for lead-loss). The table gives the potential drop along the filament and the filament current, as well as the observed emission, while the last column gives the value of I (calc.) as taken from a curve plotted from the data in Table IV.

TABLE VI

Observed and calculated thermionic emission in a tube whose thoriated filament and manner of exhaustion were similar to those of the commercial 201A tubes.

Filament current (amp)	P. D. along filament (volts)	T	Emission at 100 volts (milliamp)	I (obs)	I (calc)
0.22	4.00	1825	24.0	0.595	0.550
.20	3.36	1740	9.7	.253	.220
.18	2.88	1650	3.05	.084	.076
.16	2.32	1550	0.82	.025	.021

The difference between I (obs.) and I (calc.) is easily accounted for by the effect of anode voltage. Recalculated for zero field strength the values of I (obs.) would have to be decreased about 10 to 15 percent.

As a matter of fact, numerous series of observations on commercial radio-trons containing thoriated filaments show uniformly good agreement with the values given in Table IV, after allowances are made for lead losses and probable error in temperature determination, provided, of course, that care has been taken to activate the filament completely.

VARIATION IN EMISSION WITH DEGREE OF ACTIVATION

Langmuir has defined θ , the fraction of the surface covered with thorium atoms, thus:

$$\theta_1 = (b_\theta - b_W) / (b_{Th} - b_W) \quad (5)$$

where b_θ , b_{Th} and b_W represent the work functions for the partly covered surface, completely covered surface, and pure tungsten respectively.

For approximate calculation of θ , Langmuir has also used the relation

$$\theta_{II} = (\log I_\theta - \log I_W) / (\log I_{Th} - \log I_W) \quad (6)$$

where I_θ is the emission observed for the incompletely covered surface, I_W is the emission for pure tungsten, and I_{Th} is the emission for a surface completely covered with thorium.

Of these two methods for calculating θ , the first is the correct one from a theoretical point of view and should be used when values of the constant b_θ are available. On the other hand, Eq. (6) is very convenient to use in

practice, and usually leads to values of θ which are not very different from those obtained by use of the more rigorous equation.

The condition which has to be fulfilled in order that $\theta_I = \theta_{II}$ is easily determined as follows: Assume $I_\theta = A_\theta T^2 e^{-b_\theta/T}$ with similar relations involving A_{Th} and A_W for the fully activated and pure tungsten surfaces respectively. Then

$$\theta_I = \frac{\log(A_\theta/A_W) - \beta_\theta/T}{\log(A_{Th}/A_W) - \beta/T}$$

where $\beta = b_{Th} - b_W$ and $\beta_\theta = b_\theta - b_W$. But $\theta_{II} = \beta_\theta/\beta$; hence $\theta_I = \theta_{II}$ if

$$\frac{\beta_\theta}{\beta} = \frac{\log(A_\theta/A_W)}{\log(A_{Th}/A_W)}$$

i.e., if

$$\log A_\theta = \log A_W - \beta_\theta(\log A_W - \log A_{Th})/\beta \quad (7)$$

That is, $\log A_\theta$ should be a *linear function* of β_θ . As will be shown, the experimental data do not lead to any such conclusion, and, therefore, the two definitions cannot be equivalent.

EMISSION DATA ON PARTLY ACTIVATED SURFACES

The most accurate series of data of this nature were taken with the tube K-364 described above. While emission data were also taken for different degrees of activation with tube K-363, they were not considered as very reliable. Firstly, for lower values of θ the emission at low temperatures decreased so much that with the instruments available no emission measurements could be obtained at temperatures below about $1300^\circ - 1400^\circ\text{K}$, while at higher temperatures (about 1650°K) the filaments begin to activate (that is, thorium diffusion begins to occur) at a rate, which, although very slow, is sufficiently great to interfere with accurate measurements. For pure tungsten itself, the lowest temperature at which emission data could be taken, with the instruments used, is about 1500°K . Therefore, it proved extremely difficult to obtain reliable emission data on deactivated surfaces for which θ approaches 0.20.

Table VII summarizes the results obtained with K-364 for different states of activation. The values of θ were calculated by means of Eq. (5) using the values $b_{Th} = 30,500$, $b_W = 52,400$.

TABLE VII
Results obtained with tube K-364 for different states of filament activation.

θ	A	b_θ	$\log_{10} A$
0.95	1.50	31,460	0.176
.83	2.08	34,150	.318
.72	3.74	36,570	.573
.56	7.76	40,070	.890
.43	10.86	42,840	1.037
.25	15.81	47,050	1.199
.18	(8.2)	48,360	.914

Plotting $\log A_\theta$ against b_θ (see Fig. 3) it is observed that above a minimum value (corresponding to $b_\theta = 31,500$) four out of six points lie on a straight line passing through the value of $\log A = 1.78$ which corresponds to pure tungsten. The values of A for $\theta = 0.25$ and $\theta = 0.18$ were obtained from data which were not nearly as reliable as those obtained for larger values of θ .

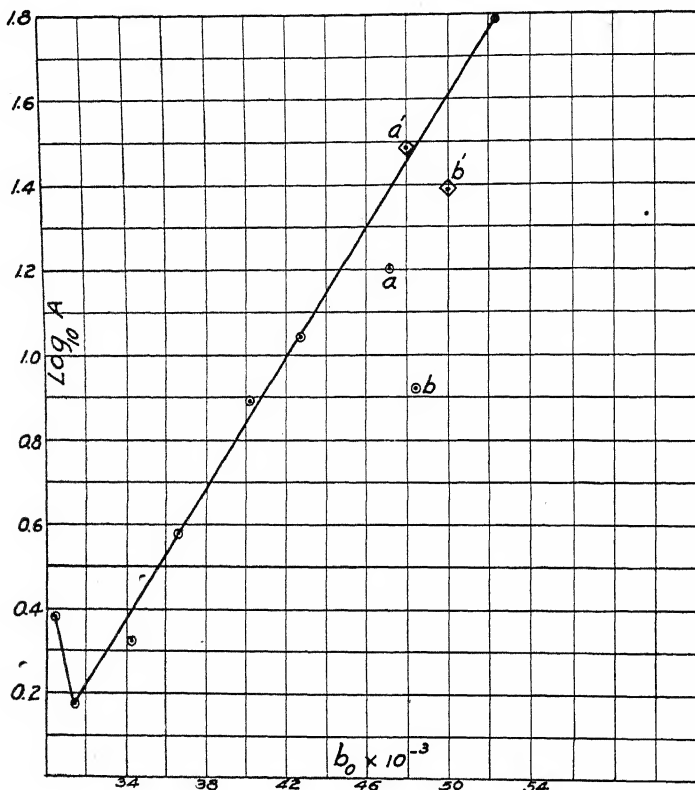


Fig. 3. Plot of $\log A_\theta$ against b_θ .

In a discussion of these results with Dr. Kingdon, he suggested that a formula of the form

$$A_\theta = A_W(1-\theta)^n + A_{Th}\theta^n$$

might fit the observed data, since such an expression passes through a minimum value as θ is decreased. Empirically, it was found that $n = 2.5$ gives a better agreement with the observations than larger or smaller values of n , but it is even less satisfactory than the linear relation between $\log A_\theta$ and b_θ suggested above.

One fact that must be considered is this, that a relatively small change in b_θ affects the value of A_θ a great deal. Thus, in the case of $b_\theta = 47,050$, if this value is decreased to $b_\theta = 48,000$, the resulting value of A_θ for constant emission at $T = 1500$, is found to be 29.8, which brings this point almost on the straight line.

Similarly for constant emission at $T=1500$, the values $A_\theta=24.6$ and $b_\theta=50,000$ correspond to $A_\theta=8.2$ and $b_\theta=48,360$. It should be stated that the emission data on which the latter values were based were taken over the range $T=1421$ to $T=1575$, which was undoubtedly too low a range for any great degree of accuracy.

From these considerations it would appear that the actual observations are not in disagreement with the tentative conclusion that from $\theta=0.95$ to $\theta=0$, $\log A$ varies linearly with b_θ (and therefore with θ).

Observations on other tubes, although not so accurate, were found to be in qualitative agreement with the observations discussed above in the conclusion that A_θ passes through a minimum value for a value of θ close to unity, as b_θ is increased.

DISCUSSION OF RESULTS

In the earlier paper published by the writers,¹ the work function b_0 for a completely activated surface was given as 34,100. This was calculated on the assumption that $A=60.2$. However, it was observed that the actual slope of $\log (I/T^2)$ against $1/T$ gave consistently lower values of b and it was assumed that this was probably due to errors in temperature scale. Since then, Dr. Jones has completed his work on this problem and on the basis of his results the earlier emission data are found to be in very good agreement with the data given in this paper.

K. H. Kingdon³ has also published emission data for thoriated tungsten, for both the completely activated and incompletely activated surfaces. Using the guard ring principle he obtains for $\theta=1$, the values $A=7$, $b_0=31,200$ (at anode potential of 150 volts), and for partly activated surfaces, the relation

$$A_\theta = (7^\theta + 60^{1-\theta} - 1) \text{ amps}/(\text{cm}^2\text{deg.}^2)$$

Values of θ were calculated from observed values of b_θ by means of Eq. (5).

The filament temperatures were determined from the heating current and Dr. Kingdon believes that the accuracy of his temperature determination was therefore not as great as that obtained in the present investigation. At $T=1000$, the emission calculated on the basis of Kingdon's constants is practically identical with that given in Table IV, while at $T=1500$, Kingdon's constants lead to a value 50 percent greater, which is probably to be accounted for by two sources of error: (1) failure to correct for effect of anode voltage, and (2) difference of about 1 percent in temperature at the upper point of his working range.

Kingdon's observations on the variation of A_θ with b_θ are in qualitative agreement with those obtained in the present work, but there is a lack of quantitative agreement.

INTERPRETATION OF OBSERVED VALUE OF A FOR COMPLETELY COVERED FILM OF THORIUM ON TUNGSTEN

Careful measurements on tungsten, molybdenum and tantalum in this laboratory, as well as similar measurements by Germer and Davisson on

tungsten and by C. Zwikker⁸ on tungsten and thorium lead to the conclusion that for at least these four metals the constant A has the value 60.2 (within the probable limits of error in determination of temperatures).

The writers believe that this conclusion is probably valid for all pure metals (subject to slight differences due to effect of surface charge, as pointed out by Bridgman⁹). On the other hand, the present observations for the case of monatomic layers of thorium on tungsten, Kingdon's measurements for caesium on tungsten, and the results obtained for Wehnelt cathodes show that for these surfaces A is less than 60.2.

It is of interest in this connection to point out that while A is less than 60.2 for a monatomic layer of thorium on tungsten, the value of b for the monatomic layer is less than that for metallic thorium, as is evidenced by the published data of Zwikker and is also confirmed by recent measurements in this laboratory on some thorium wire kindly provided by Dr. Myers of the Research Laboratory of the Westinghouse Company.

Also some recent measurements in this laboratory on monatomic layers of zirconium on tungsten¹⁰ show that in this case $A = 5$ and $b_0 = 36,500$, while for metallic zirconium Zwikker gives the values $A = 3000$, $b_0 = 52,200$. Thus the emission over the range of working temperatures is lower for metallic zirconium than for the film.

There is, therefore, every reason for believing that for all cases where we have a monatomic layer of a more electropositive metal on another metal, the value of A is less than 60.2. On the other hand, for surfaces more or less partly covered with oxygen, A is greater than this value, and the same conclusion apparently holds true in all cases where we have a monatomic layer of a more electronegative element, as, for instance, phosphorus or iodine on tungsten.¹¹

The significance of these deviations in the value of A from the so-called constant value is probably to be found in a consideration of Bridgman's theory of the effect of surface charges and of the validity of the third law for monatomic films. The discussion of this subject must, however, be deferred for further consideration in a paper by Dr. L. Tonks and the first named writer, which will appear in the near future.

RESEARCH LABORATORY,
GENERAL ELECTRIC COMPANY,
December 31, 1926.

⁸ C. Zwikker, Proc. Royal Academ. Amsterdam **29**, 792 (1926).

⁹ P. Bridgman, Phys. Rev. **14**, 306 (1909).

¹⁰ To be published in the near future.

¹¹ As shown by observations made by the writers.

NEUTRALIZATION OF THE DEFLECTING FIELD IN A BRAUN TUBE WITH EXTERNAL ELECTRODES

By L. T. JONES AND A. M. CRAVATH

ABSTRACT

The field of the external electrodes is rapidly neutralized by the collection of ions and electrons on the tube walls so that the deflection is not simply proportional to the applied voltage. The neutralization proceeds like the discharge of a condenser through a resistance for which the time constant is $RC = \tau$. This time constant τ , which is a reciprocal measure of the rate of neutralization, was calculated from current measurements made with internal electrodes together with the dimensions of the tube, and was also measured directly by photographing the variation of deflection with time, the respective values for a certain tube being 0.002 sec. calculated, and from 0.001 to 0.005 sec. measured under different conditions. The deflection of the beam is found as a function of τ and the applied voltage, and in particular the expressions for amplitude and phase of deflection for sinusoidal applied voltage are derived, the results being

$$D = V_0 S \cos \delta \sin (2\pi f t + \delta)$$

$$\delta = \cot^{-1} 2\pi f \tau$$

where D is beam deflection, V_0 the applied voltage, f the frequency, and S is a constant of the tube.

1. INTRODUCTION

THE present paper deals with a problem which arose in the investigation of Jones and Tasker¹ on the Braun tube with external electrodes, namely, the determination and explanation of the relation between deflection of the beam, and the applied voltage and time. The type of tube used is shown in Figures 1 and 5, and its functioning is described in the previous paper.

When a potential difference is suddenly applied to the external electrodes, the beam is of course deflected at first, but the electrons returning from the end of the tube are drawn to the wall next the positive electrode and the positive mercury ions formed by collision with the mercury vapor atoms are drawn to the wall next the negative electrode. The field inside the tube is thus rapidly neutralized and soon becomes zero. Neutralization also occurs when an alternating voltage is applied, the result being a change in phase and amplitude.

A quantitative theory for the latter case was developed in this laboratory in an unpublished paper by R. A. Jack. In the present paper the theory is modified and generalized and checked by comparing the neutralizing current of ions and electrons necessary to give the observed neutralization with the observed current between large internal electrodes in a tube otherwise similar.

¹ Jones, and Tasker, Jour. Opt. Soc. Am. 9, 471 (1924).

2. THEORETICAL DEVELOPMENT OF EQUATIONS FOR THE DEFLECTION

If, leaving other things unchanged, we were to silver the parts of the inner surface of the walls of the tube which lie between the external electrodes, thus obtaining insulated internal electrodes, the collection of ions and electrons on the tube walls would not be changed on the average, but would merely be somewhat differently distributed because of the more uniform potential distribution. We shall therefore treat the problem as if there exists such a pair of internal electrodes, B_1 and B_2 , between the external electrodes A_1 and A_2 . B_1 and B_2 are charged inductively from A_1 and A_2 and then discharged by the current of ions and electrons. We shall make the further assumption, to be discussed later, that this ion-and-electron neutralization current is proportional to the potential difference V between B_1 and B_2 , i.e., that the ions and electrons act like a high resistance R connected between B_1 and B_2 . Since the beam deflection is proportional to the potential difference between the walls, our problem is to find this potential difference V . In the general electrostatic equations

$$\left. \begin{aligned} V_{B1} &= p_{B1B1}Q_{B1} + p_{B1B2}Q_{B2} + p_{B1A1}Q_{A1} + p_{B1A2}Q_{A2} \\ V_{B2} &= p_{B2B1}Q_{B1} + p_{B2B2}Q_{B2} + p_{B2A1}Q_{A1} + p_{B2A2}Q_{A2} \\ V_{A1} &= p_{A1B1}Q_{B1} + p_{A1B2}Q_{B2} + p_{A1A1}Q_{A1} + p_{A1A2}Q_{A2} \\ V_{A2} &= p_{A2B1}Q_{B1} + p_{A2B2}Q_{B2} + p_{A2A1}Q_{A1} + p_{A2A2}Q_{A2} \end{aligned} \right\} \quad (1)$$

V_{B1} is the potential of B_1 , etc., the p 's are the potential coefficients, constants of the tube, and the Q 's are the quantities of electricity. In general $p_{\alpha\beta} = p_{\beta\alpha}$. From this and the symmetry of the apparatus we have:

$$\left. \begin{aligned} p_{A1B2} &= p_{B2A1} = p_{A2B1} = p_{B1A2} \\ p_{A1B1} &= p_{B1A1} = p_{A2B2} = p_{B2A2} \\ p_{A1A2} &= p_{A2A1}, \quad p_{B1B2} = p_{B2B1} \\ p_{A1A1} &= p_{A2A2}, \quad p_{B1B1} = p_{B2B2} \end{aligned} \right\} \quad (2)$$

The above equations give

$$\begin{aligned} V &= V_{B1} - V_{B2} = (Q_{B1} - Q_{B2}) \{ p_{B1B1} - p_{B1B2} - (p_{B1A1} - p_{B1A2})^2 / (p_{A1A1} - p_{A1A2}) \} \\ &\quad + (V_{A1} - V_{A2})(p_{B1A1} - p_{B1A2}) / (p_{A1A1} - p_{A1A2}) = (Q + V_a C_a) / C_b \end{aligned} \quad (3)$$

where $Q = \frac{1}{2}(Q_{B1} - Q_{B2})$ is the quantity of electricity transferred in neutralization, V_a is the potential difference applied to the external electrodes, and C_a and C_b are constants. To determine the significance of C_a , suppose B_1 and B_2 to be connected. Then $V = 0$, and

$$C_a = -Q/V_a$$

Hence we see that C_a is the ratio of the charge induced on the electrodes B_1 and B_2 to the inducing potential difference applied to the electrodes A_1 and A_2 . Next, short-circuit A_1 and A_2 , making $V_a = 0$. Then

$$C_b = Q/V$$

and we see that C_b is the capacity between B_1 and B_2 when A_1 and A_2 are connected together.

Differentiating Eq. (3) with respect to time gives

$$\frac{dV}{dt} = \frac{C_a dV_a/dt + i}{C_b}$$

We have assumed

$$i = -V/R$$

where the minus sign appears because the positive direction of i is the direction which gives positive Q_{B1} and is hence against the field. The equation now becomes

$$\frac{dV}{dt} = \frac{C_a dV_a/dt - V/R}{C_b}$$

for which the solution is

$$V = \frac{C_a}{C_b} e^{-t/RC_b} \left(\int e^{t/RC_b} \frac{dV_a}{dt} dt + \text{const.} \right) \quad (4)$$

We see that the characteristics of the tube enter in two terms, the constants C_a/C_b , and RC_b . The first, C_a/C_b , depends on the dimensions and positions of the electrodes, and merely affects the scale of the deflections. The more important term is the second, RC_b , which influences the variation of deflection with time. It is the time constant for the exponential discharge of B_1 and B_2 through R when A_1 and A_2 are short circuited. We shall call it the time constant of the tube and designate it by τ . Since the deflection of the beam, D , is proportional to V , (4) gives

$$D = S e^{-t/\tau} \left(\int e^{t/\tau} \frac{dV_a}{dt} dt + \text{const.} \right) \quad (5)$$

where S is a constant. This is the general equation for the deflection in terms of the applied voltage and time.

The deflection was photographed. The deflecting voltage V_a was that across a condenser of capacity C_1 which was being charged and discharged through a resistance R_1 , the time constant being $C_1 R_1 = \kappa$. For these cases

$$V_a = V_0 (1 - e^{-t/\kappa}) \quad \text{and} \quad V_a = V_0 e^{-t/\kappa}$$

For both charge and discharge Eq. (5) now gives

$$D = \left\{ S V_0 / (\kappa / \tau - 1) \right\} (e^{-t/\kappa} - e^{-t/\tau}) \quad (6)$$

the only difference between the two cases being a reversal of the direction of deflection. The simple case of an instantaneously applied or removed constant voltage is obtained by making $\kappa = 0$. Eq. (6) then reduces to the simple exponential decay

$$D = S V_0 e^{-t/\tau} \quad (7)$$

If the applied voltage is sinusoidal, i.e., $V_a = V_0 \sin \omega t$, Eq. (5) gives

$$\begin{aligned} D &= \left\{ V_0 S \tau \omega / (1 + \tau^2 \omega^2)^{1/2} \right\} \sin (\omega t + \cot^{-1} \tau \omega) \\ &= V_0 S \cos \delta \sin (\omega t + \delta) \end{aligned} \quad (8)$$

where $\delta = \cot^{-1} \omega \tau$ is the angle by which the deflection *leads* the applied voltage.

The above theory was checked in two ways: first, by comparing the shape of photographic deflection curves with the shape of the curves predicted by the above equations, and secondly by the more significant method of comparing the value of τ found from the observed deflection with the value calculated from R and C_b . The determination of R requires the measurement of the neutralizing current for known potential difference between the walls.

3. MEASUREMENTS OF NEUTRALIZING CURRENT

To find R we used special tubes, Fig. 1, and measured the currents between large internal electrodes about 3×10 cm spaced 1.3 cm apart which took the place of the tube walls or "electrodes" B_1 and B_2 of the tube with

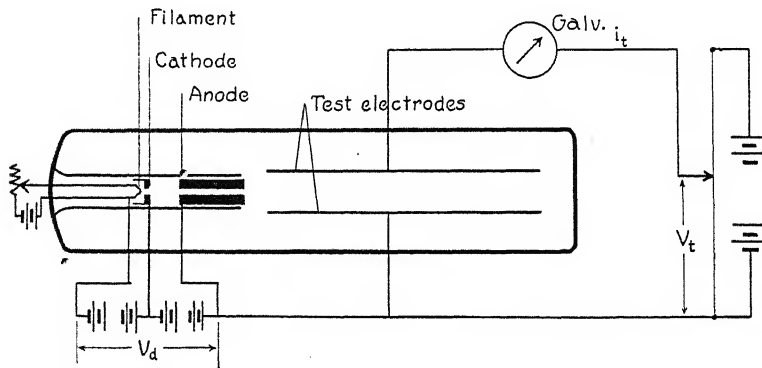


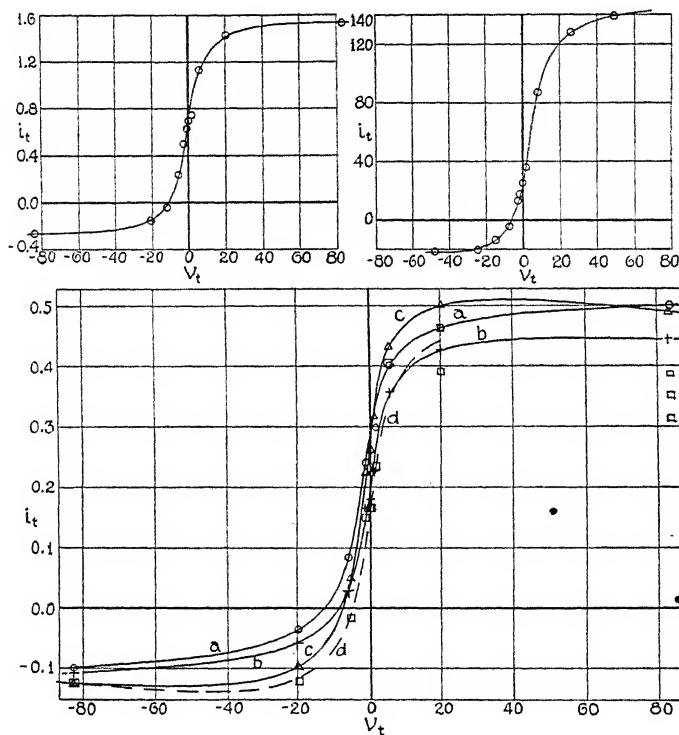
Fig. 1. Tube and connections for current measurements with internal electrodes.

external electrodes. The filaments, cathodes, anodes, and atmospheres in these tubes were the same as in the tube with external electrodes except that tube No. 1 had a slow leak and was fitted with a side tube containing thorium which could be heated to renew the vacuum.

Figs. 2, 3, and 4 show the galvanometer current i_t as a function of the potential difference between the electrodes V_t . The four curves of Fig. 4 were obtained to show the effect of varying the accelerating voltage, V_d . The absolute values of V_d were not accurately measured, but the differences are reliable. Fig. 3 taken with tube No. 2 shows the effect of increasing the beam current 250 times relative to Fig. 4. We see that practically the only difference between the various curves is in the scale of ordinates. At a given voltage they all show about the same fraction of the saturation current.

Equal and like quantities of electricity on each of the opposite walls of a tube with external electrodes would not produce any potential difference and hence would not affect the beam deflection. Rate of neutralization is

proportional to the *difference* between the currents to the opposite walls. When $V_t = 0$, each electrode receives half the return electron current from the beam, and the neutralization current is zero. The neutralizing current is therefore $i_t - i_{t_0}$ where i_{t_0} is the value of i_t when $V_t = 0$. For large V_t it approaches a saturation value which ranges from 3×10^{-7} amperes for tube No. 1 with a beam so faint as to be just visible in a daylighted room to 7×10^{-5} amperes for tube No. 2 which had a very bright beam. About 7



Figs. 2, 3, and 4. i_t , the current to test electrodes in microamperes, as a function of V_t , the voltage between test electrodes.

	Fig. 2 1	Fig. 3 2	Fig. 4a 1	Fig. 4b 1	Fig. 4c 1	Fig. 4d 1
Tube No.:						
Accelerating voltage V_a :	740	445	750	600	400	300
Beam current i_b in microamperes:	1.2	120	0.4	0.33	0.38	
Resistance to neutralization in megohms:	10	0.12	26	30	26	33
Positive ions per beam electron:	0.21	0.17	0.25	0.32	0.33	0.4

volts, or 5 volts per cm, gives half the saturation current. For small values of V_t the neutralizing current is proportional to the potential difference and we can obtain R , the resistance to neutralizing current, from the initial slopes of the curves. The values are given with the curves. R is found to be inversely proportional to the beam current as might be expected, the values of Ri_b (ohms \times amperes) being 12, 11, and 15 for curves 2, 3, and 4a. When the deflections with external electrodes were being observed, the transverse fields

between the walls rose considerably above the range for which the current is proportional to field. Our assumption of a constant R which was used in developing the equations for deflection therefore leads to results that are little more than qualitative.

The distance between the walls of the tube used in measuring the deflections with external electrodes (Fig. 5) averaged about four times the distance between the electrodes of the tubes used for the current measurements. If in these tubes the same field produces the same neutralizing current, the potential differences and resistances will have the ratio four, and for the tube used in measuring deflection

$$R = (12/i_b) \times 4 = 50/i_b$$

From the dimensions and material we find

$$C_b = 10^{-10} \text{ farads.}$$

hence

$$\tau = RC_b = 50 \times 10^{-10}/i_b$$

If we put i_b in microamperes and τ in thousandths of a second, then $\tau i_b = 5$.

The approximate number of positive ions formed by each beam electron can also be determined from the curves. The galvanometer current i_t is made up of two parts: the electrons originally in the beam which have struck the end of the tube and are returning, and the electrons and positive ions formed by collision with gas molecules. When V_t is positive and large enough for saturation, all of the original electrons of the beam and in addition all the electrons formed by collision are drawn through the galvanometer. For large negative V_t , only the positive ions are drawn through the galvanometer, and the saturation current gives their number. This is also the number of electrons produced by collision. Therefore subtracting the saturation current for negative V_t from that for positive V_t gives immediately the total beam current. This has been checked independently. Hence the number of positive ions formed per beam electron is simply the ratio of the positive saturation current to the difference between the two saturation currents. The values, given with the curves, lie between 0.4 and 0.17, showing that neutralization is principally due to the original electrons of the beam rather than to new ions and electrons produced by collision. The data of Compton and Van Voorhis² on probability of ionization by electron impact would give 0.18 ions per electron in these tubes for 350 volt electrons, but they do not extend to the higher velocities with which most of the present measurements were made.

4. MEASUREMENTS OF DEFLECTION WITH EXTERNAL ELECTRODES

The tube, electrical connections, and photographic arrangement used are shown in Fig. 5. The beam current i_b was measured by closing the galvanometer switch which was open during deflection observations.

² Compton and Van Voorhis, Phys. Rev. 26, 436 (1925).

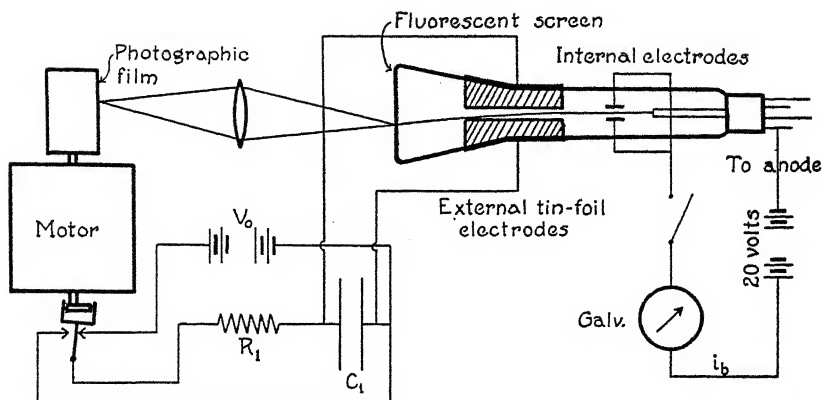


Fig. 5. Tube and connections used for deflection measurements.

In the simple case $R_1=0$ a constant voltage V_0 is suddenly applied and removed. Fig. 6 is an example of the deflection obtained. Here Eq. (7) applies and τ can be calculated from the deflections at two different times,

$$\tau = \frac{t_2 - t_1}{\ln D_1/D_2}$$

In comparing different curves where i_b varies, τi_b should be constant since

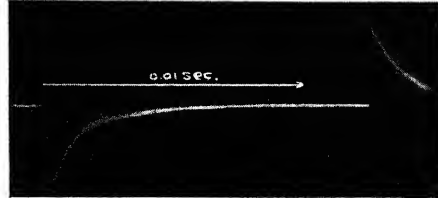


Fig. 6. Deflection produced by suddenly applying and removing voltage on external electrodes.

we found Ri_b constant. The results are given in Table I. The average agrees with the value calculated from the current measurements, and we see here

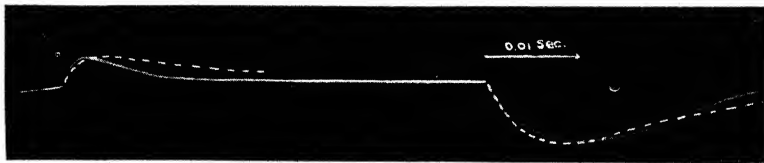


Fig. 7. Deflection when external electrodes are connected to a condenser which is alternately charged and discharged through a resistance. Dashed curve is calculated.

the same approach to saturation that we found in the current measurements; the values of τ increase with increasing field and deflection. Moreover, the

two branches of the curves, caused respectively by application and removal of the voltage, give different values of τ , the difference being specially great when V_0 is large. A similar asymmetry is noticeable in the curves taken with $R_1 \neq 0$, e.g., Fig. 7, and is sometimes observed with sinusoidal applied voltage. It is due to the fact that one electrode is maintained at a fairly constant potential while the other varies. When the latter becomes suddenly more positive, electrons are attracted to the wall next it and neutralization is rapid. When it suddenly becomes more negative, the electrons are repelled toward the anode or "plate" through which the beam emerges, and the

TABLE I

Showing the values of τ obtained in different ways. The values or sets of values for each film refer to the two branches. The times τ and t_1 and t_2 are given in thousandths of seconds. The current i_t is given in microamperes.

From the rate of decrease of deflection after sudden application or removal of constant voltage V_0						From the magnitude of maximum deflection				
τ	ri_t	t_1	t_2	Film	V_0	τ	ri_t	Film	V_0	R_1
4.62	15	4.4	7.5	#12	220	1.93	3.69	#2	45	500
3.57	11.7	7.5	10			0.91	1.75			
2.75	9.0	10	12.7							
2.40	7.85	2.5	4.6			1.43	2.94	#3	95	300
1.66	5.42	4.6	6.0			1.02	2.10			
1.36	4.44	6.0	7.4			3.45	6.55	#5	220	5000
2.3	6.10	0.0	0.44	#4	70	1.28	2.44			
0.99	2.62	0.44	1.32	(Fig. 6)		5.48	10.2	#6	220	7000
1.68	4.45	1.32	3.30			1.76	3.34	(Fig. 7)		
1.83	4.85	0.00	0.38							
1.16	3.07	0.38	1.1			1.1	2.6	From the magnitude of deflection with 60 cycles		
1.17	3.10	1.1	2.0			2.0	5.0	Calculated from measured neutralization current		

relatively few positive ions which are attracted give a relatively slow neutralization.

Fig. 7 is an example of the deflection obtained when both capacity and resistance are in circuit. The dotted curve is that given by Eq. (6). The constant S was found from the initial deflection of Fig. 6, $D = V_0 S$. R_1 was known. The value of C_1 used was the average calculated from the initial slopes of all similar curves. τ was found from the maxima. The results for all curves obtained are given in Table I.

The magnitude of the deflection produced by a 60-cycle sinusoidal voltage was measured and τ was calculated from Eq. (8). The result, also given in Table I, agrees with the other values.

CONCLUSION

Current measurements with large internal metal electrodes show that the electron and ion current has the order of magnitude and variation with

field that is necessary to explain the deflections observed with external electrodes. For small applied voltages, the tube acts as if the inner surfaces of the walls between the external plates were electrodes connected through a resistance which is inversely proportional to the beam current.

Neutralization is principally due to the original electrons of the beam which have struck the end of the tube and are returning, rather than to new ions and electrons produced by collision.

DEPARTMENT OF PHYSICS,
UNIVERSITY OF CALIFORNIA.
January 5, 1927

THE INDEX OF REFRACTION OF WATER FOR SHORT CONTINUOUS WAVES

By L. E. McCARTY AND L. T. JONES

ABSTRACT

The index of refraction of water for short continuous waves (300 to 700 cm) was measured from the phase difference resulting between two portions of a wave, one portion of which had passed through the dielectric. The phase difference was detected and measured by the rotation of the Lissajous figure, formed on the screen of a cathode ray oscillograph, due to the simultaneous action on the cathode beam of two tuned circuits receiving the two portions of the wave. The two circuits were attached to the opposite pairs of deflector plates of the oscillograph. The index of refraction was calculated from the relation $\mu = m\lambda/d + 1$, where λ is the wave-length, d the thickness of intervening dielectric in one path, and m the fraction of a period by which the wave passing through the dielectric is retarded relative to the one passing through air. The results are in good agreement with the electrical refractive index found by other methods, i.e., about 9, and approximately constant over the range of frequencies used. Brief reference is made to a method by which it is hoped to measure the dielectric constant under conditions identical with those existing in the measurement of the index of refraction, to be used in conjunction with the latter, in testing Maxwell's relation between index of refraction and dielectric constant.

THE work described in this paper represents the first part of an experimental test of Maxwell's relation between refractive index and dielectric constant, $K = \mu^2$, especially for such substances as water and alcohol, for which a very great discrepancy has been observed, and under more nearly identical conditions than have obtained in previous experiments. Inasmuch as most of the earlier tests of the relation were based on values of the refractive index and dielectric constant measured at vastly different frequencies and sometimes at different temperatures, it was not to be expected that verification would be complete. Both refractive index and dielectric constant depend on frequency and temperature. Numerous investigations extending from about 1895 to the present time have shown that the discrepancies are much reduced when the quantities to be compared are measured under more nearly similar conditions.¹ P. Drude² measured the reduction in wavelength suffered by short damped electromagnetic waves (40 to 600 cms) on passing from air to water along a Lecher Wire system, and obtained about 9 for the electrical refractive index of water, a result in very close agreement with the theory. This result has been confirmed by many others using various methods, and wave-lengths varying from a few millimeters to several meters. The importance of the temperature factor was shown by the experiments of

¹ See Fleming and Dewar, Proc. Roy. Soc. Lond. 61, 2 (1897) for a summary of the work done before 1897.

² P. Drude, Wied. Ann. 54, 352-370 (1895); 55, 633-655 (1895); 58, 1-20 (1896).

Dewar and Fleming just referred to. In view of this close dependence of index of refraction and dielectric constant on frequency and temperature it appears that in order to have a fair and decisive test of Maxwell's relation the two quantities involved must be measured under absolutely identical conditions; and the purpose of this experiment, therefore, was to measure in a single experiment, under conditions as nearly identical as possible, the two quantities entering into Maxwell's relation. The only part of this plan which has been carried out so far is the development of the method and its application to the measurement of the refractive index of water at a few frequencies of the order of 10^8 cycles per second. The results so far obtained are in agreement with those already found.

In this method the refractive index is computed directly from the phase difference introduced between two portions of a wave by the retardation of one portion in passing through the dielectric. The two parts of the wave were picked up by two tuned circuits attached to the opposite pairs of deflector plates of a cathode ray oscillograph, and the phase difference measured from the rotation of the resulting Lissajous figure. The arrangement of apparatus is shown in the accompanying diagram, Fig. 1.

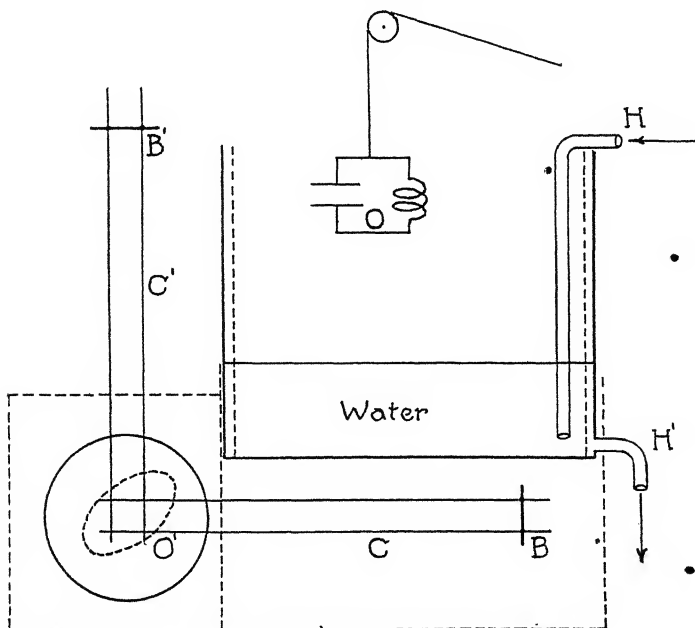


Fig. 1. Schematic diagram of apparatus.

O is a simple vacuum tube oscillating circuit (5 to 7.5 watts) suitable for generating short waves. It was suspended from a pulley over a glass water tank of dimensions $1 \times 0.5 \times 0.5$ meters. By means of the hose H and H' the depth of water could be varied continuously. The circuits C and C' received the waves traversing the water and air paths, respectively, and the

two alternating electromotive forces induced in the circuits acted simultaneously, at right angles, on the electron beam causing it to trace an ellipse on the oscillograph screen O'. The shape of the ellipse depends on the amplitudes and phase difference of the two impressed e.m.f.'s. The oscillograph was of the ordinary type⁸ with internal deflector plates. The oscillograph was enclosed by a screen of iron wire of 0.5 inch mesh, and circuit C was screened from all directions except the side next the water with 1/8 inch iron screen. A lens and film holder were placed in front of the oscillograph. The wave-lengths were measured on a Lecher bridge system in the usual manner.

The procedure followed in taking a series of observations or photographs, such as that shown in Fig. 2, was somewhat as follows: A thin layer of water was run into the tank to correct for the capacity effect of the water on

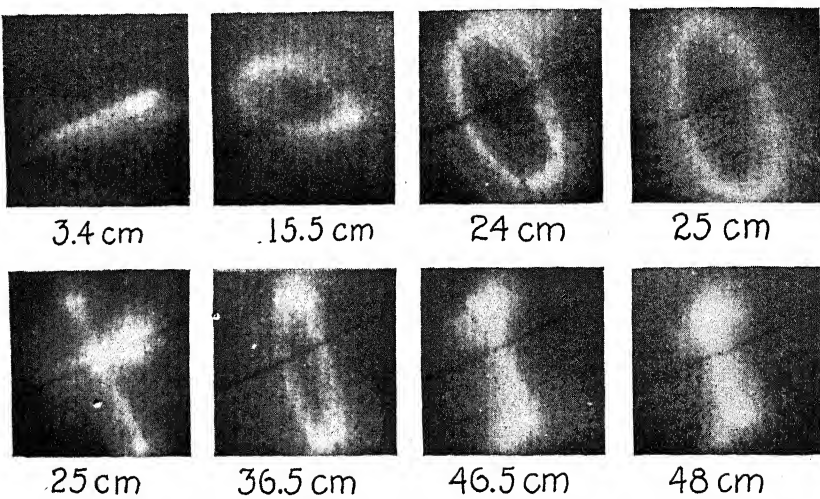


Fig. 2. Photographs of Lissajous figures for various depths of water.

circuit C. The circuits were then tuned by means of the adjustable bridges B and B' until they gave a convenient sized figure on the oscillograph screen. If the figure was not approximately a straight line it was usually made so by slight adjustment in the position of the oscillator, thickness of water layer or by changing the inductance in circuit C'. The hydrant was then opened, water run into the tank, and the various phases of the ellipse photographed, and the corresponding depths of water read. Similar sets of observations were made with the water flowing out. The water flow was stopped during an exposure. The figures below the photographs in Fig. 2 represent the depth of water at which the phase occurred. The fifth exposure is a double exposure showing the direction and amplitude of each vibration separately. The directions of vibration remained constant, but the amplitudes varied in the different exposures. On account of the time required to make a series

⁸ Jones & Tasker, J.O.S.A. 9, 471 (1924).

of exposures and the mishaps which often occurred during an unusually long run, it was found that more and better data could be secured by simply observing and recording a number of values of the depth, with the water alternately rising and falling, corresponding to certain definite forms of the figure (straight line or maximum ellipse) which were used in the computations. Two such series of readings are given in Table I. The first two

TABLE I

Containing recorded thickness of dielectric corresponding to the straight line position shown in Fig. 2 for $\lambda = 702$ cm.

Lower straight line position Upper straight line position

Water Flowing in Depth cm	Water Flowing out Depth cm	Water Flowing in Depth cm	Water Flowing out Depth cm
Phase change 180°.			
3.5	4.0	47.0	46.9
3.4	3.0	47.1	48.0
3.4	3.5	47.9	47.2
2.8	3.1	47.0	48.2
3.6	3.3	48.0	47.6
3.8	4.0	48.0	48.0
4.1	3.6	(Tank overflowed)	
3.9	3.3		
4.1	3.3		
Aver. 3.26	3.11	47.50	47.67
Final Aver.	3.18	$d=44.4$ cm	$m=0.5$
			$\mu=8.9$
Phase change 90°			
1.2	1.5	23.0	22.5
1.3	1.8	23.1	22.8
.8	1.0	23.0	23.0
.5	1.0	23.1	23.2
1.0	1.5	23.0	22.8
1.0	1.0	23.0	23.2
.9	1.1	22.9	22.7
1.2	.9	22.9	23.0
.8	.9	23.0	22.6
.7	.6	23.1	22.8
Aver. 9.4	1.13	23.01	22.86
Final Aver.	1.04	$d=21.9$ cm	$m=0.25$
			$\mu=9.0$

columns of the first set give depths of water read as the figure passed through a straight line position in one quadrant and the last two give the depths read as it passed a straight line position in an adjacent quadrant. The readings in the second set have a similar meaning except that the last two columns were taken as the figure passed through the maximum ellipse. The depths in the first and third columns of each set were read with water flowing into the tank, the second and fourth columns with water flowing out. The readings in adjacent columns were taken alternately in pairs.

Before presenting the results it will be necessary to refer to certain practical difficulties encountered in connection with screening and measurement of the rotations, and to explain how they were surmounted. It was soon

apparent that other factors besides changes in phase difference were operating to produce peculiar irregularities in the rotation of the ellipse. Investigation showed that they were due to irregular variations in amplitude of the vibrations, caused apparently, by such effects as resonance, reflection and standing waves, mutual interactions between the circuits, and absorption. All the irregularities were not accounted for and it seemed impossible to eliminate or to correct for them by analysis of the rotations. For this reason it was decided to avoid their effects altogether by basing the calculations on phase changes which were caused by multiples of 90° rotations, and in most cases on changes from a straight line position in one quadrant to a straight line in an adjacent quadrant. An analysis of the pseudo-rotations caused by amplitude changes alone shows, first, that the rotation is always confined to a single quadrant, and, second that it cannot cause a change of shape of the figure from a straight line to an ellipse, or vice versa. In case an ellipse degenerates into a straight line as a result of one of the component amplitudes becoming zero, this line will always lie along one of the axes. Hence it is at least safe to assume that the rotation between straight line positions in adjacent quadrants is due to phase change alone regardless of any irregularities in between, which may be due to both causes; and it is fairly certain that a change from a straight line position not along an axis to a maximum ellipse, or circle, is caused by a phase change of 90° . This point is illustrated, though not nearly so well as in many other observed cases, by the series of photographs in Fig. 2. In the first place it is obvious from these photographs that the amplitudes of the vibration in both circuits has changed, that in circuit C' having been reduced as the depth of water increased while that in C increased. These photographs also indicate an actual rotation of the axes of the figure through slightly more or less than 90° , depending on whether the rotation is considered as clockwise or counter-clockwise. It seemed to be clockwise. The first approximate straight line position, corresponding to 3.4 cms of water, appears to be nearly in the line with one of the axes, but the subsequent changes and the other straight line position could not well be explained by amplitude changes alone. Besides, the observations, which were more complete and accurate, showed that the best value of the lower position corresponded to 3.18 cm and was more inclined to the direction of vibration produced by C' . The results in Table 2, with the one exception noted, were computed from consecutive straight line positions in adjacent quadrants, assumed to be due to 180° phase changes in circuit C .

The equation giving the relation between index of refraction, phase difference, wave-length, and thickness of dielectric is derived as follows: Let t_1 be the time required for the wave to pass from the source to the detector by the air-path, a distance D cm, and t_2 the time required to pass through the dielectric of thickness d cms and a distance $D-d$ cms of air-path.

Then $t_1 = D/c$, and $t_2 = \mu d/c + (D-d)/c$ where c is the velocity of the wave in air. Also

$$t_2 - t_1 = d(\mu - 1)/c$$

But $t_2 - t_1 = mT$, where T is the period (λ/c) and m is the fraction of a cycle of phase difference introduced. Then

$$\mu = m\lambda/d + 1$$

As previously stated the wave-length λ was measured by means of a Lecher system. A crystal and milliammeter or a vacuum thermocouple was used to indicate the position of the nodes. The thickness of dielectric d required to make $m = \frac{1}{2}$ was read directly from a meter bar standing against the inside wall of the tank. The method of computing the average values of d for $\lambda = 702$ cm is indicated in Table I, also the substitutions and calculation of μ for this wave-length. The other values of μ shown in Table II were

TABLE II
Showing measured values of λ , m and d with corresponding values of μ .

λ cm	m	d cm	μ
702	{ $\frac{1}{4}$ $\frac{1}{2}$ $\frac{1}{4}$	{ 21.9 44.4	{ 9.0 8.9
670	$\frac{1}{2}$	45.3	8.4
500	$\frac{1}{2}$	31.6	8.9
496	$\frac{1}{2}$	29.8	9.3
425	$\frac{1}{2}$	27.2	8.8
384	$\frac{1}{2}$	22.7	9.4
332	$\frac{1}{2}$	20.0	9.3

computed in a similar manner except that the amount of data used for the two shortest waves was less than for the longer waves. The small size of the ellipse made it very difficult to obtain accurate data at the short wavelengths.

The values of μ for the different wave lengths used are seen in Table II to be almost constant and in substantial agreement with those obtained by others with different methods. The degree of accuracy of the experiment does not warrant any conclusions as to the slight variations shown. The indistinctness referred to by J. B. Johnson,⁴ due to the time required for the beam to produce the ionization necessary for focusing, did not cause trouble as had been feared. There was some erratic behavior of the spot at certain times at all frequencies, but it did not appear to be any worse at frequencies of 10^8 than at 10^6 where haziness was observed by Johnson. The difficulty experienced in making observations at the shortest wave-lengths appeared to be due to the small size of the figures, resulting from lack of sufficient power at these high frequencies, rather than to haziness caused by incomplete focusing. The broadening of the figure in some of the photographs shown was due to a division of the beam into two parts, apparently two points of emission at the filament.

It is planned to make a direct measurement of dielectric constant at exactly this same frequency and temperature by substitution of a part of the same specimens used in the refractive index determination between the plates of

⁴ J. B. Johnson, J.O.S.A. 6, 701 (1922).

the variable air condenser in the oscillating circuit and noting the distance of separation of the plates required to tune it back to the original wave-length as indicated by resonance with the same length of the Lecher system. This is a slight modification of the method described in Bulletin No. 74 of the U. S. Bureau of Standards. A rough preliminary trial has been made but no reliable results have yet been obtained.

In order to apply this method to other dielectrics with smaller indices of refraction, it will be necessary to make certain refinements and to eliminate some of the causes leading to irregular changes in amplitude so that small phase changes may be detected. It should be possible to detect and measure fairly small rotations by a null method, i.e. by bringing the figure back to its original position.

DEPARTMENT OF PHYSICS,
UNIVERSITY OF CALIFORNIA.
February 24, 1927.

THE HIGH FREQUENCY RESISTANCE OF A BUREAU OF STANDARDS TYPE VARIABLE AIR CONDENSER

By S. L. BROWN, C. F. WIEBUSCH AND M. Y. COLBY.

ABSTRACT

A method is described whereby the high frequency resistance of variable air condensers is measured with an accuracy of one percent. Data are given showing the resistance of a Bureau of Standards Type 0.0035 μf condenser at wave-lengths from 40 to 175 meters and at different positions on the scale. The values obtained range from 0.0283 ohms at 119 meters and 174° scale setting (range 0° to 180°), to 0.150 ohms at 63 meters and 20° condenser setting. The resistance increases rapidly towards the lower positions on the scale, and also increases with wave-length.

Experimental check of the calculated values of the high frequency resistance of large conductors:—The resistance of single turn coils of B and S No. 8, 2, 00, and 0000 annealed copper wire were measured at wave-lengths from 40 to 175 meters. These values were compared with the calculated values and were found to check to within two percent in most cases and the discrepancies may easily be ascribed to experimental errors.

IT HAS been considered quite permissible by many writers either wholly to neglect, or to use an approximate value for, the high frequency resistance of low-loss air condensers, in comparison with the total resistance of the circuit in which they were included. It is the purpose of this paper to show that, in cases where the total resistance of the circuit is low, not only the resistance of the condenser, but also its variation with frequency and setting must be taken into account.

The plan followed in the investigation made was to measure the total resistance of a tuned circuit in which the condenser was included and then separate the condenser resistance from that of the remainder of the circuit. The resistance variation method so frequently used for measuring the resistance of tuned circuits does not give, without modification, sufficiently accurate results in low resistance circuits. In order to obtain reliable values for the condenser resistance by this method the resistance of the remainder of the circuit should be as small as possible; otherwise the condenser resistance may be entirely concealed by experimental errors in the value of the total resistance. But this condition cannot be realized as long as it is necessary to include the resistance of an ammeter in the circuit. Furthermore, in previous descriptions¹ of the use of this method for determining the total resistance of the circuit, the separation of the condenser resistance from that of the remainder of the circuit involves the use of inordinately high values of total resistance. This necessitates the use of considerable power and close coupling; consequently there is an appreciable percentage of error, the absolute value of which might easily be greater than the resistance of the condenser.

¹ C. D. Callis, Phil. Mag. (7) 1, 428-432 (1926).

In the description of one method² of ascertaining the condenser resistance, the calculated value of the resistance of the circuit exclusive of the condenser is subtracted from the total resistance. But this procedure can not be justified because of the lack of experimental verification of these formulas when large wire and very high frequencies are used.

The differential calorimeter has been used by R. R. Ramsey³ in determining the resistance of a "low-loss" condenser at one setting. Although based on a fundamental principle, it is with considerable difficulty that calorimetric measurements can be made to yield results of a high degree of accuracy, even though comparatively elaborate apparatus is used. This is well illustrated by the fact that, in the article referred to, the value of the condenser resistance given is the average of values ranging from 0.05 to 0.15 ohms.

In the measurements subsequently described, the condenser resistance constituted at least half the total resistance of a tuned circuit consisting of nothing but the condenser and one circular turn of very large copper wire. A sensitive vacuum tube voltmeter⁴ was used to measure the voltage across the condenser at resonance.

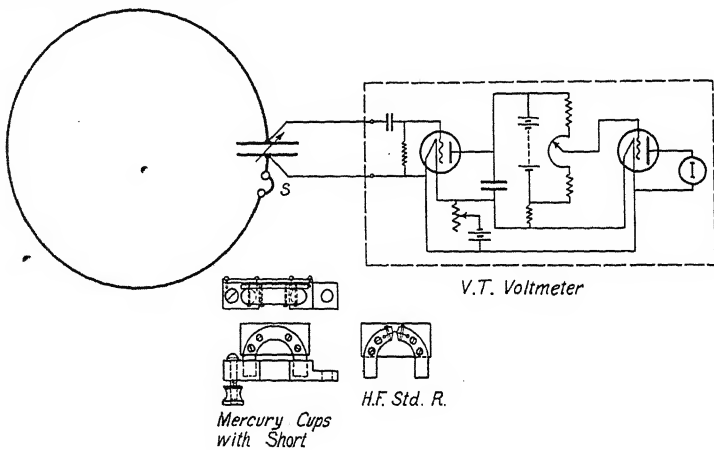


Fig. 1. Diagram of circuit.

The circuit used in these measurements is shown in Fig. 1. The condenser whose resistance was measured was a Bureau of Standards Type .0035 μ f variable air condenser fitted with a micrometer adjustment. The inductance consisted of one circular turn of B & S No. 0000 annealed bare copper wire. One end of the coil was connected directly to one terminal of the condenser while the other end was connected to the opposite condenser terminal through a short circuit *S* dipping into mercury cups. The short circuit was made of about 10 cm of No. 0000 copper wire bent so as to fit into the mercury cups. The standard resistances were exact duplicates of the short *S* except

² Weyl and Harris, Proceedings of the Institute of Radio Engineers 13, 109-121 (1925).

³ R. R. Ramsey, Phil. Mag. (7) 2, 1213-1218 (1926).

⁴ M. Y. Colby, Journal of Sci. Instruments 3, 342 (1926).

that about two or three millimeters of the large copper wire was cut out and replaced by an equal length of manganin wire of small enough cross section to make the skin effect negligible at even higher frequencies than any here employed. The mercury cups were held together by a strip of bakelite. The construction of the mercury cups and the standard resistance is shown in detail in Fig. 1. The construction was such that the short circuit could be quickly replaced by a standard resistance without varying the contact resistance and without altering the size, position or configuration of the circuit in the least. The vacuum tube voltmeter was calibrated with 60 cycle a.c. using a noninductive slide wire resistance. The constant voltage a.c. supply necessary for this calibration was obtained by operating a motor generator set from storage batteries.

The measurements were made in the following manner. The circuit was very loosely coupled to a high frequency oscillator made portable by mounting on a cart. The distance between the oscillator and the circuit was from 10 to 50 feet, depending on the amount of induction required. The coefficient of coupling calculated from observations of the current in the oscillator circuit, current in the tuned circuit, and the constants of the two circuits was of the order of 1×10^{-6} , while the power used by the tuned circuit was from 5×10^{-4} to 5×10^{-5} watts. The condenser was adjusted to the desired setting and the frequency of the oscillator varied until the two circuits were in tune. The circuit was then very accurately tuned to resonance by means of the micrometer adjustment. The resonant voltage E_x indicated by the voltmeter was observed; the short S was then replaced by the standard resistance R_s and the new value E_s of the resonant voltage observed. The total resistance R_x of the circuit is given by the relation

$$R_x = \frac{R_s}{E_x/E_s - 1}$$

Similar measurements were made at two other settings of the condenser.

A coil of No. 00 copper wire was then substituted for the coil of 0000 wire, and its length was adjusted until its inductance was exactly equal to that of the first coil. The resistance of the new circuit was measured at the same three settings of the condenser and at the same wave-lengths as in the first case. This series of three measurements was again repeated using a coil of No. 2 wire. Thus at each of the three settings of the condenser, three values of the condenser resistance plus the coil resistance were obtained, the coil resistance being different in each case.

If the three loops of different size wire were of the same length, these three values of total circuit resistance R_x plotted against the reciprocals of the diameters D of the corresponding wires would be expected, from theoretical considerations, to give a straight line cutting the resistance axis at the resistance of the condenser R_c . But since the small wire has more inductance per unit length than the large, the three loops of equal inductance vary slightly in length, the loops of smaller wire, of course, being shorter. Therefore R_x would not be expected to be a straight line function of $1/D$ and equal to R_c when $1/D$ equals zero. However, if the clearly justifiable assumption

is made, that the loop resistance is directly proportional to the length l of the wire, the values obtained for R_x would be expected to lie on the straight line,

$$R_x = R_c + Kl/D$$

Accordingly, in each case, the three values of R_x corresponding to a particular wave-length and condenser setting were plotted against l/D and the resulting curve is a straight line. One of these curves is shown in Fig. 2, the intercept being the condenser resistance corresponding to the wavelength and condenser setting indicated.

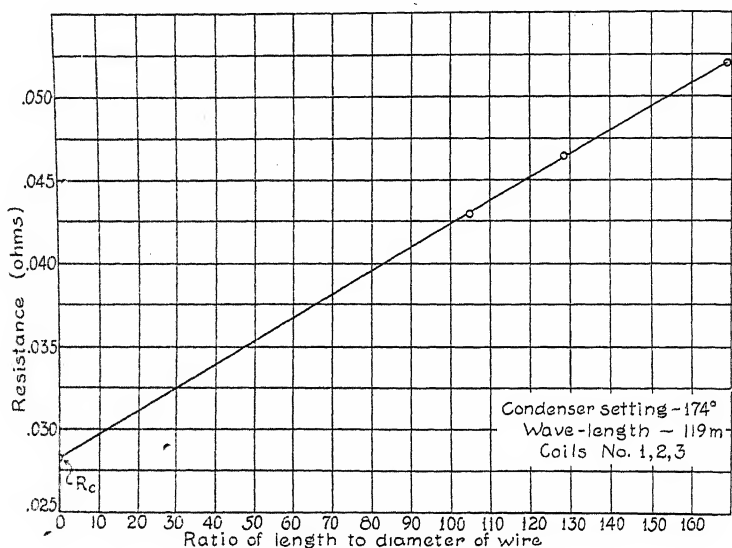


Fig. 2. Graph showing method of separating condenser resistance from coil resistance.

Using another set of larger coils, the values of the resistance of the condenser at the same three settings, but at longer wave-lengths, were determined. Table I shows the six values of condenser resistance R_c obtained by this method. In every case two resistance standards were used, one having a higher resistance and the other a lower resistance than that of the circuit being measured. These standards were measured on a Kelvin double bridge and were accurate to less than one-tenth of one percent at the frequencies used. Standards made of No. 36 and No. 42 manganin wire were checked against one another and were found to agree at all frequencies used. From ten to thirty observations were made in each measurement, the maximum variation usually being less than two percent, and the mean of these values was then taken as the total resistance of the circuit.

As a further check on the validity of the results given here, very careful measurements of the diameters of the wires were made and their high frequency resistance calculated. The agreement between the observed and the calculated⁵ values shown in Table I is as close as could be expected in

⁵ Bureau of Standards, Circular No. 74.

TABLE I

Values of condenser resistance, R_c , and of the resistance of coils whose specifications are given in Table II.

Condenser setting	Capacity in μf	λ	Coil	R_z	R_c	R of coil	R of coil calculated
20	483	43.4 m	1	.136 ohm		.023 ohm	.024 ohm
20	483	43.4	2	.144		.031	.030
20	483	43.4	3	.152	.113 ohm	.039	.038
80	1797	83.0	1	.0593		.0173	.0172
80	1797	83.0	2	.0623		.0203	.0212
80	1797	83.0	3	.0696	.0420	.0276	.0276
174	3840	119	1	.0431		.0148	.0147
174	3840	119	2	.0466		.0183	.0180
174	3840	119	3	.0517	.0283	.0234	.0236
20	483	63.0	4	.190		.040	.039
20	483	63.0	6	.208		.058	.061
20	483	63.0	7	.258	.150	.108	.112
80	1797	119	4	.0764		.0272	.0274
80	1797	119	5	.0825		.0333	.0332
80	1797	119	6	.0936	.0492	.0444	.0445
174	3840	172	4	.0542		.0237	.0231
174	3840	172	5	.0579		.0274	.0278
174	3840	172	6	.0676	.0305	.0371	.0372

TABLE II

Coil specifications.

Coil	Wire Size	Diameter	Length
1	0000	1.172 cm	123 cm
2	00	.904	116
3	2	.645	109
4	0000	1.167	238
5	00	.920	227
6	2	.649	214
7	8	.320	194

view of the fact that the wire resistance was usually only a small part of the total resistance measured.

It was found necessary to keep the room in which the measurements were made at a constant temperature, since the variation of the resistance of the circuit with temperature was appreciable.

A more exhaustive investigation of the variation of the resistance of condensers with setting and frequency, as well as with temperature, is now in progress, and the authors expect to be able in the near future to present, in more detail, data concerning these three phases of condenser resistance.

HIGH FREQUENCY LABORATORY,
DEPARTMENT OF PHYSICS,
UNIVERSITY OF TEXAS.
March 17, 1927.

NOTE ON THE PLANE WAVE IN A GAS

BY SATYENDRA RAY

ABSTRACT

Effect of amplitude on velocity of a plane wave in a gas.—In a former paper (Phys. Rev. 28, 229, 1926) it was pointed out that the velocity of a transverse wave along a string is not independent of the amplitude and that for different frequencies to travel with the same velocity the ratio a/λ must be constant, as for light waves (Zeits. f. Physik 8, 112, 1921). The same result is here proved for plane longitudinal waves in air.

AS AN exact equation governing wave motion in air for a plane wave with finite amplitude Lord Rayleigh gives the relation

$$\left(\frac{dy}{dx}\right)^{\gamma+1} \frac{d^2y}{dt^2} = \frac{\gamma P_0}{\rho_0} \frac{d^2y}{dx^2}, \quad (1)$$

where x denotes the equilibrium abscissa and y the actual abscissa in the wave. We note in passing that when the wave is very flat, y is very nearly identical with x and the coefficient (dy/dx) on the left hand side becomes equal to unity. The equation therefore reduces to the form

$$\frac{d^2y}{dt^2} = \frac{\gamma P_0}{\rho_0} \frac{d^2y}{dx^2} \quad (2)$$

of which the solution is

$$y = F(x+vt) + \phi(x-vt). \quad (3)$$

We seek to investigate the displacement wave by putting

$$y = x + \xi, \quad (4)$$

so that Lord Rayleigh's equation becomes

$$\left(1 + \frac{d\xi}{dx}\right)^{\gamma+1} \frac{d^2\xi}{dt^2} = \frac{\gamma P_0}{\rho_0} \frac{d^2\xi}{dx^2}. \quad (5)$$

The condition of "flatness" makes $d\xi/dx$ approximately zero so the Eq. (5) reduces to the form

$$\frac{d^2\xi}{dt^2} = v^2 \frac{d^2\xi}{dx^2}, \quad (6)$$

where $v = (\gamma P_0 / \rho_0)^{1/2}$. In the most general case, however,

$$\frac{d^2\xi}{dt^2} = (v')^2 \frac{d^2\xi}{dx^2}, \quad (7)$$

where

$$\begin{aligned} v' &= v(1 + d\xi/dx)^{-(\gamma+1)/2} \\ &= v[1 + Ad\xi/dx + B(d\xi/dx)^2 + \dots] \end{aligned} \quad (8)$$

and where A , B , etc., are constants.

If ξ be given by the equation

$$\begin{aligned} \xi &= a \sin 2\pi x/\lambda, \\ d\xi/dx &= 2\pi(a/\lambda) \cos 2\pi x/\lambda, \end{aligned}$$

so that the expression for the average value of $d\xi/dx$, $(d\xi/dx)^2$, etc., are functions of a/λ and so is therefore the value of v , which we can determine to as many powers of a/λ as we like.

We content ourselves here with only noting the result that, in common with the results obtained with light vibrations, the velocity of propagation of plane sound waves in air is the same only for geometrically similar waves, the value of the velocity being given in a functional form by the expression

$$v' = vf(a/\lambda). \quad (9)$$

UNIVERSITY OF LUCKNOW,
January 12, 1927.

BOOK REVIEWS

Properties and Testing of Magnetic Materials. THOMAS SPOONER.—This monograph makes available in one place a mass of information hitherto so scattered in engineering publications as largely to miss the attention of physicists. Only ferromagnetic materials are dealt with, and among these the emphasis is upon the commercial materials of widest use, the data concerning electrical (silicon steel) sheet being especially complete.

Part I (187 pages) deals with measurable magnetic properties and with their relations to each other and to the history or momentary state of the material. Fundamental theory is deliberately omitted and the critical reader will find a looseness in the use of units which is probably unavoidable in a work which reports so exactly the present official language of electrical engineering. For example, the following appears on page 9: "The ferric induction is equal to $B - H$, where B is expressed in gausses and H in gilberts per centimeter." In all that relates to high and medium magnetizations under d.c. excitation and under a.c. excitations whether of one or two frequencies, the author may be followed with confidence. His treatment of very low magnetizations is less complete, e.g., there is no mention of Rayleigh's formula for hysteresis at such low inductions that μ is expressible as a linear function of H , and the interesting changes of reversible permeability with changes in superposed d.c. are not discussed although the hysteresis losses for wider displaced a.c. loops are fully treated.

The experimenter will find in Part II (146 pages) a more complete and discriminating account of ferromagnetic test methods than is elsewhere to be found. Though engineering requirements are kept in mind the author has not hesitated to describe research apparatus when any advantage in accuracy or scope can be attained by its use.

Part III (36 pages) deals in general terms with some engineering applications and with magnetic analysis. It is almost independent of Parts I and II, the independence extending even to the repetition of arguments already presented and the duplication of one cut.

The paper, printing, binding and indexing are good. The cuts suffer in many cases from over-reduction. References to periodical literature are not all in the same form and Roman numerals, now generally abandoned, frequently appear. A few errors should be noted. On page xiv μ is omitted from the numerator of the fraction defining permeance and from the denominator of that defining reluctance. On page 6, equation (14), if E is E_{rms} , B should be B_m . On page 45 the resistivity of Co should be near 10, not 100. On page 51, line 4, the statement should be that the effect of magnetization is to increase electrical resistance. On page 208, line 1, read "a small fraction of" for "several times." On page 303, in equation (88), a factor 4 has been omitted from the denominator of the right-hand side. Pp. xiv+385, 6×9, 223 figs., McGraw-Hill, New York, 1927. Price \$5.00.

L. W. MCKEEHAN

Sternhaufen. P. TEN BRUGGENCATE. (Siebenter Band, Naturwissenschaftliche Monographien und Lehrbücher.)—This small book on star clusters is of value in bringing together into available form his elaborate unpublished doctoral thesis and several subsequent contributions to scientific journals. Since the subject of globular clusters was rapidly developed a decade ago by the large telescopes, the thesis by ten Bruggencate is the most extensive critical survey of the field.

The distances of the globular clusters and the methods developed in determining these distances have played significant rôles in all recent measures and estimates of the dimensions of the Galaxy and of the remoteness of the extra-galactic stellar systems. It is well known that Bohlin, Shapley, Charlier, Schouten, Curtiss, Kapteyn, and others have been far from accord concerning the value of the methods employed and the value found for the distances. Ten Bruggencate's methodical survey of methods has shown clearly the weaknesses of the deductions by Kapteyn, Schouten, Charlier, and those who found the clusters near at hand and

populated with dwarfish stars; and he agrees in the main with the results obtained at Mount Wilson, which show the enormous remoteness of most of the clusters.

He discusses also the distribution laws for stars in globular clusters and correctly intimates that the vast amount of theoretical study in this field is of very little value. It is an illusion to compare such star systems with gases in equilibrium, and especially to deduce distributional laws from a hopelessly prejudiced sampling of the data.

The monograph also takes up the star counts by Pease and Shapley, the forms of globular clusters, the forms of open clusters, and especially the data on the colors and apparent magnitudes. Too much weight is given, in the reviewer's opinion, to irregularities in the Farbenhelligkeitsdiagramm. The observational data seem to be overworked (again in the opinion of the reviewer who made practically all of the observations and feels their uncertainties); but ten Bruggencate, through a possible overemphasis, is directing attention to an important future need in observational work. Moreover, he is fairly cautious in places where the temptation to speculate on the cosmogonic setting of the clusters must be almost irresistible. Pp. iv + 158, 36 figs., 4 plates. Julius Springer, Berlin, 1927. Price 15.00 R.M. unbound, 16.50 R.M. bound.

HARLOW SHAPLEY

Astronomy. A Revision of Young's Manual of Astronomy. HENRY NORRIS RUSSELL, RAYMOND SMITH DUGAN, JOHN QUINCY STEWART.—A generation ago the text-books of the late Charles A. Young were the standard for colleges and secondary schools, and his *General Astronomy* was used throughout the land. This was followed in 1902 by the *Manual of Astronomy* of intermediate grade adapted to students without mathematical training. It has been well known for ten years that Russell was working on a revision of Young's Manual, and this has at last appeared under the authorship of Russell, Dugan, and Stewart. The division of the labor is not indicated in the text, but the production of such a work is a three-man job in any case.

The two volumes might be characterized respectively as covering the old and the new in astronomy. Volume I, *The Solar System*, follows Young's text pretty closely, though everything has been checked and revised, and many new illustrations have been provided. The pedagogical value of the work is greatly enhanced by a list of valuable exercises at the end of each chapter.

It is in Volume II, *Astrophysics and Stellar Astronomy*, that the modern progress of the science is demonstrated. The original chapters on the stars which covered one hundred pages have been expanded several fold and entirely re-written. In this volume are also included chapters on the analysis of light, the solar spectrum, atomic theory, and the origin of spectra. This second volume makes a most convenient text for those astronomers whose knowledge of physics antedates some of the revolutionary changes in that science. It has been said that the most striking exemplifications of modern physics are to be found among the stars, e.g., the tests of the theory of relativity, the annihilation of matter, the density of the companion of Sirius, and so on, and students will find such things here in their astronomical setting. The chapter on the constitution and evolution of the stars gives results of the latest theories by such workers as Russell, Eddington, and Jeans, and will probably impress the general reader that there is much more to astronomy than the dull routine of exact measurement.

The exposition is simple and clear, and the work may be heartily recommended to the intelligent layman. The reviewer does not admire the excessive use of parentheses (characteristic of the style of the senior author), for most mortals cannot operate two trains of thought simultaneously, but not every mind from Princeton can be limited to a single track.

The mechanical production of the books is first-class, the division into two volumes of convenient size facilitating the work of teachers who desire to provide separate semester courses. The moderately thin paper enables a great amount of material to be put in a small compass, and the reproductions of modern astronomical photographs are good but do not represent the last word in pictorial effect. However, there is no need to search for minor blemishes in this monumental work; it will remain as the standard text and reference book for the serious student for a long time to come.

Volume I, xi + 470 + xxi pp., 190 figs.; Volume II, xi + 462 + xxx pp., 127 figs., Ginn & Co., 1927. Price \$2.48 per volume.

JOEL STEBBINS

Lehrbuch der Electrodynamik. Band 1. J. FRENKEL.—This excellent text consists of four sections: an introduction on vector and tensor analysis; electromagnetic effects independent of the time; electromagnetic effects dependent on the time; the relativity theory. In his vector notation the author has departed from the awkward continental use of parentheses for scalar product and brackets for vector product, and has adopted a notation very nearly the same as that advocated by Gibbs. In fact the chief divergence from Gibbs' notation is in the omission of the dot between the vectors forming a scalar product. The cross is used to designate vector product, unit vectors are employed, and ∇F and $\nabla \times F$ are used as alternatives to $\operatorname{div} F$ and $\operatorname{rot} F$ respectively. The gradient, divergence and rotation (curl) are defined by integrals over closed surfaces, a procedure which has the advantage of emphasizing from the start the invariance of these expressions for rotations of the coordinate axes.

The author introduces the subject of electrostatics from the standpoint of the elementary dipole and adopts the novel procedure of defining the electric intensity as the ratio of the maximum mechanical torque on the dipole to its electric moment. Steady currents are considered early in this section, and the subjects of electrostatics and magnetostatics are discussed in parallel rather than in series. No effort is made to take up in detail the solution of electrostatic problems by the use of spherical harmonics.

Maxwell's equations are developed early in the third section and much of this section is devoted to the electrodynamics of the electron. Among the topics of discussion are retarded potentials, the field of an oscillating dipole, electromagnetic waves, retarded and simultaneous fields of a moving point charge, the electromagnetic theory of mass, electromagnetic energy and radiation, energy of translation and of rotation of the Lorentz electron, the magneton.

The final section contains the usual topics connected with the special relativity theory, including the representation of E and H as components of a six-vector, and the various compact formulations of the more important electromagnetic relations in four dimensional tensor language. The relativity mechanics is also developed for the case of a particle in external electric and magnetic fields, and the Hamilton-Jacobi partial differential equation is set up. Applications are given, such as the revolution of an electron about a positive nucleus as in the Bohr model of the hydrogen atom.

The arrangement of topics is along conventional historical lines in that the subject of electromagnetism is developed fairly completely before the introduction of the relativity principle. In the reviewer's opinion a more logical treatment is assured by inverting the order and basing the whole subject of electrodynamics on the relativity principle as in the emission theory. Pp. x+365. Julius Springer, Berlin, 1926. Price unbound R.M. 28.50, bound, R.M. 29.70.

LEIGH PAGE

Leitfaden der Praktischen Experimentalphysik für Vorlesung und Unterricht. REINHARD MECKE and ANTON LAMBERTZ.—Those who can read German will find this book a helpful guide in setting up lecture demonstrations for classes in first or second year physics. It is, however, as the preface indicates, nothing more nor less than a reprint of a portion of Vol. 1 of Geiger and Scheel's recently published many-volumed "Handbuch der Physik." The book is much smaller and more concise than such works on physical demonstrations as those of Weinhold and of Frick, and contains but little on general lecture-room equipment. On the other hand it offers useful hints on the conduct of lectures, and is rich in diagrams, tables, and numerical data for blackboard presentation. Most of us who have experienced the vicissitudes of lecture-demonstrating will agree with the authors that "an experimental lecture is both a *Kunstwerk* and a *Kunststück*!" Most of the demonstrations are of the familiar and well-established sort. Among the evidences of up-to-dateness may be mentioned the demonstrations of magnetic hysteresis by means of the cathode-ray oscillograph, photo-electricity, the neon tube, the Johnsen-Rahbek effect, three-electrode vacuum tubes, and alpha ray tracks. A few minor errors have been noted; for example, an inconsistency in the list of overtones on page 41, the interchanging of oxygen and nitrogen in Table 24 on page 59, and an erroneous value for the melting point of zinc on page 48. Pp. vi+195. Springer, Berlin, 1926. Price, unbound R.M. 9.60, bound R.M. 10.80.

W. G. CADY

Müller-Pouillet's, *Lehrbuch der Physik*, 11th edition, 3rd vol., 1st half. *Physikalische, chemische, und technische Thermodynamik*. (including Heat Conduction), edited by ARNOLD EUCKEN with the cooperation of U. EBBECKE, M. JAKOB, A. MAGNUS, F. POLLITZER, F. SAUERWALD, R. SUHRMANN, and G. ZERKOWITZ.—The section of this standard work dealing with heat has been entirely rewritten since the tenth edition. The large amount of new material has necessitated dividing it into two volumes; the first volume, which is the one under review, deals with the phenomenological aspects of heat, while a second volume is promised dealing with the various aspects of kinetic theory. It is impossible in a review of this character to do much more than indicate the contents, which are as follows:

Introduction

General Part

A. Experimental Methods

- Thermometry
- Calorimetry

B. The Fundamental Laws of Thermodynamics

- The first law
- The second law

Historical survey of the development of the principles of thermodynamics

Special Part

I. Systems at Uniform Temperature

A. Homogeneous one-component systems

- Characteristic equation
- Thermal equation of state

B. Heterogeneous one-component systems

- Equilibrium between different states of aggregation
- Energy changes accompanying phase changes
- Surface phenomena

Velocity phenomena during change of phase.

C. Homogeneous systems of more than one component

- General properties of mixtures and solutions
- Equilibrium in gaseous mixtures and solutions
- Transient phenomena accompanying the establishment of equilibrium

D. Heterogeneous systems of more than one component

- The equilibrium of heterogeneous systems from the phenomenological point of view
- Thermodynamic treatment of special systems of more than one component
- Boundary surface phenomena
- Transformation and reaction velocity

II. Systems not at uniform temperature

A. Thermal processes neglecting the effects of work

- Equilibrium and chemical reaction velocity
- Heat conduction

B. Technical processes with generation of work

- General thermodynamic fundamentals of thermodynamic engines
- Thermodynamic engines with external combustion
- Thermodynamic engines with internal combustion

C. Technical processes with absorption of work

- Compression of gases
- Transport of heat with expenditure of work (Refrigerating machines and thermal pumps)
- Separation of gaseous mixtures

Appendix

Physiology of heat

In general the work seems to have been brought thoroughly up to date, and will prove to be a most valuable reference book, many parts of which can be used, as suggested by the title, for the instruction of advanced students. The major part of the book was written by A. Eucken, which of itself is sufficient guarantee of its authoritative character. It is perhaps surprising that in a book of this scope no mention is made of the thermodynamic properties of crystals, which can best be treated, as was done by Voight, by methods entirely thermodynamic in spirit.

The disconcerting aspect of all this recent German activity in producing indispensable reference books is that it does not appear where the average library is to get the money to buy them all, nor does it appear how the publishers can escape financial loss. Pp. xviii+1185, 575 figs. Friedr. Vieweg und Sohn, Braunschweig, 1926.

P. W. BRIDGMAN

The Enlarged Heat Drop Tables. HERBERT MOSS.—For the British Engineer Callendar's steam tables (E. Arnold and Co., London, 1924) are standard. The tendency everywhere in steam engineering is to push up the boiler pressure so that the current tables are becoming inadequate for considerable pioneering work. The available experimental data for these higher pressures are increasingly scanty and uncertain, particularly above 300°C. Hence, Moss has taken Callendar's systems of equations which agree satisfactorily over the known experimental region and has used them to cover the range from 400 to 2000 lbs/sq. in. Ultimately, any extrapolation must be checked by experimental work. This is a tedious and difficult job, so that perhaps such extrapolated data are the best temporary expedient. These "adiabatic heat drop" tables give the heat per lb. of steam convertible into mechanical work by an ideal Rankine cycle working between the specified limits; the Rankine cycle being accepted in British practice as the most satisfactory ideal approximation to an actual engine. Such an energy quantity is dependent on both pressure limits and on the temperature rise above saturation, being particularly sensitive to the low pressure. To cover both limits the heat quantity is given in successive tables, each for a particular low pressure, where each table lists this heat for saturation pressures from 400 to 2000 lb/sq. in. and also for temperature rise above saturation up to 300°F (superheats). This requires rather large steps in the tabulation, but it is claimed interpolation may be made with about the accuracy (in the sense of consistency) of the tables. In this connection, reference might be made to the work being done by the Am. Soc. of Mech. Eng. through their committee on "Steam Research," progress reports of which are published yearly in "Mechanical Engineering." There is a very definite need for further data on the properties of water, say above 300°C. Pp. 88, Edward Arnold, London, and Longmans Green, New York, 1925. Price \$3.75.

J. R. ROEBUCK

Enlarged Mollier Diagram for Saturated and Superheated Steam. H. L. CALLENDAR.—This table puts in graphical form the results of Callendar's work on steam. The chart is 66×80 cm and covers the pressure range of 0.2 to 2000 lbs per sq. in. and the temperature range of 100 to 700°F. Along with the equations and tables it forms the basis for Moss's heat drop tables. Curves also give the volume superheat, pressure, and temperature relations. To help in using the very complicated figure, part of the lines and symbols are printed in red. It is a well-printed diagram on good paper. Edward Arnold and Co., London, for the British Electrical and Allied Industries Association, 1926, and Longmans Green and Co., New York. Price \$1.35.

J. R. ROEBUCK

Fogs and Clouds. W. J. HUMPHREYS.—This is an entertaining little book which can be counted upon to provide a few hours of pleasant and instructive reading, with the privilege of looking at some remarkable photographs. Physicists, *qua* physicists, will probably be interested most by the chapters entitled *Evaporation and Precipitation*, *Fogs*, and *Cloud Miscellany*. In these, Mr. Humphreys has given, among many other bits of diverse information,

a description of the processes of formation and dissolution of clouds; a catalogue of the sorts of condensation-nuclei that occur in the air, and notions about the number of these and the sizes of the droplets of fog or rain which form around them; many interesting facts about the sizes and localities and velocities of clouds; a theory of the genesis of rain; and commemorations of some of the pioneers in the study of clouds. In the closing chapter, *Cloud Splendors*, the author gives a theory of lightning, and much information about the haloes, coronae, parhelia and other luminous phenomena due to water-droplets or ice-crystals in the sky. Physicists will wish that the arguments for the theories and the ways in which some of the data were obtained had been given in greater detail; but Mr. Humphreys would probably retort that he has satisfied that desire in other books, and designed this as a popular presentation. The central and longest chapter, *Cloud Forms*, contains an official list of definitions of the various types of cloud, expanded by further descriptions and illustrated by multitudes of pictures. I fear that even after repeated re-reading of this chapter, one would hardly be able to look up at the sky and instantly classify whatever sort of cloud he might see there floating—that is probably an art to be learned only by first-hand experience and demonstration in the field; but, as one who hitherto has known by name no form of cloud except the cumulus and the nimbus, I hope to be able to recognize at least the cirrus and the stratus henceforward. It is interesting to read of clouds which remain stationary while the wind and the water drift through them, condensing on the windward and evaporating on the leeward side. Not many scientific books are written in so vivacious, witty and lucid a style, although even this one is marred by some long sentences not written carefully enough to be clear, by a trace of turgidity in some of the poetic passages, and by the use of *wonder* and *master* as adjectives. The illustrations, as I have intimated, are numerous and many among them are superb; one would give much to witness some of the phenomena which Mr. Humphreys or his friends have caught with their cameras, and would pray to be spared from seeing some of the others. Pp. xvii + 104, 93 figs.; Williams & Wilkins Company, Baltimore, 1926. Price \$4.00.

KARL K. DARROW

Stereoscopic Drawings of Crystal Structures. Edited by M. VON LAUE AND R. VON MISES.—It is well known that spacial models are indispensable for the study of crystal structure. This collection of stereoscopic pictures has been prepared to supply that need without the cost and the large amount of space needed for the usual wire models. There are twenty-four stereoscopic drawings accompanied by a booklet containing an explanation of each in English and in German. The drawings have been selected to show the fourteen Bravais lattices and eight different crystal structures of the simpler sort. These are rocksalt, caesium chloride, zincblende, diamond, white tin, wurtzite, fluorspar, cuprite, and cadmium iodide. The names and interatomic distances of other crystals belonging to these eight types are also given. These drawings cannot be said to entirely replace good spacial models which can be examined at will from any desired orientation, but their convenience and low cost makes them very useful accessories in the study of crystal structure.—43 pp., 3 figs. + 24 plates. Julius Springer, Berlin 1926. Price 15 M.

JOSEPH VALASEK

Handbuch der Physikalischen Optik. Edited by E. GEHRCKE. Vol. I. First Half.—Following the recent rapid advances in physical optics it has become desirable to have an up to date summary of the present status of the subject. This set of books is therefore very welcome at this time. In general, the authors have adhered to the original intention of confining the first volume to classical or wave optics and the second to modern or quantum optics. Thus the first volume begins with several chapters on photometry including spectrophotometry, colorimetry, and recording photometry. This is followed by a chapter on the velocity of light and several chapters on refraction, the first of which deals with the instruments and methods used in its measurement. An excellent discussion is given of refraction and dispersion in general, and this is followed by a chapter on the relations of refraction to chemical composition and physical state. However, the physical bases for the various refraction and dispersion theories are reserved for another part of the book. Here one finds only the discussion of the formulas in the light of experimental results. There is considerable space devoted to re-

fraction by media with continually varying indices and to astronomical and terrestrial refraction. The last chapter is on interference and its many applications in experimental optics. There are many references throughout the book, making it easy to get further information on any of the subjects when desired. Pp. 470+VIII, 233 figs. Verlag von Johann Ambrosius Barth, Leipzig 1926. Price 40 R.M.

JOSEPH VALASEK

Handbuch der Physikalischen Optik. Edited by E. GEHRKE, Vol. II. First Half.—The first half of volume one has been reviewed above. Volume two begins with photochemical laws and reactions. This is naturally followed by a chapter on photography which deals with both the chemical and physical sides of the subject. In view of recent interest in photographic photometry, an important section is that on sensitometry and the theory of the photographic plate. Applications of photography to technical reproduction are also given, and so are the various methods of color photography. The remainder of the book is concerned with some of the problems of spectroscopy. This subject is here taken up from the empirical point of view with the emphasis largely on apparatus, technique, and discussions of results, rather than on the mathematical development of the theory. The subject matter includes spectral analysis in general, fine structure of spectral lines, photo- and chemi-luminescence spectra, radiation potentials, and series laws in line spectra. The various chapters are written by well known authorities in their respective fields. Numerous references facilitate the looking up of further information. In all, this is an excellent work for which there has been a great need in view of the growing importance of physical optics as the center of interest in physics of today. Pp. 418+V, 166 figs. Verlag von Johann Ambrosius Barth, Leipzig 1927. Price 37.50 R.M.
unbound.

JOSEPH VALASEK

PROCEEDINGS
OF THE
AMERICAN PHYSICAL SOCIETY

MINUTES OF THE WASHINGTON MEETING, APRIL 22-23, 1927

The 145th regular meeting of the American Physical Society was held at the National Academy of Sciences in Washington, D. C. on Friday and Saturday, April 22 and 23, 1927. The presiding officers were Professor Karl T. Compton, President of the Society, and Professor Henry G. Gale, Vice-president of the Society.

On Friday evening there was a dinner for the members of the Society and their friends at the Hotel Raleigh. The speakers at this dinner were Professor R. A. Millikan, Dr. E. E. Slosson, and Professor P. M. Debye.

At the regular meeting of the Council held on Friday, April 22, 1927, three were transferred from membership to fellowship and nineteen were elected to membership. *Transferred from Membership to Fellowship:* F. S. Brackett, J. J. Hopfield, and R. de L. Kronig. *Elected to Membership:* Charles S. Allen, Howard H. Brinton, C. J. Campbell, C. C. Cole, W. E. Curtis, Ralph K. Day, Milan W. Garrett, Newell S. Gingrich, Philip C. Jones, S. C. Lind, Noel C. Little, H. E. Marsh, Wm. Crawford McKissack, Jr., J. Howard McMillen, John G. Moorhead, Charles A. Rinde, Harry Rolnick, Henry Semat, and Lloyd P. Smith.

The regular program of the American Physical Society consisted of 94 papers, numbers 12, 14, 21, 35, 37, 43, 44, 46, 61, 72, 87, 88, 91, 92, 93, and 94 being read by title. The abstracts of these papers are given in the following pages. An Author Index will be found at the end.

HAROLD W. WEBB, *Secretary*

ABSTRACTS

1. **A thermo-magnetic effect on gases.** NOEL C. LITTLE, Bowdoin College.—If a temperature gradient is maintained in a gas completely enclosed by a metal box placed between the poles of an electro-magnet, the isothermal surfaces in the gas are warped upon the excitation of the field, provided the field is non-uniform. That the effect varies with the nature of the gas was shown by a thermo-couple placed midway between the ends of the pole pieces where the temperature gradient was 15 degrees per centimeter. When a field of 15 kilograms was excited, drops in temperature were observed as follows: in air 16 degrees, in oxygen 18 degrees, in nitrogen and carbon dioxide none, in hydrogen 6.6 degrees, in propane 16 degrees.

2. **Critical potentials of copper.** RICHARD HAMER and SURAIN SINGH, University of Pittsburgh.—Critical potentials of copper have been investigated in the region up to 30 Volts. The method adopted was to search for repeatedly occurring breaks in the current potential curves when a copper cylinder and insulated central copper rod suspended in a highly evacuated quartz tube were heated to about 700°C. The measurement of the potentials was made to depend on the determination by a potentiometer of the e.m.f. across a standard resistance

in the same portion of the series of standard resistances as that across which the applied potentials were taken. This permits the measurement of critical potentials to be made as accurately as desired. The breaks or changes of slope were taken to indicate the critical potentials and were checked by plotting the differential curves from the observed deflections for the applied equal changes in potential. The preliminary results for copper are as follows: 3.3, 7.9, 14.2, 19.5 and 25.3 volts for the range mentioned.

3. The significance of photo-electric conduction in crystals. A. M. MACMAHON, University of Chicago.—The numerous successes of the Rutherford-Bohr atom model suggest interesting possibilities which the conception may have when applied, with appropriate modifications, to the phenomena of the solid state—e. g., the conduction of electricity. An explanation of the light-sensitiveness of certain crystalline substances, particularly selenium, follows at once. Simultaneous differential equations, whose solution leads to an expression of the same form as the empirically determined one (Phys. Rev. 29, 219 (1927)) relating the change in current through a specimen to the time of illumination, are readily obtained upon the assumption of a shift to either of two distinct configurations of the outer electrons when light is absorbed. The picture seems more plausible than those of molecular changes, proposed by previous investigators to account for the exposure and recovery characteristics of selenium, and is in agreement with x-ray analyses which show that the crystal lattice is not perceptibly disturbed even under strong illumination. An explanation of the effect of previous illumination is afforded, and the transmitted action discovered by Brown and Sieg (Phil. Mag. 28, 497 (1914)) interpreted. This view of the conduction of electricity gives physical meaning to electrical resistance in agreement with the approach to perfect conductivity found for the metals at very low temperatures.

4. Relation between light intensity and photo-current in selenium. R. J. PIERSOL, Westinghouse Research Laboratory, East Pittsburgh.—This is a continuation of work previously reported (Phys. Rev. 29, 362 (1927)) in which the variation of photo-sensitivity with temperature pointed to the theory that selenium conductivity is photo-electric. Present work on white light and ten spectral frequencies shows a linear relation within experimental error between the light intensity and the square of the photo-current. This data is shown in the form of curves for the various colors of light. The results are further substantiation of the photo-electric theory of selenium conductivity.

5. Photo-electric threshold of bismuth crystals. T. J. PARMLEY, Cornell University.—Single bismuth crystals were grown according to Bridgman's method. The apparatus was mounted in a bell jar and evacuated to a pressure of 10^{-6} mm. Then a razor blade as the effective edge was used to open the crystal along a plane and the specimen was moved into position in a Faraday cylinder where readings were taken, the mechanical operations being controlled by external electromagnets. The light source included a quartz mercury vapor lamp and quartz monochromator. Saturation currents were measured by means of a Dolezalek electrometer of 1500 mm per volt sensitivity connected directly to the crystal. The photo-electric threshold of a freshly prepared surface was found to lie between 2804 and 2894 A. Fatigue curves extending over approximately an hour's time were obtained.

6. Effect of oxygen on photo-electric emission from potassium. L. R. KOLLER, General Electric Co.—Some measurements were made to determine the effect of adsorbed oxygen on the photo-sensitivity of a potassium photo-electric cell. Sufficient oxygen was admitted to form an adsorbed layer one atom deep. This cleaned up almost at once and no change in sensitivity was observed. Oxygen was then admitted in doses of about 100 microns. There was no appreciable change in photo-sensitivity until after 355 microns had been adsorbed. The next 800 microns resulted in a three-fold increase in sensitivity. After this, each dose resulted in an immediate drop in sensitivity followed by a gradual recovery, but for each successive dose, the drop was to a new low level and the recovery less complete. The explanation of these phenomena lies in the absorption of oxygen by the potassium. Small quantities

diffuse in so that no oxide is left on the surface. After the potassium is nearly saturated, the diffusion in is slowed down so that the effect on the surface can be observed. The gradual recovery takes place as the oxide diffuses in and a fresh potassium surface is formed. Eventually the potassium is all converted to oxide and the sensitivity is completely destroyed.

7. Electron emission and diffusion constants for tungsten filaments containing various oxides. S. DUSHMAN, D. DENNISON and N. B. REYNOLDS, General Electric Company.—In general the emission phenomena observed for these filaments are similar to those observed by I. Langmuir with tungsten containing thoria. Reduction of the oxide occurs at a very high temperature and activation at a lower temperature. None of the monatomic films produced in this manner are as stable as those obtained with thoria, owing both to more rapid diffusion and evaporation. This makes it difficult to obtain accurate emission data for completely covered films. Using the equation $I = AT^2e^{-b/T}$, the values of A and b obtained for different films are as follows:

Metal	Yt	La	Ce	Zr	U	Th
A	7.0	8.0	8.0	5.0	3.2	3.0
B	31,300	31,500	31,500	36,500	33,000	30,500

Measurements have also been made on diffusion constants (d) and rates of evaporation (E) for these films. The following table gives a summary of results obtained for 4 mil filaments at $T = 2000$. The values for Th are taken from Langmuir's paper.

Atom	$d \times 10^{11} (\text{cm}^2 \text{ sec.}^{-1})$	Heat of Diffusion $\times 10^8 (\text{atoms/cm}^2 \text{ sec.})$	Atomic Weight
U	1.3	100,000	> Th 238.5
Th	5.9	94,000	232
Ce	95.	83,000	1450 140.3
Zr	324	78,000	68 91.
Yt	1820	62,000	89.

8. Theory of the shot effect. HAROLD A. WHEELER, Johns Hopkins University.—The shot effect, described by Schottky, is the phenomenon of current fluctuations in a stream of electrons limited by random emission, as from a hot filament. Previous derivations of the magnitude of the shot effect have been based on equations derived in the abstract by the theory of probability. In the present paper, a simple derivation of the equation, $(I_0^2)_{\text{mean}} = eI_a/2RC$ (I_a = average space current), is given in terms of the familiar discharge current in a simple series circuit (R, C, L). This is followed by a Fourier integral derivation of the continuous frequency spectrum of the current fluctuations: $d(I^2)_m/d\omega = eI_a/\pi$. The simple derivation is thereby linked with former work and the correctness of the assumptions verified.

9. A study of the lag of the Kerr effect for several liquids as a function of the wave-length of the light. J. W. BEAMS, National Research Fellow, and Ernest O. Lawrence, National Research Fellow, Yale University.—We have shown that an upper limit to a possible lag of the Kerr effect in carbon bisulphide is $3 \times 10^{-9} \text{ sec}$. However, measurable lags have recently been observed for various liquids (method described in J. O. S. A. & R. S. I., 13, 597(1926); also paper by Beams and Allison in press). The differences between the lags of the Kerr effect for several liquids have now been investigated as a function of the wave-length of the light. The results indicate that the lag differences are independent of the light wave-length. The following are the excess lags over a possible lag in carbon bisulphide: Bromoform $3.3 \times 10^{-9} \text{ sec}$; Chloroform $3.8 \times 10^{-9} \text{ sec}$; Ether $6.0 \times 10^{-9} \text{ sec}$.

10. The instantaneity of the photo-electric effect. ERNEST O. LAWRENCE, National Research Fellow, and J. W. Beams, National Research Fellow, Yale University.—The grid and potassium coated plate of a three electrode photo-electric cell were attached in series with a bias battery across one of two condensers which in turn were connected in parallel with a spark gap. The arrangement was such that when the potential across the spark gap was nearly a maximum the field between the photo-cell plate and grid was such as to draw electrons to the grid and on to the collecting electrode. A definite time after the discharge of the spark

(equal to the wire path connecting photo-cell to spark gap divided by the velocity of light) the field reversed, thereby preventing electrons from leaving the plate. By varying the wire path this device permitted a study of the times of ejection of electrons by short flashes of light from the spark, produced by an earlier described method. Our experiments indicate that electrons start coming off a potassium surface the instant light falls on the surface and cease being emitted the moment the illumination is cut off, within a possible experimental error of 3×10^{-9} sec.

11. Polarization of resonance radiation in strong magnetic fields. Breadth of spectral lines. A. ELLETT, University of Iowa.—The polarization of resonance radiation excited by the D lines has been measured for various states of polarization of the exciting light and for magnetic fields up to 3500 gauss. With the electric vector of the exciting light parallel to the magnetic field the polarization reaches a value of 49 ± 1 percent in a field of 500 to 600 gauss and does not change with further increase of the field. With the electric vector perpendicular to the field the polarization reaches a value of $32.8 \pm .5$ percent at 500 gauss and remains constant to 1200 to 2000 gauss depending on the breadth of the exciting line. This line breadth may be made so small that first one and then both of the perpendicular components of D_2 fall outside the exciting line. D_2 excited by the inner perpendicular component alone is completely polarized. From the magnitude of the fields at which these components cease to be excited it is evident that the line breadth is about what one expects from Doppler shift alone, though it may exceed this slightly.

12. The magnetic moment of helium and molecular hydrogen. IRVIN H. SOLT, University of Cincinnati.—A narrow beam of molecules or atoms was produced by means of two slits, $.03 \times 2.2$ mm, three centimeters apart. The space between the slits was connected to a mercury vapor pump. The beam passed through a non-homogeneous magnetic field produced by a pair of pole pieces, one wedge shaped and the other slotted, after the manner of Stern and Gerlach. The beam was explored by a platinum wire $.017$ mm in diameter and 2.5 mm long which formed one arm of a Wheatstone bridge. No influence of the magnetic field on the beam was observed for a gradient of about 1.5×10^5 gauss per cm. The experiments are being continued with a view toward increasing the sensitivity of the apparatus so that other gases can be investigated.

13. The magnetic moment of atomic iodine. JOHN B. TAYLOR and T. E. PHIPPS, University of Illinois.—The magnetic properties of atomic iodine have been investigated in an apparatus which is a modification of that used by the authors in the determination of the magnetic moment of the hydrogen atom. The iodine was dissociated in an electrically heated tiny quartz tube furnace and the ray of atoms received on a liquid air cooled glass target, which had been first coated with a thin film of mercury. This was a very sensitive detector. A multiple separation of the ray in a magnetic field, corresponding to a magnetic moment of two, has been predicted spectroscopically for the iodine atom. The rather imperfect images thus far obtained show a distinct deflection of the ray, and apparently such a multiple separation into more than two lines corresponding to a magnetic moment greater than one. This latter point and the relative intensities of the lines cannot yet be decided with certainty.

14. Method of measuring the distribution of magnetic fields. J. TYKOCINSKI-TYKOCINER and J. KUNZ, University of Illinois.—The following method has been developed for the determination of field inhomogeneity between pole pieces as used in the magnetic moment measurements of atomic rays. Two bronze ribbons carrying a mirror and stretched on a frame move between the poles of an electromagnet whose field distribution in the air gap has to be determined. By means of two micrometer screws the frame can be moved either along or across the field. From the deflection of the mirror produced by direct currents passing through one of the wires and then through the other and then through both of them the magnetic field intensity and its gradient can be determined from point to point. Satisfactory results were obtained when currents of equal intensity flow through both wires simultaneously. For a current i_1 flowing through both wires in the same direction the angular deflection is

$\tan \alpha_1/2 = c(H_2 - H_1)i_1/d$ for a current i_1 flowing in opposite direction $\tan \alpha_2/2 = c(H_2 + H_1)i_2/d$ where H_1 and H_2 are the magnetic field intensities, c is a constant and d the distance between the wires. For small angles α the following relations are obtained $H_1 = d(a_1/i_1 + a_2/i_2)/4cD$ $H_2 = d(a_1/i_1 - a_2/i_2)/4cD$ and $\partial H/\partial x = (H_2 - H_1)/d = a_1/2ci_1D$, where D is the distance between the scale and mirror, and a_1, a_2 are the scale readings corresponding to the angles α_1 and α_2 .

15. The origin of the magnetic fields of sun spots. W. F. G. SWANN, Yale University.—Recently the writer has developed a modification of the laws of electrodynamics according to which among other things, a neutral rotating sphere should give rise to a magnetic field which at the pole is proportional to Dv^4 where D is the density and v the peripheral velocity. A sun spot is usually regarded as a U-shaped structure with appreciable rotation confined to a depth of the photosphere comparable with the diameter of the spot. As regards order of magnitude we should thus expect that the magnetic field of a sun spot would be comparable with that of a sphere rotating with the same peripheral velocity. According to this, if subscript s refers to the sun spot and e to the earth $H_s/H_e = (D_sv_s^4)/(D_ev_e^4)$. Taking H_e as 0.5 for the poles, $D_e = 5.5$, $v_e = 0.5$ kilometer per second, $D_s = 4 \times 10^{-5}$, we find that the value of v_s necessary to account for a value of H_s equal to 2000 gauss is 80 kilometers per second. This value is not unreasonable for a sun spot. On applying the theory to the planet Jupiter we calculate a magnetic field of the order 50,000 gauss for that planet.

16. Magnetic susceptibility of single-crystal metals. C. NUSBAUM, Case School of Applied Science.—The magnetic susceptibility of single-crystals of bismuth and antimony has been measured by a modified form of Terry torsion balance. The single-crystals of these metals are characterized by a three-fold axis of rotational symmetry, with the cleavage planes perpendicular to the principal axis. The crystals are rotated around an axis perpendicular to the principal axis of the crystal. The mass susceptibility (χ) for bismuth in a direction parallel to the principal axis is 1.13×10^{-6} and in a perpendicular direction 1.32×10^{-6} dyne-cms. Corresponding values for antimony are 0.497×10^{-6} and 1.38×10^{-6} , respectively.

17. Results of earth-resistivity surveys in connection with the study of earth-currents at Watheroo, Western Australia and Ebro, Spain. W. J. ROONEY and O. H. GRISH, Department of Terrestrial Magnetism, Carnegie Institution of Washington.—To supplement the potential registrations and so ascertain the earth-current density, earth-resistivity surveys have been made at the Magnetic Observatory of the Carnegie Institution of Washington, Watheroo, Western Australia, and at Ebro Observatory, Tortosa, Spain. At Watheroo, situated on a sandy plain, the resistivity at the surface varies with position from 90 to more than 4,000,000 ohms per centimeter cube. The mean values for the region are extremely low, the average to depths of 60 to 100 meters being 700. Beyond this depth the values increase slowly, reaching 5,000 for 600-meter depths, the greatest explored. At the Ebro Observatory, located in the valley of the river Ebro the resistivity, although generally low near the surface, is always higher than that at Watheroo when depths beyond 30 meters are included in the measurements. The average value to 100-meter depths is 9,600 and increases to a little over 12,000 for 300 meter depths, the greatest explored there. Records of potential gradient for a number of years give values approximately one magnitude higher at Ebro than at Watheroo. The resistivity results, therefore, indicate that the current density is of about the same magnitude at both places.

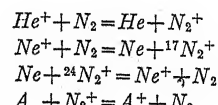
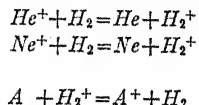
18. The Hall effect and resistance of sputtered tellurium films. F. W. WARBURTON, Cornell University.—According to Eldridge and Page the Hall coefficient should be proportional to resistance, but Mackeown's experiments with thin films have shown that the Hall e.m.f. remains constant when the resistance changes by aging. The present experiment was undertaken to find the relation of the Hall coefficient to resistance when the latter is changed by temperature or by means other than aging. Preliminary results show that the Hall e.m.f. in very thin films of tellurium is directly proportional to resistance, both when the temperature coefficient of resistance is positive, as well as when it is negative but is independent of change in resistance due to absorbed gas.

19. Magnetic properties of iron in high frequency alternating current fields. JOHN R. MARTIN, Case School of Applied Science.—A number of investigators have studied the losses due to eddy currents and hysteresis in iron when placed in high frequency alternating current fields, but the results obtained are in wide disagreement. Using a new method, the author has investigated the variation of this loss with the frequency for several areas of cross section. The total loss is considered as the equivalent of an absorbing resistance and by measuring the value of this resistance at resonance, the loss may be determined from the I^2R relation. With magnetizing currents of 3, 4 and 5 ampere-turns per cm, the measurements are made on short iron cylinders of various cross sectional areas, at frequencies ranging from 5.20×10^6 to 9.08×10^6 cycles per second. The loss is found to increase with frequency in the small samples and to decrease with frequency in the larger. At any particular frequency the loss is an inverse function of the area. This is due to the magnetic shielding effect of eddy currents in the large samples and the disagreement between previous investigations may thus be explained.

20. On refraction in moving media. N. GALLI-SHOHAT, University of Michigan.—For light passing from vacuum to a moving medium it is customary to construct a "relative ray" with the help of Fresnel's drag coefficient $(1 - 1/n^2)$. If one applies Fermat's principle both to this ray and to the wave normal, it may be shown that only one of them obeys Snell's Law. The variation of one path affects the other in such a way that it would be necessary to neglect first order terms in v/c in order to preserve Fresnel's form of the drag coefficient. It is possible however to preserve Snell's law for both rays by a modification of the drag coefficient so that it depends on the angle of incidence and assumes the customary form for normal incidence.

21. The theory of the magnetic nature of gravity and electrons. CORNELIO L. SAGUI, Castelnuovo dei Sabbioni, Italy.—In a preceding paper Balmer's series were derived from equation $(x^2 + x)/2 = y$ and other possibilities as to their behavior were investigated. The attempt is made to give a physical meaning to those mathematical results by considering the structure of an atom as an assembly of protons and electrons. Electrons are considered as an assembly of a large number of electromagnetic quanta and reasons are given for their negative electric charge. Again, a proton would result from an assembly of electrons and its positive charge is considered as due to a symmetrical difference in its structure, resulting in the opposite to an electron. The Einstein's equation $eV = h\nu$ was considered in the light of the theory and frequencies ν were supposed to be due to the splitting up of the electrons themselves into smaller units of energy. The effect would be wholly a mechanical one. The atomic fluorescent absorption, the Compton effect, the phenomena of absorption of light by atoms and their re-radiation, as well as the Brownian movements are all investigated from the point of view of the electromagnetic quantum theory.

22. Ionization by collisions of the second kind in mixtures of hydrogen and nitrogen with the rare gases, GAYLORD P. HARNWELL, Princeton University.—The behavior of ionized mixtures of hydrogen and of nitrogen with helium, neon, and argon separately have been investigated by means of a positive ray analysis. (See abstract No. 24, New York Meeting, Feb. 26, 1927.) Due to the secondary products of ionization the variation with pressure of the types of ions present was found to be more complicated than in the rare gas mixtures previously studied. However, in all cases so far investigated the results are in agreement with those predicted on the basis of a type of collision of the second kind resulting in ionization of atoms by collisions with ions of atoms of higher ionizing potentials. These processes are represented by the following equations:



In these cases as in pure rare gas mixtures the interchange was found to be most probable when the difference between the ionizing potentials was least.

23. The dissociation of hydrogen chloride by positive ion impact. WALTER M. NIELSEN, Duke University.—Positive ions from a heated sodium phosphate source were projected between two electrodes, P_1 and P_2 , towards a third electrode, P_3 . The hydrogen chloride, fed into the tube through a fine capillary, was generated by dropping H_2SO_4 onto $NaCl$. With a mean free path of about 2cms, and with a potential on P_1 such as to prevent positive ions from reaching it, and with a small drawing out potential for positive ions on P_2 and P_3 , currents were measured for increasing values of the driving potential, V_F . No negative current to P_1 was observed below 34 volts. Above this value of the driving potential the ratio of negative current to total positive ion current increased rapidly with increase in the driving potential. The positive currents were of the order of 1×10^{-9} amperes, the negative of the order of 2×10^{-10} amperes. A magnetic field of about 500 gauss was applied so as to prevent secondary electrons from leaving any of the accelerating or collecting electrodes. The driving potential at which a negative current is first observed is lowered by an increase in the drawing out potential of P_2 and P_3 , but is not affected by an increase in the retarding potential of P_1 . The experiment does not indicate the products of dissociation.

24. Combination of hydrogen and oxygen by electric discharges and x-rays. ROGERS D. RUSK, North Central College.—A study has been made of the combination of hydrogen and oxygen in the Geissler tube discharge, low-voltage arc, electrodeless discharge and by exposure to x-rays. Rates of combination were measured at pressures varying from 1mm to .01mm and with different proportions of the gases. In the low-voltage arc, the rate of combination per milliampere of arc current was abnormally small after making due allowance for the catalytic action of the coated platinum filament, which set in quite regularly with the filaments used at $65^{\circ}C$ (thermocouple measurement.) This suggests that in the low-voltage arc combination occurs mostly at or near the cathode. The logarithmic decrease in rates of combination in the other cases indicates that combination is a matter of gaseous collision. The results agree with the notion that combination is proportional to number of ions present, and in the Geissler tube discharge approximately 0.12 molecules of water per ion were formed at a pressure of .1mm in equivalent volumes.

25. The dissociation of hydrogen by electrons. A. L. HUGHES and A. M. SKELLETT, Washington University.—The dissociation of hydrogen, through which electrons are driven, may be the direct result of a collision between an electron and a hydrogen molecule, or it may be due to a secondary process, in which the dissociation actually results from a collision between a neutral hydrogen molecule and an ionized (or excited) molecule which itself had been produced by an electron impact. At sufficiently low pressures, the number of molecules dissociated should be proportional to the pressure if the effect be a direct one, but proportional to the square of the pressure if the effect be a secondary effect. Using the yield of dissociated hydrogen molecules at different pressures as a criterion, the experiments are decisively against the effect as being a secondary effect. Investigation shows that if the mean free path of the ionized (or excited) molecule be abnormally small, the above criterion may not be able to distinguish between the two possible processes at pressures available. Provided that the mean free path is not less than one three hundredth of that of the normal molecule, these experiments are decisively against the interpretation that dissociation is a secondary process.

26. Some observations on the nature of the nitrogen afterglow. A. G. WORTHING, Nela Research Laboratory and University of Pittsburgh.—Three 6-inch spherical glass bulbs symmetrically joined by large glass tubing were filled with nitrogen (1 to 5mm). Discharges in one bulb caused sudden visible streamings to the other bulbs. After the filling of the bulbs, the afterglow stream, which was produced by a single impulsive discharge, was completely stopped near the exit. It formed an umbrella-shaped luminous cloud which was many times as bright as the afterglow elsewhere in the bulb. After many discharges, the resistance to the passage of the afterglow broke down, and the afterglow carriers seemed to pass unhindered to the other bulbs. The most probable explanation suggests either that the afterglow carriers or that some of the agents active in the production of these carriers are electrically charged.

Some experiments with a tube (approximately 200mm of A, 0.4 mm of N₂) seem to indicate that this effect is limited to the early stages following a discharge. These observations do not seem to support the view that the afterglow has its origin in impacts of neutral unexcited nitrogen atoms and molecules.

27. The scattering of electrons by a nickel crystal. C. DAVISSON and L. H. GERMER, Bell Telephone Laboratories, Inc.—In bombarding a {111} surface of a single crystal of nickel with a beam of electrons of uniform speed it has been found that, for certain definite bombarding speeds, there are beams of scattered electrons leaving the crystal in perfectly sharp directions. A simple correlation between these directions and the directions taken by diffracted beams of x-rays can be stated as follows. If the known crystal structure of nickel were contracted by a factor of 0.7 in a direction parallel to the incident beam then among all the diffracted x-ray beams those ten sets of beams which correspond to the longest x-ray wave-lengths would coincide in position with ten observed sets of electron beams. The wave-lengths of the wave disturbances which could give rise to these beams are quite accurately given by $\lambda = h/mv$, in accordance with the wave mechanics. In addition to these ten sets of electron beams there are three other such sets for electrons below 200 volts. These three sets seem not to observe the symmetry required by the known structure of the nickel crystal, and they offer strong evidence that there exists in this crystal a structure which has not been hitherto observed for nickel.

28. O- and N-energy levels in the secondary emission of hot tungsten. HERMANN E. KREFFT, General Electric Company, Nela Park.—While critical potentials found by Richardson and Chalklin in the soft x-radiation of tungsten agree fairly with computations of its O and N-energy levels from x-ray data, there does not seem to be such a relation between these levels and breaks found by Petry on the secondary emission curve. If, however, the secondary emission is measured with the tungsten at about 1200° K, a number of breaks are easily obtained at primary velocities of v_p = 5 to 750 volts on the curve showing the number of secondary electrons per primary as a function of v_p . The electrode arrangement is similar to the one described by Petry. A very considerable break occurs at a primary velocity of 70.5 volts (corrected), this one also being the most prominent break above 25 volts. With cold tungsten only a slight indication of this break is obtained. This break is undoubtedly due to the O₁-level of the tungsten atom, the value 70.5 volts, or $v_p/R = 5.2$, being in excellent agreement with the value given by Bohr and Coster. The greater part of the other breaks agree well with measurements of Richardson and Chalklin and with the values for the N₁, N₂ and N₃ levels computed by Nishina. The secondary emission of other metals near tungsten will have to be studied before a definite interpretation of these breaks can be made. This work is being continued.

29. Reflection of electrons from molybdenum. W. R. HAM, Pennsylvania State College.—The apparatus in use consists of: (1) a source of steady direct current; (2) water-cooled Coolidge tubes with molybdenum anti-cathodes; (3) a constant flow calorimeter for measuring the heat developed at the anti-cathode; (4) a method of applying retarding potentials varying from zero to full impressed p.d. to the outside surface of the glass of the tube, while the tube is being run at a particular impressed voltage. (1000–22,000 volts). Since the power input, the heat generated at the anti-cathode, and the velocity distribution of reflected electrons are all measured, the percent of reflected electrons relative to incident electrons may be plotted against velocity of reflected electrons. A large percentage of reflection occurs at velocity corresponding approximately to 2900 volts. Peaks of reflection seem to occur as the impressed p.d. passes the critical potentials for the L levels and also probably the K level of molybdenum. The total number reflected is in general more than 100 percent of the incident electrons but much the larger part of this number have relatively slow velocities. Different tubes behave much alike and there is little evidence that residual gas has any effect on the results.

30. Velocity distribution and 180° scattering of low velocity electrons from iron. H. E. FARNSWORTH, Brown University.—The curve expressing ratio of secondary to primary electron current as a function of accelerating potential for both iron and copper show prominent

maxima and minima in the low velocity region. If these are due to atomic inelastic collisions one might expect to find evidence of this from a measure of the velocity distribution of the secondary electrons. Such measurements for iron show no evidence of inelastic collisions. These results, together with the fact that the above mentioned maxima and minima are obtained only after heating the metal at a critical temperature, are interpreted to mean that sudden changes in slope in the low velocity region of the secondary electron curve for metals are not an atomic phenomenon but are characteristic of the arrangement of atoms at the surface. The apparatus was such that those electrons leaving the iron target nearly normally, fell on an insulated disk concentric with the primary beam thus giving a measure of the fraction leaving approximately normally. This fraction, for primary velocities of a few volts, is much greater than that to be expected from the cosine distribution law, and decreases rapidly with increasing primary velocity to about 30 volts. Observations subsequent to baking the target at 350° C but previous to heating at red heat did not show this distribution.

31. A theory of the normal cathode fall. K. T. COMPTON and P. M. MORSE, Princeton University.—Use is made of the experimental value of the cathode fall of potential V_n and Townsend's empirical equation for the number of ionizing collisions α per unit path by an electron, together with the principle that the potential drop is distributed throughout the fall space so as to give maximum current. Thence is deduced the law $pd_n = A$ for the product of the pressure p and cathode fall space d_n , and acceptable values of the constant A are calculated for various gases. Certain dependence of d_n on cathode material is predicted, in conformity with observations. Distribution of ionization throughout the fall space is also calculated, and the results prove that a cathode in an ionized gas must be a much more copious emitter of electrons under positive ion bombardment than is a degassed metal. Introduction of Poisson's equation leads to the known law for normal current density $(j/p)^{1/2} = B$, and gives values of B which are approximately correct. At several points second order corrections are neglected, and the boundary conditions are not very satisfactorily known. Yet the theory seems to be distinctly promising in this field, in which there has been no previous tenable theory.

32. Heats of condensation of electrons and positive ions on molybdenum. C. C. VAN VOORHIS and K. T. COMPTON, Princeton University.—A small molybdenum sphere was supported in a region of intense gas ionization by three fine wires, two of which formed a thermocouple to measure its temperature, while the third carried the current of the incoming ions. Space potential and mean electronic energies \bar{V} were found by using the sphere as an exploring electrode. Its rate of heating due to an increment Δi in the electron current reaching it against a small retarding field was measured and equated to $\Delta i(\bar{V} + \phi)$, whence the heat of electron condensation ϕ was found to be 4.76 volts in argon; 4.77 or 5.01 volts in nitrogen; and 4.04 or 4.35 volts in hydrogen. The double values follow different treatments of the surface. The probable error of measurement is less than 1 percent, but uncertainty regarding the specific heat of molybdenum causes some uncertainty in the absolute values. Similar measurements of the heating effect of a positive ion of argon gave about one volt, which indicates that less than half of the energy of neutralization of the gas ion at the surface, is absorbed by the metal. ϕ_- and ϕ_+ are involved in the theory of gas discharges. Incidentally, confirmatory evidence was found for Langmuir's "high speed electrons."

33. The method of least squares vs. the arithmetic method of obtaining the slope of a straight line. R. C. SPENCER, Westinghouse Lamp Company, Bloomfield, N. J.—This discussion applies particularly to the case where the abscissas are spaced equidistantly. To illustrate: Let $t_1, t_2, \dots, t_r, \dots, t_s, \dots, t_N$ be the times of N transits of a torsion pendulum. Let the difference, $(t_r - t_s) = T(r-s)$, have a weight of unity. Then the period, $T = (t_r - t_s)/(r-s)$, will have a weight of $(r-s)^2$ because the error in $(t_r - t_s)$ has been divided by $(r-s)$. In general we will use only n observations, discarding the inner ones. The weight of the period as calculated by the method of least squares is $(N-1)^2 + (N-3)^2 + (N-5)^2 \dots$ to $\frac{1}{2}n$ terms. The weight of the arithmetic solution is $\frac{1}{2}n(N-\frac{1}{2}n)$. The arithmetic method has a maximum weight when the inner third of the observations are discarded. Tables are given comparing the two methods.

The arithmetic method can be used on a standard motor driven calculating machine by pressing the numbers 1, 2, 3 etc. up to $n/2$ and down again to 0. The sum will give the period, T , in fifths of seconds times $\frac{1}{2}n(N - \frac{1}{2}n)$. A mechanical spring model is described. The potential energy at equilibrium is a minimum, and is proportional to the sum of the squares of the spring displacements. Therefore, the equilibrium position gives the least square solution of the system.

34. Log, semi-log, and uniform coördinator. II. R. A. CASTLEMAN, JR., Bureau of Standards.—A log, semi-log, and uniform *coördinator*, (a combination of plotting instrument and computing instrument) has been designed with special reference to its usefulness in the physics or physical engineering laboratory. The device employs a drawing board, a T-square, two slide rules and certain machined accessories. One rule is attached along one edge of the drawing board, while the other is attached to the T-square, whose shoe is arranged to bear on a straight-edge of the former slide-rule. Indices attached to the T-square and a suitable slider make possible: (a) coordination of the three kinds mentioned above; (b) quick and easy change from plotting to computing; (c) quick and easy change from one side of the T-square blade to the other. Each rule carries three sizes of log and one of uniform scales, thus furnishing practically all needed combinations. The use of a somewhat similar device in the special cases of power and exponential-finding has been pointed out in previous articles.

35. Shielding from vibrations. R. C. HARTSOUGH, Western Electric Company, Inc.—The shielding of sensitive apparatus from vibration by the use of thin inflated rubber bags has been found to approach 100 percent. Three bags are generally used and interconnected so that they all have exactly the same pressure. A pressure of 50cm of water and approximately four pounds mass on each bag gave perfect shielding for all ordinary vibrations. An interferometer mounted on a quartz fibre was shielded so effectively that the fringe system was quiet, even with persons walking in the room.

36. A redetermination of the Newtonian constant of gravitation. PAUL R. HEYL, Bureau of Standards.—The present accepted value of the Newtonian constant of gravitation rests upon the independent work of Boys and Braun done thirty years ago. It is 6.66×10^{-8} , with an uncertainty of one unit in the third significant figure. About three years ago the Bureau of Standards undertook a redetermination of this constant with the object of obtaining another decimal place. The results so far obtained confirm the present accepted value and add the desired figure 6.664. The method was that of a torsion pendulum in a vacuum, as used by Braun.

37. A resonance method for the determination of the universal constant of gravitation. JACOB KUNZ, University of Illinois.—Two comparatively large spheres placed on a table are made to carry out undamped simple harmonic motion. Between these spheres there are suspended two small spheres, connected by a light bar, in a vacuum. The harmonic motion of the outer spheres induce forced oscillations of the inner spheres, which become large when their natural frequency coincides with the impressed frequency. The differential equation of the motion has been developed. It is much more complicated than the classical differential equation of resonance. The present differential equation has been solved by a method of successive approximations.

38. Variation of gold plated screw-knob weights with atmospheric humidity. A. T. PIENKOWSKY and E. S. FOWLE, Bureau of Standards.—Many gold plated weights of the common screw-knob type have been found to change by excessive amounts with changes in the humidity of the air. Measurements were made on the sets of the weights from 1 gram to 50 grams inclusive, from each set. When the relative humidity changed from 30 percent to 70 percent, the first set yet noted changed nearly 3 mg in 8 days, and was still gaining rapidly. When the humidity was lowered to 30 percent again, these weights promptly returned to their original value. In the 18 sets first tested, more than half the sets changed more than 0.5 mg for the same

conditions, while about 0.1 to 0.2 mg seems to be the smallest change that occurs with such sets. These weights were from both American and foreign makers. Several variable sets were boiled in water with the knobs out and with the adjusting material removed so far as practicable. The variations then dropped to about 0.2 mg. Weighings were made without removing the sets from a box in which the humidity was controlled, but the standards and balance were outside this box, and therefore not affected by the changes in humidity.

39. Thermal expansion of some nickel steels. PETER HIDNERT and W. T. SWEENEY, Bureau of Standards.—Data on the linear thermal expansion of some nickel steels containing from 36 to 42 percent nickel, have recently been obtained for various temperature ranges between room temperature and 500°C. The expansion curve of each steel showed a critical point by an abrupt increase in the rate of expansion. The nickel steels containing from 38.4 to 42.2 percent nickel expand less than invar for the temperature range from 20° to 500°C. Additional alloys having a greater range of coefficients are being tested. The following table gives a comparison of the results obtained.

Nickel Content Per cent	Critical Point °C	Average Coefficient of Expansion per Degree Centigrade	
		20° C to Critical Point $\times 10^{-6}$	Critical Point to 500° C $\times 10^{-6}$
36.4	260	3.1	14.4
36.9	260	3.3	14.7
38.4	300	3.5	14.4
41.0	340	5.1	14.2
42.2	340	5.5	13.6

40. The resolving power of the ears. ARTHUR LOWELL BENNETT, Union College. (Introduced by P. I. Wold.)—The resolving power of the ears will be defined for use here as the shortest time interval between two successive sound impulses, the first occurring in one ear and the second in the other, for which interval the observer can distinguish in which ear the first impulse occurred. When the interval becomes quite small the sounds merge into each other but, through the binaural sense, one is still made aware of the difference in time of arrival. A rotating disc with two brush contactors, one of which could be displaced angularly, made it possible to send two impulses separated by a small time interval measurable to a hundred thousandth of a second. Data taken on eleven observers show that every observer was able to distinguish with certainty at one one-thousandth of a second and that the limit for the average observer is one tenth of this or less. One exceptional observer was found whose limit was less than one millionth of a second.

41. The surface tensions of the molten elements as functions of the temperature. I. Copper. E. E. LIBMAN, National Research Fellow, University of Illinois.—Copper is melted in a square box with a capillary side tube by means of a high vacuum, water cooled, molybdenum wound furnace of special design. The temperature is measured by means of the resistance of the molybdenum furnace winding. An x-ray photograph is taken through the entire furnace and the capillary depression and depression of the surface at the walls of the square box is measured on the photographic films. This gives two observations for the two unknowns, surface tension and angle of contact. The method, as usual, gives not the surface tension directly but the "capillary constant" (twice the surface tension divided by the product of the density of the molten material and the acceleration of gravity) from which the surface tension can be obtained when the density of the molten material is known. In this way the capillary constants of copper have been determined over a range of temperature from the melting point 1083°C to about 1400°C, and the error is estimated not to exceed 2 percent. The capillary constant of copper at its melting point is .301 cm² and decreases linearly with rise in temperature to .269 cm² at 1375°C.

42. Variation of surface tension of oils with the temperature. GEORGE WINCHESTER, Rutgers University.—The surface tension of several high flash point oils has been measured at temperatures up to 550°F during the last two or three years by the maximum bubble pressure

method. The densities of the oils were linear functions of the temperature up to 450°F. Between 300° and 550°F Mendeleeff's equation for an ideal liquid is verified within the limits of experimental error, estimated at about 0.4 of a dyne. Below 300°F the surface tension decreases faster than the temperature rises. The critical temperature is calculated from the formula, $T = a - bt$.

43. Influence of electrolytic ions upon moisture of steam. (Analogue of Wilson cloud experiment.) ARTHUR W. EWELL, Worcester Polytechnic Institute.—Bubbles of vapor, breaking at the free surface of a liquid, inevitably throw some liquid into the vapor space and, if the vapor is continuously drawn away, some of this liquid will accompany the vapor—a phenomena known technically as "priming." An apparatus was designed, which permitted quite accurate measurements of the priming of pure water, and of various solutions. It was found that priming increases with the density and viscosity of the solution, and decreases with the number of electrolytic ions present. The addition to water of such a salt as sodium or potassium chloride, which highly dissociates, and increases the density and viscosity but little, reduces the priming. As gaseous ions in a vapor facilitate the formation of liquid bubbles, so electrolytic ions in a liquid (probably by reduction of surface tension) facilitate the formation of vapor bubbles, and thus produce quieter boiling and less priming. Slightly dissociated salts, such as lead acetate, increase the priming on account of the large increase which they produce in the density, and solutes showing no dissociation, such as cane sugar, increase the priming still more.

44. Relations in connection with the reversible mixing of substances in the condensed state at the absolute zero of temperature. R. D. KLEEMAN, Union College.—The properties of the quantities associated with the reversible mixing of substances in the condensed state, initially under the pressure of their vapors at the absolute zero of temperature, have been investigated on the basis of the theoretical results previously communicated (Phys. Rev. 29, 369 (1927)). It is shown that: $H_m = 0$, $(\partial H_m / \partial T)_v = 0$, $(\partial^2 H_m / \partial T^2)_v = 0$, $(\partial H_m / \partial T)_p = 0$, $(\partial^2 H_m / \partial T^2)_p = 0$, $dH_m / dT_p = 0$, $d^2 H_m / dT^2 = 0$, $p_m = 0$, $(\partial p_m / \partial T)_v = 0$, $(\partial^2 p_m / \partial T^2)_v = 0$, $(\partial p_m / \partial T)_p = 0$, $(\partial^2 p_m / \partial T^2)_p = 0$, $d p_m / dT = 0$, $d^2 p_m / dT^2 = 0$, $A = 0$, $(\partial A / \partial T)_v = 0$, $(\partial^2 A / \partial T^2)_v = 0$, $(\partial A / \partial T)_p = 0$, $(\partial^2 A / \partial T^2)_p = 0$, $dA / dT = 0$, $d^2 A / dT^2 = 0$, where H_m denotes the heat absorbed during the process of mixing the substances, A the external work done, p_m the increase in internal energy, p the pressure, v the volume, and T the absolute temperature. A total differential coefficient indicates that the substances are kept under the pressures of their vapors during a change in temperature. Accordingly the mixing of substances, including different forms of the same substance, is under these conditions not attended by a change in entropy and internal energy. The formulas: $T\Delta S = H_m = p_m + A = \Delta U + A$, $\Delta U = T(\partial A / \partial T)_v - A$, $\Delta U = T(\partial A / \partial T)_p - A$, $\Delta U = T(dA / dT) - A$, it can then be shown, hold for all temperatures, where S denotes the controllable entropy and U the controllable internal energy.

45. The vacuum tube oscillator. D. G. BOURGIN, Lehigh University.—The functional dependence of total filament emitted current on grid and plate voltages is formally approximated by $i_p + i_g = A[1 - \exp\{- (E_p + \mu E_g)^2\}]$ for $E_p + \mu E_g > 0$ where A is the saturation value of the current and the other symbols are standard notation. (The approximation may be improved by considering this to be the initial term in an expansion in terms of Hermite polynomials). This relation is made the basis for the "second order" treatment of the Hartley oscillator. By applying Kirchoff's laws to the equivalent network, three simultaneous differential equations of the third order are derived connecting the variable grid and plate voltages and currents, and the current in the oscillatory circuit. These equations are restricted to the case that the phase difference between E_p and E_g is closely 180° and that the general conditions for efficiency indicated by Prince are satisfied. Only the fundamental is considered. By tabulating the values of the Fourier series coefficient for the fundamental in the expansion of $\exp\{- (a + b \sin x)^2\}$ it becomes possible to use a combined analytical and graphical method to determine the amplitudes, phase relationships and fundamental frequency. The approximation for the grid current is, as yet, not wholly satisfactory.

46. A device to draw characteristic curves of vacuum tubes automatically. G. C. CAMPBELL and G. W. WILLARD, University of Minnesota.—The usual circuit for obtaining characteristic curves was used. The grid-potential was varied continuously throughout the desired range by a modified W. G. Pye drum rheostat of the potentiometer type driven by a synchronous motor through speed reducing gears. A Leeds & Northrup recording pyrometer of the potentiometer type, connected across a standard resistance in the plate circuit, automatically drew the grid-potential plate-current curve in rectangular coordinates. The paper roll of the recording instrument was driven by the same motor that varied the grid-potential in order to insure uniformity. The instrument worked well with currents as low as 0.5 millampere for full scale deflection which interpreted graphically means the maximum ordinate permitted by the width of the coordinate paper which was ten inches. Obviously, smaller currents require a larger resistance in the shunt to give sufficient potential drop for full scale deflection which reduces the sensitivity of the instrument and fixes the low current limit for satisfactory operation with any given galvanometer in the recording instrument. Characteristic curves of a higher order of accuracy than are usually obtained by plotting points were drawn in from five to ten minutes depending on the reducing gears used.

47. Space charge as a cause of negative resistance in a triode. LEWI TONKS, General Electric Co.—Oscillations occurring in a tuned circuit connected to grid and plate of a triode have been obtained by Gill (Phil. Mag. **49**, 993, (1925)) when the grid potential was 40 volts and plate potential 8 volts. These were ascribed to unstable space charge in the tube. In the present paper the mathematical theory for the case of plane parallel electrodes is first presented and later applied qualitatively to the case of cylindrical electrodes. The existence of a virtual cathode may cause negative resistance in both plate and grid circuit under emission limited operation, but for the case of space charge limited operation negative resistance is at most very small. The theory has a possible bearing on very short wave generation by the method of Barkhausen and Kurz (Phys. Zeit. **21**, 1 (1920)).

48. Electric absorption currents in solid dielectrics. HUBERT H. RACE, Cornell University. (Introduced by F. K. Richtmyer).—The lower electrode of a guard-ring condenser containing specimen under test was connected, either (A) to constant potential or (B) to ground. The upper electrode was connected to a quadrant electrometer and an adjustable air condenser. This insulated system was maintained at ground potential by controlling voltage on the air condenser. Thus charge, (A) and discharge, (B), curves were obtained as functions of time (t). Using plates in intimate contact with specimen, potential was applied until current became constant at I_a , the true conduction current. Then potential was removed and the following relation was observed for certain materials: $i(\text{charge}) - I_a = -i(\text{discharge}) = i_a$ (1). For these materials, of which hard rubber is a good example, an approximate straight line was obtained between $\log i_a$ and $\log t$, so that the current i_a , due to absorption, may be represented by the equation: $i_a = (c/t)^b$ (2) where b and c are determinable constants. Tests were also made with an air gap between specimen and upper plate. Eq. (2) was still found true but eq. (1) was not.

49. Effect of temperature on polarization capacity and resistance for gold and platinum electrodes in different concentrations of sulphuric acid and at different audible frequencies. E. E. ZIMMERMAN, Cornell University.—Measurements of polarization capacity together with corresponding values of cell resistance have been made for gold and platinum electrodes in sulphuric acid solutions at temperatures varying from 0°C to about 90°C. Measurements were made by means of an a.c. bridge using frequencies from 650 to 3900 cycles. For platinum electrodes in a 12.7 percent solution of H_2SO_4 , the temperature coefficient is positive and has a value of about 0.37 of a microfarad, for one electrode of unit area, per degree rise in temperature. The value decreases at the upper range of temperatures and also with decreasing concentration. For gold electrodes, the average value of the temperature coefficient is about one-tenth of that for platinum. In contrast to the results with platinum, the value of temperature coefficient increases at the upper part of the temperature range. Cell resistance, with platinum electrodes, decreases with increasing temperature while with gold electrodes the

resistance, especially at higher temperatures, increases with temperature. For both metals, the temperature coefficient of capacity decreases with increasing frequency. Incidentally, studies of variation of capacity and cell resistance with varying frequency have been made at constant temperature. Also, decay curves have been obtained for gold electrodes after hydrogen polarization. No such decay curve could be obtained using platinum electrodes.

50. Analysis and applications of wave filter determinants. FRANCIS D. MURNAGHAN and HAROLD A. WHEELER, Johns Hopkins University.—In the study of the electric wave filter comprising a finite line of recurrent sections, the simultaneous equations in currents and voltages yield determinants of a known type. By the method of difference equations, various typical determinants are evaluated and expressed in terms of convenient substitutions. Special attention is given to the finite cases involving (1) terminal conditions and (2) two recurrent sections in alternating succession. Procedures are given and simple formulas developed applying the determinants to (1) free oscillation frequencies of finite, conservative lines and (2) steady state response of finite, non-dissipative Campbell filters, terminated by any values of resistance, as a function of the frequency of the applied alternating voltage. Proceeding to the infinite line by a novel method, the iterative impedance and propagation exponent are derived. The definition of complex electric impedance is outlined to show the fundamental differential equations involved and thereby make the work equally applicable to other systems with similar differential equations.

51. Formal unification of gradient, divergence, and curl, by means of an infinitesimal operational volume. VLADIMÍR KARAPETOFF, Cornell University.—Besides the usual definitions of gradient, divergence, and curl, familiar to physicists, some German writers on Vector Analysis (Runge, Spicrein, von Ignatowsky) define these quantities as ratios of certain integrals of a scalar or vector function, taken over a small closed surface, to the volume comprised within the surface, when both tend to the limit zero. By properly choosing the *shape of an infinitesimal operational volume*, around the point under consideration, and its *position with respect to the lines of force, integrations can be done away with, and it is not necessary to reduce the results to the limit zero*. The above operators thus become symbols for certain forms of *space derivatives*, independent of fixed axes of coordinates. The results throw additional light on the *physical nature* of divergence and curl. The operational volume may be so chosen and placed as to give the *total magnitude of the curl vector*, and not only its components.

52. Surface layers produced by activated nitrogen. CARL KENTY and LOUIS A. TURNER, Princeton University.—A one mil tungsten wire at about 450°C placed in a stream of nitrogen shows a large decrease in resistance when the active nitrogen produced by a condensed discharge reaches it. The same effect is produced by bombarding still nitrogen in the neighborhood of the filament with electrons. In a tube having a large nickel anode the minimum accelerating voltage for producing a detectable effect is 10.8 volts but it is considerably higher (about 21 volts) in a tube having a hot tungsten filament anode. The decrease of resistance is attributed to the formation of a surface layer which increases the emissivity of the filament, thereby lowering its temperature. The effect increases with the pressure in the range from 0.04 to 5 mm. The film is removed by flashing the filament or pumping out the gas. The effect is apparently produced by a neutral substance, being independent of the potential of the test filament. Active nitrogen also causes a large reduction of the thermionic current from a tungsten filament. Such an effect is obtained with ordinary nitrogen in the hot anode tube, a saturation current reached at 15 volts being reduced at voltages above 21.

53. Simultaneous ionization and excitation of molecules on collision with foreign ions. O. S. DUFFENDACK and H. L. SMITH, University of Michigan.—The spectrum of a low-voltage arc in a mixture of 90 percent helium and 10 percent CO contains the Comet Tail, First Negative, and Baldet-Johnson bands of CO^+ strongly developed. In neon and CO the Comet Tail bands are strong, the First Negative weak, and the Baldet-Johnson absent. None appear in an argon-CO mixture. The introduction into the discharge of twice as many electrons from an auxiliary filament as from the cathode failed to increase the intensities of the bands if their

accelerating voltage was less than the ionizing potential of the rare gas, even though it was above the excitation potential of the bands. Hence these bands were not excited by electron impacts either upon the CO^+ ions or upon the CO molecules. To determine whether excited atoms or ions were effective in producing these bands, nitrogen was substituted for CO. Its negative bands appeared strongly in helium and in neon mixtures. As their excitation potential is above the strong radiating potentials of neon, their excitation must be due to the ions. We conclude that an ion may ionize a molecule and excite the resulting ion to the degree the ionizing potential of the one exceeds that of the other.

54. Residual ions and critical restriking potential in mercury arcs. M. L. Pool, University of Chicago. (Introduced by A. J. Dempster).—Using as a collector for electrons a 4 mil wire and for positive ions an anode which completely surrounds a hot cathode the rate of removal is given by $n = n_0 e^{-kt}$ where $k = 240$ for all voltages during the first $1/75$ sec. After $1/300$ sec the space charge sheaths about the anode and wire are 2 mm in thickness and 1 mm in radius respectively. These sheaths rapidly expand in size and within $1/50$ sec. fill the entire arc space. Replacing the wire by a larger collector the arc space has been swept free of ions within $1/500$ sec. The restriking of a mercury arc at the lowest radiating potential is explained by means of the large concentration of electrons and ions which exist near the filament. There electrons will have energies up to 5 volts. When the arc is stopped these electrons will diffuse into the filament and in order to repel them the filament must be made 5 volts negative with respect to the gas. If the filament is made still more negative electrons can leave the filament and the arc restrikes through ionization of the metastable atoms formed by continual recombination.

55. The fine structure of the mercury line 3650 Å. W. H. McCURDY, National Research Fellow, Johns Hopkins University.—The fine structure of the Hg line 3650 Å has been studied by means of crossed Lummer-Gehrke plates of quartz. The results show that this line consists of five components within the limits of the observations. The separations are -45 , -32 , -20 , 0 , $+102$ mA. The main component is found to be single within the limits of the plates but under certain arc conditions it is found to appear reversed. Nagoaka, Siguira and Mishima have studied all the strong lines of the mercury arc spectrum and they give as the structure of the main component a group of three lines with weaker ones on each side. The structure of the main component in their results may be due to broadening of the line and partial reversal due to the type of arc used. It is possible that their results on the line 2967 Å may also be incorrect for the same reason, as the main component of this line also shows absorption under some conditions. This shows the importance of the source in fine structure work.

56. Zeeman-effect of the fine structure components of $\lambda 2536$ of mercury. WALTER A. MACNAIR, National Research Fellow, Bureau of Standards.—Preliminary results of an extended study of the Zeeman-effect of $\lambda 2536$ of mercury show that the five fine structure components split into triplets, the perpendicular components of which behave as the perpendicular components of 322 normal triplets with no Paschen-Back effect in fields up to 5000 gauss, the present limit of the magnet being used. The parallel or central components of the five triplets show some peculiarities in fields of 3000 gauss and over.

57. H_3 as a possible emitter of the secondary hydrogen spectrum. CHARLES J. BRASEFIELD, Princeton University.—Positive ray analysis of the ions in a discharge in hydrogen show that H_3^+ is by far the predominant ion, except at very low pressures. In an attempt to correlate the proportion of H_3^+ with the intensity of the lines of the secondary spectrum, photographs were taken of the discharge operated under two different conditions; (1) in which no H_3 ions were detectable and (2) in which the number of H_3 ions was quite appreciable. The second type discharge showed marked enhancement of the Fulcher bands in the red and blue, which was at first attributed to H_2 . However, when the electron velocities were determined by the Langmuir exploring electrode method, and the results compared with the curves obtained by Lowe showing the variation of intensity of the secondary lines with the energy of

the exciting electrons (Trans. Roy. Soc. Canada, 20, 217 (1926)) it was found that the observed change in intensity could adequately be accounted for by change in electron velocity. Very little evidence was found to support the bands recently found by Allen and Sandeman which they ascribe to H₃.

58. Theory of the Stark-effect in the arc spectra of helium. J. STUART FOSTER, McGill University, Fellow of the International Education Board (in Copenhagen).—In this application of the perturbation theory of the quantum mechanics of Heisenberg quantitative displacements and intensities replace the less definite qualitative explanation afforded by the correspondence principle in the earlier Bohr theory. Following Kramers, the hydrogen atom is considered to be perturbed by (1) an inner and entirely central field which effectively replaces the time mean position of the inner helium electron as well as its resonance action, and (2) a uniform external electric field. As a first approximation, the perturbation matrix $H_1(n, m, k)$ therefore contains, within a region of given n and m , (1) diagonal terms which denote the differences (at zero field) between the hydrogen and the parhelium (or the orthohelium) spectral terms identified by the various k values, and (2) terms due to the applied field, and identical with those recently given by Pauli and by Schroedinger in the theory of the Stark-effect in hydrogen. The various Stark patterns as well as great variations in the displacements and intensities previously observed by the writer over a wide range of field strengths are faithfully reproduced in the theory. An interesting feature in accord with the observations is the vanishing of a few components at certain field strengths and their re-appearance at higher fields. Displacements of the following line groups have been calculated at seven field strengths: $\lambda\lambda$ 4922, 4388, 3965, 3614, 4472, 4026, 3188, and 2945. The intensities have been calculated at 10, 40, and 100 kv/cm.

59. The light absorption of liquefied gases. F. G. BRICKWEDDE and W. A. MACNAIR, Bureau of Standards.—For the study of the absorption of liquefied gases, the continuous spectrum of hydrogen was used for wave-lengths 2000–3700 Å, a bromine cell cutting out wave-lengths greater than this, and the light from an incandescent bulb was used for wave-lengths 3400–6500. The absorption spectra were photographed with a Hilger E2 quartz spectrograph. The liquefied gases were contained in a cylindrical, quartz Dewar flask—inside diameter 22 mm—mounted in front of the slit of the spectrograph. The results obtained with liquid oxygen were found to be in essential agreement with the results published by W. W. Shaver (Trans. Roy. Soc. of Canada, 15, 7 (1921)), except for a number of new bands not previously recorded. Three of these obviously belong to the system of broad bands found by Shaver, extending between wave-lengths 2600 and 2800. No absorption was found in liquid nitrogen between wave-lengths 2000 and 6500, and no absorption in liquid hydrogen between wave-lengths 2000 and 3800.

60. Reproducible liquid filters for the determination of the color temperatures of incandescent lamps. RAYMOND DAVIS and K. S. GIBSON, Bureau of Standards.—A series of filters has been devised, reproducible from specification, by means of which any Planckian energy distribution from 2300° to 4000°K may be converted to the color of mean Washington sunlight. Given a simple photometer, a lamp standardized at some one temperature in the above range, and the proper filter, a second lamp may then be calibrated at as many temperatures as is desired by preparing the respective filters. The solutions required for any given filter are contained in a two-chamber glass cell, one chamber containing a one-centimeter thickness of an aqueous solution of copper sulphate, pyridine, and mannite, the other, a one-centimeter thickness of an acidified aqueous mixture of copper sulphate and cobalt ammonium sulphate. Careful spectrophotometric measurements from 350 to 750 m μ were made on medium concentrations of the three component solutions, and the validity of Beer's law studied over the range of concentrations necessary. The respective concentrations were then varied until the color characteristics of the source-and-filter combinations were, by computation, all identical with that for mean sunlight.

61. The fluorescence of sodium vapor. R. W. WOOD and E. L. KINSEY, Johns Hopkins University.—Sodium vapor contained in a Wood sodium tube was excited by monochromatic radiation in the blue-green region obtained by sunlight and a monochromator. Although the exciting radiation corresponded only to a molecular absorption band group in the blue-green region and to no absorption lines in the sodium atom, the "D" lines appeared in the fluorescence spectrum when the pressure of the residual gas was around 4 mm. The phenomenon was not obtained at lower or higher pressures. Bands appearing in the region surrounding the "D" lines in the fluorescence spectrum under white light excitation were studied. They have been definitely determined to appear only at pressures of the residual gases (hydrogen and nitrogen) around 6 mm. Approximate monochromatic excitation shows them to be excited only by wave-lengths in their own region. Absorption spectra obtained with both a two meter and twenty foot spectrograph so far fail to reveal these bands. The introduction of small quantities of potassium failed to effect the appearance of these bands.

62. Spark spectrum of nickel. A. G. SHENSTONE, Princeton University.—The following terms of Ni II have been identified:—1. Low set in order $^4F'$, $^2F'$, $^4P'$, $^2P'$, 4D all from the structure d^8s . 2. Intermediate set (d^8p) $^4D'$, $^2D'$, $^4G'$, $^2G'$, 4F , 2F ; $^4S'$, 4P , $^4D'$ and a large number of levels unidentified. 3. A high $^4F'$, $^2F'$ (d^8 , s). These terms account for about two-thirds of the lines including practically every strong line. Zeeman effects indicate that the g-values of $^4F'$, $^2F'$ and the corresponding intermediate triad are probably regular. The g-values of $^4P'$ etc., are certainly irregular as are also the intervals. All terms are inverted except that 4G_6 is higher than 4G_5 . The predicted lowest term 2D (d^9) would give lines outside the present observed region and has not been found. The two $^4F'$, $^2F'$ terms belong to a sequence (d^8 , s) and give a calculated I. P. of about 17.4 volts. The same peculiarities of convergence and interval are present in this $^4F'$, $^2F'$ series as were evident in the corresponding series of Cu II, Ni I and Pd I (d^9s).

63. Terms arising from similar and dissimilar electrons. D. T. WILBER, H. E. WHITE and R. C. GIBBS, Cornell University.—Following the scheme of Hund for similar s, p and d electrons, the terms arising from similar f electrons have been worked out and tabulated. Tables have also been prepared for one and two electrons, where in the latter case these electrons are dissimilar, i. e., have either different total or different azimuthal quantum numbers, and also for three electrons two of which are similar. In the tables for similar electrons we have indicated, in parenthesis, the total number of possible configurations of p (=number of possible values of m_a times the number of possible values of m_e) things taken q (=total number of electrons in consideration) at a time. These tables are found not only to be of frequent use but also to bring out certain rules that may be applied in determining spectral terms arising from any electron configuration.

64. Multiplets in the spectra of Cr(III) and Mn(III). R. C. GIBBS and H. E. WHITE, Cornell University.—Following the method previously reported by us for the identification of multiplets in other isoelectronic systems of the first long period it has been found possible to extend the multiplet designated as $^5F - ^5G$ for four electron systems (involving the transition $4p3d^3 \rightarrow 4s3d^3$) from Ti(I) and V(II) to Cr(III) and also the multiplet designated as $^6D - ^6F$ for five electron systems (involving the transition $4p3d^4 \rightarrow 4s3d^4$) from V(I) and Cr(II) to Mn(III). The twelve lines of the 5FG multiplet of Cr(III) and the fourteen lines of the 6DF multiplet of Mn(III) all follow the usual rule of relative intensities. These and other data enable us to extend further the systematic arrangement of radiated frequencies arising from the transition of an electron from a $4p$ to a $4s$ orbit in the presence of 0, 1, 2, 3 etc. 3d electrons, for elements in the first long period from K to Cu. The Moseley diagrams for the deepest lying terms arising from $d^{n-1}s$ and $d^{n-1}p$ configurations for these elements not only give very straight lines but also reveal a regular and systematic displacement in passing successively from one iso-electronic system to another.

65. The sodium and potassium absorption bands. W. R. FREDRICKSON, WILLIAM W. WATSON, and J. RINKER, University of Chicago.—The blue-green Na_2 and the red K_2 absorp-

tion bands have been photographed with a dispersion of 1.3A per mm. Vibrational quantum numbers have been assigned, with the following formulas giving the frequencies of the heads:

$$\begin{aligned} \text{Na}_2:v &= 20301.62 + (123.84n' - 0.79n'^2) - (157.57n'' - 0.57n'^2) \\ K_2:v &= 15368.63 + (74.46n' - 0.21n'^2) - (91.94n'' - 0.39n'^2) \end{aligned}$$

Using Wood's resonance series data, the lines in the Na_2 bands are arranged into singlet P , Q , R branches, a result in accord with Mulliken's prediction of a $^1S-^1P$ electronic transition. The resonance doublets have one component on the R , the other on the P branch, with $\Delta j = 2$; most of the singlets fall on Q branches. All of Wood's magnetic rotation lines lie on P and R branches. The usual P , Q , R combination principle holds. The band origins are very close to the heads; B'_0 is 0.17 cm^{-1} . The K_2 bands appear to have four branches, indicating doublet P , R arrangement. If weak Q branches are present near the heads, they cannot be detected. The K_2 bands might involve a $^1P-^1P$ transition (suggested by Mulliken) and it is shown that both 1S and 1P initial molecular states are plausible.

66. The rotational and vibrational specific heat of a diatomic gas, the molecules of which have a doublet P normal state. ENOS E. WIRMER, National Research Fellow, Harvard University.—As is well known, the rotational and vibrational specific heat of a diatomic gas, the molecules of which have a single electronic state as the normal level, when plotted as a function of the temperature, shows the following characteristics. The curve rises more or less abruptly from zero at the absolute zero to a value in the neighborhood of R , after which the curve is almost flat until the vibrational energy begins to add its contribution. R is the gas constant in calories per degree (1.986). If, however, the normal electronic level is double, the specific heat curve presents in general in addition to this initial rise in the neighborhood of the absolute zero a secondary rise at the temperatures at which molecules begin to exist in the upper component of the doublet in appreciable numbers. After this second rise, which carries the curve above the value R , the curve again declines, tending to the value R , until vibration begins to add its contribution. A good example of the doublet type is nitric oxide. The specific heat of this gas was computed from the band spectrum data of Jenkins, Barton, and Mulliken. At 50°K . its specific heat is $1.33R$.

67. Recoil electrons from aluminum. A. A. BLESS, Cornell University.—On the Compton theory of scattering the maximum energy of the recoil electrons is given by $E = h\nu_0 2\alpha / (1+2\alpha)$. On the assumption made by C. T. R. Wilson that x-rays on scattering spread in spherical waves the maximum energy of recoil electrons would be about $1/4$ that given above. Experiments on recoil electrons have been made with a molybdenum water cooled tube and aluminum as the scattering substance. Preliminary results using the magnetic spectrometer method show the presence of a band the high velocity edge of which agrees fairly well with the value predicted by Compton. The band shifted properly with the change of the field.

68. X-ray absorption formulas. S. J. M. ALLEN, University of Cincinnati.—Wetzel, using the new wave mechanics of Schroedinger, and applying it to photo-electric effect, has recently developed a formula for the absorption of high frequency x-rays for the K series. By the aid of Moseley's law the formula can be put in such form that it can be compared with experimental data. For a single element this formula is:

$$(\mu/\rho)_K = k_1\lambda^3 + k_2\lambda^{3.5} + k_3\lambda^{2.5} + \sigma/\rho$$

Using the same exponents of λ , empirical formulas can be found which agree, within experimental error, with existing data. The elements, Al, Fe, Cu, Ag, Sn, and Pb, have been considered from $\lambda = .081$ to $\lambda = 1.934 \text{ \AA}$, and it has been found that such a formula fits the experimental data quite well through the entire range of λ for the K series. It also appears that such a formula fits the L series of Fe, Cu, and Pb, but that the L series of Ag and Sn, and the M series of Pb can be best expressed by two parameters. The complete formula for Ag is: $(\mu/\rho)_{\text{total}} = (400\lambda^3 - 30\lambda^{3.5} + 80\lambda^{2.5})_K + (97\lambda^3 - 35\lambda^{3.5})_L + (1/6.5)(\tau/\rho_L)_M$ etc. $\frac{1}{\rho}\sigma/\rho, \sigma/\rho = .35$ at $\lambda = .08 \text{ \AA}$, and increases slowly with λ . From this formula, $J_k = (\tau/\rho_K + \tau/\rho_L + \tau/\rho_M$ etc.) $(\tau/\rho_L + \tau/\rho_M$ etc.) is not a constant but varies with λ .

69. Molecular space array in liquid primary normal alcohols: the cybotatic state. G. W. STEWART and ROGER M. MORROW, University of Iowa.—Examination of liquid normal primary alcohols, methyl to lauryl, by Mo K α x-radiation, gives diffraction curves which are readily and consistently interpreted by the following: (a) There is a fluid molecular space array, called the "cybotatic" rather than "crystalline" state. (b) The alcohol molecules are parallel and separated by the most probable distance of 4.6 Å. (c) The length of the molecules increases in equal amounts with each addition of CH₂; this increase is 1.3 Å or approximately the distance between C atoms in crystalline form. (d) The above interpretations are in full accord with all known facts and especially to be noted is the agreement with the surface film molecular arrangement of similar compounds studied by Adam. The experiments and discussion refer to liquids that are optically isotropic. They are an extension of the work of numerous observers on the well known x-ray diffraction x-ray halo in liquids. The general conclusion is that *the cybotatic state or cybotaxis, is common in liquids and lends itself readily to a better understanding of the nature of a solution and solution phenomena, such as osmosis.*

70. X-rays of long wave-length from a ruled grating. F. L. HUNT, Bureau of Standards.—By the use of a grating ruled on glass (200 lines per mm), at grazing incidence (20° to 40°), in vacuum, the following lines have been obtained: M α of platinum, (6Å); K α of aluminum, (8.3Å); L α of copper, (13.3Å), all in the first three orders; the L α of iron, (17.7Å) and of chromium, (21.5Å), in the first order; and the K α of carbon, (45Å), in the first two orders. A water-cooled metal x-ray tube with a hot lime-coated platinum cathode, which permitted the use of an unprotected photographic plate, was connected directly to the spectrometer with no absorbing film between the anti-cathode and the plate. Two 0.5 mm steel slits 20 cm apart were mounted between the tube and the grating. The distance from the grating to the plate was from 10 to 30 cm. The voltage applied to the tube was 10 kilovolts, the current 10 milliamperes, and the time of exposure from 20 minutes to 1 hour. The wave-lengths were determined with reference to the first order L α of copper which was used in computing the zero position of the direct beam. The angle of incidence on the grating and the effective distance from the grating to the photographic plate were determined experimentally. These preliminary measurements agree within approximately 0.1Å with the values determined by reflection from crystals.

71. An explanation of Whiddington's rule for x-ray electrons. E. C. WATSON, California Institute of Technology.—In Whiddington's pioneer work on the velocities of electrons ejected by x-rays, the very remarkable observation was made that the incident radiation was able to eject an electron only when its frequency was double the value corresponding to the energy level of the electron concerned. Robinson, however, in his extensive study by the same method was unable to confirm this result. Robinson worked with electrons ejected approximately at right-angles to the x-ray beam, while Whiddington studied those leaving the radiator in the forward direction of the x-ray beam, and it can be shown that his rule resulted from this procedure together with the fact that x-ray plates become relatively insensitive to electrons whose HP velocity is less than 300. β -ray spectra have been taken at various angles with the x-ray beam, and lines which are forbidden by Whiddington's rule appear when the electrons leave the radiator approximately at right-angles to the x-ray beam but disappear when electrons leaving in the direction of the x-ray beam are studied. This is in agreement with the work reported at the Los Angeles Meeting (Abstract no. 24, March 5, 1927) and also with the work in gases by the expansion chamber method.

72. On a gyromagnetic electron-theory of the Compton effect. LOUIS VESSOT KING, McGill University.—In the following classical theory of the Compton effect, it is supposed that electrons are carried forward in a beam of monochromatic radiation of high frequency. The equations of motion of the electron, taking into account the variation of mass with velocity, may be solved by successive approximation. The electron describes a trajectory of sinusoidal form whose period differs slightly from that of the incident radiation, while the resultant velocity depends on the magnitude of the electric intensity in the electromagnetic wave. The dis-

turbing couples on the gyromagnetic electrons are provided by couples arising from the corresponding magnetic field. On inserting these conditions in the gyromagnetic equations of line radiation (*Gyromagnetic Electrons and a Classical Theory of Radiation and Atomic Structure*, Louis Carrier, Mercury Press, Montreal), it is found that a certain group of electrons (whose velocities give rise to a natural precessional frequency synchronizing with that of the disturbing couple) will precess by resonance, emitting line radiation of frequency differing slightly from that of the incident beam. Since the precessing electron moves forward while radiating, the application of the classical Doppler principle gives the well-known complete formula for the Compton effect.

73. Iron crystals. L. W. MCKEEHAN, Bell Telephone Laboratories, Inc.—It has been found possible to grow long crystals in iron wire by making use of the allotropic transformation which occurs at about 900°C. The method is to heat, in an inert atmosphere, a portion of the wire between two mercury contacts by passing direct or alternating current through it and then to cause the heated portion to travel along the wire either by moving the support carrying the contacts or by moving the wire itself. The hottest part of the wire should be at 1400°C or higher. Under these conditions a very steep temperature gradient exists at the point where face-centered cubic (γ) crystals, stable at high temperatures, are being replaced by body-centered cubic (α) crystals, stable at lower temperatures, and at a favorable velocity of travel a single α crystal will grow to a length of 20 centimeters or more in wire 1 millimeter in diameter. The chemical purity and previous mechanical history of the iron seem relatively unimportant. Irregularity in tension on the wire and torsional stresses in it result in twinning. Twins may either appear as small inclusions or as complete changes in orientation with the twinning plane traversing the entire cross-section of the wire. The twinning plane is of the form {211}. The magnetic and magnetostrictive properties of the long crystals appear in some respects to differ from those of crystals prepared by others by the method of over-strain and annealing.

74. The purification of helium. J. WILLIAMSON COOK, Bureau of Standards.—Helium, containing 2.91 percent air (mostly nitrogen) plus a trace of hydrogen and neon, was passed at a slow rate and at atmospheric pressure, over activated cocoanut charcoal which had been thoroughly outgassed at from 300° to 400°C. With the charcoal cooled to -78°C. all air was adsorbed by the charcoal, leaving helium with only a trace of neon and hydrogen when observed spectroscopically. The charcoal was 100 percent efficient for removing air until its saturation limit was approached, when its efficiency failed almost instantly and completely. At lower temperatures, considerably more air was adsorbed but the saturation limit was not quite so abrupt. The amount of air, in cubic centimeters, which was adsorbed per gram of charcoal, up to the saturation limit, was 7 cc at -78°C; 152 cc at -182°C; 217 cc at -209°C. Relative observations, at liquid air temperature, indicated that if the hydrogen was first removed chemically, the charcoal would then adsorb more neon than when the hydrogen and neon were both present in the helium.

75. Duration of atomic hydrogen. JOSEPH KAPLAN, Johns Hopkins University. (Introduced by R. W. Wood.)—A large bulb of 3 liters capacity was sealed to the middle of a Wood's hydrogen tube and the atomic hydrogen formed in the discharge tube was allowed to enter the bulb. It was found that atomic hydrogen could be detected, by means of a speck of Welsbach mantle, three seconds after the discharge was shut off. The piece of Welsbach was quite large which indicated that there was still probably considerable atomic hydrogen in the bulb even after three seconds. Certain other effects, such as small white infected spots on the glass, which were due to atomic hydrogen, were observed for as long as six seconds after the discharge was discontinued. There were indications that the atomic hydrogen lasted as long as 10 seconds, but, because of impurities in the tube, these indications may have been due to something else. It has also been shown that in the absence of water, a surface is a much better catalyst than when water is adsorbed on it. The present experimental proof of the role of water has, however, been made away from the discharge tube, in which other complicated reactions might occur.

76. Structure and isotope effect in the alpha bands of boron monoxide. F. A. JENKINS National Research Fellow, Harvard University.—The α bands of BO excited by active nitrogen have been photographed with high dispersion. They are electronic doublets, each component having four branches designated R_1 , (R_2+Q_1) , (Q_2+P_1) , and P_2 , of which the two central ones are relatively more intense. This structure has been interpreted by Mulliken as due to a $^2P \rightarrow ^2S$ transition. The missing lines support this designation, since there is one in the Q_1-Q_2 series for the higher frequency system, while there are three for the lower. The 2P doublet is therefore *inverted*. Quantum analysis of the $(\frac{1}{2}, \frac{1}{2})$ and $(\frac{1}{2}, 1\frac{1}{2})$ higher frequency sub-bands shows that the rotational terms in the initial state are of the form $B'(j^2 - \sigma^2)$, $\sigma = \frac{1}{2}$, and in the final state $B''(j - \epsilon)^2$, $\epsilon = \pm \frac{1}{2}$, with j integral. There is a close σ -type doubling in the initial state, but "crossing over" in the Q transitions allows the coalescence of R_2 with Q_1 , and Q_2 with P_1 . The origins of the $(\frac{1}{2}, \frac{1}{2})$ bands of $B^{10}O$ and $B^{11}O$ are separated by 1.547 \AA , exactly the amount required for half-integral vibrational quantum numbers. Analysis of this $B^{10}O$ band gives smaller moments of inertia than those obtained for $B^{11}O$, but identical inter-nuclear distances, namely $r_0' = 1.352 \times 10^{-8} \text{ cm}$ and $r_0'' = 1.208 \times 10^{-8} \text{ cm}$.

77. Band structure and intensities, atomic and molecular electronic states, in diatomic hydrides. ROBERT S. MULLIKEN, New York University, Washington Square College.—Theoretical intensity formulas applicable to $^2P \rightarrow ^2S$ and $^2S \rightarrow ^2P$ molecular electronic transitions have been obtained, for Hund's case *b*. The observed branches (six intense branches), intensity relations, missing lines, etc., in the CaH, MgH ($^2P \rightarrow ^2S$), OH, CH $\lambda\lambda 3900$ ($^2S \rightarrow ^2P$) bands agree well with the theory. As the 2P separation increases, through ZnH, CdH, to HgH (all $^2P \rightarrow ^2S$), and the 2P state approaches Hund's case *a*, a gradual transition occurs to the HgH type, with twelve strong branches. In OH (as expected), apparently also in CH, the 2P doublet is inverted; elsewhere it is normal. The intensity relations, probable missing lines, and occurrence of twelve strong branches (different from those in HgH), show that CH $\lambda 4300$ is $^2D \rightarrow ^2P$. Probably the three levels 2P , 2D , 2S involved in CH $\lambda\lambda 4300$ and 3900 are derived, by the addition of a normal hydrogen atom, from the lowest levels, 3P , 1D , 1S of the carbon atom (the latter two metastable, unlike 2D and 2S of CH); the OH levels 2P and 2S similarly from 3P and 1S of oxygen; and the 2P and 2S levels of the metal hydrides from the lowest levels (1S , 3P) of the metal atoms.

78. Zeeman effect in AgH, AlH, ZnH, and MgH bands. WILLIAM W. WATSON and B. PERKINS JR., University of Chicago.—The AgH bands are absolutely unaffected by magnetic fields of any strength, thus verifying the assignment $^1S - ^1S$ to these bands. The results for the $\lambda 4240$ AlH band ($^1S - ^1P$) are similar to those given by Kemble and Mulliken for the $\lambda 5610$ CO band ($^1P - ^1S$). The first R lines are broadened, the spread of the R(1) components being approximately half normal separation, in agreement with Van Vleck's "rigid-coupling" formula, if $j' = 1$. The first P and Q lines are diffusely broadened. In the $\lambda 4326$ ZnH band results at medium field strength are in agreement with Hulthen's except for the R_1 lines. These show a broadening for low m 's, as do the R_2 lines. The P_1 and P_2 lines are unaffected at any field strength. Both the Q_1 and Q_2 lines split up into "loose-coupling" wide doublets ($\Delta v = 2 \times$ normal separation for low m 's.) A first order "rigid-coupling" effect on the Q lines at low fields apparently occurs, but measurements are uncertain. In the MgH bands the narrow doublets fuse into single lines more intense in the center and slightly narrower than the original doublets.

79. The excitation of the spectrum of CO_2 . G. W. FOX, O. S. DUFFENDACK and E. F. BARKER, University of Michigan.—Pure CO_2 flowing continuously through a hot cathode discharge tube was excited by electron impacts at low voltages. The tube consists of two compartments separated by a diaphragm having a small aperture covered with platinum gauze through which the electrons from an oxide coated filament enter the impact chamber. The flow of gas was in the direction opposite to that of the electrons; thus dissociation products were swept out through the pump and no diffusion into the region of observation occurred. The gas pressure was controlled by regulating the rate of flow. Under these conditions the spectrum observed

is altogether different from that produced in stagnant gas, and is attributed to the molecule of CO_2 . The glow is violet and its spectrum consists of several systems of bands extending from 5000 Å to 2850 Å. Most of these bands are degraded toward the red. They have sharp edges, and occur in distinct groups. One group lying near 2880 Å seems unique. It consists of two double edged bands each having oppositely degraded branches with a very narrow band between their edges. When the flow is stopped the familiar sky blue of CO appears at once, and the spectrum consists mainly of the positive bands of CO.

80. Ultra-violet absorption and emission spectra of carbon monoxide. J. J. HOPFIELD and R. T. BIRGE, University of California.—New emission and absorption spectrograms of CO have been measured and analyzed. Many irregularities in some previous data by others have been eliminated. By gradually varying the pressure of CO in the receiver of the spectrograph from 0.05 to 850 mm, nine absorption systems, between $\lambda 920$ and $\lambda 2064.5$ have been obtained. These represent transitions from the normal level to *all* of the previously known excited electronic levels (Phys. Rev., 28, 1157 (1926)) and to four new levels at 58927, 92923,* 99730, and 105270 cm^{-1} . Other absorption systems are present but are too blended for certain analysis. The new data permit many satisfactory tests of the combination principle, and give as a direct evaluation of the previously known levels, 48438* to 48534,* 64765,* 83812* (poor) 86926,* and 91923,* cm^{-1} . Band systems are found in emission also, for transitions from starred levels directly to the normal. The strongest absorption is to the highest levels. Three of the higher levels have a vibration frequency almost identical with that of the normal state, and this fact, coupled with the absence of a Q branch in the correlated bands, predicts unique features in the appearance of the bands which are experimentally verified.

81. A comprehensive form of energy level diagram for atoms. RAYMOND T. BIRGE, University of California.—A type of diagram is suggested which may include, at least theoretically, all energy levels of an atom and its singly, doubly, etc. charged ion, provided that not more than one electron is in an excited level. A general scheme is proposed for designating the levels in accordance with the present interpretation of complex spectra. Such a diagram exhibits all possible relations between the lines of ordinary spectral series, the enhanced series of the variously charged ion, the ordinary x-ray lines, the enhanced (spark) x-ray lines, the critical absorption limits, and the so-called discontinuities in the absorption limits. With emission represented as a downward transition, the x-ray energy levels appear inverted with the K level highest. All levels for the neutral atom are represented by parallel sets of vertical columns, grouped in one section. Similarly all levels of the singly charged atom, in an adjoining section. Transitions representing monochromatic radiation never cross the division between sections. All critical absorption limits do cross. Double electron jumps are not represented, as the number of types of possible levels, with more than one electron in an excited state, is prohibitively great for convenient representation.

82. The shift in a near infra-red absorption band of some benzene derivatives. JAMES BARNEs, Bryn Mawr College.—By means of a grating spectroscope and plates sensitized with neocyanine absorption bands of benzene and of some of its derivatives have been photographed and their wave-lengths measured. The dispersion of the spectrometer as used was approximately 39.8 Å to the millimeter. The results are believed to be accurate to ± 5 Å. The wave-lengths of the center of the absorption bands of the substances used are as follows:

	$\lambda(\text{\AA})$		$\lambda(\text{\AA})$
Benzene	8741	M-Xylene	8793
Toluene	8758	P-Xylene	8808
Ethylbenzene	8772	Diethylbenzene	8799
O-Xylene	8781	Mesitylene	8844

With an absorption cell 80 cms in length benzene shows an absorption band at 7134 Å. Some interesting conclusions can be drawn from these results. Their explanation in the light of present theories regarding band spectra will be briefly discussed.

83. The infra-red absorption spectra of acetylene (C_2H_2), ethylene (C_2H_4), and ethane (C_2H_6). CHARLES F. MEYER and AARON LEVIN, University of Michigan.—The absorption spectra of the above gases are being investigated by means of a grating spectrometer. The curves show fine structure of an interesting and, in some cases, an extremely regular nature. They are the first which show resolution of bands into ultimate lines for molecules containing more than one heavy atom. That is, all bands of the vibrational-rotational type which have hitherto been analyzed, originate from molecules which contain hydrogen and only one atom of another kind. Investigators have felt that the bands of other molecules, on account of the higher moment of inertia involved, and consequent closer spacing of the lines, were unresolvable. This is shown to be untrue for the gases under investigation. The measurements extend to nearly 15μ and have thus been carried to considerably longer wave-lengths than any previous work with high dispersion.

84. The infra-red spectrum of ammonia. W. F. COLBY and E. F. BARKER, University of Michigan.—The absorption band for ammonia at 10μ has been observed with high dispersion, and analyzed as two overlapping bands with zero branches at 10.3μ and 10.7μ . Each band has the same general structure. About twelve lines have been observed in each branch, the spacing being somewhat different in the two bands, about 18.9 cm^{-1} for one and 20.4 cm^{-1} for the other. There is very little convergence. It is suggested that these two bands result from the two transitions $1/2 \rightarrow 3/2, 3/2 \rightarrow 5/2$ (or perhaps $1/2 \rightarrow 5/2, 3/2 \rightarrow 7/2$) for the same normal vibration of the molecule. The slight change in line spacing is due to coupling. Other ammonia bands previously reported are interpreted in terms of two different types of transition, one in which the second rotational quantum number changes (1.9μ and 2.2μ) and the other where it does not change (6μ and harmonics). The band at 10μ belongs to the latter class. Possible values of the two moments of inertia for the symmetrical pyramid NH_3 are obtained.

85. The infra-red reflection spectra of some carbonates. E. K. PLYLER, University of North Carolina.—A rock salt prism was used to examine the spectra of some carbonates. As the source of radiation a material called Globar was used. It was found to be about four times as intense as a Nernst glower in the region of 7μ . The structure of the band of selective reflection of calcium carbonate was studied by reflecting the radiation from the surface of a clear piece of calcite. The slit width was .07 mm. Maxima were found at 6.36μ , 6.54μ , and 6.62μ . These different maxima are probably due to the isotopes of calcium. If the three maxima are caused by the isotopic effect, then calcium should have three isotopes rather than two. The reflection spectra for iron carbonate had two maxima. Dolomite also had two maxima.

86. Intensity relations and band structure in bands of the violet CN type. ROBERT S. MULLIKEN, New York University, Washington Square College.—Theoretical intensity formulas applicable to bands of the violet CN ($^3S \rightarrow ^2S$) type are obtained, assuming Hund's case b. These predict two Q branches (RQ and PQ) which should appear as weak satellite series, one accompanying the familiar double P branch, the other, the R branch. These Q branches should decrease in intensity from their first members. The first RQ (or PQ) line should accompany the otherwise single first line of the R (or P) branch (all other P and R lines are truly double); this result is in agreement with Hulthén's results on the CaH "B" bands. In the P (and R) branches, the doublet component corresponding to the parallel orientation (+ ϵ) of the electron spin vector should be appreciably more intense than that corresponding to the antiparallel orientation (- ϵ) for low j values. Treating the doublets (and their satellites) as unresolved single lines, the intensities should be exactly as in $^1S \rightarrow ^1S$ bands (CuH, HCl). These predictions seem to be confirmed in the CaH, N_2^+ , and violet CN bands. Thus the theory appears to afford a satisfactory explanation of the observed lines and intensity relations in $^2S \rightarrow ^2S$ bands, removing previous difficulties and uncertainties in interpretation.

87. Some unclassified lines of oxygen in the ultraviolet. J. J. HOPFIELD, University of California.—Some of the ultraviolet lines of the arc spectrum of oxygen not yet fitted into series are $\lambda 1152$ and a triplet $\lambda\lambda 988.67, 990.13$, and 990.73 . These are among the strongest

lines and no doubt belong to OI. The triplet is perhaps an unresolved group similar to one in sulphur at $\lambda 1480$ (unpublished work) which contains eight lines, the normal triplet separation occurring twice. The discrepancy of the separations of the above triplet of oxygen from the normal separation may be explained on this basis. $\lambda 1152$ is always accompanied by a diffuse band or group on its ultraviolet side. Two single lines $\lambda\lambda 1217.62$ and 999.47 , the latter measured with the carbon line $\lambda 1037.021$ as standard, occur in the arc spectrum of oxygen with relative intensities of 5 and 7 respectively, the separation of these lines being 17925.6 cm^{-1} . The green aurora line attributed to oxygen has a frequency 17924.7 cm^{-1} . The difference between these two values is 0.9 cm^{-1} , so that the two numbers are identical to within limits of experimental error. This tends to indicate that this aurora line $\lambda 5577.35 \text{ I. A.}$ is related to the two ultraviolet lines of oxygen, the most plausible relation being that the ultraviolet lines have a common initial or final state and the aurora line represents the transition between their respective final or initial states.

88. X-ray absorption and valence. W. B. MOREHOUSE, Westinghouse Lamp Company.—Experiments reported at the Washington Meetings, April, 1926, suggested that the absorption of heterogeneous x-rays by an element depends upon its valence. Results obtained from the same reactions using zirconium filtered beams indicate the same general results, but the magnitude appears to be somewhat greater, which suggests that the effect may be different for different wave-lengths. From a combination of Moseley's Law with the absorption law it can be shown that at the absorption limit, $d\tau_a/\tau_a = 6db/(N-b)$ where τ_a = atomic absorption coefficient at the short wave-length side of the K limit, b = screening constant, and N = atomic number which indicates that if the screening constant changes the absorption coefficient will change. Existing data shows that the emission and absorption spectra depend upon the valence; in general the higher the valence the shorter the wave-length, which from Moseley's law indicates that the screening constant decreases, which in turn indicates qualitatively that the absorption coefficient should decrease with increase in valence. Calculations from the difference in wave-length of the L limits for iodine in the free state and iodine in sodium iodide gives a decrease in absorption of approximately 0.4 percent which is in agreement with experimental results. Hence with change of valence there must be a slight change in the electron configuration of the atom. (This work was done at Cornell University.)

89. Report on the ether-drift experiments at Cleveland in 1927. DAYTON C. MILLER, Case School of Applied Science.—The ether-drift interferometer which was used at Mount Wilson in California in the experiments of 1921-1926 has been mounted on the campus at Case School of Applied Science in Cleveland. Only minor changes, suggested by experience, have been made in the apparatus. Special precautions have been taken to obviate troubles caused by vibration from city traffic. A series of observations which will extend throughout the year, comparable with those made at Mount Wilson, is now in progress. The results for the first epoch of the series indicate an effect of the same order of magnitude as was obtained at Mount Wilson and consistent with the conclusions previously announced.

90. The photo-electromotive force in selenium. R. L. HANSON, Cornell University. (Introduced by F. K. Richtmyer.)—A detailed study was made of the e.m.f. developed in a selenium cell by illumination, an effect originally discovered by Adams and Day in 1876 and later observed by Fritts, Uljanin and others. Careful investigation has shown this not to be a thermal e.m.f. The results of the investigation up to date are the following: (1) For the same illumination the e.m.f. is independent of the current through the cell. (2) Over wide ranges the e.m.f. is directly proportional to the intensity of illumination. (3) For the same intensity of illumination the e.m.f. is a maximum in the region $\lambda = 490$.

91. Charge Density in the new mechanics. R. M. LANGER, Naval Research Laboratory, Washington, D. C. (Introduced by G. Breit.)—The Schrödinger expression for the electric moment can be written $\mu^2 - 1 = N_1/(\nu_1^2 - \nu^2) + N_2/(\nu_2^2 - \nu^2) + N_3/(\nu_3^2 - \nu^2) + \dots$. This is the form of the classical dispersion formula in which the N_i 's indicate the number of oscillators capable of emitting the frequencies ν_i . For the case of the hydrogen atom the first terms have

the numerical values 1.52, 0.28, 0.06 and the sum of the series gives a value for the refractive index which is larger than that found experimentally (Proc. Nat. Acad. 12, 639 (1926)). But if we say that in the expression of $\psi\bar{\psi}$ for atoms originally in the state k acted on by a light wave, the terms of the form $C_{nk}u_nu_k$ can be taken quite literally as indicating the presence of charge distributions described as to extension by $u_n u_k$ and as to concentration by C_{nk} , and if we say that these just as other ordinary atoms, electrons or molecules are subject to collisions in the kinetic theory sense, then we find since the higher states $u_n u_k$ occupy such large volumes that at the pressures of the experiments (about 1 mm) they collide so often that their contribution to the coherent scattering and therefore to the refractive index is greatly diminished. So far from being a difficulty, what was apparently a discrepancy between theory and experiment becomes on this point of view, evidence in favor of what some may regard as a rather extreme form of the theory.

92. A method for determining sound transmission. F. R. WATSON, University of Illinois.—A sound generated in an electric loud speaker by means of an electron tube oscillating circuit is situated on one side of a test wall, or inside a "sound-proof" room. On the other side of the partition is an observer who listens to the transmitted sound. A comparison sound is set up by a microphone placed a fixed small distance in front of the loud speaker, which transmits an electric current through a transformer and variable resistance to a pair of head telephones worn by the observer. The resistance is varied until the telephone tone just masks the sound transmitted through the partition. This measurement is repeated when the observer stands near the loud speaker, which is reckoned as 100 percent. The ratio of the measurements of the transmitted sound to the direct (100 percent) sound gives the percentage of sound transmitted. Preliminary measurements of sound proof rooms gave satisfactory results.

93. Excitation of CuII spectrum by positive neon ions. O. S. DUFFENDACK AND J. G. BLACK, University of Michigan.—The method of Duffendack and Smith of employing positive ions to excite the spectrum of a once-ionized molecule with the exclusion of higher spark spectra was applied to copper. Low-voltage arcs of 20 milliamperes at 25 volts were maintained in mixtures of argon and copper and neon and copper in a tungsten furnace apparatus and their spectra photographed with a Hilger E2 quartz spectrograph. The pressure of the copper vapor was regulated by controlling the temperature of the furnace so that the green arc lines were faintly visible in a direct vision spectroscope. Under these conditions, the argon mixture failed to produce any spark lines. In neon the lines from the levels corresponding to the $(3d)^0 (4p)$ and $(3d)^0 (5s)$ configurations were strongly developed. These results are in accord with Shennstone's (Phys. Rev. 29, 380, (1927)) analysis of the spark spectrum as the $(3d)^0 (4p)$ levels lie at 15.9 to 16.8 volts and the $(3d)^0 (5s)$ at 21.0 to 21.4 volts above the normal state of the copper atom. Thus argon ions (15.4 volts) just fail to produce the lower state and neon ions (21.5 volts) can just produce both. In the neon mixture the lines from the higher level were considerably more intense relative to those from the lower level than they are in the ordinary spark.

94. The Stark effect in neon. J. S. FOSTER AND W. ROWLES, McGill University.—By employing a rather strong Lo Surdo source in which a maximum field of 130,000 v/cm was developed, the earlier observations by Nyquist have been somewhat extended. The observed symmetrical Stark patterns for the line groups of higher order (notably $2p_i - 6q$ and $2p_i - 7g$) are remarkably hydrogen-like in character. In these groups the complex nature of the initial states is not detected by the Hilger E1 spectrograph. On the other hand, each of the lines $2p_i - 4f$ and $2p_i - 5f$ appears as a doublet and the two members of the doublet present Stark-effects which are nearly identical. This effect is similar to that noted in orthohelium, where the multiplicity is in the final state. The initial terms involved in the production of the group of new lines which commonly appear in the electric field are more hydrogen-like than the diffuse terms, and consequently the majority of these lines have exceptionally large displacements. On the present plates some are displaced more than 50A. Another large group of new lines appear, however, without appreciable displacements, but with intensities which increase rapidly with the field. These ionized neon lines simply indicate the proportion of Ne^+ atoms in the various fields.

AUTHOR INDEX

- Allen, S. J. M.—No. 68
 Barker, E. F.—see Colby
 ——see Fox
 Barnes, James—No. 82
 Beams, J. W. and Ernest O. Lawrence—No. 9
 Beams, J. W.—see Lawrence
 Bennett, Arthur Lowell—No. 40
 Birge, Raymond T.—No. 81
 Birge, Raymond T.—see Hopfield
 Black, J. G.—see Duffendack
 Bless, A. A.—No. 67
 Bourgin, D. G.—No. 45
 Brasfield, Charles J.—No. 57
 Brickwedde, F. G. and W. A. MacNair
 —No. 59
 Campbell, G. C. and G. W. Willard—No. 46
 Castleman, R. A., Jr.—No. 34
 Colby, W. F. and E. F. Barker—No. 84
 Compton, K. T. and P. M. Morse—No. 31
 Compton, K. T.—see Van Voorhis
 Cook, J. Williamson—No. 74
 Davis, Raymond and K. S. Gibson—No. 60
 Davisson, C. and L. H. Germer—No. 27
 Dennison, D.—see Dushman
 Duffendack, O. S. and J. G. Black—No. 93
 Duffendack, O. S. and H. L. Smith—No. 53
 Duffendack, O. S.—see Fox
 Dushman, S., D. Dennison and N. B.
 Reynolds—No. 7
 Ellett, A.—No. 11
 Ewell, Arthur W.—No. 43
 Farnsworth, H. E.—No. 30
 Foster, J. Stuart—No. 58
 Foster, J. Stuart and W. Rowles—No. 94
 Fowle, E. S.—see Pienkowsky
 Fox, G. W., O. S. Duffendack and E. F.
 Barker—No. 79
 Frederickson, W. R., William W. Watson,
 and J. Rinker—No. 65
 Galli-Shohat, N.—No. 20
 Germér, L. H.—see Davisson
 Gibbs, R. C. and H. E. White—No. 64
 Gibbs, R. C.—see Wilber
 Gibson, K. S.—see Davis
 Gish, O. H.—see Rooney
 Ham, W. R.—No. 29
 Hamer, Richard and Surain Singh—No. 2
 Hanson, R. L.—No. 90
 Harnwell, Gaylord P.—No. 22
 Hartsough, R. C.—No. 35
 Heyl, Paul R.—No. 36
 Hidnert, Peter and W. T. Sweeney—No. 39
 Hopfield, J. J.—No. 87
 Hopfield, J. J. and R. T. Birge—No. 80
 Hughes, A. L. and A. M. Skellett—No. 25
 Hunt, F. L.—No. 70
 Jenkins, F. A.—No. 76
 Kaplan, Joseph—No. 75
 Karapetoff, Vladimir—No. 51
 Kenty, Carl and Louis A. Turner—No. 52
 King, Louis Vessot—No. 72
 Kinsey, E. L.—see Wood
 Kleeman, R. D.—No. 44
 Koller, L. R.—No. 6
 Krefft, Hermann E.—No. 28
 Kunz, Jacob—No. 37
 Kunz, Jacob—see Tykocinski-Tykociner
 Langer, R. M.—No. 91
 Lawrence, Ernest O. and J. W. Beams—
 No. 10
 Lawrence, Ernest O.—see Beams
 Levin, Aaron—see Meyer
 Libman, E. E.—No. 41
 Little, Noel C.—No. 1
 MacMahon, A. M.—No. 3
 MacNair, Walter A.—No. 56
 MacNair, Walter A.—see Brickwedde
 McCurdy, W. H.—No. 55
 McKeehan, L. W.—No. 73
 Martin, John R.—No. 19
 Meyer, Charles F. and Aaron Levin—No. 83
 Miller, Dayton C.—No. 89
 Morehouse, W. B.—No. 88
 Morrow, Roger M.—see Stewart
 Morse, P. M.—see Compton
 Mulliken, Robert S.—Nos. 77 and 86
 Murhaghan, Francis D. and Harold A.
 Wheeler—No. 50

- Nielsen, Walter M.—No. 23
Nusbaum, C.—No. 16
- Parmley, T. J.—No. 5
Phipps, T. E.—see Taylor
Pienkowsky, A. T. and E. S. Fowle—No. 38
Piersol, R. J.—No. 4
Plyler, E. K.—No. 85
Pool, M. L.—No. 54
- Race, Hubert H.—No. 48
Reynolds, N. B.—see Dushman
Rinker, J.—see Frederickson
Rooney, W. J. and O. H. Gish—No. 17
Rowles, W.—see Foster
Rusk, Rogers D.—No. 24
- Sagui, Cornelio L.—No. 21
Shenstone, A. G.—No. 62
Singh, Surain—see Hamer
Skellett, A. M.—see Hughes
- Smith, H. L.—see Duffendack
Solt, Irvin H.—No. 12
Spencer, R. C.—No. 33
Stewart, G. W. and Roger M. Morrow—No. 69
Swann, W. F. G.—No. 15
Sweeney, W. T.—see Hidnert
- Taylor, John B. and T. E. Phipps—No. 13
Tonks, Lewi—No. 47
Turner, Louis A.—see Kenty
Tykocinski-Tykociner, J. and J. Kunz—No. 14
- Van Voorhis, C. C. and K. T. Compton—No. 32
- Warburton, F. W.—No. 18
Watson, E. C.—No. 71
Watson, F. R.—No. 92
Watson, William W. and B. Perkins, Jr.—No. 78
Watson, William W.—see Frederickson
Wheeler, Harold A.—No. 8
Wheeler, Harold A.—see Murnaghan
White, H. E.—see Gibbs
White, H. E.—see Wilber
Wilber, D. T., H. E. White and R. C. Gibbs—No. 63
Willard, G. W.—see Campbell
Winchester, George—No. 42
Witmer, Enos E.—No. 66
Worthing, A. G.—No. 26
Wood, R. W. and E. L. Kinsey—No. 61
- Zimmermann, E. E.—No. 49

AUTHOR INDEX TO VOLUME 29

- References with (A) are merely to abstracts of papers presented at meetings of the Physical Society.
- Alexeievsky, A. P. Some remarks on the formation of negative ions—752(A)
- Allen, S. J. M. X-ray absorption formulas—918(A)
- Allis, W. P. and Hans Mueller. Wave theory of the electron—361(A)
- Allison, Fred. Effect of wave-length on the differences in the lags of the Faraday effect behind the magnetic field for various liquids—370(A)
——— (see Beams, J. W.)—161
- Allison, Samuel K. Reflection of x-rays by crystals as a problem in the reflection of radiation by parallel planes—375, 748(A)
- Anderson, S. H. Striking potentials of metallic arcs in vacuo—750(A)
——— (see Ostenson, Floyd C.)—753(A)
- Babcock, Harold D. Study of the infra-red solar spectrum with the interferometer—748(A)
- Barker, E. F. (see Colby, W. F.)—923(A)
——— (see Fox, G. W.)—921(A)
——— (see Stinchcomb, G. A.)—213(A)
- Barnes, James. The shift in a near infra-red absorption band of some benzene derivatives—922(A)
- Barrett, C. S. and J. A. Bearden. The polarizing angle for x-rays—352(A)
- Barton, Henry A. Ionization in HCl vapor—608(A)
——— (see Jenkins, Francis A.)—211(A)
- Bateman, H. Motion of an airship in a variable horizontal wind—755(A)
- Baudisch, O. (see Welo, L. A.)—612(A)
- Bauer, Louis A. Cosmic aspects of atmospheric electricity—371(A)
- Baxter, Warren P. (see Dalton, Robert H.)—248
- Bayley, P. L. X-ray coloration of kunzite and hiddeinite—353(A)
- Beams, J. W. and Fred Allison. Differences in the time lags of the Faraday effect behind the magnetic field in various liquids—161
- Beams, J. W. and Ernest O. Lawrence. New method of determining the time of appearance and time of duration of spectrum lines in spark discharges—357(A)
——— Study of the lag of the Kerr effect for several liquids as a function of the wave-length of the light—903(A)
- Beams, J. W. (see Lawrence, Ernest O.)—903(A)
- Bearden, J. A. Measurement and interpretation of the intensity of x-rays reflected from sodium chloride and aluminum—20
——— (see Barrett, C. S.)—352(A)
- Becker, J. A. Life history of an adsorbed atom of Cs—364(A)
- Begeman, Hilda (see McDowell, Louise S.)—367(A)
- Bennett, Arthur Lowell. Resolving power of the ears—911(A)
- Bennett, R. D. Some properties of Geiger counters—363(A)
- Birge, R. T. Comprehensive form of energy level diagram for atoms—922(A)
——— and A. Christy. The titanium bands—212(A)
——— and J. J. Hopfield. Ultra-violet band spectra of nitrogen—356(A)
——— (see Hopfield, J. J.)—922(A)
- Black, J. G. (see Duffendack, O. S.)—358(A), 925(A)
- Blake, F. C., James Lord and A. E. Focke. Solid solutions of chromium and nickel and of iron and nickel—206(A)
- Bless, A. A. Recoil electrons from aluminum—918(A)
- Bobrovnikoff, N. T. The spectra of comets—210(A)
- Boord, Cecil E. (see Smith, Alpheus W.)—355(A)
- Bourgin, David G. Molecular fields—368(A)
——— Line intensities in the HCl fundamental band—794
——— Vacuum tube oscillator—912(A)
- Bowen, I. S. Series spectra of B, C, N, O and F—231
——— Series spectra of ionized phosphorus, P_{II} —510, 749(A)
——— (see Millikan, R. A.)—749(A)
- Bozorth, Richard M. and F. E. Haworth. Crystal structure of magnesium platinocyanide heptahydrate—233
- Brasefield, Charles J. H₃ as a possible emitter of the secondary hydrogen spectrum—915(A)
- Breit, G. Suggestion of an explanation of the long life of metastable atoms—361(A)
——— Book Reviews—200, 348, 601
- Brewer A. Keith. Factors influencing thermionic emission—752(A)
- Brickwedde, F. G. and W. A. MacNair. Light absorption of liquified gases—916(A)

- Bridgman, P. W. Breakdown of atoms at high pressures—188
 —— Book Reviews—201, 202, 349, 897
- Brown, S. L. and M. Y. Colby. Electrical measurements at radio frequencies—717
- Brown, S. L., C. F. Wiebusch and M. Y. Colby. High frequency resistance of a Bureau of Standards type variable air condenser—887
- Bush, V. and King E. Gould. Temperature distribution along a filament—337
- Butts, Donald C. A., Thomas E. Huff and Frederick Palmer, Jr. A preliminary report on the study of the emission spectra and surface tension alterations in experimental animal tumors—219(A)
- Cady, W. G. Shear mode of crystal vibration—617(A)
 —— Book Reviews—199, 896
- Cajori, Florian. Book Reviews—197, 346, 492
- Campbell, G. C. and G. W. Willard. Device to draw characteristic curves of vacuum tubes automatically—913(A)
- Carman, A. P. and K. H. Hubbard. Determination of the dielectric constant of air by a discharge method—217(A), 299
- Castleman, R. A., Jr. Log, semi-log, and uniform coordinator—910(A).
- Cheney, E. W. Measurement of index of refraction of gases at higher temperatures—292
- Christy, A. (see Birge, R. T.)—212(A)
- Clarke, Harry. Measurement of x-rays used for therapy—605(A)
- Coblentz, W. W. Tests of a new selective radiometer of molybdenite—615(A)
 —— and C. W. Hughes. New selective radiometer of molybdenite—365(A)
 —— and C. O. Lampland. Radiometric measurements on the planet, Mars, 1926—372(A)
- Colby, M. Y. (see Brown, S. L.)—717, 887
- Colby, W. F. and E. F. Barker. Infra-red spectrum of NH₃—923(A)
- Compton, K. T. and P. M. Morse. Theory of the normal cathode fall—909(A)
- Compton, K. T. (see Van Voorhis, C. C.)—909(A)
- Constantinides, Philip A. Electrical properties and nature of active nitrogen—215(A),
- Cook, J. Williamson. Purification of helium—920(A)
- Cravath, A. M. (see Jones, L. T.)—871
- Crew, W. H. and E. O. Hulbert. Pressures in discharge tubes, Part I, Long slim tubes—609(A)
 —— Number of radiating atoms in a hydrogen discharge tube—843
- Dalton, Robert H. and Warren P. Baxter. Velocity distribution of electrons issuing from small holes—248
- Darrow, Karl K. Book Reviews—493, 898
- Davey, Wheeler P. Theory of the mechanism of crystal growth—206(A)
 —— Book Review—492
- Davis, Raymond and K. S. Gibson. Reproducible liquid filters for the determination of the color temperature of incandescent lamps—916(A)
- Davission, C. and L. H. Germer. Scattering of electrons by a nickel crystal—908(A)
- Dawson, L. H. Movements of striae in discharge tubes under varying pressures—610(A)
 —— Piezo-electricity of crystal quartz—216(A), 532
- Del Rosario, C. Low pressure electric discharge in intense electric fields—360(A)
- Dennison, D. (see Dushman, S.)—903(A)
- Dickenson, R. G. (see Mitchell, A. C. G.)—751(A)
- Doan, Richard L. Refraction of x-rays by method of total reflection—205(A)
- Duane, William. General radiation from a very thin target—606(A)
- DuBridge, Lee A. Photoelectric properties of thoroughly outgassed Pt—451
- Duffendack, O. S. and J. G. Black. Energy level studies on metallic vapors using a high temperature tungsten furnace—358(A)
 —— Excitation of Cu(II) spectrum by positive Ne ions—925(A)
- Duffendack, O. S. and H. L. Smith. Simultaneous ionization and excitation of molecules on collision with foreign ions—914(A)
- Duffendack, O. S. (see Fox, G. W.)—921(A)
 —— (see Wolfe, R. A.)—209(A)
- Dunn, Hugh K. Changes in photoelectric threshold of Hg—693
- Durbin, F. M. Dependence of the free path of potassium ions in various gases on their velocity—215(A)
- Dushman, S., D. Dennison and M. B. Reynolds. Electron emission and diffusion constants for tungsten filaments containing various oxides—903(A)
- Dushman, S. and Jessie W. Ewald. Electron emission from thoriated tungsten—857
- Dymond, E. G. Electron scattering in He—433
- Eastman, E. D. Book Review—494
- Edwards, R. L. Magnetic properties of evaporated nickel and iron films—321
- Eldridge, John A. Critical potentials of the spark lines of mercury—213(A)
 ——, Alexander Ellett and Harry F. Olson. Polarization of light excited by electron impact—207(A)

- Ellett, Alexander.** Impact polarization and the spinning electron—207(A)
 —Polarization of resonance radiation in strong magnetic fields. Breadth of spectral lines—904(A)
 —(see Eldridge, John A.)—207(A)
- Ellis, Joseph W.** Infra-red absorption by the N-H bond; in aniline and alkyl anilines—356(A)
 —New infra-red absorption bands in methane—750(A)
- Ellsworth, Vivian M. and J. J. Hopfield.** Oxygen bands in the ultra-violet—79
- Epstein, Paul S.** Magnetic dipole in Schroedinger's theory—750(A)
 —Remark on the theory of the Trouton and Noble experiment—753(A)
- Erikson, Henry A.** Dependence of ionic mobility on the nature of the medium—369(A)
 —Nature of gaseous ions—215(A)
- Ewald, Jessie W.** (see Dushman, S.)—857
- Ewell, Arthur W.** Influence of electrolytic ions upon moisture of steam—912(A)
- Farnsworth, H. E.** Velocity distribution and 180° scattering of low velocity electrons from Fe—908(A)
- Focke, A. E.** (see Blake, F. C.)—206(A)
- Foote, Paul D.** Ionization of Hg vapor by 2537—609(A)
 —(see Mohler, F. L.)—141
- Foster, J. Stuart.** Theory of the Stark effect in the arc spectra of helium—916(A)
 —and W. Rowles. The Stark effect in neon—925(A)
- Fowle, E. S.** (see Pienkowsky, A. T.)—910(A)
- Fox, G. W., O. S. Duffendack and E. F. Barker.** Excitation of the spectrum of CO₂—921(A)
- Frank, N. H.** Propagation of electromagnetic waves along coaxial cylindrical conductors separated by two dielectrics—365(A)
- Franklin, William S.** Significance and scope of the idea of frequency in physics—362(A)
- Frayne, John G. and Charles W. Jarvis.** Stages in excitation of spectrum of In—357(A), 673
- Fredrickson, W. R., William W. Watson and J. Rinker.** Na and K absorption bands—917(A)
- Friauf, James B.** Crystal structure of magnesium di-zincide—34, 353(A)
- Gale, Henry G. and George S. Monk.** Band spectrum, continuous emission, and continuous absorption of fluorine gas—211(A)
- Galli-Shohat, N.** Refraction in moving media—906(A)
- Gartlein, C. W.** Arc spectrum of Ge—357(A)
- Germer, L. G.** (see Davisson, C.)—908(A)
- Gibbs, R. C. and H. E. White.** Some relations in the spectra of stripped atoms—359(A)
 —Two electron multiplets of first and second long periods—359(A)
 —Multiplets in two electron systems of the first long period—426
 —Multiplets in the spectra of Cr(III) and Mn (III)—917(A)
 —Multiplets in the spectra of V(III)—606(A)
 —Multiplets in the three electron systems of the first long period—655
- Gibbs, R. C., D. T. Wilber and H. E. White.** Terms arising from similar and dissimilar electrons—790, 917(A)
- Gibson, K. S.** (see Davis, Raymond)—916(A)
- Gish, O. H.** (see Rooney, W. J.)—905(A)
- Gortner, Ross Aiken.** Book Reviews—198, 348
- Gould, King E.** (see Bush, V.)—337
- Gray, J. A. and B. W. Sargent.** Absorption of betarays—351(A)
- Ham, W. R.** Equations for thermionic emission—607(A)
 —Interpretation of data dealing with thermionic emission—364(A)
 —Reflection of electrons from Mo—908(A)
- Hamer, Richard and Surain Singh.** Critical potentials of Cu—901(A)
 —Critical potentials of Fe—608(A)
- Hanson, R. L.** Photoelectromotive force in selenium—924(A)
- Harnwell, Gaylord P.** Evidence for collisions of the second kind in the rare gases—608(A)
 —Inelastic collisions in ionized gas mixtures—611(A)
 —Ionization by collisions of the second kind in mixtures of hydrogen and nitrogen with the rare gases—830, 906(A)
 —Ionization by collisions of the second kind in the rare gases—683
- Harkins, William D. and H. A. Shadduck.** The synthesis and disintegration of atoms as shown by an application of the Wilson cloud-track method—207(A)
- Harrington, E. A.** X-ray diffraction measurements on some of the pure compounds concerned in the study of Portland cement—353(A)
- Harrington, G. F. and A. M. Opsahl.** Technique of the Dufour cathode ray oscilloscope for the study of short time occurrences—364(A)
- Harrison, J. R.** Subfundamental piezo-electric vibrations in quartz plates—366(A)
 —Theory and applications of low frequency piezo-electric vibrations in quartz plates—617(A)

- Hartig, H. E. and H. B. Wilcox. Absolute method for measuring the velocity of fluids—485
- Hartsough, R. C. Shielding from vibrations—910(A)
- Havighurst, R. J. Electron distribution in the atoms of crystals. Sodium chloride and lithium, sodium and calcium fluorides—1
- Haworth, F. E. (see Bozorth, Richard M.)—223
- Heaps, C. W. Hall effect in Bi with small magnetic fields—332
- Henderson, Joseph E. Pseudo photographic effect of slow electrons—360(A)
- Hepburn, Ann B. Carbon monoxide band excitation potentials—212(A)
- Hertel, K. L. A study of the polarization of light from hydrogen canal rays—214(A), 848
- Herzfeld, K. F. Atomic properties which make an element a metal—701
- Heyl, Paul R. Redetermination of the Newtonian constant of gravitation—910(A)
- Hidnert, Peter and W. T. Sweeney. Thermal expansion of graphite—371(A)
- Thermal expansion of beryllium—616(A)
- Thermal expansion of some nickel steels—911(A)
- Hoag, J. Barton. Extreme ultra-violet spectra using large angles of incidence—208(A)
- Hopfield, J. J. Absorption spectra in the extreme ultra-violet—356(A)
- Some unclassified lines of oxygen in the ultra-violet—923(A)
- (see Birge, R. T.)—356(A)
- (see Ellsworth, Vivian M.)—79
- and R. T. Birge. Ultra-violet absorption and spectra of CO—922(A)
- Horovitz, Karl. Investigation of metal films by x-ray analysis—352(A)
- Determination of the surface area of adsorbers—617(A)
- Houston, William V. A compound interferometer for fine structure work—210(A), 478
- Interferometer measurements on the Balmer series—749(A)
- Fine structure of the helium arc spectrum—749(A)
- Hoyt, F. C. Book Review—197
- Hubbard, K. H. (see Carman, A. P.)—217(A), 299
- Huff, Thomas E. (see Butts, Donald C. A.)—219(A)
- Hughes, C. W. (see Coblenz, W. W.)—365(A)
- Hughes, A. Ll. and L. W. Jones. Distribution of energy among electrons rebounding from He atoms—214(A)
- Hughes, A. Ll. and A. M. Skellett. Hot Wire vacuum gauge—365(A)
- Dissociation of hydrogen by electrons—907(A)
- Hulbert, E. O. Absorption of radio waves in the upper atmosphere—865(A), 706
- (see Crew, W. H.)—609(A), 843
- Hull, Albert W. and J. M. Hyatt. Secondary electron emission from Mo—214(A)
- Hunt, F. L. X-rays of long wave-length from a ruled grating—919(A)
- Hulthén, E. Band spectrum of calcium hydride—97
- Hutchisson, Elmer. Energy of the crossed-orbit model of the hydrogen molecule—270
- Quantum theory of the specific heat of HCl—360(A)
- Hyatt, J. M. Secondary electron emission produced by positive Cs ions—214(A)
- (see Hull, Albert W.)—214(A)
- Ives, Herbert E. and G. R. Stilwell. Photoelectric emission as a function of composition in Na-K alloys—252, 363(A)
- Jarvis, Charles W. Ionization and resonance potentials in Ga and In—442
- (see Frayne, John G.)—357(A), 673
- Jauncey, G. E. M. Intensity of reflection of x-rays by crystals and the Compton effect—206(A)
- Intensity of scattered x-rays and the Compton effect—605(A)
- Theory of the intensity of scattered x-rays—757
- Jenkins, Francis A. Line spectra of isotopes of Hg and Cl—50
- Structure and isotope effect in the alpha bands of BO—921(A)
- (see Kemble, E. C.)—607(A)
- , Henry A. Barton and Robert S. Mulliken. Beta bands of NO—211(A)
- Johnson, E. H. Many-lined spectrum of sodium hydride—85
- Johnson, J. B. Thermal agitation of electricity in conductors—367(A)*
- Johnson, Thomas H. Absolute ionization vacuum gauge—610(A)
- Jones, Arthur Taber. Nodal lines of bells—616(A)
- Jones, Ernest J. Excitation of Hg vapor by positive ions—611(A)
- Jones, L. T. and A. M. Cravath. Neutralization of the deflecting field in a Braun tube with external electrodes—871
- Jones, L. T. (see McCarty, L. E.)—880
- Jones, L. W. (see Hughes, A. Ll.)—214(A)
- Jones, T. J. Probability of ionization of Hg vapor by electron impact—822
- Kaplan, Joseph. Duration of atomic hydrogen—920(A)

- Karapetoff, Vladimir. Mechanical forces between electric currents and saturated magnetic fields—367(A)
- Formal unification of gradient, divergence, and curl, by means of an infinitesimal operational volume—914(A)
- Kegerreis, Roy. Heat energy of x-rays—775
- Kemble, E. C. and F. A. Jenkins. Quantitative test of Hund's theory of doublet bands of the OH type—607(A)
- Kennard, E. H. Excitation of fluorescence in fluorescein—466
- Kent, Norton A., Lucien B. Taylor and Hazel Pearson. Fine structure of the Balmer lines—748(A)
- Kenty, Carl and Louis A. Turner. Surface layers produced by activated nitrogen.—914(A)
- Keys, David A. Note on the auroral green line 5577—209(A)
- Kimball, A. L. and D. E. Lovell. Internal friction in solids—616(A)
- King, Arthur S. Spectra of the high-current vacuum arc—359(A)
- King, Louis Vessot. On a gyromagnetic electron theory of the Compton effect—919(A)
- Kingsbury, B. A. Direct comparison of the loudness of pure tones—373(A), 588
- Kinsey, E. L. (see Wood, R. W.)—917(A)
- Kirkpatrick, Paul. Polarization factor in x-ray reflection—632
- Kleeman, Richard D. General theory of the electrical properties of surfaces of contact—368(A)
- Absolute zero of the externally controllable entropy and internal energy of a substance or mixture—369(A)
- Properties of substances and mixtures in the condensed state at the absolute zero of temperature—614(A)
- Relations in connection with the reversible mixing of substances in the condensed state at absolute zero—912(A)
- Klein, Elias. Constancy of the flashing period of a neon glow-lamp—610(A)
- Knudsen, V. O. Measurement of sound-absorption in a room—753(A)
- Kollar, L. R. Effect of oxygen on photoelectric emission from potassium—902(A)
- Krefft, Hermann E. O and N energy levels in the secondary emission of hot tungsten—903(A)
- Kronig, P. de L. Book Review—601
- and I. I. Rabi. Symmetrical top in the undulatory mechanics—262
- Kunz, Jacob. Theory of the specific heat of methane—220(A)
- Resonance method for the determination of the universal constant of gravitation—910(A)
- (see Tykocinski-Tykociner, J.)—904(A)
- Kurrelmeyer, B. Optical absorption and photoelectric conductivity of sulphur crystals—615(A)
- Laird, Elizabeth R. Absorption in region of soft x-rays—41
- Reflection of soft x-rays—605(A)
- Lampland, C. O. (see Coblenz, W. W.)—372(A)
- Langer, R. M. Charge density in the new mechanics —924(A)
- Langmuir, Irving. (see Tonks, Lewi)—524, 614(A)
- Lansing, William D. An electronic theory of passivity—216(A)
- Laporte, O. Screening constants from optical data—650
- (see Sommerfeld, A.)—208(A)
- Lawrence, Ernest O. Length of radiation quanta—361(A)
- Ultra-ionization potentials of Hg—609(A)
- (see Beams, J. W.)—357(A), 361(A), 903(A)
- and J. W. Beams. The instantaneity of the photoelectric effect—903(A)
- Lemon, Harvey B. Some laboratory observations bearing on the spectra of comets—210(A)
- Levin, Aaron (see Meyer, Charles F.)—923(A)
- Libman, E. E. Surface tensions of the molten elements as functions of temperature. I. Cu—911(A)
- Lilienfeld, J. E. and C. H. Thomas. High pressure powder contact rectifier—367(A)
- Linder, Ernest G. Thermoelectric effect in single crystal zinc—221(A), 554
- Lindsay, George A. (see Van Dyke, George D.)—205(A)
- Lindsay, R. B. Carbon atom model and the structure of diamond—497
- Note on "pendulum" orbits in atomic models —612(A)
- Little, Noel C. Thermomagnetic effect in gases—901(A)
- Loeb, Leonard B. Mobilities of ions in hydrogen gas mixtures and the constitution of the ion—751(A)
- Loomis, F. W. Correlation of the fluorescent and absorption spectra of iodine—112
- New series in the spectrum of fluorescent iodine—355(A)
- Vibrational levels in the blue-green band system of Na—607(A)
- Lord, James. (see Blake, F. C.)—206(A)
- Loughridge, D. H. Direction of photoelectric emission—751(A)
- Lovell, D. E. (see Kimball, A. L.)—616(A)
- Lubovitch, Vladimir P. Infrared spectrum of Hg—355(A)

- MacDougall, F. H. Book Reviews—494, 495, 602
- MacMahon, A. M. New measurements upon the light sensitiveness of crystalline selenium—219(A)
—The significance of photoelectric conduction in crystals—902(A)
- MacNair, Walter A. Secondary radiation and polarization of resonance radiation in Cd—677
—Zeeman effect of the fine structure components of $\lambda 2536$ of Hg—915(A)
(see Brickwedde)—916(A)
- Martin, John R. Magnetic properties of iron in high frequency alternating current fields—906(A)
- Masius, Morton. Calculation of changes of function involving factorials as applied to entropy calculations—613(A)
- McCarty, L. E. and L. T. Jones. Index of refraction of water for short continuous waves—880
- McCurdy, W. H. Fine structure of the mercury line 3650A—915(A)
- McDonald, Frank C. An investigation of some hydrocarbon bands—212(A)
- McDowell, Louise S. and Hilda Begeman. Correlation between power loss, dielectric constant and conductivity of various glasses—367(A)
- McKeehan, L. W. Iron crystals—920(A)
—Book Reviews—745, 746, 894
- McKinstry, A. (see Morton, W. B.)—192
- McLennan, J. C. and I. Walerstein. Fluorescence spectra in metallic vapours excited by the light in the mercury arc—208(A)
- Meggers, W. F. and F. M. Walters, Jr. Absorption spectra of Fe, Co and Ni—358(A)
- Meggers, W. F. (see Russell, Henry Norris)—606(A)
- Mendenhall, H. E. Vacuum switch—754(A)
- Meyer, Charles F. and Aaron Levin. Infrared absorption spectra of C_2H_2 , C_2H_4 , and C_2H_6 —923(A)
- Miller, Dayton C. Report on the ether-drift experiments at Cleveland in 1927—924(A)
- Miller, Frederic H. Resonance in alternating currents containing a single harmonic—546
- Miller, L. F. Relation of heat transmission to humidity in insulating materials—370(A)
- Millikan, R. A. and I. S. Bowen. Relationships in the spectra of the first row of the periodic table—750(A)
- Mitchell, A. C. G. and R. G. Dickinson. Effect of added gases on ammonia decomposition by optically excited Hg vapor—751(A)
- Mohler, F. L. Excitation of spectra by atomic hydrogen—354(A), 419
— and Paul D. Foote. Electron collisions in Co—141
- Monk, George S. (see Gale, Henry G.)—211(A)
- Mooney, Melvin. New electrophoretic mobility formula—217(A)
—New electrophoresis cell—218(A)
- Morehouse, W. B. X-ray absorption and valence—924(A)
—Effect of chemical combination on x-ray absorption—765
- Morrow, Roger M. (see Stewart, G. W.)—919(A)
- Morse, P. M. (see Compton, K. T.)—909(A)
- Morton, W. B. and A. McKinstry. Continuous motion produced by vibration—192
- Mueller, Hans. Activity of monovalent ions—216(A)
(see Allis, W. P.)—361(A)
- Mulliken, Robert S. Intensity relations and electronic states in spectra of diatomic molecules—211(A)
—Electronic states and band spectrum structure in diatomic molecules: III, Intensity relations—391
—Electronic states and band spectrum structure in diatomic molecules: IV, Hund's theory; second positive nitrogen and Swan bands; alternating intensities—637
—Intensity relations and band structure in bands of the violet CN type—923(A)
—Band structure and intensities, atomic and molecular electronic states, in diatomic hydrides—921(A)
(see Jenkins, Francis A.)—211(A)
- Murnaghan, Francis D. and Harold A. Wheeler. Analysis and applications of wave-filter determinants—914(A)
- Muskat, Morris (see Smith, Alpheus W.)—663
- Nathanson, J. B. Variation with state of the optical constants of Cs—369(A)
- Nicholas, Warren W. A system of structures for atomic nuclei—612(A)
—X-ray isochromats of Cu taken in different directions relative to the cathode stream—619
- Nielsen, Walter M. Dissociation of HCl by positive ion impact—907(A)
- Nusbaum, C. Magnetic susceptibility of single-crystal elements—370(A)
—Magnetic susceptibility of single-crystal metals—905(A)
- Nye, Arthur W. Measurement of wave-length of light in water—753(A)
- Nyquist, H. Thermal agitation in conductors—614(A)
- Olson, Harry F. Polarization of $\lambda 2537$ of Hg—207(A)
(see Eldridge, J. A.)—207(A)

- Opsahl, A. M. (see Harrington, G. F.)—364(A)
- Ostenson, Floyd C. and S. H. Anderson. End corrections of pipes as a function of frequency—753(A)
- Page, Leigh. Book Reviews—349, 896
- Palmer, Frederick, Jr. (see Butts, Donald C. A.)—219(A)
- Parmley, T. J. Photoelectric threshold of Bi crystals—902(A)
- Pauling, Linus. Influence of a magnetic field on the dielectric constant of a diatomic dipole gas—145
—Electron affinity of hydrogen and the second ionization potential of lithium—285
- Pearson, Hazel. (see Kent, Norton A.)—748(A)
- Pease, C. S. (see Smith, Alpheus W.)—355(A)
- Perkins, B., Jr. (see Watson, William W.)—921(A)
- Phipps, T. E. and John B. Taylor. Magnetic moment of the hydrogen atom—218(A), 309
- Phipps, T. E. (see Taylor, John B.)—904(A)
- Pienkowski, A. T. and E. S. Fowle. Variations of gold-plated screw knob weights with atmospheric humidity—910(A)
- Piersol, Robert J. Influence of temperature on selenium photosensitivity—362(A)
—Relation between light intensity and photocurrent in selenium—902(A)
- Plyler, E. K. Infrared reflection spectra of some carbonates—923(A)
- Podolsky, Boris. On King's classical theory of atomic structure 750(A)
- Poindexter, F. E. New instrument for measuring surface tension—221(A)
- Pomeroy, William C. Quantum analysis of band spectrum of aluminum oxide—59
- Pool, M. L. Post-arc conductivity and metastable states in Hg—610(A)
—Residual ions and critical restriking potential in Hg arcs—915(A)
- Purks, J. H. and C. M. Slack. Possible dependence of frequency of characteristic x-radiation on the temperature of the target—352(A)
- Rabi, I. I. Principal magnetic susceptibilities of crystals—174
(see Kronig, R. de L.)—262
- Race, Hubert H. Electric absorption currents in solid dielectrics—913(A)
- Rashevsky, N. Theory of the heats of fusion—220(A)
- Ray, Satyendra. Note on the plane wave of a gas—892
- Reynolds, N. B. (see Dushman, S.)—903(A)
- Reyerson, L. H. Book Review—746
- Richardson, Burt and Paul. Measuring the evaporation from a body of water—755(A)
- Richtmeyer, R. K. and L. S. Taylor. Relative probabilities of the photoelectric emission of electrons from Ag to Au—353(A)
—Further test of the theories of absorption of x-rays—606(A)
- Rinker, J. (see Fredrickson, W. R.)—917(A)
- Robards, W. M. Resistance of copper wires at very high frequencies—165
- Roebuck, J. R. Book Review—898
- Rogers, R. A. M series x-ray absorption spectra of Os, Ir, and Pt—205(A)
- Rooney, W. J. and O. H. Gish. Results of earth resistivity surveys in connection with the study of the earth currents at Watheroo, Western Australia and Ebro, Spain—905(A)
- Rowles, W. (see Foster, J. Stuart)—925(A)
- Rudnick, Philip. (see Watson, William W.)—413
- Rudy, Richard. Metastable neon and argon—359(A)
- Rusk, Rogers D. Resonance glow in hydrogen discharge tube—213(A)
—The 29 volt critical potential of hydrogen—354(A)
—Combination of hydrogen and oxygen by electric discharges and x-rays—907(A)
- Russell, Henry Norris. Calculation of spectroscopic terms derived from equivalent electrons—782
—and W. F. Meggers. Analysis of the arc and spark spectra of Sc—606(A)
- Russell, H. W. Potential of photoactive cells containing fluorescent electrolytes—615(A)
- Sagui, Cornelio L. Theory of the magnetic nature of gravity—371(A)
—Theory of the magnetic nature of gravity and the Balmer series—618(A)
—Theory of the magnetic nature of gravity and electrons—906(A)
- Sargent, B. W. (see Gray, J. A.)—351(A)
- Sawyer, R. A. and F. R. Smith. Spectra of boron—357(A)
- Schneider, W. A. Actino-electric effects in argentite—363(A)
- Seemann, Herman E. Thermal conductivity of fused quartz as a function of temperature—616(A)
- Shadduck, H. A. (see Harkins, William D.)—207(A)
- Shapley, Harlow. Book Review—894
- Shenstone, A. G. Spark spectrum of Cu II—209(A), 380
—Spark spectrum of Ni—917(A)

- Simon, A. W. On the electrostatics of the thunder-storm—754(A)
- Singh, Surain (see Hamer, Richard)—608(A), 901(A)
- Skellett, A. M. (see Hughes, A. L.)—365(A), 907(A)
- Slack, C. M. (see Purks, J. H.)—352(A)
- Smede, L. Temperature variations in wires heated by alternating current—614(A)
- Smith, Alpheus W., Cecil E. Boord and C. S. Pease. The absorption of ultra-violet light by organic vapors—355(A)
- Smith, Alpheus W. and Morris Muskat. Absorption spectra of Ga, In, Mn, Cr, Ni, and Co in under-water sparks—663
- Smith, F. R. (see Sawyer, R. A.)—357(A)
- Smith, H. L. (see Duffendack, O. S.)—914(A)
- Smith, Sinclair. A vertical seismometer—755(A)
- Smith, T. Townsend. Effect of a variation from the condition for achromatism in lenses—220(A)
- Solt, Irvin H. Magnetic moment of He and H₂—904(A)
- Sommer, L. A. Zeeman effect and structure of arc spectra of Cu and Rh—358(A)
- Sommerfeld, A. and O. Laporte. Spectroscopic interpretation of the magneton numbers in the iron group—208(A)
- Sorenson, Royal W. Effect of oil in storage on lightning discharge—754(A)
- Spencer, R. C. Method of least squares vs. the arithmetic method of obtaining the slope of a straight line—909(A)
- Stebbins, Joel. Book Review—895
- Stewart, G. W. Theory of the Herschel-Quincke tube—220(A)
- Book Review—494
- and Roger M. Morrow. Molecular space array in liquid primary normal alcohols: the cybotactic state—919(A)
- Stilwell, G. R. (see Ives, Herbert E.)—252, 363(A)
- Stinchcomb, G. A. and E. F. Barker. Fine structure of three infrared absorption bands of NH,—213(A)
- Stuhlman, Otto. Possible relation between radiation and ionization potentials of iron—354(A)
- Swann, W. F. G. Measurements of the variation of residual ionization in air with pressure at different altitudes—372(A)
- Origin of the magnetic fields of sun spots—905(A)
- Sweeney, W. T. (see Hidnert, Peter)—371(A), 616(A), 911(A)
- Swenson, David F. Book Review—197
- Takemchi, T. Scattering of particles by an Einstein center—186
- Tate, John T. Book Reviews—346, 602, 747
- Taylor, John B. and T. E. Phipps. Magnetic moment of atomic iodine—904(A)
- Taylor, John B. (see Phipps, T. E.)—218(A), 309
- Taylor, Lauriston. A type of oscillation hysteresis—617(A)
- Taylor, Lucien B. (see Kent, Norton A.)—748(A)
- Taylor, L. S. (see Richtmyer, F. K.)—353(A), 606(A)
- Taylor, Paul B. Theory of cell with liquid junction—369(A)
- Terry, Earle M. Factors affecting the constancy of quartz piezo-electric oscillators—366(A)
- Thomas, C. H. (see Lilienfeld, J. E.)—367(A)
- Tonks, Lewi. Space charge as a cause of negative resistance in a triode—913(A)
- and Irving Langmuir. On the surface heat of charging—524, 614(A)
- Tschudi, E. W. Spectral intensity distribution in a hydrogen discharge—354(A)
- Turner, Louis A. (see Kenty, Carl)—914(A)
- Tykocinski-Tykokiner, J. Precise determination of frequency by means of piezo-electric oscillators—366(A)
- Shielded oscillator for Hertzian waves—217(A)
- Velocity selector for atomic rays—611(A)
- and J. Kunz. Method of measuring the distribution of magnetic fields—904(A)
- Valasek, Joseph. Relative intensities of some lines in the Hg spectrum—817
- Book Reviews—492, 496, 603, 899, 900
- Valasek, Leila M. Transformation period of the initial positive air ion—542
- Vallarta, M. S. On the condition of validity of macromechanics—613(A)
- Van Dyke, George D. and George A. Lindsay. X-ray L absorption edges of elements Sn to Ru inclusive—205(A)
- Van Vleck, J. H. A general proof of the Langevin-Debye formula and the susceptibilities of O₂ and NO—613(A)
- Dielectric constants and magnetic susceptibilities in the new quantum mechanics—727
- Book Reviews—202, 491
- Van Voorhis, C. C. and K. T. Compton. Heats of condensation of electrons and positive ions on Mo—909(A)
- Wait, G. R. On the effects of dust, smoke, and relative humidity upon the potential gradient and the positive and negative conductivities of the atmosphere—372(A)

- Wait, G. R. Magnetic permeability of iron and magnetite in high frequency alternating fields—566
Walerstein, I. (See McLennan, J. C.)—208(A)
Walters, F. M., Jr. (see Meggers, W. F.)—358(A)
Warburton, F. W. Hall effect and resistance of sputtered Te films—905(A)
Waterman, A. T. Electrical resistance of metals as a function of pressure—368(A)
Watson, E. C. The velocity and number of the photoelectrons ejected by x-rays as a function of the angle of emission—751(A)
——— Spacial distribution of the photoelectrons ejected by x-rays—752(A)
——— Explanation of Whiddington's rule for x-ray electrons—919(A)
Watson, F. R. A method for determining sound transmission—925(A)
——— Optimum conditions for music in rooms—220(A)
Watson, William W. and B. Perkins, Jr. Zeeman effect in AgH, AlH, ZnH and MgH bands—921(A)
Watson, William W. and Philip Rudnick. Rotational terms in the MgH bands—413
Watson, William W. (see Frederickson, W. R.)—917(A)
Weatherby, B. B. (see Wolf, A.)—135
Webster, D. L. Book Review—346
Weigle, J. J. Effect of a magnetic field on the dielectric constant—362(A)
Welo, L. A. and O. Baudisch. Magnetic moments of iron in complex salts—612(A)
Welsh, George B. The periodicity of photoelectric thresholds—615(A)
Wenner, Frank. Principle governing the distribution of current in systems of linear conductors—218(A)
Wheeler, Harold A. Theory of the shot effect—903(A)
——— (see Murnaghan, Francis D.)—914(A)
White, H. E. (see Gibbs, R. C.)—359(A), 426, 606(A), 917(A); 655, 917(A), 790
Whitney, W. T. Michelson-Gale earth-tide experiment repeated in Pasadena, California—755(A)
Wiebusch, C. F. (see Brown, S. L.)—887
Wilber, D. T. (see Gibbs, R. C.)—917(A), 790
Wilcox, H. B. (see Hartig, H. E.)—485
Wilkins, T. R. New theory of the origin of the actinium series—352(A)
Willard, G. W. (see Campbell, G. C.)—913(A)
Williams, E. H. Magnetic susceptibility of rare earth metals—218(A)
Williams, S. R. An unusual magnetostrictive effect in Monel metal—370(A)
Winans, J. G. Collisions of the second kind between zinc and mercury atoms—213(A)
Winchester, George. Variation of surface tension of oils with the temperature—911(A)
Wissink, G. M. (see Woodrow, Jay W.)—219(A)
Witmer, Enos E. Quantization of the rotational energy of the polyatomic molecule by the new wave mechanics—362(A)
——— Rotational and vibrational specific heat of a diatomic gas, the molecules of which have a doublet *P* normal state—918(A)
Wolf, A. and B. B. Weatherby. Absorption coefficient of helium for its own radiation—135
Wolfe, R. A. and O. S. Duffendack. Excitation of arc spectrum of N—209(A)
Wood, R. W. Physical and biological effects of high frequency sound waves of great intensity—373(A)
——— Demonstration of an improved form of Rijke tube of high efficiency. A lecture experiment in acoustics—373(A)
——— and E. L. Kinsey. The fluorescence of Na vapor—917(A)
Woodrow, Jay W. and G. M. Wissink. Fluorescence and chemiluminescence of cod liver oil—219(A)
Worthing, A. G. Some observations on the nature of the nitrogen afterglow—907(A)
Zeleny, John. Striated discharge in H₂ and He—609(A)
Zemansky, Mark W. Diffusion of imprisoned resonance radiation in Hg vapor—513
Zimmerman, E. E. Effect of temperature on polarization capacity and resistance for Au and Pt electrodes in different concentrations of sulphuric acid and at different audible frequencies—913(A)
Zinszer, Harvey A. Shadowgraph method as applied to a study of the electric spark—752(A)
Zumstein, R. V. Absorption spectrum of antimony vapor—209(A)
Zwickly, F. Phenomena depending on the change of elastic frequencies in solid bodies with pressure—579, 754(A)

ANALYTIC SUBJECT INDEX TO VOLUME 29

Reference with (A) are merely to abstracts of papers presented at meetings of the Physical Society.

- Absorption of light (see also Electrical oscillations, Spectra, x-rays)
 - By aniline and alkyl anilines, infra-red, J. W. Ellis—356(A)
 - By CH₄, new infra-red bands, J. W. Ellis—751(A)
 - By fluorescein, relation to fluorescence, E. H. Kennard—466
 - By He for its own radiation, A. Wolf, B. B. Weatherby—135
 - By kunzite and hiddenite, colored by x-rays, P. L. Bayley—353(A)
 - By liquified gases, F. G. Brickwedde and W. A. MacNair—916(A)
 - By organic vapors, in ultra-violet, A. W. Smith, C. E. Boord, C. S. Pease—355(A)
 - By sulphur crystals, relation to photoelectric conductivity, B. Kurrelmeyer—615(A)
- Acoustics
 - absorption in room, measurement, V. O. Knudsen—753(A)
 - End corrections of pipes as function of frequency, F. C. Ostenson, S. H. Anderson—753(A)
 - Herschel-Quincke tube, theory, G. W. Stewart—220(A)
 - Loudness of pure tones, comparison, B. A. Kingsbury—373(A), 588
 - Method for measuring velocity of fluids, H. E. Hartig, H. B. Wilcox—485
 - Nodal lines of bells, A. T. Jones—616(A)
 - Optimum conditions for music in rooms, F. R. Watson—220(A)
 - Plane waves in gases, S. Ray—892
 - Resolving power of ears, A. L. Bennett—911(A)
 - Rijke tube of high efficiency, demonstration, R. W. Wood—373(A)
 - Transmission of sound, method for determining, F. R. Watson—925(A)
 - Ultrasonic waves, physical and biological effects, R. W. Wood—373(A)
- Actino-electric (see Photoelectric)
- Activated gases (see also collisions of second kind, Metastable atoms)
 - Active nitrogen, afterglow, A. G. Worthing—907(A)
 - Active nitrogen, electric properties and nature, P. A. Constantinides—215(A)
 - Activated gases (cont.)
 - Active nitrogen, surface layers produced by, C. Kenty, L. A. Turner—914(A)
- Activity, chemical
 - Of monovalent ions, H. Mueller—216(A)
- Adsorption
 - Of Cs on W, life history, J. A. Becker—364(A)
 - Surface area of adsorbers, determination, K. Horovitz—617(A)
 - Surface layers on W, produced by active nitrogen, C. Kenty, L. A. Turner—914(A)
- Aerodynamics
 - Motion of airship in variable horizontal winds, H. Bateman—755(A)
- Affinity, electron
 - Of H₂, L. Pauling—285
- Alpha particles
 - Scattering by Einstein center, T. Takeuchi—186
- Arcs
 - High-current, vacuum, spectra, A. S. King—359(A)
 - In H₂, 29 volt critical potential, R. D. Rusk—354(A)
 - In Hg vapor, post-arc conductivity, M. A. Pool—610(A)
 - In Hg vapor, residual ions and restriking potentials, M. L. Pool—915(A)
 - In N₂-He mixture, spectra, R. A. Wolfe, O. S. Duffendack—209(A)
 - Metallic, in vacuo, striking potentials, S. H. Andersen—750(A)
- Atmospheric electricity
 - Cosmic aspects, L. A. Bauer—371(A)
 - Effects of dust, smoke, and humidity, G. R. Wait—372(A)
- Atomic radii
 - Of Pt and Mg atoms, R. M. Bozorth, F. E. Haworth—223
- Atomic rays
 - Velocity selector, J. Tykocinski-Tykociner—611(A)

Atomic structure

- Breakdown at high pressures, P. W. Bridgman—188
 Energy level diagrams, comprehensive form, R. T. Birge—922(A)
 Electron distribution from x-ray measurements, R. J. Havighurst—1
 Electron distribution from x-ray measurements, J. A. Bearden—20
 King's classical theory, B. Podolsky—751(A)
 Metastable atoms, explanation of long life, G. Breit—361(A)
 Of carbon, structure of diamond, R. B. Lindsay—497
 Pendulum orbits, R. B. Lindsay—612(A)
 Structures of nuclei, W. W. Nicholas—612(A)

Aurora

- Auroral green line 5577, from discharge in He-O₂ and A-O₂ mixtures, D. A. Keys—209(A)

Beta-rays

- Absorption in Al, C, Cu, Pb, and Sn, J. A. Gray, B. W. Sargent—351(A)

Book Reviews

- Alexander, Jerome (editor); Colloid Chemistry—Theoretical and Applied—198
 Ambronn, Hermann, and Frey, Albert; Polarisations-Mikroskop, seine Anwendung in der Kolloidforschung und in der Farberei—492
 ten Bruggencate, P.; Sternhaufen—894
 Brunet, Pierre.; Les Physiciens Hollandais et la méthode Experimentale en France au XVIII^e Siecle—197
 Callender, H. L.; Enlarged Mollier Diagram for Saturated and Superheated Steam—898
 Clark, George L.; Applied X-rays—746
 Crandall, Irving B.; Theory of Vibrating Systems and Sound—494
 Darrow, Karl K.; Introduction to Contemporary Physics—346
 Du Noüy, P. Lecomte; Surface Equilibria of Biological and Organic Colloids—495
 Einstein, Albert; Investigations on the Theory of the Brownian Movement—747
 Eyraud, Henri; Les Equations de la Dynamique de L'Ether—349
 Forestier, A.; L'Énergie Rayonnante—603
 Franck, J., and Jordon, P.; Anregung von Quantensprungen durch Stoesse—346
 Fenkel, J.; Lehrbuch der Elektrodynamik Bd. I—896
 Gehrcke, E. (editor); Handbuch der Physikalischen Optik Vol. I First half—899
 Gehrcke, E. (editor); Handbuch der Physikalischen Optik Vol. II First half—900
 Geiger, H. and Scheel, Karl; Handbuch der Physik. B. I. Geschichte der Physik; Vorlesungstechnik—346
 Geiger, H., and Scheel, Karl; Handbuch der Physik, Bd. II. Elementare Einheiten und Ihre Messung—202
 Geiger, H., and Scheel, Karl; Handbuch der Physik. Bd. IX. Theorien der Wärme—201
 Geiger, H., and Scheel, Karl; Handbuch der Physik. Bd. XI. Anwendung der Thermodynamik—201
 Geiger, H., and Scheel, Karl; Handbuch der Physik. Bd. XXIII. Quanten—202
 Graetz, L.; Handbuch der Elektrizität und des Magnetismus. Bd. V—Lieferung I—200
 Haas, Arthur; Die Welt der Atome—493
 Hale, George Ellery; Beyond the Milky Way—496
 v. Hevesy, Georg; Das Element Hafnium—602
 Hinchenwood, C. N.; Thermodynamics (For Students of Chemistry)—494
 Holborn, L., and von Angerer, E.; Handbuch der Experimental Physik Vol. I, Messmethoden und Messtechnik—199
 Humphreys, W. J.; Fogs and Clouds—898
 Juvet, G.; Mechanique Analytique et Théorie des Quanta—197
 von Laue, M., and von Mises, R. (editors); Stereoscopic Drawings of Crystal Structures—899
 Lewis, Gilbert N.; The Anatomy of Science—349
 Liesegang, Raphael Ed.; Kolloidchemie—348
 Mark, Herman; Die Verwendung der Röntgenstrahlen in Chemie und Technik. Bd. XIV—745
 Mecke, Reinhard and Lambertz, Anton; Leitfaden der Praktischen Experimentalphysik für Vorlesung und Unterricht—896
 Moss, Herbert; The Enlarged Heat Drop Tables—898
 Müller-Pouillet; Lehrbuch der Physik. Bd. II—603
 Müller-Pouillet; Lehrbuch der Physik. Bd. III, First half. Physikalische, chemische und technische Thermodynamik—897
 Ostwald, Wolfgang; Practical Colloid Chemistry—746
 Planck, Max; Treatise on Thermodynamics—747
 Reilly, Joseph, Roe, William Norman and Wheeler, Thomas Sherlock; Physico-chemical Methods—494
 Rideal, E. K.; An Introduction to Surface Chemistry—495
 Russell, Henry Norris, Dugan, Raymond, Smith and Stewart, John Quincy; Astronomy—895

- Schroedinger, E.; Abhandlungen zur Wellenmechanik—601
- Senter, George; Outline of Physical Chemistry—602
- Smekal, Adolf; Allgemeine Grundlagen der Quantenstatistik und Quantentheorie—601
- Sommerfeld, Arnold; Three Lectures on Atomic Physics—491
- Spooner, Thomas; Properties and Testing of Magnetic Materials—894
- Stoner, Edmund C.; Magnetism and Atomic Structure—348
- Troland, Leonard T.; The Mystery of Mind—197
- Tutton, A. E. H.; Crystalline Form and Chemical Constitution—491
- Walsh, John W. T.; Photometry—496
- Webster, D. L., Farwell, H. W., and Drew, E. R.; General Physics for Colleges—199
- Wohlwill, Emil; Galilei und sein Kampf für die Copernicanische Lehre—492
- Braun tube**
With external electrodes, neutralization of field, L. T. Jones, A. M. Cravath—871
- Canal Rays**
Of hydrogen, polarization of light, K. L. Hertel—214(A), 848
- Cathode fall**
Theory, K. T. Compton, P. M. Morse—909(A)
- Cells**
Electrolytic with liquid junction, theory, P. B. Taylor—369(A)
Electrophoresis, new type, M. Mooney—218(A)
- Charge density**
Interpretation in new mechanics, R. M. Langer—924(A)
- Chemical reaction**
Combination of H_2 and O_2 by discharges and x-rays, R. D. Rusk—907(A)
Decomposition of NH_3 by excited Hg, effect of added gases, A. C. G. Mitchell, R. G. Dickinson—751(A)
Duration of atomic hydrogen, J. Kaplan—000(A)
Effect on x-ray absorption, W. B. Morehouse—924(A), 765
- Chemiluminescence**
Of cod-liver oil, J. W. Woodrow, G. M. Wissink—219(A)
- Collisions of the second kind** (see also Activated gases)
Between Zn and excited Hg atoms, J. G. Winans—213(A)
- Between active nitrogen and iodine, P. Constantinides—215(A)
- Decomposition of NH_3 by excited Hg, A. C. G. Mitchell, R. G. Dickinson—751(A)
- Effect on diffusion of resonance radiation in Hg vapor, M. W. Zemansky—513
- Evidence for, in the rare gases, G. P. Harnwell—608(A)
- Excitation of Cu(II) spectrum by positive neon ions, O. S. Duffendack, J. G. Black—925(A)
- Excitation of spectra by atomic hydrogen, F. L. Mohler—419, 354(A)
- Inelastic collisions in ionized gas mixtures, G. P. Harnwell—611(A)
- Ionization by, in rare gases, G. P. Harnwell—683
- Ionization by, in mixtures of H_2 and N_2 with the rare gases, G. P. Harnwell—906(A), 830
- Ionization and excitation by collisions with foreign ions, O. S. Duffendack, H. L. Smith—914(A)
- Colloids**
Electrophoretic mobility formula, M. Mooney—217(A)
- Electrophoresis cell, new type, M. Mooney—218(A)
- Comets**
Spectra, N. T. Bobrovnikoff—210(A)
Spectra, laboratory observations, H. B. Lemon—210(A)
- Compton effect** (see x-rays, scattering)
- Crystals**
Photoelectric conduction, significance, A. M. MacMahon—902(A)
Theory of growth, W. P. Davey—206(A)
- Crystals, single**
of Fe, new method of producing, L. W. McKeehan—920(A)
Of Ni, scattering of electrons by, C. Davisson, L. H. Germer—908(A)
Of Zn, thermoelectric effect, E. G. Linder—221(A), 554
Of various elements, susceptibility, C. Nusbaum—370(A)
- Crystal structure**
Of diamond, theory, R. B. Lindsay—497
Of $MgZn_2$, J. B. Friauf—34, 353(A)
Of magnesium platinocyanide heptahydrate, R. M. Bozorth, F. E. Haworth—223
Of solid solutions of Cr and Ni and of Fe and Ni, F. C. Blake, J. Lord, A. E. Focke—206(A)

Cybotatic state

Molecular space array in primary normal alcohols, G. W. Stewart, R. M. Morrow—919(A)

Dielectric constants

- Of air, determination by discharge method, A. P. Carman, K. H. Hubbard—217(A), 299
- Of diatomic dipole gases, influence of magnetic field, L. Pauling—145
- Of gases, effect of magnetic field, J. J. Weigle—362(A).
- Of glasses, relation to power loss and conductivity, L. S. McDowell, H. Begeman—367(A)
- Theory, in the new quantum mechanics, J. H. Van Vleck—727

Dielectrics

Solid, electric absorption currents, H. H. Race—913(A)

Diffraction (see also x-rays)

Of soft x-rays by ruled grating, F. L. Hunt—919 (A)

Diffusion

- Of resonance radiation in Hg vapor, M. W. Zemansky—513
- Of U, Th, Ce, Zr, Yt in hot tungsten, constants of, S. Dushman, D. Dennison, N. B. Reynolds—903(A)

Discharge of electricity in gases (see also Spark discharge)

- Geiger counters, properties, R. D. Bennett—363 (A)
- In He-O₂, A-O₂ mixtures, spectra, D. A. Keys—209(A)
- In H₂, resonance glow, R. D. Rusk—213(A)
- In H₂, spectral intensity distribution, E. W. Tschudi—254(A)
- In H₂ and He, pressure effects on striae, J. Zeleny—609(A)
- In H₂, number of radiating atoms, W. H. Crew, E. O. Hulbert—843
- In H₂, He, N₂, air, CO, CO₂, pressure effects on striae, L. H. Dawson—610(A)
- In H₂-O₂ mixtures, rate of combination, R. D. Rusk—907(A)
- Normal cathode fall, theory, K. T. Compton, P. M. Morse—909(A)
- Pressures in long slim discharge tubes, W. H. Crew, E. O. Hulbert—609(A)

Discharge of electricity in high vacua

with intense electric field, C. Del Rosario—360(A)

Disintegration of atoms

As shown by Wilson cloud-tracks, W. D. Harkins, H. A. Shadduck—207(A)

Dissociation

- Of H₂, by electron impact, A. Ll. Hughes, A. M. Skellett—907(A)
- Of HCl, by positive ion impact, W. M. Nielsen—907(A)

Ears

Resolving power of the ears, A. L. Bennett—911 (A)

Earth Currents

At Watheroo, western Australia, and Ebro, Spain, W. L. Rooney, O. H. Gish—905(A)

Earth tides

At Pasadena, W. T. Whitney—755(A)

Elastic oscillations

- Continuous motion produced by, W. B. Morton, A. McKinstry—192
- In crystals, shear mode, W. G. Cady—617(A)
- In quartz, factors affecting constancy, E. M. Terry—366(A)
- In quartz, subfundamentals, J. R. Harrison—366(A)
- In solids, change with pressure, F. Zwicky—579, 755(A)

Electrical capacity

Polarization capacity for Au and Pt electrodes, E. E. Zimmerman—913(A)

Electrical conductivity and resistance

- Of active nitrogen, P. A. Constantinides—215(A)
- Of air condenser, high frequency, S. L. Brown, C. F. Wiebusch, M. Y. Colby—887
- Of Cu wires, high frequency, W. M. Roberds—165
- Of electrolytic cells with Au and Pt electrodes, E. E. Zimmerman—913(A)
- Of elements, atomic properties which determine, K. F. Herzfeld—701
- Of glasses, relation to power losses, L. S. McDowell, H. Begeman—367(A)
- Of metals, effect of pressure, F. Zwicky—579, 755(A)
- Of metals, effect of pressure, A. T. Waterman—368(A)
- Of Se, light sensitiveness, A. M. MacMahon—219(A)
- Of Se, light sensitiveness, R. J. Piersol—902(A)
- Of Se, influence of temperature, R. J. Piersol—362(A)
- Of Te films, and Hall effect, F. W. Warburton—905(A)

Electrical currents

Absorption currents in solid dielectrics, H. H. Race—913(A)

Distribution in systems of conductors, theory, F. Wenner—218(A)

Electrical measurements (see also Electrical conductivity)

At radio frequencies, S. L. Brown, M. Y. Colby—717

Determination of dielectric constant of air by discharge method, A. P. Carman, K. H. Hubbard—217(A), 299

Electrical oscillations and waves

Absorption of radio waves in upper atmosphere, E. O. Hulbert—365(A), 706

High frequency magnetic properties of Fe, J. R. Martin—906(A)

High frequency permeability of iron and magnetite, G. R. Wait—566

High frequency resistance of air condenser, S. L. Brown, C. F. Wiebusch, M. Y. Colby—887

High frequency resistance of Cu wire, W. M. Roberds—165

Measurements at radio frequencies, S. L. Brown, M. Y. Colby—717

Propagation along coaxial conductors, N. H. Frank—365(A)

Refractive index of water for short waves, L. E. McCarty, L. T. Jones—880

Resonance in alternating current circuits, F. H. Miller—546

Shielded oscillator for Hertzian waves, J. Tykocinski-Tykociner—217(A)

Type of oscillation hysteresis, L. Taylor—617(A)

Electrolytes

Activity of monovalent ions, H. Mueller—216(A)

E. m. f. of cells with fluorescent electrolytes, H. W. Russell—615(A)

Polarization capacity and resistance for Au and Pt electrodes, E. E. Zimmerman—913(A)

Theory of cell with liquid junction, P. B. Taylor—369(A)

Theory of surfaces of contact, R. D. Kleeman—368(A)

Electromagnetic theory

Distribution of currents in linear conductors, F. Wenner—218(A)

Forces between currents and magnetic fields, V. Karapetoff—367(A)

Gyromagnetic electron theory of Compton effect, L. V. King—919(A)

King's theory of atomic structure, B. Podolsky—750(A)

Electromagnetic theory (cont.)

Origin of magnetic fields of sun spots, W. F. G. Swann—905(A)

Propagation of waves along coaxial conductors, N. H. Frank—365(A)

Refraction in moving media, N. Galli-Shohat—906(A)

Scattering by Einstein center, T. Takeuchi—186

Trouton-Noble experiment, P. S. Epstein—753(A)

Unification of grad, div, curl, V. Karapetoff—914(A)

Electromotive force

At surfaces of contact, R. D. Kleeman—368(A)

In conductors, due to thermal agitation, J. B. Johnson—367(A)

In conductors, due to thermal agitation, H. Nyquist—614(A)

Photo-e. m. f. in Se, R. L. Hanson—924(A)

Electrons

Affinity of H₂ for, L. Pauling—285

Distribution in crystal atoms, R. J. Havighurst—1

Distribution in crystal atoms, J. A. Bearden—20

Heat of condensation on Mo, C. C. VanVoorhis, K. T. Compton—909(A)

Photographic effect, J. E. Henderson—360(A)

Pulling electrons out of metals, C. Del Rosario—360(A)

Surface heat of charging, L. Tonks, I. Langmuir—524, 614(A)

Spinning, relation to impact polarization, A. Ellett—207(A)

Spinning, theory of Compton effect, L. V. King—919(A)

Velocity distribution, after passing diaphragms, R. H. Dalton, W. P. Baxter—248

Wave theory of, W. P. Allis, H. Mueller—361(A)

Electrons, energy states (see also Potentials, critical; spectra; spectroscopic terms)

Comprehensive energy level diagram, R. T. Birge—922(A)

In C atom, R. B. Lindsay—497

In CO, F. L. Mohler, P. D. Foote—141

In Cu, O. S. Duffendack, J. G. Black—358(A)

In diatomic molecules, R. S. Mulliken—211(A), 391, 637

In diatomic hydrides, R. S. Mulliken—921(A)

In In vapor, J. G. Frayne, C. W. Jarvis—357(A)

O and N levels in tungsten, H. E. Krefft—908(A)

Pendulum orbits, R. B. Lindsay—612(A)

Electrons, impacts, reflection, scattering

Impact polarization and spinning electron, A. Ellett—207(A)

- Electrons, impacts, reflection, scattering (cont.)**
- Impact polarization, in Hg, J. A. Eldridge, A. Ellett, H. F. Olson—207(A)
 - In CO, critical potentials, F. L. Mohler, P. D. Foote—141
 - In He, energy distribution of scattered electrons, A. Ll. Hughes, L. W. Jones—214(A)
 - In He, energy and angular distribution of scattered electrons, E. G. Dymond—433
 - On Fe, velocity distribution of secondaries, H. E. Farnsworth—908(A)
 - On Mo, number and energy of secondaries, W. R. Ham—908(A)
 - On Mo, number of secondaries as function of incident velocity, A. W. Hull, L. M. Hyatt—214(A)
 - On Ni, single crystal, angular distribution of scattered electrons, C. Davission, L. H. Germer—908(A)
- Electrons in metals**
- Effects due to thermal agitation, H. Nyquist—614(A)
 - E. m. f. due to thermal agitation, J. B. Johnson—367(A)
- Electrons, photoelectric (see Photoelectric effect)**
- Electrons, secondary (see also Electron impacts)**
- Produced by positive Cs ions, J. M. Hyatt—214(A)
- Electrophoresis**
- Cell, new type, M. Mooney—218(A)
 - Mobility formula, M. Mooney—217(A)
- Electrostatics**
- Of the thunderstorm, A. W. Simon—754(A)
- Ether-drift**
- Report on experiments at Cleveland, 1927, D. C. Miller—924(A)
- Evaporation of water**
- From large bodies of water, measurements, B. and P. Richardson—755(A)
- Faraday effect**
- Lag behind the magnetic field for various liquids, J. W. Beams, F. Allison—161
 - Lag behind the magnetic field, effect of wavelength, F. Allison—370(A)
- Films**
- Of metals, x-ray analysis, K. Horovitz—352(A)
 - Of Ni and Fe, magnetic properties, R. L. Edwards—321
- Filters for light**
- Liquid, for determination of color temperatures, R. Davis, K. S. Gibson—916(A)
- Fine Structure**
- Of Balmer lines, N. A. Kent, L. B. Taylor, H. Pearson—748(A)
 - Of Balmer lines, W. V. Houston—749(A)
 - Compound interferometer for fine structure work, W. V. Houston—210(A), 478
 - Of He arc spectrum, W. V. Houston—749(A)
 - Of Hg 3650A, W. H. McCurdy—915(A)
 - Of Hg 2536A, Zeeman effect, W. A. MacNair—915(A)
 - Of infra-red absorption bands of NH₃, G. A. Stinchcomb, E. F. Barker—213(A)
- Fluorescence (see also Spectra, fluorescence)**
- Of Cd vapor, W. A. MacNair—677
 - Of cod-liver oil, J. W. Woodrow, G. M. Wissink—219(A)
 - Of fluorescein, E. H. Kennard—466
 - Of iodine vapor, relation to absorption, F. W. Loomis—112
 - Of iodine vapor, new series, F. W. Loomis—355(A)
 - Of metallic vapors, by Hg arc, J. C. McLennan, I. Walerstein—208(A)
 - Of Na vapor, R. W. Wood, E. L. Kinsey—917(A)
 - Of Zn induced by impact with excited Hg, J. G. Winans—213(A)
 - Potential of photoactive cell with fluorescent electrolytes, H. W. Russell—615(A)
- Free path (see also Electron impacts)**
- Of K ions, as function of velocity, F. M. Durbin—215(A)
- Frequency**
- Precise determination of, J. Tykocinski-Tykociner—366(A)
 - Significance in physics, W. S. Franklin—362(A)
- Friction**
- Internal, in solids, A. L. Kimball, D. E. Lovell—616(A)
- Geiger counters**
- Some properties of, R. D. Bennett—363(A)
- Geophysics**
- Earth currents at Watheroo, Western Australia, and Ebro, Spain, W. J. Rooney, O. H. Gish—905(A)
 - Earth tides in Pasadena, W. T. Whitney—755(A)
 - Vertical seismometer, S. Smith—755(A)
- Gravitation**
- Constant, redetermination, P. R. Heyl—910(A)
 - Constant, resonance method for determining, J. Kunz—910(A)

Hall effect

In Bi, with small magnetic fields, C. W. Heaps—332
In Te films, F. W. Warburton—905(A)

Heat

Energy of x-rays, R. Kegerreis—775
Surface heat of charging, L. Tonks, I. Langmuir—524, 614(A)
Of condensation of electrons on Mo, C. C. VanVoorhis, K. T. Compton—909(A)
Of fusion, theory, N. Rashevsky—220(A)

Heaviside layer

Absorption of radio waves in upper atmosphere, E. O. Hulbert—365(A), 706

Helium

Purification of, J. W. Cook—910(A)

Herschel-Quincke tube

Theory of, G. W. Stewart—220(A)

Humidity

Effect on heat transmission in insulating materials, L. F. Miller—370(A)
Effect on gold plated, screw-knob weights, A. T. Pienkowsky, E. S. Fowle—000(A)

Impact fluorescence (see Fluorescence)**Instruments (see also Measurements, methods)**

Interferometer, compound, for fine structure work, W. V. Houston—210(A), 478
Neon glow lamp, E. Klein—610(A)
Oscillograph, Dufour, G. F. Harrington, A. M. Opsahl—364(A)
Radiometer, of molybdenite, W. W. Coblenz, C. W. Hughes—365(A): test of, W. W. Coblenz—615(A)

Shield from vibrations, R. C. Hartsough—910(A)
Spectrograph, vacuum, of large incident angle, J. B. Hoag—208(A)
Surface tension, new instrument for measuring, F. E. Poindexter—221(A)
Vacuum gauge, ionization, absolute, T. H. Johnson—610(A)
Vacuum gauge, hot wire, A. Ll. Hughes, A. M. Skellett—365(A)
Vacuum switch, H. E. Mendenhall—754(A)
Vacuum tube oscillator, theory, D. G. Bourgin—912(A)
Velocity selector, for atomic rays, J. Tykocinski-Tykociner—611(A)

Intensity relations in spectra (see also Spectra)

In bands of CN type, R. S. Mulliken—923(A)

In bands of diatomic hydrides, R. S. Mulliken—921(A)

In bands of diatomic molecules, R. S. Mulliken—211(A), 391, 637

In fundamental HCl band, D. G. Bourgin—794

Of some lines of Hg, J. Valasek—817

In spectra of isotopes of Hg and Cl, F. A. Jenkins—50

Interferometers

Applied to study of infra-red solar spectrum, H. D. Babcock—748(A)

Compound, for fine structure work, W. V. Houston—210(A), 478

Measurements on Balmer series, W. V. Houston—749(A)

Ionization by electron impact (see also Potentials, critical)

In HCl, analysis of ions formed, H. A. Barton—608(A)

In Hg vapor, probability as function of velocity, T. J. Jones—822

In Hg vapor, ultra-ionization potentials, E. O. Lawrence—609(A)

In Ga and In vapor, critical potentials, C. W. Jarvis—442

Ionization by collisions of second kind

In mixtures of H₂ and N₂ with rare gases, G. P. Harnwell—611(A), 906(A)

In rare gases, G. P. Harnwell—683
simultaneous ionization and excitation, O. S. Duffendack, H. L. Smith—914(A)

Ionization by radiation (see photoelectric effect)**Ionization gauge**

Absolute vacuum gauge, T. H. Johnson—610(A)

Ionization potentials (see Potentials critical)**Ions (see also Mobility)**

Dissociation of HCl by positive Na ions, H. M. Nielsen—907(A)

Excitation of Hg spectrum by positive K ion impact, E. J. Jones—611(A)

Formation of negative ions, theory, A. P. Alexievska—752(A)

Heats of condensation of positive ions on Mo, C. C. VanVoorhis, K. T. Compton—909(A)

Nature of gaseous ions, H. A. Erikson—215(A)

Nature of gaseous ions, L. B. Loeb—752(A)

Of K, dependence of free path on velocity, F. M. Durbin—215(A)

Residual, in Hg arc, M. L. Pool—915(A)

Secondary electron emission produced by Cs ions, J. M. Hyatt—214(A)

Transformation period of initial positive air ion, L. M. Valasek—542

Ions, electrolytic

Activity of monovalent ions, H. Mueller—216(A)
Influence of, on moisture in steam, A. W. Ewell
—912(A)

Isotopes

Of B, alpha bands of BO, F. A. Jenkins—921(A)
Of Hg and Cl, spectra, F. A. Jenkins—50

Kerr effect

Lag behind the magnetic field, J. W. Beams,
E. O. Lawrence—903(A)

Lenses

Effect of variation from condition for achro-
matism, T. T. Smith—220(A)

Magnetic dipole

In Schroedinger's theory, P. S. Epstein—751(A)

Magnetic fields

In sun spots, origin of, W. F. G. Swann—905(A)
Method of measuring, J. Tykocinski-Tykociner,
J. Kunz—904(A)

Magnetic properties (see also Hall effect)

Magnetic moment of atomic iodine, J. B. Taylor,
T. E. Phipps—904(A)

Magnetic moment of He and H₂, I. H. Solt—
904(A)

Magnetic moment of atomic hydrogen, T. E.
Phipps, J. B. Taylor—218(A), 309

Magnetic moments of Fe in complex salts, L. A.
Welo, O. Baudisch—612(A)

Magneto-striction in monel metal, S. R. Williams
—370(A)

Of Fe, in high frequency fields, J. R. Martin—
906(A)

Of evaporated Ni and Fe films, R. L. Edwards
—321

Permeability of Fe and magnetite in high fre-
quency fields, G. R. Wait—566

Susceptibilities in new quantum mechanics, J. H.
VanVleck—727

Susceptibilities, principal, of crystals, I. I. Rabi
—174

Susceptibilities of O₂ and NO, J. H. VanVleck—
613(A)

Susceptibilities of rare earth metals, E. H. Wil-
liams—218(A)

Susceptibility of single crystal metals, C. Nus-
baum—905(A)

Susceptibility of single crystal elements, C.
Nusbaum—370(A)

Thermomagnetic effect in gases, N. C. Little—
901(A)

Magneton numbers

In the Fe group, spectroscopic interpretation,
A. Sommerfeld, O. Laporte—208(A)

Mathematics

Formal unification of grad, div, curl by operational
volume, V. Karapetoff—914(A)

Log, semi-log and uniform coordinator, R. A.
Castleman—910(A)

Method of least square vs. arithmetic method of
determining slope of straight line, R. C.
Spencer—909(A)

Variation of functions involving factorials, M.
Masius—613(A)

Wave-filter determinants, analysis and applica-
tion, F. D. Murnaghan, H. A. Wheeler—914(A)

Measurements, methods (see also Instruments)

Of determining sound transmission, F. R. Watson
—925(A)

Of determining frequencies piezo-electrically, J.
Tykocinski-Tykociner—366(A)

Of determining gravitational constant, J. Kunz
—910(A)

Of drawing tube-characteristics automatically,
G. C. Campbell, G. W. Willard—913(A)

Of measuring principal magnetic susceptibilities
of crystals, I. I. Rabi—174

Of measuring magnetic field distribution, J.
Tykocinski-Tykociner, J. Kunz—904(A)

Of measuring velocity of fluids, H. E. Hartig,
H. B. Wilcox—485

Of studying short time occurrences, G. F. Harring-
ton, A. M. Opsahl—364(A)

Mechanics, quantum

Charge density in wave mechanics, R. M. Langer
—924(A)

General proof of Langevin—Debye formula and
susceptibilities of O₂ and NO, J. H. VanVleck
—613(A)

Influence of magnetic field on dielectric constant,
L. Pauling—145

Magnetic dipole in wave mechanics, P. S. Epstein
—750(A)

On conditions of validity of macro-mechanics,
M. S. Vallarta—613(A)

Symmetrical top in wave mechanics, R. de L.
Kronig, I. I. Rabi—262

Wave theory of electron, W. P. Allis, H. Mueller
—361(A)

Wave mechanics, application to quantization of
rotational energy of molecules, E. E. Witmer
—362(A)

Metastable atoms

Explanation of long life, G. Breit—361(A)

Metastable atoms (cont.)

- In Hg, post-arc conductivity, M. L. Pool—610(A)
- In Hg, residual ions and restriking potentials, M. L. Pool—915(A)
- In Ne and A, R. Rudy—359(A)

Meteorological physics

- Effect of oil in storage on lightning discharge, R. W. Sorenson—754(A)
- Electrostatics of thunderstorm, A. W. Simon—754(A)

Michelson-Morley experiment

- Ether-drift experiments in Cleveland, 1927, D. C. Miller—924(A)

Mobility of ions

- Dependence on nature of medium, H. A. Erikson—369(A)
- In hydrogen gas mixtures, L. B. Loeb—751(A)
- Nature of gaseous ions, H. A. Erikson—215(A)
- Transformation period of initial positive ion, L. M. Valasek—542

Molecular fields (see Molecular structure)**Molecular space array**

- In liquid primary normal alcohols, G. W. Stewart, R. M. Morrow—919(A)

Molecular structure

- Constants of AlO, moment of inertia, nuclear separation, W. C. Pomeroy—59
- Electronic states and band structure in diatomic molecules III, R. S. Mulliken—391
- Energy levels in CO, F. L. Mohler, P. D. Foote—141
- Energy of crossed orbit model of H₂, E. Hutchison—270
- Molecular fields, D. G. Bourgin—368(A)
- Of NaH, moments of inertia and nuclear separation, E. H. Johnson—85
- Of NO, F. A. Jenkins, H. A. Barton, R. S. Mulliken—211(A)
- Quantization of rotational energy, E. E. Witmer—362(A)
- Rotational and vibrational specific heat of diatomic molecules, E. E. Witmer—918(A)
- Vibrational levels in Na₂; F. W. Loomis—607(A)

Multiplets

- In Cr (III) and Mn (III), R. C. Gibbs, H. E. White—917(A)
- In three electron systems of first long period, R. C. Gibbs, H. E. White—655
- In two-electron systems of first long period, R. C. Gibbs, H. E. White—426
- In V (III), R. C. Gibbs, H. E. White—606(A)
- Two-electron multiplets in first and second long periods, R. C. Gibbs, H. E. White—359(A)

Neon glow lamp

- Constancy of flashing period, E; Klein—610(A)

Nodal lines

- Of bells, A. T. Jones—816(A)

Nuclear structure

- System for atomic nuclei, W. W. Nicholas—612(A)
- Synthesis and disintegration of atoms, W. D. Harkins, H. A. Shadduck—207(A)

Optical constants

- Of Cs, variation with state, J. B. Nathanson—369(A)

Optics, geometrical

- Lenses, effect of variation from condition of achromatism, T. T. Smith—220(A)

Oscillators

- Piezo-electric, quartz plate, theory and application, J. R. Harrington—617(A)
- Piezo-electric, quartz, for determining frequencies, J. Tykocinski-Tykokiner—366(A)
- Piezo-electric, quartz plate, subfundamentals, J. R. Harrington—366(A)
- Piezo-electric, quartz, factors influencing constancy, E. M. Terry—366(A)
- Vacuum tube, shielded, for Hertzian waves, J. Tykocinski-Tykokiner—217(A)
- Vacuum tube, theory, D. G. Bourgin—912(A)
- Vacuum tube, oscillation hysteresis, L. Taylor—617(A)

Oscillograph

- Dufour, technique for short time occurrences, G. F. Harrington, A. M. Opsahl—364(A)

Passivity

- Electronic theory of, W. D. Lansing—216(A)

Penetrating radiation

- Variation of residual ionization with pressure at different altitudes, W. F. G. Swann—372(A)

Photoelectric conduction

- In argenite, W. A. Schneider—363(A)
- In crystals, significance, A. M. MacMahon—902(A)
- In molybdenite, W. W. Coblenz, C. W. Hughes—365(A)
- In molybdenite, tests, W. W. Coblenz—615(A)
- In Se, relation to light intensity, R. J. Piersol—902(A)
- In Se, influence of temperature, R. J. Piersol—363(A)
- In sulphur crystals, relation to absorption, B. Kurrelmeyer—615(A)
- Photoelectromotive force in Se, R. L. Hanson—924(A)

- Photoelectric emission of electrons**
- Direction of, D. H. Loughridge—751(A)
 - By x-rays, explanation of Whiddington's rule, E. C. Watson—919(A)
 - By x-rays, relative probabilities for elements Ag to Au, F. K. Richtmyer, L. S. Taylor—353(A)
 - By x-rays, spatial distribution, E. C. Watson—752(A)
 - By x-rays, velocity and number for various angles, E. C. Watson—751(A)
 - From K, effect of oxygen, L. R. Koller—902(A)
 - From thoroughly outgassed Pt, L. A. Dubridge—451
 - From Na-K alloys, as function of composition, H. E. Ives, G. R. Stilwell—252, 363(A)
 - Instantaneity of, E. O. Lawrence, J. W. Beams—903(A)
 - Threshold, in Hg, changes, H. K. Dunn—693
 - Thresholds, periodicity with atomic number, G. B. Welsh—615(A)
 - Threshold, from Bi crystals, T. J. Parmley—902 (A)
- Photopionization of gases**
- Of Hg vapor, by 2537, P. D. Foote—609(A)
- Photographic effects**
- Of slow electrons, J. E. Henderson—360(A)
- Piezo-electric effects (see also Oscillators)**
- In crystal quartz, L. H. Dawson—216(A), 532
 - In crystals, shear mode of vibration, W. G. Cady—617(A)
 - In quartz, subfundamental vibrations, J. R. Harrison—366(A)
 - In quartz, theory and application, J. R. Harrison—617(A)
- Polarization of radiation (see also x-rays)**
- Excited by electron impact, theory, J. A. Eldridge, A. Ellett, H. F. Olson—207(A)
 - Excited by electron impact, spinning electron, A. Ellett—207(A)
 - From hydrogen canal rays, K. L. Hertel—214(A), 848
 - Of resonance radiation in strong magnetic fields, A. Ellett—404(A)
 - Of Hg 2537, in magnetic field, H. F. Olson—207(A)
 - Of resonance radiation in Cd, W. A. MacNair—677
- Potentials, critical**
- For Cu, excitation of soft x-rays, R. Hamer, S. Singh—901(A)
 - For Fe, relation between radiation and ionization potentials, O. Stuhlman—354(A)
 - For Fe, excitation of soft x-rays, R. Hamer, S. Singh—608(A)
- In CO, for band spectra, A. B. Hepburn—212(A)
 - In Cu (II), Ni (I), Pd (I), A. G. Shenstone—209(A)
 - In Ga and In vapor, C. W. Jarvis—442
 - In H₂, the 29 volt critical potential, R. D. Rusk—354(A)
 - In Hg vapor, for spark lines, J. A. Eldridge—213(A)
 - In Hg vapor, ultra-ionization potentials, E. O. Lawrence—609(A)
 - In Hg vapor, critical restriking potentials for arc, M. L. Pool—915(A)
 - In In vapor, stages in excitation of spectrum, J. G. Frayne, C. W. Jarvis—673
 - In metal arcs, striking potentials, S. H. Anderson—750(A)
 - Of Li atom, second ionization potential, theory, L. Pauling—285
- Proceedings of the American Physical Society**
- Chicago Meeting, November 26–27, 1926—204
 - Philadelphia Meeting, December 28–30, 1926—350
 - New York Meeting, February 25–26, 1927—604
 - Los Angeles Meeting, March 5, 1927—749
 - Washington Meeting, April 22–23, 1927—901
- Pyrometry**
- Liquid filters for determination of color temperatures, R. Davis, K. S. Gibson—916(A)
- Quantization**
- Of rotational energy in molecules by new wave mechanics, E. E. Witmer—362(A)
- Quantum mechanics (see Mechanics)**
- Quantum of radiation**
- Length of, E. O. Lawrence, J. W. Beams—361(A)
- Quantum theory (see also Mechanics)**
- Of specific heat of HCl, E. Hutchisson—360(A)
- Radioactivity**
- Origin of actinium series, new theory, T. R. Wilkins—352(A)
 - Absorption of beta-rays, J. A. Gray, B. W. Sargent—351(A)
 - Synthesis and disintegration of atoms, W. D. Harkins, H. A. Shadduck—207(A)
- Radiometers and measurements**
- Measurements on planet, Mars, W. W. Coblenz, C. O. Lampland—372(A)
 - New, selective radiometer of molybdenite, W. W. Coblenz, C. W. Hughes—365(A); tests, W. W. Coblenz—615(A)

Rectifiers

High pressure powder rectifier, J. E. Lilienfeld, C. H. Thomas—367(A)

Reflection (see X-rays)**Refraction**

In moving media, N. Galli-Shohat—906(A)

Refractive index

Of gases at higher temperatures, E. W. Cheney—292

Of water, measurement, A. W. Nye—753(A)

Of water, for short electric waves, L. E. McCarty, L. T. Jones—880

Relativity

Theory of Trouton-Noble experiment, P. S. Epstein—753(A)

Report of ether-drift experiments in Cleveland, 1927, D. C. Miller—924(A)

Residual ionization

Variation with pressure at various altitudes, W. F. G. Swann—372(A)

Residual rays from crystals

Infra-red reflection spectra of some carbonates, E. K. Plyler—923(A)

Shift with pressure, F. Zwicky—579, 755(A)

Resonance

In a. c. circuits, F. H. Miller—546

Resonance potentials (see Potentials, critical)**Resonance radiation**

Diffusion in Hg vapor, M. W. Zemansky—513

Polarization of Hg 2537, H. F. Olson—207(A)

Polarization in strong magnetic fields, A. Ellett—904(A)

Rijke tube

Improved form of high efficiency, R. W. Wood—373(A)

Screening constants

From optical data, O. Laporte—650

Seismometer

Vertical seismometer, S. Smith—755(A)

Shot effect

Theory, H. A. Wheeler—903(A)

Solid solutions

Of Ni-Cr and Ni-Fe, crystal structure, F. C. Blake, J. Lord, A. E. Focke—206(A)

Space charge

In triode, cause of negative resistance, L. Tonks—913(A)

Spark discharge

Study by the shadowgraph method, H. A. Zinzser—752(A)

Time of appearance and duration of spectrum lines, J. W. Beams, E. O. Lawrence—357(A)

Specific heats

Of methane, theory of, J. Kunz—220(A)

Rotational and vibrational, of diatomic gas, theory E. E. Witmer—918(A)

Of HCl, quantum theory, E. Hutchisson—360(A)

Spectra, atomic

Of B, C, N, O, F, I, S. Bowen—231

Of B, R. A. Sawyer, F. R. Smith—357(A)

Of Cr (III) and Mn (III), multiplets, R. C. Gibbs, H. E. White—917(A)

Of Cu, in hydrogen furnace, O. S. Duffendack, J. G. Black—358(A)

Of Cu, by collisions of second kind, O. S. Duffendack, H. L. Smith—914(A)

Of Cu (II), by positive neon ions, O. S. Duffendack, J. G. Black—925(A)

Of Cu and Rh, Zeeman effect, L. A. Sommer—358(A)

Of Cu (II), A. G. Shenstone—209(A), 380

Of Fe, Cr, Ti, Mg, Cu, Si, in high-current vacuum arc, A. S. King—359(A)

Of Fe, Co, Ni, absorption, W. F. Meggers—358(A)

Of Fe group, magneton numbers, A. Sommerfeld, O. Laporte—208(A)

Of first and second long period elements, two-electron multiplets, H. E. White, R. C. Gibbs—359(A)

Of first long period, three-electron multiplets, R. C. Gibbs, H. E. White—655

Of first long period elements, two-electron multiplets, R. C. Gibbs, H. E. White—426

Of first period elements, relations, R. A. Millikan, I. S. Bowen—749(A)

Of Ga, In, Mn, Cr, Ni, Co, absorption in underwater sparks, A. Smith, M. Muskat—663

Of Ge, arc, C. W. Gartlein—357(A)

Of He, Stark effect, J. S. Foster—916 (A)

Of Hg and Cli, isotopes, F. A. Jenkins—50

Of Hg, infra-red, V. P. Lubovich—355(A)

Of Hg, relative intensities, J. Valasek—817

Of ionized P, I. S. Bowen—749(A), 510

Of Na, K, Cs, Mg, Cd, Zn, Hg, Tl, by atomic hydrogen, F. L. Mohler—354(A), 419

Of Ne, Stark effect, J. S. Foster, W. Rowles—925(A)

Of Ni, spark, A. G. Shenstone—917(A)

Of oxygen, ultra-violet, J. J. Hopfield—923(A)

Of Sb, absorption, R. V. Zumstein—209(A)

Of Sc, arc and spark, analysis; H. N. Russell, W. F. Meggers—606(A)

- Spectra, atomic (cont.)**
- Of stripped atoms, relations, R. C. Gibbs, H. E. White—359(A)
 - Of V (III), multiplets, R. C. Gibbs, H. E. White—606(A)
- Spectra, auroral**
- Note on the auroral green line 5577, D. A. Keys—209(A)
- Spectra, excitation of**
- Of CO₂, by electron impact, G. W. Fox, O. S. Duffendack, E. F. Barker—921(A)
 - Of Cu and CuH, in hydrogen furnace, O. S. Duffendack, J. G. Black—358(A)
 - Of Cu, by collisions of second kind, O. S. Duffendack, H. L. Smith—914(A)
 - Of Cu (II), by positive neon ions, O. S. Duffendack, J. G. Black—925(A)
 - Of Hg, spark lines, critical potentials, J. A. Elbridge—213(A)
 - Of Hg, by positive ion impact, E. J. Jones—611(A)
 - Of In, by electron impact, J. G. Frayne, C. W. Jarvis—357(A), 673
 - Of N, by electron impact in mixture with He, R. A. Wolfe, O. S. Duffendack—209(A)
 - Of Na, K, Cs, Mg, Cd, Zn, Hg, Tl, by atomic hydrogen, F. L. Mohler—354(A), 419
- Spectra, fluorescent**
- Of iodine, correlation with absorption, R. W. Loomis—112
 - Of iodine, new series, F. W. Loomis—355(A)
 - Of Na vapor, R. W. Wood, E. L. Kinsey—917(A)
 - Of S, Se, Te, Bi vapors excited by Hg arc, J. C. McLennan, I. Walerstein—208(A)
- Spectra, molecular**
- Of AgH, AlH, ZnH, MgH, Zeeman effect, W. W. Watson, B. Perkins—921(A)
 - Of AlO, quantum analysis, W. C. Pomeroy—59
 - Of benzene derivatives, shift of absorption bands, J. Barnes—922(A)
 - Of BO, structure and isotope effect in alpha bands, F. A. Jenkins—921(A)
 - Of CaH, E. Hulthen—97
 - Of C₂H₂, C₂H₄, C₂H₆, infra-red absorption, C. F. Meyer, A. Levin—923(A)
 - Of CH₄, new infra-red absorption bands, J. W. Ellis—751(A)
 - Of CO, ultra-violet emission and absorption, J. J. Hopfield, R. T. Birge—922(A)
 - Of CO, A. B. Hepburn—212(A)
 - Of CO₂, G. W. Fox, O. S. Duffendack, E. F. Barker—921(A)
 - Of CuH, O. S. Duffendack, J. G. Black—358(A)
 - Of fluorine, continuous emission and absorption, H. G. Gale, G. S. Monk—211(A)
- Of hydrocarbons, F. C. McDonald—212(A)
- Of iodine, absorption, F. W. Loomis—112
- Of MgH, rotational terms, W. W. Watson, P. Rudnick—413
- Of Na, vibrational levels in blue-green bands, F. W. Loomis—607(A)
- Of Na and K, absorption bands, W. R. Fredrickson, W. W. Watson, J. Rinker—917(A)
- Of NaH, many-lined spectrum, E. H. Johnson—85
- Of NH₃, infra-red bands, fine structure, G. A. Stinchcomb, E. F. Barker—213(A)
- Of NH₃, infra-red, W. F. Colby, E. F. Barker—923(A)
- Of N₂, air, C₂H₂, CO, extreme ultra-violet absorption, J. J. Hopfield—356(A)
- Of N₂, ultra-violet, R. T. Birge, J. J. Hopfield—356(A)
- Of NO, beta bands, F. A. Jenkins, H. A. Barton, R. S. Mulliken—211(A)
- Of O₂ in ultra-violet, V. Ellsworth, J. J. Hopfield—79
- Of Ti, quantum analysis, R. T. Birge, A. Christy—212(A)
- Stark effect**
- In He arc spectrum, theory, J. S. Foster—916(A)
 - In Ne, J. S. Foster, J. W. Rowles—925(A)
- Sun spots**
- Origin of magnetic fields of, W. F. G. Swann—905(A)
- Surface tension**
- New instrument for measuring, F. E. Poindexter—221(A)
 - Of molten copper, as function of temperature, E. E. Libman—911(A)
 - Of oils, variation with temperature, G. Winchester—911(A)
- Surface layers**
- On W, produced by active nitrogen, C. Kenty, L. A. Turner—914(A)
- Susceptibility (see Magnetic properties)**
- Temperature**
- Distribution along a wire, V. Bush, K. E. Gould—337
 - Variations in wires heated by a. c., L. Smeele—614(A)
- Thermal conductivity**
- Of fused quartz as function of temperature, H. E. Seemann—616(A)
 - Of insulating materials, affected by humidity, L. F. Miller—370(A)

Thermal expansion

- Of Be, P. Hidnert, W. T. Sweeney—616(A)
 Of graphite, P. Hidnert, W. T. Sweeney—371(A)
 Of nickel steels, P. Hidnert, W. T. Sweeney—911
 (A)
 Of quartz, E. W. Cheney—292

Thermionic emission of electrons

- Effect of surface layers produced by active nitrogen, C. Kenty, L. A. Turner—914(A)
 Emission and diffusion constants for tungsten containing various oxides, S. Dushman, D. Dennison, N. B. Reynolds—903(A)
 Equations for, W. R. Ham—607(A)
 Factors influencing, A. K. Brewer—752(A)
 From thoriated tungsten, S. Dushman, J. W. Ewald—857(A)
 Interpretation of data, W. R. Ham—364(A)
 Shot effect, theory, H. A. Wheeler—903(A)
 Space charge as cause of negative resistance, L. Tonks—913(A)
 Surface heat of charging, L. Tonks, I. Langmuir—524, 614(A)

Thermodynamics

- Absolute zero of entropy and energy, R. D. Kleeman—369(A)
 Properties of substances in condensed state at absolute zero, R. D. Kleeman—614(A)
 Reversible mixing of substance in condensed state at absolute zero, R. D. Kleeman—912(A)

Thermoelectric effects

- In single crystal Zn, E. G. Linder—221(A), 554

Thermomagnetic effects

- In gases, N. C. Little—901(A)

Trouton-Noble experiment

- Theory of, P. S. Epstein—753(A)

Ultrasonic rays

- Physical and biological effect, R. W. Wood—373
 (A)

Undulatory mechanics (see Mechanics)**Vacuum tubes (see also Thermionic emission)**

- Device to draw characteristic curves automatically, G. C. Campbell, G. W. Willard—913(A)
 Oscillator, theory, D. G. Bourgin—912(A)
 Oscillation, hysteresis, L. Taylor—617(A)
 Space charge as cause of negative resistance in, L. Tonks—913(A)

Vacuum switch

- New type, H. E. Mendenhall—754(A)

Valence

- Effect on x-ray absorption, W. B. Morehouse—924(A)

Velocity selector

- For atomic rays, J. Tykocinski-Tykociner—611
 (A)

Vibrations

- Continuous motion produced by, W. B. Morton, A. McKinstry—192
 Shielding from, R. C. Hartsough—910(A)

Viscosity

- Internal, in solids, A. L. Kimball, D. E. Lovell—616(A)

Wave mechanics (see Mechanics)**Weights**

- Variation with humidity of gold-plated, screw-knob, A. T. Pienkowsky, E. S. Fowle—910(A)

Wireless (see Electrical oscillations)**Work function (see Thermionic emission)****X-rays absorption**

- Formulas, S. J. M. Allen—918(A)
 L absorption edges, Sn to Ru, G. D. Van Dyke, G. A. Lindsay—205(A)
 M series absorption of Os, Ir, Pt, R. A. Rogers—205(A)
 Of celluloid, air, H₂, for soft x-rays, E. R. Laird—41
 Relation to valence, W. B. Morehouse—924(A)
 Test of theories, F. K. Richtmyer, L. S. Taylor—606(A)

X-ray analysis (see Crystal structure)**X-rays, characteristic**

- Possible dependence on temperature, J. H. Purks, C. M. Slack—352(A)

X-rays, chemical effects

- Coloration of kunzite and hiddenite, P. L. Bayley—353(A)
 Combination of H₂ and O₂, R. D. Rusk—907(A)

X-rays, diffraction

- By ruled gratings, F. L. Hunt—919(A)
 Measurements on compounds in Portland cement, E. A. Harrington—353(A)

X-rays, general radiation

- From very thin target, W. Duane—606(A)

X-rays, energy

- For therapeutic use, H. Clark—605(A)
 Heat energy, R. Kegerreis—775
 Of soft x-rays, 40-610 v., E. R. Laird—41

- X-ray isochromats**
Of Cu, taken in different directions, W. W. Nicholas—619
- X-rays, polarization**
Polarization angle, C. S. Barrett, J. A. Bearden—352(A)
Polarization factor in reflection, P. Kirkpatrick—632
- X-rays, reflection and scattering**
By crystals, Compton effect, G. E. M. Jauncey—206(A)
By crystals, theory, S. K. Allison—375, 749(A)
From NaCl and Al, electron distribution, J. A. Bearden—20
From NaCl, Li F, NaF, CaF₂, electron distribution, R. J. Havighurst—1
Gyromagnetic electron theory of Compton effect, L. V. King—919(A)
Intensity, Compton effect, G. E. M. Jauncey—605(A)
Intensity, theory, G. E. M. Jauncey—757
Of soft x-rays, E. R. Laird—605(A)
Polarization factor in reflection, P. Kirkpatrick—632
- X-ray refraction**
By total reflection, R. L. Doan—205(A)
- X-rays, soft**
Absorption, E. R. Laird—41
- Diffraction, by grating, F. L. Hunt—919(A)
From Cu, critical potentials, R. Hamer, S. Singh—901(A)
From Fe, critical potentials, R. Hamer, S. Singh—608(A)
O and N levels of tungsten, H. E. Krefft—902(A)
Reflection of, E. R. Laird—605(A)
- X-rays, photoelectric effect**
Explanation of Whiddington's rule, E. C. Watson—919(A)
Probabilities of photo-emission, Ag to Au, F. K. Richtmyer, L. S. Taylor—353(A)
Recoil electrons from Al, A. A. Bless—918(A)
Spatial distribution of photoelectrons, E. C. Watson—752(A)
Velocity and number of photoelectrons as function of angle, E. C. Watson—751(A)
- X-rays, therapeutic**
Measurement of x-rays used for therapy, H. Clarke—605(A)
- Zeeman effect**
In AgH, AlH, ZnH, MgH bands, W. W. Watson, B. Perkins—921(A)
Of arc spectra of Cu and Rh, L. A. Sommer—358(A)
Of fine structure components of 2536 of Hg, W. A. MacNair—915(A)